BEILSTEIN JOURNAL OF ORGANIC CHEMISTRY

Synthesis in the glycosciences II

Edited by Thisbe K. Lindhorst

Imprint

Beilstein Journal of Organic Chemistry
www.bjoc.org
ISSN 1860-5397
Email: journals-support@beilstein-institut.de

The *Beilstein Journal of Organic Chemistry* is published by the Beilstein-Institut zur Förderung der Chemischen Wissenschaften.

Beilstein-Institut zur Förderung der Chemischen Wissenschaften
Trakehner Straße 7–9
60487 Frankfurt am Main
Germany
www.beilstein-institut.de

Beilstein Journal of Organic Chemistry

Synthesis in the glycosciences II

Thisbe K. Lindhorst

Editorial

Open Access

Address:
Otto Diels Institute of Organic Chemistry, Christiana Albertina University of Kiel, Otto-Hahn-Platz 3/4, 24098 Kiel, Germany

Email:
Thisbe K. Lindhorst - tklind@oc.uni-kiel.de

Beilstein J. Org. Chem. **2012,** *8,* 411–412.
doi:10.3762/bjoc.8.45

Received: 14 March 2012
Accepted: 15 March 2012
Published: 20 March 2012

This article is part of the Thematic Series "Synthesis in the glycosciences II".
The Thematic Series is dedicated to Professor Hans Paulsen on the occasion of his 90th birthday.

Guest Editor: T. K. Lindhorst

In 2010 the Beilstein Journal of Organic Chemistry launched a Thematic Series entitled "Synthesis in the glycosciences" with 14 contributions from renowned research groups in carbohydrate chemistry [1-14]. This series impressively demonstrated the power and the passion, the creativity and the cleverness of modern synthetic glycoscience. But this success is on a continuing journey. Thus, "Synthesis in the glycosciences II" has been started, and it gives me pleasure to introduce you to this Thematic Series today.

Here I have decided not to limit the field of the glycosciences to just synthetic chemistry but to let the contributions strike out as far as this intriguing field of science allows us go. It is interesting to see that, following this editorial approach, the diversity of titles reflects the diversity of carbohydrate chemistry and biology. There is no other class of natural products with a comparable potential for molecular diversity. There are no other biopolymers so difficult to assemble as the oligosaccharides. And there is no other cell organelle that is less understood in its detailed biochemical function and the meaning of its supramolecular identity than the glycocalyx. Hence, the field of "glycomics" may comprise a rather infant field of the "omics era", but it is certainly one of the most exciting and promising divisions of modern chemistry.

The many different works contributed to this Thematic Series impressively demonstrate the variety in the glycosciences. Fantasy and imagination have led to novel glycoconjugate architectures and glycobiological experiments. Expertise and rational planning have allowed the utilization of carbohydrates in stereoselective synthesis and the employment of enzymes in oligosaccharide synthesis. Analytical and pharmacological knowhow have disclosed polysaccharide and glycoconjugate structures, their biological effects and their potential as carbohydrate drugs. Boldness and interdisciplinary communication have opened the field for many medical applications benefitting human health, such as in tumor diagnosis, tumor treatment and vaccination.

One of the objectives of the glycosciences is to unravel the secrets of carbohydrate biology in living systems. For this endeavour, chemical, biological and physical concepts and

experiments have been equally important and equally challenging. In addition computer-aided methods, such as molecular dynamics studies of carbohydrates and glycoconjugates, have added valuable information about the characteristics of carbohydrate assembly. Furthermore, the field of glycobioinformatics has been recently invented and has started to assist researchers in managing an unprecedented number of structures and amount of biological information [15].

In this second captivating Thematic Series, the pride of the glycosciences is the answer to prejudice about a field which has been underestimated for most of the 20th century. Many facets of the comprehensive field of the glycosciences will be found in this Thematic Series. It has been a pleasure to orchestrate this sound, and resounding, collection. I am thankful to the authors who have earned the credits of this volume and to the entire Beilstein editorial team who have been tremendously positive, enthusiastic and serviceable. The secret of achievement is to hold a picture of a successful outcome in the mind. The outcome of this successful Thematic Series is a survey giving a representative example of "sweet" diversity.

Thisbe K. Lindhorst

Kiel, March 2012

References

1. Lindhorst, T. K. *Beilstein J. Org. Chem.* **2010,** *6,* No. 16. doi:10.3762/bjoc.6.16
2. Wang, A.; Hendel, J.; Auzanneau, F.-I. *Beilstein J. Org. Chem.* **2010,** *6,* No. 17. doi:10.3762/bjoc.6.17
3. Schmidt, D.; Thiem, J. *Beilstein J. Org. Chem.* **2010,** *6,* No. 18. doi:10.3762/bjoc.6.18
4. Fascione, M. A.; Turnbull, W. B. *Beilstein J. Org. Chem.* **2010,** *6,* No. 19. doi:10.3762/bjoc.6.19
5. Jiménez Blanco, J. L.; Ortega-Caballero, F.; Ortiz Mellet, C.; García Fernández, J. M. *Beilstein J. Org. Chem.* **2010,** *6,* No. 20. doi:10.3762/bjoc.6.20
6. Schitter, G.; Scheucher, E.; Steiner, A. J.; Stütz, A. E.; Thonhofer, M.; Tarling, C. A.; Withers, S. G.; Wicki, J.; Fantur, K.; Paschke, E.; Mahuran, D. J.; Rigat, B. A.; Tropak, M.; Wrodnigg, T. M. *Beilstein J. Org. Chem.* **2010,** *6,* No. 21. doi:10.3762/bjoc.6.21
7. Minuth, T.; Boysen, M. M. K. *Beilstein J. Org. Chem.* **2010,** *6,* No. 23. doi:10.3762/bjoc.6.23
8. Homann, A.; Qamar, R.; Serim, S.; Dersch, P.; Seibel, J. *Beilstein J. Org. Chem.* **2010,** *6,* No. 24. doi:10.3762/bjoc.6.24
9. Karch, F.; Hoffmann-Röder, A. *Beilstein J. Org. Chem.* **2010,** *6,* No. 47. doi:10.3762/bjoc.6.47
10. Šardzik, R.; Noble, G. T.; Weissenborn, M. J.; Martin, A.; Webb, S. J.; Flitsch, S. L. *Beilstein J. Org. Chem.* **2010,** *6,* 699–703. doi:10.3762/bjoc.6.81
11. Sundgren, A.; Lahmann, M.; Oscarson, S. *Beilstein J. Org. Chem.* **2010,** *6,* 704–708. doi:10.3762/bjoc.6.80
12. Lindhorst, T. K.; Bruegge, K.; Fuchs, A.; Sperling, O. *Beilstein J. Org. Chem.* **2010,** *6,* 801–809. doi:10.3762/bjoc.6.90
13. Lindhorst, T. K.; Märten, M.; Fuchs, A.; Knight, S. D. *Beilstein J. Org. Chem.* **2010,** *6,* 810–822. doi:10.3762/bjoc.6.91
14. Léo, P.-M.; Morin, C.; Philouze, C. *Beilstein J. Org. Chem.* **2010,** *6,* 1022–1024. doi:10.3762/bjoc.6.115
15. Hicks, M. G.; Kettner, C., Eds. *Proceedings of the International Beilstein Symposium on Glyco-Bioinformatics – Bits 'n' Bytes of Sugars,* Potsdam, Germany, Oct 4–8, 2009; Beilstein-Institut: Frankfurt am Main, Germany, 2010. http://www.beilstein-institut.de/en/symposia/overview/proceedings/2009-glycobioinformatics/ (accessed March 14, 2012).

License and Terms

Beilstein Journal of Organic Chemistry

Acceptor-influenced and donor-tuned base-promoted glycosylation

Stephan Boettcher[1], Martin Matwiejuk[2] and Joachim Thiem[*1]

Full Research Paper

Open Access

Address:
[1]Department of Chemistry, Faculty of Science, University of Hamburg, Martin-Luther-King-Platz 6, 20146 Hamburg, Germany and [2]Glycom A/S, c/o DTU, Building 201, Anker Engelunds Vej 1, DK-2800 Kgs. Lyngby, Denmark

Email:
Joachim Thiem[*] - thiem@chemie.uni-hamburg.de

* Corresponding author

Keywords:
glycosylation; oxyanion; reactivity; regioselectivity

Beilstein J. Org. Chem. **2012,** *8,* 413–420.
doi:10.3762/bjoc.8.46

Received: 06 January 2012
Accepted: 06 March 2012
Published: 20 March 2012

This article is part of the Thematic Series "Synthesis in the glycosciences II".

Guest Editor: T. K. Lindhorst

Abstract

Base-promoted glycosylation is a recently established stereoselective and regioselective approach for the assembly of di- and oligosaccharides by using partially protected acceptors and glycosyl halide donors. Initial studies were performed on partially methylated acceptor and donor moieties as a model system in order to analyze the key principles of oxyanion reactivities. In this work, extended studies on base-promoted glycosylation are presented by using benzyl protective groups in view of preparative applications. Emphases are placed on the influence of the acceptor anomeric configuration and donor reactivities.

Introduction

For the assembly of oligosaccharides the complex and challenging control of regio- and stereochemistry has to be solved. Various contributions have facilitated enormously the access to complex oligosaccharide structures so far; however, regioselective and stereoselective glycosylations remain difficult and alternative concepts are welcome, and should be considered and studied.

Recently regioselective and β-stereospecific glycosylations employing saccharide oxyanions have been presented. Initial studies on base-promoted glycosylations were elaborated on partially methylated glucopyranosides as model systems. This systematic approach allowed determination of the preferred positions for glycosylation and the establishment of an oxyanion reactivity scale. In addition to studies with different base promoters and donors, the first successful conversions with benzylated acceptor and donor moieties were reported [1-3].

This novel glycosylation method could substantially reduce the need to apply protecting-group chemistry. Also, the β-specificity and base-promoted activation without any heavy-metal salt or Lewis acid are useful for synthetic applications. To

develop the synthetic potential and evolve this method into an applicable alternative pathway towards di-, tri- or oligosaccharides, more research needs to be done.

So far, glycosylation reactions have been conducted by employing methyl α-glycopyranoside acceptors. Therefore, it was of particular interest to test the base-promoted glycosylation methodology with methyl β-glycopyranosides. Hence monobenzylated methyl α- and β-D-glycopyranosides were synthesized, then fucosylated by employing the base-promoted glycosylation methodology, and analysed with respect to the absolute and relative yields.

In addition, donor reactivity in base-promoted glycosylation reactions was investigated by employing partially benzylated methyl α- and β-D-glycopyranosides and donor halide mixtures.

Results and Discussion

To answer the questions above, monobenzylated methyl α- and β-D-gluco- and galactopyranosides **1**–**6** were selected as acceptor moieties (Figure 1) and synthesized by employing standard protecting-group chemistry. After base activation of the acceptor hydroxy groups, glycosylation was performed with the perbenzylated glycopyranosyl chlorides **7**–**9** (Figure 2).

The synthesis of the monobenzylated glucopyranosyl acceptors **1**–**4** started with benzylidenation [4] of compound **10** and **11**, respectively (Scheme 1). As the next step, monobenzylation of **12** and **13** by phase-transfer catalysis [5] afforded derivatives **14**–**17**. Subsequent cleavage of the benzylidene protecting group [4] gave the target compounds **1**–**4** in yields of up to 95%.

Preparation of the 3-*O*-monobenzylated methyl α- and β-D-galactopyranosyl acceptors **5** and **6** was achieved via stannylidene acetals [6] (Scheme 2). Compound **18** was subjected to a one-step synthesis with Bu_2SnO and BnBr, affording target

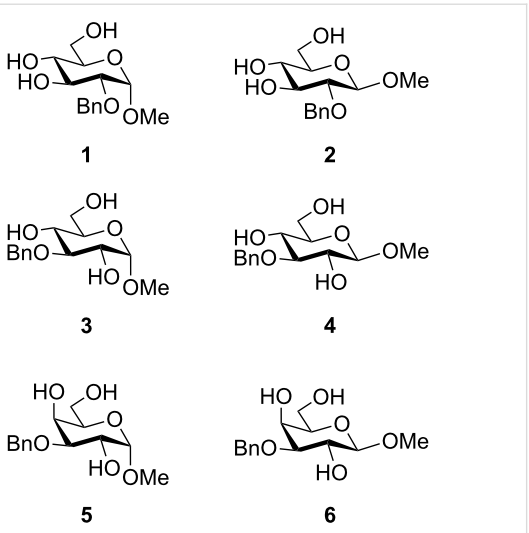

Figure 1: Monobenzylated methyl α- and β-D-gluco- and galactopyranoside acceptors **1**–**6**.

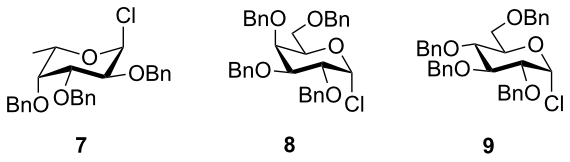

Figure 2: Benzylated glycopyranosyl halide donors **7**–**9**.

compound **5**. The synthetic route for the methyl β-glycopyranoside acceptor **6** started with benzylidenation [4] of **19**, followed by monobenzylation via intermediate stannylidene acetal formation [6] and subsequent cleavage of the benzylidene group [4].

Formation of the perbenzylated α-fucopyranosyl chloride was achieved according to [2]. Starting with peracetylated derivatives **22** and **23**, a five-step synthesis was performed in each

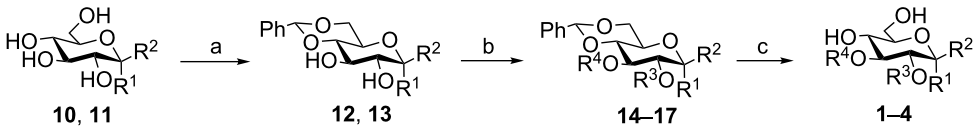

	R^1	R^2	
10	OMe	H	**12** (76%)
11	H	OMe	**13** (58%)

	R^1	R^2	R^3	R^4	
14 (51%)	OMe	H	OBn	H	**1** (76%)
15 (49%)	H	OMe	OBn	H	**2** (78%)
16 (23%)	OMe	H	H	OBn	**3** (95%)
17 (36%)	H	OMe	H	OBn	**4** (80%)

Scheme 1: Synthesis of monobenzylated glucopyranosyl acceptors **1**–**4**. Reagents and conditions: (a) Benzaldehyde dimethylacetal, camphorsulfonic acid, ACN, 80 °C, 0.5–19 h; (b) NaOH, Bu_4NHSO_4, DCM, BnBr, 14–17 h, reflux; (c) MeOH, H_2O, HCl, 2–22 h, reflux.

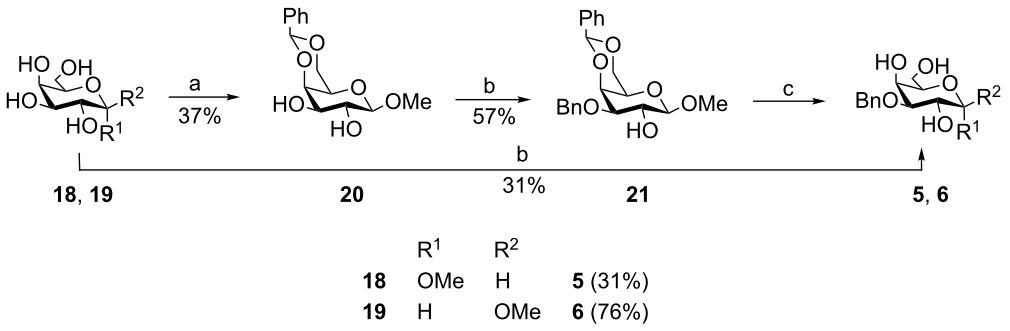

Scheme 2: Synthesis of 3-*O*-monobenzylated gluco- und galactopyranosyl acceptors **5** and **6**. Reagents and conditions: (a) Benzaldehyde dimethylacetal, camphorsulfonic acid, ACN, 80 °C, 2.5 h; (b) dibutyltin oxide, toluene, BnBr, 24 h, reflux; (c) MeOH, H_2O, HCl, 2–22 h, reflux.

case to obtain the galacto- and glucopyranosyl donors **8** and **9** (Scheme 3). Initially, peracetates **22** and **23** were converted into the thioglycopyranosides **24** and **25** with $BF_3{\cdot}Et_2O$/thiophenole [7]. Subsequent deacetylation [8] and benzylation [9] afforded compounds **28** and **29**, whose thioglycosidic bonds were cleaved with NBS in water/acetone [10]. Finally, treatment with oxalyl chloride [11] gave the α-glycopyranosyl chlorides **8** and **9** in high yields.

The results of the base-promoted glycosylation of monobenzylated methyl α- and β-D-glycopyranosides with fucopyranosyl chloride **7** are summarized in Table 1. Fucosylation of the 2-*O*-benzylated α-derivative **1** gave predominantly the β-(1→6)-linked disaccharide **33**. Conversion of the 3-*O*-benzylated methyl α-D-glucopyranoside **3** resulted in β-(1→2) **34** and β-(1→6) disaccharides **35** in a ratio of ca. 1:9. By glycosylation of the 3-*O*-benzylated methyl α-D-galactopyranoside **5** with **7** only the β-(1→6)-linked disaccharide **37** was found. Thus, in all α-methyl glycopyranoside acceptors **1**, **3** and **5**, successful glycosidic bond formations with high regioselectivity towards position 6 were observed. These findings can be understood by the presence of adjacent hydroxy groups on acceptors **1**, **3** and **5**, such as 4,6-diol and/or 3,4,6-triol structures, respectively. After deprotonation the negative charge is dispersed by hydrogen bonding of unreacted hydroxy groups and located predominantly at position 6 due to the higher acidity of OH-6 [3]. Additionally, the basicity of the oxyanions stabilized by hydrogen bonding is decreased in comparison to isolated oxyanions, and this favours glycosidic bond formation over elimination.

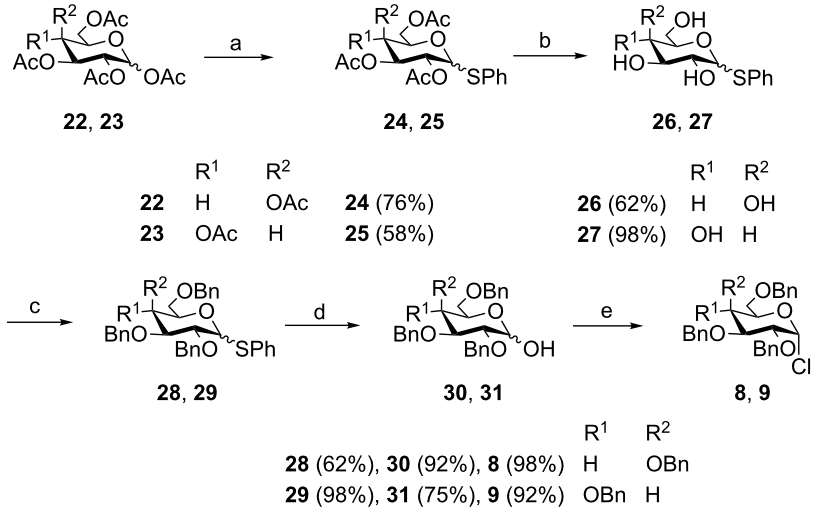

Scheme 3: Synthesis of 2,3,4,6-tetra-*O*-benzyl-α-D-galactopyranosyl chloride (**8**) and 2,3,4,6-tetra-*O*-benzyl-α-D-glucopyranosyl chloride (**9**). Reagents and conditions: (a) 1. DCM, PhSH, $BF_3{\cdot}Et_2O$, 0 °C, 1 h; 2. 4–5 d, rt; (b) MeOH, NaOMe, Amberlite IR 120 (H^+), rt, 4–15 h; (c) 1. DMF, NaH, 0 °C, 1–2 h; 2. BnBr, 0 °C → rt, 16–40 h; (d) acetone/H_2O (10:1), NBS, rt, −45 °C, 10 min to 5 h; (e) DCM, DMF, oxalyl chloride, 1 h, rt.

Table 1: Glycosylation results for acceptors **1**–**6** with NaH as base and 2,3,4-tri-*O*-methyl-α-L-fucopyranosyl chloride (Fuc-Cl, **7**) as donor.[a]

Acceptor	Products	Yield [%][b]	Relative yield [%][c]			
			β-(1→2)	β-(1→3)	β-(1→4)	β-(1→6)
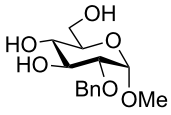 **1**	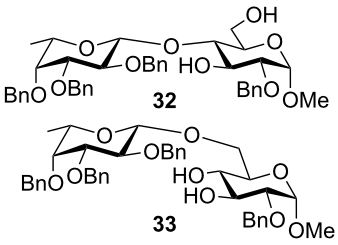 **32** **33**	25	■[d]	–	40	60
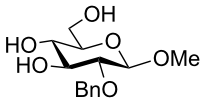 **2**	no reaction	–	■	–	–	–
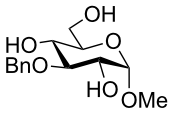 **3**	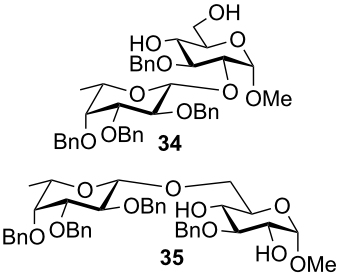 **34** **35**	48[e]	13	■	–	87
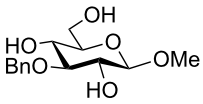 **4**	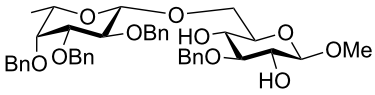 **36**	30	–	■	–	>98
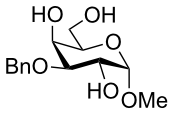 **5**	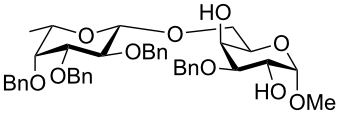 **37**	33	–	■	–	>98
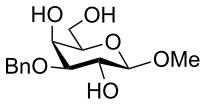 **6**	no reaction	–	–	■	–	–

[a]General reaction conditions: NaH (1.1–1.3 equiv), DMF, rt, 1 h, then donor **7** (1.0 equiv), rt, 4 h to 7 d; [b]total yield of possible disaccharide regioisomers; [c]after separation by column chromatography; [d]■: benzylated position, no linkage possible; [e] [1].

Surprisingly glycosylation of the corresponding β-glucopyranosides **2**, **4**, and **6** only showed conversion for the 3-*O*-benzylated glucopyranosyl derivative **4**. Acceptors **2** and **6** did not react at all with the fucopyranosyl chloride **7**. Obviously, the anomeric configuration in the acceptor structure has a noticeable effect on the glycosylation, resulting in lower oxyanion reactivity for methyl β-glycopyranosides. The considerable effect of the anomeric configuration on the reactivity of remote hydroxy groups may be rationalized by stereoelectronic effects [12]. Moreover, the lower reactivities of the methyl β-glycopyranosides may also be dependent on the decreased solubility of the partially deprotonated methyl β-glycospyranosides in the solvent used.

The results of base-promoted glycosylations with donor mixtures are shown in Table 2. Reaction of the 3-*O*-benzylated α-D-glucopyranoside **3** with an equimolar mixture of the fuco- and galactopyranosyl donors **7** and **8** gave both β-(1→6)-linked disaccharides **35** and **38** in 20% yield, with a ratio of 85% in favour of the fucosylated product. The corresponding β-configured acceptor **4** yielded only the β-(1→6)-linked galactosylated disaccharide **39** in poor yield (5%). With the same acceptors,

Table 2: Reactivity studies of acceptors **3** and **4** with donors **7**–**9**.[a]

Acceptor	Donor (equimolar mixture)	Products	Yield [%][b]	Ratio [%]
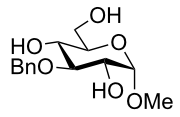 **3**	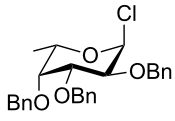 **7** 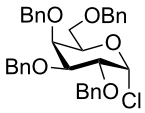 **8**	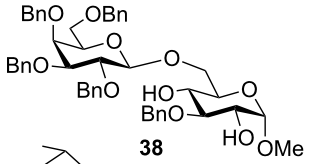 **38** 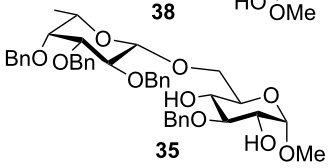 **35**	20	Gal/Fuc 15:85[c]
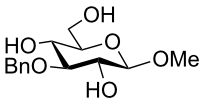 **4**	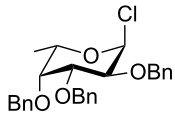 **7** 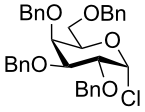 **8**	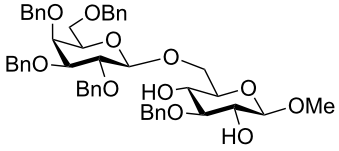 **39**	5	Gal only
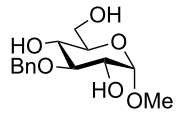 **3**	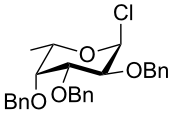 **7** 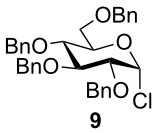 **9**	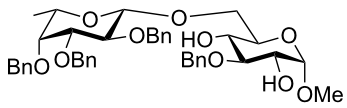 **35**	15	Fuc only
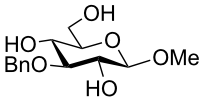 **4**	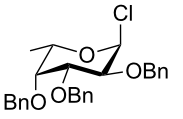 **7** 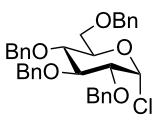 **9**	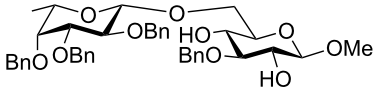 **36**	14	Fuc only

[a]General reaction conditions: NaH (1.1–1.3 equiv), DMF, rt, 1h, then donor **7** and **8** or **7** and **9** (1.0 equiv), rt, 4 h to 7 d; [b]total yield of possible disaccharide regioisomers; [c]ratio determined by ^{1}H NMR.

equimolar mixtures of the perbenzylated fuco- and glucopyranosyldonors **7** and **9** gave just the β-(1→6)-fucosylated products **35** and **36** in corresponding yields of 15% and 14%. Furthermore, a mixture of galacto- and glucopyranosyl donors **8** and **9** was employed, but this did not show any reaction at all. In all cases, disaccharide yields from donor mixtures were significantly lower; as rational of which, some unknown kind of interaction between the donors may be assumed.

Conclusion

These studies gave evidence that the configuration of the anomeric centre of acceptors has a decisive influence on the base-promoted glycosylation approach, but which so far cannot be explained. Several α-monobenzyl acceptors (**1**, **3** and **5**) and their β counterparts (**2**, **4** and **6**) were synthesized and coupled with the perbenzylated fucopyranosyl donor **7**. Whereas all α-glycosidic acceptors gave disaccharides in moderate to acceptable yields, only the β-glycosidic acceptor **4** reacted, to give the dissacharide in much lower yield.

Furthermore, a comparison between the reactivities of several donor mixtures was established. For this purpose the perbenzylated donors **7**–**9** were synthesized and reacted in equimolar mixtures with acceptors **3** and **4**. The fucopyranosyl donor **7** showed the highest reactivity, followed by the galactopyranosyl donor **8**. The glucopyranosyl donor **9** showed no reaction at all. It turned out that the disaccharide yields from the mixtures were significantly lower, indicating unknown interactions between donors.

In cases with low yields or even no glycosylation products at all, elimination became the dominant reaction and led to the corresponding glycals. Hence, and based on the workup, the recovery of glycosyl halides was neither practicable nor achieved.

Experimental

General: All reagents were purchased from commercial sources and used as received. Sodium hydride (NaH) was used

as a 60% suspension in paraffin. TLC was performed on Merck silica gel 60 F_{254} plates. Compounds were detected by UV and/or by treatment with EtOH/H_2SO_4 (9:1) and subsequent heating. Column chromatography was performed with Merck/Fluka silica gel 60 (230–400 mesh). Solvents for column chromatography were distilled prior to use. ^{1}H and ^{13}C NMR spectra were recorded with Bruker AMX-400 or Bruker AV-400 spectrometers (400 MHz for ^{1}H, 100 MHz for ^{13}C) and calibrated by using the solvent residual peak. In $CDCl_3$ TMS was used for calibration. Melting points were measured with an Apotec melting point apparatus. Optical rotations were obtained by using a Krüss Optronic P8000 polarimeter (589 nm, 25 °C). HRMS (ESI) were recorded with a Thermo Finnigan MAT 95XL mass spectrometer. MS (MALDI–TOF) were recorded with a Bruker Biflex II (positive reflection mode, matrix: 2,5-dihydroxybenzoic acid). Relative yields of disaccharide mixtures were determined by integration of the signals in the ^{1}H NMR spectra of the anomeric or other well-separated protons. The abbreviation "dd~vt" stands for a double doublet that turns into a virtual triplet because of similar coupling constants. Physical and NMR data for **34** and **35** were published previously [1].

General Procedure: Base-promoted glycosylations: The acceptor molecule (1.0 mmol) was dissolved in dry dimethylformamide (2–4 mL), and sodium hydride (1.1–1.3 mmol for each hydroxy group; as a 60% suspension in paraffin) was added. After being stirred for one hour under argon at room temperature, the donor (1.0 mmol for each hydroxy group; donor-mixtures 0.5 mmol of each donor) dissolved in dry dimethylformamide (2–4 mL) was successively added to the reaction. After stirring for 4–100 h, methanol (2 mL) was added. The crude product was purified by flash column chromatography (petroleum ether/ethyl acetate, 2:1 v/v).

Methyl 3-*O*-benzyl-β-D-glucopyranoside (4): Prepared by hydrolysis of **17** [5] with hydrochloric acid [2]. Compound **17** (3.49 g, 9.37 mmol), MeOH (80 mL), H_2O (8.0 mL), 2 N HCl (1.0 mL), 21.5 h, reflux. Yield: 80% (2.13 g, 7.49 mmol), colourless solid, mp 105 °C. $[\alpha]_D^{25}$ −7.7 (*c* 1.0, H_2O); ^{1}H NMR (400 MHz, MeOD) δ 7.47–7.43 (m, 2H, H_{ar}), 7.36–7.24 (m, 3H, H_{ar}), 4.92 (d, $J_{C(3)OCH2Ph\text{-}A,B}$ = 11.1 Hz, 1H, C(3)-O-CH_2-Ph-A), 4.88 (d, 1H, C(3)-O-CH_2-Ph-B), 4.21 (d, $J_{1,2}$ = 7.3 Hz, 1H, H-1), 3.90 (dd, $J_{6A,6B}$ = 11.8 Hz, 1H, H-6A), 3.69 (dd, 1H, H-6B), 3.48–3.42 (m, 1H, H-3), 3.41–3.38 (m, 1H, H-4), 3.37–3.34 (m, 1H, H-2), 3.32–3.28 (m, $J_{5,6A}$ = 2.3 Hz, $J_{5,6B}$ = 5.8 Hz, 1H, H-5) ppm; ^{13}C NMR (100 MHz, MeOD) δ 140.4, 129.2, 129.0, 128.5 (C_{ar}), 105.5 (C-1), 86.3 (C-4), 77.9 (C-5), 76.0 (C(3)-O-*C*H_2-Ph), 75.3 (C-2), 71.5 (C-3), 62.7 (C-6), 57.3 (-O-*C*H_3) ppm; HRMS–ESI (*m*/*z*): [M + Na]$^+$ calcd for $C_{14}H_{20}O_6Na$, 307.1158; found, 307.1150.

Methyl 2-*O*-benzyl-4-*O*-(2,3,4-tri-*O*-benzyl-β-L-fucopyranosyl)-α-D-glucopyranoside (32) and Methyl 2-*O*-benzyl-6-*O*-(2,3,4-tri-*O*-benzyl-β-L-fucopyranosyl)-α-D-glucopyranoside (33): Prepared according to the general procedure. Compound **1** (70 mg, 0.25 mmol), NaH (31 mg, 0.77 mmol), **7** (335 mg, 0.739 mmol), DMF (20 mL). Yield: 43 mg (0.061 mmol, 25%), yellow sirup, relative yield **32**:**33** = 40:60 (^{1}H NMR).

32: ^{1}H NMR (400 MHz, $CDCl_3$) δ 7.31–7.19 (m, 20H, H_{ar}), 4.89 (d, 1H, C(4')-CH_2-Ph-A), 4.80 (d, $J_{C(2')OCH2Ph\text{-}A,B}$ = 10.9 Hz, 1H, C(2')-CH_2-Ph-A), 4.77 (d, 1H, C(2')-CH_2-Ph-B), 4.70–4.53 (m, 5H, $J_{C(4')OCH2Ph\text{-}A,B}$ = 11.6 Hz, C(2)-CH_2-Ph-A/B, C(3')-CH_2-Ph-A/B, C(4')-CH_2-Ph-B), 4.59 (d, $J_{1',2'}$ = 7.8 Hz, 1H, H-1'), 4.50 (d, $J_{1,2}$ = 3.8 Hz, 1H, H-1), 4.02–3.96 (m, 1H, H-3), 3.96–3.90 (m, 1H, H-6A), 3.74 (dd~vt, 1H, H-2'), 3.62–3.56 (m, 1H, H-6B), 3.53–3.50 (m, 2H, H-4, H-5), 3.48–3.46 (m, 1H, H-4'), 3.46–3.40 (m, $J_{5',6'}$ = 6.7 Hz, 2H, H-3', H-5'), 3.28 (dd, $J_{2,3}$ = 9.6 Hz, 1H, H-2), 3.27 (s, 3H, -OCH_3), 1.10 (d, 3H, H-6') ppm; ^{13}C NMR (100 MHz, $CDCl_3$) δ 128.4, 128.4, 128.3, 128.2, 128.2, 128.1, 127.9, 127.8, 127.7, 127.7, 127.6 (C_{ar}), 104.7 (C-1'), 98.4 (C-1), 82.4 (C-3'), 79.1 (C-2'), 78.9 (C-4), 78.5 (C-2), 76.2 (C-4'), 75.5 (C(2')-O-*C*H_2-Ph), 74.8 (C(4')-O-*C*H_2-Ph), 73.6 (C-3), 73.2 (C(3')-O-*C*H_2-Ph), 73.1 (C(2)-O-*C*H_2-Ph), 70.9 (C-5'), 69.6 (C-5), 61.8 (C-6), 55.2 (-O*C*H_3), 16.7 (C-6') ppm.

33: ^{1}H NMR (400 MHz, $CDCl_3$) δ 7.33–7.19 (m, 20H, H_{ar}), 4.89 (d, 1H, C(4')-CH_2-Ph-A), 4.85 (d, 1H, C(2')-CH_2-Ph-A), 4.75–4.53 (m, $J_{C(2')OCH2Ph\text{-}A,B}$ = 10.9 Hz, $J_{C(4')OCH2Ph\text{-}A,B}$ = 11.6 Hz, 6H, C(2')-CH_2-Ph-B, C(2)-CH_2-Ph-A/B, C(3')-CH_2-Ph-A/B, C(4')-CH_2-Ph-B), 4.55 (d, $J_{1,2}$ = 3.8 Hz, 1H, H-1), 4.28 (d, $J_{1',2'}$ = 7.8 Hz, 1H, H-1'), 4.07–3.99 (m, 1H, H-6A/B), 3.88–3.85 (m, 1H, H-3), 3.76–3.70 (m, 1H, H-2', H-5), 3.62–3.59 (m, 1H, H-4), 3.47–3.45 (m, 1H, H-4'), 3.44–3.39 (m, $J_{5',6}$ = 6.3 Hz, 2H, H-3', H-5'), 3.27–3.24 (m, 1H, H-2), 3.23 (s, 1H, -OCH_3), 1.10 (d, 1H, H-6') ppm; ^{13}C NMR (100 MHz, $CDCl_3$) δ 138.8, 138.4, 137.8, 128.5, 128.5, 128.4, 128.2, 128.0, 127.9, 127.7, 127.6, 127.6, 127.5 (C_{ar}), 104.2 (C-1'), 97.9 (C-1), 82.3 (C-3'), 79.4 (C-2'), 79.1 (C-2), 79.1 (C-5), 76.3 (C-4'), 75.0, 74.7, 73.2, 73.0 (-O-*C*H_2-Ph), 72.6 (C-3), 70.6 (C-5'), 70.1 (C-4), 68.8 (C-6), 55.2 (-O*C*H_3), 16.7 (C-6') ppm; MALDI–TOF–MS (DHB, positive mode; *m*/*z*): [M + Na]$^+$ calcd for $C_{41}H_{48}O_{10}Na$, 723.3; found, 723.5.

Methyl 3-*O*-benzyl-6-*O*-(2,3,4-tri-*O*-benzyl-β-L-fucopyranosyl)-β-D-glucopyranoside (36): (a) Prepared according to the general procedure: Compound **4** (71 mg, 0.25 mmol), NaH (31 mg, 0.71 mmol), **7** (350 mg, 0.774 mmol), DMF (16 mL). Yield: 53 mg (0.074 mmol, 30%). (b) Prepared according to the general procedure by using a donor mixture: Compound **4**

(65 mg, 0.23 mmol), NaH (30 mg, 0.75 mmol), **7** (150 mg, 0.330 mmol)/**9** (182 mg, 0.325 mmol), DMF (18 mL). Yield: 22 mg (0.031 mmol, 14%), yellow sirup. $[\alpha]_D^{25}$ −106 (*c* 0.31, $CHCl_3$); ^{1}H NMR (400 MHz, $CDCl_3$) δ 7.42–7.27 (m, 20H, H_{ar}), 4.99 (d, $J_{C(4')OCH2Ph\text{-}A,B}$ = 11.6 Hz, 1H, C(4')-O-CH_2-Ph-A), 4.93 (d, $J_{C(2')OCH2Ph\text{-}A,B}$ = 10.7 Hz, 1H, C(2')-O-CH_2-Ph-A), 4.91 (d, $J_{C(3)OCH2Ph\text{-}A,B}$ = 11.3 Hz, 1H, C(3)-O-CH_2-Ph-A), 4.86 (d, 1H, C(3)-O-CH_2-Ph-B), 4.79 (d, $J_{C(3')OCH2Ph\text{-}A,B}$ = 11.7 Hz, 1H, C(3')-O-CH_2-Ph-A), 4.76 (d, 1H, C(2')-O-CH_2-Ph-B), 4.72 (d, 1H, C(3')-O-CH_2-Ph-B), 4.69 (d, 1H, C(4')-O-CH_2-Ph-B), 4.36 (d, $J_{1',2'}$ = 7.5 Hz, 1H, H-1'), 4.19 (d, $J_{1,2}$ = 7.5 Hz, 1H, H-1), 4.15 (dd, $J_{6A,6B}$ = 11.0 Hz, 1H, H-6A), 3.86–3.79 (m, 3H, H-2', H-4, H-6B), 3.57–3.38 (m, $J_{5,6A}$ = 4.1 Hz, $J_{5',6A}$ = 6.6 Hz, 6H, H-2, H-3, H-3', H-4', H-5, H-5'), 3.51 (s, 1H, -OCH_3), 1.17 (d, 3H, H-6') ppm; ^{13}C NMR (100 MHz, $CDCl_3$) δ 138.7, 138.6, 138.5, 138.5, 138.4, 128.7, 128.5, 128.5, 128.4, 128.3, 128.2, 128.1, 128.0, 127.9, 127.9, 127.8, 127.6 (C_{ar}), 104.0 (C-1'), 103.7 (C-1), 83.5 (C-3) 82.4 (C-3'), 79.0 (C-2'), 76.2 (C-4'), 75.2, 74.7, 74.6, 73.2 (-O-*C*H_2-Ph), 74.6 (C-5), 73.9 (C-2), 70.8 (C-4), 70.6 (C-5'), 69.1 (C-6), 56.9 (-OCH_3), 16.7 (-CH_3) ppm; HRMS–ESI (*m*/*z*): $[M + Na]^+$ calcd for $C_{41}H_{48}O_{10}Na$, 723.3145; found, 723.3136.

Methyl 3-*O*-benzyl-6-*O*-(2,3,4-tri-*O*-benzyl-β-L-fucopyranosyl)-β-D-galactopyranoside (37): Prepared according to the general procedure. Compound **5** (72 mg, 0.25 mmol), NaH (26 mg, 0.65 mmol), **7** (343 mg, 0.731 mmol), DMF (10 mL). Yield: 58 mg (0.083 mmol, 33%), colourless solid, mp 98 °C. $[\alpha]_D^{25}$ +72 (*c* 0.2, $CHCl_3$); ^{1}H NMR (400 MHz, $CDCl_3$) δ 7.42–7.25 (m, 20H, H_{ar}), 4.99 (d, 1H, -O-CH_2-Ph), 4.90 (d, 1H, -O-CH_2-Ph), 4.82–4.75 (m, $J_{1,2}$ = 4.0 Hz, 3H, H-1, -O-CH_2-Ph), 4.73 (d, 1H, -O-CH_2-Ph), 4.71 (d, 1H, -O-CH_2-Ph), 4.56 (s, 2H, -O-CH_2-Ph), 4.40 (d, $J_{1',2'}$ = 7.8 Hz, 1H, H-1'), 4.16–4.13 (m, 1H, H-4), 4.01 (dd, $J_{6A,6B}$ = 8.8 Hz, 1H, H-6A), 3.98 (dd, $J_{2,3}$ = 9.8 Hz, 1H, H-2), 3.93–3.89 (m, $J_{5,6A}$ = 4.3 Hz, $J_{5,6B}$ = 8.6 Hz, 1H, H-5), 3.86 (dd, 1H, H-6B), 3.82 (dd, $J_{2',3'}$ = 9.5 Hz, 1H, H-2'), 3.62–3.55 (m, 2H, H-3, H-4'), 3.53 (dd, $J_{3',4'}$ = 3.0 Hz, 1H, H-3'), 3.51–3.44 (m, $J_{5',6'}$ = 6.5 Hz, 1H, H-5'), 3.39 (s, 3H, OCH_3), 1.19 (d, 3H, H-6') ppm; ^{13}C NMR (100 MHz, $CDCl_3$) δ 128.6, 128.5, 128.4, 128.3, 127.9, 127.8, 127.6, 127.6, 127.6 (C_{ar}), 103.9 (C-1'), 99.5 (C-1), 82.5 (C-3'), 79.4 (C-2'), 78.4 (C-3), 76.2 (C-4'), 75.1, 74.6, 73.2, 71.7 (-O-*C*H_2-Ph), 70.5 (C-5'), 68.6 (C-2), 68.1 (C-5), 67.3 (C-6), 66.0 (C-4), 55.4 (OCH_3), 16.8 (C-6') ppm; HRMS–ESI (*m*/*z*): $[M + Na]^+$ calcd for $C_{41}H_{48}O_{10}Na$, 723.3135; found, 723.3140.

Methyl 3-*O*-benzyl-6-*O*-(2,3,4,6-tetra-*O*-benzyl-β-D-galactopyranosyl)-α-D-glucopyranoside (38): (a) Prepared according to the general procedure: Compound **3** (70 mg, 0.25 mmol), NaH (32 mg, 0.80 mmol), **8** (415 mg, 0.742 mmol), DMF (20 mL). Yield: 20 mg (0.025 mmol, 10%). (b) Prepared according to the general procedure by using a donor mixture: Compound **3** (70 mg, 0.25 mmol), NaH (30 mg, 0.75 mmol), **7** (170 mg, 0.375 mmol)/**8** (208 mg, 0.372 mmol), DMF (20 mL). Yield: 34 mg (0.042 mmol, 20%). Relative yield **35**:**38** = 85:15. Slightly yellow sirup. $[\alpha]_D^{25}$ +53.4 (*c* 0.70, $CHCl_3$); ^{1}H NMR (400 MHz, $CDCl_3$) δ 7.34–7.19 (m, 25H, H_{ar}), 4.89–4.84 (m, 3H, -O-CH_2-Ph), 4.73–4.61 (m, 5H, H-1, -O-CH_2-Ph), 4.52 (d, 1H, -O-CH_2-Ph), 4.41–4.31 (m, $J_{1',2'}$ = 7.5 Hz, 3H, H-1', -O-CH_2-Ph), 4.09–4.01 (m, 1H, H-6A), 3.83–3.80 (m, 1H, H-4), 3.77 (dd~vt, 1H, H-2'), 3.73–3.66 (m, 2H, H-5', H-6B), 3.56–3.42 (m, 7H, H-2, H-3, H-3', H-4', H-5, H-6'A/B), 3.29 (s, 1H, -OCH_3) ppm; ^{13}C NMR (100 MHz, $CDCl_3$) δ 138.7, 138.7, 128.5, 128.4, 128.4, 128.3, 128.2, 128.1, 128.1, 128.0, 127.9, 127.8, 127.6, 127.5, 127.5 (C_{ar}), 104.2 (C-1'), 99.3 (C-1), 82.7 (C-3), 82.3 (C-3'), 79.3 (C-2'), 75.2, 74.9, 74.5, 73.6, 73.0 (-O-*C*H_2-Ph), 73.5 (C-4), 73.5 (C-4'), 72.6 (C-2), 70.8 (C-5), 70.2 (C-5'), 69.2 (C-6), 68.7 (C-6'), 55.3 (-O*C*H_3) ppm; HRMS–ESI (*m*/*z*): $[M + Na]^+$ calcd for $C_{48}H_{54}O_{11}Na$, 829.3564; found, 829.3545.

Methyl 3-*O*-benzyl-6-*O*-(2,3,4,6-tetra-*O*-benzyl-β-D-galactopyranosyl)-β-D-glucopyranoside (39): Prepared according to the general procedure by using a donor mixture: Compound **4** (65 mg, 0.23 mmol), NaH (29 mg, 0.73 mmol), **7** (151 mg, 0.334 mmol)/**8** (175 mg, 0.313 mmol), DMF (16 mL). Yield: 8.6 mg (0.011 mmol, 5%). Yellow sirup. $[\alpha]_D^{25}$ −9.6 (*c* 0.40, $CHCl_3$); ^{1}H NMR (400 MHz, $CDCl_3$) δ 7.31–7.19 (m, 25H, H_{ar}), 4.88–4.82 (m, 3H, -O-CH_2-Ph), 4.74–4.69 (m, 2H, -O-CH_2-Ph), 4.66–4.62 (m, 2H, -O-CH_2-Ph), 4.52 (d, 1H, -O-CH_2-Ph), 4.42–4.30 (m, 2H, -O-CH_2-Ph), 4.37 (d, $J_{1,2}$ = 3.5 Hz, 1H, H-1), 4.08–4.03 (m, $J_{6A,6B}$ = 10.8 Hz, 1H, H-6A), 4.06 (d, $J_{1',2'}$ = 7.6 Hz, 1H, H-1'), 3.82–3.80 (m, 1H, H-4), 3.78–3.74 (m, 1H, H-2), 3.74 (dd, 1H, H-6B), 3.56–3.42 (m, $J_{5,6B}$ = 6.0 Hz, 6H, H-3, H-4', H-5, H-5', H-6'A/B), 3.39 (dd, $J_{2',3'}$ = 9.8 Hz, 1H, H-2'), 3.36 (s, 1H, -OCH_3), 3.31 (dd~vt, 1H, H-3') ppm; ^{13}C NMR (100 MHz, $CDCl_3$) δ 138.6, 128.6, 128.4, 128.4, 128.3, 128.3, 128.2, 128.2, 128.2, 128.1, 128.0, 127.9, 127.8, 127.8, 127.6, 127.5 (C_{ar}), 104.0 (C-1), 103.6 (C-1'), 83.7 (C-3'), 82.2 (C-3), 79.1 (C-2), 75.2, 74.7, 74.5, 73.5, 72.9 (-O-*C*H_2-Ph), 73.5 (C-4), 74.6 (C-5), 74.2 (C-2'), 73.4 (C-4), 71.4 (C-5'), 69.3 (C-6), 68.7 (C-6'), 57.1 (-O*C*H_3) ppm; MALDI–TOF–MS (DHB, positive mode; *m*/*z*): $[M + Na]^+$ calcd for $C_{48}H_{54}O_{11}Na$, 829.36; found, 830.1.

References

1. Matwiejuk, M.; Thiem, J. *Chem. Commun.* **2011,** *47,* 8379–8381. doi:10.1039/c1cc11690h
2. Matwiejuk, M.; Thiem, J. *Eur. J. Org. Chem.* **2011,** 5860–5878. doi:10.1002/ejoc.201100861
3. Matwiejuk, M.; Thiem, J. *Eur. J. Org. Chem.* **2012**. doi:10.1002/ejoc.201101708

4. Demchenko, A. V.; Pornsuriyasak, P.; de Meo, C. *J. Chem. Educ.* **2006,** *83,* 782–784. doi:10.1021/ed083p782
5. Garegg, J.; Iversen, T.; Oscarson, S. *Carbohydr. Res.* **1976,** *50,* C12–C14. doi:10.1016/S0008-6215(00)83867-7
6. David, S.; Hanessian, S. *Tetrahedron* **1985,** *41,* 643–663. doi:10.1016/S0040-4020(01)96443-9
7. Charbonnier, F.; Penadés, S. *Eur. J. Org. Chem.* **2004,** 3650–3656. doi:10.1002/ejoc.200400141
8. Zemplén, G.; Pacsu, E. *Ber. Dtsch. Chem. Ges.* **1929,** *62,* 1613–1614. doi:10.1002/cber.19290620640
9. Girard, C.; Miramon, M.-L.; de Solminihac, T.; Herscovici, J. *Carbohydr. Res.* **2002,** *337,* 1769–1774. doi:10.1016/S0008-6215(02)00206-9
10. Nicolaou, K. C.; Seitz, S. P.; Papahatjis, D. P. *J. Am. Chem. Soc.* **1983,** *105,* 2430–2434. doi:10.1021/ja00346a053
11. Iversen, T.; Bundle, D. R. *Carbohydr. Res.* **1982,** *103,* 29–40. doi:10.1016/S0008-6215(82)80005-0
12. Pedersen, C. M.; Olsen, J.; Brka, A. B.; Bols, M. *Chem.–Eur. J.* **2011,** *17,* 7080–7086. doi:10.1002/chem.201100020

License and Terms

Beilstein Journal of Organic Chemistry

Synthesis of heteroglycoclusters by using orthogonal chemoselective ligations

Baptiste Thomas[1], Michele Fiore[1], Isabelle Bossu[1], Pascal Dumy[1] and Olivier Renaudet[*1,2]

Letter

Open Access

Address:
[1]Département de Chimie Moléculaire, UMR-CNRS 5250 & ICMG FR 2607, Université Joseph Fourier, PB 53, 38041 Grenoble Cedex 9, France and [2]Institut Universitaire de France, 103 Boulevard Saint-Michel, 75005 Paris, France

Email:
Olivier Renaudet[*] - olivier.renaudet@ujf-grenoble.fr

* Corresponding author

Keywords:
chemoselective ligation; click chemistry; cyclopeptide; heteroglycocluster; oxime

Beilstein J. Org. Chem. **2012,** *8,* 421–427.
doi:10.3762/bjoc.8.47

Received: 20 January 2012
Accepted: 29 February 2012
Published: 20 March 2012

This article is part of the Thematic Series "Synthesis in the glycosciences II".

Guest Editor: T. K. Lindhorst

Abstract

Synthetic heteroglycoclusters are being subjected to increasing interest due to their potential to serve as selective ligands for carbohydrate-binding proteins. In this paper, we describe an expedient strategy to prepare cyclopeptides displaying well-defined distributions and combinations of carbohydrates. By using both oxime ligation and copper(I)-catalyzed alkyne–azide cycloaddition, two series of compounds bearing binary combinations of αMan, αFuc or βLac in an overall tetravalent presentation, and either 2:2 or 3:1 relative proportions, have been prepared.

Introduction

Multivalent interactions between carbohydrates and proteins play key roles in diverse biological events, including fertilization, cell–cell communication, host–pathogen interactions, immune response and cancer metastasis [1]. Synthetic molecules displaying multiple copies of a sugar binding motif, called (homo)glycoclusters, represent attractive tools for studying these complex recognition processes as well as for developing biological applications, for example, the inhibition of infections by pathogens such as viruses or bacteria [2-5]. In a suitable density and spatial display, clusters of carbohydrate indeed allow multiple contacts with a target protein, thus increasing avidity by means of the "glycoside cluster effect" [6,7]. While the recent progress in glycomics has led to the design of glycoclusters active at nanomolar concentration [8-10], the achievement of selective binding remains challenging because of the close structural similarities of the binding sites of proteins specific for the same carbohydrate moiety.

Interestingly, recent reports have highlighted that the association of different sugar units instead of a single motif, namely heteroglycocluster, reflects the presence of sugars found in native biological systems more closely than homoglycocluster does. Although recognition mechanisms are not fully understood, these studies suggest that heteroglycoclusters should interact with proteins through distinct binding sites, which may influence both affinity and selectivity [11-25]. In this context, we previously reported a combinatorial procedure to prepare libraries of heteroglycoclusters displaying sugars and/or amino acids at randomized positions on a topological cyclopeptide scaffold [26]. Deconvolution of the resulting libraries by affinity chromatography allowed the selection of heteroglycoclusters that were proved to be useful for exploring the surrounding regions of the binding pocket in a model lectin. Although it is easy to handle, this combinatorial procedure leads to the formation of inseparable mixtures of regioisomers, which precludes their utilization for further assays with relevant biological targets. In order to circumvent this drawback, we herein report the synthesis of similar heteroglycoclusters by using a protocol based on orthogonal chemoselective ligations. Two series of compounds containing different combinations of two different sugars have been designed (Figure 1). In one series (heteroglycocluster 2:2), two αMan, αFuc and/or βLac are conjugated at alternate positions into the tetravalent cyclopeptide sequence, whereas the second series (heteroglycocluster 3:1) contains one of a given sugar and three of another.

Results and Discussion

Glycoclusters are classically constructed from a molecular scaffold containing multiple anchoring sites that can be functionalized with sugars by using a single coupling reaction. By contrast, the chemical access of heteroglycoclusters is not trivial because it requires the controlled conjugation of different sugars at a precise position into the scaffold to obtain a well-defined distribution. Taking advantage of our experience in bioconjugation methods, we decided to explore two chemoselective strategies to achieve this purpose. We first selected the oxime ligation since we have previously used this approach successfully for the preparation of sophisticated molecular systems, such as synthetic vaccines [27,28], immunomodulators [29], lectin ligands [30] or vectors of hepatocytes [31]. As the second strategy, we have chosen the well-known copper(I)-catalyzed alkyne–azide cycloaddition (CuAAC) [32,33], which is intensively exploited for the conjugation of sugars to both molecular and biological systems [34,35]. Besides being fully compatible with carbohydrate and peptide chemistries, oximation and CuAAC reactions offer the advantage of being orthogonal [36,37], therefore allowing a controlled assembly process with a minimized risk of side reactions. The 2:2 series of heteroglycoclusters was prepared from the aminooxy [38-40] and propargyl [41] glycosides **1**-**3** (Figure 1) and the cyclopeptide **4** (Scheme 1). This scaffold containing two lysines (Lys) functionalized with an aldehyde and two norleucines (Nle) bearing an azide group was prepared by using a strategy adapted from the procedure described previously [42].

In the first step, two copies of aminooxy αMan **1a**, αFuc **2a** and βLac **3a** were coupled to **4**, affording divalent oxime-linked compounds **5-Man**, **5-Fuc**, and **5-Lac**, respectively. The oxime ligation was performed at 37 °C in aqueous acidic buffer with 2 equiv of sugars per anchoring site. After 3 h, complete reac-

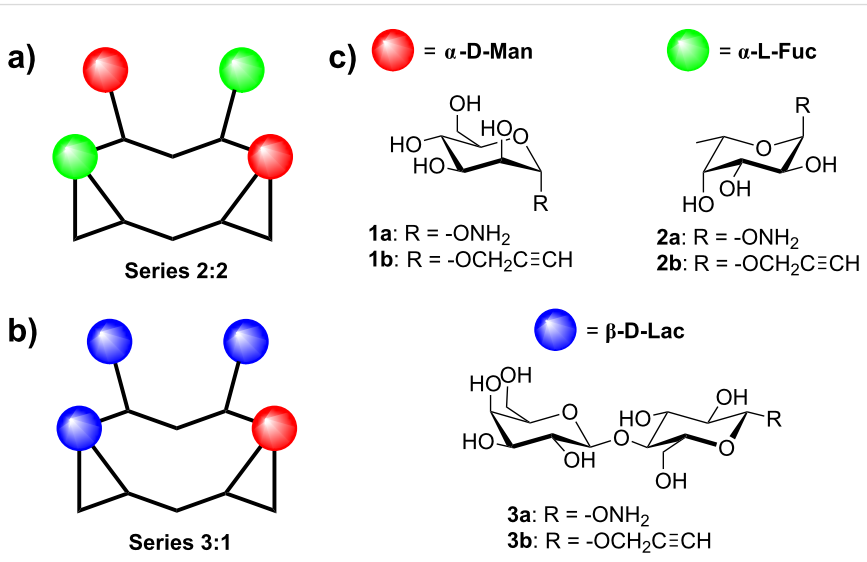

Figure 1: (a) Schematic representation of a heteroglycocluster of the 2:2 series containing Man and Fuc. (b) Schematic representation of a heteroglycocluster of the 3:1 series containing Lac and Man. (c) Structure of carbohydrates used for the construction of heteroglycoclusters.

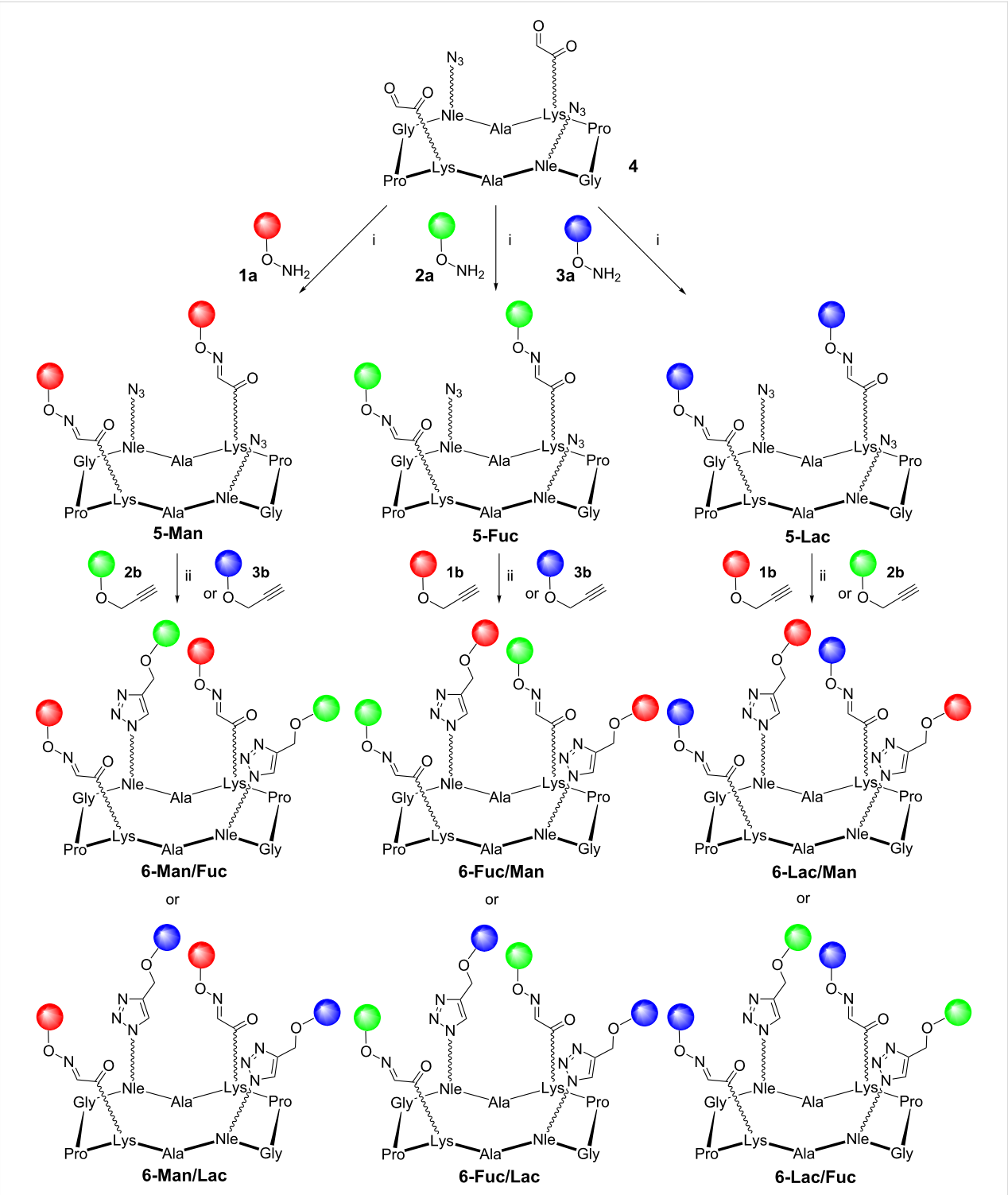

Scheme 1: Synthesis of heteroglycoclusters of the 2:2 series. Reagents and conditions: (i) 0.1% TFA in H_2O; (ii) Cu micropowder, *t*-BuOH, $AcONH_4$ 100 mM pH 7.4 (1:1, *v*/*v*). The wavy bond represents the aliphatic part (i.e., $(CH_2)_4$) of the lysine (Lys) and the norleucine (Nle) side chain.

tions were observed by analytical HPLC. The excess of sugar was then quenched by the addition of acetone, and the resulting crude mixtures were used for CuAAC without further purification. The efficiency of CuAAC clearly depends on the experimental conditions [34,35]. The choice of the solvent and of the copper(I) catalyst (delivered either using CuI, copper micropowder, or $CuSO_4$ and sodium ascorbate as reducing agent) and the utilization of microwave or ultrasonic irradiation are para-

meters that can influence the reaction kinetics, improve the yields and sometimes prevent side reactions. In a previous study, we observed that a tetravalent glycocluster can be obtained in good yields and as a unique 1,4-regioisomer by using a catalytic amount of copper micropowder in a mixture of isopropanol and ammonium acetate buffer [42]. Therefore we decided to follow similar conditions in this study with propargyl glycosides αMan **1b**, αFuc **2b** and βLac **3b**. Here again, each reaction occurred quantitatively, as shown in RP-HPLC profiles of the crude reaction mixtures (see Supporting Information File 1). After removal of solid copper by filtration and semi-preparative HPLC, six tetravalent heteroglycoclusters combining two sugars (e.g., **6-Man/Fuc**, **6-Man/Lac**, **6-Fuc/Man**, **6-Fuc/Lac**, **6-Lac/Man** and **6-Lac/Fuc**) were obtained in excellent conversion rate and purity and unambiguously characterized by mass spectrometry (Table 1).

To demonstrate the reliability of our protocol, a new series of 3:1 heteroglycoclusters was prepared from the same carbohydrate building blocks and the cyclopeptide **7**. Similar experimental conditions were followed, with the exception of the stoichiometry of reagents (see Experimental section). In this series, one oxime linkage was formed from **7** by using aminooxy αMan **1a**, αFuc **2a** and βLac **3a**, and three CuAAC reactions were subsequently performed with propargyl glycosides αMan **1b**, αFuc **2b** and βLac **3b** as described above (Scheme 2).

No difference in reactivity from the previous 2:2 series was observed, thereby confirming the efficiency of this strategy for the preparation of well-defined heteroglycoclusters.

Conclusion

In this paper we have described an expedient and controlled assembly protocol to prepare heteroglycoclusters similar to those obtained previously from randomized combinatorial libraries [26]. Following two orthogonal chemoselective reactions, cyclopeptides **4** and **7** were successively reacted with aminooxy glycosyls **1**–**3a** and propargyl glycosides **1**–**3b.** Twelve novel oxime and triazole linked-heteroglycoclusters displaying well-defined distributions and combinations of carbohydrates were thus obtained in excellent yields and purity.

Experimental

Standard procedures for the heteroglycocluster assembly

Series 2:2

A solution of **4** (4.0 mg, 3.4 μmol) and **2a** (2.6 mg, 14.2 μmol, 4 equiv) was stirred at 37 °C in 0.1% TFA in H_2O (400 μL). After 3 h, analytical HPLC revealed the total conversion of **4a** into **5-Fuc**. Analytical HPLC: t_R 9.34 min (gradient: 5 to 100% B in 20 min); ESI$^+$–MS (m/z): [M + Na]$^+$ calcd for $C_{60}H_{96}N_{20}O_{22}Na$, 1471.7; found, 1471.8. After the addition of acetone (100 μL) to the crude, the reaction mixture was lyophilized, then resuspended with t-BuOH/$AcONH_4$ 100 mM pH 7.4 (500 μL, 1:1 v/v). Compound **1b** (4.0 mg, 10.5 μmol, 3 equiv) and copper micropowder (455 μg, 7.0 μmol) were next added to the solution and the resulting mixture was left under stirring at room temperature. After 4 h, copper was removed by centrifugation and the supernatant purified by semipreparative HPLC. Compound **6-Fuc/Man** was obtained in 91% yield

Table 1: Outcome of the orthogonal ligation procedure.

compound	yield[a]	MS calcd[b]	MS found[c]	t_R (min)[d]
6-Man/Fuc	83%	1885.9 ($C_{78}H_{124}N_{20}O_{34}$)	1886.0	7.79
6-Man/Lac	99%	2242.9 ($C_{90}H_{145}N_{20}O_{46}$)	2242.3	7.43
6-Fuc/Man	98%	1885.9 ($C_{78}H_{124}N_{20}O_{34}$)	1886.0	7.73
6-Fuc/Lac	98%	2210.0 ($C_{90}H_{145}N_{20}O_{44}$)	2210.3	7.62
6-Lac/Man	94%	2242.9 ($C_{90}H_{145}N_{20}O_{46}$)	2242.2	7.31
6-Lac/Fuc	93%	2210.0 ($C_{90}H_{145}N_{20}O_{44}$)	2210.3	7.60
8-Man/Fuc	85%	1880.9 ($C_{79}H_{126}N_{21}O_{32}$)	1881.1	7.88
8-Man/Lac	87%	2415.0 ($C_{97}H_{156}N_{21}O_{50}$)	2415.4	7.30
8-Fuc/Man	91%	1912.9 ($C_{79}H_{126}N_{21}O_{34}$)	1913.2	7.66
8-Fuc/Lac	90%	2400.0 ($C_{97}H_{156}N_{21}O_{49}$)	2399.3	7.46
8-Lac/Man	89%	2092.0 ($C_{85}H_{136}N_{21}O_{40}$)	2091.2	7.46
8-Lac/Fuc	91%	2043.9 ($C_{85}H_{136}N_{21}O_{37}$)	2043.1	7.83

[a]Yields were calculated by integrating the peak corresponding to the expected compound in the crude HPLC profile. Isolated yields are given in the Experimental section. [b]Calculated mass for [M + H]$^+$. [c]MS analysis was performed by electrospray ionization method in positive mode. [d]RP-HPLC retention time using a linear gradient A/B, 95:5 to 0:100 in 20 min, flow: 1.0 mL/ min, λ = 214 nm and 250 nm (column: nucleosil 300-5 C_{18}; solvent A: 0.09% TFA in H_2O, solvent B: 0.09% TFA in 90% acetonitrile).

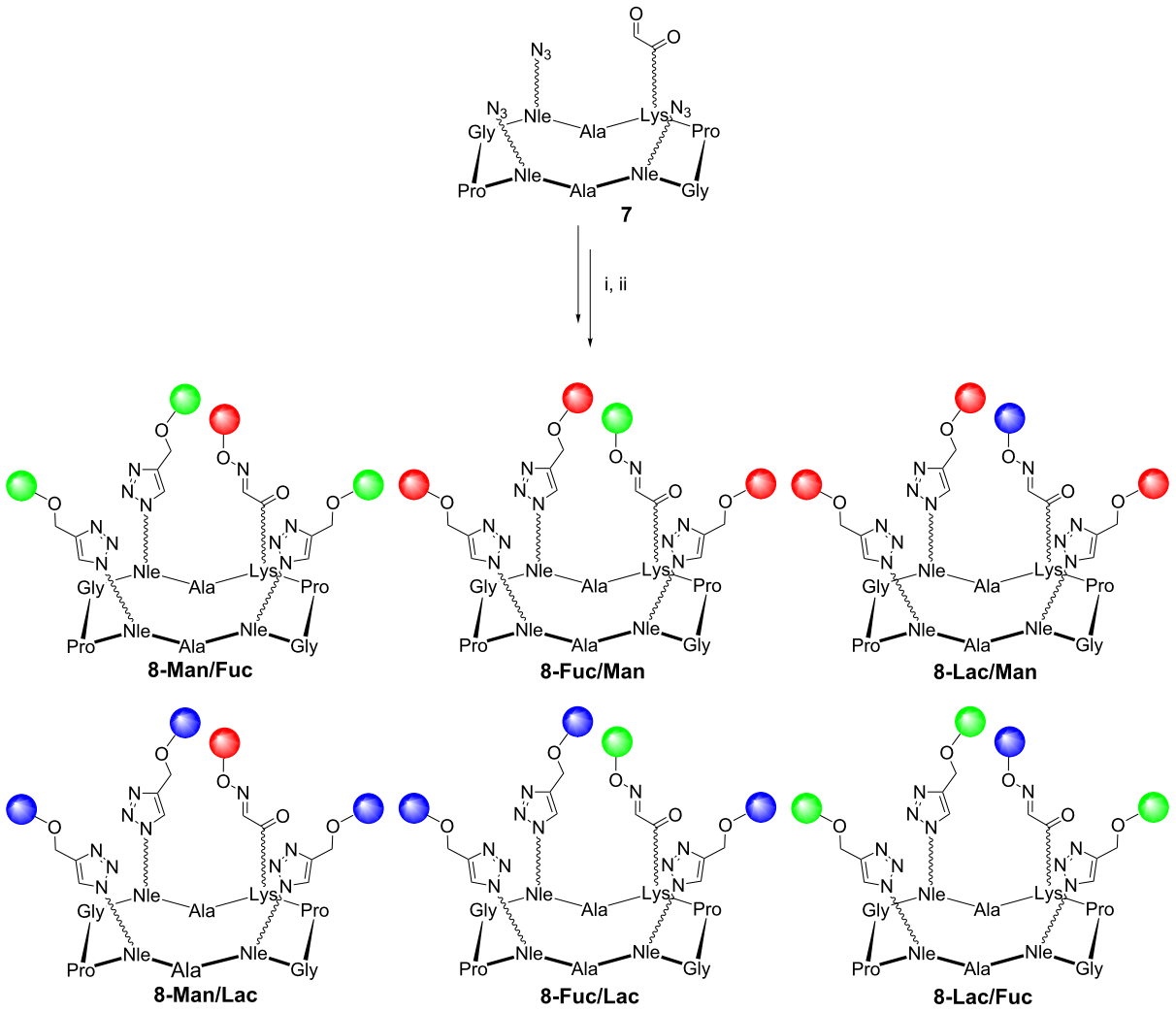

Scheme 2: Synthesis of heteroglycoclusters of the 3:1 series. Reagents and conditions: (i) **1a**, **2a** or **3a**, 0.1% TFA in H_2O; (ii) **1b**, **2b** or **3b**, Cu micropowder, *t*-BuOH, $AcONH_4$ 100 mM pH 7.4 (1:1, *v*/*v*).

(5.9 mg). Analytical RP-HPLC: t_R 7.73 min (gradient: 5 to 100% B in 20 min); ^{1}H NMR (400 MHz, D_2O) δ 8.07 (s, 1H, H_{trz}), 8.06 (s, 1H, H_{trz}), 7.81 (s, 1H, H_{ox}), 7.80 (s, 1H, H_{ox}), 5.62 (d, $J_{1,2}$ = 4.0 Hz, 1H, H-1_{Fuc}), 5.60 (d, $J_{1,2}$ = 4.0 Hz, 1H, H-1_{Fuc}), 4.99 (bs, 2H, 2H-1_{Man}), 4.86–4.68 (m, 6H, $2H_{\alpha Lys/Nle}$, $2CH_{2propargyl}$), 4.47–4.35 (m, 10H, $2H_{\alpha Lys/Nle}$, $2CH_{2\varepsilon Nle}$, $2H_{\alpha Ala}$, $2H_{\alpha Pro}$), 4.16–3.63 (m, 28H, $2CH_{2\alpha Gly}$, $2CH_{2\delta Pro}$, 2H-2_{Fuc}, 2H-3_{Fuc}, 2H-4_{Fuc}, 2H-5_{Fuc}, 2H-2_{Man}, 2H-3_{Man}, 2H-4_{Man}, 2H-5_{Man}, $2CH_2$-6_{Man}), 3.36–3.20 (m, 4H, $4H_{\varepsilon Lys}$), 2.39–2.29 (m, 2H, $2H_{\beta Pro}$), 2.16–1.27 (m, 36H, $4CH_{2\beta Lys/Nle}$, $4CH_{2\delta Lys/Nle}$, $4CH_{2\gamma Lys/Nle}$, $2H_{\beta Pro}$, $2CH_{2\gamma Pro}$, $2CH_{3Ala}$), 1.22 (d, $J_{5,6}$ = 6.0 Hz, 6H, $2CH_{3Fuc}$); ESI^+–MS (*m*/*z*): $[M + H]^+$ calcd for $C_{78}H_{124}N_{20}O_{34}$, 1885.9; found, 1886.0. Compounds **6-Man/Fuc**, **6-Man/Lac**, **6-Fuc/Lac**, **6-Lac/Man** and **6-Lac/Fuc** were prepared following the same experimental conditions.

Series 3:1

A solution of **7** (6.6 mg, 5.9 μmol) and **2a** (2.2 mg, 1.2 μmol, 2 equiv) was stirred at 37 °C in 0.1% TFA in H_2O (600 μL). After 3 h, analytical HPLC revealed the total conversion of **7** into the corresponding monovalent intermediate. Analytical HPLC t_R 10.57 min (gradient: 5 to 100% B in 20 min); ESI^+–MS (*m*/*z*): $[M + H]^+$ calcd for $C_{52}H_{84}N_{21}O_{17}$, 1274.6; found, 1274.8. After the addition of acetone (100 μL) to the crude, the reaction mixture was lyophilized, then resuspended with *t*-BuOH/$AcNH_4$ 100 mM pH 7.4 (600 μL, 1:1 *v*/*v*). Compound **1b** (10 mg, 27 μmol, 4.5 equiv) and copper micropowder (600 μg, 10 μmol) were next added to the solution and the resulting mixture was left under stirring at room temperature. After 4 h, copper was removed by centrifugation and the supernatant purified by semipreparative HPLC. Compound

8-Fuc/Man was obtained in 88% yield (10.0 mg). Analytical RP-HPLC: t_R 7.66 min (gradient: 5 to 100% B in 20 min); ^{1}H NMR (400 MHz, D_2O) δ 8.05 (s, 1H, H_{trz}), 8.02 (s, 2H, H_{trz}), 7.79 (s, 1H, H_{ox}), 5.61 (d, $J_{1,2}$ = 4.0 Hz, 1H, H-1_{Fuc}), 5.60 (d, $J_{1,2}$ = 4.0 Hz, 1H, H-1_{Fuc}), 4.99 (bs, 3H, 3H-1_{Man}), 4.85–4.66 (m, 8H, $2H_{\alpha Lys/Nle}$, $3CH_{2propargyl}$), 4.48–4.32 (m, 12H, $2H_{\alpha Lys/Nle}$, $3CH_{2\varepsilon Nle}$, $2H_{\alpha Ala}$, $2H_{\alpha Pro}$), 4.15–3.64 (m, 30H, $2CH_{2\alpha Gly}$, $2CH_{2\delta Pro}$, H-2_{Fuc}, H-3_{Fuc}, H-4_{Fuc}, H-5_{Fuc}, 3H-2_{Man}, 3H-3_{Man}, 3H-4_{Man}, 3H-5_{Man}, $3CH_2$-6_{Man}), 3.29–3.19 (m, 2H, $2H_{\varepsilon Lys}$), 2.40–2.30 (m, 2H, $2H_{\beta Pro}$), 2.15–1.28 (m, 36H, $4CH_{2\beta Lys/Nle}$, $4CH_{2\delta Lys/Nle}$, $4CH_{2\gamma Lys/Nle}$, $2H_{\beta Pro}$, $2CH_{2\gamma Pro}$, $2CH_{3Ala}$), 1.22 (d, $J_{5,6}$ = 6.6 Hz, 3H, CH_{3Fuc}); ESI$^+$–MS (*m*/*z*): $[M + H]^+$ calcd for $C_{79}H_{126}N_{21}O_{34}$, 1912.9; found, 1913.2. Compounds **8-Man/Fuc**, **8-Man/Lac**, **8-Fuc/Lac**, **8-Lac/Man** and **8-Lac/Fuc** were prepared under the same experimental conditions.

Supporting Information

The Supporting Information file contains analytical details of all heteroglycoclusters of series 2:2 (**6-Man/Fuc**, **6-Man/Lac**, **6-Fuc/Man**, **6-Fuc/Lac**, **6-Lac/Man** and **6-Lac/Fuc**) and 3:1 (**8-Man/Fuc**, **8-Man/Lac**, **8-Fuc/Man**, **8-Fuc/Lac**, **8-Lac/Man** and **8-Lac/Fuc**) described in this article.

Supporting Information File 1

Crude RP-HPLC profiles and ESI-MS spectra for the heteroglycoclusters.
[http://www.beilstein-journals.org/bjoc/content/supplementary/1860-5397-8-47-S1.pdf]

Acknowledgements

This work was supported by the Université Joseph Fourier (UJF) and the Centre National de la Recherche Scientifique (CNRS). We are grateful to the "Communauté d'agglomération Grenoble-Alpes Métropole" (Nanobio program) for access to the facilities of the Synthesis platform. Financial support from the "Cluster de Recherche Chimie de la Région Rhône-Alpes" (B.T.) and from the pôle Chimie, Sciences du vivant et de la santé, Bioingénierie of UJF (M. F.) are duly acknowledged.

References

1. Varki, A. *Glycobiology* **1993,** *3,* 97–130. doi:10.1093/glycob/3.2.97
2. Chabre, Y. M.; Roy, R. *Adv. Carbohydr. Chem. Biochem.* **2010,** *63,* 165–393. doi:10.1016/S0065-2318(10)63006-5
3. Imberty, A.; Chabre, Y. M.; Roy, R. *Chem.–Eur. J.* **2008,** *14,* 7490–7499. doi:10.1002/chem.200800700
4. Pieters, R. J. *Org. Biomol. Chem.* **2009,** *7,* 2013–2025. doi:10.1039/b901828j
5. Renaudet, O.; Spinelli, N., Eds. *Synthesis and biological applications of glycoconjugates;* Bentham Science Publishers Ltd.: U.A.E., 2011.
6. Lee, Y. C.; Lee, R. T. *Acc. Chem. Res.* **1995,** *28,* 321–327. doi:10.1021/ar00056a001
7. Lundquist, J. J.; Toone, E. J. *Chem. Rev.* **2002,** *102,* 555–578. doi:10.1021/cr000418f
8. Kitov, P. I.; Sadowska, J. M.; Mulvey, G.; Armstrong, G. D.; Ling, H.; Pannu, N. S.; Read, R. J.; Bundle, D. R. *Nature* **2000,** *403,* 669–672. doi:10.1038/35001095
9. Touaibia, M.; Wellens, A.; Shiao, T. C.; Wang, Q.; Sirois, S.; Bouckaert, J.; Roy, R. *ChemMedChem* **2007,** *2,* 1190–1201. doi:10.1002/cmdc.200700063
10. Joosten, J. A. F.; Loimaranta, V.; Appeldoorn, C. C. M.; Haataja, S.; El Maate, F. A.; Liskamp, R. M. J.; Finne, J.; Pieters, R. J. *J. Med. Chem.* **2004,** *47,* 6499–6508. doi:10.1021/jm049476+
11. Horan, N.; Yan, L.; Isobe, H.; Whitesides, G. M.; Kahne, D. *Proc. Natl. Acad. Sci. U. S. A.* **1999,** *96,* 11782–11786. doi:10.1073/pnas.96.21.11782
12. Gómez-García, M.; Benito, J. M.; Rodríguez-Lucena, D.; Yu, J.-X.; Chmurski, K.; Ortiz Mellet, C.; Gutiérrez Gallego, R.; Maestre, A.; Defaye, J.; Garcia Fernández, J. M. *J. Am. Chem. Soc.* **2005,** *127,* 7970–7971. doi:10.1021/ja050934t
13. Ramström, O.; Lehn, J.-M. *ChemBioChem* **2000,** *1,* 41–48. doi:10.1002/1439-7633(20000703)1:1<41::AID-CBIC41>3.0.CO;2-L
14. Ramström, O.; Lohmann, S.; Bunyapaiboonsri, T.; Lehn, J.-M. *Chem.–Eur. J.* **2004,** *10,* 1711–1715. doi:10.1002/chem.200305551
15. Gómez-García, M.; Benito, J. M.; Gutiérrez-Gallego, R.; Maestre, A.; Ortiz Mellet, C.; García Fernández, J. M.; Jiménez Blanco, J. L. *Org. Biomol. Chem.* **2010,** *8,* 1849–1860. doi:10.1039/b920048g
16. Ortega-Muñoz, M.; Perez-Balderas, F.; Morales-Sanfrutos, J.; Hernandez-Mateo, F.; Isac-García, J.; Santoyo-Gonzalez, F. *Eur. J. Org. Chem.* **2009,** 2454–2473. doi:10.1002/ejoc.200801169
17. Deguise, I.; Lagnoux, D.; Roy, R. *New J. Chem.* **2007,** *31,* 1321–1331.
18. Katajisto, J.; Karskela, T.; Heinonen, P.; Lönnberg, H. *J. Org. Chem.* **2002,** *67,* 7995–8001. doi:10.1021/jo026053b
19. Patel, A.; Lindhorst, T. K. *Eur. J. Org. Chem.* **2002,** 79–86. doi:10.1002/1099-0690(20021)2002:1<79::AID-EJOC79>3.0.CO;2-1
20. Geng, J.; Mantovani, G.; Tao, L.; Nicolas, J.; Chen, G.; Wallis, R.; Mitchell, D. A.; Johnson, B. R. G.; Evans, S. D.; Haddleton, D. M. *J. Am. Chem. Soc.* **2007,** *129,* 15156–15163. doi:10.1021/ja072999x
21. Ladmiral, V.; Mantovani, G.; Clarkson, G. J.; Cauet, S.; Irwin, J. L.; Haddleton, D. M. *J. Am. Chem. Soc.* **2006,** *128,* 4823–4830. doi:10.1021/ja058364k
22. Fiore, M.; Chambery, A.; Marra, A.; Dondoni, A. *Org. Biomol. Chem.* **2009,** *7,* 3910–3913. doi:10.1039/b912686d
23. Lindhorst, T. K.; Bruegge, K.; Fuchs, A.; Sperling, O. *Beilstein J. Org. Chem.* **2010,** *6,* 801–809. doi:10.3762/bjoc.6.90
24. Liang, C.-H.; Wang, S.-K.; Lin, C.-W.; Wang, C.-C.; Wong, C.-H.; Wu, C.-Y. *Angew. Chem., Int. Ed.* **2011,** *50,* 1608–1612. doi:10.1002/anie.201003482
25. Gómez-García, M.; Benito, J. M.; Butera, A. P.; Ortiz Mellet, C.; García Fernández, J. M.; Jiménez Blanco, J. L. *J. Org. Chem.* **2012,** *77,* 1273–1288. doi:10.1021/jo201797b
26. Duléry, V.; Renaudet, O.; Wilczewski, M.; Van der Heyden, A.; Labbé, P.; Dumy, P. *J. Comb. Chem.* **2008,** *10,* 368–371. doi:10.1021/cc800029v
27. Renaudet, O.; BenMohamed, L.; Dasgupta, G.; Bettahi, I.; Dumy, P. *ChemMedChem* **2008,** *3,* 737–741. doi:10.1002/cmdc.200700315

28. Renaudet, O.; Dasgupta, G.; Bettahi, I.; Shi, A.; Nesburn, A. B.; Dumy, P.; BenMohamed, L. *PLoS One* **2010,** *5,* e11216. doi:10.1371/journal.pone.0011216
29. Renaudet, O.; Křenek, K.; Bossu, I.; Dumy, P.; Kádek, A.; Adámek, D.; Vaněk, O.; Kavan, D.; Gažák, R.; Šulc, M.; Bezouška, K.; Křen, V. *J. Am. Chem. Soc.* **2010,** *132,* 6800–6808. doi:10.1021/ja101296t
30. Bossu, I.; Šulc, M.; Křenek, K.; Dufour, E.; Garcia, J.; Berthet, N.; Dumy, P.; Křen, V.; Renaudet, O. *Org. Biomol. Chem.* **2011,** *9,* 1948–1959. doi:10.1039/c0ob00772b
31. Pujol, A. M.; Cuillel, M.; Renaudet, O.; Lebrun, C.; Charbonnier, P.; Cassio, D.; Gateau, C.; Dumy, P.; Mintz, E.; Delangle, P. *J. Am. Chem. Soc.* **2011,** *133,* 286–296. doi:10.1021/ja106206z
32. Tornøe, C. W.; Christensen, C.; Meldal, M. *J. Org. Chem.* **2002,** *67,* 3057–3064. doi:10.1021/jo011148j
33. Rostovtsev, V. V.; Green, L. G.; Fokin, V. V.; Sharpless, K. B. *Angew. Chem., Int. Ed.* **2002,** *41,* 2596–2599. doi:10.1002/1521-3773(20020715)41:14<2596::AID-ANIE2596>3.0.CO;2-4
34. Dondoni, A. *Chem.–Asian J.* **2007,** *2,* 700–708. doi:10.1002/asia.200700015
35. Jewett, J. C.; Bertozzi, C. R. *Chem. Soc. Rev.* **2010,** *39,* 1272–1279. doi:10.1039/b901970g
36. Galibert, M.; Renaudet, O.; Dumy, P.; Boturyn, D. *Angew. Chem., Int. Ed.* **2011,** *50,* 1901–1904. doi:10.1002/anie.201006867
37. Clavé, G.; Volland, H.; Flaender, M.; Gasparutto, D.; Romieu, A.; Renard, P.-Y. *Org. Biomol. Chem.* **2010,** *8,* 4329–4345. doi:10.1039/c0ob00133c
38. Cao, S.; Tropper, F. D.; Roy, R. *Tetrahedron* **1995,** *51,* 6679–6686. doi:10.1016/0040-4020(95)00325-3
39. Renaudet, O.; Dumy, P. *Org. Biomol. Chem.* **2006,** *4,* 2628–2636. doi:10.1039/b604391g
40. Duléry, V.; Renaudet, O.; Philouze, C.; Dumy, P. *Carbohydr. Res.* **2007,** *342,* 894–900. doi:10.1016/j.carres.2007.02.003
41. Fernandez-Megia, E.; Correa, J.; Rodriguez-Meizoso, I.; Riguera, R. *Macromolecules* **2006,** *39,* 2113–2120. doi:10.1021/ma052448w
42. Bossu, I.; Berthet, N.; Dumy, P.; Renaudet, O. *J. Carbohydr. Chem.* **2011,** *30,* 458–468. doi:10.1080/07328303.2011.590260

License and Terms

Beilstein Journal of Organic Chemistry

Facile synthesis of nitrophenyl 2-acetamido-2-deoxy-α-D-mannopyranosides from ManNAc-oxazoline

Karel Křenek[1], Petr Šimon[1], Lenka Weignerová[1], Barbora Fliedrová[1,2], Marek Kuzma[1] and Vladimír Křen[*1]

Full Research Paper

Open Access

Address:
[1]Institute of Microbiology, Academy of Sciences of the Czech Republic, Vídeňská 1083, CZ – 142 20, Prague, Czech Republic and [2]Department of Biochemistry, Charles University in Prague, Hlavova 8, CZ – 128 40, Prague, Czech Republic

Email:
Vladimír Křen* - kren@biomed.cas.cz

* Corresponding author

Keywords:
α-ManNAc; glycosidase; glycosylation; nitrophenyl; oxazoline

Beilstein J. Org. Chem. **2012,** *8,* 428–432.
doi:10.3762/bjoc.8.48

Received: 20 January 2012
Accepted: 06 March 2012
Published: 20 March 2012

This article is part of the Thematic Series "Synthesis in the glycosciences II".

Guest Editor: T. K. Lindhorst

Abstract

The synthetic procedures for a large-scale preparation of *o*- and *p*-nitrophenyl 2-acetamido-2-deoxy-α-D-mannopyranoside are described. The synthetic pathway employs the glycosylation of phenol with ManNAc oxazoline, followed by nitration of the aromatic moiety yielding a separable mixture of the *o*- and *p*-nitrophenyl derivative in a 2:3 ratio.

Introduction

Hexosamines are fundamental structural elements and precursors of the peptidoglycan and membrane lipopolysaccharide layer as well as of capsular polysaccharides in Gram-negative bacteria. *N*-Acetyl-D-mannosamine (ManNAc) has been found to be, presumably, the strongest monosaccharidic ligand for the natural killer cells (NK-cells) activating protein NKR-P1 [1], and some ManNAc-containing oligosaccharides (e.g., Glc*p*NAc-β-(1→4)Man*p*NAc) have been identified to be strong immunoactivators [2]. Detection of ManNAc by the immune system is probably very important for recognizing bacterial infection, as this carbohydrate is an unambiguous signal of a microbial invader [3]. In the somatic cells (vertebrates) there are no structures composed of ManNAc. This carbohydrate is a precursor of sialic acid(s). The pathogenicity of some bacterial strains occurring in their R-forms (R stands for rough: virulent, containing ManNAc in the capsular structures) and S-forms (S stands for smooth: nonvirulent, lower level of ManNAc in the capsules) is related partly to the content of ManNAc. Thus, ManNAc units play a significant role in bacterial pathogenicity and virulence (e.g., *Streptococcus pneumoniae*) [4,5]. Surprisingly, glycosidases active upon β-Man*p*NAc and α-Man*p*NAc glycosides are not known so far. Therefore, the building blocks for the chemical synthesis of ManNAc-containing compounds, as well as the substrates for the hypothetical α-*N*-acetyl-mannopyranosidase, are required.

This paper describes new robust and effective methods for the synthesis of both *o*-nitrophenyl 2-acetamido-2-deoxy-α-D-

mannopyranoside (**7**) and *p*-nitrophenyl 2-acetamido-2-deoxy-α-D-mannopyranoside (**8**) usable as practical chromogenic substrates for the screening of such enzymes.

Results and Discussion

The first reported preparation of *p*-nitrophenyl 2-acetamido-2-deoxy-α-D-mannopyranoside (*p*NP-α-ManNAc, **8**) was described in [6], starting from 2-acetamido-2-deoxy-D-glucose and providing the product in 2% overall yield. We have previously published [7] a 9-step synthesis of *p*NP-α-ManNAc (**8**) from commercially available methyl α-D-glucopyranoside with an overall yield of 1.5%. Later, Popelová et al. [8] published a concise synthesis starting either from D-glucose (5 steps, 1.5% yield) or from methyl 4,6-*O*-benzylidene-α-D-glucopyranoside (5 steps, 23%). Unfortunately, in our hands this synthetic procedure did not afford the published yields, namely in the triflate and consequent azide substitution steps.

Oxazolines, such as **3**, have been used as glycosylation agents in the preparation of glycoproteins [9,10], various alcohol glycosides [11,12], phosphates [13] and oligosaccharides [12]. To the best of our knowledge, glycosylation of phenolic OH with oxazoline has not been accomplished so far. Therefore, we decided to test oxazoline **3** [14] glycosylation in our synthetic approach.

Synthetic pathway

The synthesis (see Scheme 1) was started from commercially available 2-acetamido-2-deoxy-D-mannopyranose (**1**, ManNAc), which was converted to its peracetate **2** (Ac_2O/py/DMAP (cat.), 90%). A crude mixture of peracetylated ManNAc **2** was treated with trifluoromethanesulfonic acid [14] affording oxazoline **3** in 75% yield.

The glycosylation of phenol and *p*-nitrophenol with oxazoline **3** was extensively tested. We tested a large array of reaction conditions, including variation of catalyst (copper(II) chloride [12,15], 2,2-diphenyl-1-picrylhydrazyl, zinc chloride, tin(IV) chloride) and solvent (CH_2Cl_2, THF, toluene, benzene), all of which were not successful. Finally, we found that trimethylsilyl trifluoromethanesulfonate in dichloromethane [11] was capable of catalyzing the oxazoline ring opening with phenol to afford α-phenyl glycoside **4** in a reasonable 56% yield. This reaction was also tested with *p*-nitrophenol; however, the required *p*-nitrophenyl glycoside **6** was produced under these conditions only in trace amounts (observed by TLC). Our and previously published results [11] indicate that the deactivation of phenol by the electron-withdrawing nitro group substantially decreases its reactivity in the glycosylation reaction with oxazoline and, on the other hand, the presence of electron-donating groups increases the yields.

The resulting phenyl glycoside **4** was treated with a solution of red fuming nitric acid in acetic acid [16], producing a mixture of *o*-nitrophenyl glycoside **5** (22% yield) and *p*-nitrophenyl glycoside **6** (34% yield) in approximately 2:3 ratio, which was separated by flash chromatography. Zemplén deacetylation of **4** and **5** afforded the title compounds **7** and **8** in almost quantitative yields.

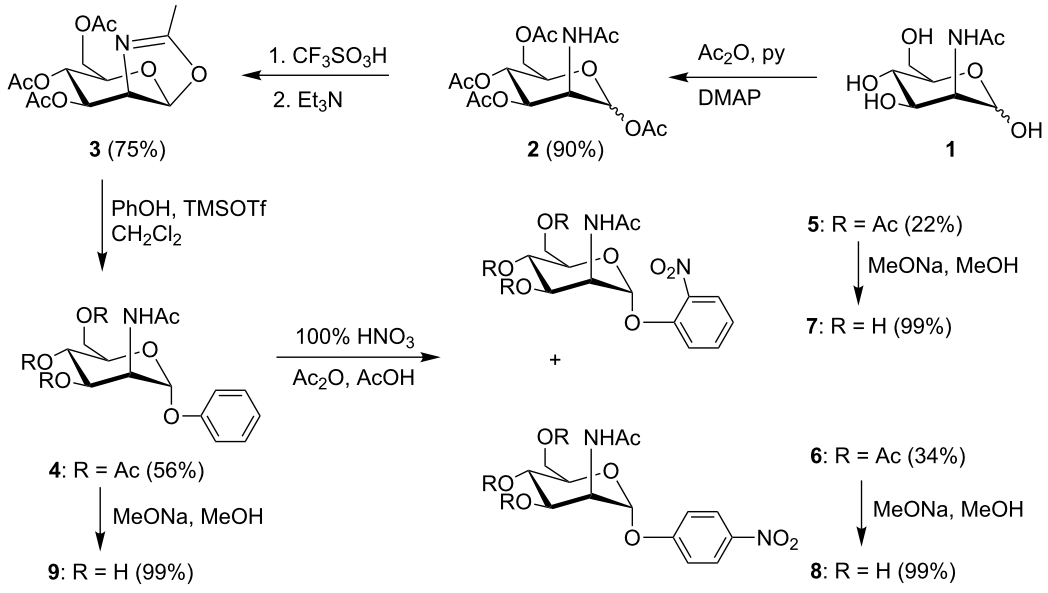

Scheme 1: Synthetic pathway.

Conclusion

In conclusion, a simple and robust procedure for the synthesis of *o*- and *p*-nitrophenyl 2-acetamido-2-deoxy-α-D-mannopyranoside (**7** and **8**) from commercially available ManNAc, via its oxazoline, is described affording an overall total yield of both **7** and **8** of over 21%, including the purification steps.

Experimental

General methods

All chemicals were purchased from Sigma-Aldrich, except for 2-acetamido-2-deoxy-D-mannose, which was purchased from BIOSYNTH AG, Staad, CH. The reactions were monitored by TLC with precoated silica gel 60 F_{254} aluminium sheets from Merck, detected with UV light and/or charred with sulfuric acid (5% in EtOH). The compounds were purified either by column flash chromatography with silica gel 60 (230–240 mesh, Merck) or by gel permeation chromatography with Sephadex LH20 from Sigma Aldrich. The solvents were distilled and dried according to the standard procedures before use.

NMR spectroscopy

NMR spectra were recorded on a Bruker Avance III 400 MHz spectrometer (400.13 MHz for ^{1}H, 100.55 MHz for ^{13}C at 30 °C) and a Bruker Avance III 600 MHz spectrometer (600.23 MHz for ^{1}H, 150.93 MHz for ^{13}C at 30 °C) in CD_3OD or $CDCl_3$ (Sigma-Aldrich). Residual signals of the deuterated solvents were used as internal standards (for CD_3OD δ_H 3.330 ppm, δ_C 49.30 ppm, for $CDCl_3$ δ_H 7.265 ppm, δ_C 77.23 ppm). NMR experiments ^{1}H NMR, ^{13}C NMR, gCOSY, gHSQC, and gHMBC were performed using the manufacturer's software. ^{1}H NMR and ^{13}C NMR spectra were zero filled to fourfold data points and multiplied by a window function before Fourier transformation. A two-parameter double-exponential Lorentz–Gauss function was applied for ^{1}H to improve resolution, and line broadening (1 Hz) was applied to get a better ^{13}C signal-to-noise ratio. Chemical shifts are given on a δ-scale with the digital resolution justifying the reported values to three (δ_H) or two (δ_C) decimal places.

The anomeric configuration of *manno*-structures was determined based on the value of ^1J (C-1, H-1) [17], which was measured by using gHMQC or gHSQC with retained direct coupling constants between directly bonded carbon and hydrogen.

Mass spectrometry

Mass spectra were measured on MALDI–TOF/TOF ultraFLEX III mass spectrometers (Bruker-Daltonics). Positive spectra were calibrated externally by using the monoisotopic $[M + H]^+$ ions of PepMixII calibrant (Bruker-Daltonics). For the MALDI experiment 0.4 μL of sample dissolved in 50% acetonitrile was allowed to dry at ambient temperature on the target and overlaid with matrix solution (either 2,5-dihydroxybenzoic acid, DHB or α-cyano-4-hydroxycinnamic acid, CCA). The spectra were collected in reflectron mode.

Phenyl 2-acetamido-2-deoxy-3,4,6-tri-*O*-acetyl-α-D-mannopyranoside (4): 2-Methyl-(3,4,6-tri-*O*-acetyl-1,2-dideoxy-β-D-mannopyrano)-[2,1:4',5']-2-oxazoline [18] **3** (280 mg, 0.85 mmol) was dissolved in 10 mL of dry dichloromethane. To this solution, phenol (250 mg, 2.66 mmol, 3 equiv) and trimethylsilyl trifluoromethanesulfonate (0.2 mL, 0.73 mmol, 1 equiv) were added. The reaction mixture was stirred at room temperature for 3 days (monitored by TLC on silica gel, chloroform/acetone 8:1). The reaction mixture was evaporated to dryness in vacuo. The product was isolated by column chromatography (silica gel, chloroform/acetone 20:1) as a white solid (200 mg, 56%). ^{1}H NMR (400 MHz, $CDCl_3$) δ 2.015 (s, 3H, 6-Ac), 2.022 (s, 3H, 3-Ac), 2.048 (s, 3H, 4-Ac), 2.080 (s, 3H, 2-Ac), 4.022 (dd, J = 2.4, 12.2 Hz, 1H, H-6u), 4.104 (ddd, J = 2.4, 5.6, 10.2 Hz, 1H, H-5), 4.265 (dd, J = 5.6, 12.2 Hz, 1H, H-6d), 4.821 (ddd, J = 1.6, 4.7, 8.9 Hz, 1H, H-2), 5.168 (dd, J = 10.2, 10.2 Hz, 1H, H-4), 5.475 (d, J = 1.6 Hz, 1H, H-1), 5.564 (dd, J = 4.7, 10.2 Hz, 1H, H-3), 5.919 (d, J = 8.9 Hz, 1H, 2-NH), 7.047 (m, 1H, H-*para*), 7.075 (m, 2H, H-*ortho*), 7.291 (m, 2H, H-*meta*); ^{13}C NMR (100 MHz, $CDCl_3$) δ 20.60, 20.70 (3 x q, 3-Ac, 4-Ac, 6-Ac), 23.29 (q, 2-Ac), 50.51 (d, C-2), 62.14 (t, C-6), 65.99 (d, C-4), 68.67 (d, C-5), 68.89 (d, C-3), 97.12 (d, C-1), 116.49 (d, C-*ortho*), 122.99 (d, C-*para*), 129.56 (d, C-*meta*), 155.60 (s, C-*ipso*), 169.82 (s, 3-CO), 169.94 (s, 4-CO), 170.15 (s, 2-CO), 170.40 (s, 6-CO).

***o*-Nitrophenyl 2-acetamido-2-deoxy-3,4,6-tri-*O*-acetyl-α-D-mannopyranoside (5) and *p*-nitrophenyl 2-acetamido-2-deoxy-3,4,6-tri-*O*-acetyl-α-D-mannopyranoside (6):** Compound **4** (1.1 g, 2.59 mmol) was dissolved in a mixture of acetic anhydride (10 mL) and glacial acetic acid (2 mL). The solution was cooled to 0 °C in an ice bath, and red fuming nitric acid (≥99.5%, 0.5 mL) was added in one portion under stirring. The reaction mixture was stirred overnight, allowing the ice bath to melt and warm up to ambient temperature. The reaction mixture was diluted by an ice–water mixture (50 mL), stirred for an additional 30 min, and neutralized by the saturated aqueous solution of $NaHCO_3$. After extraction with methylene dichloride (3 × 50 mL), the combined organic layers were washed with 50 mL of sodium bicarbonate solution and 50 mL of water. After drying (Na_2SO_4) the organic phase was evaporated and chromatographed (silica gel, chloroform/acetone 5:1). *o*-Nitrophenyl derivative **5** was isolated as a white solid (270 mg, 22%) and *p*-nitrophenyl derivative **6** was isolated as a white solid (410 mg, 34%).

(**5**) ^{1}H NMR (400 MHz, $CDCl_3$) δ 2.032 (s, 3H, 3-Ac), 2.039 (s, 3H, 6-Ac), 2.080 (s, 3H, 4-Ac), 2.104 (s, 3H, 2-Ac), 4.042 (dd, *J* = 2.2, 12.3 Hz, 1H, H-6u), 4.212 (ddd, *J* = 2.2, 5.2, 10.2 Hz, 1H, H-5), 4.286 (dd, *J* = 5.2, 12.3 Hz, 1H, H-6d), 4.812 (ddd, *J* = 1.8, 4.8, 7,7 Hz, 1H, H-2), 5.213 (dd, *J* = 10.2, 10.2 Hz, 1H, H-4), 5.593 (dd, *J* = 4.8, 10.2 Hz, 1H, H-3), 5.750 (d, *J* = 1.8 Hz, 1H, H-1), 5.909 (d, *J* = 7.7 Hz, 1H, 2-NH), 7.170 (ddd, *J* = 1.2, 7.4, 8.2 Hz, 1H, H-4´), 7.329 (dd, *J* = 1.2, 8.5 Hz, 1H, H-6´), 7.544 (ddd, *J* = 1.7, 7.4, 8.5 Hz, 1H, H-5´), 7.905 (dd, *J* = 1.7, 8.2 Hz, 1H, H-3´); ^{13}C NMR (100 MHz, $CDCl_3$) δ 20.62, 20.63, 20.65 (3 x q, 3-Ac, 4-Ac, 6-Ac), 23.28 (q, 2-Ac), 50.68 (d, C-2), 61.97 (t, C-6), 65.52 (d, C-4), 68.33 (d, C-3), 69.68 (d, C-5), 97.34 (d, C-1), 117.24 (d, C-6´), 122.82 (d, C-4´), 125.88 (d, C-3´), 134.09 (d, C-5´), 140.58 (s, C-2´), 148.66 (s, C-1´), 169.20 (s, 3-CO), 170.07 (s, 4-CO), 170.32 (s, 6-CO), 170.47 (s, 2-CO).

(**6**) ^{1}H NMR (400 MHz, $CDCl_3$) δ 2.028 (s, 3H, 6-Ac), 2.047 (s, 3H, 3-Ac), 2.065 (s, 3H, 4-Ac), 2.109 (s, 3H, 2-Ac), 4.02* (m, 1H, H-5), 4.03* (m, 1H, H-6u), 4.273 (dd, *J* = 5.6, 12.4 Hz, 1H, H-6d), 4.818 (ddd, *J* = 1.6, 4.8, 8.4 Hz, 1H, H-2), 5.196 (dd, *J* = 10.2, 10.3 Hz, 1H, H-4), 5.555 (dd, *J* = 4.8, 10.3 Hz, 1H, H-3), 5.629 (d, *J* = 1.6 Hz, 1H, H-1), 5.905 (d, *J* = 8.4 Hz, 1H, 2-NH), 7.205 (m, 2H, H-*ortho*), 8.225 (m, 2H, H-*meta*) (* = HSQC readout); ^{13}C NMR (100 MHz, $CDCl_3$) δ 20.59, 20.62, 20.67 (3 x q, 3-Ac, 4-Ac, 6-Ac), 23.28 (q, 2-Ac), 50.42 (d, C-2), 61.94 (t, C-6), 65.58 (d, C-4), 68.35 (d, C-3), 69.31 (d, C-5), 96.89 (d, C-1), 116.47 (d, C-*ortho*), 125.82 (d, C-*meta*), 143.19 (s, C-*para*), 160.22 (s, C-*ipso*), 169.68 (s, 3-CO), 169.86 (s, 4-CO), 170.26 (s, 6-CO), 170.36 (s, 2-CO).

***o*-Nitrophenyl 2-acetamido-2-deoxy-α-D-mannopyranoside (7):** Compound **5** (270 mg, 0.58 mmol) was dissolved in dry methanol (2 mL) and three drops of NaOMe in MeOH (35%, w/w) were added. The reaction mixture was stirred at ambient temperature for 20 minutes. The solution was directly loaded onto the gel permeation chromatography column (Sephadex LH-20) with methanol as a mobile phase (2 mL/min, UV detection 254 nm). The product was isolated as a white solid (197 mg, 99%). ^{1}H NMR (400 MHz, CD_3OD) δ 2.070 (s, 3H, 2-Ac), 3.660 (ddd, *J* = 2.3, 4.5, 10.0 Hz, 1H, H-5), 3.761 (dd, *J* = 2.5, 12.0 Hz, 1H, H-6u), 3.756 (dd, *J* = 9.7, 9.9 Hz, 1H, H-4), 3.824 (dd, *J* = 4.5, 12.0 Hz, 1H, H-6d), 4.183 (dd, *J* = 4.9, 9.7 Hz, 1H, H-3), 4.541 (dd, *J* = 1.7, 4.9 Hz, 1H, H-2), 5.689 (d, *J* = 1.7 Hz, 1H, H-1), 7.188 (ddd, *J* = 1.2, 7.4, 8.1 Hz, 1H, H-4´), 7.515 (dd, *J* = 1.2, 8.5 Hz, 1H, H-6´), 7.612 (ddd, *J* = 1.7, 7.4, 8.5 Hz, 1H, H-5´), 7.854 (dd, *J* = 1.7, 8.1 Hz, 1H, H-3´); ^{13}C NMR (100 MHz, CD_3OD) δ 22.93 (q, 2-Ac), 54.36 (d, C-2), 62.23 (t, C-6), 68.14 (d, C-4), 70.43 (d, C-3), 76.04 (d, C-5), 99.65 (d, C-1), 118.74 (d, C-6´), 123.58 (d, C-4´), 126.51 (d, C-3´), 135.52 (d, C-5´), 142.17 (s, C-2´), 150.50 (s, C-1´), 174.61 (s, 2-CO); MS–MALDI–TOF (*m*/*z*): 365.1 $[M + Na]^+$ (DHB), 365.1 $[M + Na]^+$ (CCA).

***p*-Nitrophenyl 2-acetamido-2-deoxy-α-D-mannopyranoside (8):** Compound **6** (400 mg, 0.85 mmol) was deacetylated and purified as described for compound **7** yielding **8** as a white solid (290 mg, 99%). ^{1}H NMR (400 MHz, CD_3OD) δ 2.078 (s, 2-Ac3H,), 3.562 (ddd, *J* = 2.4, 4.7, 9.9 Hz, 1H, H-5), 3.746 (dd, *J* = 2.4, 12.0 Hz, 1H, H-6u), 3.752 (dd, *J* = 9.7, 9.9 Hz, 1H, H-4), 3.812 (dd, *J* = 4.7, 12.0 Hz, 1H, H-6d), 4.164 (dd, *J* = 4.9, 9.7 Hz, 1H, H-3), 4.544 (dd, *J* = 1.7, 4.9 Hz, 1H, H-2), 5.657 (d, *J* = 1.7 Hz, 1H, H-1), 7.300 (m, 2H, H-*ortho*), 8.230 (m, 2H, H-*meta*). ^{13}C NMR (100 MHz, CD_3OD) δ 22.93 (q, 2-Ac), 54.28 (d, C-2), 62.23 (t, C-6), 68.20 (d, C-4), 70.51 (d, C-3), 75.79 (d, C-5), 99.09 (d, C-1), 118.05 (d, C-*ortho*), 127.00 (d, C-*meta*), 144.21 (s, C-*para*), 162.80 (s, C-*ipso*), 174.66 (s, 2-CO); MS–MALDI–TOF (*m*/*z*): 365.1 $[M + Na]^+$ (DHB), 365.1 $[M + Na]^+$ (CCA).

Phenyl 2-acetamido-2-deoxy-α-D-mannopyranoside (9): Compound **4** (50 mg, 0.12 mmol) was deacetylated and purified as described for compound **7**, yielding **9** as a white solid (35 mg, 99%). ^{1}H NMR (400 MHz, CD_3OD) δ 2.067 (s, 3H, 2-Ac), 3.654 (m, 1H, H-5), 3.73* (m, 1H, H-6u), 3.75* (m, 1H, H-4), 3.838 (dd, *J* = 4.2, 11.9 Hz, 1H, H-6d), 4.178 (dd, *J* = 4.8, 9.6 Hz, 1H, H-3), 4.525 (dd, *J* = 1.7, 4.8 Hz, 1H, H-2), 5.466 (d, *J* = 1.7 Hz, 1H, H-1), 7.023 (m, 1H, H-*para*), 7.110 (m, 2H, H-*ortho*), 7.298 (m, 2H, H-*meta*) (* - HSQC readouts); ^{13}C NMR (100 MHz, CD_3OD) δ 22.95 (q, 2-Ac), 54.64 (d, C-2), 62.22 (t, C-6), 68.35 (d, C-4), 70.81 (d, C-3), 75.06 (d, C-5), 99.22 (d, C-1), 118.00 (d, C-*ortho*), 123.79 (d, C-*para*), 130.83 (d, C-*meta*), 157.95 (s, C-*ipso*), 174.53 (s, 2-CO); MS–MALDI–TOF (*m*/*z*): 320.1 $[M + Na]^+$ (DHB), 320.1 $[M + Na]^+$ (CCA).

Acknowledgements

Support from the Czech Science Foundation grant P207/10/0321, EU project NOVOSIDES FP7-KBBE-2010-4-265854 (MŠMT 7E11011), and ESF COST Chemistry CM1102 project is acknowledged.

References

1. Krist, P.; Herkommerová-Rajnochová, E.; Rauvolfová, J.; Semeňuk, T.; Vavrušková, P.; Pavlíček, J.; Bezouška, K.; Petruš, L.; Křen, V. *Biochem. Biophys. Res. Commun.* **2001,** *287,* 11–20. doi:10.1006/bbrc.2001.5537
2. Sedmera, P.; Přikrylová, V.; Bezouška, K.; Rajnochová, E.; Thiem, J.; Křen, V. *J. Carbohydr. Chem.* **1998,** *17,* 1351–1357. doi:10.1080/07328309808002358
3. Attolino, E.; Bonaccorsi, F.; Catelani, G.; D'Andrea, F.; Křenek, K.; Bezouška, K.; Křen, V. *J. Carbohydr. Chem.* **2008,** *27,* 156–171. doi:10.1080/07328300802030845

4. Lee, C. J.; Fraser, B. A. *J. Biol. Chem.* **1980,** *255,* 6847–6853.
5. Lee, C. J.; Banks, S. D.; Li, J. P. *Crit. Rev. Microbiol.* **1991,** *18,* 89–114. doi:10.3109/10408419109113510
6. Yoshimura, J.; Sakai, H.; Oda, N.; Hashimoto, H. *Bull. Chem. Soc. Jpn.* **1972,** *45,* 2027–2031. doi:10.1246/bcsj.45.2027
7. Krist, P.; Kuzma, M.; Pelyvás, I. F.; Simerská, P.; Křen, V. *Collect. Czech. Chem. Commun.* **2003,** *68,* 801–811. doi:10.1135/cccc20030801
8. Popelová, A.; Kefurt, K.; Hlaváčková, M.; Moravcová, J. *Carbohydr. Res.* **2005,** *340,* 161–166. doi:10.1016/j.carres.2004.11.002
9. Rich, J. R.; Withers, S. G. *Nat. Chem. Biol.* **2009,** *5,* 206–215. doi:10.1038/nchembio.148
10. Hollósi, M.; Kollát, E.; Laczkó, I.; Medzihradsky, K. F.; Thurin, J.; Otvös, L., Jr. *Tetrahedron Lett.* **1991,** *32,* 1531–1534. doi:10.1016/S0040-4039(00)74264-X
11. Lopin, C.; Jacquinet, J.-C. *Angew. Chem., Int. Ed.* **2006,** *45,* 2574–2578. doi:10.1002/anie.200503551
12. Wittmann, V.; Lennartz, D. *Eur. J. Org. Chem.* **2002,** 1363–1367. doi:10.1002/1099-0690(200204)2002:8<1363::AID-EJOC1363>3.0.CO;2-#
13. Heidlas, J. E.; Lees, W. J.; Pale, P.; Whitesides, G. M. *J. Org. Chem.* **1992,** *57,* 146–151. doi:10.1021/jo00027a028
14. Freese, S. J.; Vann, W. F. *Carbohydr. Res.* **1996,** *281,* 313–319. doi:10.1016/0008-6215(95)00345-2
15. Subramanian, V.; Moume-Pymbock, M.; Hu, T.; Crich, D. *J. Org. Chem.* **2011,** *76,* 3691–3709. doi:10.1021/jo102411j
16. Weissmann, B. *J. Org. Chem.* **1966,** *31,* 2505–2509. doi:10.1021/jo01346a018
17. Bock, K.; Pedersen, C. *J. Chem. Soc., Perkin Trans. 2* **1974,** 293–297. doi:10.1039/P29740000293
18. Yamayaki, T.; Warden, C. H.; Herscovics, A.; Jeanloz, R. W. *Carbohydr. Res.* **1980,** *79,* C9–C12. doi:10.1016/S0008-6215(00)85143-5

License and Terms

Beilstein Journal of Organic Chemistry

Synthesis of fluorinated maltose derivatives for monitoring protein interaction by ^{19}F NMR

Michaela Braitsch[1], Hanspeter Kählig[1], Georg Kontaxis[2], Michael Fischer[1], Toshinari Kawada[3], Robert Konrat[*2] and Walther Schmid[*1]

Full Research Paper

Open Access

Address:
[1]Department of Organic Chemistry, University of Vienna, Währinger Strasse 38, A-1090 Vienna, Austria, [2]Department of Structural and Computational Biology, Max F. Perutz Laboratories, University of Vienna, Campus Vienna Biocenter 5, A-1030 Vienna, Austria and [3]Graduate School of Life and Environmental Sciences, Kyoto Prefectural University, Sakyo-Ku, Kyoto 606-8522, Japan

Email:
Robert Konrat[*] - robert.konrat@univie.ac.at;
Walther Schmid[*] - walther.schmid@univie.ac.at

* Corresponding author

Keywords:
fluorination; ^{19}F NMR; maltose-binding protein (MBP); maltose derivatives; protein interaction

Beilstein J. Org. Chem. **2012,** *8,* 448–455.
doi:10.3762/bjoc.8.51

Received: 16 January 2012
Accepted: 08 March 2012
Published: 27 March 2012

This article is part of the Thematic Series "Synthesis in the glycosciences II".

Guest Editor: T. K. Lindhorst

Abstract

A novel reporter system, which is applicable to the ^{19}F NMR investigation of protein interactions, is presented. This approach uses 2-F-labeled maltose as a spy ligand to indirectly probe protein–ligand or protein–protein interactions of proteins fused or tagged to the maltose-binding protein (MBP). The key feature is the simultaneous NMR observation of both ^{19}F NMR signals of gluco/manno-type-2-F-maltose-isomers; one isomer (α-gluco-type) binds to MBP and senses the protein interaction, and the nonbinding isomers (β-gluco- and/or α/β-manno-type) are utilized as internal references. Moreover, this reporter system was used for relative affinity studies of fluorinated and nonfluorinated carbohydrates to the maltose-binding protein, which were found to be in perfect agreement with published X-ray data. The results of the NMR competition experiments together with the established correlation between ^{19}F chemical shift data and molecular interaction patterns, suggest valuable applications for studies of protein–ligand interaction interfaces.

Introduction

In recent years, we have witnessed significant improvements in NMR spectroscopy, especially as a powerful tool for studying protein–ligand and protein–protein interactions [1,2]. Based on tremendous gains in sensitivity due to high-field spectrometers and cryogenic-probe technology, unprecedented structural and functional information can be obtained on biologically important protein–ligand systems and protein complexes [2]. To overcome the well-known and inherent problem of molecular weight

limitation of current NMR spectroscopy, which renders direct protein observation of the interaction partners infeasible, an indirect observation technique for the detection of protein interactions was recently established [3]. It utilizes the relaxation properties of a small-molecular-weight reporter ligand that reversibly binds to a ligand binding domain, which in turn is fused to the interacting protein of interest. Subsequent protein–protein interaction leads to an additional increase of the molecular weight of the complex and can efficiently be probed by following the NMR relaxation changes of the ligand (e.g., selective T_1 or T_2, which reflect the effective molecular weight). Due to this indirect detection scheme no isotope labeling of the protein interaction partners is required and consumption of protein material is reduced.

The concept presented here relies on the development of an indirect ^{19}F-detected NMR reporter system with possibilities for internal control for the study of protein-binding events. The benefits of fluorine (^{19}F) NMR detection for ligand-based NMR screening applications as well as for ^{19}F magnetic resonance imaging (MRI) have been convincingly demonstrated in the past [4-11]. The usage of the fluorine NMR alleviates most of the problems encountered with ^{1}H observation, such as signal overlap and problems with the dynamic range. Additionally, the ^{19}F nucleus with 100% natural abundance and a magnetogyric ratio comparable to ^{1}H is highly sensitive and, due to its large chemical shift anisotropy (CSA), very responsive to changes of molecular weight that accompany the binding events.

We thus anticipate ^{19}F detection to be a general and versatile probe for indirect NMR studies of protein-binding and interaction events. Biological systems often require sophisticated buffer systems for stabilization and solubility, thus leading to severe spectral overlap and problems with the dynamic range (e.g., intense buffer and solvent peaks). These drawbacks are particularly present in the case of membrane-bound (or attached) proteins, in which additional peaks originate from membrane lipids and raise severe technical problems. However, indirect detection techniques should always be cross-checked with reference experiments and suitable controls, to demonstrate selectivity of binding and to exclude systematic errors (e.g., nonspecific binding or aggregation, and/or viscosity changes due to increased protein concentration). Ideally, the system of choice would thus be a mixture of reporter ligands consisting of one ^{19}F-labeled reporter ligand and another chemically similar (also ^{19}F-labeled) reference compound lacking the affinity to the ligand binding domain.

Here we describe the possibility of monitoring protein interactions by ^{19}F NMR, known as fluorine chemical-shift anisotropy and exchange for screening (FAXS) [5-7], with internal control by using 2-F labeled maltose as a reporter system. The rationale for choosing maltose lies in the fact that maltodextrin/maltose-binding protein (MBP) is a generally applicable protein fusion tag with beneficial solution properties and therefore widely used in molecular biology [12,13].

MBP belongs to the family of periplasmic binding proteins, which are involved in active transport processes of small molecules into gram-negative bacteria through their function as an initial high-affinity binding component; furthermore, these proteins participate as sensors for signaling during chemotaxis [14]. MBP binds maltodextrin and linear oligosaccharides of up to eight α(1→4)-linked glucose (Glc) units with micromolar affinities [15,16]. X-ray structural data (PDB ID codes 1-DMB and 1ANF) demonstrated that the MBP (370 residues, M_r = 41 kDa) consists of two globular domains joined by a hinge-bending region, in which the ligand binding site is located in a cleft between the two domains. MBP exists in two different conformations: The ligand-free "open" form, exposing the binding site, and in the presence of a ligand, the "closed" form, trapping the ligand to provide contacts from both domains [17-19]. The number of protein–sugar hydrogen bonds associated with maltose and MBP is 12, excluding those with water and between glucose units. The reducing glucose unit (g_1) makes about twice as many direct hydrogen bonds with MBP as the nonreducing glucose unit (g_2) does (Figure 1). But there is some evidence for the importance of hydrogen bonds and van der Waals interactions for the oligosaccharide binding as well [20-22].

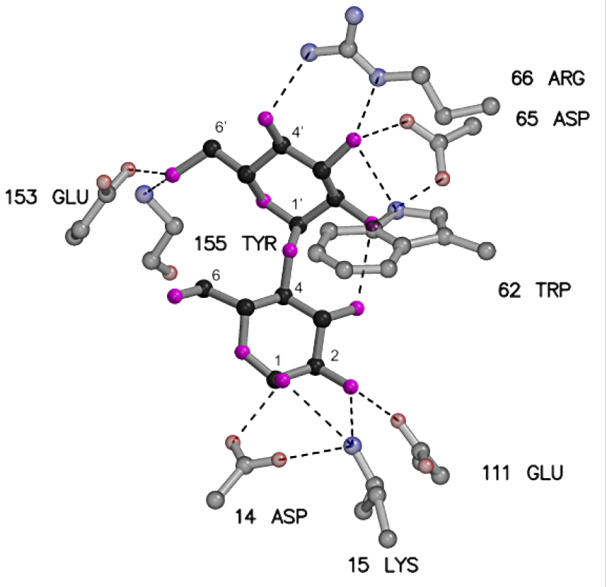

Figure 1: Schematic diagram of the network of hydrogen bonds in the binding pocket of the complex between MBP and maltose (PDB ID code 1ANF); hydrogen bonds are shown as dashed lines.

Specifically, the 2-OH and the 2′-OH moieties are involved in an intricate hydrogen bonding network including the carboxy group of Glu111 and Asp65 and the amino group of Lys15 and Trp62, respectively. We thus decided to synthesize 2-^{19}F-labeled maltose. By replacing the OH group by fluorine and modifying the stereochemistry at position 2, different binding affinities of the anomeric mixture of the two resulting diastereomers were expected (Figure 2). The gluco-type 2-F-maltose, in which the fluorine atom occupies the equatorial position of g_1 of maltose, should display comparable binding affinities to maltose itself, whereas the manno-type 2-F-maltose was expected to lose its affinity due to the axial orientation of the fluorine atom.

This ^{19}F-labeled reporter experiment (FAXS) [5-7] was additionally used to measure the relative binding affinities of various fluorinated and nonfluorinated maltose derivatives to MBP in competitive titration experiments. The incorporation of fluorine in different positions into maltose allows fine tuning of the carbohydrate affinities to the maltose-binding protein.

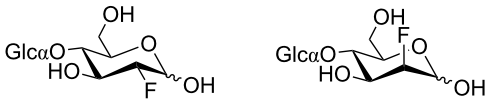

Figure 2: 2-^{19}F-Maltose reporter system: Nonstereoselective fluorine labeling at the 2-position of maltose leads to a 2/1 mixture of two epimeric forms [left: gluco-type; right: manno-type]. Only the gluco-type isomer of 2-deoxy-2-fluoro-maltose retains the affinity to the maltose-binding protein (MBP).

Results and Discussion

Syntheses

The synthesis of the 2-F-maltose reporter system was performed following a modified protocol developed by Dax et al. [23,24]. Starting from maltose (**1**), disaccharide α-bromide **3** was obtained in excellent yield by a standard acetylation procedure and subsequent treatment with hydrobromic acid in glacial acetic acid (Scheme 1) [25]. Treatment of bromide **3** with Zn and *N*-methylimidazole [26] afforded the protected maltal derivative **4**, which was transformed to the target compounds by

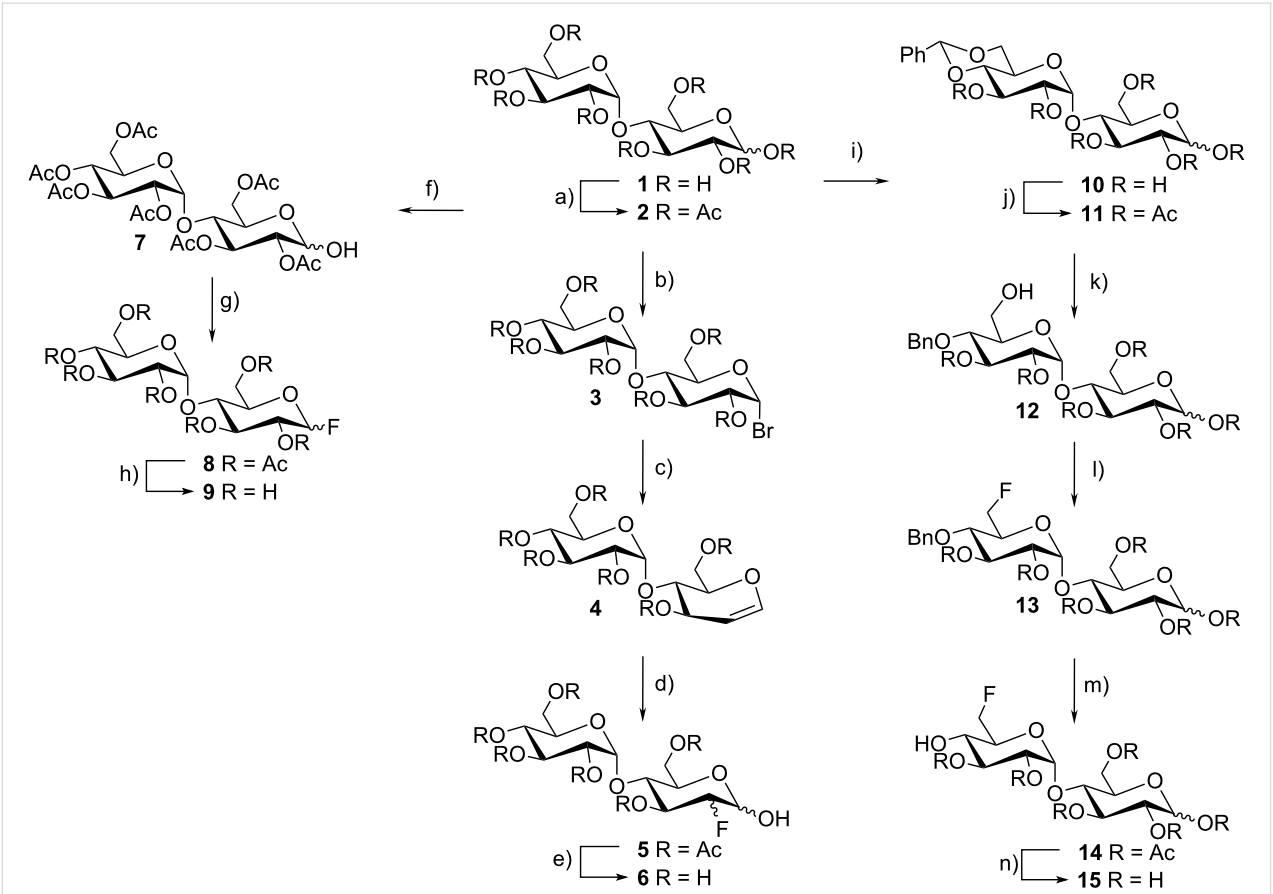

Scheme 1: Syntheses of maltose derivatives; reagents and conditions: (a) Ac_2O, Pyr, 97%; (b) HBr, AcOH, 99%; (c) Zn, *N*-methylimidazole, ethyl acetate, 74%; (d) Selectfluor®, CH_3NO_2, 40%; (e) NaOMe, MeOH, 99%; (f) NH_2NH_2·HOAc, DMF, 94%; (g) DAST, CH_2Cl_2, 89%; (h) NaOMe, MeOH, 99%; (i) α,α-dimethoxytoluene, *p*-TosOH, DMF, 79%; (j) Ac_2O, Pyr, 93%; (k) BH_3·THF, Bu_2BOTf, THF 56%; (l) microwave reaction, DAST, collidine, CH_2Cl_2, 79%; (m) Pd/C, H_2, ethylacetate, 64%; (n) NaOMe, MeOH, 75%.

utilizing Selectfluor® as a fluorinating agent [23,27,28] in a nitromethane solution. The mixture of anomeric 2-fluoro derivatives **5** with gluco- and manno-type stereochemistry was analyzed by ^{19}F NMR, thus showing a gluco (α/β = 1/1) to manno (α/β = 2/1) ratio of 2/1. Final deprotection with sodium methoxide yielded the deprotected fluoro-derivatives **6**.

Maltosyl fluoride **9** was obtained by deprotection of the anomeric acetyl group of compound **2** with hydrazine acetate [29] yielding derivative **7**, followed by nucleophilic fluorination with DAST [30,31] generating the diasteriomeric mixture **8**. The α-anomer was isolated by HPLC and subsequent Zemplén saponification of the remaining acetate protecting groups yielded the α-maltosyl fluoride **9**. However, the β-maltosyl fluoride turned out to be rather unstable. Decomposition of the unprotected fluorinated sugar to maltose and hydrofluoric acid started immediately in D_2O-solution. Therefore only the α-maltosyl fluoride was used for the binding studies. The regioselective reductive ring opening of benzylidene acetals in the maltose derivative **11** was performed with a complex of BH_3/Bu_2BOTf at −70 °C [32,33]. Fluorination with DAST [34,35] was performed in a sealed tube for 1 h at 80 °C under microwave conditions. The deprotection of the benzyl group was achieved with Pd/C [36], followed by a Zemplén saponification to obtain product **15**. Starting from 4′,6′-*O*-benzylidene maltose **10** [37], the primary alcohol was protected as *tert*-butyldimethylsilyl ether followed by standard peracetylation (Scheme 2). Treatment of the silyl protecting group with an excess of Deoxofluor [38] yielded the 6-F-maltose derivatives **18**. Final deprotection with acetic acid [37,39] and sodium methoxide yielded compound **20**.

The synthesis of the galacto-type derivative **23** started from peracetylated benzylidene maltose **11** [37]. Deprotection [37] with acetic acid followed by microwave fluorination with DAST [34,35] yielded a mixture of fluorinated disaccharides: The desired product **22** [39] was isolated by column chromatography and Zemplén deprotection yielded derivative **23**.

Binding studies using the 2-F-maltose reporter system

The binding properties of the two stereoisomers of 2-^{19}F-labeled maltose (gluco- and manno-type) to the maltose-binding protein and a MBP-V53 fusion protein comprising five V3 modules of the LDL receptor in a linear tandem arrangement (V33333) were analyzed. As can be seen in Figure 3 and Figure 4, the stereoisomers of 2-F labeled maltose clearly exhibit different changes in the transverse relaxation rates upon addition of approx. 0.1 equiv of MBP. The significant change in line width was only observed for the interacting α-2-F-maltose. In contrast, the transverse relaxation remained nearly unchanged for the manno-type epimers and the β-gluco-type isomer. This observation corresponds to the anomeric preference described by Gehring et al. [40]. The numeric specifity of MBP with a 2.7-fold higher affinity for α- versus β-maltose was demonstrated by tritium NMR spectroscopy [40-42]. In addition, the β-anomer can be bound in two different modes, probably corresponding to the closed- and open-domain conformations of MBP; but only the α-anomer complex has been observed in X-ray structures of MBP with maltose [21].

Furthermore we used this technique for probing the interactions between 2-F-maltose and the MBP-V53 [43,44] fusion protein,

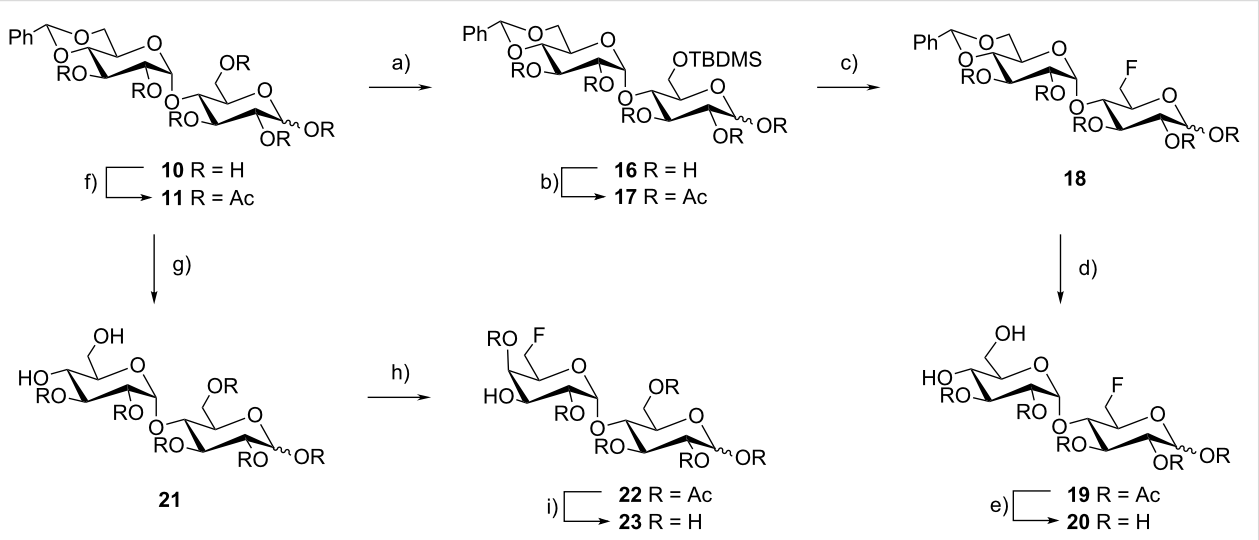

Scheme 2: Synthesis of the maltose- and galacto-type derivatives; reagents and conditions: (a) TBDMS-Cl, imidazole, DMF, 43%; (b) Ac_2O, Pyr, quant.; (c) Deoxofluor, CH_2Cl_2, 17%; (d) conc. AcOH, 73%; (e) NaOMe, MeOH, 40%, (f) Ac_2O, Pyr, 93%; (g) conc. AcOH, 76%; (h) DAST, collidine, CH_2Cl_2, 30%; (i) NaOMe; MeOH, quant.

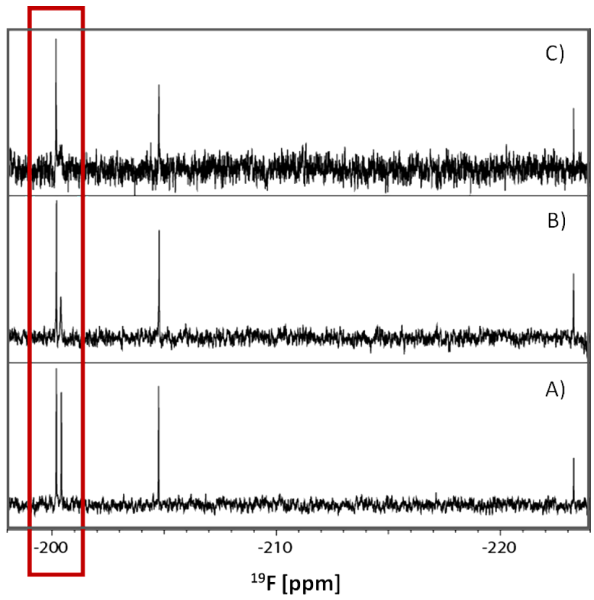

Figure 3: 1-D ^{19}F NMR: Experimental demonstration of differential binding of gluco- and manno-type 2-F-labeled maltose (2 mM) in the free form (A); bound to maltose-binding protein (200 μM) (B); and bound to MBP-V53 fusion protein (200 μM) (C). Highlighted area shows the gluco-type region. Spectra were recorded on a Bruker Avance DRX 600 MHz spectrometer by using a conventional 1-D pulse sequence. Up to 512 scans were acquired without signal suppression via T2 relaxation filter.

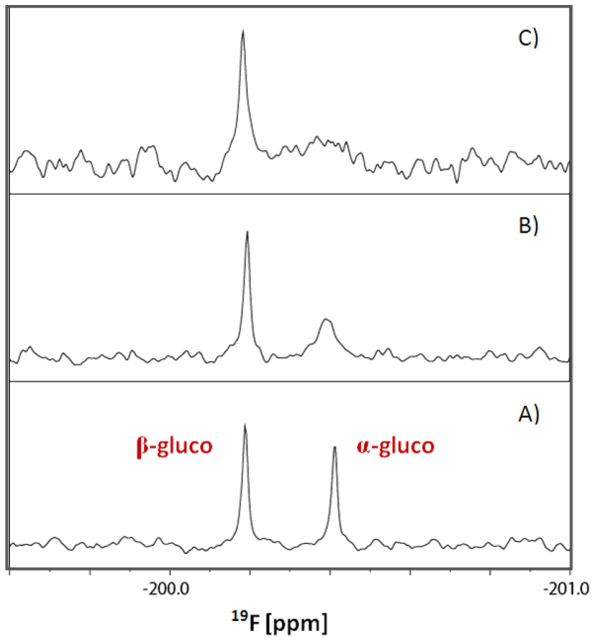

Figure 4: ^{19}F NMR expansion (of Figure 3) of the gluco-type region of the 2-F-maltose reporter system.

which has almost twice the molecular weight of MBP alone. Upon the addition of 0.1 equiv again, the expected increase of the transverse relaxation rate was observed through the specific and significant binding of the α-gluco-type isomer to the MBP-V53 fusion protein. The larger resulting molecular weight is reflected in a further (proportional) increase of the line broadening (Figure 4). In a similar way, noncovalent protein–protein interactions would increase the effective molecular weight by transient binding and result in a consequently increased line width, which can be quantified to derive affinities. This clearly demonstrates both the binding selectivity of the α-gluco-type and the feasibility of the β-gluco-type and manno-type isomers, serving as internal reference compounds to rule out nonspecific binding and interactions (e.g., changes in viscosity). It should be noted that the detection limit of protein binding improves with decreasing ligand concentration, and thus even smaller protein and ligand concentrations can be used in the experiment [45]. Full exploitation of this effect, however, requires high performance ^{19}F NMR probes (e.g., cryoprobes).

Relative affinity studies using the 2-F-maltose reporter system

The 2-F-maltose FAXS reporter system [5-7] was further used for studying the relative binding affinities of natural and artificial maltose derivatives to MBP. The initial experiments were performed with maltose, maltotriose, maltohexose and cellobiose, as well as the artificial α-methyl glucoside. The well-known ability of MBP to bind exclusively to linear maltooligosaccharides or maltodextrins of up to eight α(1→4)-linked glucose units was confirmed by competitive titration and ^{19}F NMR experiments. The displacement of α-gluco-2-F-maltose was already observed by the addition of 0.04 equiv of maltose. Similar results were obtained for the malto-oligosaccharides, maltotriose and maltohexose as well. In contrast, α-methyl glucoside and cellobiose showed no binding. To specify the precise hydroxy groups that are directly involved in hydrogen bonding to MBP, further competition experiments were performed with different fluorinated maltose derivatives. Change, i.e., reduction in the line width of the α-2-F-maltose signal, could be observed if the competitor had a higher affinity than the α-2-F-maltose itself; caused by the release of α-2-F-maltose from the binding pocket of the maltose-binding protein. An overview of the results of the titration experiments is shown in Figure 5. The stepwise addition of equivalent amounts of single fluorinated maltose derivatives to the 2-F-maltose reporter system allows a direct comparison of the relative affinities of the competitors to MBP. The 6-F-maltose is the most efficient competitor with an affinity equal to maltose, α-maltosyl fluoride and 6′-F-maltose. The 6′-F-“galacto”-maltose derivative does not bind to MBP at all.

Note that the competitive binding experiments shown in Figure 5 allow for the direct extraction of dissociation

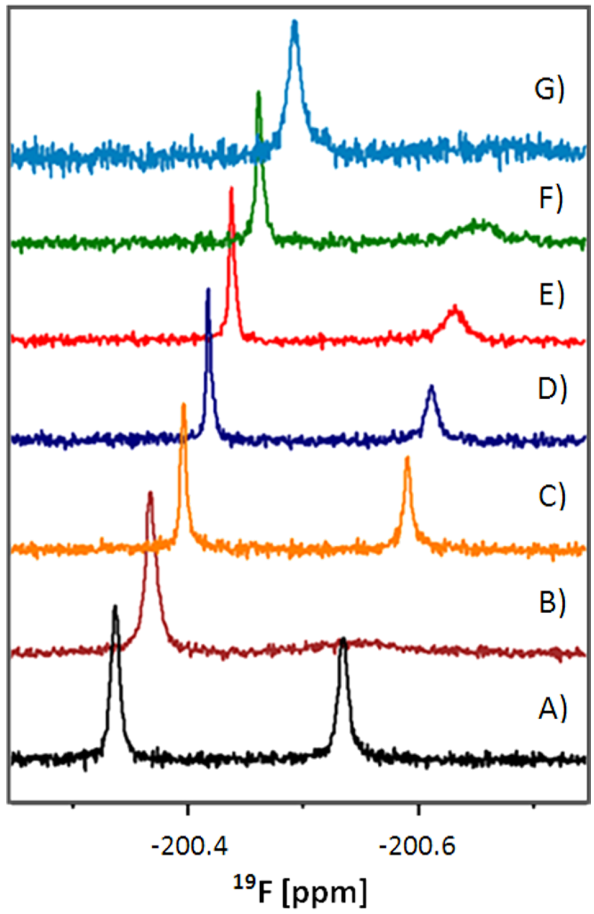

Figure 5: Competitive titration with the 2-F-maltose reporter system and ^{19}F NMR: only the important section of the gluco-type isomers is shown. (A) 2-F-maltose, (B) 2-F-maltose bound to MBP, (C–G) addition of 0.125 equiv of the following maltose derivatives: (C) 6-F-maltose, (D) maltose, (E) α–maltosyl fluoride, (F) 6′-F-maltose, (G) 6′-F-"galacto"-maltose. Spectra were recorded on a Bruker Avance DRX 600 MHz spectrometer by using a conventional 1-D pulse sequence. Up to 128 scans were acquired without signal suppression via T2 relaxation filter.

constants, as was shown by Dalvit and co-workers [46,47]. This would offer additional valuable experimental possibilities for a quantitative analysis of protein–ligand interactions but is beyond the scope of the present paper. Fluorinated substrate analogues perturb the hydrogen bonding network in the substrate binding pocket to a certain extent. Therefore it is not always possible for the ligand to be bound with an optimal hydrogen-bonding geometry. These results are fully consistent with published X-ray data. For instance, in the case of 2-F-maltose, the 2-OH acts simultaneously as a hydrogen-bond acceptor for the Nε of Lys15 and as a bond donor to the carboxylate of Glu111, and the 2-F fluorine can only be a (limited) acceptor, thus leaving some of the H-bonds "frustrated". It is worth comparing these findings with recently reported correlations between ^{19}F chemical shifts and fluorine–protein interaction patterns [48,49]. Shielded fluorine atoms, due to their increased electron density, are preferentially involved in direct hydrogen-bonding interactions with donor groups of the protein. Although the 2-F fluorine is significantly shielded (about −200 ppm), and thus an ideal hydrogen-bond acceptor binding of 2-F-maltose is impaired due to the hydrogen-bond donor activity of the 2-OH group (to the carboxylate of Glu111). In that respect, introducing the fluorine into the 6-position results in a smaller energetic penalty (compared to the 2-F-maltose), because no direct H-bonds between the ligand and MBP are involved, and only indirect water-mediated interactions are concerned (data not shown). Therefore the affinity is higher in that case. Similar arguments apply in the other cases. It is, however, possible to "fine tune" the affinity between the ligand binding domain and the reporter ligand by using differently fluorinated maltose derivatives in which different hydroxy groups are substituted by fluorine. Thus the affinity of the reporter ligand can be "customized" for ligand competition assays or for specific studies of protein–ligand and protein–protein interactions to match the affinities between the interaction partners. For example, small affinities or proteins with a relatively low molecular weight are more easily detected with high-affinity ligands, whereas strongly interacting proteins or high-molecular-weight protein ligands can be better studied with low-affinity ligands.

Conclusion

We have demonstrated that 2-deoxy-2-F-maltose can be effectively used as a reporter system to study protein-binding interactions by ^{19}F NMR. The particular benefit of this novel reporter system is the simultaneous accessibility of reference molecules (nonbinding manno-type and β-gluco-type 2-F-maltose isomers), which serve as internal standards, to rule out nonspecific binding and interactions, and thus increasing the reliability of this method. The 2-F-maltose reporter system was used to study the ligand binding affinity to MBP. "Fine tuning" by the regioselective fluorination of single hydroxy groups of maltose was used to define the important hydroxy groups that are responsible for the hydrogen bonding network and therefore for binding to the protein. The results of the competitive titration are in perfect agreement with the X-ray data published [21] previously. Additionally, the different binding affinities of selectively ^{19}F-labeled maltose derivatives to MBP illustrate how the recently established correlation between ^{19}F chemical shift data and molecular interaction patterns [48,49] can be used to delineate details of protein–ligand interaction interfaces. Together with efficient synthetic approaches to fluorinated derivatives, this offers exciting perspectives for rational programs for drug design. Experiments to explore these possibilities are currently underway in our laboratories. Applications of the reporter system to biological material inherently giving

strong background signals (e.g., membrane-bound protein receptors) should be straightforward, having the advantage that ^{19}F signals can be detected with high sensitivity and without any background, and should broaden the applicability of this approach.

Supporting Information

Supporting Information File 1

Detailed experimental procedures and spectral data of compounds **2**–**4**, **6**, **7**, **9**, **11**–**15**, **17**, **18**, **20**–**23**.
[http://www.beilstein-journals.org/bjoc/content/supplementary/1860-5397-8-51-S1.pdf]

Acknowledgements

The MBP and MBP-V53 fusion protein samples were provided by J. Wruss and D. Blaas of the Department of Medical Biochemistry of the Medical University of Vienna. Financial support by the Wiener Wissenschafts-, Forschungs- und Technologiefond (WWTF), project LS162 is gratefully acknowledged.

References

1. Bonvin, A. M. J. J.; Boelens, R.; Kaptein, R. *Curr. Opin. Chem. Biol.* **2005,** *9,* 501–508. doi:10.1016/j.cbpa.2005.08.011
2. Zuiderweg, E. R. P. *Biochemistry* **2002,** *41,* 1–7. doi:10.1021/bi011870b
3. Ludwiczek, M. L.; Baminger, B.; Konrat, R. *J. Am. Chem. Soc.* **2004,** *126,* 1636–1637. doi:10.1021/ja039149b
4. Tengel, T.; Fex, T.; Emtenäs, H.; Almqvist, F.; Sethson, I.; Kihlberg, J. *Org. Biomol. Chem.* **2004,** *2,* 725–731. doi:10.1039/B313166A
5. Dalvit, C.; Flocco, M.; Veronesi, M.; Stockman, B. J. *Comb. Chem. High Throughput Screening* **2002,** *5,* 645–650.
6. Dalvit, C.; Fagerness, P. E.; Hadden, D. T. A.; Sarver, R. W.; Stockman, B. J. *J. Am. Chem. Soc.* **2003,** *125,* 7696–7703. doi:10.1021/ja034646d
7. Dalvit, C. *Concepts Magn. Reson., Part A* **2008,** *32A,* 341–372. doi:10.1002/cmr.a.20121
8. Mizukami, S.; Takikawa, R.; Sugihara, F.; Hori, Y.; Tochio, H.; Wälchli, M.; Shirakawa, M.; Kikuchi, K. *J. Am. Chem. Soc.* **2008,** *130,* 794–795. doi:10.1021/ja077058z
9. Jackson, J. C.; Hammill, J. T.; Mehl, R. A. *J. Am. Chem. Soc.* **2007,** *129,* 1160–1166. doi:10.1021/ja064661t
10. Kreutz, C.; Kählig, H.; Konrat, R.; Micura, R. *J. Am. Chem. Soc.* **2005,** *127,* 11558–11559. doi:10.1021/ja052844u
11. Cobb, S. L.; Murphy, C. D. *J. Fluorine Chem.* **2009,** *130,* 132–143. doi:10.1016/j.jfluchem.2008.11.003
12. Terpe, K. *Appl. Microbiol. Biotechnol.* **2003,** *60,* 523–533. doi:10.1007/s00253-002-1158-6
And references cited therein.
13. Medintz, I. L.; Deschamps, J. R. *Curr. Opin. Biotechnol.* **2006,** *17,* 17–27. doi:10.1016/j.copbio.2006.01.002
14. Quiocho, F. A.; Ledvina, P. S. *Mol. Microbiol.* **1996,** *20,* 17–25. doi:10.1111/j.1365-2958.1996.tb02484.x
15. Kellermann, O.; Szmelcman, S. *Eur. J. Biochem.* **1974,** *47,* 139–149. doi:10.1111/j.1432-1033.1974.tb03677.x
16. Miller, D. M., III; Olson, J. S.; Pflugrath, J. W.; Quiocho, F. A. *J. Biol. Chem.* **1983,** *258,* 13665–13672.
17. Wemmer, D. E. *Proc. Natl. Acad. Sci. U. S. A.* **2003,** *100,* 12529–12530. doi:10.1073/pnas.2335923100
18. Shilton, B. H.; Shuman, H. A.; Mowbray, S. L. *J. Mol. Biol.* **1996,** *264,* 364–376. doi:10.1006/jmbi.1996.0646
19. Tang, C.; Schwieters, C. D.; Clore, G. M. *Nature* **2007,** *449,* 1078–1082. doi:10.1038/nature06232
20. Spurlino, J. C.; Lu, G. Y.; Quiocho, F. A. *J. Biol. Chem.* **1991,** *266,* 5202–5219.
21. Quiocho, F. A.; Spurlino, J. C.; Rodseth, L. E. *Structure* **1997,** *5,* 997–1015. doi:10.1016/S0969-2126(97)00253-0
22. Evenäs, J.; Tugarinov, V.; Skrynnikov, N. R.; Goto, N. K.; Muhandiram, R.; Kay, L. E. *J. Mol. Biol.* **2001,** *309,* 961–974. doi:10.1006/jmbi.2001.4695
23. Dax, K.; Albert, M.; Ortner, J.; Paul, B. J. *Carbohydr. Res.* **2000,** *327,* 47–86. doi:10.1016/S0008-6215(00)00022-7
24. Braitsch, M.; Fischer, M.; Hollaus, R.; Lentsch, C.; Lichtenecker, R.; Nagl, M.; Nowikow, C.; Schmoelzer, C.; Schmid, W. Synthetic Tools for Addressing Biological and Medicinal Chemical Questions. In *Joint Meeting on Medical Chemistry,* June 24–27, 2009; Budapest, Hungary; pp 21–26.
25. Hehre, E. J.; Brewer, C. F.; Genghof, D. S. *J. Biol. Chem.* **1979,** *254,* 5942–5950.
26. Broddefalk, J.; Nilsson, U.; Kihlberg, J. *J. Carbohydr. Chem.* **1994,** *13,* 129–132. doi:10.1080/07328309408009183
27. Ortner, J.; Albert, M.; Weber, H.; Dax, K. *J. Carbohydr. Chem.* **1999,** *18,* 297–316. doi:10.1080/07328309908543997
28. Nyffeler, P. T.; Gonzales Durón, S.; Burkart, M. D.; Vincent, S. P.; Wong, C.-H. *Angew. Chem., Int. Ed.* **2005,** *44,* 192–212. doi:10.1002/anie.200400648
29. Excoffier, G.; Gagnaire, D.; Utille, J.-P. *Carbohydr. Res.* **1975,** *39,* 368–373. doi:10.1016/S0008-6215(00)86150-9
30. Toshima, K. *Carbohydr. Res.* **2000,** *327,* 15–26. doi:10.1016/S0008-6215(99)00325-0
31. Lal, G. S.; Pez, G. P.; Pesaresi, R. J.; Prozonic, F. M.; Cheng, H. *J. Org. Chem.* **1999,** *64,* 7048–7054. doi:10.1021/jo990566+
32. Jiang, L.; Chan, T.-H. *Tetrahedron Lett.* **1998,** *39,* 355–358. doi:10.1016/S0040-4039(97)10599-8
33. Hernández-Torres, J. M.; Achkar, J.; Wei, A. *J. Org. Chem.* **2004,** *69,* 7206–7211. doi:10.1021/jo048999m
34. Withers, S. G.; MacLennan, D. J.; Street, I. P. *Carbohydr. Res.* **1986,** *154,* 127–144. doi:10.1016/S0008-6215(00)90028-4
35. Mersch, C.; Wagner, S.; Hoffmann-Röder, A. *Synlett* **2009,** 2167–2171. doi:10.1055/s-0029-1217566
36. Chong, J. M.; Sokoll, K. K. *Org. Prep. Proced. Int.* **1993,** *25,* 639–647. doi:10.1080/00304949309356259
37. Takeo, K.; Shinmitsu, K. *Carbohydr. Res.* **1984,** *133,* 135–145. doi:10.1016/0008-6215(84)85189-7
38. Ye, S.; Rezende, M. M.; Deng, W.-P.; Herbert, B.; Daly, J. W.; Johnson, R. A.; Kirk, K. L. *J. Med. Chem.* **2004,** *47,* 1207–1213. doi:10.1021/jm0303599
39. Best, W. M.; Stick, R. V.; Tilbrook, D. M. G. *Aust. J. Chem.* **1997,** *50,* 13–18. doi:10.1071/C96078
40. Gehring, K.; Williams, P. G.; Pelton, J. G.; Morimoto, H.; Wemmer, D. E. *Biochemistry* **1991,** *30,* 5524–5531. doi:10.1021/bi00236a027

41. Duan, X.; Hall, J. A.; Nikaido, H.; Quiocho, F. A. *J. Mol. Biol.* **2001,** *306,* 1115–1126. doi:10.1006/jmbi.2001.4456
42. Gehring, K.; Zhang, X.; Hall, J.; Nikaido, H.; Wemmer, D. E. *Biochem. Cell Biol.* **1998,** *76,* 189–197. doi:10.1139/o98-060
43. Moser, R.; Snyers, L.; Wruss, J.; Angulo, J.; Peters, H.; Peters, T.; Blaas, D. *Virology* **2005,** *338,* 259–269. doi:10.1016/j.virol.2005.05.016
44. Nicodemou, A.; Petsch, M.; Konecsni, T.; Kremser, L.; Kenndler, E.; Casasnovas, J. M.; Blaas, D. *FEBS Lett.* **2005,** *579,* 5507–5511. doi:10.1016/j.febslet.2005.09.013
45. Vulpetti, A.; Hommel, U.; Landrum, G.; Lewis, R.; Dalvit, C. *J. Am. Chem. Soc.* **2009,** *131,* 12949–12959. doi:10.1021/ja905207t
46. Dalvit, C.; Gossert, A. D.; Coutant, J.; Piotto, M. *Magn. Reson. Chem.* **2011,** *49,* 199–202. doi:10.1002/mrc.2733
47. Dalvit, C.; Fasolini, M.; Flocco, M.; Knapp, S.; Pevarello, P.; Veronesi, M. *J. Med. Chem.* **2002,** *45,* 2610–2614. doi:10.1021/jm011122k
48. Dalvit, C.; Vulpetti, A. *ChemMedChem* **2011,** *6,* 104–114. doi:10.1002/cmdc.201000412
49. Dalvit, C.; Vulpetti, A. *ChemMedChem* **2012,** *7,* 262–272. doi:10.1002/cmdc.201100483

License and Terms

Beilstein Journal of Organic Chemistry

Electrochemical generation of 2,3-oxazolidinone glycosyl triflates as an intermediate for stereoselective glycosylation

Toshiki Nokami[1], Akito Shibuya[1], Yoshihiro Saigusa[1], Shino Manabe[*2], Yukishige Ito[2,3] and Jun-ichi Yoshida[*1]

Letter

Open Access

Address:
[1]Department of Synthetic Chemistry and Biological Chemistry, Kyoto University, Nishikyo-ku Kyoto 615-8510 Japan, [2]Advanced Science Institute, RIKEN, Hirosawa, Wako, Saitama 351-0198, Japan and [3]ERATO JST, Hirosawa, Wako, Saitama 351-0198, Japan

Email:
Shino Manabe[*] - smanabe@riken.jp; Jun-ichi Yoshida[*] - yoshida@sbchem.kyoto-u.ac.jp

* Corresponding author

Keywords:
amino sugar; anomerization; electrochemical oxidation; glycosylation; thioglycoside

Beilstein J. Org. Chem. **2012,** *8,* 456–460.
doi:10.3762/bjoc.8.52

Received: 11 January 2012
Accepted: 06 March 2012
Published: 28 March 2012

This article is part of the Thematic Series "Synthesis in the glycosciences II".

Guest Editor: T. K. Lindhorst

Abstract

Glycosyl triflates with a 2,3-oxazolidinone protecting group were generated from thioglycosides by low-temperature electrochemical oxidation. The glycosyl triflates reacted with alcohols to give the corresponding glycosides β-selectively at low temperatures. However, α-selectivity was observed in the absence of base at elevated reaction temperatures. In situ generated triflic acid promotes the isomerization of β-products to α-products.

Introduction

Stereoselective formation of glycosidic linkages is the key issue in oligosaccharide synthesis, because both 1,2-*trans* and 1,2-*cis* aminoglycosides are ubiquitous in biologically active oligosaccharides [1-5]. The 1,2-*trans* aminoglycosides, which are found in Nod factor [1] and lipid A [2], can be easily prepared by protecting the 2-amino group with phthaloyl or carbamate groups [6]. On the other hand, 1,2-*cis* glycosidic linkages are still difficult to make with perfect stereoselectivity. Although 2-azido-substituted glycosyl donors are commonly used for the preparation of 1,2-*cis* glycosidic linkages of amino sugars [7,8], the selectivity highly depends on the nature of the glycosyl acceptors and reaction conditions. In the last decade, 2,3-oxazolidinone protected 2-amino-2-deoxy-glycosides have been developed as glycosyl donors for the stereoselective synthesis of amino sugars [9-24]. These glycosyl donors afford the corresponding glycosides in a 1,2-*trans* or 1,2-*cis* selective manner by action with various types of glycosyl acceptors. However, it is still uncertain whether glycosyl triflate intermediates [25], which were detected by NMR, play an important role in the stereoselective formation of both α- and β-isomers.

We have developed an electrochemical method to generate and accumulate highly reactive glycosyl triflates by low-temperature electrochemical oxidation of thioglycosides [26-30]. Although Kerns and Ye have already reported a chemically generated glycosyl triflate equipped with an acetylated 2,3-oxazolidinone protecting group [11,19], we envisioned that the electrochemically generated glycosyl triflate with a 2,3-oxazolidinone protecting group could be a useful intermediate to reveal stereoselectivity in glycosylations via glycosyl triflate intermediates. In this paper, we report the generation, accumulation, and characterization by low-temperature NMR analyses, of the corresponding glycosyl triflates. Electrochemical glycosylation of the thioglycoside donor with 2,3-oxazolidinone protecting group gave both 1,2-*trans* linkages in the presence of a base at low temperatures and 1,2-*cis* glycosidic linkages in the absence of a base at elevated temperatures.

Results and Discussion

We began by conducting the electrochemical oxidation of 2,3-oxazolidinone thioglycosides **1a**–**1c** in the absence of a glycosyl acceptor at low temperatures in order to generate and accumulate the corresponding glycosyl triflates (Scheme 1). Low-temperature NMR measurements of the anodic solution were carried out to confirm the structure of the glycosyl triflates. For example, the anodic solution obtained by the electrochemical oxidation of thioglycoside **1a** (4 mA, 1 h) exhibited a single set of peaks for glycosyl triflate **2a** in the ^{1}H NMR spectrum at −80 °C (Figure 1). In contrast to the previous reports by Kerns and Ye, the corresponding β-triflate was not observed under these conditions [11,19]. The small coupling constant of the anomeric proton (J = 2.1 Hz) indicates α-configuration of the anomeric triflate. The ^{1}H and ^{13}C NMR chemical shifts of the anomeric protons and carbons of glycosyl triflates **2a**–**c** are listed in Table 1. In all cases, the starting thioglycosides **1a**–**c** were quantitatively converted to the corresponding glycosyl triflates **2a**–**c,** which have α-configuration of the anomeric triflate. Although the chemical shift of the anomeric proton H-1 of glycosyl triflate **2a** appears at a lower chemical shift (6.89 ppm) than those of glycosyl triflates **2b** (5.97 ppm) and **2c** (5.95 ppm), the chemical shift of the anomeric carbon is around 100 ppm in all cases and the corresponding cross peaks of the anomeric protons and carbons were observed in HMQC spectra.

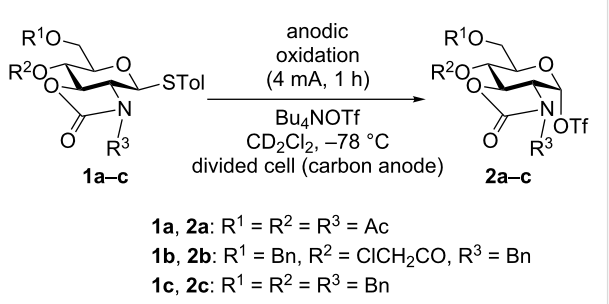

Scheme 1: Electrochemical conversion of thioglycosides to glycosyl triflates.

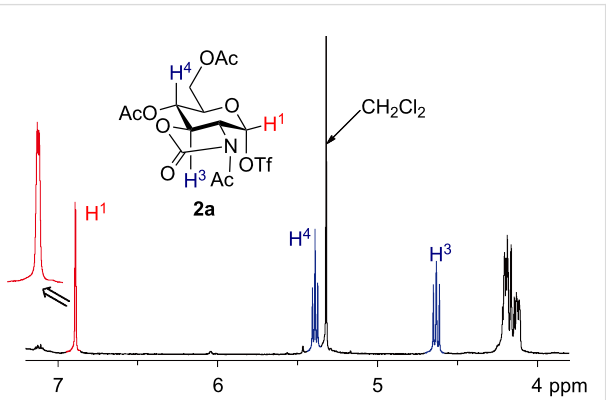

Figure 1: ^{1}H NMR spectrum of glycosyl triflate **2a**.

Table 1: ^{1}H- and ^{13}C NMR chemical shifts of the anomeric proton and carbon of glycosyl triflates **2a**–**c**.

entry	glycosyl triflate	^{1}H NMR [δ (ppm)[a], J (Hz)[b]]	^{13}C NMR [δ (ppm)[a]]
1	**2a**	6.89, 2.1[c]	99.9
2	**2b**	5.97, singlet	99.9
3	**2c**	5.95, singlet	100.7

[a]chemical shift; [b]coupling constant; [c]doublet.

Using electrochemically generated glycosyl triflate **2a**, the stereoselectivity of the glycosylation was investigated by the addition of five equiv of various alcohols (Table 2). In accordance with our previous results [26,29], high β-selectvity was observed with highly reactive alcohols (Table 2, entries 1 and 2). On the other hand, less nucleophilic alcohols, such as benzyl alcohol and CF_3CH_2OH, gave the corresponding glycosides in lower β-selectivity than methanol or ethanol (Table 2, entries 3 and 4) [31].

Next, we examined the electrochemical activation of thioglycoside **1a** to generate glycosyl triflate **2a** in the presence of glycosyl acceptor **7**. In order to improve the yield and the stereoselectivity of glycosylation, we examined the effects of the reaction temperature and base (Table 3). Although poor β-selectivity and yield were observed at low temperatures in the absence of a base (Table 3, entry 1), the addition of an organic base such as 2,6-di-*tert*-butyl-4-methylpyridine (DTBMP), significantly improved the β-selectivity and yield (Table 3, entry 2). In both cases small amounts of the α-isomers of the

Table 2: Glycosylation of electrochemically generated glycosyl triflate **2a**.

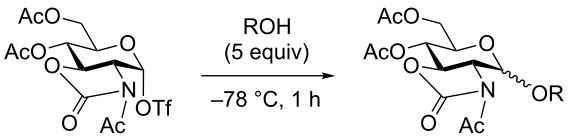

2a **3–6**

entry	ROH	product: yield[a], ratio (α to β)[b]
1	MeOH	**3**: 76% (<1 to >99)
2	EtOH	**4**: 71% (<1 to >99)
3	BnOH	**5**: 89% (9 to 91)
4	CF_3CH_2OH	**6**: 82% (15 to 85)

[a]isolated yields; [b]determined by ^{1}H NMR.

starting thioglycoside **9** and glucal **10** were obtained as byproducts (Table 3, entries 1 and 2). The yield was further increased and the formation of byproducts was suppressed by raising the reaction temperature to 0 °C (Table 3, entry 3). On the other hand, the corresponding α-isomer of disaccharide **8α** was obtained as a major product together with the anomerized donor **9** when the reaction was performed at 0 °C in the absence of DTBMP (Table 3, entry 4). These anomerizations may be caused by the endocyclic cleavage reaction [22-24], which is often observed for pyranosides with a 2,3-*trans* carbamate group, under acidic conditions. The yield of disaccharide **8** was improved by raising the temperature to 0 °C after the completion of electrolysis at −78 °C (Table 3, entry 5). The fact that disaccharide **8** was obtained in higher yields (59% to 78%) and that only a trace amount of α-isomer **9** (4%) was obtained strongly suggests that the isomerization of thioglycoside donor **1a** occurs during the electrolysis at 0 °C. It is noteworthy that the α- and β-glycosides could be selectively prepared from the same glycosyl donor with a 2,3-*trans* carbamate group, simply by changing the reaction conditions.

In order to confirm that the anomerization of **8β** to **8α** could take place under the reaction conditions, we examined the acid-mediated isomerization of the β-isomer of disaccharide **8β** to the α-isomer **8α** (Scheme 2). Triflic acid (TfOH) must be generated in situ by the reaction of glycosyl triflate **2a** with alcohols. Thus, TfOH (1.0 equiv) and tetrabutylammonium triflate (Bu_4NOTf) (5.0 equiv), which was used as a supporting electrolyte for electrolysis, were added to a CH_2Cl_2 solution of the β-isomer of disaccharide **8β** at 0 °C. After stirring at 0 °C for 1 h, the reaction was quenched by the addition of Et_3N. The α-isomer of the disaccharide **8α** was obtained in 83% yield as a single isomer. This experiment shows that the α-product **8α** is the isomerization product of the β-isomer **8β** as a result of endocyclic cleavage, as shown in Scheme 2.

Table 3: Electrochemical glycosylation in the presence of glycosyl acceptor.

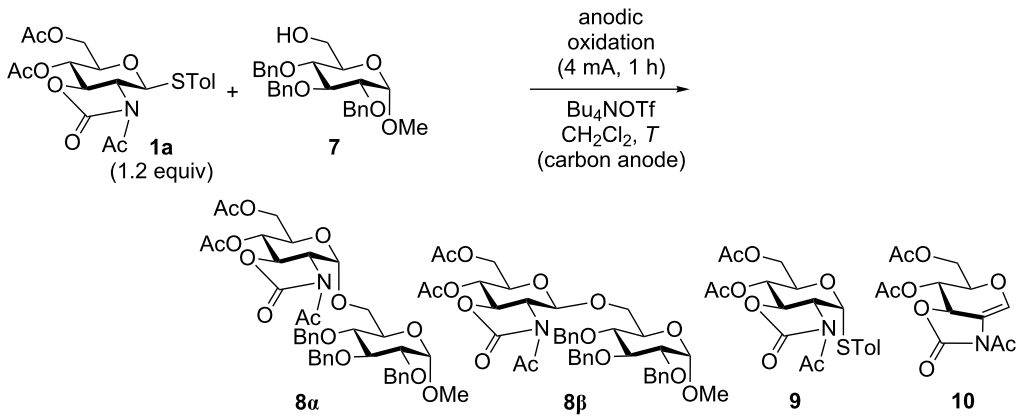

entry	*T*	base	product: yield, ratio (**8α** to **8β**)[a]		
1	−78 °C	–	**8**[b]: 36% (46 to 54)	**9**: <3%[c]	**10**: 34%[c]
2	−78 °C	DTBMP[d]	**8**: 60% (4 to 96)	**9**: <3%[c]	**10**: 24%[c]
3	0 °C	DTBMP[d]	**8**: 79% (3 to 97)	**9**: trace	**10**: trace
4	0 °C	–	**8**: 59% (α only)	**9**: 29%[c]	**10**: 2%[c]
5	−78 °C then 0 °C[e]	–	**8**: 78% (α only)[f]	**9**: 4%[c]	**10**: 8%[c]

[a]determined by ^{1}H NMR; [b]**1a** (ca 15%) was recovered; [c]yields are based on **1a**; [d]5.0 equiv; [e]the reaction temperature was raised after electrolysis; [f]**1a** (ca 6%) was recovered.

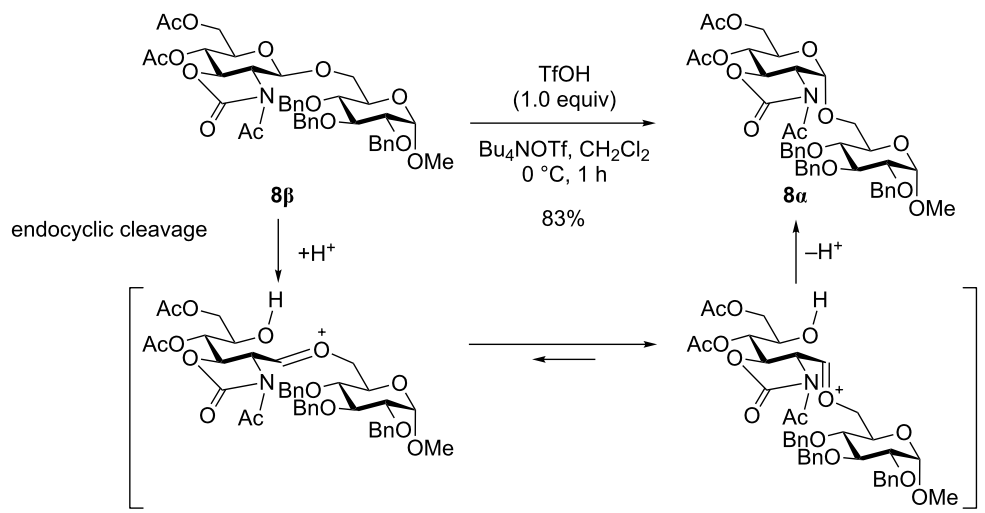

Scheme 2: Triflic acid mediated isomerization of β-glycoside.

Conclusion

In conclusion, we have achieved the electrochemical generation and accumulation of glycosyl triflates equipped with the 2,3-oxazolidinone protecting group. This glycosyl triflate intermediate reacted with alcohols of high reactivity to afford β-glycosides as kinetic products. The α-products were also obtained at elevated temperatures after anomerization of the β-products, as both Oscarson and our group have previously reported [18,22-24]. Namely, α- and β-glycosides were obtained from 2,3-oxazolidinone donors by changing the reaction conditions. Further investigations to reveal the scope and limitations of the glycosylation reaction using electrochemically generated glycosyl triflates are in progress in our laboratory.

Supporting Information

Supporting Information File 1

Experimental procedures, spectral data of glycosyl triflates and new compounds, and ^{1}H- and ^{13}C NMR spectra.
[http://www.beilstein-journals.org/bjoc/content/supplementary/1860-5397-8-52-S1.pdf]

Acknowledgements

This work was financially supported in part by the Grants-in-Aid for Scientific Research on Innovative Areas (No. 2015) from the MEXT. S. M. thanks Grants-in-Aid for Scientific Research (C) from JSPS (grant number 21590036) and Ms. Akemi Takahashi for her technical assistance. T. N. thanks Meiji Seika Kaisha, Ltd. Award in Synthetic Organic Chemistry. The authors thank Dr. Keiko Kuwata and Ms. Sakiko Goto for MS analyses.

References

1. Long, S. R. *Plant Cell* **1996,** *8,* 1885–1898. doi:10.1105/tpc.8.10.1885
2. Raetz, C. R. H.; Whitfield, C. *Annu. Rev. Biochem.* **2002,** *71,* 635–700. doi:10.1146/annurev.biochem.71.110601.135414
3. Werz, D. B.; Ranzinger, R.; Herget, S.; Adibekian, A.; von der Lieth, C.-W.; Seeberger, P. H. *ACS Chem. Biol.* **2007,** *2,* 685–691. doi:10.1021/cb700178s
4. Hu, Y.-P.; Lin, S.-Y.; Huang, C.-Y.; Zulueta, M. M. L.; Liu, J.-Y.; Chang, W.; Hung, S.-C. *Nat. Chem.* **2011,** *3,* 557–563. doi:10.1038/nchem.1073
5. Petitou, M.; von Boeckel, C. A. A. *Angew. Chem., Int. Ed.* **2004,** *43,* 3118–3133. doi:10.1002/anie.200300640
6. Banoub, J.; Baullanger, P.; Lafont, D. *Chem. Rev.* **1992,** *92,* 1167–1195. doi:10.1021/cr00014a002
7. Paulsen, H.; Kolář, Č.; Stenzel, W. *Chem. Ber.* **1978,** *111,* 2358–2369. doi:10.1002/cber.19781110630
8. Lemieux, R. U.; Ratcliffe, R. M. *Can. J. Chem.* **1979,** *57,* 1244–1251. doi:10.1139/v79-203
9. Benakli, K.; Zha, C.; Kerns, R. J. *J. Am. Chem. Soc.* **2001,** *123,* 9461–9462. doi:10.1021/ja0162109
10. Kerns, R. J.; Zha, C.; Benakli, K.; Liang, Y.-Z. *Tetrahedron Lett.* **2003,** *44,* 8069–8072. doi:10.1016/j.tetlet.2003.09.058
11. Wei, P.; Kerns, R. J. *J. Org. Chem.* **2005,** *70,* 4195–4198. doi:10.1021/jo047812o
12. Boysen, M.; Gemma, E.; Lahmann, M.; Oscarson, S. *Chem. Commun.* **2005,** 3044–3046. doi:10.1039/b503651h
13. Manabe, S.; Ishii, K.; Ito, Y. *J. Am. Chem. Soc.* **2006,** *128,* 10666–10667. doi:10.1021/ja062531e
14. Manabe, S.; Ishii, K.; Ito, Y. *J. Org. Chem.* **2007,** *72,* 6107–6115. doi:10.1021/jo070669p
15. Geng, Y.; Zhang, L.-H.; Ye, X.-S. *Chem. Commun.* **2008,** 597–599. doi:10.1039/b712591g
16. Geng, Y.; Zhang, L.-H.; Ye, X.-S. *Tetrahedron* **2008,** *64,* 4949–4958. doi:10.1016/j.tet.2008.03.103
17. Manabe, S.; Ishii, K.; Ito, Y. *Trends Glycosci. Glycotech.* **2008,** *20,* 187–202. doi:10.4052/tigg.20.187

18. Olsson, J. D. M.; Eriksson, L.; Lahmann, M.; Oscarson, S. *J. Org. Chem.* **2008,** *73,* 7181–7188. doi:10.1021/jo800971s
19. Geng, Y.; Ye, X.-S. *Synlett* **2010,** 2506–2512. doi:10.1055/s-0030-1258557
20. Manabe, S.; Ishii, K.; Ito, Y. *Eur. J. Org. Chem.* **2011,** 497–516. doi:10.1002/ejoc.201001278
21. Manabe, S.; Aihara, Y.; Ito, Y. *Chem. Commun.* **2011,** *47,* 9720–9722. doi:10.1039/c1cc13172a
22. Manabe, S.; Ishii, K.; Hashizume, D.; Koshino, H.; Ito, Y. *Chem.–Eur. J.* **2009,** *15,* 6894–6901. doi:10.1002/chem.200900064
23. Manabe, S.; Ito, Y. *Tetrahedron Lett.* **2009,** *50,* 4827–4829. doi:10.1016/j.tetlet.2009.05.119
24. Satoh, H.; Manabe, S.; Ito, Y.; Lüthi, H. P.; Laino, T.; Hutter, J. *J. Am. Chem. Soc.* **2011,** *133,* 5610–5619. doi:10.1021/ja201024a
25. Crich, D. *J. Org. Chem.* **2011,** *76,* 9193–9209. doi:10.1021/jo2017026
26. Nokami, T.; Shibuya, A.; Tsuyama, H.; Suga, S.; Bowers, A. A.; Crich, D.; Yoshida, J.-i. *J. Am. Chem. Soc.* **2007,** *129,* 10922–10928. doi:10.1021/ja072440x
27. Nokami, T.; Shibuya, A.; Yoshida, J.-i. *Trends Glycosci. Glycotech.* **2008,** *20,* 175–185. doi:10.4052/tigg.20.175
28. Nokami, T.; Tsuyama, H.; Shibuya, A.; Nakatsutsumi, T.; Yoshida, J.-i. *Chem. Lett.* **2008,** *37,* 942–943. doi:10.1246/cl.2008.942
29. Nokami, T.; Shibuya, A.; Manabe, S.; Ito, Y.; Yoshida, J.-i. *Chem.–Eur. J.* **2009,** *15,* 2252–2255. doi:10.1002/chem.200802293
30. Nokami, T.; Nozaki, Y.; Saigusa, Y.; Shibuya, A.; Manabe, S.; Ito, Y.; Yoshida, J.-i. *Org. Lett.* **2011,** *13,* 1544–1547. doi:10.1021/ol200242u
31. The observed stereoselectivity was determined kinetically; however, the possibility of the isomerization of the β-isomer to the thermodynamically more stable α-isomer cannot be excluded.

Beilstein Journal of Organic Chemistry

Synthesis and biological evaluation of nojirimycin- and pyrrolidine-based trehalase inhibitors

Davide Bini[1], Francesca Cardona[2], Matilde Forcella[1], Camilla Parmeggiani[2,3], Paolo Parenti[4], Francesco Nicotra[1] and Laura Cipolla[*1]

Full Research Paper

Open Access

Address:
[1]Department of Biotechnology and Biosciences, University of Milano-Bicocca, Piazza della Scienza 2, 20126 Milano, Italy, [2]Department of Chemistry "Ugo Schiff", University of Florence, Polo Scientifico e Tecnologico, Via della Lastruccia 3–13, 50019 Sesto Fiorentino, Florence, Italy, [3]CNR-INO U. O. S. Sesto Fiorentino c/o LENS, Via Nello Carrara 1, 50019 Sesto Fiorentino, Florence, Italy and [4]Department of Environmental Sciences, University of Milano-Bicocca, Piazza della Scienza 1, 20126 Milano, Italy

Email:
Laura Cipolla[*] - laura.cipolla@unimib.it

* Corresponding author

Keywords:
glycosidases inhibitors; iminosugars; nojirimycins; pyrrolidines; trehalases

Beilstein J. Org. Chem. **2012,** *8,* 514–521.
doi:10.3762/bjoc.8.58

Received: 12 January 2012
Accepted: 06 March 2012
Published: 05 April 2012

This article is part of the Thematic Series "Synthesis in the glycosciences II".

Guest Editor: T. K. Lindhorst

Abstract

A small set of nojirimycin- and pyrrolidine-based iminosugar derivatives has been synthesized and evaluated as potential inhibitors of porcine and insect trehalases. Compounds **12**, **13** and **20** proved to be active against both insect and porcine trehalases with selectivity towards the insect glycosidase, while compounds **10**, **14** and **16** behaved as inhibitors only of insect trehalase. Despite the fact that the activity was found in the micromolar range, these findings may help in elucidating the structural features of this class of enzymes of different origin, which are still scarcely characterised.

Introduction

Trehalase (EC3.2.1.28) is a glycosidase that catalyses trehalose (α-D-glucopyranosyl-α-D-glucopyranoside **1**, Figure 1) [1-3] hydrolysis. It was found initially at the end of the 19th century in *Aspergillus niger* [4] and *S. cerevisiae* [5], and has since then been reported in several other organisms, including mammals, where it is found both in the kidney brush border membranes [6] and in the intestinal villae membranes [7]. While the role of trehalase in the kidney has not been elucidated yet (trehalose is absent in blood), in the intestine it hydrolyses ingested trehalose [8]. However, trehalose hydrolysis is fundamental for insect flight [9], growth resumption of resting cells, and spore germination in fungi.

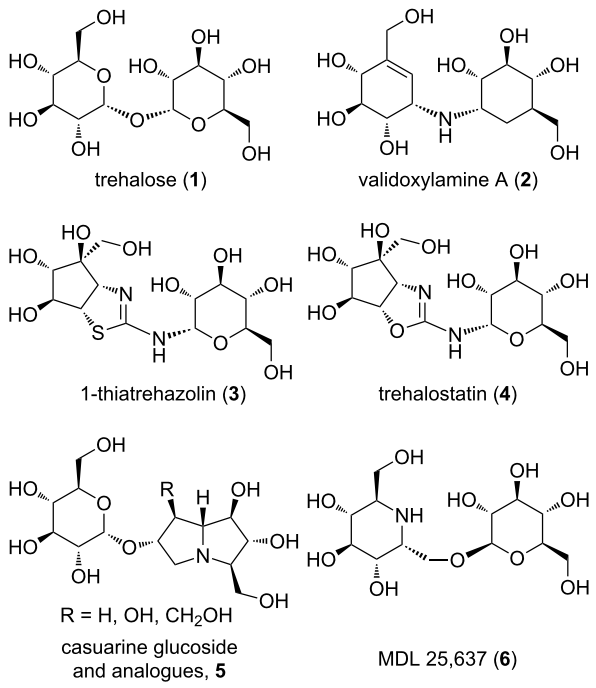

Figure 1: Structure of trehalose (**1**), validoxylamine A (**2**), 1-thiatrehazolin (**3**), trehalostatin (**4**), casuarine glucoside and analogues **5**, and MDL 25,637 (**6**).

Trehalase is an inverting glycosidase [10], belonging to the GH37 family of the carbohydrate-active enzyme (CAZy) classification [11], and despite its abundance in nature, few details are known of its function and properties. The first 3D structure of a trehalase (Tre37A from *E. coli*) in a complex with inhibitors (validoxylamine A (**2**) and 1-thiatrehazolin (**3**) Figure 1; protein data bank (PDB) entries 2JF4 and 2JG0 [12]) shows the presence of two subsites: Subsite +1 accommodating the leaving-group, the "recognition" site, and subsite −1 as the "catalytic" site.

Due to the biological relevance of trehalose and trehalase, several trehalose mimetics have been proposed as potential fungicides or antibiotics [13], such as trehalostatin (**4**) [1,14] and some iminosugar glycoconjugates, e.g., **5** or MDL 25,637 (**6**) [1,15,16] (Figure 1). In this work we report the synthesis and the biological activity of a small set of nojirimycin- and pyrrolidine-based iminosugar derivatives and their preliminary biological evaluation as inhibitors against porcine and insect trehalase from *C. riparius*.

Results and Discussion

In previous studies by us and other research groups it was reported that 1-deoxynojirimycin (**7**) and its benzyl urea derivative **8** (Figure 2) [17,18] are trehalase inhibitors. It is worth noting that they have the nojirimycin ring in common with the trehalose mimetic compound **6** (Figure 1). Furthermore, it was also reported that pyrrolidine derivatives (i.e., DAB-1, **9**, Figure 2) [19] may act as trehalase inhibitors, in particular as competitive inhibitors with affinity to the catalytic site [19]. In general, it is well known that a key issue in the design of glycosidase inhibitors is specificity, for example, 1-deoxynojirimycin (**7**) is a glycosidase inhibitor in the low micromolar range, but despite its activity it lacks specificity. In this study we wish to gain further insights into the recognition requirements of the catalytic site of porcine (as the mammalian counterpart) and insect trehalase from *Chironomus riparius*. Both nojirimycin and pyrrolidine derivatives fall into the class of catalysis-site-targeting inhibitors [19].

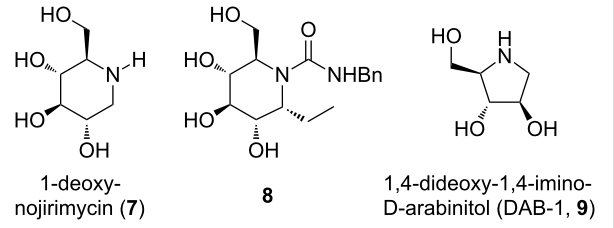

Figure 2: Structure of nojirimycin-based (**7**, **8**) and pyrrolidine-based (**9**) leads.

On the basis of these considerations, we designed and synthesized nojirimycin and pyrrolidine derivatives **10**–**21** (Figure 3), bearing different groups on the nitrogen atom and on the adjacent carbon. We did not expect a high value of inhibition, since, as already reported [19], good inhibitors must have a pseudodisaccharide structure, which ensures the synergistic interactions of an aminocyclitol or a nitrogen-containing heterocycle with the catalytic site, and of a sugar or cyclitol unit with the recognition site. However, this work may highlight relevant structural features of the catalytic site that can give access to specific inhibitors.

In general, the compounds were synthesized with the aim of understanding whether the presence of substituents on the nitrogen atom and/or a short- or medium-sized alkyl chain at position 1 (numbering of the parent aldose) can somehow influence the activity and selectivity. In addition, the pyrrolidine derivatives **14**–**16** and **17**–**19** possess a "α-D-arabino" and a "β-D-ribo" configuration, respectively, which may affect the activity and selectivity towards porcine and insect trehalase. Finally, we also included two pyrrolidine derivatives **20** and **21**, differing in the alkylation position with a C_8 alkyl chain (Figure 3). These two compounds can help answer whether a medium-sized lipophylic chain can be accommodated into the catalytic site, and whether any difference could be due to the positioning of the chain itself. Only the "α-D-arabino-config-

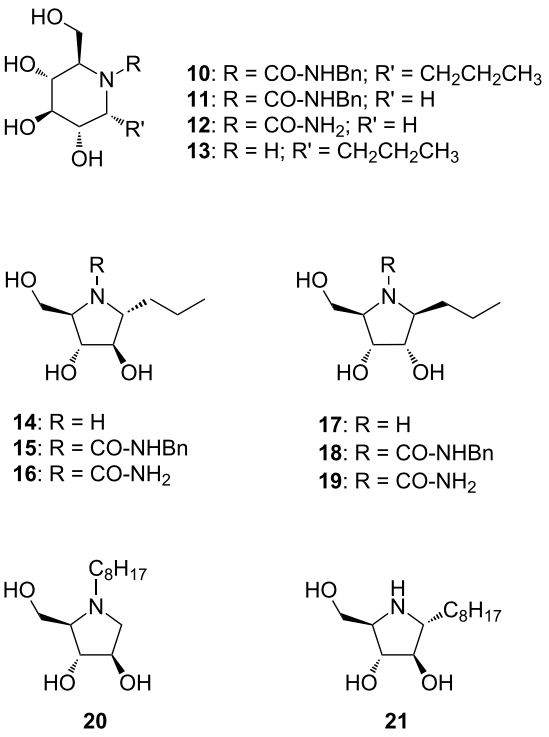

Figure 3: Structures of potential inhibitors **10**–**21**.

ured" pyrrolidines **20**, **21** were considered here, since preliminary data showed that "β-D-ribo-configured" pyrrolidines were not active at all (for details, see Enzyme assays).

Chemical synthesis

Based on the structure of lead compound **8** (Figure 2), which showed some selectivity towards insect trehalase from *C.riparius* [18], we envisaged the possibility to synthesize a few nojirimycin and pyrrolidine derivatives bearing a benzyl urea moiety and a different alkyl substituent on the adjacent carbon (**10**, **11**, **15** and **18**, Figure 3). Thus the presence of a benzyl urea moiety was expected to be a common feature of the majority of the iminosugar derivatives (piperidines and pyrrolidines). However, during the final deprotection step by hydrogenolysis, the reaction resulted in the formation of the disubstituted urea **10** or, unexpectedly, monosubstituted ureas **12**, **16** and **19** (Figure 3), depending on the starting material.

Pyrrolidine derivatives were synthesized with different stereochemistry on the five-membered ring (i.e., compounds **14**, **16** versus **17**, **19**, Figure 3), in order to elucidate whether this feature could be relevant for enzyme recognition, and with a sterically demanding alkyl chain positioned either at the nitrogen atom or at the adjacent carbon (i.e., compounds **20** and **21**, Figure 3).

Nojirimycin-based derivatives **10**, **12** and **13**

Compounds **10** and **12** were synthesized from the corresponding protected nojirimycin derivatives **22** [20] (Scheme 1A) and **24** [21] (Scheme 1B). Cbz deprotection of compound **22** (Scheme 1A) followed by reaction with benzyl isocyanate in dimethoxyethane at 85 °C afforded urea **23** (15% yield over two steps). Reaction of compound **24** directly with benzyl isocyanate in dimethoxyethane at 85 °C afforded urea **25** in 72% yield (Scheme 1B).

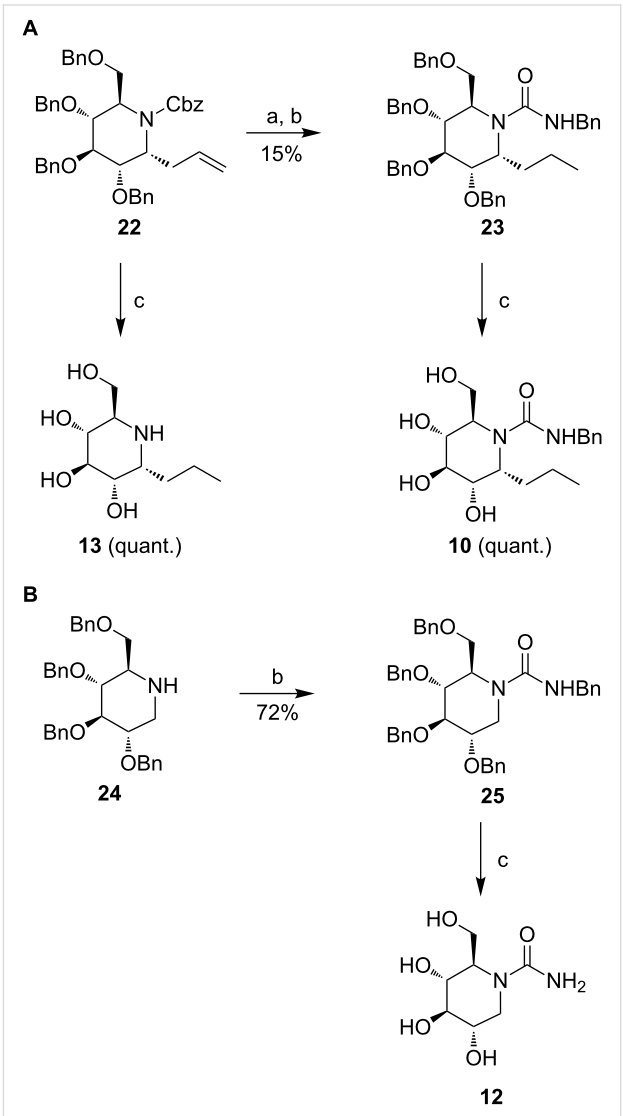

Scheme 1: Synthesis of nojirimycin-based inhibitors **10**,**12** and **13**. Reagents and conditions: (a) H_2, Pd/C, NH_4OAc, EtOH, rt, 10 h; (b) benzyl isocyanate, DME, 85 °C, 2 h; (c) H_2, $Pd(OH)_2$/C, EtOAc/EtOH 1:1, rt, 5 d.

The hydrogenolysis of benzyl ureas **23** and **25** unexpectedly proceeded in a different manner. Derivative **23** afforded benzyl nojirimycin urea **10** in quantitative yield (Scheme 1A), while derivative **25**, under the same reaction conditions gave mono-

substituted urea **12** in 83% purity, as determined by NMR (Scheme 1B). Impurities, which could not be separated from the title compound, were due to small amounts of the benzyl urea that could not be fully hydrolysed, even after prolonged reaction times.

In order to figure out whether the benzyl urea moiety might have any effect on the activity and specificity against trehalases, derivative **13** was also synthesized by direct hydrogenolysis of starting compound **22** (Scheme 1A). Any activity difference between inhibitor **10** and **13** must be ascribed to the presence of the benzyl urea group instead of the free nojirimycin NH.

Pyrrolidine-based compounds **14**, **16**, **17** and **19–21**

Pyrrolidine derivatives **14**, **16**, **17** and **19** were obtained from the corresponding pyrrolidines **26** and **27** [22], by following the same synthetic steps used for nojirimycin derivatives, as outlined in Scheme 2. Direct hydrogenolysis of **26** and **27** afforded quantitatively the compounds **14** and **17**, respectively. Cbz deprotection of **26** and **27** followed by reaction with benzyl isocyanate in dimethoxyethane at 85 °C produced ureas **28** and **29** in 47 and 50% overall yields, respectively. As previously observed, hydrogenolysis of **28** and **29** afforded monosubstituted ureas **16** and **19**, with loss of the *N*-benzyl group. In addition, while derivative **19** was obtained with comparable purity (85%) to compound **12**, deprotection of intermediate **28** afforded monosubstituted urea **16** in only 58% purity.

In addition, pyrrolidines **20** and **21** were synthesized in a few steps from nitrone **30** [23]. Catalytic hydrogenation over Pd/C followed by reductive amination in the presence of octanal and $NaBH_3CN$ afforded compound **20** in 33% yield over two steps (Scheme 3). Grignard addition of octylmagnesium bromide to nitrone **30** proceeded cleanly and gave stereoselectively the "all trans" hydroxypyrrolidine **31** as a single adduct in 84% yield, with a stereoselectivity that was in accordance with previously reported Grignard additions on the same nitrone [24]. Final catalytic hydrogenation over Pd/C gave pyrrolidine **21**, which was recently synthesized by an enantioselective strategy [25], in 73% yield.

Enzyme assays

Synthesized compounds **10**, **12**–**14**, **16**, **17** and **19**–**21** were tested for their inhibitory activity against insect (*C. riparius*) and porcine kidney trehalase. All data are summarised in Figure 4 and Table 1.

Even if the synthesis unexpectedly afforded a structurally quite heterogeneous set of compounds, biological data give some hints toward the design of selective inhibitors of trehalases of

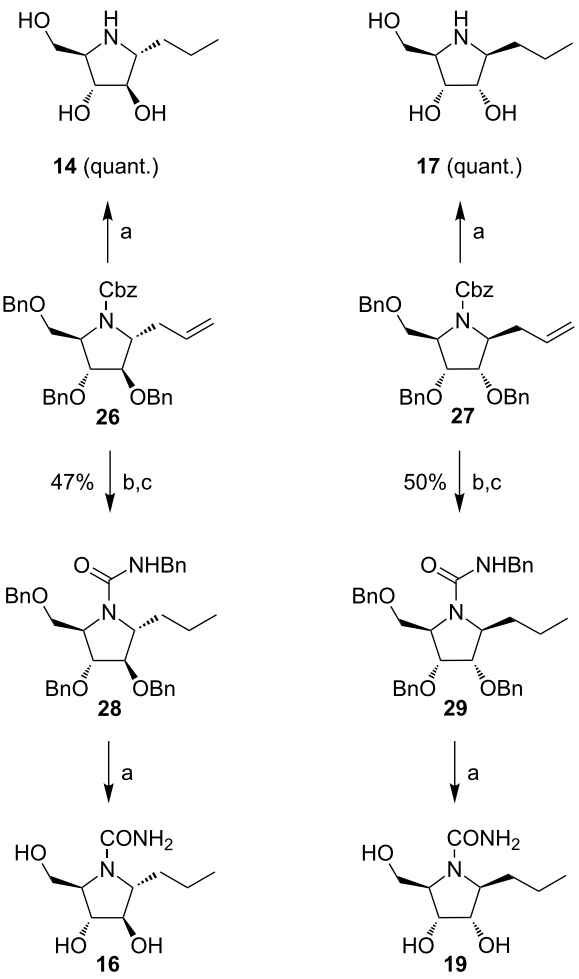

Scheme 2: Synthesis of pyrrolidine derivatives **14**, **16**, **17** and **19**. Reagents and conditions: (a) H_2, $Pd(OH)_2$/C, EtOAc/EtOH 1:1, rt, 5 d; (b) H_2, Pd/C, NH_4OAc, EtOH, rt, 10 h; (c) benzyl isocyanate, DME, 85 °C, 2 h.

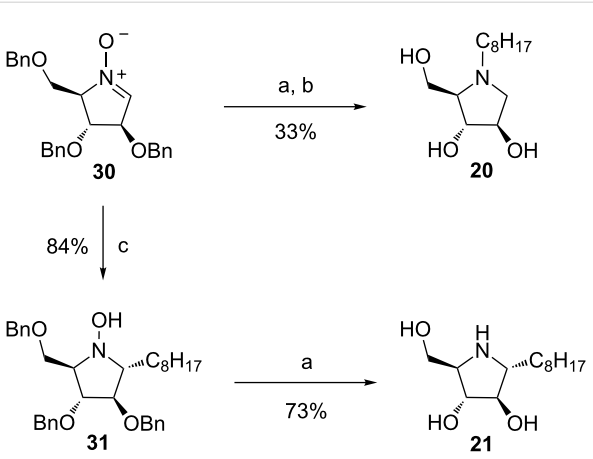

Scheme 3: Synthesis of pyrrolidines **20** and **21**. Reagents and conditions: (a) H_2, Pd/C, MeOH, HCl; (b) octanal, $NaBH_3CN$, MeOH, AcOH rt; (c) $C_8H_{17}MgBr$ (2 M in Et_2O), THF, −75 °C to rt (3 h).

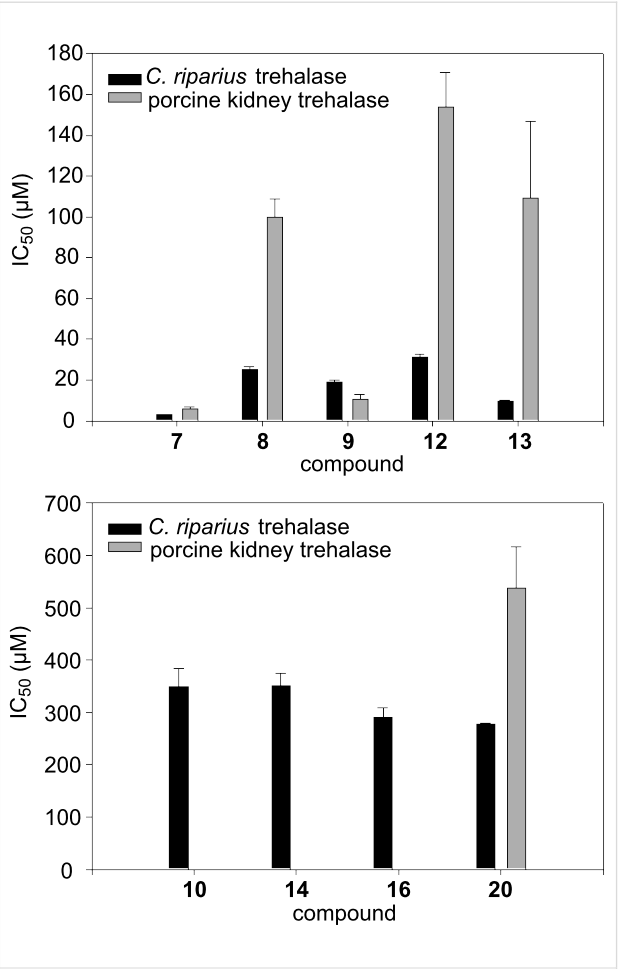

Figure 4: Histogram of the inhibitory activity of compounds **7**–**10**, **12**–**14**, **16** and **20**. Derivatives **10**, **14** and **16** showed no activity against porcine kidney trehalase.

different origin. Trehalase activity was measured through a coupled assay with glucose-6-phosphate dehydrogenase and hexokinase according to Wegener et al. [26]. To examine the potential of each compound as a trehalase inhibitor, screening assays of potential inhibitors were carried out at a fixed concentration of 1 mM. For the most active compounds, dose–response curves were established to determine the IC_{50} values. Experiments were performed in the presence of increasing concentrations of the inhibitor at a fixed substrate concentration close to the K_m value (0.5 mM for *C. riparius* trehalase and 2.5 mM for porcine trehalase). Initial rates as a function of inhibitor concentration were fitted to the following equation:

$$\frac{v_i}{v} = \frac{1}{1+\left(\frac{[I]}{IC_{50}}\right)^n}$$

where v_i and v are the initial rate in the presence and in the absence of the inhibitor, respectively, [I] is the inhibitor concentration, IC_{50} is the inhibitor concentration producing half-maximal inhibition, and n is the Hill coefficient.

In the nojirimycin series (compounds **10**, **12** and **13**) the most active compound was derivative **13**, with IC_{50} values close to 1-deoxynojirimycin (**7**) for insect trehalase inhibition (Table 1). Interestingly, compound **13** was found to be around ten times more active towards insect trehalase than to porcine trehalase, hence more specific than lead compound **7** (only twice as active on insect trehalase), suggesting that a short alkyl chain at C-1, together with the free NH group in the ring account for the good activity and specificity.

Table 1: Inhibition of trehalase activity. Fixed amounts of *C. riparius* and kidney porcine trehalases were incubated in the presence of fixed concentrations (K_m) of trehalose and increasing concentrations of the indicated inhibitors. Parameters were calculated as described in the text. Data are (means ± SE) of three independent experiments.

Compound	IC_{50} *C. riparius* trehalase (μM)	IC_{50} porcine kidney trehalase (μM)
7	2.8 ± 0.34[a]	5.96 ± 0.62[b]
8	25.0 ± 1.60[a]	100.0 ± 8.82[a]
9	19.0 ± 0.95[a]	10.6 ± 2.42[a]
10	349.0 ± 35	no inhibition
12	31.0 ± 1.82	154.0 ± 17
13	9.70 ± 0.30	109.0 ± 38
14	350.0 ± 24	no inhibition
16	290.0 ± 18	no inhibition
17	no inhibition	no inhibition
19	no inhibition	no inhibition
20	277.0 ± 2.63	537.0 ± 80
21	no inhibition	no inhibition

[a]values from [18]; [b]values from [13].

Comparing the activity of lead **7** with compound **12**, it appears that substitution on the nitrogen atom of the ring causes a drop in activity; however, a good degree of selectivity (five times) towards the insect glycosidase is maintained.

When substituents are introduced both on the nitrogen of the ring and at C-1, as in compound **10**, a further drop of activity can be observed for insect trehalase inhibition (IC_{50} 2.8 μM → 31.0 μM → 349.0 μM for **7** → **12** → **10**), together with complete loss of activity against the porcine enzyme (IC_{50} 5.96 μM → 154.0 μM → no inhibition for **7** → **12** → **10**), thus maximising selectivity. The inhibition of the trehalase activity of **8** is 25 μM and of **10** is 349 μM: Elongation of the ethyl chain of compound **8** to the propyl group of inhibitor **10** causes a more than ten-fold drop in activity against insect trehalase.

Analysis of the pyrrolidine set (**14**, **16**, **17** and **19**–**21**) immediately shows that the "β-D-ribo-configured" pyrrolidines **17** and **19** do not possess any activity against either enzyme. As for the "α-D-arabino-configured" pyrrolidines, the presence of a sterically demanding substituent (C_8 alkyl chain) at C-1 (compound **21**) is detrimental for the inhibition of both trehalases, while shorter chains, as in **14**, are accepted only by the catalytic site of insect trehalase, thus imparting selectivity in inhibition. In contrast, when the C_8 alkyl chain is positioned on the nitrogen (compound **20**) both enzymes can accommodate the inhibitor in the catalytic pocket, with a preference for the insect trehalase. Furthermore, the presence of substituents both on the nitrogen of the ring and at C-1, as in compound **16**, slightly increases the activity against insect trehalase (IC_{50} 350.0 μM → 290.0 μM for **14** → **16**).

It is worth noting that the introduction of small substituents on lead pyrrolidine **9**, either at the nitrogen atom or at the adjacent carbon, affords compounds less active than **9**, but with reversed specificity (**9** is twice more active on porcine trehalase, while **14**, **16** and **20** are more active on insect enzyme).

Conclusion

The design and synthesis of enzyme inhibitors can often provide information about the mechanism of action and chemical topography of the active site of the enzyme under consideration. We proposed the synthesis of a small set of iminosugar derivatives, which in some cases resulted in selective inhibitors of trehalases of different origin, despite the fact that their activity was in the micromolar range. The most active and specific inhibitor was compound **13**, characterised by a nojirimycin ring with a propyl group at C-1. Compared to lead 1-deoxynojirimycin (**7**), the presence of the propyl group in **13** causes a slight decrease of activity, but nevertheless imparting a ten-fold selectivity towards insect trehalase. In general, the collected data clearly indicate that the catalytic sites of trehalases from porcine kidney and insects have different recognition requirements, which can be exploited for the future design of specific inhibitors.

Further studies are needed in order to characterise the synthesized compounds in terms of their inhibitory activity against other glycosidases of interest, such as maltase, isomaltase, sucrase, glucoamylase, lactase and α-amylase.

Experimental

Synthesis

General methods

Solvents were dried over molecular sieves for at least 24 h prior to use, when required. When dry conditions were required, the reaction was performed under Ar or N_2 atmosphere. Thin-layer chromatography (TLC) was performed on silica gel $60F_{254}$ coated glass plates (Merck) with UV detection when possible, or spots were visualized by charring with a conc. H_2SO_4/EtOH/H_2O solution (10:45:45 v/v/v), or with a solution of $(NH_4)_6Mo_7O_{24}$ (21 g), $Ce(SO_4)_2$ (1 g), conc. H_2SO_4 (31 mL) in water (500 mL) and then heating to 110 °C for 5 min. Flash column chromatography was performed on silica gel 230–400 mesh (Merck). Routine ^1H and ^{13}C NMR spectra were recorded on a Varian Mercury instrument at 400 MHz (^1H) and 100.57 MHz (^{13}C) or on a Varian Gemini 200 MHz instrument 50.29 MHz (^{13}C) where stated. Chemical shifts are reported in parts per million downfield from TMS as an internal standard; *J* values are given in Hz. Mass spectra were recorded on a System Applied Biosystems MDS SCIEX instrument (Q TRAP, LC/MS/MS, turbo ion spray) or on a System Applied Biosystem MDS SCIEX instrument (Q STAR elite nanospray). ESI full MS were recorded on a Thermo LCQ instrument by direct inlet; relative percentages are shown in brackets. Elemental analyses (C, H, N) were performed on a Perkin-Elmer series II 2400 analyzer, and all synthesized compounds showed a purity of more than 95%.

General procedure for hydrogenolysis (compounds 10, 12, 13, 14, 16, 17, 19): A 0.02 M solution of the appropriate compound dissolved in EtOAc/EtOH 1:1 was treated with $Pd(OH)_2$/C (100 wt %). The reaction mixture was stirred for 5 d under a H_2 atmosphere. Palladium was then removed by filtration through a Celite pad followed by washing with EtOH and water. Evaporation of the solvents afforded the corresponding deprotected compounds in quantitative yields.

General procedure for Cbz deprotection: To a 0.2 M solution of the appropriate compound dissolved in EtOH, crystallized NH_4OAc (0.5 equiv) and Pd/C (5 wt %) were added. The reaction mixture was stirred overnight under a H_2 atmosphere.

Palladium was then removed by filtration through a Celite pad followed by washing with EtOH. The solvent was removed under reduced pressure and crude amine was used for the benzyl isocyanate reaction (see general procedure for details).

General procedure for benzyl isocyanate reaction: To a 0.07 M solution of the appropriate compound dissolved in dry DME, benzyl isocyanate (2 equiv) was added and the reaction mixture was heated under reflux. After 2 h the solvent was evaporated under reduced pressure. The residue was purified on a silica gel column with a suitable eluent. See Supporting Information File 1 for full experimental data.

Enzyme assays

All enzyme assays were performed in triplicate at 30 °C by using sample volumes varying from 5 to 20 µL in 1 mL test tubes and using a Cary3 UV–vis spectrophotometer. Enzyme activities were analyzed by Cary Win UV application software for Windows XP. The specific activity (U mg^{-1}) was expressed as µmol min^{-1}(mg protein)$^{-1}$. Values were expressed as mean ± SE of replicated.

Supporting Information

Supporting Information File 1

Full experimental data.
[http://www.beilstein-journals.org/bjoc/content/supplementary/1860-5397-8-58-S1.pdf]

Acknowledgements

We gratefully acknowledge University of Milano-Bicocca FAR 2009, MIUR (PRIN2008/24M2HX) and Ente CRF for financial support.

References

1. Bini, D.; Cardona, F.; Gabrielli, L.; Russo, L.; Cipolla, L. Trehalose mimetics as inhibitors of trehalose processing enzymes. In *Carbohydr. Chem.;* Rauter, A. P., Ed.; Royal Society of Chemistry, 2011; Vol. 37, pp 259–302. doi:10.1039/9781849732765-00259
2. Ohtake, S.; Wang, Y. J. *J. Pharm. Sci.* **2011,** *100,* 2020–2053. doi:10.1002/jps.22458
3. Elbein, A. D.; Pan, Y. T.; Pastuszak, I.; Carroll, D. *Glycobiology* **2003,** *13,* 17R–27R. doi:10.1093/glycob/cwg047
4. Bourquelot, M. E. M. *Compt. Rend. Soc. Biol. IX* **1893,** *5,* 653.
5. Fischer, E. *Ber. Dtsch. Chem. Ges.* **1895,** *28,* 1432–1438.
6. Yoneyama, Y.; Lever, J. E. *J. Cell. Physiol.* **1987,** *131,* 330–341. doi:10.1002/jcp.1041310305
7. Dahlqvist, A. *Anal. Biochem.* **1968,** *22,* 99–107. doi:10.1016/0003-2697(68)90263-7
8. Ruf, J.; Wacker, H.; James, P.; Maffia, M.; Seiler, P.; Galand, G.; von Kieckebusch, V.; Semenza, A. G.; Mantei, N. *J. Biol. Chem.* **1990,** *265,* 15034–15039.
9. Thompson, S. N. *Adv. Insect. Physiol.* **2003,** *31,* 205–285. doi:10.1016/S0065-2806(03)31004-5
10. Defaye, J.; Driguez, H.; Henrissat, B.; Bar-Guilloux, E. *Carbohydr. Res.* **1983,** *124,* 265–273. doi:10.1016/0008-6215(83)88462-6
11. Coutinho, P. M.; Henrissat, B. In *Recent Advances In Carbohydrate Bioengineering;* Gilbert, H. J.; Davies, G. J.; Henrissat, B.; Svensson, B., Eds.; Royal Society of Chemistry: Cambridge, 1999; pp 3–12.
12. Gibson, R. P.; Gloster, T. M.; Roberts, S.; Warren, R. A. J.; Storch De Gracia, I.; García, A.; Chiara, J. L.; Davies, G. J. *Angew. Chem., Int. Ed.* **2007,** *46,* 4115–4119. doi:10.1002/anie.200604825
13. Asano, N. *Glycobiology* **2003,** *13,* 93R–104R. doi:10.1093/glycob/cwg090
14. El Nemr, A.; El Ashry, E. S. H. *Adv. Carbohydr. Chem. Biochem.* **2011,** *65,* 45–114. doi:10.1016/B978-0-12-385520-6.00003-0
15. Cardona, F.; Parmeggiani, C.; Faggi, E.; Bonaccini, C.; Gratteri, P.; Sim, L.; Gloster, T. M.; Roberts, S.; Davies, G. J.; Rose, D. R.; Goti, A. *Chem.–Eur. J.* **2009,** *15,* 1627–1636. doi:10.1002/chem.200801578
16. Cardona, F.; Goti, A.; Parmeggiani, C.; Parenti, P.; Forcella, M.; Fusi, P.; Cipolla, L.; Roberts, S. M.; Davies, G. J.; Gloster, T. M. *Chem. Commun.* **2010,** *46,* 2629–2631. doi:10.1039/b926600c
17. Kameda, Y.; Asano, N.; Yamaguchi, T.; Matsui, J. *J. Antibiot.* **1987,** *40,* 563–565.
18. Forcella, M.; Cardona, F.; Goti, A.; Parmeggiani, C.; Cipolla, L.; Gregori, M.; Schirone, R.; Fusi, P.; Parenti, P. *Glycobiology* **2010,** *20,* 1186–1195. doi:10.1093/glycob/cwq087
19. Asano, N.; Kato, A.; Matsui, K. *Eur. J. Biochem.* **1996,** *240,* 692–698. doi:10.1111/j.1432-1033.1996.0692h.x
20. Cipolla, L.; Reis Fernandes, M.; Gregori, M.; Airoldi, C.; Nicotra, F. *Carbohydr. Res.* **2007,** *342,* 1813–1830. doi:10.1016/j.carres.2007.04.002
21. Wennekes, T.; Lang, B.; Leeman, M.; van der Marel, G. A.; Smits, E.; Weber, M.; van Wiltenburg, J.; Wolberg, M.; Aerts, J. M. F. G.; Overkleeft, H. S. *Org. Process Res. Dev.* **2008,** *12,* 414–423. doi:10.1021/op700295x
22. Bini, D.; Forcella, M.; Cipolla, L.; Fusi, P.; Matassini, C.; Cardona, F. *Eur. J. Org. Chem.* **2011,** 3995–4000. doi:10.1002/ejoc.201100484
23. Cardona, F.; Faggi, E.; Liguori, F.; Cacciarini, M.; Goti, A. *Tetrahedron Lett.* **2003,** *44,* 2315–2318. doi:10.1016/S0040-4039(03)00239-9
24. Delso, I.; Tejero, T.; Goti, A.; Merino, P. *Tetrahedron* **2010,** *66,* 1220–1227. doi:10.1016/j.tet.2009.12.030
25. Natori, Y.; Imahori, T.; Murakami, K.; Yoshimura, Y.; Nakagawa, S.; Kato, A.; Adachi, I.; Takahata, H. *Bioorg. Med. Chem. Lett.* **2011,** *21,* 738–741. doi:10.1016/j.bmcl.2010.11.112
26. Wegener, G.; Tschiedel, V.; Schlöder, P.; Ando, O. *J. Exp. Biol.* **2003,** *206,* 1233–1240. doi:10.1242/jeb.00217

Beilstein Journal of Organic Chemistry

Branching out at *C*-2 of septanosides. Synthesis of 2-deoxy-2-*C*-alkyl/aryl septanosides from a bromo-oxepine

Supriya Dey and Narayanaswamy Jayaraman*

Full Research Paper

Open Access

Address:
Department of Organic Chemistry, Indian Institute of Science, Bangalore 560 012, India

Email:
Narayanaswamy Jayaraman* - jayaraman@orgchem.iisc.ernet.in

* Corresponding author

Keywords:
C–C bond formations; 2-deoxy sugars; organometallic reactions; septanosides; unsaturated sugars

Beilstein J. Org. Chem. **2012,** *8,* 522–527.
doi:10.3762/bjoc.8.59

Received: 21 January 2012
Accepted: 14 March 2012
Published: 10 April 2012

This article is part of the Thematic Series "Synthesis in the glycosciences II".

Guest Editor: T. K. Lindhorst

Abstract

This paper deals with the synthesis of 2-deoxy-2-*C*-alkyl/aryl septanosides. A range of such septanoside derivatives was synthesized by using a common bromo-oxepine intermediate, involving C–C bond forming organometallic reactions. Unsaturated, seven-membered septanoside vinyl bromides or bromo-oxepines, obtained through a ring expansion methodology of the cyclopropane derivatives of oxyglycals, displayed a good reactivity towards several acceptor moieties in C–C bond forming Heck, Suzuki and Sonogashira coupling reactions, thus affording 2-deoxy-2-*C*-alkyl/aryl septanosides. Whereas Heck and Sonogashira coupling reactions afforded 2-deoxy-2-*C*-alkenyl and -alkynyl derivatives, respectively, the Suzuki reaction afforded 2-deoxy-2-*C*-aryl septanosides. Deprotection and reduction of the 2-deoxy-2-alkenyl derivative afforded the corresponding 2-deoxy-2-*C*-alkyl septanoside free of protecting groups. The present study illustrates the reactivity of bromo-oxepine in the synthesis of hitherto unknown septanosides, branching out at *C*-2, through C–C bond formation with alkyl and aryl substituents.

Introduction

Septanoses and septanosides are unnatural, seven-membered cyclic sugars [1]. Methods of preparation and the exploration of the properties of these unnatural sugars are of high interest [2]. An early isolation of septanose was achieved through cyclization of generic hexose sugars, which afforded minor amounts of septanose, along with furanose and pyranose, which formed in major amounts [3]. Synthetic approaches to septanoses have been explored in many instances, for example, (i) hemiacetal or acetal formation from a linear precursor containing aldehyde and an appropriately positioned hydroxyl group [4-8]; (ii) Knoevenagel-type condensation of sugar aldehyde with active methylene compounds [9,10]; (iii) ring-closing

metathesis reactions of appropriately installed diene derivatives [11-13]; (iv) ring expansion of 1,2-cyclopropanated sugars [14-17]; (v) Baeyer–Villiger oxidation of inositol derivatives [18,19] and (vi) electrophile-induced cyclization [20]. We recently developed a new methodology to prepare septanosides, which involved a sequence of dihalocarbene insertion on to an oxyglycal, ring opening of the cyclopropyl moiety with a nucleophile, and oxidation and reduction reactions, so as to permit the expansion of six-membered pyranoses to seven-membered septanosides [21-23]. Features of this methodology include the formation of vinyl halide, vinyl ether, diketone and diol intermediates, which are potential sites for varied types of functionalizations. While exploring such features, we undertook the preparation of septanoside derivatives that are branched out at *C*-2, so as to afford 2-deoxy-2-*C*-alkyl/aryl derivatives, through C–C bond formations mediated by organometallic reagents. Details of the preparation of 2-deoxy-2-*C*-aryl/alkyl septanosides are described herein.

Results and Discussion

The methodology of septanoside preparation starting from an oxyglycal is shown in Figure 1 [21]. The oxygen at *C*-2 of oxyglycal **I** was retained throughout until the septanoside **V** was obtained. More importantly, vinyl halide **III** and diketone **IV** also form as intermediates of the reaction and these intermediates provide an avenue to expand the scope of the reaction sequence.

In the present work, we envisaged that **III** would form as a synthon to implement C–C bond forming reactions. Vinyl halide **2** was synthesized through a ring-expansion reaction of cyclopropanated adduct **1** (Scheme 1), as reported previously [21]. The reactivity at *C*-2 of **2** was examined by the chosen organometallic reactions, namely, Heck, Suzuki and Sonogashira coupling reactions. Heck coupling reactions [24,25] were undertaken first. Thus, the reaction of bromo-oxepine **2** with methyl acrylate was performed, in the presence of $Pd(OAc)_2$ (10 mol %) and Cs_2CO_3 in 1,4-dioxane, at 98 °C (Scheme 1), to afford diene **3**, in 70% yield. The presence of doublets at 7.80 and 5.97 ppm (J = 16.0 Hz) in the ^{1}H NMR spectrum and signals at 136.3 ppm and 119.5 ppm in the ^{13}C NMR spectrum confirmed the formation of **3**.

Having realized the synthesis of one product, reactions of **2** were performed with a few other substrates, namely, *tert*-butyl acrylate, a substrate presenting two acrylates within the molecule, styrene, and α-methyl styrene (Scheme 1). Reactions with these substrates also afforded the diene products **4**–**7**, in good

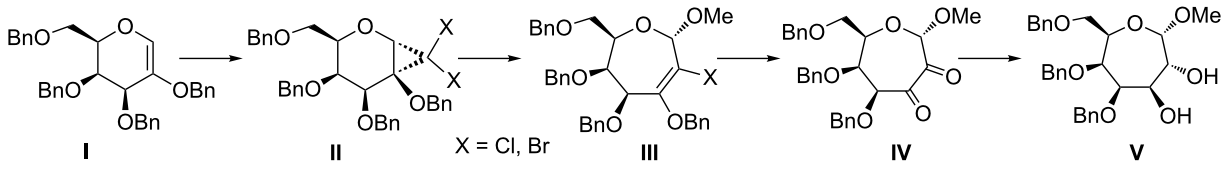

Figure 1: Synthetic route to transform oxyglycal **I** to a septanoside **V**.

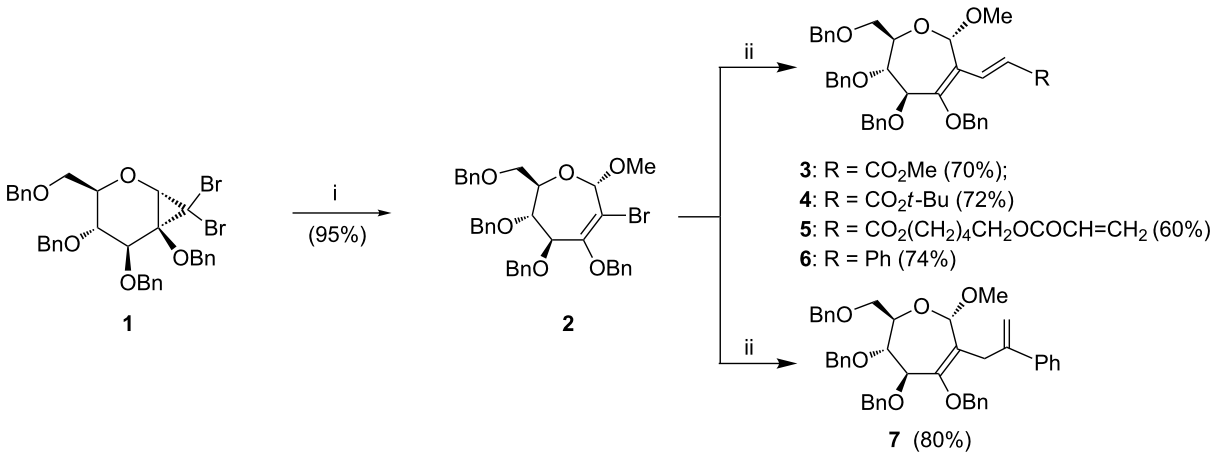

Scheme 1: Reaction conditions: (i) NaOMe, PhMe, reflux, 8 h; (ii) methyl acrylate (for **3**); *tert*-butyl acrylate (for **4**); H_2C=CHCOO$(CH_2)_5$OCOCH=CH_2 (for **5**; **2**/substrate = 1:0.57); styrene (for **6**); α-methyl styrene (for **7**); $Pd(OAc)_2$ (10 mol %), Cs_2CO_3 (1.5 molar equiv), 1,4-dioxane, 98 °C, 72 h.

yields. The anticipated two Heck coupling reactions with the substrate that presents two acrylates, could not be achieved, rather only the mono-Heck coupling product **5** was obtained. Alternative reaction conditions were attempted, for example, by using $Pd(PPh_3)_2Cl_2$ (10 mol %), instead of $Pd(OAc)_2$, while keeping other parameters of the reaction uniform, yet the double-Heck coupling product was not observed. The newly generated exocyclic olefin protons resonated as two distinct doublets in **4** at 7.72 and 5.88 ppm (J = 16.4 Hz); in **5** at 7.79 and 5.93 ppm (J = 16.4 Hz) and in **6** at 7.19 and 6.66 ppm (J = 16.8 Hz). Further, the exocyclic double-bond carbon nuclei resonated at ~136–130 and ~122 ppm in the ^{13}C NMR spectra of **4**–**6**. The reactions afforded only the (*E*)-isomer. Interestingly, when the reaction was performed with α-methyl styrene, product **7**, with an exocyclic double bond isomerization to a terminal double bond was observed. The appearance of two singlets at 5.30 and 5.14 ppm in the ^1H NMR spectrum indicated the presence of two vinylic protons in **7**. On the other hand, the exocyclic methylene moiety at *C*-2 in **7** appeared as two distinct doublets (3.88, 3.08 ppm, J = 14.4 Hz) in the ^1H NMR spectrum. Further structural assignments of **7** were performed through COSY and HSQC experiments.

Following the Heck coupling reactions on bromo-oxepine **2**, efforts were undertaken to implement C–C bond forming Suzuki and Sonogashira coupling reactions. Suzuki reactions were undertaken by involving phenylboronic acid and substituted phenylboronic acids [26,27], in the presence of $Pd(OAc)_2$ (10 mol %) and Cs_2CO_3 in 1,4-dioxane at 98 °C (Scheme 2). The reactions afforded septanosides **8–10**, which are derivatized with a phenyl substituent at *C*-2, in moderate yields. The formation of a C–C bond at *C*-2 in **8–10** was inferred by the observation of shifts of the *C*-2 nuclei signal at ~129 ppm, which in the case of bromo-oxepine was observed at 114.3 ppm. Analyses of ^1H and ^{13}C NMR spectra and mass spectra confirmed the constitution of **8–10**.

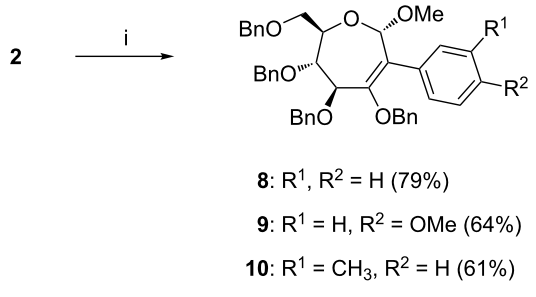

Scheme 2: Reaction conditions: (i) phenylboronic acid (for **8**); 4-methoxyphenylboronic acid (for **9**); 3-methylphenylboronic acid (for **10**); $Pd(OAc)_2$ (10 mol %), Cs_2CO_3 (1.5 molar equiv), 1,4-dioxane, 98 °C, 72 h.

The reactivity of bromo-oxepine, the key intermediate of the septanoside synthesis earlier, was explored further in the context of C–C bond formation at *C*-2, through another versatile C–C bond forming reaction, namely, Sonogashira coupling [28,29]. Reactions of **2** with acetylenes were performed in the presence of $Pd(PPh_3)_2Cl_2$ (20 mol %) and CuI (10 mol %) in a DMF/THF/Et_3N 5:3:2 solvent mixture as the optimized protocol. The use of $Pd(OAc)_2$ as a catalyst or Et_3N as the base did not promote the reaction, leading only to the recovery of the starting material. Thus, the reaction of **2** with phenylacetylene and oct-1-yne led to the formation of the corresponding 2-deoxy-2-*C*-alkynyl septanosides **11** and **12** (Scheme 3) in moderate yields. Prolonging the reaction time and increasing the catalyst loading did not increase the yields, although dehalogenation of **2** to oxepine was found to occur to a minor extent when the reaction time was increased to several days. ^{13}C NMR spectra of **11** and **12** showed resonances for the newly formed C–C bond at **11**: 108.4 ppm (*C*-2) and 95.8 ppm (*C*≡C-Ph); **12**: 109.9 ppm (*C*-2) and 97.4 ppm (*C*≡C-C_6H_{13}). Further, ^1H and ^{13}C NMR spectroscopic and mass spectrometric analyses confirmed the constitutions of **11** and **12**.

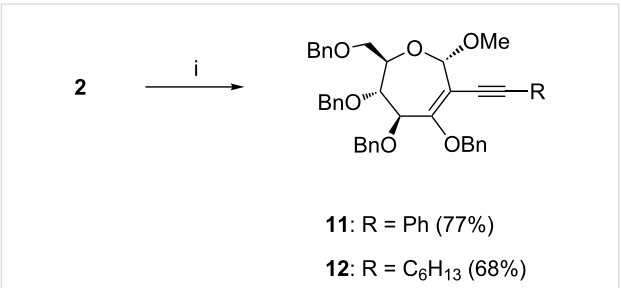

Scheme 3: Reaction conditions: (i) phenylacetylene (for **11**); oct-1-yne (for **12**); $Pd(PPh_3)_2Cl_2$ (20 mol %), CuI (10 mol %), DMF/THF/Et_3N 3:2:1, 98 °C, 72 h.

Having observed a good reactivity of bromo-oxepine **2** in C–C bond forming reactions, we used one of the 2-deoxy-2-*C*-alkyl derivatives, namely, product **4** for further reactions, leading to a 2-deoxy-2-*C*-alkyl septanoside containing free hydroxyl groups. Towards this effort, **4** was subjected first to a hydrogenolysis (Pd/C, H_2), which afforded D-*manno*-sept-3-uloside **13** as single diastereomer in good yield (Scheme 4).

The configuration of C-2 in **13** was confirmed through HMQC and COSY experiments. A doublet at 4.37 ppm with $J_{H1,H2}$ of 8.0 Hz indicated a *trans*-configuration of H-2 with respect to H-1 in **13**. The presence of sets of protons in the ^1H NMR spectrum, one at 2.05 and 1.78 ppm (multiplet) and the other at 2.21 ppm (t, J = 7.4 Hz), corresponding to exocyclic methylene moieties in **13**, resulting from the concomitant reduction of the exocyclic double bond in **4**, was also observed. The presence of

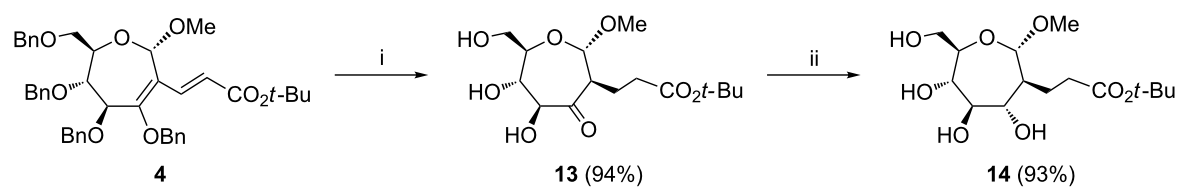

Scheme 4: Reaction conditions: (i) Pd/C (10 %), H_2, MeOH, rt, 24 h; (ii) $NaBH_4$, MeOH, 0 °C to rt, 3 h.

the ketone functionality in **13** was inferred from the resonance at 208.4 ppm in the ^{13}C NMR spectrum. Subsequent to hydrogenolysis, the treatment of **13** with $NaBH_4$ facilitated the reduction of the keto-moiety to the corresponding alcohol **14**, in an excellent yield. The *trans*-bisequatorial configuration of the hydroxyl groups at *C*-3 and *C*-4 in **14** was inferred from a $^3J_{H3,H4}$ of 12.4 Hz, in the ^1H NMR spectrum. On the other hand, the proton at *C*-2 merged with the exocyclic methylene group, leading to an inability to assess the H-2,H-3 coupling constant in **14**. Having defined the configuration of the substituent at *C*-2 in **13**, we infer a *trans*-configuration of the substituent at *C*-2 and *C*-3. The results of mass spectrometric analysis concurred with the constitutions of **13** and **14**.

Conclusion

The present study illustrates the effective application of synthetically useful bromo-oxepine for the preparation of hitherto unknown 2-deoxy-2-*C*-alkyl/aryl septanoside derivatives. C–C bond forming Heck, Suzuki and Sonogashira coupling reactions, with appropriate acrylates, arylboronic acids and alkynes, afforded the respective cross-coupled products in good yields. It is pertinent to note that the implementation of such reactions is known in seven-membered 1,2-oxazepines, so as to secure the corresponding cross-coupling products [30]. Furthermore, one of the 2-deoxy-2-*C*-alkyl septanoside derivatives was converted to a hydroxyl-group-free methyl 2-deoxy-2-*C*-alkyl septanoside. The present study illustrates the scope of seven-membered bromo-oxepines as useful substrates for the generation of 2-deoxy-2-*C*-alkyl/aryl septanosides, in addition to our previous efforts to progress such intermediates to a number septanosides and septanoside-containing di- and tri-saccharides.

Experimental

General

Chemicals were purchased from commercial sources and were used without further purification. Solvents were dried and distilled according literature procedures. Analytical TLC was performed on commercial Merck plates coated with silica gel GF254 (0.25 mm). Silica gel (230–400 mesh) was used for column chromatography. Optical rotations were recorded on a JASCO Model P-1020 polarimeter at the sodium D line at 24 °C. High-resolution mass spectra were obtained from a Q-TOF instrument by the electrospray ionization (ESI) technique. ^1H and ^{13}C NMR spectral analyses were performed on 400 MHz and 100 MHz spectrometers, respectively, with the residual solvent signal acting as the internal standard. COSY and HSQC analyses were performed on a 400 MHz NMR spectrometer.

Methyl 2-deoxy-2-*C*-(2-(*tert*-butoxycarbonyl)vinyl)-3,4,5,7-tetra-*O*-benzyl-α-D-*arabino*-hept-2-enoseptanoside (4): A solution of **2** [21] (0.05 g, 0.07 mmol) in 1,4-dioxane (1 mL) was admixed with $Pd(OAc)_2$ (1 mg, 10 mol %) under a N_2 atmosphere, and this was followed by the addition of Cs_2CO_3 (0.03 g, 0.11 mmol) and *tert*-butyl acrylate (0.02 mL, 0.153 mmol), in a sealed tube. The reaction mixture was stirred at 98 °C for 72 h, cooled, filtered, diluted with EtOAc (20 mL), washed with water (2 × 30 mL) and brine (2 × 10 mL), dried (Na_2SO_4) and concentrated in vacuo. The resulting residue was purified (hexane/EtOAc 9:1) to afford **4** (0.038 g, 72%), as an oil. R_f 0.48 (hexane/EtOAc 9:1); $[\alpha]_D$ −130.8 (*c* 1.0, $CHCl_3$); ^1H NMR (400 MHz, $CDCl_3$) δ 7.72 (d, *J* = 16.4 Hz, 1H, -C*H*=CHCO$_2$*t*-Bu), 7.33–7.24 (m, 18H, aromatic), 7.10–7.08 (m, 2H, aromatic), 5.88 (d, *J* = 16.4 Hz, 1H, -CH=C*H*CO$_2$*t*-Bu), 5.36 (s, 1H, H-1), 4.69–4.56 (m, 4H, PhCH_2), 4.48 (d, *J* = 12.0 Hz, 1H, PhCH_2), 4.43 (d, *J* = 12.0 Hz, 1H, PhCH_2), 4.33 (d, *J* = 12.0 Hz, 1H, PhCH_2), 4.24 (d, *J* = 12.0 Hz, 1H, PhCH_2), 4.21–4.17 (m, 2H, H-4 and H-6), 3.75 (dd, *J* = 8.4, 1.4 Hz, 1H, H-5), 3.63–3.57 (br, 1H, H-7a), 3.53–3.52 (br, 1H, H-7b), 3.51 (s, 3H, OMe), 1.47 (s, 9H, *t*-Bu); ^{13}C NMR (100 MHz, $CDCl_3$) δ 166.6 (C=O), 158.7 (C-3), 138.2–137.0 (aromatic), 136.4 (-*C*H=CHCO$_2$*t*-Bu), 128.4–127.5 (aromatic), 124.4 (C-2), 121.9 (-CH=*C*HCO$_2$*t*-Bu), 100.0 (C-1), 80.1 (C-5), 79.9 (C-4), 73.0 (Ph*C*H$_2$), 72.8 (Ph*C*H$_2$), 72.0 (Ph*C*H$_2$), 71.2 (Ph*C*H$_2$), 71.0 (C-6), 70.8 (C-7), 55.5 (OMe), 28.1 (*t*-Bu); HRMS–ESI (*m*/*z*): $[M + Na]^+$ calcd for 715.3247; found, 715.3245.

Methyl 2-deoxy-2-*C*-(2-phenylallyl)-3,4,5,7-tetra-*O*-benzyl-α-D-*arabino*-hept-2-enoseptanoside (7): A solution of **2** [21] (0.05 g, 0.07 mmol) in 1,4-dioxane (1 mL) was admixed with $Pd(OAc)_2$ (1 mg, 10 mol %) under a N_2 atmosphere, and was followed by the addition of Cs_2CO_3 (0.03 g, 0.11 mmol) and α-methyl styrene (0.01 mL, 0.09 mmol) in a sealed tube. The reaction mixture was stirred at 98 °C for 72 h, cooled, filtered,

diluted with EtOAc (20 mL), washed with water (2 × 30 mL) and brine (2 × 10 mL), dried (Na_2SO_4) and concentrated in vacuo. The crude reaction mixture was purified (hexane/EtOAc 92:8) to afford **7** (0.042 g, 80%), as an oil. R_f 0.60 (hexane/EtOAc 9:1); $[\alpha]_D$ −58.8 (*c* 0.5, $CHCl_3$); ^{1}H NMR (400 MHz, $CDCl_3$) δ 7.44 (d, *J* = 7.6 Hz, 2H, aromatic), 7.33–7.21 (m, 21H, aromatic), 7.18 (d, *J* = 4.8 Hz, 2H, aromatic), 5.30 (app. s, 1H, C*H*H=CPh), 5.14 (app. s, 1H, CH*H*=CPh), 4.98 (s, 1H, H-1), 4.58 (d, *J* = 12.4 Hz, 2H, PhCH_2), 4.44 (d, *J* = 12.0 Hz, 2H, PhCH_2), 4.31 (d, *J* = 10.8 Hz, 2H, PhCH_2), 4.22 (d, *J* = 11.6 Hz, 1H, PhCH_2), 4.08–4.03 (band, 3H, H-4, H-6 and PhCH_2), 3.88 (d, *J* = 14.4 Hz, 1H, -C*H*H *C*(Ph)=CH_2), 3.61 (dd, *J* = 9.2, 1.6 Hz, 1H, H-5), 3.55 (dd, *J* = 10.4, 6.4 Hz, 1H, H-7a), 3.49 (dd, *J* = 8.8, 2.0 Hz, 1H, H-7b), 3.36 (s, 3H, OMe), 3.08 (d, *J* = 14.4 Hz, 1H, -CH*H* *C*(Ph)=CH_2); ^{13}C NMR (100 MHz, $CDCl_3$) δ 150.9 (C-3), 146.3 (CH_2-*C*(Ph)=CH_2), 141.0–137.3 (aromatic), 128.3–126.6 (aromatic), 126.5 (C-2), 114.1 (C-10), 101.0 (C-1), 80.8 (C-5), 76.3 (C-4), 72.9 (Ph*C*H_2), 72.0 (Ph*C*H_2), 71.7 (Ph*C*H_2), 71.3 (Ph*C*H_2), 71.2 (C-7), 70.0 (C-6), 55.7 (OMe) 33.2 (-*C*H_2-C(Ph)=CH_2); HRMS–ESI (*m*/*z*): [M + Na]$^+$ calcd for 705.3192; found, 705.3193.

Methyl 2-deoxy-2-*C*-(*p*-methoxyphenyl)-3,4,5,7-tetra-*O*-benzyl-α-D-*arabino*-hept-2-enoseptanoside (9): A solution of **2** [21] (0.05 g, 0.07 mmol) in 1,4-dioxane (1 mL) was admixed with $Pd(OAc)_2$ (1 mg, 10 mol %) under a N_2 atmosphere, and was followed by the addition of Cs_2CO_3 (0.03 g, 0.11 mmol) and 4-methoxyphenylboronic acid (0.012 g, 0.07 mmol), in a sealed tube. The reaction mixture was stirred at 98 °C for 72 h, cooled, filtered, diluted with EtOAc (20 mL), washed with water (2 × 30 mL) and brine (2 × 10 mL), dried (Na_2SO_4) and concentrated in vacuo. The crude reaction mixture was purified (hexane/EtOAc 8:2) to afford **9** (0.033 g, 64%), as an oil. R_f 0.60 (hexane/EtOAc 8:2); $[\alpha]_D$ −9.8 (*c* 0.1, $CHCl_3$); ^{1}H NMR (400 MHz, $CDCl_3$) δ 7.38–7.11 (m, 20H, aromatic), 6.88 (d, *J* = 7.6 Hz, 2H, aromatic), 6.83 (d, *J* = 8.8 Hz, 2H, aromatic), 5.37 (s, 1H, H-1), 4.81 (d, *J* = 12.4 Hz, 1H, PhCH_2), 4.64–4.49 (m, 3H, PhCH_2), 4.40 (d, *J* = 11.6 Hz, 2H, PhCH_2), 4.32–4.29 (br, 1H, H-6), 4.28 (app. d, *J* = 11.2 Hz, 1H, H-4), 4.23 (s, 2H, PhCH_2), 3.80 (s, 3H, OMe), 3.77–3.74 (br, 1H, H-5), 3.66 (dd, *J* = 10.6, 6.4 Hz, 1H, H-7a), 3.58 (dd, *J* = 10.6, 2.4 Hz, 1H, H-7b), 3.33 (s, 3H, OMe); ^{13}C NMR (100 MHz, $CDCl_3$) δ 158.4 (aromatic), 152.3 (C-3), 138.4–137.3 (aromatic), 130.9 (aromatic), 129.0 (C-2), 128.4–127.4 (aromatic), 113.1 (aromatic), 102.2 (C-1), 80.7 (C-5), 78.3 (C-4), 73.0 (Ph*C*H_2), 72.6 (Ph*C*H_2), 72.0 (Ph*C*H_2), 71.2 (C-6), 71.1 (C-7), 55.9 (OMe), 55.2 (-C_6H_4OMe); HRMS–ESI (*m*/*z*): [M + Na]$^+$ calcd for 695.2985; found, 695.2983.

Methyl 2-deoxy-2-*C*-(octyn-1-yl)-3,4,5,7-tetra-*O*-benzyl-α-D-*arabino*-hept-2-enoseptanoside (12): A solution of **2** [21] (0.05 g, 0.07 mmol) in DMF/THF/Et_3N 5:3:2 (1 mL) was admixed with $Pd(PPh_3)_2Cl_2$ (0.01 g, 20 mol %) under a N_2 atmosphere, and was followed by the addition of CuI (0.012 g, 10 mol %) and 1-octyne (0.023 mL, 0.14 mmol), in a sealed tube. The reaction mixture was stirred at 98 °C for 72 h, cooled, filtered, diluted with EtOAc (20 mL), washed with water (2 × 30 mL) and brine (2 × 10 mL), dried (Na_2SO_4) and concentrated in vacuo. The crude reaction mixture was purified (hexane/EtOAc 9:1) to afford **12** (0.035 g, 68%), as an oil. R_f 0.30 (hexane/EtOAc 9:1); $[\alpha]_D$ +4.56 (*c* 0.1, $CHCl_3$); ^{1}H NMR (400 MHz, $CDCl_3$) δ 7.36–7.21 (m, 18H, aromatic), 7.07–7.05 (m, 2H, aromatic), 5.25 (s, 1H, H-1), 5.08 (d, *J* = 11.6 Hz, 1H, PhCH_2), 4.80 (d, *J* = 11.6 Hz, 1H, PhCH_2), 4.72 (d, *J* = 12.4 Hz, 1H, PhCH_2), 4.60 (d, *J* = 12.4 Hz, 1H, PhCH_2), 4.45 (d, *J* = 12.4 Hz, 2H, PhCH_2), 4.32 (d, *J* = 11.6 Hz, 1H, PhCH_2), 4.17 (d, *J* = 11.6 Hz, 1H, PhCH_2), 4.14–4.10 (band, 2H, H-4 and H-6), 3.68 (dd, *J* = 8.8, 2.0 Hz, 1H, H-5), 3.60 (dd, *J* = 6.0, 3.0 Hz, 1H, H-7a), 3.52–3.49 (br, 1H, H-7b), 3.48 (s, 3H, OMe), 2.37 (t, *J* = 7.2 Hz, 2H, -C≡CCH_2-), 1.55–1.51 (m, 1H, -C≡CCH$_2$CH_2-), 1.42–1.35 (m, 1H, -C≡CCH$_2$CH_2-), 1.30–1.18 (m, 6H, -C≡C(CH$_2$)$_2$(CH_2)$_3$-), 0.86 (t, *J* = 6.8 Hz, 3H, -C≡C(CH$_2$)$_5$*C*H$_3$); ^{13}C NMR (100 MHz, $CDCl_3$) δ 160.9 (C-3), 138.4–137.5 (aromatic), 128.4–127.4 (aromatic), 109.9 (C-2), 100.8 (C-1), 97.4 (-*C*≡CCH$_2$CH_2-), 80.4 (C-5), 78.6 (C-4), 75.7 (-C≡*C*CH$_2$CH$_2$-), 73.3 (Ph*C*H_2), 72.8 (Ph*C*H_2), 71.8 (Ph*C*H_2), 71.2 (Ph*C*H_2), 71.1 (C-6), 70.8 (C-7), 55.9 (OMe), 31.3 (-C≡C(CH$_2$)$_3$*C*H$_2$-), 28.6 (-C≡C(CH$_2$)$_4$*C*H$_2$-), 28.5 (-C≡CCH$_2$*C*H$_2$-), 22.5 (-C≡C(CH$_2$)$_2$*C*H$_2$-), 20.0 (-C≡C*C*H$_2$(CH$_2$)$_4$CH$_3$), 14.3 (-C≡C(CH$_2$)$_5$*C*H$_3$); HRMS–ESI (*m*/*z*): [M + Na]$^+$ calcd for 697.3505; found, 697.3507.

Methyl 2-deoxy-2-*C*-(2-(*tert*-butoxycarbonyl)ethyl)-α-D-*manno*-sept-3-uloside (13): A mixture of **4** (0.038 g, 0.054 mmol) and Pd/C (10%, 0.030 g) in MeOH (10 mL) was stirred under a positive pressure of H_2 for 24 h at rt, filtered through a celite pad, and washed with MeOH (2 × 15 mL), and the solvents were removed in vacuo to afford **13** (0.017 g, 94%), as an oil. R_f 0.3 (MeOH/$CHCl_3$ 1:1); $[\alpha]_D$ +63.12 (*c* 0.5, MeOH); ^{1}H NMR (400 MHz, CD_3OD) δ 4.37 (d, *J* = 8.0 Hz, 1H, H-1), 4.28 (app. d, *J* = 7.6 Hz, 1H, H-4), 4.08 (m, 1H, H-6), 3.85 (dd, *J* = 13.6, 2.4 Hz, 1H, H-7a), 3.73 (dd, *J* = 13.6, 4.8 Hz, 1H, H-7b), 3.46 (s, 3H, OMe), 3.35 (br, 1H, H-5), 3.22–3.17 (m, 1H, H-2), 2.21 (t, *J* = 7.4 Hz, 2H, -CH$_2$-CH_2CO$_2$*t*-Bu), 2.10–2.01 (m, 1H, -C*H*HCH$_2$CO$_2$*t*-Bu), 1.83–1.75 (m, 1H, -CH*H*CH$_2$CO$_2$*t*-Bu), 1.49 (s, 9H, *t*-Bu); ^{13}C NMR (100 MHz, CD_3OD) δ 208.4 (C-3), 175.3 (C=O), 103.4 (C-1), 84.5 (C-4), 83.1 (C-*t*-Bu), 73.2 (C-5), 71.0 (C-6), 62.7 (C-7), 56.6 (OMe), 52.2 (C-2), 33.9 (-CH$_2$*C*H$_2$CO$_2$*t*-Bu), 28.2 (*t*-Bu), 23.3 (-*C*H$_2$CH$_2$CO$_2$*t*-Bu); HRMS–ESI (*m*/*z*): [M + Na]$^+$ calcd for 357.1525; found, 357.1526.

Supporting Information

Supporting Information File 1

Experimental procedures and spectroscopic data.
[http://www.beilstein-journals.org/bjoc/content/supplementary/1860-5397-8-59-S1.pdf]

Acknowledgements

We thank the Department of Science and Technology, New Delhi, for a financial support. SD thanks Council of Scientific and Industrial Research, New Delhi, for a senior research fellowship.

References

1. Collins, P. M.; Ferrier, R. J. *Monosaccharides: Their Chemistry and Their Roles in Natural Products*. John Wiley & Sons: Chichester, UK, 1998; pp 40–42.
2. Pakulski, Z. *Pol. J. Chem.* **2006,** *80,* 1293–1326.
3. Stevens, J. D. *J. Chem. Soc. D* **1969,** 1140–1141. doi:10.1039/C29690001140
4. Stevens, J. D. *Carbohydr. Res.* **1972,** *21,* 490–492. doi:10.1016/S0008-6215(00)84936-8
5. Anet, E. F. L. J. *Carbohydr. Res.* **1968,** *8,* 164–174. doi:10.1016/S0008-6215(00)80152-4
6. Contour, M.-O.; Fayet, C.; Gelas, J. *Carbohydr. Res.* **1990,** *201,* 150–152. doi:10.1016/0008-6215(90)84232-J
7. Tauss, A.; Steiner, A. J.; Stütz, A. E.; Tarling, C. A.; Withers, S. G.; Wrodnigg, T. M. *Tetrahedron: Asymmetry* **2006,** *17,* 234–239. doi:10.1016/j.tetasy.2005.12.007
8. Sizun, G.; Dukhan, D.; Griffon, J.-F.; Griffe, L.; Meillon, J.-C.; Leroy, F.; Storer, R.; Sommadossi, J.-P.; Gosselin, G. *Carbohydr. Res.* **2009,** *344,* 448–453. doi:10.1016/j.carres.2008.12.019
9. Butcher, M. E.; Ireson, J. C.; Lee, J. B.; Tyler, M. J. *Tetrahedron* **1977,** *33,* 1501–1507. doi:10.1016/0040-4020(77)88012-5
10. Ovaa, H.; Leeuwenburgh, M. A.; Overkleeft, H. S.; van der Marel, G. A.; van Boom, J. H. *Tetrahedron Lett.* **1998,** *39,* 3025–3028. doi:10.1016/S0040-4039(98)00324-4
11. Peczuh, M. W.; Snyder, N. L. *Tetrahedron Lett.* **2003,** *44,* 4057–4061. doi:10.1016/S0040-4039(03)00849-9
12. Schmidt, B.; Biernat, A. *Chem.–Eur. J.* **2008,** *14,* 6135–6141. doi:10.1002/chem.200800567
13. Alcázar, E.; Pletcher, J. M.; McDonald, F. E. *Org. Lett.* **2004,** *6,* 3877–3880. doi:10.1021/ol0483495
14. Hoberg, J. O.; Bozell, J. J. *Tetrahedron Lett.* **1995,** *36,* 6831–6834. doi:10.1016/0040-4039(95)01387-W
15. Cousins, G. S.; Hoberg, J. O. *Chem. Soc. Rev.* **2000,** *29,* 165–174. doi:10.1039/a906932a
16. Ramana, C. V.; Murali, R.; Nagarajan, M. *J. Org. Chem.* **1997,** *62,* 7694–7703. doi:10.1021/jo970948k
17. Hewitt, R. J.; Harvey, J. E. *J. Org. Chem.* **2010,** *75,* 955–958. doi:10.1021/jo902306a
18. Fukami, H.; Koh, H.-S.; Sakata, T.; Nakajima, M. *Tetrahedron Lett.* **1968,** *9,* 1701–1704. doi:10.1016/S0040-4039(01)99032-X
19. Wang, Z.-X.; Miller, S. M.; Anderson, O. P.; Shi, Y. *J. Org. Chem.* **1999,** *64,* 6443–6458. doi:10.1021/jo9908849
20. Köver, A.; Matheu, M. I.; Díaz, Y.; Castillón, S. *ARKIVOC* **2007,** *part (iv),* 364–379.
21. Ganesh, N. V.; Jayaraman, N. *J. Org. Chem.* **2007,** *72,* 5500–5504. doi:10.1021/jo070444e
22. Ganesh, N. V.; Jayaraman, N. *J. Org. Chem.* **2009,** *74,* 739–746. doi:10.1021/jo801967s
23. Ganesh, N. V.; Raghothama, S.; Sonti, R.; Jayaraman, N. *J. Org. Chem.* **2010,** *75,* 215–218. doi:10.1021/jo901945e
24. Heck, R. F.; Nolley, J. P. *J. Org. Chem.* **1972,** *37,* 2320–2322. doi:10.1021/jo00979a024
25. de Meijere, A.; Meyer, F. E. *Angew. Chem.* **1994,** *106,* 2473–2506. doi:10.1002/ange.19941062307
26. Miyaura, N.; Yamada, K.; Suzuki, A. *Tetrahedron Lett.* **1979,** *20,* 3437–3440. doi:10.1016/S0040-4039(01)95429-2
27. Miyaura, N.; Suzuki, A. *Chem. Rev.* **1995,** *95,* 2457–2483. doi:10.1021/cr00039a007
28. Sonogashira, K.; Tohda, Y.; Hagihara, N. *Tetrahedron Lett.* **1975,** *16,* 4467–4470. doi:10.1016/S0040-4039(00)91094-3
29. Chinchilla, R.; Nájera, C. *Chem. Soc. Rev.* **2011,** *40,* 5084–5121. doi:10.1039/c1cs15071e
30. Al-Harrasi, A.; Fischer, S.; Zimmer, R.; Reissig, H.-U. *Synthesis* **2010,** 304–314. doi:10.1055/s-0029-1217126

License and Terms

Beilstein Journal of Organic Chemistry

Cyanoethylation of the glucans dextran and pullulan: Substitution pattern and formation of nanostructures and entrapment of magnetic nanoparticles

Kathrin Fiege[1], Heinrich Lünsdorf[2], Sevil Atarijabarzadeh[3] and Petra Mischnick*[1,3]

Full Research Paper

Open Access

Address:
[1]Institute for Food Chemistry, Technische Universität Braunschweig, Schleinitzstraße 20, D-38106 Braunschweig, Germany, [2]Department of Vaccinology and Applied Microbiology, EM-Unit, Helmholtz Centre for Infection Research, Inhoffenstraße 7, D-38124 Braunschweig, Germany and [3]Fiber and Polymer Technology, KTH Royal Institute of Technology, Teknikringen 56-58, SE-10044 Stockholm, Sweden

Email:
Petra Mischnick* - p.mischnick@tu-braunschweig.de

* Corresponding author

Keywords:
cyanoethyldextran; cyanoethylpullulan; ferromagnetic nanoparticles; glycan nanostructures; substitution pattern

Beilstein J. Org. Chem. **2012,** *8,* 551–566.
doi:10.3762/bjoc.8.63

Received: 16 January 2012
Accepted: 23 March 2012
Published: 13 April 2012

This article is part of the Thematic Series "Synthesis in the glycosciences II"

Guest Editor: T. K. Lindhorst

Abstract

Cyanoethylglucans with a degree of substitution in the range of 0.74 to 2.40 for dextran and 0.84 to 2.42 for pullulan were obtained by Michael addition of acrylonitrile to the glucans under various conditions. Products were thoroughly characterized, comprising elementary analysis, NMR and ATR–IR spectroscopy, and analysis of the substituent distribution in the glucosyl units by GC–FID and GC–MS of the constituting monosaccharide derivatives. Nanostructuring of the highly substituted cyanoethylpolysaccharides was performed by dialysis against a non-solvent. In the presence of ferromagnetic iron-oxide nanoparticles, multicore cyanoethylglucan-coated ferromagnetic nanoparticles were formed by selective entrapment. The specific interaction between cyano groups and iron could be proven. The size distribution and morphology of the nanoparticles were analyzed by dynamic light scattering (DLS), scanning electron microscopy (SEM) and energy-filtered transmission electron microscopy (EF–TEM) with parallel electron energy loss spectroscopy (PEELS).

Introduction

Cyanoethylation has been widely applied to polysaccharides, e.g., to cellulose [1], inulin [2], and starch [3]. Onda reported on cyanoethylation of pullulan with degrees of substitution (DS) up to 2.71 [4]. In contrast to Williamson-type etherifications, the base is not consumed in this nucleophilic addition of acrylonitrile, which is a reversible and thermodynamically controlled

reaction. While *O*-cyanoalkylglycans are of interest as such, they have also been used as precursors for amino-functionalized polysaccharides [2,5-8].

Introducing a cyanoethyl group offers various potential advantages. First, cyanoethylpolysaccharides show remarkable electric properties: These compounds used as gel electrolytes exhibited an enhanced ionic conductivity up to 2.4×10^{-3} S/cm. Thus, a lithium ion polymer battery with cyanoethylpullulan as a matrix polymer could be built with high charge/discharge efficiency [9]. Another example is a vertical electrochemical transistor based on poly(3-hexylthiophene), which was realized by making use of the film-forming qualities of cyanoethylpullulan [10].

Partial hydrophobization of polysaccharides by the introduction of nonpolar residues enables nanostructuring by self-assembly of these compounds. Heinze et al. demonstrated that hydrophobic dextran derivatives form spherical particles on the nanometer scale when a solution of the polymer material is dialyzed against the poorer solvent water. A certain degree of hydrophobicity and amphiphilic balance is necessary to form stable particles [11-14]. We also observed nanostructure formation of alkynyldextrans [15]. Embedding magnetic iron cores in the polymer particle allows for control by magnetic fields. Magnetic separation techniques or magnetic particle imaging can be performed. Applications, such as drug delivery or targeting, hyperthermia and biosensing can be realized [16-18]. Binding of stabilizing organic shells to ferric oxide nanoparticles is usually mediated by carboxylate groups [19]. The interaction of magnetic nanoparticles, coated with glucans (cellulose, pullulan and dextran), with human cells was reported by Heinze et al. [17,20].

A prerequisite for any application in pharmaceutical as well as technological fields is the structural characterization of the material. Cyanoethylation is established for polysaccharides, but the substituent pattern has only been studied for cyanoethylamylose and starch [3]. In most cases, the products have only been roughly characterized by NMR and IR spectroscopy or by elementary analysis [1,2]. Verraest described the substituent distribution in *O*-cyanoethylinulin by HPLC analysis and ^{13}C NMR spectroscopy [7]. The structure and the solution properties of cyanoethylcellulose were investigated by FT–IR and ^{13}C NMR spectroscopy, as well as by light scattering [21,22]. Cellulose and starch derivatives have been studied more extensively due to their frequent use, e.g., market share and bulk flow in industrial processing [23].

Pullulans and dextrans (Figure 1) have not received the attention these fascinating polymers deserve, due to their lower trading volume and higher price. But in recent years their

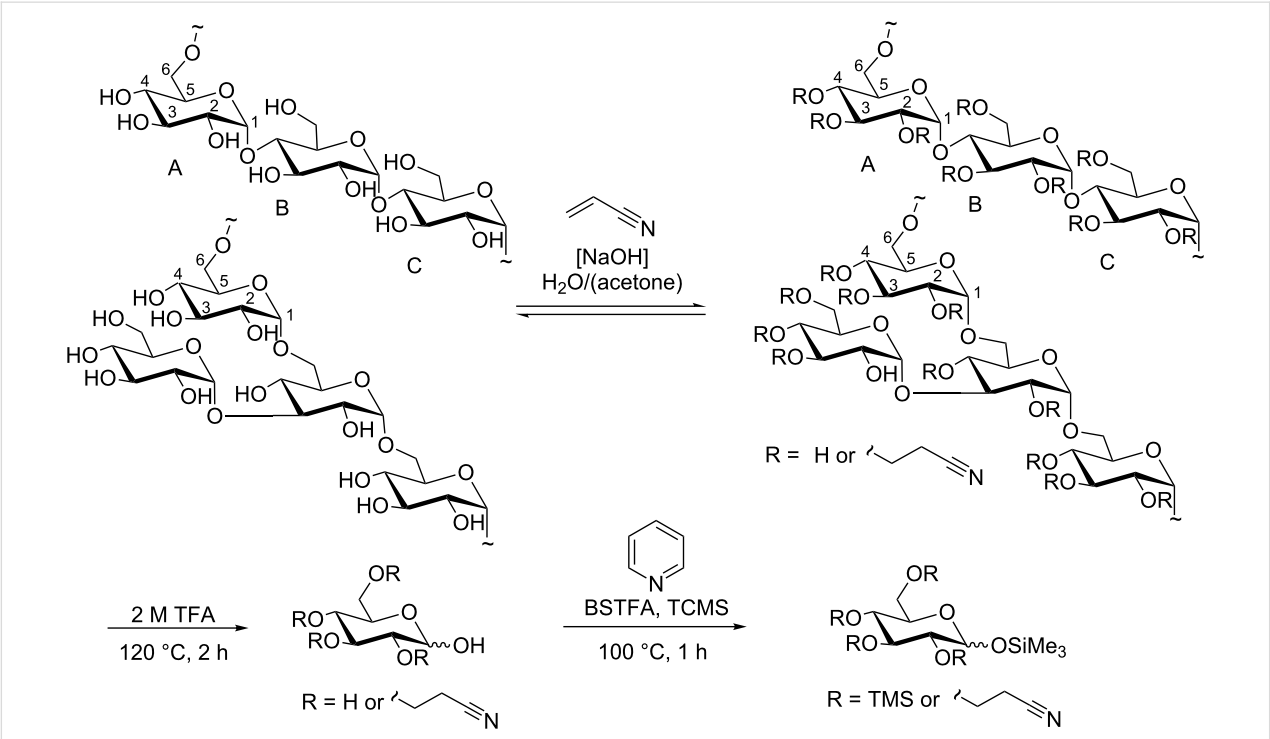

Figure 1: Polysaccharide structures of pullulan and dextran cyanoethylation with acrylonitrile and NaOH as catalyst; sample preparation for GLC/GLC–MS analysis: depolymerization and silylation.

importance for special biochemical or pharmaceutical applications, such drug delivery or biosensor technology, has grown, due to their special properties such as water solubility, low viscosity and film formation [24-27]. Pullulan is a homopolysaccharide of D-glucose secreted by *Aureobasidium pullulans*. The repeating units of this linear and regular glucan are maltotrioses (Glc-α-1→4-Glc-α-1→4-Glc), which are α-1→6-linked. Due to this linkage pattern, pullulan is very flexible and dissolves readily in water, with low viscosity. Films can be easily prepared. Pullulan is nontoxic, even edible, biocompatible and biodegradable [28,29]. Several applications in pharmaceutical and food technology have been reported. A summary for biotechnological applications of pullulan is given by Leathers [30].

Dextran is also a microbial glucan, e.g., from *Leuconostoc mesenteroides*. The main chain is α-1→6-linked and, in contrast to pullulan, randomly branched to various extent at positions O-3, O-4 and/or O-2, beside short stumps consisting of 1 to 2 glucose units; the 1–2% long-chain branching influences the properties of commercially available dextran [31-33]. Due to their nontoxicity and biocompatibility, dextrans are applied as blood-plasma expander. Dextran derivatives are used in many biomedical and bioanalytical applications [34] and are the subject of further developments in this field [35]. Therefore, we selected pullulan and dextran as candidates for a linear and a branched polysaccharide in our cyanoethylation studies. Cyanoethylglucans of different DS values were produced. Another objective of our approach was the detailed determination of the substitution pattern on the monomer level. Furthermore, nanostructuring of highly substituted cyanoethylglucans with and without ferromagnetic nanoparticles was investigated.

Results and Discussion

Synthesis and characterization of cyanoethylglucans

Dextran (6 kDa) and pullulan (100 kDa) were reacted with different amounts of acrylonitrile (AN) and sodium hydroxide in water. According to the patent of Onda [4], acetone was applied as a solubility mediator in some reactions. Reaction conditions were varied to obtain scarcely, moderately and highly substituted cyanoethylglucans. Products were isolated and purified by dialysis. Reaction parameters are shown in Table 1. DS values ranging from 0.74 to 2.40 (dextran, CED-1–CED-3) and 0.84 to 2.42 (pullulan, CEP-1–CEP-3) were obtained by GLC analysis. Up to a DS of around 1.50, the products were still water-soluble. Derivatives with a DS above 2 showed good solubility in acetone, DMSO or DMF. Product

Table 1: Conditions and results of cyanoethylation of dextran (6 kDa) and pullulan (100 kDa) with acrylonitrile (AN) and NaOH.

sample			CED-1	CED-2	CED-3	CEP-1	CEP-2	CEP-3
reaction conditions	mass educt	[g]	1.20	1.20	0.50	1.20	1.20	0.50
		[mmol/glc]	7.4	7.4	3.1	7.4	7.4	3.1
	H_2O	[mL]	4	4	5	4	4	5
	acetone	[mL]	–	1	4.75	–	1	4.75
	NaOH	[equiv/glc]	0.2	0.2	2	0.2	0.2	2
	AN	[mL]	1.9	1.9	4.65	1.9	1.9	4.65
		[equiv/glc]	4	4	23	4	4	23
	time	[h]	0.5	0.5	24	0.5	0.5	24
	temperature	[°C]	45	45	20	45	45	20
	mass product	[g]	1.23	1.30	0.77	1.17	1.29	0.71
DS	$DS_{EA(N)}$[a]		0.86	1.46	2.68	0.90	1.35	2.32
	$DS_{EA(CN)}$[b]		0.91	1.55	2.72	0.97	1.42	2.32
	$DS_{NMR(1)}$[c]		1.01	1.81	2.37	–	–	–
	part. $DS_{NMR(2)}$ at O-2[d]		0.47 (46.1)	0.72 (39.6)	–	–	–	–
	$DS_{NMR(3)}$[e]		0.97	1.61	2.51	0.89	1.31	2.43
	DS_{GC}[f]		0.74	1.39	2.40	0.84	1.52	2.42
	DS_{GC}[g]		0.85	1.52	2.52	0.91	1.55	2.48
yield[h]			77–83	86–74	82–86	74–76	72–75	79–81

[a]DS calculated from elementary analysis (based on N content). [b]DS calculated from elementary analysis (based on C/N ratio). [c]DS calculated from ^{1}H NMR according to Equation 1. [d]Partial DS in position 2 calculated from ^{1}H NMR according to Equation 2, % of total $DS_{NMR(1)}$. [e]DS calculated from ^{1}H NMR according to Equation 3. [f]DS calculated from GLC analysis; only cyanoethyl derivatives considered. [g]DS calculated from GLC analysis; *O*-carboxyethyl side products (TMS esters) are included. [h]Range calculated based on the lowest and highest DS value obtained by the different methods a–c, e and f.

characterization was carried out by elementary analysis (EA), ^{1}H NMR spectroscopy, and infrared spectroscopy (ATR–IR). Gas–liquid chromatography (GLC) in combination with mass spectrometry (MS) was employed for the analysis of glucose derivatives after depolymerization of the cyanoethylglucans.

The DS of heterogenic atoms containing polysaccharide derivatives can be followed by elementary analysis. To avoid misinterpretations due to impurities of the polymer sample, it should be checked whether the DS usually calculated from the nitrogen content is in accordance with the ratios of the other elements. Therefore, we evaluated the DS_{EA} from the N content and additionally from the C/N ratio. Results are given in Table 1. $DS_{EA(C/N)}$ was 0 to 7.8% higher than $DS_{EA(N)}$. In the following the functionalized glucans were investigated by ATR–IR spectroscopy. The characteristic C≡N stretching vibration was detected at 2250 cm^{-1} increasing with DS, while the intensity of the OH stretching (3400 cm^{-1}) decreased, with the maximum being shifted to higher wavenumbers (→ less hydrogen bonding). No side products, such as amides or carboxylates (as hydrolysis products of nitrile groups), or only traces thereof, were observed [21]. ATR–IR spectra of native dextran and the cyanoethyl ethers are shown in Figure 2. Figure 3 shows the ATR–IR spectra for pullulan and the corresponding cyanoethyl ethers.

^{1}H NMR spectroscopy is a versatile and fast method for qualitative and quantitative structural analysis. Figure 4 presents the ^{1}H NMR spectra of cyanoethyldextrans CED-2 and CED-3 in comparison with the unmodified polysaccharide. DMSO-d_6 was used as a solvent for the derivatives with a DS > 2 and D_2O for the less-substituted polyglucans.

The spectra of *O*-cyanoethylglucans show strong peak broadening and therefore worse resolution compared to the starting material (Figure 4 and Figure 5). The signal at 2.82 ppm in D_2O and 2.75 ppm in DMSO is assigned to the methylene group

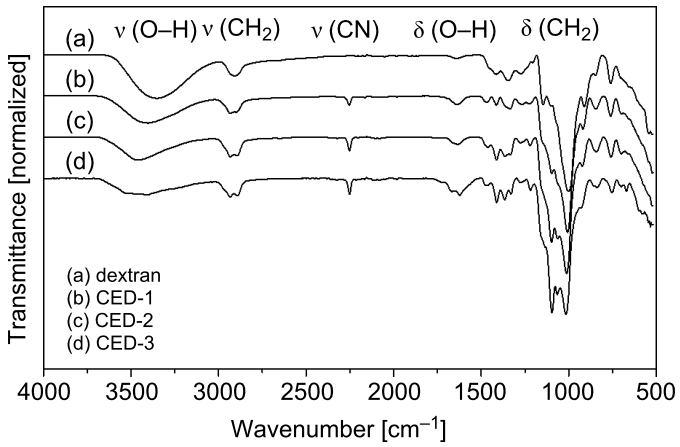

Figure 2: ATR–IR spectra of (a) dextran, 6 kDa, and cyanoethyldextrans (b–d) CED-1–3.

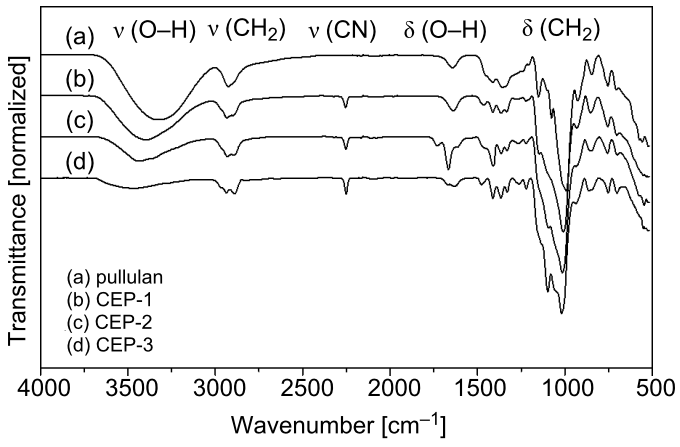

Figure 3: ATR–IR spectra of (a) pullulan, 100 kDa, and cyanoethylpullulans (b–d) CEP-1–3.

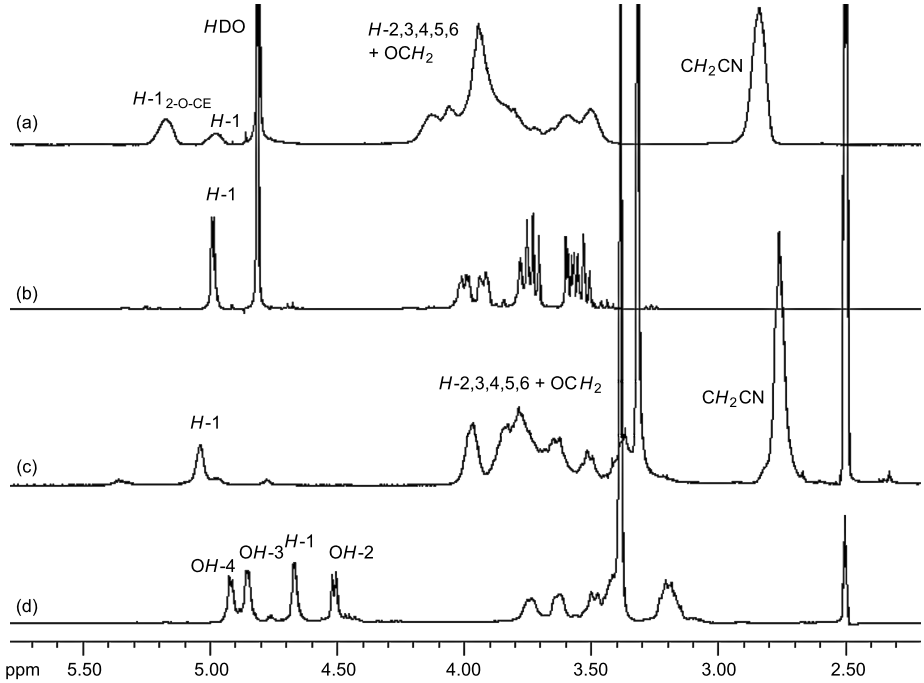

Figure 4: ^{1}H NMR spectra (300 MHz) of (a) CED-2 ($DS_{NMR(1)}$ = 1.81) in D_2O; (b) dextran, native in D_2O; (c) CED-3 ($DS_{NMR(1)}$ = 2.37) in DMSO-d_6; (d) dextran, native in DMSO-d_6; calibrated with solvent signals.

adjacent to the cyano function (CH_2–CN). The remaining protons of the cyanoethyl substituent overlap with sugar ring protons in the range of 3.3–4.2 ppm. As a result of 2-*O*-substitution, *H*-1 is shifted downfield. For the α-1→6-glucosyl residues of dextrans (in D_2O) it is shifted from 4.97 to 5.16 ppm. The average DS value was calculated from the ratio of the signal integrals of the methylene group adjacent to the nitrile group, to the summarized integrals of *H*-1 (Equation 1). DS evaluation in position 2 is also possible (Equation 2).

$$DS_{CE} = \frac{\frac{1}{2}\int CH_2CN}{\int H\text{-}1 + \int H\text{-}1_{2-O-CE}} \quad (1)$$

$$DS_{2-O-CE} = \frac{\int H\text{-}1_{2-O-CE}}{\int H\text{-}1 + \int H\text{-}1_{2-O-CE}} \quad (2)$$

For cyanoethylated pullulan, the situation is more complex as is obvious from Figure 5. While the NMR spectrum of the native pullulan in D_2O is well resolved with *H*-1 signals at 4.90 (α-1→6-Glc, ring C), 5.30 ppm (α-1→4-Glc, ring A) (α-1→4-Glc, ring B), the signals are shifted downfield by *O*-cyanoethylation and peak broadening occurs, probably due to a poorer solution state of the much more hydrophobic derivatives, and higher viscosity. The region of the anomeric protons becomes very complex and is difficult to integrate. It is assumed that for the 2-*O*-cyanoethylglucoses, the *H*-1 of the glucosyl residues A, B and C (Figure 1) are differentiated by ^{1}H NMR spectroscopy. In DMSO the OH resonances overlap with *H*-1 protons (Figure 5c and Figure 5d) [36]. The signals are shifted by substitution and the resolution becomes poor. Nevertheless, DS can alternatively be estimated from the integral of the CE-methylene group at 2.82 and the sugar ring protons, which are corrected for the equal contribution by the CE substituent according to Equation 3.

$$DS_{CE} = \frac{\frac{1}{2}\int CH_2CN}{\frac{1}{6}\left(\int H2,3,4,5,6_{a,b} - \int CH_2CN\right)} \quad (3)$$

To gain more detailed insight into the distribution of substituents in the glucosyl units, the cyanoethylated glucans were hydrolyzed and subsequently trimethylsilylated. The resulting trimethylsilyl *O*-cyanoethyl-*O*-trimethylsilyl-α,β-D-glucosides were analyzed by GLC–FID [3]. Peaks were assigned according to the position of cyanoethylation by GC–MS (Figure 6). Pairs of α- and β-glucosides were observed for each pattern. In addition, minor peaks of *O*-carboxyethyl derviatives (as $SiMe_3$ esters) were observed, since hydrolysis of the cyano group could not be avoided completely. However, quantitative evaluation, with and without considering these side

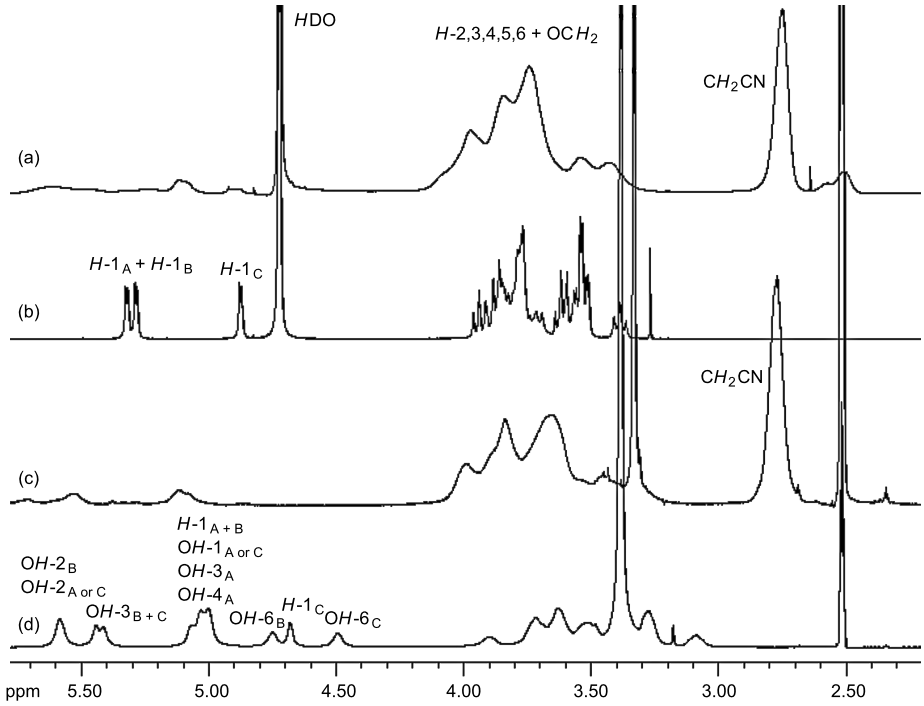

Figure 5: ^{1}H NMR spectra (400 MHz) of (a) CEP-2 ($DS_{NMR(3)}$ = 1.31) in D_2O; (b) pullulan, native in D_2O; (c) CEP-3 ($DS_{NMR(3)}$ = 2.43) in DMSO-d_6; (d) pullulan, native in DMSO-d_6; calibrated with solvent signals.

products, did not effect significant differences in the relative substituent distribution, but only an underestimation of the average DS_{GC} of up to 12%. Obviously, the rate of hydrolysis of the peripheral CN groups is decoupled from the carbohydrate backbone and thus independent of the position. Both DS_{GC} values are given in Table 1.

Based on monomer analysis, a statistical evaluation can be performed. Neglecting 6-*O*-substitution at terminal residues, eight different constituents are expected for cyanoethyldextran: unsubstituted (s_0), monosubstituted at position 2, 3, or 4 (s_2, s_3, s_4), disubstituted at positions 2,3, 2,4, or 3,4 (s_{23}, s_{24}, s_{34}), and 2,3,4-tri-*O*-substituted glucose (s_{234}). For pullulan, 6-, 2,6-, 3,6-, and 2,3,6-patterns must be additionally considered. With the exception of 6-*O*-CE-glc, these patterns were not detected for cyanoethyldextrans. The tetra-*O*-substituted glucosyl unit (s_{2346}), a possible product of the terminal residue, was neither detected for pullulan nor for dextran ethers.

For the statistical evaluation of the monomer data of cyanoethyldextrans, substitution at O-6 was neglected, i.e., 6,*n*-*O*-substituted glucosyl units were added to the *n*-*O*-substituted group. The number of monomer patterns considered was thus reduced to eight. In case of pullulan, consisting of α-1→6 linked maltotriose repeating units (Figure 1), patterns including 4- or 6-*O*-substitution were weighted according to their availability of 1:2 calculated for a random distribution. Random patterns were calculated considering the partial DS values determined for the different OH groups. The results of monomer analysis and statistical evaluation are summarized in Table 2. The peak areas from GLC–FID measurements were corrected according to the effective response concept [37].

CED-1 and CEP-1, modified without the cosolvent acetone, showed the lowest DS values. Upon addition of 1 mL acetone (Table 1), while the other parameters of the reaction were maintained, the DS value increased by nearly 100% (CED-2 and CEP-2). The highest DS values were achieved under the conditions according to Onda (CED-3 and CEP-3) [4]. In this approach acetone and acrylonitrile were used in the same ratio. The base concentration and reaction time were increased (2 equiv NaOH/glc) and the reaction was performed at rt. Acetone acts as a solvent intermediator and probably improves the contact of acrylonitrile and glucan. In addition, it keeps the product in a solution state, even at increasing DS.

The results of GLC analysis demonstrate that the thermodynamically controlled regioselectivity for the cyanoethylation follows the order O-2 > O-4 > O-3 for all CE-dextrans. The order of partial DS values for CE-pullulans changes with increasing DS (and thus with the reaction conditions), in favor of the primary 6-OH. Considering the relative proportions of the OH groups,

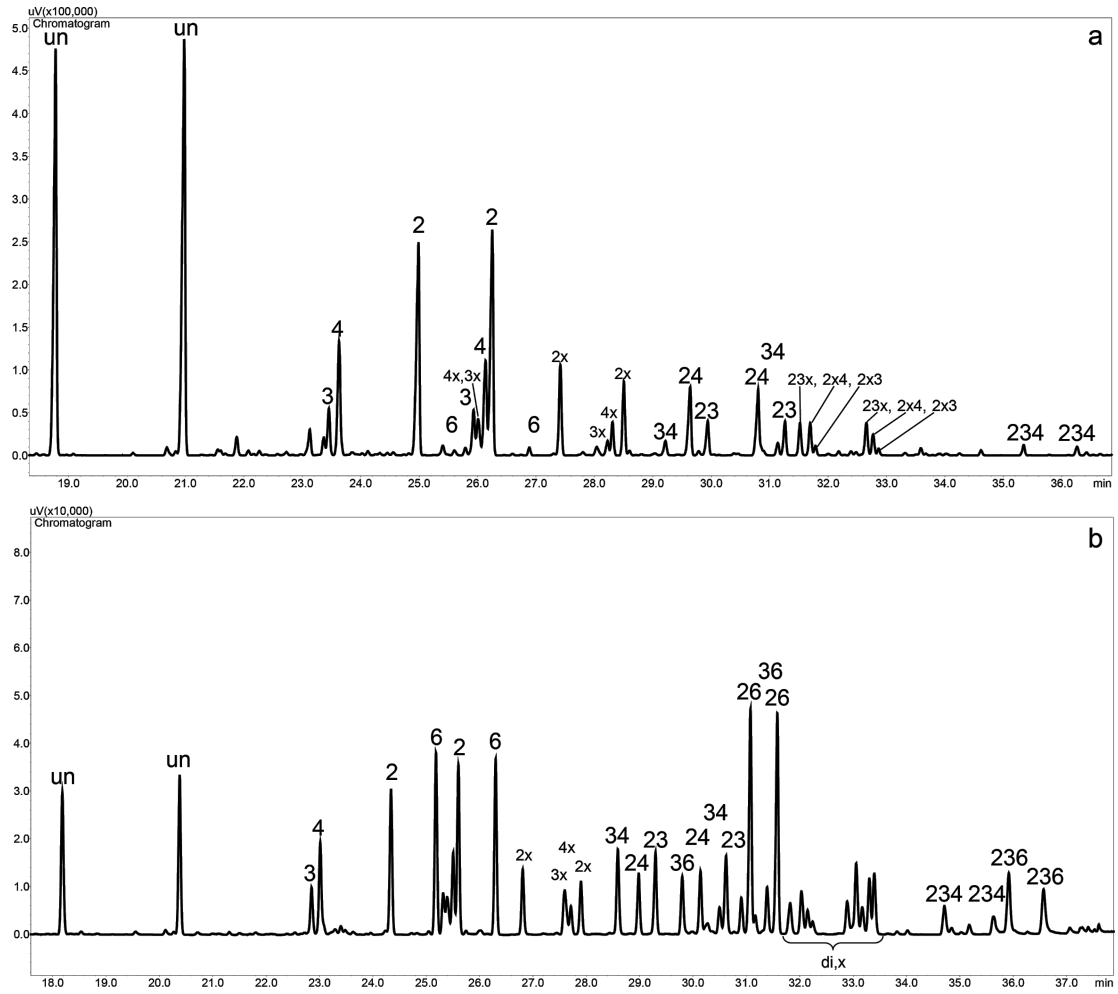

Figure 6: Gas chromatogram of hydrolyzed and trimethylsilylated cyanoethylglucans; (a) CED-1 (DS_{GC} = 0.74); (b) CEP-2 (DS_{GC} = 1.52); x = side products with hydrolyzed cyanonitrile, i.e., carboxyethyl-TMS-ester group; di,x = 3x,6CE, 2 or 4x,CE, 2x,6CE, 3x,6CE, 2 or 4x,CE, 2x,6CE); un: unsubstituted glc.

Table 2: Monomer composition [mol %] (s_n) of un-, mono-, di- and tri-substituted glucose units (c_n) (DS_{GC} calculated without *O*-carboxyethyl dervia-tives) and partial degrees of substitution (x_n) at position 2, 3, 4, 6; H_1: heterogeneity parameter.

		CED-1	CED-2	CED-3	CEP-1	CEP-2	CEP-3
monomer composition [mol %]	s_0	43.20	14.97	2.29	37.90	11.32	0.49
	s_2	24.61	21.76	2.92	25.39	11.82	1.05
	s_3	4.85	5.39	2.65	4.28	3.52	0.88
	s_4	11.86	12.19	3.38	3.65	6.86	1.26
	s_6				9.02	13.98	6.63
	s_{23}	4.02	11.41	13.58	2.94	7.03	3.69
	s_{24}	8.46	21.36	6.80	2.97	5.23	1.12
	s_{26}				6.28	19.66	15.07
	s_{34}	1.80	4.46	15.39	4.20	5.26	6.54
	s_{36}				1.62	4.81	10.14
	s_{234}	1.20	8.46	52.99	0.33	3.34	16.53
	s_{236}				1.41	7.17	36.60

Table 2: Monomer composition [mol %] (s_n) of un-, mono-, di- and tri-substituted glucose units (c_n) (DS_{GC} calculated without *O*-carboxyethyl dervia-tives) and partial degrees of substitution (x_n) at position 2, 3, 4, 6; H_1: heterogeneity parameter. (continued)

number of cyanoethyl groups	c_0	43.20	14.97	2.29	37.90	11.32	0.49
	c_1	41.31	39.34	8.95	42.35	36.17	9.82
	c_2	14.28	37.23	35.78	18.01	41.99	36.55
	c_3	1.20	8.46	52.99	1.74	10.51	53.14
partial DS values	x_2	0.38	0.63	0.76	0.39	0.54	0.74
	%	52.12	45.27	31.85	47.05	35.76	30.56
	x_3	0.12	0.30	0.85	0.15	0.31	0.74
	%	16.15	21.35	35.34	17.69	20.52	30.70
	x_4	0.23	0.46	0.79	0.11	0.21	0.25
	%	31.73	33.38	32.81	13.35	13.64	10.50
	x_6				0.18	0.46	0.68
	%				21.92	30.07	28.24
	DS	**0.74**	**1.39**	**2.40**	**0.84**	**1.52**	**2.42**
	H_1[a]	0.30	0.39	0.51	0.43	0.43	0.55

[a] $H_1 = \sqrt{\sum_{i=0}^{234} \Delta s_i^2} / n$, $\Delta s_i = s_i$ (theor.) – s_i, with s_i = mol fraction of glucose units substituted in position i, n = 8 for dextran, n = 12 for pullulan; (mean values calculated by twofold determination of the molar composition of the corresponding TMS derivatives by GLC–FID).

namely 3:3:1:2 for O-2, O-3, O-4, and O-6, the degree of conversion follows the order O-6 > O-4 > O-2 > O-3 for CEP-2 (DS = 1.52), with the three secondary OH being equalized for CEP-3 (DS = 2.42). Only for CEP-1, with the lowest DS (0.84), the most acidic 2-OH dominates, and 4-OH shows higher conversion than primary O-6. Comparing pullulan with dextran, the preference for 2-*O*-cyanoethylation is less pronounced in pullulans, in which one third of the 4-OH is "substituted" by the primary 6-OH. In former work, we found a higher preference for 6-O-substitution (50%) over 2-O-substitution (37%) for exclusively α-1→4-linked amyloses reacted in an aqueous paste [3]. The heterogeneity parameter H_1 indicates the average deviation of experimental data from a random distribution, taking into account the relative partial DS values (x_i) found for the various OH groups. A DS dependency of H_1 is inherent when employing this equation, since DS is limited to the range of 0–3. The highest heterogeneity can be calculated at medium DS values of around 1.5. Approximating the limits (DS = 0 and 3), less deviation is possible. The evaluated heterogeneity values are low, as was expected for a thermodynamically controlled reaction [38]. Minor deviations from the random model are within experimental error. Corresponding graphics are shown in Figure 7 and Figure 8.

By all three of the methods applied, similar DS values were obtained. Elementary analysis is a fast method employing the entire material. However, it is important not only to take the nitrogen content for the estimation of DS, but also to check whether the relative amounts of C and H are in accordance with this, since the N content can be lowered by nitrogen-free impurities or be enhanced by residual side products from the reagent. DS_{GC} values calculated by including the *O*-carboxyethyl derivatives were in good agreement with the DS_{EA}. The DS_{GC} calculated values without these side products were decreased. This is plausible, since the side reaction mentioned makes the product pattern even more complex and does not allow detection and identification of all minor components, thus discriminating the DS. NMR spectroscopy can be applied to the intact polymer and gives more detailed information than EA. However, broadening and splitting of peaks into different types of H_1 depending on the position of linkage and substitution makes it difficult to assign and integrate all relevant resonance signals. This is obvious from the differences obtained when employing different signals for the calculation (Equation 1 and Equation 3). Only after depolymerization it was possible to determine the detailed substitution pattern by GLC analysis.

In general, good isolated yields in the range from 72 to 86% were achieved (Table 1). The DS values strongly increased upon the addition of acetone as a solubility mediator (CED-2 and CEP-2). No side products, such as amides or carboxylates, or only traces thereof, were detectable for the CE glucans, as proved by IR and NMR measurements (^{1}H and ^{13}C). A homopolymerization of acrylonitrile could be excluded since the DS_{EA} from N and C/N were very close and only moderately enhanced compared to the DS_{GC}.

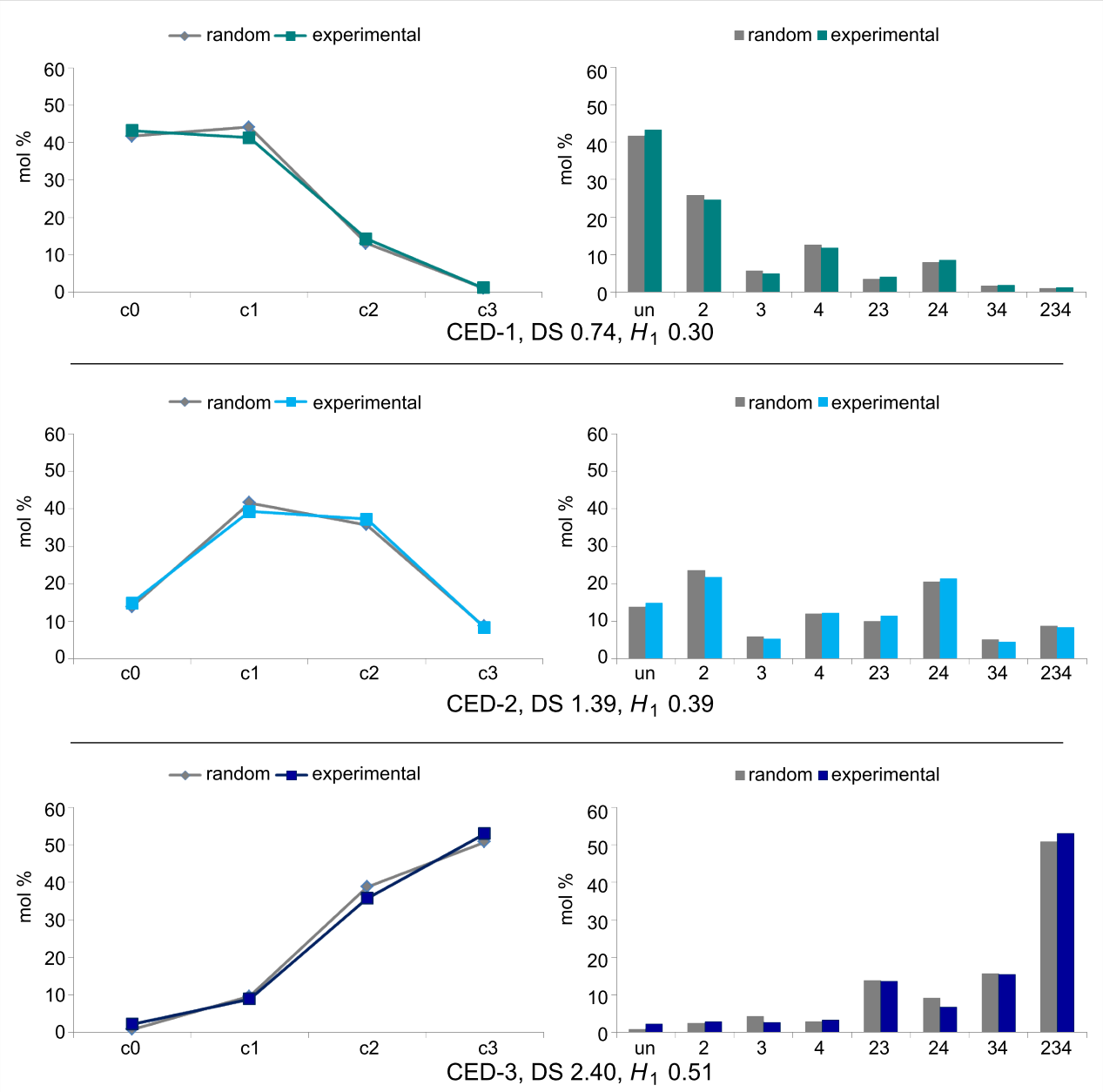

Figure 7: Experimentally determined substituent distribution in the glucosyl units (glc) of cyanoethyldextrans CED-1–3 (blue) compared with a random distribution (gray). Left: ci = the fraction of i-fold-substituted glucosyl units (mol %); right: un = unsubstituted glc; the numbers assign the substituted positions, e.g., 234 = 2,3,4-tri-*O*-cyanoethyl glc; H_1 heterogeneity parameter for the standard deviation as defined in Table 2.

Nanostructures of cyanoethylglucans

In the next step the ability of cyanoethylglucans to form nanoparticles was investigated [12-14,39]. DMSO solutions of the cyanoethylpolysaccharides CEP-3 (DS_{GC} = 2.42) and CED-3 (DS_{GC} = 2.40) were submitted to dialysis against water. Only the derivatives with a DS value >2 formed regular particles that were stable in water for several weeks without precipitation [13]. Furthermore, the same procedure was performed in the presence of ferromagnetic iron oxide nanoparticles. The magnetic cores were prepared by a precipitation process of Fe(II) and Fe(III) chlorides (molar ratio 1.7:1.0) with aqueous ammonia solution [40,41]. After ultrasonic treatment the resulting particles were fixed with strong magnets and washed with distilled water. Monodisperse and regularly shaped iron oxide nanoparticles were obtained as shown by TEM (Figure 9). The iron concentration of the nanoparticle dispersion, as analyzed with inductively coupled plasma optical emission spectroscopy (ICP–OES), was 37.2 g/kg. The particle size was calculated by image data processing of the TEM micrograph resulting in a mean diameter of 12.2 nm ± 2.6 nm. The hydro-

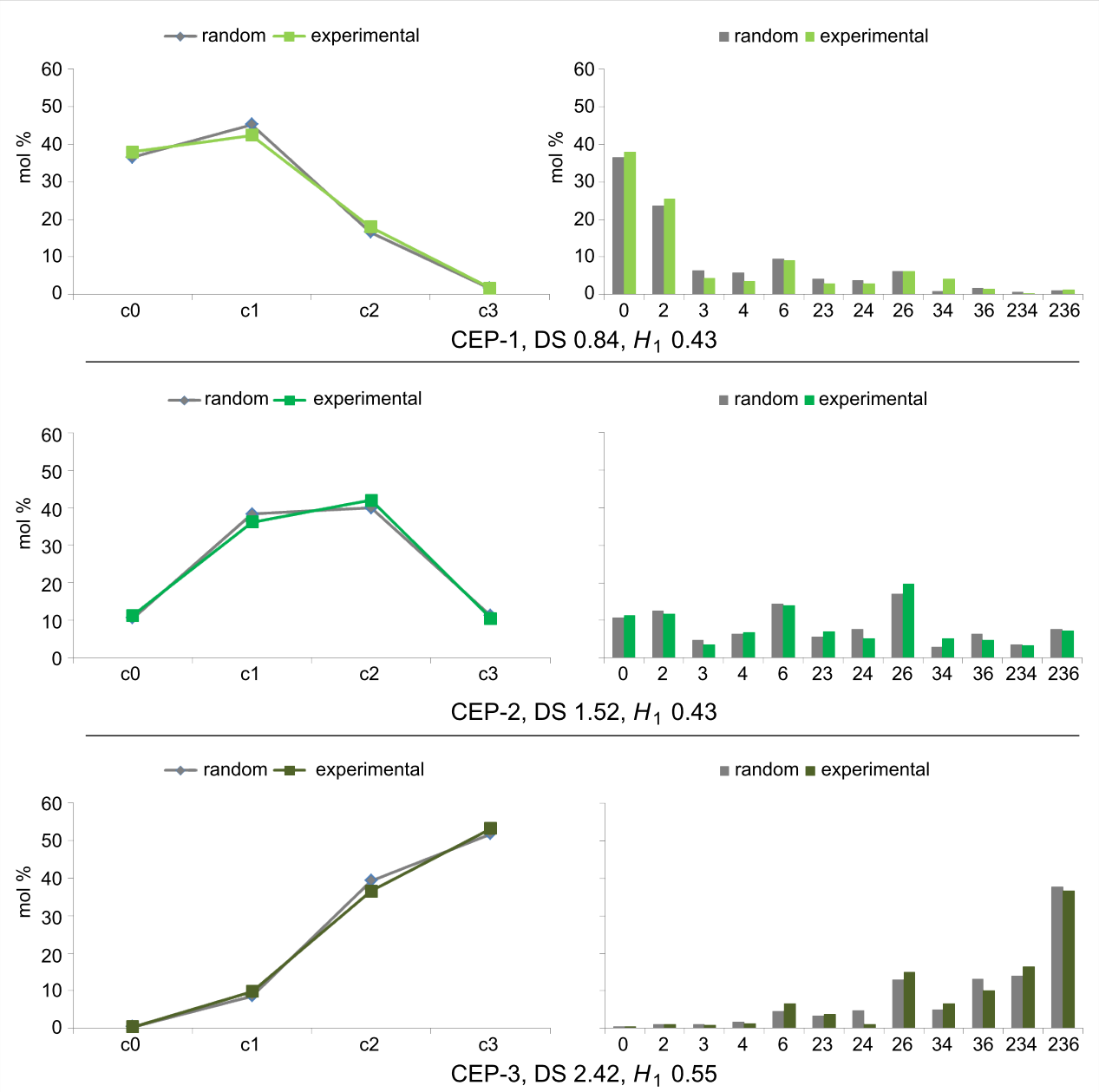

Figure 8: Experimentally determined substituent distribution in the glucosyl units (glc) of cyanoethylpullulans CEP-1–3 (green) compared to a random pattern (gray). Left: c_i = the fraction of i-fold-substituted glucosyl units (mol %); right: un = unsubstituted glc; the numbers assign the substituted positions, e.g., 234 = 2,3,4-tri-*O*-cyanoethyl glc; H_1 heterogeneity parameter for the standard deviation as defined in Table 2.

dynamic diameter was estimated at 27 nm by dynamic light scattering (DLS) measurements. Agglomeration or aggregation processes were prohibited by pH stabilization. At pH 2 the iron oxide dispersion is stable for several months without precipitation.

After the dialysis process of the high-DS cyanoethyldextran and pullulan (20 mg, CED-3, DS_{GC} = 2.40; CEP-3, DS_{GC} = 2.42) the hydrodynamic diameter of the particles was determined by DLS. Additionally, scanning electron microscopy (SEM) micrographs were recorded. Using SEM the morphology of polysaccharide particles is accessible. The parameters and results of the DLS and SEM measurements are summarized in Table 3.

DLS measurements were in good agreement with the evaluation of the electron microscopy images. According to the micrographs, the morphology of the cyanoethyl nanoparticles can be considered as spherical. Representative SEM pictures of CEP-3 + Fe-np (Table 3, entry 2) are shown in Figure 10.

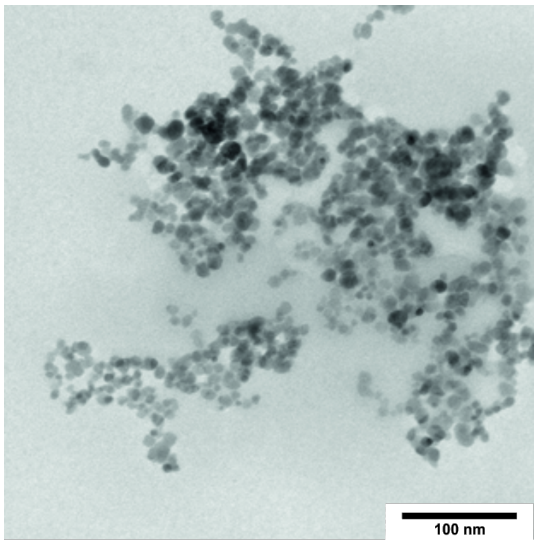

Figure 9: TEM micrograph of iron oxide nanoparticles prepared from an aqueous dispersion.

The influence of different amounts of ferromagnetic nanoparticle dispersion was investigated (10–200 µL or equivalently 0.0067–0.1332 mmol Fe/0.07 mmol glucosyl units, or 0.165 mmol CE). Independent preparation of the ferromagnetic nanoparticles has the advantage that nanostructuring can be performed on a small scale. Coprecipitation methods, in which magnetic particles are formed and simultaneously coated, require higher amounts of polymer [42] (up to gram scale) and deliver irregularly shaped particles [13]. Increasing the amount of metal oxide from 0.0133 to 0.1332 mmol iron (20–200 µL) with 20 mg polymer (= 0.07 mmol glucosyl units, respective 0.165 mmol CE) resulted in smaller particles (Table 3). The upper limit is 200 µL ferrofluid (0.1332 mmol Fe/0.165 mmol CE). Below this limit the whole of the iron core is entrapped. Higher amounts of iron oxide resulted in multimodal, aggregated particles and precipitation. Interestingly, the smallest particles were formed without iron oxide (Table 3, entry 6 and 7, 260 nm, respectively 331 nm). Magnetic properties depend on the amount of iron and can be adjusted by varying the

Table 3: Parameters and characterization of nanostructures formed from CED-3 and CEP-3, in the absence and presence of ferromagnetic nanoparticles, by DLS and SEM measurements; 20 mg of cyanoethylglucan was used for each entry (= 0.07 mmol glucosyl units).

sample	CE-glucan[a]	iron oxide nanoparticle dispersion		diameter		
		[µL]	Fe [mmol]	DLS [nm]	SEM ± [b] [nm]	No[c]
1	CEP-3	10	0.0067	611	613 ± 174	(69)
2	CEP-3	20	0.0133	399	388 ± 93	(335)
3	CED-3	10	0.0067	337	514 ± 205	(92)
4	CED-3	20	0.0133	444	451 ± 113	(27)
5	CED-3	200	0.1332	252	–	
6	CEP-3	–	–	241	260 ± 57	(182)
7	CED-3	–	–	203	331 ± 71	(308)

[a]20 mg (= 0.07 mmol glucosyl units, or 0.165 mmol CE); [b]standard deviation; [c]number of evaluated particles

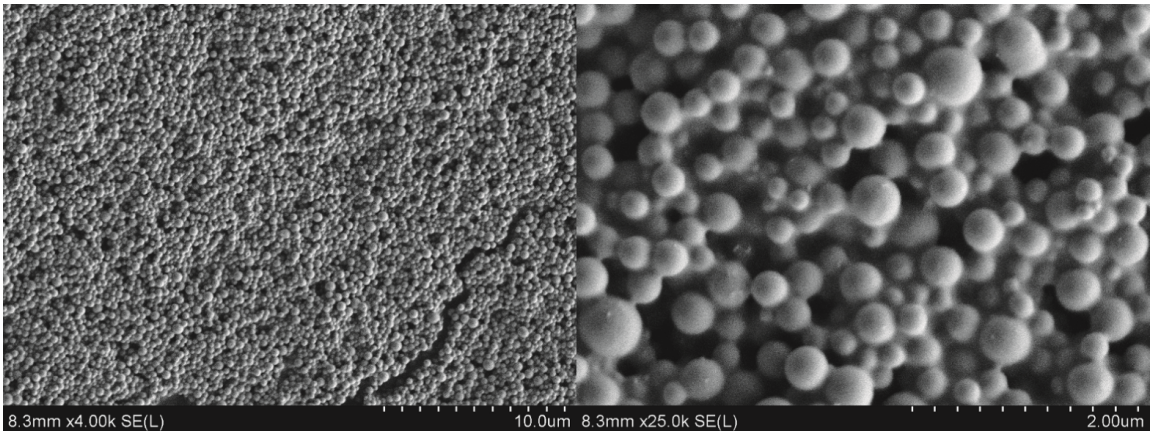

Figure 10: SEM micrographs of CEP-3 with iron oxide nanoparticles, (Table 3, entry 2).

doping of the glucan particles with iron. Nanostructuring of cyanoethyldextrans and cyanoethylpullulans show no significant differences, although in one case a branched polymer with 6 kDa and on the other hand a 100 kDa linear macromolecule was employed.

Energy-filtered transmission electron microscopy (EF–TEM) is an appropriate method to characterize the structure, morphology and the redox state of metal-containing nanoparticles. Parallel electron energy loss spectroscopy (PEELS) analyses were performed with the uncoated and coated iron oxide nanoparticles in Figure 11. The energy loss functions have been summed from 690 to 740 eV. Figure 11c shows the Fe $L_{2,3}$ edge spectra of the uncoated iron oxide particles (red line) relative to the polysaccharide coated particles (blue line) and a reference iron, Fe(0) spectrum (dashed black line) [43]. The intensity is comparably low (Figure 12c) due to the particle size, exceeding the ideal thickness of 30 to 40 nm for EELS analysis. Nevertheless, a typical intensity profile of Fe $L_{2,3}$ can be seen, at an energy resolution of 1.2 eV. The uncoated metal oxide particles show

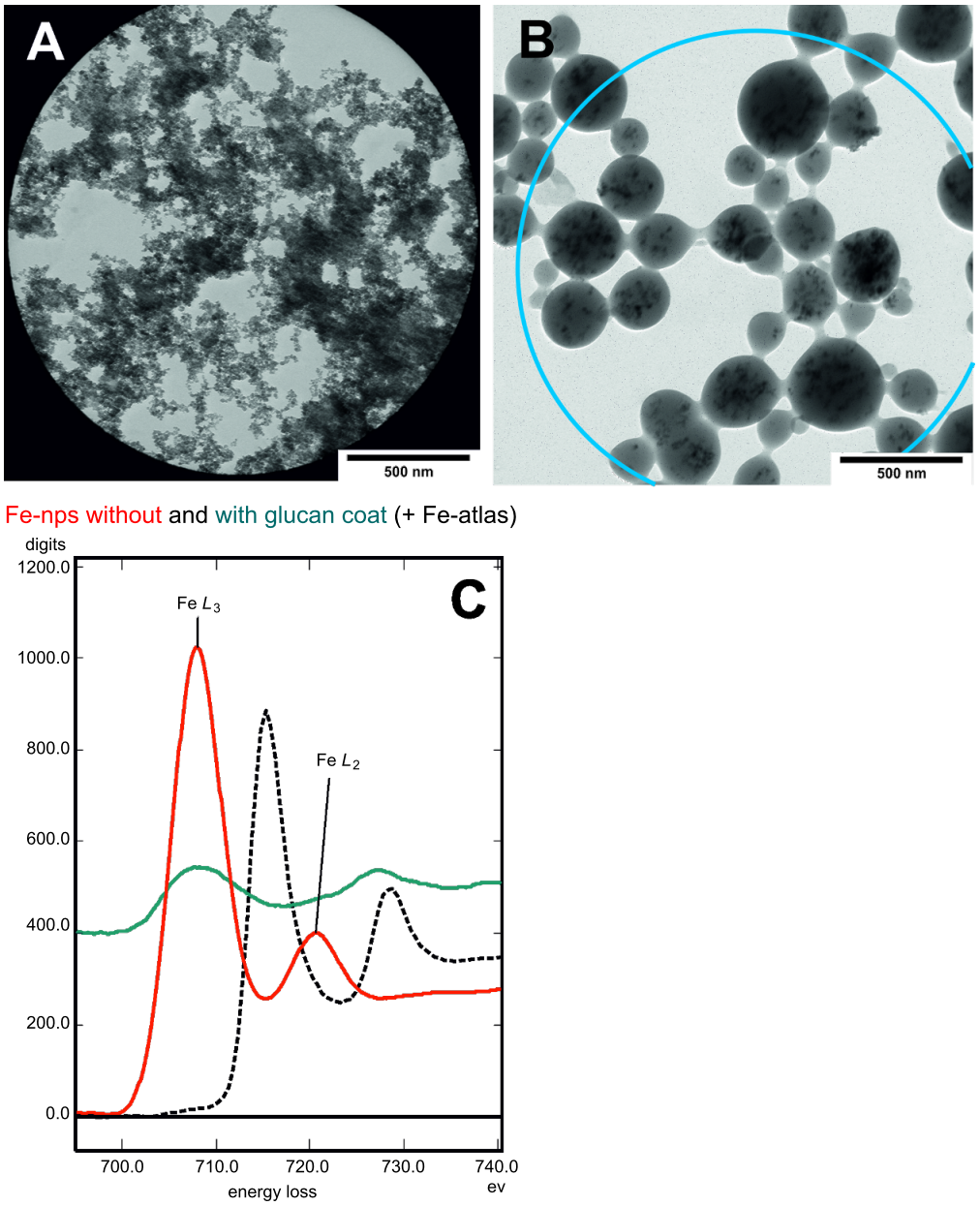

Figure 11: TEM micrograph of (a) uncoated iron oxide nanoparticles; (b) of CEP-3 + iron oxide nanoparticles (no stain), Table 3, entry 1; (c) PEELS measurements of uncoated iron oxide particles (red line), polysaccharide coated particles (blue line) and the Fe(0) atlas reference spectrum (black, dashed line); PEELS measuring areas are shown as aperture in A and circle in B; for details see text.

maxima of 708.2 eV and 720.7 eV for the L_3 respective L_2 edge. In the case of the coated particles, the maxima were determined at 711.4 eV for L_3 and 728.9 eV for the L_2 edge, showing a significant chemical shift, and differences in the spin orbit splitting, i.e., 17.5 eV for coated iron oxide cores versus 12.5 eV for noncoated particles were observed, based on individual measurements. The L_3–L_2 peak maxima distance is defined as the spin orbit splitting for "white-line" elements, such as transition elements and lanthanides, and the L_3/L_2 ratio is indicative of the oxidation state of the element [44,45]. Cressey described the possibility to characterize multiple valence states of 3*d* metals by *L*-edge spectra [46]. By comparing our data with theirs, it is shown that Fe^{2+} and Fe^{3+} are present. The spin orbit splitting reflects the influence of the electronic state of the iron oxide core and obviously an interaction with the nitrile groups should be considered [45,47].

Entrapping of iron oxide cores during the carbohydrate nanostructuring process is proven by the electron micrographs. Figure 12 shows the net iron distribution, colored red, in the multicore particles in detail. Due to the material thickness, which is beyond the ideal 30–40 nm, common for EELS measurements, only iron oxide particles near the surface show strong intensity signals. No free iron particles were detected on the carbon foil of the electron microscopic grid or in the waste water after the dialysis step, proving that all of the iron was specifically bound by the cyanoethylglucans. The hydrophobic cyanoethyl groups are expected to "hide" inside the particles, but depending on the distribution of these residues, some can also be directed towards the water phase. These substituents may bind iron oxide particles additionally. This observation could indicate that some cyanoethyl groups are available for further transformation of the outer sugar shell, e.g., amino functionalization followed by coupling with bioactive molecules. In conclusion, it was shown, that the magnetic iron cores were captured by the cyanoethyl-functionalized polysaccharides.

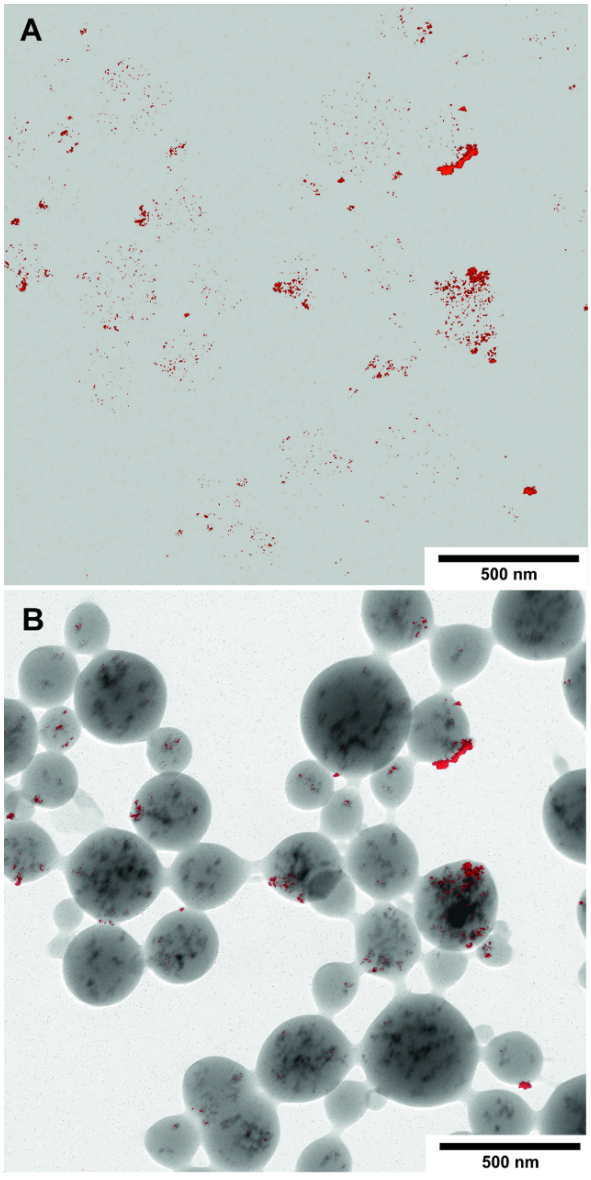

Figure 12: ESI Fe distribution maps of CEP-3 with iron oxide nanoparticle (Table 3, entry 1). (A) Net Fe, shown in red. Because of the signal dimensions, much of the signal intensity is lost, leading to only a weak mapping signal within the corresponding particles; (B) Fe map (red) overlaid on the zero-loss image.

Conclusion

Cyanoethylation by Michael addition is a versatile tool for polysaccharide modification. The hydrophobic substituents were introduced up to a DS of ca. 2.4 through choice of the appropriate conditions. Average reactivity of the α-glucans dextran and pullulan was very similar. The order of substitution was O-2 > O-4 > O-3 for dextran, while the relative degree of conversion changed with the DS from O-2 > O-4 > O-6 > O-3, in favor of primary O-6 for pullulan. The substituents present are randomly distributed in the glucosyl units, which is typical for reversible reactions and always favored in aqueous systems. High cyanoethylated glucans form regularly shaped nanostructures with diameters in the range of 260 to 613 nm. When dialysis was performed in the presence of ferromagnetic nanoparticles, glucan-coated multicore ferromagnetic nanostructures were formed. Quantitative entrapment of iron oxide during dialysis is obviously based on interactions of the cyanoethyl residues with the iron oxide core particles, as is indicated by TEM and PEELS measurements. Further modification of the cyanoethylglucans and their respective nanostructures by transformation to aminopropyl derivatives is under progress. These new particles possess great potential as precursors for amino-functionalized, magnetic architectures and electrochemical applications.

Experimental

Materials

Dextran from *Leuconostoc ssp*. (6 kDa) and pullulan (100 kDa) were purchased from Fluka. Acrylonitrile (AN) was supplied from Janssen. DMSO [puriss, absolute, over molecular sieves ($H_2O \leq 0.01\%$), $\geq 99.5\%$ (GC)] was obtained from Sigma-Aldrich. Deionized water was used. Dialysis was performed with molecular porous dialysis membranes (molecular weight cut off 3.5 kDa) from Spectrum Laboratories. Bidistilled water was chosen for ICP–OES sample preparation.

Instrumentation

^{1}H NMR spectra were acquired on a Bruker AMX 300 spectrometer or a Bruker AMX 400 MHz Advance spectrometer at rt (around 5 mg sample in D_2O or DMSO-d_6). Chemical shifts are given in ppm relative to the residual solvent signals. ATR–IR spectra were recorded by using a Bruker Tensor 27 attenuated total reflectance infrared (ATR–IR) spectrometer. Elementary analysis (EA) was performed on a Thermoquest EA 1112 analyser. The data given is always the average of two measurements.

Gas–liquid chromatography (GLC) analysis was carried out with a GLC–FID instrument Shimadzu GC 2010 with a Phenomenex Zebron ZB5-MS column (30 m, i.d. 0.25 mm, film thickness 0.25 mm and 1.5 m). H_2 (40 cm s^{-1}, linear velocity mode) was used as a carrier gas. Data were recorded with a Shimadzu GC Solution Chromatography Data System (version 2.3). Peaks were identified by gas chromatography/mass spectrometry (GLC–MS) analysis. Conditions: injector 250 °C, temperature program: 60 °C (1 min); 20 °C/min to 130 °C, 4 °C/min to 260 °C, 50 °C/min to 310 °C (10 min), splitless. GLC–MS: Agilent 6890 GC (ZB5-MS column, 30 m, inner diameter 0.25 mm, film thickness 0.25 mm and 1.5 m) and a JEOL GC mate II bench-top double-focusing magnetic sector mass spectrometer. The iron content was determined with a Radialen ICP–OEC Vista MPX, from Varian, (power 1.20 kW, plasma gas 15 L/min (Ar), auxiliary gas 1.5 L/min (Ar), atomizer pressure 240 kPa, pump speed 20 rps). Atom emission lines: ion emission lines: 234.350/238.204/239.563/259.940/260.709/261.187 nm, and internal reference line: Ar, 470.067 nm. Sample preparation: 0.408 g iron nanoparticle dispersion was dissolved by adding 5 mL HCl (37%) and subsequently diluted to 100 mL with bidistilled water (ultrapure). Calibration was carried out with an external standard solution: Fe 10.000 mg/L (Specpure, Fa. Alfa Aesar).

Particle size determination

The hydrodynamic size was determined by using a Zetasizer Ver 6.0.1, Malvern Instruments Ltd. Scanning electron micrographs were recorded with a Hitachi S-4800 FE-SEM (Tokyo, Japan) at KTH, Sweden. Samples were prepared by putting a drop of each sample on the carbon film covered the metal studs and allowing it to dry. Samples were kept for at least 48 h in the desiccator prior to the analysis. Transmission electron micrographs were obtained by using a EF–TEM Libra 120 plus Zeiss microscope operated at 120 kV. The samples were adsorbed to a hydrophilized carbonfilm, which was supported by a Cu grid (carbon only, copper 300 square mesh) and dried at rt. All images, PEELS and ESI-sets were recorded with a 2×2k SharpEye cooled CCD camera (Tröndle, Moorenweiss, Germany) and directed by the ITEM software (OSIS, Münster, Germany). PEELS spectra (main settings: emission current = 2 μA; spectrum magnification 100×; illumination aperture = 0.5 mrad; spectrum registration = 5 s;) and ESI series (magnification 12500×; spectrometer entrance aperture = 100 μm; slit width = 9 eV; illumination aperture = 0.8 mrad; image registration = 50 s; E_{max}: 712 eV; W1: 690 eV; W2: 660 eV; emission current: 2 μA) of Fe and oxygen were processed, following adaptively the workflow as described by Hedrich et al. [48].

Cyanoethylation

Samples with DS < 2

The glucan (1200 mg, 7.4 mmol glc 100 kDa pullulan or 6 kDa dextran) was dissolved in water, and NaOH (60 mg, 0,2 equiv/glc) and acrylonitrile (1,941 μL, 4 equiv/glc) were added. In syntheses of CED-2 and CEP-2 1 mL, acetone was added. The mixture was stirred at 45 °C for 30 min. The product was purified from low-molecular-weight reagents and by-products by dialysis and freeze dried.

Samples with DS > 2

According to Onda [4], acrylonitrile (4.65 mL, 23 equiv/glc) and acetone (4.75 mL) were added to a solution of the polysaccharide (500 mg, 3.08 mmol glc 100 kDa pullulan or 6 kDa dextran) in water and NaOH (250 mg, 2 equiv/glc). The solution was stirred for 24 h at rt. The product was dissolved by the addition of acetone and precipitated by adding water three times.

Elementary analysis: CED-1: C, 47.65; H, 6.12; N, 5.79; CED-2: C, 50.06; H, 5.82; N, 8.53; CED-3: C, 54.60; H, 5.96; N, 12.23; CEP-1: C, 47.08; H, 6.27; N, 5.99; CEP-2: C, 50.10; H, 6.02, N 8.10; CEP-3: C, 54.55; H, 6.23; N, 11.41.

IR (diamant–ATR): $\tilde{\nu}$ = 3465 (s, OH, depending on DS), 2923, 2893 (m, CH, CH_2, aliph.), 2252 (w, C≡N, nitrile), 1640 (m, OH), 1167, 1467, 1409, 1324, 1271 (m, CH), 1099, 1009 (s, C-O).

^{1}H NMR of CED-1 and CED-2: ^{1}H NMR (D_2O, 300 MHz) δ (ppm) 5.19 (1H, *H*-1,substituted at position 2), 5.00 (1H, *H*-1,

unsubstituted), 4.20–3.37 (6H + DS × 2H, *H*-2,3,4,5,6a,b + OCH_2), 2.82 (2H, CH_2CN); CED-3: ^{1}H NMR (DMSO-d_6, 400 MHz) δ (ppm) 5.03 (1H, *H*-1), 5.40–4.64 O*H*-4, O*H*-3, O*H*-2 overlapped by *H*-1 shifted due to substitution), 4.10–3.62 (6H + DS × 2H, *H*-2,3,4,5,6,ab + OCH_2), 2.76 (2H, CH_2CN).

^{1}H NMR of CEP-1 and CEP-2: ^{1}H NMR (D_2O, 300 MHz) δ (ppm) 5.77–4.86 (O*H*-2, O*H*-3, of glucosyl unit A, B and C + *H*-1, substituted and unsubstituted of glucosyl unit A, B and C), 4.21–3.36 (6H, H-2,3,4,5,6,a,b + OCH_2), 2.80 (2H, CH_2CN); CEP-3: ^{1}H NMR (DMSO-d_6, 400 MHz) δ (ppm) 5.95–4.75 (O*H*-2, O*H*-3, of glucosyl unit A, B and C + *H*-1, substituted and unsubstituted, glucosyl unit A,B and C), 4.11–3.20 (6H, *H*-2,3,4,5,6,a,b + OCH_2), 2.77 (2H, CH_2CN).

Monomer analysis of cyanoethylpolysaccharides

The monomer composition of cyanoethyl derivatives was determined by GLC (twofold determination) after hydrolysis and trimethylsilylation according to [3]. The effective carbon response concept was applied for quantitative GLC–FID evaluation [37]. Peak areas were corrected by multiplication with the following factors: TMS O-CE/O-TMS-Glc: un- ≡ 1.0000, mono- 1.0694, di- 1.1491, and trisubstituted 1.2416; carboxyethyl-TMS-ester (from hydrolysis of the nitrile group): mono- 0.9250, di- 0.9840 (CH_2CH_2COOTMS/CE), 0.8605 (2 × CH_2CH_2COOTMS), trisubstituted 1.0511 (2 × CH_2CH_2COOTMS/CE).

Preparation of nanoscaled structures

Iron nanoparticle dispersion

A solution of a mixture of Fe(II) and Fe(III) chlorides in a molar ratio of 1.7:1.0 was prepared in distilled water. Aqueous ammonia solution (25 mL, 25%) was added and the mixture was heated at 70 °C for 30 min. After ultrasonic treatment the resulting particles were fixed with strong magnets, and the nonmagnetic products were removed by washing with distilled water three times and adjusted to pH 2.1 with HCl [17,40,41].

Polysaccharide nanoparticles

Polysaccharide (20 mg) was dissolved in 5 mL DMSO. Nanoparticles of cyanoethylglucans were prepared by a dialysis process against water [12]. For entrapping of iron oxide nanoparticles, various portions were mixed with the cyanoethylpolysaccharides before dialysis.

Acknowledgements

The authors are thankful to Dr. Ilka Grabs and Prof. Dr. Georg Garnweitner, Institute for Particle Technology, TU Braunschweig, for fruitful discussions and the opportunity of using their DLS instrument. Furthermore, the authors thank Prof. Dr. Thomas Heinze, Friedrich-Schiller-Universität Jena, for the introduction to the preparation of ferromagnetic nanoparticels. Thanks also go to Mrs. Christiane Schmidt, Institute for Ecological Chemistry, TU Braunschweig, for performing ICP-OES measurements, and Dennis Rosebrock, Institute for Robotics and Process Control, TU Braunschweig for the image data processing program.

References

1. Volkert, B.; Wagenknecht, W.; Mai, M. Structure-Property Relationship of Cellulose Ethers – Influence of the Synthetic Pathway on Cyanoethylation. In *Cellulose Solvents: For Analysis, Shaping and Chemical Modification;* Liebert, T. F.; Heinze, T. J.; Edgar, K. J., Eds.; ACS Symposium Series, Vol. 1033; American Chemical Society: Washington DC, 2010; pp 319–341.
2. Verraest, D. L.; da Silva, L. P.; Peters, J. A.; van Bekkum, H. *Starch/Staerke* **1996,** *48,* 191–195. doi:10.1002/star.19960480509
3. Gonera, A.; Goclik, V.; Baum, M.; Mischnick, P. *Carbohydr. Res.* **2002,** *337,* 2263–2272. doi:10.1016/S0008-6215(02)00115-5
4. Onda, Y.; Muto, H.; Suzuki, H. Cyanoethylpullulan. U. S. Patent 4,322,524, March 30, 1982.
5. Gonera, A.; Mischnick, P.; Ukeda, H. *Enzyme Microb. Technol.* **2004,** *34,* 248–254. doi:10.1016/j.enzmictec.2003.10.008
6. Ademovic, Z.; Gonera, A.; Mischnick, P.; Klee, D. *Biomacromolecules* **2006,** *7,* 1429–1432. doi:10.1021/bm050591r
7. Verraest, D. L.; Peters, J. A.; Kuzee, H. C.; Raaijmakers, H. W. C.; van Bekkum, H. *Carbohydr. Res.* **1997,** *302,* 203–212. doi:10.1016/S0008-6215(97)00127-4
8. Verraest, D. L.; Zitha-Bovens, E.; Peters, J. A.; van Bekkum, H. *Carbohydr. Res.* **1998,** *310,* 109–115. doi:10.1016/S0008-6215(98)00174-8
9. Yoshida, H.; Takei, F.; Sawatari, N. *Fujitsu Sci. Tech. J.* **2002,** *38,* 39–45.
10. Taniguchi, M.; Kawai, T. *Appl. Phys. Lett.* **2004,** *85,* 3298–3300. doi:10.1063/1.1801167
11. Hornig, S.; Heinze, T. *Carbohydr. Polym.* **2007,** *68,* 280–286. doi:10.1016/j.carbpol.2006.12.007
12. Hornig, S.; Heinze, T. *Biomacromolecules* **2008,** *9,* 1487–1492. doi:10.1021/bm8000155
13. Hornig, S.; Heinze, T.; Becer, C. R.; Schubert, U. S. *J. Mater. Chem.* **2009,** *19,* 3838–3840. doi:10.1039/b906556n
14. Liebert, T.; Hornig, S.; Hesse, S.; Heinze, T. *J. Am. Chem. Soc.* **2005,** *127,* 10484–10485. doi:10.1021/ja052594h
15. Tahir, M. N.; Bork, C.; Risberg, A.; Horst, J. C.; Komoß, C.; Vollmer, A.; Mischnick, P. *Macromol. Chem. Phys.* **2010,** *211,* 1648–1662. doi:10.1002/macp.200900700
16. Likhitkar, S.; Bajpai, A. K. *Carbohydr. Polym.* **2012,** *87,* 300–308. doi:10.1016/j.carbpol.2011.07.053
17. Wotschadlo, J.; Liebert, T.; Heinze, T.; Wagner, K.; Schnabelrauch, M.; Dutz, S.; Müller, R.; Steiniger, F.; Schwalbe, M.; Kroll, T. C.; Höffken, K.; Buske, N.; Clement, J. H. *J. Magn. Magn. Mater.* **2009,** *321,* 1469–1473. doi:10.1016/j.jmmm.2009.02.069
18. McCarthy, J. R.; Weissleder, R. *Adv. Drug Delivery Rev.* **2008,** *60,* 1241–1251. doi:10.1016/j.addr.2008.03.014
19. Kawaguchi, T.; Hanaichi, T.; Hasegawa, M.; Maruno, S. *J. Mater. Sci.: Mater. Med.* **2001,** *12,* 121–127. doi:10.1023/A:1008961709559

20. Hornig, S.; Biskup, C.; Gräfe, A.; Wotschadlo, J.; Liebert, T.; Mohr, G. J.; Heinze, T. *Soft Matter* **2008,** *4,* 1169–1172. doi:10.1039/b800276b
21. Chatterjee, P. K.; Conrad, C. M. *J. Polym. Sci., Part A-1* **1966,** *4,* 233–243. doi:10.1002/pol.1966.150040115
22. Li, Q.; Wu, P.; Zhou, J.; Zhang, L. *Cellulose* **2011,** *19,* 161–169. doi:10.1007/s10570-011-9609-9
23. Mischnick, P.; Momcilovic, D. Chemical Structure Analysis of Starch and Cellulose Derivatives. In *Advances in Carbohydrate Chemistry and Biochemistry;* Horton, D., Ed.; Academic Press, 2010; Vol. 64, pp 117–210. doi:10.1016/S0065-2318(10)64004-8
24. Kawahara, K.; Ohta, K.; Miyamoto, H.; Nakamura, S. *Carbohydr. Polym.* **1984,** *4,* 335–356. doi:10.1016/0144-8617(84)90049-3
25. De Geest, B. G.; Van Camp, W.; Du Prez, F. E.; De Smedt, S. C.; Demeester, J.; Hennink, W. E. *Chem. Commun.* **2008,** 190–192. doi:10.1039/b714199h
26. Kuroda, K.; Fujimoto, K.; Sunamoto, J.; Akiyoshi, K. *Langmuir* **2002,** *18,* 3780–3786. doi:10.1021/la011454s
27. Na, K.; Lee, E. S.; Bae, Y. H. *J. Controlled Release* **2003,** *87,* 3–13. doi:10.1016/S0168-3659(02)00345-0
28. Kimoto, T.; Shibuya, T.; Shiobara, S. *Food Chem. Toxicol.* **1997,** *35,* 323–329. doi:10.1016/S0278-6915(97)00001-X
29. European Food Safety Authority. *EFSA J.* **2004,** *89,* 1–35.
30. Leathers, T. D. *Appl. Microbiol. Biotechnol.* **2003,** *62,* 468–473. doi:10.1007/s00253-003-1386-4
31. Larm, O.; Lindberg, B.; Svensson, S. *Carbohydr. Res.* **1971,** *20,* 39–48. doi:10.1016/S0008-6215(00)84947-2
32. Rolland-Sabaté, A.; Mendez-Montealvo, M. G.; Colonna, P.; Planchot, V. *Biomacromolecules* **2008,** *9,* 1719–1730. doi:10.1021/bm7013119
33. Fahner, E. M.; Großmann, G. H.; Ebert, K. H. *Makromol. Chem.* **1984,** *185,* 2205–2212.
34. Heinze, T.; Liebert, T.; Heublein, B.; Hornig, S. In *Functional Polymers based on Dextran;* Klemm, D., Ed.; Advances in Polymer Science, Vol. 205; Springer: Berlin/Heidelberg, 2006; pp 199–291.
35. van Dijk, M.; Rijkers, D. T. S.; Liskamp, R. M. J.; van Nostrum, C. F.; Hennink, W. E. *Bioconjugate Chem.* **2009,** *20,* 2001–2016. doi:10.1021/bc900087a
36. Bruneel, D.; Schacht, E.; De Bruyn, A. *J. Carbohydr. Chem.* **1993,** *12,* 769–778. doi:10.1080/07328309308019006
37. Sweet, D. P.; Shapiro, R. H.; Albersheim, P. *Carbohydr. Res.* **1975,** *40,* 217–225. doi:10.1016/S0008-6215(00)82604-X
38. Vollmer, A.; Voiges, K.; Bork, C.; Fiege, K.; Cuber, K.; Mischnick, P. *Anal. Bioanal. Chem.* **2009,** *395,* 1749–1768. doi:10.1007/s00216-009-3013-4
39. Liebert, T.; Hornig, S.; Hesse, S.; Heinze, T. *Macromol. Symp.* **2005,** *223,* 253–266. doi:10.1002/masy.200550518
40. Khalafalla, S.; Reimers, G. *IEEE Trans. Magn.* **1980,** *16,* 178–183. doi:10.1109/TMAG.1980.1060578
41. Massart, R. *IEEE Trans. Magn.* **1981,** *17,* 1247–1248. doi:10.1109/TMAG.1981.1061188
42. Hong, X.; Guo, W.; Yuan, H.; Li, J.; Liu, Y.; Ma, L.; Bai, Y.; Li, T. *J. Magn. Magn. Mater.* **2004,** *269,* 95–100. doi:10.1016/S0304-8853(03)00566-3
43. Reimer, L.; Zepke, U.; Moesch, J.; Schulze-Hillert, S.; Ross-Messemer, M.; Probst, W.; Weimer, E. *EELSpectroscopy. A Reference Handbook of Standard Data for Interpretation of Electron Energy Loss Spectra and for Generation of Electron Spectroscopic Images;* Institute of Physics, University of Münster: Münster, Germany, and Carl Zeiss, Electon Optics Division: Oberkochen, Germany, 1992.
44. Egerton, R. F. *Electron Energy-Loss Spectroscopy in the Electron Microscope;* Plenum Press: New York, London, 1996.
45. van Aken, P. A.; Liebscher, B.; Styrsa, V. J. *Phys. Chem. Miner.* **1998,** *25,* 323–327. doi:10.1007/s002690050122
46. Cressey, G.; Henderson, C. M. B.; Laan, G. *Phys. Chem. Miner.* **1993,** *20,* 111–119. doi:10.1007/BF00207204
47. Garvie, L. A. J.; Craven, A. J.; Brydson, R. *Am. Mineral.* **1994,** *79,* 411–425.
48. Hedrich, S.; Lünsdorf, H.; Kleeberg, R.; Heide, G.; Seifert, J.; Schlömann, M. *Environ. Sci. Technol.* **2011,** *45,* 7685–7692. doi:10.1021/es201564g

License and Terms

Beilstein Journal of Organic Chemistry

2-Allylphenyl glycosides as complementary building blocks for oligosaccharide and glycoconjugate synthesis

Hemali D. Premathilake and Alexei V. Demchenko*

Full Research Paper

Open Access

Address:
Department of Chemistry and Biochemistry, University of Missouri – St. Louis, One University Boulevard, St. Louis, MO 63121, USA

Email:
Alexei V. Demchenko* - demchenkoa@umsl.edu

* Corresponding author

Keywords:
carbohydrates; glycosylation; leaving group; oligosaccharides; orthogonal strategy; selective activation

Beilstein J. Org. Chem. **2012,** *8,* 597–605.
doi:10.3762/bjoc.8.66

Received: 06 February 2012
Accepted: 23 March 2012
Published: 18 April 2012

This article is part of the Thematic Series "Synthesis in the glycosciences II".

Guest Editor: T. K. Lindhorst

Abstract

The *O*-allylphenyl (AP) anomeric moiety was investigated as a new leaving group that can be activated for chemical glycosylation under a variety of conditions, through both direct and remote pathways. Differentiation between the two activation pathways was achieved in a mechanistic study. The orthogonal-type activation of the AP moiety along with common thioglycosides allows for the execution of efficient oligosaccharide assembly.

Introduction

Current knowledge about the key roles of carbohydrates is still limited. However, thanks to the explosive growth of the field of glycobiology in recent years, we have already learned that carbohydrates are involved in a broad range of vital biological processes (e.g., fertilization, anti-inflammation, immuno-response, joint lubrication, antigenic determination) [1]. Carbohydrates are also involved in many harmful processes (e.g., bacterial and viral infections, development of tumors, metastasis, tissue rejection, congenital disorders). The fact that many of these processes are directly associated with the pathogenesis of deadly diseases, including AIDS, cancer, pneumonia, septicemia, hepatitis and malaria [2-4], has been particularly stimulating for major scientific efforts in the field of modern glycosciences. The traditional chemical synthesis of oligosaccharides is lengthy because it involves multiple manipulations of protecting and/or leaving groups between glycosylation steps [5]. Many advanced strategies that shorten the oligosaccharide assembly by minimizing or even eliminating additional manipulations between coupling steps, are based either on chemoselective or on selective activation of leaving groups [6]. The use of selective activation [7] offers more flexibility than that of the chemoselective activation which relies on the nature of the protecting groups [8], and Ogawa's orthogonal strategy is conceptually the most attractive approach

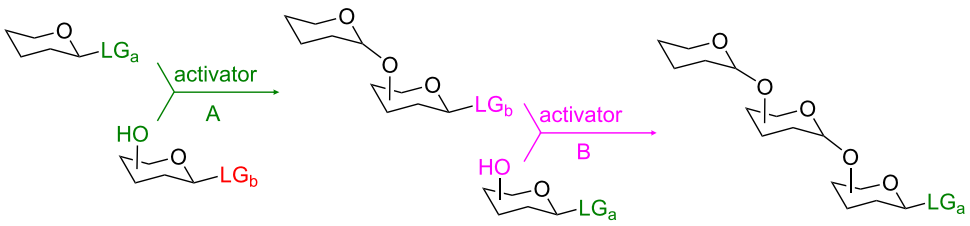

Scheme 1: Orthogonal strategy introduced by Ogawa et al.

that has been developed to date [9-12]. This technique implies the use of two orthogonal leaving groups, LG_a and LG_b, the selective activation of which can be reiterated to give streamlined access to oligosaccharides (Scheme 1).

Yet, the orthogonal strategy remains underdeveloped, with too few examples to become universally applicable. Only Ogawa's *S*-phenyl (SPh) versus fluoride [9,10,13] and our thioimidate-based approaches [14-16] are known. A very promising orthogonality was shown for *O*-pentenyl versus *O*-propargyl glycosides by Hotha et al. [17] and for *S*-glycosyl *O*-methyl phenylcarbamothioate (SNea) versus thioglycosides/thioimidates by us [18], but still their applicability to multistep synthesis remains to be proven. Working to expand this concept, our group reported a related, albeit less flexible, semiorthogonal approach with the use of *S*-ethyl and *O*-pentenyl leaving groups [19], which was later extended to fluoride/*O*-pentenyl combination by Fraser-Reid and Lopez [20]. Oxygen- [21] and sulfur-based [22] leaving groups fit into many expeditious strategies for oligosaccharide synthesis [6]. However, suitable reaction conditions for the orthogonal activation of these two classes of leaving groups are yet to be found. Commonly, *O*-glycosides are too stable to be used as effective glycosyl donors [21]. Pent-4-enyl *O*-glycosides introduced by Fraser-Reid are unique in this category of leaving groups, because they can be glycosidated under mild conditions by using I^+ generated in situ. Also this method has its limitations since I^+ can also activate thioglycosides. Indeed, only the semiorthogonality of the *O*-pentenyl and SEt leaving groups could be established [19]. Additionally, 4-pentenol is rather expensive ($ 323/50 g, Aldrich), and although *O*-pentenyl can be introduced from the anomeric acetate directly, the most economical synthesis includes a three-step protocol, with halide, orthoester, and the rearrangement of the latter to glycoside.

Results and Discussion

As a part of the ongoing research effort to develop versatile building blocks, we present herein the development of a new *ortho*-allylphenyl (AP) leaving group. In line with other efforts [23-26], the AP group was specifically designed to address the drawbacks of *O*-pentenyl glycosides and to create a more flexible approach for oligosaccharide synthesis. Concomitantly with our studies, Hung et al. came up with essentially the same idea and reported the synthesis of AP mannosides and their activation for *O*-mannosylation in the presence of ICl/AgOTf [27].

The following considerations driving our efforts were of particular relevance. First, chemists have been making aryl glycosides for some 130 years [28], and many excellent protocols for their synthesis are available [29]. We determined that AP glycosides can be readily obtained from the corresponding peracetate by using inexpensive 2-allylphenol ($ 35/100 g, Aldrich) in the presence of $BF_3{\cdot}Et_2O$. For instance, acetylated AP β-D-glucopyranoside was obtained in 92% yield. Second, we anticipated that the same promoters used for *O*-pentenyl activation [30] can also activate the AP leaving group. However, since AP glycosides bear structural features of both aryl and pentenyl glycosides, they should offer a more versatile activation profile than either class of the leaving group. Our working hypothesis is that activation of the AP leaving group with I^+ takes place by the formation of an epi-iodonium ion, which is then opened with the anomeric oxygen, similarly to that known for *O*-pentenyl glycosides [30]. It is possible that the activation of the AP leaving group can also be achieved with TMSOTf or $BF_3{\cdot}Et_2O$ via the direct anomeric activation pathway, which was expected to become the key feature of the AP-mediated glycosylation approach in comparison to that of both *O*-pentenyl or thioglycosides. As a result, this pathway may offer a suitable platform for developing a fully orthogonal approach in combination with thioglycosides.

To pursue this methodology we obtained a range of differently protected AP glucosides, including perbenzylated **1a**, perbenzoylated **1b**, and derivative **1c** equipped with the superarming protecting-group pattern (2-*O*-benzoyl-3,4,6-tri-*O*-benzyl) [31]. For comparison, we also obtained the AP donor **1d** of the D-galacto series. With glycosyl donors **1a**–**d** in hand, we began evaluating their applicability to chemical glycosylation using a range of standard glycosyl acceptors **2**–**5** [18]. Encouragingly, the reaction of glycosyl donor **1a** with the primary glycosyl acceptor **2** in the presence of TMSOTf was completed within 15 min and provided the corresponding disaccharide **6a** in 82%

yield (Table 1, entry 1). As expected, when a control experiment was set up with MeOTf, no glycosylation of **2** took place (Table 1, entry 2). The fact that the AP group in **1a** can be activated with TMSOTf, but not with MeOTf, offers a basis for exploring its orthogonality to thioglycosides. This is because thioglycosides show a completely opposite reactivity trend, namely no reaction with TMSOTf and smooth glycosylation with MeOTf [32].

Table 1: Glycosylation of AP glycosyl donors **1a–d**.

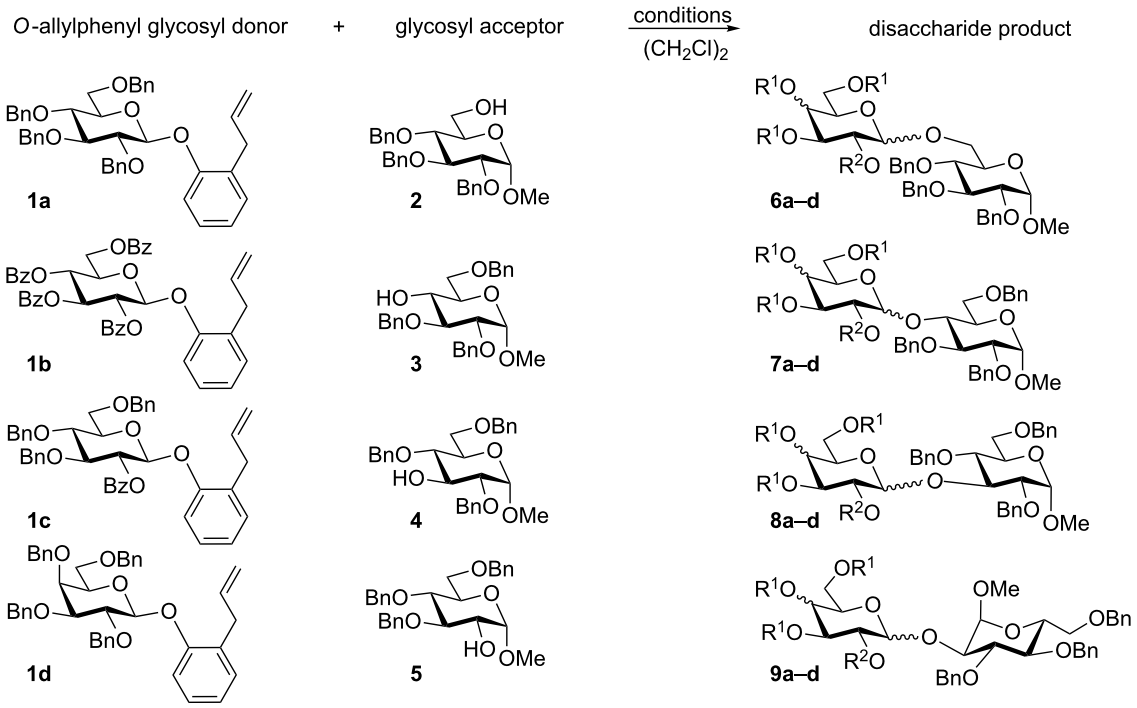

a: $R^1 = R^2$ = Bn (Glc); **b**: $R^1 = R^2$ = Bz (Glc); **c**: R^1 = Bn, R^2 = Bz (Glc); **d**: $R^1 = R^2$ = Bn (Gal)

entry	donor + acceptor	conditions[a]	time	product (yield, α/β ratio)
1	**1a** + **2**	TMSOTf, rt	15 min	**6a** (82%, 2.7/1)
2	**1a** + **2**	MeOTf, rt	24 h	no reaction
3	**1a** + **2**	NIS/TMSOTf, 0 °C	40 min	**6a** (80%, 1.4/1)
4	**1a** + **2**	NIS/TfOH, 0 °C	15 min	**6a** (90%, 1/1.5)
5	**1a** + **3**	NIS/TfOH, 0 °C	4 h	**7a** (73%, 1.2/1)
6	**1a** + **4**	NIS/TfOH, 0 °C	30 min	**8a** (82%, 1.0/1)
7	**1a** + **5**	NIS/TfOH, 0 °C	3 h	**9a** (72%, 1/1.3)
8	**1b** + **2**	MeOTf, rt	24 h	no reaction
9	**1b** + **2**	TMSOTf, rt	24 h	no reaction
10	**1b** + **2**	NIS/TMSOTf, 0 °C	6 h	**6b** (77%, β only)
11	**1b** + **2**	NIS/TfOH, 0 °C	2 h	**6b** (71%, β only)
12	**1b** + **5**	NIS/TfOH, 0 °C	3 h	**9b** (78%, β only)
13	**1c** + **2**	MeOTf, rt	24 h	no reaction
14	**1c** + **2**	TMSOTf, −20 °C	2.5 h	**6c** (73%, β only)
15	**1c** + **2**	NIS/TMSOTf, 0 °C	10 min	**6c** (84%, β only)
16	**1c** + **2**	NIS/TfOH, −20 °C	15 min	**6c** (93%, β only)
17	**1d** + **2**	NIS/TfOH, 0 °C	15 min	**6d** (85%, 1.5/1)
18	**1d** + **3**	NIS/TfOH, 0 °C	4 h	**7d** (81%, 1.2/1)
19	**1d** + **4**	NIS/TfOH, 0 °C	30 min	**8d** (82%, 1.0/1)
20	**1d** + **5**	NIS/TfOH, 0 °C	2 h	**9d** (80%, 3.0/1)

[a]performed in the presence of molecular sieves 4 Å (or 3 Å in MeOTf-promoted reactions, entries 2, 8, and 13).

NIS/TMSOTf is a powerful promoter for the activation of both *O*-pentenyl and thioglycosides. It was also found to be effective for the activation of AP glycosyl donor **1a**, upon which disaccharide **6a** was obtained in 80% yield. Even faster reaction and higher yield was obtained by using the NIS/TfOH promoter system, wherein the resulting disaccharide **6a** was obtained in 90% yield (Table 1, entry 4). The latter reaction conditions were chosen for use in the investigation of the glycosylation of the secondary glycosyl acceptors **3**–**5**.

These couplings were also proven to be feasible, and the corresponding disaccharides **7a**–**9a** were obtained in 72–82% yield (Table 1, entries 5–7). As anticipated, the reactivity of the perbenzoylated (disarmed) counterpart **1b** was significantly lower than that of **1a**, and TMSOTf-promoted glycosylation of **1b** was practically ineffective (Table 1, entry 9). This observation along with the fact that the armed AP leaving group in **1a** can be readily activated with TMSOTf (Table 1, entry 1) suggests that AP glycosides can be applied in accordance with the classic armed–disarmed strategy [33]. NIS-promoted glycosylations of **1b** have proven to be of preparative value and the desired disaccharides **6b** and **9b** were isolated in 71–78% yield (Table 1, entries 10–12). In order to gain a more flexible activation profile for the synthesis of 1,2-trans glycosides, we also investigated AP glycosyl donor **1c**, bearing a superarming protecting-group pattern [31]. As expected, all of the previously established activation conditions were very effective, and glycosylation of **1c** with acceptor **2** readily produced disaccharide **6c** (Table 1, entries 14–16). Again, particularly efficient was the NIS/TfOH-promoted reaction wherein disaccharide **6c** was isolated in 93% yield (Table 1, entry 16). To broaden the scope of the AP approach, we tested its applicability to the synthesis of D-galactosides, which are a highly important and abundant sugar series. All glycosylations of AP donor **1d** proceeded smoothly in the presence of NIS/TfOH and the corresponding disaccharides **6d**–**9d** were obtained in 80–85% yield (Table 1, entries 17–20). To verify the two anticipated activation pathways by which the AP group may depart, all components of the key experiments (Table 1, entries 1 and 3) wherein glycosyl donor **1a** reacted with glycosyl acceptor **2** in the presence of TMSOTf and NIS/TMSOTf, respectively, were separated and analyzed. In the TMSOTf-promoted reaction, (*o*-allylphenoxy)trimethylsilane (**10**) was isolated and identified by comparison with analytical data obtained from a commercial sample. This result suggests that the activation of the AP moiety with TMSOTf takes place through the anomeric oxygen atom (**A**, Pathway A, Scheme 2). In the NIS/TMSOTf-promoted reaction, 2-iodomethyl-2,3-dihydrobenzofuran (**11**) [34] was isolated and its identity was proven by spectral methods indicating that activation with I^+ takes place through the remote allyl moiety (**B**, Pathway B). In addition, in the latter experiment we detected the presence of adduct **12**, which was formed as the result of a competing attack of the glycosyl acceptor oxygen, as opposed to endocyclization of **B** through the anomeric oxygen leading to oxacarbenium intermediate **C**.

In accordance with Fraser-Reid's armed–disarmed approach, electronically activated (armed) glycosyl donors are chemoselectively activated over deactivated (disarmed) glycosyl acceptors bearing the same type of leaving group [30,35]. To explore this avenue, we obtained a disarmed (benzoylated) 6-OH AP glycosyl acceptor **13** (Supporting Information File 1), which was coupled with the armed AP glycosyl donor **1a** in the presence of TMSOTf. As anticipated, this reaction was feasible and the expected disaccharide **14** was obtained in 78% yield (Table 2, entry 1). With the ultimate goal of developing distinct orthogonal differentiation of AP and thioglycosides, we next obtained glycosyl acceptor **15** [36] equipped with an ethylthio leaving group. TMSOTf-promoted chemoselective glycosylation between building blocks **1a** and **15** produced the expected disaccharide **16** in 71% yield (Table 2, entry 2).

In a selective activation fashion, glycosyl acceptors **17** [37] and **19** [38], equipped with *S*-tolyl (STol) and *S*-phenyl leaving groups, respectively, were glycosylated with AP glycosyl donor **1a** to afford disaccharides **18** and **20** in 75 and 90% yield, respectively (Table 2, entries 3 and 4). Also the disarmed SPh acceptor **21** [39] led to disaccharide **22** in 98% yield. The synthesis of a 1,2-trans-linked disaccharide was also possible with glycosyl donor **1c** leading to the corresponding β-linked disaccharide **23** in 75% yield (Table 2, entry 6). This series of experiments clearly demonstrates that the AP leaving group can be reliably activated with TMSOTf in the presence of *S*-alkyl/aryl leaving groups. We next investigated glycosyl acceptor **25** equipped with the AP leaving group. MeOTf-promoted glycosylation of SEt, STaz, STol, and SPh glycosyl donors **24** [40], **27** [14], **28** [41], and **29** [42], respectively, with acceptor **25** afforded the respective disaccharide **26** in 78–97% yield (Table 2, entries 7–10). These series of results indicates a completely orthogonal character of AP and the thioglycosides. To expand this observation, disaccharide **26** was coupled with thioglycoside acceptor **21** in the presence of TMSOTf leading to trisaccharide **30** in 90% (Scheme 3). Since **30** is equipped with the SPh anomeric leaving group, it is available for further chain elongation directly. In a similar fashion, thioglycoside disaccharide **16** was coupled with AP acceptors **25** and **13** in the presence of MeOTf to afford trisaccharides **31** and **32** in 50 and 80% yield, respectively. Since these trisaccharides are equipped with the AP leaving group, their direct application to further chain elongation can be envisaged.

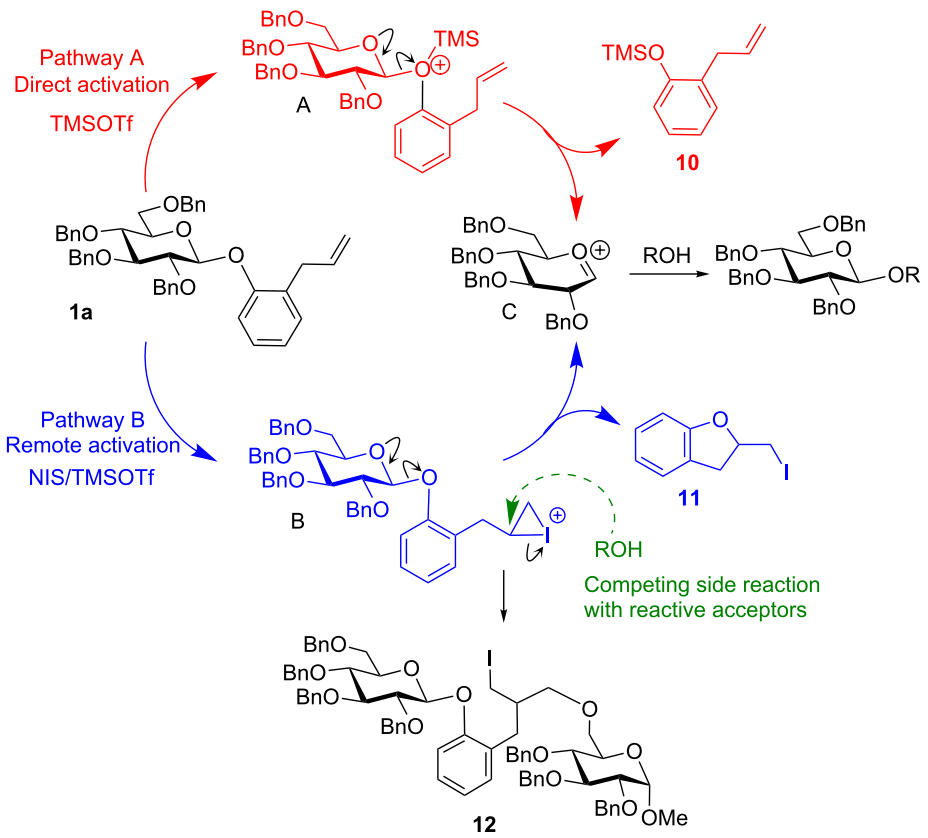

Scheme 2: Determination of the AP activation pathways.

Table 2: AP glycosides as glycosyl donors and acceptors in chemoselective and selective activations.

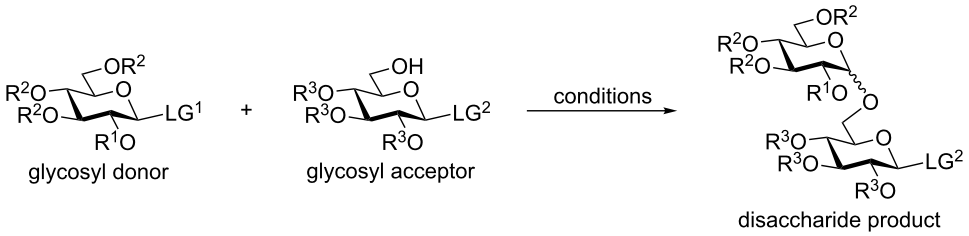

entry	donor; acceptor	promoter[a]	time	product (yield, α/β ratio)
1	**1a** (LG^1 = OAP, R^1 = R^2 = Bn); **13** (LG^2 = OAP, R^3 = Bz)	A	10 min	**14** (78%, 1.0/1)
2	**1a**; **15** (LG^2 = SEt, R^3 = Bn)	A	15 min	**16** (71%, 1.0/1)
3	**1a**; **17**(LG^2 = STol, R^3 = Bz)	A	1 h	**18** (75%, 2.4/1)
4	**1a**; **19** (LG^2 = SPh, R^3 = Bn)	A	1 h	**20** (90%, 1.0/1)
5	**1a**; **21** (LG^2 = SPh, R^3 = Bz)	A	2 h	**22** (98%, 1.8/1)
6	**1c** (LG^1 = OAP, R^1 = Bz, R^2 = Bn); **21**	A	30 min	**23** (75%, β only)

Table 2: AP glycosides as glycosyl donors and acceptors in chemoselective and selective activations. (continued)

7	**24** (LG^1 = SEt, R^1 = R^2 = Bn); **25** (LG^2 = OAP, R^3 = Bn)	B	2 h	**26** (82%, 1.8/1)
8	**27** (LG^1 = STaz, R^1 = R^2 = Bn); **25**	B	1 h	**26** (78%, 1.0/1)
9	**28** (LG^1 = STol, R^1 = R^2 = Bn); **25**	B	4 h	**26** (97%, 1.2/1)
10	**29** (LG^1 = SPh, R^1 = R^2 = Bn); **25**	B	6 h	**26** (90%, 1.0/1)

[a]performed in the presence of molecular sieves 4 Å (A: TMSOTf) or 3 Å (B: MeOTf) at rt or 0 °C (entry 6).

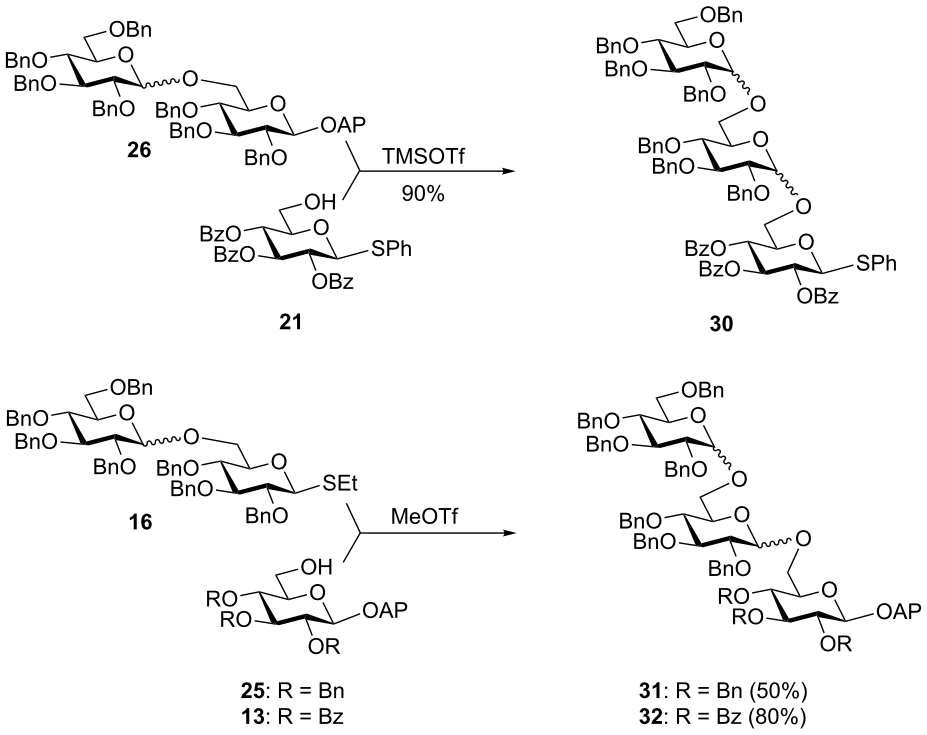

Scheme 3: AP building blocks in oligosaccharide synthesis.

Conclusion

In conclusion, we investigated the *O*-allylphenyl (AP) anomeric moiety as a new leaving group that can be activated for chemical glycosylation under a variety of conditions including Lewis acid and iodonium ion mediated pathways. The two activation pathways were confirmed by a mechanistic study. We also demonstrated that the application of the AP moiety allows executing oligosaccharide assembly by an orthogonal concept. The application of the AP glycosides may stretch well beyond their initial intended purpose because the alkene moiety can be utilized in a variety of other modes. Similar to that of *O*-pentenyl [30], it can be temporarily deactivated toward the I^+ activation pathway by the addition of Br_2, which can be reverted as needed (active–latent strategy). Direct conjugation of the AP moiety to biomolecules, monolayers, arrays, etc., should be possible by executing thiol–ene chemistry [43], ozonolysis/reductive amination [44-46], or other ligation protocols [47,48].

Experimental

General remarks

Column chromatography was performed on silica gel 60 (EM Science, 70–230 mesh), reactions were monitored by TLC on Kieselgel 60 F_{254} (EM Science). The compounds were detected by examination under UV light and by charring with 10% sulfuric acid in methanol. Solvents were removed under reduced pressure at <40 °C. CH_2Cl_2 and $ClCH_2CH_2Cl$ were distilled from CaH_2, directly prior to application.

Anhydrous DMF (EM Science) was used as received. Methanol was dried by heating under reflux with magnesium methoxide, distilled and stored under argon. Pyridine and acetonitrile were dried by heating under reflux with CaH_2 and then distilled and stored over molecular sieves (3 Å). Molecular sieves (3 Å or 4 Å), used for reactions, were crushed and activated in vacuo at 390 °C during 8 h in the first instance and then for 2–3 h at 390 °C directly prior to application. DOWEX MONOSPHERE 650C (H) was washed three times with MeOH and stored under MeOH. Optical rotations were measured with a Jasco P-1020 polarimeter. ^{1}H NMR spectra were recorded in $CDCl_3$ at 300 MHz; ^{13}C NMR spectra were recorded in $CDCl_3$ at 75 MHz (Bruker Avance) or 125 MHz (Varian). Anomeric ratios were determined by comparison of the integral intensities of the respective groups of signals in the ^{1}H NMR spectra. HRMS determinations were made with the use of a JEOL MStation (JMS-700) mass spectrometer.

Synthesis of glycosides

Typical MeOTf-promoted glycosylation procedure (Method A). A mixture of glycosyl donor (0.11 mmol), glycosyl acceptor (0.10 mmol), and freshly activated molecular sieves (3 Å, 300 mg) in 1,2-dichloroethane (1.4 mL) was stirred under argon for 1 h. MeOTf (0.33 mmol) was added and the reaction mixture was monitored by TLC. Upon completion (Table 1, Table 2), the solid was filtered off and the residue was rinsed with CH_2Cl_2. The combined filtrate (30 mL) was washed with 20% aq $NaHCO_3$ (10 mL) and water (3 × 10 mL). The organic layer was separated, dried with $MgSO_4$ and concentrated in vacuo. The residue was purified by silica gel column chromatography (ethyl acetate/hexanes gradient elution) to afford the corresponding oligosaccharide.

Typical TMSOTf-promoted glycosylation procedure (Method B). A mixture of glycosyl donor (0.11 mmol), glycosyl acceptor (0.10 mmol), and freshly activated molecular sieves (4 Å, 150 mg) in 1,2-dichloroethane (1.6 mL) was stirred under argon for 1 h. TMSOTf (0.22 mmol) was added and the reaction mixture was monitored by TLC. Upon completion (Table 1, Table 2), the solid was filtered off and the residue was rinsed with CH_2Cl_2. The combined filtrate (30 mL) was washed with 20% aq $NaHCO_3$ (10 mL) and water (3 × 10 mL). The organic layer was separated, dried with $MgSO_4$ and concentrated in vacuo. The residue was purified by silica gel column chromatography (ethyl acetate/hexanes gradient elution) to afford the corresponding oligosaccharide.

Typical NIS/TfOH-promoted glycosylation procedure (Method C). A mixture of glycosyl donor (0.11 mmol), glycosyl acceptor (0.10 mmol), and freshly activated molecular sieves (4 Å, 150 mg) in 1,2-dichloroethane (1.6 mL) was stirred under argon for 1 h. NIS (0.22 mmol) and TfOH (0.022 mmol) were added and the reaction mixture was monitored by TLC. Upon completion, the mixture was diluted with CH_2Cl_2, the solid was filtered off, and the residue was rinsed with CH_2Cl_2. The combined filtrate (30 mL) was washed with 10% aq $Na_2S_2O_3$ (10 mL) and water (3 × 10 mL). The organic layer was separated, dried with $MgSO_4$ and concentrated in vacuo. The residue was purified by silica gel column chromatography (ethyl acetate/hexanes gradient elution) to afford the corresponding oligosaccharide.

Typical NIS/TMSOTf-promoted glycosylation procedure (Method D). A mixture of glycosyl donor (0.11 mmol), glycosyl acceptor (0.10 mmol), and freshly activated molecular sieves (4 Å, 150 mg) in 1,2-dichloroethane (1.6 mL) was stirred under argon for 1 h. NIS (0.22 mmol) and TMSOTf (0.022 mmol) were added and the reaction mixture was monitored by TLC. Upon completion, the mixture was diluted with CH_2Cl_2, the solid was filtered off, and the residue was rinsed with CH_2Cl_2. The combined filtrate (30 mL) was washed with 10% aq $Na_2S_2O_3$ (10 mL) and water (3 × 10 mL). The organic layer was separated, dried with $MgSO_4$ and concentrated in vacuo. The residue was purified by silica gel column chromatography (ethyl acetate/hexanes gradient elution) to afford the corresponding oligosaccharide.

Supporting Information

Supporting Information File 1

Experimental procedures, extended experimental data, ^{1}H and ^{13}C NMR spectra for all new compounds.
[http://www.beilstein-journals.org/bjoc/content/supplementary/1860-5397-8-66-S1.pdf]

Acknowledgements

This work was supported by an award from the NIGMS (GM077170). H. D. P. is grateful to UMSL Graduate School for proving her with the Dissertation Fellowship. Dr. Winter and Mr. Kramer (UM – St. Louis) are thanked for HRMS determinations.

References

1. Varki, A.; Cummings, R. D.; Esko, J. D.; Freeze, H. H.; Stanley, P.; Bertozzi, C. R.; Hart, G. W.; Etzler, M. E. *Essentials of Glycobiology;* CSH Press: New York, 2009.
2. Witczak, Z. J. Carbohydrates as new and old targets for future drug design. In *Carbohydrates in Drug Design;* Witczak, Z. J.; Nieforth, K. A., Eds.; Marcel Dekker Inc.: New York, 1997; pp 1–37.
3. Wong, C.-H., Ed. *Carbohydrate-Based Drug Discovery;* Wiley-VCH: Weinheim, 2003. doi:10.1002/3527602437

4. Klyosov, A. A.; Witczak, Z. J.; Platt, D., Eds. *Carbohydrate Drug Design;* ACS Symposium Series, Vol. 932; ACS: Washington, 2006. doi:10.1021/bk-2006-0932
5. Zhu, X.; Schmidt, R. R. *Angew. Chem., Int. Ed.* **2009,** *48,* 1900–1934. doi:10.1002/anie.200802036
6. Smoot, J. T.; Demchenko, A. V. *Adv. Carbohydr. Chem. Biochem.* **2009,** *62,* 161–250. doi:10.1016/S0065-2318(09)00005-5
7. Kaeothip, S.; Demchenko, A. V. *Carbohydr. Res.* **2011,** *346,* 1371–1388. doi:10.1016/j.carres.2011.05.004
8. Premathilake, H. D.; Demchenko, A. V. *Top. Curr. Chem.* **2011,** *301,* 189–221. doi:10.1007/128_2010_106
9. Kanie, O.; Ito, Y.; Ogawa, T. *J. Am. Chem. Soc.* **1994,** *116,* 12073–12074. doi:10.1021/ja00105a066
10. Ito, Y.; Kanie, O.; Ogawa, T. *Angew. Chem., Int. Ed. Engl.* **1996,** *35,* 2510–2512. doi:10.1002/anie.199625101
11. Paulsen, H. *Angew. Chem., Int. Ed. Engl.* **1995,** *34,* 1432–1434. doi:10.1002/anie.199514321
12. Kanie, O. Orthogonal Strategy in Oligosaccharide Synthesis. In *Carbohydrates in Chemistry and Biology;* Ernst, B.; Hart, G. W.; Sinaý, P., Eds.; Wiley-VCH: Weinheim, New York, 2000; pp 407–426. doi:10.1002/9783527618255.ch16
13. Kanie, O.; Ohtsuka, I.; Ako, T.; Daikoku, S.; Kanie, Y.; Kato, R. *Angew. Chem., Int. Ed.* **2006,** *45,* 3851–3854. doi:10.1002/anie.200600433
14. Demchenko, A. V.; Pornsuriyasak, P.; De Meo, C.; Malysheva, N. N. *Angew. Chem., Int. Ed.* **2004,** *43,* 3069–3072. doi:10.1002/anie.200454047
15. Pornsuriyasak, P.; Demchenko, A. V. *Chem.–Eur. J.* **2006,** *12,* 6630–6646. doi:10.1002/chem.200600262
16. Kaeothip, S.; Pornsuriyasak, P.; Rath, N. P.; Demchenko, A. V. *Org. Lett.* **2009,** *11,* 799–802. doi:10.1021/ol802740b
17. Vidadala, S. R.; Thadke, S. A.; Hotha, S. *J. Org. Chem.* **2009,** *74,* 9233–9236. doi:10.1021/jo901837z
18. Ranade, S. C.; Kaeothip, S.; Demchenko, A. V. *Org. Lett.* **2010,** *12,* 5628–5631. doi:10.1021/ol1023079
19. Demchenko, A. V.; De Meo, C. *Tetrahedron Lett.* **2002,** *43,* 8819–8822. doi:10.1016/S0040-4039(02)02235-9
20. López, J. C.; Uriel, C.; Guillamón-Martín, A.; Valverde, S.; Gómez, A. M. *Org. Lett.* **2007,** *9,* 2759–2762. doi:10.1021/ol070753r
21. Kim, K.-S.; Jeon, H.-B. Anomeric transglycosylation. In *Handbook of Chemical Glycosylation: Advances in Stereoselectivity and Therapeutic Relevance;* Demchenko, A. V., Ed.; Wiley-VCH: Weinheim, Germany, 2008; pp 185–223.
22. Zhong, W.; Boons, G.-J. Glycoside synthesis from 1-Sulfur/Selenium-Substituted Derivatives: Thioglycosides in Oligosaccharide Synthesis. In *Handbook of Chemical Glycosylation: Advances in Stereoselectivity and Therapeutic Relevance;* Demchenko, A. V., Ed.; Wiley-VCH: Weinheim, Germany, 2008; pp 261–303.
23. Rodebaugh, R.; Fraser-Reid, B. *Tetrahedron* **1996,** *52,* 7663–7678. doi:10.1016/S0040-4020(96)00349-3
24. Rodebaugh, R.; Fraser-Reid, B. *J. Am. Chem. Soc.* **1994,** *116,* 3155–3156. doi:10.1021/ja00086a068
25. Lee, J.-C.; Pan, G.-R.; Kulkarni, S. S.; Luo, S.-Y.; Liao, C.-C.; Hung, S.-C. *Tetrahedron Lett.* **2006,** *47,* 1621–1624. doi:10.1016/j.tetlet.2005.12.127
26. Fortin, M.; Kaplan, J.; Pham, K.; Kirk, S.; Andrade, R. B. *Org. Lett.* **2009,** *11,* 3594–3597. doi:10.1021/ol901313z
27. Luo, S.-Y.; Tripathi, A.; Zulueta, M. M. L.; Hung, S.-C. *Carbohydr. Res.* **2012,** in press. doi:10.1016/j.carres.2012.01.022
28. Michael, A. *Am. Chem. J.* **1879,** *1,* 305–312.
29. Jacobsson, M.; Malmberg, J.; Ellervik, U. *Carbohydr. Res.* **2006,** *341,* 1266–1281. doi:10.1016/j.carres.2006.04.004
30. Fraser-Reid, B.; Udodong, U. E.; Wu, Z.; Ottosson, H.; Merritt, J. R.; Rao, C. S.; Roberts, C.; Madsen, R. *Synlett* **1992,** 927–942. doi:10.1055/s-1992-21543
And references therein.
31. Mydock, L. K.; Demchenko, A. V. *Org. Lett.* **2008,** *10,* 2103–2106. doi:10.1021/ol800345j
32. Lönn, H. *J. Carbohydr. Chem.* **1987,** *6,* 301–306. doi:10.1080/07328308708058879
33. Fraser-Reid, B.; Wu, Z.; Udodong, U. E.; Ottosson, H. *J. Org. Chem.* **1990,** *55,* 6068–6070. doi:10.1021/jo00312a004
34. Sheng, S.; Hu, M.; Wu, D.; Cai, M.; Huang, X. *Lett. Org. Chem.* **2009,** *6,* 345–348.
35. Mootoo, D. R.; Konradsson, P.; Udodong, U. E.; Fraser-Reid, B. *J. Am. Chem. Soc.* **1988,** *110,* 5583–5584. doi:10.1021/ja00224a060
36. Fei, C.; Chan, T. H. *Acta Chim. Sin. (Engl. Ed.)* **1989,** 258–264.
37. Huang, X.; Huang, L.; Wang, H.; Ye, X.-S. *Angew. Chem., Int. Ed.* **2004,** *43,* 5221–5224. doi:10.1002/anie.200460176
38. Pfäffli, P. J.; Hixson, S. H.; Anderson, L. *Carbohydr. Res.* **1972,** *23,* 195–206. doi:10.1016/S0008-6215(00)88025-8
39. Sliedregt, L. A. J. M.; van der Marel, G. A.; van Boom, J. H. *Tetrahedron Lett.* **1994,** *35,* 4015–4018. doi:10.1016/S0040-4039(00)76728-1
40. Kaeothip, S.; Pornsuriyasak, P.; Demchenko, A. V. *Tetrahedron Lett.* **2008,** *49,* 1542–1545. doi:10.1016/j.tetlet.2007.12.105
41. France, R. R.; Compton, R. G.; Davis, B. G.; Fairbanks, A. J.; Rees, N. V.; Wadhawan, J. D. *Org. Biomol. Chem.* **2004,** *2,* 2195–2202. doi:10.1039/b316728c
42. Dinkelaar, J.; de Jong, A. R.; van Meer, R.; Somers, M.; Lodder, G.; Overkleeft, H. S.; Codée, J. D. C.; van der Marel, G. A. *J. Org. Chem.* **2009,** *74,* 4982–4991. doi:10.1021/jo900662v
43. Hoyle, C. E.; Bowman, C. N. *Angew. Chem., Int. Ed.* **2010,** *49,* 1540–1573. doi:10.1002/anie.200903924
44. Rele, S. M.; Iyer, S. S.; Baskaran, S.; Chaikof, E. L. *J. Org. Chem.* **2004,** *69,* 9159–9170. doi:10.1021/jo049092r
45. Noti, C.; de Paz, J. L.; Polito, L.; Seeberger, P. H. *Chem.–Eur. J.* **2006,** *12,* 8664–8686. doi:10.1002/chem.200601103
46. Jeon, I.; Iyer, K.; Danishefsky, S. J. *J. Org. Chem.* **2009,** *74,* 8452–8455. doi:10.1021/jo901682p
47. Pozsgay, V.; Kubler-Kielb, J. Conjugation Methods toward Synthetic Vaccines. In *Carbohydrate-Based Vaccines;* Roy, R., Ed.; ACS Symposium Series, Vol. 989; 2008; pp 36–70. doi:10.1021/bk-2008-0989.ch003
48. Payne, R. J.; Wong, C.-H. *Chem. Commun.* **2010,** *46,* 21–43. doi:10.1039/b913845e

Beilstein Journal of Organic Chemistry

An easy α-glycosylation methodology for the synthesis and stereochemistry of mycoplasma α-glycolipid antigens

Yoshihiro Nishida*[1], Yuko Shingu[2], Yuan Mengfei[1], Kazuo Fukuda[1], Hirofumi Dohi[1], Sachie Matsuda[2] and Kazuhiro Matsuda[2]

Full Research Paper

Open Access

Address:
[1]Chiba University, Graduate School of Advanced Integration Science, Matsudo 271-8510, Chiba, Japan and [2]M. Biotech. Co. Ltd., Setagaya-ku, Fukazawa 2-1-3-1103,Tokyo 158-0081, Japan

Email:
Yoshihiro Nishida* - YNishida@faculty.chiba-u.jp

* Corresponding author

Keywords:
cytoplasm membrane; glycolipid antigen; glycosylation; mycoplasma; stereochemistry

Beilstein J. Org. Chem. **2012,** *8,* 629–639.
doi:10.3762/bjoc.8.70

Received: 15 January 2012
Accepted: 28 March 2012
Published: 24 April 2012

This article is part of the Thematic Series "Synthesis in the glycosciences II".

Guest Editor: T. K. Lindhorst

Abstract

Mycoplasma fermentans possesses unique α-glycolipid antigens (GGPL-I and GGPL-III) at the cytoplasm membrane, which carry a phosphocholine group at the sugar primary (6-OH) position. This paper describes a practical synthetic pathway to a GGPL-I homologue ($C_{16:0}$) and its diastereomer, in which our one-pot α-glycosylation method was effectively applied. The synthetic GGPL-I isomers were characterized with ^{1}H NMR spectroscopy to determine the equilibrium among the three conformers (*gg*, *gt*, *tg*) at the acyclic glycerol moiety. The natural GGPL-I isomer was found to prefer *gt* (54%) and *gg* (39%) conformers around the lipid tail, while adopting all of the three conformers with equal probability around the sugar position. This property was very close to what we have observed with respect to the conformation of phosphatidylcholine (DPPC), suggesting that the *Mycoplasma* glycolipids GGPLs may constitute the cytoplasm fluid membrane together with ubiquitous phospholipids, without inducing stereochemical stress.

Introduction

Mycoplasmas constitute a family of gram-positive microbes lacking rigid cell walls. They are suspected to be associated with human immune diseases, in either direct or indirect ways, although the molecular mechanism is not fully understood [1]. In recent biochemical studies, *Mycoplasma* outer-membrane lipoproteins [2,3] and glycolipids [4-6] are thought to serve not only as the main antigens but also as probable pathogens. Also in our research team, Matsuda et al. [7-10] isolated a new class of α-glycolipid antigens (GGPL-I and GGPL-III, Figure 1) from *M. fermentans*. Another α-glycolipid (MfGL-II), which has a chemical structure very close to GGPL-III, was identified and characterized by other groups [11-14].

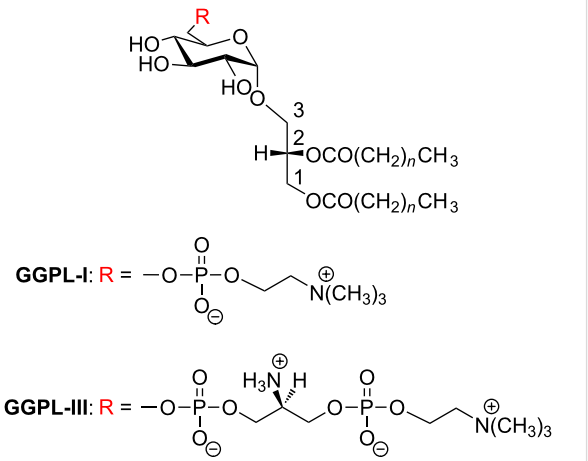

Figure 1: Absolute chemical structures of *M. fermentans* α-glycolipid antigens, GGPL-I and GGPl-III (GGPL: Glycosyl-*sn*-glycerophospholipid).

Absolute chemical structures of GGPL-I [15] and GGPL–III [16] have already been established by chemical syntheses of stereoisomers; these α-glycolipids have a common chemical backbone of 3-*O*-(α-D-glucopyranosyl)-*sn*-glycerol carrying phosphocholine at the sugar primary (6-OH) position. The fatty acids at the glycerol moiety are saturated, namely palmitic acid ($C_{16:0}$) and stearic acid ($C_{18:0}$). GGPL-I has a structural feature analogous to 1,2-di-*O*-palmitoyl phosphatidylcholine (DPPC) as a ubiquitous cell membrane phospholipid. Apparently, GGPLs are amphiphilic compounds that can form certain self-assembled structures under physiological conditions [12,13] and may give physicochemical stress on the immune system of the host [17]. In fact, our research team has proven that these α-glycolipid antigens have certain pathogenic functions [18,19]. In order to exploit their biological functions in detail, it is necessary to obtain these α-glycolipids in sufficient amounts. Thus, both genetic [20-22] and chemical synthetic approaches [23,24] are being followed, although no practical way has yet been established. In this paper, we report a chemical access to both a natural GGPL-I homologue ($C_{16:0}$) and its diastereomer **I-a** and **I-b**, in which our one-pot α-glycosylation methodology [25,26] is effectively applied. The two GGPL-I isomers prepared thereby were characterized with ^{1}H NMR spectroscopy, in terms of configuration and conformation at the asymmetric glycerol moiety.

Results and Discussion

A practical synthetic access to GGPL-I homologues

GGPL-I provides two key asymmetric centers to be controlled, literally, in the synthetic pathway. One is the configuration at the chiral glycerol moiety, and another is the sugar α-glycoside linkage. In former synthetic works on 3-*O*-(α-D-glycopyranosyl)-*sn*-glycerol [27-30], chiral 1,2-*O*-isopropylidene-*sn*-glycerol has often been employed [29,30] as the acceptor substrate for different α-glycosylation reactions. In this case, however, attention should be paid to the acid-catalyzed migration of the dimethylketal group [23,29-31]. In our synthetic pathway, chiral (*S*)- or (*R*)-glycidol is employed as an alternative source of the chiral glycerol to circumvent this problem. In an established synthetic approach, 6-*O*-acetyl-2,3,4-tri-*O*-benzyl protected sugar **1** [23] is used as the donor and treated with a reagent combination of CBr_4 and Ph_3P (Appel–Lee reagent) in either CH_2Cl_2 or DMF solvent, or a mixture of the two (Scheme 1). For the reaction in CH_2Cl_2, *N*,*N*,*N'*,*N'*-tetramethylurea (TMU) is added after in situ formation of α-glycosyl bromide **2**, which

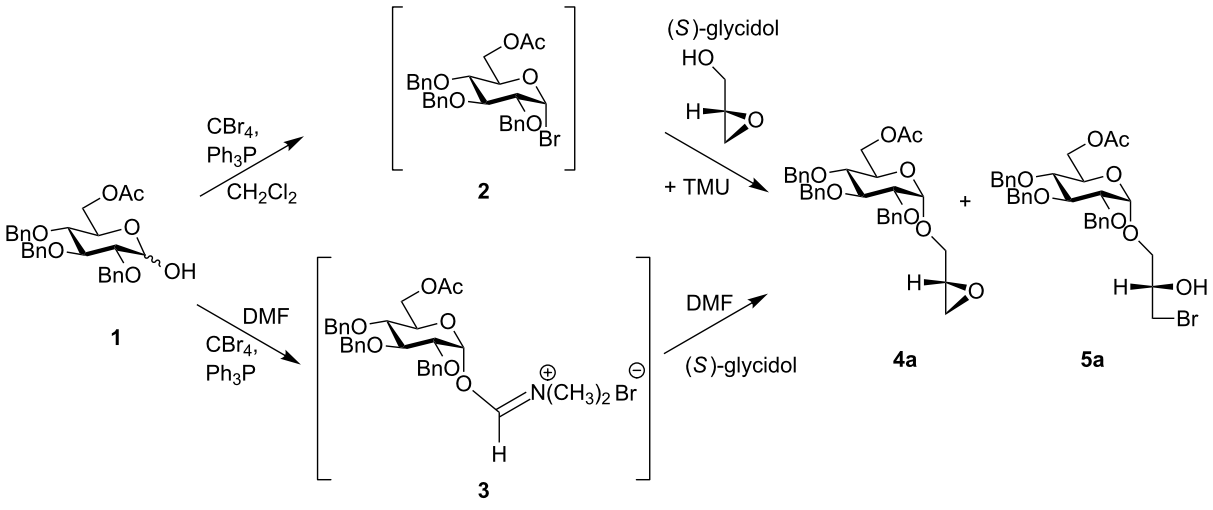

Scheme 1: An established synthetic pathway to α-glycosyl-*sn*-glycerols **4a** and **5a**. A reagent combination of CBr_4 and Ph_3P (Appel–Lee reagent) is utilized in either CH_2Cl_2 or DMF as solvent.

equilibrates with a more reactive β-glycosyl bromide species [32]. In the pathway using DMF, the α-glycosylation is routed via α-glycosyl cationic imidate **3**, which was predicted in former studies [33] and evidenced in our preceding NMR and MS study [25,26].

The reaction between **1** and (*S*)-glycidol in CH_2Cl_2 (+ TMU) gave a mixture of epoxy compound **4a** (60–70%) and bromide **5a** (30–40%). In **5a**, the oxirane ring was opened by nucleophilic Br^- ions produced by Ph_3P and CBr_4. Also in the DMF-promoted reaction, a mixture of **4a** (70–90%) and **5a** (10–30%) was derived. In both reaction pathways, however, the glycosylation was α-selective (α:β ≥ 90:10, yields >80%) and not accompanied by isomerization at the glycerol moiety.

A mixture of **4a** and **5a** was used in the following chemical transformation (Scheme 2). First, a *lyso*-glycolipid **6a** was derived after deprotection at the sugar hydroxymethyl position and S_N2 substitution with cesium palmitate at the glycerol *sn*-1 position. Then, this compound was converted to glycolipid **8a** after sequential reaction of the temporary *tert*-butyldimethylsilyl (TBDMS) -protected sugar, and O-acylation at the glycerol 2-OH position to give **7a**, followed by removal of the TBDMS protecting group. For introducing the phosphocholine group at the sugar 6-OH position, we employed a phosphoroamidite method using 1*H*-tetrazole as a promoter [34]. First, **8a** was treated with 2-cyanoethyl-*N*,*N*,*N*',*N*'-tetraisopropyl phosphorodiamidite in the presence of 1*H*-tetrazole, and then with choline tosylate to give **9a**. After removal of the sugar *O*-benzyl group by catalytic hydrogenolysis, the GGPL-I homologue **I-a** was obtained. In the same way, the GGPL-I *sn*-isomer **I-b** was derived from a mixture of **4b** and **5b** available from the reaction between **1** and (*R*)-glycidol (Scheme 1 and Scheme 2b).

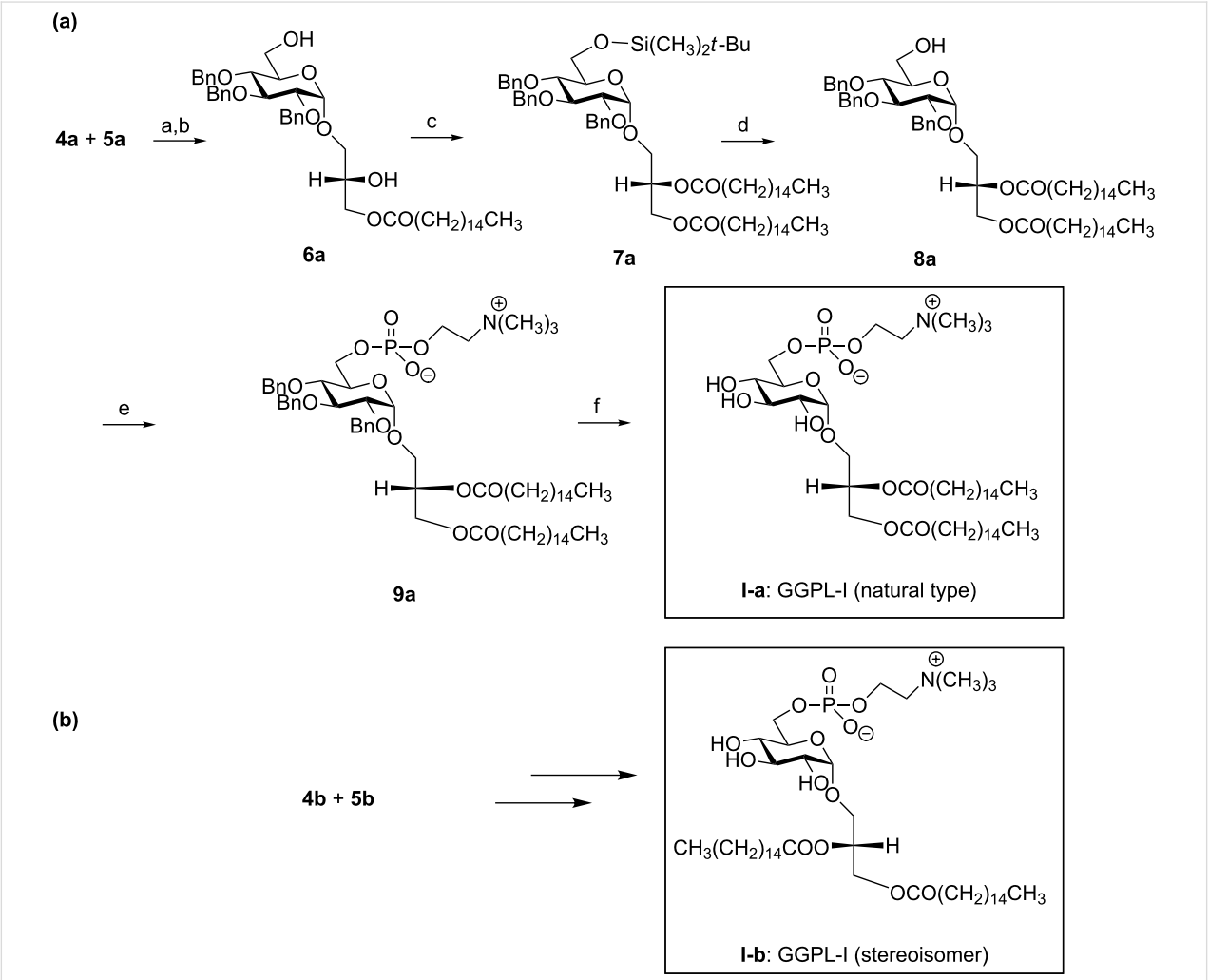

Scheme 2: Syntheses of GGPL-I homologue **I-a** and its isomer **I-b**. Conditions: (a) K_2CO_3, CH_3OH; (b) cesium palmitate in DMF; (c) TBDMS chloride then palmitoyl chloride in pyridine + DMAP; (d) TFA in CH_3OH; (e) (i) 2-cyanoethyl-*N*,*N*,*N*',*N*'-tetraisopropyl phosphorodiamidite, 1*H*-tetrazole and MS-4 Å in CH_2Cl_2; (ii) choline tosylate, 1*H*-tetrazole, (iii) *m*CPBA, (iv) aq. NH_3 in CH_3OH, (f) H_2, $Pd(OH)_2$/C in CH_3OH.

^{1}H NMR characterization of **I-a**, **I-b** and the related glycerolipids

^{1}H NMR spectroscopy provides a useful tool for discriminating between the two GGPL-I isomers as shown in Figure 2. A clear difference was observed in the chemical shifts of the glycerol methylene protons as designated by "a" and "b". Conversely, little difference was observed between the *sn*-isomers at the sugar H-1 signal as well as at the glycerol H-2 (Table 1). Natural GGPL-I and GGPL-III gave ^{1}H NMR data very close to those of **I-a**, indicating that both have a common skeleton of 3-*O*-(α-D-glucopyranosyl)-*sn*-glycerol [15,16].

The glycerol moiety has two C–C single bonds. By free rotation, each of them is allowed to have three staggered conformers of *gg* (*gauche-gauche*), *gt* (*gauche-trans*) and *tg* (*trans-gauche*) (Figure 3). In solution and also in self-

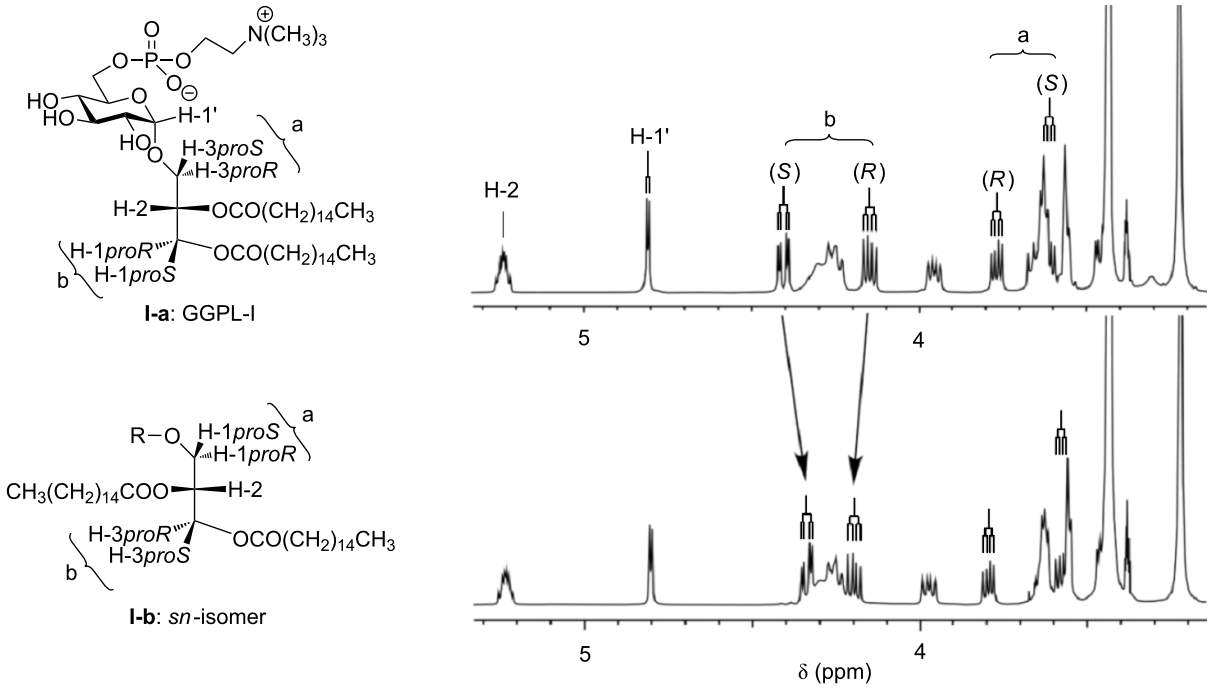

Figure 2: ^{1}H NMR spectra of **I-a** and **I-b** (500 MHz, 25 °C, $CDCl_3/CD_3OD$ 10:1). The assignment of *sn*-glycerol methylene protons (H_{proR} and H_{proS}) was performed on the basis of our preceding studies on deuterium-labeled glycerols [35-37] and α(1→6)-linked disaccharides [38-40].

Table 1: ^{1}H NMR data (500 MHz) of **I-a**, **I-b**, and their precursors (**9a** and **9b**).

Compound	δ [ppm] (^3J and ^2J [Hz])					
	glucose	*sn*-glycerol moiety				
	H-1'	H-1		H-2	H-3	
		proR	*proS*		*proR*	*proS*
I-a[a]	4.80 (3.5)	4.14 (6.5)	4.40 (3.5, 12.0)	5.24	3.76 (5.5)	3.61 (5.5, 11.0)
9a	4.70 (3.5)	4.17 (6.5)	4.38 (3.0, 12.0)	5.22	3.72 (5.5)	3.52 (6.0, 11.0)
I-b[a]	4.80 (3.5)	3.80 (6.0)	3.57 (5.5,11.0)	5.23	4.34 (3.5)	4.20 (6.5,12.0)
9b	4.74 (3.5)	3.76 (5.5)	3.57 (5.5, 11.0)	5.23	4.37 (3.0)	4.19 (6.5, 12.0)

[a]These α-glycolipids were dissolved in a mixture of $CDCl_3$ and CD_3OD (10:1) at 11.2 mM concentration.

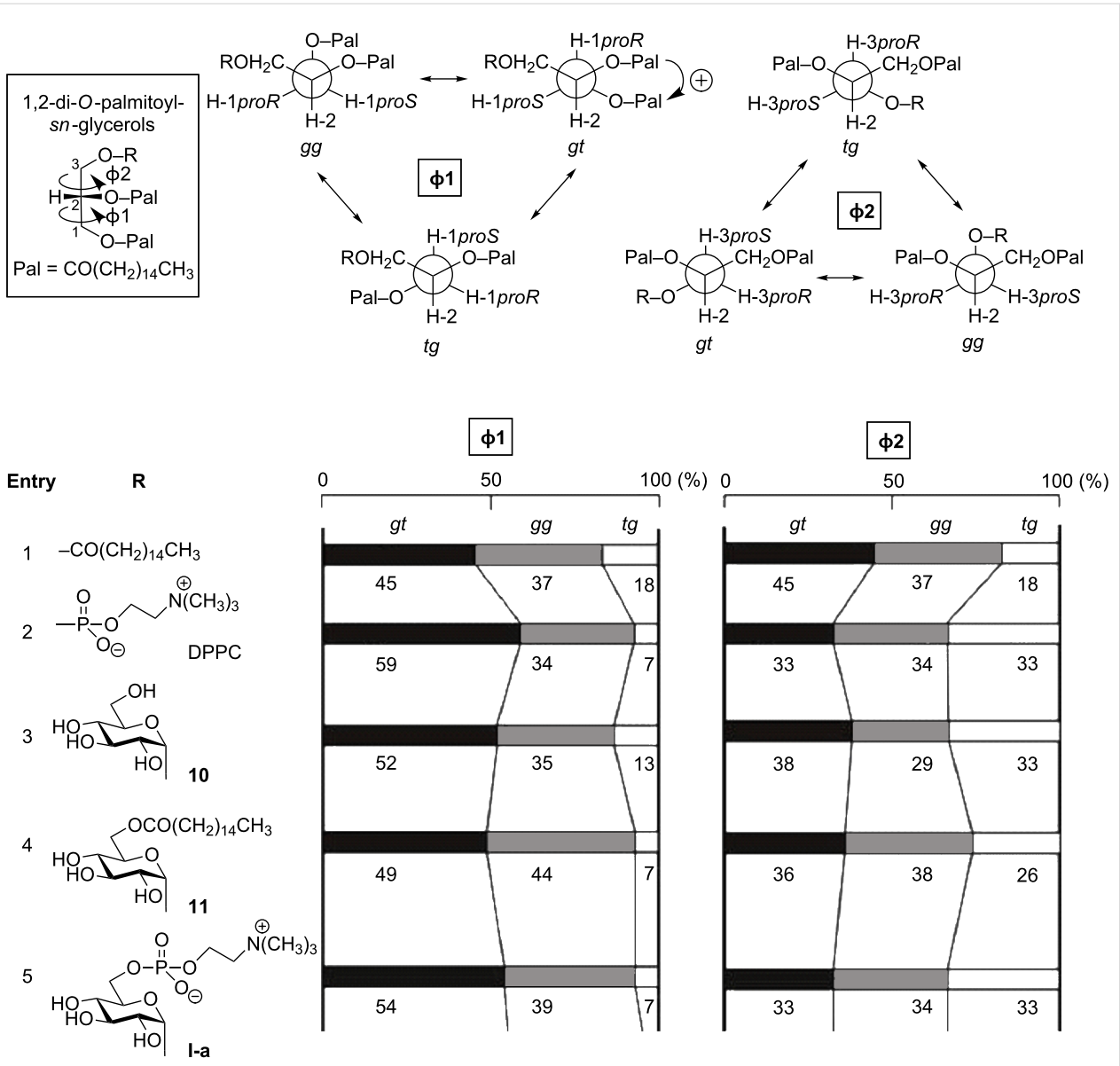

Figure 3: Distributions of *gg*, *gt* and *tg*-conformers in 3-substituted *sn*-glycerols at 11 mM in solutions of $CDCl_3$ and CD_3OD (10:1) at 298 K.

contacting liquid-crystalline states, these conformers are thought to equilibrate with each other. In this study, we calculated time-averaged populations of the three conformers by means of ^{1}H NMR spectroscopy. As we reported in a preceding paper [41], the Karplus-type equation proposed by Haasnoot et al.[42] was adapted as follows:

$$2.8gg + 3.1gt + 10.7tg = {}^3J_{H2,H1S} \text{ (or } {}^3J_{H2,H3R})$$

$$0.9gg + 10.7gt + 5.0tg = {}^3J_{H2,H1R} \text{ (or } {}^3J_{H2,H3S}) \text{ and}$$

$$gg + gt + tg = 1.$$

In this equation, a perfect staggering (Φ1 and Φ2 = +60, −60 or 180 degree) is assumed for every conformer. Figure 3 summarizes the results for a series of 3-substituted 1,2-di-*O*-palmitoyl-*sn*-glycerols, which involve tripalmitin (Figure 3, entry 1), DPPC (1,2-di-*O*-palmitoylphosphatidylcholine) (Figure 3, entry 2), and GGPL-I homologues (Figure 3, entries 3–5). In a solution state with a mixture of $CDCl_3$ and CD_3OD (10:1) as the solvent and at a concentration of 11.2 mM, tripalmitin adopts the three conformers in the ratio of *gt* (45%), *gg* (37%) and *tg* (18%). In comparison with this symmetric lipid, the asymmetric phospholipid (DPPC) favors the *gt*-conformer more strongly around the tail lipid moiety along the *sn*-1,2 position, while disfavoring the *tg*-conformer, in the ratio of *gt* (59%), *gg*

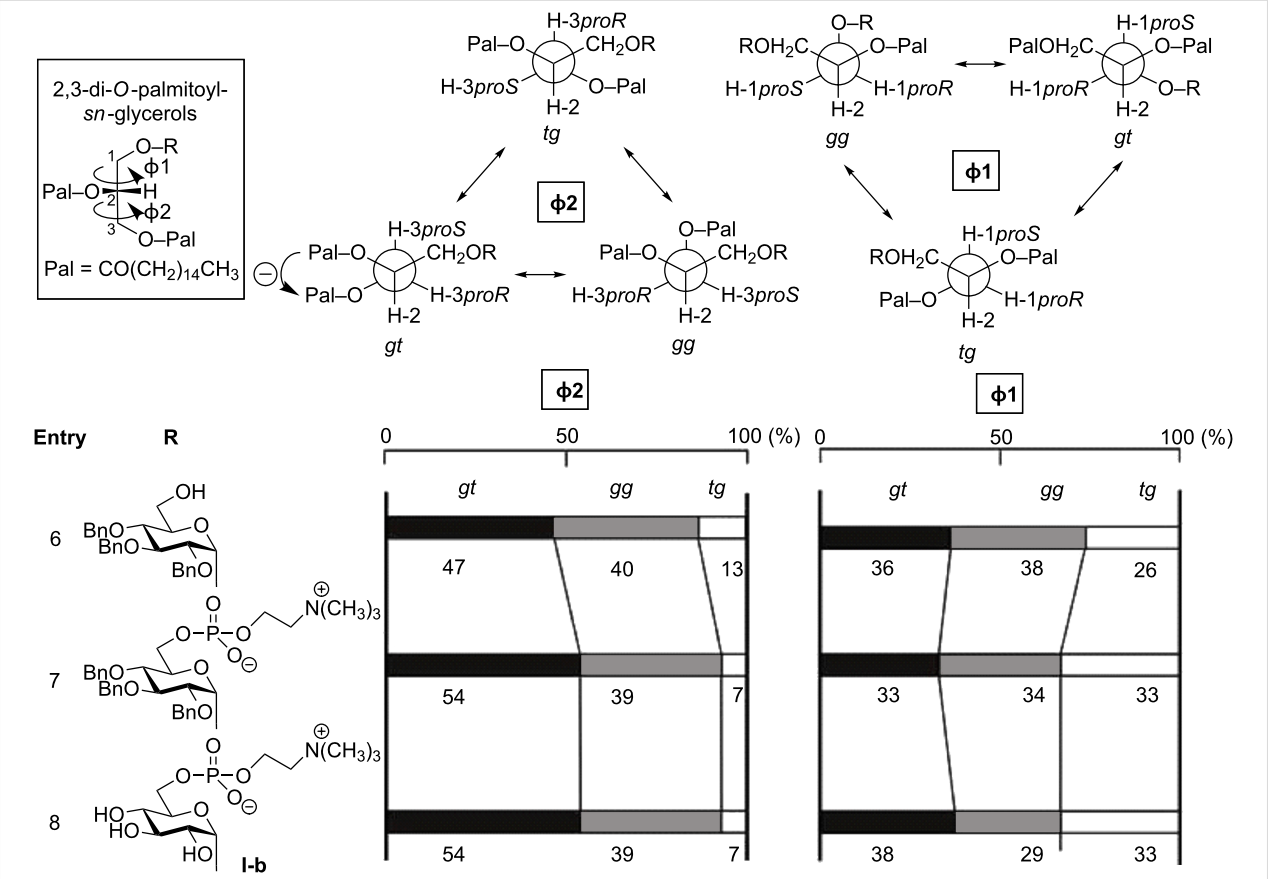

Figure 4: Distributions of *gg*, *gt* and *tg*-conformers in 1-substituted *sn*-glycerols. In these *sn*-isomers, Φ1 and Φ2 represent the dihedral angles around the C–C single bond at the glycerol *sn*-2,3 and 1,2-position, respectively.

(34%) and *tg* (7%). The head phosphate moiety along the *sn*-2,3 position adopts the three conformers in equilibrated populations (*gg* = *gt* = *tg*).

3-*O*-(α-D-glucopyranosyl)-*sn*-glycerolipids **10** and **11** (Figure 3, entries 3 and 4) were found to have conformational properties very similar to DPPC; the lipid tail moiety prefers the *gauche* conformations (*gt* and *gg*), while the sugar moiety allows a random conformation. Here, it should be mentioned that the conformer distribution coincides between **I-a** (Figure 3, entry 5) and DPPC (Figure 3, entry 2) at the head moiety [*gt* (33%), *gg* (34%) and *tg* (33%)].

The above analysis was carried out also for the stereoisomer **I-b** and the related glycolipids (Figure 4, entries 6–8). The isomer (Figure 4, entry 8) showed an overall conformational property similar to **I-a** and DPPC (Figure 5), although a small difference was observed in the conformer distribution at the sugar head moiety. However, it should be recognized here that the helical direction (helicity) of the *gt* conformer in **I-b** is reversed (anti-clockwise) from the case of DPPC and GGPL-I (clockwise), as depicted in Figure 3 and Figure 4.

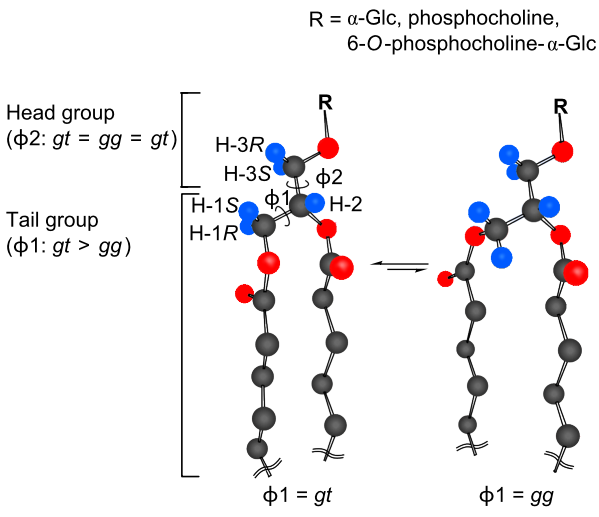

Figure 5: A common conformational property of GGPL-I and DPPC. The tail lipid moiety favors two *gauche*-conformers of *gt* and *gg* (*gt* > *gg* >> *tg*), while the head moiety takes three conformers in averaged populations (*gt* = *gg* = *tg*).

Conclusion

We have proposed a synthetic pathway to a GGPL-I homologue and its stereoisomer, in which our one-pot α-glycosylation methodology was effectively applied. We envisage that the simple method will allow us to prepare a variety of α-glycolipid antigens other than GGPLs and to prove their biological significance [43]. By the ^{1}H NMR conformational analysis, which was based on our former studies on deuterium-labeled *sn*-glycerols and sugars, we have proven that GGPL-I and other 3-*O*-(α-D-glucopyranosyl)-*sn*-glycerolipids have a common conformational property at the chiral glycerol moiety: The lipid tail moiety prefers two *gauche*-conformations (*gg* and *gt*) in the order *gt* > *gg* >> *tg,* while the sugar head moiety adopts three conformers in an averaged population (*gg* = *gt* = *tg*). At the lipid tail position, the *gt*-conformer with clockwise helicity is predominant over the anticlockwise *gg*-conformer. The observed conformation was very close to what we have seen in DPPC (Figure 5). Although these results were based on the solution state in a solvent mixture of $CHCl_3$ and CH_3OH (10:1), it may be possible to assume that the mycoplasma GGPLs and the related 3-*O*-(α-D-glycopyranosyl)-*sn*-glycerolipids can constitute cytoplasm membranes in good cooperation with ubiquitous phospholipids without inducing stereochemical stress at the membrane.

The GGPL-I isomer **I-b** showed an overall conformational property similar to the natural isomer **I-a** and DPPC. However, it should be mentioned here that the chiral helicity of *gt*-conformers in **I-b** is reversed (anticlockwise) from the clockwise helicity of DPPC and GGPL-I. The difference in chirality seems critical in biological recognition events and also in physicochemical contact with other chiral constituents in cell membranes [44,45].

Experimental

General methods

Infrared (IR) spectra were recorded on a JASCO FT/IR-230 Fourier transform infrared spectrometer on KBr disks. All ^{1}H NMR (500 MHz) spectra were recorded by using a Varian INOVA-500 or Varian Gemini 200. ^{1}H chemical shifts are expressed in parts per million (δ ppm) by using an internal standard of tetramethylsilane (TMS = 0.000 ppm). Mass spectra were recorded with a JEOL JMS 700 spectrometer for fast atom bombardment (FAB) spectra. Silica gel column chromatography was performed on silica gel 60 (Merck 0.063–0.200 mm and 0.040–0.063 mm) and eluted with a mixture of toluene and ethyl acetate or a mixture of $CHCl_3$ and CH_3OH in gradient modes (100:0 to 80:20). For purification of phosphocholine-containing products, a chromatographic column packed with Iatrobeads (IATRON LABORATORIES INC., 6RS-8060) was applied and eluted with a mixture of CH_3OH and $CHCl_3$ in gradient modes. For thin-layer chromatography (TLC) analysis, Merck precoated TLC plates (silica gel 60 F_{254}, layer thickness 0.25 mm) and Merck TLC aluminum roles (silica gel 60 F_{254}, layer thickness 0.2 mm) were used. All other chemicals were purchased from Tokyo Kasei Kogyo Co., Ltd., Kishida Chemical Co., Ltd., and Sigma–Aldrich Chemical Company Co, Int., and were used without further purification.

A typical procedure for the one-pot α-glycosylation: CBr_4 (1.6 g, 6.09 mmol) and Ph_3P (2.02 g, 6.09 mmol) were added to a solution of 6-*O*-acetyl-2,3,4-tri-*O*-benzyl-D-glucose (**1**) (1.0 g, 2.03 mmol) in 10 mL of DMF and stirred for 3 h at rt. Then, (*S*)-glycidol (301 mg, 4.06 mmol) was added to the reaction mixture and stirred for 14 h at rt. Products were diluted with a mixture of toluene and ethyl acetate (10:1), and the solution was washed with saturated aq. $NaHCO_3$ and aq. NaCl solution, dried and concentrated. The residue was purified by silica gel column chromatography in toluene and ethyl acetate to give a mixture of **4a** and **5a** (the ratio changed with reaction time) as colorless syrup. The total yield of **4a** and **5a** was between 80% and 90%.

3-*O*-(2,3,4-tri-*O*-benzyl-α-D-glucopyranosyl)-1,2-di-*O*-palmitoyl-*sn*-glycerols 8a and 8b: K_2CO_3 (379 mg, 2.74 mmol) was added to the mixture of **4a** and **5a** (1 g, 1.83 mmol based on **4a**) in CH_3OH (20 mL) and stirred for 1 h at rt. The reaction mixture was neutralized, washed with water, dried, and concentrated. The residue was dried under reduced pressure and directly subjected to the next reaction. A mixture of caesium palmitate (2.7 g, 7.3 mmol) in DMF (40 mL) was heated at 100–110 °C, to which the DMF solution of the above residue was added slowly. The reaction mixture was stirred for 2 h at 110 °C, cooled to rt, and then filtered through a pad of Celite powder with ethyl acetate. The filtrate was washed with saturated aq. NaCl solution, dried, and concentrated. The residue was purified by silica gel column chromatography to give **6a** as a colorless syrup (830 mg, 60% yield). To a solution of **6a** (300 mg, 0.39 mmol) in pyridine (20 mL), TBDMS chloride (107 mg, 0.71 mmol) and 4-*N,N*-dimethylaminopyridine (cat.) were added. The reaction mixture was stirred for 12 h at rt, treated with methanol (2 mL) for 3 h and concentrated. The residue was purified by silica gel column chromatography in a mixture of toluene and ethyl acetate. The main product was dissolved in pyridine (20 mL) and then reacted with palmitoyl chloride (162 mg, 0.59 mmol) for 3 h at rt. The reaction mixture was treated with methanol (2 mL) and then concentrated with toluene. The residue was dissolved in a mixture of CH_3OH and CH_2Cl_2 (1:1, 20 mL) and treated with trifluoroacetic acid (1 mL) for 2 h at rt. After concentration, the residue was purified by silica gel column chromatography in a mixture of toluene and ethyl acetate to give **8a** as a white waxy solid

(0.32 g, 81% yield from **6a**). $[\alpha]_D^{30}$ +21.1 (*c* 1.0, $CHCl_3$); IR (KBr, film): 3413, 2923, 2853, 1736, 1630, 1457, 1361, 1158, 1069, 736 cm^{-1}; ^1H NMR (500 MHz, $CDCl_3$): δ_H 7.40–7.23 (m, 5H × 3, -$CH_2C_6H_5$), 5.23 (m, 1H, glycerol H-2), 4.96–4.64 (d, 2H × 3,-$CH_2C_6H_5$), 4.70 (d, 1H, *J* = 3.5 Hz, H-1), 4.40 (dd, 1H, *J* = 4.0 and 12.0 Hz, glycerol H-1_{proS}), 4.19 (dd, 1H, *J* = 6.0 and 12.0 Hz, glycerol H-1_{proR}), 3.96 (dd, 1H, *J* = 9.5 and 9.5 Hz, H-3), 3.72 (dd, 1H, *J* = 5.5 and 10.5 Hz, glycerol H-3_{proR}), 3.72 and 3.66 (b, 2H, H-6_{ProR} and H-6_{proS}), 3.65 (m, 1H, H-5), 3.54 (dd, 1H, *J* = 5.5 and 10.5 Hz, glycerol H-3_{proS}), 3.50 (dd, 1H, *J* = 9.5 and 10.0 Hz, H-4), 3.49 (dd, 1H, *J* = 3.5 and 9.5 Hz, H-2), 2.29 (m, 2H × 2, -OCOC$H_2$$CH_2(CH_2)_{12}CH_3$), 1.58 (b, 2H × 2, -OCOCH$_2$C$H_2$$(CH_2)_{12}CH_3$), 1.25 (b, 24H × 2, -OCOCH$_2$CH$_2$(CH_2)$_{12}$CH$_3$), 0.88 (t, 3H × 2, *J* = 7.0 Hz, -OCOCH$_2$CH$_2$(CH$_2$)$_{12}$CH_3); FABMS *m*/*z*: $[M + Na]^+$ 1023.7.

In the same way as derived for the synthesis of **8a**, (*R*)-glycidol and **6b** (0.30 g, 0.39 mmol) was used for the synthesis of **8b** (0.30 g, 77% yield). $[\alpha]_D^{32}$ +18.5 (*c* 1.0, $CHCl_3$); IR (KBr, film): 3452, 2924, 2854, 1739, 1586, 1455, 1296, 1159, 1095, 710 cm^{-1}; ^1H NMR (500 MHz, $CDCl_3$): δ_H 7.40–7.23 (m, 5H × 3, -$CH_2C_6H_5$), 5.23 (b, 1H, glycerol H-2), 4.96–4.63 (d, 2H × 3,-$CH_2C_6H_5$), 4.75 (d, 1H, *J* = 3.5 Hz, H-1), 4.38 (dd, 1H, *J* = 3.5 and 12.0 Hz, glycerol H-3_{proR}), 4.21 (dd, 1H, *J* = 6.5 and 12.0 Hz, glycerol H-3_{proS}), 3.96 (dd, 1H, *J* = 9.5 and 9.5 Hz, H-3), 3.73 (dd, 1H, *J* = 6.0 and 11.0 Hz, glycerol H-1_{proS}), 3.76 and 3.66 (b, 2H, H-6_{ProR} and H-6_{proS}), 3.65 (m, 1H, H-5), 3.57 (dd, 1H, *J* = 5.5 and 11.0 Hz, glycerol H-1_{proR}), 3.51 (dd, 1H, *J* = 9.5 and 10.0 Hz, H-4), 3.50 (dd, 1H, *J* = 3.5 and 9.5 Hz, H-2), 2.29 (b, 2H × 2, -OCOC$H_2$$CH_2(CH_2)_{12}CH_3$), 1.59 (b, 2H × 2, -OCOCH$_2$C$H_2$$(CH_2)_{12}CH_3$), 1.25 (b, 24H × 2, -OCOCH$_2$CH$_2$(CH_2)$_{12}$CH$_3$), 0.88 (t, 3H × 2, *J* = 7.0 Hz, -OCOCH$_2$CH$_2$(CH$_2$)$_{12}$CH_3); FABMS *m*/*z*: $[M + Na]^+$ 1023.7.

A phosphorodiamidite method for the synthesis of **I-a**

(a) The reaction vessel was kept under anhydrous conditions with Ar gas in the presence of molecular sieves (50%w/w), and a solution of **8a** (0.20 g, 0.20 mmol) and 2-cyanoethyl-*N*,*N*,*N*',*N*'-tetraisopropyl phosphorodiamidite (90.4 mg, 0.30 mmol) in 10 mL of CH_2Cl_2 was injected. 1*H*-tetrazole (28.4 mg, 0.40 mmol) was added and stirred for 2 h at rt. Then 1*H*-tetrazole (42.6 mg, 0.60 mmol, 3.0 equiv) and choline tosylate (220.3 mg, 0.8 mmol: thoroughly dried overnight under vacuum) were added to the reaction mixture and stirred for 1.5 h at rt. The reaction was quenched by the addition of water (1 mL), and then *m*-chloroperbenzoic acid (51.8 mg, 0.3 mmol) was added at 0 °C and stirred for 10 min at rt. The reaction mixture was washed with 10 % aq. Na_2SO_3 solution, saturated aq. $NaHCO_3$ solution, water and saturated aq. NaCl solution, dried and concentrated. The residue was dissolved in a mixture of CH_3OH (10 mL) and 30% aq. NH_3 (1 mL) and stirred for 15 min at rt. The reaction mixture was concentrated, and the residue was purified by column chromatography (IATROBEADS in a mixture of $CHCl_3$ and CH_3OH) to give **9a** (186 mg, 80% yield). $[\alpha]_D^{26}$ +13.0 (*c* 0.45, $CHCl_3$); IR (KBr, film): 3301, 2929, 2856, 2537, 1731, 1577, 1419, 1216, 1093, 925, 788, 746; ^1H NMR (500 MHz, $CDCl_3$): δ_H 7.35–7.25 (m, 5H × 3, -$CH_2C_6H_5$), 5.22 (m, 1H, glycerol H-2), 4.93–4.61 (d, 2H × 3, -$CH_2C_6H_5$), 4.70 (d, 1H, *J* = 3.5 Hz, H-1), 4.38 (dd, 1H, *J* = 3.0 and 12.0 Hz, glycerol H-1_{proS}), 4.19 (b, 2H, choline -$CH_2CH_2N^+(CH_3)_3$), 4.17 (dd, 1H, *J* = 6.5 and 12.0 Hz, glycerol H-1_{proR}), 4.15 and 4.02 (m, 2H × 2, H-6_{ProR} and H-6_{proS}), 3.93 (dd, 1H, *J* = 9.0 and 9.5 Hz, H-3), 3.72 (dd, 1H, *J* = 5.5 and 11.0 Hz, glycerol H-3_{proR}), 3.71 (b, 1H, H-5), 3.62 (t, 1H, H-4), 3.58 (b, 2H, choline -$CH_2CH_2N^+(CH_3)_3$), 3.52 (dd, 1H, *J* = 6.0 and 11.0 Hz, glycerol H-3_{proS}), 3.46 (dd, 1H, *J* = 3.5 and 9.5 Hz, H-2), 3.15 (s, 9H, -$POCH_2CH_2N^+(CH_3)_3$), 2.28 (m, 2H × 2, -OCOC$H_2$$CH_2(CH_2)_{12}CH_3$), 1.58 (b, 2H × 2, -OCOCH$_2$C$H_2$$(CH_2)_{12}CH_3$), 1.25 (b, 24H × 2, -OCOCH$_2$CH$_2$(CH_2)$_{12}$CH$_3$), 0.88 (t, 3H × 2, *J* = 7.0 Hz, -OCOCH$_2$CH$_2$(CH$_2$)$_{12}$CH_3); FABMS *m*/*z*: $[M + Na]^+$ 1188.7.

(b) Compound **9a** (0.18 g, 0.15 mmol) was hydrogenated with $Pd(OH)_2$/C (8 mg) under atmospheric pressure in a mixture of CH_3OH (10 mL) and acetic acid (0.1 mL) for 7 h at rt. The reaction mixture was neutralized by the addition of Et_3N, filtered and concentrated. The residue was purified by column chromatography with IATROBEADS (CH_3OH and $CHCl_3$) to give **I-a** (101 mg, 75% yield). $[\alpha]_D^{31}$ +18.7 (*c* 1.0, $CHCl_3$/CH_3OH 10:1); IR (KBr, film): 3372, 2927, 2852, 1731, 1573, 1469, 1112, 975, 727; ^1H NMR (500 MHz, $CDCl_3$/CD_3OD 10:1): δ_H 5.23 (m, 1H, glycerol H-2), 4.80 (d, 1H, *J* = 3.5 Hz, H-1), 4.39 (dd, 1H, *J* = 3.5 and 12.0 Hz, glycerol H-1_{proS}), 4.30 (b, 2H, -$CH_2CH_2N^+(CH_3)_3$), 4.24 and 3.95 (b, 2H, H-6_{ProR} and H-6_{proS}), 4.14 (dd, 1H, *J* = 6.5 and 12.0 Hz, glycerol H-1_{proR}), 3.75 (dd, 1H, *J* = 5.5 and 11.0 Hz, glycerol H-3_{proR}), 3.67 (b, 2H, choline-$CH_2CH_2N^+(CH_3)_3$), 3.65 (b, 1H × 2, H-3 and H-5), 3.61 (dd, 1H, *J* = 5.5 and 11.0 Hz, glycerol H-3_{proS}), 3.56 (b, 1H, H-4), 3.46 (b, 1H, H-2), 3.22 (s, 9H, -$POCH_2CH_2N^+(CH_3)_3$), 2.31 (m, 2H × 2, -OCOC$H_2$$CH_2(CH_2)_{12}CH_3$), 1.60 (b, 2H × 2, -OCOCH$_2$C$H_2$$(CH_2)_{12}CH_3$), 1.25 (b, 24H × 2, -OCOCH$_2$CH$_2$(CH_2)$_{12}$CH$_3$), 0.88 (t, 3H × 2, *J* = 7.0 Hz, -OCOCH$_2$CH$_2$(CH$_2$)$_{12}$CH_3); HRMS–FAB (*m*/*z*): $[M + Na]^+$ calcd for $C_{46}H_{90}NO_{13}PNa$, 918.6048; found, 918.6028.

In the same way as described above, **9b** (180 mg) was derived from **8b** (200 mg, 0.20 mmol) in 76% yield and converted to the GGPL-I isomer **I-b** [70 mg, 81% yield from **9b** (120 mg)]. **9b:** $[\alpha]_D^{26}$ +8.1 (*c* 0.62, $CHCl_3$); IR (KBr, film): 3413, 2923, 2857,

1735, 1461, 1241, 1097, 744, 495, 445; ^{1}H NMR (500 MHz, $CDCl_3$): δ_H 7.35–7.23 (m, 5H × 3, -$CH_2C_6H_5$), 5.23 (b, 1H, glycerol H-2), 4.94–4.64 (d, 2H × 3,-$CH_2C_6H_5$), 4.74 (d, 1H, J = 3.5 Hz, H-1), 4.37 (dd, 1H, J = 3.0 and 12.0 Hz, glycerol H-3$_{proR}$), 4.23 (b, 2H, choline-$CH_2CH_2N^+(CH_3)_3$), 4.19 (dd, 1H, J = 6.5 and 12.0 Hz, glycerol H-3$_{proS}$), 4.16 and 4.09 (b, 2H, H-6$_{proR}$ and H-6$_{proS}$), 3.94 (dd, 1H, J = 9.5 and 9.5 Hz, H-3), 3.76 (dd, 1H, J = 5.5 and 11.0 Hz, glycerol H-1$_{proS}$), 3.72 (m, 1H, H-5), 3.61 (dd, 1H, J = 9.0 and 9.5 Hz, H-4), 3.60 (b, 2H, choline-$CH_2CH_2N^+(CH_3)_3$), 3.57 (dd, 1H, J = 5.5 and 11.0 Hz, glycerol H-1$_{proR}$), 3.49 (dd, 1H, J = 3.5 and 9.5 Hz, H-2), 3.20 (s, 9H, choline-$CH_2CH_2N^+(CH_3)_3$), 2.28 (dd, 2H × 2, J = 7.5 and 15 Hz, -$OCOCH_2CH_2(CH_2)_{12}CH_3$), 1.58 (b, 2H × 2, -$OCOCH_2CH_2(CH_2)_{12}CH_3$), 1.25 (b, 24H × 2, -$OCOCH_2CH_2(CH_2)_{12}CH_3$), 0.88 (t, 3H × 2, J = 7.0 Hz, -$OCOCH_2CH_2(CH_2)_{12}CH_3$); FABMS m/z: $[M + Na]^+$ 1188.7.

I-b: $[\alpha]_D^{31}$= +10.7 (c 1.0, $CHCl_3/CH_3OH$ 10:1); IR (KBr film): 3390, 2919, 2856, 1731, 1463, 1228, 1074, 964, 711; ^{1}H NMR (500 MHz, $CDCl_3/CD_3OD$ 10:1): δ_H 5.24 (m, 1H, glycerol H-2), 4.80 (d, 1H, J = 3.5 Hz, H-1), 4.34 (dd, 1H, J = 3.5 and 12.0 Hz, glycerol H-3$_{proR}$), 4.28 (b, 2H, choline-$CH_2CH_2N^+(CH_3)_3$), 4.25 and 3.97 (b, 2H, H-6$_{ProR}$ and H-6$_{proS}$), 4.20 (dd, 1H, J = 7.0 and 12.0 Hz, glycerol H-3$_{proS}$), 3.80 (dd, 1H, J = 6.0 and 11.0 Hz, glycerol H-1$_{proS}$), 3.63 (b, 1H × 2, H-3 and H-5), 3.63 (b, 2H, choline-$CH_2CH_2N^+(CH_3)_3$), 3.58 (dd, 1H, J = 5.5 and 11.0 Hz, glycerol H-1$_{proR}$), 3.55 (b, 1H, H-4), 3.46 (dd, 1H, H-2), 3.22 (s, 9H, choline-$CH_2CH_2N^+(CH_3)_3$), 2.31 (dd, 2H × 2, J = 7.5 and 15 Hz, -$OCOCH_2CH_2(CH_2)_{12}CH_3$), 1.60 (b, 2H × 2, -$OCOCH_2CH_2(CH_2)_{12}CH_3$), 1.26 (b, 24H × 2, -$OCOCH_2CH_2(CH_2)_{12}CH_3$), 0.88 (t, 3H × 2, J = 7.0 Hz, -$OCOCH_2CH_2(CH_2)_{12}CH_3$); HRMS–FAB ($m/z$): $M + Na]^+$ calcd for $C_{46}H_{90}NO_{13}PNa$, 918.6048; found, 918.6078.

3-*O*-(α-D-glucopyranosyl)-1,2-di-*O*-palmitoyl-*sn*-glycerol (10, entry 3): Compound **10** was obtained as a waxy solid (73 mg, 83% yield) from **8a** (120 mg, 0.12 mmol) by catalytic hydrogenation under the same reaction conditions as those described above for the preparation of **I-a**. $[\alpha]_D^{30}$ +27.2 (c 1.0, $CHCl_3/CH_3OH$ 10:1); IR (KBr, film): 3411, 2919, 2851, 1739, 1587, 1465, 1158, 1053, 720 cm^{-1}; ^{1}H NMR (500 MHz, $CDCl_3/CD_3OD$ 10:1): δ_H 5.25 (m, 1H, glycerol H-2), 4.83 (d, 1H, J = 3.5 Hz, H-1), 4.40 (dd, 1H, J = 3.5 and 12.0 Hz, glycerol H-1$_{proS}$), 4.16 (dd, 1H, J = 6.5 and 12.0 Hz, glycerol H-1$_{proR}$), 3.82 (dd, 1H, J = 5.5 and 10.5 Hz, glycerol H-3$_{proR}$), 3.78 (d, 2H, J = 3.5 Hz, H-6$_{proR}$ and H-6$_{proS}$), 3.65 (t, 1H, J = 9.5 and 9.5 Hz, H-3), 3.62 (dd, 1H, J = 6.0 and 10.5 Hz, glycerol H-3$_{proS}$), 3.56 (dt, 1H, H-5), 3.44 (dd, 1H, J = 3.5 and 9.5 Hz, H-2), 3.42 (dd, 1H, J = 8.5 and 10.0 Hz, H-4), 2.32 (dt, 2H × 2, -$OCOCH_2CH_2(CH_2)_{12}CH_3$), 1.61 (b, 2H × 2, -$OCOCH_2CH_2(CH_2)_{12}CH_3$), 1.26 (b, 24H × 2, -$OCOCH_2CH_2(CH_2)_{12}CH_3$), 0.88 (t, 3H × 2, J = 7.0 Hz, -$OCOCH_2CH_2(CH_2)_{12}CH_3$); HRMS–FAB ($m/z$): $[M + Na]^+$calcd for $C_{41}H_{78}O_{10}Na$, 753.5493;found, 753.5519.

3-*O*-(6-*O*-palmitoyl-α-D-glucopyranosyl)-1,2-di-*O*-palmitoyl-*sn*-glycerol (11, entry 4): A mixture of **8a** (120 mg, 0.12 mmol) and palmitoyl chloride (165 mg, 0.6 mmol) in pyridine was stirred at rt for 3 h and then treated with CH_3OH (1 mL) for 3 h. After concentration in vacuo, the residue was purified on silica gel (toluene/ethyl acetate). The main product (138 mg) was dissolved in a mixture of cyclohexene/ethanol 1:4 and subjected to catalytic hydrogenation at atmospheric pressure in the presence of $Pd(OH)_2$/C (50 mg). The product was purified by silica gel column chromatography ($CH_3OH/CHCl_3$) to afford **11** (99 mg, 85% yield from **8a**). $[\alpha]_D^{30}$ +20.9 (c 1.0, $CHCl_3/CH_3OH$ 10:1); IR (KBr, film): 3414, 2919, 2851, 1739, 1605, 1465, 1375, 1176, 1054, 720 cm^{-1}; ^{1}H NMR (500 MHz, $CDCl_3/CD_3OD$ 10:1): δ_H 5.25 (m, 1H, glycerol H-2), 4.82 (d, 1H, J = 4.0 Hz, H-1), 4.40 (dd, 1H, J = 3.5 and 12.0 Hz, glycerol H-1$_{proS}$), 4.34 and 4.30 (dd × 2, 2H, J = 5.0 and 12.0, 2.5 and 12.0 Hz, H-6$_{proR}$ and H-6$_{proS}$), 4.16 (dd, 1H, J = 6.5 and 12.0 Hz, glycerol H-1$_{proR}$), 3.82 (dd, 1H, J = 5.0 and 10.5 Hz, glycerol H-3$_{proR}$), 3.73 (m, 1H, H-5), 3.65 (dd, 1H, J = 9.0 and 9.5 Hz, H-3), 3.61 (dd, 1H, J = 5.5 and 10.5 Hz, glycerol H-3$_{proS}$), 3.45 (dd, 1H, J = 4.0 and 9.5 Hz, H-2), 3.33 (dd, 1H, J = 9.0 and 10.0 Hz, H-4), 2.33 (m, 2H × 3, -$OCOCH_2CH_2(CH_2)_{12}CH_3$), 1.61 (b, 2H × 3, -$OCOCH_2CH_2(CH_2)_{12}CH_3$), 1.26 (b, 24H × 3, -$OCOCH_2CH_2(CH_2)_{12}CH_3$), 0.88 (t, 3H × 3, J = 7.0 Hz, -$OCOCH_2CH_2(CH_2)_{12}CH_3$); HRMS–FAB ($m/z$): $[M + Na]^+$ calcd for $C_{57}H_{108}O_{11}Na$, 991.7789; found, 991.7832.

Acknowledgements

This work was supported by the Industrial Technology Research Grant Program from New Energy and Industrial Technology Development Organization (NEDO) of Japan and from the Science & Technology Project for a Safe & Secure Society from the Ministry of Education, Culture, Sports, Science and Technology (MEXT) of Japan.

References

1. Rawadi, G. *Microbes Infect.* **2000,** *2,* 955–964. doi:10.1016/S1286-4579(00)00395-6
2. Shimizu, T.; Kida, Y.; Kuwano, K. *Immunology* **2004,** *113,* 121–129. doi:10.1111/j.1365-2567.2004.01937.x
3. Romero, F.; Moreno, E.; Ruiz-Bravo, A.; Jiménez-Valera, M. *Curr. Microbiol.* **2004,** *48,* 237–239. doi:10.1007/s00284-003-4134-1
4. Rottem, S. *Biochim. Biophys. Acta, Rev. Biomembr.* **1980,** *604,* 65–90. doi:10.1016/0005-2736(80)90585-4
5. Boggs, J. M. *Biochim. Biophys. Acta* **1987,** *906,* 353–404.

6. Toujima, S.; Kuwano, K.; Zhang, Y.; Fujimoto, N.; Hirama, M.; Oishi, T.; Fukuda, S.; Nagumo, Y.; Imai, H.; Kikuchi, T.; Arai, S. *Microbiology (Reading, U. K.)* **2000,** *146,* 2317–2323.
7. Matsuda, K.; Kasama, T.; Ishizuka, I.; Handa, S.; Yamamoto, N.; Taki, T. *J. Biol. Chem.* **1994,** *269,* 33123–33128.
8. Matsuda, K.; Li, J.-L.; Harasawa, R.; Yamamoto, N. *Biochem. Biophys. Res. Commun.* **1997,** *233,* 644–649. doi:10.1006/bbrc.1997.6443
9. Li, J.-L.; Matsuda, K.; Takagi, M.; Yamamoto, N. *J. Immunol. Methods* **1997,** *208,* 103–113. doi:10.1016/S0022-1759(97)00135-X,
10. Matsuda, K.; Li, J.-L.; Ichinose, S.; Harasawa, R.; Saito, M.; Yamamoto, N. *Microbiol. Immunol.* **2000,** *44,* 695–702.
11. Zähringer, U.; Wagner, F.; Rietschel, E. T.; Ben-Menachem, G.; Deutsch, J.; Rottem, S. *J. Biol. Chem.* **1997,** *272,* 26262–26270. doi:10.1074/jbc.272.42.26262
12. Ben-Menachem, G.; Byström, T.; Rechnitzer, H.; Rottem, S.; Rilfors, L.; Lindblom, G. *Eur. J. Biochem.* **2001,** *268,* 3694–3701. doi:10.1046/j.1432-1327.2001.02277.x
13. Brandenburg, K.; Wagner, F.; Müller, M.; Heine, H.; Andrä, J.; Koch, M. H. J.; Zähringer, U.; Seydel, U. *Eur. J. Biochem.* **2003,** *270,* 3271–3279. doi:10.1046/j.1432-1033.2003.03719.x
14. Yavlovich, A.; Katzenell, A.; Tarshis, M.; Higazi, A. A.-R.; Rottem, S. *Infect. Immun.* **2004,** *72,* 5004–5011. doi:10.1128/IAI.72.9.5004-5011.2004
15. Nishida, Y.; Ohrui, H.; Meguro, H.; Ishizawa, M.; Matsuda, K.; Taki, T.; Handa, S.; Yamamoto, N. *Tetrahedron Lett.* **1994,** *35,* 5465–5468. doi:10.1016/S0040-4039(00)73526-X
16. Nishida, Y.; Takamori, Y.; Ohrui, H.; Ishizaka, I.; Matsuda, K.; Kobayashi, K. *Tetrahedron Lett.* **1999,** *40,* 2371–2374. doi:10.1016/S0040-4039(99)00191-4
17. Matsuda, K. Phosphocholine-containing glycoglycerolipids of Mycoplasma fermentans as a pathogen of rheumatoid arthritis: possible role of Mycoplasma fermentans GGPLs in the pathogenesis of neuroendocrine-immune abnormalities.. In *Recent research developments in neuroscience;* Pandalai, S. G., Ed.; Research Signpost: India, 2004; Vol. 1, pp 15–23.
18. Kawahito, Y.; Ichinose, S.; Sano, H.; Tsubouchi, Y.; Kohno, M.; Yoshikawa, T.; Tokunaga, D.; Hojo, T.; Harasawa, R.; Nakano, T.; Matsuda, K. *Biochem. Biophys. Res. Commun.* **2008,** *369,* 561–566. doi:10.1016/j.bbrc.2008.02.079
19. Sato, N.; Oizumi, T.; Kinbara, M.; Sato, T.; Funayama, H.; Sato, S.; Matsuda, K.; Takada, H.; Sugawara, S.; Endo, Y. *FEMS Immunol. Med. Microbiol.* **2010,** *59,* 33–41. doi:10.1111/j.1574-695X.2010.00657.x
20. Fujiwara, M.; Ishida, N.; Asano, K.; Matsuda, K.; Nomura, N.; Nishida, Y.; Harasawa, R. *J. Vet. Med. Sci.* **2010,** *72,* 805–808. doi:10.1292/jvms.09-0572
21. Ishida, N.; Irikura, D.; Matsuda, K.; Sato, S.; Sone, T.; Tanaka, M.; Asano, K. *Curr. Microbiol.* **2009,** *58,* 535–540. doi:10.1007/s00284-009-9362-6
22. Ishida, N.; Irikura, D.; Matsuda, K.; Sato, S.; Sone, T.; Tanaka, M.; Asano, K. *J. Biosci. Bioeng.* **2010,** *109,* 341–345. doi:10.1016/j.jbiosc.2009.09.049
23. Shingu, Y.; Nishida, Y.; Dohi, H.; Matsuda, K.; Kobayashi, K. *J. Carbohydr. Chem.* **2002,** *21,* 605–611. doi:10.1081/CAR-120016858
24. Shingu, Y.; Nishida, Y.; Dohi, H.; Kobayashi, K. *Org. Biomol. Chem.* **2003,** *1,* 2518–2521. doi:10.1039/b303984f
25. Nishida, Y.; Shingu, Y.; Dohi, H.; Kobayashi, K. *Org. Lett.* **2003,** *5,* 2377–2380. doi:10.1021/ol034269+
26. Shingu, Y.; Miyachi, A.; Miura, Y.; Kobayashi, K.; Nishida, Y. *Carbohydr. Res.* **2005,** *340,* 2236–2244. doi:10.1016/j.carres.2005.07.020
27. Gigg, R.; Penglis, A. A. E.; Conant, R. *J. Chem. Soc., Perkin Trans. 1* **1977,** 2014–2017. doi:10.1039/P19770002014
28. Mannock, D. A.; Lewis, R. N.; McElhaney, R. N. *Chem. Phys. Lipids* **1990,** *55,* 309–321. doi:10.1016/0009-3084(90)90169-R
29. Gordon, D. M.; Danishefsky, S. J. *J. Am. Chem. Soc.* **1992,** *114,* 659–663. doi:10.1021/ja00028a036
30. Imai, H.; Oishi, T.; Kikuchi, T.; Hirama, M. *Tetrahedron* **2000,** *56,* 8451–8459. doi:10.1016/S0040-4020(00)00793-6
31. Shvets, V. I.; Bashkatova, A. I.; Evstigneeva, R. P. *Chem. Phys. Lipids* **1973,** *10,* 267–285. doi:10.1016/0009-3084(73)90006-6 And see the related references cited therein.
32. Lemieux, R. U.; Hendriks, K. B.; Stick, R. V.; James, K. *J. Am. Chem. Soc.* **1975,** *97,* 4056–4062. doi:10.1021/ja00847a032
33. Lu, S.-R.; Lay, Y.-H.; Chen, J.-H.; Liu, C.-Y.; Mong, K.-K. T. *Angew. Chem.* **2011,** *123,* 7453–7458. doi:10.1002/ange.201100076 And see the related references cited therein.
34. Hayakawa, Y.; Kataoka, M. *J. Am. Chem. Soc.* **1997,** *119,* 11758–11762. doi:10.1021/ja970685b
35. Nishida, Y.; Uzawa, H.; Hanada, S.; Ohrui, H.; Meguro, H. *Agric. Biol. Chem.* **1989,** *53,* 2319–2326. doi:10.1271/bbb1961.53.2319
36. Uzawa, H.; Nishida, Y.; Hanada, S.; Ohrui, H.; Meguro, H. *J. Chem. Soc., Chem. Commun.* **1989,** 862–863. doi:10.1039/C39890000862
37. Uzawa, H.; Nishida, Y.; Ohrui, H.; Meguro, H. *J. Org. Chem.* **1990,** *55,* 116–122. doi:10.1021/jo00288a024
38. Ohrui, H.; Nishida, Y.; Watanabe, M.; Hori, H.; Meguro, H. *Tetrahedron Lett.* **1985,** *26,* 3251–3254. doi:10.1016/S0040-4039(00)98164-4
39. Nishida, Y.; Hori, H.; Ohrui, H.; Meguro, H.; Uzawa, J.; Reimer, D.; Sinnwell, V.; Paulsen, H. *Tetrahedron Lett.* **1988,** *29,* 4461–4464. doi:10.1016/S0040-4039(00)80522-5
40. Hori, H.; Nishida, Y.; Ohrui, H.; Meguro, H.; Uzawa, J. *Tetrahedron Lett.* **1988,** *29,* 4457–4460. doi:10.1016/S0040-4039(00)80521-3
41. Nishida, Y.; Hori, H.; Ohrui, H.; Meguro, H. *J. Carbohydr. Chem.* **1988,** *7,* 239–250. doi:10.1080/07328308808058917
42. Haasnoot, C. A. G.; de Leeuw, F. A. A. M.; Altona, C. *Tetrahedron* **1980,** *36,* 2783–2790. doi:10.1016/0040-4020(80)80155-4
43. Matsuda, K. Antigens: Lipids. In *Encyclopedia of Life Science*; John Wiley and Sons: Chichester, U. K., 2002; pp. 748–755.
44. Koynova, R. D.; Kuttenreich, H. L.; Tenchov, B. G.; Hinz, H. J. *Biochemistry* **1988,** *27,* 4612–4619. doi:10.1021/bi00413a005
45. Mannock, D. A.; Lewis, R. N.; McElhaney, R. N.; Akiyama, M.; Yamada, H.; Turner, D. C.; Gruner, S. M. *Biophys. J.* **1992,** *63,* 1355–1368. doi:10.1016/S0006-3495(92)81713-7

Beilstein Journal of Organic Chemistry

Carbohydrate-auxiliary assisted preparation of enantiopure 1,2-oxazine derivatives and aminopolyols

Marcin Jasiński[1,2], Dieter Lentz[1,§] and Hans-Ulrich Reissig[*1]

Full Research Paper

Open Access

Address:
[1]Institut für Chemie und Biochemie, Freie Universität Berlin, Takustr. 3, D-14195 Berlin, Germany and [2]Department of Organic and Applied Chemistry, University of Łódź, Tamka 12, PL-91-403 Poland

Email:
Hans-Ulrich Reissig* - hreissig@chemie.fu-berlin.de

* Corresponding author
§ Responsible for X-ray crystal-structure determination

Keywords:
aminopolyols; carbohydrates; chiral auxiliaries; lithiated alkoxyallenes; 1,2-oxazines; pyrroles; pyrrolidines; samarium diiodide

Beilstein J. Org. Chem. **2012,** *8,* 662–674.
doi:10.3762/bjoc.8.74

Received: 27 January 2012
Accepted: 28 March 2012
Published: 30 April 2012

This article is part of the Thematic Series "Synthesis in the glycosciences II".

Guest Editor: T. K. Lindhorst

Abstract

An approach to enantiopure hydroxylated 2*H*-1,2-oxazine derivatives is presented utilizing the [3 + 3] cyclisation of lithiated alkoxyallenes and an L-erythrose-derived *N*-glycosyl nitrone as precursors. This key step proceeded only with moderate diastereoselectivity, but allowed entry into both enantiomeric series of the resulting 3,6-dihydro-2*H*-1,2-oxazines. Their enol ether double bond was then subjected to a hydroboration followed by an oxidative work-up, and finally the auxiliary was removed. The described three-step procedure enabled the synthesis of enantiopure hydroxylated 1,2-oxazines. Typical examples were treated with samarium diiodide leading to enantiopure acyclic aminopolyols. We also report on our attempts to convert these compounds into enantiopure hydroxylated pyrrolidine derivatives.

Introduction

During the last few decades carbohydrate-derived nitrones have turned out to be particularly attractive tools for the synthesis of structurally complex compounds [1-4]. Employed mainly as 1,3-dipoles in cycloadditions [5,6] or as imine analogues in nucleophilic additions [7,8], these nitrones very often furnish the corresponding products in a highly selective manner. In this context, reactions of lithiated alkoxyallenes with enantiopure nitrones are particularly of interest since they lead by a [3 + 3] cyclisation process to 1,2-oxazine derivatives with excellent diastereoselectivity [9]. We previously reported on the unusually diverse synthetic potential of carbohydrate-derived 1,2-oxazines allowing the smooth and flexible preparation of various highly functionalised compounds, including de novo syntheses of carbohydrates and their mimetics, as well as *N*-heterocycles [10-12]. Although the reactions of lithiated alkoxyallenes, with nitrones bearing substituents with stereogenic centres at the carbon atom, were studied in our group in great detail [13], *N*-glycosyl-substituted nitrones have so far not

been used as electrophiles for this purpose. This type of nitrone has been introduced and broadly studied by Vasella and co-workers [14-20] and has also been used by other groups [21-25]. They observed moderate to high diastereoselectivities for 1,3-dipolar cycloadditions and for nucleophilic additions. Successful applications of these easily removable auxiliaries in the syntheses of biologically active agents were also reported [26-31]. Apart from the obvious reactivity of *N*-glycosyl nitrones of type **1** leading to five-membered heterocycles **A** or to *N*,*N*-disubstituted hydroxylamine derivatives **B**, a twofold nucleophilic addition of an excess of organometallic reagents furnishing compounds of type **C** ($Nu^1 = Nu^2$) was described and discussed by Goti et al. (Scheme 1) [32]. In selected examples, the synthesis of differently substituted products ($Nu^1 \neq Nu^2$) was possible by consecutive additions of the appropriate Grignard reagents [33]. Here we report on the application of a nitrone with an L-erythronolactone-derived auxiliary for the synthesis of 3,6-dihydro-2*H*-1,2-oxazine derivatives of type **D**. Their selected transformations, including hydroboration of the enol ether moiety, oxidative work-up, glycosyl cleavage, and samarium diiodide-induced reactions, are presented as well.

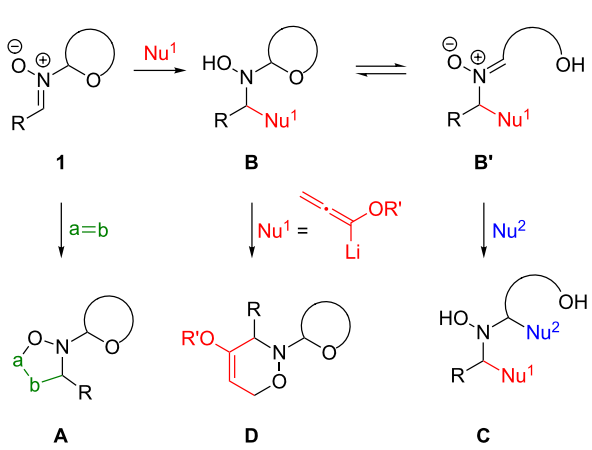

Scheme 1: Reactivity of *N*-glycosyl nitrones **1** towards dipolarophiles and nucleophiles leading to products of type **A**, **B**, **C** and **D**.

Results and Discussion

In continuation of our recent exploration of L-erythrose-derived nitrones for the synthesis of 3,6-dihydro-2*H*-1,2-oxazine derivatives [34], we turned our attention to benzaldehyde-derived nitrone **1a**, which is readily available in a three-step procedure starting from L-arabinose. L-Erythronolactone was first prepared [35] and was subsequently treated with *N*-benzylhydroxylamine [36], and the resulting product was oxidised with activated MnO_2 [37] to furnish the desired compound **1a** in 51% overall yield. The initial experiment with **1a** was carried out under typical conditions with 2.4 equiv of lithiated methoxyallene at −78 °C in THF. Similarly to previous results for more rigid cyclic nitrones [38], the formation of the intermediate *N*-hydroxylamines **2** (Scheme 2) was clearly observed. These primarily formed compounds were not isolated, but (in the presence of a drying agent) they underwent slow cyclisation in Et_2O solution at room temperature to furnish the desired 1,2-oxazine derivative as a mixture of separable diastereomers (3*S*)-

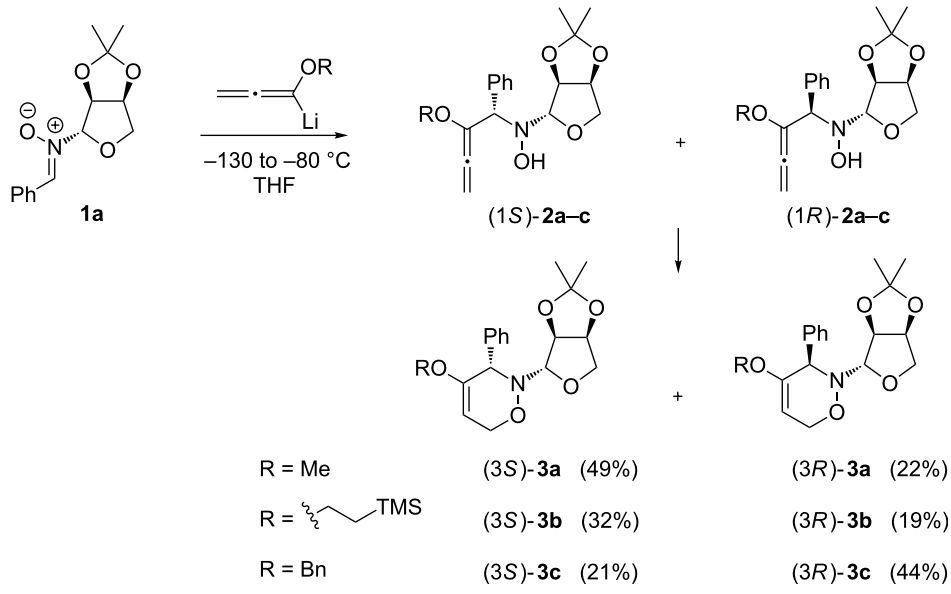

Scheme 2: Additions of lithiated alkoxyallenes to L-erythrose-derived nitrone **1a** leading to 3,6-dihydro-2*H*-1,2-oxazine derivatives **3** via the respective *N*-hydroxylamines **2**.

Table 1: Selected reaction conditions of nitrone **1a** with lithiated methoxyallene.

entry	lithiated methoxyallene (equiv)[a]	*T* (°C)	time (h)	(3*S*)-**3a** / (3*R*)-**3a** ratio[b]	yield[c] [%]
1	10.0	−78	1.0	–	traces[d]
2	3.0	−78	1.0	3:1	26
3	2.4	−78	1.0	3:1	33
4	2.2	−78	1.0	3:1	38
5	1.5	−78	1.0	2.5:1	26
6	2.2	−100 → −80	1.0	2:1	51
7	2.2	−130 → −80	1.5	2:1	75

[a]Reactions performed in 1.1 mmol scale with respect to **1a**. [b]Crude product. [c]Combined yield of isolated (3*S*)-**3a** and (3*R*)-**3a**. [d]Only the major diastereomer (3*S*)-**3a** was detected.

3a and (3*R*)-**3a** in 25% and 8% yield, respectively (Table 1, entry 3). The 1,2-oxazines were accompanied by a complex mixture of by-products, from which only two compounds **4** (1%) and **5** (3%) could be isolated in pure form (Figure 1). After tedious optimisation with respect to stoichiometry, temperature, time, concentration, etc. (selected results are presented in Table 1), we found that running the reaction from −130 to −80 °C, followed by standing overnight at room temperature, allowed the synthesis of **3a** with an overall yield of 75% and a ratio of diastereomers of ca. 2:1 (49% and 22% after separation of the isomers, Table 1, entry 7). When the reaction was scaled up to 3.50 g of **1a** the expected diastereomers of 1,2-oxazines **3a** were obtained with no decrease in yield (78%). As illustrated in Scheme 2, lithiated (2-trimethylsilyl)ethoxyallene and benzyloxyallene were also examined under the optimised reaction conditions and furnished the expected diastereomers of 1,2-oxazine derivatives **3b** and **3c** in 51% and 65% yield, respectively.

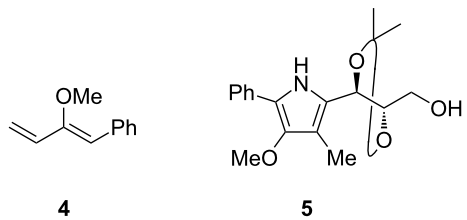

Figure 1: By-products **4** and **5** isolated from the reaction of nitrone **1a** with lithiated methoxyallene.

The mixtures of diastereomers of crude 1,2-oxazines **3a**–**c** were easily separated by standard column chromatography and characterised by spectroscopic methods. However, in certain cases additional purification was necessary to obtain analytically pure samples. The absolute configuration of the newly generated stereogenic centre could not be determined based on NMR techniques. For instance, in the ^{1}H NMR spectra of the diastereomeric products (3*S*)-**3a** and (3*R*)-**3a**, the signals of the benzylic protons assigned to C-3 of the 1,2-oxazine ring appear as singlets at 4.85 and 4.48 ppm, respectively. Due to the unhindered rotation of the auxiliary moiety similar correlation peaks in NOE experiments were observed for both isomers. Fortunately, the minor product (3*R*)-**3a** isolated as an amorphous solid could be recrystallised from ethyl acetate solution to give crystals suitable for an X-ray crystallographic analysis (Figure 2). The X-ray analysis of (3*R*)-**3a** shows a well-defined half-chair conformation of the 1,2-oxazine ring, with four carbon atoms in plane and with ONCC and OCCC torsion angles of −60° and 13°, respectively. The bulky *N*-substituent occupies a pseudo-equatorial position and the phenyl group is in a pseudo-axial position. Since characteristic shift patterns in the ^{1}H NMR spectra for both diastereomeric series are observed, the con-

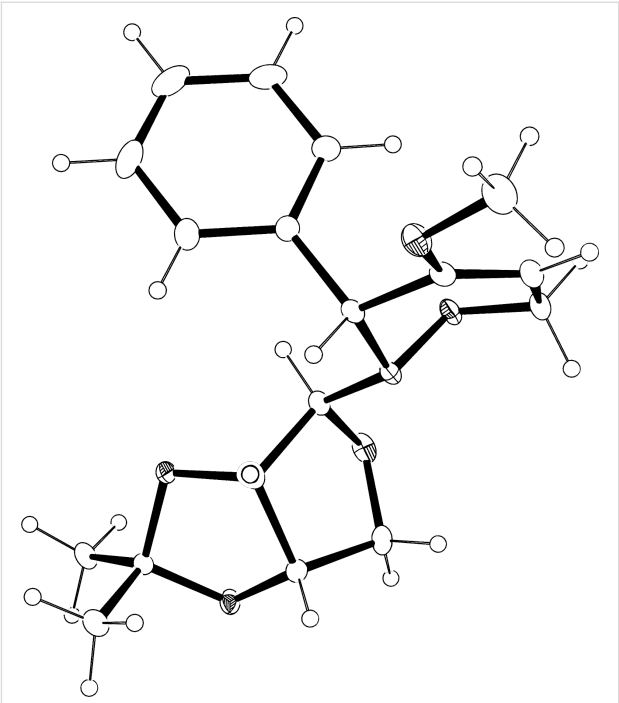

Figure 2: Single-crystal X-ray analysis of (3*R*)-**3a** (ellipsoids are drawn at a 50% probability level).

figuration at C-3 of the TMSE derivatives (**b**) and benzyloxy analogues (**c**) could be assigned as well with high certainty.

The stereochemical outcome observed for the reactions studied also deserves some comment. Whereas lithiated methoxy- and TMS-ethoxyallene yielded the diastereomers in ca. 2:1 ratio, in the case of lithiated benzyloxyallene a significant switch of the selectivity to an approximate 1:2 ratio was observed. According to the model proposed in the literature [7,18,20] for the addition of nucleophiles, the stereochemical course is governed by a competition of steric and electronic effects. As presented in Figure 3, the bulky benzyloxy substituent favours the *anti*-addition and hence yields the (3*R*)-configured product as the major compound. In contrast, the less hindered lithiated methoxyallene enables a *syn*-attack supported by a "kinetic anomeric effect", stabilizing the respective transition state [20] and furnishing the (3*S*)-configured 1,2-oxazine. In all tested examples the level of diastereoselectivity was only low to moderate, and the interpretation should therefore not be exaggerated. Alternative conformations explaining the results are certainly possible.

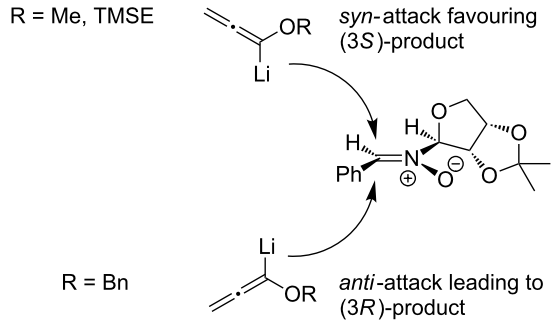

Figure 3: Model proposed for the addition of lithiated allenes to nitrone **1a**.

The fragmentation of the primarily formed allenyl *N*-hydroxylamines of type **2** leading to 1,3-dienes such as **4** (Figure 1) by retro-nitroso-ene reaction was discussed in earlier work [13], but the formation of pyrrole derivative **5** is unprecedented for the reactions of nitrones and lithiated alkoxyallenes. The ^{1}H NMR spectrum of **5** shows four singlets (3H each) assigned to three methyl groups and one methoxy substituent. Additionally, a broad singlet at δ = 8.98 ppm attributed to the NH functionality, an OH group at 2.11 ppm (dd, $J \approx$ 4.0, 8.1 Hz) coupling with the adjacent methylene group, and a characteristic set of multiplets of the [1,3]dioxolane and the phenyl moieties could be found. The signals of four quaternary carbon atoms in the ^{13}C NMR spectrum evidenced the presence of the pyrrole structure. Finally, the HMBC experiment proved the proposed substitution pattern at the pyrrole ring. HRMS and elemental analysis allowed identification of **5** as a 2,3,4,5-tetrasubstituted pyrrole derivative.

As shown in Table 1, entries 1–3, a higher excess of lithiated methoxyallene resulted in a significant decrease in the yield of 1,2-oxazine derivatives. For example, in the case of 10 equiv of lithiated methoxyallene (Table 1, entry 1) only a trace amount of (3*S*)-**3a** (<5%) and numerous side products were found in the crude product, including compound **5**. On the other hand, no pyrrole **5** could be detected when only a slight excess of methoxyallene was used (Table 1, entry 5) or when the reaction was performed at lower temperatures (Table 1, entries 6 and 7). These observations prompted us to postulate that the surprising formation of **5** is the result of a double addition of lithiated methoxyallene to nitrone **1a** as illustrated in Scheme 3, the crucial step being the (reversible) opening of the tetrahydrofuran ring of the primary addition product **E**. The resulting new nitrone **F** can then react with the second equiv of lithiated methoxyallene to give the double adduct **G**. After aqueous work-up, hydroxylamine derivative **H** underwent a ring-closure to 1,2-oxazetidine derivative **I**. It is known that this class of compounds can suffer a thermally induced [2 + 2] cycloreversion involving N–O bond cleavage [39,40], which, in our case, led to the formation of methyl acrylate and imine **J**. This imine underwent subsequent cyclisation to zwitterion **K** and two proton shifts, probably via 3-exomethylene compound **L,** finally led to pyrrole **5**. This mechanism is certainly speculative but offers a possibility to explain the formation of the tetrasubstituted pyrrole **5**. The structure of the intermediate double-addition product **H** suggests that other by-products may be formed, e.g., two different *N*-allenylmethyl-substituted 3,6-dihydro-2*H*-1,2-oxazines or an isomeric pyrrole derivative. The numerous sets of signals in the ^{1}H NMR spectrum as well as additional spots seen on TLC of the crude reaction mixtures support this assumption, but none of these possible by-products could be isolated.

With respect to the enormous importance of polyhydroxylated *N*-heterocycles as carbohydrate-mimicking glycosidase inhibitors [41-45], the introduction of an additional hydroxyl moiety into 1,2-oxazine derivatives was an essential goal in several studies by our group [34,46-48]. A series of 5-hydroxy-1,2-oxazine derivatives was successfully prepared by the well known hydroboration/oxidation protocol, with yields and selectivities strongly depending on the relative configuration of the employed 1,2-oxazine derivative and on the presence of additives [34,48]. In general, *syn*-configured 1,2-oxazines (with respect to the relative configuration at C-3 and the neighbouring stereogenic centre at the carbohydrate-derived C-3-substituent) were found to be excellent substrates, leading to the desired alcohols exclusively with very high degrees of stereose-

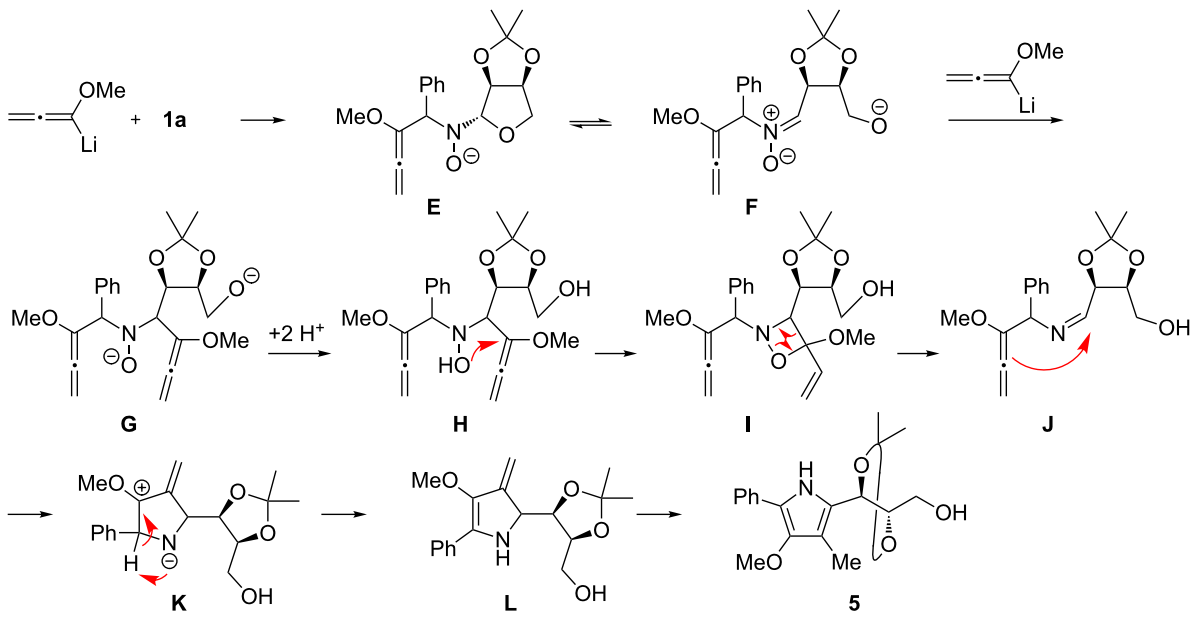

Scheme 3: Speculative mechanistic suggestion for the formation of tetrasubstituted pyrrole derivative **5**.

lectivity. In an extension of these studies, selected compounds of type **3** were hydroxylated following the general methodology. As shown in Scheme 4, each of the (3*S*)-configured 1,2-oxazines **3a** and **3b** furnished a pair of hydroxylated products **6**, **7** and **8**, **9**, respectively, in high combined yields (83% and 93%) and almost the same ratio (approximately 3:2) of *cis*-*trans*/*trans*-*trans* isomers. The stereoselectivity for this series is apparently only low. On the other hand, for (3*R*)-**3a** a ca. 3:1 ratio of hydroxylated products was observed based on the ^{1}H NMR spectrum of the crude mixture; however, the minor product **10** was isolated in 13% yield only, whereas the major product was obtained in a satisfying 66% yield. We assume that the observed low facial selectivity results predominantly from the moderate hindrance exhibited by the neighbouring phenyl substituent, which in the case of the (3*S*)-series probably occupies a pseudo-equatorial position in the half-chair conformation of the 3,6-dihydro-2*H*-1,2-oxazine derivatives **3**. The higher stereoselectivity of the hydroboration of (3*R*)-**3a** is probably caused by the pseudo-axial location of the phenyl group (as evidenced by the X-ray analysis, Figure 2), shielding one side more efficiently. The carbohydrate-derived *N*-substituent is relatively far away from the two reacting carbon atoms and very likely has no strong, direct influence on the observed diastereoselectivities.

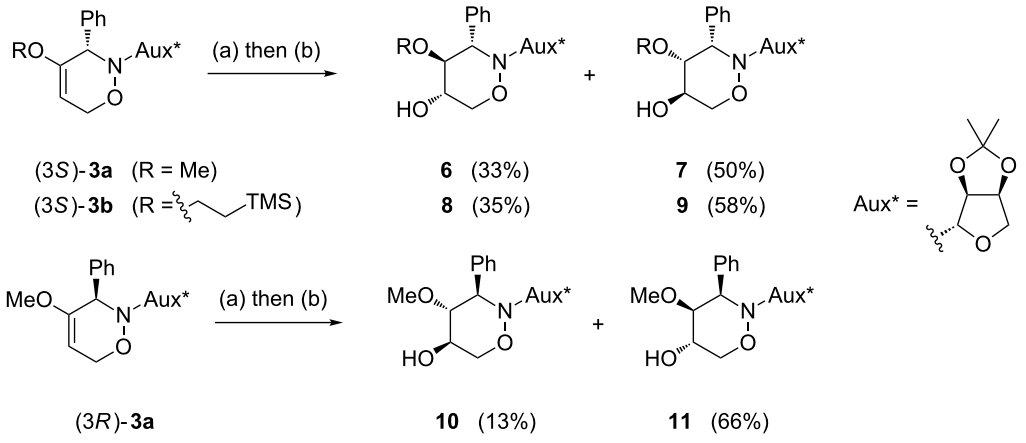

Scheme 4: Introduction of a 5-hydroxy group into 1,2-oxazine derivatives **3** by a hydroboration/oxidation protocol; (a) BH_3·THF (4.0 equiv), THF, −30 °C to rt, 3 h; (b) NaOH, H_2O_2 (30%), −10 °C to rt, overnight.

All products **6**–**11** obtained by the hydroboration/oxidation protocol were easily purified and separated by column chromatography and finally deprotected by treatment with acid. This afforded a series of the desired, highly functionalised tetrahydro-2*H*-1,2-oxazine derivatives **12**–**15**, including *ent*-**12** and *ent*-**13** (Table 2). Reaction of the *trans*-*trans*-configured 4-methoxy-1,2-oxazines **6** and **10** with a methanolic solution of HCl (1 M) at elevated temperatures enabled the smooth

Table 2: Acid-induced cleavages of *N*- and *O*-protective groups of 5-hydroxy-1,2-oxazine derivatives **6**–**11**; conditions: (a) HCl (1 M) in MeOH, 40 °C, 3.5 h; (b) DOWEX-50, EtOH, 50 °C, 4 d; (c) BBr_3 (3 equiv), CH_2Cl_2, −78 °C (1 h) then rt, overnight.

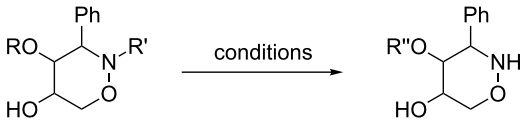

R = Me, TMSE
R' = Aux*, H

R'' = Me, TMSE, H

entry	*N*-glycosyl 1,2-oxazine	conditions	product	yield	mp/$[\alpha]_D^{22}$
1	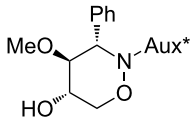 **6**	(a)	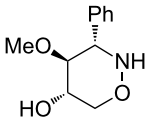 **12**	79%	110–112 °C/ +60.1 (*c* 1.05, $CHCl_3$)
2	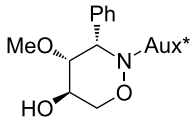 **7**	(a)	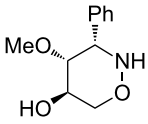 **13**	83%	112–113 °C/ +47.9 (*c* 1.00, $CHCl_3$)
3	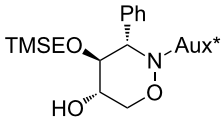 **8**	(b)[a]	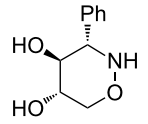 **14**	78%	153–154 °C/ +33.8 (*c* 1.05, CH_3OH)
4	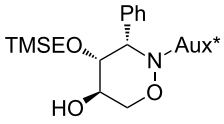 **9**	(a) then (b)	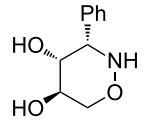 **15**	75%[b]	190–192 °C/ +65.6 (*c* 1.26, CH_3OH)
5	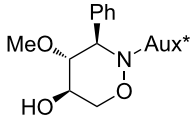 **10**	(a)	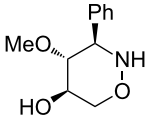 *ent*-**12**	84%	110–112 °C/ −61.5 (*c* 1.18, $CHCl_3$)
6	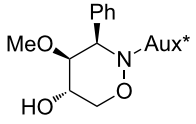 **11**	(a)	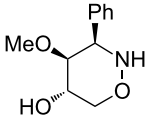 *ent*-**13**	92%	110–113 °C/ −48.8 (*c* 1.10, $CHCl_3$)
7	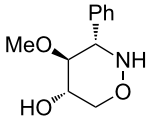 **12**	(c)	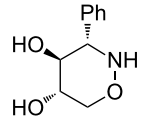 **14**	18%	—[c]

[a]Reaction time prolonged to 10 days; [b]overall yield for two steps; [c]melting point and spectroscopic data correspond with the sample of compound **14** obtained from **8** (Table 2, entry 3).

cleavage of the glycosyl bond to give the *N*-unsubstituted derivatives **12** and *ent*-**12** in high yields (Table 2, entries 1 and 5). The *cis*-*trans*-configured compound pair **7** and **11** provided similar results, yielding the expected enantiomers **13** and *ent*-**13** (Table 2, entries 2 and 6). As expected, the enantiomers show nicely matching optical rotations with opposite sign. In the case of the TMSE-protected derivative **9**, selective removal of the *N*-protective group could be achieved under the applied conditions. After prolonged reaction times (16 h) there was no significant change in the tested sample. A complete deprotection of **9** leading to dihydroxylated compound **15** was possible in high overall yield (75%) by using ion-exchange resin DOWEX-50 at 50 °C (Table 2, entry 4). As shown for compound **8**, simultaneous cleavage was also possible, and the analytically pure compound **14** was isolated in comparable yield (Table 2, entry 3). Alternatively, demethylation of **12** by treatment with boron tribromide at low temperatures [49] also provided the expected compound **14** (Table 2, entry 7); however, the analytically pure sample of this compound could only be isolated in 18% yield. Therefore, the protocol applying a TMS-ethyl substituent as a more easily removable O-protective group turned out to be much more effective. All enantiopure 1,2-oxazines **12**–**15** were isolated as colourless crystals, which were prone to sublimation.

The ^{1}H NMR spectrum of *trans*–*trans* configured **14** also deserves a short comment. Similarly to the previously described 2,4- and 2,5-dimethyltetrahydro-1,2-oxazine derivatives [50], significant long-range couplings could be observed in the ^{1}H NMR spectrum. The low-field shifted multiplet (4.12–4.19 ppm) assigned to the equatorial 6-H showed additional couplings of <2.5 Hz. However, due to 4-H/5-H overlapping, selective decoupling of this complex spin system was not possible. An indirect proof for the observed phenomenon was found in the ^{1}H NMR spectrum (Supporting Information File 2) of **14** prior to purification, i.e., still containing BBr_3, which acts here as a shift reagent. The influence of the coordinated boron species resulted not only in a strong low-field shift but it also simplified the spectrum, and thus, only geminal and vicinal couplings (J = 12.2 Hz and J = 5.4 Hz) for the equatorial 6-H could be found. On the other hand, a possible nitrogen and/or ring inversion usually measurable at lower temperatures should be taken into account [51]. As expected, no significant changes in the shift pattern were observed in a series of ^{1}H NMR spectra measured at elevated temperatures, both in methanol-d_4 (up to 50 °C) and DMSO-d_6 (up to 80 °C). Moreover, in the ^{13}C NMR spectrum only one set of sharp signals was observed.

Due to their similarity to carbohydrate derivatives, hydroxylated 1,2-oxazines such as **12**–**15** may already have interesting biological activity, but their functional groups also open several options for subsequent transformations into other relevant compound classes. By reductive ring opening the corresponding amino polyols should be accessible. Since compounds of type **12** contain a benzylamine substructure, standard methods that may possibly attack this moiety, such as catalytic hydrogenation, should be avoided. As an alternative, samarium diiodide is an attractive reagent for this purpose. Apart from its extraordinary potential for the formation of new carbon–carbon bonds [52-54], the cleavage of N–O bonds in a chemoselective fashion is also well documented [55-57]. The application of samarium diiodide for 1,2-oxazine ring opening allowed efficient syntheses of numerous polyhydroxylated heterocycles, such as pyrrolidine [46], azetidine [47], furan [58], and pyran derivatives [59]. Gratifyingly, the treatment of tetrahydro-2*H*-1,2-oxazine derivatives **12** and **13** with an excess of SmI_2 in tetrahydrofuran smoothly provided the expected amino alcohols **16** and **17** in excellent yields (Scheme 5).

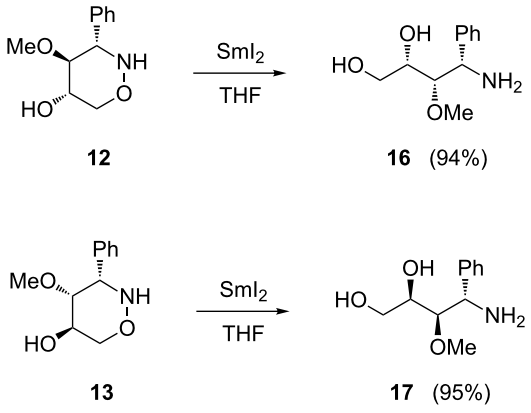

Scheme 5: Samarium diiodide-induced ring opening of tetrahydro-2*H*-1,2-oxazine derivatives **12** and **13**.

In order to compare the behaviour of a compound still bearing the *N*-auxiliary, we converted tetrahydro-2*H*-1,2-oxazine **7** into the *O*-benzylated derivative **18** under standard conditions (Scheme 6). Treatment of this protected compound with samarium diiodide furnished a complex mixture of products from which only the two amino alcohols **19** and **20** were isolated, in low yield. The formation of **20** could be explained by a subsequent SmI_2-mediated reduction of the C=N bond formed by ring opening of **19**, which contains a hemiaminal moiety. This suggestion is supported by the ^{1}H NMR spectrum of **19** in which a second set of signals could be easily detected. Thus, the direct use of 1,2-oxazine derivatives still containing the carbohydrate-derived auxiliary at the nitrogen is apparently not sufficiently selective during samarium diiodide-promoted reactions.

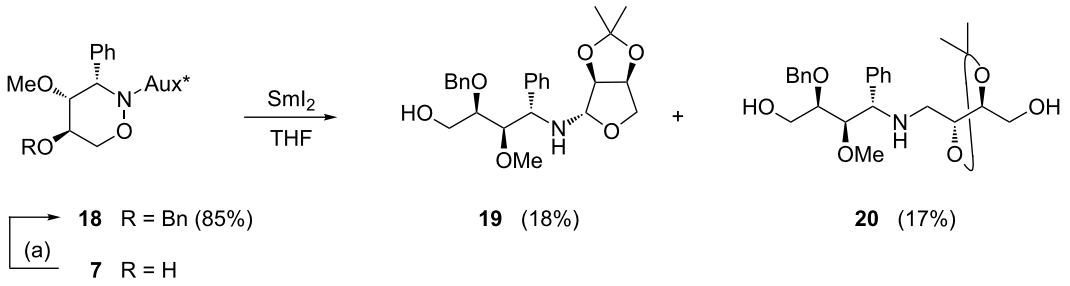

Scheme 6: Reaction of tetrahydro-2*H*-1,2-oxazine **18** with samarium diiodide. (a) NaH (1.4 equiv), BnBr (1.2 equiv), DMF, 0 °C to rt, overnight.

The successful transformation of *N*-benzyl-substituted tetrahydro-2*H*-1,2-oxazine derivatives into polyhydroxylated pyrrolidine derivatives [46] prompted us to select compound **13** as a precursor and to examine the described methods with this substrate. First, the free hydroxy group was protected as a trimethylsilyl ether and, after SmI_2-induced ring opening, the expected product **22** was clearly identified based on TLC monitoring. However, the attempted isolation and purification of this compound by column chromatography provided amino alcohol **17** as the only product in high yield (92%). The limited stability of the TMS protective group is evident from the results presented in Scheme 7. Treatment of freshly prepared unpurified **22** with an excess of mesyl chloride and triethylamine yielded a complex product mixture. The isolated compounds **23**–**26** clearly indicate that the migration of the TMS group not only takes place in an intramolecular fashion to the terminal hydroxy function to furnish **24**, but it also occurs intermolecularly leading to the disilylated mesylamide **23**. The desired pyrrolidine derivative **25** was obtained only as a minor product (5%). The major isolated component, *N*,*O*-dimesylated pyrrolidine **26** (35%) derives from **25** by TMS-cleavage and subsequent mesylation of the OH group.

To overcome these apparent difficulties, *tert*-butyldimethylsilyl-protected compound **27** was prepared. Samarium diiodide-mediated ring opening under standard conditions furnished the expected amino alcohol **28** in excellent yield (Scheme 8). An attempted cyclisation of **28** using tosyl chloride in the presence of triethylamine was not successful but led to *N*-tosylated compound **31** in 24% yield. A partial epimerisation at the benzylic position and slow decomposition of precursor **28** could also be observed under the reaction conditions applied, and none of the desired pyrrolidine derivatives could be found in the crude product. Purification on a silica gel column yielded two fractions containing a mixture of the C-4 epimeric *N*,*O*-ditosylated compounds (14%, ca. 1:1 ratio) and a mixture of the respective tosylamides (41%, ca. 4:1 ratio). Additional chromatography of the latter fraction enabled isolation of compound **31** in the pure state (24%). Isolation of other by-products was not possible.

Fortunately, the use of mesyl chloride was more efficient to achieve cyclisation of **28**. Application of this reagent afforded pyrrolidine derivative **29** in acceptable overall yield. The different reaction outcome observed for the transformations of

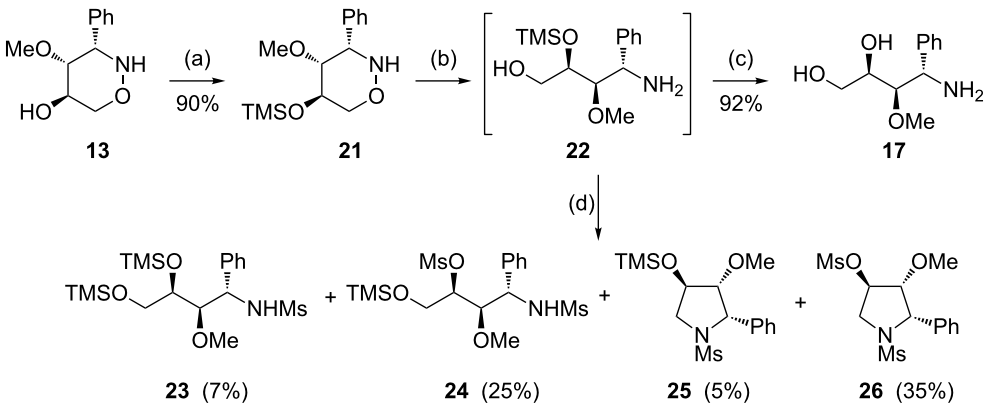

Scheme 7: Attempted synthesis of pyrrolidine derivatives from precursor **13**. (a) TMSCl (1.5 equiv), imidazole, DMAP, CH_2Cl_2, rt, overnight; (b) SmI_2, THF, 1.5 h, rt; (c) $CHCl_3$, rt, overnight; (d) MsCl (4 equiv), Et_3N, CH_2Cl_2, rt, overnight.

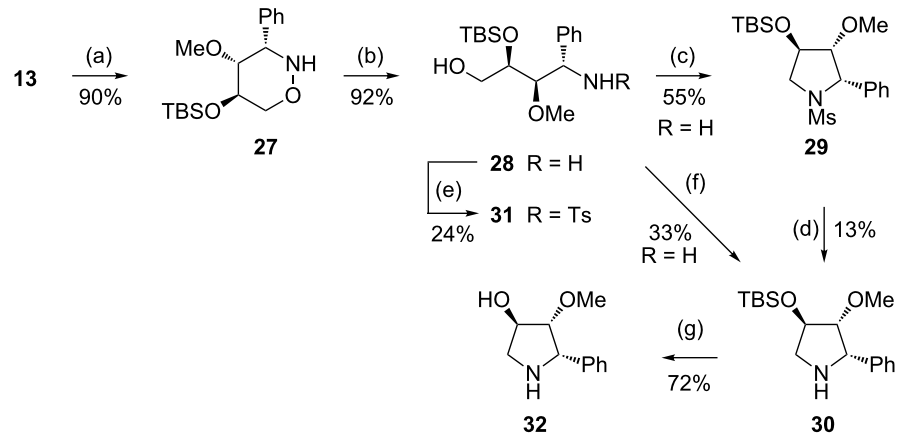

Scheme 8: Synthesis of TBS-protected tetrahydro-2*H*-1,2-oxazine **27** and its transformation into pyrrolidine derivatives **29**, **30** and **32**. (a) TBSCl (2.0 equiv), imidazole, DMAP, CH_2Cl_2, rt, 5 d; (b) SmI_2, THF, 1.5 h, rt; (c) MsCl (2.0 equiv), Et_3N, CH_2Cl_2, rt, overnight; (d) LDA (5.4 equiv), rt, 16 h; (e) *p*TsCl (2.2 equiv), Et_3N, CH_2Cl_2, rt, overnight; (f) CBr_4 (1.2 equiv), PPh_3 (1.2 equiv), Et_3N (1.1 equiv), CH_2Cl_2, rt, overnight; (g) HCl (1 M) in MeOH, rt, 3 d.

28 with the two sulfonyl chlorides is probably a consequence of the bulkiness of the TBS group. The small sulfene intermediate, generated from mesyl chloride, smoothly reacts with the terminal OH group to give the respective mesylate, which subsequently cyclises to afford pyrrolidine **29**. On the other hand, the more bulky tosyl chloride competitively attacks the amino group. As illustrated in Scheme 8, the attempted conversion of **29** into the free secondary amine **30** by treatment with LDA [60] was not very efficient. The target compound was accompanied by a mixture of dihydropyrrole derivatives, which were very likely formed by deprotonation at the benzylic position and subsequent elimination.

Finally, freshly prepared unpurified **28** was subjected to the conditions of an Appel reaction [61] providing, after 16 hours at room temperature, pyrrolidine derivative **30** in 33% yield. Again, the relatively low efficacy could be explained by the destructive role of the base required for the subsequent cyclisation step. Cleavage of the TBS-moiety under acidic conditions furnished the desired hydroxylated pyrrolidine **32** in good yield. An attempted direct conversion of the unprotected amino diol **17** into **32** by treatment with tetrabromomethane in the presence of triphenylphosphine gave no satisfactory results, possibly due to the formation of the corresponding oxirane and its diverse, subsequent reactions.

Conclusion

We achieved the efficient synthesis of enantiopure hydroxylated tetrahydro-2*H*-1,2-oxazine derivatives using, in the key step, lithiated alkoxyallenes and a phenyl-substituted nitrone **1a** bearing an L-erythronolactone-derived auxiliary as starting materials. Moderate levels of diastereoselectivity were observed for the formation of the 1,2-oxazine ring and for the subsequent hydroboration step. However, due to the easy separation of the formed products by standard column chromatography, the presented protocol opens up access to enantiopure products with both absolute configurations in different relative configurations, in a relatively short time. The described procedure supplements known protocols employing terpene units [62] and carbohydrate-derived auxiliaries [63,64] for the asymmetric synthesis of the 1,2-oxazine derivatives. More recently, the use of (–)-menthol as a chiral auxiliary was presented for the separation of diastereomeric 6*H*-1,2-oxazines [65,66]. Subsequent transformations of the newly prepared tetrahydro-2*H*-1,2-oxazines, utilizing samarium diiodide as the key reagent for the chemoselective ring opening, enable a smooth access to novel phenyl-substituted aminopolyols. Their transformation into hydroxylated pyrrolidine derivatives so far proceeds only with moderate efficacy, but this may certainly be optimised in the future.

Experimental

General methods. Reactions were generally performed under an inert atmosphere (argon) in flame-dried flasks. Solvents and reagents were added by syringe. Solvents were purified with a MB SPS-800-dry solvent system. Triethylamine was distilled from CaH_2 and stored over KOH under an atmosphere of argon. Other reagents were purchased and used as received without further purification unless stated otherwise. Products were purified by flash chromatography on silica gel (230–400 mesh, Merck or Fluka). Unless stated otherwise, yields refer to analytically pure samples. NMR spectra were recorded with Bruker (AC 250, AC 500, AVIII 700) and JOEL (ECX 400, Eclipse 500) instruments. Chemical shifts are reported relative

to TMS or solvent residual peaks (^{1}H: δ = 0.00 ppm [TMS], δ = 3.31 ppm [CD_3OD], δ = 7.26 ppm [$CDCl_3$]; ^{13}C: δ = 49.0 ppm [CD_3OD], δ = 77.0 ppm [$CDCl_3$]). Integrals are in accordance with assignments and coupling constants are given in Hertz. All ^{13}C NMR spectra are proton-decoupled. For detailed peak assignments, 2D spectra were measured (COSY, HMQC, HMBC). IR spectra were measured with a Nexus FT-IR spectrometer fitted with a Nicolet Smart DuraSample IR ATR. MS and HRMS analyses were performed with a Varian Ionspec QFT-7 (ESI–FT ICRMS) instrument. Elemental analyses were obtained with a Vario EL or a Vario EL III (Elementar Analysensysteme GmbH) instrument. Melting points were measured with a Reichert apparatus (Thermovar) and are uncorrected. Optical rotations ($[\alpha]_D$) were determined with a Perkin–Elmer 241 polarimeter at the temperatures given. Single crystal X-ray data were collected with a Bruker SMART CCD diffractometer (Mo Kα radiation, λ = 0.71073 Å, graphite monochromator); the structure solution and refinement was performed by using SHELXS-97 [67] and SHELXL-97 [67] in the WINGX system [68]. CCDC-864241 contains the supplementary crystallographic data for this paper. These data can be obtained free of charge from the Cambridge Crystallographic Data Centre via http://www.ccdc.cam.ac.uk/data_request/cif.

Typical procedure for the preparation of 1,2-oxazine derivatives by addition of a lithiated alkoxyallene to nitrone **1a** (Procedure 1)

Lithiated methoxyallene was generated under an atmosphere of dry argon by treating a solution of methoxyallene (357 mg, 0.42 mL, 5.06 mmol) in dry THF (20 mL) with *n*-BuLi (2.5 M in hexanes; 2.0 mL, 5.0 mmol) at −40 °C. After 5 min, the resulting mixture was cooled to −130 °C (*n*-pentane/liq. N_2 bath), and a solution of nitrone **1a** (606 mg, 2.30 mmol) in dry THF (15 mL) was added under vigorous stirring. The partially solidified mixture was allowed to reach −80 °C within 1.5 h and was quenched with water. Then, warming to room temperature was followed by extraction with Et_2O (3 × 25 mL), and the combined organic layers were stirred overnight with the drying agent ($MgSO_4$). When cyclisation of the primarily formed allene adducts was complete (TLC monitoring, hexane/ethyl acetate 4:1, *p*-anisaldehyde stain) the solvents were removed in vacuo to yield a light orange oil (763 mg). The crude material was filtered through a short silica gel pad (hexane/ethyl acetate 3:1) to yield a mixture of diastereomers (574 mg, 75%, 2:1 ratio), which were separated by column chromatography (silica gel, hexane/ethyl acetate 7:1, gradient to 5:1) to give (3*S*)-**3a** (380 mg, 49%, first eluted) as a pale yellow oil and (3*R*)-**3a** (170 mg, 22%) as a colourless solid. An analytically pure sample of (3*R*)-**3a** was obtained by recrystallisation from ethyl acetate.

(3*S*,3a'*S*,4'*S*,6a'*S*)-2-(2',2'-Dimethyltetrahydrofuro[3,4-*d*][1,3]dioxol-4'-yl)-4-methoxy-3-phenyl-3,6-dihydro-2*H*-[1,2]oxazine ((3*S*)-3a): $[\alpha]_D^{22}$ +133.4 (*c* 1.12, $CHCl_3$); ^{1}H NMR ($CDCl_3$, 700 MHz) δ 1.32, 1.41 (2 s, 3H each, 2 Me), 3.47 (s, 3H, OMe), 4.03 (d, *J* = 9.5 Hz, 1H, 6'-H), 4.23–4.27 (dd_{br}, *J* ≈ 3.5, 9.5 Hz, 1H, 6'-H), 4.30 (dd, *J* = 4.3, 13.7 Hz, 1H, 6-H), 4.40 (s, 1H, 4'-H), 4.62 (dt_{br}, *J* ≈ 2.0, 13.7 Hz, 1H, 6-H), 4.85 (s_{br}, 1H, 3-H), 4.87 (dt_{br}, *J* ≈ 1.3, 4.3 Hz, 1H, 5-H), 4.88–4.90 (m, 2H, 3a'-H, 6a'-H), 7.26–7.33, 7.34–7.38 (2 m, 5H, Ph) ppm; ^{13}C NMR ($CDCl_3$, 126 MHz) δ 24.5, 26.3 (2 q, 2 Me), 54.8 (q, OMe), 63.5 (d, C-3), 67.3 (t, C-6), 76.6 (t, C-6'), 81.2, 84.2 (2 d, C-3a', C-6a'), 92.1 (d, C-5), 94.7 (d, C-4'), 111.6 (s, C-2'), 128.0, 128.3, 129.7, 136.2 (3 d, s, Ph), 154.9 (s, C-4) ppm; IR (ATR) $\tilde{\nu}$: 3085–2840 (=C-H, C-H), 1670 (C=C), 1225, 1075, 1055 (C-O) cm^{-1}; ESI–TOF (*m*/*z*): $[M + Na]^+$ calcd for $C_{18}H_{23}NNaO_5$, 356.1474; found, 356.1479; Anal. calcd for $C_{18}H_{23}NO_5$ (333.4): C, 64.85; H, 6.95; N, 4.20; found: C, 64.81; H, 6.98; N, 4.15.

(3*R*,3a'*S*,4'*S*,6a'*S*)-2-(2',2'-Dimethyltetrahydrofuro[3,4-*d*][1,3]dioxol-4'-yl)-4-methoxy-3-phenyl-3,6-dihydro-2*H*-[1,2]oxazine ((3*R*)-3a): mp 110–113 °C; crystals suitable for X-ray analysis were obtained from AcOEt solution by cooling (fridge); Crystal data: $C_{18}H_{23}NO_5$, *M* = 333.37, orthorhombic, *a* = 5.6042(12) Å, *b* = 16.756(4) Å, *c* = 17.839(4) Å, α = 90.00°, β = 90.00°, γ = 90.00°, *V* = 1675.2(6) Å^3, *T* = 133(2) K, space group *P*2(1)2(1)2(1), *Z* = 4, Mo Kα, 23651 reflections measured, 4186 independent reflections (R_{int} = 0.0178). R_1 = 0.0307 ($I > 2\sigma(I)$); $wR(F^2)$ = 0.0782 (all data); GOOF(F^2) = 1.048. $[\alpha]_D^{22}$ −87.0 (*c* 1.36, $CHCl_3$); ^{1}H NMR ($CDCl_3$, 500 MHz) δ 1.34, 1.44 (2 s, 3H each, 2 Me), 3.49 (s, 3H, OMe), 3.89 (d, *J* = 9.9 Hz, 1H, 6'-H), 4.03 (dd, *J* = 4.0, 9.9 Hz, 1H, 6'-H), 4.41 (ddd, *J* = 1.7, 3.2, 14.3 Hz, 1H, 6-H), 4.48 (s_{br}, 1H, 3-H), 4.54 (ddd, *J* = 1.6, 2.4, 14.3 Hz, 1H, 6-H), 4.72 (s, 1H, 4'-H), 4.80 (dd, *J* = 4.0, 6.1 Hz, 1H, 6a'-H), 4.90 (t_{br}, *J* ≈ 3.0 Hz, 1H, 5-H), 5.03 (d, *J* = 6.1 Hz, 1H, 3a'-H), 7.27–7.34, 7.36–7.40 (2 m, 5H, Ph) ppm; ^{13}C NMR ($CDCl_3$, 126 MHz) δ 24.7, 26.3 (2 q, 2 Me), 54.6 (q, OMe), 63.6 (d, C-3), 65.2 (t, C-6), 74.5 (t, C-6'), 81.1 (d, C-6a'), 81.5 (d, C-3a'), 91.7 (d, C-5), 96.4 (d, C-4'), 112.0 (s, C-2'), 127.8, 128.3, 129.0, 138.1 (3 d, s, Ph), 153.1 (s, C-4) ppm; IR (ATR) $\tilde{\nu}$: 3060–2840 (=C-H, C-H), 1675 (C=C), 1220, 1100, 1050 (C-O) cm^{-1}; ESI–TOF (*m*/*z*): $[M + Na]^+$ calcd for $C_{18}H_{23}NNaO_5$, 356.1474; found, 356.1470; Anal. calcd for $C_{18}H_{23}NO_5$ (333.4): C, 64.85; H, 6.95; N, 4.20; found: C, 64.85; H, 6.83; N, 4.11.

Typical procedure for hydroborations of 1,2-oxazines (Procedure 2)

To a solution of 1,2-oxazine (3*S*)-**3a** (268 mg, 0.80 mmol) in dry THF (20 mL), a solution of BH_3·THF (1 M in THF, 3.2 mL, 3.2 mmol) was added at −30 °C. The solution was warmed to

room temperature and stirred for 3 h, then cooled to −10 °C and an aq NaOH solution (2 M, 4.8 mL) followed by H_2O_2 (30%, 1.6 mL) were added. Stirring at room temperature was continued overnight. After addition of a sat. aq $Na_2S_2O_3$ solution, the layers were separated, the water layer was extracted with Et_2O (3 × 15 mL), the combined organic layers were dried with $MgSO_4$ and filtered, and the solvents were removed under reduced pressure. The crude products (321 mg, 3:2 ratio) were separated by chromatography column (silica gel, hexane/ethyl acetate 1:1) to give 5-hydroxy-1,2-oxazines **6** (92 mg, 33%, first eluted) and **7** (141 mg, 50%) as hygroscopic, colourless semisolids.

(3*S*,4*S*,5*S*,3'a*S*,4'*S*,6'a*S*)-2-(2',2'-Dimethyltetrahydrofuro[3,4-*d*][1,3]dioxol-4'-yl)-4-methoxy-3-phenyl-[1,2]oxazinan-5-ol (6): $[\alpha]_D^{22}$ +131.2 (*c* 1.02, $CHCl_3$); ^{1}H NMR ($CDCl_3$, 500 MHz) δ 1.28, 1.35 (2 s, 3H each, 2 Me), 2.60 (d, *J* = 1.9 Hz, 1H, OH), 2.90 (s, 3H, OMe), 3.41 (ddd, *J* = 1.4, 6.7, 9.4 Hz, 1H, 4-H), 3.66–3.72 (m, 2H, 5-H, 6-H), 3.93 (d, *J* = 9.4 Hz, 1H, 3-H), 3.93 (d, *J* = 9.5 Hz, 1H, 6'-H), 4.07 (dd, *J* ≈ 11, 16 Hz, 1H, 6-H), 4.19 (dd, *J* = 4.4, 9.5 Hz, 1H, 6'-H), 4.41 (s, 1H, 4'-H), 4.81 (dd, *J* = 4.4, 6.1 Hz, 1H, 6a'-H), 4.86 (d, *J* = 6.1 Hz, 1H, 3a'-H), 7.28–7.42 (m, 5H, Ph) ppm; ^{13}C NMR ($CDCl_3$, 126 MHz) δ 24.5, 26.2 (2 q, 2 Me), 60.5 (q, OMe), 67.6 (d, C-3), 70.6 (d, C-5), 71.4 (t, C-6), 77.4 (t, C-6'), 81.3 (d, C-6a'), 84.4 (d, C-3a'), 87.6 (d, C-4), 94.8 (d, C-4'), 111.7 (s, C-2'), 128.3, 128.8*, 136.8 (2 d, s, Ph) ppm; *higher intensity; IR (ATR) $\tilde{\nu}$: 3440 (O-H), 3090–2830 (=C-H, C-H), 1205, 1055 (C-O) cm^{-1}; ESI–TOF (*m*/*z*): $[M + Na]^+$ calcd for $C_{18}H_{25}NNaO_6$, 374.1580; found, 374.1581; Anal. calcd for $C_{18}H_{25}NO_6$ (351.4): C, 61.52; H, 7.17; N, 3.99; found: C, 61.43; H, 7.15; N, 3.85.

(3*S*,4*R*,5*R*,3a'*S*,4'*S*,6a'*S*)-2-(2',2'-Dimethyltetrahydrofuro[3,4-*d*][1,3]dioxol-4'-yl)-4-methoxy-3-phenyl-[1,2]oxazinan-5-ol (7): $[\alpha]_D^{22}$ +138.2 (*c* 1.41, $CHCl_3$); ^{1}H NMR ($CDCl_3$, 500 MHz) δ 1.28, 1.34 (2 s, 3H each, 2 Me), 2.44 (d, *J* = 7.7 Hz, 1H, OH), 3.10 (s, 3H, OMe), 3.21 (m_c, 1H, 4-H), 3.75 (s_{br}, 1H, 5-H), 3.82 (d, *J* = 12.2 Hz, 1H, 6-H), 3.94 (d, *J* = 9.4 Hz, 1H, 6'-H), 4.21 (dd, *J* = 4.6, 9.4 Hz, 1H, 6'-H), 4.36 (dd, *J* = 1.4, 12.2 Hz, 1H, 6-H), 4.45 (d, *J* = 2.3 Hz, 1H, 3-H), 4.60 (s, 1H, 4'-H), 4.81 (t_{br}, *J* ≈ 5.2 Hz, 1H, 6a'-H), 4.94 (d, *J* = 6.1 Hz, 1H, 3a'-H), 7.24–7.31, 7.42–7.45 (2 m, 5H, Ph) ppm; ^{13}C NMR ($CDCl_3$, 126 MHz) δ 24.5, 26.3 (2 q, 2 Me), 59.3 (q, OMe), 62.7 (d, C-3), 65.3 (d, C-5), 71.0 (t, C-6), 77.5 (t, C-6'), 80.4 (d, C-4), 81.1 (d, C-6a'), 84.5 (d, C-3a'), 95.6 (d, C-4'), 111.6 (s, C-2'), 127.8, 128.3, 129.5, 136.4 (3 d, s, Ph) ppm; IR (ATR) $\tilde{\nu}$: 3455 (O-H), 3090–2830 (=C-H, C-H), 1215, 1085, 1050 (C-O) cm^{-1}; ESI–TOF (*m*/*z*): $[M + Na]^+$ calcd for $C_{18}H_{25}NNaO_6$, 374.1580; found, 374.1579; Anal. calcd for $C_{18}H_{25}NO_6$ (351.4): C, 61.52; H, 7.17; N, 3.99; found: C, 61.43; H, 7.17; N, 3.87.

Typical protocol for glycosyl bond cleavage (Procedure 3)

1,2-Oxazine **6** (425 mg, 1.21 mmol) was dissolved in 1 N HCl in MeOH (14 mL) and heated at 40 °C for 3.5 h (TLC monitoring, hexane/AcOEt 1:2, potassium permanganate stain). Then the mixture was allowed to reach room temperature, quenched with sat. aq $NaHCO_3$ solution and extracted with Et_2O (3 × 30 mL). The combined organic layers were dried with $MgSO_4$ and filtered, and the solvents were removed. The purification by column chromatography (silica gel, dichloromethane/methanol 40:1) yielded **12** (201 mg, 79%) as a colourless solid.

(3*S*,4*S*,5*S*)-4-Methoxy-3-phenyl-[1,2]oxazinan-5-ol (12): mp 110–112 °C; $[\alpha]_D^{22}$ +60.1 (*c* 1.05, $CHCl_3$); ^{1}H NMR ($CDCl_3$, 500 MHz) δ 3.02 (s, 3H, OMe), 3.37 (t_{br}, *J* ≈ 8.5 Hz, 1H, 4-H), 3.71–3.81 (m, 2H, 5-H, 6-H), 3.91 (d, *J* = 9.2 Hz, 1H, 3-H), 4.14 (dd, *J* = 4.1, 9.7 Hz, 1H, 6-H), 2.60, 5.48 (2 s_{br}, 2H, NH, OH), 7.31–7.38, 7.40–7.43 (2 m, 5H, Ph) ppm; ^{13}C NMR ($CDCl_3$, 126 MHz) δ 60.4 (q, OMe), 67.0 (t, C-3), 70.9 (d, C-5), 72.3 (t, C-6), 86.9 (d, C-4), 128.4, 128.6, 128.7, 136.3 (3 d, s, Ph) ppm; IR (ATR) $\tilde{\nu}$: 3405–3260 (O-H, N-H), 3065–2830 (=C-H, C-H), 1105, 1055 (C-O) cm^{-1}; ESI–TOF (*m*/*z*): $[M + H]^+$ calcd for $C_{11}H_{16}NO_3$, 210.1130; found, 210.1127; Anal. calcd for $C_{11}H_{15}NO_3$ (209.2): C, 63.14; H, 7.23; N, 6.69; found: C, 63.14; H, 7.23; N, 6.66.

Typical procedure for the reactions with samarium diiodide (Procedure 4)

To a solution of SmI_2 (ca. 0.1 M in THF, 15 mL, ~1.5 mmol) at room temperature was added dropwise a solution of 5-hydroxy-1,2-oxazine **12** (102 mg, 0.49 mmol) in degassed THF (10 mL). After the mixture was stirred for 3 h it was quenched with sat. aq sodium potassium tartrate solution and extracted with Et_2O (20 mL), and then with CH_2Cl_2 (3 × 15 mL). The combined organic layers were dried with $MgSO_4$, filtered and the solvents were removed under reduced pressure to give the spectroscopically pure product as a yellow oil in almost quantitative yield. Filtration through a short silica gel pad (dichloromethane/methanol 15:1) yielded **16** (97 mg, 94%) as a colourless oil.

(2*S*,3*S*,4*S*)-4-Amino-3-methoxy-4-phenylbutane-1,2-diol (16): $[\alpha]_D^{22}$ +12.2 (*c* 1.48, $CHCl_3$); ^{1}H NMR ($CDCl_3$, 500 MHz) δ 3.31 (dd, *J* = 2.1, 5.3 Hz, 1H, 3-H), 3.39 (s, 3H, OMe), 3.57 (dd, *J* = 4.6, 11.1 Hz, 1H, 1-H), 3.72 (dd, *J* = 6.1, 11.1 Hz, 1H, 1-H), 3.77–3.80 (m, 1H, 2-H), 4.58 (d, *J* = 5.3 Hz, 1H, 4-H), 7.28–7.33, 7.36–7.43 (2 m, 5H, Ph) ppm; ^{13}C NMR ($CDCl_3$, 126 MHz) δ 55.9 (d, C-4), 59.3 (q, OMe), 63.4 (t, C-1), 70.7 (d, C-2), 83.0 (d, C-3), 127.1, 128.1, 128.8, 138.6 (3 d, s, Ph) ppm; IR (ATR) $\tilde{\nu}$: 3490–3230 (O-H, N-H), 3065–2810 (=C-H, C-H), 1075 (C-O) cm^{-1}; ESI–TOF (*m*/*z*): $[M + H]^+$ calcd for $C_{11}H_{18}NO_3$, 212.1292; found, 212.1282.

Supporting Information

Supporting Information File 1

Experimental procedures and characterisation data.
[http://www.beilstein-journals.org/bjoc/content/supplementary/1860-5397-8-74-S1.pdf]

Supporting Information File 2

^{1}H NMR and ^{13}C NMR spectra of synthesised compounds.
[http://www.beilstein-journals.org/bjoc/content/supplementary/1860-5397-8-74-S2.pdf]

Acknowledgements

Generous support of this work by the Foundation for Polish Science (postdoctoral fellowship to M. J.), the Deutsche Forschungsgemeinschaft, and Bayer Healthcare is most gratefully acknowledged. We also thank Dr. R. Zimmer for valuable discussions and help during the preparation of the manuscript.

References

1. Merino, P. In *Science of Synthesis;* Padwa, A., Ed.; Thieme: Stuttgart, Germany, 2004; Vol. 1, p 511.
2. Gothelf, K. V.; Jørgensen, K. A. *Chem. Rev.* **1998,** *98,* 863–910. doi:10.1021/cr970324e
3. Merino, P.; Tejero, T. *Molecules* **1999,** *4,* 169–179. doi:10.3390/40700169
4. Revuelta, J.; Cicchi, S.; Goti, A.; Brandi, A. *Synthesis* **2007,** 485–504. doi:10.1055/s-2007-965914
5. Osborn, H. M. I.; Gemmell, N.; Harwood, L. M. *J. Chem. Soc., Perkin Trans. 1* **2002,** 2419–2438. doi:10.1039/b200549m
6. Fišera, L. *Top. Heterocycl. Chem.* **2007,** *7,* 287–323. doi:10.1007/7081_2007_076
7. Lombardo, M.; Trombini, C. *Synthesis* **2000,** 759–774. doi:10.1055/s-2000-6269
8. Merino, P.; Franco, S.; Merchan, F. L.; Tejero, T. *Synlett* **2000,** 442–454. doi:10.1055/s-2000-6555
9. Schade, W.; Reissig, H.-U. *Synlett* **1999,** 632–634. doi:10.1055/s-1999-2662
10. Brasholz, M.; Reissig, H.-U.; Zimmer, R. *Acc. Chem. Res.* **2009,** *42,* 45–56. doi:10.1021/ar800011h
11. Pfrengle, F.; Reissig, H.-U. *Chem. Soc. Rev.* **2010,** *39,* 549–557. doi:10.1039/B914356D
12. Bouché, L.; Reissig, H.-U. *Pure Appl. Chem.* **2012,** *84,* 23–36. doi:10.1351/PAC-CON-11-09-20
13. Helms, M.; Schade, W.; Pulz, R.; Watanabe, T.; Al-Harrasi, A.; Fišera, L.; Hlobilová, I.; Zahn, G.; Reissig, H.-U. *Eur. J. Org. Chem.* **2005,** 1003–1019. doi:10.1002/ejoc.200400627
14. Vasella, A. *Helv. Chim. Acta* **1977,** *60,* 1273–1295. doi:10.1002/hlca.19770600417
15. Aebischer, B.; Vasella, A. *Helv. Chim. Acta* **1983,** *66,* 789–794. doi:10.1002/hlca.19830660310
16. Vasella, A.; Voeffray, R.; Pless, J.; Huguenin, R. *Helv. Chim. Acta* **1983,** *66,* 1241–1252. doi:10.1002/hlca.19830660424
17. Huber, R.; Knierzinger, A.; Obrecht, J.-P.; Vasella, A. *Helv. Chim. Acta* **1985,** *68,* 1730–1747. doi:10.1002/hlca.19850680629
18. Bernet, B.; Krawczyk, E.; Vasella, A. *Helv. Chim. Acta* **1985,** *68,* 2299–2311. doi:10.1002/hlca.19850680825
19. Huber, R.; Vasella, A. *Helv. Chim. Acta* **1987,** *70,* 1461–1476. doi:10.1002/hlca.19870700603
20. Huber, R.; Vasella, A. *Tetrahedron* **1990,** *46,* 33–58. doi:10.1016/S0040-4020(01)97582-9
21. Mancini, F.; Piazza, M. G.; Trombini, C. *J. Org. Chem.* **1991,** *56,* 4246–4252. doi:10.1021/jo00013a032
22. Fišera, L.; Al-Timari, U. A. R.; Ertl, P.; Prónayová, N. *Monatsh. Chem.* **1993,** *124,* 1019–1029. doi:10.1007/BF00814148
23. Cicchi, S.; Marradi, M.; Corsi, M.; Faggi, C.; Goti, A. *Eur. J. Org. Chem.* **2003,** 4152–4161. doi:10.1002/ejoc.200300353
24. Fässler, R.; Frantz, D. E.; Oetiker, J.; Carreira, E. M. *Angew. Chem., Int. Ed.* **2002,** *41,* 3054–3056. doi:10.1002/1521-3773(20020816)41:16<3054::AID-ANIE3054>3.0.CO;2-B
25. Ritter, T.; Carreira, E. M. *Angew. Chem., Int. Ed.* **2005,** *44,* 936–938. doi:10.1002/anie.200461934
26. Mzengeza, S.; Whitney, R. A. *J. Org. Chem.* **1988,** *53,* 4074–4081. doi:10.1021/jo00252a035
27. Ashwell, M.; Guo, X.; Sinnot, M. L. *J. Am. Chem. Soc.* **1992,** *114,* 10158–10166. doi:10.1021/ja00052a011
28. Basha, A.; Henry, R.; McLaughlin, M. A.; Ratajczyk, J. D.; Wittenberger, S. J. *J. Org. Chem.* **1994,** *59,* 6103–6106. doi:10.1021/jo00099a052
29. Lantos, I.; Flisak, J.; Liu, L.; Matsuoka, R.; Mendelson, W.; Stevenson, D.; Tubman, K.; Tucker, L.; Zhang, W.-Y.; Adams, J.; Sorenson, M.; Garigipati, R.; Erhardt, K.; Ross, S. *J. Org. Chem.* **1997,** *62,* 5385–5391. doi:10.1021/jo9621736
30. Tamura, O.; Kanoh, A.; Yamashita, M.; Ishibashi, H. *Tetrahedron* **2004,** *60,* 9997–10003. doi:10.1016/j.tet.2004.08.023
31. Borrello, L.; Chiacchio, U.; Corsaro, A.; Pistarà, V.; Iannazzo, D. *ARKIVOC* **2009,** *viii,* 112–124.
32. Bonanni, M.; Marradi, M.; Cicchi, S.; Faggi, C.; Goti, A. *Org. Lett.* **2005,** *7,* 319–322. doi:10.1021/ol047691e
33. Bonanni, M.; Marradi, M.; Cicchi, S.; Goti, A. *Synlett* **2008,** 197–202. doi:10.1055/s-2007-1000934
34. Jasiński, M.; Lentz, D.; Reissig, H.-U. *Eur. J. Org. Chem.* accepted. doi:10.1002/ejoc.201200158
35. Thompson, D. K.; Hubert, C. N.; Wightman, R. H. *Tetrahedron* **1993,** *49,* 3827–3840. doi:10.1016/S0040-4020(01)90234-0
36. Dondoni, A.; Perrone, D. *Tetrahedron* **2003,** *59,* 4261–4273. doi:10.1016/S0040-4020(03)00631-8
37. Cicchi, S.; Marradi, M.; Goti, A.; Brandi, A. *Tetrahedron Lett.* **2001,** *42,* 6503–6505. doi:10.1016/S0040-4039(01)01222-9
38. Pulz, R.; Cicchi, S.; Brandi, A.; Reissig, H.-U. *Eur. J. Org. Chem.* **2003,** 1153–1156. doi:10.1002/ejoc.200390169
39. Moderhack, D.; Lorke, M. *Angew. Chem., Int. Ed. Engl.* **1980,** *19,* 45–46. doi:10.1002/anie.198000451
40. Schaumann, E.; Ketcham, R. *Angew. Chem., Int. Ed. Engl.* **1982,** *21,* 225–247. doi:10.1002/anie.198202253
And references cited therein.
41. Winchester, B. G. *Tetrahedron: Asymmetry* **2009,** *20,* 645–651. doi:10.1016/j.tetasy.2009.02.048
42. Davis, B. G. *Tetrahedron: Asymmetry* **2009,** *20,* 652–671. doi:10.1016/j.tetasy.2009.03.013
43. Asano, N. *Cell. Mol. Life Sci.* **2009,** *66,* 1479–1492. doi:10.1007/s00018-008-8522-3

44. Benalla, W.; Bellahcen, S.; Bnouham, M. *Curr. Diabetes Rev.* **2010,** *6,* 247–254. doi:10.2174/157339910791658826
45. Moreno-Clavijo, E.; Carmona, A. T.; Moreno-Vargas, A. J.; Molina, L.; Robina, I. *Curr. Org. Synth.* **2011,** *8,* 102–133. doi:10.2174/157017911794407700
46. Pulz, R.; Al-Harrasi, A.; Reissig, H.-U. *Org. Lett.* **2002,** *4,* 2353–2355. doi:10.1021/ol0260573
47. Dekaris, V.; Reissig, H.-U. *Synlett* **2010,** 42–46. doi:10.1055/s-0029-1218531
48. Dekaris, V.; Pulz, R.; Al-Harrasi, A.; Lentz, D.; Reissig, H.-U. *Eur. J. Org. Chem.* **2011,** 3210–3219. doi:10.1002/ejoc.201100230
49. McOmie, J. F. W.; Watts, M. L.; West, D. E. *Tetrahedron* **1968,** *24,* 2289–2292. doi:10.1016/0040-4020(68)88130-X
50. Riddell, F. G. *Tetrahedron* **1975,** *31,* 523–525. doi:10.1016/0040-4020(75)85023-X
51. Riddell, F. G. *Tetrahedron* **1981,** *37,* 849–858. doi:10.1016/S0040-4020(01)97649-5
52. Edmonds, D. J.; Johnston, D.; Procter, D. J. *Chem. Rev.* **2004,** *104,* 3371–3404. doi:10.1021/cr030017a
53. Nicolaou, K. C.; Ellery, S. P.; Chen, J. S. *Angew. Chem., Int. Ed.* **2009,** *48,* 7140–7165. doi:10.1002/anie.200902151
54. Beemelmanns, C.; Reissig, H.-U. *Chem. Soc. Rev.* **2011,** *40,* 2199–2210. doi:10.1039/c0cs00116c
55. Chiara, J. L.; Destabel, C.; Gallego, P.; Marco-Contelles, J. *J. Org. Chem.* **1996,** *61,* 359–360. doi:10.1021/jo951571q
56. Keck, G. E.; Wager, T. T.; McHardy, S. F. *Tetrahedron* **1999,** *55,* 11755–11772. doi:10.1016/S0040-4020(99)00486-X
57. Jung, S. H.; Lee, J. E.; Koh, H. Y. *Bull. Korean Chem. Soc.* **1998,** *19,* 33–35.
58. Bressel, B.; Egart, B.; Al-Harrasi, A.; Pulz, R.; Reissig, H.-U.; Brüdgam, I. *Eur. J. Org. Chem.* **2008,** 467–474. doi:10.1002/ejoc.200700792
59. Al-Harrasi, A.; Reissig, H.-U. *Angew. Chem., Int. Ed.* **2005,** *44,* 6227–6231. doi:10.1002/anie.200501127
60. Ritter, T.; Stanek, K.; Larrosa, I.; Carreira, E. M. *Org. Lett.* **2004,** *6,* 1513–1514. doi:10.1021/ol049514j
61. Appel, R. *Angew. Chem., Int. Ed. Engl.* **1975,** *14,* 801–811. doi:10.1002/anie.197508011
62. Arnold, T.; Reissig, H.-U. *Synlett* **1990,** 514–516. doi:10.1055/s-1990-21147
63. Arnold, T.; Orschel, B.; Reissig, H.-U. *Angew. Chem., Int. Ed. Engl.* **1992,** *31,* 1033–1035. doi:10.1002/anie.199210331
64. Defoin, A.; Joubert, M.; Heuchel, J.-M.; Strehler, C.; Streith, J. *Synthesis* **2000,** 1719–1726. doi:10.1055/s-2000-8214
65. Buchholz, M.; Hiller, F.; Reissig, H.-U. *Eur. J. Org. Chem.* **2002,** 2838–2843. doi:10.1002/1099-0690(200208)2002:16<2838::AID-EJOC2838>3.0.CO;2-O
66. Zimmer, R.; Buchholz, M.; Collas, M.; Angermann, J.; Homann, K.; Reissig, H.-U. *Eur. J. Org. Chem.* **2010,** 4111–4121. doi:10.1002/ejoc.201000425
67. Sheldrick, G. M. *Acta Crystallogr., Sect. A* **2008,** *64,* 112–122. doi:10.1107/S0108767307043930
68. Farrugia, L. J. *J. Appl. Crystallogr.* **1999,** *32,* 837–838. doi:10.1107/S0021889899006020

License and Terms

Beilstein Journal of Organic Chemistry

Sonogashira–Hagihara reactions of halogenated glycals

Dennis C. Koester and Daniel B. Werz*

Full Research Paper

Open Access

Address:
Institut für Organische und Biomolekulare Chemie, Georg-August-Universität Göttingen, Tammannstr. 2, 37077 Göttingen, Germany

Email:
Daniel B. Werz* - dwerz@gwdg.de

* Corresponding author

Keywords:
C-glycosides; enyne; glycals; reductive/oxidative refunctionalization; Sonogashira–Hagihara reaction

Beilstein J. Org. Chem. **2012,** *8,* 675–682.
doi:10.3762/bjoc.8.75

Received: 01 March 2012
Accepted: 04 April 2012
Published: 02 May 2012

This article is part of the Thematic Series "Synthesis in the glycosciences II".

Guest Editor: T. K. Lindhorst

Abstract

Herein, we report on our findings of the Sonogashira–Hagihara reaction with 1-iodinated and 2-brominated glycals using several aromatic and aliphatic alkynes. This Pd-catalyzed cross-coupling reaction presents a facile access to alkynyl *C*-glycosides and sets the stage for a reductive/oxidative refunctionalization of the enyne moiety to regenerate either *C*-glycosidic structures or pyran derivatives with a substituent in position 2.

Introduction

Carbohydrates are key players in a plethora of biological processes, such as cell-development, metastasis, cell–cell aggregation and viral infection [1-4]. Many different monosaccharide units and the large variety of possibilities to link two subunits result in an immense variety of highly complex biomolecules [5-7]. In order to mimic certain subunits of oligosaccharides, e.g., for the inhibition of glycosidases or glycosyltransferases, modified mono- or disaccharides have come into the focus of medicinal chemists [8,9]. An important class of carbohydrate mimetics are the *C*-glycosides [10-13]. In such compounds the oxygen of the *O*-glycosidic bond is substituted by a methylene unit rendering them stable to enzymatic degradation or hydrolysis. During the past decades *C*-glycosides have emerged as valuable synthetic targets, not only for medicinal chemists, but also for methodologists [8]. In particular, glycals have transpired as versatile building blocks in the synthesis of various *C*-glycosides. Most of the reported preparations of alkyl- and aryl-*C*-glycosides rely on glycals as starting materials. Transition-metal-catalyzed cross-coupling reactions play a key role in the assembly of these structures; thus, many metalated glycals have been employed in their synthesis. Scheme 1 provides a brief overview.

In 1990 Beau and co-workers utilized 1-stannylated glycals of type **1** in a Stille cross-coupling for the synthesis of aryl-*C*-glycosides such as **2** (R = Ar) [14,15]. To generate these

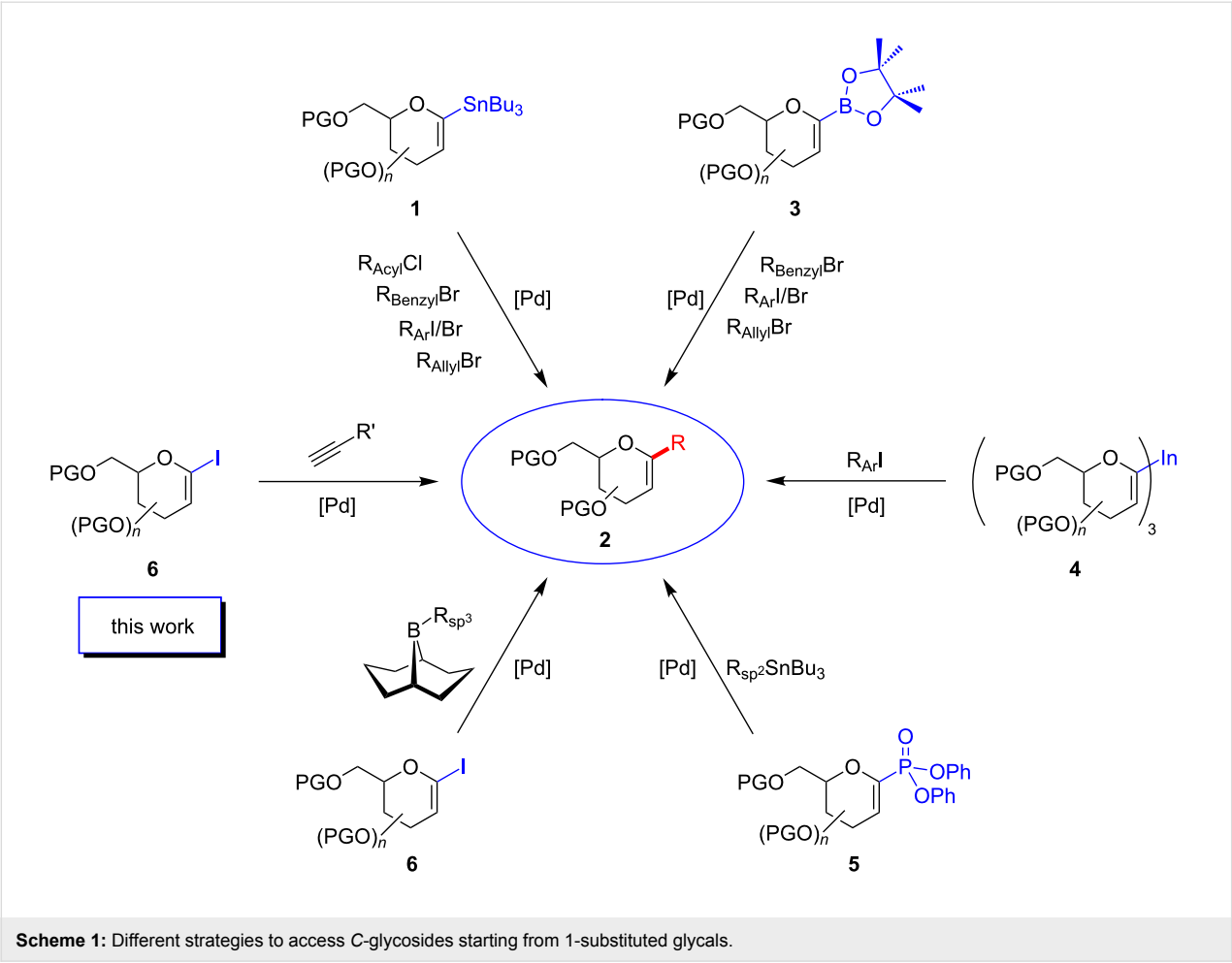

Scheme 1: Different strategies to access *C*-glycosides starting from 1-substituted glycals.

1-substituted glycals a prefunctionalization of the pseudo-anomeric carbon is mandatory. Recent advances in the field of C–H functionalization allowed for the mild and selective borylation of unfunctionalized glycals. Starting from persilylated glycals Ishikawa and Miyaura applied an Ir-catalyzed C–H-functionalization with B_2pin_2 to obtain 1-borylated glycals, such as **3**, in excellent yields and selectivity. They elegantly demonstrated the use of these compounds in the synthesis of aryl-, allyl- and benzyl-*C*-glycosides [16]. The group of Minehan described another fascinating approach to aryl-*C*-glycosides in 2003 [17]. They showed that aryl-*C*-glycosides can be prepared from glycalyl indium(III) compounds (e.g., **4**) in a Pd-catalyzed cross-coupling reaction with iodoarenes.

However, it is not only metalated sugar derivatives that have prevailed in the synthesis of *C*-glycosides, but also some electrophilic coupling reagents, such as glycalyl phosphates, and bromo- and iodoglycals. Glycal phosphates of type **5** were employed as electrophiles in a Stille cross-coupling reaction [18]. These building blocks exhibit a high stability and efficiency in their formation and are therefore particularly interesting. In a careful optimization study, Tan and co-workers found that several alkenes hydroborated in situ with 9-BBN can be utilized in a Suzuki–Miyaura coupling with iodoglucals **6** to yield aliphatic *C*-glycosides [19]. This method impressively demonstrates the power of the Suzuki–Miyaura coupling in the formation of $C(sp^2)$–$C(sp^3)$ bonds for the preparation of carbohydrate mimetics. Friesen and co-workers reported on a synthesis of aryl-*C*-glycosides employing different metalated arenes with persilylated 1-iodoglucals [20]. These proved to be particularly reactive to organozinc and organoboron compounds, whereas Hayashi successfully disclosed an approach to react simple stannylated or even electron-poor olefins with 2-bromoglucals in Stille and Heck reactions, respectively [21]. The dienes obtained during these transformations were successfully converted in Diels–Alder reactions to afford carbocyclic chiral compounds with a sugar backbone.

In 2008, Gagné introduced a Ni-mediated Negishi coupling to synthesize alkyl- and aryl-*C*-glycosides from glycosyl halides [22]. Worthy of note is that this transformation displays a $C(sp^3)$–$C(sp^3)$ coupling in the case of alkyl-*C*-glycosides and a

$C(sp^2)$–$C(sp^3)$ coupling in the preparation of aryl-*C*-glycosides. Although the diasteroselectivity of the reaction is highly dependent on the type of monosaccharide, this approach is unique due to its use of fully functionalized sugars, thus avoiding further refunctionalization steps to obtain the native *C*-glycoside.

Results and Discussion

Despite the numerous organometallic reactions performed with substituted glycals, to the best of our knowledge there has been no in-depth study of the synthesis of 1- and 2-alkynylated glycals by means of the Sonogashira–Hagihara reaction to date. Herein, we wish to report on our findings with respect to the reaction of persilylated 1-iodoglucal **7** and peracetylated 2-bromogalactal **10** with readily available alkynes **8a**–**8h**. We became interested in this chemistry whilst searching for a method to synthesize (1→6)-linked *C*-glycosidic disaccharide mimetics [23]. The simplicity of the transformation, the mild reaction conditions, and the commercial availability of the catalyst render this method highly useful for the preparation of internal alkynes [24].

We started our investigations with the persilylated 1-iodoglucal **7**, which is easily available by a sequence of lithiation and iodination from the parent, fully TIPS-protected congener [25]. The Sonogashira reaction was carried out under standard conditions. $Pd(PPh_3)_2Cl_2$ was used as catalyst, and CuI served as cocatalyst. The reaction was performed at room temperature for 12 h in neat triethylamine acting as the solvent as well as base. As coupling partners, a variety of commercially available alkynes as depicted in Table 1 were investigated. The yields proved to be good to excellent (72% to 92%). Aromatic as well as aliphatic alkynes could be employed for this reaction leading to excellent results. Fluorinated alkynyl-*C*-glycosides (Table 1, entry 4) may be readily functionalized at the aromatic core, whereas TMS-protected enynes (Table 1, entry 6) allow for further manipulations on the alkynyl residue. Our previous studies also revealed that even carbohydrate-derived alkynes can be utilized under these reaction conditions in an efficient manner [23].

Our recent interest in domino reactions starting with 2-brominated glycals [26-28] motivated us to investigate also the behav-

Table 1: Sonogashira–Hagihara reactions of 1-iodoglucal **7** with different alkynes **8a**–**8h**.

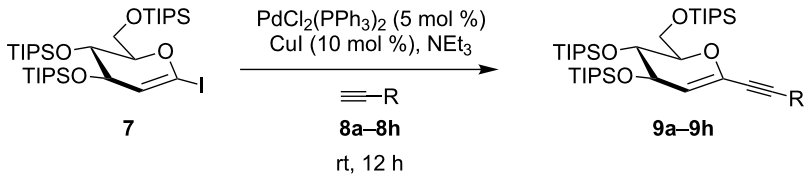

7 **8a–8h** **9a–9h**

entry	alkyne	product	yield [%][a]
1	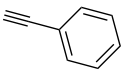 **8a**	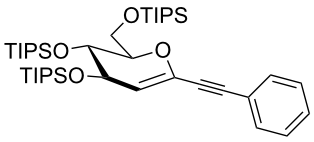 **9a**	92
2	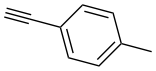 **8b**	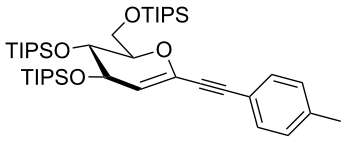 **9b**	72
3	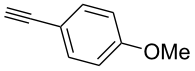 **8c**	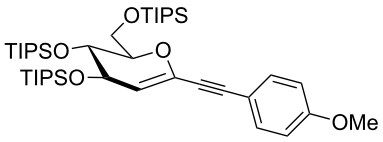 **9c**	86

Table 1: Sonogashira–Hagihara reactions of 1-iodoglucal **7** with different alkynes **8a**–**8h**. (continued)

4	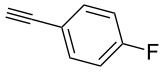 **8d**	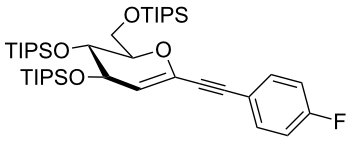 **9d**	82
5	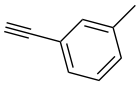 **8e**	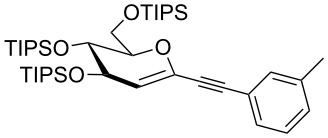 **9e**	90
6	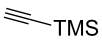 **8f**	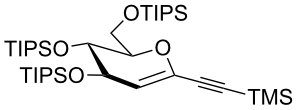 **9f**	79
7	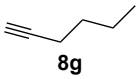 **8g**	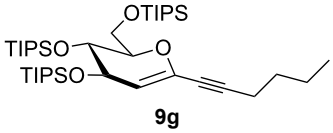 **9g**	83
8	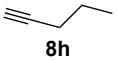 **8h**	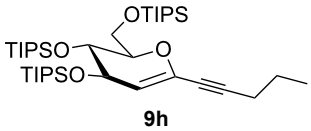 **9h**	90

[a]Isolated yields.

iour of peracetylated 2-bromogalactal **10** in Sonogashira–Hagihara reactions (Table 2). We found that **10** is much less reactive than **7**. This may be due to a more facile oxidative addition to the C–I bond compared to the C–Br bond. Furthermore, we assume that the electron density at C-2 of the sugar core is particularly high, rendering the 2-palladated glycal a bad electrophile towards electron-poor or electron-neutral alkynes. To push the reaction an elevated temperature was necessary, and only moderate yields were obtained.

Efforts to react perbenzylated 2-chloro-1-iodoglucal **12** in a twofold Sonogashira reaction with an excess of phenylacetylene resulted in a chemoselective monoalkynylation of the pseudo-anomeric position in quantitative yield (Scheme 2). Even the use of an elevated temperature did not lead to the formation of an enediyne. Further refunctionalization of the enynes was achieved by selective reduction of the triple bond by making use of Raney nickel (Table 3). We found that the electron-rich enol ether moiety remains untouched, when reaction times of less than four hours were chosen in the case of the enynes **9e**–**9h**. It should be noted that methanol was a crucial part of the solvent mixture, otherwise no reaction was observed. Interestingly, when we employed the perbenzylated enyne **9ea** the yield of the alkyne-reduced product decreased tremendously. A mixture of completely reduced products was obtained. Thus, we assume that not only electronic effects, but also the sterically encumbered TIPS groups render the reduction of the olefinic moiety much more difficult.

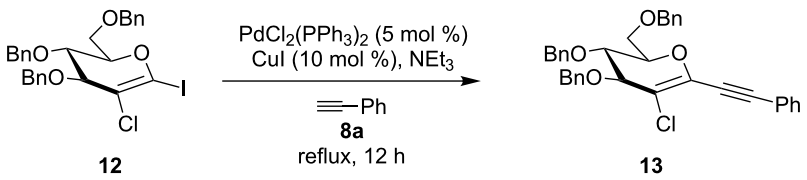

Scheme 2: Sonogashira–Hagihara reaction of 1-iodo-2-chloroglucal **12** with phenylacetylene (**8a**) to afford **13**.

Table 2: Sonogashira–Hagihara reactions of 2-bromogalactal **10** with different alkynes.

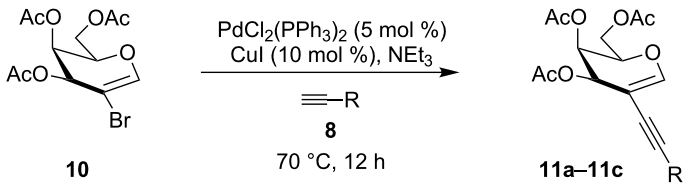

entry	alkyne	product	yield [%][a]
1	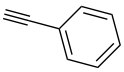 **8a**	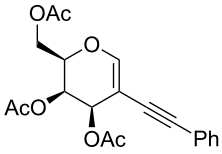 **11a**	66
2	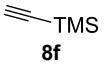 **8f**	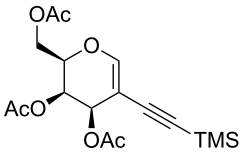 **11b**	45
3	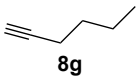 **8g**	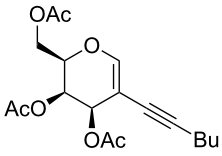 **11c**	traces

[a]Isolated yields.

Table 3: Reduction of carbohydrate-derived enynes **9e–9h** and **11a–11b**.

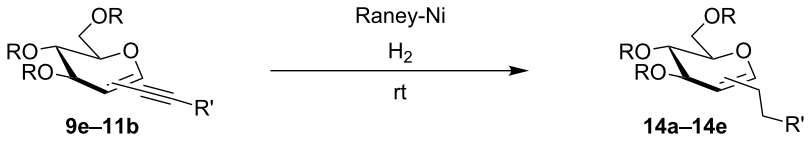

entry	substrate	time [h]	solvent	product	yield [%][a]
1	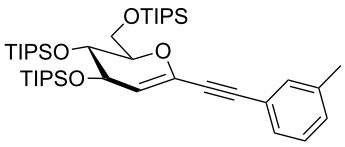 **9e**	3	MeOH:THF (1:1)	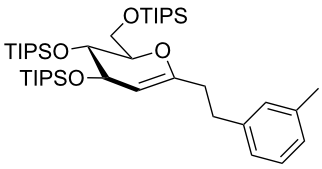 **14a**	88
2	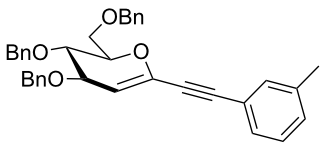 **9ea**	12	MeOH:THF (1:1)	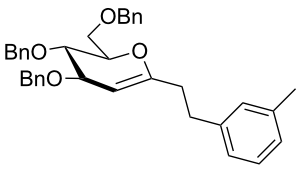 **14b**	11

Table 3: Reduction of carbohydrate-derived enynes **9e**–**9h** and **11a**–**11b**. (continued)

3	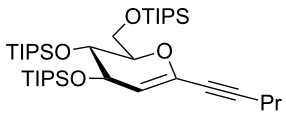 **9h**	4	MeOH:THF (1:1)	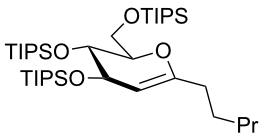 **14c**	63
4	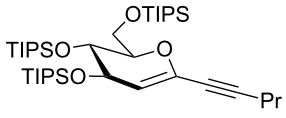 **9e**	4	THF	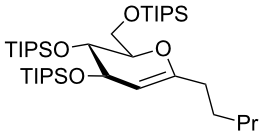 **14c**	0
5	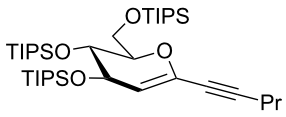 **9e**	7	MeOH:THF (1:1)	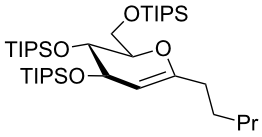 **14c**	58
6[b,c]	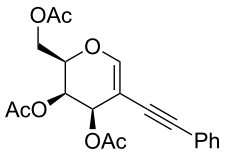 **11a**	12	MeOH:DCM:EtOAc (3:1:1)	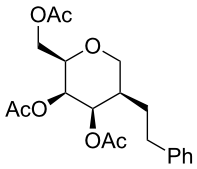 **14d**	97
7[b]	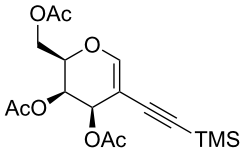 **11b**	12	MeOH:DCM:EtOAc (3:1:1)	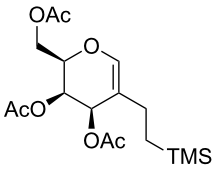 **14e**	86

[a]Isolated yields; [b]Pearlman's catalyst ($Pd(OH)_2/C$) was used instead of Raney-Ni; [c]Fully reduced carbohydrate mimetic was observed; a final proof of the stereochemistry by NOESY effects was not possible due to strongly overlapping signals. However, the stereochemistry given is highly reasonable because of the shielding of the top face by three substituents [29].

In contrast to the other enynes the carbohydrate derivative **11a** was fully reduced in a diastereoselective manner and in excellent yield to the pyran **14d** by employing Pearlman's catalyst (rt, overnight), whereas in the case of enyne **11b**, under the same reaction conditions, only the triple bond was reduced to furnish enol ether **14e** selectively.

In three cases we further functionalized the 1-alkylated glycals by an epoxidation/epoxide-opening sequence [30-33]. Dimethyldioxirane (DMDO) was used as a neutral epoxidation reagent leading to a facial-selective epoxide formation [34-36]. The so-obtained highly reactive acetal epoxide was either attacked by a superhydride, such as $LiBHEt_3$ [31], or by a Lewis acidic hydrogen transfer agent, such as DIBAL-H [32,33]. In the former case, an S_N2-type reaction takes place leading to the α-*gluco*-configured *C*-glycoside **15a** in a moderate yield of 30% (Table 4). The aluminium centre coordinates the epoxide oxygen allowing the hydride to attack from the same side, leading to β-configured alkyl-*C*-glycosides. The epoxidation/ring-opening sequence of TIPS-protected glucals proved to be challenging; for the respective product **15c** only a yield of 13% was observed.

Conclusion

We investigated the behaviour of 1-iodinated and 2-brominated glycals in Sonogashira–Hagihara cross-coupling reactions with various alkylated and arylated alkynes. 1-Alkynylated glycals were obtained in very good yields whereas the alkynylation in position 2 gave poorer results. Chemoselective reduction of the triple bond in the resulting enyne system by the action of Raney-Ni furnished enol ethers, which could be readily refunctionalized. Methanol proved to be an essential co-solvent in order to execute the Ni-catalyzed reduction. The enol ether double bond could be further hydroxylated by an epoxidation/

Table 4: Diastereoselective epoxidation/epoxide opening sequence employing different hydride sources to afford **15a–15c**.

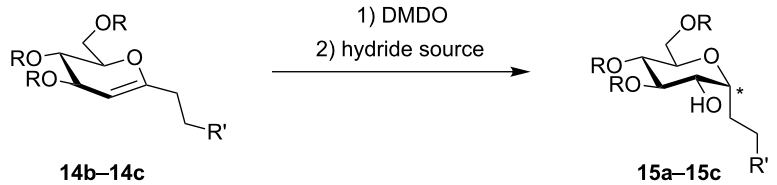

14b–14c **15a–15c**

entry	substrate	product	yield [%][a]
1[b]	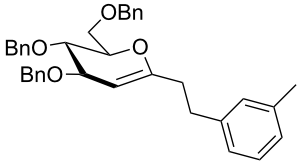 **14b**	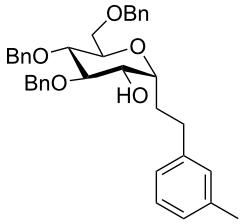 **15a**	30
2[c]	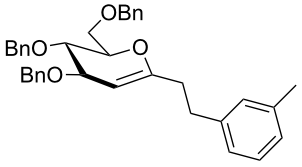 **14b**	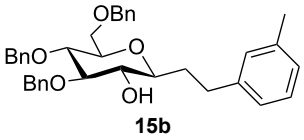 **15b**	40
3[c]	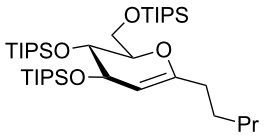 **14c**	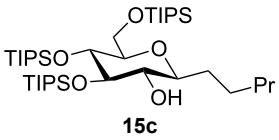 **15c**	13

*Stereochemistry depending on the hydride source; [a]Isolated yields; [b]$LiBHEt_3$ was employed as a hydride source; [c]DIBAL-H was employed as a hydride source.

epoxide opening sequence. Depending on the hydride source α- and β-configured alkyl-*C*-glycosides were obtained diastereoselectively in moderate yield. These investigations with respect to the Sonogashira–Hagihara coupling complement the rich organometallic chemistry that has already been performed with borylated, stannylated and phosphorylated glycals.

Supporting Information

Supporting Information containing all experimental details and analytical data of all new compounds given in this article as well as their ^1H and ^{13}C NMR spectra is provided.

Supporting Information File 1

Experimental procedures, analytical data and NMR spectra.
[http://www.beilstein-journals.org/bjoc/content/supplementary/1860-5397-8-75-S1.pdf]

Acknowledgements

This work was supported by the Deutsche Forschungsgemeinschaft and the Fonds der Chemischen Industrie (Emmy Noether Fellowship to D.B.W. and Dozentenstipendium to D.B.W.). D.C.K. is grateful to the Fonds der Chemischen Industrie for a Ph.D. fellowship. The authors acknowlegde Reinhard Machinek (University of Göttingen) for giving every possible support during NMR spectroscopy measurements. Martin Pawliczek is acknowledged for a donation of 2-bromogalactal. The authors also thank Professor Dr. Lutz F. Tietze (University of Göttingen) for helpful discussions and generous support of our work.

References

1. Seeberger, P. H.; Werz, D. B. *Nature* **2007,** *446,* 1046–1051. doi:10.1038/nature05819
2. Varki, A. *Glycobiology* **1993,** *3,* 97–130. doi:10.1093/glycob/3.2.97
3. Dwek, R. A. *Chem. Rev.* **1996,** *96,* 683–720. doi:10.1021/cr940283b

4. Lorenz, B.; Álvarez de Cienfuegos, L.; Oelkers, M.; Kriemen, E.; Brand, C.; Stephan, M.; Sunnick, E.; Yüksel, D.; Kalsani, V.; Kumar, K.; Werz, D. B.; Janshoff, A. *J. Am. Chem. Soc.* **2012,** *134,* 3326–3329. doi:10.1021/ja210304j
5. Werz, D. B.; Ranzinger, R.; Herget, S.; Adibekian, A.; von der Lieth, C.-W.; Seeberger, P. H. *ACS Chem. Biol.* **2007,** *2,* 685–691. doi:10.1021/cb700178s
6. Laine, R. A. *Glycobiology* **1994,** *4,* 759–767. doi:10.1093/glycob/4.6.759
7. Adibekian, A.; Stallforth, P.; Hecht, M.-L.; Werz, D. B.; Gagneux, P.; Seeberger, P. H. *Chem. Sci.* **2011,** *2,* 337–344. doi:10.1039/c0sc00322k
8. Koester, D. C.; Holkenbrink, A.; Werz, D. B. *Synthesis* **2010,** 3217–3242. doi:10.1055/s-0030-1258228
9. Sears, P.; Wong, C.-H. *Angew. Chem.* **1999,** *111,* 2446–2471. doi:10.1002/(SICI)1521-3757(19990816)111:16<2446::AID-ANGE2446>3.0.CO;2-4
   Angew. Chem. Int. Ed. **1999,** *38,* 2300–2324. doi:10.1002/(SICI)1521-3773(19990816)38:16<2300::AID-ANIE2300>3.0.CO;2-6
10. Rouzaud, D.; Sinaÿ, P. *J. Chem. Soc., Chem. Commun.* **1983,** 1353–1354. doi:10.1039/C39830001353
11. Giese, B.; Hoch, M.; Lamberth, C.; Schmidt, R. R. *Tetrahedron Lett.* **1988,** *29,* 1375–1378. doi:10.1016/S0040-4039(00)80300-7
12. Postema, M. H. D.; Piper, J. L.; Komanduri, V.; Lei, L. *Angew. Chem.* **2004,** *116,* 2975–2978. doi:10.1002/ange.200353478
    Angew. Chem. Int. Ed. **2004,** 43, 2915–2918. doi:10.1002/anie.200353478
13. Wiebe, C.; Schlemmer, C.; Weck, S.; Opatz, T. *Chem. Commun.* **2011,** *47,* 9212–9214. doi:10.1039/c1cc13078a
14. Dubois, E.; Beau, J.-M. *J. Chem. Soc., Chem. Commun.* **1990,** 1191–1192. doi:10.1039/C39900001191
15. Dubois, E.; Beau, J.-M. *Carbohydr. Res.* **1992,** *228,* 103–120. doi:10.1016/S0008-6215(00)90552-4
16. Kikuchi, T.; Takagi, J.; Isou, H.; Ishiyama, T.; Miyaura, N. *Chem.–Asian J.* **2008,** *3,* 2082–2090. doi:10.1002/asia.200800157
17. Lehmann, U.; Awasthi, A.; Minehan, T. *Org. Lett.* **2003,** *5,* 2405–2408. doi:10.1021/ol0345428
18. Nicolaou, K. C.; Shi, G.-Q.; Gunzner, J. L.; Gärtner, P.; Yang, Z. *J. Am. Chem. Soc.* **1997,** *119,* 5467–5468. doi:10.1021/ja970619+
19. Potuzak, J. S.; Tan, D. S. *Tetrahedron Lett.* **2004,** *45,* 1797–1801. doi:10.1016/j.tetlet.2003.12.006
20. Friesen, R. W.; Loo, R. W.; Sturino, C. F. *Can. J. Chem.* **1994,** *72,* 1262–1272. doi:10.1139/v94-160
21. Hayashi, M.; Tsukada, K.; Kawabata, H.; Lamberth, C. *Tetrahedron* **1999,** *55,* 12287–12294. doi:10.1016/S0040-4020(99)00727-9
22. Gong, H.; Gagné, M. R. *J. Am. Chem. Soc.* **2008,** *130,* 12177–12183. doi:10.1021/ja8041564
23. Koester, D. C.; Leibeling, M.; Neufeld, R.; Werz, D. B. *Org. Lett.* **2010,** *12,* 3934–3937. doi:10.1021/ol101625p
24. Sonogashira, K.; Tohda, Y.; Hagihara, N. *Tetrahedron Lett.* **1975,** *16,* 4467–4470. doi:10.1016/S0040-4039(00)91094-3
25. Friesen, R. W.; Loo, R. W. *J. Org. Chem.* **1991,** *56,* 4821–4823. doi:10.1021/jo00016a003
26. Leibeling, M.; Koester, D. C.; Pawliczek, M.; Schild, S. C.; Werz, D. B. *Nat. Chem. Biol.* **2010,** *6,* 199–201. doi:10.1038/nchembio.302
27. Leibeling, M.; Koester, D. C.; Pawliczek, M.; Kratzert, D.; Dittrich, B.; Werz, D. B. *Bioorg. Med. Chem.* **2010,** *18,* 3656–3667. doi:10.1016/j.bmc.2010.03.004
28. Leibeling, M.; Milde, B.; Kratzert, D.; Stalke, D.; Werz, D. B. *Chem.–Eur. J.* **2011,** *17,* 9888–9892. doi:10.1002/chem.201101917
29. Cobo, I.; Matheu, M. I.; Castillón, S.; Boutureira, O.; Davis, B. G. *Org. Lett.* **2012,** *14,* 1728–1731. doi:10.1021/ol3003139
30. Halcomb, R. L.; Danishefsky, S. J. *J. Am. Chem. Soc.* **1989,** *111,* 6661–6666. doi:10.1021/ja00199a028
31. Inoue, M.; Yamashita, S.; Tatami, A.; Miyazaki, K.; Hirama, M. *J. Org. Chem.* **2004,** *69,* 2797–2804. doi:10.1021/jo049877x
32. Krishnamurthy, S.; Schubert, R. M.; Brown, H. C. *J. Am. Chem. Soc.* **1973,** *95,* 8486–8487. doi:10.1021/ja00806a067
33. Majumder, U.; Cox, J. M.; Johnson, H. W. B.; Rainier, J. D. *Chem.–Eur. J.* **2006,** *12,* 1736–1746. doi:10.1002/chem.200500993
34. Adam, W.; Chan, Y.-Y.; Cremer, D.; Gauss, J.; Scheutzow, D.; Schindler, M. *J. Org. Chem.* **1987,** *52,* 2800–2803. doi:10.1021/jo00389a029
35. Düfert, A.; Werz, D. B. *J. Org. Chem.* **2008,** *73,* 5514–5519. doi:10.1021/jo800692z
36. Alberch, L.; Cheng, G.; Seo, S.-K.; Li, X.; Boulineau, F. P.; Wei, A. *J. Org. Chem.* **2011,** *76,* 2532–2547. doi:10.1021/jo102382r

License and Terms

Beilstein Journal of Organic Chemistry

Synthesis and antiviral activities of spacer-linked 1-thioglucuronide analogues of glycyrrhizin

Christian Stanetty[1,§], Andrea Wolkerstorfer[2,§], Hassan Amer[1], Andreas Hofinger[1], Ulrich Jordis[3], Dirk Claßen-Houben[2] and Paul Kosma[*1]

Full Research Paper

Open Access

Address:
[1]Department of Chemistry, University of Natural Resources and Life Sciences-Vienna, Muthgasse 18, A-1190 Vienna, Austria, [2]Savira Pharmaceuticals GmbH, Veterinärplatz 1, A-1210 Vienna, Austria and [3]Institute of Applied Synthetic Chemistry, Vienna University of Technology, Getreidemarkt 9, A-1060 Vienna, Austria

Email:
Paul Kosma[*] - paul.kosma@boku.ac.at

* Corresponding author
§ These authors contributed equally to this work

Keywords:
antiviral activity; carbenoxolone; glycyrrhizin; influenza A virus; thioglycoside; triterpene

Beilstein J. Org. Chem. **2012,** *8,* 705–711.
doi:10.3762/bjoc.8.79

Received: 09 March 2012
Accepted: 12 April 2012
Published: 08 May 2012

This article is part of the Thematic Series "Synthesis in the glycosciences II".

Guest Editor: T. K. Lindhorst

Abstract

The influenza virus infection remains a significant threat to public health and the increase of antiviral resistance to available drugs generates an urgent need for new antiviral compounds. Starting from the natural, antivirally active compound glycyrrhizin, spacer-bridged derivatives were generated with improved antiviral activity against the influenza A virus infection. Simplified analogues of the triterpene saponin glycyrrhizin containing 1-thio-β-D-glucuronic acid residues have been prepared in good yields by alkylation of 3-amino and 3-thio derivatives of glycyrrhetinic acid with a 2-iodoethyl 1-thio-β-D-glucopyranosiduronate derivative. The spacer-connected 3-amino derivatives were further transformed into N-acetylated and N-succinylated derivatives. The deprotected compounds containing these carboxylic acid appendices mimic the glycon part of glycyrrhizin as well as the hemisuccinate derivative of glycyrrhetinic acid, carbenoxolone. Antiviral activities of the compounds were determined in a biological test based on influenza A virus-infected cells, wherein the 3-(2-thioethyl)-*N*-acetylamino- and 3-(2-thioethyl)-thio-linked glucuronide derivatives were effective inhibitors with IC_{50} values as low as 54 μM.

Introduction

The triterpene saponin glycyrrhizin (**GL**) and its aglycon glycyrrhetinic acid (**GA**) are the main triterpene components of licorice roots and harbor various pharmacological activities, including antitumor, anti-inflammatory, antioxidant and antiviral properties [1,2]. The antiviral activities have been reported to be directed against a broad spectrum of viruses comprising herpes-, corona-, alpha-, and flaviviruses, HIV, Epstein–Barr virus, influenza A virus (IAV), vaccinia and

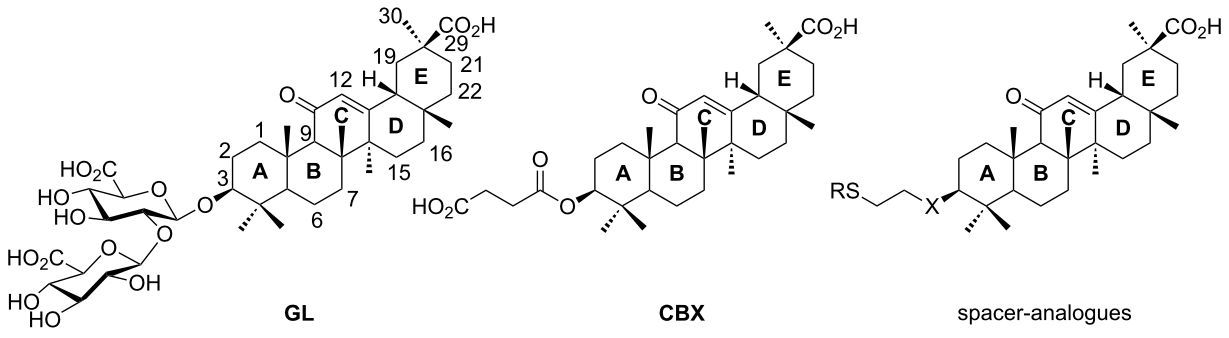

Figure 1: Structure of glycyrrhizin (**GL**), carbenoxolone (**CBX**), and spacer analogues.

polio type I viruses as examples [3-8]. In particular anti-influenza virus activities have been described, although the underlying mechanisms of action are diverse [9-12]. In order to evaluate the potential antiviral properties of glycyrrhizin derivatives, we set out to modify the chemical environment in the vicinity of ring A of glycyrrhetinic acid. The envisaged modifications should assess the impact of acidic groups, which reside at the glucuronic acid residues in the β-(1→2)-linked disaccharide unit of **GL**, with respect to antiviral properties (Figure 1).

Previously, ring A modified derivatives of glycyrrhetinic acid were prepared containing 3-amino, 3-thio and 1-thio groups, allowing for an extension of the oleanolic acid unit with spacer groups as well as facile covalent attachment of carboxyalkyl groups by alkylation or acylation reactions [13,14]. For the compounds included in this investigation, the size of the spacer group was selected to closely match the formal distances between the A-ring and the carboxylic acid function present in the glucopyranosiduronic residues of the parent compound glycyrrhizin (**GL**) and in the hemisuccinate moiety of the glycyrrhetinic acid derivative carbenoxolone (**CBX**) [15] (Figure 1). For the sake of clarity, the nomenclature and numbering for the triterpene system as used throughout this report is illustrated in Figure 1. In order to enhance resistance against enzymatic cleavage by glucuronidases, the glucuronic acid residue was introduced through a stable thioglycosidic linkage.

Results and Discussion

Synthesis of 3-amino derivatives

Commercially available methyl (2,3,4-tri-*O*-acetyl-D-glucopyranosyl)uronate bromide (**1**) was first reacted with potassium thioacetate in DMF to furnish the known 1-thioacetyl derivative **2** in 82% yield [16]. Subsequent treatment of **2** with sodium methoxide, under controlled conditions at low temperature (−60 °C → −45 °C), provided the corresponding glucuronyl 1-thiol **3** in 89% yield [17,18]. Reaction of **3** with an excess of 1,2-dibromoethane (3–4 equiv) in DMF in the presence of sodium hydride, with the strict exclusion of oxygen, afforded the 2-bromoethyl 1-thioglycoside **4** in 80% yield. Under these conditions formation of the bis-substitution product **5** (3%) and the disulfide oxidation product of 1-thiol **3** was observed in only very minor quanities. The corresponding 2-iodoethyl derivative **6** was prepared by a Finkelstein reaction from the bromoethyl 1-thioglycoside **4** in 95% yield (Scheme 1).

The previously reported 3β-amino derivative of the diphenylmethyl ester of glycyrrhetinic acid **7** [19] was then used for the introduction of the spacer-extended 1-thio-glucopyranosiduronate residue. Coupling of the 3β-amino derivative **7** with two equivalents of the 2-iodoethyl glycoside **6** in DMF in the presence of Hünig base proceeded smoothly to provide the alkylated amine **8** in 79% yield without the formation of a bis-alkylated product (Scheme 2), whereas the use of the corresponding bromide **4** resulted in a significantly slower reaction.

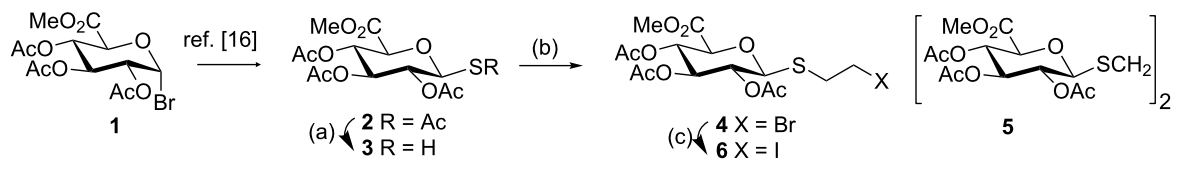

Scheme 1: Synthesis of methyl 2-haloethyl 1-thio-glucuronide derivatives: (a) 1 M NaOMe, MeOH, −60 °C to −45 °C, 89% ; (b) $Br(CH_2)_2Br$, NaH, DMF, −5 °C (80% for **4**, 3% for **5**); (c) NaI, acetone, 4 °C, 16 h, 95%.

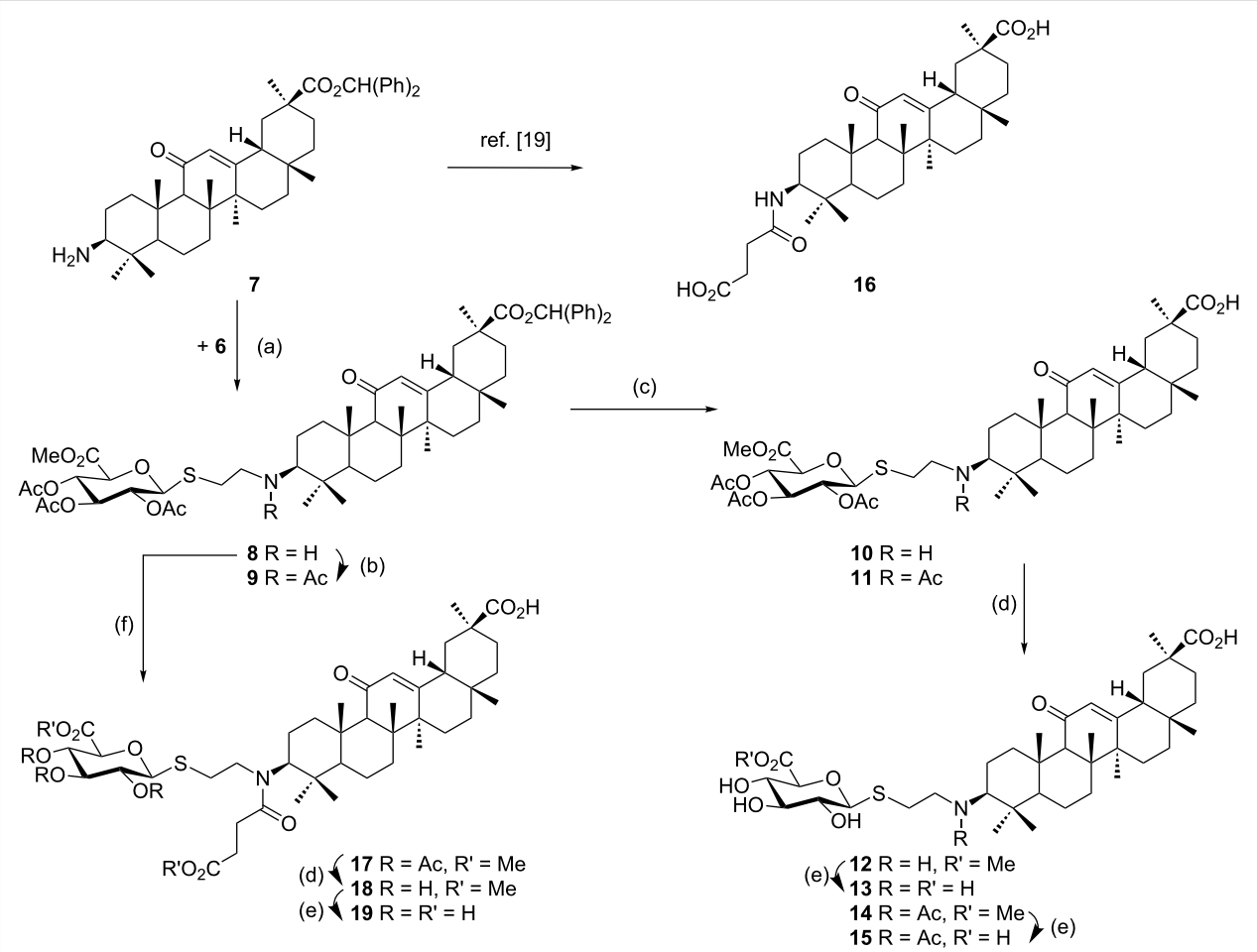

Scheme 2: Synthesis of thioalkylglucuronide **GA** derivatives: (a) DMF, DIPEA, 45–50 °C, 16 h, 79%; (b) TEA, Ac_2O, DCM, 0 °C, 2 h, 96%; (c) anisole, TFA, DCM, rt, 3 h (75% for **10**, 89% for **11**); (d) 0.1 M NaOMe, MeOH, 0 °C (89% for **12**, 97% for **14**, 99% for **18**); (e) 0.2 M NaOH, MeOH, rt, 3 h (91% for **13**, ~quant. for **15**, 99% for **19**); (f) $MeO_2C(CH_2)_2COCl$ in DCM, DIPEA, 0 °C to rt, 90 min, then anisole, TFA, DCM, 0 °C, 3 h, 83% for two steps.

At elevated temperature, elimination leading to the corresponding hexenuronic acid derivative was observed (structure not shown). The secondary amino group in compound **8** was subjected to further derivatization by N-acetylation (triethylamine, acetic anhydride), which gave compound **9** in 96% yield. Deprotection of the ethyl 1-thio-glucuronide derivatives **8** and **9** was achieved by acid-catalyzed cleavage of the diphenylmethyl ester group with TFA/anisole (as carbocation scavenger), giving the monoacid derivatives **10** and **11** in 75% and 89% yield, respectively. Subsequent transesterification of **10** and **11** with methanolic NaOMe afforded the deacetylated methyl ester glucuronide derivatives **12** and **14**, respectively, which were finally fully deprotected by hydrolysis of the methyl ester group with 0.2 M methanolic NaOH to furnish the diacid derivatives **13** and **15**, in high overall yield.

A second series of compounds was designed as glucuronide-extended amide derivatives of the previously reported carbenoxolone analogue **16** [20,21]. Reaction of the 3-amino group of **8** with the monomethyl ester of succinic acid chloride in dichloromethane in the presence of Hünig base was followed by deblocking of the diphenylmethyl ester group to afford **17** in a combined yield of 83%. The acetyl groups of **17** were removed under Zemplén conditions to afford the dimethyl ester **18**. Alkaline hydrolysis of the ester groups eventually gave the triacid derivative **19** in good yield. In contrast to the straightforward chemical transformations, analysis of the NMR spectra of this series of compounds was challenging and the N-acylated derivatives **9**, **11**, **14**, **15** and **17**–**19** revealed complex spectra. Whereas the secondary amides of 3β-amino-glycyrrhetinic acid derivatives displayed coherent NMR signals [22,23], the tertiary amides frequently exist as mixtures of *cis*/*trans* rotamers leading to the duplication of signals [24,25]. The steric congestion at position 3 exerted by the two adjacent methyl groups may additionally contribute to the restricted rotation of the amide linkage. Thus, in the ^{1}H NMR spectra of the *N*-acetyl-

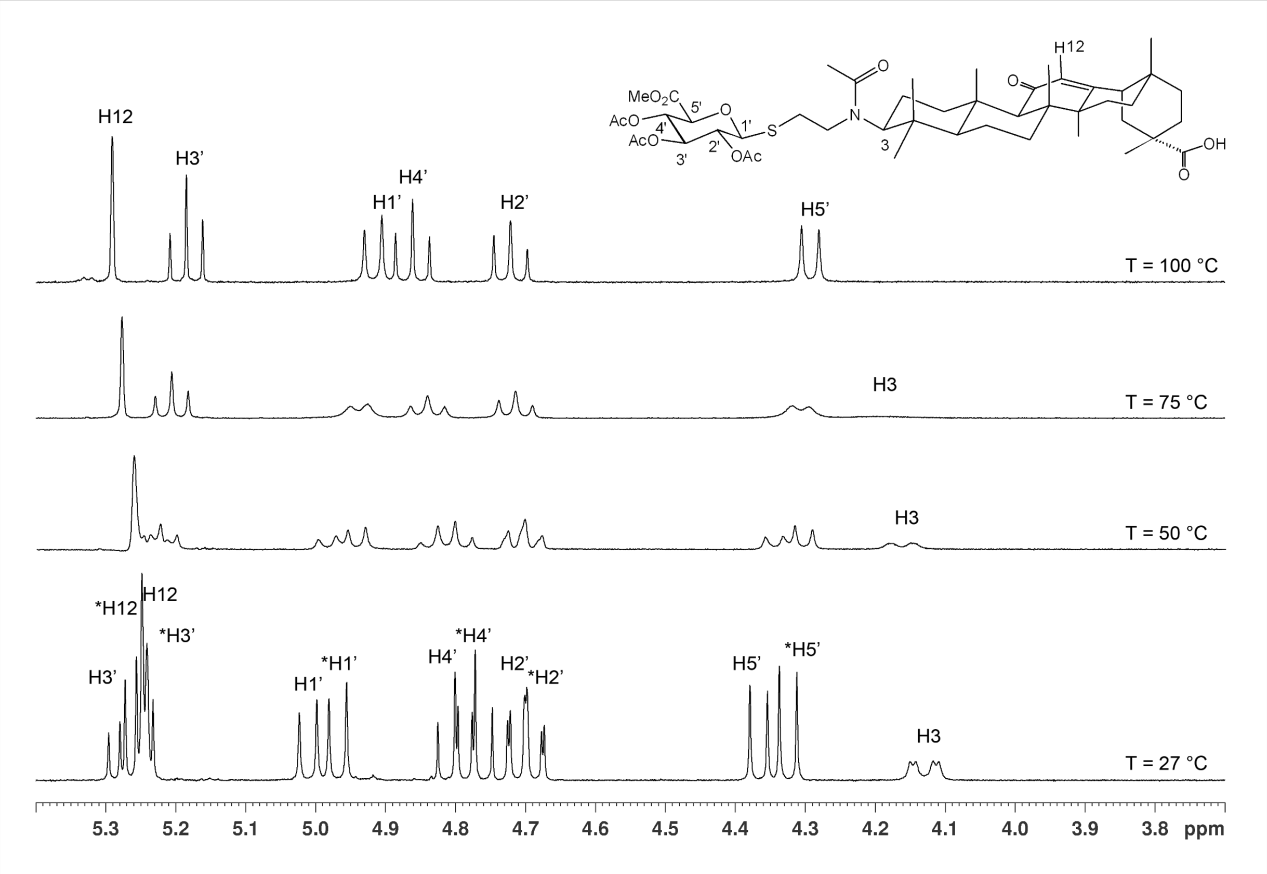

Figure 2: 400 MHz ^{1}H NMR expansion plots of the carbohydrate region of compound **11**, recorded at various temperatures.

and *N*-succinyl derivatives, recorded at room temperature, two sets of signals in an approximate 6:4 ratio were observed. Reversible coalescence of these signal groups was observed upon heating a solution of the *N*-acetyl derivative **11** up to 100 °C in DMSO-d_6 and subsequent cooling to room temperature (Figure 2), supporting the assignment of two signal data sets for two rotamers. The orientation of the amide carbonyl group in the rotamers also had a pronounced effect on the NMR chemical shifts of carbon and proton signals in ring A, which led to a shift of H-3 to lower field (δ 4.47) and to a shielding of C-3 (δ 59.9) for the minor isomer, whereas the inverse effects were seen for the major rotamer (δ for H-3 at 3.36 and δ for C-3 at 66.7). Similar, but less-pronounced effects were observed for the respective ^{1}H and ^{13}C signals at position 5 of ring A (see Supporting Information File 1).

Synthesis of 3-thio derivatives

Complementing the series of the 3β-amino series, related 3-thio derivatives were employed for the spacer elongation [14]. The previously reported 1,2-dehydro-3-thiol derivative **20** was subjected to alkylation with the 2-iodoethyl 1-thioglucuronide compound **6** in the presence of K_2CO_3 to furnish the thioether-bridged glucuronide triterpene **21** in 60% yield. Deprotection of **21** was performed in two steps as described for **10**, which furnished the methyl ester derivative **22** and the glucuronic acid compound **23**, respectively, in good yields (Scheme 3).

Antiviral activities

For biological testing the compounds were dissolved in DMSO and diluted in cell culture medium to a maximum final DMSO concentration of 1%. For determination of the cytotoxicity of the compounds, MDCK cells were treated with compound concentrations ranging from 3.1 μM to 250 μM for 48 h and then cell viability was determined as a surrogate endpoint for cytotoxicity. Except for the aglycons of **GL**, namely glycyrrhetinic acid (**GA**) and the hemisuccinate carbenoxolone (**CBX**), which showed CC_{50} values (half-maximal cytotoxic concentration) of 7.4 μM and 17.8 μM, respectively, none of the compounds tested were toxic at concentrations up to 250 μM. **GL** was not toxic at 2500 μM (Table 1). The antiviral activity of the compounds was determined by infecting MDCK cells with influenza A H3N2 virus and treating them with different concentrations of compounds at the same time. Most compounds prevented virus-induced cytopathicity and restored cell viability compared to virus-infected control cells. The antiviral activity of glycyrrhizin (**GL**) against influenza and other viruses

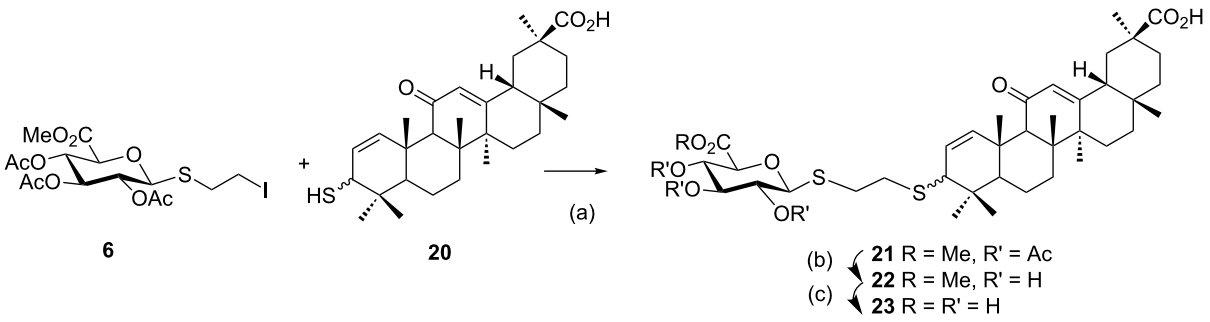

Scheme 3: Synthesis of 3-thioether-bridged glucuronide derivatives: (a) K_2CO_3, acetone, 60%; (b) 0.8 M NaOMe, MeOH, 71%; (c) 0.2 M NaOH, MeOH, 95% .

reported in the literature was confirmed in this study resulting in an IC_{50} of 1026 µM (Table 1). **GA** and **CBX** did not show any antiviral activity at nontoxic concentrations. Compounds **12**, **13**, **14**, **15**, **18** and **19**, which possess a (1-thio-β-D-glucopyranosyluronic acid)ethylamino substituent at position 3 of **GA** did not show toxicity at concentrations up to 250 µM, but showed enhanced antiviral activity compared to **GL**. Good activities were found for compounds **12** and **18** with IC_{50} values of 220.4 µM and 125 µM, respectively, being between 4.7-fold to 8-fold more active compared to the lead compound **GL**. The methyl ester **14** containing the N-acetylated spacer group was approximately 14-fold more active compared to **GL**, reflected by an IC_{50} value of 72.1 µM. The free acid **15** displayed an IC_{50} value in the same range as the methyl ester **14**. Replacement of the *N*-acetyl group of **14** with a methylsuccinyl group (**18**) did not improve the activity; however, the compound was still active with an IC_{50} value of 125 µM. The cleavage of both methyl ester groups of this compound resulted in compound **19** and led to the loss of antiviral activity up to the highest concentration tested (250 µM). Compound **16** containing only the *N*-succinyl substituent is a close analogue to **CBX** bearing an amide instead of the ester group. Unlike **CBX**, which is toxic at low concentrations, **16** was not toxic but inactive, indicating that the glucuronic acid moiety is associated with the antiviral properties. This was further supported by the data obtained with compound **23** containing a 1-thioethyl-linked glucuronic acid residue at position 3 of 1,2-dehydro-glycyrrhetinic acid. Compound **23** showed good activity with an even lower IC_{50} value of 54 µM compared to **15**, and exhibited also no cytotoxicity at the concentrations tested.

Table 1: Cytotoxic concentration 50% (CC_{50}) of compound-treated uninfected cells and antiviral activities, shown as half-maximal inhibitory concentration (IC_{50}) values of glycyrrhizin (**GL**) analogues.

Compound	Substructure	CC_{50} [µM]	IC_{50} [µM]
GL	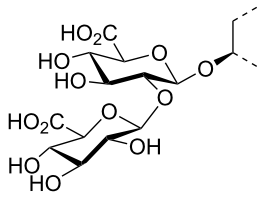	>2500	1026 ± 181
GA		7.4 ± 0.05	nd[a]
CBX	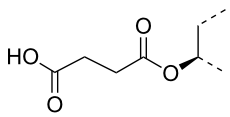	17.8 ± 2.3	nd[a]
12	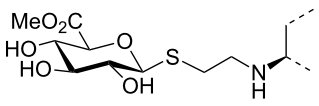	>250	220.4 ± 41

Table 1: Cytotoxic concentration 50% (CC_{50}) of compound-treated uninfected cells and antiviral activities, shown as half-maximal inhibitory concentration (IC_{50}) values of glycyrrhizin (**GL**) analogues. (continued)

13	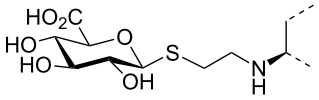	>250	nd (>250)[b]
14	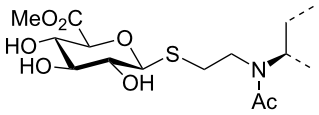	>75	72.1 ± 19.1[c]
15	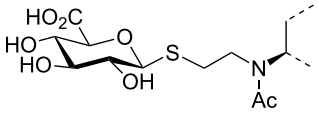	>250	87 ± 7.9
16	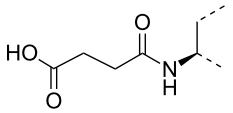	>250	nd (>250)[b]
18	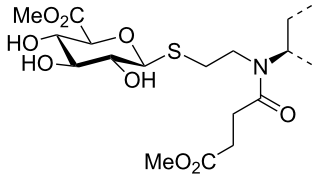	>250	125 ± 15.9
19	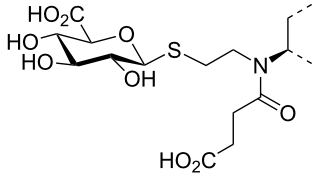	>250	nd (>250)[b]
23	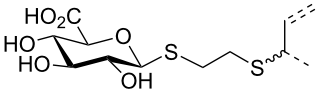	>250	54 ± 13

[a]nd not determined due to cytotoxicity; [b]nd (>250) no detectable antiviral activity up to 250 μM; [c]approximate value, since the compound precipitates at concentrations >75 μM.

Conclusion

3-Amino and 3-thio derivatives of glycyrrhetinic acid served as versatile scaffolds for the attachment of glycosyl extensions through high-yielding alkylation reactions. The glucuronide derivatives linked via a thioethyl spacer group to the oleanolic acid unit exhibited no toxicity at concentrations up to 250 μM and significantly enhanced the anti-influenza virus activity of the natural triterpene glycoside glycyrrhizin.

Supporting Information

Supporting Information File 1

Experimental details for the preparation of compounds **2**–**19** and **21**–**23** as well as the biological assays.
[http://www.beilstein-journals.org/bjoc/content/supplementary/1860-5397-8-79-S1.pdf]

Acknowledgements

The work was supported by the ZIT Zentrum für Innovation und Technologie GmbH (Vienna Spot of Excellence: 182081). We thank Michaela Mutzl, Barbara Butzendobler and Eva Zingler for the performance of antiviral activity assays and David Baum and Karin Hofbauer for technical assistance in the organic syntheses of precursors.

References

1. Baltina, L. A. *Curr. Med. Chem.* **2003,** *10,* 155–171.
2. Schwarz, S.; Csuk, R. *Bioorg. Med. Chem.* **2010,** *18,* 7458–7474. doi:10.1016/j.bmc.2010.08.054
3. Lampis, G.; Deidda, D.; Pinza, M.; Pompei, R. *Antiviral Chem. Chemother.* **2001,** *12,* 125–131.
4. Cinatl, J.; Morgenstern, B.; Bauer, G.; Chandra, P.; Rabenau, H.; Doerr, H. W. *Lancet* **2003,** *361,* 2045–2046. doi:10.1016/S0140-6736(03)13615-X

5. Crance, J. M.; Scaramozzino, N.; Jouan, A.; Garin, D. *Antiviral Res.* **2003,** *58,* 73–79. doi:10.1016/S0166-3542(02)00185-7
6. Hattori, T.; Ikematsu, S.; Koito, A.; Matsushita, S.; Maeda, Y.; Hada, M.; Fujimaki, M.; Takatsuki, K. *Antiviral Res.* **1989,** *11,* 255–261. doi:10.1016/0166-3542(89)90035-1
7. Harada, S. *Biochem. J.* **2005,** *392,* 191–199. doi:10.1042/BJ20051069
8. Lin, J.-C. *Antiviral Res.* **2003,** *59,* 41–47. doi:10.1016/S0166-3542(03)00030-5
9. Pompei, R.; Paghi, L.; Ingianni, A.; Uccheddu, P. *Microbiologica* **1983,** *6,* 247–250.
10. Utsunomiya, T.; Kobayashi, M.; Pollard, R. B.; Suzuki, F. *Antimicrob. Agents Chemother.* **1997,** *41,* 551–556.
11. Wolkerstorfer, A.; Kurz, H.; Bachhofner, N.; Szolar, O. *Antiviral Res.* **2009,** *83,* 171–178. doi:10.1016/j.antiviral.2009.04.012
12. Michaelis, M.; Geiler, J.; Naczk, P.; Sithisarn, P.; Leutz, A.; Doerr, H. W.; Cinatl, J., Jr. *PLoS One* **2011,** *6,* e19705. doi:10.1371/journal.pone.0019705
13. Claßen-Houben, D.; Kueenburg, B.; Kosma, P.; Jordis, U.; Stanetty, C.; Szolar, O.; Wolkerstorfer, A. Antiviral Triterpene Derivatives. EP 2 258 713 A1, Dec 8, 2010.
14. Amer, H.; Mereiter, K.; Stanetty, C.; Hofinger, A.; Czollner, L.; Beseda, I.; Jordis, U.; Kueenburg, B.; Claßen-Houben, D.; Kosma, P. *Tetrahedron* **2010,** *66,* 4390–4402. doi:10.1016/j.tet.2010.03.098
15. Jellinck, P. H.; Monder, C.; McEwen, B. S.; Sakai, R. R. *J. Steroid Biochem. Mol. Biol.* **1993,** *46,* 209–213. doi:10.1016/0960-0760(93)90296-9
16. Florio, P.; Thomson, R. J.; von Itzstein, M. *Carbohydr. Res.* **2000,** *328,* 445–448. doi:10.1016/S0008-6215(00)00228-7
17. MacDougall, J. M.; Zhang, X.-D.; Polgar, W. E.; Khroyan, T. V.; Toll, L.; Cashman, J. R. *J. Med. Chem.* **2004,** *47,* 5809–5815. doi:10.1021/jm049554t
18. Cao, H.; Yu, B. *Tetrahedron Lett.* **2005,** *46,* 4337–4340. doi:10.1016/j.tetlet.2005.04.088
19. Beseda, I.; Czollner, L.; Shah, P. S.; Khunt, R.; Gaware, R.; Kosma, P.; Stanetty, C.; del Ruiz-Ruiz, M. C.; Amer, H.; Mereiter, K.; Da Cunha, T.; Odermatt, A.; Claßen-Houben, D.; Jordis, U. *Bioorg. Med. Chem.* **2010,** *18,* 433–454. doi:10.1016/j.bmc.2009.10.036
20. Ijichi, S.; Tamagaki, S. *Chem. Lett.* **2005,** *34,* 356–357. doi:10.1246/cl.2005.356
21. Brieskorn, C. H.; Eschelbach, H. *Arch. Pharm.* **1979,** *312,* 752–762. doi:10.1002/ardp.19793120907
22. Stanetty, C.; Czollner, L.; Koller, I.; Shah, P.; Gaware, R.; Da Cunha, T.; Odermatt, A.; Jordis, U.; Kosma, P.; Claßen-Houben, D. *Bioorg. Med. Chem.* **2010,** *18,* 7522–7541. doi:10.1016/j.bmc.2010.08.046
23. Csuk, R.; Schwarz, S.; Siewert, B.; Kluge, R.; Ströhl, D. *Eur. J. Med. Chem.* **2011,** *46,* 5356–5369. doi:10.1016/j.ejmech.2011.08.038
24. Zhou, C. C.; Stewart, K. D.; Dhaon, M. K. *Magn. Reson. Chem.* **2005,** *43,* 41–46. doi:10.1002/mrc.1501
25. Stewart, W. E.; Siddall, T. H., III. *Chem. Rev.* **1970,** *70,* 517–551. doi:10.1021/cr60267a001

License and Terms

Beilstein Journal of Organic Chemistry

Chemo-enzymatic modification of poly-*N*-acetyllactosamine (LacNAc) oligomers and *N,N*-diacetyllactosamine (LacDiNAc) based on galactose oxidase treatment

Christiane E. Kupper[1], Ruben R. Rosencrantz[1], Birgit Henßen[1], Helena Pelantová[2], Stephan Thönes[1], Anna Drozdová[2], Vladimir Křen[2] and Lothar Elling[*1]

Full Research Paper

Open Access

Address:
[1]Laboratory for Biomaterials, Institute for Biotechnology and Helmholtz-Institute for Biomedical Engineering, RWTH Aachen University, Worringer Weg 1, Aachen, 52074, Germany and [2]Institute of Microbiology, Academy of Sciences of the Czech Republic, Videnska 1083, Prague 4, CZ 14220, Czech Republic

Email:
Lothar Elling[*] - l.elling@biotec.rwth-aachen.de

* Corresponding author

Keywords:
chemo-enzymatic synthesis; galactose oxidase; glycosyltransferase; LacDiNAc; poly-*N*-acetyllactosamine

Beilstein J. Org. Chem. **2012,** *8,* 712–725.
doi:10.3762/bjoc.8.80

Received: 27 January 2012
Accepted: 12 April 2012
Published: 09 May 2012

This article is part of the Thematic Series "Synthesis in the glycosciences II".

Guest Editor: T. K. Lindhorst

Abstract

The importance of glycans in biological systems is highlighted by their various functions in physiological and pathological processes. Many glycan epitopes on glycoproteins and glycolipids are based on *N*-acetyllactosamine units (LacNAc; Galβ1,4GlcNAc) and often present on extended poly-LacNAc glycans ([Galβ1,4GlcNAc]$_n$). Poly-LacNAc itself has been identified as a binding motif of galectins, an important class of lectins with functions in immune response and tumorigenesis. Therefore, the synthesis of natural and modified poly-LacNAc glycans is of specific interest for binding studies with galectins as well as for studies of their possible therapeutic applications. We present the oxidation by galactose oxidase and subsequent chemical or enzymatic modification of terminal galactose and *N*-acetylgalactosamine residues of poly-*N*-acetyllactosamine (poly-LacNAc) oligomers and *N,N*-diacetyllactosamine (LacDiNAc) by galactose oxidase. Product formation starting from different poly-LacNAc oligomers was characterised and optimised regarding formation of the C6-aldo product. Further modification of the aldehyde containing glycans, either by chemical conversion or enzymatic elongation, was established. Base-catalysed β-elimination, coupling of biotin–hydrazide with subsequent reduction to the corresponding hydrazine linkage, and coupling by reductive amination to an amino-functionalised poly-LacNAc oligomer were performed and the products characterised by LC–MS and NMR analysis.

Remarkably, elongation of terminally oxidised poly-LacNAc glycans by β3GlcNAc- and β4Gal-transferase was also successful. In this way, a set of novel, modified poly-LacNAc oligomers containing terminally and/or internally modified galactose residues were obtained, which can be used for binding studies and various other applications.

Introduction

N-Acetyllactosamine (LacNAc; Galβ1,4GlcNAc) structures are important carriers of glycan epitopes, such as ABH or Lewis blood group determinants. Some of these are present on extended poly-*N*-acetyllactosamine glycans (poly-LacNAc; $[Gal\beta1,4GlcNAc]_n$) which serve as spacers and additional information carriers [1-5]. Poly-LacNAc itself was identified as a recognition motif of galectins, which are an important class of mammalian lectins [6,7]. Another LacNAc related epitope is LacDiNAc (GalNAcβ1,4GlcNAc), which is especially well-known from parasitic nematodes and trematodes [8,9]. In humans, LacDiNAc-containing glycans trigger the cellular immune response of natural killer cells [10-12]. Scientific interest in the synthesis of naturally occurring and modified LacNAc and poly-LacNAc glycans is high, as they can be used for the detailed investigation of lectin binding modes and their biological function, and as possible diagnostic markers or therapeutic agents [13-16]. Naturally occurring poly-LacNAc glycans and furthermore epitopes thereof, such as fucosylated, sialylated and branched glycans, are widely used in the analysis of galectin–glycan interaction in glycan arrays [7,17-19]. Efforts have especially been made regarding the development and evaluation of galectin inhibitors as therapeutic agents [20-23]. For example, chemically modified mono- and disaccharides as well as thiodigalactosides have been investigated [21,24-27]. Another modification strategy is the use of galactose oxidase, which can be combined with different chemical modifications. Galactose oxidase is a copper-containing enzyme that catalyses the oxidation of the C6-hydroxyl group of nonreducing D-galactose residues [28,29]. Several subsequent modifications, such as site-specific labelling of glycoconjugates with hydrazide or hydroxylamine reagents [30-34], coupling with amino-modified glycan moieties [35], chemical oxidation of the carbonyl to a carboxyl group in the synthesis of immunoreactive neo-glycosaminoglycans [12], and the synthesis of deoxysugars [36], have been reported. The specific properties of galactose oxidase, such as activity and substrate spectrum, have been altered by directed evolution [34,37]. However, although galactose oxidase was discovered decades ago [38,39] and is widely used, the formation of different products during the enzymatic conversion of D-galactose is still not yet completely understood and controllable. The main products of the galactose oxidase reaction are the aldehyde, which occurs as a hydrate in aqueous solution, the corresponding galacturonic acid, and an α,β-unsaturated aldehyde as a dehydrated side product [40-42]. The occurrence of these products seems to vary depending on the synthesis parameters in different applications [12,42-44].

We here investigate the oxidation of LacNAc and LacDiNAc terminated poly-*N*-acetyllactosamine glycans, recently synthesised by our group [11,45], with subsequent chemical conversion of the 6-aldehyde group to the corresponding α,β-unsaturated aldehyde by base-catalysed β-elimination (Scheme 1). The galactose 6-aldehydes of poly-LacNAc oligomers were chemically converted to their corresponding α,β-unsaturated aldehydes under elevated temperature at alkaline pH in almost quantitative yield. In this way defined oxidised poly-LacNAc oligomer structures are easily obtained by galactose oxidase treatment and subsequent heating of the reaction mixture. The corresponding 6-aldehyde LacNAc oligomers were used as substrates in further elongation reactions with glycosyltransferases (Scheme 2). Remarkably, the terminally oxidised poly-LacNAc oligomers could be elongated by β3GlcNAc-transferase and subsequently by β4Gal-transferase. These results pave the way for the synthesis of a set of novel, modified poly-LacNAc glycan structures containing terminally and/or internally oxidised galactose residues for further chemical conversions. As an example, the 6-aldehydes of poly-LacNAc oligomers were converted with (+)-biotinamidohexanoic acid hydrazide (BACH), resulting in biotin-labelled poly-LacNAc glycans (Scheme 3). Moreover, the amine group obtained after deprotection of the NH_2-linker of poly-LacNAc oligomers was utilised for the reductive amination of 6-aldehyde groups of oxidised poly-LacNAc oligomers (Scheme 4). In this way, chemically branched poly-LacNAc glycans are synthesised that resemble natural, branched poly-LacNAc glycans (I-antigens) of glycoproteins and glycolipids.

Results and Discussion

Evaluation of Gal- and GalNAc terminated poly-LacNAc oligomers as substrates of galactose oxidase

The activity of galactose oxidase from *Dactylium dendroides* with LacNAc **1a**, Gal-terminated poly-LacNAc oligosaccharides **1b**–**d** and LacDiNAc **2** (Scheme 1) was investigated by a photometric-activity assay and by HPLC analysis. Compared to methyl β-D-galactopyranoside the galactose oxidase showed a relative activity of about 4% for all tested

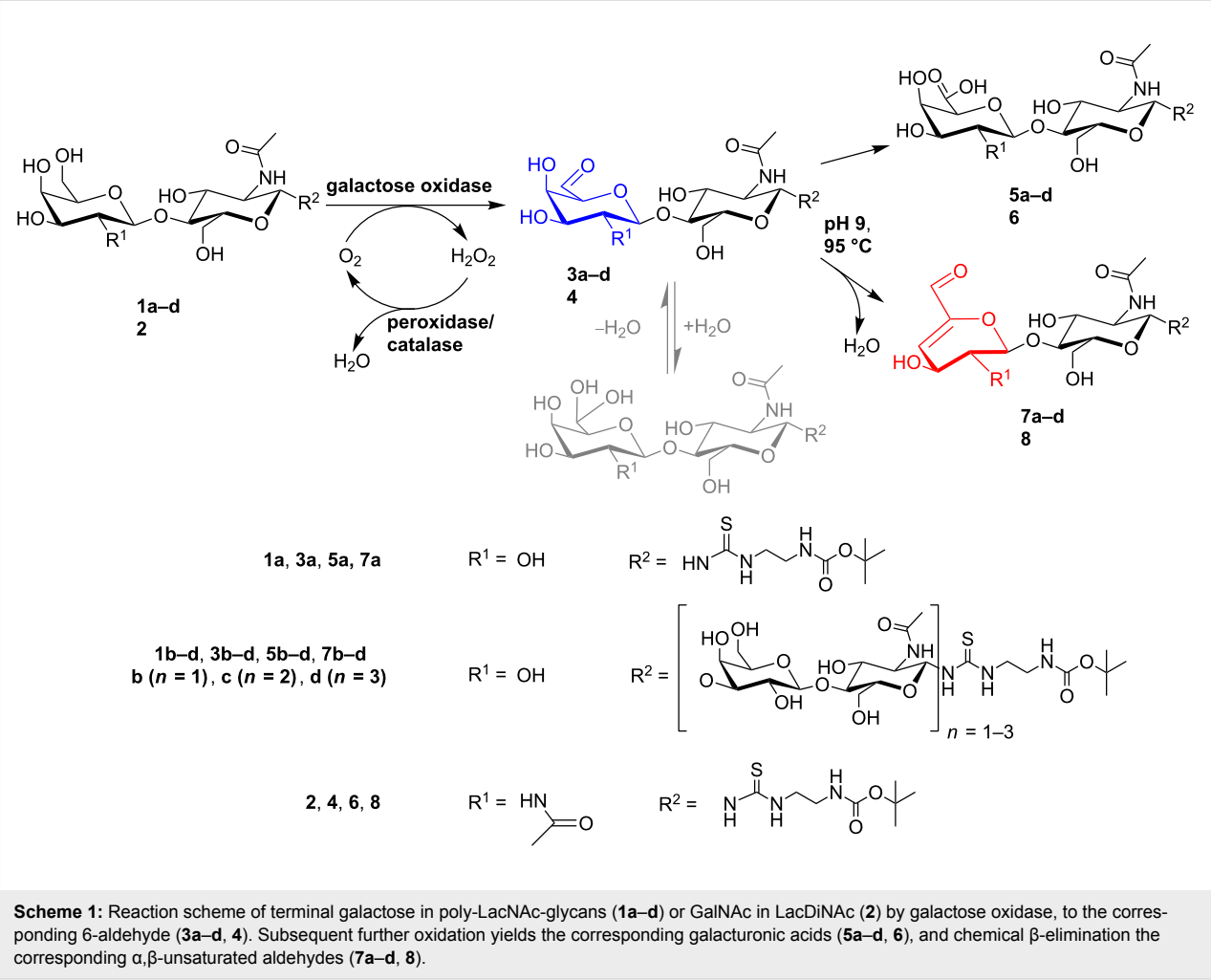

Scheme 1: Reaction scheme of terminal galactose in poly-LacNAc-glycans (**1a–d**) or GalNAc in LacDiNAc (**2**) by galactose oxidase, to the corresponding 6-aldehyde (**3a–d**, **4**). Subsequent further oxidation yields the corresponding galacturonic acids (**5a–d**, **6**), and chemical β-elimination the corresponding α,β-unsaturated aldehydes (**7a–d**, **8**).

saccharides (**1a**–**d** and **2** were measured at a standard concentration of 1 mM glycan, Figure S2 in Supporting Information File 1), which is sufficient for the semipreparative production of oxidised products. The methyl β-galactoside was chosen as a reference substance because of the comparable linkage at the anomeric C-atom and its known high activity [38]. No activity could be seen with odd-numbered (GlcNAc-terminated) poly-LacNAc–linker–*t*-Boc oligosaccharides, either by photometric or by HPLC analysis, even after long reaction times (data not shown). This confirms that galactose oxidase accepts only terminal galactose residues of poly-LacNAc glycans, as previously concluded for the oxidation of raffinose and plant arabinogalactan polysaccharides [36,46]. Standard enzymatic reactions were performed in sodium phosphate buffer pH 6 and analysed by HPLC after the enzymatic reaction was stopped at 95 °C at different reaction times. Three main products could be detected with all tested substrates (Scheme 1, Figure S3 in Supporting Information File 1). The products from the conversion of the tetrasaccharide **1b** and LacDiNAc **2** could be assigned according to their molecular mass as the corresponding aldehydes **3b** and **4**, the corresponding α,β-unsaturated aldehyde products **7b** and **8**, and the galacturonic acid products **5b** and **6**, as depicted in Table S1 in Supporting Information File 1 [42,44]. The formation of the corresponding uronic acids, whether chemically or enzymatically catalysed, was not further investigated. The formation of the 6-aldehydes **3a** and **3c** and the α,β-unsaturated aldehydes **7a** and **7c** for the conversion of **1a** and **1c**, was also confirmed by ESI–MS analysis (Table S1 and Figure S13 in Supporting Information File 1). Conversion of **1d** (Figure S4 in Supporting Information File 1, compared to **1c**) was followed by HPLC and gave similar product patterns to those seen for **1a**, **1b** and **1c**.

However, we asked if β-elimination is catalysed by galactose oxidase or is chemically driven by the applied reaction conditions. The products (88% **3b**, 10% **5b** and 2% **7b**) obtained after conversion of **1b** and termination of the galactose oxidase reaction by heat were incubated in 50 mM sodium phosphate buffer (varying pH as indicated) at different temperatures for different time periods, without the addition of enzyme (Figure S5 in

Supporting Information File 1). We observed that the α,β-unsaturated aldehyde **7b** is formed independently of the enzyme. We concluded that dehydration of the 6-aldehyde **3b** occurs chemically at high temperatures and alkaline pH values. Similar reactions at elevated temperatures and different pH values were previously described for the synthesis of α,β-unsaturated aldehydes of α,β-galactosides, lactose, and raffinose [36,42,47]. In summary, the detailed product analysis by HPLC and ESI–MS provides evidence for the chemical conversion of the aldehyde to the corresponding α,β-unsaturated aldehyde by base-catalysed β-elimination.

Optimisation of galactose oxidase reaction with poly-LacNAc glycans as substrates for the synthesis of 6-aldehydes

In the following experiments the oxidation of **1b** was optimised for the formation of the 6-aldehyde **3b**. No significant effect of pH (between 5 and 8) could be detected for the initial reaction rate of galactose oxidase (between 20 and 23% conversion in the first 15 min) and no marked effect on enzyme stability for the tested reaction times was detected. The pH optimum for galactose oxidase is described to be neutral to slightly acidic [48]. Different pH values were chosen for the oxidation reaction in previous studies [33,42,44,49]. We found a small preference for the formation of galacturonic acid at neutral pH, as previously described by Parikka and Tenkanen [42]. Taking these data and our results regarding the formation of acid and α,β-unsaturated aldehyde into account, we chose pH 6 for further galactose oxidase reactions.

Hydrogen peroxide is known to inhibit galactose oxidase activity [50,51]. Therefore, we tested reaction mixtures with catalase and a mixture of catalase and peroxidase, as well as peroxidase alone, for their conversion capabilities. All tested mixtures led to the same maximum, almost quantitative conversion after 24 h reaction time at pH 6, while a control sample without any additional catalase or peroxidase showed a distinctly reduced conversion. Surprisingly, the use of peroxidase alone already showed optimal conversion rates at least as good as with catalase, although a classical, appropriate donor substrate for the peroxidase was not present in the reaction. In other studies peroxidase has been shown to increase the activity of galactose oxidase, which may improve the reaction in such a way as to overcome the inhibitory effects [42,52,53]. The surface-to-volume-ratio was kept high to ensure sufficient oxygen transfer through the solvent surface. Accordingly, (semi-)preparative reactions were performed in open glass vessels to increase the transfer rate in comparison to closed ones.

Optimised reaction conditions for the conversion of **1b** yielded 94% 6-aldehyde **3b** with minimum formation of the α,β-unsaturated aldehyde **7b** (Table 1). Substrates **1a**, **1c** and **1d** gave comparable conversion rates and yields (Table 1 and Figure S4 in Supporting Information File 1). In addition, compound **2** was oxidised with basically the same conversion rate and in similar yields. Quantitative conversion of all the substrates to their corresponding 6-aldehydes without the formation of α,β-unsaturated aldehydes was achieved by avoiding heat treatment and by removal of galactose oxidase by ultrafiltration instead. In contrast, small amounts of α,β-unsaturated aldehydes were formed when the reactions were stopped with heat, as shown in Table 1.

Semipreparative synthesis (>5 mg scale) of the 6-aldehydes **3a–c** was performed for subsequent further modification. Product isolation was accomplished by preparative HPLC with overall yields (based on substrate amount) of 35 to 55%. The products **3a**, **3b** and **3c** were characterised by LC–ESI–MS (Table S1 and Figure S13 in Supporting Information File 1). **3a** and **3b** were additionally confirmed by ^{1}H- and ^{13}C NMR analysis (Experimental section and Table NMR 1 and Table NMR 2 in Supporting Information File 2). During evaporation of the solvents under moderate heat (40–60 °C), small amounts of α,β-unsaturated aldehyde impurities **7a–c** (approx. 1–5%) were formed. The corresponding LacDiNAc 6-aldehyde **4** was

Table 1: Conversion of poly-LacNAc oligomers **1a–d** with galactose oxidase under optimised conditions (pH 6, 24 h, 10 µmol substrate, 15.5 U galactose oxidase and 322 U peroxidase). The 6-aldehydes **3a–d** were obtained in 84–94% yield. A small fraction of α,β-unsaturated aldehydes **5a–d** was formed due to termination of the reaction by heating for 3 min at 95 °C.

substrate	peak fraction according to HPLC analysis (%)			
	educt **1a–d**	6-aldehyde **3a–d**	galacturonic acid **5a–d**	α,β-unsaturated aldehyde **7a–d**
1a	9	84	2	5
1b	0	94	1	5
1c	0	94	1	5
1d	0	92	0	8

produced and isolated on a smaller scale (<1 mg) and analysed by LC–ESI–MS (Table S1 and Figure S13 in Supporting Information File 1).

Chemical conversion of 6-aldehydes to their corresponding α,β-unsaturated aldehydes

As the α,β-unsaturated aldehydes (**7a**–**d**) may also be interesting products for the evaluation of protein–glycan interactions, we decided to produce these for further analysis. To characterise and optimise the chemical conversion of 6-aldehydes to their corresponding α,β-unsaturated aldehydes (Scheme 1) the time course of the conversion of the 6-aldehydes **3a** and **3b** at pH 9 and 95 °C was monitored. HPLC analyses revealed the formation of the desired α,β-unsaturated aldehydes and several separated side products (Figure S6 in Supporting Information File 1). Complete conversion of **3a** (Figure S7 in Supporting Information File 1) and **3b** (Figure 1) was achieved within 30 min reaction time at pH 9 and 95 °C. After 15–20 min reaction time the product mixture contained up to 90% α,β-unsaturated aldehyde. However, with longer incubation the fraction of side products increased. Schoevaart et al. assumed the formation of more than 30 products under conditions of heat, with increased production rates at alkaline pH [43]. Therefore the side products were not further investigated.

The semipreparative synthesis of the α,β-unsaturated aldehydes **7a**–**c** was accomplished by the conversion of **3a**–**c** at 95 °C at pH 9 for 15 min. The products were isolated by preparative HPLC and characterised by LC–ESI–MS (Table S1 and Figure S13 in Supporting Information File 1). ^{1}H- and ^{13}C NMR analysis (Table NMR 3 and Table NMR 4 in Supporting Information File 2) was performed for **7a** and **7b**. The corresponding LacDiNAc α,β-unsaturated aldehyde **8** was synthesised on an analytical scale and analysed by ESI–MS (Table S1 and Figure S13 in Supporting Information File 1). This proves the formation of an α,β-unsaturated product also for the GalNAc-residue, which has, to the best of our knowledge, not been reported before.

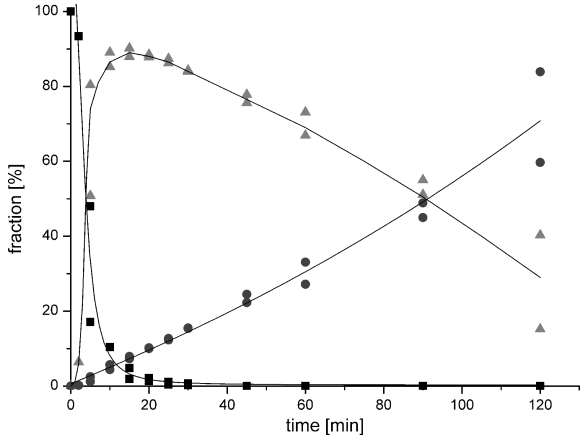

Figure 1: Conversion of **3b** (squares) to the corresponding α,β-unsaturated aldehyde **7b** (triangles) and side products (circles) at 95 °C and pH 9. Percentages of the products were calculated by integration of HPLC signals at 254 nm in relation to the sum of all peak integrals at 254 nm. Shown are single values of two independent conversions.

Enzymatic elongation of modified poly-LacNAc oligomers

The 6-aldehydes **3a**,**b** (see Scheme 2A for **3a**), the α,β-unsaturated aldehydes **7a**,**b**, and the biotinylated poly-LacNAc glycans **15a**,**b** (see Scheme 3B) were tested as substrates for further enzymatic conversion with β3GlcNAc-transferase and MBP-His$_6$-α3Gal-transferase [45,54] on an analytical scale. HPLC analysis indicated that **3a**,**b** as well as **15a**,**b** were accepted as substrates by both glycosyltransferases (Figure 2 and Figure S8 in Supporting Information File 1). In contrast, the α,β-unsaturated aldehydes **7a**,**b** are not accepted as substrates by the tested glycosyltransferases.

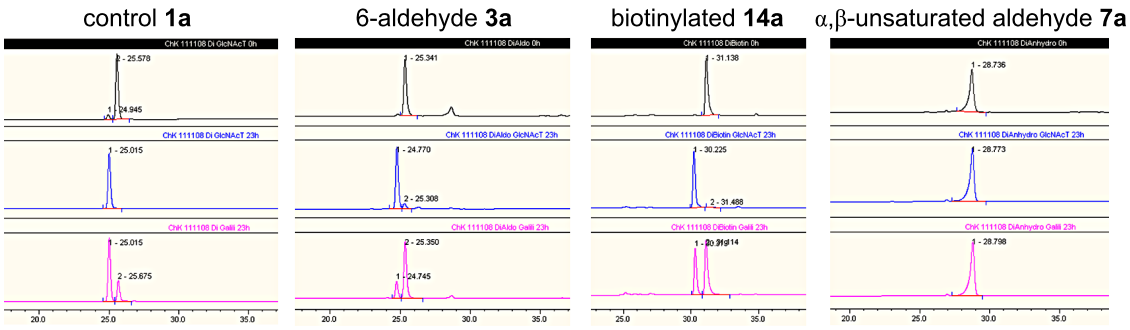

Figure 2: HPLC analysis for the conversion of modified LacNAc oligomers **3a, 15a**, and **7a** with β3-GlcNAc-transferase and MBP-His$_6$-α3Gal-transferase. LacNAc–linker–*t*-Boc **1a** served as control. The upper panel (black) shows the substrates under the initial reaction conditions. The middle panel (blue) depicts the conversion with β3-GlcNAc-transferase after 23 h and the lower panel (magenta) the conversion with MBP-His$_6$-α3Gal-transferase after 23 h. The 6-aldehyde of LacNAc (**3a**) and the C6-biotinylated LacNAc (**15a**) are substrates for enzymatic elongation, while the α,β-unsaturated aldehyde derivative of LacNAc (**7a**) is not accepted by either glycosyltransferase.

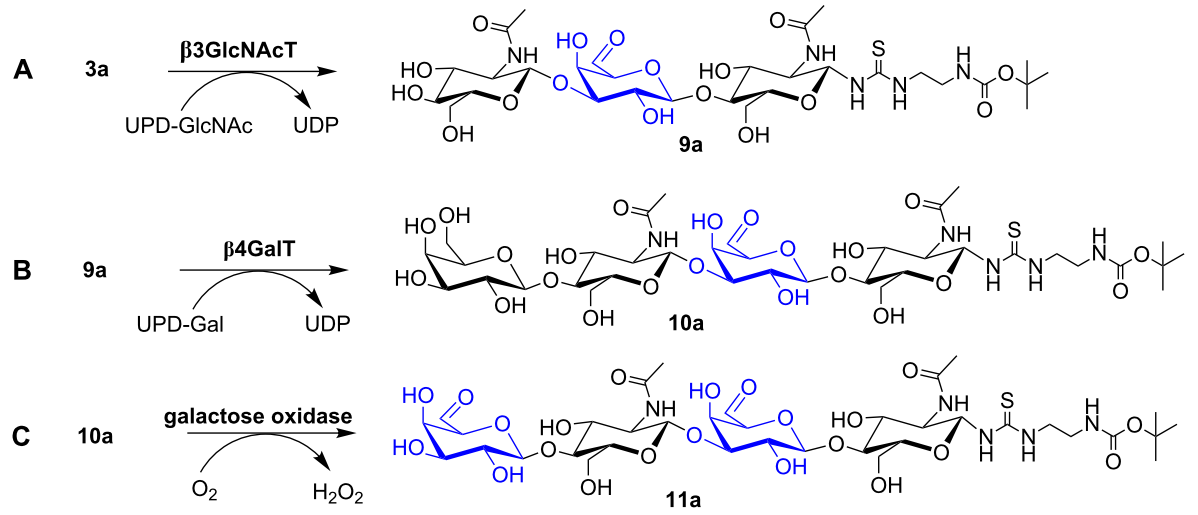

Scheme 2: Enzymatic modifications of oxidised poly-LacNAc oligomers. **A:** Elongation of LacNAc-6-aldehyde **3a** by β3-*N*-acetylglucosaminyltransferase (β3GlcNAc-transferase) leads to internally modified trisaccharide **9a**. **B:** The trisaccharide **9a** was further elongated by β4-galactosyltransferase (β4GalT) to yield the di-LacNAc derivative **10a** with an internal C6-oxidised galactose moiety. This reaction proves the synthesis of poly-LacNAc oligomers with internal C6-oxidised galactose units. **C:** Subsequent oxidation of the terminal galactose unit of **10a** showing the potential to produce terminally as well as internally oxidised and modified poly-LacNAc oligomers (**11a**).

The reaction of **3a** with β3GlcNAc-transferase (Scheme 2A) was analysed by ESI–MS (Table S1 and Figure S13 in Supporting Information File 1) and revealed the formation of trisaccharide **9a** with an internal 6-aldehyde group. Moreover, further elongation of **9a** by β4Gal-transferase yielded the product **10a** (Scheme 2B) as analysed by ESI–MS (Table S1 and Figure S13 in Supporting Information File 1). A second oxidation round led to the production of a tetrasaccharide that shows an internal and a terminal 6-aldehyde group (**11a**, see Scheme 2C, Table S1 and Figure S13 in Supporting Information File 1). These results open a range of new possibilities to synthesise poly-LacNAc glycans with internally and/or terminally modified galactose moieties.

Labelling of 6-aldehydes of poly-LacNAc oligomers

The 6-aldehyde products of poly-LacNAc oligomers **3a**–**c** were further reacted with BACH (**12**) to incorporate a site-specific biotin label for subsequent detection of immobilised glycans. Conversion with **12** and subsequent reduction were performed according to a standard procedure optimised in our laboratory [33]. The reactions were followed by HPLC analysis (Figure S9 and Figure S10 in Supporting Information File 1). Conversion rates of substrates **3a**–**c** were comparable, leading to 80–85% conversion after 24 h with no improvement for longer incubation times. Reduction with $Na[BH_3(CN)]$ was performed in a frozen state at −20 °C leading to complete reduction after 24 h (Scheme 3A). Products **15a**–**c** were purified by preparative HPLC in yields between 32 and 72% (based on initial 6-aldehyde amount) and confirmed by ESI–MS (Table S1 and Figure S13 in Supporting Information File 1). The structures of products **15a** and **15b** were characterised by ^1H- and ^{13}C NMR analysis (Experimental section and Table NMR 5–NMR 7 in Supporting Information File 2). The product **9a**, bearing an internal aldehyde group, was also modified with **12** yielding **14a**, as shown in Scheme 3A and Figure S11 in Supporting Information File 1.

Chemical conjugation at 6-aldehydes of modified poly-LacNAc oligomers

An especially interesting coupling reaction was performed to yield chemically branched poly-LacNAc oligomers (Scheme 4). The 6-aldehyde products **3a** as well as **10a** were used for coupling of a deprotected poly-LacNAc–linker–NH_2 glycan (**17**), which was synthesised as described previously [45,55]. On an analytical scale, a heptasaccharide–linker–NH_2 glycoconjugate **17** was coupled to the aldehyde groups of **3a** or **10a** by reductive amination leading to the chemically branched poly-LacNAc glycan structures **18** and **19**, respectively. Products **18** and **19** were isolated by analytical HPLC and confirmed by ESI–MS (Table S1 and Figure S13 in Supporting Information File 1). Our first experiments gave only low product yields of about 10–15% before purification, due to the formation of different side products at a reaction temperature of 60 °C and long incubation time (Figure S12 in Supporting Information File 1). No further optimisation was performed but would be required for better conversion of poly-LacNAc oligosaccharide substrates, especially regarding the reaction temperature as

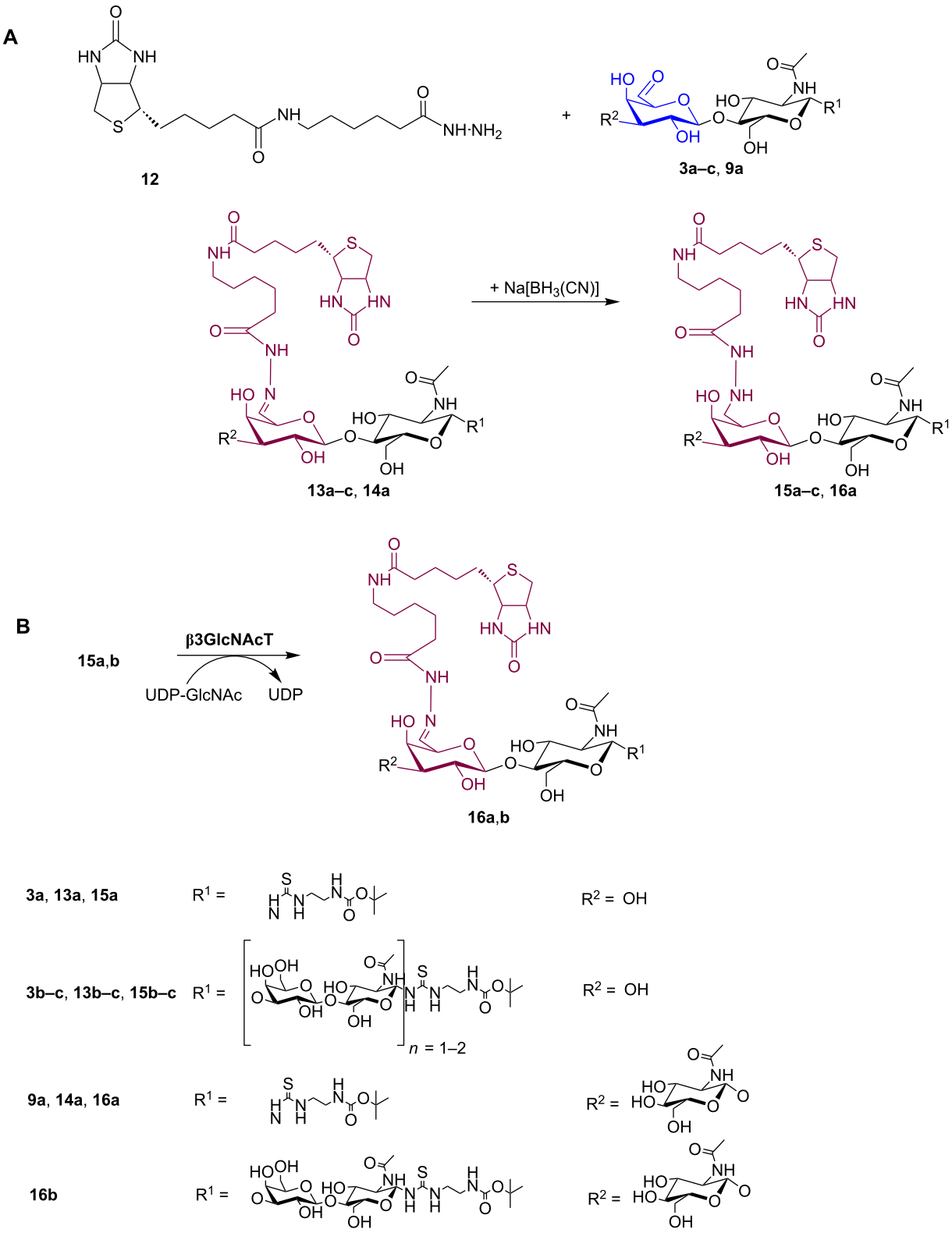

Scheme 3: A: Labelling of poly-LacNAc oligomers **3a–c** and **9a** with biotin hydrazide derivative BACH (**12**) yielding the hydrazone products (**13a–c** and **14a**); **13a–c** and **14a** were subsequently reduced with Na[BH_3(CN)] to the corresponding hydrazines (**15a–c** and **16a**). **B:** Elongation of biotinylated LacNAc (**15a**) and biotinylated tetrasaccharide (**15b**) by β3-*N*-acetylglucosaminyltransferase (β3GlcNAc-transferase) leads to an internally modified trisaccharide **16a** as the enzymatic elongation of the biotinylated LacNAc **13a** shown in **A**, or pentasaccharide (**16b**), respectively.

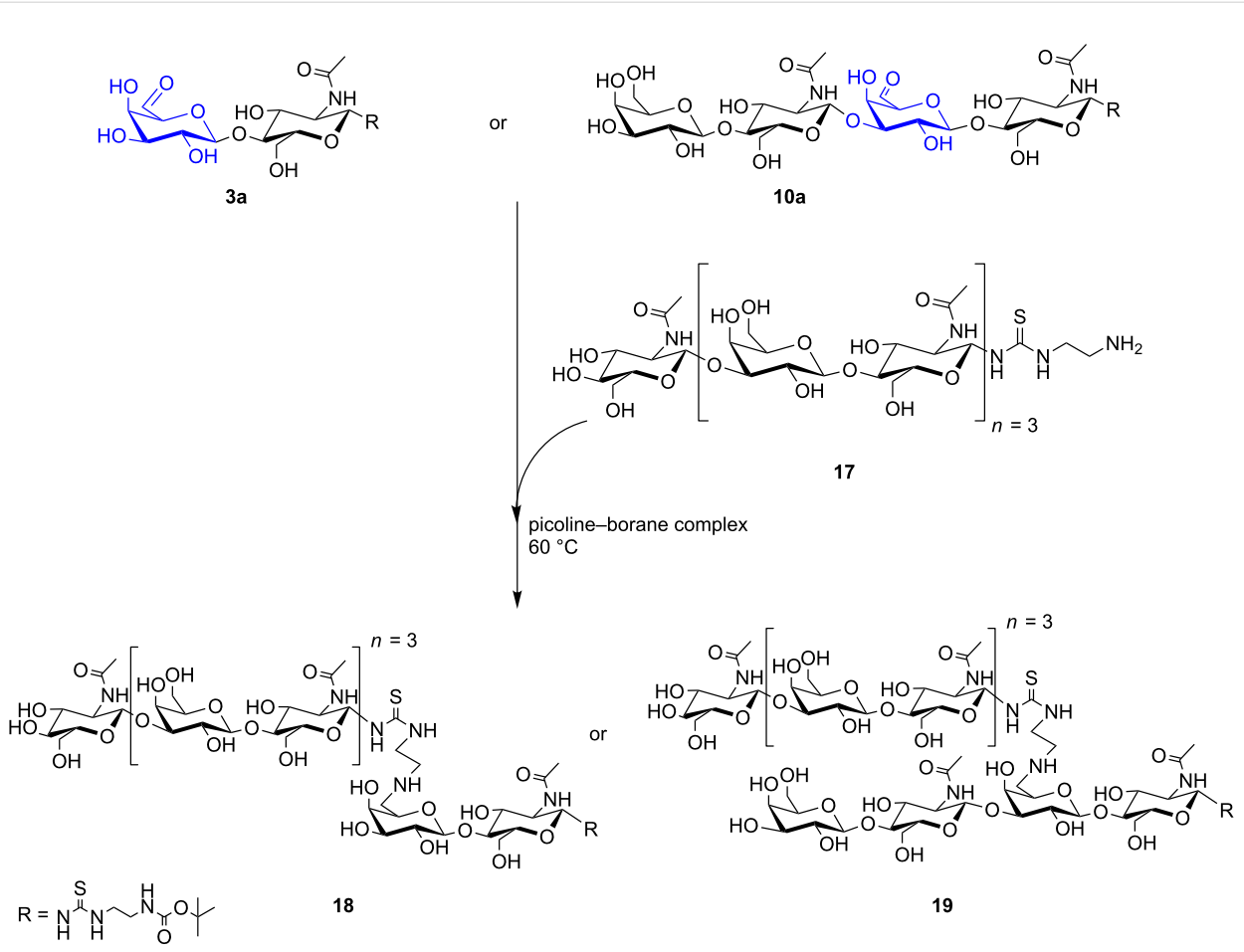

Scheme 4: Chemical conjugation of oxidised poly-LacNAc oligomers with heptasaccharide–linker–NH_2 (**17**) by reductive amination. Beside the main products (**18** and **19**) several byproducts are formed.

heating of the reaction mixture leads to the formation of α,β-unsaturated aldehydes. By branching, the avidity of glycans has been shown to increase, which is important for the binding affinity of lectins [56,57]. The chemically branched poly-LacNAc glycans may, moreover, serve as analogues to naturally occurring I-antigens (β1,6-branched poly-LacNAc) [58,59]. The I-antigen structures have so far been synthesised by chemical routes [60,61]. A similar coupling of oligosaccharides has already been shown by Rodriguez et al. on peptides, but no branching site in the glycans was introduced in their study [35]. In summary, these novel neo-glycoconjugates are interesting tools for extensive binding studies of a variety of glycan binding proteins (lectins, antibodies) and for possible therapeutic applications.

Conclusion

Novel poly-LacNAc derivatives have been produced on a micro-gram scale, which can be used for binding studies with different glycan-binding proteins, for the evaluation of binding mechanisms and biological functions. Our present study gives further insight into the reaction of galactose oxidase with poly-LacNAc substrates and has led to optimised reaction conditions, proving also the chemical conversion of 6-aldehydes under alkaline conditions to the corresponding α,β-unsaturated aldehydes. By means of ultrafiltration instead of heating, at moderate pH values, the chemical formation of α,β-unsaturated aldehydes was avoided, giving rise to a series of poly-LacNAc oligomer 6-aldehydes as a novel class of neo-glycoconjugates. We here also demonstrate, for the first time, that poly-LacNAc oligomers with terminal galactose 6-aldehyde moieties are substrates for glycosyltransferases. In this way, further poly-LacNAc glycans carrying terminal and/or internal galactose 6-aldehyde units can be built up. Incorporation of the aldehyde group gives rise to further modification with different amines, hydroxylamines, and hydrazides. Thereby modifications that introduce various chemical properties can be incorporated and tested for their influence on protein binding and biological function. The synthesised products could be valuable tools to follow

glycan immobilisation on biomaterial surfaces. Preliminary results already demonstrate that biotinylated poly-LacNAc oligosaccharides (with deprotected NH_2-linker) are detectable by streptavidin-peroxidase-detection after immobilisation on amine-reactive microtiter plates (data not shown). These products offer also the possibility of direct comparison between binding to soluble and immobilised poly-LacNAc glycans. This is especially important as it was shown that the presentation mode and the valency of glycans have a high impact on protein-binding regulation [62,63]. Binding analysis of different galectins to these novel poly-LacNAc derivatives is currently under investigation.

The production of poly-LacNAc chains with one or more modified galactose residues will allow further insight in detailed protein-glycan binding mechanisms. In the past mainly glycan-modified poly-LacNAc structures have been used to evaluate galectin affinity for internal and terminal galactose moieties [7,64]. In contrast, modified poly-LacNAc structures synthesised in this study could refine binding analysis by the incorporation of bulky residues, such as biotin, or more subtle modifications, such as an aldehyde group [65,66]. Terminal and internal aldehyde groups could be further used for the introduction of different functionalities, such as alkyne or azide groups, to facilitate orthogonal click-chemistry reactions [67]. Moreover, branched poly-LacNAc glycan structures were synthesised, which are interesting binding ligands for a variety of glycan-binding proteins. These novel chemically branched structures may serve as analogues for branched N-glycans.

Experimental

Materials

Galactose oxidase was purchased from Worthington (Lakewood, NJ) and peroxidase from Merck (Darmstadt, Germany). Restriction enzymes and alkaline phosphatase were supplied by Fermentas (St. Leon Roth, Germany). The used chemicals were purchased either from Sigma-Aldrich (Taufkirchen, Germany) or Carl Roth (Karlsruhe, Germany) and used without further purification.

Analytical methods

Chromatography and mass spectrometry

Analytical HPLC measurements were carried out on a Dionex LC–MS System using LiChrospher® 100RP 18-5µ EC or Multokrom 100-5 C18 250 × 4 mm (both CS Chromatographie, Langerwehe, Germany) columns. The following methods were used: A: Isocratic separation of poly-LacNAc–linker–*t*-Boc glycans by using 15% MeCN in water with 0.1% formic acid added as a mobile phase at 0.5 mL/min flow rate. B: Gradient separation of LacDiNAc-compounds by applying a gradient from 11–50% MeCN in water over a time course of 50 min at a flow rate of 0.5 mL/min. C: Gradient separation of oxidation products was performed by the use of 10–15% MeCN in water at 0.5 mL/min flow rate. For preparative purification of poly-LacNAc–linker–*t*-Boc compounds, a HPLC-system from Knauer (Berlin, Germany) was used in combination with a Eurospher 100-10 C18, 250 × 20 mm column (Knauer, Berlin, Germany), which was generally described elsewhere [45]. Purification took place with the same mobile phases as described above but at a flow rate of 12.5 mL/min. The products were fractionated manually. Detection of all glycans was possible at 205 nm and 254 nm. Qualitative fast monitoring of reaction progress was also done by thin-layer chromatography on 0.2 mm silica gel 60 (ALUGRAM® Xtra SIL G/UV254, Macherey&Nagel, Germany) with either isopropanol/30% ammonia/H_2O (7:2:1) or ethylacetate/methanol/H_2O/acetic acid (4:2:1:0.1) as mobile phases. Isolated products were analysed by HPLC/ESI mass spectrometry (Thermo Finnigan Surveyor® MSQ™) using the following settings: negative ESI ionization, probe temperature: 400 °C; needle voltage: 4.5 kV; cone voltage: 100 V. Ten microlitres of a 0.1 mM glycan solution were concentrated on a Multospher 120 RP 18 HP-3µ (60 × 2 mm), applying a flow rate of 0.2 mL/min using 50% MeCN in water as a mobile phase. Nonpurified products **5b** and **6** were analysed from the reaction mixture by using HPLC method A without formic acid and ESI mass spectrometry as described.

NMR spectroscopy

NMR spectra and data may be found in Supporting Information File 2. NMR spectra were measured on a Bruker AVANCE III 600 MHz spectrometer (600.23 MHz for ^{1}H, 150.93 MHz for ^{13}C, and 60.82 MHz for ^{15}N) in D_2O at 30 °C. The residual signal of the solvent was used as an internal standard (δ_H 4.508). The carbon spectra were referenced to the signal of acetone (δ_C 30.50). ^{1}H NMR, ^{13}C NMR, COSY, HSQC, HMBC, HSQC-TOCSY, and 1-D TOCSY spectra were measured by using the standard software from the manufacturers. Chemical shifts are given in δ-scale [ppm], and coupling constants in hertz. The digital resolution enabled us to report chemical shifts of protons to three and carbon chemical shifts to two decimal places. Some hydrogen chemical shifts were read out from HSQC and are reported to two decimal places. For compounds **3a** and **3b** the anomeric configuration (β) of galactose units was determined from the $J_{H\text{-}1,H\text{-}2}$ coupling constants. The glycosidic linkage was deduced by using heteronuclear correlations in the HMBC experiment (bold printed in tables) and confirmed by the downfield glycosylation shift of the involved carbons (C-4 for Glc, C-3 for Gal). Chemical shifts of GlcNAc carbons C-2 agree with N-acetylation. Because of isomerism on the NH-C=S bond, signals of H-1^A and CS were not detected. Chemical shifts of terminal C-6 and H-6 (87.98 and 4.861 ppm in **3a**, 88.14 and 4.955 ppm in **3b**) indicate the

presence of a geminal diol (the hydrate was formed). The NMR structure assignment of **7a** and **7b** was achieved as described for the above-mentioned products **3a** and **3b**. The α,β-unsaturated aldehyde structure of compounds **7a** and **7b** was proven by the presence of a C4–C5 double bond in the terminal saccharide unit. For compounds **15a** and **15b** the HSQC-TOCSY experiment was fundamental for the assignment of particular proton spin systems of individual saccharide units, the $–N(CH_2)_2N–$ and $–(CH_2)_5N–$ groups of spacers, and the spin system $–(CH_2)_4CHCH(N–)CH(N–)CH_2–$ of biotin. The anomeric configuration (β) of all saccharide units was determined from the $J_{H\text{-}1,H\text{-}2}$ coupling constants. Chemical shifts of GlcNAc carbons C-2 agree with *N*-acetylation. Because of isomerism on the NH–C=S bond, protons H-1^A resonate as two broad singlets. The above-mentioned spin systems were put together by using information extracted from the $^1H,^{13}C$ HMBC experiment (diagnostic correlations are bold printed in the Tables NMR 5 and NMR 6 in Supporting Information File 2). The glycosidic linkage was also demonstrated by the downfield glycosylation shift of the involved carbons (C-4 for Glc, C-3 for Gal). The structure of **15b** was supported by the $^1H,^{15}N$ HMBC experiment. The extracted $^1H,^{15}N$ contacts of seven nitrogen atoms (see the Table NMR 7 in Supporting Information File 2) confirmed the connection of particular spin systems; the remaining three nitrogens in the molecule were not detected.

Synthesis and isolation of linear poly-LacNAc–linker–*t*-Boc glycans

Linear poly-LacNAc–linker–*t*-Boc oligomers with defined chain length (**1a**–**d** and protected **17**) were synthesised as described previously with minor variations [45]. Briefly, two Leloir-glycosyltransferases, human β1,4-galactosyltransferase-1 (β4Gal-transferase) [68] and the β1,3-*N*-acetylglucosaminyltransferase from *Helicobacter pylori* (β3GlcNAc-transferase) [69], as well as UDP-Glc/GlcNAc 4'-epimerase from *Campylobacter jejuni* [70] were recombinantly produced in *E. coli,* purified and combined in a one-pot-synthesis. LacNAc–linker–*t*-Boc (5 mM), synthesised as described previously [45,55], was incubated as starting acceptor substrate together with UDP-α-D-glucose (UDP-Glc) and UDP-α-D-*N*-acetylglucosamine (UDP-GlcNAc) as donor substrates in 100 mM HEPES-NaOH-buffer pH 7.2, 25 mM KCl, 1 mM DTT, 1 mM $MnCl_2$, 1 mM $MgCl_2$, 2 U/mL alkaline phosphatase approx. 5 mU/mL β4Gal-transferase, approx. 25 mU/mL β3GlcNAc-transferase and approx. 3.5 U/mL UDP-Glc/GlcNAc 4'-epimerase for 48 h to 72 h. In order to yield even- or odd-numbered poly-LacNAc glycans, the reactions were stopped by ultrafiltration (molecular weight cut off at 30 kDa) and subsequently terminated by the addition of β4Gal-transferase, UDP-Glc/GlcNAc 4'-epimerase and UDP-Glc, or β3GlcNAc-transferase and UDP-GlcNAc, as described above, and incubation for 24 h. The isolation of single, defined poly-LacNAc–linker–*t*-Boc-glycans (**1a**–**d** and protected **17**) out of the product mixture was carried out by preparative reversed-phase HPLC (method A mobile phase). After evaporation of the solvent, the products were dissolved in water and appropriate stock solutions were stored at −20 °C. Reaction progress and final products (**1a**–**d** and protected **17**) were analysed by analytical reversed-phase HPLC applying method A and assigned by comparison to defined standards [45]. Concentration was determined by integration of the peak area and calculated against a linear calibration regression of GlcNAc–linker–*t*-Boc.

Synthesis and isolation of LacDiNAc-*t*-Boc

LacDiNAc-*t*-Boc (**2**) was synthesised as described previously with some modifications [11]. To increase enzyme stability after purification, the buffer was exchanged to storage buffer (100 mM MOPS, 25 mM KCl, pH 6.8) and 20% glycerol was added to reduce protein precipitation. To reach an improved conversion of the acceptor substrate, UDP-GlcNAc was used in 1.25-fold excess. Reaction mixtures of 5 mM GlcNAc–linker–*t*-Boc, 6.25 mM UDP-GlcNAc, recombinant mutant human galactosyltransferase 1 (His_6-propeptide-cat-β4-galactosyltransferase Y284L) (approx. 5 mU/mL), recombinant UDP-Glc/GlcNAc 4'-epimerase from *Campylobacter jejuni* (approx. 3.5 U/mL), 2 mM $MnCl_2$ and 2 U/mL alkaline phosphatase were incubated for 48 h to 72 h to achieve quantitative or almost quantitative conversion. Isolation of **2** was performed as described above by preparative reversed-phase HPLC applying the mobile phase of method B. The reaction progress and final product were analysed with HPLC, method B.

Deprotection of heptasaccharide–linker–NH_2: synthesis of **17**

Deprotection of the poly-LacNAc oligomer (**17**) was performed as described previously, except that sugars were not lyophilised but instead dissolved in water and stored at −20 °C [55]. Deprotection was controlled by HPLC using method A. As for protected glycans, the concentration was determined by integration of the peak area and calculated against the GlcNAc–linker–*t*-Boc standard regression curve.

Photometric galactose oxidase activity assay

Galactose oxidase activity was determined by the oxidation of 2,2'-azino-bis(3-ethylbenzothiazolin-6-sulfonic acid) (ABTS) as described previously with some modifications [71]. The assay was performed on microtiter plates by using 100 µL total volume. The standard assay contained 100 mM sodium phosphate buffer pH 6 (saturated with oxygen by flushing pure oxygen into the buffer for 10 min), 2 mM ABTS, 1 mM substrate (methyl β-D-galactoside as standard, **1a**–**d** and **2**) and

6 U/mL peroxidase. The reaction was started by the addition of 0.5 U/mL galactose oxidase. The reaction mixture was incubated at 30 °C and an increase of absorption at 405 nm was detected. Enzyme activity was determined from the linear reaction rate.

Oxidation of **1a–d** and **2**

Standard oxidation reactions were performed in oxygen-saturated sodium phosphate buffer (50 mM, pH 6, saturated by flushing pure oxygen into the buffer for 10 min). Open glass vessels were used to allow easy oxygen transfer, and the reaction mixtures were incubated at 30 °C under gentle mixing at 60 rpm for 5.5 h. For the oxidation of 10 µmol *t*-Boc-saccharide (**1a**–**d**, **2**), 15.5 U galactose oxidase and 322 U peroxidase were used. Samples were taken to control the progress of the synthesis and the reactions were stopped for 5 min at 95 °C, unless mentioned differently. After centrifugation for 20 min the supernatant was analysed as described below. Preparative batch reactions were stopped by ultrafiltration (molecular weight cut off at 10 kDa) to reduce the formation of α,β-unsaturated aldehydes. On an analytical scale, variations of the standard procedure were assessed, for example, different pH values, enzyme amounts or reaction time. For the analysis of oxidation reactions, reversed-phase HPLC utilizing method C was performed. Qualitative fast monitoring of the reaction progress was also done by TLC. Isolation of single products (**3a**–**c**, **4**) was performed by preparative HPLC as described above with the mobile phase of method C. NMR analysis confirmed the structure of products **3a** (Figure NMR 1 and Table NMR 1 in Supporting Information File 2) and **3b** (Figure NMR 2 and Table NMR 2 in Supporting Information File 2).

Chemical conversion of 6-aldehydes to α,β-unsaturated aldehydes

To analyse the chemical conversion of 6-aldehydes (**3a**,**b**) to the corresponding α,β-unsaturated aldehydes (**7a**,**b**), purified aldehydes or mixtures from a galactose oxidase reaction (88% aldehyde **3b**, 2% α,β-unsaturated aldehyde **7b** and 10% acid **5b**) were incubated in 50 mM sodium phosphate buffer as indicated at different pH values and various temperatures, for specific time periods. After incubation the sample was directly cooled down on ice. Formation of α,β-unsaturated aldehyde was monitored by reversed phase HPLC with method A. The conversion for Figure 1 was calculated as

$$\text{conversion} = \frac{5\text{b}}{3\text{b}+5\text{b}} - \frac{5\text{b}_{\text{initial}}}{3\text{b}_{\text{initial}}+5\text{b}_{\text{initial}}}.$$

The structures of **7a** and **7b** were confirmed by NMR experiments. The corresponding spectra and data are shown in Supporting Information File 2 (Figure NMR 3 and Table NMR 3 represent **7a** and Figure NMR 4 and Table NMR 4 represent **7b**).

Biotinylation of 6-aldehydes of poly-LacNAc oligomers

The biotinylation of 6-aldehydes **3a**–**c** was performed using biotin-amidohexanoic acid hydrazide (**12**) (BACH) according to a modified protocol from our previous work [33,49]. BACH (3.5 equiv) was added to 1 equiv isolated aldehyde (**3a**–**c**), or oxidation reaction mixture containing **3a-c**, in 25 mM sodium phosphate buffer (pH 6). The reaction was controlled directly by reversed-phase HPLC (method B) or TLC (isopropanol/30% ammonia/water 7:2:1). After 24–48 h at maximum conversion, 30 equiv of $Na[BH_3(CN)]$ (with reference to *t*-Boc-glycan) were added to the reaction mixture and the mixture was frozen at −20 °C. Samples were analysed again by HPLC and TLC. The product was purified by preparative HPLC as described above (mobile phase of method B), and the structure of **15a** and **15b** was confirmed by NMR analysis. The measured spectra and assigned data are found in Supporting Information File 2. Figure NMR 5 and Table NMR 5 correspond with **15a**, while Figure NMR 6 as well as Table NMR 6 and Table NMR 7 show the results for **15b**.

Enzymatic elongation of modified poly-LacNAc oligomers

Modified di- and tetra-saccharides (**3a**,**b**, **7a**,**b** and **15a**,**b**) were incubated with β3GlcNAc-transferase and 1.2-fold excess of UDP-GlcNAc, as described above. Elongation of **3a**,**b**, **7a**,**b** and **15a**,**b** with recombinant murine α3-galactosyltransferase (MBP-His_6-α3Gal-transferase) was performed in 100 mM MES–NaOH pH 6, 25 mM KCl, 2 mM $MnCl_2$ using 1.2-fold excess of UDP-α-D-galactose (UDP-Gal). MBP-His_6-α3Gal-transferase was cloned from an expression plasmid previously used by our group [54]. NdeI and XhoI restriction sites were incorporated by PCR. The primer sequences were: 5′-GGGAATTCCATATGGGCCATCATCATCATCAT-CACAGTTCGAGTGTCGAGAC-3′ and 3′-CCGTCT-GTTTTCTCATATTAAACCAATCTTTATTACAGATTAT-TGAGCTCCGCCC-5′. The insert was digested with restriction enzymes NdeI and XhoI and ligated into the pCWori+ derivate JHP1032 described by Logan et al., which was digested with restriction enzymes NdeI and SalI, resulting in the expression vector pMisGali [69]. Expression was performed in *E.coli* BL21(DE3) in a 2.5 L Minifors fermenter (Infors HT, Bottmingen, Switzerland) by using 1.5 L TB medium containing 100 mM phosphate buffer, maintaining a pH of 7.5, and 100 µg/mL Ampicillin. After inoculation with 40 mL preparatory culture, fermentation was performed at 37 °C, 1100 rpm and 4.0 vvm mass flow. Upon reaching the stationary

phase, a change of the fermentation temperature to 25 °C was followed by the addition of isopropyl β-D-thiogalactopyranoside (IPTG) yielding a concentration of 1 mM. Additionally a feed (approx. 0.1 mL/min) of 50% (v/v) glycerol in water was applied. Cultivation was terminated 2 h after IPTG addition, yielding 60 g cells (wet weight) per litre of media. Purification was done by IMAC as described elsewhere [45]. Reactions were controlled by using reversed-phase HPLC (method B). Elongation of **9a** with galactose was performed by incubation with approx. 5 mU/mL β4Gal-transferase and 1.2-fold excess of UDP-Gal, as described previously for the synthesis of poly-LacNAc glycans [45].

Reductive amination of poly-LacNAc aldehydes **3a** and **10a** with deprotected poly-LacNAc-linker glycan **17**

Aldehyde-modified glycans (**3a** and **10a**) were incubated with two-fold excess of deprotected hepta-saccharide–linker–NH_2 (**17**), 1.5-fold excess of picoline–borane complex and two-fold excess of acetic acid in methanol:H_2O mixture (approx. 6:1) [72-74]. Reaction mixtures were incubated at 60 °C for 19 h. The analysis and small-scale isolation of products **18** and **19** were performed by reversed-phase HPLC using method A and ESI–MS.

Supporting Information

Supporting Information File 1

Additional diagrams, HPLC chromatograms and ESI–MS spectra.
[http://www.beilstein-journals.org/bjoc/content/supplementary/1860-5397-8-80-S1.pdf]

Supporting Information File 2

NMR data and spectra.
[http://www.beilstein-journals.org/bjoc/content/supplementary/1860-5397-8-80-S2.pdf]

Acknowledgements

L. E. and C. E. K. acknowledge financial support by the DFG within the Research Training Group 1035 “BioInterface” and by the excellence initiative of the German federal and state governments through ERS@RWTH Aachen University. L. E. acknowledges financial support by the DFG (project EL 135/10-1). L. E. and V. K. are thankful for financial support from the EU-COST action CM0701 (MSMT OC09045). The authors thank Dipl.-Ing. Dennis Hirtz for excellent technical assistance and Dr. W. W. Wakarchuck (National Research Council of Canada) for providing the plasmids for β3GlcNAc-transferase and UDP-Glc/GlcNAc 4′-epimerase.

References

1. Demetriou, M.; Granovsky, M.; Quaggin, S.; Dennis, J. W. *Nature* **2001,** *409,* 733–739. doi:10.1038/35055582
2. Lau, K. S.; Partridge, E. A.; Grigorian, A.; Silvescu, C. I.; Reinhold, V. N.; Demetriou, M.; Dennis, J. W. *Cell* **2007,** *129,* 123–134. doi:10.1016/j.cell.2007.01.049
3. Ujita, M.; McAuliffe, J.; Hindsgaul, O.; Sasaki, K.; Fukuda, M. N.; Fukuda, M. *J. Biol. Chem.* **1999,** *274,* 16717–16726. doi:10.1074/jbc.274.24.16717
4. Wang, S. H.; Wu, S. W.; Khoo, K. H. *Proteomics* **2011,** *11,* 2812–2829. doi:10.1002/pmic.201000794
5. Zhou, D. *Curr. Protein Pept. Sci.* **2003,** *4,* 1–9. doi:10.2174/1389203033380304
6. Song, X. Z.; Xia, B. Y.; Stowell, S. R.; Lasanajak, Y.; Smith, D. F.; Cummings, R. D. *Chem. Biol.* **2009,** *16,* 36–47. doi:10.1016/j.chembiol.2008.11.004
7. Stowell, S. R.; Arthur, C. M.; Mehta, P.; Slanina, K. A.; Blixt, O.; Leffler, H.; Smith, D. F.; Cummings, R. D. *J. Biol. Chem.* **2008,** *283,* 10109–10123. doi:10.1074/jbc.M709545200
8. Wuhrer, M.; Koeleman, C. A. M.; Fitzpatrick, J. M.; Hoffmann, K. F.; Deelder, A. M.; Hokke, C. H. *Glycobiology* **2006,** *16,* 991–1006. doi:10.1093/glycob/cwl020
9. van Die, I.; Cummings, R. D. *Glycobiology* **2010,** *20,* 2–12. doi:10.1093/glycob/cwp140
10. Drozdová, A.; Bojarová, P.; Křenek, K.; Weignerová, L.; Henssen, B.; Elling, L.; Christensen, H.; Jensen, H. H.; Pelantová, H.; Kuzma, M.; Bezouška, K.; Krupová, M.; Adámek, D.; Slámová, K.; Křen, V. *Carbohydr. Res.* **2011,** *346,* 1599–1609. doi:10.1016/j.carres.2011.04.043
11. Bojarová, P.; Křenek, K.; Wetjen, K.; Adamiak, K.; Pelantová, H.; Bezouška, K.; Elling, L.; Křen, V. *Glycobiology* **2009,** *19,* 509–517. doi:10.1093/glycob/cwp010
12. Fialová, P.; Namdjou, D. J.; Ettrich, R.; Přikrylová, V.; Rauvolfová, J.; Křenek, K.; Kuzma, M.; Elling, L.; Bezouška, K.; Křen, V. *Adv. Synth. Catal.* **2005,** *347,* 997–1006. doi:10.1002/adsc.200505041
13. Gustafsson, A.; Holgersson, J. *Expert Opin. Drug Discovery* **2006,** *1,* 161–178.
14. Horlacher, T.; Seeberger, P. H. *Chem. Soc. Rev.* **2008,** *37,* 1414–1422. doi:10.1039/b708016f
15. Paulson, J. C.; Blixt, O.; Collins, B. E. *Nat. Chem. Biol.* **2006,** *2,* 238–248. doi:10.1038/nchembio785
16. Schmaltz, R. M.; Hanson, S. R.; Wong, C. H. *Chem. Rev.* **2011,** *111,* 4259–4307. doi:10.1021/cr200113w
17. Blixt, O.; Head, S.; Mondala, T.; Scanlan, C.; Huflejt, M. E.; Alvarez, R.; Bryan, M. C.; Fazio, F.; Calarese, D.; Stevens, J.; Razi, N.; Stevens, D. J.; Skehel, J. J.; van Die, I.; Burton, D. R.; Wilson, I. A.; Cummings, R.; Bovin, N.; Wong, C. H.; Paulson, J. C. *Proc. Natl. Acad. Sci. U. S. A.* **2004,** *101,* 17033–17038. doi:10.1073/pnas.0407902101
18. Hirabayashi, J.; Hashidate, T.; Arata, Y.; Nishi, N.; Nakamura, T.; Hirashima, M.; Urashima, T.; Oka, T.; Futai, M.; Muller, W. E.; Yagi, F.; Kasai, K. *Biochim. Biophys. Acta* **2002,** *1572,* 232–254. doi:10.1016/S0304-4165(02)00311-2
19. Song, X. Z.; Lasanajak, Y.; Xia, B. Y.; Heimburg-Molinaro, J.; Rhea, J.; Ju, H.; Zhao, C. M.; Molinaro, R.; Cummings, R.; Smith, D. *Glycobiology* **2010,** *20,* 1466. doi:10.1093/glycob/cwq137
20. Johnson, K. D.; Glinskii, O. V.; Mossine, V. V.; Turk, J. R.; Mawhinney, T. P.; Anthony, D. C.; Henry, C. J.; Huxley, V. H.; Glinsky, G. V.; Pienta, K. J.; Raz, A.; Glinsky, V. V. *Neoplasia* **2007,** *9,* 662–670.

21. Oberg, C. T.; Leffler, H.; Nilsson, U. J. *Chimia* **2011,** *65,* 18–23. doi:10.2533/chimia.2011.18
22. Papaspyridonos, M.; McNeill, E.; de Bono, J. P.; Smith, A.; Burnand, K. G.; Channon, K. M.; Greaves, D. R. *Arterioscler., Thromb., Vasc. Biol.* **2008,** *28,* 433–440. doi:10.1161/ATVBAHA.107.159160
23. Pieters, R. J. *ChemBioChem* **2006,** *7,* 721–728. doi:10.1002/cbic.200600011
24. Giguère, D.; Bonin, M. A.; Cloutier, P.; Patnam, R.; St-Pierre, C.; Sato, S.; Roy, R. *Bioorg. Med. Chem.* **2008,** *16,* 7811–7823. doi:10.1016/j.bmc.2008.06.044
25. Öberg, C. T.; Noresson, A. L.; Leffler, H.; Nilsson, U. J. *Chem.–Eur. J.* **2011,** *17,* 8139–8144. doi:10.1002/chem.201003247
26. Sörme, P.; Qian, Y. N.; Nyholm, P. G.; Leffler, H.; Nilsson, U. J. *ChemBioChem* **2002,** *3,* 183–189. doi:10.1002/1439-7633(20020301)3:2/3<183::AID-CBIC183>3.0.CO;2-#
27. van Scherpenzeel, M.; Moret, E. E.; Ballell, L.; Liskamp, R. M. J.; Nilsson, U. J.; Leffler, H.; Pieters, R. J. *ChemBioChem* **2009,** *10,* 1724–1733. doi:10.1002/cbic.200900198
28. Ettinger, M. J.; Kosman, D. J. In *Copper proteins;* Spiro, T. G., Ed.; Metal Ions in Biology, Vol. 3; Wiley-Interscience: New York, 1981; pp 219–261.
29. Mazur, A. W. Galactose Oxidase – Selected Properties and Synthetic Applications. In *Enzymes in carbohydrate synthesis;* Bednarski, M. D.; Simon, E. S., Eds.; ACS Symposium Series, Vol. 466; American Chemical Society: Washington, DC, 1991; pp 99–110. doi:10.1021/bk-1991-0466.ch008
30. Gahmberg, C. G.; Hakomori, S. *J. Biol. Chem.* **1973,** *248,* 4311–4317.
31. Itaya, K.; Gahmberg, C. G.; Hakomori, S. I. *Biochem. Biophys. Res. Commun.* **1975,** *64,* 1028–1035. doi:10.1016/0006-291X(75)90150-3
32. Wilchek, M.; Bayer, E. A. *Methods Enzymol.* **1987,** *138,* 429–442. doi:10.1016/0076-6879(87)38037-1
33. Bülter, T.; Schumacher, T.; Namdjou, D. J.; Gutièrrez Gallego, R.; Clausen, H.; Elling, L. *ChemBioChem* **2001,** *2,* 884–894. doi:10.1002/1439-7633(20011203)2:12<884::AID-CBIC884>3.0.CO;2-2
34. Rannes, J. B.; Ioannou, A.; Willies, S. C.; Grogan, G.; Behrens, C.; Flitsch, S. L.; Turner, N. J. *J. Am. Chem. Soc.* **2011,** *133,* 8436–8439. doi:10.1021/ja2018477
35. Rodriguez, E. C.; Winans, K. A.; King, D. S.; Bertozzi, C. R. *J. Am. Chem. Soc.* **1997,** *119,* 9905–9906. doi:10.1021/ja971633p
36. Schoevaart, R.; Kieboom, T. *Top. Catal.* **2004,** *27,* 3–9. doi:10.1023/B:TOCA.0000013536.27551.13
37. Delagrave, S.; Murphy, D. J.; Rittenhouse Pruss, J. L.; Maffia, A. M., III; Marrs, B. L.; Bylina, E. J.; Coleman, W. J.; Grek, C. L.; Dilworth, M. R.; Yang, M. M.; Youvan, D. C. *Protein Eng.* **2001,** *14,* 261–267. doi:10.1093/protein/14.4.261
38. Avigad, G.; Asensio, C.; Horecker, B. L.; Amaral, D. *J. Biol. Chem.* **1962,** *237,* 2736–2743.
39. Cooper, J. A. D.; Smith, W.; Bacila, M.; Medina, H. *J. Biol. Chem.* **1959,** *234,* 445–448.
40. Kelleher, F. M.; Bhavanandan, V. P. *J. Biol. Chem.* **1986,** *261,* 1045–1048.
41. Bonnet, V.; Duval, R.; Rabiller, C. *J. Mol. Catal. B: Enzym.* **2003,** *24–25,* 9–16. doi:10.1016/S1381-1177(03)00065-1
42. Parikka, K.; Tenkanen, M. *Carbohydr. Res.* **2009,** *344,* 14–20. doi:10.1016/j.carres.2008.08.020
43. Schoevaart, R.; Kieboom, T. *Carbohydr. Res.* **2001,** *334,* 1–6. doi:10.1016/S0008-6215(01)00166-5
44. Matsumura, S.; Kuroda, A.; Higaki, N.; Hiruta, Y.; Yoshikawa, S. *Chem. Lett.* **1988,** 1747–1750. doi:10.1246/cl.1988.1747
45. Rech, C.; Rosencrantz, R. R.; Křenek, K.; Pelantová, H.; Bojarová, P.; Römer, C. E.; Hanisch, F. G.; Křen, V.; Elling, L. *Adv. Synth. Catal.* **2011,** *353,* 2492–2500. doi:10.1002/adsc.201100375
46. Parikka, K.; Leppanen, A. S.; Pitkanen, L.; Reunanen, M.; Willfor, S.; Tenkanen, M. *J. Agric. Food Chem.* **2010,** *58,* 262–271. doi:10.1021/jf902930t
47. Ohrui, H.; Nishida, Y.; Higuchi, H.; Hori, H.; Meguro, H. *Can. J. Chem.* **1987,** *65,* 1145–1153. doi:10.1139/v87-191
48. Hamilton, G. A.; Adolf, P. K.; de Jersey, J.; DuBois, G. C.; Dyrkacz, G. R.; Libby, R. D. *J. Am. Chem. Soc.* **1978,** *100,* 1899–1912. doi:10.1021/ja00474a042
49. Namdjou, D.-J.; Sauerzapfe, B.; Schmiedel, J.; Dräger, G.; Bernatchez, S.; Wakarchuk, W. W.; Elling, L. *Adv. Synth. Catal.* **2007,** *349,* 314–318. doi:10.1002/adsc.200606169
50. Mendonça, M. H.; Zancan, G. T. *Arch. Biochem. Biophys.* **1987,** *252,* 507–514. doi:10.1016/0003-9861(87)90058-0
51. Kwiatkowski, L. D.; Adelman, M.; Pennelly, R.; Kosman, D. J. *J. Inorg. Biochem.* **1981,** *14,* 209–222. doi:10.1016/S0162-0134(00)80001-X
52. Radin, N. S.; Evangelatos, G. P. *J. Lipid Res.* **1981,** *22,* 536–541.
53. Tressel, P.; Kosman, D. J. *Biochem. Biophys. Res. Commun.* **1980,** *92,* 781–786. doi:10.1016/0006-291X(80)90771-8
54. Brinkmann, N.; Malissard, M.; Ramuz, M.; Römer, U.; Schumacher, T.; Berger, E. G.; Elling, L.; Wandrey, C.; Liese, A. *Bioorg. Med. Chem. Lett.* **2001,** *11,* 2503–2506. doi:10.1016/S0960-894X(01)00474-7
55. Sauerzapfe, B.; Křenek, K.; Schmiedel, J.; Wakarchuk, W. W.; Pelantová, H.; Křen, V.; Elling, L. *Glycoconjugate J.* **2009,** *26,* 141–159. doi:10.1007/s10719-008-9172-2
56. André, S.; Lahmann, M.; Gabius, H. J.; Oscarson, S. *Mol. Pharmaceutics* **2010,** *7,* 2270–2279. doi:10.1021/mp1002416
57. Dam, T. K.; Gabius, H. J.; André, S.; Kaltner, H.; Lensch, M.; Brewer, C. F. *Biochemistry* **2005,** *44,* 12564–12571. doi:10.1021/bi051144z
58. Twu, Y. C.; Hsieh, C. Y.; Lin, M.; Tzeng, C. H.; Sun, C. F.; Yu, L. C. *Blood* **2009,** *115,* 2491–2499. doi:10.1182/blood-2009-07-231993
59. Yu, L. C.; Lin, M. *Curr. Opin. Hematol.* **2011,** *18,* 421–426. doi:10.1097/MOH.0b013e32834baae9
60. Matsuzaki, Y.; Ito, Y.; Ogawa, T. *Tetrahedron Lett.* **1992,** *33,* 6343–6346. doi:10.1016/S0040-4039(00)60969-3
61. Whitfield, D. M.; Pang, H.; Carver, J. P.; Krepinsky, J. J. *Can. J. Chem.* **1990,** *68,* 942–952. doi:10.1139/v90-147
62. Rapoport, E. M.; André, S.; Kurmyshkina, O. V.; Pochechueva, T. V.; Severov, V. V.; Pazynina, G. V.; Gabius, H.-J.; Bovin, N. V. *Glycobiology* **2008,** *18,* 315–324. doi:10.1093/glycob/cwn009
63. André, S.; Frisch, B.; Kaltner, H.; Desouza, D. L.; Schuber, F.; Gabius, H. J. *Pharm. Res.* **2000,** *17,* 985–990. doi:10.1023/A:1007535506705
64. Leppänen, A.; Stowell, S.; Blixt, O.; Cummings, R. D. *J. Biol. Chem.* **2005,** *280,* 5549–5562. doi:10.1074/jbc.M412019200
65. Lobsanov, Y. D.; Gitt, M. A.; Leffler, H.; Barondes, S. H.; Rini, J. M. *J. Biol. Chem.* **1993,** *268,* 27034–27038.
66. Seetharaman, J.; Kanigsberg, A.; Slaaby, R.; Leffler, H.; Barondes, S. H.; Rini, J. M. *J. Biol. Chem.* **1998,** *273,* 13047–13052. doi:10.1074/jbc.273.21.13047

67. Kolb, H. C.; Finn, M. G.; Sharpless, K. B. *Angew. Chem., Int. Ed.* **2001,** *40,* 2004–2021. doi:10.1002/1521-3773(20010601)40:11<2004::AID-ANIE2004>3.0.CO;2-5
68. Sauerzapfe, B.; Namdjou, D.-J.; Schumacher, T.; Linden, N.; Křenek, K.; Křen, V.; Elling, L. *J. Mol. Catal. B: Enzym.* **2008,** *50,* 128–140. doi:10.1016/j.molcatb.2007.09.009
69. Logan, S. M.; Altman, E.; Mykytczuk, O.; Brisson, J. R.; Chandan, V.; St. Michael, F.; Masson, A.; Leclerc, S.; Hiratsuka, K.; Smirnova, N.; Li, J. J.; Wu, Y. Y.; Wakarchuk, W. W. *Glycobiology* **2005,** *15,* 721–733. doi:10.1093/glycob/cwi057
70. Bernatchez, S.; Szymanski, C. M.; Ishiyama, N.; Li, J. J.; Jarrell, H. C.; Lau, P. C.; Berghuis, A. M.; Young, N. M.; Wakarchuk, W. W. *J. Biol. Chem.* **2005,** *280,* 4792–4802. doi:10.1074/jbc.M407767200
71. Petersen, A.; Steckhan, E. *Bioorg. Med. Chem.* **1999,** *7,* 2203–2208. doi:10.1016/S0968-0896(99)00152-2
72. Cosenza, V. A.; Navarro, D. A.; Stortz, C. A. *ARKIVOC* **2011,** *(vii),* 182–194.
73. Ruhaak, L. R.; Steenvoorden, E.; Koeleman, C. A. M.; Deelder, A. M.; Wuhrer, M. *Proteomics* **2010,** *10,* 2330–2336. doi:10.1002/pmic.200900804
74. Sato, S.; Sakamoto, T.; Miyazawa, E.; Kikugawa, Y. *Tetrahedron* **2004,** *60,* 7899–7906. doi:10.1016/j.tet.2004.06.045

License and Terms

Beilstein Journal of Organic Chemistry

Synthesis and antifungal properties of papulacandin derivatives

Marjolein van der Kaaden[1], Eefjan Breukink[2] and Roland J. Pieters[*1]

Full Research Paper

Open Access

Address:
[1]Department of Medicinal Chemistry and Chemical Biology. Utrecht Institute for Pharmaceutical Sciences, Utrecht University, P.O. Box 80082, 3508 TB Utrecht, The Netherlands and [2]Department of Biochemistry of Membranes, Bijvoet Centre for Biomolecular Research, Utrecht University, Padualaan 8, Utrecht, The Netherlands

Email:
Roland J. Pieters[*] - R.J.Pieters@uu.nl

* Corresponding author

Keywords:
antifungal agents; carbohydrate; papulacandins; spiroketal

Beilstein J. Org. Chem. **2012,** *8,* 732–737.
doi:10.3762/bjoc.8.82

Received: 08 March 2012
Accepted: 24 April 2012
Published: 14 May 2012

This article is part of the Thematic Series "Synthesis in the glycosciences II".

Guest Editor: T. K. Lindhorst

Abstract

Derivatives of an antifungal agent that targets the β-(1,3)-D-glucan synthase, papulacandin D, were synthesized and tested for activity. The papulacandin D structure contains a challenging benzannulated spiroketal unit, which is introduced in a palladium-catalyzed cross-coupling reaction of a glycal silanolate and an aryl iodide followed by an oxidative spiroketalization. Four different variants were made, differing in the nature of the acyl side chain with respect to the length, and in the number and stereochemistry of the double bonds. Moderate biological activity was observed for the derivatives with a side chain based on palmitic acid and linoleic acid.

Introduction

In recent years, a steady increase in the incidence of opportunistic fungal infections in immunocompromised patients has been observed [1]. Treatment failure is frequent and mortality is unacceptably high in high-risk patients [2]. Reasons for this include delayed diagnosis, toxicity and low bioavailability of current drugs, and the development of antifungal drug resistance [1]. Clearly, there is a need for new antifungal therapeutics. The papulacandins are a series of naturally occurring antifungal agents whose isolation and characterization were initially reported by Traxler and co-workers in 1977 (Figure 1) [3,4]. They contain a benzannulated spiroketal unit, which has been the signature of a wide series of bioactive natural products [5] and has inspired ample synthetic activity [5-8]. The papulacandins A–E were isolated from the fermentation broths of *Papularia sphaerosperma* [3]. They block the synthesis of β-(1,3)-D-glucan by inhibition of β-(1,3)-D-glucan synthase [9-12]. The β-(1,3)-D-glucan is an integral and essential component of the fungal cell wall [13] and the dominant glucan in the cell wall of most medically important fungi, and therefore it is a target that is being actively pursued [14]. The papulacandins have demonstrated a very high specific activity against several yeasts, but they are largely inactive against filamentous fungi, bacteria and

protozoa [3]. Recently, in a direct comparison, papulacandin B was shown to be superior in some aspects compared to the drug caspofungin and a few drug candidates [15]. Its interesting biological activity has stimulated the search for new members of the papulacandin family, and several new compounds that are structurally related have been isolated, such as chaetiacandein [16,17], L-687,781 [18,19], Mer-WF3010 [20,21], BU-4794F [22], fusacandins [23,24], saricandin and PF-1042 [25], corynecandin [26,27] and the F-10748 series [28]. These structures vary mostly with respect to the two partially unsaturated acyl chains on the sugars. Small changes in these fatty acid tails have only small effects on the activity. However, more drastic changes in these tails or the lack of one of the tails drastically reduce activity, in comparison with the most active member of this family: papulacandin B. For the papulacandins it was shown that the substituted galactose is not essential for activity, since papulacandin D is still active, but it does increase the potency. Apparently, the situation is different for the related disaccharide saricandan carrying different acyl chains, for which the monosaccharide analogue was not active [29]. Removing the galactose acyl chain from papulacandin B results in material that can still inhibit the target (in a spheroplasts glucan synthesis assay) but cannot reach the target site of *C. albicans* [12]. The same is true for the hydrogenated form of papulacandin D [12]. Clearly some form of unsaturation is needed to maintain biological activity, but it is not known to what extent unsaturation (and alkylation and/or hydroxylation) needs to be present for the compound to reach the target site.

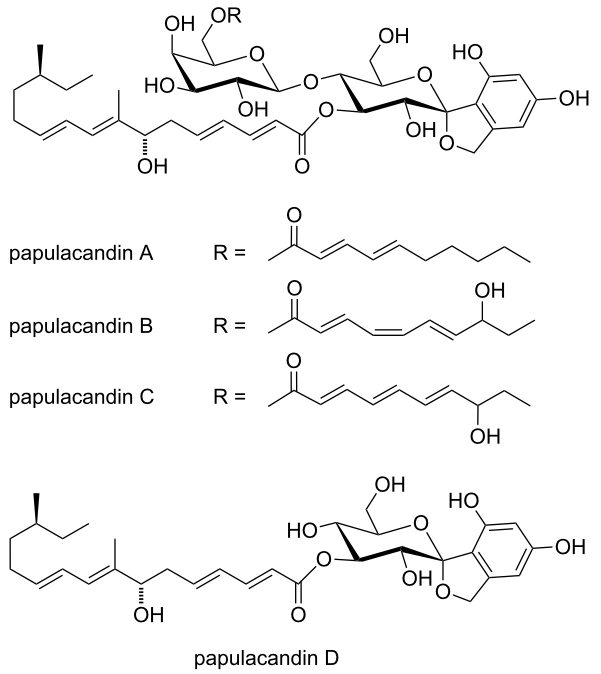

Figure 1: The papulacandins.

The papulacandins represent a synthetic challenge and as such the class has stimulated numerous synthetic studies. So far, only the total synthesis of papulacandin D, the simplest member of the family, has been published. This was reported by two different research groups [30-33] and additionally a number of different synthetic routes [34-38] to the spiroketal core structure have been published, including a hetero Diels–Alder reaction [39], a palladium(0)-catalyzed coupling [40-45] and a condensation reaction [46,47]. We herein report our efforts on the synthesis of papulacandin derivatives by total synthesis and the evaluation of their antifungal properties. The synthetic approach is largely based on the Denmark route [31] with a few notable deviations.

Results

The synthesis started with the anomeric aromatic group, i.e., the eventual spiroketal group of the glucose, to be introduced as an aryliodide with an ortho hydroxymethylene as in **12**. The commercially available 3,5-dihydroxybenzoic acid (**1**) was esterified, followed by benzylation of the aromatic hydroxy groups and reduction of the ester to the primary alcohol to give **7** (Scheme 1). This compound was iodinated by using *N*-iodosuccinimide (NIS), and finally the free hydroxy group was protected with a pivaloyl group to give aryl iodide **12**. Derivatives **13** and **14**, providing alternative core structures, were prepared similarly.

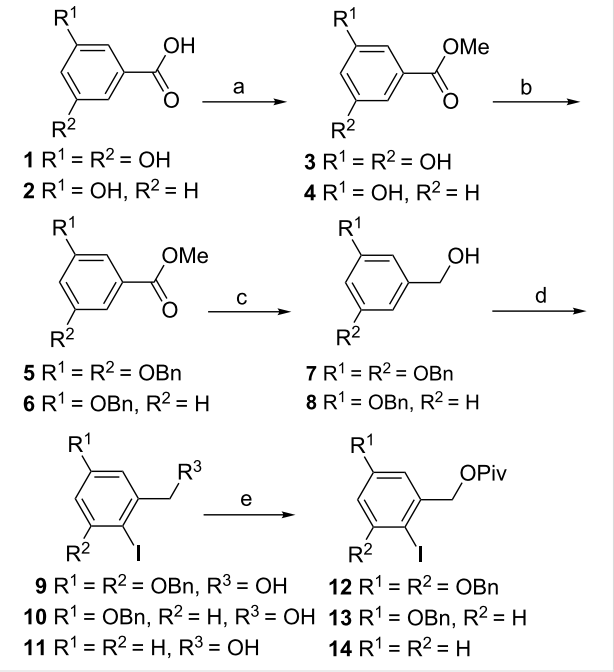

Scheme 1: (a) H_2SO_4, MeOH, reflux, 18 h, **3**: 98%; (b) BnBr, K_2CO_3, acetone, reflux, 18 h; (c) $LiAlH_4$, THF, rt, 10–30 min, **7**: 92% over three steps, **8**: 65% over three steps; (d) NIS, $CHCl_3$, rt, 18 h, **9** and **11** quant. or I_2, CF_3COOAg, $CHCl_3$, rt, 1 h, **10**: 96%; (e) pivaloyl chloride, pyridine, CH_2Cl_2, rt, 3–18 h, **12**: 95% over 2 steps, **13**: 96%, **14**: 98%.

The glucose moiety at the core of the structure, as present in papulacandin D, was approached from glycal **15**. The aim was to obtain a silanol such as **22** for coupling to an aryl iodide in the palladium-catalyzed cross-coupling reactions of silanolates, as pioneered and applied by the Denmark group (Scheme 2) [48]. The synthesis started with the saponification of **15**, followed by the protection of O-4 and O-6 by using di-*tert*-butylsilyl bis(trifluoromethanesulfonate). Subsequent protection of O-3 with TES-Cl, gave the fully protected glucal **18**. According to Denmark et al. [31], lithiation and silylation of **18** should give **20**, but in our hands a more complicated mixture resulted. We concluded that under our conditions deprotonation of the protecting group (protons α to silicon) may be competitive with the desired α-lithiation next to oxygen. Use of the more substituted TIPS silyl protecting group in **19** indeed solved this problem and yielded **21** in almost quantitative yield. Additional test reactions confirmed this trend as the corresponding 3,4,6-tri-*O*-(triisopropylsilyl)-D-glucal (**52**) yielded a single product after lithiation (Supporting Information File 1) and the 3,4,6-tri-*O*-(*tert*-butyldimethylsilyl)-D-glucal gave a mixture of products. Finally, compound **21** was oxidized to give silanol building block **22**.

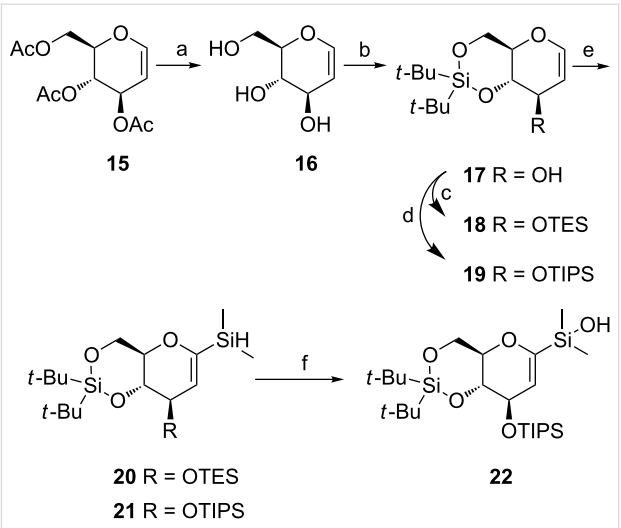

Scheme 2: (a) NaOMe in MeOH, MeOH, rt, 1 h, 96%; (b) $(t\text{-Bu})_2Si(OTf)_2$, pyridine, DMF, −40 °C to rt, 2 h, 90%; (c) TESCl, pyridine, CH_2Cl_2, rt, 18 h, 93%; (d) TIPSCl, imidazole, DMF, 60 °C, 2 d, 74%; (e) *t*-BuLi, Me_2SiHCl, Et_2O, −78 °C to rt, 3 h, **20**: no yield, **21**: 99%; (f) $[RuCl_2(p\text{-cymene})]_2$, H_2O, benzene/CH_3CN, rt, 4 h, 95%.

With building blocks **13** and **22** in hand, the palladium-catalyzed cross-coupling reaction was performed by using $Pd_2(dba)_3$ to give **23** (Scheme 3). Then the pivaloyl ester was selectively cleaved by using DIBAL-H, followed by oxidative spiroketalization under basic conditions to give the α- and β-anomers **29**, which were separable using column chromatog-

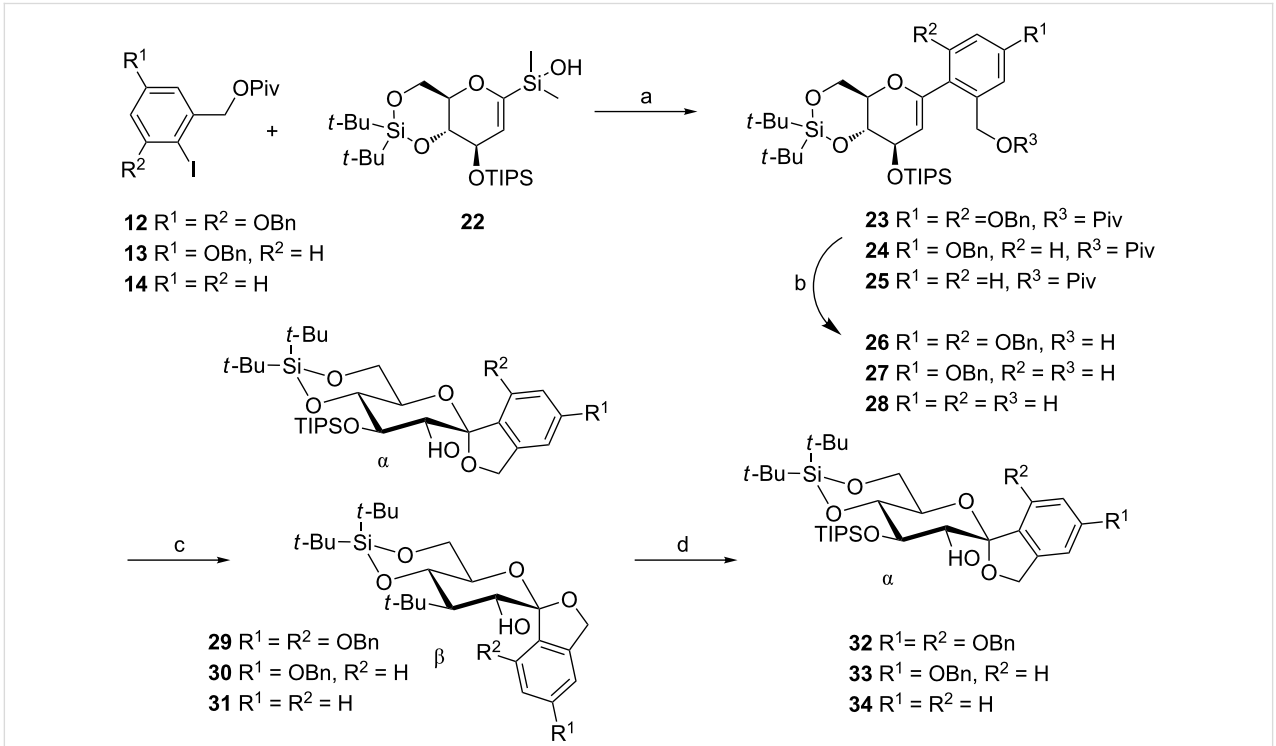

Scheme 3: (a) $Pd_2(dba)_3{\cdot}CHCl_3$, NaO*t*-Bu, toluene, 50 °C, 6–20 h, **23**: 72%, **24**: 79%, **25**: 62%; (b) DiBAL-H, CH_2Cl_2, −78 °C to rt, 0.5–1 h, **26**: 86%, **27**: 70%, **28**: 75%; (c) *m*-CPBA, $NaHCO_3$, CH_2Cl_2, 0 °C to rt, 2–2.5 h; (d) HCl, $CHCl_3$, rt, 1 h, **32**: 91% over two steps, **33**: 83% over two steps, **34**: 86% over two steps.

raphy. However this was not necessary: The β-anomer could readily be converted into the more stable α-anomer **32** by using a solution of 0.1 M HCl in chloroform. Similarly, the related iodides **14** and **15** performed well in this sequence yielding **33** and **34**.

The first step in the synthesis of the mimics of papulacandin D was debenzylation of **32**, since these groups cannot be removed in the presence of olefines in the final product side chain (Scheme 4). The liberated hydroxy groups were reprotected with MOM groups by using MOM-Cl to give **36**. Then the glucose O(3) needed to be selectively deprotected for the incorporation of the fatty acid tail. Unfortunately, this was not possible from **36** because of the use of the more stable TIPS group in this synthesis. Therefore, the cyclic silyl protecting group was first removed by using TBAHF in THF, followed by the deprotection of the TIPS group with TBAF and reintroduction of the cyclic silyl protecting group, giving **39**. To circum-

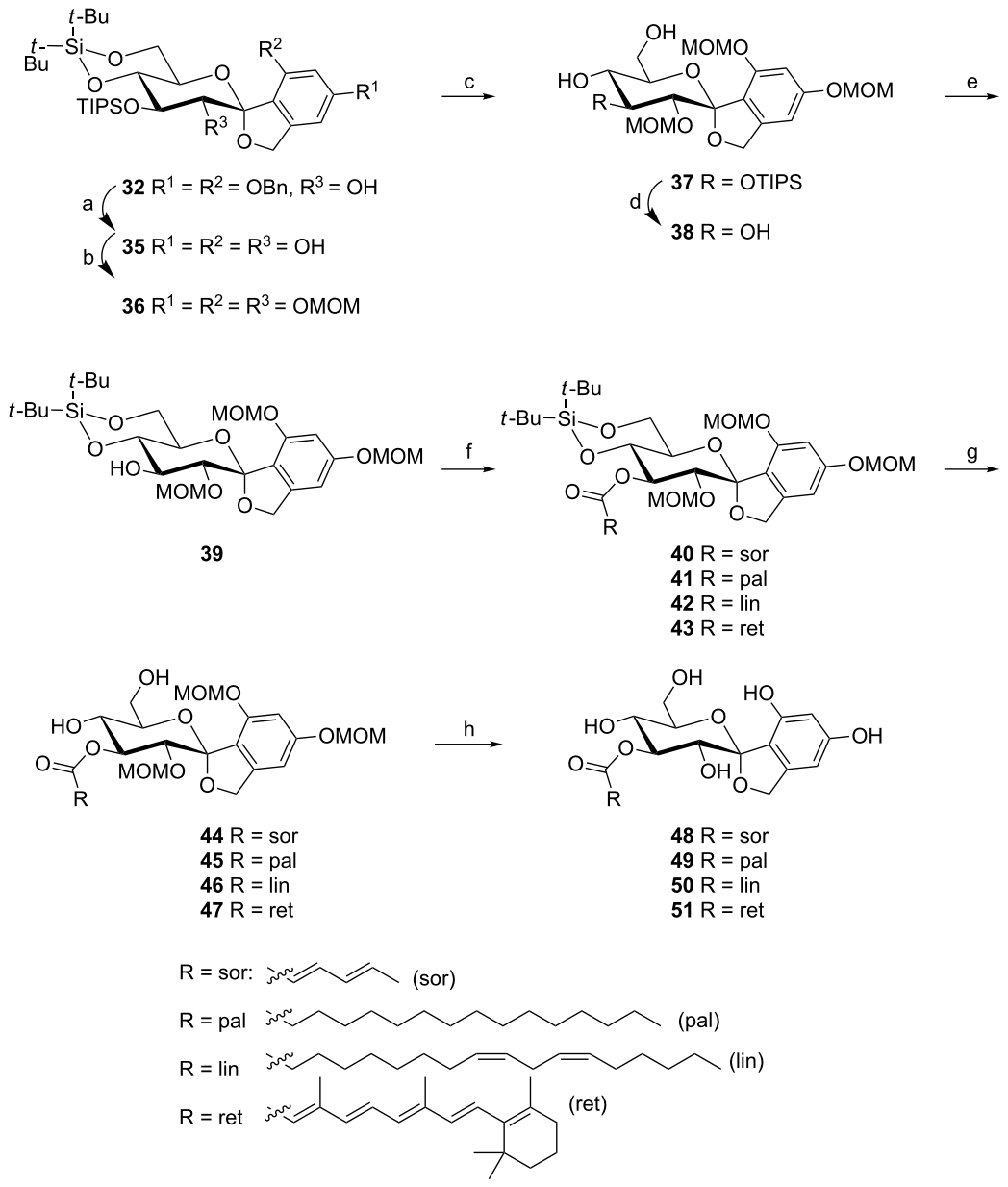

Scheme 4: (a) Pd/C, $NaHCO_3$, H_2, THF, rt, 1.5 h, 98%; (b) MOMCl, DiPEA, DMAP, CH_2Cl_2, rt, 4 d, 78%; (c) TBAHF, THF, rt, 2 d, 84%; (d) TBAF·$3H_2O$, THF, rt, 3 d; (e) *t*-$Bu_2Si(OTf)_2$, pyridine, DMF, −40°C to rt, 2 h, 84% over two steps; (f) RCOOH, NEt_3, 2,4,6-trichlorobenzoyl chloride, toluene, rt, 1 h, **39**, DMAP, toluene, rt, 3 h, **40**: 89%, **41**: quant., **42**: 92%, **43**: 90%; (g) TBAHF, THF, rt, 2–3 d, **44**: 25%, **45**: 85%, **46**: 86%, **47**: 39%; (h) Dowex 50 × 8, MeOH, 50 °C, 20 h **48**: 13%, **50**: 43%, **51**: 7% or $Sc(OTf)_3$, 1,3-propanediol, CH_3CN, 50 °C, 3 h, **49**: 9%, isolated yields after preparative HPLC and lyophilization.

vent this problem a silanol building block analogue of **22** bearing three TIPS protecting groups was also used (Supporting Information File 1).

At this stage, four commercially available side-chain acids, comprising variations in their degree of unsaturation, length and branching, were coupled: sorbic acid (sor), palmitic acid (pal), linoleic acid (lin) and *trans*-retinoic (ret) acid. Their coupling by 2,4,6-trichlorobenzoyl chloride to **39** gave the desired compounds **40**–**43** in good yields. Following this the cyclic disilyl protecting group was removed by TBAHF yielding **44**–**47**. Finally, removal of the MOM group proved to be a challenge. The use of Dowex (50 × 8) acidic resin in dry MeOH gave the most consistent results, but also the use of $Sc(OTf)_3$ in dry acetonitrile in the presence of 1,3-propanediol [49] yielded the deprotected product. The final compounds were purified by preparative HPLC. Due to some degradation during deprotection, the final yields were low. For **51** no clear NMR spectra could be obtained, possibly caused by aggregation. This was not a problem for the other three compounds.

The final products were tested for inhibition of *Candida albicans*. No inhibition was observed for the all-*trans*-retinoic acid derivative **51** and the sorbic acid derivative **48**. The MIC for the linoleic acid derivative **50** was measured as 100 μg/mL. The saturated palmitic acid derivative **49** was slightly more potent with an MIC of 88 μg/mL.

Discussion

Starting from glycal the synthesis of papulacandin D derivatives was undertaken with an initial focus on the acyl side chain, a clearly sensitive area for activity. The synthesis followed the general approach of Denmark et al. [31] with the palladium-catalyzed cross-coupling reactions of silanolates as its main feature. In our hands the reaction between glycal **18** and *t*-BuLi gave a mixture of products, possibly due to competing deprotonation of the hydrogens α to the Si in the TES group. Moving to the more substituted TIPS group at this position gave a clean reaction and allowed us to proceed, albeit with a more complicated endgame. It should be pointed out that the unplanned synthetic route eventually taken here due to the troublesome lithiation of glycal **18**, led us to compound **37**. This compound opens the way to a total synthesis of disaccharides such as the papulacandins A–C. Selective protection of the hydroxy group of C(6) followed by glycosylation of the hydroxy group at C(4), should accomplish this.

In our biological assay we did not see any activity for the sorbic acid derivative **48**, suggesting that this tail may be too short to be effective. The same was true for the retinoic acid derivative **51**, but its identity was also uncertain due to instability. Some activity was observed for linoleic acid derivative **50**, which contains two *cis* double bonds in contrast to the four *trans* double bonds of papulacandin D. The highest activity was observed for the saturated palmitic acid derivative **49**, whose tail was of the same length as the one from papulacandin D. The fact that we observed some activity with **49** is encouraging, since this was not the case for the hydrogenated form of papulacandin D [12], although that compound was able to block the target in vitro. This could be the case for the compounds described here as well, but this was not investigated. In summary, we synthesized a number of papulacandin D derivatives with differing acyl side chains. Even though the compounds were moderately active at best it is clear that the side chains are of crucial importance. The synthetic route taken will allow future variation of the aromatic core and will extend the synthesis to the more potent disaccharide papulacandins.

Supporting Information

Supporting Information File 1

Synthetic procedures, the biological assay procedure and spectral data.
[http://www.beilstein-journals.org/bjoc/content/supplementary/1860-5397-8-82-S1.pdf]

Acknowledgements

The Utrecht Institute for Pharmaceutical Sciences (UIPS) is gratefully acknowledged for support of this research.

References

1. Mathew, B. P.; Nath, M. *ChemMedChem* **2009,** *4,* 310–323. doi:10.1002/cmdc.200800353
2. Pound, M. W.; Townsend, M. L.; Dimondi, V.; Wilson, D.; Drew, R. H. *Med. Mycol.* **2011,** *49,* 561–580. doi:10.3109/13693786.2011.560197
3. Traxler, P.; Gruner, J.; Auden, J. A. L. *J. Antibiot.* **1977,** *30,* 289–296. doi:10.7164/antibiotics.30.289
4. Traxler, P.; Fritz, H.; Fuhrer, H.; Richter, W. J. *J. Antibiot.* **1980,** *33,* 967–978. doi:10.7164/antibiotics.33.967
5. Sperry, J.; Wilson, Z. E.; Rathwell, D. C. K.; Brimble, M. A. *Nat. Prod. Rep.* **2010,** *27,* 1117–1137. doi:10.1039/b911514p
6. Liu, G.; Wurst, J. M.; Tan, D. S. *Org. Lett.* **2009,** *11,* 3670–3673. doi:10.1021/ol901437f
7. Yamamoto, Y.; Yamashita, K.; Hotta, T.; Hashimoto, T.; Kikuchi, M.; Nishiyama, H. *Chem.–Asian J.* **2007,** *2,* 1388–1399. doi:10.1002/asia.200700077
8. Subrahmanyam, A. V.; Palanichamy, K.; Kaliappan, K. P. *Chem.–Eur. J.* **2010,** *16,* 8545–8556. doi:10.1002/chem.201000482
9. Baguley, B. C.; Römmele, G.; Gruner, J.; Wehrli, W. *Eur. J. Biochem.* **1979,** *97,* 345–351. doi:10.1111/j.1432-1033.1979.tb13120.x
10. Pérez, P.; Varona, R.; Garcia-Acha, I.; Duran, A. *FEBS Lett.* **1981,** *129,* 249–252. doi:10.1016/0014-5793(81)80176-7
11. Varona, R.; Pérez, P.; Durán, A. *FEMS Microbiol. Lett.* **1983,** *20,* 243–247. doi:10.1111/j.1574-6968.1983.tb00125.x

12. Römmele, G.; Traxler, P.; Wehrli, W. *J. Antibiot.* **1983,** *36,* 1539–1542. doi:10.7164/antibiotics.36.1539
13. Debono, M.; Gordee, R. S. *Annu. Rev. Microbiol.* **1994,** *48,* 471–497. doi:10.1146/annurev.mi.48.100194.002351
14. Hector, R. F.; Bierer, D. E. *Exp. Opin. Ther. Pat.* **2011,** *21,* 1597–1610. doi:10.1517/13543776.2011.603899
15. Martins, I. M.; Cortés, J. C. G.; Muñoz, J.; Belén Moreno, M.; Ramos, M.; Clemente-Ramos, J. A.; Durán, A.; Ribas, J. C. *J. Biol. Chem.* **2011,** *286,* 3484–3496. doi:10.1074/jbc.M110.174300
16. Komori, T.; Yamashita, M.; Tsurumi, Y.; Kohsaka, M. *J. Antibiot.* **1985,** *38,* 455–459. doi:10.7164/antibiotics.38.455
17. Komori, T.; Itoh, Y. *J. Antibiot.* **1985,** *38,* 544–546. doi:10.7164/antibiotics.38.544
18. VanMiddlesworth, F.; Omstead, M. N.; Schmatz, D.; Bartizal, K.; Fromtling, R.; Bills, G.; Nollstadt, K.; Honeycutt, S.; Zweerink, M.; Garrity, G.; Wilson, K. E. *J. Antibiot.* **1991,** *44,* 45–51. doi:10.7164/antibiotics.44.45
19. VanMiddlesworth, F.; Dufresne, C.; Smith, J.; Wilson, K. E. *Tetrahedron* **1991,** *47,* 7563–7568. doi:10.1016/S0040-4020(01)88280-6
20. Kaneto, R.; Chiba, H.; Agematu, H.; Shibamoto, N.; Yoshioka, T.; Nishida, H.; Okamoto, R. *J. Antibiot.* **1993,** *46,* 247–250. doi:10.7164/antibiotics.46.247
21. Chiba, H.; Kaneto, R.; Agematu, H.; Shibamoto, N.; Yoshioka, T.; Nishida, H.; Okamoto, R. *J. Antibiot.* **1993,** *46,* 356–358. doi:10.7164/antibiotics.46.356
22. Aoki, M.; Andoh, T.; Ueki, T.; Masuyoshi, S.; Sugawara, K.; Oki, T. *J. Antibiot.* **1993,** *46,* 952–960. doi:10.7164/antibiotics.46.952
23. Jackson, M.; Frost, D. J.; Karwowski, J. P.; Humphrey, P. E.; Dahod, S. K.; Choi, W. S.; Brandt, K.; Malmberg, L.-H.; Rasmussen, R. R.; Scherr, M. H.; Flamm, R. K.; Kadam, S.; McAlpine, J. B. *J. Antibiot.* **1995,** *48,* 608–613. doi:10.7164/antibiotics.48.608
24. Hochlowski, J. E.; Whittern, D. N.; Buko, A.; Alder, L.; McAlpine, J. B. *J. Antibiot.* **1995,** *48,* 614–618. doi:10.7164/antibiotics.48.614
25. Chen, R. H.; Tennant, S.; Frost, D.; O'Beirne, M. J.; Karwowski, J. P.; Humphrey, P. E.; Malmberg, L.-H.; Choi, W.; Brandt, K. D.; West, P.; Kadam, S. K.; Clement, J. J.; McAlpine, J. B. *J. Antibiot.* **1996,** *49,* 596–598. doi:10.7164/antibiotics.49.596
26. Gunawardana, G.; Rasmussen, R. R.; Scherr, M.; Frost, D.; Brandt, K. D.; Choi, W.; Jackson, M.; Karwowski, J. P.; Sunga, G.; Malmberg, L.-H.; West, P.; Chen, R. H.; Kadam, S.; Clement, J. J.; McAlpine, J. B. *J. Antibiot.* **1997,** *50,* 884–886. doi:10.7164/antibiotics.50.884
27. Gunawardana, G. P.; Frost, D.; Jackson, M.; Karwowski, J. P.; Rasmussen, R. R. Antifungal corynecandin. U.S. Patent 5,863,773, Jan 26, 1999.
28. Ohyama, T.; Iwadate-Kurihara, Y.; Hosoya, T.; Ishikawa, T.; Miyakoshi, S.; Hamano, K.; Inukai, M. *J. Antibiot.* **2002,** *55,* 758–763. doi:10.7164/antibiotics.55.758
29. Hamdouchi, C.; Sanchez-Martinez, C. *Synthesis* **2001,** 833–840. doi:10.1055/s-2001-13399
30. Barrett, A. G. M.; Peña, M.; Willardsen, J. A. *J. Org. Chem.* **1996,** *61,* 1082–1100. doi:10.1021/jo951895e
31. Denmark, S. E.; Regens, C. S.; Kobayashi, T. *J. Am. Chem. Soc.* **2007,** *129,* 2774–2776. doi:10.1021/ja070071z
32. Kobayashi, T.; Regens, C. S.; Denmark, S. E. *J. Synth. Org. Chem., Jpn.* **2008,** *66,* 616–628. doi:10.5059/yukigoseikyokaishi.66.616
33. Denmark, S. E.; Kobayashi, T.; Regens, C. S. *Tetrahedron* **2010,** *66,* 4745–4759. doi:10.1016/j.tet.2010.03.093
34. McDonald, F. E.; Zhu, H. Y. H.; Holmquist, C. R. *J. Am. Chem. Soc.* **1995,** *117,* 6605–6606. doi:10.1021/ja00129a030
35. Parker, K. A.; Georges, A. T. *Org. Lett.* **2000,** *2,* 497–499. doi:10.1021/ol991346l
36. Balachari, D.; O'Doherty, G. A. *Org. Lett.* **2000,** *2,* 863–866. doi:10.1021/ol0000253
37. Balachari, D.; O'Doherty, G. A. *Org. Lett.* **2000,** *2,* 4033–4036. doi:10.1021/ol006662a
38. Ahmed, M. M.; O'Doherty, G. A. *Tetrahedron Lett.* **2005,** *46,* 4151–4155. doi:10.1016/j.tetlet.2005.04.073
39. Danishefski, S.; Phillips, G.; Ciufolini, M. *Carbohydr. Res.* **1987,** *171,* 317–327. doi:10.1016/S0008-6215(00)90895-4
40. Rosenblum, S. B.; Bihovsky, R. *J. Am. Chem. Soc.* **1990,** *112,* 2746–2748. doi:10.1021/ja00163a042
41. Friesen, R. W.; Sturino, C. F. *J. Org. Chem.* **1990,** *55,* 2572–2574. doi:10.1021/jo00296a005
42. Friesen, R. W.; Sturino, C. F. *J. Org. Chem.* **1990,** *55,* 5808–5810. doi:10.1021/jo00310a004
43. Dubois, E.; Beau, J.-M. *J. Chem. Soc., Chem. Commun.* **1990,** 1191–1192. doi:10.1039/C39900001191
44. Dubois, E.; Beau, J.-M. *Tetrahedron Lett.* **1990,** *31,* 5165–5168. doi:10.1016/S0040-4039(00)97832-8
45. Dubois, E.; Beau, J.-M. *Carbohydr. Res.* **1992,** *223,* 157–167. doi:10.1016/0008-6215(92)80014-R
46. Schmidt, R. R.; Frick, W. *Tetrahedron* **1988,** *44,* 7163–7169. doi:10.1016/S0040-4020(01)86084-1
47. Czernecki, S.; Perlat, M. C. *J. Org. Chem.* **1991,** *56,* 6289–6292. doi:10.1021/jo00022a014
48. Denmark, S. E.; Baird, J. D. *Chem.–Eur. J.* **2006,** *12,* 4954–4963. doi:10.1002/chem.200600034
49. Oriyama, T.; Watahiki, T.; Kobayashi, Y.; Hirano, H.; Suzuki, T. *Synth. Commun.* **2001,** *31,* 2305–2311. doi:10.1081/SCC-100104830

License and Terms

Beilstein Journal of Organic Chemistry

Formation of carbohydrate-functionalised polystyrene and glass slides and their analysis by MALDI-TOF MS

Martin J. Weissenborn[1], Johannes W. Wehner[2], Christopher J. Gray[1], Robert Šardzík[1], Claire E. Eyers[*1], Thisbe K. Lindhorst[*2] and Sabine L. Flitsch[*1]

Full Research Paper

Open Access

Address:
[1]School of Chemistry & Manchester Interdisciplinary Biocentre, The University of Manchester, 131 Princess Street, Manchester, M1 7DN, United Kingdom and [2]Otto Diels Institute of Organic Chemistry, Christiana Albertina University of Kiel, Otto-Hahn-Platz 3/4, 24098 Kiel, Germany

Email:
Claire E. Eyers* - Claire.eyers@manchester.ac.uk;
Thisbe K. Lindhorst* - tklind@oc.uni-kiel.de;
Sabine L. Flitsch* - sabine.flitsch@manchester.ac.uk

* Corresponding author

Keywords:
carbohydrate array; conductive tape; MALDI-TOF MS; nonconductive surface; trityl-mediated adhesion

Beilstein J. Org. Chem. **2012,** *8,* 753–762.
doi:10.3762/bjoc.8.86

Received: 10 February 2012
Accepted: 02 May 2012
Published: 21 May 2012

This article is part of the Thematic Series "Synthesis in the glycosciences II".

Associate Editor: A. Kirschning

Abstract

Glycans functionalised with hydrophobic trityl groups were synthesised and adsorbed onto polystyrene and glass slides in an array format. The adsorbed glycans could be analysed directly on these minimally conducting surfaces by MALDI-TOF mass spectrometry analysis after aluminium tape was attached to the underside of the slides. Furthermore, the trityl group appeared to act as an internal matrix and no additional matrix was necessary for the MS analysis. Thus, trityl groups can be used as simple hydrophobic, noncovalently linked anchors for ligands on surfaces and at the same time facilitate the in situ mass spectrometric analysis of such ligands.

Introduction

Microarrays have become valuable tools in the high-throughput analysis of biological interactions and have promising applications for the development of diagnostic devices in clinical environments [1]. The initial success with DNA microarrays has prompted investigations into other biomolecular ligands, such as protein, peptide and carbohydrate arrays [2,3]. An

important aspect of this field is the immobilisation of such ligands on solid array surfaces, which can be polymers, such as polystyrene, or glass or gold, i.a. [4-7]. The challenge for immobilisations is in the efficiency of coupling and analysis of the attached ligands to ensure quality control.

Noncovalent attachment of biomolecules to hydrophobic surfaces has been used for a long time in ELISA assays and is attractive because no coupling reagents are required. However, it requires inherent hydrophobicity in the biomolecule or attachment of a hydrophobic tether. The latter has been used highly successfully by the Feizi group as part of the neoglycolipid array technology [8]. More recently, two groups [7,9] have reported the application of hydrophobic tethers for binding to polystyrene slides for glycan analysis. Initially, simple alkyl chains were used as tethers [9] but more recently, Wong and co-workers improved on this technology by using trityl-derived glycans, which are easily attached to glycans and were reported to bind strongly to polystyrene (Figure 1A) [7].

The attachment of glycans to the surface was generally confirmed indirectly by lectin binding, which severely limits the ligands that can be interrogated to those that can be detected by carbohydrate-binding proteins.

To overcome this limitation, we were interested in developing label-free methods for ligand detection on these polystyrene surfaces, and have investigated the use of matrix-assisted laser desorption/ionisation time-of-flight (MALDI-TOF) mass spectrometry (MS) analysis (Figure 1B), which has been highly successful on ligands immobilised on gold plates [10]. MALDI-TOF MS requires an electrically conducting surface and a matrix for analysis. The matrix is typically cocrystallised with the sample, which can lead to irregular surfaces, which can be a problem for reproducible analysis, especially when used in array format as a high-throughput tool. To avoid the use of such a matrix, we were interested in investigating trityl functionalisation, which has the potential for self-formation of a matrix (self-matrix) for MS analysis, at the same time as acting as a hydrophobic tether [11-13]. However, polystyrene has only minimal innate electrical conductivity and to our knowledge has never been used successfully, unmodified, as a target for MALDI-TOF MS analysis. Based on previous work one predicts that photoelectrons generated by UV laser irradiation are not dissipated by the polymeric surface. These photoelectrons distort the local electric field causing a significant loss in resolution of the analyte ions and a nonlinear shift in the mass-to-charge ratio [14].

Previous attempts to get around this issue have involved coating polymer or glass surfaces with a thin membrane of conductive material, such as gold, carbon or indium-tin oxide [15-17], or the addition of electron-accepting additives, such as methyl viologen dichloride hydrate [14]. The addition of electron-accepting additives, however, did not completely suppress the mass shifts observed during MALDI-TOF MS on low-conduc-

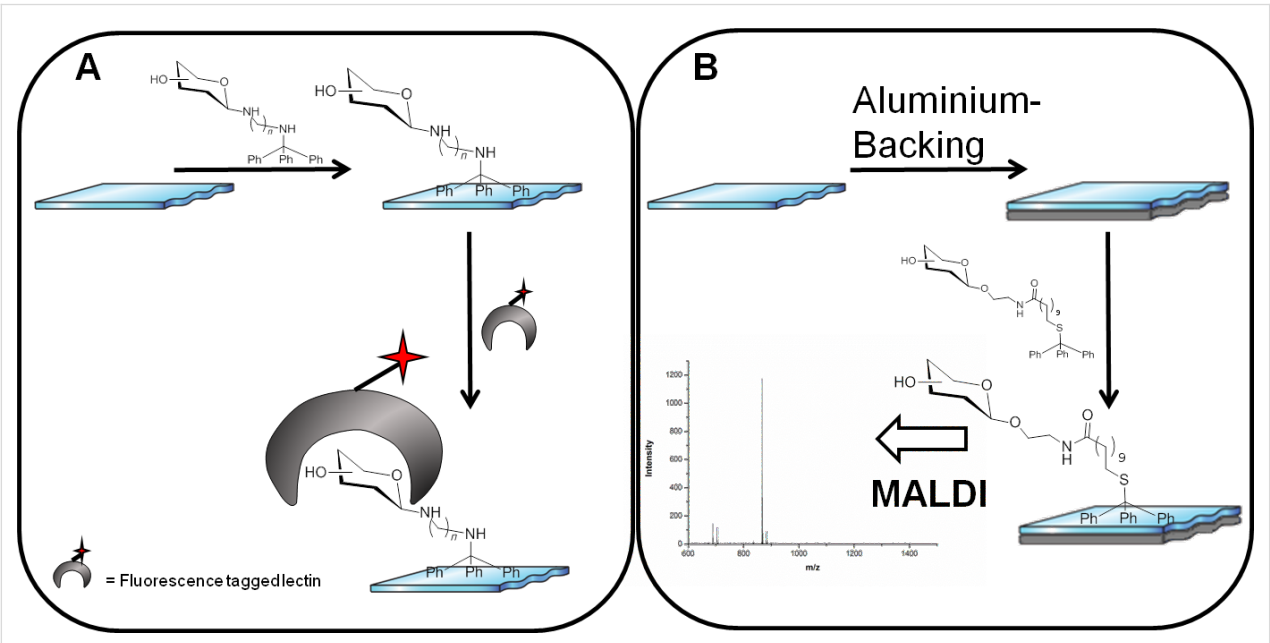

Figure 1: Carbohydrate arrays on polystyrene slides can be obtained by noncovalent immobilisation of tritylated saccharide derivatives. (A) Lectin-mediated analysis of carbohydrate arrays [7]. (B) The new concept of label-free MALDI-TOF MS analysis by aluminium-backing of polystyrene or glass slides.

tivity supports. Additionally, glass slides coated with conductive material are expensive and limited in their utility [14].

In order to address these issues, we have investigated a simple and cheap method to enable MALDI-TOF MS analysis on minimally conductive supports by applying a commercially available aluminium tape to the underside of glass and polystyrene slides. This has allowed us to make standard microscope slides suitable for MALDI-TOF MS analysis.

Results and Discussion

The hydrophobic trityl tethers chosen for our studies consisted of *S*-tritylated instead of *N*-tritylated groups, which were used previously [7]. This followed the idea of "orthogonal" surface functionalisation. Thus, a thiol group would make the tethers generally compatible with other platforms in our laboratories, such as through the formation of SAMs on gold [18] or by coupling into maleimide-functionalised surfaces in a chemoselective fashion [19].

For the initial studies two carbohydrate derivatives, **5** and **7**, were synthesised. The α-D-mannoside **5** would be useful in a bacterial adhesion inhibition assay against the bacterial lectin FimH [20,21]. The second glycoside **7** has been used previously for well-established enzymatic surface modifications [22]. Both these compounds can be synthesised by starting from commercially available 11-mercaptoundecanoic acid (**1**), which is tritylated with **2** in a straightforward synthesis, in 98% yield, following the procedure of Kovács et al. [23] (Scheme 1). The acid **3** was coupled with either of the aminoethyl glycosides **4** [24-26] or the GlcNAc derivative **6** [27], which were prepared according to literature procedures. For the coupling a combination of HBTU/DIPEA or HATU/DIPEA in dry DMF was applied yielding 74% of **5** and 71% of **7**.

The analysis of molecules on materials such as polystyrene by MALDI-TOF MS is difficult and irreproducible, largely due to their minimal electrical conductivity. To our knowledge, successful MS analysis on such surfaces has not been reported. In order to circumvent this issue, commercially available aluminium tape was applied to the underside of a polystyrene microscope slide.

The tape significantly enhanced both the signal intensity and resolution of MALDI-TOF MS analysis of the Man–Trt compound **5** (Figure 2). Furthermore, we observed that analysis of the Man–Trt compound **5** could not only be performed in the absence of any additional matrix [11,12], but under these conditions a modest increase in mass-spectrometric resolution was also observed. Such self-matrix properties are very convenient, yielding more robust and reproducible analyses, and negating the need to search for "sweet spots", as no crystal formation is required, in contrast to conventional MALDI-TOF MS analysis.

Interestingly, both Na and K cation adducts of Man–Trt **5** and its disulfide **8** were observed (Scheme 2). The relative ratios of the monomer **5** and the disulfide **8** were found to be concentration-dependent in the analysis on stainless steel (Supporting

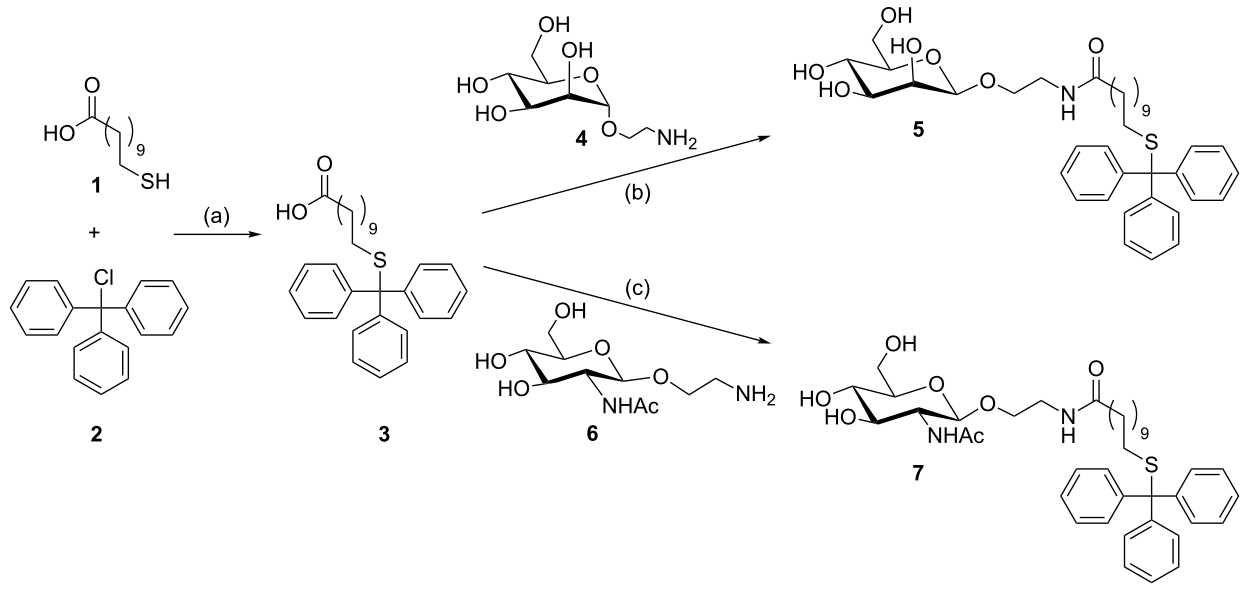

Scheme 1: Synthesis of the tritylated compounds **3** [28], **5** and **7**: (a) dichloromethane, 2.5 h, rt, 98%, (b) HBTU/DIPEA, dry DMF, overnight, rt, 74%, (c) HATU/DIPEA, dry DMF, 3 h, rt, 71%.

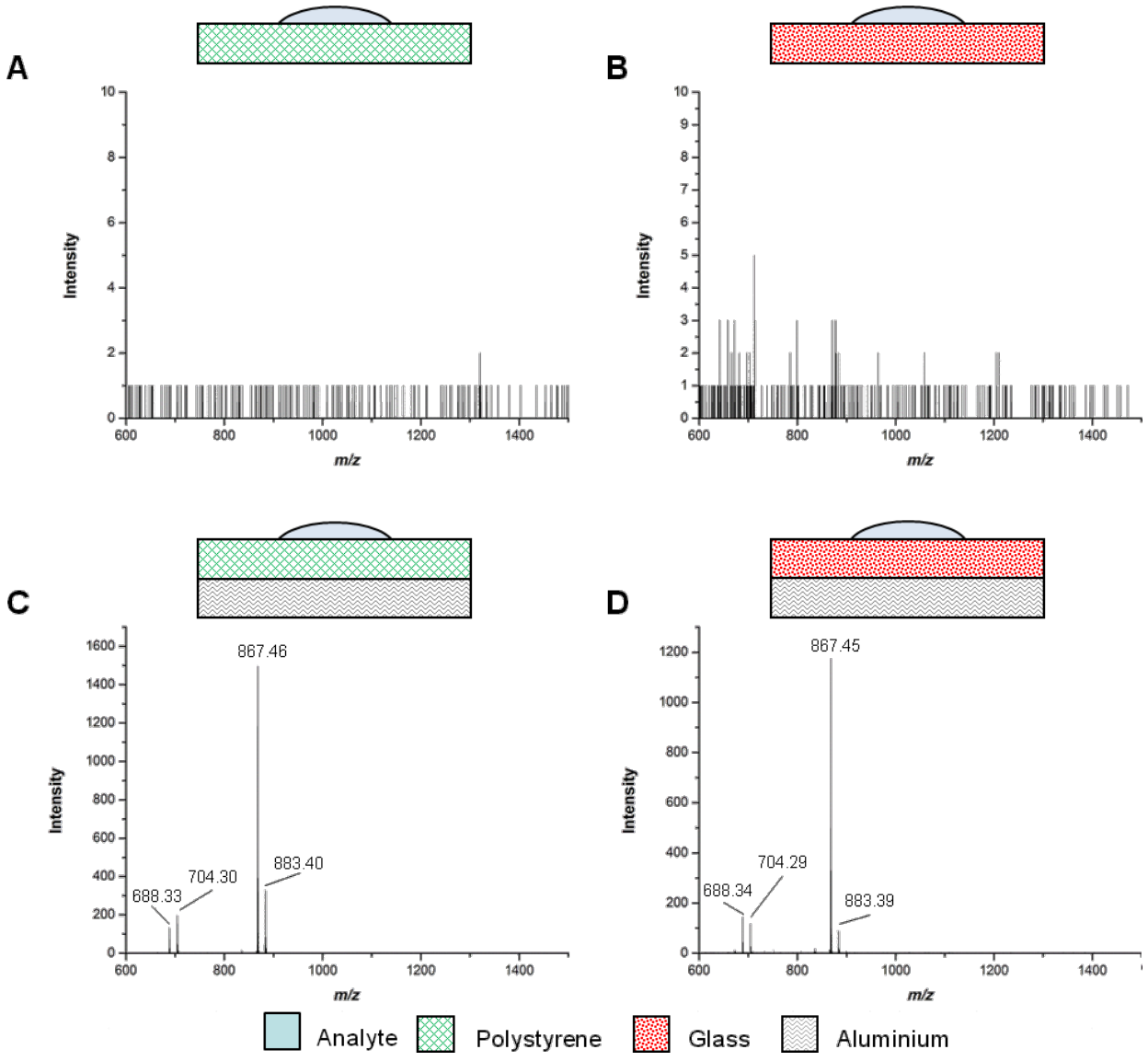

Figure 2: Comparison of the polystyrene and glass surfaces with and without aluminium backing by matrix-free MALDI-TOF MS analysis. Each spot contains 15 nmol Man–Trt (**5**): (A) polystyrene without aluminium; (B) glass without aluminium; (C) polystyrene with aluminium and (D) glass with aluminium. The peaks at *m*/*z* of 688.3, 704.3, 867.5 and 883.4 correspond to [**5** + Na]$^+$, [**5** + K]$^+$, [**8** + Na]$^+$, and [**8** + K]$^+$, respectively.

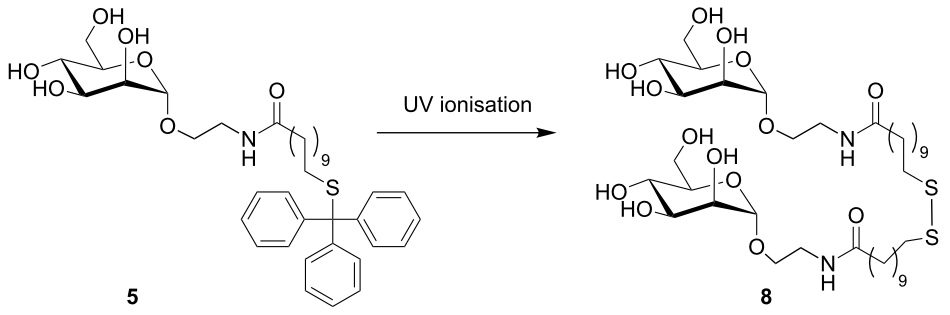

Scheme 2: The Man–Trt compound **5** forms the disulfide **8** during UV ionisation in MALDI-TOF MS analysis.

Information File 1). It was observed that at 15 nmol, almost exclusively the disulfide **8** was detected. Conversely at 50 pmol only K^+ and Na^+ adducts of Man–Trt **5** were found.

We were interested to see whether the addition of the aluminium tape would also enhance signals on surfaces other than polystyrene, and we therefore assessed the influence of the conductive tape on analysis using glass slides, which are widely used in protein-, peptide- and glycoarrays [2,29,30]. As observed with the polystyrene slides, the resolution and signal intensity of MALDI-TOF MS analysis (Figure 2) was dramatically improved following application of the aluminium tape to the back of the glass slides.

Next, the limit of detection of MS analysis of aluminium-backed polystyrene and glass slides was compared (Figure 3), using dilutions of the analyte Man–Trt **5** from 15 nmol to 50 pmol. The resolution between the two supports was compar-

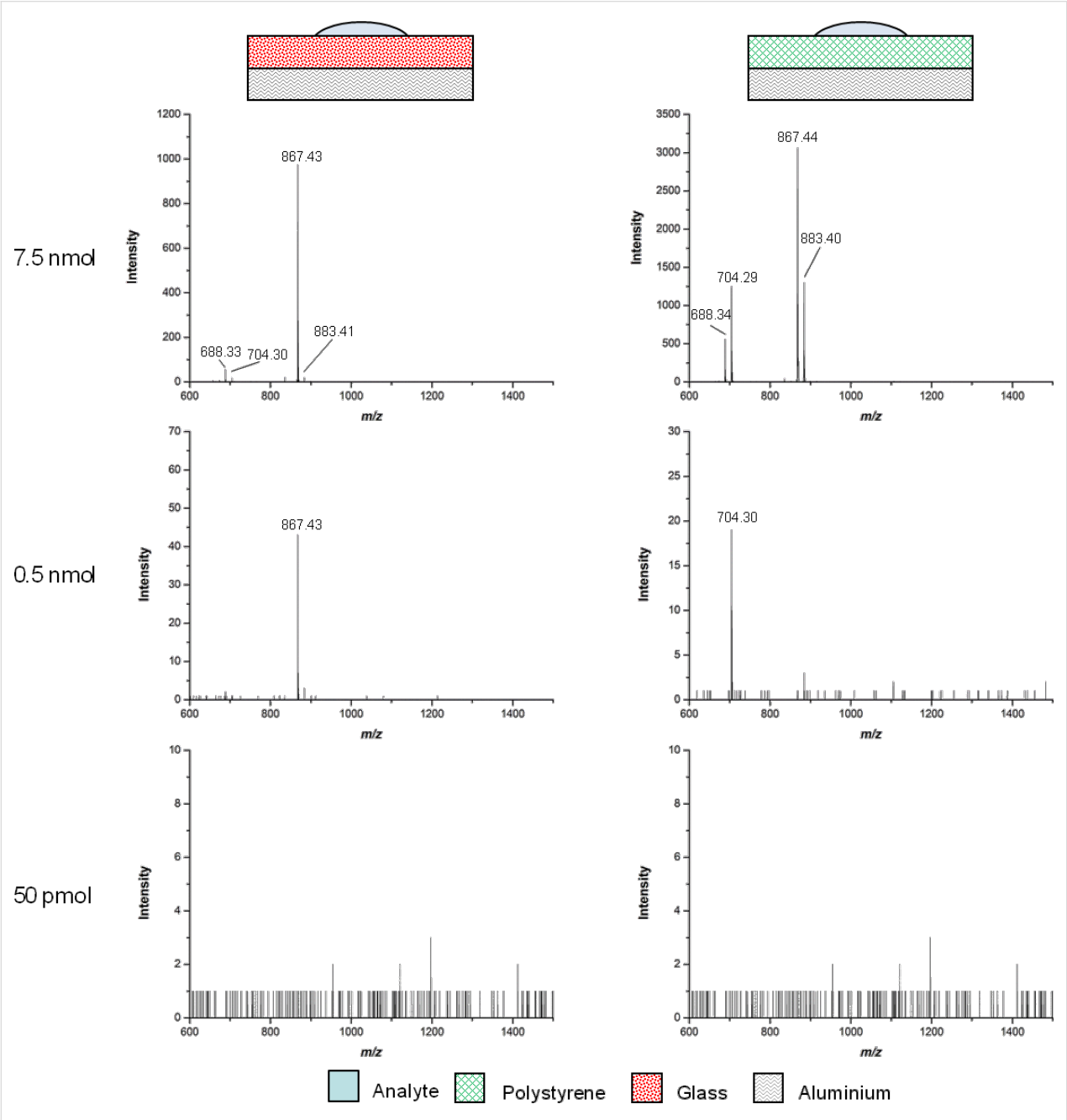

Figure 3: Limit-of-detection analysis of **5** on aluminium-backed glass and polystyrene slides. Both systems showed the MALDI-TOF MS detection limit at 0.5 nmol. The peaks at *m/z* of 688.3, 704.3, 867.4 and 883.4 correspond to [**5** + Na]$^+$, [**5** + K]$^+$, [**8** + Na]$^+$, and [**8** + K]$^+$, respectively.

able and analysis showed that Man–Trt **5** could still be detected at a concentration of 0.5 nmol for aluminium-backed polystyrene and glass slides.

After application of trityl samples, the polystyrene and glass slides were gently washed with 1 µL of water (washing procedure 1). Subsequent analysis by MALDI-TOF MS showed no noticeable change to the prewashed samples, confirming the trityl-group-mediated noncovalent adhesion of the ligands to the surfaces. On the other hand, much more rigorous washing under running distilled water (washing procedure 2) caused a significant reduction in signal on the polystyrene slide (Figure 4). Analysis of the glass slide, however, showed only a slight decrease in signal intensity even after three rigorous washes.

We were intrigued by the role of the aluminium backing and decided to investigate it in more detail. The aluminium backing was applied in three different ways: First, the entire underside of the slide was covered as in the previous experiments. Second, only a narrow strip of tape was applied to the back of the slide, making sure that the strip was in contact with the frame of the slide adapter (Figure 5). This configuration should still allow for efficient dissipation of any produced photoelectrons. Spots were analysed directly over and also next to the strip. The results showed similar intensity and resolution as for the fully aluminium-backed polystyrene slide (Supporting Information File 1, Figures S2 and S3). Third, only a small aluminium rectangle was attached to the back of the polystyrene slide, this time making sure that there was no electrical contact to the slide

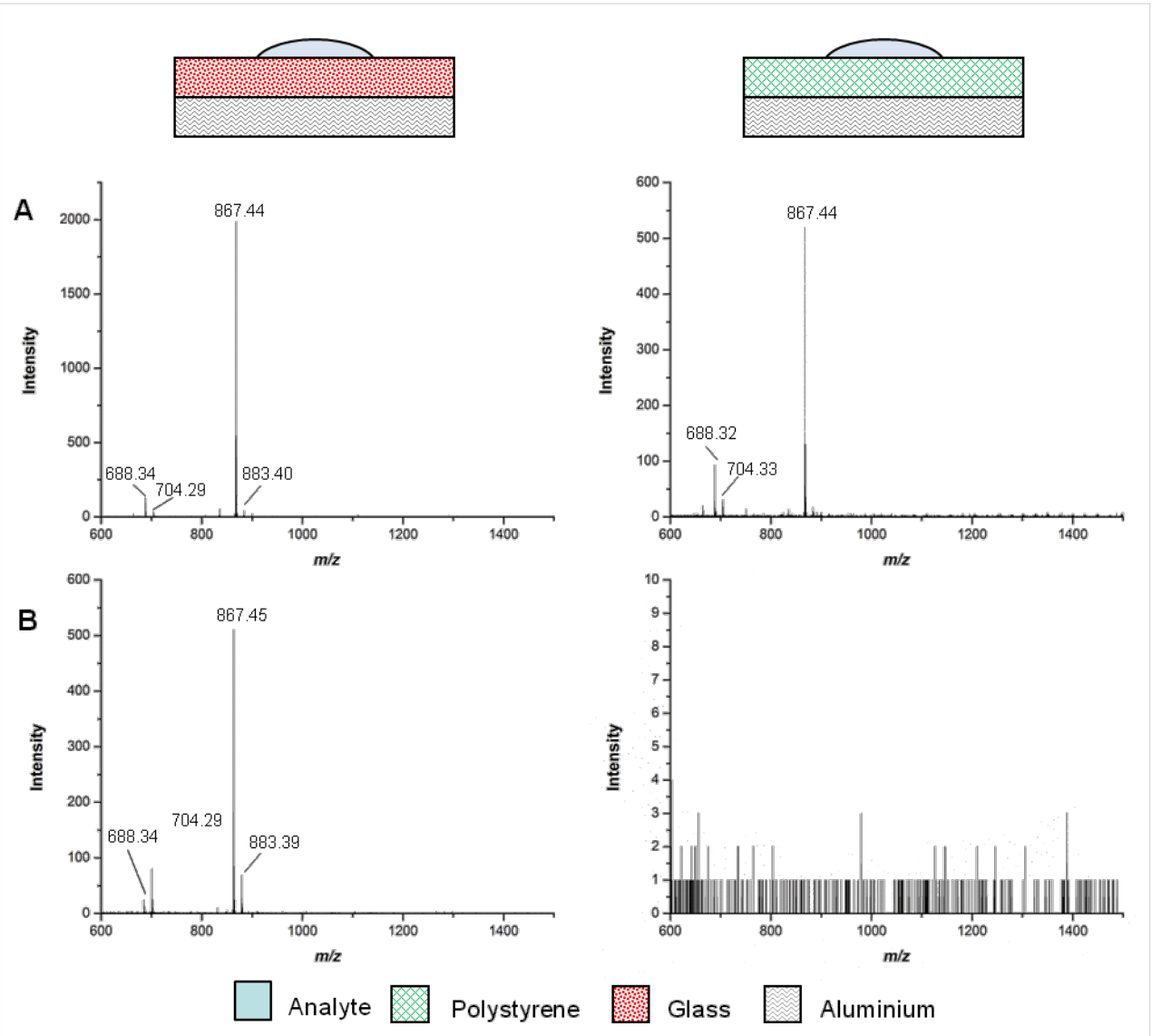

Figure 4: Comparison of MALDI-TOF MS spectra on the aluminium-backed polystyrene and glass slides after washing. (**A**) At 7.5 nmol following washing procedure 1 and (**B**) at 15 nmol following washing procedure 2.

frame (Supporting Information File 1, Figures S4 and S5). In this last case very poor signals, both in resolution and intensity, were observed, which were analogous to the non-aluminium-backed polystyrene slide. Thus, contact of the tape to the slide adapter frame appears to be essential for good signal intensity, but it is not necessary to cover the slide fully.

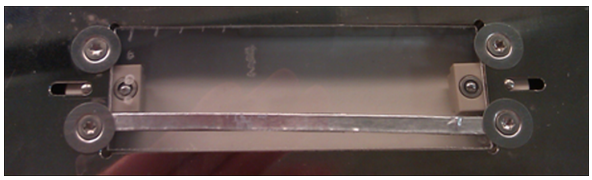

Figure 5: Photo of the aluminium strip on the back of the polystyrene support.

Given that the MS analysis on the polystyrene was successful, we attempted an enzymatic galactosylation of GlcNAc–Trt **7** using bovine β-(1→4)-galactosyltransferase (β-(1→4)-GalT, EC 2.4.1.38) on the polystyrene slides. This enzymatic transformation has proven to be a very reproducible and robust reaction, which appears to proceed to completion on gold arrays [31] and is routinely performed in our laboratory. After treatment of slides containing GlcNAc–Trt **7** with the enzyme by using previously reported procedures [31], followed by washing procedure 1, neither product nor starting material could be observed by MALDI-TOF MS analysis. In fluorescence-assisted studies this problem is mostly overcome by blocking with nonfluorescent milk proteins or BSA; however, in MALDI-TOF MS analysis the blocking proteins would also be ionised and consequently quench the signal [32].

Conclusion

Successful MALDI-TOF MS analysis on minimally conductive surfaces was achieved by application of aluminium tape. Polystyrene and glass surfaces were spotted with the analyte Man–Trt **5** and were analysed over a range of concentrations and after washing. This new technique enables the direct analysis of any noncovalent glycoarray on glass and polystyrene. So far, our attempts to study enzymatic reactions on the modified polystyrene surface have been unsuccessful and will require further investigation.

Experimental

General experimental section for the saccharide synthesis

Commercially available starting materials and reagents were used without further purification. Reactions requiring dry conditions were performed under an atmosphere of nitrogen. Anhydrous DMF was purchased.

2-Aminoethyl α-D-mannopyranoside (**4**) [24-26] and 2-aminoethyl 2-acetamido-2-deoxy-β-D-glucopyranoside (**6**) [27] were prepared according to the literature. Reactions were monitored by thin-layer chromatography using silica gel 60 GF_{254} on aluminium foil (Merck) with detection by UV light and charring with sulfuric acid in EtOH (10%). Preparative MPLC was performed on a Büchi apparatus using a LiChroprep Si 60 (40–60 mm, Merck) column for normal-phase silica-gel chromatography. Analytical HPLC was performed on a Merck Hitachi LaChrom L-7000 series apparatus with a LiChrospher 100 RP-8 (5 µm, Merck) column. ^{1}H and ^{13}C NMR spectra were recorded on a Bruker DRX-500 spectrometer. NMR spectra were calibrated with respect to the solvent peak. 2D NMR techniques (COSY, HSQC, HMBC) were used for full assignment of the spectra. ESI-MS measurements were performed on a Mariner ESI-TOF 5280 instrument (Applied Biosystems). High-resolution mass spectra (HRMS) were obtained with the Waters Micromass LCT-TOF mass spectrometer. MALDI-TOF mass spectra were recorded on a Bruker Biflex-III 19 kV instrument with Cl-CCA (4-chloro-α-cyanocinnamic acid) or DHB (2,5-dihydroxybenzoic acid) as matrix. Optical rotation was measured on a Perkin-Elmer polarimeter 341 (Na-D-line: 589 nm, length of cell 1 dm). IR spectra were recorded on a Perkin-Elmer Paragon 1000 FTIR spectrometer. For sample preparation a Golden Gate diamond ATR unit with a sapphire stamp was used.

11-Tritylsulfanylundecanoic acid (**3**) [28]

Chlorotriphenylmethane (**2**, 2.53 g, 9.07 mmol) was dissolved in dichloromethane. 11-Mercaptoundecanoic acid (**1**, 2.00 g, 9.15 mmol) dissolved in dichloromethane (60 mL) was added dropwise over 1 h. The reaction mixture was stirred for 1.5 h at ambient temperature until TLC (cyclohexane/ethyl acetate 3:1) indicated no further conversion. The reaction mixture was washed with H_2O (50 mL), the organic layer was dried over $MgSO_4$, and the solvent was removed under reduced pressure. The crude product was purified by MPLC (100 g silica column, A: cyclohexane, B: ethyl acetate, A: 90% → 40%, 120 min) yielding **3** (4.10 g, 8.90 mmol, 98%) as a colourless solid.

R_f 0.61 (methanol/dichloromethane 3:18); mp 80–82 °C; HPLC t_R 7.31 min (A = water, B = methanol, A: 20%, 10 min, 1.2 mL/min); ^{1}H NMR (500 MHz, CD_3OD, 300 K) δ 7.38 (m_c, 6H, $H_{aryl,Trt}$), 7.25 (m_c, 6H, $H_{aryl,Trt}$), 7.19 (m_c, 3H, $H_{aryl,Trt}$), 2.18 (t, ^3J = 7.6 Hz, 2H, HO(O)CCH_2CH$_2$), 2.11 (t, ^3J = 7.4 Hz, 2H, CH_2STrt), 1.59 (q, ^3J = 7.9 Hz, ^3J = 7.0 Hz, 2H, HO(O)CCH$_2CH_2$), 1.37–1.09 (m, 14H, CH$_2CH_2$CH$_2$) ppm; ^{13}C NMR (125 MHz, CD_3OD, 300 K) δ 179.3 (*C*(O)OH), 146.5 (3 $C_{aryl,Trt}$), 130.8 (6 $CH_{aryl,Trt}$), 128.8 (6 $CH_{aryl,Trt}$), 127.6 (3 $CH_{aryl,Trt}$), 67.6 ($C_{quart,Trt}$), 36.5 (HO(O)CCH_2CH$_2$), 32.9 (CH_2STrt), 30.5, 30.4, 30.4, 30.3, 30.1, 30.0, 29.7 (7

$CH_2CH_2CH_2$), 26.9 (HN(O)CCH$_2$$CH_2$) ppm; MALDI-TOF MS (DHB) *m/z*: 483.13 $[M + Na]^+$, 499.10 $[M + K]^+$; HRMS–ESI (*m/z*): $[M + Na]^+$ calcd for $C_{30}H_{36}NNaO_2S$, 483.2328; found, 483.2343; IR (ATR–IR) ṽ: 3384, 3189, 3056, 2923, 2850, 1651, 1594, 1489, 1444, 1419, 1032, 770, 740, 695, 674, 621 cm^{-1}.

2-((11-Tritylsulfanylundecanoyl)amino)ethyl α-D-mannopyranoside (**5**)

11-Tritylsulfanylundecanoic acid (**3**, 750 mg, 1.63 mmol) and HBTU (743 mg, 1.96 mmol) were dried for 2 h under vacuum, and then dry DMF (5 mL) and DIPEA (400 µL, 2.33 mmol) were added, and the mixture was stirred for 20 min under a nitrogen atmosphere at ambient temperature. Simultaneously, in a different reaction vessel aminoethyl mannoside **4** (438 mg, 1.96 mmol) was dried for 2 h under vacuum, and then dissolved in dry DMF (5 mL), and DIPEA (160 µL, 931 µmol) was added. The mixture was stirred for 20 min under a nitrogen atmosphere at ambient temperature. The reaction mixture with the preactivated 11-tritylsulfanylundecanoic acid (**3**) was cooled to 0 °C, the solution of mannoside **4** was added and the resulting mixture was stirred under a nitrogen atmosphere at ambient temperature overnight. All volatile compounds were removed under reduced pressure and the crude product was subjected to MPLC (150 g silica column, A: dichloromethane, B: methanol, A: 99% → 90%, 120 min) and another round of MPLC (125 g silica column, A: ethyl acetate, B: methanol, A: 99% → 90%, 120 min) yielding **5** (808 mg, 1.21 mmol, 74%) as a colourless foam.

R_f 0.16 (methanol/dichloromethane, 1:9); HPLC t_R = 5.49 min (A = water, B = methanol, A: 20%, 10 min, 1.2 mL/min); $[\alpha]_D^{20}$ +23.7 (*c* 0.5, MeOH); ^{1}H NMR (500 MHz, CD_3OD, 300 K) δ 7.38 (m_c, 6H, $H_{aryl,Trt}$), 7.27 (m_c, 6H, $H_{aryl,Trt}$), 7.20 (dt, ^3J = 7.3 Hz, ^4J = 1.3 Hz, 3H, $H_{aryl,Trt}$), 4.76 (d, ^3J = 1.7 Hz, 1H, H1$_{Man}$), 3.83 (dd, ^2J = 11.6 Hz, ^3J = 2.3 Hz, 1H, H6a$_{Man}$), 3.80 (dd, ^3J = 1.7 Hz, ^3J = 3.3 Hz, 1H, H2$_{Man}$), 3.77–3.67 (m, 3H, O*CH*HCH$_2$NH, H3$_{Man}$, H6b$_{Man}$), 3.60 (dd~t, ^3J = 9.5 Hz, 1H, H4$_{Man}$), 3.56–3.50 (m, 2H, H5$_{Man}$, OCH*H*CH$_2$NH), 3.41 (ddd, ^2J = 14.0 Hz, ^3J = 6.3 Hz, ^3J = 4.6 Hz, 1H, OCH$_2$C*H*HNH), 3.35 (ddd, ^2J = 14.0 Hz, ^3J = 6.7 Hz, ^3J = 4.7 Hz, 1H, OCH$_2$CH*H*NH), 2.19 (t, ^3J = 7.6 Hz, 2H, HN(O)CCH_2CH$_2$), 2.12 (t, ^3J = 7.4 Hz, 2H, CH_2STrt), 1.59 (q, ^3J = 7.6 Hz, ^3J = 7.3 Hz, 2H, HN(O)CCH$_2$$CH_2$), 1.38–1.10 (m, 14H, 7 CH$_2$$CH_2CH_2$) ppm; ^{13}C NMR (125 MHz, CD_3OD, 300 K) δ 176.5 (*C*(O)NH), 146.5 (3 $C_{aryl,Trt}$), 130.8 (6 $CH_{aryl,Trt}$), 128.8 (6 $CH_{aryl,Trt}$), 127.7 (3 $CH_{aryl,Trt}$), 101.7 (C1$_{Man}$), 74.8 (C5$_{Man}$), 72.6 (C3$_{Man}$), 72.1 (C2$_{Man}$), 68.6 (C4$_{Man}$), 67.3 ($C_{quart,Trt}$), 67.3 (OCH_2CH$_2$NH), 62.9 (C6$_{Man}$), 40.2 (OCH$_2$$CH_2$NH), 37.1 (HN(O)C$CH_2CH_2$), 32.9 ($CH_2$STrt), 30.5, 30.4, 30.4, 30.3, 30.1, 30.0, 29.7 (7 CH$_2$$CH_2CH_2$), 27.0 (HN(O)CCH$_2$$CH_2$) ppm; MALDI-TOF MS (DHB) *m/z*: 688.11 $[M + Na]^+$, 704.08 $[M + K]^+$; HRMS–ESI (*m/z*): $[M + Na]^+$ calcd for $C_{40}H_{54}N_2NaO_7S$, 729.3544; found, 729.3506; IR (ATR–IR) ṽ: 3293, 2923, 2852, 1645, 1548, 1488, 1443, 1253, 1132, 1057, 1031, 975, 810, 741, 697, 676, 616 cm^{-1}.

2-((11-Tritylsulfanylundecanoyl)amino)ethyl 2-acetamido-2-deoxy-β-D-glucopyranoside (**7**)

11-Tritylsulfanylundecanoic acid (**3**, 18.2 mg, 39.5 µmol) and HATU (30.0 mg, 79.0 µmol) were dried for 1 h under vacuum. Then, dry DMF (2 mL) and DIPEA (7.00 µL, 40.9 µmol) were added, and the mixture was stirred for 20 min under a nitrogen atmosphere at ambient temperature. Simultaneously, in a different reaction vessel 2-aminoethyl 2-acetamido-2-deoxy-β-D-glucopyranoside (**6**, 11.5 mg, 43.5 µmol) was dried for 1 h under vacuum and dissolved in dry DMF (1 mL), and then DIPEA (7.00 µL, 40.9 µmol) was added. The mixture was stirred for 20 min under a nitrogen atmosphere at ambient temperature. The solution of **6** in dry DMF was added to the preactivated 11-tritylsulfanylundecanoic acid (**3**) and it was stirred under a nitrogen atmosphere at ambient temperature for 3 h. All volatile compounds were removed under reduced pressure and the crude product was subjected to MPLC (50 g silica column, A: dichloromethane, B: methanol, A: 99% → 85%, 180 min) yielding **7** (19.7 mg, 27.9 µmol, 71%) as a colourless lyophylisate.

R_f 0.21 (methanol/dichloromethane, 3:18); HPLC t_R 5.44 min (A = water, B = methanol, A: 20%, 10 min, 1.2 mL/min); $[\alpha]_D^{20}$ −1.6 (*c* 0.1, methanol); ^{1}H NMR (500 MHz, CD_3OD, 300 K) δ 7.39 (m_c, 6H, $H_{aryl,Trt}$), 7.28 (m_c, 6H, $H_{aryl,Trt}$), 7.21 (m_c, 3H, $H_{aryl,Trt}$), 4.39 (d, ^3J = 8.4 Hz, 1H, H1$_{GlcNAc}$), 3.88 (dd, ^2J = 11.8 Hz, ^3J = 2.2 Hz, 1H, H6a$_{GlcNAc}$), 3.82 (ddd, ^2J = 10.6 Hz, ^3J = 6.7 Hz, ^3J = 4.5 Hz, 1H, O*CH*HCH$_2$NH), 3.67 (dd, ^2J = 11.8 Hz, ^3J = 5.8 Hz, 1H, H6b$_{GlcNAc}$), 3.67–3.59 (m, 2H, H2$_{GlcNAc}$, OCH*H*CH$_2$NH), 3.43 (dd, ^3J = 10.4 Hz, ^3J = 8.3 Hz, 1H, H3$_{GlcNAc}$), 3.40–3.36 (m, 1H, OCH$_2$*CH*HNH), 3.40–3.26 (m, 3H, OCH$_2$CH*H*NH, H4$_{GlcNAc}$, H5$_{GlcNAc}$), 2.18 (t, ^3J = 7.6 Hz, 2H, HN(O)CCH_2CH$_2$), 2.12 (t, ^3J = 7.4 Hz, 2H, CH_2STrt), 1.98 (s, 3H, NHAc), 1.59 (m, 2H, HN(O)CCH$_2$$CH_2$), 1.38–1.10 (m, 14H, 7 CH$_2$$CH_2CH_2$) ppm; ^{13}C NMR (125 MHz, CD_3OD, 300 K) δ 176.4 (HN*C*(O)CH$_2$), 173.9 (HN*C*(O)CH$_3$), 146.5 (3 $C_{aryl,Trt}$), 130.8 (6 $CH_{aryl,Trt}$), 128.8 (6 $CH_{aryl,Trt}$), 127.7 (3 $CH_{aryl,Trt}$), 102.9 (C1$_{GlcNAc}$), 78.0 (C5$_{GlcNAc}$), 76.1 (C3$_{GlcNAc}$), 72.1 (C4$_{GlcNAc}$), 69.2 (OCH_2CH$_2$NH), 67.3 ($C_{quart,Trt}$), 62.8 (C6$_{GlcNAc}$), 57.3 (C2$_{GlcNAc}$), 40.6 (OCH$_2$$CH_2$NH), 37.1 (HN(O)C$CH_2CH_2$), 32.9 ($CH_2$STrt), 30.5, 30.4, 30.4, 30.3, 30.1, 30.0, 29.7 (7 CH$_2$$CH_2CH_2$), 27.0 (HN(O)CCH$_2$$CH_2$), 23.0 (HNC(O)$CH_3$) ppm; MALDI-TOF MS (DHB) *m/z*: 729.48 $[M + Na]^+$, 745.45 $[M + K]^+$; HRMS–ESI (*m/z*): $[M + Na]^+$ calcd for

$C_{40}H_{54}N_2NaO_7S$, 729.3544; found, 729.350; IR (ATR–IR) ṽ: 3270, 2924, 2852, 1640, 1549, 1488, 1443, 1373, 1156, 1109, 1080, 1033, 896, 742, 698, 616 cm^{-1}.

Array washing

Washing procedure 1

Distilled water (1 μL) was spotted over the dried analyte spot and was subsequently drawn back up with the pipette. This was repeated three times. The slides were then allowed to dry under atmospheric conditions.

Washing procedure 2

The MALDI target slide was washed with cool distilled water (making sure the spot was not directly under the tap) for 6 s at a flow rate of 3 L/min and then dried under a stream of nitrogen.

MALDI-TOF MS analysis of tritylated compounds

Unless otherwise stated all MALDI-TOF MS experiments were carried out on an Ultraflex II instrument (Bruker Daltonics, USA) in positive reflectron mode in the absence of a matrix. Spectra were acquired over the mass range 600–2500 *m*/*z* with 500 shots (57% laser energy) per spectrum and a laser firing rate of 200 Hz. Data were processed and analysed with FlexAnalysis software (Bruker Daltonics, USA) by using the default integration settings. Smoothing and baseline subtraction was performed on each spectrum by using the default settings in FlexAnalysis. Calibration was either performed before the analysis on the Ultraflex II instrument or afterwards in FlexAnalysis by using Man–Trt **5** as an internal calibrant for polystyrene and glass slides and a tryptic digest of Qcal protein as the calibrant for the steel target [33].

Polystyrene slides were manufactured by Goodfellows, U.K., and standard glass microscope slides, purchased from Yancheng Huida Medical Instruments Co., China, were used. Conductive aluminium tape was purchased from Farnell, U.K., and attached to the back of the nonconductive polystyrene and glass slides. The slides were mounted on to MTP Slide-Adapter II (Bruker) for analysis. Tritylated sugar in methanol (0.5 μL) was applied to the surface and the solvent was allowed to evaporate under atmospheric conditions. Unless otherwise stated, the spots were washed by following procedure 1.

Supporting Information

Supporting Information File 1

Enzyme expression and MALDI MS spectra.
[http://www.beilstein-journals.org/bjoc/content/supplementary/1860-5397-8-86-S1.pdf]

Acknowledgements

We thank Dr Stephan Mohr and Dr Jeremy Hawkes for providing us with the polystyrene slides; and Dr Niels-Christian Reichardt, Javier Calvo Martinez, Dr Sonia Serna and Dr Antonio Sanchez-Ruiz for help with the initial MALDI-TOF MS analysis. This work was supported by the Royal Society (Wolfson Award to SLF) and the European Commission's Seventh Framework Programme (FP7), which funded the EuroGlycoArrays ITN (MJW) and GlycoBioM (RS, SLF, CEE). JWW was supported by the Evonik Foundation and CJG by a BBSRC-funded doctoral training award.

References

1. Cao, B.; Li, R.; Xiong, S.; Yao, F.; Liu, X.; Wang, M.; Feng, L.; Wang, L. *Appl. Environ. Microbiol.* **2011,** *77,* 8219–8225. doi:10.1128/AEM.05914-11
2. Berrade, L.; Garcia, A. E.; Camarero, J. A. *Pharm. Res.* **2011,** *28,* 1480–1499. doi:10.1007/s11095-010-0325-1
3. Blixt, O.; Head, S.; Mondala, T.; Scanlan, C.; Huflejt, M. E.; Alvarez, R.; Bryan, M. C.; Fazio, F.; Calarese, D.; Stevens, J.; Razi, N.; Stevens, D. J.; Skehel, J. J.; van Die, I.; Burton, D. R.; Wilson, I. A.; Cummings, R.; Bovin, N.; Wong, C.-H.; Paulson, J. C. *Proc. Natl. Acad. Sci. U. S. A.* **2004,** *101,* 17033–17038. doi:10.1073/pnas.0407902101
4. Weissenborn, M. J.; Castangia, R.; Wehner, J. W.; Šardzík, R.; Lindhorst, T. K.; Flitsch, S. L. *Chem. Commun.* **2012,** *48,* 4444–4446. doi:10.1039/c2cc30844d
5. Serna, S.; Yan, S.; Martin-Lomas, M.; Wilson, I. B. H.; Reichardt, N.-C. *J. Am. Chem. Soc.* **2011,** *133,* 16495–16502. doi:10.1021/ja205392z
6. Voglmeir, J.; Šardzík, R.; Weissenborn, M. J.; Flitsch, S. L. *OMICS* **2010,** *14,* 437–444. doi:10.1089/omi.2010.0035
7. Zou, L.; Pang, H.-L.; Chan, P.-H.; Huang, Z.-S.; Gu, L.-Q.; Wong, K.-Y. *Carbohydr. Res.* **2008,** *343,* 2932–2938. doi:10.1016/j.carres.2008.08.021
8. Fukui, S.; Feizi, T.; Galustian, C.; Lawson, A. M.; Chai, W. *Nat. Biotechnol.* **2002,** *20,* 1011–1017. doi:10.1038/nbt735
9. Bryan, M. C.; Plettenburg, O.; Sears, P.; Wong, C.-H. *Abstr. Pap. - Am. Chem. Soc.* **2002,** *224,* U181.
10. Šardzík, R.; Green, A. P.; Laurent, N.; Both, P.; Fontana, C.; Voglmeir, J.; Weissenborn, M. J.; Haddoub, R.; Grassi, P.; Haslam, S. M.; Widmalm, G.; Flitsch, S. L. *J. Am. Chem. Soc.* **2012,** *134,* 4521–4524. doi:10.1021/ja211861m
11. Thiery, G.; Shchepinov, M. S.; Southern, E. M.; Audebourg, A.; Audard, V.; Terris, B.; Gut, I. G. *Rapid Commun. Mass Spectrom.* **2007,** *21,* 823–829. doi:10.1002/rcm.2895
12. Ustinov, A. V.; Shmanai, V. V.; Patel, K.; Stepanova, I. A.; Prokhorenko, I. A.; Astakhova, I. V.; Malakhov, A. D.; Skorobogatyi, M. V.; Bernad, P. L.; Khan, S.; Shahgholi, M.; Southern, E. M.; Korshun, V. A.; Shchepinov, M. S. *Org. Biomol. Chem.* **2008,** *6,* 4593–4608. doi:10.1039/b810600b
13. Aumüller, I.; Lindhorst, T. K. *Eur. J. Org. Chem.* **2006,** 1103–1108. doi:10.1002/ejoc.200500900
14. Ibáñez, A. J.; Muck, A.; Svatoš, A. *J. Mass Spectrom.* **2007,** *42,* 634–640. doi:10.1002/jms.1192
15. Altelaar, A. F. M.; van Minnen, J.; Jiménez, C. R.; Heeren, R. M. A.; Piersma, S. R. *Anal. Chem.* **2005,** *77,* 735–741. doi:10.1021/ac048329g

16. Scherl, A.; Zimmermann-Ivol, C. G.; Di Dio, J.; Vaezzadeh, A. R.; Binz, P.-A.; Amez-Droz, M.; Cochard, R.; Sanchez, J.-C.; Glückmann, M.; Hochstrasser, D. F. *Rapid Commun. Mass Spectrom.* **2005,** *19,* 605–610. doi:10.1002/rcm.1831
17. Li, X.; Wilm, M.; Franz, T. *Proteomics* **2005,** *5,* 1460–1471. doi:10.1002/pmic.200401023
18. Laurent, N.; Haddoub, R.; Voglmeir, J.; Wong, S. C. C.; Gaskell, S. J.; Flitsch, S. L. *ChemBioChem* **2008,** *9,* 2592–2596. doi:10.1002/cbic.200800481
19. Houseman, B. T.; Gawalt, E. S.; Mrksich, M. *Langmuir* **2003,** *19,* 1522–1531. doi:10.1021/la0262304
20. Hartmann, M.; Lindhorst, T. K. *Eur. J. Org. Chem.* **2011,** 3583–3609. doi:10.1002/ejoc.201100407
21. Hartmann, M.; Horst, A. K.; Klemm, P.; Lindhorst, T. K. *Chem. Commun.* **2010,** *46,* 330–332. doi:10.1039/b922525k
22. Laurent, N.; Voglmeir, J.; Flitsch, S. L. *Chem. Commun.* **2008,** 4400–4412. doi:10.1039/b806983m
23. Kupihár, Z.; Schmél, Z.; Kovács, L. *Molecules* **2000,** *5,* M144–U3. doi:10.3390/M144
24. Kleinert, M.; Röckendorf, N.; Lindhorst, T. K. *Eur. J. Org. Chem.* **2004,** 3931–3940. doi:10.1002/ejoc.200400239
25. Lindhorst, T. K.; Kötter, S.; Krallmann-Wenzel, U.; Ehlers, S. *J. Chem. Soc., Perkin Trans. 1* **2001,** 823–831. doi:10.1039/B009786L
26. Dahmén, J.; Frejd, T.; Grönberg, G.; Lave, T.; Magnusson, G.; Noori, G. *Carbohydr. Res.* **1983,** *116,* 303–307. doi:10.1016/0008-6215(83)88120-8
27. Šardzík, R.; Noble, G. T.; Weissenborn, M. J.; Martin, A.; Webb, S. J.; Flitsch, S. L. *Beilstein J. Org. Chem.* **2010,** *6,* 699–703. doi:10.3762/bjoc.6.81
28. Ryan, D.; Parviz, B. A.; Linder, V.; Semetey, V.; Sia, S. K.; Su, J.; Mrksich, M.; Whitesides, G. M. *Langmuir* **2004,** *20,* 9080–9088. doi:10.1021/la048443u
29. MacBeath, G.; Schreiber, S. L. *Science* **2000,** *289,* 1760–1763.
30. Weinrich, D.; Jonkheijm, P.; Niemeyer, C. M.; Waldmann, H. *Angew. Chem., Int. Ed.* **2009,** *48,* 7744–7751. doi:10.1002/anie.200901480
31. Šardzík, R.; Sharma, R.; Kaloo, S.; Voglmeir, J.; Crocker, P. R.; Flitsch, S. L. *Chem. Commun.* **2011,** *47,* 5425–5427. doi:10.1039/c1cc10745c
32. Deere, J.; McConnell, G.; Lalaouni, A.; Maltman, B. A.; Flitsch, S. L.; Halling, P. J. *Adv. Synth. Catal.* **2007,** *349,* 1321–1326. doi:10.1002/adsc.200700044
33. Eyers, C. E.; Simpson, D. M.; Wong, S. C. C.; Beynon, R. J.; Gaskell, S. J. *J. Am. Soc. Mass Spectrom.* **2008,** *19,* 1275–1280. doi:10.1016/j.jasms.2008.05.019

License and Terms

Beilstein Journal of Organic Chemistry

Triterpenoid saponins from the roots of *Acanthophyllum gypsophiloides* Regel

Elena A. Khatuntseva[1], Vladimir M. Men'shov[1], Alexander S. Shashkov[2], Yury E. Tsvetkov[1], Rodion N. Stepanenko[3], Raymonda Ya. Vlasenko[3], Elvira E. Shults[4], Genrikh A. Tolstikov[4], Tatjana G. Tolstikova[4], Dimitri S. Baev[4], Vasiliy A. Kaledin[5], Nelli A. Popova[5], Valeriy P. Nikolin[5], Pavel P. Laktionov[6], Anna V. Cherepanova[6], Tatiana V. Kulakovskaya[7], Ekaterina V. Kulakovskaya[7] and Nikolay E. Nifantiev[*1]

Full Research Paper

Open Access

Address:
[1]Laboratory of Glycoconjugate Chemistry, N. D. Zelinsky Institute of Organic Chemistry, Russian Academy of Sciences, Leninsky prospect 47, 119991 Moscow, Russian Federation, [2]Laboratory of NMR spectroscopy, N. D. Zelinsky Institute of Organic Chemistry, Russian Academy of Sciences, Leninsky prospect 47, 119991 Moscow, Russian Federation, [3]Institute of Immunology, Ministry of Health and Social Development of Russian Federation, Kashirskoe Chaussee, 24/2, 115478 Moscow, Russian Federation, [4]Laboratory of Pharmacological Researches N. N. Vorozhtsov Novosibirsk Institute of Organic Chemistry, Siberian Branch of the Russian Academy of Sciences, prospect Acad. Lavrent'eva, 9, 630090 Novosibirsk, Russian Federation, [5]Institute of Cytology and Genetics Siberian Branch of the Russian Academy of Sciences, 10 prospect Acad. Lavrent'eva, 630090 Novosibirsk, Russian Federation, [6]Institute of Chemical Biology and Fundamental Medicine, Siberian Branch of the Russian Academy of Sciences, 8 prospect Acad. Lavrent'eva, 630090 Novosibirsk, Russian Federation and [7]G. K. Skryabin Institute of Biochemistry and Physiology of Microorganisms, Russian Academy of Sciences, 142290 Pushchino, Moscow region, Russian Federation

Email:
Nikolay E. Nifantiev[*] - nen@ioc.ac.ru

* Corresponding author

Keywords:
Acanthophyllum gypsophiloides; adjuvant; hemolysis; NMR; saponin; structure

Beilstein J. Org. Chem. **2012,** *8,* 763–775.
doi:10.3762/bjoc.8.87

Received: 13 March 2012
Accepted: 03 May 2012
Published: 23 May 2012

This article is part of the Thematic Series "Synthesis in the glycosciences II".

Guest Editor: T. K. Lindhorst

Abstract

Two new triterpenoid saponins **1** and **2** were isolated from the methanol extract of the roots of *Acanthophyllum gypsophiloides* Regel. These saponins have quillaic acid or gypsogenin moieties as an aglycon, and both bear similar sets of two oligosaccharide chains, which are 3-*O*-linked to the triterpenoid part trisaccharide α-L-Ara*p*-(1→3)-[α-D-Gal*p*-(1→2)]-β-D-Glc*p*A and pentasac-

charide β-D-Xyl*p*-(1→3)-β-D-Xyl*p*-(1→3)-α-L-Rha*p*-(1→2)-[β-D-Qui*p*-(1→4)]-β-D-Fuc*p* connected through an ester linkage to C-28. The structures of the obtained saponins were elucidated by a combination of mass spectrometry and 2D NMR spectroscopy. A study of acute toxicity, hemolytic, anti-inflammatory, immunoadjuvant and antifungal activity was carried out. Both saponins **1** and **2** were shown to exhibit immunoadjuvant properties within the vaccine composition with keyhole limpet hemocyanin-based immunogen. The availability of saponins **1** and **2** as individual pure compounds from the extract of the roots of *A. gypsophiloides* makes it a prospective source of immunoactive agents.

Introduction

Triterpenoid saponins [1] occur in many plant species and have a diverse range of properties [2]. Nowadays, a steadily growing number of publications [3-10] are aimed at research on saponins as potential adjuvants, with an urgent demand due to the fast development of immunotherapy methods. Among the most efficient saponin adjuvants are the components of a complex mixture of triterpenoids extracted from the bark of *Quillaja saponaria* Molina, which are used in veterinary vaccines [4]. One of the best known products of this origin is the less toxic and more stable fraction QS-21 [8], which is included now into a vast range of pilot vaccine compositions against viral infections [11-13] and cancer [14-17].

Meanwhile, the search for abundant, nontoxic, stable and individual saponin adjuvants is still urgent. This explains the enormous interest in investigations into saponins, particularly concerning the study of the relationships between their structure, adjuvant activity and toxicity [5,7]. In this paper we report the isolation and structural assessment of two saponins from the roots of *A. gypsophiloides* Rgl. (Turkestan soap root) with the further investigation of their toxicity, hemolytic activity, anti-inflammatory, antifungal and adjuvant properties. The roots of *A. gypsophiloides* Rgl. are an easily available raw material, which was reported [18] to comprise a saponin with a structure that is close to that of the extremely efficient adjuvant QS-21. *A. gypsophiloides* Rgl. is a member of the genus *Caryophyllaceae* (for other saponins see [19-22]), which is widely spread in mountain areas of central Asia. The crude saponin-containing fraction from the roots of *A. gypsophiloides* Rgl. has been known to be an excellent foaming agent for food and nutrition industry, and its composition has previously been under investigation [18].

Results and Discussion

The methanolic extract of the dried powdered roots of *A. gypsophiloides* was concentrated, and the crude mixture of saponins was precipitated from methanol by the addition of acetone and subjected to reversed-phase C18 HPLC. Compounds **1** and **2** (Figure 1) were isolated as white amorphous powders. Compound **1** exhibited in the HRMS (ESI) the $[M + Na]^+$ peak at *m*/*z* 1681.7071, indicating a molecular weight compatible with the molecular formula $C_{75}H_{118}O_{40}$. Compound **2** exhibited the $[M + Na]^+$ peak at *m*/*z* 1665.7181, consistent with the molecular formula $C_{75}H_{118}O_{39}$. GLC analysis of the acetylated (*S*)-2-octyl glycosides derived after full acid hydrolysis of compound **1** revealed the presence of D-galactose (D-Gal), L-arabinose (L-Ara), 6-deoxy-D-glucose (D-Qui), D-xylose (D-Xyl), L-rhamnose (L-Rha), D-fucose (D-Fuc), and D-glucuronic acid (D-GlcA). Similar investigation of compound **2** revealed the same sugar composition as for compound **1**.

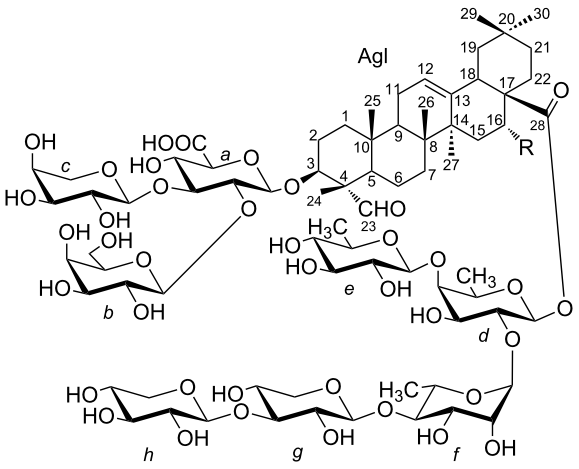

Figure 1: Saponins from *A. gypsophiloides* **1**, R = OH and **2**, R = H.

The structures of both compounds **1** and **2** were confirmed on the basis of their ^{1}H NMR, ^{13}C NMR, APT, COSY, TOCSY, ROESY, HSQC, and HMBC spectra. In accordance with the earlier reports [18] on structures of saponins from *A. gypsophiloides*, the aglycons of compound **1** and **2** were supposed to comprise quillaic acid (16-α-hydroxygypsogenin) and gypsogenin, respectively. This assumption was in good agreement with the detection of characteristic signals for six methyl groups in the ^{1}H (Table 1) and ^{13}C NMR (Table 2) spectra of **1** and **2**. Furthermore, the presence of these aglycons was unambiguously confirmed by the good agreement between ^{13}C NMR shifts of aglycon moieties of **1** and **2** and signals of aglycons for described bidesmosides comprising quillaic acid [21] and gypsogenin [21].

Table 1: ^{1}H and ^{13}C NMR data (δ, ppm) of the triterpene units of compounds **1** and **2** (500 MHz, pyridine-d_5/D_2O 1:1).[a]

Comp.	C-1 *H-1*	C-2 *H-2*	C-3 *H-3*	C-4	C-5 *H-5*	C-6 *H-6*	C-7 *H-7*	C-8	C-9 *H-9*	C-10	C-11 *H-11*	C-12 *H-12*	C-13	C-14	C-15 *H-15*
1	38.3 *1.53* *0.91*	25.2 *2.28* *1.97*	85.3 *4.06*	55.9	48.3 *1.37*	20.7 *1.40* *1.01*	32.8 *1.62* *1.49*	40.4	47.0 *1.75*	36.3	23.9 *1.91* *1.86*	122.7 *5.37*	144.1	42.2	35.9 *2.04* *1.89*
2	38.2 *1.51* *0.94*	25.1 *2.29* *1.97*	85.4 *4.10*	56.0	48.2 *1.43*	20.8 *1.43* *1.08*	32.6 *1.62* *1.48*	40.2	47.8 *1.66*	36.3	23.8 *1.87* *1.82*	122.8 *5.37*	144.1	42.5	28.7 *1.81* *1.42*
Comp.	C-16 *H-16*	C-17	C-18 *H-18*	C-19 *H-19*	C-20	C-21 *H-21*	C-22 *H-22*	C-23 *H-23*	C-24 *H-24*	C-25 *H-25*	C-26 *H-26*	C-27 *H-27*	C-28	C-29 *H-29*	C-30 *H-30*
1	73.9 *5.01*	47.9	41.6 *3.27*	47.4 *2.57* *1.24*	29.3	35.8 *2.19* *1.26*	31.5 *2.28* *2.04*	211.6 *9.71*	10.7 *1.43*	16.0 *0.88*	17.6 *0.96*	27.3 *1.68*	177.1	33.1 *0.94*	24.6 *0.96*
2	23.3 *2.05* *1.75*	47.9	42.1 *2.99*	46.4 *1.68* *1.17*	30.8	33.9 *1.25* *1.14*	32.4 *1.82* *1.66*	211.5 *9.63*	10.7 *1.43*	15.8 *0.85*	17.5 *0.92*	26.1 *1.24*	176.4	33.2 *0.93*	23.7 *0.85*

[a]^{1}H NMR chemical shifts are italicized.

Table 2: ^{1}H and ^{13}C NMR data (δ, ppm; *J*, Hz) for carbohydrate units of compounds **1** and **2** (500 MHz, pyridine-d_5/D_2O 1:1).

Units, atoms	**1**		**2**	
	δ_C	δ_H (*J*)	δ_C	δ_H (*J*)
→2,3)-GlcA (*a*)				
1	103.4	4.83, d (7.8)	103.4	4.82, d (7.3)
2	77.7	4.26	77.7	4.27
3	85.0	4.30	85.0	4.31
4	71.6	4.16	71.6	4.17
5	77.7	4.26	77.7	4.27
6	175.2		175.2	
Gal (*b*)				
1	103.2	5.33, d (7.7)	103.2	5.33, d (7.5)
2	72.8	4.14	72.8	4.14
3	74.4	4.09	74.5	4.08
4	70.3	4.31	70.3	4.31
5	76.5	3.97	76.5	3.97
6(a, b)	62.2	4.33, 4.17	62.1	4.35, 4.17
Ara (*c*)				
1	104.0	5.16, d (7.5)	104.0	5.17, d (7.5)
2	72.4	4.23	72.4	4.23
3	73.7	4.12	73.8	4.12
4	69.3	4.28	69.4	4.28
5(a, b)	67.2	4.34, 3.95	67.2	4.34, 3.95
→2,4)-Fuc (*d*)				
1	94.4	5.78, d (8.1)	94.5	5.80, d (8.1)
2	74.6	4.43	75.1	4.41

Table 2: ^{1}H and ^{13}C NMR data (δ, ppm; *J*, Hz) for carbohydrate units of compounds **1** and **2** (500 MHz, pyridine-d_5/D_2O 1:1). (continued)

3	76.3	4.20	76.0	4.19
4	83.2	4.12	83.0	4.12
5	71.9	4.03	71.8	4.02
6	17.1	1.52	17.1	1.52
Qui (*e*)				
1	105.6	4.92, d (7.8)	105.6	4.92, d (7.8)
2	75.6	3.81	75.6	3.80
3	77.0	3.99	77.1	4.00
4	76.1	3.53	76.1	3.53
5	72.9	3.69	72.9	3.70
6	18.2	1.51	18.2	1.51
→4)-Rha (*f*)				
1	101.2	6.01 s (<1)	101.2	5.97 s (<1)
2	71.1	4.62	71.1	4.62
3	71.8	4.41	71.8	4.43
4	83.7	4.15	83.7	4.18
5	68.3	4.26	68.7	4.28
6	18.3	1.65	18.4	1.68
→3)-Xyl (*g*)				
1	106.1	5.06, d (8.5)	105.9	5.09, d (7.7)
2	74.7	3.92	74.7	3.91
3	86.5	4.02	86.4	4.01
4	68.8	3.99	68.8	4.00
5(a, b)	66.2	4.18, 3.58	66.2	4.18, 3.58
Xyl (*h*)				
1	104.9	5.03, d (8.8)	104.9	5.04, d (7.6)
2	74.7	3.92	74.7	3.91
3	77.0	4.01	77.1	4.01
4	70.2	4.09	70.2	4.09
5(a, b)	66.5	4.30, 3.69	66.5	4.30, 3.68

Analysis of COSY and TOCSY spectra of both **1** and **2** revealed the presence of the following residues: β-Glc*p*A (residue *a*), β-Gal*p* (residue *b*), α-Ara*p* (residue *c*), β-Fuc*p* (residue *d*), β-Qui*p* (6-deoxy-β-Glc*p*, residue *e*), α-Rha*p* (residue *f*), β-Xyl*p* (residues *g* and *h*). The HSQC spectrum confirmed the structures of the triterpene aglycon and showed the positions of the substitutions within the oligosaccharide fragments (Table 1 and Table 2). The ROESY spectra (identical for compounds **1** and **2**) disclosed the sequence of the residues in two oligosaccharides and their location at the C-3 and C-28 of the aglycon. Thus, the location of GlcA (residue *a*) at the position 3 of the triterpene was established from the presence of a correlation peak 1*a*/3Agl (Figure 2 and Figure 3). Correlation peaks 1*b*/2*a* and 1*c*/3*a* correspond to substitutions of the residue *a* by terminal *b* at the position 2 and by terminal *c* at the position 3. Esterification of the position 1 of Fuc (residue *d*) with the carboxy group of the triterpene was unambiguously shown by the high-field shift of C-1 (94.4 ppm), being indirectly confirmed with the long-range correlation peak in the ROESY spectra 16Agl/3*d*. The sequence of the other residues was disclosed from the presence of the correlation peaks 1*e*/4*d*, 1*f*/2*d*, 1*g*/4*f* and 1*g*/4*h* (Figure 2). HMBC spectra finally confirmed the structure of the aglycons and the sequence of the residues. Thus, the correlation peak 1*d*/28Agl evidenced the location of Fuc (residue *d*) as the esterified substituent at C-28 of the triterpene (Figure 4). The other inter-residue correlation peaks were in agreement with the structure of oligosaccharides established from analysis of the ROESY spectra.

Characteristic chemical shifts in the ^{13}C NMR spectrum of **2** (δ_C 85.4 ppm for C-3 and δ_C 176.4 ppm for C-28 of the aglycon) evidence the bidesmosidic nature of the genin, which is glycosydated at C-3 and esterified to an oligosaccharide. The structures of both the trisaccharide and pentasaccharide frag-

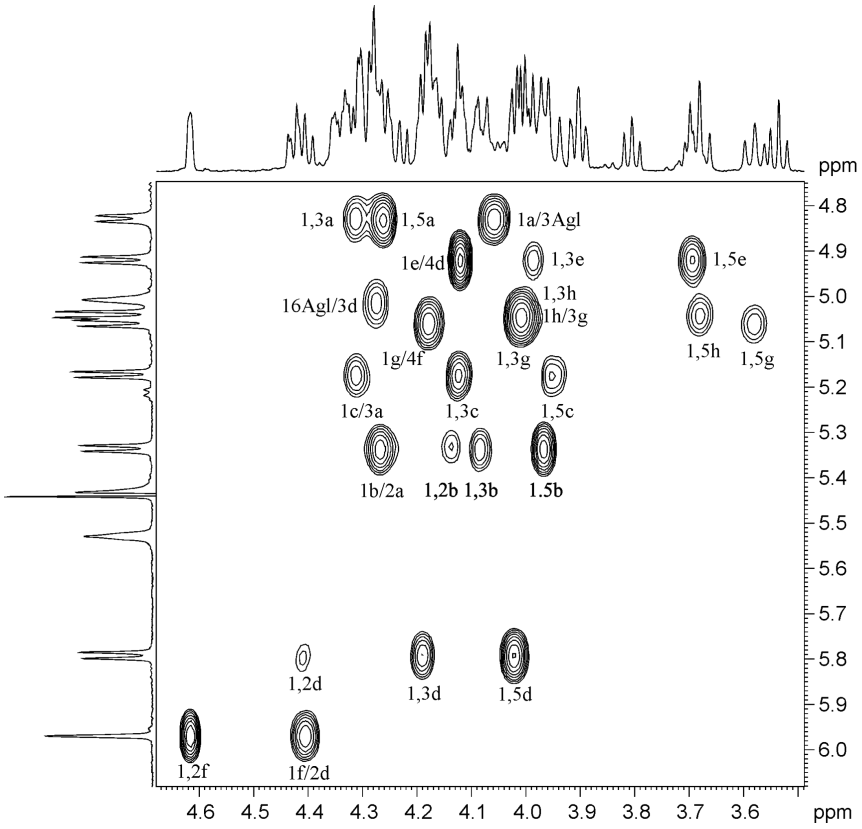

Figure 2: Part of a 2D ROESY spectrum of compound **1**. The corresponding parts of the ^{1}H NMR spectrum are shown along the axes. Arabic numerals refer to atoms in sugar residues denoted by letters, as shown for compounds **1** and **2**. Slashes are used for the designation of inter-residual interactions.

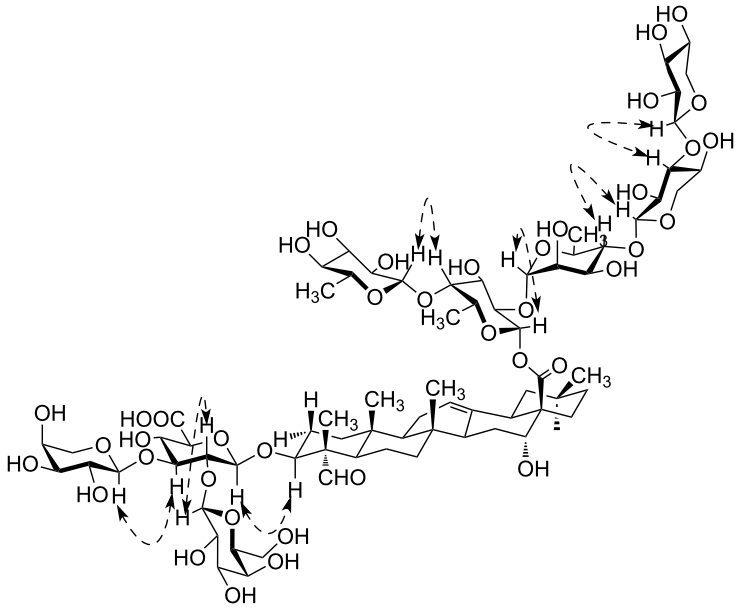

Figure 3: Key ROESY (dashed line) correlations for compound **1**.

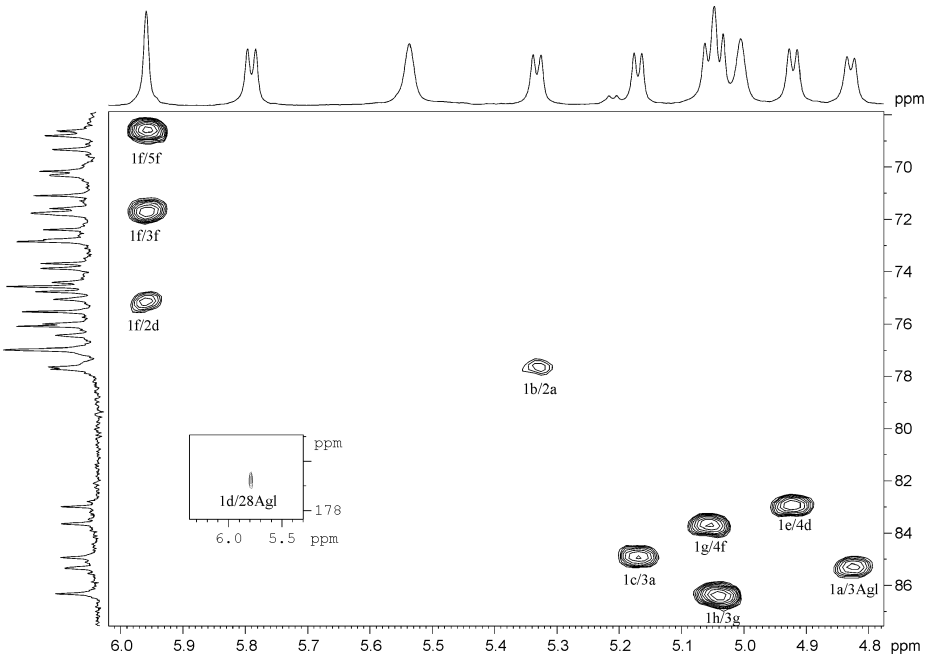

Figure 4: Part of the HMBC spectrum of compound **1**. ^{1}H and ^{13}C NMR spectra are shown along the horizontal and vertical axes, respectively. Arabic numerals before a slash refer to protons and after a slash refer to carbons in sugar residues denoted by letters, as shown for compounds **1** and **2**.

ments of compound **2** are similar to those established for compound **1**. Thus the structure of **2** was elucidated as gypsogenin 28-*O*-β-D-xylopyranosyl-(1→3)-β-D-xylopyranosyl-(1→3)-α-L-rhamnopyranosyl-(1→2)-[6-deoxy-β-D-glucopyranosyl-(1→4)]-β-D-fucopyranosyl ester 3-*O*-α-L-arabinopyranosyl-(1→3)-[β-D-galactopyranosyl-(1→2)]-β-D-glucuronopyranoside.

It should be noted that the elucidated structures of **1** and **2** are different from those reported earlier [18]. In the published structures β-D-Qui*p* (residue *e*) is located at O-2 of the β-Fuc*p* (residue *d*), and the trisaccharide moiety β-D-Xyl-(1→3)-β-D-Xyl-(1→3)-α-L-Rha is at O-4.

The acute-toxicity study of saponins **1** and **2** was carried out on albino mice. The median lethal dose (LD_{50}) was determined after a single dose administered through the oral or intraperitoneal route. The obtained data show that, in the case of oral administration of the studied compounds, LD_{50} was in the range of 304 ± 55 mg/kg for compound **1** and 252 ± 57 mg/kg for compound **2** with $p < 0.05$ (t). In the case of intraperitoneal administration, the LD_{50} was in the range of 15.1 ± 5.6 mg/kg for compound **1** and 5.4 ± 2.8 mg/kg for compound **2** with $p < 0.05$ (t). The immense difference between the values of LD_{50} in oral and intraperitoneal tests evidences low or no absorption of saponins in the intestine. However, it remains to be studied whether traces or decomposition products of ingested saponins enter the blood stream through the permeable membranes of mucosal cells.

For compounds **1**, **2** and saponin from *Quillaja* bark (Sigma) as a reference compound, the study on in vitro hemolysis was carried out. The obtained data confirmed high hemolytic activity of the *Quillaja* bark saponin, which caused 100% of hemolysis at a minimal hemolytic concentration of 5.5 μg/mL. Saponins **1** and **2** exhibited much lower hemolytic activity (Table 3): 50% hemolysis was observed at concentrations 11–18 μg/mL. Hemolysis of 85–95% for compounds **1** and **2** was observed at 62.5 μg/mL, whereas saponins QS-17, 18, and 21 from *Quillaja* bark were reported [23] to cause hemolysis at

Table 3: Hemolytic activities (%) of compounds **1** and **2** at different concentrations. The hemolytic activities of saline and distilled water were used as minimal and maximal hemolytic controls, respectively. $n = 3$ tests. Mean $p < 0.05$ vs saline group.

Saponin	Percentage of hemolysis (concentration of saponin in saline, μg/mL)						
1	84.5 ± 4.4 (62.5)	76.5 ± 3.3 (25)	75.1 ± 1.6 (12.5)	8.6 ± 3 (5)	8.3 ± 2.4 (2.5)	0.7 ± 1.2 (0.5)	0 ± 1.6 (0)
2	93.4 ± 4.5 (62.5)	90.8 ± 4.2 (25)	15.8 ± 1.4 (12.5)	12.0 ± 1.7 (5)	11.2 ± 2.3 (2.5)	10.0 ± 1.4 (0.5)	0 ± 1.6(0)

concentrations of 7–25 μg/mL. These results are in good agreement with our expectations based on the factors that are known to accompany low hemolytic activity, i.e., the bidesmosidic nature of compounds **1** and **2**, the presence of glucuronic acid at C-3 of the aglycone, and the absence of a lipid moiety.

Histamine-induced acute inflammation in the paws of the mice was used as a classical model of edema formation for the study of the anti-inflammatory activity of saponins. Two methods of saponin administration were used, namely oral (Table 4) and intraperitoneal (Table 5). In the first experiment, six groups of eight mice each were treated orally with compound **1** (20 mg/kg, 50 mg/kg), compound **2** (20 mg/kg, 50 mg/kg), indomethacin (20 mg/kg), and water (control). One hour after receiving the agents, each animal received a subcutaneous injection of 0.05 mL 0.1% histamine in the right, hind paw. The edema was measured 5 hours after the histamine injection. The anti-inflammatory effect was assessed by the decrease in the index of edema compared with the control group, which is defined as the percentage difference between the mass of the healthy and the inflamed paw, relative to the mass of the healthy paw.

In general, the anti-inflammatory effect of saponins **1** and **2** given intraperitoneally was dose-dependent, whereas that in the experiment with oral administration was not. Within the experiment based on oral administration, compound **1** did not show any reliable anti-inflammatory action. Data given in Table 5 evidences the more pronounced anti-inflammatory properties of compound **2** as compared to compound **1** in the experiment based on intraperitoneal administration.

The influence of saponins **1** and **2** on the vessel endothelium was assessed via determination of interleukin-6 (IL-6) production in primary human umbilical vein endothelial cells (HUVEC). These cells were found to express various pattern-recognizing receptors (PRRs), including TLR4 [24], and can produce pro-inflammatory cytokines, including IL-6, IL-8 and IL-1β, upon stimulation with bacterial and viral components, such as lipopolysaccharides (LPS) and double-stranded RNA (dsRNA) [25].

HUVEC were cultivated in the presence of saponins **1** and **2** at nontoxic concentrations, i.e., 1 and 5 μg/mL, as determined by EZ4U test, and reference compounds LPS from *E. coli* and dsRNA analogue poly(I:C). Measurement of IL-6 production did not show any effect of saponins **1** and **2** on IL-6 secretion, either by testing intact endothelial cells or cells pre-stimulated with LPS or poly(I:C) (Figure 5), indicating that at nontoxic concentrations saponins are not able to induce an innate immune response in endothelium. Thus we can conclude that compounds **1** and **2** are not prone to cause inflammation of the vessel endothelium.

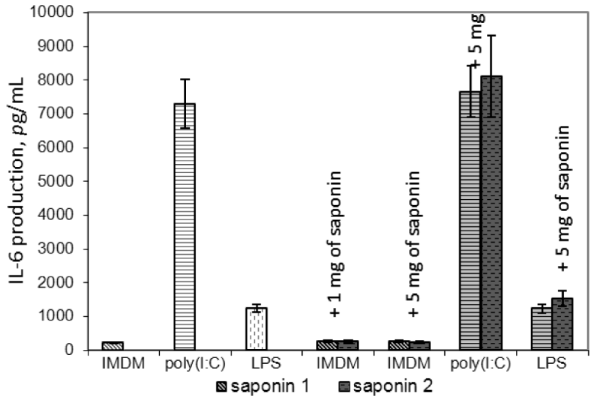

Figure 5: IL-6 production of primary endotheliocytes in the presence of compounds **1** and **2**. Error bars represent the standard deviation in each point.

Table 4: Anti-inflammatory effect of compounds **1** and **2** (oral administration).

parameter	dose in mg/kg					
	Water	**1**, 20	**2**, 20	**1**, 50	**2**, 50	Indomethacin, 20
Index of edema (%)	23.51 ± 5.18	20.23 ± 4.97	16.39 ± 5.49*	19.14 ± 5.79	24.57 ± 5.81***	15.79 ± 5.17*

*p < 0.05, ***p < 0.001 compared with control.

Table 5: Anti-inflammatory effect of compound **1** and **2** (intraperitoneal administration).

parameter	dose in mg/kg					
	Water	**1**, 1.25	**2**, 1.25	**1**, 2.5	**2**, 2.5	Indomethacin, 20
Index of edema (%)	28.22 ± 6.07	24.06 ± 9.11	17.32 ± 7.6**	14.88 ± 5.17***	12.28 ± 3.94***	19.43 ± 6.7*

*p < 0.05, ** p < 0.01, ***p < 0.001 compared with control.

To estimate the adjuvant properties of compounds **1** and **2** a series of test immunizations was carried out by using the synthetic vaccine neoglycoconjugate α-NeuAc-(2→3)-β-Gal*p*-(1→4)-β-Glc*p*-KLH (3'SL-KLH) on the basis of 3'-sialyllactoside (3'SL) ligands and keyhole limpet hemocyanin (KLH) protein carrier [26]. Four groups of mice were immunized with 40 μg of 3'SL-KLH together with 50 μg of compound **1** or **2**, or saponin from *Quillaja* bark, or without an adjuvant, and the specific anti-3'SL IgM and IgG responses were evaluated. For saponins **1** and **2**, a significant specific response was observed in comparison with the control vaccine formulation with antigen alone (Table 6). High serum titers of IgM and IgG antibodies were registered in the vaccination with compound **1** as adjuvant, though the IgG level did not achieve the level measured in the experiment with saponin from *Quillaja* bark. Titers of those antibodies in the experiment with saponin **2** were rather low. We can conclude, that in combination with 3'SL-KLH, antigen compound **1** showed significant adjuvant properties and, hence, can be considered as a prospective component of vaccine formulations.

Table 6: Serum titer data for antisera against 3'SL-polyacrylamide cover antigen obtained by immunization with 3'SL-KLH neoglycoconjugate with adjuvants **1**, **2**, and saponin from *Quillaja* bark, or without an adjuvant.

adjuvant	IgM	IgG
no adjuvant	1/1600	1/800
saponin **1**	1/102400	1/51200
saponin **2**	1/12800	1/6400
saponin from *Quillaja* bark	1/25600	1/204800

As many saponins are known to exhibit antifungal activities [2], we examined the ability of compounds **1** and **2** to suppress the proliferation of four test cultures: Basidiomycetous yeasts *Cryptococcus terreus*, *Filobasidiella neoformans*, and ascomycetous yeasts *Saccharomyces cerevisiae* and *Candida albicans*. The data in Table 7 demonstrate that compounds **1** and **2** exhibit antifungal activity against both ascomycetous and basidiomycetous yeasts, including the medically important *C. albicans* and *F. neoformans*. Saponins are known to be more effective against basidiomycetous yeast and at acidic pH act similarly to natural detergents, such as cellobiose lipids [27]. Growth inhibition experiments showed (Figure 6, Table 7), that the lower pH 4.0 favored antifungal activity of saponins **1** and **2**. At pH 7.0 neither compound **1** nor **2** inhibited the growth of *C. albicans* and *F. neoformans*. However, at pH 4.0 both saponins exhibited suppressing properties against these two strains. Notably, compound **2** was totally inactive against *S. cerevisiae* at both pH values. The liquid medium test involving

Table 7: Growth inhibition zones (Figure 6) of *C. terreus* (*C.t.*), *S. cerevisiae* (*S.c.*), *F. neoformans* (*F.n.*) and *C. albicans* (*C.a.*) in the presence of compounds **1** and **2** at pH 7.0 and 4.0.

pH	compound	amount,	diameter of growth inhibition zone, mm			
		mg/disc	*C.t.*	*S.c.*	*F.n.*	*C.a.*
7.0	**1**	1.0	n.d.[a]	n.d.	0	0
		0.5	12	10	0	0
		0.25	7	0	0	0
		0.1	0	0	0	0
		0.05	0	0	0	0
	2	1.0	n.d.	n.d.	0	0
		0.5	0	0	0	0
		0.25	0	0	0	0
		0.1	0	0	n.d.	n.d.
		0.05	0	0	n.d.	n.d.
4.0	**1**	1.0	n.d.	n.d.	n.d.	14
		0.5	18	10	15	10
		0.25	14	5	10	0
		0.1	10	0	n.d.	n.d.
		0.05	0	0	n.d.	n.d.
	2	1.0	n.d.	n.d.	n.d.	14
		0.5	13	0	15	7
		0.25	10	0	0	0
		0.1	10	0	n.d.	n.d.
		0.05	0	0	n.d.	n.d.

[a]n.d. not determined.

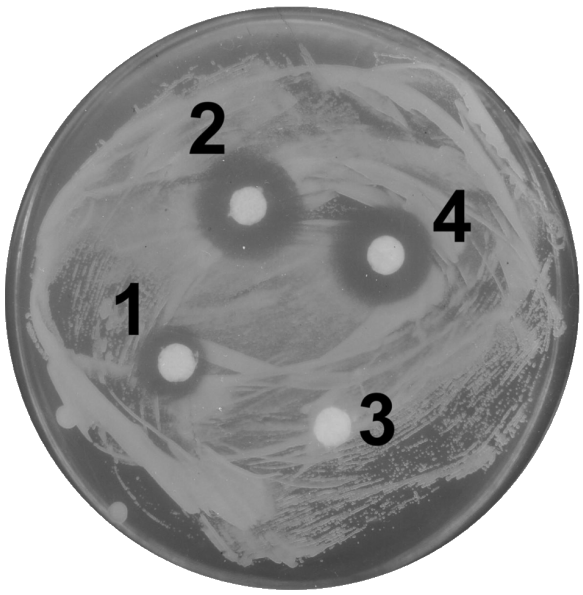

Figure 6: Growth inhibition zones for *F. neoformans* IGC 3957 in the presence of compounds **1** and **2** at pH 4.0. Compound **1**: (1) 0.25 mg/disc, (2) 0.5 mg/disc; compound **2**: (3) 0.25 mg/disc, (4) 0.5 mg/disc.

F. neoformans showed only slight differences between saponins **1** and **2** (Table 8).

Table 8: Viability (%) of *F. neoformans* IGC 3957 treated with compounds **1** and **2** at pH 4.0.

	concentration, mg/mL			
compound	0	0.49	0.97	1.87
1	100	66 ± 5.6	11 ± 0.1	4 ± 0.3
2	100	93 ± 7.2	18 ± 1.8	6 ± 0.5

Conclusion

Thus, the structures of two easily available novel saponins **1** and **2** were elucidated, and they were shown to exhibit low hemolytic activity, low oral and intraperitoneal toxicity, and an inability to induce inflammation in the vessel endothelium. Meanwhile, compounds **1** and **2** exhibited prominent immune-stimulating properties and can be considered as a prospective adjuvant in combination with KLH-based neoglycoconjugates. The antifungal activity of saponins **1** and **2** was also examined on four yeast species.

Experimental

General experimental procedures. Optical rotation values were measured on a JASCO DIP-360 polarimeter at 22 ± 2 °C. NMR spectra were recorded on Bruker DRX-500 and Bruker AM-300 instruments in D_2O/pyridine-d_5 with TMS as internal reference. High-resolution mass spectra (HRMS) were measured on a Bruker microTOF II instrument by using electrospray ionization (ESI) [28]. The measurements were done in a positive-ion mode (interface capillary voltage: 4500 V) or in a negative-ion mode (3200 V); mass range from *m*/*z* 50–3000 Da; external or internal calibration was achieved with electrospray calibrant solution (Fluka). A syringe injection was used for solutions in acetonitrile, methanol, or water (flow rate 3 μL/min). Nitrogen was applied as a dry gas; the interface temperature was set to 180 °C. High-performance liquid chromatography (HPLC) was carried out on a C18 reversed-phase column (Ascentis C18, 5 μm, 250 × 21.2 mm, 65% MeOH, 35% of 0.05 M aq. solution of NH_4HCO_3) with the use of a UV detector at 210 nm. Analysis of purity was carried out on a C18 reversed-phase column (IBM C18, 5 μm, 250 × 4.5 mm) with eluent and detection as described above.

Statistical analysis. Statistical significance was determined by the Student's *t*-test. *P* values less than 0.05 were considered to be significant. The Kaplan–Meier and one-way ANOVA analysis was used to establish statistical significance for the in vivo experiments.

Plant material. The roots of *A. gypsophiloides* Rgl. were collected in September 2005 on a mountainside in the Chimkent region, Kazakhstan and were identified by Prof. P. G. Gorovoi (G.B. Elyakov Pacific Institute of Bioorganic Chemistry, Far Eastern Branch, Russian Academy of Sciences). A herbarium specimen (herbarium no. 03025) has been deposited at the Herbarium of Novosibirsk Botanical Garden; Russia. Saponin from *Quillaja* bark was purchased from Sigma–Aldrich (S4521) and used without further purification.

Extraction and isolation. Dried and finely powdered roots of *A. gypsophiloides* (490 g) were heated in methanol (5 × 800 mL) under reflux for 10 h, filtered, and concentrated to yield the extract (86.5 g, 17.6%). This extract was dissolved in methanol (87 mL) and precipitated by the addition of acetone (750 mL). The resulting precipitate was filtered and dried in a vacuum desiccator over dry KOH (fraction A, 14.5 g, 3.0%). The mother liquid was concentrated and subjected to silica gel column chromatography; elution with a mixture of $CHCl_3$/MeOH/H_2O 130:70:15 gave 29.3 g of an amorphous residue, which was dissolved in 500 mL of 2-propanol and 0.2 mL of acetic acid and evaporated under reduced pressure to remove residual water. The residue was triturated with 20 mL of methanol and the slurry was diluted with acetone (160 mL). The formed precipitate was filtered and dried to give 22.2 g of total glycosides (fraction B). Combined fractions A and B (36.7 g) were subjected to preparative HPLC (Ascentis C18, 5 μm, 250 × 21.2 mm) using a mixture of 65% methanol and 35% 0.05 M aq. solution of NH_4HCO_3 to yield 18.35 g of compound **1** (3.7% starting from the root powder) and 15.42 g of compound **2** (3.1% starting from the root powder) as ammonium salts. The purity of **1** and **2** was assessed by analytical C18 reversed-phase HPLC and varied in a range of 97–99%.

Monosaccharide analyses. Compounds **1** and **2** were hydrolyzed with 2 M CF_3CO_2H (120 °C, 2 h) and the absolute configurations of the monosaccharides were determined by GLC of acetylated (*S*)-(+)-2-octyl glycosides according to the published method [29]. GLC was performed using an Agilent 7820A chromatograph equipped with an HP-5 fused silica column (0.25 mm × 30 m) using a temperature program of 160 °C to 290 °C (7 °C min^{-1}).

3-*O*-[β-D-Galactopyranosyl-(1→2)-[α-L-arabinopyranosyl-(1→3)]-β-D-glucuronopyranosyl]quillaic acid 28-β-D-xylopyranosyl-(1→3)-β-D-xylopyranosyl-(1→3)-α-L-rhamnopyranosyl-(1→2)-[6-deoxy-β-D-glucopyranosyl-(1→4)]-β-D-fucopyranosyl ester (1): white amorphous solid; $[\alpha]^{20}_D$ −5.0 (*c* 1, H_2O); ^1H and ^{13}C NMR data, see Table 1 and Table 2; HRMS–ESI$^+$ (*m*/*z*): $[M + Na]^+$ calcd for $C_{75}H_{118}O_{40}Na$, 1681.7097; found, 1681.7071.

3-*O*-[β-D-Galactopyranosyl-(1→2)-[α-L-arabinopyranosyl-(1→3)]-β-D-glucuronopyranosyl]gypsogenin 28-β-D-xylopyranosyl-(1→3)-β-D-xylopyranosyl-(1→3)-α-L-rhamnopyranosyl-(1→2)-[6-deoxy-β-D-glucopyranosyl-(1→4)]-β-D-fucopyranosyl ester (2): white amorphous solid; $[\alpha]^{20}_{D}$ 5.0 (*c* 1, H_2O); ^1H and ^{13}C NMR data, see Table 1 and Table 2; HRMS–ESI$^+$ (*m*/*z*): $[M + Na]^+$ calcd for $C_{75}H_{118}O_{39}Na$, 1665.7148; found, 1665.7181.

Acute-toxicity assay. Albino, nonbreeding, sexually mature male mice from SPF-vivarium of SB RAS weighing 20–25 g were used in the test. All research involving laboratory animals was carried out in accordance with The Guidelines for the Care and Use of Laboratory Animals. Mice were housed in appropriate caging facilities and allowed food and water ad libitum.

Oral route: The experiment involved 50 male mice. Animals were selected at random and divided into five groups, each consisting of 10 mice. The control group received only pelleted food and water. The other four groups received pelleted food and water along with varying doses of compounds **1** or **2**, at either 50.0 mg/kg, 100.0 mg/kg, 250.0 mg/kg or 500.0 mg/kg. Saponins were given by single oral gavage in the prescribed doses by using a feeding cannula. The acute LD_{50} toxicity of saponins **1** and **2** was calculated on the basis of the mortality data collected within seven days by using Probit Analysis 1.0 software with $p < 0.05$.

Intraperitoneal route. The experiment involved 50 male mice. Animals were selected at random and divided into five groups, each consisting of 10 mice. The control group received only pelleted food and water. The other four groups received pelleted food and water and were inoculated once intraperitoneally with solutions of varying doses of saponins **1** or **2**, at either 0.50 mg/kg, 5.0 mg/kg, 10 mg/kg or 50.0 mg/kg in saline. The acute LD_{50} toxicity of saponins **1** and **2** was calculated on the basis of the mortality data collected within seven days using Probit Analysis 1.0 software with $p < 0.05$.

Hemolysis assay. Red blood cells were obtained from Wistar sexually mature rats of both sexes from SPF-vivarium of SB RAS, weighing 200–250 g. Blood was collected from neck vessels in standard plastic tubes containing 3.8% solution of sodium citrate. Aliquots of 7 mL of citrated blood (volume ratio of blood to sodium citrate 9:1) were washed with sterile non-pyrogenic saline (0.89% sodium chloride). Washing was performed by adding an equal volume of saline solution to an aliquot of citrated blood and subsequent centrifugation at 180 g for 5 min, after which the supernatant was discarded, and the procedure repeated three times. Harvested erythrocytes were diluted with saline to obtain a suspension of 0.5% hematocrit. Samples containing 0.5 mL of cell suspension were mixed with 0.5 mL of saline solutions (145 mM, isotonic conditions) containing the investigated saponins in concentrations of 5, 10, 15, 25, 50, 75, 100, 250, 500 μg/mL. Samples were stirred continuously for 30 min at 37 °C and then centrifuged at 70*g* for 10 min. The content of free hemoglobin in the supernatant was measured by spectrophotometric analysis at a wavelength of 412 nm (spectrophotometer Cary 50, Varian). Hemoglobin concentration in the supernatant was expressed as a percentage of hemoglobin concentration in the supernatant of cells, which were totally hemolysed by the addition of distilled water. The absorbance of samples with 0% hemolysis was registered for samples with saline and used as a blank measurement. The degree of hemolysis, depending on the concentration of saponin was calculated by using Probit Analysis 1.0 software.

Anti-inflammatory activity. Albino, nonbreeding, sexually mature male mice from SPF-vivarium of SB RAS weighing 20–25 g were used in the test. All research involving laboratory animals was carried out in accordance with The Guidelines for the Care and Use of Laboratory Animals. Mice were housed in appropriate caging facilities and allowed food and water ad libitum.

Oral route: Six groups of eight mice were treated orally with saponin **1** (20 mg/kg, 50 mg/kg), saponin **2** (20 mg/kg, 50 mg/kg), and indomethacin (20 mg/kg) in Twin-80 water solution (control). One hour after receiving the agents, each animal received a subcutaneous injection of 0.05 mL 0.1% histamine in the right hind paw. The edema was measured 5 h after the histamine injection as the difference in weight between the paw that was administered histamine, and a healthy paw. The anti-inflammatory effect was assessed by the decrease in index of edema compared with the control group. The index of edema is defined as the ratio of the difference between the masses of the inflamed and healthy paws to the mass of the healthy paw in percent: $(Mi - Mh) / Mh \times 100\%$; Mi: mass of inflamed paw, Mh: mass of healthy paw. A probability of $p < 0.05$ was considered significant.

Intraperitoneal route: Six groups of eight mice were treated intraperitoneally with saponin **1** (1.25 mg/kg, 2.5 mg/kg), saponin **2** (1.25 mg/kg, 2.5 mg/kg) and indomethacin orally (20 mg/kg) in Twin-80 water solution (control). One hour after receiving the agents, each animal received a subcutaneous injection of 0.05 mL 0.1% histamine in the right hind paw. The edema was measured 5 h after the histamine injection as the difference in weight between the paw that was administered histamine, and a healthy paw. The anti-inflammatory effect was assessed as described above.

Cytotoxicity, cell proliferation test and endotoxin test

Cell cultures: Primary endothelial cells were obtained from the human umbilical vein [30] and cultivated in Iscove's Modified Dulbecco's Medium (IMDM, Gibco, USA, 42200-014) with 10% fetal bovine serum (FBS) (Gibco, USA, 10106), 100 μg/mL streptomycin, and 100 μg/mL penicillin (IMDM-FBS) at 37 °C with 5% CO_2. Primary endotheliocytes were seeded on 0.5% gelatin precoated (Sigma, USA, G-2500) culture dishes or microplate wells and were detached with 0.1% collagenase solution (Gibco, USA, 17104-019). To examine the cytotoxic and pro-inflammatory effects of saponins, primary endotheliocytes were seeded at a density of 7×10^3 cells per well of a 48-well microplate. Sixteen hours after seeding, cells were washed with IMDM, and 200 μL (48-well plate) of IMDM-FBS with saponins (from 1 to 100μg/mL) was added and cultivated for a subsequent 24 h.

EZ4U test: After incubation with saponins, cells were washed with IMDM-FBS and cultivated with 100 μL of fresh IMDM-FBS containing components of EZ4U kit (EZ4U, Biomedica, Austria) for a subsequent 24 h. After incubation, the culture supernatants were transferred into a 96-well plate and the optical density was registered in a Multiscan plate reader at 450 nm (SDB NP Puschino, Russia). All experiments were performed in triplicate.

LAL test: All components contacting with cells were tested for endotoxin contamination by using the LAL gel clot test as recommended by the producers (Associate of Cape Cod Incorporated, USA).

IL-6 release assay: Primary endotheliocytes were incubated in the IMDM-FBS with saponins at noncytotoxic concentrations (1 and 5 μg/mL) in the absence or in presence of LPS (100 ng/mL) or poly-(I:C) (Sigma, USA, P9582, 100 μg/mL) at 37 °C, 5% CO_2 for 24 h. For positive control, cells were incubated in the presence of 100 μg/mL of poly-(I:C) or 100 ng/mL of LPS from *E. coli* (LPS) (Sigma, USA, L2755). Cells were incubated in IMDM-FBS for 24 h, culture medium was removed, and cells were centrifuged at 1500*g* and preserved at −20 °C. The IL-6 concentration in the samples was determined by using a commercial ELISA kit (Vector-Best, Russia, A-8768) according to the protocol suggested by the manufacturer. All experiments were performed in triplicate.

Studies of adjuvant activity: *Animals.* Female Swiss mice (eight weeks old) of the C57B1/6J breed were purchased from the "Stolbovaya", Russia, and rodent laboratory chow and tap water were provided ad libitum. Mice were maintained under a controlled temperature (22 ± 2 °C) and humidity under a 12/12 h light/dark cycle. All the procedures were carried out in strict accordance with the International Legislation on the Use and Care of Laboratory Animals.

Glycoconjugate vaccine preparation: Conjugate (3'SL-KLH [28]) of α-NeuAc-(2→3)-β-Gal*p*-(1→4)-β-Glc*p* ligands with keyhole limpet hemocyanin carrier (KLH), bearing 5% mass of indicated carbohydrate, was used as an immunogen, and saponins **1** and **2** and saponin from *Quillaja* bark were used as adjuvants. All samples were filtered through 0.22 μm Micropore® filters and kept at 4 °C prior to use.

Immunization: Four groups of seven mice each were immunized intramuscularly thrice, on days 0, 14, and 84 with a mixture of 40 μg of conjugate and 50 μg of different saponins (or without adjuvant for the control group) in PBS as a vehicle in a total vaccine volume of 200 μL.

ELISA: Sera from inoculated mice were collected on day 91 post-inoculation (p.v.) of the first dose of vaccine and pooled. The titers for IgG and IgM against α-NeuAc-(2→3)-β-Gal*p*-(1→4)-β-Glc*p* were determined in an indirect ELISA as previously described [31]. ELISA plates (96-well, Nunc Maxisorp) were coated with a cover polyacrylamide antigen [28] with α-NeuAc-(2→3)-β-Gal*p*-(1→4)-β-Glc*p* moieties. Coating was performed with a 10 μg/mL in 0.1 M bicarbonate buffer solution at 4 °C overnight. Wells were washed three times with PBS containing 0.05% Tween 20 (PBS-T) and blocked with 1% solution of HSA in PBS-T. Diluted sera (100 μL) collected from the mice in PBS-T was added to wells and incubated overnight at 4 °C. The plates were washed three times with PBS-T, and goat anti-mouse IgG or IgM peroxidase conjugate (Jackson Immuno Research) in 1:1500 dilution (PBS-T) was added to the wells. Plates were then incubated for 1 h at 37 °C and washed, and substrate (*o*-phenylenediamine, 0.4 mg/mL in 0.1 M phosphate-citrate buffer with 0.0013% H_2O_2) was added to each well. Plates were then incubated for 25 min at 37 °C, after which the reaction was terminated by adding 50 μL per well of 2 N H_2SO_4. The optical density (OD) was measured in an ELISA plate reader at 492 nm. Data were expressed as the mean OD value of the samples minus the mean OD value of the control wells. The value of the OD for the control group was less than 0.1 (dilution 1/100 and more). Antibody levels in the sera of all samples were higher than the control ($p < 0.05$).

Antifungal activity

Strains and culture conditions: The basidiomycetous yeasts *Cryptococcus terreus* VKM Y-2253 (All-Russian Collection of Microorganisms), *Filobasidiella neoformans* IGC 3957 (Portuguese Yeast Culture Collection, Centro de Biologia, Portugal), and ascomycetous yeasts *Saccharomyces cerevisiae*

VKM Y-1173 (All-Russian Collection of Microorganisms), *Candida albicans* JCM 1542 (Japan Collection of Microorganisms) were used as test-cultures. Strains were maintained on malt agar slants at 5 °C. *S. cerevisiae* VKM Y-1173 was grown in YPD medium containing glucose (20 g/L), yeast extract (10 g/L) and peptone (20 g/L; Sigma, USA) under shaking at 30 °C for 24 h. *Candida albicans*, *Filobasidiella neoformans*, and *Cryptococcus terreus* were grown under the same conditions for 48 h in YPD medium containing glucose (20 g/L), yeast extract (4 g/L), peptone (5 g/L).

Antifungal activity assay: Sterile 5 mm diameter glass microfiber filter discs GF/A (Whatman, UK) were placed onto the surface of a solid medium in Petri dishes inoculated with test cultures. Two media were used: YPD containing 0.5% glucose, 0.2% yeast extract, 0.25% peptone, 2% agar, and 0.04 M citrate–phosphate buffer (pH 4.0), and YPD with 2% agar (pH 7.0). Aliquots of saponin solutions in deionized water were pipetted onto discs. The plates were incubated at 24 °C for 2–3 days until growth of the lawn strain appeared, and the diameters of the growth inhibition zones were measured. For the assay of cell viability the suspension of the cells *F. neoformans* (3×10^6 cells mL^{-1}) was treated with saponins in 0.01 M citrate buffer (pH 4.0) at room temperature for 1 h. Thereafter, the samples were diluted by the same buffer and inoculated on YPD agar. Three days later, the number of colonies was determined. The samples without saponins were used as a control. All experiments were repeated twice. Fresh solutions of saponins in deionized water were used.

Acknowledgements

We wish to acknowledge financial support from the Ministry of Education and Science of the Russian Federation (contract 16.512.11.2089) and the Interdisciplinary Integration project #93 of the Siberian branch of RAS.

References

1. Vincken, J.-P.; Heng, L.; de Groot, A.; Gruppen, H. *Phytochemistry* **2007,** *68,* 275–297. doi:10.1016/j.phytochem.2006.10.008
2. Francis, G.; Kerem, Z.; Makkar, H. P. S.; Becker, K. *Brit. J. Nutr.* **2002,** *88,* 587–605. doi:10.1079/BJN2002725
3. Sun, H.-X.; Xie, Y.; Ye, Y.-P. *Vaccine* **2009,** *27,* 1787–1796. doi:10.1016/j.vaccine.2009.01.091
4. Rajput, Z. I.; Hu, S.-h.; Xiao, C.-w.; Arijo, A. G. *J. Zhejiang Univ., Sci., B* **2007,** *8,* 153–161. doi:10.1631/jzus.2007.B0153
5. Kensil, C. R. Methods in Molecular Medicine. In *Vaccine Adjuvants;* O'Hagan, D. T.; Walker, J. M., Eds.; Methods in Molecular Medicine, Vol. 42; Springer: New York, 2000; pp 259–271. doi:10.1385/1-59259-083-7:259
6. Skene, C. D.; Sutton, P. *Methods* **2006,** *40,* 53–59. doi:10.1016/j.ymeth.2006.05.019
7. Press, J. B.; Reynolds, R. C.; May, R. D.; Marciani, D. J. Structure/function relationships of immunostimulating saponins. In *Bioactive natural Products (Part E);* Rahman, A.-u., Ed.; Studies in Natural Products Chemistry, Vol. 24; Elsevier, 2000; pp 131–174. doi:10.1016/S1572-5995(00)80045-9
8. Kensil, C. R.; Kammer, R. *Expert Opin. Invest. Drugs* **1998,** *7,* 1475–1482. doi:10.1517/13543784.7.9.1475
9. Fleck, J. D.; Kauffmann, C.; Spilki, F.; Lencina, C. L.; Roehe, P. M.; Gosmann, G. *Vaccine* **2006,** *24,* 7129–7134. doi:10.1016/j.vaccine.2006.06.059
10. Katselis, G. S.; Estrada, A.; Gorecki, D. K. J.; Barl, B. *Can. J. Physiol. Pharmacol.* **2007,** *85,* 1184–1194. doi:10.1139/Y07-109
11. Evans, T. G.; McElrath, M. J.; Matthews, T.; Montefiori, D.; Weinhold, K.; Wolff, M.; Keefer, M. C.; Kallas, E. G.; Corey, L.; Gorse, G. J.; Belshe, R.; Graham, B. S.; Spearman, P. W.; Schwartz, D.; Mulligan, M. J.; Goepfert, P.; Fast, P.; Berman, P.; Powell, M.; Francis, D. *Vaccine* **2001,** *19,* 2080–2091. doi:10.1016/S0264-410X(00)00415-1
12. Kennedy, J. S.; Co, M.; Green, S.; Longtine, K.; Longtine, J.; O'Neill, M. A.; Adams, J. P.; Rothman, A. L.; Yu, Q.; Johnson-Leva, R.; Pal, R.; Wang, S.; Lu, S.; Markham, P. *Vaccine* **2008,** *26,* 4420–4424. doi:10.1016/j.vaccine.2008.05.090
13. Vandepapelière, P.; Horsmans, Y.; Moris, P.; Van Mechelen, M.; Janssens, M.; Koutsoukos, M.; Van Belle, P.; Clement, F.; Hanon, E.; Wettendorff, M.; Garçon, N.; Leroux-Roels, G. *Vaccine* **2008,** *26,* 1375–1386. doi:10.1016/j.vaccine.2007.12.038
14. Ragupathi, G.; Meyers, M.; Adluri, S.; Howard, L.; Musselli, C.; Livingston, P. O. *Int. J. Cancer* **2000,** *85,* 659–666. doi:10.1002/(SICI)1097-0215(20000301)85:5<659::AID-IJC11>3.0.CO;2-5
15. Gilewski, T.; Ragupathi, G.; Bhuta, S.; Williams, L. J.; Musselli, C.; Zhang, X.-F.; Bencsath, K. P.; Panageas, K. S.; Chin, J.; Hudis, C. A.; Norton, L.; Houghton, A. N.; Livingston, P. O.; Danishefsky, S. J. *Proc. Natl. Acad. Sci. U. S. A.* **2001,** *98,* 3270–3275. doi:10.1073/pnas.051626298
16. Ragupathi, G.; Slovin, S. F.; Adluri, S.; Sames, D.; Kim, I. J.; Kim, H. M.; Spassova, M.; Bornmann, W. G.; Lloyd, K. O.; Scher, H. I.; Livingston, P. O.; Danishefsky, S. J. *Angew. Chem.* **1999,** *111,* 590–594. doi:10.1002/(SICI)1521-3757(19990215)111:4<590::AID-ANGE590>3.0.CO;2-A
Angew. Chem., Int. Ed. **1999**, *38*, 563–566. doi:10.1002/(SICI)1521-3773(19990215)38:4<563::AID-ANIE563>3.0.CO;2-3
17. Sabbatini, P. J.; Ragupathi, G.; Hood, C.; Aghajanian, C. A.; Juretzka, M.; Iasonos, A.; Hensley, M. L.; Spassova, M. K.; Ouerfelli, O.; Spriggs, D. R.; Tew, W. P.; Konner, J.; Clausen, H.; Rustum, N. A.; Danishefsky, S. J.; Livingston, P. O. *Clin. Cancer Res.* **2007,** *13,* 4170–4177. doi:10.1158/1078-0432.ccr-06-2949
18. Putieva, Z. M.; Gorovitch, T. T.; Kondratenko, E. S.; Abubakirov, N. K. *Chem. Nat. Compd.* **1979,** *15,* 148–151. doi:10.1007/BF00570786
19. Böttger, S.; Melzig, M. F. *Phytochem. Lett.* **2011,** *4,* 59–68. doi:10.1016/j.phytol.2010.08.003
20. Kondratenko, E. S.; Putieva, Z. M.; Abubakirov, N. K. *Chem. Nat. Compd.* **1981,** *17,* 303–317. doi:10.1007/BF01185255
21. Nie, W.; Luo, J.-G.; Kong, L.-Y. *Carbohydr. Res.* **2010,** *345,* 68–73. doi:10.1016/j.carres.2009.08.015

22. Jia, Z.; Koike, K.; Sahu, N. P.; Nikaido, T. Triterpenoid saponins from Caryophyllaceae family. In *Studies in Natural Product Chemistry;* Rahman, A.-u., Ed.; Elsevier: Amsterdam, 2002; Vol. 26, Part G, pp 3–61. doi:10.1016/S1572-5995(02)80004-7
23. Kensil, C. R.; Patel, U.; Lennik, M.; Marciani, D. *J. Immunol.* **1991,** *146,* 431–437.
24. Faure, E.; Thomas, L.; Xu, H.; Medvedev, A. E.; Equils, O.; Arditi, M. *J. Immunol.* **2001,** *166,* 2018–2024.
25. Harcourt, J. L.; Hagan, M. K.; Offermann, M. K. *J. Interferon Cytokine Res.* **2000,** *20,* 1007–1013. doi:10.1089/10799900050198453
26. Khatuntseva, E. A.; Yudina, O. N.; Tsvetkov, Y. E.; Grachev, A. A.; Stepanenko, R. N.; Vlasenko, R. Y.; Lvov, V. L.; Nifantiev, N. E. *Russ. Chem. Bull.* **2006,** *55,* 2095–2102. doi:10.1007/s11172-006-0554-y
27. Kulakovskaya, T. V.; Shashkov, A. S.; Kulakovskaya, E. V.; Golubev, W. I. *FEMS Yeast Res.* **2005,** *5,* 919–923. doi:10.1016/j.femsyr.2005.04.006
28. Belyakov, P. A.; Kadentsev, V. I.; Chizhov, A. O.; Kolotyrkina, N. G.; Shashkov, A. S.; Ananikov, V. P. *Mendeleev Commun.* **2010,** *20,* 125–131. doi:10.1016/j.mencom.2010.05.001
29. Leontein, K.; Lönngren, J. Determination of the absolute configuration of sugars by gas–liquid chromatography of their acetylated 2-octyl glycosides. In *Lipopolysaccharides, Separation and analysis. Glycosylated polymers;* BeMiller, J. N.; Whistler, R. L.; Shaw, D. H., Eds.; Methods in Carbohydrate Chemistry, Vol. 9; John Wiley & Sons: Hoboken, NJ, 1993; pp 87–89.
30. Jaffe, E. A.; Nachman, R. L.; Becker, C. G.; Minick, C. R. *J. Clin. Invest.* **1973,** *52,* 2745–2756. doi:10.1172/JCI107470
31. Stepanenko, R. N.; Vlasenko, R. Y.; Tsvetkov, Y. E.; Khatuntseva, E. A.; Novikova, E. M.; Verner, I. K.; Nifantiev, N. E.; Petrov, R. V. *Immunologia* **2010,** *2,* 86–92.

License and Terms

Beilstein Journal of Organic Chemistry

An easily accessible sulfated saccharide mimetic inhibits in vitro human tumor cell adhesion and angiogenesis of vascular endothelial cells

Grazia Marano[1,2], Claas Gronewold[1,3], Martin Frank[1,4], Anette Merling[1], Christian Kliem[1], Sandra Sauer[1], Manfred Wiessler[1], Eva Frei[1] and Reinhard Schwartz-Albiez[*1,§]

Full Research Paper

Open Access

Address:
[1]German Cancer Research Center (DKFZ), Im Neuenheimer Feld 280, 69120 Heidelberg, Germany, [2]Calvatis GmbH, Dr.-Albert-Reimann-Str. 16a, 68526 Ladenburg, Germany, [3]Kao Germany GmbH, Pfungstädter Str. 92–100, 64297 Darmstadt/Eberstadt, Germany, and [4]Biognos AB, Generatorsgatan 1, 41705 Goeteborg, Sweden

Email:
Reinhard Schwartz-Albiez[*] - r.s-albiez@dkfz.de

* Corresponding author
§ Tel: +49 6221 423713

Keywords:
angiogenesis; biomimetic synthesis; carbohydrates; in silico blind docking; melanoma cells

Beilstein J. Org. Chem. **2012,** *8,* 787–803.
doi:10.3762/bjoc.8.89

Received: 01 February 2012
Accepted: 11 May 2012
Published: 29 May 2012

This article is part of the Thematic Series "Synthesis in the glycosciences II".

Guest Editor: T. K. Lindhorst

Abstract

Oligosaccharides aberrantly expressed on tumor cells influence processes such as cell adhesion and modulation of the cell's microenvironment resulting in an increased malignancy. Schmidt's imidate strategy offers an effective method to synthesize libraries of various oligosaccharide mimetics. With the aim to perturb interactions of tumor cells with extracellular matrix proteins and host cells, molecules with 3,4-bis(hydroxymethyl)furan as core structure were synthesized and screened in biological assays for their abilities to interfere in cell adhesion and other steps of the metastatic cascade, such as tumor-induced angiogenesis.

The most active compound, (4-{[(β-D-galactopyranosyl)oxy]methyl}furan-3-yl)methyl hydrogen sulfate (GSF), inhibited the activation of matrix-metalloproteinase-2 (MMP-2) as well as migration of the human melanoma cells of the lines WM-115 and WM-266-4 in a two-dimensional migration assay. GSF inhibited completely the adhesion of WM-115 cells to the extracellular matrix (ECM) proteins, fibrinogen and fibronectin.

In an in vitro angiogenesis assay with human endothelial cells, GSF very effectively inhibited endothelial tubule formation and sprouting of blood vessels, as well as the adhesion of endothelial cells to ECM proteins. GSF was not cytotoxic at biologically active concentrations; neither were 3,4-bis{[(β-D-galactopyranosyl)oxy]methyl}furan (BGF) nor methyl β-D-galactopyranoside nor

3,4-bis(hydroxymethyl)furan, which were used as controls, eliciting comparable biological activity. In silico modeling experiments, in which binding of GSF to the extracellular domain of the integrin $\alpha_v\beta_3$ was determined, revealed specific docking of GSF to the same binding site as the natural peptidic ligands of this integrin. The sulfate in the molecule coordinated with one manganese ion in the binding site.

These studies show that this chemically easily accessible molecule GSF, synthesized in three steps from 3,4-bis(hydroxymethyl)furan and benzoylated galactose imidate, is nontoxic and antagonizes cell physiological processes in vitro that are important for the dissemination and growth of tumor cells in vivo.

Introduction

Adhesion of mammalian cells to the extracellular matrix (ECM) is mediated by protein–protein and protein–carbohydrate interactions. Alterations in the expression of cell-surface molecules lead to the dissemination of metastatic cells from tumor tissue [1,2]. Cell surface molecules in melanoma, which are important for their metastatic property, have been intensely investigated. Among these, integrins, which are hetero-dimeric integral membrane proteins, are involved in protein–protein mediated adhesion of cells to the extracellular matrix (ECM).

Aberrant levels of several integrins have been observed in malignant melanomas. While some integrins such as $\alpha_6\beta_1$ and $\alpha_v\beta_5$ are down-regulated, others such as $\alpha_v\beta_3$, $\alpha_4\beta_1$ and $\alpha_3\beta_1$ are up-regulated [3]. Integrins bind to ECM-proteins and this constitutes the strongest interaction in the adhesion processes. The importance of the fibrinogen receptor $\alpha_v\beta_3$ in malignancy is well described for melanomas [4]. It is also a prerequisite for the activation of pro-MMP-2, a secreted metalloprotease important for cell migration through the basal layer [5].

Due to the vast variability of branched saccharide chains, more specific interactions between cells and the ECM and among cells are mediated by binding of proteins such as lectins to oligosaccharides. Upon progression to higher malignancy, the glycosylation patterns of glycoproteins and glycosphingolipids on tumor cell surfaces undergo several alterations [6]. These changes are closely associated with distinct cellular processes, such as adhesion to the ECM, and modulation of the tumor-associated microenvironment, which represent advantages for the capacity of the cell to invade the host tissue and to secure undisturbed growth [7]. The glycosylation pattern of tumor cells is therefore the focus in the development not only of new tools for tumor diagnosis and monitoring but also in the design of new anticancer drugs [8]. Attempts have been made to mount an immune response against tumor oligosaccharides by carbohydrate vaccines [9] and also to inhibit adhesive processes, such as the interaction between oligosaccharides and lectins, by synthetic carbohydrate analogues [10-13].

Based on Schmidt's imidate strategy [14], we have developed a method for the synthesis of a library of saccharide-mimetics containing furans. Furan, especially as its bis-hydroxymethylated derivative, was chosen as a core molecule because it mimics a furanose but without an optically active center, making the synthesis of defined molecules much easier than on a furanose core. Synthetically it is easily accessible and is a dienophile, which allows attachment of marker molecules in a Diels–Alder reaction, leaving the hydroxy groups of the carbohydrate moieties unaffected [15]. With biotin-labeled Diels–Alder products of branched saccharide mimetics, discrete staining patterns were observed on surfaces of human epithelial tumor cells, but not on immortalized normal fibroblasts. Screening of the library to find members with anti-adhesive properties showed that 3,4-bis{[(β-D-galactopyranosyl)oxy]methyl}furan (BGF) could inhibit the adhesion of murine B16F10 melanoma cells to several ECM-proteins [15].

Probably, more important than uncharged saccharides are carbohydrates that contain acidic residues, such as sialic acids or sulfated saccharides. Glycosaminoglycans (GAG) are long polysaccharide chains containing sulfated saccharides of uronic acids (either iduronic or glucuronic acid) and glucosamine or galactosamine as repetitive disaccharide units. GAGs exist at the cell-surface as well as in the ECM and are attached to proteins [16]. Furthermore, the overexpression of the charged blood group antigen sialyl Lewis^x consisting of the terminal NeuNAcα2-3Galβ1-4(Fucα1-3)GlcNAc-group is correlated with carcinogenesis. It is recognized and bound by selectins, which are a subgroup of lectins that play an important role as cell-surface molecules [17]. Molecular dynamics simulations have shown that furans with two saccharides bound to hydroxymethyl groups show a nearly perfect alignment with each of the three terminal saccharides in Lewis^y [15], another member of the Lewis histo blood group family, which is involved in tumor cell adhesion [18] as well as in tumor-induced angiogenesis [19]. To further develop the molecules found to be biologically active in our earlier study, and because charged saccharides are important in tumor cell interactions, we decided to include a charged pharmacophor. Here, we describe the synthesis of (4-{[(β-D-galactopyranosyl)oxy]methyl}furan-3-yl)methyl hydrogen sulfate (GSF), which is a bifunctional saccharide mimetic consisting of a bis-hydroxymethylated furan core, a

galactose residue and a sulfate group. It represents a mimetic of the GAG-subunit and may interact with the cell-surface or the ECM. We report the inhibitory capacity of the lead compound GSF to block adhesion and migration both of tumor cells and vascular endothelial cells and endothelial-cell-mediated angiogenesis. Surprisingly, GSF may not only block carbohydrate–protein interactions but also integrin-mediated protein–protein interactions, and thus, represents a strong candidate for the design of saccharide mimetics to be used as antitumor drugs.

Results and Discussion

Syntheses of saccharide mimetics

Glycosylation of 3,4-bis(hydroxymethyl)furan (**1**) with 1.0 equiv imidate **2** in CH_2Cl_2 afforded 48% of monosaccharide **3**. The synthesis of (4-{[(β-D-galactopyranosyl)oxy]methyl}furan-3-yl)methyl hydrogen sulfate (GSF, **5**) was modified by using trimethylamine sulfur trioxide instead of pyridinsulfoxide. The advantage was a short reaction time of 5 h at 50–55 °C instead of at room temperature (rt). One equiv of the benzoylated furan galactoside **3** was reacted with five equiv of trimethylamine sulfur trioxide in DMF at 55 °C. After purification on silica with CH_2Cl_2/CH_3OH (5:1) the sulfate **4** was isolated in a yield of 95%.

Deprotection of the sulfated benzoylated furan **4** was carried out with freshly prepared sodium methylate in methanol at rt. After 10 h GSF (**5**) was obtained in a yield of 85%. It was found to be important that after the debenzoylation the aqueous medium be neutralized with 0.1 M HCl under control of a pH-meter, to pH 7.2. Under the highly acidic conditions induced by a Dowex H^+ ion-exchange resin, the free sulfate decomposes. The product was purified by silica gel chromatography (CH_3CN/H_2O, 95:5).

3,4-bis{[(β-D-galactopyranosyl)oxy]methyl}furan (BGF, **7**) was synthesized by glycosylating **1** with 2.5 equiv of imidate **2** to yield 60% benzoylated BGF **6**. After deprotection with CH_3ONa in CH_3OH, the reaction mixture was neutralized by the addition of ion-exchange resin (Dowex WX8 H^+) to yield 61% BGF (**7**) after recrystallization (Scheme 1).

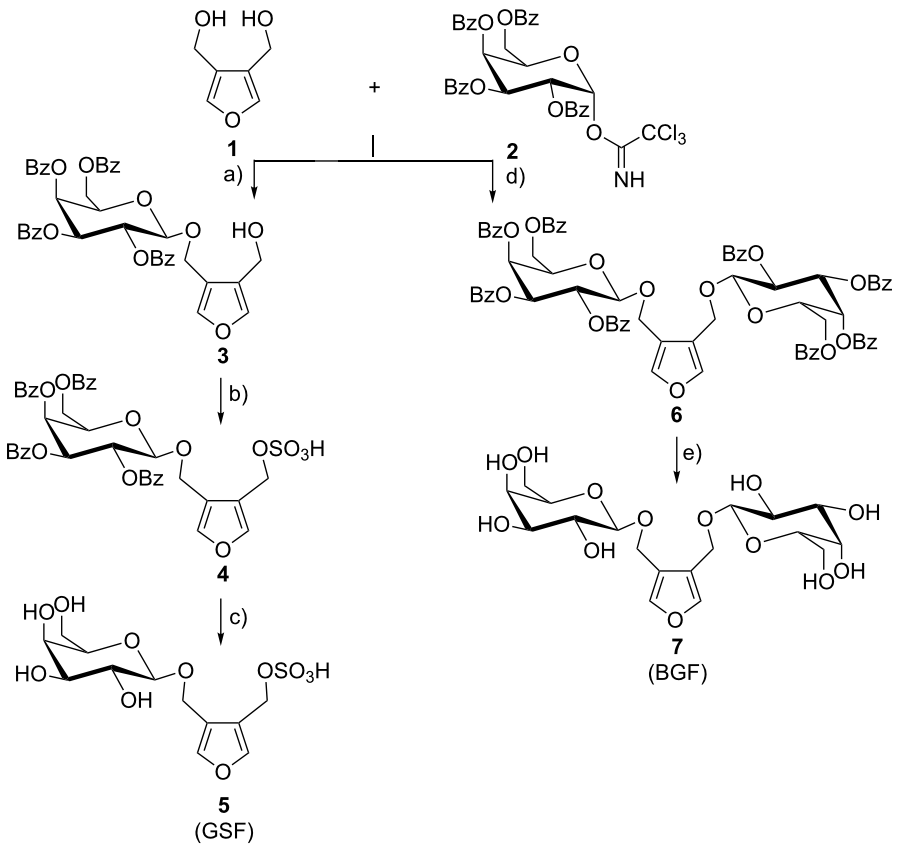

Scheme 1: Synthesis of (4-{[(β-D-galactopyranosyl)oxy]methyl}furan-3-yl)methyl hydrogen sulfate (GSF, **5**) and 3,4-bis{[(β-D-galactopyranosyl)oxy]methyl}furan (BGF, **7**); (a) 1 equiv 3,4-bis(hydroxymethyl)furan (**1**) and 1 equiv imidate **2** in CH_2Cl_2, TMSOTf, 0 °C, 2 h, yield: 48%; (b) 1 equiv **3** with 5 equiv $NMe_3{\cdot}SO_3$ in DMF, 55 °C, 5 h, yield: 95%; (c) NaOMe in MeOH, 10 h, rt, adjustment to pH 7.2 with 0.1 M HCl, yield: 85%; (d) 1 equiv 3,4-(bis-hydroxymethyl)furan (**1**) and 2.5 equiv imidate **2** in CH_2Cl_2, TMSOTf, 0 °C, 2 h, yield: 60%; (e) NaOMe in MeOH at 50 °C, neutralization with Dowex WX8 H^+, yield: 61%.

Analysis of cytotoxic effects of GSF toward human cells

Two human melanoma cell lines, WM-115, isolated from a primary cancer, and WM-266-4, isolated from its cutaneous metastasis, were used to initially screen the compounds. To exclude the idea that the observed effects of the synthesized compounds on the cell properties were caused by the compound killing the cells, the cytotoxicity was determined over time with the sulforhodamine-B assay. As an example, the growth of WM-115 cells over a period of 72 h with increasing concentrations of GSF is shown in Figure 1.

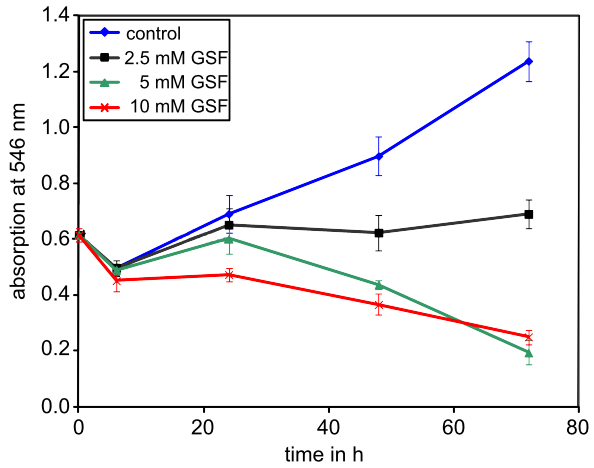

Figure 1: Effects of increasing concentrations of (4-{[(β-D-galactopyranosyl)oxy]methyl}furan-3-yl)methyl hydrogen sulfate (GSF) upon the growth of human melanoma cells WM-115. Cell densities were measured by staining adherent and fixed cells with sulforhodamine-B and solubilizing the dye with Tris base. Absorbance was determined at 546 nm. Absorbance values are proportional to cell numbers.

GSF had a cytostatic effect at 2.5 mM beyond 24 h and exhibited cytotoxic effects after 48 h at 5 mM. We also performed cytotoxicity assays by counting cells after trypan-blue staining for disrupted membranes, but the standard deviations are quite high with this assay. Here, 5 mM GSF resulted in 40% dead WM-266-4 cells after 48 h, while only 10% of the WM-115 cells were dead. At earlier time points, which are relevant for the assays described below, only 10 mM GSF was toxic to WM-266-4, and lower concentrations had no effect. The melanoma cells isolated from the cutaneous metastasis therefore seem to be a bit more sensitive. Therefore, GSF is a mildly toxic compound with an IC_{50} of more than 10 mM after 48 h.

In the cell adhesion assays described, cells were exposed to GSF for a very short period of 2 h. Up to 6 h no effect of GSF up to a concentration of 10 mM was observed (Figure 1). In addition, the viability of the cells in cell adhesion assays after incubation with the test compounds was checked in each assay by using trypan blue, and even at the highest concentration of 40 mM no cytotoxicity was detectable.

BGF up to a concentration of 40 mM was neither cytotoxic nor cytostatic to cells of these two melanoma lines. The human endothelial cells HBMEC-60 showed a similar sensitivity to GSF as the WM-115 cells, for which incubations beyond 72 h led to the arrest of cell growth at 5 mM, and 10 mM was cytotoxic after these long incubation times.

Inhibition of melanoma cell adhesion by a sulfated saccharide mimetic

In order to investigate the potential of the synthesized saccharide mimetics to interfere with the binding of the human melanoma line WM-115 to ECM proteins, we used a standard adhesion assay. Cells were radioactively labeled with [methyl-^{3}H]-thymidine and we found a linear relation between the incorporated radioactivity and the number of cells, between 1×10^4 and 7×10^4 cells. To find the optimal conditions for WM-115 cells, their adhesion to increasing amounts of fibrinogen and fibronectin from 0.1–2 µg per well was measured. WM-115 cells showed maximum adhesion to both proteins at amounts of 0.5 µg/well, when wells were coated as described in the experimental section. The number of adherent cells varied between 40% and 70% of the 5×10^4 cells added to one well. Reproducible values of around 50% adherence of cells were reached when cells were grown for 48 h before radioactive labeling. In general, more cells adhered to fibronectin than to fibrinogen.

WM-266-4 cells derived from the metastasis show a completely different growth and adhesion behavior compared to the cells isolated from the primary melanoma. Only 20–30% of the cells seeded on fibronectin or fibrinogen attached after 1 h. Results with inhibitors were therefore very difficult to perform, because the variation in attached cells in control wells was very high. Under normal culture conditions we always observed a lot of detached but viable cells. In wound-healing assays WM-266-4 cells very rapidly closed the wounds but were never as dense as WM-115 cells upon confluence. We therefore only used WM-115 cells for adhesion assays. These properties may point to high motility of a metastasis-derived cell line.

Our earlier results had shown oligosaccharide mimetics containing furan as the core molecules to modulate cell–ECM interactions. Especially 3,4-bis{[(β-D-galactopyranosyl)oxy]methyl}furan (BGF) had shown bioactivity by blocking the adhesion of murine B16F10 melanoma cells to murine fibronectin [15]. We have now obtained similar results with the human WM-115 melanoma, for which we observed a 30% reduction of the adhesion to human fibrinogen without any dose dependence between 5–40 mM BGF (Figure 2A). One-way

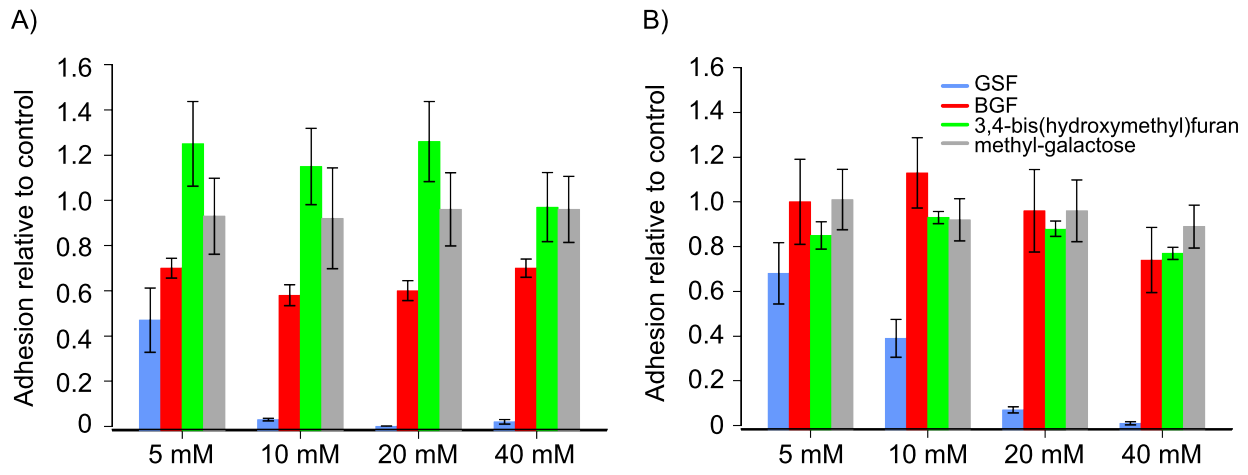

Figure 2: Inhibition of adhesion of WM-115 cells to fibrinogen (A), or to fibronectin (B) with increasing concentrations of (4-{[(β-D-galactopyranosyl)oxy]methyl}furan-3-yl)methyl hydrogen sulfate (GSF) (blue bars), 3,4-bis{[(β-D-galactopyranosyl)oxy]methyl}furan (BGF) (red bars), 3,4-bis(hydroxymethyl)furan (green bars), or methyl β-D-galactopyranoside (grey bars). Radioactively labeled cells were exposed to the compounds in medium for 1 h, then aliquots of the medium with 5×10^4 cells were seeded into a well precoated with the extracellular matrix protein and incubated for a further 1 h. Nonadherent cells were washed off and adherent cells quantified by liquid scintillation counting. Means of four values ± SD relative to cells adhering in the absence of the compounds are shown.

ANOVA analysis of variance showed the inhibition to be significant ($p < 0.001$) pointing to an optimal concentration of 10–20 mM BGF. In the presence of GSF we obtained a significant concentration-dependent decrease of adhesion to fibrinogen (one-way ANOVA $p < 0.001$), down to 3% adherent cells with 10 mM GSF. No inhibition could be seen with methyl β-D-galactopyranoside or 3,4-bis(hydroxymethyl)furan, demonstrating the importance of the sulfate- and the galactosyl-group as bioactive parts of the molecule.

The cell adhesion to fibronectin decreased significantly (one-way ANOVA $p < 0.001$) in a dose-dependent manner in the presence of GSF until cell binding was completely blocked at 40 mM (Figure 2B). No significant inhibition by either BGF, 3,4-bis(hydroxymethyl)furan, or methyl β-D-galactopyranoside was observed. In both experiments data analysis by two-way ANOVA showed significance for substance and concentration both with $p < 0.001$. The extent of inhibition of adhesion to fibronectin by GSF was weaker than to fibrinogen.

In the GSF molecule both the sugar and the sulfate moiety can interfere in several ways with cell–ECM binding. Carbohydrate–protein interactions may be inhibited by GSF binding to cell surface lectins, thereby perturbing the binding of the cell to the highly glycosylated ECM proteins [20], or by binding to lectin-like domains on fibronectin. The negatively charged sulfate group could also block cell–ECM interactions by interfering with heparin binding sites on fibronectin [21] and fibrinogen [22], which recognize the sulfated groups of cell-surface-expressed GAGs. GSF could mimic the highly sulfated GAG-building block. The result would be a reduction of free binding sites on the cell surface for natural ligands, such as sialyl-Lewis^x, sialyl-Lewis^a or GAG.

By completely blocking the cell adhesion of WM-115 cells to fibrinogen and fibronectin with GSF we inhibited all interactions of cells with the ECM. To characterize the affected interactions in more detail, cells were incubated with peptidic integrin ligands and GSF in combination.

The RGD motif (an arginine–glycine–aspartic acid peptide sequence) is recognized and bound by several integrins including $\alpha_v\beta_3$ and $\alpha_5\beta_1$. The sequence glutamic acid–isoleucine–leucine–aspartic acid–valine (EILDV) is the binding motif of ligands of the $\alpha_4\beta_1$ integrin. Both motifs are part of the amino acid sequence of fibronectin.

In initial experiments we investigated the inhibition of cell adhesion to fibronectin with increasing concentrations of the RGD-containing peptide: glycine–arginine–glycine–aspartic acid–serine–proline (GRGDSP) or EILDV. Neither peptide, up to 2 mM, completely inhibited adhesion of WM-115 cells to fibronectin. We then decided to combine the peptidic integrin ligands with GSF to see if an antagonism or additive effect upon cell adhesion occurs. For these experiments we chose 1 mM GRGDSP, 2 mM EILDV and 5 mM GSF.

A complete inhibition of cell adhesion to fibronectin was observed in the presence of 1 mM GRGDSP plus 2 mM EILDV (Figure 3), and, as shown in Figure 2B, with GSF concentrations of 40 mM. On the one hand, there was no detectable carbohydrate–protein interaction, because the combined synthetic peptidic integrin ligands completely blocked cell adhesion to fibronectin, but on the other hand, cell adhesion could be inhibited with the sulfated saccharide mimetic GSF, probably by interfering with protein–protein interactions. The effects of the single agents were additive, showing that they probably interact at different sites that are important for adhesion. The effect of GSF on cell adhesion is dependent on ECM proteins, since WM-115 cell adhesion on plastic was not influenced by GSF up to 20 mM. At 40 mM, only 40% inhibition of adhesion was observed (data not shown).

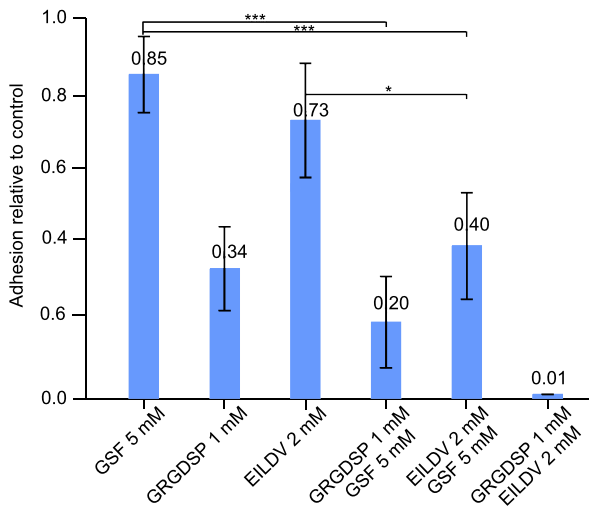

Figure 3: Inhibition of adhesion of melanoma cells WM-115 to fibronectin-coated plastic by 5 mM (4-{[(β-D-galactopyranosyl)oxy]methyl}furan-3-yl)methyl hydrogen sulfate (GSF), 1 mM glycine–arginine–glycine–aspartic acid–serine–proline (GRGDSP), 2 mM glutamic acid–isoleucine–leucine–aspartic acid–valine (EILDV), 1 mM GRGDSP plus 5 mM GSF, 2 mM EILDV plus 5 mM GSF, 1 mM GRGDSP plus 2 mM EILDV. Cells were radioactively labeled and incubated in the presence of the compounds indicated for a total of 2 h. Nonattached cells were then washed away and the remaining cells quantified by their radioactivity. Means of four values ± SD relative to cells adhering in the absence of the compounds are shown. One-way ANOVA followed by Bonferroni's Multiple Comparison Test showed combinations with GSF to be significant as indicated; * = $p < 0.05$, *** = $p < 0.001$.

Moitessier et al. [23] synthesized a combinatorial library of carbohydrate mimetics, based on xylose, as inhibitors of the integrins $\alpha_{IIb}\beta_3$ and $\alpha_v\beta_3$ and blocked binding to the natural ligand RGD, as reviewed by Gruner et al. [24]. Gottschalk and Kessler [25] created a β-D-mannose-containing inhibitor of $\alpha_4\beta_1$ based on in silico modeled structures.

In silico analysis of GSF interaction with integrins

Our data showing similar inhibition of melanoma cell attachment to fibronectin by GSF as by the combined integrin ligand peptides, also points to an interaction of GSF with integrins. To find possible binding sites for GSF, we used a "blind docking" approach to screen the protein surface of the extracellular domain of $\alpha_v\beta_3$, the crystal structure of which was published by Xiong et al. [26]. In an initial validation study, we performed multiple blind-docking experiments using the cyclic peptide Cilengitide® (cyclo-[RGDfN(Me)V]) [27] as a ligand. The orientation of the pentapeptide Cilengitide and its binding to the binding site formed by the α and β chains of $\alpha_v\beta_3$ reproduced the published X-ray structure with high accuracy.

The method thus validated was then used to dock GSF in silico to the same surface area. This resulted in two binding sites. One site was identical to the binding site described for the RGD motif [28] of the cyclic peptide and a second binding site was located inside the β-propeller domain of the α_v domain (Figure 4A). This binding site is probably a nonfunctional site since it is most likely not accessible for "surface bound" molecules such as ECM proteins. It is therefore possible that GSF blocks the functional binding site of natural ligands and the synthetic cyclic peptide Cilengitide (Figure 4B), explaining the observed interference with the adhesion of melanoma (Figure 2) and endothelial cells (Figure 7) to the extracellular matrix protein.

In order to investigate the molecular interactions of GSF in the RGD binding site of the integrin molecule in more detail we performed molecular dynamics (MD) simulation in explicit water. The MD simulation was started from the docked position of the GSF ligand. GSF slightly changed its position during the MD simulation, in which the sulfate group moved to the position that was occupied by the carboxylate group of the aspartic acid in the cyclic peptide (Figure 4C). The galactose forms several hydrogen bonds with the protein. A surface-water density analysis based on a MD simulation of the unligated protein in water revealed that the furan oxygen atom in GSF occupies the position of a (predicted) surface water-binding site.

Impact of (4-{[(β-D-galactopyranosyl)oxy]methyl}furan-3-yl)methyl hydrogen sulfate (GSF) on melanoma cell migration

Migration of malignant tumor cells is an important step in the process of metastasis. Diverse members of the integrin family as well as MMPs have been shown to play a crucial role in the motility of cells [29-31]. Using a two-dimensional migration assay, we observed the effect of GSF on migration of the human

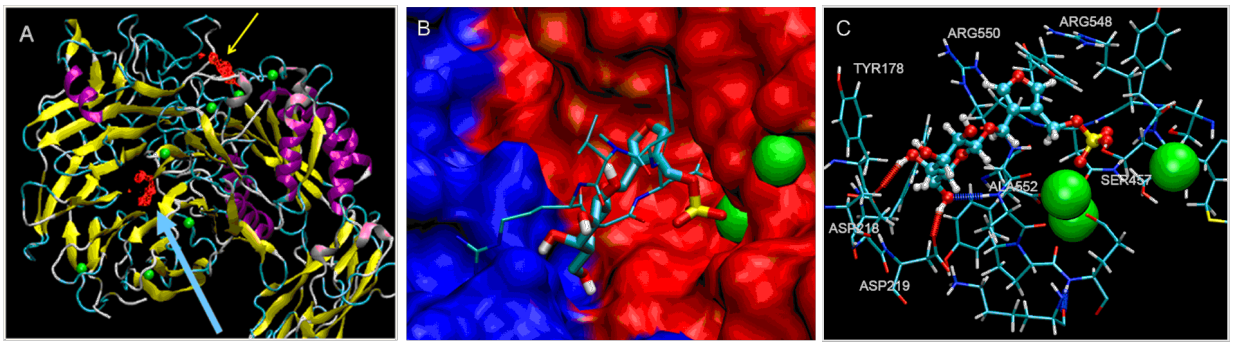

Figure 4: In silico blind-docking (A, B) and molecular dynamic simulations (C) of (4-{[(β-D-galactopyranosyl)oxy]methyl}furan-3-yl)methyl hydrogen sulfate (GSF) on the extracellular domain of the integrin $\alpha_v\beta_3$. A: The blind-docking studies showed a preferred binding of GSF (red) to the binding site of the natural peptide ligands on $\alpha_v\beta_3$ (yellow arrow). An additional binding site was predicted to be located inside the β-propeller domain of the α chain (blue arrow). B: Close-up of the binding site between the α_v (blue) and the β_3 (red) chain of the integrin showing the synthetic pentapeptide cyclo-[RGDfN(Me)V] with thin lines and GSF in broader lines. Carbon, oxygen, nitrogen and sulfur are shown in blue, red, dark blue, and yellow, respectively. The manganese ions are represented as green spheres. C: Molecular dynamics simulation in water of the GSF molecule showing hydrogen bonds of the galactose moiety with the amino acids in the binding site of integrin $\alpha_v\beta_3$ (Gal(OH4) with ASP218 and Gal(OH6) with ASP219/ALA552). The sulfate coordinates with one of the manganese ions.

melanoma lines WM-115 and WM-266-4 into a wound scratched into an intact cell monolayer.

The migration rates of the two untreated cell lines are clearly different. While WM-115 cells from the original tumor needed about 24 h for the wound to close (Figure 5), the WM-266-4 cells derived from the metastasis of the same primary tumor are about three times faster, almost completely closing the wound within 8 h.

Incubation of the WM cells with GSF at concentrations that inhibit integrin-mediated cell adhesion, leads also to interference of the cell migration. GSF at a concentration of 5 mM diminished the number of WM-115 cells migrating into the wound after 24 h (Figure 5), and as shown in Figure 1 this is not due to a toxic effect of GSF. The influence on WM-266-4 cells was even more pronounced. These cells changed their morphology after 8 h by rounding up without complete detachment of the cells. After 24 h no more attached cells could be

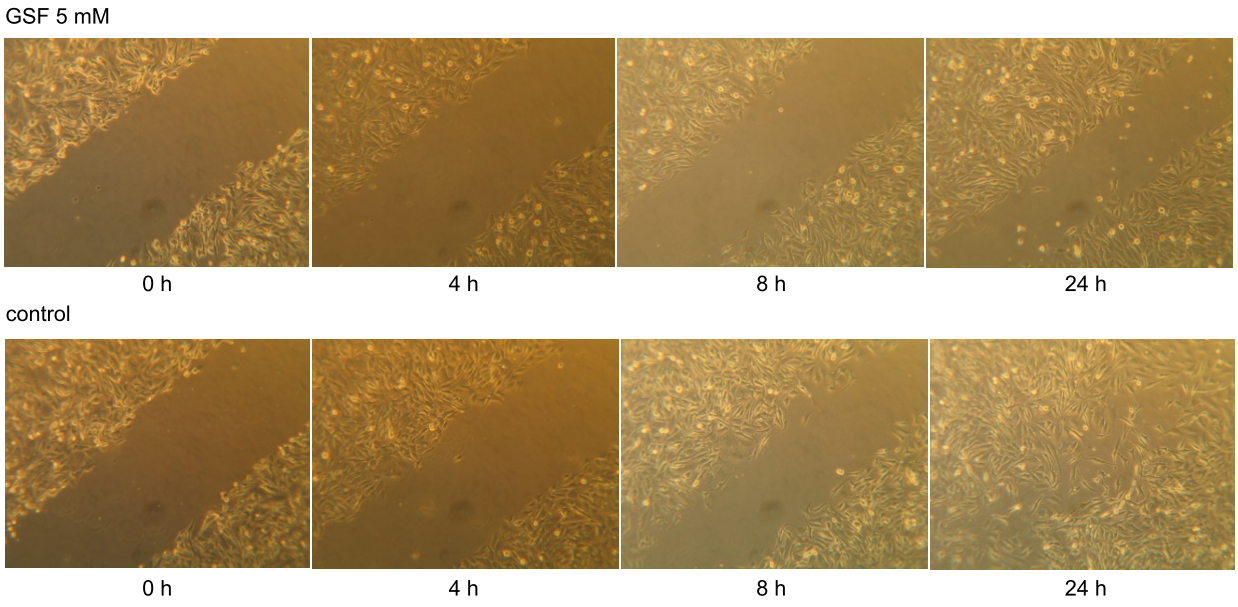

Figure 5: Intact cell monolayers of WM-115 cells in 12-well plates were wounded with a 100 µL pipette tip and washed three times with serum-free medium. Complete medium either containing 5 mM (4-{[(β-D-galactopyranosyl)oxy]methyl}furan-3-yl)methyl hydrogen sulfate (GSF) (upper row) or without GSF (lower row) was added to the wells, and cell migration into the wound was observed by microscopy after 0, 4, 8 and 24 h.

detected, but the detached cells were still viable (trypan-blue exclusion test) (data not shown). Binding of GSF to $\alpha_v\beta_3$ probably leads to the loosening of focal adhesion plaques and detachment of cells from their adjacent matrix. This interaction would also explain a weaker effect of GSF on WM-115 cells, because their star-like, lamellipodic structure contains more focal adhesions than the filopodia of WM-266-4. These results confirm the assumption of an antagonistic effect of GSF on cell-surface molecules such as integrins.

Impairment of MMP-2 activity by GSF

Matrix metalloproteinases (MMP) play a critical role in the invasion of tumor cells and metastasis formation. MMP-2, an ECM degrading gelatinase, is directly associated with tumor progression in a variety of cancer diseases [32]. The importance of active MMP-2 in melanoma progression is summarized in a review [33].

Because GSF inhibited the $\alpha_v\beta_3$-mediated adhesion of WM-115 cells to fibrinogen, it may also influence the activation of MMP-2. The enzymatic activity of gelatinases such as MMP-2 can be determined in serum-free medium in which cells were grown for several days, i.e., serum-free conditioned medium (SFCM). After separation of proteins by electrophoresis in a polyacrylamide gel containing gelatin, the gelatinolytic activity can be determined after renaturation of the enzymes and visualized by staining the gel with Coomassie blue, in which white bands in a blue gel show enzymatic activity at the molecular weight of the enzymes. This process is called zymography and was performed to study the activation status of MMP-2 after incubation of the melanoma cells with GSF. Functionally active MMP-2 (64 kD) was found in SFCM in which WM-115 and WM-266-4 cells had been incubated while no bands of the proforms could be observed (Figure 6A, lanes „control“).

Bands were identified as MMP-2 in a Western blot with an anti-MMP-2 antibody (Figure 6B). With increasing concentrations of GSF the active MMP-2 form disappeared and the intermediate (68 kD) and inactive proform (72 kD) were detectable in SFCM from both cell lines (Figure 6A). In SFCM of WM-115

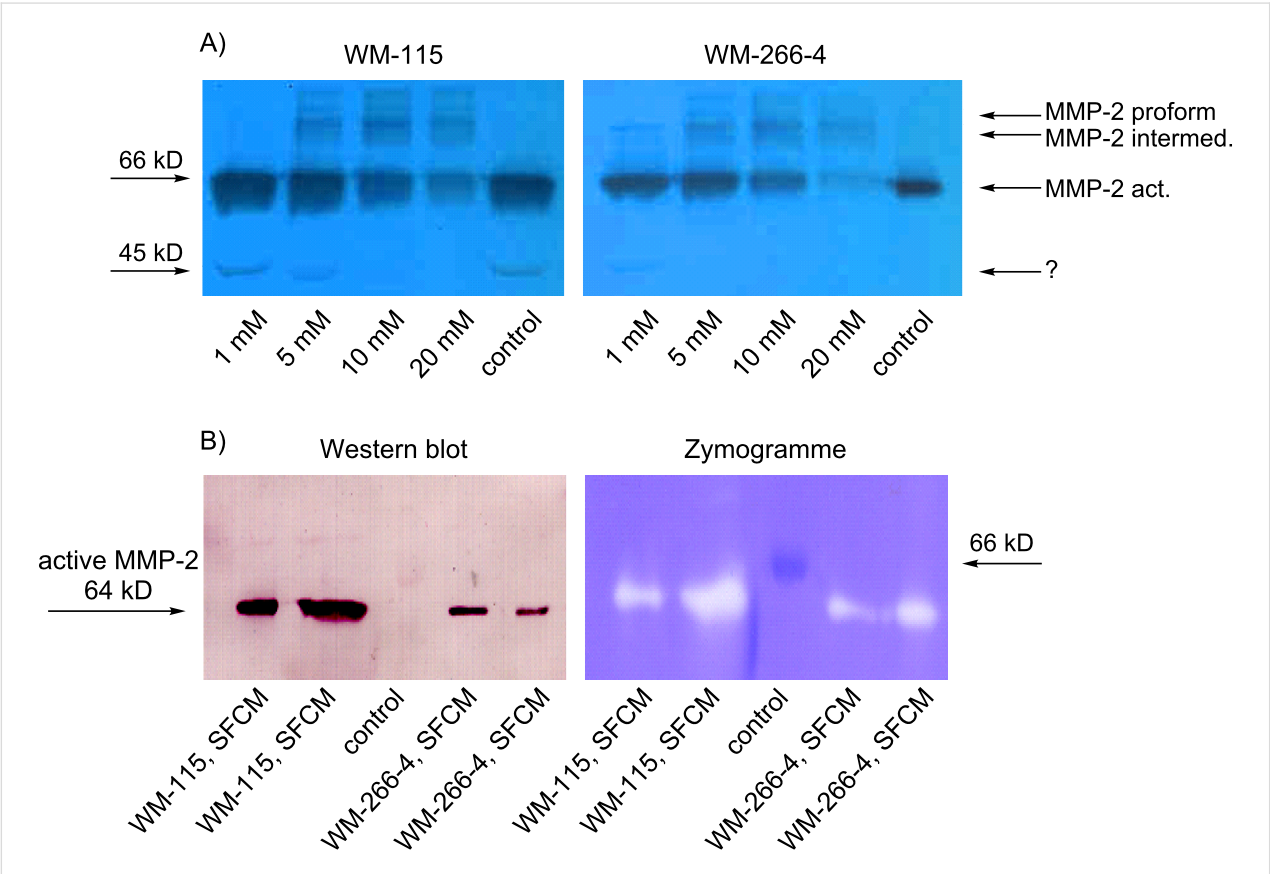

Figure 6: A: Zymograms (color inverted) of serum-free conditioned medium of melanoma cells treated with (4-{[(β-D-galactopyranosyl)oxy]methyl}furan-3-yl)methyl hydrogen sulfate (GSF) for 24 h at the concentrations indicated. Dark bands are the result of gelatinolytic activity of the proteins migrating into the gel. Molecular weights in kilodalton (kD) are indicated on the left. B: Western blot on the left analyzed with anti-MMP-2 antibodies showing that the gelatinolytic activity determined in parallel in the gel on the right is caused by activated MMP-2. “Control” lane is a molecular weight standard (albumin).

cells an unknown gelatinolytic band of 45 kD appeared in the samples, which disappeared also with higher concentrations of GSF. Incubation of the cells with 20 mM GSF showed an overall reduction of the gelatinolytic activity, probably due to a cytotoxic effect of GSF at higher concentrations in serum-free medium, which is a stressful condition for cells routinely cultivated in the presence of 10% fetal bovine serum (FBS) (Figure 1).

Brooks et al. [5] proposed an activation model for MMP-2 in which the gelatinase is recruited to the cell surface by the binding of pro-MMP-2 and active MMP-2 to integrin $\alpha_v\beta_3$. After cleavage, active MMP-2 is liberated and degrades ECM components such as collagen type IV. Hofmann et al. [34] proposed a second activation model, which is also associated with binding of the pro-MMP-2 to $\alpha_v\beta_3$ in addition to membrane-bound matrix metalloprotease MT1-MMP, suggesting that this integrin plays a crucial role in MMP-2 activation.

Teti et al. [35] observed increasing MMP-2 activity after incubation with the $\alpha_v\beta_3$-integrin-ligand GRGDSP, similar to the activation seen upon binding of cells to fibronectin or fibrinogen. However, GSF, which inhibits cell adhesion to both ECM-proteins, inhibits the cleavage of the MMP-2 pro-sequence.

A GSF–$\alpha_v\beta_3$ interaction could directly or allosterically inhibit binding of pro-MMP-2 to the integrin, and our in silico blind-docking studies (Figure 4) have shown GSF to bind to another domain on $\alpha_v\beta_3$ in addition to the RGD binding site. Alternatively, GSF could bind to the ECM and thereby inhibit cell adhesion and MMP-2 activation. The lack of inhibition of cell adhesion to plastic by GSF points to such a mechanism. A reduction of the gelatinase MMP-2 and its proforms could also be caused by lower pro-MMP-2 expression upon GSF binding or its cellular uptake.

Effects of saccharide mimetics on adhesion, migration and tubule formation of vascular endothelial cells

Endothelial cells play a central role in the process of angiogenesis, which is stimulated and regulated by a complex network of chemo- and cytokine-signaling. One of the pivotal angiogenic factors is the vascular endothelial growth factor (VEGF); in addition, the initial steps of angiogenesis may also be stimulated by inflammatory growth factors, such as the tumor necrosis factor (TNF) [35-39]. During the first stages of vessel formation endothelial cells have to adhere to and migrate along the extracellular matrix, build contacts between each other, and finally form tubules [40,41].

In order to evaluate the influence of saccharide mimetics on endothelial vessel formation we studied the effects of GSF and BGF in several in vitro endothelial cell assays. For our studies we used a transformed human endothelial cell line (HBMEC-60) derived from bone marrow [42], which, in its biological characteristics, is similar to primary endothelial cells, such as human umbilical cord vein endothelial cells (HUVEC) [19,43].

The influence of GSF on the adhesion of HBMEC-60 endothelial cells to ECM components was tested using plates coated with fibronectin, laminin or collagen. Addition of GSF to the cells in medium inhibited the adhesion of these cells to all three matrix components in a dose-dependent fashion (Figure 7). Cell adhesion was strongest to fibronectin and collagen, and weaker to laminin in the absence of GSF. A significant inhibition of adhesion to fibronectin was observed at a concentration of 5 mM GSF (approximately 28% inhibition). This result is similar to that obtained with GSF-mediated inhibition of adhesion of WM-115 melanoma cells to fibronectin (Figure 2). At concentrations of 10 mM GSF adhesion to all three ECM components was inhibited by about 40%.

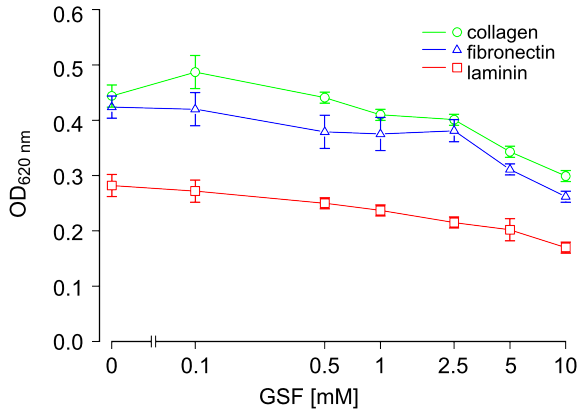

Figure 7: Adhesion of HBMEC-60 to extracellular matrix proteins. Prior to the adhesion experiments, HBMEC-60 cells were incubated for 30 min with (4-{[(β-D-galactopyranosyl)oxy]methyl}furan-3-yl)methyl hydrogen sulfate (GSF) at the concentrations indicated. The cells were then seeded onto plates coated with fibronectin, collagen or laminin. After 30 min nonadherent cells were removed, and adherent cells were fixed, stained with methylene blue, and washed; the cell-bound dye was then extracted and the absorption determined photometrically. In some experiments cells were also stimulated with TNF as described in the Experimental section. TNF pretreatment of cells resulted in virtually the same adhesive properties as without TNF and with a significant inhibition of adhesion by GSF at 5 mM. The values shown are the mean and SD of six replicates. The same results were obtained in two independent experiments.

In a subsequent step, we assessed the influence of GSF on the migration of HBMEC-60 cells through 8 µm pores in polycarbonate transwells coated with extracellular matrix proteins. For

this assay endothelial cells were stimulated before seeding into the plates, with either VEGF or TNF as indicated. Inhibition of migration and adhesion to the lower side of the transwells was observed at a concentration of 1 mM GSF and increased up to 10 mM for all three matrix components, although to different extents. Two-way ANOVA analysis showed significant effects of concentration ($p < 0.001$) and substance ($p < 0.001$) on migration. One-way ANOVA showed significant ($p < 0.001$) concentration dependence for GSF on all three matrix proteins. The strongest inhibitory effects were obtained after TNF stimulation at a concentration of 10 mM GSF on collagen-coated plates (Figure 8). It has to be noted that BGF, though much weaker than GSF, also inhibited migration and adhesion (data not shown).

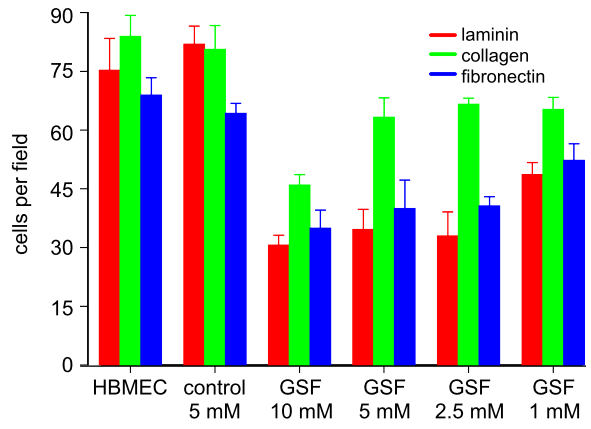

Figure 8: Effect of (4-{[(β-D-galactopyranosyl)oxy]methyl}furan-3-yl)methyl hydrogen sulfate (GSF) on transmigration of HBMEC-60 cells on transwell plates with 8 µm pores and adhesion to matrix components on the lower side of the wells. Cells were stimulated with TNF, then GSF or 3,4-bis(hydroxymethyl)furan (control), or medium only (HBMEC), were added. Cells were seeded into transwell inserts coated with extracellular matrix proteins as indicated. After incubation for 30 min nonadherent cells were washed away, and cells sticking to the proteins were fixed, stained and quantified. Shown is an exemplary experiment with TNF-stimulated HBMEC-60 cells. The experiments were performed in triplicate and in three independent experiments for each extracellular matrix protein.

As described earlier, migration of WM-115 (Figure 5) and WM-266-4 melanoma cells observed in a two-dimensional migration assay system was also inhibited by GSF. It therefore seems that adhesion and migration both of human tumor and endothelial cells are affected by GSF, pointing to a more general mechanism, possibly mediated by several different forms of integrin that adhere to either, collagen, fibronectin or laminin. Besides perturbing integrin-ECM protein–protein interactions, GSF may also interfere with ionic forces between charged ECM proteins and cells due to the negative charge of the sulfate.

In order to investigate cell biological features that are more specific for endothelial cells, we looked at contact and network formation between endothelial cells under the influence of saccharide mimetics as measured in the matrigel-assay. The cells were prestimulated with either VEGF or TNF for 24 h and then added to the plates coated with a complex extracellular matrix (matrigel). Network formation of cells in the presence of mimetics was observed after an overnight incubation period. As shown in Figure 9A, a concentration of 2.5 mM GSF already severely disturbed the formation of interendothelial cell contacts, and at higher GSF concentrations no contacts at all were built. It has to be noted that at a concentration of 5 mM GSF, and to a somewhat lesser extent also at 10 mM GSF, the endothelial cells were still viable such that GSF disturbs the initial phases of their networking rather than their viability and proliferation.

Although the in silico studies described earlier predict an interaction of GSF with the RGD binding site on integrins, and integrin $\alpha_v\beta_3$ antagonists have been shown to block angiogenesis [45], we cannot rule out that this saccharide mimetic also competes with cell-surface-bound oligosaccharides interacting with the respective binding partners on neighboring cells. In this respect our results are reminiscent of a previous study in which we described the inhibition of endothelial networking by monoclonal antibodies against the histo blood group oligosaccarides Lewis^y and H and further by siRNA inhibition of the fucosyltransferase FUT1 and GDP-4-keto-6-deoxymannose-epimerase/reductase (FX-protein) [19]. The FX-protein is required for de novo synthesis of GDP-fucose from GDP-mannose [46], whereas FUT 1 catalyzes the α_2 fucosylation of blood group H type 1 and Lewis^y oligosaccharides. The fucosylated oligosaccharides Lewis^y and H are strongly expressed on the cellular extensions that form the first contacts between endothelial cells. From these experiments we concluded that fucosylation of oligosaccharide chains is necessary for the first steps in the lining-up of endothelial cells and ensuing tubule formation. In our earlier study we reported that bis-glycosylated 3,4-bis(hydroxymethyl)furan derived saccharide mimetics containing fucose and galactose or two galactoses showed good structural agreements with the terminal oligosaccharides of Lewis^y by in silico MD simulation, and at the same time these mimetics showed biological activities [15]. Lewis^y has been reported to be part of the oligosaccharide moiety of the $\alpha_5\beta_1$ integrin interacting with fibronectin [47]. Therefore, the inhibitory activity of GSF with regard to integrin-mediated processes may be caused by blockade of the RGD site as well as by interfering with the oligosaccharides of the respective integrin. Further studies are needed to show whether GSF indeed interacts with oligosaccharide binding sites on cells and therefore contributes to the inhibition of cell–cell communication.

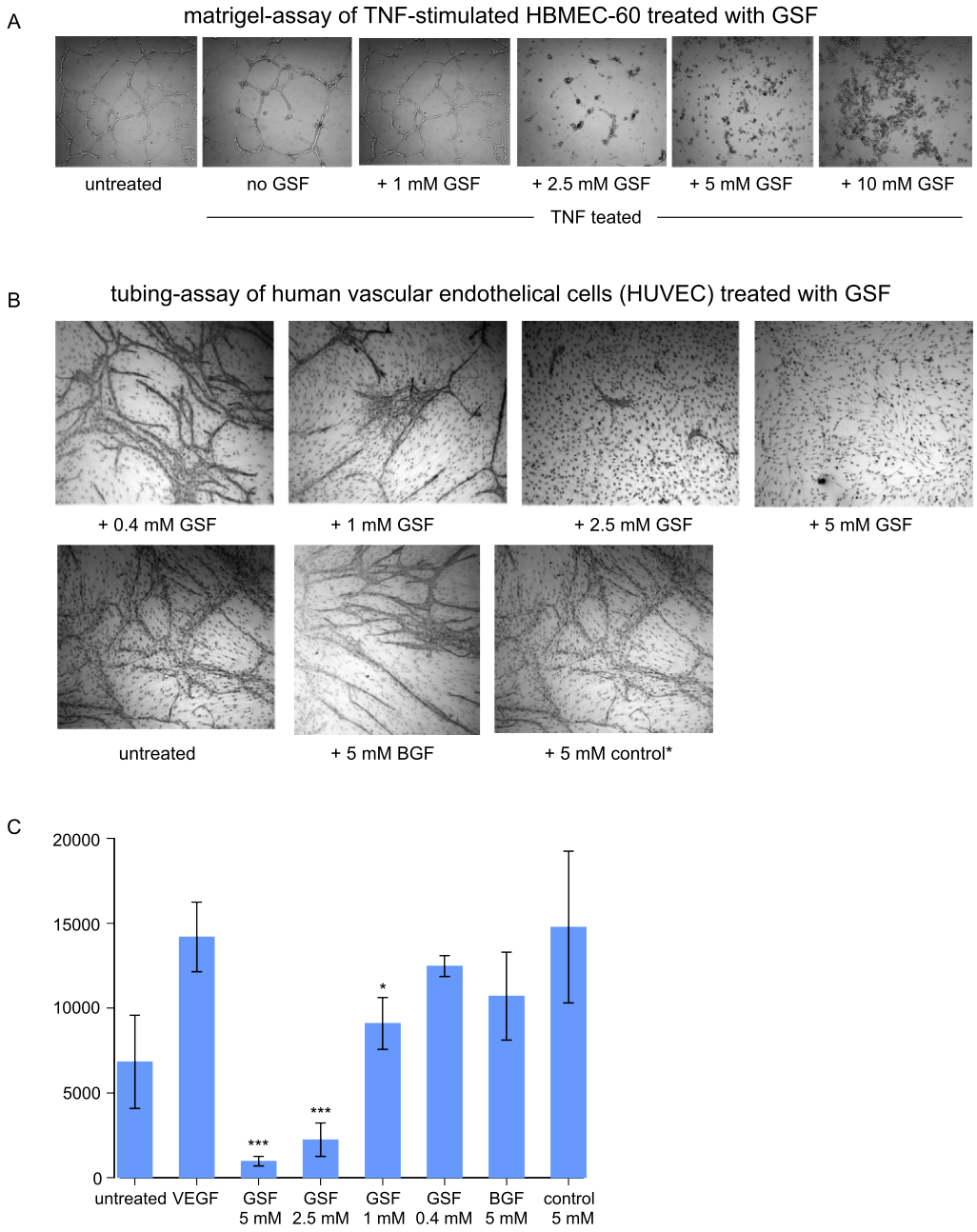

Figure 9: Influence of saccharide mimetics on endothelial networking (matrigel-assay) (A) and tube formation (B,C). A: The matrigel-assay is used to assess the initial stages of tube formation, i.e., the lining-up and subsequent formation of networks between endothelial cells. In the experiment shown, cells were stimulated with TNF or left untreated for 24 h, then (4-{[(β-D-galactopyranosyl)oxy]methyl}furan-3-yl)methyl hydrogen sulfate (GSF) was added in the concentrations indicated. The cells were then seeded onto the matrigel, which consists of a solubilized complex basement membrane of the EHS mouse tumor [44], and incubated overnight. B: The tubing assay measures the formation of endothelial tubules in a coculture of HUVEC and fibroblast cells (dots seen in the background). VEGF, which is necessary for proper in vitro tubule formation, was added at day 0 to the cells together with GSF or 3,4-bis{[(β-D-galactopyranosyl)oxy]methyl}furan (BGF) in the concentrations indicated. As one control, tubule formation is shown with VEGF only (untreated) or with 3,4-bis(hydroxymethyl)furan (5 mM control*). The growth media including growth factors and the respective mimetics were changed at days 4 and 7. At day 9 the medium was removed and the endothelial cells were stained with a monoclonal antibody against the cell surface antigen CD31 to allow evaluation of tubule formation. The assay was performed in three independent experiments with the same results in terms of the GSF effect. C: The tubule formation as observed under the microscopic was quantitatively analyzed using Angiosys 1.0 software, which counts the total tubule length, number of tubules and junctions between different tubules. Here, we show the results for total tubule length of an experiment performed as shown in panel B. The values are means and standard deviations of three experiments, * = $p < 0.05$, *** = $p < 0.001$ of the GSF exposed cells compared to VEGF alone. ANOVA one-way analysis of variance showed the concentration dependence of the GSF effect to be significant with $p < 0.0001$. The results for the other parameters reflected the same tendency of inhibitory capacity of GSF with increasing concentrations.

As expected from the results of the matrigel assay, GSF also inhibited the sprouting of endothelial cells and their tubule formation in the long-term tube-formation assay of HUVEC cells cocultivated with fibroblasts in a dose-dependent manner (Figure 9B and Figure 9C). An inhibitory effect of GSF could be already observed at a concentration of 0.4 mM and increasingly in a dose-dependent manner up to 5 mM GSF. In contrast, even 5 mM BGF showed a very minor effect on tubule formation, indicating that GSF had a specific inhibitory effect on in vitro angiogenesis.

Conclusion

We have described the synthesis of the lead compound (4-{[(β-D-galactopyranosyl)oxy]methyl}furan-3-yl)methyl hydrogen sulfate (GSF) and its possible biological application with regard to the inhibition of tumor cell adhesion to an extracellular matrix, and to interference with endothelial cell-mediated angiogenesis. GSF thus targets three important aspects of metastasis, namely tumor cell invasion, the adhesion of the cells to extracellular matrix proteins, and the ensuing angiogenesis enabling tumor growth. These properties make this lead compound interesting for further development as an anti-cancer drug. The integrins $\alpha v\beta_3$ and $\alpha_5\beta_1$ are highly expressed on activated endothelia of tumor tissues and, thus, represent ideal targets for cancer treatment. In this respect, GSF may occupy the same binding site on these integrins as the cyclic RGD pentapeptide Cilengitide®, which targets the integrins $\alpha v\beta_3$ and $\alpha_5\beta_1$. Cilengitide has been described as a strong inhibitor of angiogenesis and is currently under investigation in several clinical trials for the treatment of recurrent malignant glioblastoma [48]. GSF, due to its direct anti-tumor and anti-angiogenic effect, may represent a new class of small-molecule anticancer drugs. Although anti-angiogenic drugs such as the monoclonal antibody Avastin®, which blocks the activity of VEGF, are already in clinical use for tumor therapy, they cannot prevent overall progression of malignant cancers. This may be due to the tumors mounting a resistance against these treatments, e.g., by using mechanisms of blood-vessel formation other than VEGF-mediated ones. Therefore, there is a strong need to develop new anti-angiogenic drugs for tumor treatment. Saccharide mimetics, as shown here, may have an excellent potential, not only because of their inhibition of angiogenesis but also because of their ability to directly interfere with mechanisms that are essential for metastasis formation.

An advantage of saccharide mimetics such as GSF, also in comparison to more complex oligosaccharide mimetics, is their chemically easy accessibility and their potential for further derivatization. In this respect, GSF is a lead compound, which upon minor variations in its molecular structure, such as the introduction of a second sulfate or the replacement of the sulfate by a halogen, may become even more potent [49]. Further systematic tests are needed to investigate the structure–activity relationship.

Experimental

General

Commercially available reagents and anhydrous solvents were used without further purification unless stated otherwise. TMSOTf was from Acros, Geele, Belgium, all other chemicals were from either Sigma-Fluka, Taufkirchen, Germany, Fisher Scientific, Schwerte, Germany or Merck Schuchardt, Darmstadt, Germany. Thin-layer chromatography was performed on TLC plates Si 60 F_{254} (Merck) in petroleum ether (PE), ethyl acetate (EE) or other solvents as indicated, and compounds were visualized under UV and after spraying with a cerium-molybdate spray reagent (20 g ammonium molybdate, 0.4 g cerium(IV) sulfate in 400 mL 10% sulfuric acid) or vanillin–sulfuric acid spray reagent (1% vanillin in 15% sulfuric acid). Column chromatography was performed on silica gel (63–200 mesh, particle size 60 Å, MP Biomedicals, Eschwege, Germany), Dowex WX8 H^+ was from Serva, Heidelberg, Germany. Analytical HPLC was performed on a Jasco HPLC system by using a Lichrosphere-RP18 (e)-5µ, 250/4 mm column for reversed-phase chromatography unless stated otherwise. The UV detector was set to 210 nm to monitor the signals of the analytes.

^{1}H and ^{13}C NMR spectra were recorded on a Bruker AM 250 (250 MHz for ^{1}H and 63 MHz for ^{13}C) instrument (Bruker, Rheinstetten, Germany) with Me_4Si ($\delta = 0$) as the internal standard. Mass spectrometry electrospray ionization (ESI–MS) measurements were recorded on a Finnigan MAT TSQ 7000 instrument. All measurements were performed at the central spectroscopy unit of the DKFZ.

Synthesis of 3,4-bis{[(β-D-galactopyranosyl)oxy]methyl}furan (BGF, 7): 2,3,4,6-Tetra-*O*-benzoyl-β-D-galactopyranose was synthesized by ChemCon GmbH (Freiburg, Germany). 2,3,4,6-Tetra-*O*-benzoyl-β-D-galactopyranosyl trichloroacetimidate (**2**) was synthesized according to Schmidt et al. [14]. 3,4-Bis(hydroxymethyl)furan (**1**) was synthesized according to [50].

For 3,4-bis{[(2,3,4,6-tetra-*O*-benzoyl-β-D-galactopyranosyl)oxy]methyl}furan (**6**) TMSOTf (100 µL) was added to a solution of furan **1** (1.28 g, 10 mmol) and imidate **2** (18.5 g, 25.0 mmol) in dry CH_2Cl_2 (150 mL) at −40 °C. The reaction was stirred for 2 h at 0 °C and then extracted with aq. $NaHCO_3$ (100 mL) and H_2O (100 mL). After evaporation of the solvent the product was recrystallized from PE/EE, 1:1. The bis-galactoside **6** (7.70 g, 6 mmol) was obtained in 60% yield as a white

foam. TLC (PE/EE 3:1) R_f 0.1; ESI–MS (*m/z*): 1285.4 $[M + H]^+$ (2), 1302.5 $[M + NH_4]^+$ (10), 1307.4 $[M + Na]^+$ (100); HPLC: (*n*-hexane/THF 80:20→50:50 in 10 min, Purosphere-Si80-5µ, 125/4 mm) t_R7.9 min; ^{1}H NMR (250 MHz, $CDCl_3$) δ 3.80 (dt, $J_{4',5'}$ = 1 Hz, $J_{5',6a'} = J_{5',6b'}$= 6.5 Hz, 2H, 2 H5′), 4.11 (d, $J_{1',2'}$ = 7.8 Hz, 2H, 2 H1′), 4.21 (d, $J_{O\text{-}CHa,O\text{-}CHb}$ = 11.4 Hz, 2H, 2 O-CH_a), 4.34 (dd, $J_{6a',6b'}$ = 11.2 Hz, 2H, 2 $H6_a$′), 4.57 (dd, 2H, 2 $H6_b$′), 4.63 (d, 2H, 2 O-CH_b), 5.41 (dd, 2H, $J_{2',3'}$ = 10.4 Hz, $J_{3',4'}$ = 3.5 Hz, 2 H3′), 5.66 (dd, 2H, 2 H2′), 5.84 (dd, 2H, 2 H4′), 8.09–7.19 (m, 42H, 40 Ar-H, H2, H5); ^{13}C NMR (63 MHz, $CDCl_3$) δ 61.62, 62.00 (2 C6′, 2 O-CH_2), 68.06, 69.82, 71.15, 71.40 (2 C2′, 2 C3′, 2 C4′, 2 C5′), 99.68 (2 C1′), 120.32 (C3, C4), 128.30, 128.57, 128.71, 128.83, 129.00, 129.48, 129.63, 129.74, 129.87, 130.02, 133.29, 133.38, 133.59 (48 Ar-C), 142.41 (C2, C5), 164.90, 165.54, 165.98 (8 CO).

Deprotection to 3,4-bis{[(β-D-galactopyranosyl)oxy]methyl}furan (BGF, **7**): The bis-galactoside **6** (2.00 g, 1.56 mmol) was added to a freshly prepared solution of sodium (0.5 g) in methanol (50 mL). The resulting suspension was heated to 50 °C until it was clear. When debenzoylation of **6** was complete (monitored by TLC) the solution was neutralized with Dowex WX8 H^+, the solvent evaporated, the product dissolved in H_2O (50 mL) and extracted twice with diethylether (50 mL), the H_2O evaporated and the product crystallized from methanol. BGF (**7**, 430 mg, 0.95 mmol) was obtained with 61% yield as a white foam. TLC ($CHCl_3$/EtOH 4:1) R_f 0.8; ESI–MS (*m/z*): 453.0 $[M + H]^+$ (12), 470.1 $[M + NH_4]^+$ (28), 475.0 $[M + Na]^+$ (100), 922.5 $[2M + H]^+$ (2), 927.4 $[2M + Na]^+$ (5); HPLC: (CH_3CN/H_2O 0:100→100:0 in 40 min) t_R 5.8 min; ^{1}H NMR (250 MHz, D_2O) δ 3.53 (dd, $J_{1',2'}$ = 7.7 Hz, $J_{2',3'}$ = 9.9 Hz, 2H, 2 H2′), 3.63 (dd, $J_{3',4'}$ = 3.4 Hz, 2H, 2 H3′), 3.69 (ddd, $J_{4',5'}$ = 0.9 Hz, $J_{5',6a'}$ = 4.3 Hz, $J_{5',6b'}$ = 7.8 Hz, 2H, 2 H5′), 3.75 (dd, $J_{6a',6b'}$ = 11.5 Hz, 2H, 2 $H6_a$′), 3.82 (dd, 2H, 2 $H6_b$′), 3.92 (dd, 2H, 2 H4′), 4.47 (d, 2H, 2 H1′), 4.71 (d, $J_{O\text{-}CHa,O\text{-}CHb}$ = 11.8 Hz, 2H, 2 O-CH_a), 4.92 (d, 2H, 2 O-CH_b), 7.64 (s, 2H, H2, H5); ^{13}C NMR (63 MHz, D_2O) δ 65.58, 65.80 (2 C6′, 2 O-CH_2), 73.25, 75.26, 77.39, 79.73 (2 C2′, 2 C3′, 2 C4′, 2 C5′), 105.90 (2 C1′), 124.83 (C3, C4), 148.07 (C2, C5).

Synthesis of (4-{[(β-D-galactopyranosyl)oxy]methyl}furan-3-yl)methyl hydrogen sulfate (GSF, 5): 3-Hydroxymethyl-4-{[(2,3,4,6-tetra-O-benzoyl-β-D-galactopyranosyl-1-yl)-oxy]methyl}furan (**3**) was synthesized by adding TMSOTf (100 µL) to an ice cooled solution of furan **1** (2.92 g, 22.3 mmol) and imidate **2** (17.2 g, 22.3 mmol) in dry CH_2Cl_2 (150 mL). The reaction was stirred for 2 h at 0 °C, and 1 h at rt, and then stopped by neutralization with triethylamine. The solvent was evaporated and the product purified by silica gel column chromatography (PE/EE = 7:3→1:1). The monoglycoside **3** (7.2 g, 10.1 mmol) was obtained with 48% yield as a white foam. TLC (PE/EE 7:3) R_f 0.27; HPLC: (CH_3CN/H_2O, 0:100→100:0 in 60 min) t_R 53 min; ESI–MS (*m/z*): 729.4 $[M + Na]^+$ (100); ^{1}H NMR (250 MHz, $CDCl_3$) δ 4.36 (m, 3H, CH_2-furan, H5′), 4.46 (dd, $J_{5',6a'}$ = 6.3 Hz, $J_{6a',6b'}$ = 11.4 Hz, 1H, $H6_a$′), 4.67 (d, *J* = 12.2 Hz, 1H, CH_aOGal), 4.70 (dd, $J_{5',6b'}$ = 6.5 Hz, 1H, $H6_b$′), 4.88 (d, 1H, CH_bOGal), 4.94 (d, $J_{1',2'}$ = 7.9, 1H, H1′), 5.61 (dd, $J_{2',3'}$ = 10.4 Hz, $J_{3',4'}$ = 3.7 Hz, 1H, H3′), 5.84 (dd, 1H, H2′), 6.00 (dd, 1H, H4′), 7.4–8.12 (m, 22H, 20 Ar-H, H2, H5); ^{13}C NMR (63 MHz, $CDCl_3$) δ 55.62 (CH_2OH), 62.21 (CH_2OGal), 69.72, 71.15, 71.2, 76.38 (C2′, C3′, C4′, C5′), 99.7 (C1′), 120.26 (C3), 124.2 (C4), 128.1–133.6 (20 × CBz), 142.4 (C2, C5), 164.7–166.1 (4 × CO).

Synthesis of (4-{[2,3,4,6-tetra-O-benzoyl-β-D-galactopyranosyl)oxy]methyl}furan-3-yl)methyl hydrogen sulfate (**4**): To a solution of furan **3** (5.0 g, 7.08 mmol) in dry DMF (35 mL), $NMe_3{\cdot}SO_3$ (4.92 g, 35.4 mmol) was added. The reaction mixture was stirred for 5 h at 55 °C, the solvent evaporated and the product purified by silica gel column chromatography ($CHCl_3$/MeOH 5:1). Compound **4** (5.4 g, 6.8 mmol) was obtained in 95% yield as a white solid. TLC ($CHCl_3$/MeOH 5:1) R_f 0.1; ESI–MS (*m/z*): 785.2 $[M - H]^-$ (100); HPLC: (CH_3CN/H_2O 0:100→100:0 in 60 min) t_R 34 min; ^{1}H NMR (250 MHz, $CDCl_3$) δ 4.31 (dd, $J_{4',5'}$ = 1.4 Hz, $J_{5,6a'} = J_{5',6b'}$ = 6.9 Hz, 1H, H5′), 4.38 (dt, $J_{6a',6b'}$ = 12.2 Hz, 1H, H6a′), 4.48 (d, $J_{CHaOGal,ChbOGal}$ = 12.8 Hz, 1H, CH_aOGal), 4.63 (dd, 1H, H6b′), 4.65 (d, 1H, CH_bOGal), 4.77 (s, 2H, CH_2OSO_3), 4.96 (d, $J_{1',2'}$ = 7.1 Hz, 1H, H1′), 5.64 (dd, $J_{2',3'}$ = 11.0 Hz, $J_{3',4'}$ = 2.8 Hz, 1H, H3′), 5.69 (dd, 1H, H2′), 5.93 (dd, 1H, H4′), 7.6–8.0 (m, 22H, 20 Ar-H, H2, H5); ^{13}C NMR (63 MHz, $CDCl_3$) δ 55.06 (CH_2OSO_3), 61.48 (C6′), 62.07 (CH_2OGal), 68.11, 69.08, 70.08, 71.51 (C2′, C3′, C4′, C5′), 100.01 (C1′), 119.23, 120.78 (C3, C4), 128.1–133.5 (20 × CBz), 142.1, 143.06 (C2, C5), 165.50, 165.60, 165.68, 166.64 (4 × CO).

Deprotection to (4-{[(β-D-galactopyrano-syl)oxy]methyl}furan-3-yl)methyl hydrogen sulfate (GSF, **5**): Solid, powdered $NaOCH_3$ (170 mg, 3.15 mmol) was added to a solution of furan **4** (1.0 g, 1.27 mmol) in dry methanol (20 mL), and the reaction mixture was stirred for 10 h at rt. The solvent was then evaporated, and the product was dissolved in water (10 mL), adjusted to pH 7.2 with 0.1 M HCl, and extracted three times with diethyl ether. The aqueous layer was lyophilized. GSF (**5**, 400 mg 1.08 mmol) was obtained with 85% yield as a white powder. TLC (CH_3CN/H_2O 9:1): R_f 0.7; HPLC: (CH_3CN/H_2O 2:98) t_R 5 min; ESI–MS (*m/z*): 369.0 $[M - H]^-$ (100); ^{1}H NMR (250 MHz, D_2O) δ 3.53 (dd, $J_{2',3'}$ = 9.8 Hz, $J_{1',2'}$ = 7.7 Hz, 1H, H2′), 3.64 (dd, $J_{3',4'}$ = 3.2 Hz, 1H, H3′), 3.73 (ddd, $J_{5',6a'}$ = 5.9 Hz, $J_{5',6b'}$ = 6.3 Hz, $J_{5',4'}$ = 1.6 Hz, 1H, H5′), 3.81 (dd, $J_{6a',6b}$ = 12.4 Hz, 1H, H6a′), 3.83 (dd, 1H, H6b′), 3.94 (dd, 1H, H4′),

4.48 (d, 1H, H1′), 4.68 (d, $J_{CHaOGal,ChbOGal}$ = 11.5 Hz, 1H, CH_aOGal), 4.90 (d, 1H, CH_bOGal), 5.07 (s, 2H, CH_2OSO_3), 7.65 (s, 1H, H5), 7.68 (s, 1H, H2); ^{13}C NMR (63 MHz, DMSO-d_6) δ 58.4, 60.5, 60.6 (CH_2OSO_3, CH_2OGal, C6′), 68.2, 70.6, 73.4, 75.2 (C2′, C3′, C4′, C5′), 102.6 (C1′), 121.3, 121.7 (C3, C4), 141.49, 141.52 (C2, C5).

In silico blind-docking and molecular dynamics simulations

A flexible docking approach using AUTODOCK 3.05 [51] was applied to screen a large part of the surface of the protein for potential binding sites. The complete β-propeller domain of α_v and the βA domain of β_3 were extracted from the crystal structure of the extracellular segment of integrin $\alpha_v\beta_3$ (pdb code 1L5G) [26] and used as a (rigid) receptor for docking. In an initial test calculation the cyclic peptide ligand Cilengitide® (cyclo-[RGDfN(Me)V]) [48] present in the X-ray structure [26] was redocked to the receptor in a "blind-docking" approach in which the search space covered almost the complete receptor surface (grid dimensions: 120 × 80 × 80, resolution 0.75 Å).

The input files for AUTODOCK were created with the help of "AutoDockTools" [52]. The genetic algorithm with local search option (GA-LS) as implemented in AUTODOCK was used to dock the flexible ligand. One hundred AUTODOCK jobs were started in parallel each performing 10 GA-LS runs, giving rise to 1000 individual GA-LS docking runs in total. For each GA-LS docking run 1,000,000 energy evaluations were performed. The Conformational Analysis Tools (CAT) program was used to merge the output data of the AUTODOCK runs, to perform the analysis of the entire dataset, and to organize the results in such a way that areas on the protein surface exhibiting a strong binding affinity could be easily visualized by using standard display programs.

In order to refine the docked structure of GSF a molecular dynamics (MD) simulation of the complex was performed by using AMBER [53]. The atomic partial charges and the topology files for GSF were prepared with *antechamber*. The final input files for *sander* were built with *tleap*. The MD simulations were run at 300 K in explicit water, by using periodic boundary conditions and following established standard protocols.

Cell lines and culture conditions

The human melanoma cell lines WM-115 and WM-266-4 were obtained from the American Type Culture Collection (Manassas, VA). The WM-115 line was derived from a primary tumor and the WM-266-4 line from a cutaneous metastasis of the same patient. Both lines were maintained in Eagle's minimum essential medium (MEM) with Earle's salts (Biochrom, Berlin, Germany), 2 mM *L*-glutamine (PAA, Cölbe, Germany), 1 mM sodium pyruvate (Biochrom, Berlin, Germany), 0.1 mM nonessential amino acids (Biochrom, Berlin, Germany), 1.5 g/L $NaHCO_3$ (Biochrom, Berlin, Germany) and 10% fetal bovine serum (FBS) (PAN Biotech, Aidenbach, Germany). Both lines were grown in a 5% CO_2 atmosphere at temperatures of 34.5 °C (WM-115) or 37 °C (WM-266-4). Cells were passaged once a week by using 0.05% trypsin, 0.02% EDTA in PBS (PAA, Cölbe, Germany) to detach cells.

HBMEC-60 (retrovirally immortalized human-bone-marrow-derived endothelial) cells, kindly provided by Dr. E. van der Schoot (Sanguin, Amsterdam, The Netherlands) and originally described by Rood et al. [42], were grown in endothelial-specific culture medium (endothelial cell basal medium, PromoCell, Heidelberg, Germany), supplemented with 20% (v/v) FBS (Biochrom, Berlin, Germany), 1 µg/mL hydrocortisone, 0.1 ng/mL human epidermal growth factor and 1ng/mL human basal fibroblast growth factor, as recommended by the manufacturer. Cells used for the assays described below were mycoplasm free as verified by DAPI-staining of DNA and a PCR based mycoplasm test (Venor GeM-OneStep, Minerva Biolabs, Berlin, Germany).

Cytotoxicity test

Cytotoxicity of GSF was tested using the sulforhodamine B (SRB) assay. Cells (1.3×10^4/ well) were seeded into a 96-well plate and after 24 h incubation 2.5 to 10 mM of saccharide mimetics were added to the medium. After 24, 48 or 72 h the medium was gently removed and cells were fixed for 5 min at −20 °C with MeOH/HOAc, 95:5. After being washed three times with H_2O and dried, the cells were stained with 0.4% SRB in 1% HOAc for 30 min. Wells were washed three times with 1% HOAc before the bound dye was dissolved with 10 mM Tris (pH 10.5). The absorbance at 546 nm was measured by using a microplate reader (µ-Quant, BIO-TEK Instruments Inc., Winooski, VT). The means and SD of quadruplicates were calculated.

Experimental conditions for human melanoma cells

Adhesion assay: To coat flexible 96-well plates (polyvinyl chloride (PVC), Falcon, Becton-Dickinson, Heidelberg, Germany) with human plasma ECM proteins, 0.5 µg human fibronectin (Invitrogen Karlsruhe, Germany) or 0.5 µg human fibrinogen (Calbiochem, Schwalbach, Germany) dissolved in 50 µL H_2O was added to the wells and incubated overnight at 4 °C. Nonspecific binding sites were blocked with 200 µL of 1% bovine serum albumin (BSA) solution in phosphate-buffered saline (PBS). To control for nonspecific adherence to

the PVC surface, cell adhesion was also measured on noncoated PVC plates.

Nearly confluent monolayers of WM-115 cells (48 h growth) were labeled with [methyl-^{3}H]-thymidine (spec. activity 1.16–31.5 TBq/mmol, Hartmann Analytic, Braunschweig, Germany), 1.48 MBq/10^6 cells/mL and incubated for 16 h at their respective temperatures. Cells were detached with 0.05% EDTA and washed three times in assay-medium (serum-free MEM-medium with Earle's salts containing 0.25 mM $MnCl_2$ and 0.1% BSA). Test compounds (the compounds described above, and methyl-β-D-galactose (Fluka, Taufkirchen, Germany), the peptides GRGDSP (Calbiochem, Darmstadt, Germany) or EILDV (synthesized by R. Pipkorn, DKFZ) were dissolved in assay medium and the cells were incubated therein for 1 h. For the adhesion assays on PVC, the assay medium contained no BSA. To each coated well 5×10^4 cells were added, and after 1 h nonadherent cells were removed by three consecutive washing steps with PBS. Wells were cut out and transferred into scintillation vials, and then 5 mL scintillation cocktail (Ultima Gold, PerkinElmer, Boston, MA) was added and [^{3}H] quantified by using a scintillation-counter (TriCarb 2200CA, Packard, Downers Grove, IL). Attached cells were quantified with a standard curve, which was performed for each assay, relating the cell number to [^{3}H]-radioactivity. The number of adherent cells relative to the 5×10^4 cells/well were calculated and related to the control incubations without test compounds. Standard deviations were calculated according to Bishop [54], taking the SD of the control into account.

Cell migration (wound healing) assay: Intact cell monolayers of WM-115 or WM-266-4 cells in 12-well plates (Becton Dickinson, Heidelberg, Germany) were wounded with a 100 µL pipette tip and washed three times with serum-free medium. Complete medium containing GSF was added to the wells and cell migration into the wound was observed by microscopy after 2, 4, 8 and 24 h and compared with migration in medium without GSF.

Matrix metalloprotease (MMP) assays: Zymographic analyses. Cells grown for 48 h were treated with GSF for 24 h in serum-free medium. Medium was removed and centrifuged for 8 min at 300*g*. Samples containing equal amounts of protein (determined by Lowry's method) were separated under nonreducing conditions in a 7.5% sodium dodecyl sulfate-polyacrylamide gel (SDS-PAGE) polymerized together with 0.1% gelatin. After electrophoresis, gels were washed twice in 2.5% Triton X-100 and four times in H_2O before overnight incubation in gelatinase buffer (0.02% Brij 35, Tris-HCl 50 mM, NaCl 150 mM, $CaCl_2$ 10 mM, pH 7.6). Gelatinolytic activity was visualized by Coomassie-blue staining.

Western blot of MMP-2. Samples were prepared as described for zymography and separated in a 7.5% polyacrylamide gel under reducing conditions. Proteins were electroblotted onto nitrocellulose sheets (Schleicher & Schuell, Dassel, Germany) and the blots blocked for 30 min with 5% milk powder in PBS. Incubation with the primary mouse anti MMP-2 antibody (MAB13431, Chemicon, Temecula, Canada) in PBS with 0.5% human serum albumin was carried out overnight. After washing with PBS containing 0.1% tween-20 membranes were incubated for 4 h at rt with a rabbit anti-mouse alkaline phosphatase conjugated antibody (Dako, Glostrup, Denmark) in PBS with 0.5% human serum albumin. After additional washes the binding of the secondary antibody was visualized by BCIP/NBT-Blue (Sigma, Taufkirchen, Germany) as substrate.

Experimental conditions for human endothelial cell assays

Adhesion assay: For endothelial cell adhesion assays we used 96-well microtiter plates precoated either with laminin, fibronectin (both supplied by Becton Dickinson, Heidelberg, Germany) or collagen I (supplied by Greiner Bioscience, Frickenhausen, Germany). Cells were pre-incubated with the respective mimetic compounds in the concentrations indicated, for 30 min on ice. Prior to use, microtiter plates were washed with phosphate-buffered saline (PBS), then 4×10^4 cells/100 µL culture medium without FBS or growth factors, and with or without mimetic compounds, were added to each well and cultivated for 30 min at 37 °C in a 5% CO_2 atmosphere. Subsequently, the culture medium was decanted, and then the cells were washed twice in PBS and adherent cells fixed in 4% formaldehyde (v/v) in PBS for 5 min at rt. Subsequently, the fixation solution was removed, the plates were air dried and washed with 0.01 M borate, and the cells were stained in 1% methylene blue dissolved in 0.01 M borate for 10 min at rt. The staining solution was removed, and the cells were washed in water. The plates were air dried again and incubated with 200 µL/well of extraction buffer (0.1 M HCl/EtOH, 1:1 (v/v)) for 30 min at rt. Absorption was measured in an ELISA reader at 620 nm to quantify adherent cells. For certain experiments, cells were stimulated with 40 ng/mL human recombinant tumor necrosis factor (TNF) (PromoCell) 24 h prior to the test. Experiments were performed with six replicates.

Migration assay: In an endothelial migration assay, polycarbonate transwells (8 µm pore size, Corning Costar) were coated on the lower side with laminin, fibronectin or collagen type I (10 µg/mL in PBS each for 1 h at 37 °C) and were inserted into 24-well plates. Endothelial cells were plated at a density of 4×10^5 cells/mL (100 µL/insert) into transwells in endothelial medium as described above, with or without 40 ng/mL TNF or 20 ng/mL VEGF and mimetic compounds, as indicated. After

incubation for 30 min at 37 °C nonadherent cells were removed, and cells on the transwells were washed with PBS and fixed in 4% paraformaldehyde for 10 min at rt, washed again and stained in the dark with Hoechst 33342 DNA dye (Invitrogen), washed twice with PBS at rt and then stored at 4 °C until photographical documentation of the microscopy image and further counting of adherent stained cells.

Matrigel in vitro angiogenesis assay: The assay was performed as previously described [43]. Cells were preincubated with either 40 ng/mL TNF or 20 ng/mL VEGF for 24 h at 37 °C, before the cells (4×10^4 cells/well in 300 µL medium) were added to 48-well plates coated with matrigel. The cells on matrigel plates were incubated overnight, with or without test compounds, in concentrations as indicated, at 37 °C, before the cellular networks were documented photographically and the networks quantified by a computational image-evaluation program.

Tubing in vitro angiogenesis assay: The cell preparation kit of TCS (Buckingham, UK) was used to perform the endothelial tubule formation assay. Cocultures of cells consisting of fibroblasts and human umbilical cord vein endothelial cells (HUVEC) were incubated in 24-well plates. On day 1, VEGF (20 ng/mL) and the test compounds in concentrations as indicated were added to the cell culture. The growth medium including growth factors and test substances was changed at days 4 and 7 of cell culture. At day 9 the medium was removed from the cell culture, and the cells were washed and fixed in 70% EtOH (v/v) for 30 min at rt, followed by a washing step and incubation in MeOH/30% H_2O_2, 40:1 (v/v) for 10 min at rt. The cells were washed, then incubated with a monoclonal antibody against the CD31 antigen (Dako, Hamburg, Germany), which is specifically expressed on endothelial cells. They were then diluted 1:20 for 30 min, and, after a washing step, incubated with a secondary goat anti-mouse IgG antibody coupled to biotin (Dako) for 20 min, followed by a washing step and incubation with streptavidin coupled to horseradish peroxidase for 20 min. Antibody reactivity was visualized by adding AEC (3-amino-9-ethylcarbazole) chromogen substrate (Dako) to the cells for 14 min in the dark. Enzymatic reaction was stopped by washing with water. Wells were sealed with mounting medium and microscopic quantitative analysis of tube formation was performed with the software Angiosys 1.0, TCS (Cellworks). Statistical analyses were performed with GraphPad PRISM version 5.

Acknowledgements

This study was kindly supported by a grant to Dr. Schwartz-Albiez from the "Deutsche José Carreras Leukämie-Stiftung" (project DJCLS R10/32f). Part of this work and Grazia Marano was funded by the DBU (Deutsche Bundesstiftung Umwelt) (project 22597-31). ChemCon GmbH (ChemCon Part G, Freiburg i. Br., Germany) was partner in the project and is commended for the syntheses of the protected saccharides used in the syntheses described.

References

1. Ahmad, A.; Hart, I. R. *Crit Rev. Oncol. Hematol.* **1997,** *26,* 163–173. doi:10.1016/S1040-8428(97)10002-6
2. Ruoslahti, E. *Adv. Cancer Res.* **1999,** *76,* 1–20. doi:10.1016/S0065-230X(08)60772-1
3. Nesbit, M.; Herlyn, M. *Invasion Metastasis* **1994,** *14,* 131–146.
4. Mitjans, F.; Meyer, T.; Fittschen, C.; Goodman, S.; Jonczyk, A.; Marshall, J. F.; Reyes, G.; Piulats, J. *Int. J. Cancer* **2000,** *87,* 716–723. doi:10.1002/1097-0215(20000901)87:5<716::AID-IJC14>3.0.CO;2-R
5. Brooks, P. C.; Strömblad, S.; Sanders, L. C.; von Schalscha, T. L.; Aimes, R. T.; Stetler-Stevenson, W. G.; Quigley, J. P.; Cheresh, D. A. *Cell* **1996,** *85,* 683–693. doi:10.1016/S0092-8674(00)81235-0
6. Fukuda, M. *Cancer Res.* **1996,** *56,* 2237–2244.
7. Kannagi, R.; Izawa, M.; Koike, T.; Miyazaki, K.; Kimura, N. *Cancer Sci.* **2004,** *95,* 377–384. doi:10.1111/j.1349-7006.2004.tb03219.x
8. Dube, D. H.; Bertozzi, C. R. *Nat. Rev. Drug Discovery* **2005,** *4,* 477–488. doi:10.1038/nrd1751
9. Allen, J. R.; Harris, C. R.; Danishefsky, S. J. *J. Am. Chem. Soc.* **2001,** *123,* 1890–1897. doi:10.1021/ja002779i
10. Oetke, C.; Brossmer, R.; Mantey, L. R.; Hinderlich, S.; Isecke, R.; Reutter, W.; Keppler, O. T.; Pawlita, M. *J. Biol. Chem.* **2002,** *277,* 6688–6695. doi:10.1074/jbc.M109973200
11. Heidecke, C. D.; Lindhorst, T. K. *Chem.–Eur. J.* **2007,** *13,* 9056–9067. doi:10.1002/chem.200700787
12. Fuster, M. M.; Brown, J. R.; Wang, L.; Esko, J. D. *Cancer Res.* **2003,** *63,* 2775–2781.
13. Shirota, K.; Kato, Y.; Irimura, T.; Kondo, H.; Sugiyama, Y. *Biol. Pharm. Bull.* **2001,** *24,* 316–319. doi:10.1248/bpb.24.316
14. Schmidt, R. R.; Castro-Palomino, J. C.; Retz, O. *Pure Appl. Chem.* **1999,** *71,* 729–744. doi:10.1351/pac199971050729
15. Kim, E. Y.-L.; Gronewold, C.; Chatterjee, A.; von der Lieth, C.-W.; Kliem, C.; Schmauser, B.; Wiessler, M.; Frei, E. *ChemBioChem* **2005,** *6,* 422–431. doi:10.1002/cbic.200400092
16. Sasisekharan, R.; Shriver, Z.; Venkataraman, G.; Narayanasami, U. *Nat. Rev. Cancer* **2002,** *2,* 521–528. doi:10.1038/nrc842
17. Schwartz-Albiez, R. Inflammation and Glycosciences. In *The Sugar Code;* Gabius, H., Ed.; Wiley-VCH: Weinheim, Germany, 2009; pp 447–463.
18. Li, F.; Lin, B.; Hao, Y.; Li, Y.; Liu, J.; Cong, J.; Zhu, L.; Liu, Q.; Zhang, S. *Int. J. Mol. Sci.* **2010,** *11,* 3748–3759. doi:10.3390/ijms11103748
19. Moehler, T. M.; Sauer, S.; Witzel, M.; Andrulis, M.; Garcia-Vallejo, J. J.; Grobholz, R.; Willhauck-Fleckenstein, M.; Greiner, A.; Goldschmidt, H.; Schwartz-Albiez, R. *J. Cell. Physiol.* **2008,** *215,* 27–36. doi:10.1002/jcp.21285
20. Yanagishita, M. *Acta Pathol. Jpn.* **1993,** *43,* 283–293.
21. Brooks, S. A.; Dwek, M. V.; Schuhmacher, U. *Functional and Molecular Glycobiology;* BIOS Scientific Publishers Ltd.: Oxford, 2002.
22. Yakovlev, S.; Gorlatov, S.; Ingham, K.; Medved, L. *Biochemistry* **2003,** *42,* 7709–7716. doi:10.1021/bi0344073
23. Moitessier, N.; Minoux, H.; Maigret, B.; Chrétien, F.; Chapleur, Y. *Lett. Pept. Sci.* **1998,** *5,* 75–78. doi:10.1007/BF02443442

24. Gruner, S. A. W.; Locardi, E.; Lohof, E.; Kessler, H. *Chem. Rev.* **2002,** *102,* 491–514. doi:10.1021/cr0004409
25. Gottschalk, K.-E.; Kessler, H. *Angew. Chem., Int. Ed.* **2002,** *41,* 3767–3774. doi:10.1002/1521-3773(20021018)41:20<3767::AID-ANIE3767>3.0.CO;2-T
26. Xiong, J.-P.; Stehle, T.; Zhang, R.; Joachimiak, A.; Frech, M.; Goodman, S. L.; Arnaout, M. A. *Science* **2002,** *296,* 151–155. doi:10.1126/science.1069040
27. Friess, H.; Langrehr, J. M.; Oettle, H.; Raedle, J.; Niedergethmann, M.; Dittrich, C.; Hossfeld, D. K.; Stöger, H.; Neyns, B.; Herzog, P.; Piedbois, P.; Dobrowolski, F.; Scheithauer, W.; Hawkins, R.; Katz, F.; Balcke, P.; Vermorken, J.; van Belle, S.; Davidson, N.; Esteve, A. A.; Castellano, D.; Kleeff, J.; Tempia-Caliera, A. A.; Kovar, A.; Nippgen, J. *BMC Cancer* **2006,** *6,* No. 285. doi:10.1186/1471-2407-6-285
28. Barczyk, M.; Carracedo, S.; Gullberg, D. *Cell Tissue Res.* **2010,** *339,* 269–280. doi:10.1007/s00441-009-0834-6
29. Melchiori, A.; Mortarini, R.; Carlone, S.; Marchisio, P. C.; Anichini, A.; Noonan, D. M.; Albini, A. *Exp. Cell Res.* **1995,** *219,* 233–242. doi:10.1006/excr.1995.1223
30. Mitra, A.; Chakrabarti, J.; Chattopadhyay, N.; Chatterjee, A. *J. Environ. Pathol. Toxicol. Oncol.* **2003,** *22,* 93–100. doi:10.1615/JEnvPathToxOncol.v22.i2.20
31. Lauffenburger, D. A.; Horwitz, A. F. *Cell* **1996,** *84,* 359–369. doi:10.1016/S0092-8674(00)81280-5
32. Yamamoto, M.; Mohanam, S.; Sawaya, R.; Fuller, G. N.; Seiki, M.; Sato, H.; Gokaslan, Z. L.; Liotta, L. A.; Nicolson, G. L.; Rao, J. S. *Cancer Res.* **1996,** *56,* 384–392.
33. Hofmann, U. B.; Houben, R.; Bröcker, E.-B.; Becker, J. C. *Biochimie* **2005,** *87,* 307–314. doi:10.1016/j.biochi.2005.01.013
34. Hofmann, U. B.; Westphal, J. R.; Van Kraats, A. A.; Ruiter, D. J.; Van Muijen, G. N. P. *Int. J. Cancer* **2000,** *87,* 12–19. doi:10.1002/1097-0215(20000701)87:1<12::AID-IJC3>3.0.CO;2-A
35. Teti, A.; Farina, A. R.; Villanova, I.; Tiberio, A.; Tacconelli, A.; Sciortino, G.; Chambers, A. F.; Gulino, A.; Mackay, A. R. *Int. J. Cancer* **1998,** *77,* 82–93. doi:10.1002/(SICI)1097-0215(19980703)77:1<82::AID-IJC14>3.0.CO;2-B
36. Carmeliet, P. *Nature* **2005,** *438,* 932–936. doi:10.1038/nature04478
37. Auguste, P.; Lemiere, S.; Larrieu-Lahargue, F.; Bikfalvi, A. *Crit Rev. Oncol. Hematol.* **2005,** *54,* 53–61. doi:10.1016/j.critrevonc.2004.11.006
38. Sethi, G.; Sung, B.; Aggarwal, B. B. *Front Biosci.* **2008,** *13,* 5094–5107. doi:10.2741/3066
39. Naldini, A.; Carraro, F. *Curr. Drug Targets. Inflamm. Allergy* **2005,** *4,* 3–8. doi:10.2174/1568010053622830
40. Carmeliet, P.; Jain, R. K. *Nature* **2011,** *473,* 298–307. doi:10.1038/nature10144
41. Ramjaun, A. R.; Hodivala-Dilke, K. *Int. J. Biochem. Cell Biol.* **2009,** *41,* 521–530. doi:10.1016/j.biocel.2008.05.030
42. Rood, P. M.; Calafat, J.; von dem Borne, A. E.; Gerritsen, W. R.; van der Schoot, C. E. *Eur. J. Clin. Invest.* **2000,** *30,* 618–629. doi:10.1046/j.1365-2362.2000.00672.x
43. Willhauck-Fleckenstein, M.; Moehler, T. M.; Merling, A.; Pusunc, S.; Goldschmidt, H.; Schwartz-Albiez, R. *Angiogenesis.* **2010,** *13,* 25–42. doi:10.1007/s10456-010-9162-4
44. Kleinman, H. K.; McGarvey, M. L.; Hassell, J. R.; Star, V. L.; Cannon, F. B.; Laurie, G. W.; Martin, G. R. *Biochemistry* **1986,** *25,* 312–318. doi:10.1021/bi00350a005
45. Rüegg, C.; Dormond, O.; Foletti, A. *Endothelium* **2002,** *9,* 151–160. doi:10.1080/10623320213635
46. Becker, D. J.; Lowe, J. B. *Glycobiology* **2003,** *13,* 41R–53R. doi:10.1093/glycob/cwg054
47. Yan, L.-M.; Lin, B.; Zhu, L.-C.; Hao, Y.-Y.; Qi, Y.; Wang, C.-Z.; Gao, S.; Liu, S.-C.; Zhang, S.-L.; Iwamori, M. *Biochimie* **2010,** *92,* 852–857. doi:10.1016/j.biochi.2010.02.012
48. Mas-Moruno, C.; Rechenmacher, F.; Kessler, H. *Anti-Cancer Agents Med. Chem.* **2010,** *10,* 753–768. doi:10.2174/187152010794728639
49. Frank, M.; Frei, E.; Marano, G.; Meister, B.; Schwartz-Albiez, R. New saccharide mimics and their use as inhibitors of angiogenesis and metastasis formation. European Patent Application 11000103.9-2101, Jan 7, 2011.
50. Cook, M. J.; Forbes, E. J. *Tetrahedron* **1968,** *24,* 4501–4508. doi:10.1016/S0040-4020(01)96287-8
51. Morris, G. M.; Goodsell, D. S.; Halliday, R. S.; Huey, R.; Hart, W. E.; Belew, R. K.; Olson, A. J. *J. Comput. Chem.* **1998,** *19,* 1639–1662. doi:10.1002/(SICI)1096-987X(19981115)19:14<1639::AID-JCC10>3.0.CO;2-B
52. Auto Dock Tools, The Molecular Graphics Laboratory. http://autodock.scripps.edu/ (accessed Aug 19, 2011).
53. Case, D. A.; Cheatham, T. E., III; Darden, T.; Gohlke, H.; Luo, R.; Merz, K. M., Jr.; Onufriev, A.; Simmerling, C.; Wang, B.; Woods, R. J. *J. Comput. Chem.* **2005,** *26,* 1668–1688. doi:10.1002/jcc.20290
54. Bishop, Y. *Discrete multivariate analysis: Theory and practice;* MITPr: Cambridge, MA, 1997.

License and Terms

Beilstein Journal of Organic Chemistry

Synthetic glycopeptides and glycoproteins with applications in biological research

Ulrika Westerlind

Review

Open Access

Address:
Gesellschaft zur Förderung der Analytischen Wissenschaften e.V., ISAS – Leibniz Institute for Analytical Sciences, Otto-Hahn-Str. 6b, D-44227 Dortmund, Germany, Tel: (+49)231-1392 4215, Fax: (+49)231-1392 4850

Email:
Ulrika Westerlind - ulrika.westerlind@isas.de

Keywords:
glycopeptide binding; glycopeptides; glycoprotein synthesis; solid-phase peptide synthesis; synthetic vaccines

Beilstein J. Org. Chem. **2012,** *8,* 804–818.
doi:10.3762/bjoc.8.90

Received: 04 February 2012
Accepted: 22 May 2012
Published: 30 May 2012

This article is part of the Thematic Series "Synthesis in the glycosciences II".

Guest Editor: T. K. Lindhorst

Abstract

Over the past few years, synthetic methods for the preparation of complex glycopeptides have been drastically improved. The need for homogenous glycopeptides and glycoproteins with defined chemical structures to study diverse biological phenomena further enhances the development of methodologies. Selected recent advances in synthesis and applications, in which glycopeptides or glycoproteins serve as tools for biological studies, are reviewed. The importance of specific antibodies directed to the glycan part, as well as the peptide backbone has been realized during the development of synthetic glycopeptide-based anti-tumor vaccines. The fine-tuning of native chemical ligation (NCL), expressed protein ligation (EPL), and chemoenzymatic glycosylation techniques have all together enabled the synthesis of functional glycoproteins. The synthesis of structurally defined, complex glycopeptides or glyco-clusters presented on natural peptide backbones, or mimics thereof, offer further possibilities to study protein-binding events.

Introduction

The majority of human proteins are co- or post-translationally modified by mono- or oligosaccharides. The glycoprotein saccharides contribute physiochemical properties, influencing protein conformation or increasing stability against proteolytic activity. With their unique structural diversity and complexity, carbohydrates attached on proteins or lipids are involved in numerous cell-surface binding events, such as cell growth and differentiation, cell proliferation, cell adhesion, binding of pathogens, fertilization and immune responses [1,2]. Furthermore, glycans assist in intracellular protein folding and transport. Pathogenic processes, such as chronic inflammation, viral and bacterial infections, tumor growth and metastasis, and autoimmune disorders, all involve glycan cell–cell or cell–external-agent communication [3-5]. The availability of structurally defined glycopeptides and glycoproteins, which contain information about the glycan structure and glycosylation sites, is valuable for functional biological studies. Glycopeptides have, for instance, been applied to evaluate the role of con-

formational and proteolytic stability [6]. In other studies, synthetic glycopeptides have been employed in vaccines to induce specific immune responses or for the inhibition of protein-binding events [7-10]. This review is written with the intention to highlight a few recent reports describing the synthesis and application of synthetic glycopeptides and glycoproteins. For a more detailed description of this field of research, the reader is guided to other excellent reviews [6-18].

Review

Glycopeptide-based vaccines

Specific immune recognition, in which the glycan and the peptide backbone contribute to the binding epitope, is of particular interest for the development of safe immunotherapy and immunodiagnostics. Since the discovery, by Springer et al., that glycoproteins on the outer cell membrane of epithelial tumor cells have an altered glycosylation consisting of the Thomsen-Friedenreich (T-) antigen and its precursor T_N-antigen structure, the synthesis and evaluation of anti-tumor vaccines have been a topic of intense research [19]. During the past few years, the synthesis and evaluation of glycopeptide-based mucin anti-tumor vaccines have dominated this research area [7,20-24].

Mucins are a class of extensively glycosylated proteins expressed on the surface of epithelial cells or secreted in mucus. Among them, mucin 1 (MUC1) is expressed on almost all epithelial tissues. Changes of the cell-surface protein glycosylation together with MUC1 protein overexpression, results in the formation of tumor-specific epitopes consisting of both the formed short saccharides, e.g., T_N, T, sialyl-T_N and sialyl-T, and the mucin tandem repeat peptide region, which is exposed due to the aberrant glycosylation (Figure 1) [25-27]. A number of synthetic glycopeptide vaccines with the MUC1 tumor associated glycopeptide epitope as target have recently been prepared. Variation of glycan structure, number of glycans per repeat, and the sites for glycan attachment on the MUC1 peptide backbone were explored. For the induction of a strong and specific immune response, different immuno-stimulants were connected to the mucin glycopeptides. Among the immuno-stimulants, the Toll-like receptor 2 (TLR2) ligand, tripalmitoyl-(*S*)-glyceryl lipopeptide Pam_3-Cys-Ser-$(Lys)_4$ (Pam_3CSK_4) and carrier proteins, such as tetanus toxoid (T.Tox.), have been successfully applied in MUC1 anti-tumor vaccines [28-30]. T_H-cell peptides included in two- or three-component vaccines and multivalent glycopeptide dendrimer vaccines have furthermore been evaluated [31-33].

Synthetic MUC1-tetanus toxoid conjugate vaccines have proven to be particularly interesting. Tetanus toxoid vaccines conjugated to other antigens have been administered to humans. During immunization in mice, highly specific and strong immune responses were induced in a number of cases [28,29,34]. Furthermore, several antibodies induced by the vaccines showed specific recognition of tumor cells.

The MUC1 tandem repeat glycopeptides were synthesized on solid-phase, according to the Fmoc strategy, by using Fmoc protected amino acids and Fmoc glycosyl amino acid building blocks in a stepwise fashion. After cleavage from resin and removal of the protecting groups the MUC1 glycopeptides (**1**–**5**) could be conjugated through diethyl squarate to the tetanus toxoid carrier protein (Scheme 1). Immunological evaluation of MUC1 glycopeptide vaccines containing a sialyl-T_N, a T-antigen, or a difluoro-T-antigen on different positions in the tandem repeat (**6**–**10**), showed that high antibody titers were induced in almost all of the immunized mice. Evaluation of the generated antibodies provided evidence that specific immune responses were elicited towards the MUC1 antigens present in the vaccines. FACS analysis with serum antibodies induced by the MUC1 vaccines **7**–**10** showed that they all recognize MCF-

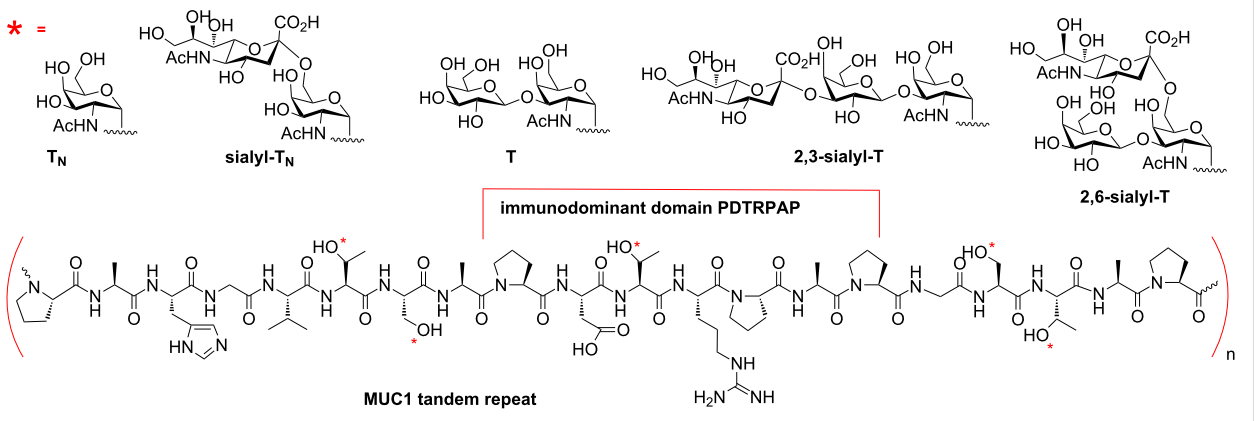

Figure 1: Tumor-associated glycosylation on MUC1 tandem repeat peptides.

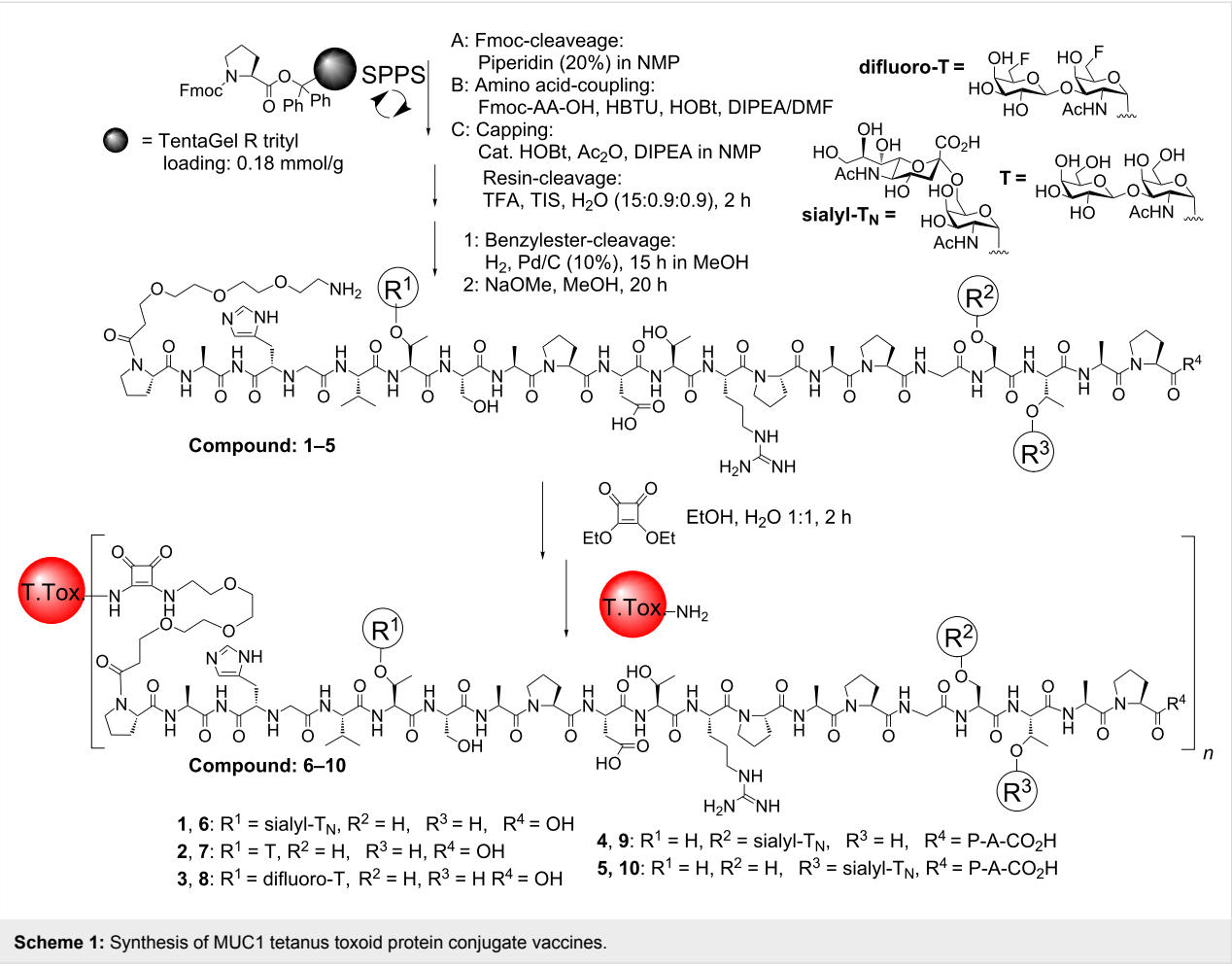

Scheme 1: Synthesis of MUC1 tetanus toxoid protein conjugate vaccines.

7 breast-cancer cells. The serum from mice immunized with vaccine **9** was further evaluated through mammary carcinoma tissue-staining experiments. A gradual increase of the tissue staining was found, resulting from a strong binding to the advanced G3-phase tumor tissue. Taken together, these results show that a selective immune response discriminating between healthy and diseased tissue can be efficiently obtained [28,29,34].

A number of two- or three-component vaccines containing a Toll-like receptor-2 (TLR2) ligand have, moreover, been synthesized and evaluated [35-38]. These self-adjuvanting vaccines avoid invoking an immune response to the immune carrier, a problem commonly seen upon employing protein conjugate vaccines. The synthesis of two-component vaccines with a Pam_3Cys TLR2 ligand connected to T_N, T and sialyl-T MUC1 glycopeptides was recently described (Scheme 2) [35]. The Pam_3CSK_4 lipopeptide fragment **13** was prepared by Fmoc solid-phase synthesis, including protected amino-acid side chains after resin cleavage. Subsequently, different T_N, T and sialyl-T MUC1 glycopeptides (**2**, **11**, **12**) were prepared and fully deprotected. Peptide synthesis was followed by fragment condensation employing HATU and HOAt and after additional deprotection steps, resulting in the formation of the lipopeptide vaccine constructs **14–16**. Immunization of the vaccines in mice showed that a specific immune response was induced in all mice although not with the high antibody titers found upon employing MUC1 tetanus toxoid vaccines [35]. In a later study, two- and three-component vaccines were synthesized and compared by immunological evaluation. The three component vaccines, containing an extra tetanus toxoid T-cell peptide epitope, showed a stronger immune response when the MUC1 peptides were glycosylated, whereas the nonglycosylated two- and three-component vaccines did not show any difference in antibody titers [36]. Recently, a three-component vaccine consisting of a MUC1 T_N-glycopeptide, a polio peptide T-cell epitope and the Pam_3CSK_4 lipopeptide immune-stimulant was prepared by liposome-mediated native chemical ligation. Mice immunized with the three-component vaccine were injected with breast-cancer tumor cells, and were found to be significantly more resistant to tumor growth compared to control mice [37]. Vaccines with multivalent MUC1 T- and T_N-glyco-

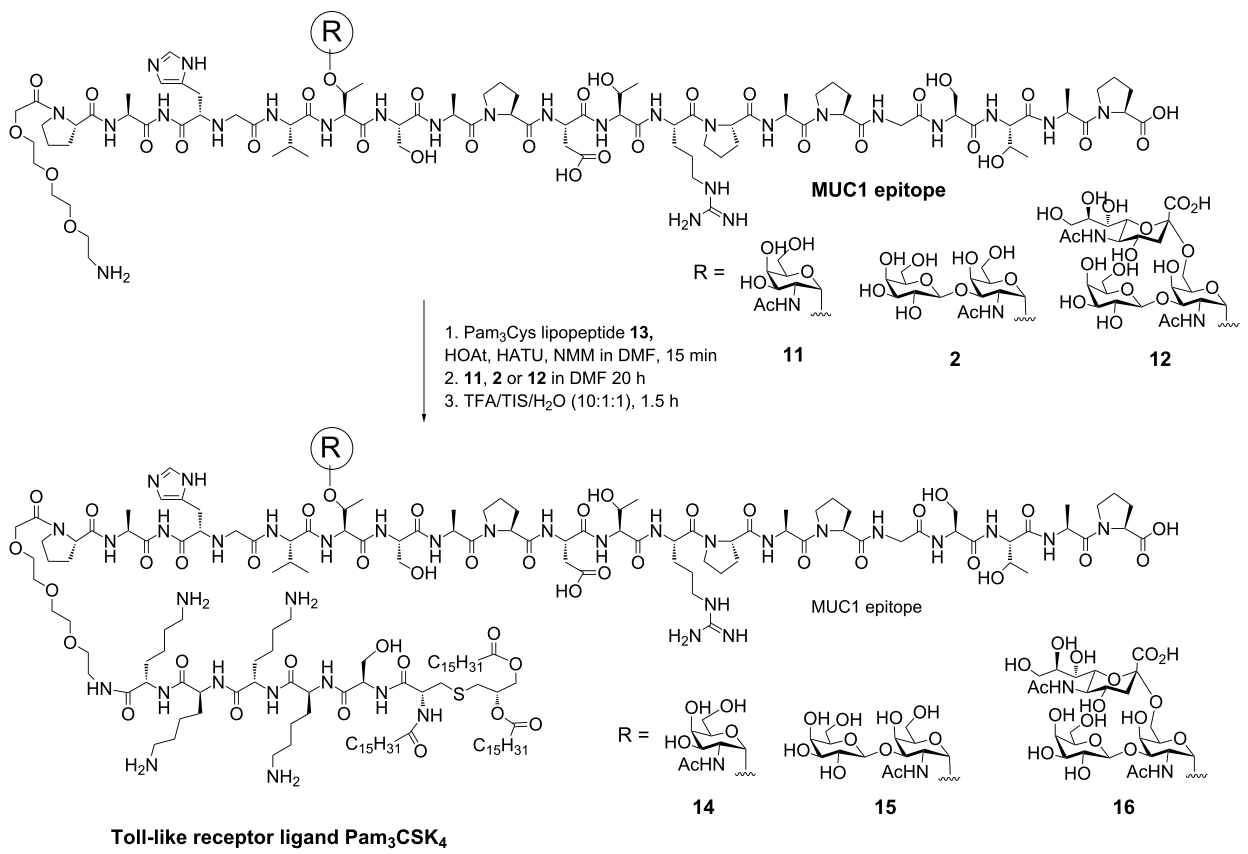

Scheme 2: T_N, T and sialyl-T MUC1 Pam_3Cys two-component vaccines.

peptides were efficiently conjugated through azide/alkyne click chemistry to the Pam_3CSK_4 lipopeptide immune-stimulant. The recently reported vaccines are currently under immunological investigation [38].

Synthetic glycoproteins

An important task for chemists is to make homogenous glycoproteins and complex glycopeptides available for biological research. Studies of glycosylation effects on protein conformation, stability and structure–activity relationships (SAR) are a few examples of the applications of synthetic glycoproteins. Since the discovery of native chemical ligation (NCL) by Kent and co-workers, numerous efforts have been made to prepare challenging protein targets [39-44]. In the NCL method, a native amide bond is formed by coupling of a C-terminal thioester with the N-terminal cysteine, followed by a S→N acyl shift. The development of a variant of NCL, namely expressed protein ligation (EPL), has further made it possible to efficiently prepare large proteins without the size limitations set by ordinary peptide synthesis [45]. Bertozzi and co-workers introduced the NCL and EPL techniques for glycoprotein synthesis by preparation of a number of GalNAc containing *O*-glycoproteins, such as the antimicrobial protein diptericin, the cytokine lymphotactin and the leukocyte adhesion molecule ligand GlyCAM-1 [46-48]. By repeated NCL couplings of mucin tandem repeats, MUC2 and MUC1 tandem repeat polypeptides have been prepared, and such polypeptides are useful for the development of anti-tumor vaccines [49,50]. The bovine ribonuclease C glycoprotein (RNase C) has been used as a model system for the preparation of homogenous *N*-glycoproteins, employing NCL and EPL for coupling between a *N*-glycopeptide and other peptide/protein fragments [51-53]. The glycoprotein contains eight cysteines locked up as disulfide bridges, which need to be correctly folded to obtain an active enzyme [54-56]. In one study, a complex type *N*-glycopeptide (fragment **17**) was prepared by standard Fmoc-SPPS followed by sequential NCL [51]. The *N*-glycopeptide fragment RNase 26–39 (**17**) was prepared with a thioester in the C-terminal and a thiazolidine protected cysteine at the N-terminus. The chemical ligation was performed by coupling of the *N*-glycopeptide thioester RNase 26–39 (**17**) and the expressed protein fragment 40–124 (**18**) containing a N-terminal cysteine, employing thiophenol and tris(2-carboxyethyl)phosphine (TCEP). The obtained RNase fragment 26–124 (**19**) was then treated with *N*-methoxyamine (0.2 M, pH 3–4, 4 h) to remove the protecting group on the

N-terminal cysteine. Ligation of the RNase fragment 26–124 (**20**) to the thioester peptide fragment RNase 1-25 (**21**) was followed to give RNase fragment 1–124 (**22**). The formed RNase C protein was then folded by treatment with glutathione disulfide (GSSG) resulting in an active RNase C enzyme **(23)** (Scheme 3).

Recently, the 111-amino-acid long β-subunit of human follicle-stimulating hormone (hFSH) glycoprotein was prepared, containing two complex type *N*-glycans, modified with core fucose and terminal sialic acid glycan residues [57]. The FSH β-subunit was prepared by sequential native chemical ligation. Initially, a larger C-terminal fragment, (β-FSH 28–111) was obtained by ligation of two shorter synthetically prepared peptides followed by sequential coupling of two N-terminal glycopeptide fragments (β-FSH 1–19 and 20–27) employing standard NCL conditions. Binding of the hFSH glycoprotein to its receptor stimulates the maturation of follicles and the production of estrogene in females, and maintains spermatogenesis in males [58]. Recombinant FSH, which is heterogeneously glycosylated, is currently used in the clinic for treatment of disorders associated with infertility [59]. Studies on mice have further indicated that FSHs reduce tumor growth [60]. The synthesis of different homogenous glycosylated FSH proteins to investigate SAR would therefore be highly desirable.

Another clinically relevant glycoprotein prepared by NCL and EPL is erythropoietin (EPO), a red-blood-cell stimulant used for the treatment of renal anaemia [61]. EPO consists of 166 amino-acid residues with four glycosylation sites, one O-glycosylation site positioned at serine 126 and three N-glycosylation sites positioned at aspargines 24, 38 and 83. EPO has been found to contain multiple glycoforms and the efficacy of EPO is heavily dependent on the type and extent of glycosylation [62,63]. The synthesis of homogeneously glycosylated EPO for improvements in therapy is therefore desirable.

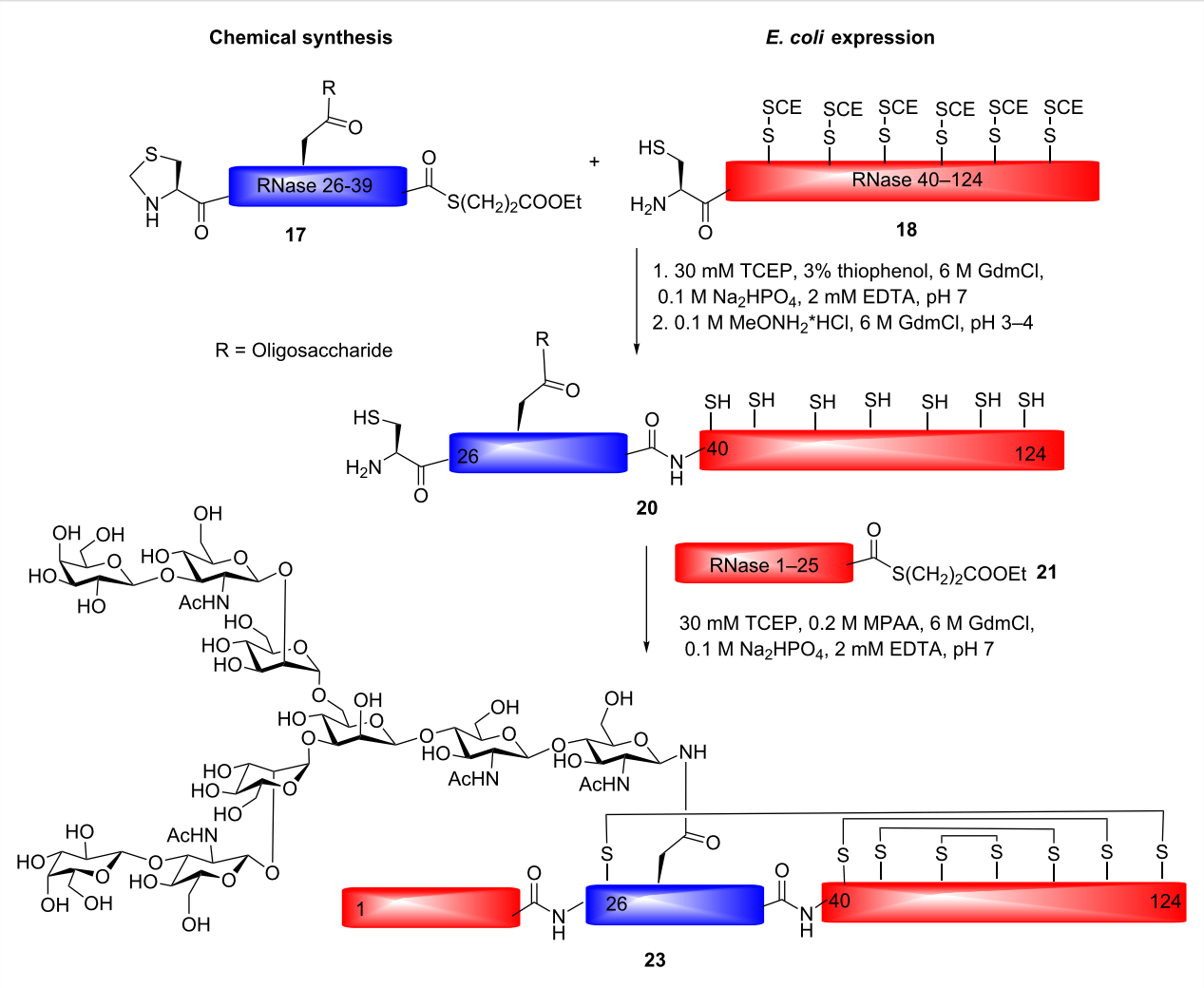

Scheme 3: Preparation of RNase C by sequential NCL.

Kajihara and co-workers have prepared a number of erythropoietin analogues by expressed protein ligation [64,65]. Complex-type *N*-glycans were attached through coupling to side-chain cysteine residues employing the haloacetamide method, forming a non-native linkage to the peptide backbone (Scheme 4). Due to *E. coli* expression of fragment 33–166, the natural sites for glycosylation 38, 83 and 126 could not be modified, and instead, glycosylations were incorporated at other unnatural positions. The synthetic EPO analogues modified with two or three complex type *N*-glycans, were evaluated in a cell proliferation assay showing that the analogues induced cell-proliferation in vitro. However, cell-proliferation activity in vivo was very weak for both analogues.

Danishefsky and co-workers prepared a number of erythropoietin glycopeptide fragments to improve the native chemical ligation methodology [14,66-68]. Recently the complete EPO protein was prepared by sequential NCL containing four glycosylation sites [69].

Although traditional NCL has resulted in advancements in the preparation of synthetic proteins, there is still a need for better methods that are independent of the relatively low abundance of the cysteine residue for a broad application of NCL in protein synthesis. To meet these needs, efforts are being made to improve the NCL ligation method, e.g., auxiliary based protocols, desulfurization methods or sugar-assisted chemical ligation (SAL) are all examples of expanded NCL techniques [70-77].

According to the auxiliary-based ligation strategy, a thiol-containing mimic replaces the N-terminal cysteine; the mimic group is then cleavable after ligation with the C-terminal thioester peptide fragment. The auxiliary-based coupling strategy employing the 4,5,6-trimethoxy-2-mercaptobenzoyl (Tmb) group is illustrated in Scheme 5. Two glycopeptide fragments are coupled together under reductive conditions. The *ortho*-thiophenolic moiety rearranges, forming a C-terminal thioester, followed by coupling to the N-terminal peptide fragment containing a thiol auxiliary. After coupling, the Tmb auxiliary could be removed by treatment with 95% trifluoroacetic acid (TFA). In spite of the strong-acid treatment required, the glycosidic bonds were reported to stay intact (Scheme 5) [70,78].

Although applicable in glycopeptide ligation, the Tmb auxiliary strategy is of limited use in glycoprotein synthesis, due to the harsh conditions employed for auxiliary removal. Further-

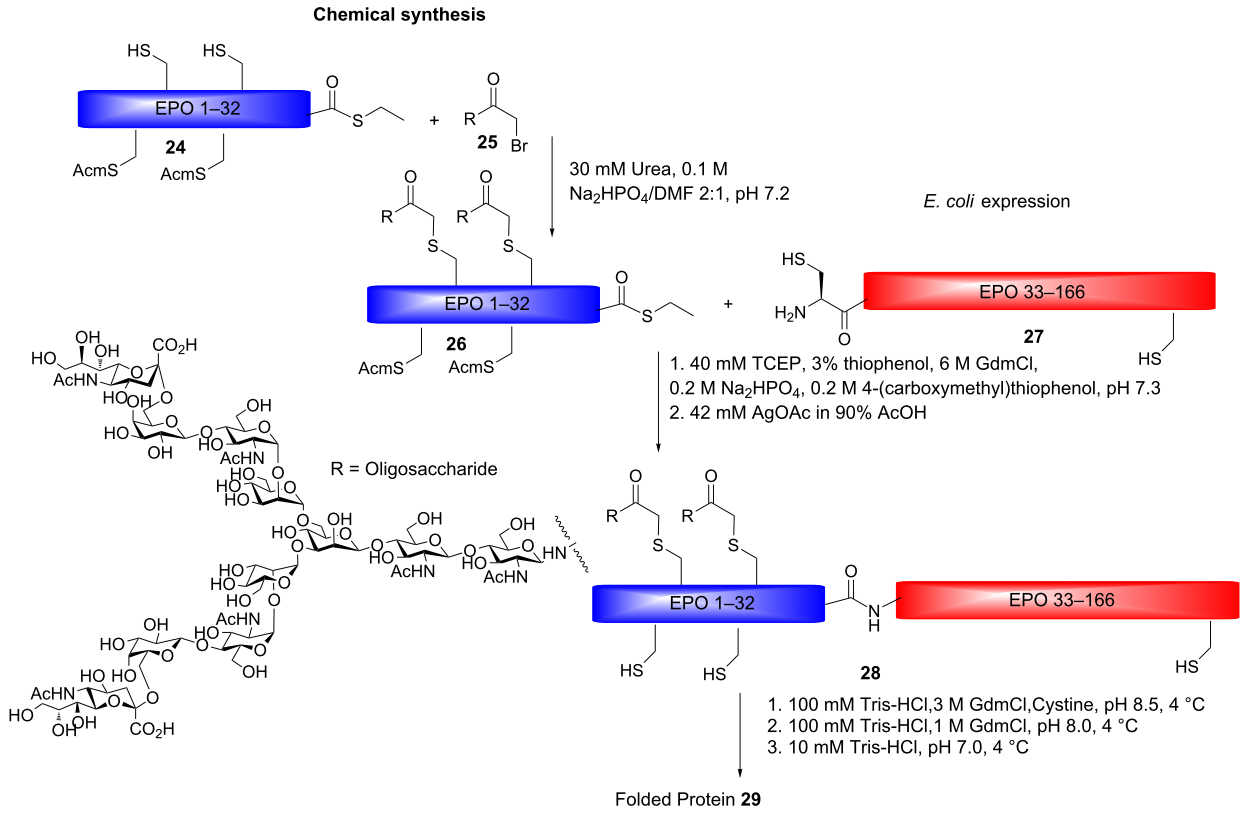

Scheme 4: Preparation of an EPO analogue modified with complex type *N*-glycans at position 24 and 30.

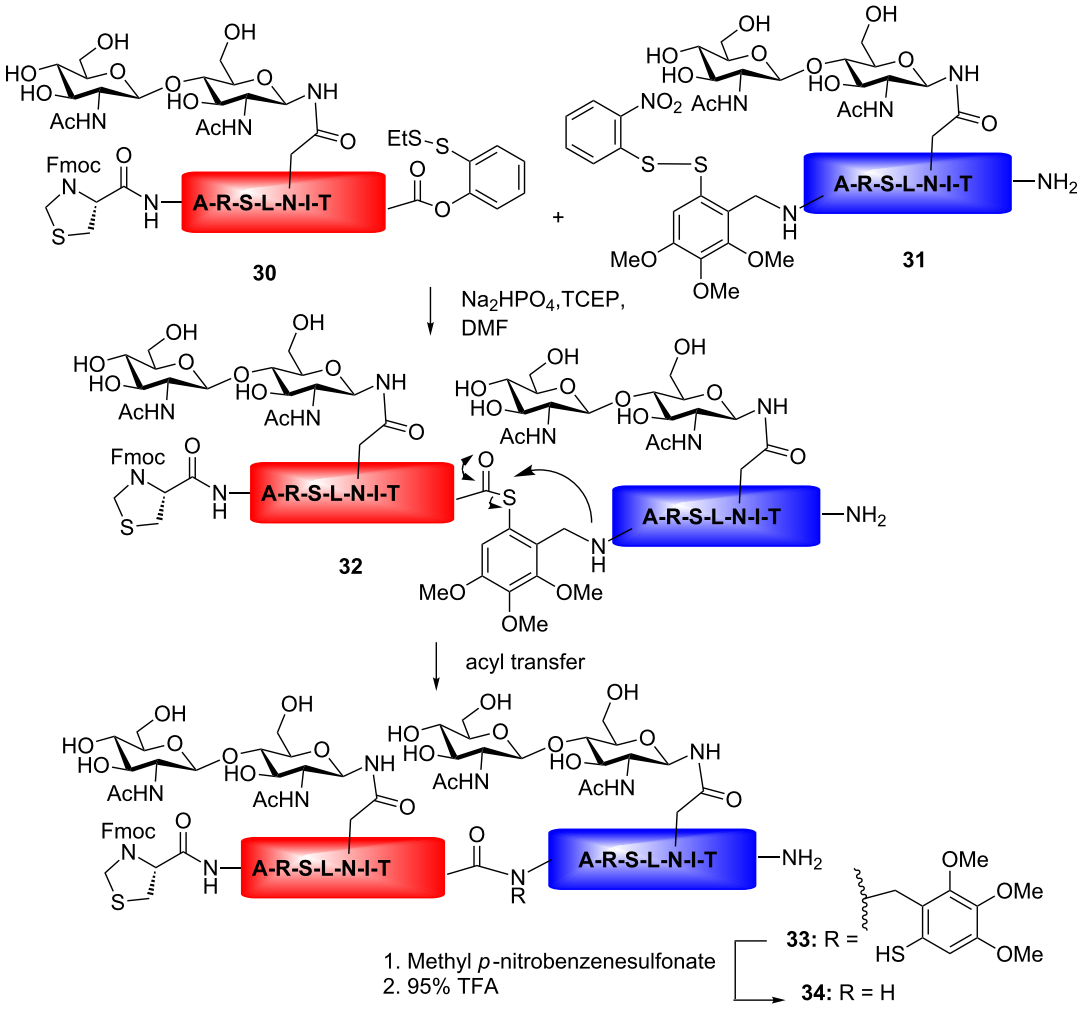

Scheme 5: Auxiliary-assisted NCL of two glycopeptide fragments.

more, due to steric hindrance by the auxiliary group, the reactivity of the amine group is reduced resulting in longer coupling times and lower yields. Therefore, the auxiliary method is mainly applied when the ligation site contains a glycine residue. To avoid these limitations, a ligation methodology has been developed with the thiol group linked to the amino-acid side-chain functional groups. After ligation the side-chain thiol could be removed by Raney nickel treatment. Employing the desulfurization methodology, thiol amino acids could be converted to alanine, valine, phenylalanine and threonine residues [71-76]. As an alternative to Raney nickel reduction, a radical-induced desulfurization method was recently reported [76]. An example of the desulfurization method is illustrated in Scheme 6. After the NCL-reaction, the γ-thiol valine at the ligation site could be converted to a valine by treatment with tris(2-carboxyethyl)phosphine (TCEP), *t*-BuSH, and the water-soluble radical initiator VA-044 [73]. The radical-induced desulfurization method has also been applied in the total synthesis of an EPO glycoprotein analogue [69].

Another promising path to prepare homogenous glycoproteins is represented by chemoenzymatic synthesis. Both glycosyltransferases and endoglycosidases have been applied in the synthesis or modulation of the glycan structure of glycopeptides and glycoproteins [79,80]. The chemoenzymatic strategy based on transglycosylation activity of endo-β-*N*-acetylglucosaminidase (ENGase) deserves particular attention. Two ENGases have commonly been applied in glycopeptide/glycoprotein synthesis, Endo-A specific for high-mannose glycans and Endo-M operating on both high-mannose and complex type *N*-glycans [81-83]. These enzymes can, in contrast to glycosyltransferases, by means of a one-step reaction attach large oligo-

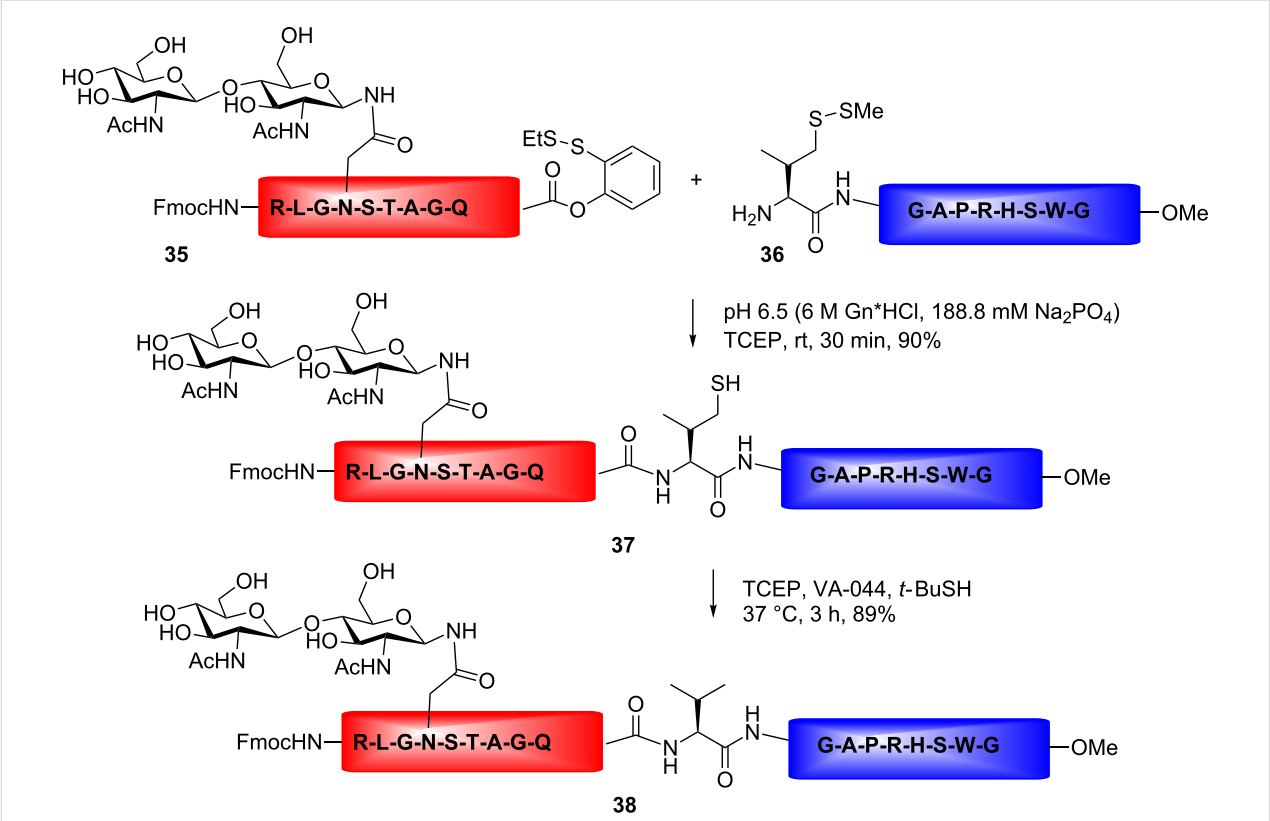

Scheme 6: NCL of a glycopeptide fragment, generating valine by desulfurization at the ligation site.

saccharides to a GlcNAc polypeptide. Until recently, the application of the transglycosylation reaction was of limited use, due to competing enzyme hydrolysis of the formed glycopeptide/protein. By use of oxazoline transition-state analogue substrates, the rate for the transglycosylation reaction was increased and thereby the slower product hydrolysis reaction could be avoided [84,85]. A number of successful preparations of *N*-glycopeptides and *N*-glycoproteins have since then been successfully prepared by using oxazoline oligosaccharide donors; the synthesis of a HIV gp120 glycopeptide fragment, the HIV gp41 peptide, and the RNase B glycoprotein are a few examples [84,86-89]. The glycan remodeling approach is particularly interesting for glycoprotein synthesis. This method was employed in the synthesis of two RNase B glycoproteins modified with either high-mannose or complex type *N*-glycans [87]. The bovine RNase B glycoprotein **39** used in this study contained a mixture of high-mannose glycoforms; by treatment with endoglycosidase H (Endo-H), these glycans could be hydrolytically cleaved leaving the GlcNAc monosaccharide still attached to the protein. By treatment with a complex type glycan oxazoline donor and an Endo-M mutant or a high-mannose oxazoline donor and an Endo-A mutant, two different homogenous glycoproteins **40** and **41** were formed (Scheme 7) [87].

Glycopeptide binding events

Carbohydrates on proteins and lipids play critical roles in cell–cell and cell–external-agent binding events. Efforts in the preparation of diverse carbohydrate structures immobilized in a microarray format have made carbohydrates accessible for numerous functional studies of protein-binding recognition [90-92]. In addition to the glycan structure, multivalency and orientation are important for the presentation of glycan ligands, and, in addition, the peptide backbone of the glycoprotein is sometimes a part of the binding recognition domain. Synthetic glycopeptides with natural multivalent presentation of glycan structures may function as tools for the investigation of protein-binding events. Applications of glycopeptides in a microarray format are desirable for such binding studies. Evaluation of antibody binding epitopes in vaccine and biomarker discovery is one recent example of glycopeptide microarrays [93,94].

Multivalency and orientation for glycan presentation have been shown to be important for the inhibition of microbe and lectin binding [95-105]. The synthesis of glycoclusters/dendrimers is an area of research aimed at tackling the increasing problems with bacterial multi-antibiotic resistance. Microbe adherence to the glycans on the tissue cell surface is essential for an infection to progress. As a consequence, mutations of the pathogen

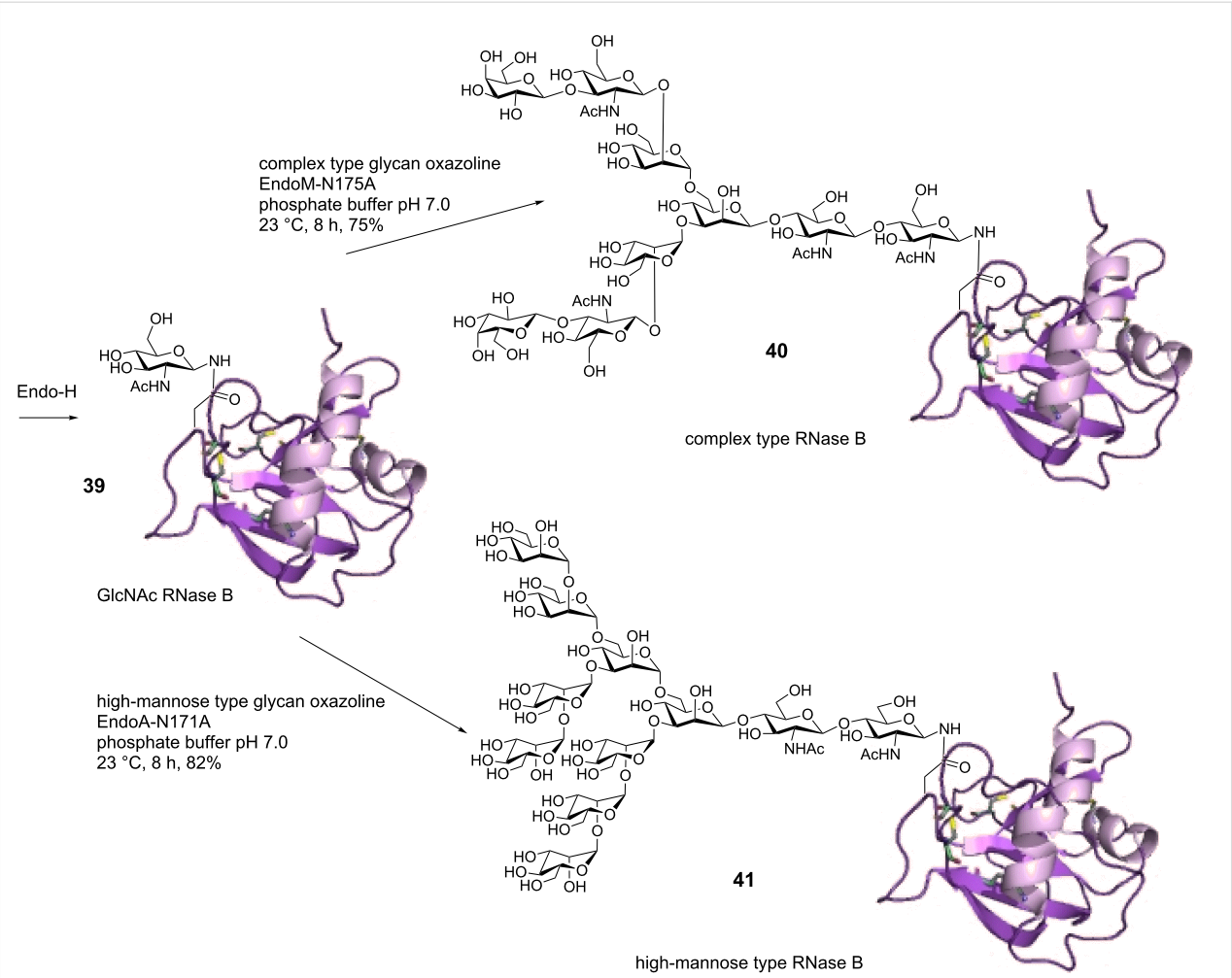

Scheme 7: Synthesis of homogeneous glycoproteins by chemoenzymatic glycan remodeling.

adhesion proteins, resulting in a loss of cell-surface binding recognition are not very likely to occur. Interference with the microbe binding events by employing an anti-adhesive strategy could therefore be very efficient. In several microbe and lectin binding studies, glycopeptide based glycoclusters/dendrimers were applied, employing linear peptide backbones, cyclic peptide scaffolds or multi-lysine scaffolds [106-118].

The pentavalent cholera toxin protein secreted by *Vibrio cholerae,* causes severe diarrhea and massive dehydration upon binding and entrance into the intestinal epithelial cells [119]. The AB_5-type toxin consists of one toxic ADP-ribosyltransferase and five lectin subunits that bind to the gangloside GM1 ligands on the epithelial cell surface [120]. The cholera-toxin–GM1 complex is one of the most well characterized protein–carbohydrate interactions [95-99]. Development of inhibitors targeting the cholera-toxin protein–carbohydrate binding events is a novel strategy for disease prevention and therapy as well as for detection of the toxin in patient samples. Binding studies to GM1 ligands have clearly demonstrated the importance of multivalency in protein–carbohydrate binding recognition [95-99,120]. In one study, a 380,000 (47,000/sugar)-fold affinity enhancement and an IC_{50} of 50 pM was reported, by comparison of a GM1 monovalent derivative with the multivalent inhibitor [121]. The X-ray crystal structure of the cholera-toxin–GM1-ganglioside complex has shown that most of the protein contacts are given to the terminal galactose unit [122]. With this knowledge in hand, dendrimers based on readily available galactose monosaccharide ligands have been prepared and evaluated [123].

The type 1 fimbriated *Echerichia coli* is a pathogen responsible for urinary tract infections with millions of cases every year [124]. The type 1 fimbriae have been identified to be a major contributor to these infections [125,126]. The FimH lectin on type 1 fimbriae is an attractive target for the inhibition of

α-mannose-mediated cell adhesion [127-131]. Previous X-ray studies have proven that the FimH lectin has a monovalent binding site recognizing α-*D*-mannose [132,133]. In close proximity to the mannose-binding crevice, two tyrosine residues form the "tyrosine gate" [134]. By π–π stacking interactions with the aromatic tyrosine residues, monovalent α-mannose ligands containing hydrophobic aglycons, have shown increased binding affinities [128,135,136]. Employing multivalent ligands, the binding affinity to FimH could be further increased [137-139]. In one study, the FimH inhibition of mannosylated di- and tetravalent lysine core dendrimers resulted in 455- and 2000-fold increases relative to a monovalent mannose residue [114]. The observed multivalency effects are not fully understood. In a recent study, mannose di- and trivalent glycopeptides were evaluated for their inhibition of FimH binding [107]. The valency, conformational properties, and spatial arrangement of the attached mannose residues were evaluated. Glycopeptides containing an aromatic aglycon showed increased affinity to FimH due to interactions with the FimH tyrosine gate; this effect was more pronounced by the divalent glycopeptides. In accordance with other studies, it could be concluded that the distance between the mannoside ligands was important, showing stronger inhibition for the divalent glycopeptide with a larger spatial ligand distance (Figure 2) [140-142].

In another study, a combinatorial library of fucosyl-peptide dendrimers was synthesized and screened for binding to the fucose-specific lectin (LecB) from *Pseudomonas aeruginosa*, a pathogen causing severe infections in patients leading to chronic inflammation in the airways [106,143]. Previously, it was found that the LecB protein was important for biofilm formation [144-146]. In the screening for LecB inhibitors, one glycopeptide dendrimer, FD2 **49** (C-FucLysPro-Leu)$_4$(LysPheLysIle)$_2$LysHisIleNH$_2$, showed particularly strong LecB inhibition (FD2 IC_{50} = 0.14 μM and L-fucose IC_{50} = 11 μM) [106]. The glycopeptide dendrimer was able to completely inhibit *P. aeruginosa* biofilm formation at a concentration of 50 μM and established biofilms from wild-type strain and clinical isolates could be completely dispersed. In a later study, analogues of FD2 **49** were prepared; in one of them the L-amino acids were replaced by D-amino acids (D-FD2, **51**) to avoid proteolytic cleavage of the peptide construct [147]. Interestingly, it was found that the D-FD2 **51** glycopeptide

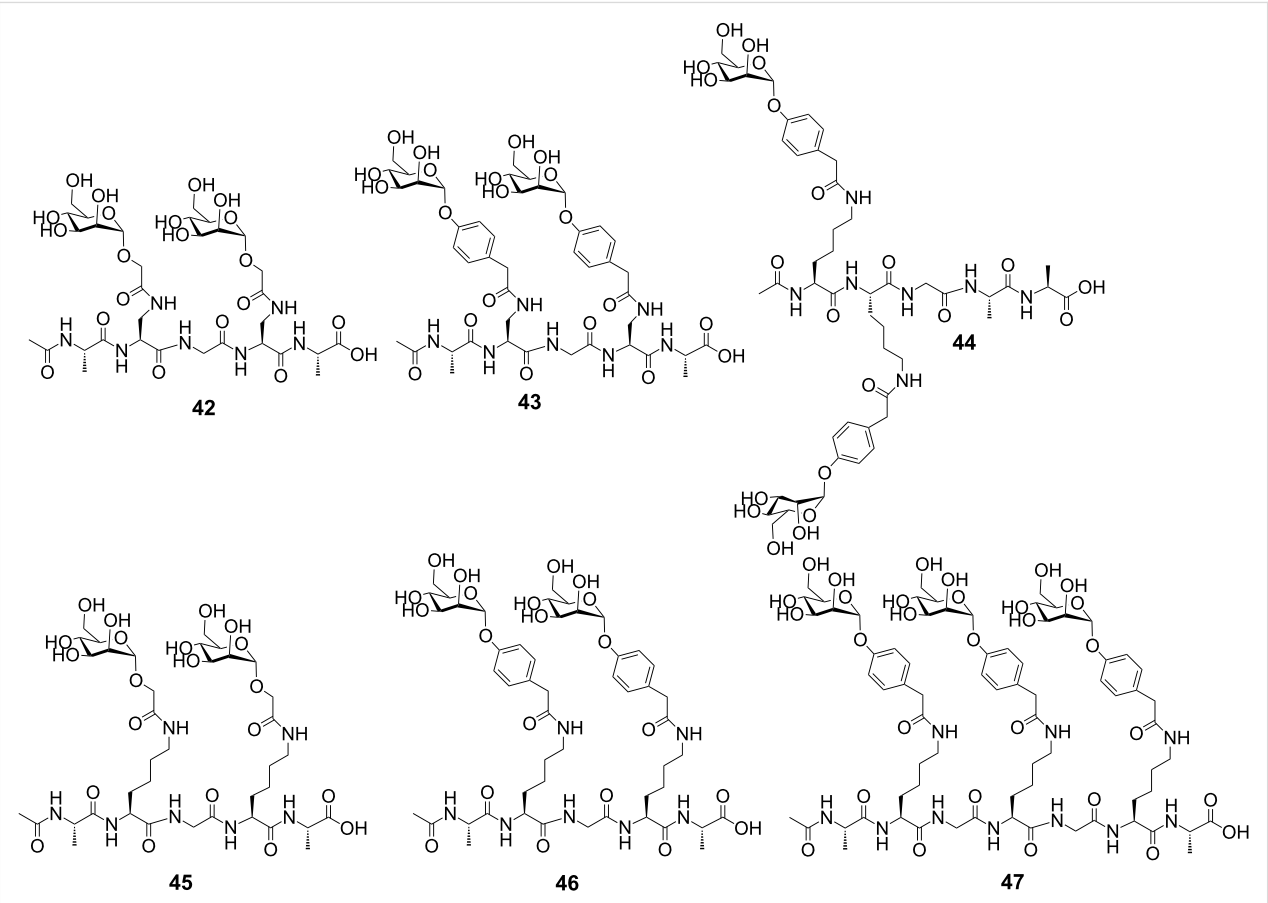

Figure 2: Di- and trivalent glycopeptide dendrimers evaluated for FimH inhibition.

dendrimer showed a slightly weaker binding affinity to LecB, but the *P. aeruginosa* biofilm inhibitory properties remained, whereas D-FD2 **51**, in contrast to FD2 **49**, was completely resistant to proteolysis (Table 1) [147].

Considering the favorable properties of the FD2 LecB inhibitor, an identical peptide dendrimer backbone was employed for the development of inhibitors of the galactose-specific *P. aeruginosa* lectin LecA [148]. By incorporation of hydrophobic groups to the galactose anomeric position, the affinity to LecA could be further enhanced. The most potent LecA inhibitor from these studies, GalAG2, showed a 4000-fold increase in hemagglutination inhibition activity and 875-fold increase in binding (K_d) to LecA compared with D-galactose [148]. Similar to the LecB inhibitor FD2, complete inhibition of biofilm formation was observed.

Conclusions

Recent developments of synthetic methodologies have enabled the preparation of complex glycopeptides and glycoproteins. The availability of structurally defined material has further made it possible to apply glycopeptides in biological studies. The development of glycopeptide anti-tumor vaccines and the synthesis of homogenous glycoproteins and glycopeptide dendrimers for the inhibition of microbe binding events are examples described in this review. The development of methods in the synthesis of homogenous glycoproteins may result in new therapeutic applications. Better understanding of protein glycosylation will help to identify new protein targets for immunotherapy. The synthesis and application of glycopeptide microarrays is an upcoming topic, which will offer multivalent presentation and fine-tuning in studies of specific protein-binding events.

Table 1: Synthesis of LecB glycopeptide dendrimer ligands for biofilm inhibition.

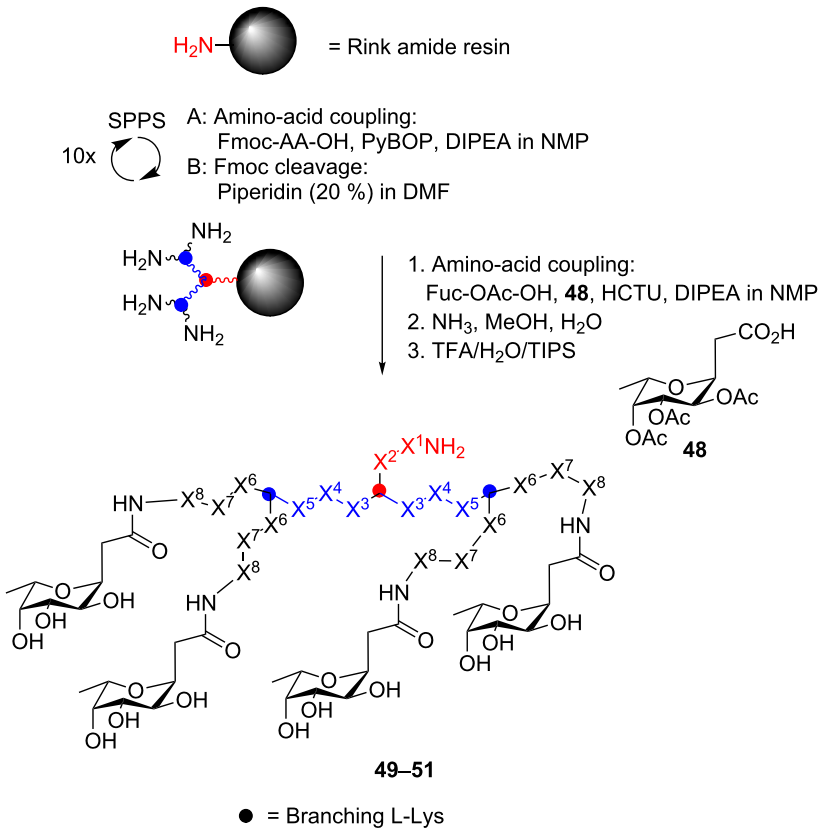

	X^8	X^7	X^6	X^5	X^4	X^3	X^2	X^1
FD2 (**49**)	Lys	Pro	Leu	Phe	Lys	Ile	His	Ile
Leu-**FD2** (**50**)	Lys	Pro	Leu	Phe	Lys	Leu	His	Leu
D-**FD2** (**51**)	D-Lys	D-Pro	D-Leu	D-Phe	D-Lys	D-Leu	D-His	D-Leu

References

1. Lis, H.; Sharon, N. *Eur. J. Biochem.* **1993,** *218,* 1–27. doi:10.1111/j.1432-1033.1993.tb18347.x
2. Dwek, R. A. *Chem. Rev.* **1996,** *96,* 683–720. doi:10.1021/cr940283b
3. Kim, Y. J.; Varki, A. *Glycoconjugate J.* **1997,** *14,* 569–576. doi:10.1023/A:1018580324971
4. Geyer, H.; Geyer, R. Glycobiology of Viruses. In *Carbohydrates in Chemistry and Biology;* Ernst, B.; Hart, G. W.; Sinaj, P., Eds.; Wiley-VCH: Weinheim, Germany, 2008; pp 821–838. doi:10.1002/9783527618255.ch89
5. Moncada, D. M.; Kammanadiminti, S. J.; Chadee, K. *Trends Parasitol.* **2003,** *19,* 305–311. doi:10.1016/S1471-4922(03)00122-3
6. Meyer, B.; Möller, H. *Top. Curr. Chem.* **2007,** *267,* 187–251. doi:10.1007/128_2006_078
7. Becker, T.; Dziadek, S.; Wittrock, S.; Kunz, H. *Curr. Cancer Drug Targets* **2006,** *6,* 491–517. doi:10.2174/156800906778194577
8. Pudelko, M.; Bull, J.; Kunz, H. *ChemBioChem* **2010,** *11,* 904–930. doi:10.1002/cbic.201000029
9. Sebestik, J.; Niederhafner, P.; Jezek, J. *Amino Acids* **2011,** *40,* 301–370. doi:10.1007/s00726-010-0707-z
10. Mintzer, M. A.; Dane, E. L.; O'Toole, G. A.; Grinstaff, M. W. *Mol. Pharmaceutics* **2012,** *9,* 342–354. doi:10.1021/mp2005033
11. Westerlind, U.; Kunz, H. Advances in *N*- and *O*-Glycopeptide Syntehsis – A Tool to Study Glycosylation and Develop New Therapeutics. In *Amino Acids, Peptides; Proteins in Organic Chemistry;* Hughes, A. B., Ed.; Wiley-VCH: Weinheim, Germany, 2011; Vol. 4, pp 321–358. doi:10.1002/9783527631827.ch10
12. Haase, C.; Seitz, O. *Top. Curr. Chem.* **2007,** *267,* 1–36. doi:10.1007/128_043
13. Herzner, H.; Reipen, T.; Schultz, M.; Kunz, H. *Chem. Rev.* **2000,** *100,* 4495–4538. doi:10.1021/cr990308c
14. Yuan, Y.; Chen, J.; Wan, Q.; Wilson, R. M.; Danishefsky, S. *J. Pept. Sci.* **2010,** *94,* 373–384. doi:10.1002/bip.21374
15. Gamblin, D. P.; Scanlan, E. M.; Davis, B. G. *Chem. Rev.* **2009,** *109,* 131–163. doi:10.1021/cr078291i
16. Kajihara, Y.; Yamamoto, N.; Okamoto, R.; Hirano, K.; Murase, T. *Chem. Rec.* **2010,** *10,* 80–100. doi:10.1002/tcr.200900024
17. Westerlind, U.; Kunz, H. *Carbohydr. Chem.* **2010,** *36,* 1–37. doi:10.1039/9781849730891-00001
18. Warren, D. J.; Geng, X.; Danishefsky, S. J. *Top. Curr. Chem.* **2007,** *267,* 109–141. doi:10.1007/128_031
19. Springer, G. F. *Science* **1984,** *224,* 1198–1206. doi:10.1126/science.6729450
20. Taylor-Papadimitriou, J.; Burchell, J.; Miles, D. W.; Dalziel, M. *Biochim. Biophys. Acta, Mol. Basis Dis.* **1999,** *1455,* 301–313. doi:10.1016/S0925-4439(99)00055-1
21. Beatson, R. E.; Taylor-Papadimitriou, J.; Burchell, J. M. *Immunotherapy* **2010,** *2,* 305–327. doi:10.2217/imt.10.17
22. Sørensen, A. L.; Reis, C. A.; Trap, M. A.; Mandel, U.; Ramachandran, K.; Sankaranarayanan, V.; Schwientek, T.; Graham, R.; Taylor-Papadimitriou, J.; Hollingworth, M. A.; Burchell, J.; Clausen, H. *Glycobiology* **2006,** *16,* 96–107. doi:10.1093/glycob/cwj044
23. von Mensdorff-Pouilly, S.; Moreno, M.; Verheijen, R. H. M. *Cancers* **2011,** *3,* 3073–3103. doi:10.3390/cancers3033073
24. Westerlind, U.; Kunz, H. *Chimia* **2011,** *65,* 30–34. doi:10.2533/chimia.2011.30
25. Brockhausen, I.; Yang, J.-M.; Bruchell, J.; Whitehouse, C.; Taylor-Papadimitriou, J. *Eur. J. Biochem.* **1995,** *233,* 607–617. doi:10.1111/j.1432-1033.1995.607_2.x
26. Burchell, J. M.; Mungul, A.; Taylor-Papadimitriou, J. *J. Mammary Gland Biol. Neoplasia* **2001,** *6,* 355–364. doi:10.1023/A:1011331809881
27. Lloyd, K. O.; Burchell, J.; Kudryashov, V.; Yin, B. W. T.; Taylor-Papadimitriou, J. *J. Biol. Chem.* **1996,** *271,* 33325–33334. doi:10.1074/jbc.271.52.33325
28. Kaiser, A.; Gaidzik, N.; Westerlind, U.; Kowalczyk, D.; Hobel, A.; Schmitt, E.; Kunz, H. *Angew. Chem., Int. Ed.* **2009,** *48,* 7551–7555. doi:10.1002/anie.200902564
29. Hoffmann-Röder, A.; Kaiser, A.; Wagner, S.; Gaidzik, N.; Kowalczyk, D.; Westerlind, U.; Gerlitzki, B.; Schmitt, E.; Kunz, H. *Angew. Chem., Int. Ed.* **2010,** *49,* 8498–8503. doi:10.1002/anie.201003810
30. Ingale, S.; Wolfert, M. A.; Gaekwad, J.; Buskas, T.; Boons, G.-J. *Nat. Chem. Biol.* **2007,** *3,* 663–667. doi:10.1038/nchembio.2007.25
31. Becker, T.; Kaiser, A.; Kunz, H. *Synthesis* **2009,** 1113–1122. doi:10.1055/s-0028-1088002
32. Keil, S.; Kaiser, A.; Syed, F.; Kunz, H. *Synthesis* **2009,** 1355–1369. doi:10.1055/s-0028-1088033
33. Westerlind, U.; Hobel, A.; Gaidzik, N.; Schmitt, E.; Kunz, H. *Angew. Chem., Int. Ed.* **2008,** *47,* 7551–7556. doi:10.1002/anie.200802102
34. Gaidzik, N.; Kaiser, A.; Kowalczyk, D.; Westerlind, U.; Gerlitzki, B.; Sinn, H. P.; Schmitt, E.; Kunz, H. *Angew. Chem., Int. Ed.* **2011,** *50,* 9977–9981. doi:10.1002/anie.201104529
35. Kaiser, A.; Gaidzik, N.; Becker, T.; Menge, C.; Groh, K.; Cai, H.; Li, Y.-M.; Gerlitzki, B.; Schmitt, E.; Kunz, H. *Angew. Chem., Int. Ed.* **2010,** *49,* 3688–3692. doi:10.1002/anie.201000462
36. Wilkinson, B. L.; Day, S.; Malins, L. R.; Apostolopoulos, V.; Payne, R. J. *Angew. Chem., Int. Ed.* **2011,** *50,* 1635–1639. doi:10.1002/anie.201006115
37. Lakshminarayanan, V.; Thompson, P.; Wolfert, M. A.; Buskas, T.; Bradley, J. M.; Pathangey, L. B.; Madsen, C. S.; Cohen, P. A.; Gendler, S. J.; Boons, G.-J. *Proc. Natl. Acad. Sci. U. S. A.* **2012,** *109,* 261–266. doi:10.1073/pnas.1115166109
38. Cai, H.; Huang, Z.-H.; Shi, L.; Zhao, Y.-F.; Kunz, H.; Li, Y.-M. *Chem.–Eur. J.* **2011,** *17,* 6396–6406. doi:10.1002/chem.201100217
39. Dawson, P. E.; Muir, T. W.; Clark-Lewis, I.; Kent, S. B. *Science* **1994,** *266,* 776–779. doi:10.1126/science.7973629
40. Bang, D.; Makhatadze, G. I.; Tereshko, V.; Kossiakoff, A. A.; Kent, S. B. *Angew. Chem., Int. Ed.* **2005,** *44,* 3852–3856. doi:10.1002/anie.200463040
41. Brunsveld, L.; Kuhlmann, J.; Alexandrov, K.; Wittinghofer, A.; Goody, R. S.; Waldmann, H. *Angew. Chem., Int. Ed.* **2006,** *45,* 6622–6646. doi:10.1002/anie.200600855
42. Kurpiers, T.; Mootz, H. D. *Angew. Chem., Int. Ed.* **2007,** *46,* 5234–5237. doi:10.1002/anie.200700719
43. Lahiri, S.; Brehs, M.; Olschewski, D.; Becker, C. F. W. *Angew. Chem., Int. Ed.* **2011,** *50,* 3988–3992. doi:10.1002/anie.201006686
44. Kumar, K. S. A.; Bavikar, S. N.; Spasser, L.; Moyal, T.; Ohayon, S.; Brik, A. *Angew. Chem., Int. Ed.* **2011,** *50,* 6137–6141. doi:10.1002/anie.201101920
45. Muir, T. W. *Annu. Rev. Biochem.* **2003,** *72,* 249–289. doi:10.1146/annurev.biochem.72.121801.161900

46. Shin, Y.; Winans, K. A.; Backes, B. J.; Kent, S. B. H.; Ellman, J. A.; Bertozzi, C. R. *J. Am. Chem. Soc.* **1999,** *121,* 11684–11689. doi:10.1021/ja992881j
47. Marcaurelle, L. A.; Mizoue, L. S.; Wilken, J.; Oldham, L.; Kent, S. B. H.; Handel, T. M.; Bertozzi, C. R. *Chem.–Eur. J.* **2001,** *7,* 1129–1132. doi:10.1002/1521-3765(20010302)7:5<1129::AID-CHEM1129>3.0.CO;2-W
48. Macmillan, D.; Bertozzi, C. R. *Angew. Chem., Int. Ed.* **2004,** *43,* 1355–1359. doi:10.1002/anie.200352673
49. Wilkinson, B. L.; Chun, C. K. Y.; Payne, R. J. *Pep. Sci.* **2010,** *98,* 137–146.
50. Hojo, H.; Matsumoto, Y.; Nakahara, Y.; Ito, E.; Suzuki, Y.; Suzuki, M.; Suzuki, A.; Nakahara, Y. *J. Am. Chem. Soc.* **2005,** *127,* 13720–13725. doi:10.1021/ja053711b
51. Piontek, C.; Varón Silva, D.; Heinlein, C.; Pöhner, C.; Mezzato, S.; Ring, P.; Martin, A.; Schmid, F. X.; Unverzagt, C. *Angew. Chem., Int. Ed.* **2009,** *48,* 1941–1945. doi:10.1002/anie.200804735
52. Piontek, C.; Ring, P.; Harjes, C.; Heinlein, C.; Mezzato, S.; Lombana, N.; Pöhner, C.; Püttner, M.; Varón Silva, D.; Martin, A.; Schmid, F. X.; Unverzagt, C. *Angew. Chem., Int. Ed.* **2009,** *48,* 1936–1940. doi:10.1002/anie.200804734
53. Heinlein, C.; Varón Silva, D.; Tröster, A.; Schmidt, J.; Gross, A.; Unverzagt, C. *Angew. Chem., Int. Ed.* **2011,** *50,* 6406–6410. doi:10.1002/anie.201101270
54. Baynes, J. W.; Wold, F. *J. Biol. Chem.* **1976,** *251,* 6016–6024.
55. Crook, E. M.; Mathias, A. P.; Rabin, B. R. *Biochem. J.* **1960,** *74,* 234–238.
56. Hodges, R. S.; Merrifield, R. B. *J. Biol. Chem.* **1975,** *250,* 1231–1241.
57. Nagorny, P.; Sane, N.; Fasching, B.; Aussedat, B.; Danishefsky, S. J. *Angew. Chem., Int. Ed.* **2012,** *51,* 975–979. doi:10.1002/anie.201107482
58. Smith, P. E. *J. Am. Med. Assoc.* **1927,** *88,* 158–161. doi:10.1001/jama.1927.02680290020005
59. Howles, C. M. *Hum. Reprod. Update* **1996,** *2,* 172–191. doi:10.1093/humupd/2.2.172
60. Li, Y.; Ganta, S.; Cheng, C.; Craig, R.; Ganta, R. R.; Freeman, L. C. *Mol. Cell. Endocrinol.* **2007,** *267,* 26–37. doi:10.1016/j.mce.2006.11.010
61. Jelkmann, W. *Intern. Med.* **2004,** *43,* 649–659. doi:10.2169/internalmedicine.43.649
62. Higuchi, M.; Oh-eda, M.; Kuboniwa, H.; Tomonoh, K.; Shimonaka, Y.; Ochi, N. *J. Biol. Chem.* **1992,** *267,* 7703–7709.
63. Egrie, J. C.; Grant, J. R.; Gilles, D. K.; Aoki, K. H.; Strickland, T. W. *Glycoconjugate J.* **1993,** *10,* 263. doi:10.1007/BF01209934
64. Hirano, K.; Macmillan, D.; Tezuka, K.; Tsuji, T.; Kajihara, Y. *Angew. Chem., Int. Ed.* **2009,** *48,* 9557–9560. doi:10.1002/anie.200904376
65. Kajihara, Y.; Izumi, M.; Hirano, K.; Murase, T.; Macmillan, D.; Okamoto, R. *Isr. J. Chem.* **2011,** *51,* 917–929. doi:10.1002/ijch.201100081
66. Kan, C.; Trzupek, J. D.; Wu, B.; Wan, Q.; Chen, G.; Tan, Z.; Yuan, Y.; Danishefsky, S. J. *J. Am. Chem. Soc.* **2009,** *131,* 5438–5443. doi:10.1021/ja808707w
67. Tan, Z.; Shang, S.; Halkina, T.; Yuah, Y.; Danishefsky, S. J. *J. Am. Chem. Soc.* **2009,** *131,* 5424–5431. doi:10.1021/ja808704m
68. Yuan, Y.; Chen, J.; Wan, Q.; Tan, Z.; Chen, G.; Kan, C.; Danishefsky, S. J. *J. Am. Chem. Soc.* **2009,** *131,* 5432–5437. doi:10.1021/ja808705v
69. Dong, S.; Shang, S.; Tan, Z.; Danishefsky, S. J. *Isr. J. Chem.* **2011,** *51,* 968–976. doi:10.1002/ijch.201100077
70. Offer, J.; Boddy, C. N. C.; Dawson, P. E. *J. Am. Chem. Soc.* **2002,** *124,* 4642–4646. doi:10.1021/ja016731w
71. Yan, L. Z.; Dawson, P. E. *J. Am. Chem. Soc.* **2001,** *123,* 526–533. doi:10.1021/ja003265m
72. Pentelute, B. L.; Kent, S. B. H. *Org. Lett.* **2007,** *9,* 687–690. doi:10.1021/ol0630144
73. Chen, J.; Wan, Q.; Yuan, Y.; Zhu, J.; Danishefsky, S. J. *Angew. Chem., Int. Ed.* **2008,** *47,* 8521–8524. doi:10.1002/anie.200803523
74. Crich, D.; Banerjee, A. *J. Am. Chem. Soc.* **2007,** *129,* 10064–10065. doi:10.1021/ja072804l
75. Haase, C.; Rhode, H.; Seitz, O. *Angew. Chem., Int. Ed.* **2008,** *47,* 6807–6810. doi:10.1002/anie.200801590
76. Wan, Q.; Danishefsky, S. J. *Angew. Chem., Int. Ed.* **2007,** *46,* 9248–9252. doi:10.1002/anie.200704195
77. Bennett, C. S.; Dean, S. M.; Payne, R. J.; Ficht, S.; Brik, A.; Wong, C.-H. *J. Am. Chem. Soc.* **2008,** *130,* 11945–11952. doi:10.1021/ja8010513
78. Wu, B.; Chen, J.; Warren, J. D.; Chen, G.; Hua, Z.; Danishefsky, S. J. *Angew. Chem., Int. Ed.* **2006,** *45,* 4116–4125. doi:10.1002/anie.200600538
79. Thayer, D. A.; Wong, C.-H. *Top. Curr. Chem.* **2007,** *267,* 37–63. doi:10.1007/128_032
80. Wang, L.-X. *Carbohydr. Res.* **2008,** *343,* 1509–1522. doi:10.1016/j.carres.2008.03.025
81. Yamamoto, K.; Kadowaki, S.; Watanabe, J.; Kumagai, H. *Biochem. Biophys. Res. Commun.* **1994,** *203,* 244–252. doi:10.1006/bbrc.1994.2174
82. Takegawa, K.; Yamaguchi, S.; Kondo, A.; Iwamoto, H.; Nakoshi, M.; Kato, I.; Iwahara, S. *Biochem. Int.* **1991,** *24,* 849–855.
83. Takegawa, K.; Yamaguchi, S.; Kondo, A.; Kato, I.; Iwahara, S. *Biochem. Int.* **1991,** *25,* 829–835.
84. Li, B.; Zeng, Y.; Hauser, S.; Song, H.; Wang, L.-X. *J. Am. Chem. Soc.* **2005,** *127,* 9692–9693. doi:10.1021/ja051715a
85. Heidecke, C. D.; Parsons, T. B.; Fairbanks, A. J. *Carbohydr. Res.* **2009,** *344,* 2433–2438. doi:10.1016/j.carres.2009.09.013
86. Li, H.; Li, B.; Song, H.; Breydo, L.; Baskakov, I. V.; Wang, L.-X. *J. Org. Chem.* **2005,** *70,* 9990–9996. doi:10.1021/jo051729z
87. Huang, W.; Li, C.; Li, B.; Umekawa, M.; Yamamoto, K.; Zhang, X.; Wang, L.-X. *J. Am. Chem. Soc.* **2009,** *131,* 2214–2223. doi:10.1021/ja8074677
88. Wang, L.-X.; Song, H.; Liu, S.; Lu, H.; Jiang, S.; Ni, J.; Li, H. *ChemBioChem* **2005,** *6,* 1068–1074. doi:10.1002/cbic.200400440
89. Huang, W.; Groothuys, S.; Heredia, A.; Kuijpers, B. H. M.; Rutjes, F. P. J. T.; van Delft, F. L.; Wang, L.-X. *ChemBioChem* **2009,** *10,* 1234–1242. doi:10.1002/cbic.200800741
90. Blixt, O.; Head, S.; Mondala, T.; Scanlan, C.; Huflejt, M.; Alvares, R.; Bryan, M. C.; Fazio, F.; Calarese, D.; Stevens, J.; Razi, N.; Stevens, D. J.; Skehel, J. J.; van Die, I.; Burton, D. R.; Wilson, I. A.; Cummings, R.; Bovin, N.; Wong, C.-H.; Paulson, J. C. *Proc. Natl. Acad. Sci. U. S. A.* **2004,** *101,* 17033–17038. doi:10.1073/pnas.0407902101
91. Kamena, F.; Tamborrini, M.; Liu, X.; Kwon, Y.-U.; Thompson, F.; Pluschke, G.; Seeberger, P. H. *Nat. Chem. Biol.* **2008,** *4,* 238–240. doi:10.1038/nchembio.75

92. Wang, C.-C.; Huang, Y.-L.; Ren, C.-T.; Lin, C.-W.; Hung, J.-T.; Yu, J.-C.; Yu, A. L.; Wu, C.-Y.; Wong, C.-H. *Proc. Natl. Acad. Sci. U. S. A.* **2008,** *105,* 11661–11666. doi:10.1073/pnas.0804923105
93. Westerlind, U.; Schröder, H.; Hobel, A.; Gaidzik, N.; Kaiser, A.; Niemeyer, C. M.; Schmitt, E.; Waldmann, H.; Kunz, H. *Angew. Chem., Int. Ed.* **2009,** *48,* 8263–8267. doi:10.1002/anie.200902963
94. Wandall, H. H.; Blixt, O.; Tarp, M. A.; Pedersen, J. W.; Bennett, E. P.; Mandel, U.; Ragupathi, G.; Livingston, P. O.; Hollingsworth, M. A.; Taylor-Papadimitriou, J.; Burchell, J.; Clausen, H. *Cancer Res.* **2010,** *70,* 1306–1313. doi:10.1158/0008-5472.CAN-09-2893
95. Fan, E.; Zhang, Z.; Minke, W. E.; Hou, Z.; Verlinde, C. L. M. J.; Hol, W. G. J. *J. Am. Chem. Soc.* **2000,** *122,* 2663–2664. doi:10.1021/ja993388a
96. Zhang, Z.; Merritt, E. A.; Ahn, M.; Roach, C.; Hou, Z.; Verlinde, C. L. M. J.; Hol, W. G. J.; Fan, E. *J. Am. Chem. Soc.* **2002,** *124,* 12991–12998. doi:10.1021/ja027584k
97. Merritt, E. A.; Zhang, Z.; Pickens, J. C.; Ahn, M.; Hol, W. G. J.; Fan, E. *J. Am. Chem. Soc.* **2002,** *124,* 8818–8824. doi:10.1021/ja0202560
98. Gargano, J. M.; Ngo, T.; Kim, J. Y.; Acheson, D. W. K.; Lees, W. J. *J. Am. Chem. Soc.* **2001,** *123,* 12909–12910. doi:10.1021/ja016305a
99. Arosio, D.; Vrasidas, I.; Valentini, P.; Liskamp, R. M. J.; Pieters, R. J.; Bernardi, A. *Org. Biomol. Chem.* **2004,** *2,* 2113–2124. doi:10.1039/b405344c
100. Kitov, P. I.; Sadowska, J. M.; Mulvey, G.; Armstrong, G. D.; Ling, H.; Pannu, N. S.; Read, R. J.; Bundle, D. R. *Nature* **2000,** *403,* 669–672. doi:10.1038/35001095
101. Mammen, M.; Chio, S.-K.; Whitesides, G. M. *Angew. Chem., Int. Ed.* **1998,** *37,* 2754–2794. doi:10.1002/(SICI)1521-3773(19981102)37:20<2754::AID-ANIE2754>3.0.CO;2-3
102. Lundquist, J. J.; Toone, E. J. *Chem. Rev.* **2002,** *102,* 555–578. doi:10.1021/cr000418f
103. Lindhorst, T. K. *Top. Curr. Chem.* **2002,** *218,* 201–235. doi:10.1007/3-540-45010-6_7
104. Lee, Y. C.; Lee, R. T. *Acc. Chem. Res.* **1995,** *28,* 321–327. doi:10.1021/ar00056a001
105. Turnbull, W. B.; Stoddart, J. F. *Rev. Mol. Biotechnol.* **2002,** *90,* 231–255. doi:10.1016/S1389-0352(01)00062-9
106. Johansson, E. M. V.; Crusz, S. A.; Kolomiets, E.; Buts, L.; Kadam, R. U.; Cacciarini, M.; Bartels, K.-M.; Diggle, S. P.; Cámara, M.; Williams, P.; Loris, R.; Nativi, C.; Rosenau, F.; Jaeger, K.-E.; Darbre, T.; Reymond, J.-L. *Chem. Biol.* **2008,** *15,* 1249–1257. doi:10.1016/j.chembiol.2008.10.009
107. Schierholt, A.; Hartmann, M.; Lindhorst, T. K. *Carbohydr. Res.* **2011,** *346,* 1519–1526. doi:10.1016/j.carres.2011.04.023
108. Tian, X.; Pai, J.; Baek, K.-H.; Ko, S.-K.; Shin, I. *Chem.–Asian J.* **2011,** *6,* 2107–2113. doi:10.1002/asia.201100319
109. Bossu, I.; Šulc, M.; Křenek, K.; Dufour, E.; Garcia, J.; Berthet, N.; Dumy, P.; Křen, V.; Renaudet, O. *Org. Biomol. Chem.* **2011,** *9,* 1948–1959. doi:10.1039/c0ob00772b
110. Wittmann, V.; Seeberger, S. *Angew. Chem., Int. Ed.* **2004,** *43,* 900–903. doi:10.1002/anie.200352055
111. Sprengard, U.; Schudok, M.; Schmidt, W.; Kretzschmar, G.; Kunz, H. *Angew. Chem., Int. Ed.* **1996,** *35,* 321–324. doi:10.1002/anie.199603211
112. Herzner, H.; Kunz, H. *Carbohydr. Res.* **2007,** *342,* 541–557. doi:10.1016/j.carres.2006.09.012
113. Franzyk, H.; Christensen, M. K.; Jørgensen, R. M.; Meldal, M.; Cordes, H.; Mouritsen, S.; Bock, K. *Bioorg. Med. Chem.* **1997,** *5,* 21–40. doi:10.1016/S0968-0896(96)00194-0
114. Nagahori, N.; Lee, R. T.; Nishimura, S.-I.; Pagé, D.; Roy, R.; Lee, Y. C. *ChemBioChem* **2002,** *3,* 836–844. doi:10.1002/1439-7633(20020902)3:9<836::AID-CBIC836>3.0.CO;2-2
115. Shaikh, H. A.; Sönnichsen, F. D.; Lindhorst, T. K. *Carbohydr. Res.* **2008,** *343,* 1665–1674. doi:10.1016/j.carres.2008.04.015
116. Wehner, J. W.; Lindhorst, T. K. *Synthesis* **2010,** 3070–3082. doi:10.1055/s-0030-1258157
117. Wiegand, M.; Lindhorst, T. K. *Eur. J. Org. Chem.* **2006,** 4841–4851. doi:10.1002/ejoc.200600449
118. Kolomiets, E.; Johansson, E. M. V.; Renaudet, O.; Darbre, T.; Reymond, J.-L. *Org. Lett.* **2007,** *9,* 1465–1468. doi:10.1021/ol070119d
119. Torgersen, M. L.; Skretting, G.; van Deurs, B.; Sandvig, K. *J. Cell Sci.* **2001,** *114,* 3737–3747.
120. Fan, E.; Merritt, E. A.; Verlinde, C. L. M. J.; Hol, W. G. J. *Curr. Opin. Struct. Biol.* **2000,** *10,* 680–686. doi:10.1016/S0959-440X(00)00152-4
121. Pukin, A. V.; Branderhorst, H. M.; Sisu, C.; Weijers, C. A. G. M.; Gilbert, M.; Liskamp, R. M. J.; Visser, G. M.; Zuilhof, H.; Pieters, R. J. *ChemBioChem* **2007,** *8,* 1500–1503. doi:10.1002/cbic.200700266
122. Merritt, E. A.; Kuhn, P.; Sarfaty, S.; Erbe, J. L.; Holmes, R. K.; Hol, W. G. J. *J. Mol. Biol.* **1998,** *282,* 1043–1059. doi:10.1006/jmbi.1998.2076
123. Branderhorst, H. M.; Liskamp, R. M. J.; Visser, G. M.; Pieters, R. J. *Chem. Commun.* **2007,** 5043–5045. doi:10.1039/b711070g
124. Osrin, D.; Vergnano, S.; Costello, A. *Curr. Opin. Infect. Dis.* **2004,** *17,* 217–224. doi:10.1097/00001432-200406000-00008
125. Ohlsen, K.; Oelschlaeger, T. A.; Hacker, J.; Khan, A. S. *Top. Curr. Chem.* **2009,** *288,* 109–120. doi:10.1007/128_2008_10
126. Jones, C. H.; Pinkner, J. S.; Roth, R.; Heuser, J.; Nicholes, A. V.; Abraham, S. N.; Hultgren, S. J. *Proc. Natl. Acad. Sci. U. S. A.* **1995,** *92,* 2081–2085. doi:10.1073/pnas.92.6.2081
127. Sperling, O.; Fuchs, A.; Lindhorst, T. K. *Org. Biomol. Chem.* **2006,** *4,* 3913–3922. doi:10.1039/b610745a
128. Dubber, M.; Sperling, O.; Lindhorst, T. K. *Org. Biomol. Chem.* **2006,** *4,* 3901–3912. doi:10.1039/b610741a
129. Ofek, I.; Hasty, D. L.; Sharon, N. *FEMS Immunol. Med. Microbiol.* **2003,** *38,* 181–191. doi:10.1016/S0928-8244(03)00228-1
130. Pieters, R. J. *Med. Res. Rev.* **2007,** *27,* 796–816. doi:10.1002/med.20089
131. Han, Z.; Pinkner, J. S.; Ford, B.; Obermann, R.; Nolan, W.; Wildman, S. A.; Hobbs, D.; Ellenberger, T.; Cusumano, C. K.; Hultgren, S. J.; Janetka, J. W. *J. Med. Chem.* **2010,** *53,* 4779–4792. doi:10.1021/jm100438s
132. Hung, C.-S.; Bouckaert, J.; Hung, D.; Pinkner, J.; Widberg, C.; DeFusco, A.; Auguste, C. G.; Strouse, R.; Langermann, S.; Waksman, G.; Hultgren, S. J. *Mol. Microbiol.* **2002,** *44,* 903–915. doi:10.1046/j.1365-2958.2002.02915.x
133. Bouckaert, J.; Berglund, J.; Schembri, M.; De Genst, E.; Cools, L.; Wuhrer, M.; Hung, C.-S.; Pinkner, J.; Slättegård, R.; Zavialov, A.; Choudhury, D.; Langermann, S.; Hultgren, S. J.; Wyns, L.; Klemm, P.; Oscarson, S.; Knight, S. D.; De Greve, H. *Mol. Microbiol.* **2005,** *55,* 441–455. doi:10.1111/j.1365-2958.2004.04415.x
134. Knight, S. D.; Bouckaert, J. *Top. Curr. Chem.* **2009,** *288,* 67–107. doi:10.1007/128_2008_13

135. Lindhorst, T. K.; Kötter, S.; Kubisch, J.; Krallmann-Wenzel, U.; Ehlers, S.; Křen, V. *Eur. J. Org. Chem.* **1998,** 1669–1674. doi:10.1002/(SICI)1099-0690(199808)1998:8<1669::AID-EJOC1669>3.0.CO;2-Q
136. Firon, N.; Ashkenazi, S.; Mirelman, D.; Ofek, I.; Sharon, N. *Infect. Immun.* **1987,** *55,* 472–476.
137. Touaibia, M.; Wellens, A.; Shiao, T. C.; Wang, Q.; Sirois, S.; Bouckaert, J.; Roy, R. *ChemMedChem* **2007,** *2,* 1190–1201. doi:10.1002/cmdc.200700063
138. Lindhorst, T. K.; Dubber, M.; Krallmann-Wenzel, U.; Ehlers, S. *Eur. J. Org. Chem.* **2000,** 2027–2034. doi:10.1002/1099-0690(200006)2000:11<2027::AID-EJOC2027>3.0.CO;2-L
139. Schierholt, A.; Hartmann, M.; Schwekendiek, K.; Lindhorst, T. K. *Eur. J. Org. Chem.* **2010,** 3120–3128. doi:10.1002/ejoc.201000185
140. Lahmann, M. *Top. Curr. Chem.* **2009,** *288,* 17–65. doi:10.1007/128_2008_30
141. Chabre, Y. M.; Roy, R. *Adv. Carbohydr. Chem. Biochem.* **2010,** *63,* 165–393. doi:10.1016/S0065-2318(10)63006-5
142. Touaibia, M.; Roy, R. *Mini-Rev. Med. Chem.* **2007,** *7,* 1270–1283. doi:10.2174/138955707782795610
143. Wagner, V. E.; Iglewski, B. H. *Clin. Rev. Allerg. Immunol.* **2008,** *35,* 124–134. doi:10.1007/s12016-008-8079-9
144. Mitchell, E.; Houles, C.; Sudakevitz, D.; Wimmerova, M.; Gautier, C.; Pérez, S.; Wu, A. M.; Gilboa-Garber, N.; Imberty, A. *Nat. Struct. Mol. Biol.* **2002,** *9,* 918–921. doi:10.1038/nsb865
145. Loris, R.; Tielker, D.; Jaeger, K.-E.; Wyns, L. *J. Mol. Biol.* **2003,** *331,* 861–870. doi:10.1016/S0022-2836(03)00754-X
146. Tielker, D.; Hacker, S.; Loris, R.; Strathmann, M.; Wingender, J.; Wilhelm, S.; Rosenau, F.; Jaeger, K.-E. *Microbiology* **2005,** *151,* 1313–1323. doi:10.1099/mic.0.27701-0
147. Johansson, E. M. V.; Kadam, R. U.; Rispoli, G.; Crusz, S. A.; Bartels, K.-M.; Diggle, S. P.; Cámara, M.; Williams, P.; Jaeger, K.-E.; Darbre, T.; Reymond, J.-L. *Med. Chem. Commun.* **2011,** *2,* 418–420. doi:10.1039/C0MD00270D
148. Kadam, R. U.; Bergmann, M.; Hurley, M.; Garg, D.; Cacciarini, M.; Swiderska, M. A.; Nativi, C.; Sattler, M.; Smyth, A. R.; Williams, P.; Cámara, M.; Stocker, A.; Darbre, T.; Reymond, J.-L. *Angew. Chem., Int. Ed.* **2011,** *50,* 10631–10635. doi:10.1002/anie.201104342

License and Terms

Beilstein Journal of Organic Chemistry

High-affinity multivalent wheat germ agglutinin ligands by one-pot click reaction

Henning S. G. Beckmann, Heiko M. Möller and Valentin Wittmann*

Full Research Paper

Open Access

Address:
Fachbereich Chemie and Konstanz Research School Chemical Biology (KoRS-CB), Universität Konstanz, 78457 Konstanz, Germany

Email:
Valentin Wittmann* - mail@valentin-wittmann.de

* Corresponding author

Keywords:
carbohydrates; click chemistry; cluster effect; lectins; multivalency

Beilstein J. Org. Chem. **2012,** *8,* 819–826.
doi:10.3762/bjoc.8.91

Received: 23 March 2012
Accepted: 21 May 2012
Published: 01 June 2012

This article is part of the Thematic Series "Synthesis in the glycosciences II".

Guest Editor: T. K. Lindhorst

Abstract

A series of six mono-, di-, and trivalent *N*,*N*'-diacetylchitobiose derivatives was conveniently prepared by employing a one-pot procedure for Cu(II)-catalyzed diazo transfer and Cu(I)-catalyzed azide–alkyne cycloaddition (CuAAC) starting from commercially available amines. These glycoclusters were probed for their binding potencies to the plant lectin wheat germ agglutinin (WGA) from *Triticum vulgaris* by an enzyme-linked lectin assay (ELLA) employing covalently immobilized *N*-acetylglucosamine (GlcNAc) as a reference ligand. IC_{50} values were in the low micromolar/high nanomolar range, depending on the linker between the two disaccharides. Binding enhancements β up to 1000 for the divalent ligands and 2800 for a trivalent WGA ligand, compared to *N*,*N*'-diacetylchitobiose as the corresponding monovalent ligand, were observed. Molecular modeling studies, in which the chitobiose moieties were fitted into crystallographically determined binding sites of WGA, correlate the binding enhancements of the multivalent ligands with their ability to bind to the protein in a chelating mode. The best WGA ligand is a trivalent cluster with an IC_{50} value of 220 nM. Calculated per mol of contained chitobiose, this is the best WGA ligand known so far.

Introduction

The recognition of carbohydrate structures by carbohydrate binding proteins (lectins) plays a fundamental role in numerous intra- and intercellular events during development, inflammation, immune response, cancer metastasis, and pathogen–host interactions [1,2]. Inhibition of such interactions by high-affinity ligands is of high medicinal interest for the treatment of many human diseases. However, carbohydrate–protein interactions are often characterized by low binding affinities. A possible solution to compensate for these weak individual receptor–ligand interactions is the multivalent presentation of sugar epitopes on suitable scaffolds. This principle is not only used in nature but is also a valid strategy for the construction of

artificial lectin ligands [3-13]. Prime examples are the recently described ligands for the Shiga-like [14,15] and cholera toxins [16,17] both belonging to the AB_5 family of bacterial toxins.

The frequent observation that the binding affinity of a multivalent ligand increases exponentially with the number of binding sites has been termed the glycoside cluster effect [18,19]. Due to the exponential increase of binding affinities, the cluster effect often leads to the amplification of the binding selectivity. This was experimentally demonstrated, for example, by Mortell et al. while investigating glycopolymer ligands of concanavalin A (Con A) [20]. Whereas two diastereomeric (monovalent) C-glycosidic Con A ligands displayed only a small difference in the free energies of binding to Con A, a sizable difference was measured between the corresponding multivalent C-glycosides (calculated per monovalent ligand within the glycopolymer). Such effects can be analyzed in the context of the chelate effect [21], and a number of theoretical models to treat multivalent receptor–ligand interactions have been developed [22-27]. A simple conclusion following from these analyses is that multimerization of monovalent ligands with enhanced binding affinity can lead to multivalent ligands with disproportionally enhanced avidity. A prerequisite for an effective multivalency effect, however, is that the linking spacer between the individual epitopes has the correct geometry to allow a simultaneous multipoint association, i.e., a chelating binding mode.

Wheat germ agglutinin (WGA), besides other plant lectins such as Con A, has been intensively employed as a model lectin to study the influence of the structure of multivalent ligands on the binding affinity. WGA ligands of defined structure containing two to twelve GlcNAc residues obtained either by individual synthesis [28-36] or from screening of combinatorial libraries [37,38] have been reported. WGA is a 36 kDa plant lectin composed of two identical glycine- and cysteine-rich subunits [39] and is enriched in the seeds of *Triticum vulgaris*. It is specific for terminal *N*-acetylneuraminic acid and *N*-acetylglucosamine (GlcNAc) and has been shown to inhibit fungal growth through interaction with fungal cell-wall components [40-42] and to agglutinate transformed cells in vitro [43,44].

Recently, we determined the structural basis of multivalent binding to WGA by X-ray crystallography [36] and EPR spectroscopy [45]. Crystal structure analysis of a complex of WGA and four molecules of a divalent ligand containing two GlcNAc residues showed that each ligand bridged adjacent binding sites with a distance of approx. 13–14 Å between the anomeric oxygen atoms of the GlcNAc residues. This structure confirmed for the first time that all eight sugar binding sites of the WGA dimer [46] are simultaneously functional, and provides the basis for the design of new multivalent ligands with improved binding affinity.

Besides GlcNAc, WGA also binds to chitooligosaccharides with even higher affinity. The association constant for the WGA–*N*,*N*'-diacetylchitobiose interaction, for example, has been determined to be $K \approx 5 \times 10^3$ to 2×10^4 M^{-1}. The corresponding value for binding to GlcNAc is $K \approx 2 \times 10^2$ to 1.3×10^3 M^{-1} [47]. This prompted us to design a series of multivalent WGA ligands containing two or three *N*,*N*'-diacetylchitobiose moieties. To connect the chitobiose moieties we chose several linkers of varying length and flexibility, which were, nevertheless, all expected to allow simultaneous binding to adjacent binding sites in a chelating fashion, thus, leading to especially effective ligands. In this report, we describe the preparation of such a series of multivalent WGA ligands by a one-pot procedure for diazo transfer and azide–alkyne cycloaddition [48] starting from commercially available di- and triamines and the propargyl glycoside of *N*,*N*'-diacetylchitobiose. Binding potencies were determined by an enzyme-linked lectin assay (ELLA), resulting in IC_{50} values in the low-micromolar/high-nanomolar range. A trivalent ligand has a remarkable IC_{50} value of 220 nM. Molecular dynamics calculations based on published X-ray crystal structures of WGA-ligand complexes provide an explanation for the observed binding affinities.

Results and Discussion

Synthesis of glycoclusters

The Cu(I)-catalyzed [49,50] Huisgen [3 + 2] cycloaddition [51] of azides and alkynes (CuAAC) is a frequently used method for the covalent attachment of carbohydrate epitopes to azide- or alkyne-presenting scaffolds [52-54]. Recently, we reported a convenient one-pot procedure for diazo transfer and azide–alkyne cycloaddition [48] giving access to multivalent triazole-linked structures starting from amines. For the synthesis of triazole-linked glycoclusters, commercially available amines **A1**–**A6** (Figure 1) comprising different spacer geometries were selected. These amines were employed in the sequen-

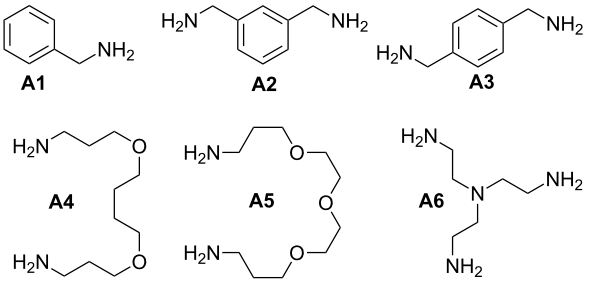

Figure 1: Amines used for the synthesis of glycoclusters.

tial one-pot procedure [48] for diazo transfer and CuAAC (Table 1). First, the Cu(II)-catalyzed diazo transfer was performed at ambient temperature until complete conversion of the amines to azides. Then, CuAAC was provoked without any workup procedure by the addition of tris(benzyltriazolylmethyl)amine [55] (TBTA), sodium ascorbate, and the propargyl glycoside **1** [56] of *N*,*N*'-diacetylchitobiose and heating of the mixture to 80 °C by microwave irradiation, until TLC showed complete consumption of the intermediate azides (see Supporting Information File 1 for full experimental data).

Table 1: Synthesis of glycoclusters **B1**–**B6** using the one-pot procedure for diazo transfer and azide-alkyne cycloaddition.

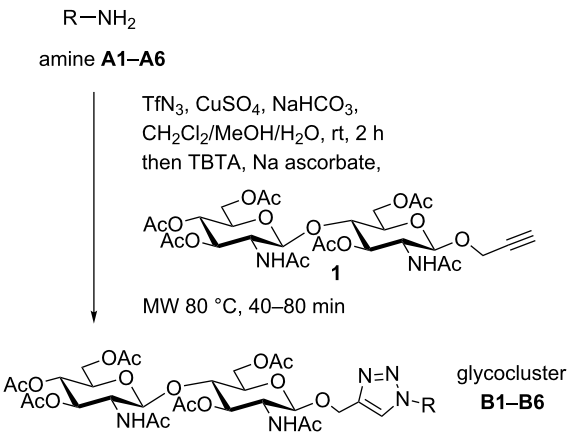

Amine	Product	Yield (%)
A1	**B1**	45
A2	**B2**	30
A3	**B3**	37
A4	**B4**	28
A5	**B5**	48[a]
A6	**B6**	6

[a]In this case the intermediate diazide **2** was isolated (cf. Scheme 1).

According to TLC all reactions (except for **B6**) proceeded with complete conversion of the amines to the desired glycoconjugates. However, some loss of material during purification of the acetylated chitobiose derivatives by flash chromatography on silica gel led to the moderate yields indicated in Table 1. Monovalent compounds resulting from partial reactions of the diamines were not observed. To exclude that the observed yields are a result of the one-pot procedure, the preparation of divalent **B5** was carried out in two separate steps (Scheme 1). Diazo transfer with **A5** gave diazide **2** in a yield of 95%. Subsequent CuAAC of isolated **2** with alkyne **1** delivered **B5** after flash chromatography in 51% yield with no observed side products. Severe loss of about 50% of the material during flash chromatography was also experienced when a pure sample of disaccharide **1** was eluted from a silica gel column for a second time. In comparison, the use of the less polar propargyl β-D-glucoside instead of **1** in the one-pot procedure with amine **A4** led to the corresponding divalent glycocluster in a yield of 86% [48]. Finally, *O*-deacetylation of the glycoclusters **B1**–**B6** under Zemplén conditions resulted in WGA ligands **C1**–**C6** (Scheme 2).

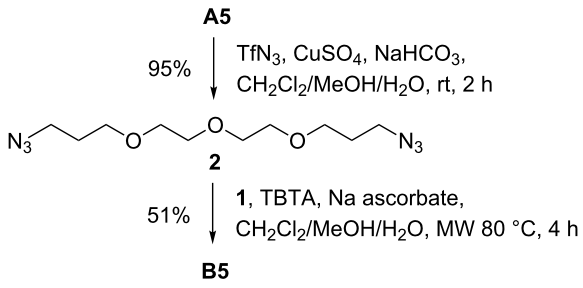

Scheme 1: Synthesis of glycocluster **B5** with isolation of the intermediate diazide **2**.

During the synthesis of trivalent compound **B6** the formation of a side product with a R_f similar to that of **B6** was observed. This is remarkable because all other reactions proceeded without the formation of side-products. The mass of this side product (*m*/*z* $[M + H]^+$ = 1500.7) corresponds to a divalent compound in which one arm of the tertiary amine is missing. Since this side product could not be isolated in pure form, we investigated the reaction of **A6** with phenylacetylene (**3**, Scheme 3). Also with this alkyne two main products were obtained which were difficult to separate by chromatography. Apart from the expected tris(triazole) **4**, the secondary amine **5** was isolated and characterized. This structure corresponds to the assumed side-product obtained during the synthesis of **B6**. A contamination of the starting material **A6** with secondary amine di(2-aminoethyl)amine was excluded. ESI–MS measurements indicated that side-product formation may already take place during the diazo transfer reaction of **A6** because the mass of the corresponding intermediate di(2-azidoethyl)amine (*m*/*z* $[M + H]^+$ = 156.2) was found. The mechanism of this side product formation is not clear. We assume that the mechanism is due to the special structure of **A6** because comparable side-product formation was not observed with any other amine used.

Determination of binding potencies by ELLA

Binding potencies of compounds **C1**–**C6**, GlcNAc, and *N*,*N*'-diacetylchitobiose were determined by an ELLA employing covalently immobilized GlcNAc as a reference ligand, as described recently [34]. GlcNAc-coated microtiter plates were incubated with mixtures of horseradish-peroxidase-labeled WGA (HRP-WGA) and synthetic WGA ligands in varying

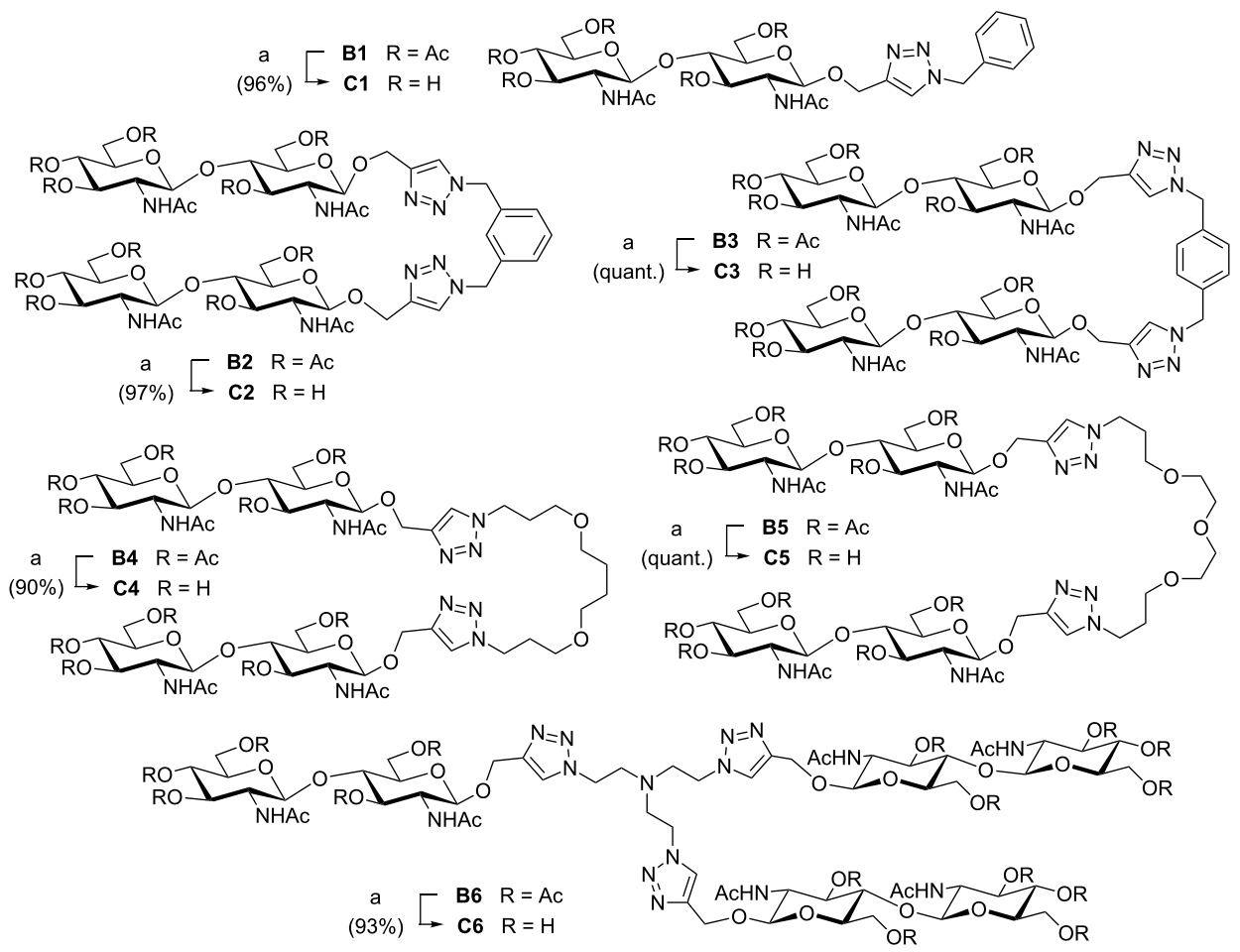

Scheme 2: Deacetylation of glycoconjugates **B1**–**B6**. (a) NaOMe, MeOH.

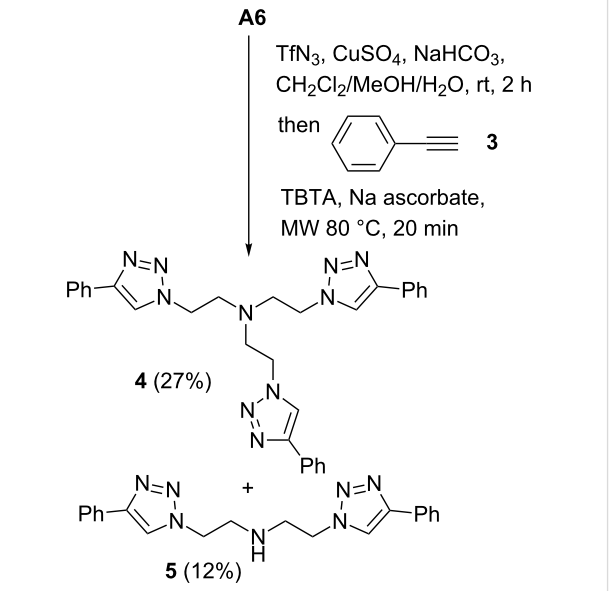

Scheme 3: Formation of side-product **5** during the synthesis of **4**.

concentrations. After incubation, the plates were washed and the remaining HRP-WGA bound to the microtiter plates was quantified by a HRP-catalyzed color reaction. Dose-response curves for inhibition of the binding of HRP–WGA to immobilized GlcNAc are shown in Figure 2. From these curves the concentrations at which the binding of HRP–WGA to GlcNAc is reduced by 50% (IC_{50} values) were determined as a measure of the potency of the synthesized inhibitors (Table 2). Also shown in Table 2 are the relative inhibitory potencies (β values) referenced to *N*,*N*'-diacetylchitobiose (β = 1).

With an 82 times lower IC_{50} value, *N*,*N*'-diacetylchitobiose is a much better inhibitor than GlcNAc, which is in accordance with the association constants determined by solution binding assays [47]. The benzyl triazolyl appendage of **C1** further enhances binding by a factor of two, probably due to additional weak hydrophobic interactions. However, introducing an additional *N*,*N*'-diacetylchitobiose epitope leads to dramatically increased affinities. The divalent chitobiose derivatives **C2**–**C5** have IC_{50} values in the low-micromolar/high-nanomolar range, with some

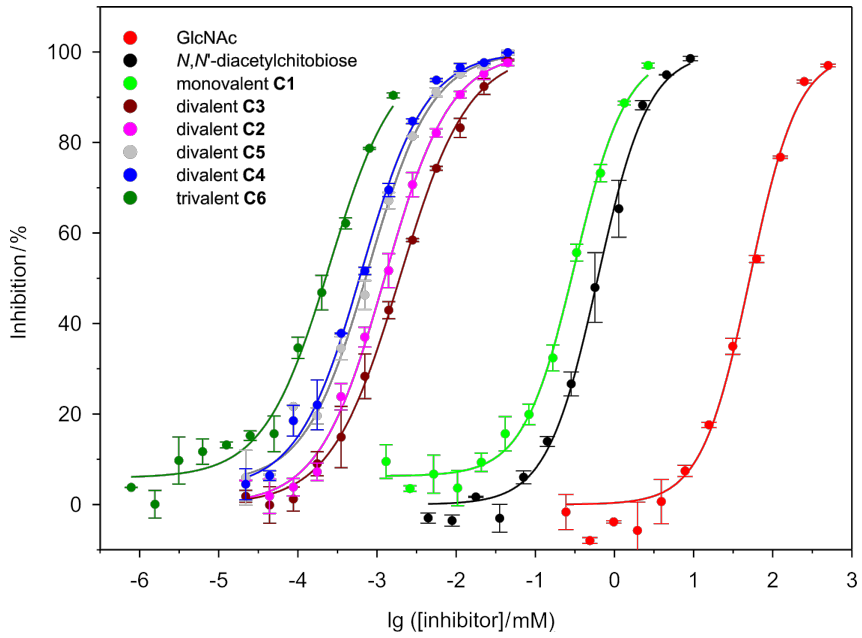

Figure 2: Dose-response curves for the inhibition of binding of HRP-labeled WGA to covalently immobilized GlcNAc by synthetic ligands **C1**–**C6**.

Table 2: Absolute and relative IC_{50} values of synthetic ligands **C1**–**C6** for inhibition of the binding of HRP-labeled WGA to covalently immobilized GlcNAc from dose-response curves shown in Figure 2.

Compound	IC_{50} (μM)	β
GlcNAc	51000	1/82
N,*N*'-diacetylchitobiose	620	1
monovalent **C1**	290	2.1
divalent **C2**	1.3	480
divalent **C3**	1.9	330
divalent **C4**	0.60	1000
divalent **C5**	0.72	860
trivalent **C6**	0.22	2800

variation due to different spacer properties. Their inhibitory potencies relative to *N*,*N*'-diacetylchitobiose are 330–1000. It is interesting to note the differences induced by differing linker geometries. Here, not the most hydrophobic linkers show strongest binding but the ones that apparently promote multivalent binding most efficiently. Whereas the flexible linkers of **C4** and **C5** lead to β values of 1000 and 860, respectively, the ligands **C2** and **C3** with the less flexible aromatic linkers have significantly lower binding potencies (β values: 480 and 330). This observation points to the possibility that the aromatic linkers cannot adopt a strain-free conformation if the ligand binds in a chelating mode to WGA. The best divalent WGA ligand is **C4** (IC_{50} 0.6 μM), which binds 1000 times stronger to WGA than *N*,*N*'-diacetylchitobiose (500 times per chitobiose residue).

As expected, clustering of carbohydrate epitopes with higher WGA binding affinity not only leads to multivalent ligands with higher absolute affinity but also to a higher binding enhancement β relative to the respective monovalent compound. Earlier, we reported WGA binding affinities of β-*O*-glycosidic divalent GlcNAc derivatives with linker lengths comparable to those of **C2**–**C5** [34]. These GlcNAc derivatives displayed β values of 80–260 relative to GlcNAc, which are much lower than the β values (330–1000, relative to *N*,*N*'-diacetylchitobiose) determined for **C2**–**C5** (Table 2). The relative potency of **C4** of 500 per chitobiose residue is even higher than that of tetra- to octavalent GlcNAc clusters [28,31-34,37]. We are aware of only one example of a divalent GlcNAc derivative with an exceptional β value of 2350 [36]. In this case, however, the GlcNAc moieties are α-*O*-glycosidically linked.

For trivalent cluster **C6** an IC_{50} value of 220 nM (660 nM per contained chitobiose) was determined, which is 2800-fold lower than that of *N*,*N*'-diacetylchitobiose or 230000-fold lower than the IC_{50} value of GlcNAc. This is one of the best WGA ligands known. Masaka et al. reported a tetravalent *N*,*N*'-diacetylchitobiose derivative with an IC_{50} value of 180 nM (720 nM per contained chitobiose) determined by a hemagglutination inhibition assay [57]. Calculating the IC_{50} value per contained chitobiose, trivalent **C6** is the better ligand. However, since such numbers are strongly dependent on the employed assay [58,59], they cannot be readily compared. Interestingly, the ligand reported by Masaka et al. led to precipitation of WGA. In this respect it is worth mentioning that we never observed precipi-

tate formation during incubation of WGA with our synthetic ligands. This suggests that in our case intermolecular multivalency (cross-linking) plays a negligible role and that the main mechanism of affinity enhancement is chelating binding to the same WGA dimer.

The 2.8-fold increased inhibition potency of **C6** over the best divalent ligand **C4** indicates that **C6** can reach only two WGA binding sites simultaneously due to its geometrical properties, which is fully in accordance with the structural investigations described below. Otherwise, a significantly stronger binding enhancement would have been expected comparable to the several-hundred-fold increase observed when moving from mono- to divalent ligand structures.

Molecular modeling

To provide a structure-based rationalization for the determined binding potencies of **C2**–**C6**, we performed molecular modeling studies. Combining information from the crystal structures of WGA3 in complex with *N*,*N*'-diacetylchitobiose (PDB ID: 1K7U) [60] and WGA3 binding to a divalent ligand presenting two GlcNAc residues (PDB ID: 2X52) [36], two *N*,*N*'-diacetylchitobiose residues were placed in a pair of adjacent primary binding sites of WGA and connected by the respective linker (see Supporting Information File 1 for details). Subsequently, the linkers were energy minimized with the chitobiose moieties fixed in their ideal positions. The models containing the various linker structures were further energy minimized with the terminal GlcNAc residues kept in their optimal positions.

Our molecular modeling studies revealed that the *para*-disubstituted aromatic linker of **C3** cannot adopt a low-energy conformation if the chitobiose residues are kept in their ideal positions in the binding sites of WGA, resulting in significant ring strain of the triazole moieties as well as the central phenyl ring. This ring strain can be reduced by slightly pulling the GlcNAc residues directly attached to the linker out of the binding site, but at the expense of a less efficient multivalent binding of the two chitobiose entities. The chitobiose groups of the divalent ligand **C4**, on the other hand, can maintain their ideal positions easily with the linker adopting an all-staggered low-energy conformation (Figure 3). Ligand **C2** allows for the positioning of its chitobiose moieties ideally in both binding sites when adopting a fully extended conformation. Ligand **C2**, and even more so ligand **C3**, possess very limited conformational freedom when adopting a chelating binding mode. Conformational changes within the linkers of **C2** and **C3** lead to

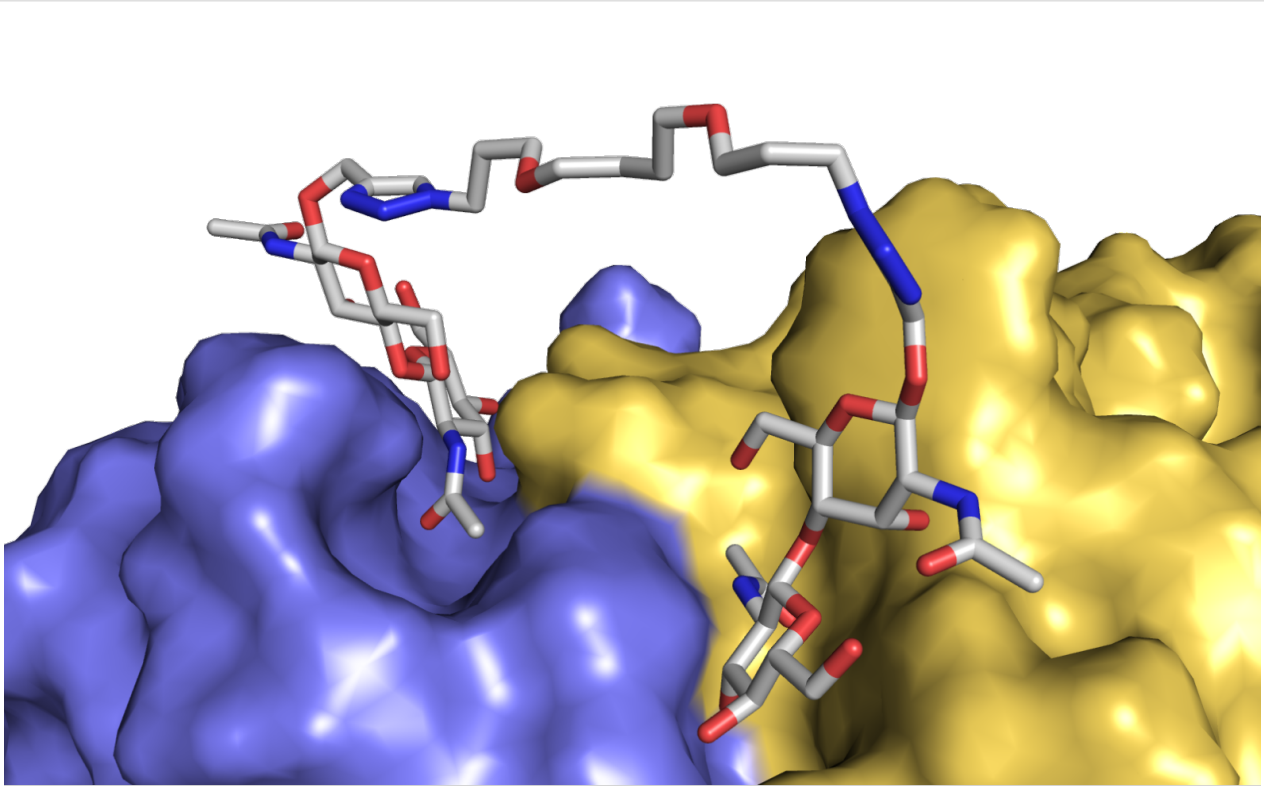

Figure 3: Molecular model of divalent ligand **C4** with its two chitobiose moieties occupying two adjacent binding sites of WGA. The linker is conformationally largely unrestricted and can adopt several low-energy conformations. WGA chain 1 is colored yellow, chain 2 is blue.

forces that pull one or the other GlcNAc/chitobiose out of its binding site. This situation may increase the entropic costs of chelating binding for these two ligands providing a further explanation for their significantly lower binding affinity.

With its linker length and flexibility, trivalent ligand **C6** is in an intermediate position between the relatively short-bridged and rigid ligands **C2** and **C3** and the more flexibly connected ligands **C4** and **C5**. With six chemical bonds between the triazole groups, **C6** can present its *N*,*N*'-diacetylchitobiose residues in rather similar distances as **C2** or **C3** having the same linker length. However, **C6** has two more rotatable bonds between pairs of chitobiose moieties leading to significantly increased conformational freedom. This is expected to facilitate binding in a chelating fashion at relatively low entropic costs. It is important to note that the third chitobiose unit of **C6** cannot reach a third carbohydrate binding site of the WGA dimer. The closest distance to another binding site is approximately 24 Å (measured between the anomeric oxygens of the inner GlcNAc residues). The 2.8-fold increased potency relative to ligand **C4** could possibly originate from the facilitated rebinding of monovalently bound trivalent ligand **C6** due to the two-fold-higher local concentration of chitobiose compared to the divalent ligands.

Conclusion

In summary, we have presented a series of *O*-glycosidically linked *N*,*N*'-diacetylchitobiose clusters that were conveniently obtained from propargyl glycoside **1** and readily available amine scaffolds by a one-pot procedure for diazo transfer and azide–alkyne cycloaddition. Binding potencies were determined by an ELLA. Divalent ligands were found to have IC_{50} values in the low-micromolar/high-nanomolar range depending on the linker between the two disaccharides. The observed binding enhancements over the monovalent ligand are significantly higher than those of comparable β-linked GlcNAc clusters. The different binding enhancements can be rationalized by molecular modeling studies that correlate the different linker geometries with their propensities to support chelating binding. The best WGA ligand is trivalent cluster **C6** with a remarkable IC_{50} value of 220 nM. Calculated per mol of contained chitobiose, this is the best WGA ligand published so far.

Supporting Information

Supporting Information File 1

Experimental procedures and analytical data for all new compounds.
[http://www.beilstein-journals.org/bjoc/content/supplementary/1860-5397-8-91-S1.pdf]

Acknowledgements

This work was supported by the Deutsche Forschungsgemeinschaft (FOR 434) and the University of Konstanz. H.S.G.B. acknowledges a fellowship according to the Landesgraduiertenförderungsgesetz.

References

1. Dwek, R. A. *Chem. Rev.* **1996,** *96,* 683–720. doi:10.1021/cr940283b
2. Varki, A.; Cummings, R. D.; Esko, J. D.; Freeze, H. H.; Stanley, P.; Bertozzi, C. R.; Hart, G. W.; Etzler, M. E., Eds. *Essentials of Glycobiology,* 2nd ed.; Cold Spring Harbor Laboratory Press: Cold Spring Harbor, NY, 2009.
3. Mammen, M.; Choi, S.-K.; Whitesides, G. M. *Angew. Chem., Int. Ed.* **1998,** *37,* 2754–2794. doi:10.1002/(SICI)1521-3773(19981102)37:20<2754::AID-ANIE2754>3.0.CO;2-3
4. Lee, Y. C.; Lee, R. T., Eds. *Neoglycoconjugates: Preparation and Applications;* Academic Press: San Diego, CA, 1994.
5. Kiessling, L. L.; Gestwicki, J. E.; Strong, L. E. *Angew. Chem., Int. Ed.* **2006,** *45,* 2348–2368. doi:10.1002/anie.200502794
6. Collins, B. E.; Paulson, J. C. *Curr. Opin. Chem. Biol.* **2004,** *8,* 617–625. doi:10.1016/j.cbpa.2004.10.004
7. Choi, S.-K. *Synthetic Multivalent Molecules. Concepts and Biomedical Applications;* John Wiley & Sons: Hoboken, NJ, 2004. doi:10.1002/0471578908
8. Ortiz Mellet, C.; Defaye, J.; García Fernández, J. M. *Chem.–Eur. J.* **2002,** *8,* 1982–1990. doi:10.1002/1521-3765(20020503)8:9<1982::AID-CHEM1982>3.0.CO;2-5
9. Lindhorst, T. K. *Top. Curr. Chem.* **2002,** *218,* 201–235. doi:10.1007/3-540-45010-6_7
10. Chabre, Y. M.; Roy, R. *Adv. Carbohydr. Chem. Biochem.* **2010,** *63,* 165–393. doi:10.1016/S0065-2318(10)63006-5
11. Dam, T. K.; Brewer, C. F. *Biochemistry* **2008,** *47,* 8470–8476. doi:10.1021/bi801208b
12. Pieters, R. J. *Org. Biomol. Chem.* **2009,** *7,* 2013–2025. doi:10.1039/b901828j
13. Wittmann, V. Synthetic Approaches to Study Multivalent Carbohydrate-Lectin Interactions. In *Highlights in Bioorganic Chemistry: Methods and Applications;* Schmuck, C.; Wennemers, H., Eds.; Wiley-VCH: Weinheim, Germany, 2004; pp 203–213. doi:10.1002/3527603727.ch2g
14. Kitov, P. I.; Sadowska, J. M.; Mulvey, G.; Armstrong, G. D.; Ling, H.; Pannu, N. S.; Read, R. J.; Bundle, D. R. *Nature* **2000,** *403,* 669–672. doi:10.1038/35001095
15. Kitov, P. I.; Mulvey, G. L.; Griener, T. P.; Lipinski, T.; Solomon, D.; Paszkiewicz, E.; Jacobson, J. M.; Sadowska, J. M.; Suzuki, M.; Yamamura, K.-i.; Armstrong, G. D.; Bundle, D. R. *Proc. Natl. Acad. Sci. U. S. A.* **2008,** *105,* 16837–16842. doi:10.1073/pnas.0804919105
16. Fan, E.; Zhang, Z.; Minke, W. E.; Hou, Z.; Verlinde, C. L. M. J.; Hol, W. G. J. *J. Am. Chem. Soc.* **2000,** *122,* 2663–2664. doi:10.1021/ja993388a
17. Merritt, E. A.; Zhang, Z.; Pickens, J. C.; Ahn, M.; Hol, W. G. J.; Fan, E. *J. Am. Chem. Soc.* **2002,** *124,* 8818–8824. doi:10.1021/ja0202560
18. Lee, Y. C.; Lee, R. T. *Acc. Chem. Res.* **1995,** *28,* 321–327. doi:10.1021/ar00056a001

19. Lundquist, J. J.; Toone, E. J. *Chem. Rev.* **2002,** *102,* 555–578. doi:10.1021/cr000418f
20. Mortell, K. H.; Weatherman, R. V.; Kiessling, L. L. *J. Am. Chem. Soc.* **1996,** *118,* 2297–2298. doi:10.1021/ja953574q
21. Jencks, W. P. *Proc. Natl. Acad. Sci. U. S. A.* **1981,** *78,* 4046–4050. doi:10.1073/pnas.78.7.4046
22. Hubble, J. *Mol. Immunol.* **1999,** *36,* 13–18. doi:10.1016/S0161-5890(98)00116-3
23. Gargano, J. M.; Ngo, T.; Kim, J. Y.; Acheson, D. W. K.; Lees, W. J. *J. Am. Chem. Soc.* **2001,** *123,* 12909–12910. doi:10.1021/ja016305a
24. Ercolani, G. *J. Am. Chem. Soc.* **2003,** *125,* 16097–16103. doi:10.1021/ja038396c
25. Kitov, P. I.; Bundle, D. R. *J. Am. Chem. Soc.* **2003,** *125,* 16271–16284. doi:10.1021/ja038223n
26. Krishnamurthy, V. M.; Semetey, V.; Bracher, P. J.; Shen, N.; Whitesides, G. M. *J. Am. Chem. Soc.* **2007,** *129,* 1312–1320. doi:10.1021/ja066780e
27. Diestler, D. J.; Knapp, E. W. *J. Phys. Chem. C* **2010,** *114,* 5287–5304. doi:10.1021/jp904258c
28. Zanini, D.; Roy, R. *Bioconjugate Chem.* **1997,** *8,* 187–192. doi:10.1021/bc970005u
29. Furuike, T.; Aiba, S. *Chem. Lett.* **1999,** *28,* 69–70. doi:10.1246/cl.1999.69
30. García-López, J. J.; Hernández-Mateo, F.; Isac-García, J.; Kim, J. M.; Roy, R.; Santoyo-González, F.; Vargas-Berenguel, A. *J. Org. Chem.* **1999,** *64,* 522–531. doi:10.1021/jo981576y
31. Furuike, T.; Aiba, S.; Nishimura, S.-I. *Tetrahedron* **2000,** *56,* 9909–9915. doi:10.1016/S0040-4020(00)00962-5
32. Consoli, G. M. L.; Cunsolo, F.; Geraci, C.; Sgarlata, V. *Org. Lett.* **2004,** *6,* 4163–4166. doi:10.1021/ol0485767
33. Yamada, A.; Hatano, K.; Koyama, T.; Matsuoka, K.; Takahashi, N.; Hidari, K. I. P. J.; Suzuki, T.; Suzuki, Y.; Terunuma, D. *Bioorg. Med. Chem.* **2007,** *15,* 1606–1614. doi:10.1016/j.bmc.2006.12.030
34. Maierhofer, C.; Rohmer, K.; Wittmann, V. *Bioorg. Med. Chem.* **2007,** *15,* 7661–7676. doi:10.1016/j.bmc.2007.08.063
35. Misawa, Y.; Masaka, R.; Maeda, K.; Yano, M.; Murata, T.; Kawagishi, H.; Usui, T. *Carbohydr. Res.* **2008,** *343,* 434–442. doi:10.1016/j.carres.2007.11.025
36. Schwefel, D.; Maierhofer, C.; Beck, J. G.; Seeberger, S.; Diederichs, K.; Möller, H. M.; Welte, W.; Wittmann, V. *J. Am. Chem. Soc.* **2010,** *132,* 8704–8719. doi:10.1021/ja101646k
37. Wittmann, V.; Seeberger, S. *Angew. Chem., Int. Ed.* **2004,** *43,* 900–903. doi:10.1002/anie.200352055
38. Wittmann, V.; Seeberger, S. *Angew. Chem., Int. Ed.* **2000,** *39,* 4348–4352. doi:10.1002/1521-3773(20001201)39:23<4348::AID-ANIE4348>3.0.CO;2-X
39. Wright, C. S. *J. Mol. Biol.* **1980,** *141,* 267–291. doi:10.1016/0022-2836(80)90181-3
40. Mirelman, D.; Galun, E.; Sharon, N.; Lotan, R. *Nature* **1975,** *256,* 414–416. doi:10.1038/256414a0
41. Laroy, K.; Weeks, G. *J. Cell Sci.* **1983,** *59,* 203–212.
42. Asensio, J. L.; Cañada, F. J.; Siebert, H.-C.; Laynez, J.; Poveda, A.; Nieto, P. M.; Soedjanaamadja, U. M.; Gabius, H.-J.; Jiménez-Barbero, J. *Chem. Biol.* **2000,** *7,* 529–543. doi:10.1016/S1074-5521(00)00136-8
43. Aub, J. C.; Sanford, B. H.; Cote, M. N. *Proc. Natl. Acad. Sci. U. S. A.* **1965,** *54,* 396–399. doi:10.1073/pnas.54.2.396
44. Aub, J. C.; Sanford, B. H.; Wang, L.-H. *Proc. Natl. Acad. Sci. U. S. A.* **1965,** *54,* 400–402. doi:10.1073/pnas.54.2.400
45. Braun, P.; Nägele, B.; Wittmann, V.; Drescher, M. *Angew. Chem., Int. Ed.* **2011,** *50,* 8428–8431. doi:10.1002/anie.201101074
46. Wright, C. S.; Kellogg, G. E. *Protein Sci.* **1996,** *5,* 1466–1476. doi:10.1002/pro.5560050803
47. Bains, G.; Lee, R. T.; Lee, Y. C.; Freire, E. *Biochemistry* **1992,** *31,* 12624–12628. doi:10.1021/bi00165a012
48. Beckmann, H. S. G.; Wittmann, V. *Org. Lett.* **2007,** *9,* 1–4. doi:10.1021/ol0621506
49. Rostovtsev, V. V.; Green, L. G.; Fokin, V. V.; Sharpless, K. B. *Angew. Chem., Int. Ed.* **2002,** *41,* 2596–2599. doi:10.1002/1521-3773(20020715)41:14<2596::AID-ANIE2596>3.0.CO;2-4
50. Tornøe, C. W.; Christensen, C.; Meldal, M. *J. Org. Chem.* **2002,** *67,* 3057–3064. doi:10.1021/jo011148j
51. Huisgen, R. *Angew. Chem., Int. Ed. Engl.* **1963,** *2,* 565–598. doi:10.1002/anie.196305651
52. Meldal, M.; Tornøe, C. W. *Chem. Rev.* **2008,** *108,* 2952–3015. doi:10.1021/cr0783479
53. Pieters, R. J.; Rijkers, D. T. S.; Liskamp, R. M. J. *QSAR Comb. Sci.* **2007,** *26,* 1181–1190. doi:10.1002/qsar.200740075
54. Dedola, S.; Nepogodiev, S. A.; Field, R. A. *Org. Biomol. Chem.* **2007,** *5,* 1006–1017. doi:10.1039/b618048p
55. Chan, T. R.; Hilgraf, R.; Sharpless, K. B.; Fokin, V. V. *Org. Lett.* **2004,** *6,* 2853–2855. doi:10.1021/ol0493094
56. Merkel, L.; Beckmann, H. S. G.; Wittmann, V.; Budisa, N. *ChemBioChem* **2008,** *9,* 1220–1224. doi:10.1002/cbic.200800050
57. Masaka, R.; Ogata, M.; Misawa, Y.; Yano, M.; Hashimoto, C.; Murata, T.; Kawagishi, H.; Usui, T. *Bioorg. Med. Chem.* **2010,** *18,* 621–629. doi:10.1016/j.bmc.2009.12.006
58. André, S.; Specker, D.; Bovin, N. V.; Lensch, M.; Kaltner, H.; Gabius, H.-J.; Wittmann, V. *Bioconjugate Chem.* **2009,** *20,* 1716–1728. doi:10.1021/bc900152w
59. Corbell, J. B.; Lundquist, J. J.; Toone, E. J. *Tetrahedron: Asymmetry* **2000,** *11,* 95–111. doi:10.1016/S0957-4166(99)00589-3
60. Muraki, M.; Ishimura, M.; Harata, K. *Biochim. Biophys. Acta* **2002,** *1569,* 10–20. doi:10.1016/S0304-4165(01)00231-8

License and Terms

Beilstein Journal of Organic Chemistry

The use of glycoinformatics in glycochemistry

Thomas Lütteke

Review

Open Access

Address:
Justus-Liebig-University Gießen, Institute of Veterinary Physiology and Biochemistry, Frankfurter Str. 100, 35392 Gießen, Germany

Email:
Thomas Lütteke - thomas.luetteke@vetmed.uni-giessen.de

Keywords:
carbohydrates; databases; glycomics; software

Beilstein J. Org. Chem. **2012,** *8,* 915–929.
doi:10.3762/bjoc.8.104

Received: 07 March 2012
Accepted: 29 May 2012
Published: 21 June 2012

This article is part of the Thematic Series "Synthesis in the glycosciences II".

Guest Editor: T. K. Lindhorst

Abstract

Glycoinformatics is a small but growing branch of bioinformatics and chemoinformatics. Various resources are now available that can be of use to glycobiologists, but also to chemists who work on the synthesis or analysis of carbohydrates. This article gives an overview of existing glyco-specific databases and tools, with a focus on their application to glycochemistry: Databases can provide information on candidate glycan structures for synthesis, or on glyco-enzymes that can be used to synthesize carbohydrates. Statistical analyses of glycan databases help to plan glycan synthesis experiments. 3D-Structural data of protein–carbohydrate complexes are used in targeted drug design, and tools to support glycan structure analysis aid with quality control. Specific problems of glycoinformatics compared to bioinformatics for genomics or proteomics, especially concerning integration and long-term maintenance of the existing glycan databases, are also discussed.

Introduction

Carbohydrates, often referred to as glycans, differ from other biopolymers such as proteins or nucleic acids in various ways. The number of different monosaccharides that are present in naturally occurring glycans is significantly higher than the number of proteogenic amino acids, or of nucleotides that form DNA or RNA strands [1,2]. Furthermore, the monosaccharides can be linked to each other in several ways, including the possibility to form branched structures. Another important difference between glycans, on the one hand, and proteins and nucleic acids, on the other hand, is visible in their biosynthesis: DNA, RNA and proteins are synthesized by copying, transcription or translation, respectively, of nucleic acids, whereas carbohydrates are built in a non-template-driven approach by the sequential action of various glycosyltransferases (GT) that add monosaccharides to an existing glycan chain, and by glycoside hydrolases (GH) that remove specific monosaccharides [3]. For this reason there is no technique available to amplify carbohydrates comparable to Polymerase Chain Reaction (PCR) or protein expression systems. Instead, carbohydrates have to be analyzed in physiological amounts. If specific and well-defined

glycans are required for experiments such as glycan arrays [4], they have to be synthesized chemically [5].

The special features of carbohydrates not only pose problems for their wet-lab analysis but also for computational approaches that deal with carbohydrates. Classical bioinformatics algorithms are developed for linear gene or protein sequences, and thus cannot be applied to branched carbohydrates. Instead, new algorithms that deal with the branching as well as with other special features of carbohydrates, such as microheterogeneity, have to be developed [6,7]. Furthermore, there are much less primary data on carbohydrates available than, e.g., on proteins, to test or train the algorithms [8]. For these reasons, glycoinformatics as a research area at the intersection of bioinformatics and chemoinformatics has been considered to be lagging behind its sister fields, such as bioinformatics for genomics or proteomics, for a long time. By now, however, glycoinformatics is coming of age and offers a variety of databases and applications that are of use to glycoscientists. Many new resources are still being developed, and efforts for a better integration of existing resources have also been started. Formats and protocols for data exchange have been specified [9,10]. Recently, the MIRAGE (Minimum Information Related to A Glycomics Experiment) consortium was founded to define checklists for the standardization of experimental glycomics data and meta information [11]. However, there is still no long-term repository of glycan structures available.

Being part of the Thematic Series "Synthesis in the glycosciences II", this overview mainly focuses on those resources that are relevant to glycan synthesis. For a more general overview of glycoinformatics resources and the development of the field over time, the reader is referred to references [12-17].

Review

Carbohydrate databases

Glycan structure databases

Various databases that collect information on carbohydrates are now available (Table 1) and new resources are still being developed. The individual databases differ in the kind of data that are stored, the number and topicality of entries, the search interfaces, and the way the data are presented to the user. They are of use to glycochemists in several ways. First of all, they provide literature references on specific carbohydrate structures, which are often difficult to find via keyword searches in general literature databases such as PubMed. However, keeping databases up to date with bibliographic references is a time-consuming task that cannot be performed automatically by computer programs because the glycan structures are often encoded graphically within the publication figures. And even when information on glycan chains is given in the text, the notation is often complex, difficult to parse, and may contain ambiguities. Therefore, database users should keep in mind that if a database does not list any reference that, e.g., deals with the synthesis of a specific glycan structure, it does not mean that there is no such reference available: it just might not have been included into the database yet. Aside from providing literature references, carbohydrate databases can also serve glycochemists as a source of information on structures that are potential targets for synthesis. For this purpose resources that feature data such as the biological source, or diseases related to a glycan structure, can be of special interest.

The first approach used to create a comprehensive collection of carbohydrate data that had been published in scientific literature, was the Complex Carbohydrate Structure Database (CCSDB) [19], which is often referred to by the name of its querying software, CarbBank [20]. Each CarbBank entry contains a glycan structure together with a bibliographic reference, and further information such as taxonomic data of the biological source, experimental methods, or related diseases are also present. When funding stopped in the mid-1990s, however, CarbBank was no longer updated and CCSDB no longer maintained. Nevertheless, its content formed the basis of several other databases that were subsequently developed. Depending on their focus, other resources have incorporated all or part of the CarbBank data, and have added further information. The Bacterial Carbohydrate Structure Database (BCSDB), for example, has incorporated ca. 4000 CarbBank entries, the structures of which are of bacterial origin, and added ca. 5000 records referring to articles that were published after the maintenance of CarbBank had stopped. BCSDB covers more than 90% of the literature in the scope of bacterial carbohydrates [18]. Data that are listed in the entries include bibliographic data, taxonomic information on the biological source, and primary data of nuclear magnetic resonance (NMR) experiments that had been performed to elucidate the structures. Other sources of NMR data are SugaBase [36], which similar to CarbBank is no longer maintained, GlycoBase (Lille), *Escherichia coli* O-antigen Database (ECODAB) [22], and Glycosciences.DB [31], the database of the Glycosciences.de web portal. Glycosciences.DB, formerly known as SweetDB [38], started to make CarbBank entries available over the internet and to provide 3D structural models of the glycan structures. These models are calculated by the Sweet-2 software [39]. NMR data were incorporated from SugaBase or manually entered from the literature. Glycosciences.DB also contains information on carbohydrate 3D structures that are available in the Protein Data Bank (PDB, [40]). Extraction and validation of carbohydrate data from PDB entries is automated to a large extent and therefore requires only minimal human interference [41], making the update of these data much less dependent of

Table 1: Carbohydrate structure databases.

Name, Ref	Main content, comments	URL	Status[a]
BCSDB (Bacterial Carbohydrate Structure Database) [18]	Glycan sequences, taxonomy, bibliography, NMR data	http://csdb.glycoscience.ru/bacterial/	D/M
CCSDB//CarbBank [19,20]	Glycan sequences, taxonomy, bibliography	–	S
CFG Glycan Structure DB [21]	Glycan sequences, taxonomy, bibliography, glycan array data	http://www.functionalglycomics.org/glycomics/molecule/jsp/carbohydrate/carbMoleculeHome.jsp	S
ECODAB (*Escherichia coli* O-antigen Database) [22,23]	Glycan sequences, NMR data, glycosyltranferases (*E. coli* glycans only)	http://www.casper.organ.su.se/ECODAB/	D/M
EUROCarbDB [24]	Glycan sequences, taxonomy, bibliography, MS data	http://www.ebi.ac.uk/eurocarb/	S
Glycobase (Dublin) [25]	Glycan sequences, taxonomy, HPLC data, MS data, bibliography	http://glycobase.nibrt.ie (registration required)	D/M
Glycobase (Lille)	Glycan sequences, taxonomy, NMR data	http://glycobase.univ-lille1.fr/base/	?
GlycoconjugateDB [26]	Glycan sequences, PDB references	http://www.glycostructures.jp	?
GlycoMapsDB [27]	Computed conformational maps	http://www.glycosciences.de/modeling/glycomapsdb/	P
GlycoNavi (JCGGDB)	Chemical reactions of carbohydrate molecules	http://ws.glyconavi.org	D/M
GlycomeDB [28-30]	Glycan sequences and taxonomic data extracted from other databases	http://www.glycome-db.org	D/M
GlycoPOD (JCGGDB GlycoProtocols Online Database)	Protocols for synthesis and analysis of glycan structures	http://jcggdb.jp/GlycoPOD/protocolListShow.action	D/M
Glycosciences.DB [31]	Glycan sequences, taxonomy, bibliography, 3D structure models, NMR data, PDB references	http://www.glycosciences.de/database/	D/M
GlycosideDB (JCGGDB)	Chemical structures of glycoconjugates, aglycones	http://jcggdb.jp/search/GlycosideDB.cgi	D/M
GlycoSuiteDB [32,33]	Glycan sequences, taxonomy, bibliography, disease, protein glycosylation sites	http://glycosuitedb.expasy.org	D/M
JCGGDB [34]	Collection of several Japanese glyco-related databases	http://jcggdb.jp/index_en.html	D/M
KEGG GLYCAN [35]	Glycan sequences, bibliography, cross-references to other KEGG resources	http://www.genome.jp/kegg/glycan/	?
MonosaccharideDB	Monosaccharide notation and properties	http://www.monosaccharidedb.org	D/M
SugaBase [36]	Glycan sequences, taxonomy, NMR data	–	S
UniCarb-DB [37]	Glycan sequences, taxonomy, LC–MS data	http://www.unicarb-db.com	D/M

[a]D/M: Database is further developed and/or maintained; P: Development/maintenance is paused, but planned to be continued; S: Development/maintenance is stopped (or, in the case of CFG resources, will be stopped soon because funding will discontinue); ?: Status unknown.

funding than that of data extracted from the literature. Carbohydrate data from the PDB are also available in the Glycoconjugate Database [26], but updates are less frequent than in Glycosciences.DB, which is updated weekly with new PDB entries.

Other databases that implemented CarbBank data are KEGG GLYCAN [35], EUROCarbDB [24], and the Glycan Structure Database of the Consortium for Functional Glycomics (CFG) [21]. KEGG GLYCAN is part of the Kyoto Encyclopedia of Genes and Genomes (KEGG) and integrates carbohydrate data with a variety of tools and information on other biomolecules. The KEGG portal has a particular focus on biosynthetic pathways. EUROCarbDB was developed to store primary data of mass spectrometry (MS), NMR and high performance liquid chromatography (HPLC) experiments. In addition to data imported from CarbBank, the database contains structures from such experiments (mainly MS data). Detailed information on the biological context in which a structure was found, is also provided. EUROCarbDB is another example of a database that is no longer being developed because the funding has stopped. However, it was developed as an open-source project. Therefore, newly funded projects such as UniCarb-DB [37] or the latest version of GlycoBase (Dublin) [25], which stores HPLC data, are able to make use of the EUROCarbDB source code

and, thus, the software does not need to be rewritten. The CFG databases are focused on various aspects of mammalian glycans. Similar to EUROCarbDB, the CFG Glycan Structure Database features CarbBank *N*- and *O*-glycan data as well as entries that have been found in MS experiments performed by CFG members or that have been synthesized by the CFG. The database is complemented with glycans from the GlycoMinds Ltd. seed database. Primary data of MS experiments and glycan array screens are also available via the CFG website. If a glycan structure has been detected to be bound by a glycan-binding protein in a CFG glycan array experiment, links to the corresponding protein pages are provided with the glycan structure entries. A link to a 3D structural model generated by the GLYCAM-Web Biomolecule Builder [42] is also given. GlycoSuiteDB [32,33], which started as a commercial database and was later made publicly accessible, differs from most other carbohydrate databases in that it provides information on proteins to which specific glycans were found to be attached, including details on glycosylation sites.

The Japan Consortium for Glycobiology and Glycotechnology DataBase (JCGGDB) [34] provides a collection of individual databases that are cross-linked with each other and currently being actively developed. Unfortunately, some resources are not fully translated to English yet, but nevertheless the portal contains various useful databases. Of those, GlycoPOD is of particular use for wet-lab scientists. GlycoPOD is a collection of lab protocols for the synthesis or analysis of carbohydrates and other glyco-related experiments. The protocols include step-by-step instructions, references, and features to rate the protocols or to post related questions. Another resource with a special focus on glycochemistry is GlycoNavi, which is a database of chemical reactions that involve carbohydrates and of the molecules involved in these reactions. Information about the chemical properties of carbohydrate molecules can also be found in general molecule databases, such as ChEBI (Chemical Entities of Biological Interest, http://www.ebi.ac.uk/chebi/) [43,44] or PubChem (http://pubchem.ncbi.nlm.nih.gov) [45]. These resources provide data that are important for chemists but are often not present in the more biology-focused carbohydrate-specific databases, such as atomic descriptions, charges, chemical synonyms, SMILES (Simplified Molecular Input Line Entry System) and InChi (IUPAC International Chemical Identifier) codes, and 3D structural information in mol2 format. However, no carbohydrate-specific search options are available. This can make it difficult to locate entries in ChEBI or PubChem especially for oligosaccharides. Introducing cross-links between carbohydrate-specific databases and the major chemical databases would not only make it easier to find specific carbohydrates, but also provide a linkage between biological and chemical information.

Databases on glycosyltransferases and glycan binding proteins

As an alternative or complement to chemical synthesis it is possible to make use of the enzymes that build or degrade the glycan chains in vivo, the glycosyltransferases or glycoside hydrolases, respectively [46-49]. To plan such experiments, however, detailed knowledge of the substrate-specificity of these enzymes is required. The same applies to glycan-binding proteins, which can be promising targets for the synthesis of glycomimetics. To some extent, knowledge of such proteins can of course be found in classical protein or enzyme databases, such as UniProt (http://www.uniprot.org) [50] or BRENDA (http://www.brenda-enzymes.info) [51]. However, these databases do not offer any glyco-specific search options. Therefore, it can be difficult to find the respective data in these general databases. There are various resources available that specifically deal with glyco-enzymes or glycan-binding proteins (Table 2). These are often much better suited as starting points for searching than the more general protein databases, not only because of the more narrow focus, but also because most of the glyco-specific protein databases contain links to corresponding entries in the more general databases, but usually not vice versa.

A major resource for glyco-enzymes (glycosyltransferases, glycoside hydrolases, polysaccharide lyases and carbohydrate esterases) as well as proteins that feature carbohydrate-binding modules is CAZy (Carbohydrate Active Enzymes). This database classifies proteins by sequence comparison and clusters them into families by using well-established bioinformatics tools such as BLAST [55] or HMMER [56]. In this way, approximately 1–3% of the proteins encoded by a typical genome are categorized as glyconzymes [52,57]. For each CAZy family, the corresponding proteins are listed (and can be filtered by subcategories, such as taxonomic kingdoms or entries with existing 3D structural information) together with links to corresponding entries in NCBI GenBank, UniProt [50] or PDB [40]. However, little information is provided about enzyme specificity, kinetics, or catalytic residues, which is crucial information if the enzymes are to be used in carbohydrate synthesis experiments. Such information can be obtained together with literature references from CAZy's sister resource CAZypedia, a wiki on glyco-enzymes.

Glyco-enzyme data are also found in KEGG Pathway and KEGG Orthology. These resources are not glyco-specific, but metabolic pathways are classified in a hierarchical system, which makes it easy to locate the glyco-related data, but also to learn about the relations between carbohydrate metabolism and other metabolic pathways. KEGG resources cover a diverse range of species of all kingdoms. In contrast, CFG GT database focuses on mammalian glycosyltransferases, and GT informa-

Table 2: Glycosyltransferase/glycan-binding protein databases.

Name, Ref	Main content, comments	URL	Status[a]
Glycosyltransferase (GT) databases			
CAZy (Carbohydrate Active enZYmes) [52]	Glyco-enzymes clustered into families by sequence comparison	http://www.cazy.org	D/M
CAZyPedia	Wikipedia-like description of GT and GH families	http://www.cazypedia.org	D/M
CFG GT DB	Enzymes for biosynthesis of mammalian glycans	http://www.functionalglycomics.org/glycomics/molecule/jsp/glycoEnzyme/geMolecule.jsp	S
GlycoGeneDB (JCGGDB)	Glyco-enzymes: genes, substrates, gene expression	http://riodb.ibase.aist.go.jp/rcmg/ggdb/	D/M
GPI Biosynthesis report [53]	Enzymes involved in biosynthesis of glycosyl phosphatidyl inositol (GPI) anchors	http://mendel.imp.ac.at/SEQUENCES/gpi-biosynthesis/	S
KEGG Pathway	Biosynthesis pathways, enzyme entries with sequence and notation data and links to other resources	http://www.genome.jp/kegg/pathway.html	D/M
KEGG Orthology	General data on enzymes and catalyzed reactions, links to specific proteins	http://www.genome.jp/kegg/ko.html	D/M
Glycan binding proteins (GBP) databases			
CFG Glycan Binding Proteins	Includes information on recognized glycan epitopes and on related diseases	http://www.functionalglycomics.org/glycomics/molecule/jsp/gbpMolecule-home.jsp	S
Genomics Resource for Animal Lectins	Description of animal lectin families	http://www.imperial.ac.uk/research/animallectins/	S
GlyAffinity	Collection of glycan array data from several resources	http://worm.mpi-cbg.de/affinity/	S
GlycoEpitopeDB [54]	Antibodies that bind to carbohydrates, glyco-epitopes recognized by the antibodies	http://www.glyco.is.ritsumei.ac.jp/epitope/	D/M
KEGG BRITE: Glycan Binding Proteins	Protein classification, links to other KEGG resources and to external databases	http://www.genome.jp/kegg-bin/get_htext?ko04091.keg	D/M
Lectin Frontier Database (JCGGDB)	Includes glycan array data	http://riodb.ibase.aist.go.jp/rcmg/glycodb/LectinSearch	D/M
LECTINES	Collection of lectin 3D structures from the PDB	http://www.cermav.cnrs.fr/lectines/	D/M
PACDB (JCGGDB Pathogen Adherence to Carbohydrate DB)	Pathogen adherence molecule, host glycan/glycoprotein ligand, bibliography	http://jcggdb.jp/search/PACDB.cgi	D/M

[a]D/M: Database is further developed and/or maintained; S: Development/maintenance is stopped (or, in the case of CFG resources, will be stopped soon because funding will discontinue).

tion in ECODAB [23] is limited to *E. coli* enzymes. GlycoGeneDB as part of the JCGGDB portal also holds data on glyco-enzymes, including information on substrate specificity, which is important when the enzymes are to be used to synthesize glycan structures in the lab.

Information on glycan-binding proteins (GBPs) or lectins is stored in various databases such as CFG GBP DB, GlycoEpitopeDB [54], the Glycan Binding Proteins section of KEGG BRITE, Lectin Frontier Database, and GlyAffinity. KEGG BRITE mainly links to other resources within and outside the KEGG portal, providing protein sequences, classifications, and information regarding related diseases. GlycoEpitopeDB provides information on antibodies that recognize specific carbohydrate epitopes and glycoproteins or glycolipids that are known to carry the epitopes.

A frequently used technique to study the epitopes, to which a GBP binds, are glycan arrays [4]. CFG Glycan Binding Proteins DB and Lectin Frontier Database store data of glycan array experiments and thus also provide information on the glycan specificity of GBPs. Glycan array data from these two resources and from other research groups are collected and available via a common interface in GlyAffinity. PACDB (Pathogen Adher-

ence Carbohydrate Database) lists glycan-binding proteins that are involved in the adherence of pathogens to the host. The data are extracted from the literature and can be accessed by pathogen names or by related diseases.

Integration of carbohydrate databases

It is obvious that a lot of knowledge on carbohydrates is stored in the databases, but also that this knowledge is widely spread over the resources. In contrast to genomics or proteomics databases, hardly any exchange of data is carried out between glycan databases. However, some attempts have been made to cross-reference corresponding entries or to allow cross-database searches. As already mentioned above, the individual databases of JCGGDB are cross-linked with each other, as well as the different KEGG resources. Links between these two initiatives also exist.

Cross-references have also been established between distinct resources. BCSDB and Glycosciences.DB, for example, allow cross-database searches, in which users can simultaneously query both resources [58]. Furthermore, there are links available between corresponding entries of the CFG Glycan Structure Database and Glycosciences.DB, but these links are not updated any more, i.e., recently added entries are not covered. Despite these first attempts, it is still rather cumbersome to search for information on a specific glycan structure, as most resources have not only developed individual interfaces, to which the user has to adapt, but they also use individual ways to encode the carbohydrate structures. CarbBank, for example, used a two-dimensional notation that is similar to IUPAC extended notation [59]. This notation is relatively easy for the human user to survey, but is difficult to handle computationally. Therefore, most databases have developed more clearly defined notations to store carbohydrate structures, such as the LINUCS notation [60] of Glycosciences.de, the LinearCode® used within the CFG databases, GlycoCT [61] in EUROCarbDB, or KCF [62] in KEGG GLYCAN. The usage of individual notations is one of the main reasons that hamper the integration of carbohydrate databases. Conversion of one notation to another is often difficult because they do not only differ in the way in which the linkages are encoded and the branching is handled, but also in the denotation of residue names. Dictionaries of frequently occurring monosaccharides can be created manually, but unusual residues, as can be found in bacterial or synthetic glycans, are difficult to handle in this way. This issue is tackled by MonosaccharideDB, which provides routines to automatically parse and encode carbohydrate residues in various notations.

GlycomeDB [28-30] aims to overcome the problem of poor integration of carbohydrate databases by collecting carbohydrate structures and taxonomy data from other databases, namely BCSDB, CarbBank, CFG, EUROCarbDB, GlycoBase (Lille), Glycosciences.DB, and KEGG GLYCAN. Carbohydrate-containing PDB entries are also included by extracting this information from Glycosciences.DB. The glycan structures are translated to a common notation (GlycoCT) by using manually curated dictionaries and MonosaccharideDB routines. Glycans are also stored in GLYDE-II encoding [63,64], which was agreed on as a general carbohydrate data-exchange format [9]. All structures in GlycomeDB can be accessed via a common interface, which allows searches by (sub-)structure, similarity, maximum common substructure, and species. Individual entries mainly provide links to the original database entries in the resources, from which the structures were obtained. This way, GlycomeDB serves as a search engine that allows users to easily navigate through several databases without having to query all resources individually. However, it does not contain further data beyond structural and taxonomic information. Integrating more data offers the possibility of performing systems biology analyses. Such approaches are served by JCGGDB, as already mentioned above, and the newly founded UniCarbKB project [65]. At the time of writing this article, however, UniCarbKB is still in a very early stage.

Statistical analyses of carbohydrate databases aid the planning of glycan synthesis

Information extracted from glycan structure databases can be useful for glycochemists not only to find potential synthesis targets but also to plan efficient synthesis approaches by providing lists of building blocks that are minimally necessary to synthesize a large number of glycan structures stored in the databases. An analysis of mammalian carbohydrate structures present in Glycosciences.DB, for example, revealed that this data set contained 3299 oligosaccharides, which are part of *N*-glycans, *O*-glycans or glycolipids from 38 mammalian species. Only ten different monosaccharides were found in this data set [66]. However, different anomeric configurations and some substitutions, such as sulfate groups, were ignored, and no distinction was made between *N*-acetylneuraminic acid (Neu5Ac) and *N*-glycolylneuraminic acid (Neu5Gc). The large number of different oligosaccharides that are formed from this relatively small number of different residues arises from the fact that the monosaccharides can be linked in several ways, which has to be considered when creating a set of building blocks for the chemical synthesis of these glycans. Nevertheless, 25 building blocks are sufficient to synthesize 60% of the mammalian glycans stored in the database, and with 36 building blocks 75% of the glycans can be created chemically [66].

The situation is much more complex where bacterial carbohydrates are concerned. The variety of different monosaccharides

as well as of different disaccharide pairs that are present in bacterial glycomes is significantly larger than in the mammalian glycome, featuring many residues that do not occur in mammals, but also exhibiting differentiation between individual classes of bacteria [1,2]. Due to the complexity of residue notation this structural diversity is a challenge for glycoinformatics, but it also offers many possibilities to synthesize carbohydrates or glycomimetics that target specific pathogen proteins. For example, oligosaccharide motifs that are found in surface carbohydrates of pathogens, but not in host organisms or in symbiotes, can serve as templates in vaccine development [67-70], and glycomimetics that block specific enzymes or lectins can be used for therapeutic purposes [71-77].

The Glycan Pathway Prediction (GPP) tool of the RINGS portal [78] can be used to predict glycans that can be obtained with a given glycan structure and a set of enzymes. If knowledge of gene expression is available, e.g., from gene microarray experiments, KEGG Gene Expression to Chemical Structure (GECS) can be used to predict the *N*-glycan chains that can be created by the expressed glyco-enzymes. Further tools that are available for the analysis and conversion of glycan sequence data are summarized in Table 3. The Glycan Fingerprints approach to calculate the degree of diversity in a set of glycan structures is a useful tool to, e.g., evaluate the glycans that are present on a glycan array [79]. GlycanBuilder [80] and DrawRings are used by some databases to enable graphical input of glycan (sub-)structure queries using icons to describe monosaccharides. Atomic pictograms as frequently used by chemists, however, are not supported by these tools.

3D Structure information for targeted drug design

Knowledge of the 3D structure of the target protein and its ligand is a prerequisite for a targeted design of therapeutic glycomimetics [74]. Protein 3D structures are stored in the Protein Data Bank (PDB, [40]). The PDB offers various options to search for proteins. Finding specific carbohydrate structures within PDB entries, however, can be difficult when using PDB queries only. Instead, glycan databases that provide links to PDB entries such as GlycoconjugateDB or Glycosciences.DB can be used. The LECTINES database lists PDB entries of lectins grouped by lectin families. Unfortunately, carbohydrate moieties in the PDB are of significantly lower quality than the protein parts [26,84-86]. Reasons for this are both the greater complexity of carbohydrates, and the fact that, while numerous validation tools are available for protein structures [87], only a few programs exist to validate carbohydrate 3D structures. The PDB carbohydrate residue check (pdb-care) tool [88] aids researchers with locating errors in carbohydrate 3D structures (3D structure-related tools are summarized in Table 4). Ramachandran-like plots of glycosidic torsions are generated by CARP [89], which compares torsions observed in a given 3D structure with computationally derived conformational maps of GlycoMapsDB [27] or with torsions present in carbohydrates in the PDB provided by glyTorsion [89]. In contrast to protein backbone torsions, unusual glycosidic torsions do not necessarily indicate errors in the 3D structure because the conformation of a carbohydrate ligand in complex with a protein can differ from the preferred conformation in solution [90,91]. Nevertheless, CARP plots can help researchers to find potential problems, as well as indicate unusual binding conformations that

Table 3: Tools to input, convert, or analyze glycan structures.

Name, Ref	Comment	URL
DrawRings	Visual editor of glycan structures	http://rings.t.soka.ac.jp/cgi-bin/tools/DrawRings/drawrings2.pl
GECS (Gene Expression to Chemical Structure) [81]	Prediction of *N*-glycan chains from gene expression data	http://www.genome.jp/tools/gecs/
GlycanBuilder [80]	Visual editor of glycan structures	http://www.glycoworkbench.org/wiki/GlycanBuilder
Glycan Fingerprints [79]	Estimation of the degree of diversity in a set of glycan structures	–
Glycan Miner [82]	Detection of motifs or significant subtrees in a set of glycan structures	http://rings.t.soka.ac.jp/cgi-bin/tools/GlycanMiner/Miner_index.pl
GPP (Glycan Pathway Predictor)	Computes *N*-glycan biosynthesis pathway for a given glycan structure	http://rings.t.soka.ac.jp/cgi-bin/tools/GPP/gpp_index.pl
LiGraph	Builds graphical representations of glycans	http://www.glycosciences.de/tools/LiGraph/
ProfilePSTMM [83]	Generates glycan profiles from glycan structure data	http://rings.t.soka.ac.jp/cgi-bin/tools/ProfilePSTMM/profile-training_index.pl
Sumo (Sugar Motif Search)	Detects frequently occurring motifs in a glycan structure	http://www.glycosciences.de/tools/sumo/

Table 4: Tools for prediction and analysis of carbohydrate/glycoprotein 3D structures.

Name, Ref	Comment	URL
BALLDock/SLICK [92,93]	Protein–carbohydrate docking	
CARP [89]	Ramachandran plot-like analysis of glycosidic torsions	http://www.glycosciences.de/tools/carp/
CAT	Conformational analysis tool, for analysis of MD trajectories	http://www.md-simulations.de/CAT/
GLYCAM Biomolecules Builder [42]	Generation of glycan models and in silico glycosylation of proteins, preparation of input files for AMBER [94,95]	http://glycam.ccrc.uga.edu/ccrc/pages/3dspt.html
Glycan Reader [96]	Detection of carbohydrates in PDB files, preparation of input files for CHARMM [97]	http://www.charmm-gui.org/input/glycan
glyProt [98]	in silico glycosylation of proteins	http://www.glycosciences.de/modeling/glyprot/
glyTorsion [89]	Statistics of torsion angles of carbohydrate structures in the PDB	http://www.glycosciences.de/tools/glytorsion/
glyVicinity [89]	Amino acids in the spatial vicinity of carbohydrates in the PDB	http://www.glycosciences.de/tools/glyvicinity/
pdb2linucs [85]	Detection of carbohydrates in PDB files	http://www.glycosciences.de/tools/pdb2linucs/
pdb-care [88]	Validation of carbohydrate 3D structure files	http://www.glycosciences.de/tools/pdbcare/
Sweet-II [39]	Prediction of carbohydrate 3D structures	http://www.glycosciences.de/modeling/sweet2/

have to be taken into account when planning the synthesis of glycomimetics.

In many cases, however, no carbohydrate ligands are present in PDB entries of glycan-binding proteins. Glycan chains of glycoproteins are also often missing, or only a fraction of a chain is present in the coordinates. In such cases, tools such as Sweet-2 [39] or GLYCAM Biomolecule Builder [42] can be used to create models of carbohydrate chains. The latter program can also perform in silico glycosylation by adding the glycan chains to a protein 3D structure, and provides input files for the AMBER [94,95] modeling programs using the GLYCAM force field [99]. Glycan 3D structures calculated by Sweet-2 can be linked to a protein with glyProt [98]. When using these tools to create conformational models of carbohydrates or glycoproteins, one should always keep in mind that these are models and do not represent the one and only "correct" conformation. As glycans are rather flexible molecules, they adopt several conformations with different populations. The conformational space of a glycan can be analyzed by molecular dynamics (MD) simulations (see in the following) [100]. For this purpose the models generated by the GLYCAM Biomolecules Builder are convenient, as this tool already provides the input files for AMBER simulations. The list of residues that are available, however, is more limited than in Sweet-2. Sulfated residues, which frequently occur in glycosaminoglycans [101], for example, are only supported by Sweet-2 at the moment. GlycanReader [96] as part of the CHARMM-GUI [102] creates CHARMM [97] input files from PDB files that contain carbohydrates. Various tools to predict the occupancy state of potential glycosylation sites from protein sequence data are available as well (Table 5).

If a protein–carbohydrate complex is to be modeled, generally available docking tools such as AutoDock [113] can be used to identify the binding position. These tools, however, often do not sufficiently consider the peculiarities of protein–carbohydrate complexes, such as CH–π interactions [13]. Therefore, BALLDock/SLICK has been developed specifically for protein–carbohydrate docking [92,93]. One of the major problems of docking algorithms in general is the identification of the correct conformation among the potential binding modes [100]. Therefore, computational docking approaches are frequently combined with wet-lab experiments, such as saturation transfer difference NMR (STD NMR) or transferred nuclear Overhauser effect (trNOE) spectroscopy [75,114-116], to reliably assign the correct conformation of the ligand on the protein surface. Such combinations of experimental and theoretical approaches are also useful to determine the conformations of natural carbohydrates or their synthetic glycan mimetics [117-119]. Results can be improved by combinations of different modeling approaches, such as docking and MD simulations [101]. To run reliable MD simulations of carbohydrate 3D structures, force fields are necessary that contain parameters for carbohydrates. In the case of glycoproteins, protein–carbohydrate complexes, or glycolipids, the force fields have to cover all types of molecules involved [100,120]. The force fields need to be extensible if not only standard monosaccharides, but also

Table 5: Prediction and analysis of glycosylation sites.

Name, Ref	Comment	URL
big-PI [103]	GPI anchor modification site prediction	http://mendel.imp.ac.at/sat/gpi/gpi_server.html
CBS prediction servers	Collection of various prediction tools, including NetNGlyc, NetOGlyc [104], NetCGlyc [105], NetGlycate [106], DictyOGlyc [107], YingOYang [108]	http://cbs.dtu.dk/services/
CKSAAP_OGlySite [109]	Prediction of mucin-type O-glycosylation sites	http://bioinformatics.cau.edu.cn/zzd_lab/CKSAAP_OGlySite/
EnsembleGly [110]	Prediction of O-, N-, and C-linked glycosylation sites	http://turing.cs.iastate.edu/EnsembleGly/
glySeq [89]	Statistical analysis of amino acids around glycosylation sites	http://www.glycosciences.de/tools/glyseq/
GPI-SOM [111]	Identification of GPI-anchor signals	http://gpi.unibe.ch
GPP [112]	Prediction of N- and O-glycosylation sites	http://comp.chem.nottingham.ac.uk/glyco/

derivatized residues are included in a simulation, which is especially important during the design of glycomimetics [121]. Parameters that affect the simulations of carbohydrates include the treatment of atom charges [122], and solvent model (several models for water are available) [100]. The question of whether to include extra terms for (exo) anomeric effects has also been discussed for a long time [13].

With increasing computational power, MD simulations of larger molecules become feasible; and timescales of simulations increase. One major bottleneck for the scientific use of MD simulations that involve carbohydrates is, therefore, the availability of tools to analyze these simulation trajectories [13]. MD software packages contain analysis tools [94,97,123], but these are tailored for analyzing simulations of proteins. Therefore, tools such as CAT (Conformational Analysis Tools) that serve the needs of glycoscientists are specifically developed [13].

Glycoinformatics in carbohydrate structure analysis

After synthesis of carbohydrate chains an assessment of the quality of the produced material is necessary to exclude wrong structures among the products. Errors in structures that are meant for use in experiments such as glycan arrays may yield incorrect results and thereby lead to mistaken conclusions. Incorrect products that are used as therapeutics can have severe results. Impurities in heparin, a widely used carbohydrate pharmaceutical, for example, can even be fatal [124-126]. The major methods for quality control comprise MS, NMR, and HPLC, all of which produce large amounts of data that have to be evaluated. Companies that develop the analytical equipment that is necessary for these techniques usually do not focus on the detection or analysis of carbohydrates and their software does not suit the needs of glycoscientists [12]. Nevertheless, various community-developed tools exist that facilitate the carbohydrate-specific interpretation of these data (Table 6).

Among the three techniques, the largest choice of tools is available for mass spectrometry. These programs commonly first try and assign residue compositions to measured mass peaks, but use different approaches to determine glycan sequences from compositional data. Some tools such as Cartoonist [127,128] and GlycoMod [132] apply constraints that are created from the knowledge of biosynthetic pathways, thus they are tailored to the analysis of biological samples rather than of chemically synthesized glycans, which do not match the biosynthetic pathways. In contrast, the mass fingerprinting approach as implemented in GlycosidIQ [137], GlypPep ID [134], or GlycoSearch-MS [136] works similarly to algorithms that are frequently used in peptide or protein identification by tools such as Mascot: Mass peaks that are observed in a spectrum are compared to theoretically derived fragment masses that are computed from glycan structures stored in a carbohydrate database. This approach, however, is limited by the content of the database that provides the templates for in silico fragmentation, which means that structures that have not been observed before or that are missing from the database will not be identified this way. This problem also applies to programs that use experimental MS^n data of oligosaccharide standards to assign MS^n fragments of larger glycans, such as GLYCH [129] or MS^n FragLib [140]. In contrast, programs such as STAT [142], StrOligo [143], or OSCAR [141] also allow de novo determination of structures because they interpret MS^n data by determining the possible compositions of parent ions according to their masses; subsequently, the masses of possible connected branching topologies are computed to match the experimentally determined data [149]. GlyQuest [139] and GlycoMiner [131] are designed for high-throughput analysis of glycopeptides that carry *N*-glycan chains. Glyco-Peakfinder [133] and

Table 6: Tools to support experimental analysis of glycans.

Name, Ref	Comment	URL
Mass spectrometry		
Cartoonist [127,128]	Template based glycan sequencing	–
GlycanMass	Calculates the mass of an oligosaccharide structure	http://web.expasy.org/glycanmass/
GLYCH [129]	De novo sequencing of glycans	–
GlycoFragment [130]	Calculation of theoretical mass fragments of glycans	http://www.glycosciences.de/tools/GlycoFragments/
GlycoMiner [131]	Glycopeptide (*N*-glycan) composition analysis	http://www.chemres.hu/ms/glycominer/
GlycoMod [132]	Prediction of oligosaccharide structures of glycoproteins from mass peaks	http://www.expasy.org/tools/glycomod/
Glyco-Peakfinder [133]	Composition annotation of glycans in MS spectra	http://www.glyco-peakfinder.org
GlycoPep ID [134]	Glycan mass fingerprinting	http://hexose.chem.ku.edu/predictiontable.php
GlycoPeptideSearch [135]	Glycan mass fingerprinting (MS/MS) of *N*-glycopeptides using GlycomeDB glycans	http://edwardslab.bmcb.georgetown.edu/software/GlycoPeptideSearch.html
Glyco-Search-MS [136]	Glycan mass fingerprinting using Glyocsciences.DB glycans	http://www.glycosciences.de/database/start.php?action=form_ms_search
GlycosidIQ [137]	Glycan mass fingerprinting using GlycoSuiteDB glycans	–
GlycoWorkbench [138]	Assists interpretation of MS spectra	http://www.glycoworkbench.org
GlyQuest [139]	Glycopeptide (*N*-glycan) analysis	–
MS^n FragLib [140]	Glycan characterization based on an MS^n fragment spectral library	–
OSCAR [141]	De novo sequencing of glycans	–
Peptoonist [127]	Identification of *N*-glycopeptides from a series of mass spectra (MS and MS/MS)	–
PMAA (Partially Methylated Alditol Acetate)	GC–MS fragmentation of permethylated monosaccharides	http://www.ccrc.uga.edu/specdb/ms/pmaa/pframe.html
STAT [142]	De novo sequencing of glycans	–
StrOligo [143]	De novo sequencing of glycans	–
NMR		
CASPER [144,145]	Simulation of NMR spectra, glycan sequence determination from chemical shifts	http://www.casper.organ.su.se/casper/
CCPN [146]	NMR annotation software	http://www.ccpn.ac.uk
GlyNest [147]	Estimation of NMR chemical shifts	http://www.glycosciences.de/sweetdb/start.php?action=form_shift_estimation
ProspectND	NMR data processing and inspection	http://prospectnd.sourceforge.net/
HPLC		
AutoGU [25]	Interpretation of HPLC data	–
GALAXY [148]	Visualization of HPLC 2D maps	http://www.glycoanalysis.info/ENG/index.html

GlycoWorkbench [138] cover the complete workflow from recorded experimental data to a fully assigned spectrum or to glycan structure determination [150]. GlycoWorkbench also facilitates upload of primary data into EUROCarbDB [24]. Furthermore, it enables user-defined residues, which is important when chemically synthesized glycans are to be analyzed. Such glycans may contain highly modified monosaccharides, protecting groups, linkers, or other kinds of nonstandard residues, which are neither included in the standard residue sets nor present in the databases used by mass-fingerprinting approaches.

Significantly fewer tools are available to aid the interpretation of HPLC or NMR spectra of carbohydrates. AutoGU [25] and GALAXY [148] assist users to interpret HPLC profiles or to visualize HPLC 2D maps, respectively. ProspectND is designed

for the signal processing of multidimensional NMR spectra. CCPN (Collaborative Computing Project for the NMR community) helps users to assign NMR spectra [146,151]. Originally designed for proteins or peptides, CCPN by now also supports carbohydrates. Other tools such as CASPER [144,145,152-154] or GlyNest [147] can be used to predict 1D NMR spectra of carbohydrates and to determine glycan sequences from chemical shifts.

Conclusion

Due to the challenges that carbohydrates pose, not only with respect to their analysis or synthesis but also in the handling of them computationally, glycoinformatics has been lagging behind other areas of bioinformatics for a long time [6], but has made good progress over the past decade and is catching up with bioinformatics for genomics or proteomics. Despite this relatively quick growth and some promising approaches to cross-reference and standardize the data [9,10,28,58,65], there is still an urgent need for better integration of the various resources [13], many of which can still be regarded as disconnected islands. Furthermore, funding for the maintenance of existing databases is required to keep useful resources up-to-date, rather than only funding new projects. The open-source idea can also help to partly overcome this dilemma. If the data and source codes that have been developed in a project are accessible to other researchers, they can be used in new projects to actually improve the existing status, rather than the wheel having to be reinvented every time by starting from scratch and redeveloping basic concepts and sources.

References

1. Herget, S.; Toukach, P. V.; Ranzinger, R.; Hull, W. E.; Knirel, Y. A.; von der Lieth, C.-W. *BMC Struct. Biol.* **2008,** *8,* No. 35. doi:10.1186/1472-6807-8-35
2. Adibekian, A.; Stallforth, P.; Hecht, M.-L.; Werz, D. B.; Gagneux, P.; Seeberger, P. H. *Chem. Sci.* **2011,** *2,* 337–344. doi:10.1039/c0sc00322k
3. Varki, A.; Cummings, R. D.; Esko, J. D.; Freeze, H. H.; Stanley, P.; Bertozzi, C. R.; Hart, G. W.; Etzler, M. E., Eds. *Essentials of Glycobiology,* 2nd ed.; Cold Spring Harbor Laboratory Press: Plainview, NY, 2009.
4. Rillahan, C. D.; Paulson, J. C. *Annu. Rev. Biochem.* **2011,** *80,* 797–823. doi:10.1146/annurev-biochem-061809-152236
5. Bernardes, G. J. L.; Castagner, B.; Seeberger, P. H. *ACS Chem. Biol.* **2009,** *4,* 703–713. doi:10.1021/cb900014n
6. von der Lieth, C.-W.; Bohne-Lang, A.; Lohmann, K. K.; Frank, M. *Briefings Bioinf.* **2004,** *5,* 164–178. doi:10.1093/bib/5.2.164
7. von der Lieth, C.-W.; Lütteke, T.; Frank, M. *Biochim. Biophys. Acta, Gen. Subj.* **2006,** *1760,* 568–577. doi:10.1016/j.bbagen.2005.12.004
8. von der Lieth, C.-W. Databases and Informatics for Glycobiology and Glycomics. In *Comprehensive Glycoscience;* Kamerling, J. P., Ed.; Elsevier: Oxford, 2007; Vol. 2, pp 329–346.
9. Packer, N. H.; von der Lieth, C.-W.; Aoki-Kinoshita, K. F.; Lebrilla, C. B.; Paulson, J. C.; Raman, R.; Rudd, P.; Sasisekharan, R.; Taniguchi, N.; York, W. S. *Proteomics* **2008,** *8,* 8–20. doi:10.1002/pmic.200700917
10. Katayama, T.; Arakawa, K.; Nakao, M.; Ono, K.; Aoki-Kinoshita, K. F.; Yamamoto, Y.; Yamaguchi, A.; Kawashima, S.; Chun, H.-W.; Aerts, J.; Aranda, B.; Barboza, L. H.; Bonnal, R. J. P.; Bruskiewich, R.; Bryne, J. C.; Fernández, J. M.; Funahashi, A.; Gordon, P. M. K.; Goto, N.; Groscurth, A.; Gutteridge, A.; Holland, R.; Kano, Y.; Kawas, E. A.; Kerhornou, A.; Kibukawa, E.; Kinjo, A. R.; Kuhn, M.; Lapp, H.; Lehvaslaiho, H.; Nakamura, H.; Nakamura, Y.; Nishizawa, T.; Nobata, C.; Noguchi, T.; Oinn, T. M.; Okamoto, S.; Owen, S.; Pafilis, E.; Pocock, M.; Prins, P.; Ranzinger, R.; Reisinger, F.; Salwinski, L.; Schreiber, M.; Senger, M.; Shigemoto, Y.; Standley, D. M.; Sugawara, H.; Tashiro, T.; Trelles, O.; Vos, R. A.; Wilkinson, M. D.; York, W.; Zmasek, C. M.; Asai, K.; Takagi, T. *J. Biomed. Semantics* **2010,** *1,* No. 8. doi:10.1186/2041-1480-1-8
11. MIRAGE Consortium. http://glycomics.ccrc.uga.edu/MIRAGE/index.php/Main_Page (accessed May 9, 2012).
12. Ranzinger, R.; Maass, K.; Lütteke, T. Bioinformatics Databases and Applications Available for Glycobiology and Glycomics. In *Functional and Structural Proteomics of Glycoproteins;* Owens, R.; Nettleship, J., Eds.; Springer: New York, 2011; pp 59–90.
13. Frank, M.; Schloissnig, S. *Cell. Mol. Life Sci.* **2010,** *67,* 2749–2772. doi:10.1007/s00018-010-0352-4
14. Lütteke, T. *ChemBioChem* **2008,** *9,* 2155–2160. doi:10.1002/cbic.200800338
15. Aoki-Kinoshita, K. F.; Kanehisa, M. *Curr. Opin. Mol. Ther.* **2006,** *8,* 514–520.
16. Peréz, S.; Mulloy, B. *Curr. Opin. Struct. Biol.* **2005,** *15,* 517–524. doi:10.1016/j.sbi.2005.08.005
17. Berteau, O.; Stenutz, R. *Carbohydr. Res.* **2004,** *339,* 929–936. doi:10.1016/j.carres.2003.11.008
18. Toukach, P. V. *J. Chem. Inf. Model.* **2011,** *51,* 159–170. doi:10.1021/ci100150d
19. Doubet, S.; Bock, K.; Smith, D.; Darvill, A.; Albersheim, P. *Trends Biochem. Sci.* **1989,** *14,* 475–477. doi:10.1016/0968-0004(89)90175-8
20. Doubet, S.; Albersheim, P. *Glycobiology* **1992,** *2,* 505. doi:10.1093/glycob/2.6.505
21. Raman, R.; Venkataraman, M.; Ramakrishnan, S.; Lang, W.; Raguram, S.; Sasisekharan, R. *Glycobiology* **2006,** *16,* 82R–90R. doi:10.1093/glycob/cwj080
22. Stenutz, R.; Weintraub, A.; Widmalm, G. *FEMS Microbiol. Rev.* **2006,** *30,* 382–403. doi:10.1111/j.1574-6976.2006.00016.x
23. Lundborg, M.; Modhukur, V.; Widmalm, G. *Glycobiology* **2010,** *20,* 366–368. doi:10.1093/glycob/cwp185
24. von der Lieth, C.-W.; Freire, A. A.; Blank, D.; Campbell, M. P.; Ceroni, A.; Damerell, D. R.; Dell, A.; Dwek, R. A.; Ernst, B.; Fogh, R.; Frank, M.; Geyer, H.; Geyer, R.; Harrison, M. J.; Henrick, K.; Herget, S.; Hull, W. E.; Ionides, J.; Joshi, H. J.; Kamerling, J. P.; Leeflang, B. R.; Lütteke, T.; Lundborg, M.; Maass, K.; Merry, A.; Ranzinger, R.; Rosen, J.; Royle, L.; Rudd, P. M.; Schloissnig, S.; Stenutz, R.; Vranken, W. F.; Widmalm, G.; Haslam, S. M. *Glycobiology* **2011,** *21,* 493–502. doi:10.1093/glycob/cwq188
25. Campbell, M. P.; Royle, L.; Radcliffe, C. M.; Dwek, R. A.; Rudd, P. M. *Bioinformatics* **2008,** *24,* 1214–1216. doi:10.1093/bioinformatics/btn090

26. Nakahara, T.; Hashimoto, R.; Nakagawa, H.; Monde, K.; Miura, N.; Nishimura, S.-I. *Nucleic Acids Res.* **2008,** *36* (Suppl. 1), D368–D371. doi:10.1093/nar/gkm833
27. Frank, M.; Lütteke, T.; von der Lieth, C.-W. *Nucleic Acids Res.* **2007,** *35* (Suppl. 1), 287–290. doi:10.1093/nar/gkl907
28. Ranzinger, R.; Herget, S.; Wetter, T.; von der Lieth, C.-W. *BMC Bioinf.* **2008,** *9,* No. 384. doi:10.1186/1471-2105-9-384
29. Ranzinger, R.; Frank, M.; von der Lieth, C.-W.; Herget, S. *Glycobiology* **2009,** *19,* 1563–1567. doi:10.1093/glycob/cwp137
30. Ranzinger, R.; Herget, S.; von der Lieth, C.-W.; Frank, M. *Nucleic Acids Res.* **2011,** *39* (Suppl. 1), D373–D376. doi:10.1093/nar/gkq1014
31. Lütteke, T.; Bohne-Lang, A.; Loss, A.; Goetz, T.; Frank, M.; von der Lieth, C.-W. *Glycobiology* **2006,** *16,* 71R–81R. doi:10.1093/glycob/cwj049
32. Cooper, C. A.; Harrison, M. J.; Wilkins, M. R.; Packer, N. H. *Nucleic Acids Res.* **2001,** *29,* 332–335. doi:10.1093/nar/29.1.332
33. Cooper, C. A.; Joshi, H. J.; Harrison, M. J.; Wilkins, M. R.; Packer, N. H. *Nucleic Acids Res.* **2003,** *31,* 511–513. doi:10.1093/nar/gkg099
34. Taniguchi, N. *IUBMB Life* **2006,** *58,* 269–272. doi:10.1080/15216540600756020
35. Hashimoto, K.; Goto, S.; Kawano, S.; Aoki-Kinoshita, K. F.; Ueda, N.; Hamajima, M.; Kawasaki, T.; Kanehisa, M. *Glycobiology* **2006,** *16,* 63R–70R. doi:10.1093/glycob/cwj010
36. van Kuik, J. A.; Hard, K.; Vliegenthart, J. F. G. *Carbohydr. Res.* **1992,** *235,* 53–68. doi:10.1016/0008-6215(92)80078-F
37. Hayes, C. A.; Karlsson, N. G.; Struwe, W. B.; Lisacek, F.; Rudd, P. M.; Packer, N. H.; Campbell, M. P. *Bioinformatics* **2011,** *27,* 1343–1344. doi:10.1093/bioinformatics/btr137
38. Loß, A.; Bunsmann, P.; Bohne, A.; Loß, A.; Schwarzer, E.; Lang, E.; von der Lieth, C.-W. *Nucleic Acids Res.* **2002,** *30,* 405–408. doi:10.1093/nar/30.1.405
39. Bohne, A.; Lang, E.; von der Lieth, C.-W. *Bioinformatics* **1999,** *15,* 767–768. doi:10.1093/bioinformatics/15.9.767
40. Berman, H. M.; Westbrook, J.; Feng, Z.; Gilliland, G.; Bhat, T. N.; Weissig, H.; Shindyalov, I. N.; Bourne, P. E. *Nucleic Acids Res.* **2000,** *28,* 235–242. doi:10.1093/nar/28.1.235
41. Lütteke, T.; von der Lieth, C.-W. *Biocatal. Biotransform.* **2006,** *24,* 147–155. doi:10.1080/10242420600598269
42. Woods Group (2005-2012) GLYCAM Web, Complex Carbohydrate Research Center, University of Georgia, Athens, GA (http://www.glycam.com).
43. Degtyarenko, K.; Hastings, J.; de Matos, P.; Ennis, M. *Curr. Protoc. Bioinformatics* 2009, *Chapter,* 14, Unit 14–19.
44. de Matos, P.; Adams, N.; Hastings, J.; Moreno, P.; Steinbeck, C. *Methods Mol. Biol.* **2012,** *803,* 273–296. doi:10.1007/978-1-61779-364-6_19
45. Wang, Y.; Xiao, J.; Suzek, T. O.; Zhang, J.; Wang, J.; Bryant, S. H. *Nucleic Acids Res.* **2009,** *37* (Suppl. 2), W623–633. doi:10.1093/nar/gkp456
46. Homann, A.; Seibel, J. *Appl. Microbiol. Biotechnol.* **2009,** *83,* 209–216. doi:10.1007/s00253-009-1989-5
47. Huang, W.; Li, C.; Li, B.; Umekawa, M.; Yamamoto, K.; Zhang, X.; Wang, L.-X. *J. Am. Chem. Soc.* **2009,** *131,* 2214–2223. doi:10.1021/ja8074677
48. Schmidt, D.; Thiem, J. *Beilstein J. Org. Chem.* **2010,** *6,* No. 18. doi:10.3762/bjoc.6.18
49. Palcic, M. M. *Curr. Opin. Chem. Biol.* **2011,** *15,* 226–233. doi:10.1016/j.cbpa.2010.11.022
50. Apweiler, R.; Martin, M. J.; O'Donovan, C.; Magrane, M.; Alam-Faruque, Y.; Antunes, R.; Barrell, D.; Bely, B.; Bingley, M.; Binns, D.; Bower, L.; Browne, P.; Chan, W. M.; Dimmer, E.; Eberhardt, R.; Fedotov, A.; Foulger, R.; Garavelli, J.; Huntley, R.; Jacobsen, J.; Kleen, M.; Laiho, K.; Leinonen, R.; Legge, D.; Lin, Q.; Liu, W.; Luo, J.; Orchard, S.; Patient, S.; Poggioli, D.; Pruess, M.; Corbett, M.; di Martino, G.; Donnelly, M.; van Rensburg, P.; Bairoch, A.; Bougueleret, L.; Xenarios, I.; Altairac, S.; Auchincloss, A.; Argoud-Puy, G.; Axelsen, K.; Baratin, D.; Blatter, M.-C.; Boeckmann, B.; Bolleman, J.; Bollondi, L.; Boutet, E.; Quintaje, S. B.; Breuza, L.; Bridge, A.; deCastro, E.; Ciapina, L.; Coral, D.; Coudert, E.; Cusin, I.; Delbard, G.; Doche, M.; Dornevil, D.; Roggli, P. D.; Duvaud, S.; Estreicher, A.; Famiglietti, L.; Feuermann, M.; Gehant, S.; Farriol-Mathis, N.; Ferro, S.; Gasteiger, E.; Gateau, A.; Gerritsen, V.; Gos, A.; Gruaz-Gumowski, N.; Hinz, U.; Hulo, C.; Hulo, N.; James, J.; Jimenez, S.; Jungo, F.; Kappler, T.; Keller, G.; Lachaize, C.; Lane-Guermonprez, L.; Langendijk-Genevaux, P.; Lara, V.; Lemercier, P.; Lieberherr, D.; de Oliveira Lima, T.; Mangold, V.; Martin, X.; Masson, P.; Moinat, M.; Morgat, A.; Mottaz, A.; Paesano, S.; Pedruzzi, I.; Pilbout, S.; Pillet, V.; Poux, S.; Pozzato, M.; Redaschi, N.; Rivoire, C.; Roechert, B.; Schneider, M.; Sigrist, C.; Sonesson, K.; Staehli, S.; Stanley, E.; Stutz, A.; Sundaram, S.; Tognolli, M.; Verbregue, L.; Veuthey, A.-L.; Yip, L.; Zuletta, L.; Wu, C.; Arighi, C.; Arminski, L.; Barker, W.; Chen, C.; Chen, Y.; Hu, Z.-Z.; Huang, H.; Mazumder, R.; McGarvey, P.; Natale, D. A.; Nchoutmboube, J.; Petrova, N.; Subramanian, N.; Suzek, B. E.; Ugochukwu, U.; Vasudevan, S.; Vinayaka, C. R.; Yeh, L. S.; Zhang, J. *Nucleic Acids Res.* **2010,** *38* (Suppl. 1), D142–D148. doi:10.1093/nar/gkp846
51. Chang, A.; Scheer, M.; Grote, A.; Schomburg, I.; Schomburg, D. *Nucleic Acids Res.* **2009,** *37* (Suppl. 1), D588–D592. doi:10.1093/nar/gkn820
52. Cantarel, B. L.; Coutinho, P. M.; Rancurel, C.; Bernard, T.; Lombard, V.; Henrissat, B. *Nucleic Acids Res.* **2009,** *37* (Suppl. 1), D233–D238. doi:10.1093/nar/gkn663
53. Eisenhaber, B.; Maurer-Stroh, S.; Novatchkova, M.; Schneider, G.; Eisenhaber, F. *Bioessays* **2003,** *25,* 367–385. doi:10.1002/bies.10254
54. Kawasaki, T.; Nakao, H.; Takahashi, E.; Tominaga, T. *Trends Glycosci. Glycotechnol.* **2006,** *18,* 267–272. doi:10.4052/tigg.18.267
55. Altschul, S. F.; Gish, W.; Miller, W.; Myers, E. W.; Lipman, D. J. *J. Mol. Biol.* **1990,** *215,* 403–410. doi:10.1016/S0022-2836(05)80360-2
56. Eddy, S. R. *Bioinformatics* **1998,** *14,* 755–763. doi:10.1093/bioinformatics/14.9.755
57. Davies, G. J.; Gloster, T. M.; Henrissat, B. *Curr. Opin. Struct. Biol.* **2005,** *15,* 637–645. doi:10.1016/j.sbi.2005.10.008
58. Toukach, P.; Joshi, H. J.; Ranzinger, R.; Knirel, Y.; von der Lieth, C.-W. *Nucleic Acids Res.* **2007,** *35* (Suppl. 1), D280–D286. doi:10.1093/nar/gkl883
59. McNaught, A. D. *Adv. Carbohydr. Chem. Biochem.* **1997,** *52,* 43–177. doi:10.1016/S0065-2318(08)60089-X
60. Bohne-Lang, A.; Lang, E.; Förster, T.; von der Lieth, C.-W. *Carbohydr. Res.* **2001,** *336,* 1–11. doi:10.1016/S0008-6215(01)00230-0
61. Herget, S.; Ranzinger, R.; Maass, K.; von der Lieth, C.-W. *Carbohydr. Res.* **2008,** *343,* 2162–2171. doi:10.1016/j.carres.2008.03.011

62. Aoki, K. F.; Yamaguchi, A.; Ueda, N.; Akutsu, T.; Mamitsuka, H.; Goto, S.; Kanehisa, M. *Nucleic Acids Res.* **2004,** *32* (Suppl. 2), W267–W272. doi:10.1093/nar/gkh473
63. Sahoo, S. S.; Thomas, C.; Sheth, A.; Henson, C.; York, W. S. *Carbohydr. Res.* **2005,** *340,* 2802–2807. doi:10.1016/j.carres.2005.09.019
64. York, W. S.; Kochut, K. J.; Miller, J. A.; Sahoo, S.; Thomas, C.; Henson, C. GLYDE-II – GLYcan structural Data Exchange using Connection Tables. http://glycomics.ccrc.uga.edu/GLYDE-II/GLYDE-description_v0.7.pdf.
65. Campbell, M. P.; Hayes, C. A.; Struwe, W. B.; Wilkins, M. R.; Aoki-Kinoshita, K. F.; Harvey, D. J.; Rudd, P. M.; Kolarich, D.; Lisacek, F.; Karlsson, N. G.; Packer, N. H. *Proteomics* **2011,** *11,* 4117–4121. doi:10.1002/pmic.201100302
66. Werz, D. B.; Ranzinger, R.; Herget, S.; Adibekian, A.; von der Lieth, C.-W.; Seeberger, P. H. *ACS Chem. Biol.* **2007,** *2,* 685–691. doi:10.1021/cb700178s
67. Snippe, H.; van Dam, J. E.; van Houte, A. J.; Willers, J. M.; Kamerling, J. P.; Vliegenthart, J. F. *Infect. Immun.* **1983,** *42,* 842–844.
68. Vliegenthart, J. F. G. *FEBS Lett.* **2006,** *580,* 2945–2950. doi:10.1016/j.febslet.2006.03.053
69. Astronomo, R. D.; Burton, D. R. *Nat. Rev. Drug Discovery* **2010,** *9,* 308–324. doi:10.1038/nrd3012
70. Avci, F. Y.; Li, X.; Tsuji, M.; Kasper, D. L. *Nat. Med.* **2011,** *17,* 1602–1609. doi:10.1038/nm.2535
71. Wilson, J. C.; von Itzstein, M. *Curr. Drug Targets* **2003,** *4,* 389–408. doi:10.2174/1389450033491019
72. Haselhorst, T.; Wilson, J. C.; Thomson, R. J.; McAtamney, S.; Menting, J. G.; Coppel, R. L.; von Itzstein, M. *Proteins* **2004,** *56,* 346–353. doi:10.1002/prot.20143
73. Russell, R. J.; Haire, L. F.; Stevens, D. J.; Collins, P. J.; Lin, Y. P.; Blackburn, G. M.; Hay, A. J.; Gamblin, S. J.; Skehel, J. J. *Nature* **2006,** *443,* 45–49. doi:10.1038/nature05114
74. von Itzstein, M. *Nat. Rev. Drug Discovery* **2007,** *6,* 967–974. doi:10.1038/nrd2400
75. Reina, J. J.; Díaz, I.; Nieto, P. M.; Campillo, N. E.; Páez, J. A.; Tabarani, G.; Fieschi, F.; Rojo, J. *Org. Biomol. Chem.* **2008,** *6,* 2743–2754. doi:10.1039/b802144a
76. Bhunia, A.; Vivekanandan, S.; Eckert, T.; Burg-Roderfeld, M.; Wechselberger, R.; Romanuka, J.; Bächle, D.; Kornilov, A. V.; von der Lieth, C.-W.; Jiménez-Barbero, J.; Nifantiev, N. E.; Schachner, M.; Sewald, N.; Lütteke, T.; Gabius, H. J.; Siebert, H.-C. *J. Am. Chem. Soc.* **2010,** *132,* 96–105. doi:10.1021/ja904334s
77. Schierholt, A.; Hartmann, M.; Lindhorst, T. K. *Carbohydr. Res.* **2011,** *346,* 1519–1526. doi:10.1016/j.carres.2011.04.023
78. Akune, Y.; Hosoda, M.; Kaiya, S.; Shinmachi, D.; Aoki-Kinoshita, K. F. *OMICS* **2010,** *14,* 475–486. doi:10.1089/omi.2009.0129
79. Rademacher, C.; Paulson, J. C. *ACS Chem. Biol.* **2012,** *7,* 829–834. doi:10.1021/cb300003z
80. Ceroni, A.; Dell, A.; Haslam, S. M. *Source Code Biol. Med.* **2007,** *2,* No. 3. doi:10.1186/1751-0473-2-3
81. Kawano, S.; Hashimoto, K.; Miyama, T.; Goto, S.; Kanehisa, M. *Bioinformatics* **2005,** *21,* 3976–3982. doi:10.1093/bioinformatics/bti666
82. Hashimoto, K.; Takigawa, I.; Shiga, M.; Kanehisa, M.; Mamitsuka, H. *Bioinformatics* **2008,** *24,* i167–i173. doi:10.1093/bioinformatics/btn293
83. Aoki-Kinoshita, K. F.; Ueda, N.; Mamitsuka, H.; Kanehisa, M. *Bioinformatics* **2006,** *22,* e25–e34. doi:10.1093/bioinformatics/btl244
84. Crispin, M.; Stuart, D. I.; Jones, E. Y. *Nat. Struct. Mol. Biol.* **2007,** *14,* 354. doi:10.1038/nsmb0507-354a
85. Lütteke, T.; Frank, M.; von der Lieth, C.-W. *Carbohydr. Res.* **2004,** *339,* 1015–1020. doi:10.1016/j.carres.2003.09.038
86. Lütteke, T. *Acta Crystallogr., Sect. D: Biol. Crystallogr.* **2009,** *65,* 156–168. doi:10.1107/S0907444909001905
87. Read, R. J.; Adams, P. D.; Arendall, W. B.; Brunger, A. T.; Emsley, P.; Joosten, R. P.; Kleywegt, G. J.; Krissinel, E. B.; Lütteke, T.; Otwinowski, Z.; Perrakis, A.; Richardson, J. S.; Sheffler, W. H.; Smith, J. L.; Tickle, I. J.; Vriend, G.; Zwart, P. H. *Structure* **2011,** *19,* 1395–1412. doi:10.1016/j.str.2011.08.006
88. Lütteke, T.; von der Lieth, C.-W. *BMC Bioinf.* **2004,** *5,* No. 69. doi:10.1186/1471-2105-5-69
89. Lütteke, T.; Frank, M.; von der Lieth, C.-W. *Nucleic Acids Res.* **2005,** *33* (Suppl. 1), D242–D246. doi:10.1093/nar/gki013
90. Raman, R.; Venkataraman, G.; Ernst, S.; Sasisekharan, V.; Sasisekharan, R. *Proc. Natl. Acad. Sci. U. S. A.* **2003,** *100,* 2357–2362. doi:10.1073/pnas.0437842100
91. Bhunia, A.; Schwardt, O.; Gäthje, H.; Gao, G.-P.; Kelm, S.; Benie, A. J.; Hricovini, M.; Peters, T.; Ernst, B. *ChemBioChem* **2008,** *9,* 2941–2945. doi:10.1002/cbic.200800458
92. Kerzmann, A.; Fuhrmann, J.; Kohlbacher, O.; Neumann, D. *J. Chem. Inf. Model.* **2008,** *48,* 1616–1625. doi:10.1021/ci800103u
93. Kerzmann, A.; Neumann, D.; Kohlbacher, O. *J. Chem. Inf. Model.* **2006,** *46,* 1635–1642. doi:10.1021/ci050422y
94. Case, D. A.; Cheatham, T. E., III; Darden, T.; Gohlke, H.; Luo, R.; Merz, K. M., Jr.; Onufriev, A.; Simmerling, C.; Wang, B.; Woods, R. J. *J. Comput. Chem.* **2005,** *26,* 1668–1688. doi:10.1002/jcc.20290
95. Case, D. A.; Darden, T. A.; Cheatham, T. E.; Simmerling, C. L.; Wang, J.; Duke, R. E.; Luo, R.; Walker, R. C.; Zhang, W.; Merz, K. M.; Roberts, B. P.; Wang, B.; Hayik, S.; Roitberg, A.; Seabra, G.; Kolossváry, I.; Wong, K. F.; Paesani, F.; Vanicek, J.; Liu, J.; Wu, X.; Brozell, S. R.; Steinbrecher, T.; Gohlke, H.; Cai, Q.; Ye, X.; Wang, J.; Hsieh, M.-J.; Cui, G.; Roe, D. R.; Mathews, D. H.; Seetin, M. G.; Sagui, C.; Babin, V.; Luchko, T.; Gusarov, S.; Kovalenko, A.; Kollman, P. A. *AMBER 11*; University of California: San Francisco, 2010.
96. Jo, S.; Song, K. C.; Desaire, H.; MacKerell, A. D., Jr.; Im, W. *J. Comput. Chem.* **2011,** *32,* 3135–3141. doi:10.1002/jcc.21886
97. Brooks, B. R.; Brooks, C. L., III; Mackerell, A. D., Jr.; Nilsson, L.; Petrella, R. J.; Roux, B.; Won, Y.; Archontis, G.; Bartels, C.; Boresch, S.; Caflisch, A.; Caves, L.; Cui, Q.; Dinner, A. R.; Feig, M.; Fischer, S.; Gao, J.; Hodoscek, M.; Im, W.; Kuczera, K.; Lazaridis, T.; Ma, J.; Ovchinnikov, V.; Paci, E.; Pastor, R. W.; Post, C. B.; Pu, J. Z.; Schaefer, M.; Tidor, B.; Venable, R. M.; Woodcock, H. L.; Wu, X.; Yang, W.; York, D. M.; Karplus, M. *J. Comput. Chem.* **2009,** *30,* 1545–1614. doi:10.1002/jcc.21287
98. Bohne-Lang, A.; von der Lieth, C.-W. *Nucleic Acids Res.* **2005,** *33* (Suppl. 2), W214–W219. doi:10.1093/nar/gki385
99. Kirschner, K. N.; Yongye, A. B.; Tschampel, S. M.; González-Outeiriño, J.; Daniels, C. R.; Foley, B. L.; Woods, R. J. *J. Comput. Chem.* **2008,** *29,* 622–655. doi:10.1002/jcc.20820
100. Woods, R. J.; Tessier, M. B. *Curr. Opin. Struct. Biol.* **2010,** *20,* 575–583. doi:10.1016/j.sbi.2010.07.005
101. Sapay, N.; Cabannes, E.; Petitou, M.; Imberty, A. *Glycobiology* **2011,** *21,* 1181–1193. doi:10.1093/glycob/cwr052
102. Jo, S.; Kim, T.; Iyer, V. G.; Im, W. *J. Comput. Chem.* **2008,** *29,* 1859–1865. doi:10.1002/jcc.20945
103. Eisenhaber, B.; Bork, P.; Eisenhaber, F. *J. Mol. Biol.* **1999,** *292,* 741–758. doi:10.1006/jmbi.1999.3069
104. Julenius, K.; Mølgaard, A.; Gupta, R.; Brunak, S. *Glycobiology* **2005,** *15,* 153–164. doi:10.1093/glycob/cwh151

105. Julenius, K. *Glycobiology* **2007,** *17,* 868–876. doi:10.1093/glycob/cwm050
106. Johansen, M. B.; Kiemer, L.; Brunak, S. *Glycobiology* **2006,** *16,* 844–853. doi:10.1093/glycob/cwl009
107. Gupta, R.; Jung, E.; Gooley, A. A.; Williams, K. L.; Brunak, S.; Hansen, J. *Glycobiology* **1999,** *9,* 1009–1022. doi:10.1093/glycob/9.10.1009
108. Gupta, R.; Brunak, S. *Pac. Symp. Biocomput.* **2002,** 310–322.
109. Chen, Y.-Z.; Tang, Y.-R.; Sheng, Z.-Y.; Zhang, Z. *BMC Bioinf.* **2008,** *9,* No. 101. doi:10.1186/1471-2105-9-101
110. Caragea, C.; Sinapov, J.; Silvescu, A.; Dobbs, D.; Honavar, V. *BMC Bioinf.* **2007,** *8,* No. 438. doi:10.1186/1471-2105-8-438
111. Fankhauser, N.; Mäser, P. *Bioinformatics* **2005,** *21,* 1846–1852. doi:10.1093/bioinformatics/bti299
112. Hamby, S. E.; Hirst, J. D. *BMC Bioinf.* **2008,** *9,* No. 500. doi:10.1186/1471-2105-9-500
113. Morris, G. M.; Huey, R.; Lindstrom, W.; Sanner, M. F.; Belew, R. K.; Goodsell, D. S.; Olson, A. J. *J. Comput. Chem.* **2009,** *30,* 2785–2791. doi:10.1002/jcc.21256
114. Bhunia, A.; Jayalakshmi, V.; Benie, A. J.; Schuster, O.; Kelm, S.; Rama Krishna, N.; Peters, T. *Carbohydr. Res.* **2004,** *339,* 259–267. doi:10.1016/j.carres.2003.09.021
115. Kuntothom, T.; Raab, M.; Tvaroška, I.; Fort, S.; Pengthaisong, S.; Cañada, J.; Calle, L.; Jiménez-Barbero, J.; Ketudat Cairns, J. R.; Hrmova, M. *Biochemistry* **2010,** *49,* 8779–8793. doi:10.1021/bi101112c
116. DeMarco, M. L.; Woods, R. J.; Prestegard, J. H.; Tian, F. *J. Am. Chem. Soc.* **2010,** *132,* 1334–1338. doi:10.1021/ja907518x
117. Kogelberg, H.; Frenkiel, T. A.; Homans, S. W.; Lubineau, A.; Feizi, T. *Biochemistry* **1996,** *35,* 1954–1964. doi:10.1021/bi9521598
118. Morando, M. A.; Nurisso, A.; Grenouillat, N.; Vauzeilles, B.; Beau, J.-M.; Cañada, F. J.; Jiménez-Barbero, J.; Imberty, A. *Glycobiology* **2011,** *21,* 824–833. doi:10.1093/glycob/cwr014
119. Säwén, E.; Stevensson, B.; Östervall, J.; Maliniak, A.; Widmalm, G. *J. Phys. Chem. B* **2011,** *115,* 7109–7121. doi:10.1021/jp2017105
120. Tessier, M. B.; DeMarco, M. L.; Yongye, A. B.; Woods, R. J. *Mol. Simul.* **2008,** *34,* 349–363. doi:10.1080/08927020701710890
121. Fadda, E.; Woods, R. J. *Drug Discovery Today* **2010,** *15,* 596–609. doi:10.1016/j.drudis.2010.06.001
122. Tschampel, S. M.; Kennerty, M. R.; Woods, R. J. *J. Chem. Theory Comput.* **2007,** *3,* 1721–1733. doi:10.1021/ct700046j
123. Van Der Spoel, D.; Lindahl, E.; Hess, B.; Groenhof, G.; Mark, A. E.; Berendsen, H. J. C. *J. Comput. Chem.* **2005,** *26,* 1701–1718. doi:10.1002/jcc.20291
124. Guerrini, M.; Beccati, D.; Shriver, Z.; Naggi, A.; Viswanathan, K.; Bisio, A.; Capila, I.; Lansing, J. C.; Guglieri, S.; Fraser, B.; Al-Hakim, A.; Gunay, N. S.; Zhang, Z.; Robinson, L.; Buhse, L.; Nasr, M.; Woodcock, J.; Langer, R.; Venkataraman, G.; Linhardt, R. J.; Casu, B.; Torri, G.; Sasisekharan, R. *Nat. Biotechnol.* **2008,** *26,* 669–675. doi:10.1038/nbt1407
125. Beyer, T.; Diehl, B.; Randel, G.; Humpfer, E.; Schäfer, H.; Spraul, M.; Schollmayer, C.; Holzgrabe, U. *J. Pharm. Biomed. Anal.* **2008,** *48,* 13–19. doi:10.1016/j.jpba.2008.06.014
126. Alban, S.; Lühn, S.; Schiemann, S.; Beyer, T.; Norwig, J.; Schilling, C.; Rädler, O.; Wolf, B.; Matz, M.; Baumann, K.; Holzgrabe, U. *Anal. Bioanal. Chem.* **2011,** *399,* 605–620. doi:10.1007/s00216-010-4169-7
127. Goldberg, D.; Bern, M.; Parry, S.; Sutton-Smith, M.; Panico, M.; Morris, H. R.; Dell, A. *J. Proteome Res.* **2007,** *6,* 3995–4005. doi:10.1021/pr070239f
128. Goldberg, D.; Sutton-Smith, M.; Paulson, J.; Dell, A. *Proteomics* **2005,** *5,* 865–875. doi:10.1002/pmic.200401071
129. Tang, H.; Mechref, Y.; Novotny, M. V. *Bioinformatics* **2005,** *21* (Suppl. 1), i431–i439. doi:10.1093/bioinformatics/bti1038
130. Lohmann, K. K.; von der Lieth, C.-W. *Proteomics* **2003,** *3,* 2028–2035. doi:10.1002/pmic.200300505
131. Ozohanics, O.; Krenyacz, J.; Ludányi, K.; Pollreisz, F.; Vékey, K.; Drahos, L. *Rapid Commun. Mass Spectrom.* **2008,** *22,* 3245–3254. doi:10.1002/rcm.3731
132. Cooper, C. A.; Gasteiger, E.; Packer, N. H. *Proteomics* **2001,** *1,* 340–349. doi:10.1002/1615-9861(200102)1:2<340::AID-PROT340>3.0.CO;2-B
133. Maass, K.; Ranzinger, R.; Geyer, H.; von der Lieth, C.-W.; Geyer, R. *Proteomics* **2007,** *7,* 4435–4444. doi:10.1002/pmic.200700253
134. Irungu, J.; Go, E. P.; Dalpathado, D. S.; Desaire, H. *Anal. Chem.* **2007,** *79,* 3065–3074. doi:10.1021/ac062100e
135. Pompach, P.; Chandler, K. B.; Lan, R.; Edwards, N.; Goldman, R. *J. Proteome Res.* **2012,** *11,* 1728–1740. doi:10.1021/pr201183w
136. Lohmann, K. K.; von der Lieth, C.-W. *Nucleic Acids Res.* **2004,** *32* (Suppl. 2), W261–W266. doi:10.1093/nar/gkh392
137. Joshi, H. J.; Harrison, M. J.; Schulz, B. L.; Cooper, C. A.; Packer, N. H.; Karlsson, N. G. *Proteomics* **2004,** *4,* 1650–1664. doi:10.1002/pmic.200300784
138. Ceroni, A.; Maass, K.; Geyer, H.; Geyer, R.; Dell, A.; Haslam, S. M. *J. Proteome Res.* **2008,** *7,* 1650–1659. doi:10.1021/pr7008252
139. Gao, H. Y. *J. Am. Soc. Mass Spectrom.* **2009,** *20,* 1739–1742. doi:10.1016/j.jasms.2009.05.012
140. Zhang, H.; Singh, S.; Reinhold, V. N. *Anal. Chem.* **2005,** *77,* 6263–6270. doi:10.1021/ac050725r
141. Lapadula, A. J.; Hatcher, P. J.; Hanneman, A. J.; Ashline, D. J.; Zhang, H.; Reinhold, V. N. *Anal. Chem.* **2005,** *77,* 6271–6279. doi:10.1021/ac050726j
142. Gaucher, S. P.; Morrow, J.; Leary, J. A. *Anal. Chem.* **2000,** *72,* 2331–2336. doi:10.1021/ac000096f
143. Ethier, M.; Saba, J. A.; Spearman, M.; Krokhin, O.; Butler, M.; Ens, W.; Standing, K. G.; Perreault, H. *Rapid Commun. Mass Spectrom.* **2003,** *17,* 2713–2720. doi:10.1002/rcm.1252
144. Lundborg, M.; Widmalm, G. *Anal. Chem.* **2011,** *83,* 1514–1517. doi:10.1021/ac1032534
145. Jansson, P.-E.; Stenutz, R.; Widmalm, G. *Carbohydr. Res.* **2006,** *341,* 1003–1010. doi:10.1016/j.carres.2006.02.034
146. Vranken, W. F.; Boucher, W.; Stevens, T. J.; Fogh, R. H.; Pajon, A.; Llinas, M.; Ulrich, E. L.; Markley, J. L.; Ionides, J.; Laue, E. D. *Proteins* **2005,** *59,* 687–696. doi:10.1002/prot.20449
147. Loß, A.; Stenutz, R.; Schwarzer, E.; von der Lieth, C.-W. *Nucleic Acids Res.* **2006,** *34* (Suppl. 2), W733–W737. doi:10.1093/nar/gkl265
148. Takahashi, N.; Kato, K. *Trends Glycosci Glycotechnol.* **2003,** *15,* 235–251. doi:10.4052/tigg.15.235
149. Packer, N. H.; Karlsson, N. G. Glycomic Mass Spectrometric Analysis and Data Interpretation Tools. In *Bioinformatics for Glycobiology and Glycomics - an Introduction;* von der Lieth, C.-W.; Lütteke, T.; Frank, M., Eds.; Wiley & Sons: Chichester, UK, 2009; pp 223–256.
150. Maass, K.; Ceroni, A. Software Tools for Semi-automatic Interpretation of Mass Spectra of Glycans. In *Bioinformatics for Glycobiology and Glycomics - an Introduction;* von der Lieth, C.-W.; Lütteke, T.; Frank, M., Eds.; Wiley & Sons: Chichester, UK, 2009; pp 257–268.

151. Fogh, R. H.; Vranken, W. F.; Boucher, W.; Stevens, T. J.; Laue, E. D. *J. Biomol. NMR* **2006,** *36,* 147–155. doi:10.1007/s10858-006-9076-z
152. Jansson, P. E.; Kenne, L.; Widmalm, G. *J. Chem. Inf. Comput. Sci.* **1991,** *31,* 508–516. doi:10.1021/ci00004a013
153. Stenutz, R.; Jansson, P.-E.; Widmalm, G. *Carbohydr. Res.* **1998,** *306,* 11–17. doi:10.1016/S0008-6215(97)10047-7
154. Lundborg, M.; Fontana, C.; Widmalm, G. *Biomacromolecules* **2011,** *12,* 3851–3855. doi:10.1021/bm201169y

License and Terms

Beilstein Journal of Organic Chemistry

Low-generation dendrimers with a calixarene core and based on a chiral C_2-symmetric pyrrolidine as iminosugar mimics

Marco Marradi*[1,§], Stefano Cicchi[1], Francesco Sansone[2], Alessandro Casnati[2] and Andrea Goti[1]

Letter

Open Access

Address:
[1]Dipartimento di Chimica "Ugo Schiff", Università degli Studi di Firenze, via della Lastruccia 13, I-50019 Sesto Fiorentino (Firenze), Italy and [2]Dipartimento di Chimica Organica e Industriale, Università degli Studi di Parma, Parco Area delle Scienze 17/A, I-43124 Parma, Italy

Email:
Marco Marradi* - mmarradi.ciber-bbn@cicbiomagune.es; Stefano Cicchi - stefano.cicchi@unifi.it; Francesco Sansone - francesco.sansone@unipr.it; Alessandro Casnati - casnati@unipr.it; Andrea Goti - andrea.goti@unifi.it

* Corresponding author
§ present address: Laboratory of GlycoNanotechnology, Biofunctional Nanomaterials Unit, CIC biomaGUNE / CIBER-BBN, Pº Miramón 182, San Sebastián E-20009, Spain

Keywords:
calixarenes; cation-responsive system; dendrimers; iminosugars; multivalency

Beilstein J. Org. Chem. **2012,** *8,* 951–957.
doi:10.3762/bjoc.8.107

Received: 28 April 2012
Accepted: 30 May 2012
Published: 26 June 2012

This article is part of the Thematic Series "Synthesis in the glycosciences II".

Guest Editor: T. K. Lindhorst

Abstract

The preparation of low-generation dendrimers based on a simple calix[4]arene scaffold by insertion of the iminosugar-analogue C_2-symmetric 3,4-dihydroxypyrrolidine is described. This methodology allows a rapid incorporation of a considerable number of iminosugar-like moieties in a reduced volume and in a well-defined geometry. The inclusion of alkali-metal ions (sodium and potassium) in the polar cavity defined by the acetamide moieties at the lower rim of the calixarene was demonstrated, which allows also the rigidification of the dendrimer structure and the iminosugar presentation in the clusters. The combination of the supramolecular properties of calixarenes with the advantage of a dendrimeric presentation of repetitive units opens up the possibility of generating well-defined multivalent and multifaceted systems with more complex and/or biologically relevant iminosugars.

Introduction

Polyhydroxylated pyrrolidines are one of the main classes of naturally occurring sugar mimics [1,2] and belong to the so-called iminosugars [3]. Several iminosugars have shown potential as therapeutics due to the ability to inhibit glycosidases and other enzymes associated with the metabolism of polysaccharides and the processing of glycoproteins [3].

Conjugation of iminosugars onto a polyvalent skeleton has been investigated only occasionally, and their properties as multivalent enzyme inhibitors gave contrasting results. Early findings indicated in fact that poor multivalent phenomena take place [4-6], but more recently moderate [7] to remarkable [8,9] effects have been reported on glycosidases. Unlike lectin-mediated interactions [10], the effect of iminosugar-based multivalent inhibitors on enzyme activity is difficult to rationalise. However, the introduction of several copies of an *N*-alkyl analogue of iminosugar 1-deoxynojirimycin onto a fullerene ball [8] or onto β-cyclodextrin [9] afforded the first pieces of evidence for a significant multivalent effect in glycosidase inhibition. These results highlight the interest in synthesizing multivalent iminosugar-conjugates with well-defined structures. In this context, we aimed at studying the feasibility of combining the supramolecular properties of multivalent scaffolds, such as calixarenes, with the advantages of a dendrimeric presentation of iminosugar analogues.

Calixarenes [11] have been widely employed in host–guest chemistry, first as ligands for small ions and neutral molecules [12,13] and, more recently, for biologically relevant molecules and macromolecules [14]. Multivalent calixarenes functionalised with carbohydrate units (glycocalixarenes) [15] have been extensively reported in the literature and represent examples of sugar clustering on macrocyclic structures [16,17]. Thanks to the "glycoside cluster effect" [18-20], glycocalixarenes can enhance the avidity of interactions between glycans and lectins [15]. Some glycocalixarenes have shown remarkable inhibition properties towards galectins [21,22] or *Pseudomonas Aeruginosa* lectin [23], the inhibition ability being dependent on the macrocyclic conformation and presentation of the glycoside units. With the purpose of expanding the valency and increasing the glycoside density, glycodendrimers have also been synthesised and their properties in protein–carbohydrate interactions have been studied [24-26]. However, the innovative frontier of combining glycodendrimeric arrangements onto a calixarene core has only occasionally been explored. To the best of our knowledge, only one example in which a glycodendrimer was built on a calixarene core has been published [27], while no examples of iminosugar-based calixarene dendrimers have been reported so far.

We report herein the synthesis of low-generation iminosugar-type calixarene-based dendrimers, demonstrating the feasibility of increasing the valency of the cluster by combining a dendrimeric arrangement of iminosugar ligands with a multivalent calixarene core.

Results and Discussion

We chose to address the conjugation of iminosugar-analogue dendrimers, based on the C_2-symmetric (3*S*,4*S*)-3,4-dihydoxypyrrolidine (**1**) unit, to a simple calix[4]arene scaffold (Figure 1). This allows a rapid increase of the valency of the iminosugar dendrimer in a reduced volume. The C_2 symmetry of pyrrolidine **1**, its ready accessibility from the "chiral pool" (L-tartaric acid) [28], and its functional groups (an anchoring amine and two transformable hydroxy groups) make it a convenient chiral AB_2 building block for the construction of dendrimers [29]. The linkable hydroxy groups of the pyrrolidine rings open up the possibility of constructing calixarene-based dendrimers [30] of higher generation. In addition to its properties as a chiral building block, pyrrolidine **1** may be considered an elemental iminosugar, and it is, by far, easier to handle and to characterise as a consequence of its symmetry. The synthesis of model iminosugar-based calixarene dendrimers may open the way for the construction of more complex systems, decorated with biologically active polyhydroxylated pyrrolidines or piperidines.

The synthesis of first- and second-generation iminosugar-based calixarene-dendrimers **2** and **3** (Figure 1) was addressed in

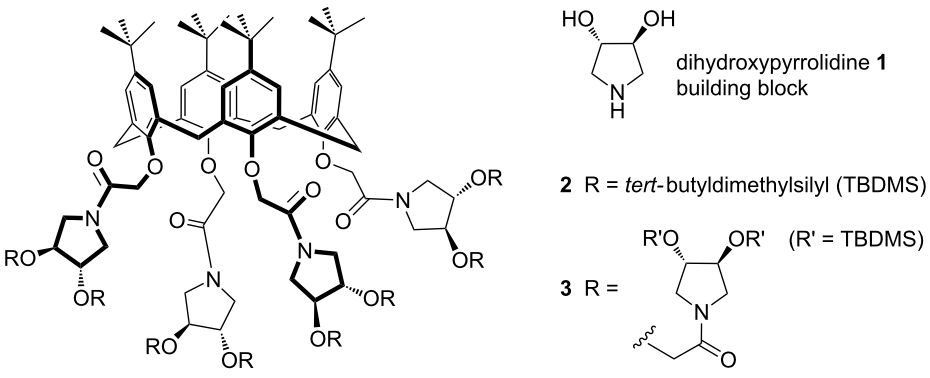

Figure 1: First (**2**) and second (**3**) generation of dendrimers based on chiral C_2-symmetric pyrrolidine **1** and having *p-tert*-butyl calix[4]arene as the scaffold.

order to prove the viability of such a strategy. A convergent synthetic approach was chosen for the conjugation of pyrrolidine **4** and pyrrolidine-based dendron **5** (see Scheme 1) to the calix[4]arene core, via intermediate **11**, in order to obtain iminosugar-based calixarene-dendrimers **2** and **3** (see Scheme 2). The starting calixarene used in this work was the commercially available *p-tert*-butyl calix[4]arene, which has the phenolic hydroxy groups at the lower rim and the *tert*-butyl groups at the upper rim. Functionalization of *p-tert*-butyl calix[4]arene was performed by standard conversion of the hydroxy groups of the lower rim to activated acetic acid succinimide ester (COOSu) moieties (compound **11**, see Scheme S2 in Supporting Information File 1). These moieties allowed the subsequent conjugation by amide bond formation between **11** and the suitably protected pyrrolidine derivatives **4** and **5** in order to obtain the calixarene-dendrimers **2** and **3**, respectively. The synthesis of (3*S*,4*S*)-3,4-bis(*tert*-butyldimethylsilyloxy)pyrrolidine (**4**) was achieved by following a reported procedure [31], via the key intermediate **6** (Scheme 1 and Supporting Information File 1). Tripyrrolidine **5** required for the second generation calixarene-dendrimer **3** was prepared starting again from the key intermediate **6**, but in this case a modified multistep synthetic procedure was necessary. First, *N*-Boc dihydroxypyrrolidine **7** was obtained from **6** through a "one pot" change of protecting group from benzyl to *tert*-butoxycarbonyl, which occurred in excellent yield by performing the catalytic hydrogenation in methanol under reflux and in the presence of Boc_2O (Scheme 1). This simple process is unprecedented and may result in a new straightforward method to convert *N*-benzyl amines into *N*-Boc amines once a series of similar compounds are screened. On the other hand, alkylation of the hydroxy groups of **7** with the 2-ethoxycarbonylmethyl linker was problematic. In fact, when sodium hydride was used as a deprotonating agent, no reaction occurred after in situ addition of ethyl bromoacetate. However, a mixture of mono-(**8'**) and di-(**8**) substituted products was obtained by using metallic potassium (Scheme 1). In spite of the poor yield (35%) of the desired product **8**, the starting material **7** and the mono-derivative **8'** could be recovered after column chromatography over silica gel, and used again for the same reaction. The *N*-protected pyrrolidine **8** was then activated for the coupling with pyrrolidine **4** in order to obtain the pyrrolidine-based dendron **5** to be used in assembling the second-generation calixarene-dendrimer **3**. In particular, succinimidyl-activated pyrrolidine **9** was obtained by hydrolysis of ester groups in **8** followed by treatment with DCC/NHS (two steps, 80% overall yield). The amide coupling was then performed by reaction of **9** with pyrrolidine **4** using DIPEA as a base, and this afforded the branched tripyrrolidine **10** in 77% yield after column chromatography over neutral aluminium oxide. The *tert*-butoxycarbonyl group was then removed in the presence of TFA to obtain the pyrrolidine-based dendron **5** (Scheme 1), which was used in the next step without further purification.

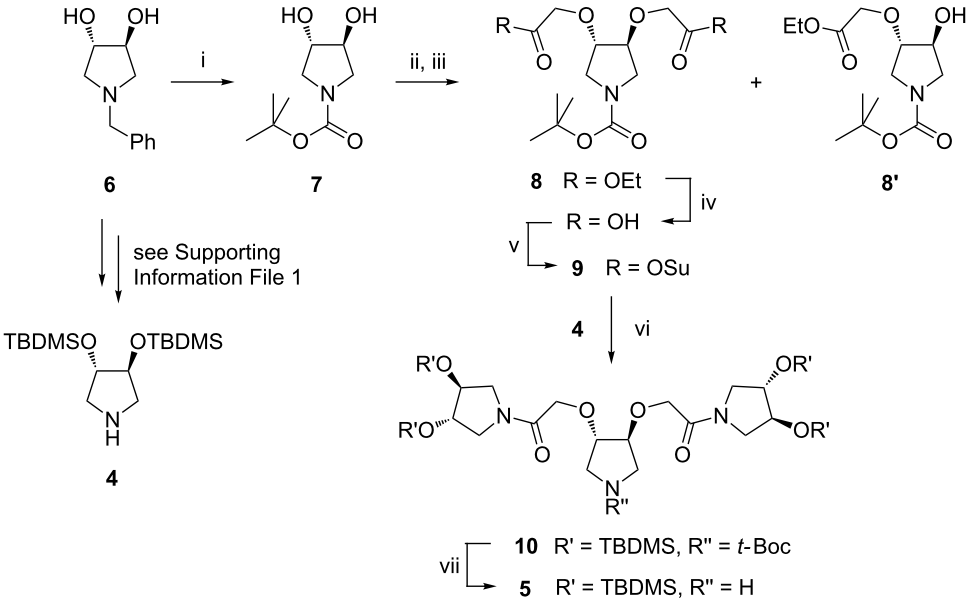

Scheme 1: Use of the key intermediate (3*S*,4*S*)-1-benzyl-3,4-dihydroxypyrrolidine (**6**) [31] for the synthesis of pyrrolidine **4** and the pyrrolidine-based dendron **5**. Reagents and conditions: i. $Pd(OH)_2$/C, MeOH, $HCOO^-NH_4^+$, Boc_2O, reflux, 3 h, 95%; ii. K, THF, 0 °C to rt, 16 h; iii. $BrCH_2CO_2Et$, 4 h, 35% (**8**) and 17% (**8'**); iv. KOH 1 N, EtOH, reflux, 3.5 h, quantitative; v. *N*-hydroxysuccinimide (NHS), AcOEt, dicyclohexylcarbodiimide (DCC), 30 °C, 72 h, 80%, (Su: succinimidyl); vi. *N*,*N*-diisopropylethylamine (DIPEA), CH_2Cl_2, 30 °C, 5 d, 77%; vii. trifluoroacetic acid (TFA), CH_2Cl_2, rt, 16 h, quantitative.

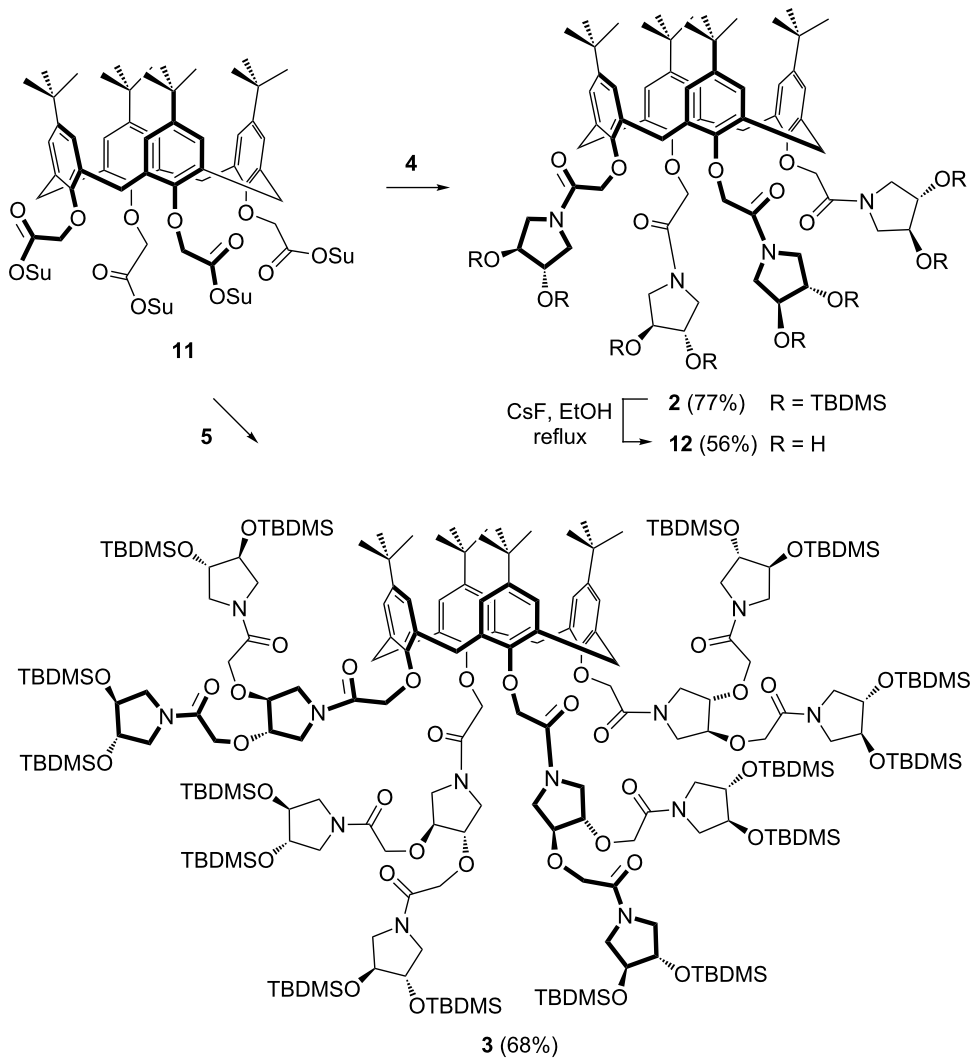

Scheme 2: Synthesis of calixarene-based dendrimers **2** and **3**. Reagents and conditions: DIPEA, CH_2Cl_2, 30 °C, 5 d, (Su: succinimidyl; TBDMS: *tert*-butyldimethylsilyl).

Using the SuO-activated calix[4]arene **11** as the scaffold, the planned convergent synthetic approach was completed to afford the first (**2**) and second (**3**) generation iminosugar-based calixarene dendrimers. The coupling between calixarene **11** and pyrrolidine derivatives **4** or **5** was performed as reported before for the synthesis of compound **10** (Scheme 1) and is shown in Scheme 2. The identity of both final compounds **2** and **3**, obtained in good yields (77% and 68%, respectively), was assessed by their spectroscopic data and elemental analysis (see Supporting Information File 1). In particular, integration ratios of the calixarene aromatic (8H, δ ≈ 7 ppm) and *tert*-butyl signals (36H, δ ≈ 1 ppm) versus those of the C*H*$_3$ of TBDMS at ca. 0 ppm were in good agreement with the number of the expected protons for dendrimers **2** and **3** (48H and 96H, respectively). Thus, an increase of the valency of a model iminosugar dihydroxypyrrolidine **4** in a controlled manner and geometry, by its conjugation to the calixarene scaffold **11** in a dendrimeric fashion, could be demonstrated. Quite interestingly, we could also prove the feasibility of the iminosugar deprotection on the calixarene dendrimer **2**. By treatment with CsF in EtOH, the eight *tert*-butyldimethylsilyl groups could be removed and the deprotected derivative **12** was obtained in 56% yield after trituration with CH_2Cl_2 and washing several times with water.

The presence of acetamide moieties at the lower rim of the dendrimers **2** and **3** prompted us to explore the possibility to use alkali metal salts as allosteric effectors in the modulation of the shape and rigidity of the iminosugar presentation by the calixarene scaffold. A common way, in fact, used to rigidify the "mobile cone" structure of tetraalkoxycalix[4]arenes is to introduce strong donating groups, such as amide or ester [32,33], on

the phenolic oxygen atoms and an alkali-metal ion. The cation, strongly coordinated by eight oxygen atoms in the polar region created at the lower rim, blocks the calixarene in a "rigid cone" structure [34], also controlling the convergence of the iminosugars.

The ability of first-generation calixarene dendrimer **2** to bind alkali-metal cations was tested by means of NMR, by solid–liquid extraction of solid alkali picrate salts into a $CDCl_3$ solution of ligand **2**. A mixture of 0.5 equiv of sodium or potassium picrate and ligand **2** showed the simultaneous presence of the peaks of the complex and of the free ligand indicating a slow exchange regime on the NMR timescale. On the other hand, the NMR analysis of a $CDCl_3$ solution of ligand **2** in the presence of an excess of metal picrate (see Figure S1 in Supporting Information File 1) allowed the stoichiometry of the complex to be established. As the picrate salts are scarcely soluble in $CDCl_3$, the comparison of the integrals of the picrate signal (a singlet of 2H, around 8.8 ppm) and of the calixarene aromatic protons (a signal of 8H at 7.00–7.10 ppm) indicated that the complexes (both with sodium and potassium) have a 1:1 stoichiometry. As it can be seen in Figure 2, and as reported also for other alkali-metal ion complexes of similar tetramide ligands [35], the cation complexation induces a strong deshielding effect on the aromatic protons of about 0.3 ppm with respect to the free calixarene (as indicated by the asterisks) as a consequence of the electron-withdrawing effect of the metal ion coordinated to the phenolic oxygen.

Quite remarkable is the up-field shift exerted by the OCH_2CON protons (empty circles in Figure 2), which is due to their positioning close to the shielding cone of the aromatic nuclei as a consequence of the C=O coordination to the metal ion (Figure 3). Interesting, and not observed for achiral calixarene tetramide ligands, is the splitting of the OCH_2CON methylene protons into an AB system (empty circles in Figure 2), which, especially in the case of the Na^+ complex, indicates a quite different chemical environment for the two geminal protons and could be the consequence of a quite twisted square antiprism of coordination around the cation [36]. Consistent shifts are observed for the methylene bridge protons (filled circles in Figure 2), which are in line with previous observations but more difficult to be rationalised also as a consequence of a slight conformational rearrangement of the calixarene scaffold. Less important shifts are obviously observed for the pyrrolidine ring protons, which are quite far from the binding region.

These results show, therefore, that, in spite of the bulky substituents present on the pyrrolidine nuclei, the amide groups can still bind alkali-metal ions quite efficiently. This encourages the use of such compounds not only to study the metal-ion effect on the organisation of iminosugars and on the rigidifica-

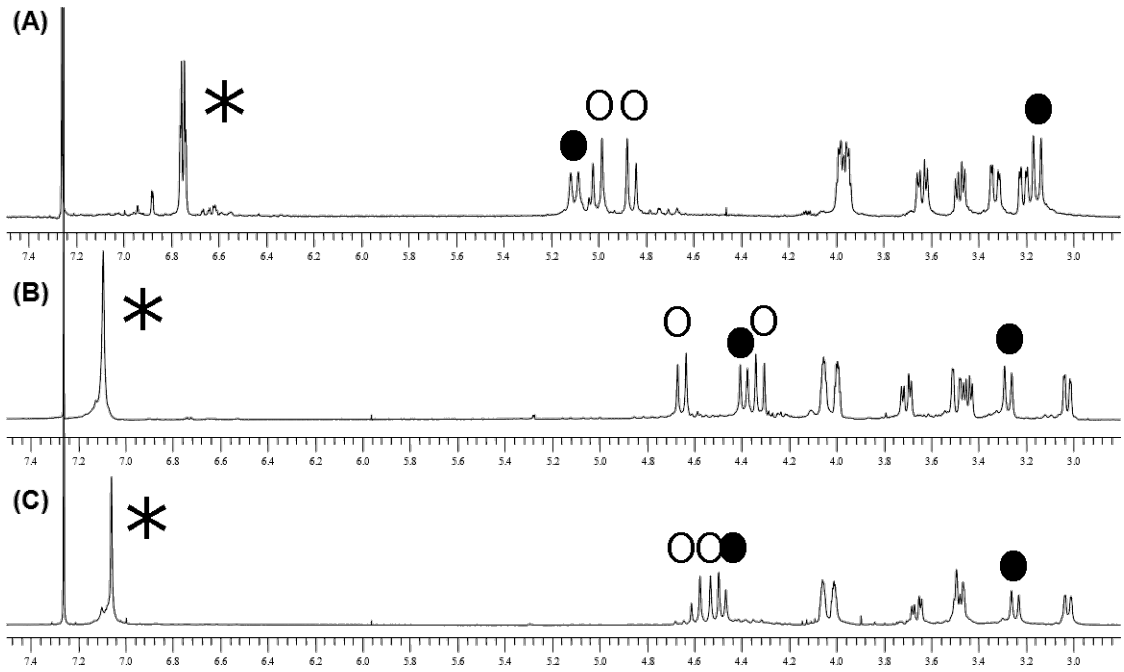

Figure 2: Expansion (about 7 to 3 ppm) of the ^{1}H NMR spectra of (A) the free ligand **2**, (B) the sodium picrate complex, and (C) the potassium picrate complex. The full spectra are reported in Supporting Information File 1 (Figure S1). Asterisks: aromatic protons; empty circles: OCH_2CON protons; filled circles: methylene bridge protons.

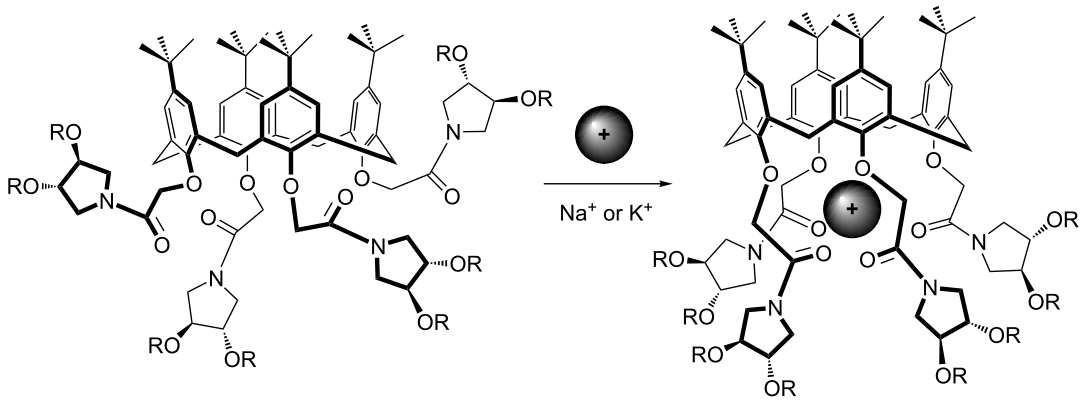

Figure 3: Schematic of the inclusion of alkali-metal ions (sodium and potassium) in the polar cavity defined by the acetamide moieties at the lower rim of the calixarene, and its effect on the rigidification of the calixarene scaffold and organisation of iminosugars.

tion of the calixarene scaffold, but also to exploit the ability of these chiral ligands to enantioselectively recognise chiral salts [37] or the ability of their transition-metal complexes to catalyse enantioselective syntheses [38,39], which are objects of current investigations.

Conclusion

The coupling of low-generation dendrons, based on the chiral C_2-symmetric dihydroxypyrrolidine **1**, with a calix[4]arene scaffold allowed the construction of novel supramolecular architectures, i.e., iminosugar-analogue-based calixarene dendrimers. The convergent synthetic approach used permits the rapid increase of the valency of the iminosugar presentation. Complexation studies with sodium or potassium picrate, carried out on the calixarene-dendrimer **2**, indicated an effective binding of the metal cation at the calixarene lower rim that induces a rigidification of the macrocyclic scaffold and, as a consequence, the convergence of the iminosugars into a restricted region of space. These chiral multivalent dendrimers could thus be interestingly engaged in enantioselective recognition and catalysis. Up to now, pyrrolidine **1** has been used both as a dendrimeric building block and iminosugar model; its substitution at the hydroxy groups with more complex and biologically active iminosugars, such as polyhydroxylated pyrrolidines, would also allow the investigation of the corresponding calixarene dendrimers in interactions with enzymatic receptors.

Supporting Information

Supporting Information File 1

Experimental procedures; spectroscopic and analytical data.
[http://www.beilstein-journals.org/bjoc/content/supplementary/1860-5397-8-107-S1.pdf]

Acknowledgements

Cassa di Risparmio di Firenze is acknowledged for granting a 400 MHz spectrometer. Maurizio Passaponti and Brunella Innocenti (Università degli Studi di Firenze) are acknowledged for technical assistance. MM thanks the Networking Research Center on Bioengineering, Biomaterials and Nanomedicine (CIBER-BBN). AC and MM acknowledge COST action CM1102. AC and FS also acknowledge PRIN200858SA98 for partial support.

References

1. Asano, N.; Nash, R. J.; Molyneux, R. J.; Fleet, G. W. J. *Tetrahedron: Asymmetry* **2000,** *11,* 1645–1680. doi:10.1016/S0957-4166(00)00113-0
2. Elbein, A. D. *Annu. Rev. Biochem.* **1987,** *56,* 497–523. doi:10.1146/annurev.bi.56.070187.002433
3. Compain, P.; Martin, O. R. *Iminosugars: From Synthesis to Therapeutic Applications;* John Wiley & Sons, Ltd: Chichester, U. K., 2007.
4. Johns, B. A.; Johnson, C. R. *Tetrahedron Lett.* **1998,** *39,* 749–752. doi:10.1016/S0040-4039(97)10616-5
5. Lohse, A.; Jensen, K. B.; Lundgren, K.; Bols, M. *Bioorg. Med. Chem.* **1999,** *7,* 1965–1971. doi:10.1016/S0968-0896(99)00116-9
6. Wennekes, T.; van den Berg, R. J. B. H. N.; Bonger, K. M.; Donker-Koopman, W. E.; Ghisaidoobe, A.; van der Marel, G. A.; Strijland, A.; Aerts, J. M. F. G.; Overkleeft, H. S. *Tetrahedron: Asymmetry* **2009,** *20,* 836–846. doi:10.1016/j.tetasy.2009.02.043
7. Diot, J.; García-Moreno, M. I.; Gouin, S. G.; Ortiz Mellet, C.; Haupt, K.; Kovensky, J. *Org. Biomol. Chem.* **2009,** *7,* 357–363. doi:10.1039/b815408b
8. Compain, P.; Decroocq, C.; Iehl, J.; Holler, M.; Hazelard, D.; Mena Barragán, T.; Ortiz Mellet, C.; Nierengarten, J.-F. *Angew. Chem., Int. Ed.* **2010,** *49,* 5753–5756. doi:10.1002/anie.201002802
9. Decroocq, C.; Rodríguez-Lucena, D.; Russo, V.; Mena Barragán, T.; Ortiz Mellet, C.; Compain, P. *Chem.–Eur. J.* **2011,** *17,* 13825–13831. doi:10.1002/chem.201102266

10. Kiessling, L. L.; Gestwicki, J. E.; Strong, L. E. *Angew. Chem., Int. Ed.* **2006,** *45,* 2348–2368. doi:10.1002/anie.200502794
11. Gutsche, C. D. *Calixarenes: An Introduction;* Royal Society of Chemistry: Cambridge, U. K., 2008.
12. Ungaro, R.; Arduini, A.; Casnati, A.; Pochini, A.; Ugozzoli, F. *Pure Appl. Chem.* **1996,** *68,* 1213–1218. doi:10.1351/pac199668061213
13. Casnati, A.; Sansone, F.; Ungaro, R. Calixarene Receptors in Ion Recognition and Sensing. In *Advances in Supramolecular Chemistry;* Gokel, G. W., Ed.; Cerberus Press Inc.: Miami, FL, U. S. A., 2003; Vol. 9, pp 165–218.
14. Sansone, F.; Baldini, L.; Casnati, A.; Ungaro, R. *New J. Chem.* **2010,** *34,* 2715–2728. doi:10.1039/c0nj00285b
15. Marra, A.; Scherrmann, M.-C.; Dondoni, A.; Ungaro, R.; Casnati, A.; Minari, P. *Angew. Chem., Int. Ed. Engl.* **1995,** *33,* 2479–2481. doi:10.1002/anie.199424791
16. Dondoni, A.; Marra, A. *Chem. Rev.* **2010,** *110,* 4949–4977. doi:10.1021/cr100027b
17. Sansone, F.; Rispoli, G.; Casnati, A.; Ungaro, R. Multivalent Glycocalixarenes. In *Synthesis and Biological Applications of Glycoconjugates;* Renaudet, O.; Spinelli, N., Eds.; Bentham Science Publishers: eBook, 2011; pp 36–63. doi:10.2174/978160805277611101010036
18. Lee, Y. C.; Lee, R. T. *Acc. Chem. Res.* **1995,** *28,* 321–327. doi:10.1021/ar00056a001
19. Kiessling, L. L.; Pohl, N. L. *Chem. Biol.* **1996,** *3,* 71–77. doi:10.1016/S1074-5521(96)90280-X
20. Lundquist, J. J.; Toone, E. J. *Chem. Rev.* **2002,** *102,* 555–578. doi:10.1021/cr000418f
21. André, S.; Sansone, F.; Kaltner, H.; Casnati, A.; Kopitz, J.; Gabius, H.-J.; Ungaro, R. *ChemBioChem* **2008,** *9,* 1649–1661. doi:10.1002/cbic.200800035
22. André, S.; Grandjean, C.; Gautier, F.-M.; Bernardi, S.; Sansone, F.; Gabius, H.-J.; Ungaro, R. *Chem. Commun.* **2011,** *47,* 6126–6128. doi:10.1039/c1cc11163a
23. Cecioni, S.; Lalor, R.; Blanchard, B.; Praly, J.-P.; Imberty, A.; Matthews, S. E.; Vidal, S. *Chem.–Eur. J.* **2009,** *15,* 13232–13240. doi:10.1002/chem.200901799
24. Chabre, Y. M.; Roy, R. *Adv. Carbohydr. Chem. Biochem.* **2010,** *63,* 165–393. doi:10.1016/S0065-2318(10)63006-5
25. Turnbull, W. B.; Stoddart, J. F. *Rev. Mol. Biotechnol.* **2002,** *90,* 231–255. doi:10.1016/S1389-0352(01)00062-9
26. Röckendorf, N.; Lindhorst, T. K. Glycodendrimers. In *Dendrimers IV. Metal Coordination, Self Assembly, Catalysis;* Vögtle, F.; Schalley, C. A., Eds.; Topics in Current Chemistry, Vol. 217; Springer: Berlin, 2001; pp 201–238.
27. Roy, R.; Kim, J. M. *Angew. Chem., Int. Ed.* **1999,** *38,* 369–372. doi:10.1002/(SICI)1521-3773(19990201)38:3<369::AID-ANIE369>3.0.CO;2-1
28. Nagel, U.; Kinzel, E.; Andrade, J.; Prescher, G. *Chem. Ber.* **1986,** *119,* 3326–3342. doi:10.1002/cber.19861191112
29. Cicchi, S.; Goti, A.; Rosini, C.; Brandi, A. *Eur. J. Org. Chem.* **1998,** 2591–2597. doi:10.1002/(SICI)1099-0690(199811)1998:11<2591::AID-EJOC2591>3.0.CO;2-Q
30. Baklouti, L.; Cheriaa, N.; Mahouachi, M.; Abidi, R.; Kom, J. S.; Kim, Y.; Vicens, J. *J. Inclusion Phenom. Macrocyclic Chem.* **2006,** *54,* 1–7. doi:10.1007/s10847-005-6994-4
31. Arakawa, Y.; Yoshifuji, S. *Chem. Pharm. Bull.* **1991,** *39,* 2219–2224. doi:10.1248/cpb.39.2219
32. Arduini, A.; Ghidini, E.; Pochini, A.; Ungaro, R.; Andreetti, G. D.; Calestani, G.; Ugozzoli, F. *J. Inclusion Phenom. Mol. Recognit. Chem.* **1988,** *6,* 119–134. doi:10.1007/BF00663045
33. Arnaud-Neu, F.; Barboso, S.; Berny, F.; Casnati, A.; Muzet, N.; Pinalli, A.; Ungaro, R.; Schwing-Weill, M.-J.; Wipff, G. *J. Chem. Soc., Perkin Trans. 2* **1999,** 1727–1738. doi:10.1039/a902001b
34. Arduini, A.; Fabbi, M.; Mantovani, M.; Mirone, L.; Pochini, A.; Secchi, A.; Ungaro, R. *J. Org. Chem.* **1995,** *60,* 1454–1457. doi:10.1021/jo00110a055
35. Arduini, A.; Pochini, A.; Reverberi, S.; Ungaro, R. *Tetrahedron* **1986,** *42,* 2089–2100. doi:10.1016/S0040-4020(01)87626-2
36. Casnati, A.; Cavallo, G.; Metrangolo, P.; Resnati, G.; Ugozzoli, F.; Ungaro, R. *Chem.–Eur. J.* **2009,** *15,* 7903–7912. doi:10.1002/chem.200900771
37. Yakovenko, A. V.; Boyko, V. I.; Kalchenko, V. I.; Baldini, L.; Casnati, A.; Sansone, F.; Ungaro, R. *J. Org. Chem.* **2007,** *72,* 3223–3231. doi:10.1021/jo062410x
38. Casolari, S.; Cozzi, P. G.; Oriolo, P.; Tagliavini, E.; Umani-Ronchi, A. *J. Chem. Soc., Chem. Commun.* **1997,** 2123–2124. doi:10.1039/a705045c
39. Pinkhassik, E.; Stibor, I.; Casnati, A.; Ungaro, R. *J. Org. Chem.* **1997,** *62,* 8654–8659. doi:10.1021/jo9706990

License and Terms

Beilstein Journal of Organic Chemistry

Synthesis and structure of tricarbonyl(η^6-arene)chromium complexes of phenyl and benzyl D-glycopyranosides

Thomas Ziegler* and Ulrich Heber

Full Research Paper

Open Access

Address:
Institute of Organic Chemistry, University of Tuebingen, Auf der Morgenstelle 18, 72076 Tuebingen, Germany

Email:
Thomas Ziegler* - thomas.ziegler@uni-tuebingen.de

* Corresponding author

Keywords:
aryl glycosides; carbohydrates; transition-metal complex; tricarbonyl(arene)chromium

Beilstein J. Org. Chem. **2012,** *8,* 1059–1070.
doi:10.3762/bjoc.8.118

Received: 14 March 2012
Accepted: 19 June 2012
Published: 11 July 2012

This article is part of the Thematic Series "Synthesis in the glycosciences II".

Guest Editor: T. K. Lindhorst

Abstract

A series of 15 glycoside-derived tricarbonyl(η^6-arene)chromium complexes were prepared in 19–87% yield by heating fully acetylated or methylated aryl O-, S-, N- and C-glycosides of D-glucopyranose and D-mannopyranose with hexacarbonylchromium. All tricarbonylchromium complexes were fully characterized. The structures of nine crystalline complexes were determined by X-ray diffraction, revealing unusual intra- and intermolecular nonclassical hydrogen bonds.

Introduction

In 1957, Fischer and Öfele published the preparation of tricarbonyl(η^6-benzene)chromium, which was the first arene tricarbonylchromium complex [1]. Since then, a plethora of transition-metal complexes of arenes have been prepared, characterized and described in the literature. Among the multitude of transition-metal complexes of aromatic compounds, however, only tricarbonyl(η^6-arene)chromium compounds are widely used for organic syntheses [2-4]. This is due to the fact that tricarbonyl(η^6-arene)chromium complexes are relatively stable compounds, which can be easily prepared and also easily reconverted into the parent arenes. Furthermore, the tricarbonylchromium group is an electron-withdrawing substituent increasing the acidity of the aromatic protons and the electrophilicity of the aromatic ring and, thus, making the arene more susceptible towards S_NAr reactions. Likewise, the benzylic and homo-benzylic positions in tricarbonyl(η^6-arene)chromium complexes are more acidic and more prone to solvolysis, nucleophilic substitution and deprotonation than in the parent arenes due to the fact that the tricarbonylchromium ligand stabilizes both benzylic and homo-benzylic carbenium ions and carbanions [5,6]. Asymmetric ortho- or meta-substituted tricarbonyl(η^6-arene)chromium compounds display planar chirality, which, in turn, makes these chiral complexes attractive catalysts for enantioselective reactions [6-8].

Despite the broad applications that tricarbonyl(η^6-arene)chromium complexes have found in organic synthesis since their discovery in 1957, only a very few tricarbonylchromium complexes of sugar derivatives are known today. Figure 1 shows the types of such carbohydrate-derived chromium complexes that have been described in the literature so far. Complexes of type **A** and **B** were obtained from the corresponding glycopyranosides and were studied as substrates for chiral-auxiliary-directed asymmetric ortholithiation and as catalysts for enantioselective Diels–Alder reactions [9-12]. Tricarbonylchromium complexes of type **C** and **D** were obtained via benzannulation of glucal-derived pentacarbonylchromium carbenes or by reaction of alkynyl C-glycosides with pentacarbonylchromium carbenes [13].

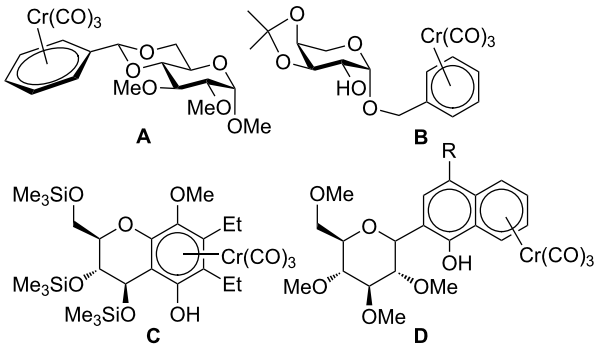

Figure 1: Known types of η^6-tricarbonylchromium complexes of sugar derivatives [9-13].

Further syntheses and characterizations of more examples of carbohydrate-derived tricarbonyl(η^6-arene)chromium complexes are highly desirable in order to allow studies of the rich chemistry of such complexes in greater detail. In this paper we describe the synthesis and structural elucidation of a series of tricarbonyl-(η^6-arene)chromium complexes of some simple phenyl and benzyl O-, N-, S- and C-glycosides.

Results and Discussion

Preparation of η^6-tricarbonylchromium complexes of glycosides

In general, tricarbonyl(η^6-arene)chromium compounds can be prepared in a wide variety of methods [4]. However, the following two methods are the most commonly employed ones: (a) ligand-exchange reaction between an arene and, most conveniently, either naphthalene–$Cr(CO)_3$ complex or $(MeCN)_3Cr(CO)_3$ in which the chromium ligand is only weakly bound [14]; (b) simply heating the arene with hexacarbonylchromium in an inert solvent (Mahaffy–Pauson method) [15,16]. Method (a) has the disadvantage that the applied chromium complexes for the ligand exchange reaction are extremely sensitive toward oxidation, due to the weakly bound chromium. For method (b) high-boiling-point solvents, such as di-*n*-butylether, decalin or dioxane, can be used. The addition of THF to these solvents was shown to prevent the excessive sublimation of $Cr(CO)_6$ during the formation of the arene–chromium complexes [17]. Therefore, we used method (b) for the preparation of tricarbonyl(η^6-arene)chromium complexes of glycosides as follows.

One equivalent of phenyl or benzyl glycoside **1** and one equivalent of $Cr(CO)_6$ were dissolved in di-*n*-butylether containing 10% THF, and the solution was stirred at 140 °C under argon and under the exclusion of light (brown glassware). After the reaction of **1** with $Cr(CO)_6$ was complete (16–96 h), the solvent was evaporated and the crude complexes **2** were purified by chromatography under argon on silica gel with *n*-hexane/ethyl acetate mixtures as eluent. Crystalline chromium complexes **2** were recrystallized from ethanol, and for suitable crystals X-ray structures were determined. Table 1 summarizes the results for the preparation of the complexes **2** from simple acetylated and methylated phenyl, benzyl and 1-*O*-benzoyl glycosides **1**. All glycosides **1a**–**k** were prepared according to literature procedures (for details see the Supporting Information File 1).

All reactions of glycosides **1a**–**k** with $Cr(CO)_6$ proceeded smoothly and gave the corresponding tricarbonyl(η^6-arene)chromium complexes **2a**–**k** in medium yield. The somewhat lower yields in some cases are due to oxidative decomposition of the products during purification by column chromatography on silica gel.

The reaction times also varied significantly between 16 and 96 h. This was due to the purity of the hexacarbonyl chromium charges we purchased from several companies. In general, however, electron-donating protecting groups in the sugar moiety accelerated the formation of the chromium complexes at the aglycon (Table 1, entries 3 and 4). Treatment of the mannose orthoester **1f** (Table 1, entry 6) under the standard conditions applied here resulted in the exclusive formation of tricarbonyl[(2,3,4,6-tetra-*O*-acetyl-α-D-mannopyranosyloxy)-η^6-benzene]chromium (**2f**) in 47% yield. In the glucose series it is well known that orthoesters similar to **1f** rearrange to the corresponding glycosides upon heating [18]. Therefore, it is very likely that **1f** isomerized to the corresponding phenyl 2,3,4,6-tetra-*O*-acetyl-α-D-mannopyranoside, which was then converted into complex **2f**. The direct complexation of orthoester **1f** is unlikely because no such chromium complex was detected. The anomeric α-configuration of **2f** was proven by decomplexation of an analytical sample with iodine in $CHCl_3$ followed by measurement of the NMR spectrum of the formed glycoside. The latter showed a CH-coupling constant at the anomeric center of 173.9 Hz, which is indicative of an

Table 1: Synthesis of η^6-tricarbonylchromium complexes **2a–k** from glycosides **1a–k** and $Cr(CO)_6$ in di-*n*-butylether/THF 9:1 at 140 °C under Ar and exclusion of light.

Entry	Glycoside **1**	Time	Complex **2**	Yield
1	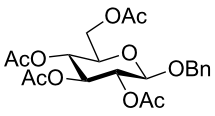 **1a**	96 h	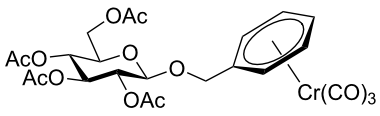 **2a**	29%
2	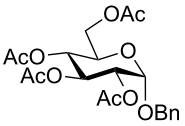 **1b**	90 h	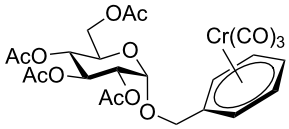 **2b**	87%
3	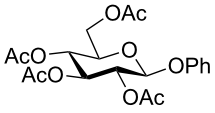 **1c**	80 h	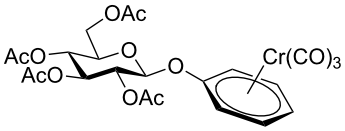 **2c**	29%
4	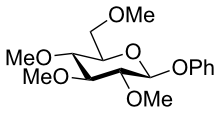 **1d**	16 h	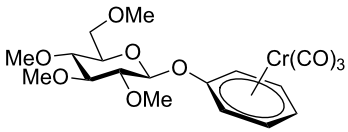 **2d**	19%
5	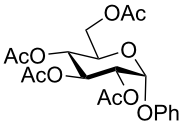 **1e**	70 h	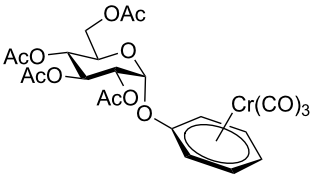 **2e**	53%
6	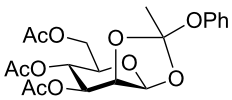 **1f**	42 h	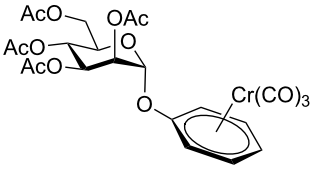 **2f**	47%
7	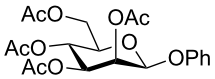 **1g**	42 h	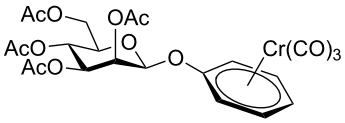 **2g**	35%
8	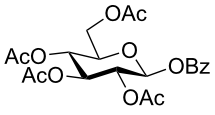 **1h**	67 h	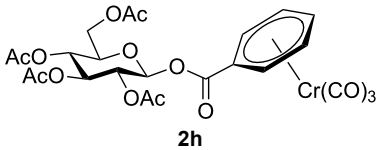 **2h**	30%
9[a]	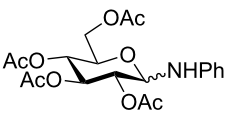 **1i**	24 h	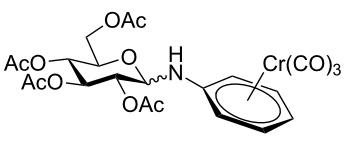 **2i**	46%

Table 1: Synthesis of η^6-tricarbonylchromium complexes **2a–k** from glycosides **1a–k** and $Cr(CO)_6$ in di-*n*-butylether/THF 9:1 at 140 °C under Ar and exclusion of light. (continued)

10	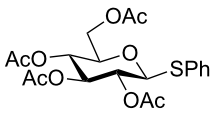 **1j**	24 h	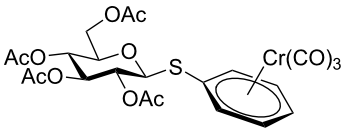 **2j**	49%
11	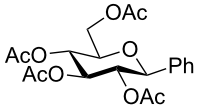 **1k**	80 h	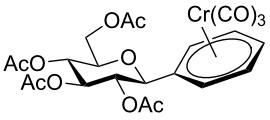 **2k**	81%

[a]Anomeric mixture α:β = 1:2.

α-anomer [19]. As additional proof for the anomeric configuration of **2f**, we also prepared β-anomer **2g** (Table 1, entry 7). For the preparation of chromium complex **2i** we used a 1:2 anomeric mixture of aminoglucoside **1i**, which did not change during the complexation (Table 1, entry 9).

For the anticipated synthesis of a glucose-derived tricarbonyl(η^6-pyridine)chromium complex we prepared glycoside **1l** by reacting acetobromoglucose with 6-*tert*-butyl-2-hydroxypyridine [20] under Helferich conditions ($Hg(CN)_2$). Only the corresponding *O*-glycoside **1l** was obtained, and no *N*-glycoside was formed in this Helferich glycosylation (Scheme 1). Sterically hindered 6-*tert*-butyl-2-hydroxypyridine was chosen as the aglycon in order to avoid complexation of hexacarbonylchromium with the basic nitrogen atom. However, all attempts to convert **1l** into the corresponding tricarbonyl(η^6-pyridine)chromium complex failed. Attempts to prepare a chromium complex of **1l** by a ligand exchange reaction with naphthalene–$Cr(CO)_3$ or $(MeCN)_3Cr(CO)_3$ were also unsuccessful (no further experimental details shown).

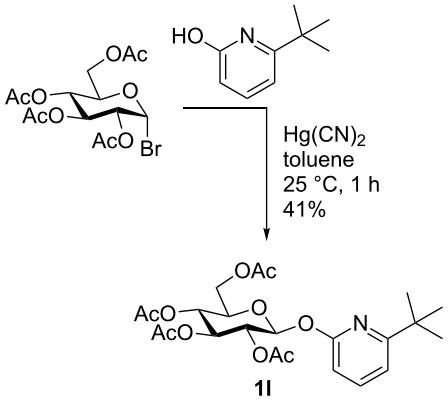

Scheme 1: Synthesis of glucoside **1l**.

Next, we also prepared some sugar-derived tricarbonylchromium complexes of glycosides having a prochiral aglycon, i.e., an ortho-substituted phenyl or benzyl aglycon. Glycosides **1m** [21] and **1q** [22] were prepared according to the respective literature procedures. Glycosides **1n**–**p** were not known in the literature and were prepared as follows: *o*-Tolyl 2,3,4-6-tetra-*O*-acetyl-β-D-glucopyranoside (**1m**) was first deacetylated (cat. NaOMe in MeOH) followed by treatment with pivaloyl chloride in pyridine to give **1n** in 86% yield. Treatment of pentaacetylglucose and 2-*tert*-butylphenol with BF_3-etherate in dichloromethane afforded **1o** in 31% yield. Glycoside **1p** was prepared by a Helferich glycosylation of *o*-methylbenzyl alcohol with acetobromoglucose. For further details see Supporting Information File 1. Table 2 summarizes the results of the complexation of glucosides **1m**–**q** affording the diastereomeric tricarbonyl(η^6-arene)chromium complexes **2m**–**q**.

Treatment of *o*-tolyl glucoside **1m** with hexacarbonylchromium under the standard conditions for 70 h afforded a 7:3 mixture of the diastereomeric tricarbonylchromium complexes **2m** in 76% overall yield (Table 2, entry 1). Upon slow crystallization of the diastereomeric mixture from ethanol, isomer ***pR*-2m** could be obtained in pure form. From the mother liquor a small amount of pure isomer ***pS*-2m** could be isolated upon repeated recrystallization as well. The absolute configuration of the planar chiral tricarbonyl(η^6-*o*-tolyl)chromium aglycon in both diastereomers **2m** could be unambiguously assigned by X-ray crystallography. Since the two diastereomers **2m** were not formed in equal amounts during complexation of glucoside **1m**, we contemplated that an even higher diastereoselectivity should be obtained when sterically more demanding aglycons or sugar moieties are present during reaction with $Cr(CO)_6$. Therefore, we also reacted glucosides **1n** and **1o** bearing either bulky pivaloyl groups or a *tert*-butyl group in the aglycon in the sugar moiety with $Cr(CO)_6$. However, no complexation could be

Table 2: Synthesis of tricarbonylchromium complexes **2m–q** from glycosides **1m–q** containing a prochiral aglycon and $Cr(CO)_6$ in di-*n*-butylether/THF 9:1 at 140 °C under Ar in the dark.

Entry	Glycoside **1**	Time	Complex **2**	Yield	Ratio[a]
1	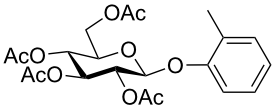 **1m**	70 h	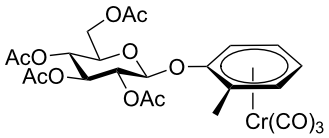 ***pR*-2m** 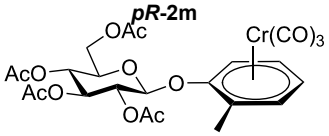 ***pS*-2m**	76%	***pR*-2m**:***pS*-2m** = 7:3[b]
2	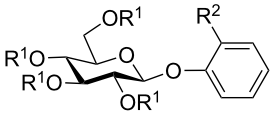 **1n** R^1 = Piv, R^2 = Me **1o** R^1 = Ac, R^2 = $C(CH_3)_3$		no product	–	–
3	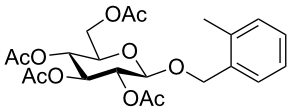 **1p**	15 h	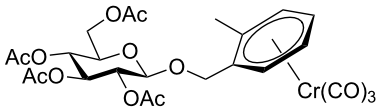 **2p**	42%	***pR*-2p**:***pS*-2p** = 1:1[c]
4	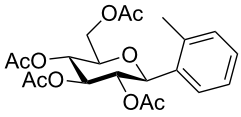 **1q**	16 h	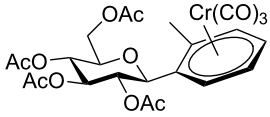 **2q**	42%	***pR*-2q**:***pS*-2q** = 1:1[c]

[a]Determined by ^1H NMR; [b]diastereomers can be separated by crystallization; [c]no separation possible.

detected even under prolonged reaction time (Table 2, entry 2). Placing the *o*-tolyl group in a position more distant from the sugar part, as in glucoside **1p** (Table 2, entry 3), or using *o*-tolyl C-glucoside **1q** (Table 2, entry 4) gave 1:1 mixtures of the corresponding diastereomers **2p** and **2q**, respectively. A separation of the diastereomers by crystallization was not possible for complexes **2p** and **2q**.

The *O*-acetylated carbohydrate-derived tricarbonyl(η^6-arene)chromium complexes prepared here can be deprotected without affecting the chromium complex, as exemplified in Scheme 2. Zemplén deacetylation of **2c** afforded tricarbonyl(β-D-glucopyranosyloxy-η^6-benzene)chromium (**3**) in quantitative yield. Glucoside **3** is a good substrate for β-glucosidases, such as almond glucosidase E.C. 3.2.1.21, and is converted into D-glucose and tricarbonyl(η^6-phenol)chromium in 98% yield.

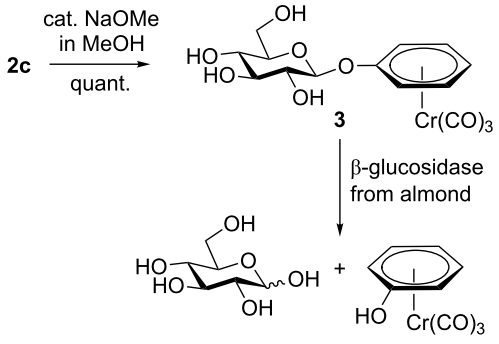

Scheme 2: Deprotection of **2c** and enzymatic cleavage of **3**.

Structures of tricarbonyl(η^6-arene)chromium complexes of glycosides

In general, complexation of glycosides **1** with $Cr(CO)_6$ to give the corresponding tricarbonyl(η^6-arene)chromium compounds **2** does not significantly affect the conformation of the sugar moieties. This is evident from the ^1H NMR spectra of compounds **2**, which show no significant change of chemical shifts and coupling constants of the carbohydrate protons compared to those of the educts **1**. As an example, Table 3 shows the chemical shifts of the protons of compounds **1a** and **2a**. All NMR signals of the sugar protons remain practically unchanged,

Table 3: Chemical shifts (δ in ppm) of the protons of compounds **1a** and **2a** derived from the ^{1}H NMR spectra of the compounds measured in acetone-d_6.

	H1	H2	H3	H4	H5	H6a	H6b	OCH_2	H_{Ar}
1a	4.83 d	4.98 t	5.25 t	5.05 t	3.97 m	4.29 dd	4.15 dd	4.87 d 4.67 d	7.28–7.34 m
2a	4.98 d	4.98 t	5.28 t	5.06 t	4.01 m	4.27 dd	4.16 dd	4.68 d 4.45 d	5.56–5.72 m

whereas the protons of the benzylic methylene group and the benzene moiety appear, as was expected, at higher fields in **2a**. Therefore, it can be concluded that the sugar rings remain in the $^4C_1$ conformation. The high-field shifts of the benzylic methylene group and the aromatic moiety are in accordance with other tricarbonyl(η^6-arene)chromium complexes. This is further confirmed by the X-ray structures obtained from crystalline chromium complexes.

For the tricarbonylchromium complexes **2a**–**e**,**j**,**k**,**m** which gave suitable crystals, structures were determined by X-ray diffraction [23]. Crystals were grown for all compounds by slow crystallization of the compounds from ethanol. The conformation of the $Cr(CO)_3$ group in relation to the aromatic ring shows some deviations compared to other tricarbonyl(η^6-arene)chromium complexes. In complexes where the benzene ring carries an electron-donating substituent, the $Cr(CO)_3$ group is preferably in an eclipsed orientation, whereas in cases where the benzene carries an electron-withdrawing substituent, a staggered conformation is commonly found [24]. Here, eclipsed conformations of the $Cr(CO)_3$ group were found in compounds **2c** and **2e**, which both carry an electron-donating glycosyloxy substituent. However, compound **2k**, which carries an electron-withdrawing substituent also shows an eclipsed conformation of the $Cr(CO)_3$ group. Likewise, all compounds **2a**, **2b**, **2d**, **2j** and **2m** show a staggered conformation of the $Cr(CO)_3$ group, although they all carry an electron-donating substituent at the benzene ring. All complexes show unusual intra- and intermolecular nonclassical hydrogen bonds [25], which will be discussed in more details for each individual X-ray structure in the following. For technical details of the X-ray structures see Supporting Information File 1.

Figure 2 shows the asymmetric unit of compound **2a**, which contains two slightly differently distorted molecules. Table 4 summarizes some selected atomic distances and angles of the two molecules in the asymmetric unit (**2aa** refers to the right molecule and **2ab** to the left one in Figure 2). Most significantly, the biggest differences are found around the benzylic methylene groups (C7 and C37, respectively). Another significant feature of **2a** that was not observed in any other complex **2** is the parallel face-to-face orientation of the two benzene rings. However, the distance of the two ring planes of 3.627 Å and the angle of 16° between the ring planes indicate no π-interaction of the two benzene rings.

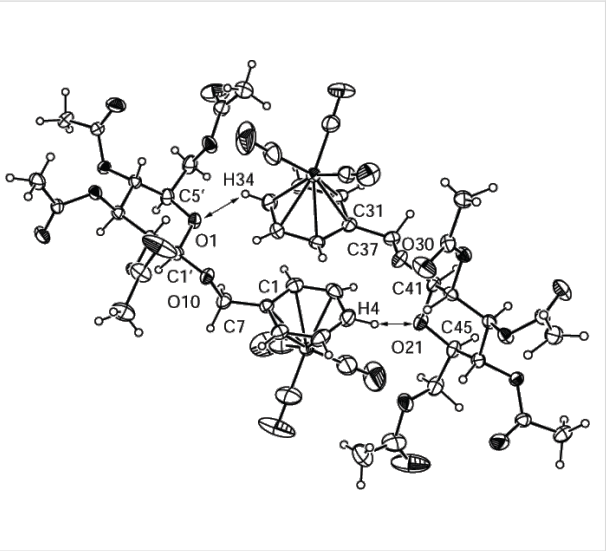

Figure 2: ORTEP-plot of the asymmetric unit containing two molecules of compound **2a** showing 30% probability ellipsoids; the arrows show the nonclassical H-bonds between O1 and H34 and O21 and H4.

Table 4: Selected corresponding distances and angles of **2aa** and **2ab**.

2aa		**2ab**	
C1'–O10	1.375 Å	C41–O30	1.378 Å
O10–C7	1.427 Å	O30–C37	1.407 Å
C7–C1	1.491 Å	C37–C31	1.477 Å
C1'–O10–C7	112.8°	C41–O30–C37	113.2°
C1–C7–O10	108.4°	C31–C37–O30	112.6°
C1'–O10–C7–C1	147.8°	C41–O30–C37–C31	157.9°

The most significant features in the crystal structure of **2a** are the two intermolecular nonclassical hydrogen bonds between O1 and H34 and O21 and H4 (Figure 2). That these hydrogen bonds are indeed true bonds is evident from the distances of 2.659 Å for O1/H34 and 2.680 Å for O21/H4 and the angles 101.9° for C1'–O1–H34, 123.7° for C5'–O1–H34, 122.8° for C41–O21–H4 and 105.6° for C41–O21–H4. These distances and angles allow protons H4 and H34 to interact with the lone pairs of the oxygen atoms O1 and O21 of the sugar rings [26]. Most likely, the two nonclassical hydrogen bonds in **2a** are the reasons why two molecules crystallize as slightly different pairs; a feature not observed in the other complexes.

Figure 3 shows the structure of compound **2b**, which is the anomer of **2a**. Once again a nonclassical hydrogen bond is responsible for the interaction of the molecules. Contrary to **2a**, in which a nonclassical H-bond was found between the oxygen of a sugar ring and the hydrogen of a benzene ring, the H-bond forms in **2b** between the oxygen of a carbonyl group (O13) and the hydrogen of an acetyl group (H26B). However, the length of this H-bond (2.212 Å) and the angles (161.6° for C≡O···H and 159.8° for C–H···O) prove the presence of the H-bond.

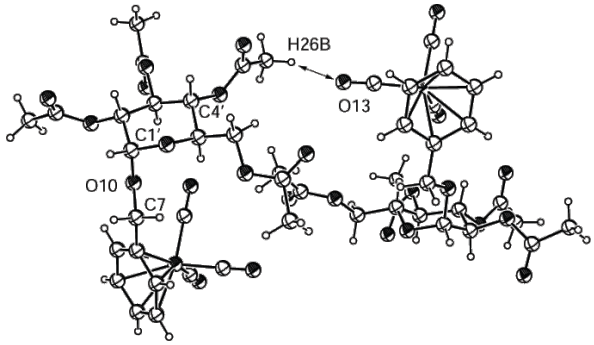

Figure 3: ORTEP-plot of the asymmetric unit showing two molecules of compound **2b** and 30% probability ellipsoids; the arrows show the nonclassical H-bonds between O13 and H26B.

Figure 4 shows the structure of compound **2c**. Once again the most significant feature is a nonclassical intermolecular hydrogen bond between the oxygen of a carbonyl group (O12) and the hydrogen (H6'A) at C6 of the neighboring molecule. Distance (2.628 Å) and C≡O···H and C–H···O angles (123 and 101.5°) are indicative of the H-bond. Compound **2c** also shows that complexation of an aromatic aglycon with tricarbonylchromium does not have any significant influence on the sugar ring. In Table 5, the distances and angles at the anomeric center of **2c** are compared to those for phenyl β-D-glucopyranoside (Ph-Glc) [27] showing that only the anomeric bond is slightly shortened upon complexation.

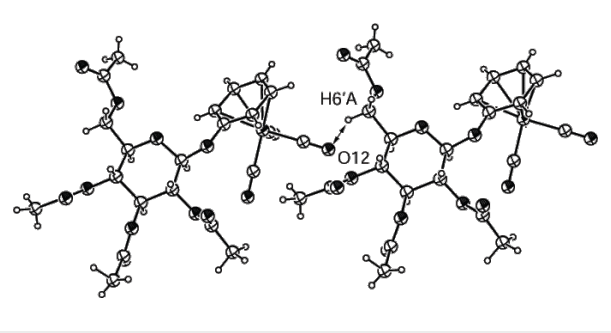

Figure 4: ORTEP-plot of the asymmetrical unit showing two molecules of compound **2c** and 30% probability ellipsoids; the arrows show the nonclassical H-bonds between O12 and H6'A.

Figure 5 shows the structure of compound **2d**, which contains a hydrogen bond between carbonyl oxygen O13 of the left molecule and hydrogen H5 of the benzene ring of the right molecule. The length of this hydrogen bond is 2.498 Å and the angles C≡O···H and C–H···O are 166.2 and 158.3°, respectively. All atomic distances and angles of the tricarbonyl(η^6-benzene)chromium aglycon are almost identical to those of the acetylated counterpart **2c**. However, in **2d**, the carbonyl groups are in a staggered conformation (like in compound **2a**) whereas in **2c** the carbonyl ligands adopt an eclipsed conformation.

Table 5: Comparison of selected distances and angles in **2c** with phenyl β-D-glucopyranoside.

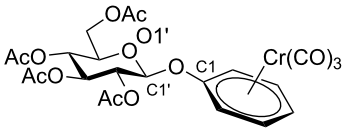

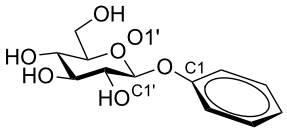

Bond	**2c**	phenyl β-D-glucopyranoside
C1'–O1	1.417 Å	1.394 Å
O1'–C1'	1.418 Å	1.434 Å
O1–C1	1.360 Å	1.388 Å
C1'–O1–C1	119.1°	118.0°
O1'–C1'–O1	106.7°	107.4°

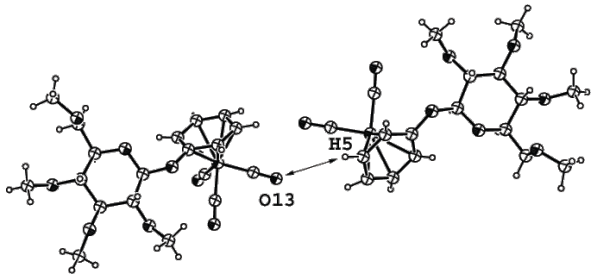

Figure 5: ORTEP-plot of the asymmetric unit showing two molecules of compound **2d** and 30% probability ellipsoids; the arrows show the nonclassical H-bonds between O13 and H5.

All bond distances and angles for both the carbohydrate moiety and the tricarbonyl(η^6-benzene)chromium aglycon in compound **2e** (Figure 6) are within the values found for all of the other complexes. The carbonyl groups adopt an eclipsed conformation like in **2c**. In the crystal, two complexed benzene rings face each other and are aligned parallel, with the tricarbonylchromium groups facing in opposite directions. One carbonyl group of each molecule is placed in between the benzene rings and, thus, allows for the formation of a "network" of three nonclassical H-bonds in the crystal. The lengths and angles of these three hydrogen bonds in **2e** are within the typical range for nonclassical H-bonds [28-31] (Table 6).

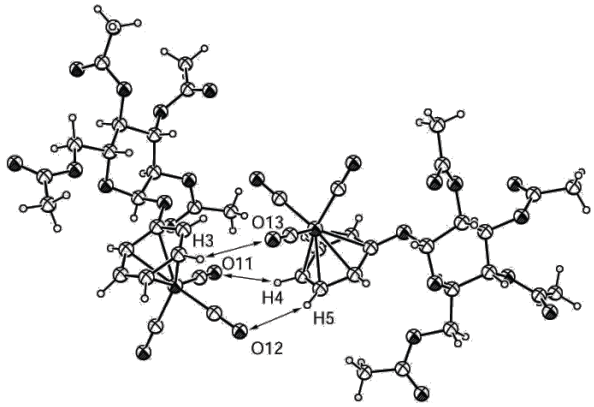

Figure 6: ORTEP-plot of the asymmetrical unit showing two molecules of compound **2e** and 30% probability ellipsoids; the arrows show the nonclassical H-bonds between O13 and H3, O11 and H4 and O12 and H5.

Figure 7 shows the crystal structure of the *S*-glycoside **2j** in which the molecules are stacked with all benzene rings in an almost symmetric parallel orientation on one side. However, an interaction of the tricarbonyl(η^6-benzene)chromium rings can be excluded because the distance between the benzene rings is, with >3.37 Å, too long for such interactions, which only occur at shorter distances [32-34]. A nonclassical hydrogen bond is found between O13 of a carbonyl group and H22a of the acetyl group at O6 of the sugar moiety. The bond lengths and angles of this H-bond are in the expected range (2.709 Å for O···H, 138.2° for angle C–H···O and 93.5° for angle C≡O···H).

Table 6: Bond lengths and angles for the nonclassical H-bonds in **2e**.

H-bond	Length C≡O···H	Angle C–H···O	Angle C≡O···H
O11–H4	2.594 Å	154.4°	94.5°
O12–H5	2.668 Å	142.5°	118.9°
O13–H3	2.656 Å	133.4°	125.6°

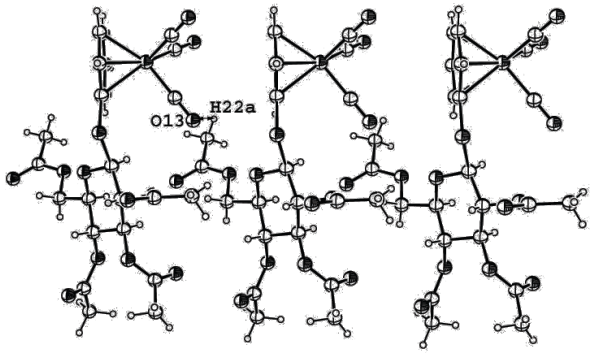

Figure 7: ORTEP-plot of the asymmetric unit showing three molecules of compound **2j** and 30% probability ellipsoids; the arrows show the nonclassical H-bonds between O13 and H22a.

The structure of the C-glycoside **2k** (Figure 8) also shows a "network" or nonclassical hydrogen bond in the crystal. The molecules group similarly to compound **2e**; however, the benzene rings between two molecules (Figure 8, molecules on the right side) are not oriented in parallel. Four nonclassical hydrogen bonds form between the oxygen atoms of three carbonyl groups (O12 and O13) and the hydrogen atoms of two methyl groups (H2' and H22a), one methylene group (H1') and one aromatic hydrogen (H6). Table 7 summarizes the bond lengths and angles of these nonclassical H-bonds.

Table 7: Bond lengths and angles for the nonclassical H-bonds in **2k**.

H-bond	Length C≡O···H	Angle C–H···O	Angle C≡O···H
O11–H6	2.714 Å	129.5°	126.3°
O13–H22a	2.719 Å	127.1°	118.9°
O13–H1'	2.720 Å	150.5°	118.4°
O12–H2'	2.632 Å	164.2°	130.3°

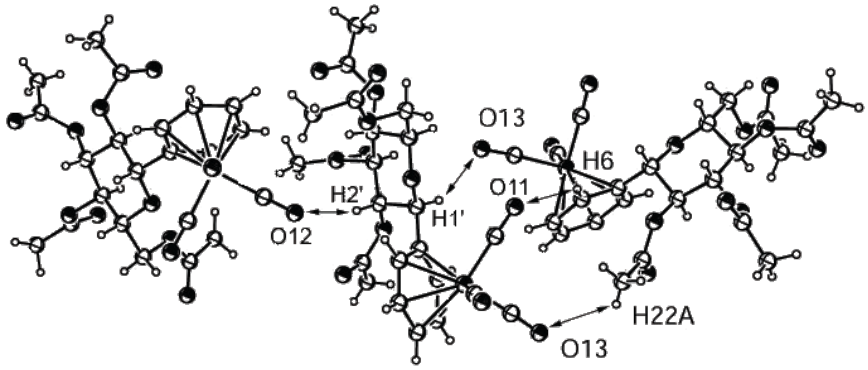

Figure 8: ORTEP-plot of the asymmetric unit showing three molecules of compound **2k** and 30% probability ellipsoids; the arrows show the nonclassical H-bonds between O12 and H2', O13 and H1', O11 and H6 and O13 and H22A.

Figure 9 and Figure 10 show the crystal structures of the two diastereomers **2m**. The isomer with (*pR*)-configuration of the tricarbonyl(η^6-benzene)chromium group (Figure 9) shows one intramolecular nonclassical hydrogen bond between carbonyl oxygen O11 and H22B of the 2-*O*-acetyl group and one intermolecular H-bond between carbonyl oxygen O13 of the right molecule and H24A of the 3-*O*-acetyl group of the left molecule. All bond lengths and angles of these hydrogen bonds are in the expected range for nonclassical H-bonds.

The structure of the diastereomer **2m** with (*pS*)-configuration of the tricarbonyl(η^6-benzene)chromium group (Figure 10) resembles compound **2j** (Figure 7) in that the benzene rings are also in a symmetric parallel orientation. However, the distance of the benzene rings is, with 3.178 Å, shorter than in **2j** but still too long for an interaction of the aromatic rings. One nonclassical hydrogen bond is found in ***pS*-2m,** between the oxygen O13 of a carbonyl group and the anomeric hydrogen H1' of the sugar moiety. The bond lengths and angles of this H-bond are also in

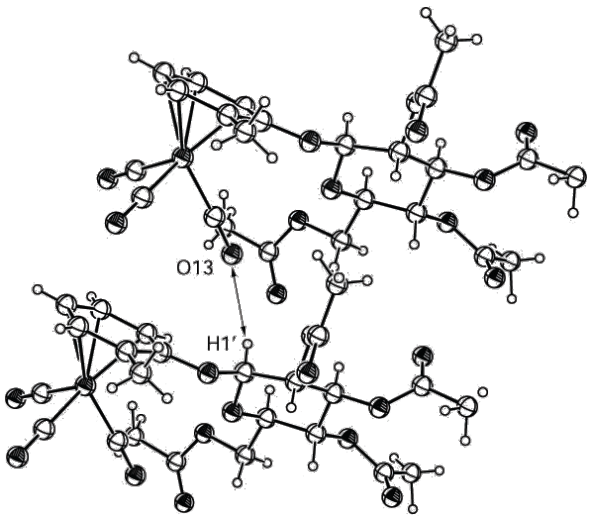

Figure 10: ORTEP-plot of the asymmetric unit showing three molecules of compound ***pS*-2m** and 30% probability ellipsoids; the arrows show the nonclassical H-bonds between O13 and H1'.

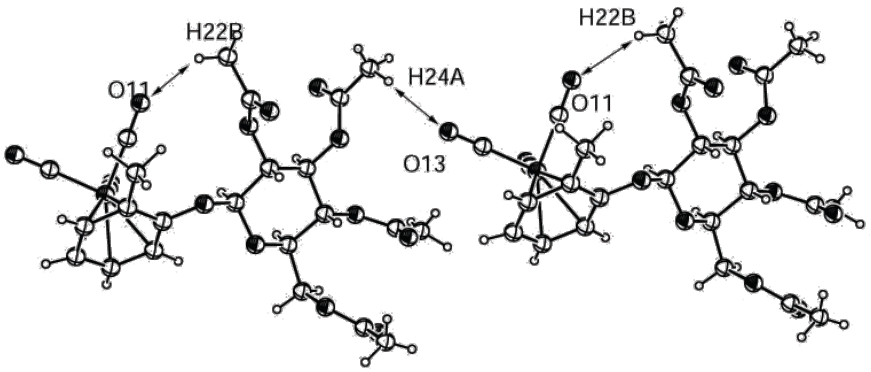

Figure 9: ORTEP-plot of the asymmetric unit showing two molecules of compound ***pR*-2m** and 30% probability ellipsoids; the arrows show the nonclassical intramolecular H-bonds between O11 and H22B and the intermolecular ones between O13 and H24A.

the expected range for nonclassical hydrogen bonds (2.699 Å for O···H, 128.7 degree for angle C–H···O and 167.3 degree for angle C≡O···H).

Conclusion

We have prepared and characterized a series of tricarbonyl(η^6-benzene)chromium complexes from phenyl and benzyl O-, N-, S- and C-glycosides, and which were hitherto unknown. The X-ray diffraction of some of these glycoside-derived tricarbonylchromium complexes revealed crystal structures that contain numerous nonclassical hydrogen bonds.

Experimental

General details. All solvents were dried and distilled prior to their use. Reactions were performed under Ar and monitored by TLC on Polygram Sil G/UV silica gel plates from Machery & Nagel. Detection was effected by charring with H_2SO_4 (5% in EtOH) or by inspection of the TLC plates under UV light. Reactions involving $Cr(CO)_6$ or chromium complexes were performed in brown glassware or in the dark. NMR spectra were recorded on a Bruker ARX 250 spectrometer at 250 MHz for proton spectra and 62.5 MHz for carbon spectra, on a Bruker Avance 400 spectrometer at 400 MHz for proton spectra and 100 MHz for carbon spectra, and on a Bruker AMX 600 spectrometer at 600 MHz for proton spectra and 150 MHz for carbon spectra. Tetramethylsilane was used at the internal standard. Chemical shifts δ are given in parts per million (ppm) and coupling constants in hertz (Hz). All NMR spectra were treated as first-order spectra. HRMS was performed on a Bruker Daltonics APEX 2 FT–ICR spectrometer. FAB–MS was performed on a Finnigan MAT TSQ 70 spectrometer and ionization with Xe. IR spectra were recorded with a Bruker Tensor 27 IR spectrometer. UV spectra were recorded with a Shimadzu UV 2102 PC spectrometer. Elemental analyses were performed on a Hekatech Euro 3000 CHN analyzer. Optical rotations were measured with a Perkin-Elmer Polarimeter 341. Melting points were determined with a Büchi B-540 apparatus and are uncorrected. Preparative chromatography was performed on silica gel (0.032–0.063 mm) from Machery & Nagel with different mixtures of solvents as eluent.

Starting materials. The following glycosides **1** were prepared according to literature procedures: Benzyl 2,3,4,6-tetra-*O*-acetyl-β-D-glucopyranoside (**1a**) [35], benzyl 2,3,4,6-tetra-*O*-acetyl-α-D-glucopyranoside (**1b**) [36], phenyl 2,3,4,6-tetra-*O*-acetyl-β-D-glucopyranoside (**1c**) [37], phenyl 2,3,4,6-tetra-*O*-methyl-β-D-glucopyranoside (**1d**) [38], phenyl 2,3,4,6-tetra-*O*-acetyl-α-D-glucopyranoside (**1e**) [39], 3,4,6-tri-O-acetyl-1,2-(1-phenoxy-1-ethylidene)-β-D-mannopyranose (**1f**) [37], phenyl 2,3,4,6-tetra-*O*-acetyl-β-D-mannopyranoside (**1g**) [40], benzoyl 2,3,4,6-tetra-*O*-acetyl-β-D-glucopyranoside (**1h**) [41], *N*-phenyl-2,3,4,6-tetra-*O*-acetyl-D-glucopyranosylamine (**1i**) [42], phenyl 2,3,4,6-tetra-*O*-acetyl-1-thio-β-D-glucopyranoside (**1j**) [43], 2,3,4,6-tetra-*O*-acetyl-β-D-glucopyranosylbenzene (**1k**) [44], 2-methylphenyl 2,3,4,6-tetra-*O*-acetyl-β-D-glucopyranoside (**1m**) [21], 2-(2,3,4,6-tetra-*O*-acetyl-β-D-glucopyranosyl)methylbenzene (**1q**) [22].

Chromium complexes: general procedure. A solution of glycoside **1** (1 mol equiv) and $Cr(CO)_6$ (1 mol equiv) in di-*n*-butylether/THF 9:1 was heated in the dark under Ar at 140 °C until TLC indicated complete consumption of **1** and was then concentrated. Chromatography of the residue under Ar with *n*-hexane/ethyl acetate 2:1 and immediate concentration of the fractions containing the chromium complex gave **2**. Crystalline complexes **2** were slowly recrystallized from ethanol. Suitable crystals were submitted to X-ray crystallographic analysis.

Tricarbonyl[(2,3,4,6-tetra-*O*-acetyl-β-D-glucopyranosyloxymethyl)-η^6-benzene]chromium (**2a**)

Treatment of **1a** (3.0 g, 6.8 mmol) and $Cr(CO)_6$ (1.50 g, 6.8 mmol) in di-*n*-butylether/THF (100 mL) for 96 h according to the general procedure afforded **2a** (1.14 g, 29%) as yellow triclinic crystals: Mp 140–141 °C (EtOH); $[\alpha]_D$ −11.0 (*c* 1.0, toluene); IR (KBr): 1952, 1895 cm^{-1}; FAB–MS (*m*/*z*): 597 $[M + Na]^+$, 574 $[M]^+$, 490 $[M - 3CO]^+$; ^1H NMR (acetone-d_6) δ 5.74–5.56 (m, 5H, H-aryl), 5.28 (t, 1H, 3-H), 5.06 (t, 1H, 4-H), 4.98 (t, 1H, 2-H), 4.98 (dd, $J_{1,2}$ = 7.3 Hz, 1H, 1-H), 4.68, 4.45 (dd, 2H, OCH_2Ph), 4.27 (dd, 1H, 6a-H), 4.16 (dd, 1H, 6b-H), 4.01 (m, 1H, 5-H), 2.06–1.94 (m, 12H, OCH_3); ^{13}C NMR (acetone-d_6) δ 234.1 (Cr-CO), 170.7, 170.3, 170.0, 169.7 (O=CO), 109.3 (C1-aryl), 100.9 (C1), 95.3, 95.2, 94.0, 93.8, 93.8 (C-aryl), 72.8 (C3), 72.6 (C5), 71.9 (C2), 70.0 (OCH_2), 69.3 (C4), 62.7 (C6), 20.6 (3C, OCH_3), 20.5 (OCH_3); Anal. calcd for $C_{24}H_{26}CrO_{13}$ (574.5): C, 50.18; H, 4.56; found: C, 50.10; H, 4.40.

Supporting Information

Supporting Information File 1

Experimental data.
[http://www.beilstein-journals.org/bjoc/content/supplementary/1860-5397-8-118-S1.pdf]

Acknowledgements

This work was financially supported by the Deutsche Forschungsgemeinschaft. We thank the groups of Professor K. Albert and Professor K. Zeller for measuring the NMR and MS spectra.

References

1. Fischer, E. O.; Öfele, K. *Chem. Ber.* **1957,** *90,* 2532–2535. doi:10.1002/cber.19570901117
2. Davies, S. G. *Organotransition Metal Chemistry: Applications to Organic Synthesis;* Pergamon Press: Oxford, U.K., 1992.
3. Beller, M.; Bolm, C. *Transition Metals for Organic Synthesis;* Wiley-VCH: Weinheim, Germany, 1998.
4. Kündig, E. P., Ed. *Transition Metal Arene π-Complexes in Organic Synthesis and Catalysts; Topics in Organometallic Chemistry*, Vol. 7; Springer, 2004. doi:10.1007/b76615
5. Semmelhack, M. F.; Clark, G. R.; Garcia, J. L.; Harrison, J. J.; Thebtaranonth, Y.; Wulff, W.; Yamashita, A. *Tetrahedron* **1981,** *37,* 3957–3965. doi:10.1016/S0040-4020(01)93270-3
6. Rosillo, M.; Domínguez, G.; Pérez-Castells, J. *Chem. Soc. Rev.* **2007,** *36,* 1589–1604. doi:10.1039/b606665h
7. Bolm, C.; Muñiz, K. *Chem. Soc. Rev.* **1999,** *28,* 51–59. doi:10.1039/a801291a
8. Pape, A. R.; Kaliappan, K. P.; Kündig, E. P. *Chem. Rev.* **2000,** *100,* 2917–2940. doi:10.1021/cr9902852
9. Rickard, C. E. F.; Woodgate, P. D.; Zhao, Z. *Acta Crystallogr., Sect. C* **1998,** *54,* 1420–1424. doi:10.1107/S0108270198005976
10. Rickard, C. E. F.; Singh, Y.; Woodgate, P. D.; Zhao, Z. *Acta Crystallogr., Sect. C* **1999,** *55,* 1475–1479. doi:10.1107/S0108270199007313
11. Han, J. W.; Son, S. U.; Chung, Y. K. *J. Org. Chem.* **1997,** *62,* 8264–8267. doi:10.1021/jo9712761
12. Shing, T. K. M.; Chow, H.-F.; Chung, I. H. F. *Tetrahedron Lett.* **1996,** *37,* 3713–3716. doi:10.1016/0040-4039(96)00648-X
13. Dötz, K.-H.; Jäkel, C.; Haase, W.-C. *J. Organomet. Chem.* **2001,** *617–618,* 119–132. doi:10.1016/S0022-328X(00)00650-1
14. Kündig, E. P.; Perret, C.; Spichiger, S.; Bernardinelli, G. *J. Organomet. Chem.* **1985,** *286,* 183–200. doi:10.1016/0022-328X(85)88005-0
15. Mahaffy, C. A. L.; Pauson, P. L. *Inorg. Synth.* **1979,** *19,* 154–158.
16. Silverthorn, W. E. *Adv. Organomet. Chem.* **1975,** *13,* 47–137. doi:10.1016/S0065-3055(08)60682-6
17. Lee, Y. T.; Choi, S. Y.; Lee, S. I.; Chung, Y. K.; Kang, T. J. *Tetrahedron Lett.* **2006,** *47,* 6569–6572. doi:10.1016/j.tetlet.2006.07.011
18. Ishido, Y.; Inaba, S.; Matsuno, A.; Yoshino, T.; Umezawa, H. *J. Chem. Soc., Perkin Trans. 1* **1977,** 1382–1390. doi:10.1039/P19770001382
19. Nunez, H. A.; Walker, T. E.; Fuentes, R.; O'Conner, J.; Serianni, A.; Barker, R. *J. Supramol. Struct.* **1977,** *6,* 535–550. doi:10.1002/jss.400060407
20. Baur, J.; Jacobson, H.; Burger, P.; Artus, G.; Berke, H.; Dahlenburg, L. *Eur. J. Inorg. Chem.* **2000,** 1411–1422. doi:10.1002/1099-0682(200007)2000:7<1411::AID-EJIC1411>3.0.CO;2-M
21. Helferich, B.; Günther, E.; Winkler, S. *Liebigs Ann. Chem.* **1934,** *508,* 192–205. doi:10.1002/jlac.19345080117
22. Panigot, M. J.; Curley, R. W., Jr. *J. Carbohydr. Chem.* **1994,** *13,* 293–302. doi:10.1080/07328309408009194
23. The supplementary crystallographic data for this paper can be obtained free of charge from The Cambridge Crystallographic Data Centre via http://www.ccdc.cam.ac.uk/data_request/cif by using the following numbers: CCDC 870827 for **2a**, CCDC 870828 for **2b**, CCDC 870829 for **2c**, CCDC 870830 for **2d**, CCDC 870831 for **2e**, CCDC 870832 for **2j**, CCDC 870833 for **2k**, CCDC 870834 for ***pR*-2m** and CCDC 870835 for ***pS*-2m**.
24. Solladié-Cavallo, A. *Polyhedron* **1985,** *4,* 901–927. doi:10.1016/S0277-5387(00)84058-9
25. Taylor, R.; Kennard, O. *J. Am. Chem. Soc.* **1982,** *104,* 5063–5070. doi:10.1021/ja00383a012
26. Chesnut, D. B. *J. Phys. Chem. A* **2000,** *104,* 11644–11650. doi:10.1021/jp002957u
27. Jones, P. G.; Sheldrick, G. M.; Clegg, W.; Kirby, A. J.; Glenn, R. *Z. Kristallogr.* **1982,** *160,* 269–274. doi:10.1524/zkri.1982.160.3-4.269
28. Brisdou, A. K.; Crossley, I. R.; Pritchard, R. G.; Warren, J. E. *Acta Crystallogr., Sect. C* **2003,** *59,* m322–m324. doi:10.1107/S0108270103013787
29. Eglin, J. L.; Smith, L. T. *Inorg. Chim. Acta* **2001,** *320,* 198–202. doi:10.1016/S0020-1693(01)00475-3
30. Bonifaci, C.; Ceccon, A.; Gambaro, A.; Ganis, P.; Santi, S.; Valle, G.; Venzo, A. *J. Organomet. Chem.* **1995,** *492,* 35–39. doi:10.1016/0022-328X(94)05280-O
31. Braga, D.; Grepioni, F.; Biradha, K.; Pedireddi, V. R.; Desiraju, G. R. *J. Am. Chem. Soc.* **1995,** *117,* 3156–3166. doi:10.1021/ja00116a020
32. Braga, D.; Grepioni, F. *Organometallics* **1991,** *10,* 2563–2569. doi:10.1021/om00054a013
33. Braga, D.; Dyson, P. J.; Grepioni, F.; Johnson, B. F. G. *Chem. Rev.* **1994,** *94,* 1585–1620. doi:10.1021/cr00030a006
34. Gambaro, A.; Ganis, P.; Manoli, F.; Polimeno, A.; Santi, S.; Venzo, A. *J. Organomet. Chem.* **1999,** *583,* 126–130. doi:10.1016/S0022-328X(99)00120-5
35. Steffan, W.; Vogel, C.; Kristen, H. *Carbohydr. Res.* **1990,** *204,* 109–120. doi:10.1016/0008-6215(90)84026-Q
36. Utamura, T.; Kuromatsu, K.; Suwa, K.; Koizumi, K.; Shingu, T. *Chem. Pharm. Bull.* **1986,** *34,* 2341–2353. doi:10.1248/cpb.34.2341
37. Dess, D.; Kleine, H. P.; Weinberg, D. V.; Kaufmann, R. J.; Sidhu, R. S. *Synthesis* **1981,** 883–885. doi:10.1055/s-1981-29631
38. Stanssens, D.; De Keukeleire, D.; Vandewalle, M. *Tetrahedron: Asymmetry* **1990,** *1,* 547–560. doi:10.1016/S0957-4166(00)80546-7
39. Audichya, T. D.; Ingle, T. R.; Bose, J. L. *Indian J. Chem.* **1973,** *11,* 704–705.
40. Montgomery, E. M.; Richtmyer, N. K.; Hudson, C. S. *J. Am. Chem. Soc.* **1942,** *64,* 690–694. doi:10.1021/ja01255a060
41. Pfander, H.; Läderach, M. *Carbohydr. Res.* **1982,** *99,* 175–179. doi:10.1016/S0008-6215(00)81907-2
42. Baker, J. W. *J. Chem. Soc.* **1928,** 1583–1593.
43. Dasgupta, F.; Garegg, P. J. *Acta Chem. Scand.* **1989,** *43,* 471–475. doi:10.3891/acta.chem.scand.43-0471
44. Hur, C. D.; Bonner, W. A. *J. Am. Chem. Soc.* **1945,** *67,* 1972–1977. doi:10.1021/ja01227a033

License and Terms

Beilstein Journal of Organic Chemistry

Synthesis of 4” manipulated Lewis X trisaccharide analogues

Christopher J. Moore and France-Isabelle Auzanneau*

Full Research Paper

Open Access

Address:
Department of Chemistry, University of Guelph, 50 Stone Rd. East, Guelph, Ontario, N1G 2W1, Canada

Email:
France-Isabelle Auzanneau* - fauzanne@uoguelph.ca

* Corresponding author

Keywords:
chlorodeoxygalactose; fluorodeoxygalactose; Lewis X analogues; oligosaccharide synthesis

Beilstein J. Org. Chem. **2012,** *8,* 1134–1143.
doi:10.3762/bjoc.8.126

Received: 25 April 2012
Accepted: 29 June 2012
Published: 23 July 2012

This article is part of the Thematic Series "Synthesis in the glycosciences II".

Guest Editor: T. K. Lindhorst

Abstract

Three analogues of the Le^x trisaccharide antigen (β-D-Gal*p*(1→4)[α-L-Fuc*p*(1→3)]-D-GlcNAc*p*) in which the galactosyl residue is modified at O-4 as a methyloxy, deoxychloro or deoxyfluoro, were synthesized. We first report the preparation of the modified 4-OMe, 4-Cl and 4-F trichloroacetimidate galactosyl donors and then report their use in the glycosylation of an *N*-acetylglucosamine glycosyl acceptor. Thus, we observed that the reactivity of these donors towards the $BF_3{\cdot}OEt_2$-promoted glycosylation at O-4 of the *N*-acetylglucosamine glycosyl acceptors followed the ranking 4-F > 4-OAc ≈ 4-OMe > 4-Cl. The resulting disaccharides were deprotected at O-3 of the glucosamine residue and fucosylated, giving access to the desired protected Le^x analogues. One-step global deprotection (Na/NH_3) of the protected 4”-methoxy analogue, and two-step deprotections (removal of a *p*-methoxybenzyl with DDQ, then Zemplén deacylation) of the 4”-deoxychloro and 4”-deoxyfluoro protected Le^x analogues gave the desired compounds in good yields.

Introduction

A glycolipid displaying the dimeric Le^x hexasaccharide (dimLe^x) has been identified as a cancer associated carbohydrate antigen, particularly prevalent in colonic and liver adenocarcinomas. In addition, an association between the fucosylation of internal GlcNAc residues in polylactosamine chains, and metastasis and tumor progression in colorectal cancers has been suggested [1-6]. Unfortunately, dimLe^x displays the Le^x trisaccharide (β-D-Gal*p*(1→4)[α-L-Fuc*p*(1→3)]-D-GlcNAc*p*), at the nonreducing end, and this antigenic determinant is also present at the surface of many normal cells and tissues, which include kidney tubules, gastrointestinal epithelial cells, and cells of the spleen and brain [7-11]. Indeed, anti-Le^x monoclonal antibodies (e.g., FH3, SH1) have been shown to recognize this Le^x antigenic determinant as it exists in the hexasaccharide

[1-6]. Therefore, as our group embarks on the development of a therapeutic anticancer vaccine utilizing the Tumor Associated Carbohydrate Antigen (TACA) dimLe^x as a target, an important factor to consider is an expected autoimmune response to the native Le^x antigen. Fortunately an internal epitope displayed by dimLe^x was discovered when monoclonal antibodies (mAbs) FH4 and SH2, raised against dimLe^x, were isolated. Indeed, these mAbs were shown to bind to the dimLe^x and trimLe^x antigens but only weakly recognise Le^x trisaccharide antigen [1-6]. With this in mind, we focus our research on the discovery of analogues of dimLe^x that can be used as safe vaccine candidates. Ideally, these analogues should display the internal epitopes that are recognized by anti-dimLe^x SH2-like antibodies while being free of those that are recognized by anti-Le^x SH1-like antibodies.

In order to abolish cross-reactivity with the Le^x antigen, we have prepared [12-14] several analogues in an attempt to identify a suitable replacement for the nonreducing end Le^x trisaccharide. In turn, we have compared the conformational behaviour of these analogues to that of the natural Le^x-OMe **1** (Figure 1) through a mixture of stochastic searches and NMR analyses [15]. The results pointed toward the preferential adoption, by all of analogues, of the stacked conformation that has been assigned for the Le^x trisaccharide [16-21]. The relative affinity of the anti-Le^x monoclonal antibody SH1 [6] for the native Le^x antigen **1** and our Le^x analogues [12-14] was examined by competitive ELISA experiments using a Le^x-BSA glycoconjugate as the immobilized ligand [15,22-24].

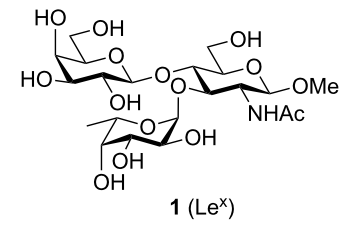

1 (Le^x)

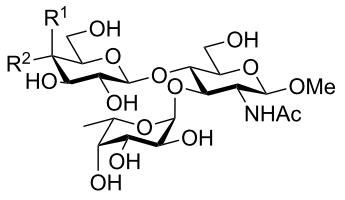

2: R^1 = H, R^2 = OH
3: R^1 = OMe, R^2 = H
4: R^1 = Cl, R^2 = H
5: R^1 = F, R^2 = H

Figure 1: Structure of Le^x and analogues **2**–**5**.

It was discovered that the Le^x analogue **2**, with a glucose unit in place of the galactose residue (Figure 1), did not bind to the SH1 mAb, even at high concentrations [15]. This discovery suggests that, to conserve cross-reactivity with the natural Le^x antigen, the nonreducing end galactose is essential, and that modifying this residue, particularly at O-4, may lead to the complete loss of this cross-reactivity [15]. Currently, it is not known what the reason for this observed loss of binding is, since the binding affinities between proteins and carbohydrates are the result of a combination of factors [25-29]. One of the main interactions is the formation of hydrogen bonds, either direct or water-mediated, between the amino acid residues of the protein and the key binding hydroxy groups of the ligand, which are arranged in clusters presented by different monosaccharide units. Other factors include favourable interactions of the nonpolar amino acid residues with the hydrophobic patches exhibited by the ligand, as well as high-energy water molecules being favourably displaced from the combining site. Binding affinity is therefore a result of combined enthalpic, entropic and solvation effects, frequently leading to a balance between favourable enthalpic and unfavourable entropic contributions [25-29]. Thus, only additional competitive ELISA studies with Le^x-OMe analogue inhibitors containing strategic manipulations at the 4” site will provide further insight into specific binding interactions [15]. The synthesis of a 4”-deoxy Le^x trisaccharide analogue was reported recently by Dong et al. [30]. Here, we report the synthesis of 4”-methyloxy, 4”-deoxychloro and 4”-deoxyfluoro Le^x-OMe analogue inhibitors **3**–**5**.

Results and Discussion

There are numerous reports in the literature of the chemical preparation of Le^x analogues [30-55], including one recent report of the synthesis of a Le^x pentasaccharide 4-deoxy at the nonreducing end galactosyl residue [30]. These syntheses follow one of three strategies: (1) the galactosylation then fucosylation of a glucosamine acceptor [30-47]; (2) the fucosylation then galactosylation of a glucosamine acceptor [48-53]; or (3) the fucosylation at O-3 of a lactosamine derivative prepared from lactose [54,55]. Our synthetic approach to prepare analogues **3**–**5** followed the first strategy [30-47] and involved the use of *N*-acetylglucosamine glycosyl acceptors **6** [14] and **8**, galactosyl donors **9**–**11**, and known fucosyl donors **12** [56] and **13** [12] (Figure 2).

Synthesis of monosaccharide building blocks 8–11

Glucosamine acceptor **8** was prepared in two steps from the known [14] benzylidene **7**: the benzylidene acetal was first hydrolyzed, and then the resulting diol (79%) was selectively benzoylated at O-6 (BzCl-collidine) giving acceptor **8** in 62% yield.

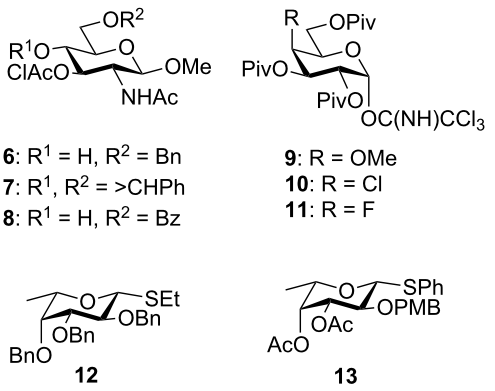

Figure 2: Monosaccharide building blocks **6**–**13**.

The syntheses of trichloroacetimidate donors **9**–**11** are described on Scheme 1; they were all prepared from the known trichloroethyl galactoside **14** [57]. Galactoside **14** was first prepared in three steps from galactose: (1) peracetylation (Ac_2O-pyridine); (2) $BF_3{\cdot}OEt_2$ activation of the anomeric acetate and glycosidation with trichloroethanol; and (3) Zemplén deacetylation. This sequence of reactions gave the desired galactoside **14** in 78% yield and as a 9:1 α/β mixture, as assessed by ^{1}H NMR. It is important to point out that the second step in this sequence of reactions used conditions very similar to those used by Risbood et al. to prepare peracetylated trichloroethyl galactopyranoside from peracetylated galactose. Indeed, in agreement with their work [57], the ratio of α-anomer isolated here suggests a late anomerization of the β-glycoside during our extended reaction time (20 h) at reflux. The 4-methyloxy trichloroacetimidate donor **9** was then prepared in four steps from the anomeric mixture of galactoside **14**. Tetraol **14** was stirred in a mixture of pyridine and dichloromethane at −10 °C and treated with 3.1 equivalents of pivaloyl chloride. Under these conditions the α-tripivaloate **15**, selectively acylated at O-2, O-3 and O-6, was obtained pure and free of β-anomer (64%). The free hydroxy group in alcohol **15** was then deprotonated with sodium hydride and allowed to react with methyl iodide, yielding the 4-OMe galactoside **16** in very good yield. In turn, trichloroethyl galactoside **16** was converted to the trichloroacetimidate donor **9** in two steps: the anomeric trichloroethyl group was removed (Zn/AcOH), and then the resulting hemiacetal was treated with trichloroacetonitrile in the presence of DBU giving the desired α-trichloroacetimidate in good yield.

A Lattrell-Dax nitrite mediated inversion [58-60] of the 4-OH in galactoside **15** provided the glucoside **17**, which was used as the common precursor to analogues **18** and **19**. Treatment with sulfuryl chloride [61] gave the 4-chloro galactoside **18** in good yield, whereas triflation at O-4 followed by S_N2 displacement of the triflate by using tetrabutylammonium fluoride [62,63] gave the 4-fluoro galactoside analogue **19** in excellent yields. As described above for the preparation of donor **9** from glycoside **16**, trichloroethyl galactosides **18** and **19** were, in turn, converted in two steps (Zn/AcOH then Cl_3CCN/DBU) to the trichloroacetimidate donors **10** and **11**, respectively, which were obtained in acceptable yields over the two steps.

Galactosylation at O-4 of *N*-acetylglucosamine acceptors

It has been well established that the hydroxy group at C-4 of *N*-acetylglucosamine is a poor nucleophile, with reduced reactivity toward glycosylation [64-66]. However, we have

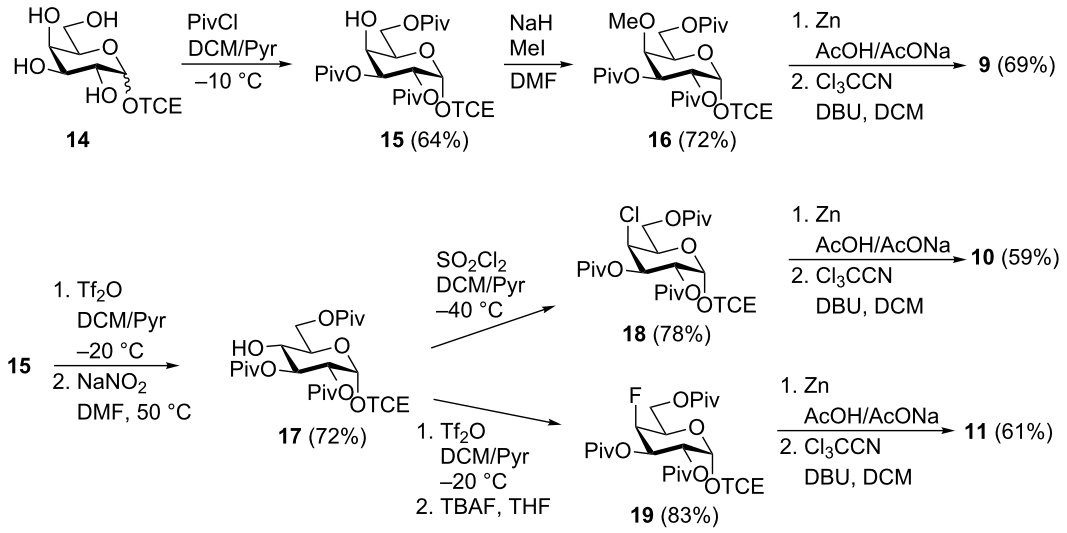

Scheme 1: Synthesis of trichloroacetimidate donors **9**–**11**.

reported the successful O-4 glycosylation of an *N*-acetylglucosamine monosaccharide acceptor using peracetylated gluco- and galactopyranose α-trichloroacetimidate donors under activation with 2 equivalents of $BF_3{\cdot}OEt_2$ at room temperature or 40 °C [14,67]. We applied similar conditions to prepare disaccharides **20**–**22** (Table 1). Glycosylation of methyl glycoside **6** with the 4-methoxy donor **9** gave the best results when the reaction was carried out at 40 °C and left to proceed for 2 hours. Under these conditions, the desired disaccharide **20** was isolated in acceptable yields (Table 1, entries 1 and 2). Our attempts to reduce the number of equivalents of donor **9** used in the reaction always resulted in a lower yield of the desired disaccharide. Glycosylation of acceptor **8** with the 4-chloro galactosyl donor **10** appeared to be slower (Table 1, entries 3–5) than that of acceptor **6** with donor **9**. The best results were obtained when the reaction was left to proceed for 3 rather than 2 hours (Table 1, entry 4), and the desired disaccharide **21** was then obtained in acceptable yield. Increasing the temperature to 60 °C did not increase the yield, presumably due to the degradation of the glycosyl donor at this higher temperature (Table 1, entry 5). Of the three glycosylations considered here, the coupling of acceptor **8** with the 4-fluoro donor **11** gave the highest yields (Table 1, entries 6 and 7). Indeed the desired disaccharide **22** was obtained in very good yields when the reaction was allowed to proceed for 2 hours at 40 °C. Once again, increasing the temperature to 60 °C offered no advantage and in fact led to a lower yield of the desired product.

From these three reactions, it is clear that the substituent at O-4 of a galactosyl donor impacts the outcome of glycosylation at O-4 of *N*-acetylglucosamine acceptors. Indeed, we have previously observed that galactosylations of such acceptors [68,69] usually result in lower yields (~70%) than those for analogous glucosylations, which usually provided around 90% of the desired disaccharides [14,67]. The results described here indicate that 4-OAc galactosyl donors perform better than the 4-Cl donor **10**, whereas the 4-OMe donor **9** performs as well as the 4-OAc analogues. In addition, of all of the galactosyl donors employed thus far in such reactions, the 4-fluorinated analogue seemed to perform the best. Thus the reactivity of galactosyl trichloroacetimidate donors towards the $BF_3{\cdot}OEt_2$-promoted glycosylation at O-4 of *N*-acetylglucosamine glycosyl acceptors seems to follow the ranking 4-F > 4-OAc ≈ 4-OMe > 4-Cl.

Table 1: Glycosylation at O-4 of glucosamine with donors **9**–**11**.[a]

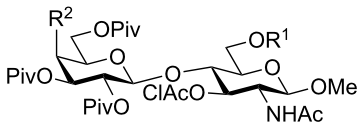

20: R^1 = Bn, R^2 = OMe
21: R^1 = Bz, R^2 = Cl
22: R^1 = Bz, R^2 = F

Entry	Acc.	Don.	*T* (°C)	Time (h)	Product (%)
1	**6**	**9**	rt[b]	2	**20** (65)
2	**6**	**9**	40[b]	2	**20** (70)
3	**8**	**10**	40[b]	2	**21** (55)
4	**8**	**10**	40[b]	3	**21** (63)
5	**8**	**10**	60[c]	2	**21** (62)
6	**8**	**11**	40[b]	2	**22** (77)
7	**8**	**11**	60[c]	2	**22** (73)

[a]Reagents and conditions: $BF_3{\cdot}Et_2O$ (2 equiv), donor **9**–**11** (5 equiv); [b]solvent: CH_2Cl_2; [c]solvent: 1,2-dichloroethane.

Preparation of the protected Le^x trisaccharide analogues

The synthesis of protected trisaccharide intermediates **26**–**28** is described in Scheme 2. First, acceptors **23**–**25** were prepared in good yields through the selective removal of the chloroacetate (thiourea) in disaccharides **20**–**22**. Fucosylation of acceptor **23** with ethylthioglycoside **12** was first attempted under NIS and TMSOTf activation at low temperature (−30 °C). Under these conditions, the desired trisaccharide **26** was isolated in 78% yield but as an 8:2 mixture of the α and β-anomers as estimated by ^{1}H NMR. Although the desired anomer **26α** could be obtained pure upon purification by HPLC, it was isolated in a less than desirable yield of 48%. We thus attempted the coupling of acceptor **23** and donor **12** under activation with excess MeOTf (5 equiv). Indeed, we have reported that such conditions allow glycosylation at O-4 of *N*-acetylglucosamine acceptors through the in situ formation of the corresponding *N*-methylimidate, temporarily masking the *N*-acetyl group in the acceptor [70,71]. Thus, we expected a similar in situ formation of the methyl imidate in acceptor **23**, which would further undergo fucosylation at O-3. However, since methylimidates are unstable when purified on silica gel, they were converted back to the acetamido before purification. Thus, once TLC had shown that all of the acceptor had been consumed, the reaction was worked up and the crude mixture was treated with Ac_2O–AcOH prior to purification by chromatography [70,71]. Under these conditions, the desired trisaccharide **26α** was obtained pure and free of the β-anomer in 77% yield.

Similar reaction conditions were applied for the glycosylation of acceptors **24** and **25** with ethylthioglycoside **13**. Interestingly, these fucosylation reactions proved to be slower and required additional equivalents of donor **13** to proceed. However, after treatment of the reaction mixtures with AcOH–Ac_2O, the desired trisaccharides **27** and **28** were isolated in good yields (Scheme 2) and exclusively as the α-fucosylated trisaccharides.

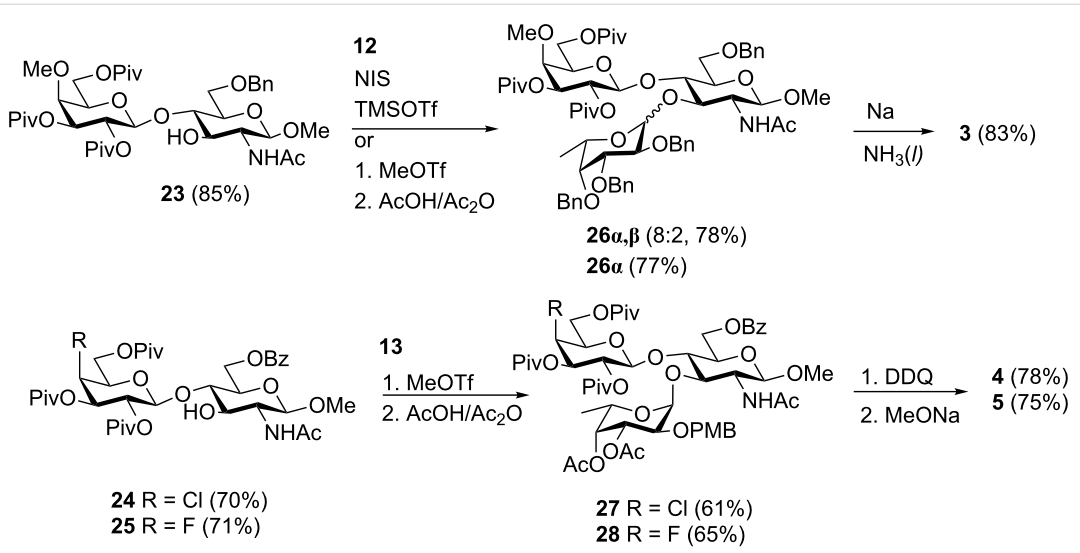

Scheme 2: Synthesis of trisaccharides **26**–**28** and deprotection reactions giving **3**–**5**.

As previously observed for other similar analogues [66,72,73], careful analysis of the ^{1}H NMR spectra acquired for trisaccharides **26α**, **27**, **28** indicated that the glucosamine residue adopted a conformation distorted from the usual $^4C_1$ chair conformation. The distorted conformations of the *N*-acetylglucosamine ring in analogues **26α**, **27**, **28** were characterized by vicinal coupling constants of 6.2–6.6 Hz measured between the ring hydrogens H-2 to H-5 of this residue, rather than the expected values of 8.0–8.3 Hz as observed, when measurable, for the same hydrogens in disaccharides **20**–**25**. In addition, although signal overlap precluded its measurement in trisaccharides **26α** and **28**, the vicinal coupling constant measured between H-1 and H-2 in trisaccharide **27** (5.2 Hz) also supported a distorted conformation for this residue (compare to the same coupling constant in compounds **23**–**25**, ~7.4 Hz).

Deprotection of trisaccharides 26–28

As described previously, the removal of various protecting groups, such as pivaloyl and benzyl groups here, can be accomplished efficiently in one step under Birch reduction conditions [15,68,69,74,75]. Thus, treatment of trisaccharide **26α** with sodium in liquid ammonia at −78 °C was followed by neutralization of the reaction mixture with AcOH and purification by gel permeation chromatography on a Biogel P2 column (water) to give the desired deprotected 4”-methoxy trisaccharide analogue **3** pure in 83% yield. Since such conditions were not compatible with the 4-chloro and 4-fluoro substituents in trisaccharides **27** and **28**, these intermediates were converted in two steps to the desired deprotected analogues **4** and **5**, respectively. Thus, removal of the *p*-methoxybenzyl group with DDQ in CH_2Cl_2/H_2O (15:1 v/v) was followed by Zemplén deacylation, giving the target Le^x analogues **4** and **5** in 78% and 75%, respectively, over the two steps. The structures of the final deprotected trisaccharides **3**–**5** were confirmed by HR–ESI mass spectrometry and NMR.

Conclusion

We describe here the efficient synthesis of three Le^x methyl glycoside derivatives (**3**–**5**) in which the galactosyl 4-hydroxy group is either methylated (**3**) or replaced by a chlorine (**4**) or fluorine (**5**). Our results seem to indicate that galactosylation at O-4 of an *N*-acetylglucosamine acceptor under activation with excess $BF_3{\cdot}OEt_2$ can be significantly affected by the nature of the substituent present at C-4 of the galactosyl donor. Indeed, the best results were obtained with the 4-fluoro galactosyl donor, whereas the 4-chloro donor reacted less efficiently than the 4-O-methyl or 4-O-acetyl donors. Overall, this study also confirms our observation [68], that galactosylations at position 4 of *N*-acetylglucosamine acceptors are usually less successful than glucosylations [14,67]. The final Le^x-OMe analogues will be used as competitive inhibitors in future ELISA experiments to provide a better understanding of the binding process between the anti-Le^x monoclonal antibody SH1 and the Le^x antigen.

Experimental

General Methods: ^{1}H (400.13 MHz) and ^{13}C NMR (100.6 MHz) spectra were recorded for compounds solubilized in $CDCl_3$ (internal standard, for ^{1}H: residual $CHCl_3$ δ 7.24; for ^{13}C: $CDCl_3$ δ 77.0), DMSO-d_6 (internal standard, for ^{1}H: residual DMSO δ 2.54; for ^{13}C: DMSO-d_6 δ 40.45), CD_3OD (internal standard, for ^{1}H: residual MeOD δ 3.31; for ^{13}C: CD_3OD δ 49.15) or D_2O [external standard 3-(trimethylsilyl)propionic acid-d_4, sodium salt (TSP) for

^{1}H δ 0.00; for ^{13}C δ 0.00]. Chemical shifts and coupling constants were obtained from a first-order analysis of one-dimensional spectra. Assignments of proton and carbon resonances were based on COSY and ^{13}C–^{1}H heteronuclear correlated experiments. ^{1}H NMR data are reported with standard abbreviations: singlet (s), doublet (d), triplet (t), doublet of doublet (dd), doublet of doublet of doublet (ddd), broad singlet (bs), broad triplet (bt), broad doublet of doublet (bdd) and multiplet (m). Mass spectra were obtained with electrospray ionization (ESI) on a high-resolution mass spectrometer. TLC were performed on precoated aluminum plates with Silica Gel 60 F_{254} and detected with UV light and/or by charring with a solution of 10% H_2SO_4 in EtOH. Compounds were purified by flash chromatography with Silica Gel 60 (230–400 mesh) unless otherwise stated. Solvents were distilled and dried according to standard procedures [76], and organic solutions were dried over Na_2SO_4 and concentrated under reduced pressure below 40 °C. HPLC purifications were run with HPLC grade solvents.

Methyl 2-acetamido-2-deoxy-3-*O*-(α-L-fucopyranosyl)-4-*O*-(4-methoxy-β-D-galactopyranosyl)-β-D-glucopyranoside (3). A solution of the protected trisaccharide **26*α*** (50 mg, 0.043 mmol) dissolved in THF (5 mL) was added to a solution of liquid NH_3 (ca. 20 mL) containing Na (72 mg, 3.13 mmol, 73 equiv) at −78 °C. After 1 h the reaction was quenched with MeOH (5 mL) and the ammonia was allowed to evaporate at rt. The remaining solution was neutralized with AcOH (220 μL, ca. 1.2 equiv to Na), and the mixture was concentrated. The resulting solid was dissolved in water and passed through a Biogel P2 column eluted with H_2O. After freeze drying, the deprotected 4”-methoxy-Le^x analogue **3** (20 mg, 0.0359 mmol, 83%) was obtained pure as a white solid. $[\alpha]_D$ = −75 (*c* 0.3, H_2O); ^{1}H NMR (400 MHz, D_2O, 295 K) δ 4.95 (d, *J* = 4.0 Hz, 1H, H-1’), 4.67 (m, 1H, H-5’), 4.32 (d, *J* = 8.2 Hz, 1H, H-1), 4.27 (d, *J* = 7.7 Hz, 1H, H-1”), 3.85 (dd, *J* = 2.0, 12.2 Hz, 1H, H-6a), 3.78–3.68 (m, 5H, H-2, H-3, H-4, H-3’, H-6b), 3.63–3.60 (m, 3H, H-4’, H-6ab”), 3.55–3.50 (m, 2H, H-2’, H-3”), 3.47–3.44 (m, 2H, H-5, H5”), 3.39 (d, *J* = 3.4 Hz, 1H, H-4”), 3.35 (s, 3H, OCH_3), 3.32 (s, 3H, OCH_3), 3.29 (m, 1H, H-2”), 1.88 (s, 3H, C(O)CH_3), 1.03 (d, *J* = 6.6 Hz, 3H, H-6’); ^{13}C NMR (100 MHz, D_2O, 295 K) δ 174.4 (C=O), 101.7 (C-1), 101.6 (C-1”), 98.7 (C-1’), 78.6 (C-4”), 75.3, 75.1, 75.0 (C-5, C-5”, C-3), 73.3 (C-4), 72.9 (C-3”), 71.9 (C-4’), 71.5 (C-2”), 69.2 (C-3’), 67.7 (C-2’), 66.7 (C-5’), 61.1 (OCH_3), 61.0 (C-6”), 59.7 (C-6), 57.1 (OCH_3), 55.6 (C-2), 22.2 (C(O)*C*H_3), 15.2 (C-6’); HRMS–ESI (*m*/*z*): [M + Na]$^+$ calcd for $C_{22}H_{39}NNaO_{15}$, 580.2217; found, 580.2223.

Methyl 2-acetamido-2-deoxy-4-*O*-(4-chloro-4-deoxy-β-D-galactopyranoside)-3-*O*-(α-L-fucopyranosyl)-β-D-glucopyranoside (4). A solution of the protected trisaccharide **27** (39 mg, 0.0347 mmol) and DDQ (12 mg, 1.5 equiv) in CH_2Cl_2 (350 μL) and H_2O (20 μL, 6% v/v) was stirred at room temperature for 2 h. The mixture was filtered over Celite and the solids were washed with CH_2Cl_2 (5 mL). The combined filtrate and washings were washed with aq saturated $NaHCO_3$ (10 mL), the aq layer was re-extracted with CH_2Cl_2 (3 × 5 mL), and the combined organic layers were dried and concentrated. Flash chromatography (EtOAc/hexanes, 1:1 → 7:3) of the residue gave a white solid (27 mg, 0.0269 mmol, 78%), which was dissolved in a methanolic solution of NaOMe (1 mL, 0.13 M) and stirred for 3 h at 50 °C. The reaction mixture was diluted with MeOH (5 mL) and de-ionized with DOWEX H^+ resin. The resin was filtered off and washed with MeOH (5 mL), and the combined filtrated and washings were concentrated. The crude product was dissolved in Milli Q water and washed with CH_2Cl_2 (5 mL). After freeze drying, the deprotected 4”-deoxy-chloro Le^x analogue **4** (15.1 mg, 0.0269 mmol, 78%) was obtained pure as an amorphous solid. $[\alpha]_D$ = −123 (*c* = 0.7, H_2O); ^{1}H NMR (400 MHz, D_2O, 295 K) δ 4.97 (d, 1H, *J* = 4.0 Hz, H-1’), 4.61 (m, 1H, H-5’), 4.38–4.30 (m, 3H, H-1, H-1”, H-4”), 3.88 (dd, *J* = 1.9, 12.3 Hz, 1H, H-6a), 3.82 (dd, *J* = 3.8, 9.7 Hz, 1H, H-3”), 3.77–3.70 (m, 7H, H-2, H-3, H-4, H-6b, H-3’, H-4’, H-5”), 3.66 (dd, *J* = 7.1, 11.7 Hz, 1H, H-6a”), 3.59–3.53 (m, 2H, H-2’, H-6b”), 3.45 (m, 1H, H-5), 3.38–3.33 (m, 4H, H-2”, OCH_3), 1.88 (s, 3H, C(O)CH_3), 1.05 (d, *J* = 6.6 Hz, 3H, H-6’); ^{13}C NMR (100 MHz, D_2O, 295 K) δ 174.4 (C=O), 102.2 (C-1”), 101.7 (C-1), 98.5 (C-1’), 75.2 (C-5), 74.4 (C-3), 73.7 (C-4), 73.6 (C-5”), 71.9 (C-4’), 71.5 (C-3”), 70.8 (C-2”), 69.3 (C-3’), 67.6 (C-2’), 66.6 (C-5’), 62.2 (C-4”), 61.6 (C-6”), 59.5 (C-6), 57.1 (OCH_3), 55.7 (C-2), 22.2 (C(O)CH_3), 15.2 (C-6’); HRMS–ESI (*m*/*z*): [M + Na]$^+$ calcd for $C_{21}H_{36}ClNNaO_{14}$, 584.1722; found, 584.1733.

Methyl 2-acetamido-2-deoxy-4-*O*-(4-deoxy-4-fluoro-β-D-galactopyranoside)-3-*O*-(α-L-fucopyranosyl)-β-D-glucopyranoside (5). Trisaccharide **28** (30 mg, 0.0271 mmol) was deprotected in two steps as described above for the preparation of trisaccharide **4**. After freeze drying, the deprotected 4”-deoxyfluoro Le^x analogue **5** (11.1 mg, 0.0203 mmol, 75%) was obtained pure as an amorphous solid. $[\alpha]_D$ = −85 (*c* 0.5, H_2O); ^{1}H NMR (400 MHz, D_2O, 295 K) δ 4.95 (d, *J* = 4.0 Hz, 1H, H-1’), 4.66 (m, 1H, H-5’), 4.65 (bdd, *J* = 2.7 Hz, $J_{H,F}$ = 50.4 Hz, 1H, H-4”), 4.39 (d, *J* = 7.8 Hz, 1H, H-1”), 4.33 (d, *J* = 8.0 Hz, 1H, H-1), 3.86 (dd, *J* = 2.0, 12.3 Hz, 1H, H-6a), 3.81–3.66 (m, 6H, H-2, H-3, H-4, H-6b, H-3’, H-3”), 3.64–3.58 (m, 4H, H-4’, H-5”, H-6ab”), 3.54 (dd, *J* = 4.0, 10.4 Hz, 1H, H-2’), 3.45 (m, 1H, H-5), 3.37–3.33 (m, 4H, H-2”, OCH_3), 1.88 (s, 3H, C(O)CH_3), 1.02 (d, *J* = 6.6 Hz, 3H, H-6’); ^{13}C NMR (100 MHz, D_2O, 295 K) δ 174.4 (C=O), 101.7 (C-1), 101.4 (C-1”), 98.7 (C-1’), 89.3 (d, $J_{C,F}$ = 177.7 Hz, C-4”), 75.2 (C-5), 74.9 (C-3), 73.4 (C-4), 73.2 (d, $J_{C,F}$ 17.6 Hz, C-5”), 71.9 (C-4’),

71.2 (C2"), 71.1 (d, $J_{C,F}$ = 18.5 Hz, C-3"), 69.2 (C-3'), 67.6 (C-2'), 66.5 (C-5'), 60.0 (C-6"), 59.6 (C-6), 57.1 (OCH_3), 55.6 (C-2), 22.2 ($C(O)CH_3$), 15.3 (C-6'); HRMS–ESI (*m*/*z*): $[M + Na]^+$ calcd for $C_{21}H_{36}FNO_{14}$, 568.2018; found, 568.2023.

Methyl 2-acetamido-6-*O*-benzyl-3-*O*-chloroacetyl-2-deoxy-4-*O*-(4-*O*-methyl-2,3,6-tri-*O*-pivaloyl-β-D-galactopyranosyl)-β-D-glucopyranoside (20). A solution of acceptor **6** (215 mg, 0.535 mmol) and trichloroacetimidate donor **9** (1.58 g, 5.0 equiv) in CH_2Cl_2 (30 mL) was stirred at 40 °C, and $BF_3{\cdot}OEt_2$ (134 μL, 2.0 equiv) was added. The reaction was allowed to proceed for 2 h at 40 °C and then quenched with Et_3N (179 μL, 2.4 equiv), and the mixture was diluted with CH_2Cl_2 (70 mL). The mixture was washed with aq saturated $NaHCO_3$ (100 mL), the aq layer was re-extracted with CH_2Cl_2 (20 mL × 3), and the combined organic layers were dried and concentrated. Flash chromatography (EtOAc/hexanes, 2:8 → 6:4) of the residue gave disaccharide **20** (312 mg, 0.375 mmol, 70%) pure as a colourless glass. $[\alpha]_D$ = −11 (*c* 0.6, CH_2Cl_2); ^{1}H NMR (400 MHz, $CDCl_3$, 296 K) δ 7.29 (m, 5H, H_{arom}), 5.95 (d, *J* = 9.2 Hz, 1H, NH), 5.08–4.99 (m, 2H, H-3, H-2'), 4.71–4.68 (m, 2H, H-3', C*H*HPh), 4.40 (d, *J* = 12.1 Hz, 1H, C*H*HPh), 4.38 (d, *J* = 7.4 Hz, 1H, H-1), 4.24–4.19 (m, 2H, H-1', H-6a'), 4.13–4.07 (m, 2H, H-6b', C*H*HCl), 4.01 (d, *J* = 15.1 Hz, 1H, C*H*HCl), 3.96–3.92 (m, 2H, H-4, H-2), 3.71 (m, 2H, H-6ab), 3.50–3.40 (m, 3H, H-5, H-4', H-5'), 3.43, 3.41 (2s, 6H, 2 × OCH_3), 1.94 (s, 3H, $C(O)CH_3$), 1.30, 1.15, 1.10 (3s, 27H, 3 × $C(CH_3)_3$); ^{13}C NMR (100 MHz, $CDCl_3$, 296 K) δ 177.9, 177.7, 176.2, 170.3, 167.3 (C=O), 137.7, 128.6, 128.1, 128.0 (Ar), 101.7 (C-1), 99.2 (C-1'), 76.3 (C-4'), 74.2 (C-5), 73.9 (C-3), 73.5 (CH_2Ph), 73.4 (C-3'), 72.1 (C-4), 72.0 (C-5'), 69.5 (C-2'), 67.7 (C-6), 61.7 (C-6'), 61.5 (OCH_3), 56.6 (OCH_3), 52.6 (C-2), 40.8 (CH_2Cl), 38.8, 38.7, 38.6 ($C(CH_3)_3$), 27.2, 27.1 ($C(CH_3)_3$), 23.3 ($C(O)CH_3$); HRMS–ESI (*m*/*z*): $[M + H]^+$ calcd for $C_{40}H_{61}ClNO_{15}$, 830.3730; found, 830.3735.

Methyl 2-acetamido-6-*O*-benzoyl-3-*O*-chloroacetyl-4-*O*-(4-chloro-4-deoxy-2,3,6-tri-*O*-pivaloyl-β-D-galactopyranosyl)-2-deoxy-β-D-glucopyranoside (21). Glycosylation of acceptor **8** (97 mg, 0.233 mmol) with trichloroacetimidate **10** (694 mg, 5.0 equiv) was performed under $BF_3{\cdot}OEt_2$ (59 μL, 2.0 equiv) activation as described above for the synthesis of disaccharide **20**. Work-up, as described above, and flash chromatography (EtOAc/hexanes, 2:8 → 6:4) of the residue gave disaccharide **21** (125 mg, 0.147 mmol, 63%) pure as a colourless glass. $[\alpha]_D$ = +9 (*c* 0.9, CH_2Cl_2); ^{1}H NMR (400 MHz, $CDCl_3$, 295 K) δ 8.00–7.41 (m, 5H, Ar), 5.87 (d, *J* = 9.3 Hz, 1H, NH), 5.27–5.16 (m, 2H, H-2', H-3), 4.86 (dd, *J* = 3.9, 10.1 Hz, 1H, H-3'), 4.61 (dd, *J* = 2.9, 12.0 Hz, 1H, H-6a), 4.51–4.47 (m, 3H, H-1, H-6b, H-1'), 4.38 (d, *J* = 3.5 Hz, 1H, H-4'), 4.35–4.30 (dd, *J* = 7.2, 11.5 Hz, 1H, H-6a'), 4.16–4.02 (m, 4H, H-2, H-6b', CH_2CCl_3), 3.91 (t, *J* = 8.3 Hz, 1H, H-4), 3.83 (bt, *J* = 6.2 Hz, 1H, H-5'), 3.72 (m, 1H, H-5), 3.45 (s, 3H, OCH_3), 1.97 (s, 3H, $C(O)CH_3$), 1.16, 1.14, 1.13 (3s, 27H, 3 × $C(CH_3)_3$); ^{13}C NMR (100 MHz, $CDCl_3$, 295 K) δ 177.8, 177.6, 176.3, 170.3, 167.3, 166.0 (C=O), 133.5, 129.6, 129.4, 128.7, 128.4 (Ar), 101.7 (C-1), 100.4 (C-1'), 73.5 (C-3), 73.4 (C-4), 72.5 (C-5), 71.6 (C-3'), 71.2 (C-5'), 68.3 (C-2'), 62.6 (C-6), 62.6 (C-6'), 57.2 (C-4'), 56.8 (OCH_3), 52.6 (C-2), 40.7 (CH_2Cl), 38.9, 38.8, 38.7 ($C(CH_3)_3$), 27.6, 27.1, 27.0, 26.9, 26.7 ($C(CH_3)_3$), 23.3 ($C(O)CH_3$); HRMS–ESI (*m*/*z*): $[M + H]^+$ calcd for $C_{39}H_{56}Cl_2NO_{15}$, 848.3027; found, 848.3009.

Methyl 2-acetamido-6-*O*-benzoyl-3-*O*-chloroacetyl-2-deoxy-4-*O*-(4-deoxy-4-fluoro-2,3,6-tri-*O*-pivaloyl-β-D-galactopyranosyl)-β-D-glucopyranoside (22). Glycosylation of acceptor **8** (91.5 mg, 0.220 mmol) with trichloroacetimidate **11** (637 mg, 5.0 equiv) was performed under $BF_3{\cdot}OEt_2$ (134 μL, 2.0 equiv) activation as described above for the synthesis of disaccharide **20**. Work-up, as described above, and flash chromatography (EtOAc/hexanes, 2:8 → 6:4) of the residue gave disaccharide **22** (143 mg, 0.172 mmol, 77%) pure as a colourless glass. $[\alpha]_D$ = +9 (*c* 2.2, CH_2Cl_2); ^{1}H NMR (400 MHz, $CDCl_3$, 295 K) δ 7.98–7.46 (m, 5H, H_{arom}), 6.00 (d, *J* = 9.3 Hz, 1H, NH), 5.21–5.16 (m, 2H, H-3, H-2'), 4.82 (ddd, *J* = 2.6, 10.3 Hz, $J_{H,F}$ = 26.9 Hz, 1H, H-3'), 4.70 (dd, *J* = 2.6 Hz, $J_{H,F}$ = 42.9 Hz, 1H, H-4'), 4.62 (m, 1H, H-6a), 4.51–4.46 (m, 3H, H-1, H-6b, H-1'), 4.29 (dd, *J* = 7.6, 11.4 Hz, 1H, H-6a'), 4.16 (dd, *J* = 5.6, 11.5 Hz, 1H, H-6b'), 4.09–4.00 (m, 3H, H-2, CH_2Cl), 3.92 (t, *J* = 8.2 Hz, 1H, H-4), 3.72 (m, 1H, H-5), 3.66 (dt, *J* = 6.4 Hz, $J_{H,F}$ = 25.8 Hz, 1H, H-5'), 3.44 (s, 3H, OCH_3), 1.97 (s, 3H, OCH_3), 1.16, 1.13 (2s, 27H, 3 × $C(CH_3)_3$); ^{13}C NMR (100 MHz, $CDCl_3$, 295 K) δ 177.8, 177.6, 176.5, 170.46, 167.3, 165.9 (C=O), 133.5, 129.5, 129.4, 128.6 (Ar), 101.6 (C-1), 99.9 (C-1'), 85.3 (d, $J_{C,F}$ = 186.4 Hz, C-4'), 73.5 (C-3), 73.4 (C-4), 72.4 (C-5), 71.2 (d, $J_{C,F}$ = 18.0 Hz, C-3'), 71.1 (d, $J_{C,F}$ = 18.0 Hz, C-5'), 68.6 (C-2'), 62.6 (C-6), 61.2 (C-6'), 56.8 (OCH_3), 52.5 (C-2), 40.6 (CH_2Cl), 38.8, 38.8, 38.7 ($C(CH_3)$), 27.1, 26.9 ($C(CH_3)$), 23.2 ($C(O)CH_3$); HRMS–ESI (*m*/*z*): $[M + H]^+$ calcd for $C_{39}H_{56}ClFNO_{15}$, 832.3323; found, 832.3344.

Methyl 2-acetamido-6-*O*-benzyl-3-*O*-(2,3,4-tri-*O*-benzyl-α-L-fucopyranosyl)-2-deoxy-4-*O*-(4-*O*-methyl-2,3,6-tri-*O*-pivaloyl-β-D-galactopyranosyl)-β-D-glucopyranoside (26). A mixture of disaccharide acceptor **23** (30 mg, 0.0398 mmol), known [56] thioethyl fucopyranoside **12** (76 mg, 0.159 mmol, 4.0 equiv), and activated powdered 4 Å molecular sieves (0.25 g) in Et_2O (3.0 mL, 0.13 M), was stirred for 1 h at rt under N_2. Then, MeOTf (23 μL, 5.0 equiv) was added, the reaction mixture was stirred for 30 min, and the reaction quenched with Et_3N (33 μL, 6.0 equiv). Solids were filtered off on Celite

and washed with CH_2Cl_2 (20 mL), and the combined filtrate and washings were washed with aq saturated $NaHCO_3$ (15 mL). The aq layer was re-extracted with CH_2Cl_2 (3 × 10 mL), and the combined organic layers were dried and concentrated. The residue was dissolved in 25% AcOH in Ac_2O (5 mL), and the solution was stirred at rt for 12 h and co-concentrated with toluene (3 × 10 mL). Flash chromatography (EtOAc/hexanes, 2:8 → 1:1) of the residue gave trisaccharide **26** (35.7 mg, 0.0305 mmol, 77%) pure as a colourless glass. $[\alpha]_D$ = −56 (*c* 0.7, CH_2Cl_2); ^{1}H NMR (400 MHz, $CDCl_3$, 296 K) δ 7.32–7.17 (m, 20H, H_{arom}), 5.96 (d, *J* = 7.6 Hz, 1H, NH), 5.14 (dd, *J* = 8.1, 10.4 Hz, 1H, H-2"), 5.04 (d, *J* = 3.6 Hz, 1H, H-1'), 4.89 (d, *J* = 11.7 Hz, 1H, C*H*HPh), 4.78–4.66 (m, 6H, H-1, H-3", 2 × CH_2Ph), 4.60 (d, *J* = 11.7 Hz, 1H, C*H*HPh), 4.56 (d, *J* = 12.1 Hz, 1H, C*H*HPh), 4.31 (m, 2H, H-1", C*H*HPh), 4.21 (m, 1H, H-5'), 4.10–4.00 (m, 4H, H-4, H-2', H-6ab"), 3.89 (t, *J* = 6.3 Hz, 1H, H-3), 3.86 (dd, *J* = 2.6, 10.1 Hz, 1H, H-3'), 3.79 (dd, *J* = 4.9, 10.1 Hz, 1H, H-6a), 3.69 (dd, *J* = 3.7, 10.1 Hz, 1H, H-6b), 3.59 (bd, *J* = 1.4 Hz, 1H, H-4'), 3.46–3.40 (m, 4H, H-2, H-5, H-4", H-5"), 3.29, 3.26 (2s, 6H, 2 × OCH_3), 1.73 (s, 3H, C(O)CH_3), 1.14–1.08 (m, 30H, H-6', 3 × C(O)C$(CH_3)_3$); ^{13}C NMR (100 MHz, $CDCl_3$, 296 K) δ 177.7, 177.6, 176.8, 170.3 (C=O), 139.1, 139.0, 138.7, 138.0, 128.5–127.0 (Ar), 100.4 (C-1), 98.8 (C-1"), 96.2 (C-1'), 79.7 (C-3'), 77.0 (C-4'), 76.5 (C-4), 76.2 (C-4"), 74.7 (*C*H_2Ph), 73.4 (C-5"), 73.3 (C-3"), 73.0, 72.6, 72.2 (3 × *C*H_2Ph), 72.0 (C-3), 71.8 (C-2'), 71.6 (C-5), 69.1 (C-2"), 68.8 (C-6), 66.6 (C-5'), 61.5 (C-6"), 61.3 (OCH_3), 56.5 (OCH_3), 53.5 (C-2) 38.8, 38.7 (*C*$(CH_3)_3$), 27.2, 27.1 (C(*C*$H_3)_3$), 23.1 (C(O)*C*H_3), 16.6 (C-6'); HRMS–ESI (*m*/*z*): $[M + H]^+$ calcd for $C_{65}H_{88}NO_{18}$, 1170.6001; found, 1170.6033.

Methyl 2-acetamido-3-*O*-(3,4-acetyl-2-*O*-paramethoxybenzyl-α-L-fucopyranosyl)-6-*O*-benzoyl-4-*O*-(4-chloro-4-deoxy-2,3,6-pivaloyl-β-D-galactopyranosyl)-2-deoxy-β-D-glucopyranoside (27). A mixture of disaccharide acceptor **24** (48 mg, 0.0622 mmol), known [12] thiophenyl fucopyranoside **13** (86 mg, 0.187 mmol, 3.0 equiv) and activated powdered 4 Å molecular sieves (0.3 g) in Et_2O (2.0 mL) was stirred 1 h at rt under N_2. MeOTf (35 μL, 5.0 equiv) was added and the reaction was allowed to proceed for 3 h at rt. More donor **13** (43 mg, 1.5 equiv) was added and the reaction was allowed to proceed for an additional 1 h at rt before being quenched with Et_3N (52 μL, 6.0 equiv). Work up of the reaction and treatment of the crude product in 25% AcOH in Ac_2O (6 mL), as well as the subsequent work-up, were carried out as described above for the synthesis of trisaccharide **26.** Flash chromatography (EtOAc/hexanes, 2:8 → 6:4) of the residue gave trisaccharide **27** (42.5 mg, 0.0379 mmol, 61%) pure as a colourless glass. $[\alpha]_D$ = –21 (*c* 0.8, CH_2Cl_2); ^{1}H NMR (400 MHz, $CDCl_3$, 295 K) δ 8.00–6.84 (m, 9H, H_{arom}), 6.01 (d, *J* = 7.6 Hz, 1H, NH), 5.32–5.24 (m, 3H, H-3', H-4', H-2"), 5.18 (d, *J* = 3.6 Hz, 1H, H-1'), 4.90 (dd, *J* = 3.8, 10.0 Hz, 1H, H-3"), 4.80 (d, *J* = 5.2 Hz, 1H, H-1), 4.72 (dd, *J* = 3.6, 11.9 Hz, 1H,H-6a), 4.65–4.52 (m, 5H, H-6b, H-5', H-1", CH_2Ph), 4.42 (bd, *J* = 3.4 Hz, 1H, H-4"), 4.39–4.34 (m, 2H, H-6ab"), 4.20 (t, *J* = 6.6 Hz, 1H, H-3), 3.96 (t, *J* = 6.4 Hz, 1H, H-4), 3.89 (dd, *J* = 3.7, 10.4 Hz, 1H, H-2'), 3.81–3.76 (m, 2H, H-5, H-5"), 3.76 (s, 3H, OCH_3), 3.58 (m, 1H, H-2), 3.34 (s, 3H, OCH_3), 2.11, 1.95, 1.86 (3s, 9H, 3 × C(O)CH_3), 1.15–1.14 (m, 30H, H-6', 3 × C$(CH_3)_3$); ^{13}C NMR (100 MHz, $CDCl_3$, 295 K) δ 177.6, 177.5, 170.5, 170.4, 169.7, 166.0, 159.2 (C=O), 133.4, 130.4, 129.7, 129.5, 128.9, 128.7 (Ar), 100.4 (C-1), 100.0 (C-1"), 96.1 (C-1'), 73.3 (C-4, C-2'), 72.6 (*C*H_2Ph), 72.2 (C-5"), 71.7 (C-4', C-3, C-5), 71.5 (C-3"), 70.4 (C-3'), 68.0 (C-2"), 65.0 (C-5'), 63.7 (C-6), 62.2 (C-6"), 57.6 (C-4"), 56.6, 55.3 (OCH_3), 53.5 (C-2) 38.9, 38.8, 38.7 (*C*$(CH_3)_3$), 27.1, 27.0, 27.0 (C(*C*$H_3)_3$), 23.2, 20.9, 20.7 (C(O)*C*H_3), 15.9 (C-6'); HRMS–ESI (*m*/*z*): $[M + H]^+$ calcd for $C_{55}H_{77}ClNO_{21}$, 1122.4677; found, 1122.4626.

Methyl 2-acetamido-3-*O*-(3,4-di-*O*-acetyl-2-*O*-*p*-methoxybenzyl-α-L-fucopyranosyl)-6-*O*-benzoyl-2-deoxy-4-*O*-(4-deoxy-4-fluoro-2,3,6-pivaloyl-β-D-galactopyranosyl)-β-D-glucopyranoside (28). A mixture of disaccharide acceptor **25** (24 mg, 0.0318 mmol), known [12] thiophenyl fucopyranoside **13** (44 mg, 0.0953 mmol, 3.0 equiv) and activated powdered 4 Å molecular sieves (0.15 g) in Et_2O (1.5 mL) was stirred for 1 h at rt under N_2. MeOTf (18 μL, 5.0 equiv) was added and the reaction was allowed to proceed for 30 min at rt. More donor **13** (44 mg, 3.0 equiv) was added and the reaction was allowed to proceed for an additional 2 h at rt before being quenched with Et_3N (27 μL, 6.0 equiv). Work up of the reaction and treatment of the crude product in 25% AcOH in Ac_2O (4 mL), as well as the subsequent work-up, were carried out as described above for the synthesis of trisaccharide **26.** Flash chromatography (EtOAc/hexanes, 2:8 → 6:4) of the residue gave trisaccharide **28** (22.8 mg, 0.0206 mmol, 65%) pure as a colourless glass. $[\alpha]_D$ = −37 (*c* 1.2, CH_2Cl_2); ^{1}H NMR (400 MHz, $CDCl_3$, 295 K) δ 8.00–6.84 (m, 9H, H_{arom}), 6.08 (d, *J* = 7.9 Hz, 1H, NH), 5.30–5.22 (m, 3H, H-3', H-4', H-2"), 5.19 (d, *J* = 3.6 Hz, 1H, H-1'), 4.87 (ddd, *J* = 2.4, 10.3 Hz, $J_{H,F}$ = 27.1 Hz, 1H, H-3"), 4.79–4.53 (m, 7H, H-1, H-6ab, H-1", H-4", CH_2Ph), 4.47 (m, 1H, H5'), 4.36–4.33 (m, 2H, H-6ab"), 4.14 (t, *J* = 6.2 Hz, 1H, H-3), 3.97 (t, *J* = 6.1 Hz, 1H, H-4), 3.90–3.83 (m, 2H, H-5, H-2'), 3.76 (s, 3H, OCH_3), 3.69–3.61 (m, 2H, H-2, H-5"), 3.34 (s, 3H, OCH_3), 2.11, 1.95, 1.87 (3s, 9H, 3 × C(O)CH_3), 1.17–1.14 (m, 30H, H-6', 3 × C$(CH_3)_3$); ^{13}C NMR (100 MHz, $CDCl_3$, 295 K) δ 177.6, 177.0, 170.5, 170.4, 169.8, 166.0, 159.2 (C=O), 133.3, 130.3, 129.7, 129.5–128.6, 113.8 (Ar), 100.5 (C-1'), 99.2 (C-1"), 95.9 (C-1), 85.4 (d, $J_{C,F}$ = 186.3 Hz, C-4"), 73.3 (C-2'), 72.9 (C-4), 72.6 (CH_2Ph), 72.1 (C-3), 71.6 (C-5), 71.1 (d, $J_{C,F}$ = 18.1 Hz, C-5"), 70.9 (d, $J_{C,F}$ =

18.5 Hz , C-3"), 70.5 (C-3', C-4'), 68.5 (C-2"), 64.9 (C-5'), 63.8 (C-6), 60.7 (C-6"), 56.6, 55.2 (OCH_3), 52.7 (C-2), 38.9, 38.8, 38.7 ($C(CH_3)_3$), 23.1 ($C(CH_3)_3$), 20.9, 20.7 ($C(O)CH_3$), 15.8 (C-6'); HRMS–ESI (m/z): $[M + H]^+$ calcd for $C_{55}H_{77}FNO_{21}$, 1106.4972; found, 1106.4956.

Supporting Information

Supporting Information File 1

Experimental procedures and characteristics for compounds **8**–**11**, **14**–**19**, **23**–**25**.
[http://www.beilstein-journals.org/bjoc/content/supplementary/1860-5397-8-126-S1.pdf]

Supporting Information File 2

^1H NMR and ^{13}C NMR for compounds **3**–**5**, **8**–**11**, **14**–**28**.
[http://www.beilstein-journals.org/bjoc/content/supplementary/1860-5397-8-126-S2.pdf]

Acknowledgements

We thank the National Science and Engineering Research Council for financial support of this work.

References

1. Fukushi, Y.; Hakomori, S.-i.; Nudelman, E.; Cochran, N. *J. Biol. Chem.* **1984,** *259,* 4681–4685.
2. Fukushi, Y.; Hakomori, S.-i.; Shepard, T. *J. Exp. Med.* **1984,** *160,* 506–520. doi:10.1084/jem.160.2.506
3. Fukushi, Y.; Kannagi, R.; Hakomori, S.-i.; Shepard, T.; Kulander, B. G.; Singer, J. W. *Cancer Res.* **1985,** *45,* 3711–3717.
4. Itzkowitz, S. H.; Yuan, M.; Fukushi, Y.; Palekar, A.; Phelps, P. C.; Shamsuddin, A. M.; Trump, B. T.; Hakomori, S.-i.; Kim, Y. S. *Cancer Res.* **1986,** *46,* 2627–2632.
5. Nakasaki, H.; Mitomi, T.; Noto, T.; Ogoshi, K.; Hanaue, H.; Tanaka, Y.; Makuuchi, H.; Clausen, H.; Hakomori, S.-i. *Cancer Res.* **1989,** *49,* 3662–3669.
6. Singhal, A. K.; Ørntoft, T. F.; Nudelman, E.; Nance, S.; Schibig, L.; Stroud, M. R.; Clausen, H.; Hakomori, S.-i. *Cancer Res.* **1990,** *50,* 1375–1380.
7. Kobata, A.; Ginsburg, V. *J. Biol. Chem.* **1969,** *244,* 5496–5502.
8. Yang, H.-J.; Hakomori, S.-i. *J. Biol. Chem.* **1971,** *246,* 1192–1200.
9. Zhang, S.; Zhang, H. S.; Cordon-Cardo, C.; Reuter, V. E.; Singhal, A. K.; Lloyd, K. O.; Livingston, P. O. *Int. J. Cancer* **1997,** *73,* 50–56. doi:10.1002/(SICI)1097-0215(19970926)73:1<50::AID-IJC9>3.0.CO;2-0
10. Satoh, J.; Kim, S. U. *J. Neurosci. Res.* **1994,** *37,* 466–474. doi:10.1002/jnr.490370406
11. Croce, M. V.; Isla-Larrain, M.; Rabassa, M. E.; Demichelis, S.; Golussi, A. G.; Crespo, M.; Lacunza, E.; Segal-Eiras, A. *Pathol. Oncol. Res.* **2007,** *13,* 130–138. doi:10.1007/BF02893488
12. Asnani, A.; Auzanneau, F.-I. *Carbohydr. Res.* **2003,** *338,* 1045–1054. doi:10.1016/S0008-6215(03)00053-3
13. Asnani, A.; Auzanneau, F.-I. *Carbohydr. Res.* **2008,** *343,* 1653–1664. doi:10.1016/j.carres.2008.04.017
14. Hendel, J. L.; Cheng, A.; Auzanneau, F.-I. *Carbohydr. Res.* **2008,** *343,* 2914–2923. doi:10.1016/j.carres.2008.08.025
15. Wang, J.-W.; Asnani, A.; Auzanneau, F.-I. *Bioorg. Med. Chem.* **2010,** *18,* 7174–7185. doi:10.1016/j.bmc.2010.08.040
16. Thøgersen, H.; Lemieux, R. U.; Bock, K.; Meyer, B. *Can. J. Chem.* **1982,** *60,* 44–57. doi:10.1139/v82-009
17. Imberty, A.; Mikros, E.; Koča, J.; Mollicone, R.; Oriol, R.; Pérez, S. *Glycoconjugate J.* **1995,** *12,* 331–349. doi:10.1007/BF00731336
18. Reynolds, M.; Fuchs, A.; Lindhorst, T. K.; Pérez, S. *Mol. Simul.* **2008,** *34,* 447–460. doi:10.1080/08927020701713878
19. Miller, K. E.; Mukhopadhyay, C.; Cagas, P.; Bush, C. A. *Biochemistry* **1992,** *31,* 6703–6709. doi:10.1021/bi00144a009
20. Haselhorst, T.; Weimar, T.; Peters, T. *J. Am. Chem. Soc.* **2001,** *123,* 10705–10714. doi:10.1021/ja011156h
21. Pérez, S.; Mouhous-Riou, N.; Nifant'ev, N. E.; Tsvetkov, Y. E.; Bachet, B.; Imberty, A. *Glycobiology* **1996,** *6,* 537–542. doi:10.1093/glycob/6.5.537
22. Bundle, D. R. *Pure Appl. Chem.* **1989,** *61,* 1171–1180. doi:10.1351/pac198961071171
23. Meikle, P. J.; Young, N. M.; Bundle, D. R. *J. Immunol. Methods* **1990,** *132,* 255–261. doi:10.1016/0022-1759(90)90037-V
24. Reimer, K. B.; Gidney, M. A. J.; Bundle, D. R.; Pinto, B. M. *Carbohydr. Res.* **1992,** *232,* 131–142. doi:10.1016/S0008-6215(00)91000-0
25. Bundle, D. R. Recognition of Carbohydrate Antigens by Antibody Binding Sites. In *Bioorganic Chemistry: Carbohydrates;* Hecht, S. M., Ed.; Oxford University Press: New York, 1999; pp 370–440.
26. Lemieux, R. U. *Acc. Chem. Res.* **1996,** *29,* 373–380. doi:10.1021/ar9600087
27. Woods, R. J. *Glycoconjugate J.* **1998,** *15,* 209–216. doi:10.1023/A:1006984709892
28. Clarke, C.; Woods, R. J.; Gluska, J.; Cooper, A.; Nutley, M. A.; Boons, G.-J. *J. Am. Chem. Soc.* **2001,** *123,* 12238–12247. doi:10.1021/ja004315q
29. Laederach, A.; Reilly, P. J. *Proteins: Struct., Funct., Bioinf.* **2005,** *60,* 591–597. doi:10.1002/prot.20545
30. Dong, D.; Gourmala, C.; Zhang, Y.; Zhang, Y. *Sci. China: Chem.* **2010,** *53,* 1963–1969. doi:10.1007/s11426-010-4060-6
31. Jacquinet, J.-C.; Sinaÿ, P. *J. Chem. Soc., Perkin Trans. 1* **1979,** 314–318. doi:10.1039/P19790000314
32. Hindsgaul, O.; Norberg, T.; Le Pendu, J.; Lemieux, R. U. *Carbohydr. Res.* **1982,** *109,* 109–142. doi:10.1016/0008-6215(82)84034-2
33. Sato, S.; Ito, Y.; Nukada, T.; Nakahara, Y.; Ogawa, T. *Carbohydr. Res.* **1987,** *167,* 197–210. doi:10.1016/0008-6215(87)80279-3
34. Jain, R. K.; Matta, K. L. *Carbohydr. Res.* **1992,** *226,* 91–100. doi:10.1016/0008-6215(92)84057-Y
35. Numomura, S.; Iida, M.; Numata, M.; Sugimoto, M.; Ogawa, T. *Carbohydr. Res.* **1994,** *263,* C1–C6. doi:10.1016/0008-6215(94)00264-9
36. Jain, R. K.; Vig, R.; Rampal, R.; Chandrasekaran, E. V.; Matta, K. L. *J. Am. Chem. Soc.* **1994,** *116,* 12123–12124. doi:10.1021/ja00105a091
37. Yan, L.; Kahne, D. *J. Am. Chem. Soc.* **1996,** *118,* 9239–9248. doi:10.1021/ja9608555
38. Lay, L.; Manzoni, L.; Schmidt, R. R. *Carbohydr. Res.* **1998,** *310,* 157–171. doi:10.1016/S0008-6215(98)00148-7
39. Figueroa-Pérez, S.; Verez-Bencomo, V. *Tetrahedron Lett.* **1998,** *39,* 9143–9146. doi:10.1016/S0040-4039(98)02104-2

40. Cao, S.; Gan, Z.; Roy, R. *Carbohydr. Res.* **1999,** *318,* 75–81. doi:10.1016/S0008-6215(99)00080-4
41. Gan, Z.; Cao, S.; Wu, Q.; Roy, R. *J. Carbohydr. Chem.* **1999,** *18,* 755–773. doi:10.1080/07328309908544034
42. Zhang, Y.-M.; Esnault, J.; Mallet, J.-M.; Sinaÿ, P. *J. Carbohydr. Chem.* **1999,** *18,* 419–427. doi:10.1080/07328309908544006
43. Zhu, T.; Boons, G.-J. *J. Am. Chem. Soc.* **2000,** *122,* 10222–10223. doi:10.1021/ja001930l
44. Zhu, T.; Boons, G.-J. *Chem.–Eur. J.* **2001,** *7,* 2382–2389. doi:10.1002/1521-3765(20010601)7:11<2382::AID-CHEM23820>3.0.CO;2-2
45. La Ferla, B.; Prosperi, D.; Lay, L.; Giovanni, R.; Panza, L. *Carbohydr. Res.* **2002,** *337,* 1333–1342. doi:10.1016/S0008-6215(02)00164-7
46. Xia, J.; Alderfer, J. L.; Locke, R. D.; Piskorz, C. F.; Matta, K. L. *J. Org. Chem.* **2003,** *68,* 2752–2759. doi:10.1021/jo020698u
47. Mukherjee, D.; Sarkar, S. K.; Chattopadhyay, P.; Chowdhury, U. S. *J. Carbohydr. Chem.* **2005,** *24,* 251–259. doi:10.1081/CAR-200058529
48. Toepfer, A.; Schmidt, R. R. *Tetrahedron Lett.* **1992,** *33,* 5161–5164. doi:10.1016/S0040-4039(00)79122-2
49. Hummel, G.; Schmidt, R. R. *Tetrahedron Lett.* **1997,** *38,* 1173–1176. doi:10.1016/S0040-4039(97)00006-3
50. Kretzschmar, G.; Stahl, W. *Tetrahedron* **1998,** *54,* 6341–6358. doi:10.1016/S0040-4020(98)00294-4
51. Manzoni, L.; Lay, L.; Schmidt, R. R. *J. Carbohydr. Chem.* **1998,** *17,* 739–758. doi:10.1080/07328309808002349
52. de la Fuente, J. M.; Penadés, S. *Tetrahedron: Asymmetry* **2002,** *13,* 1879–1888. doi:10.1016/S0957-4166(02)00480-9
53. de Paz, J.-L.; Ojeda, R.; Barrientos, A. G.; Penadés, S.; Martín-Lomas, M. *Tetrahedron: Asymmetry* **2005,** *16,* 149–158. doi:10.1016/j.tetasy.2004.11.066
54. Windmüller, R.; Schmidt, R. R. *Tetrahedron Lett.* **1994,** *35,* 7927–7930. doi:10.1016/0040-4039(94)80013-8
55. Sato, K.-i.; Seki, H.; Yoshimoto, A.; Nanaumi, H.; Takai, Y.; Ishido, Y. *J. Carbohydr. Chem.* **1998,** *17,* 703–727. doi:10.1080/07328309808002347
56. Lönn, H. *Carbohydr. Res.* **1985,** *139,* 105–113. doi:10.1016/0008-6215(85)90011-4
57. Risbood, P. A.; Reed, L. A., III; Goodman, L. *Carbohydr. Res.* **1981,** *88,* 245–251. doi:10.1016/S0008-6215(00)85538-X
58. Lattrell, R.; Lohaus, G. *Justus Liebigs Ann. Chem.* **1974,** 901–920. doi:10.1002/jlac.197419740606
59. Albert, R.; Dax, K.; Link, R. W.; Stütz, A. E. *Carbohydr. Res.* **1983,** *118,* C5–C6. doi:10.1016/0008-6215(83)88062-8
60. Dong, H.; Pei, Z.; Ramström, O. *J. Org. Chem.* **2006,** *71,* 3306–3309. doi:10.1021/jo052662i
61. Arita, H.; Ueda, N.; Matsushima, Y. *Bull. Chem. Soc. Jpn.* **1972,** *45,* 567–569. doi:10.1246/bcsj.45.567
62. Kasuya, M. C.; Ito, A.; Hatanaka, K. *J. Fluorine Chem.* **2007,** *128,* 562–565. doi:10.1016/j.jfluchem.2007.02.013
63. Subotkowski, W.; Friedrich, D.; Weiberth, F. J. *Carbohydr. Res.* **2011,** *346,* 2323–2326. doi:10.1016/j.carres.2011.07.019
64. Paulsen, H. *Angew. Chem., Int. Ed. Engl.* **1982,** *21,* 155–173. doi:10.1002/anie.198201553
65. Crich, D.; Dudkin, V. *J. Am. Chem. Soc.* **2001,** *123,* 6819–6825. doi:10.1021/ja010086b
66. Liao, L.; Auzanneau, F.-I. *Org. Lett.* **2003,** *5,* 2607–2610. doi:10.1021/ol034669x
67. Hendel, J. L.; Wang, J.-W.; Jackson, T. A.; Hardmeier, K.; De Los Santos, R.; Auzanneau, F.-I. *J. Org. Chem.* **2009,** *74,* 8321–8331. doi:10.1021/jo901616p
68. Wang, A.; Hendel, J.; Auzanneau, F.-I. *Beilstein J. Org. Chem.* **2010,** *6,* No. 17. doi:10.3762/bjoc.6.17
69. Wang, A.; Auzanneau, F.-I. *Carbohydr. Res.* **2010,** *345,* 1216–1221. doi:10.1016/j.carres.2010.03.038
70. Liao, L.; Auzanneau, F.-I. *J. Org. Chem.* **2005,** *70,* 6265–6273. doi:10.1021/jo050707+
71. Cheng, A.; Hendel, J. L.; Colangelo, K.; Bonin, M.; Auzanneau, F.-I. *J. Org. Chem.* **2008,** *73,* 7574–7579. doi:10.1021/jo801117y
72. Liao, L.; Robertson, V.; Auzanneau, F.-I. *Carbohydr. Res.* **2005,** *340,* 2826–2832. doi:10.1016/j.carres.2005.09.025
73. Ruttens, B.; Kováč, P. *Carbohydr. Res.* **2006,** *341,* 1077–1080. doi:10.1016/j.carres.2006.04.007
74. Kwon, Y.-U.; Soucy, R. L.; Snyder, D. A.; Seeberger, P. H. *Chem.–Eur. J.* **2005,** *11,* 2493–2504. doi:10.1002/chem.200400934
75. Hendel, J. L.; Auzanneau, F.-I. *Eur. J. Org. Chem.* **2011,** 6864–6876. doi:10.1002/ejoc.201101342
76. Armarego, W. L. F.; Chai, C. L. L., Eds. *Purification of Laboratory Chemicals,* 5th ed.; Elsevier, 2003.

License and Terms

Beilstein Journal of Organic Chemistry

Studies on the substrate specificity of a GDP-mannose pyrophosphorylase from *Salmonella enterica*

Lu Zou, Ruixiang Blake Zheng and Todd L. Lowary*

Full Research Paper

Open Access

Address:
Alberta Glycomics Centre and Department of Chemistry, The University of Alberta, Edmonton, AB T6G 2G2, Canada

Email:
Todd L. Lowary* - tlowary@ualberta.ca

* Corresponding author

Keywords:
chemoenzymatic synthesis; kinetics; methylation; pyrophosphorylase; sugar nucleotide

Beilstein J. Org. Chem. **2012,** *8,* 1219–1226.
doi:10.3762/bjoc.8.136

Received: 29 May 2012
Accepted: 29 June 2012
Published: 01 August 2012

This article is part of the Thematic Series "Synthesis in the glycosciences II".

Guest Editor: T. K. Lindhorst

Abstract

A series of methoxy and deoxy derivatives of mannopyranose-1-phosphate (Man*p*-1P) were chemically synthesized, and their ability to be converted into the corresponding guanosine diphosphate mannopyranose (GDP-Man*p*) analogues by a pyrophosphorylase (GDP-ManPP) from *Salmonella enterica* was studied. Evaluation of methoxy analogues demonstrated that GDP-ManPP is intolerant of bulky substituents at the C-2, C-3, and C-4 positions, in turn suggesting that these positions are buried inside the enzyme active site. Additionally, both the 6-methoxy and 6-deoxy Man*p*-1P derivatives are good or moderate substrates for GDP-ManPP, thus indicating that the C-6 hydroxy group of the Man*p*-1P substrate is not required for binding to the enzyme. When taken into consideration with other previously published work, it appears that this enzyme has potential utility for the chemoenzymatic synthesis of GDP-Man*p* analogues, which are useful probes for studying enzymes that employ this sugar nucleotide as a substrate.

Introduction

Modified sugar nucleotide analogues are valuable probes to study glycosyltransferases and other enzymes that use these activated glycosylating agents as substrates [1-5]. The synthesis of natural and non-natural sugar nucleotides is therefore a topic of continuing interest [6]. The classical method for chemically synthesizing sugar nucleotides involves the preparation of a sugar 1-phosphate derivative followed by its coupling to an activated nucleoside monophosphate to form the key pyrophosphate moiety (Figure 1A) [7]. In general, the yield of this process is low, and the purification of the product can be tedious; hence, the development of new methods to prepare sugar nucleotides remains an area of active research [6].

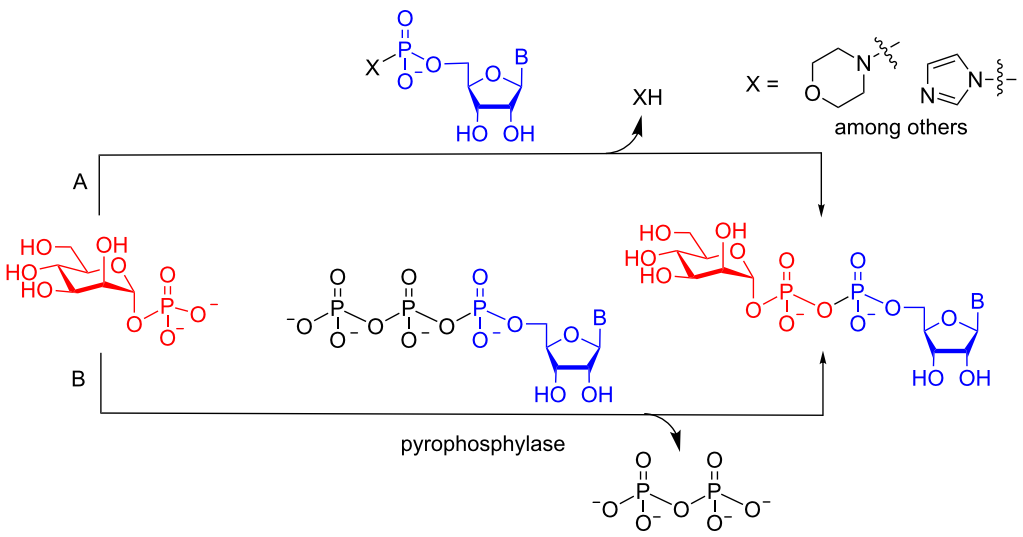

Figure 1: (A) Conventional approach for the chemical synthesis of sugar nucleotides from sugar 1-phosphates; (B) enzymatic conversion of sugar 1-phosphates into sugar nucleotides.

Although improved chemical methods have been developed [8-13], another attractive strategy is to employ a chemoenzymatic approach, in which a synthetic sugar 1-phosphate derivative is converted to the sugar nucleotide by a pyrophosphorylase (Figure 1B) [14,15]. This approach is increasingly used for the synthesis of sugar nucleotides, but a limitation is that the specificity of the pyrophosphorylase must be sufficiently broad to recognize the synthetic sugar 1-phosphate derivative. However, some of these enzymes have been demonstrated to have broad specificity, or can be engineered to have broad specificity, with regard to both the sugar 1-phosphate and nucleotide substrates [16-19].

As part of a larger study on the specificity of mannosyltransferases involved in mycobacterial glycan biosynthesis [20-22], we had the need for a panel of singly deoxygenated and methylated guanosine diphosphophosphate mannopyranose (GDP-Man) derivatives. In developing a strategy for the synthesis of these compounds, we chose to take advantage of a GDP-mannose pyrophosphorylase (GDP-ManPP) from *Salmonella enterica* [23], which had previously been shown to have a relaxed specificity for the sugar 1-phosphate moiety [24,25]. In particular, it has been shown that the enzyme will accept mannopyranosyl 1-phosphate (Man*p*-1P) derivatives deoxygenated at C-2, C-3 and C-4 (**1**–**3**, Figure 2), as well as a substrate lacking the hydroxymethyl group at C-5 (**4**) [24]. A series monoazido derivatives (**5**–**8**) were also shown to be substrates [25]. To further probe the potential of this enzyme for the chemoenzymatic synthesis of modified GDP-Man*p* derivatives, we describe here the preparation of all four singly methylated Man*p*-1P analogues **9**–**12**, as well as the 6-deoxy-Man*p*-1P derivative **13**, and an initial evaluation of their ability to serve as a substrate for *S. enterica* GDP-ManPP.

Results and Discussion

Synthesis of 2-methoxy derivative 9

The synthesis of sugar 1-phosphate **9** containing a methyl group at O-2 commenced from 3-*O*-benzyl-4,6-*O*-benzylidene-α-D-mannopyranoside **14** [26] as illustrated in Scheme 1. Methyl-

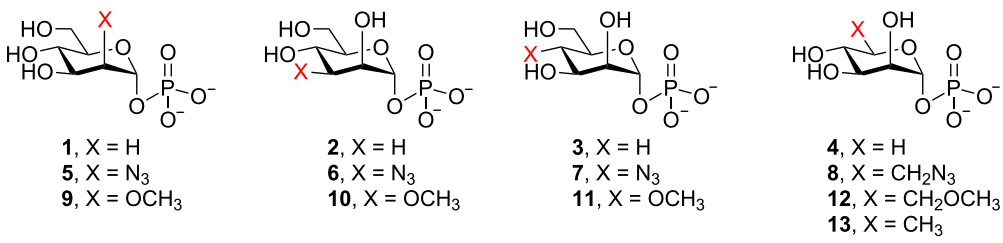

Figure 2: Structures of the Man*p*-1P derivatives (**1**–**8**) previously shown [24,25] to be substrates for *S. enterica* GDP-ManPP and analogues **9**–**13** studied in this paper.

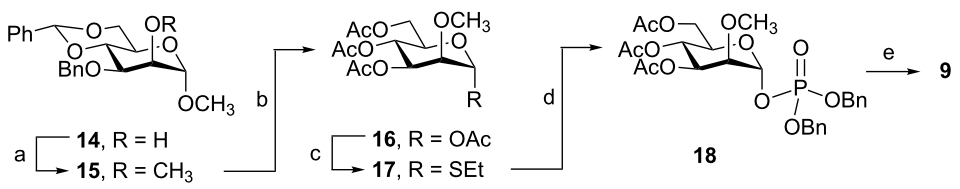

Scheme 1: Reagents and conditions: (a) CH_3I, NaH, DMF, 80%; (b) Ac_2O–HOAc–H_2SO_4, 35:15:1, 81%; (c) EtSH, $BF_3{\cdot}OEt_2$, CH_2Cl_2, 65%; (d) HO-P(O)$(OBn)_2$, NIS, AgOTf, CH_2Cl_2, 84%; (e) (i) H_2, $Pd(OH)_2$–C, toluene, Et_3N, pyridine; (ii) CH_3OH–H_2O–Et_3N, 5:2:1, 92%.

ation of the alcohol under standard conditions proceeded in 80% yield affording **15**. The benzylidene protecting group was cleaved, together with the methyl glycoside, by acetolysis giving the tetra-*O*-acetylated compound **16** in 81% yield. This glycosyl acetate was converted to the corresponding thioglycoside (**17**), which was, in turn, coupled with dibenzyl phosphate under NIS–AgOTf activation conditions, providing compound **18** in 55% yield over two steps from **16**. The anomeric stereochemistry in **18** was confirmed by the magnitude of the $^1J_{C1,H1}$, which was 177.9 Hz, consistent with α-stereochemistry as described earlier by Timmons and Jakeman for rhamnopyranosyl phosphates [27]. In the other phosphorylation reactions reported in this paper, the anomeric stereochemistry was determined in an analogous manner. Compound **18** was then deprotected in two steps, namely catalytic hydrogenolysis and then, without further purification, treatment with a mixture of CH_3OH–H_2O–Et_3N 5:2:1 to remove the acetyl groups. This series of reactions gave 2-methoxy Man*p*-1P analogue **9** in 92% overall yield from **18**.

Synthesis of 3-methoxy derivative **10**

The preparation of the 3-methoxy Man*p*-1P analogue **10** followed a route similar to that used for the synthesis of **9** (Scheme 2). Methyl 2-*O*-benzyl-4,6-*O*-benzylidene-α-D-mannopyranoside (**19**) [26] was first methylated giving **20** and then converted into glycosyl acetate **21** in 49% yield over the two steps. Subsequent thioglycosylation provided a 52% yield of **22**. The protected dibenzyl phosphate **23** was next formed by the NIS–AgOTf promoted glycosylation of dibenzyl phosphate with **22**, which afforded the desired compound, **23**, in 75% yield. Hydrogenolysis of the benzyl groups and deacylation led to the formation, in 67% yield, of Man*p*-1P derivative **10**.

Synthesis of 4-methoxy derivative **11**

As illustrated in Scheme 3, the synthesis of the 4-methoxy Man*p*-1P analogue **11** started by treatment of methyl α-D-mannopyranoside (**24**) with trityl chloride in pyridine. The product, **25**, was then converted to the isopropylidene acetal **26** in 65% overall yield from **24**. The hydroxy group in **26** was

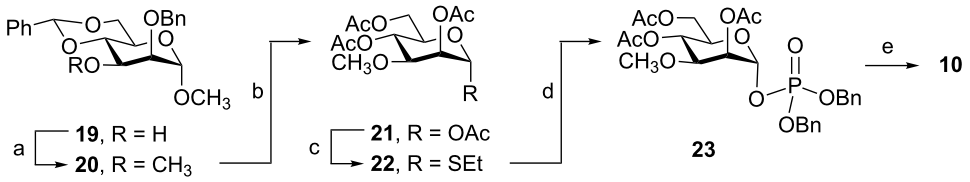

Scheme 2: Reagents and conditions: (a) CH_3I, NaH, DMF, 76%; (b) Ac_2O–HOAc–H_2SO_4, 35:15:1, 65%; (c) EtSH, $BF_3{\cdot}OEt_2$, CH_2Cl_2, 52%; (d) HO-P(O)$(OBn)_2$, NIS, AgOTf, CH_2Cl_2, 75%; (e) (i) H_2, $Pd(OH)_2$–C, toluene, Et_3N, pyridine; (ii) CH_3OH–H_2O–Et_3N, 5:2:1, 67%.

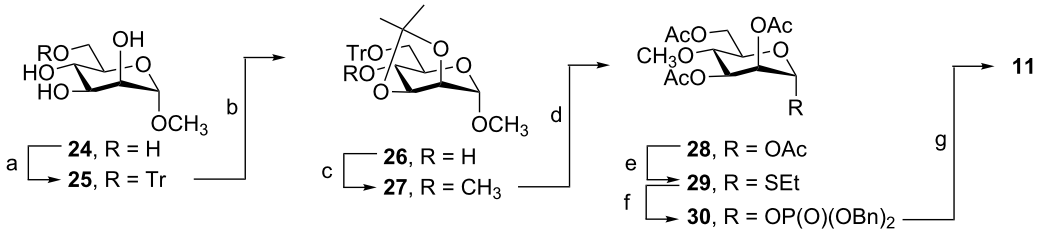

Scheme 3: Reagents and conditions: (a) TrCl, DMAP, pyridine, 85%; (b) DMP, *p*-TsOH, 76%; (c) CH_3I, NaH, DMF, 91%; (d) Ac_2O–HOAc–H_2SO_4, 35:15:1, 55%; (e) EtSH, $BF_3{\cdot}OEt_2$, CH_2Cl_2, 70%; (f) HO-P(O)$(OBn)_2$, NIS, AgOTf, CH_2Cl_2, 80%; (g) (i) H_2, $Pd(OH)_2$–C, toluene, Et_3N, pyridine; (ii) CH_3OH–H_2O–Et_3N, 5:2:1, 70%.

methylated under standard conditions (CH_3I, NaH) to give the 4-methoxy analogue **27** in 91% yield. Acetolysis of **27** to the corresponding glycosyl acetate **28**, followed by reaction with ethanethiol and $BF_3{\cdot}OEt_2$, yielded thioglycoside **29**, in a modest 39% yield from **27** over two steps. This compound was then converted to **11**, in 56% yield, as outlined above, by successive phosphorylation and deprotection.

Synthesis of 6-methoxy derivative 12

Two routes, differing in the choice of protecting groups, were explored to produce the 6-methoxy Man*p*-1P derivative **12** (Scheme 4 and Scheme 5). In one route, the C-2, C-3, and C-4 hydroxy groups of the mannose residues were protected with benzyl ethers and in the other they were protected with benzoyl esters. The overall yields of these two methods were 30% and 17%, respectively. In the first method (Scheme 4), the initial step was the conversion, in 78% yield, of the fully acetylated thioglycoside **31** [28] into silyl ether **32** by treatment with sodium methoxide and then *tert*-butyldiphenylchlorosilane in DMF. Benzylation of **32** using benzyl bromide and sodium hydride gave **33** in 84% yield. The TBDPS group was then cleaved and replaced with a methyl group to give the 6-methoxy compound **35** in 72% yield over two steps. The protected dibenzyl phosphate **36** was formed in 70% yield by phosphorylation as described for the synthesis of **9**–**11**. Catalytic hydrogenolysis in the presence of $NaHCO_3$ was used to cleave all the benzyl groups, which gave the 6-methoxy Man*p*-1P derivative **12** in 91% yield.

The second route to **12** began with methyl 2,3,4-tri-*O*-benzoyl-α-D-mannopyranoside (**37**) [29] and is illustrated in Scheme 5. Methylation of the free OH, even under mildly basic conditions (e.g., Ag_2O–$CaSO_4$), led to significant amounts of acyl group migration, and the desired product was obtained in only 52% yield. Nevertheless, enough material was produced to move forward. Acetolysis conditions were used to replace the methyl group at the anomeric center in **38** with an acetyl group, resulting in a 96% yield of **39**. Thioglycosylation, followed by coupling of the resulting thioglycoside donor **40** (obtained in 75% yield) with dibenzyl phosphate, gave phosphate **41** in a yield of 67% over the two steps. The 6-methoxy Man*p*-1P analogue **12** was obtained by catalytic hydrogenolysis of the benzyl ethers followed by treatment with CH_3OH–H_2O–Et_3N 5:2:1 providing **12** in 85% yield over two steps.

Synthesis of 6-deoxy derivative 13

The synthesis of the 6-deoxy Man*p*-1P analogue **13** used an intermediate (**37**) prepared in the course of the synthesis of the 6-methoxy analogue (Scheme 6). First, the hydroxy group of **37** was converted to the corresponding iodide in 65% yield, by using triphenylphosphine and iodine. The product, **42**, was then subjected to acetolysis and catalytic hydrogenation, which gave 6-deoxy glycosyl acetate derivative **43** in 72% yield. The subsequent thioglycosylation, phosphorylation and deprotection steps proceeded, as outlined above, to give the 6-deoxy Man*p*-1P **13** in 43% yield over four steps.

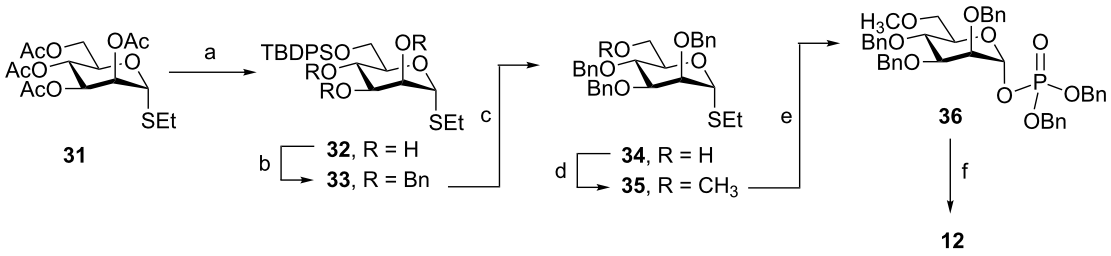

Scheme 4: Reagents and conditions: (a) (i) $NaOCH_3$, CH_3OH; (ii) TBDPSCl, imidazole, DMF, 78%; (b) BnBr, NaH, TBAI, 84%; (c) TBAF, THF, 83%; (d) CH_3I, NaH, DMF, 87%; (e) HO-P(O)$(OBn)_2$, NIS, AgOTf, CH_2Cl_2, 70%; (f) H_2, $Pd(OH)_2$–C, $NaHCO_3$, CH_3OH, 91%.

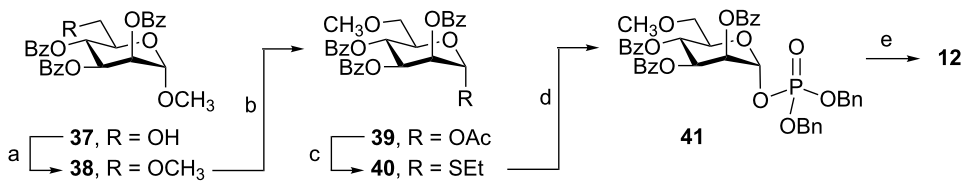

Scheme 5: Reagents and conditions: (a) Ag_2O, $CaSO_4$, CH_3I, 52%; (b) Ac_2O–HOAc–H_2SO_4, 70:30:1, 96%; (c) EtSH, $BF_3{\cdot}OEt_2$, CH_2Cl_2, 75%; (d) HO-P(O)$(OBn)_2$, NIS, AgOTf, CH_2Cl_2, 89%; (e) (i) H_2, $Pd(OH)_2$–C, toluene, Et_3N, pyridine; (ii) CH_3OH–H_2O–Et_3N, 5:2:1, 85%.

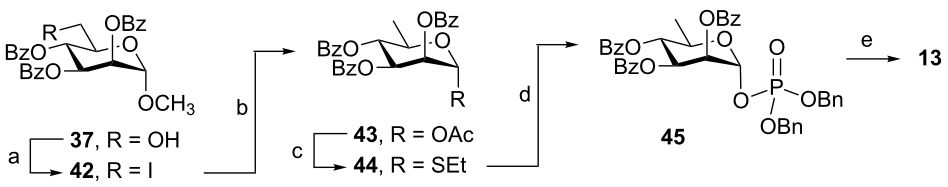

Scheme 6: Reagents and conditions: (a) PPh_3, imidazole, I_2, 65%; (b) (i) Ac_2O–HOAc–H_2SO_4, 35:15:1; (ii) Pd–C, H_2, Et_3N, EtOAc, 72%; (c) EtSH, $BF_3{\cdot}OEt_2$, CH_2Cl_2, 89%, α/β 4:1; (d) HO-P(O)(OBn)$_2$, NIS, AgOTf, CH_2Cl_2, 67%; (e) (i) H_2, Pd(OH)$_2$–C, toluene, Et_3N, pyridine; (ii) CH_3OH–H_2O–Et_3N, 5:2:1, 72%.

Evaluation of 9–13 as substrates for GDP-Man pyrophosphorylase

With **9**–**13** in hand, each was evaluated as a substrate for the *S. enterica* GDP-ManPP. Before doing that, the recombinant protein was produced and the natural substrate for the enzyme, Man*p*-1P (**46**, Figure 3), was evaluated by incubation with the enzyme and GTP. The reaction was monitored by HPLC (Figure S1 in Supporting Information File 1) and stopped when the complete consumption of GTP was observed. Simultaneous with the loss of the GTP was the appearance of the signal for a new product, which was found to elute at a retention time similar to that for an authentic sample of GDP-Man*p*. The product was isolated, and analysis by high-resolution electrospray ionization mass spectrometry revealed an ion with m/z = 604.0691, which corresponds to the $[M - H]^-$ ion (calcd m/z = 604.0699) of GDP-Man*p*.

Having established that the enzyme GDP-ManPP was active, we carried out the same incubations for **9**–**13**, and in all cases the corresponding GDP-Man*p* analogue peaks could be observed (Figure S2 in Supporting Information File 1). However, in the case of **11** and **9**, a peak corresponding to GDP, resulting from hydrolysis of the GDP-sugar, was also observed, and, in the case of **9**, a much smaller amount of the GDP-Man*p* analogue was produced. To confirm the identity of each GDP-Man*p* analogue, the product peaks were isolated and analysed by electrospray ionization mass spectrometry. For the reactions involving **9**–**12** a signal at $m/z \approx 618$ was observed, as would be expected for the $[M - H]^-$ ion of the methylated GDP-Man derivatives (**48**–**51**, Figure 4). Similarly, for the reaction with **13**, a signal at $m/z \approx 588$ was observed in the mass spectrum consistent with the 6-deoxy GDP-Man derivative **52**.

Relative activity of Man*p*-1P analogues with GDP-ManPP

After it was established that all five Man*p*-1P analogues could serve as substrates for GDP-ManPP, the relative activity with each was assessed. This was done by using an established colorimetric activity assay, which relies on the detection of the pyrophosphate (PPi, Figure 3) formed as a byproduct of the

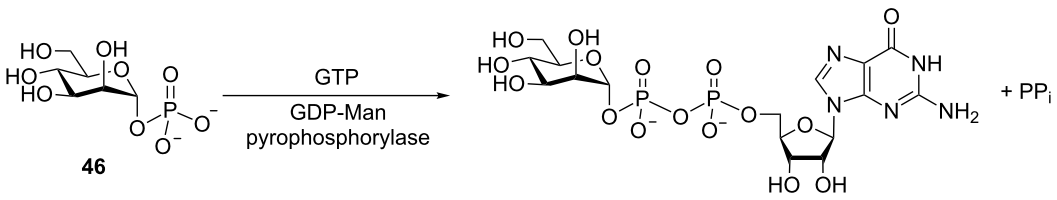

Figure 3: Reaction catalyzed by GDP-ManPP.

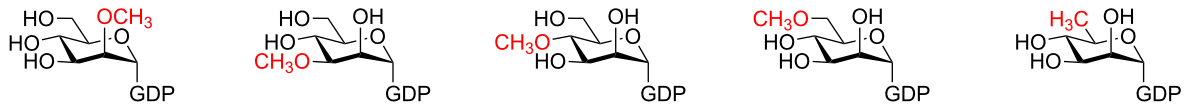

48	49	50	51	52
$[M - H]^-$ m/z = 618.0848	$[M - H]^-$ m/z = 618.0849	$[M - H]^-$ m/z = 618.0848	$[M - H]^-$ m/z = 618.0852	$[M - H]^-$ m/z = 588.0746
calcd m/z = 618.0855	calcd m/z = 618.0855	calcd m/z = 618.0855	calcd m/z = 618.0855	calcd m/z = 588.0750

Figure 4: Structure of modified GDP-Man derivatives **48**–**52** produced from **9**–**13**.

enzymatic reaction [30]. As illustrated in Figure 5, all five synthetic derivatives **9**–**13** were active as substrates, although at lower levels than the parent compound **46**. The 6-methoxy (**12**) and 6-deoxy (**13**) analogues, demonstrated moderate to good relative activities, while the 2-methoxy (**9**), 3-methoxy (**10**), and 4-methoxy (**11**) compounds showed much lower activities. For example, the 2-methoxy, 3-methoxy, and 4-methoxy analogues displayed a 6-, 14-, and 17-fold decrease relative to **46**, respectively. Because both the 6-deoxy and 6-methoxy analogues (**12** and **13**) showed relatively good activity it is likely that this hydroxy group does not interact significantly with the enzyme. On the other hand, because the 2-methoxy, 3-methoxy, and 4-methoxy compounds all showed a large decrease in activity, it is likely that these positions are bound tightly in the active site of the enzyme. A graphical summary of the substrate specificity for GDP-ManPP is shown in Figure 6.

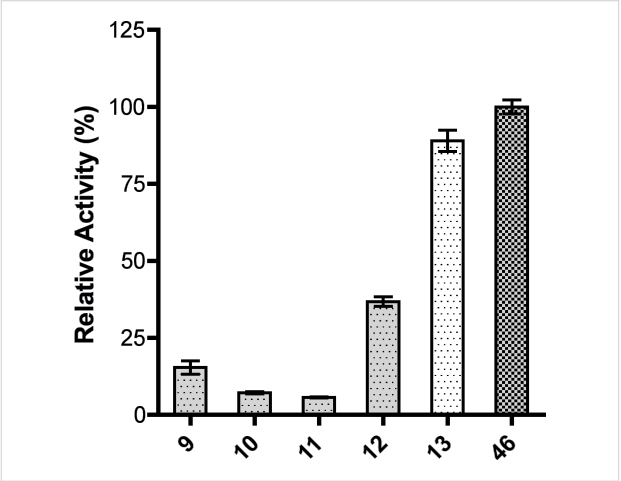

Figure 5: Comparison of the relative activity of synthetic Man*p*-1P analogues **9**–**13** for GDP-ManPP, with that of the parent compound **46**. Error bars represent the standard deviation of duplicate reactions.

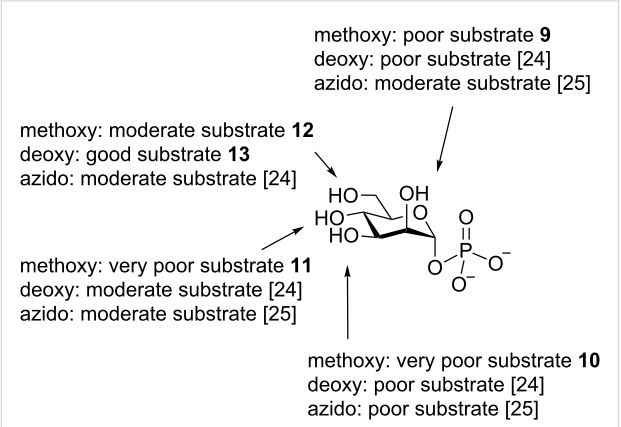

Figure 6: Summary of the substrate specificity of GDP-ManPP. Data from previous studies on the enzyme are also included as indicated [24,25].

Kinetic analysis of Man*p*-1P analogues with GDP-ManPP

To better understand how these **9**–**13** interact with GDP-ManPP, kinetic analyses were performed by using the colorimetric activity assay mentioned above (Table 1). Both the 6-methoxy Man*p*-1P (**12**) and 6-deoxy Man*p*-1P (**13**) derivatives bind relatively well to the enzyme, showing only a two- or three-fold increase in K_M, respectively, compared to the native Man*p*-1P donor **46**. The turnover rate of 6-methoxy analogue **12** is, however, much lower than the 6-deoxy counterpart (**13**) and the natural substrate **46**, as substantiated by a greater than 10-fold decrease in k_{cat}. Taken together, these results suggest that the C-6 hydroxy group does not engage in any critical hydrogen-bonding interactions and that a bulky substituent interferes with the rate of substrate turnover. The binding of the 2-methoxy (**9**) and 4-methoxy (**11**) analogues is very weak compared to the native substrate, as seen by the greater then 100-fold increase in K_M; consequently, the turnover rates are also low. The binding between 3-methoxy analogue **10** is moderate, with only a five-fold increase in the observed K_M, but it shows an extremely low turnover rate. These results all suggest that GDP-ManPP is not tolerant of bulky substituents at the C-2, C-3, and C-4 positions, which is consistent with the results obtained from their relative activity. It should be noted that these trends are consistent with earlier studies of the enzyme using deoxygenated or azido analogues [24,25].

Table 1: K_M, k_{cat}, and k_{cat}/K_M of GDP-ManPP kinetic studies.

compound	K_M (μM)	k_{cat} (min^{-1})	k_{cat}/K_M ($min^{-1}·μM^{-1}$)
9 (2-methoxy analogue)	4000 ± 1100	70 ± 11	(2 ± 1) × 10^{-2}
10 (3-methoxy analogue)	200 ± 72	5.2 ± 0.7	(2.6 ± 0.1) × 10^{-2}
11 (4-methoxy analogue)	3400 ± 870	31 ± 4.7	(9 ± 5) × 10^{-3}
12 (6-methoxy analogue)	120 ± 18	27 ± 1	0.23 ± 0.06
13 (6-deoxy analogue)	70 ± 13	300 ± 13	4 ± 1
46 (Man-1P)	40 ± 6	360 ± 16	9 ± 3

Conclusion

In this paper, we report the synthesis of a panel of methoxy and deoxy analogues of Man*p*-1P. Five analogues, **9**–**13**, in which one of the hydroxy groups was methylated or deoxygenated were generated by chemical synthesis, and the ability of these compounds to be converted to the corresponding GDP-Man*p* analogues by GDP-ManPP from *S. enterica* was evaluated. All the derivatives acted as substrates for GDP-ManPP, but with uniformly lower activity than the natural substrate Man-1P. The

results suggest that the C-2, C-3, and C-4 hydroxy groups of Man*p*-1P are bound within the active site of GDP-ManPP and the addition of a methyl group at these positions is tolerated very poorly. Conversely, the addition of a methyl group to, or deoxygenation of, O-6 had a much smaller effect, suggesting that this position protrudes from the active site, or is accommodated in a pocket that can tolerate either of these modifications. These results are consistent with earlier studies of this enzyme, which were focused on deoxygenated and azido derivatives [24,25]. Considered together, our studies and those published previously suggest that this enzyme can be used to access deoxy and azido derivatives of GDP-Man on a preparative scale, but that the synthesis of analogues containing more sterically demanding groups is likely to be only possible when the modifications are present on O-6.

Experimental

Detailed experimental procedures can be found in Supporting Information File 1.

Supporting Information

Supporting Information File 1

Detailed experimental procedures.
[http://www.beilstein-journals.org/bjoc/content/supplementary/1860-5397-8-136-S1.pdf]

Acknowledgements

This work was supported by the Alberta Glycomics Centre, the University of Alberta and the Natural Sciences and Engineering Research Council of Canada. We thank Dr. Warren Wakarchuk at the National Research Council of Canada for providing the plasmid containing the GDP-ManPP gene, and Mr. Myles B. Poulin for technical assistance on the enzyme assay.

References

1. Errey, J. C.; Mann, M. C.; Fairhurst, S. A.; Hill, L.; McNeil, M. R.; Naismith, J. H.; Percy, J. M.; Whitfield, C.; Field, R. A. *Org. Biomol. Chem.* **2009,** *7,* 1009–1016. doi:10.1039/b815549f
2. Peltier, P.; Beláňová, M.; Dianišková, P.; Zhou, R.; Zheng, R. B.; Pearcey, J. A.; Joe, M.; Brennan, P. J.; Nugier-Chauvin, C.; Ferrières, V.; Lowary, T. L.; Daniellou, R.; Mikušová, K. *Chem. Biol.* **2010,** *17,* 1356–1366. doi:10.1016/j.chembiol.2010.10.014
3. Poulin, M. B.; Zhou, R.; Lowary, T. L. *Org. Biomol. Chem.* **2012,** *10,* 4074–4087. doi:10.1039/c2ob25159k
4. Brown, C. D.; Rusek, M. S.; Kiessling, L. L. *J. Am. Chem. Soc.* **2012,** *134,* 6552–6555. doi:10.1021/ja301723p
5. Zhang, Q.; Liu, H.-w. *J. Am. Chem. Soc.* **2001,** *123,* 6756–6766. doi:10.1021/ja010473l
6. Wagner, G. K.; Pesnot, T.; Field, R. A. *Nat. Prod. Rep.* **2009,** *26,* 1172–1194. doi:10.1039/b909621n
7. Roseman, S.; Distler, J. J.; Moffatt, J. G.; Khorana, H. G. *J. Am. Chem. Soc.* **1961,** *83,* 659–663. doi:10.1021/ja01464a035
8. Arlt, M.; Hindsgaul, O. *J. Org. Chem.* **1995,** *60,* 14–15. doi:10.1021/jo00106a007
9. Timmons, S. C.; Jakeman, D. L. *Org. Lett.* **2007,** *9,* 1227–1230. doi:10.1021/ol063068d
10. Wolf, S.; Zismann, T.; Lunau, N.; Meier, C. *Chem.–Eur. J.* **2009,** *15,* 7656–7664. doi:10.1002/chem.200900572
11. Gold, H.; van Delft, P.; Meeuwenoord, N.; Codée, J. D. C.; Filippov, D. V.; Eggink, G.; Overkleeft, H. S.; van der Marel, G. A. *J. Org. Chem.* **2008,** *73,* 9458–9460. doi:10.1021/jo802021t
12. Warnecke, S.; Meier, C. *J. Org. Chem.* **2009,** *74,* 3024–3030. doi:10.1021/jo802348h
13. Mohamady, S.; Taylor, S. D. *J. Org. Chem.* **2011,** *76,* 6344–6349. doi:10.1021/jo200540e
14. Timmons, S. C.; Hui, J. P. M.; Pearson, J. L.; Peltier, P.; Daniellou, R.; Nugier-Chauvin, C.; Soo, E. C.; Syvitski, R. T.; Ferrières, V.; Jakeman, D. L. *Org. Lett.* **2008,** *10,* 161–163. doi:10.1021/ol7023949
15. Errey, J. C.; Mukhopadhyay, B.; Kartha, K. P. R.; Field, R. A. *Chem. Commun.* **2004,** 2706–2707. doi:10.1039/b410184g
16. Mizanur, R. M.; Pohl, N. L. B. *Org. Biomol. Chem.* **2009,** *7,* 2135–2139. doi:10.1039/b822794b
17. Barton, W. A.; Biggins, J. B.; Jiang, J.; Thorson, J. S.; Nikolov, D. B. *Proc. Natl. Acad. Sci. U. S. A.* **2002,** *99,* 13397–13402. doi:10.1073/pnas.192468299
18. Jiang, J.; Biggins, J. B.; Thorson, J. S. *J. Am. Chem. Soc.* **2000,** *122,* 6803–6804. doi:10.1021/ja001444y
19. Moretti, R.; Chang, A.; Peltier-Pain, P.; Bingman, C. A.; Phillips, G. N., Jr.; Thorson, J. S. *J. Biol. Chem.* **2011,** *286,* 13235–13243. doi:10.1074/jbc.M110.206433
20. Xia, L.; Zheng, R. B.; Lowary, T. L. *ChemBioChem* **2012,** *13,* 1139–1151. doi:10.1002/cbic.201200121
21. Tam, P.-H.; Lowary, T. L. *Org. Biomol. Chem.* **2010,** *8,* 181–192. doi:10.1039/b916580k
22. Tam, P.-H.; Besra, G. S.; Lowary, T. L. *ChemBioChem* **2008,** *9,* 267–278. doi:10.1002/cbic.200700391
23. Elling, L.; Ritter, J. E.; Verseck, S. *Glycobiology* **1996,** *6,* 591–597. doi:10.1093/glycob/6.6.591
24. Watt, G. M.; Flitsch, S. L.; Fey, S.; Elling, L.; Kragl, U. *Tetrahedron: Asymmetry* **2000,** *11,* 621–628. doi:10.1016/S0957-4166(99)00556-X
25. Marchesan, S.; Macmillan, D. *Chem. Commun.* **2008,** 4321–4323. doi:10.1039/b807016d
26. Tam, P.-H.; Lowary, T. L. *Carbohydr. Res.* **2007,** *342,* 1741–1772. doi:10.1016/j.carres.2007.05.001
27. Timmons, S. C.; Jakeman, D. L. *Carbohydr. Res.* **2008,** *343,* 865–874. doi:10.1016/j.carres.2008.01.046
28. Zhong, W.; Kuntz, D. A.; Ernber, B.; Singh, H.; Moremen, K. W.; Rose, D. R.; Boons, G.-J. *J. Am. Chem. Soc.* **2008,** *130,* 8975–8983. doi:10.1021/ja711248y
29. Esmurziev, A. M.; Simic, N.; Hoff, B. H.; Sundby, E. *J. Carbohydr. Chem.* **2010,** *29,* 348–367. doi:10.1080/07328303.2010.540055
30. Davis, A. J.; Perugini, M. A.; Smith, B. J.; Stewart, J. D.; Ilg, T.; Hodder, A. N.; Handman, E. *J. Biol. Chem.* **2004,** *279,* 12462–12468. doi:10.1074/jbc.M312365200

Beilstein Journal of Organic Chemistry

Automated synthesis of sialylated oligosaccharides

Davide Esposito[1,2], Mattan Hurevich[1,2], Bastien Castagner[3], Cheng-Chung Wang[4] and Peter H. Seeberger[*1,2]

Full Research Paper

Open Access

Address:
[1]Max-Planck-Institute of Colloids and Interfaces, Department of Biomolecular Systems, Am Mühlenberg 1, 14476 Potsdam, Germany, [2]Freie Universität Berlin, Institute of Chemistry and Biochemistry, Arnimallee 22, 14195 Berlin, Germany, [3]Institute of Pharmaceutical Sciences, Swiss Federal Institute of Technology (ETH) Zurich, 8093 Zurich, Switzerland and [4]Institute of Chemistry, Academia Sinica, Taipei, 11529, Taiwan

Email:
Peter H. Seeberger[*] - Peter.Seeberger@mpikg.mpg.de

* Corresponding author

Keywords:
automated synthesis; disaccharide building blocks; solid-phase synthesis; sialic acid; sialosides

Beilstein J. Org. Chem. **2012,** *8,* 1601–1609.
doi:10.3762/bjoc.8.183

Received: 25 June 2012
Accepted: 16 August 2012
Published: 21 September 2012

This article is part of the Thematic Series "Synthesis in the glycosciences II".

Guest Editor: T. K. Lindhorst

Abstract

Sialic acid-containing glycans play a major role in cell-surface interactions with external partners such as cells and viruses. Straightforward access to sialosides is required in order to study their biological functions on a molecular level. Here, automated oligosaccharide synthesis was used to facilitate the preparation of this class of biomolecules. Our strategy relies on novel sialyl α-(2→3) and α-(2→6) galactosyl imidates, which, used in combination with the automated platform, provided rapid access to a small library of conjugation-ready sialosides of biological relevance.

Introduction

Sialic acid (Sia) belongs to a family of nonulosonic acids, i.e., monosaccharides equipped with a carboxylic moiety and a nine-carbon backbone, which play a unique role in glycobiology. Sia-containing glycans mediate pathogen invasion [1] and are involved in signalling cascades, which have been extensively studied [2]. The distinctive structure of Sia confers special properties to membrane oligosaccharides [3] resulting in sialosides having exceptional biological significance. Rapid access to synthetic sialylated glycans would contribute greatly to the biological studies on this important class of molecules. The automated synthesis of oligosaccharides has been significantly improved since the first report in 2001 [4]. Currently, the platform enables the rapid assembly of complex oligosaccharides and accommodates the most commonly employed glycosylation reactions [5-7]. However, accessing sialosides by automation has been hampered by several factors. Chemical silalylation represents a significant challenge, and is usually plagued by low yields and anomeric mixtures [8]. To avoid synthetic complications, Sia has often been introduced by enzymatic methods [9]. In order to allow for access to synthetic sialosides, an intense

effort has been devoted to identifying sialic acid building blocks with superior sialylation properties [10]. In turn, only limited attention has been given to the design of more efficient nucleophiles for sialylations. In naturally occurring *N*- and *O*-glycans the terminal sialic acid residue is most often connected to the C3 or C6 hydroxy group of galactose. Therefore, differently protected galactose precursors have been exploited for sialylation reactions. The obtained disaccharides have been used to prepare synthetic sialosides [11-13]. A disaccharide building block approach is an attractive possibility for solid-phase synthesis, since it avoids performing a low yielding and unselective sialylation on a solid support.

Here, we describe a method for the rapid preparation of different sialosides relying on a new automated solid-phase synthesis platform [5]. Central to the success of this approach is the use of galactals as nucleophiles for chemical sialylation, which allows for efficient access to the novel sialyl α-(2-3) and α-(2-6) galactosyl imidate disaccharide building blocks. The combination of the automated platform and sialylated building blocks proved successful for the synthesis of representative Sia-containing oligosaccharides ready for biological evaluation.

Results and Discussion

Building-blocks preparation

Many sialylation strategies utilize building blocks that require multistep syntheses [10]. In contrast, solid-phase automated synthesis requires readily accessible building blocks that can be used in excess to drive reactions to completion. As our initial goal, we developed a method to provide sialic acid containing disaccharide glycosylating agents with minimal synthetic effort. Simple *N*-acetyl building blocks such as **1** (Figure 1) were used due to their facile syntheses, in contrast to other commonly employed *N*-5 modified building blocks [14-17]. Most of the *N*-acetyl sialic acid glycosylating agents reported in the literature can be accessed from the common intermediate **6** [18], which is prepared in two steps from commercially available Sia (Figure 1b).

Compound **6** was converted in a single step into various sialylating agents, such as the *N*-phenyl trifluoroacetimidoyl glycoside **10**, and glycosyl phosphites **8** and **1** as previously described (Table 1) [19-21]. Galactal **2** was identified recently as an efficient acceptor for sialylation [11,12]. Its efficiency can be attributed to a combination of reduced steric hindrance and good nucleophilicity of the C3 hydroxy group. Thus, galactal **2** was glycosylated with different *N*-acetyl sialic acid building blocks (Table 1).

We started our screening by comparing the glycosylation of building blocks **1**, **8** and **10** with galactal **2** under similar conditions (Table 1, entries 1–3). Sialylation with building block **8** failed to yield any disaccharide **9** (Table 1, entry 1), while glycosylating agents **10** and **1** gave moderate yields and good selectivity (Table 1, entries 2 and 3). The glycosylation of galactal **2** with phosphite **1**, which we described in the supporting information of [5], was further optimized. In particular, elevating the reaction temperature proved beneficial and disaccharide **9** was isolated in higher overall yield, albeit with a

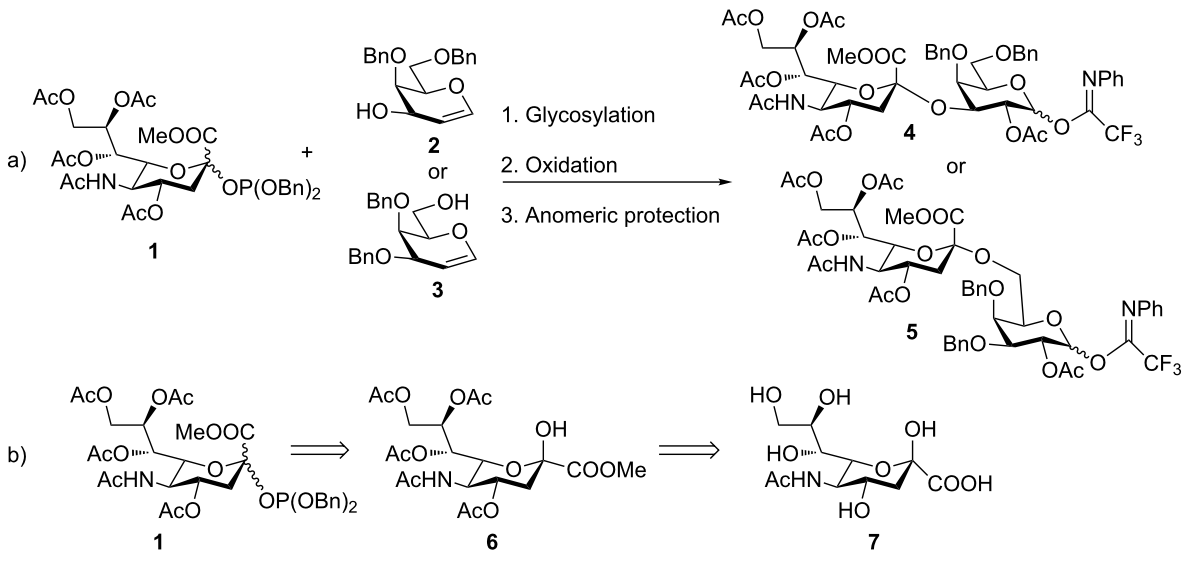

Figure 1: (a) Synthesis sequence for the preparation of building blocks **4** and **5**; (b) Retrosynthetic analysis for the preparation of **1**.

Table 1: Synthesis of building blocks **9** and **11**.

entry	glycosylating agent	nucleophile	conditions[a]	product	yield	α/β ratio
1	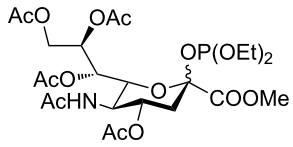 **8** (1.0 equiv)	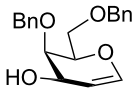 **2** (1.5 equiv)	a	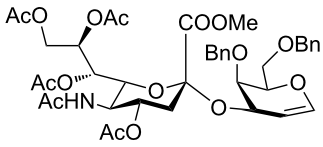 **9**	–	–
2	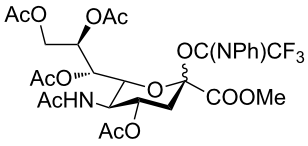 **10** (1.0 equiv)	**2** (1.5 equiv)	a	**9**	30%	9/1
3	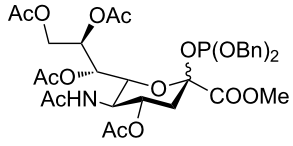 **1** (1.0 equiv)	**2** (1.5 equiv)	a	**9**	27%	9/1
4	**1** (1.0 equiv)	**2** (1.7 equiv)	b	**9**	80%	4/1
5	**1** (1.0 equiv)	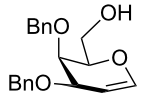 **3** (2.0 equiv)	b	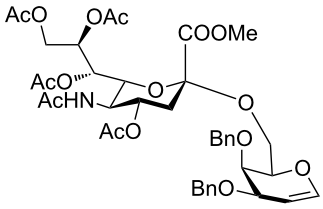 **11**	75%	2.5/1

[a]Reagents and Conditions: (a) TMSOTf (0.2 equiv), EtCN, AW-4Å MS, −78 °C; (b) TMSOTf (0.2 equiv), CH_3CN, AW-4Å MS, −42 °C.

slight decrease in selectivity. The best results were obtained by using 1.7 equivalents of **2** at −42 °C, using acetonitrile as the solvent instead of the more expensive propionitrile (Table 1, entry 4). The conditions established for the synthesis of compound **8** were applied to synthesize sialyl α-(2→6) galactal **11** (Table 1, entry 5) in good yield upon glycosylation of galactal **3** [22]. In all cases, the desired anomer was readily purified by column chromatography.

In order to convert the disaccharide products into the corresponding glycosyl imidates, the double bond in compounds **9** and **11** was oxidized by treatment with $PhI(OAc)_2$ and catalytic amounts of $BF_3{\cdot}Et_2O$ [23] and gave disaccharides **12** and **13**, respectively after acetylation (Scheme 1). Removal of the anomeric acetate mediated by hydrazine acetate provided the hemiacetals, which was followed by introduction of the anomeric *N*-phenyl trifluoroacetimidate to furnish disaccharide building blocks **4** and **5**. It should be noted that building block **4** can be prepared with higher overall yield than the recently disclosed *N*-Troc protected disaccharide building block [11] obtained with a similar method.

Solution-phase studies

In order to evaluate the utility of building block **4** for the solid-phase synthesis of sialosides we undertook a model solution-phase synthesis of the glycan portion of GM3 ganglioside **16** (Scheme 2). GM3 serves as an important receptor for viral infection [24,25] and contains the common sialyl α-(2→3) galactose motif. The key step en route to compound **16** was the glycosylation of compound **14** with building block **4** (Scheme 2), which proceeded efficiently in the presence of trimethylsilyl triflate (TMSOTf) as promoter at −10 °C to afford trisaccharide **15** with a yield of 80%. It is worth mentioning that glycosylation of an analogue of glucose **14** equipped with a benzoyl group at the C3 hydroxy position resulted in a lower glycosylation yield (36%), suggesting that an ester can lower the nucleophilicity of the vicinal C4-hydroxy. The synthesis was completed by deacetylation of compound **15** under Zemplén's conditions, followed by saponification and hydrogenolysis affording good yields of the trisaccharide **16**, equipped with an amino spacer for conjugation. The synthesis of GM3 trisaccharide **16** proved that compound **4** is efficient for installing the capping sialyl α-(2→3) galactose unit into syn-

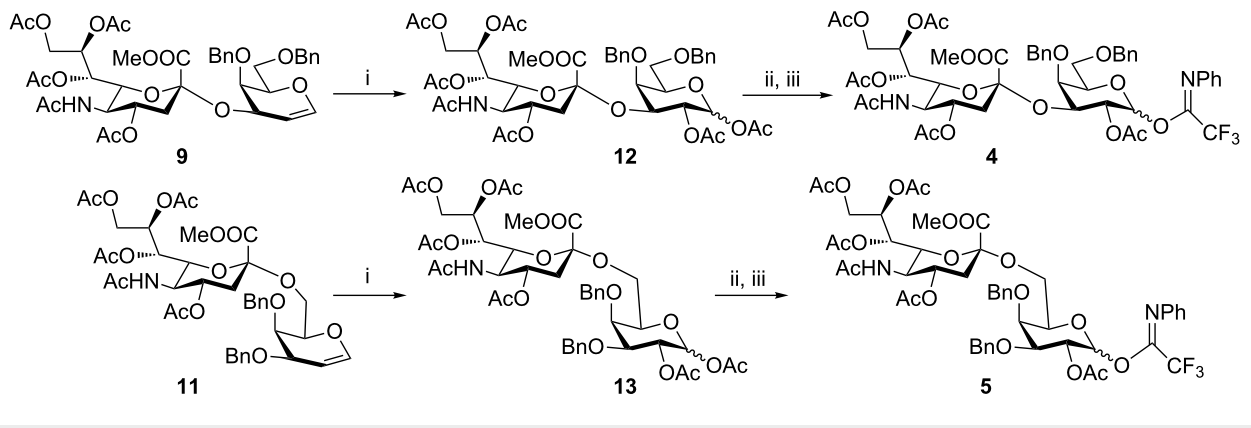

Scheme 1: Reagents and conditions: (i) $PhI(OAc)_2$, $BF_3{\cdot}Et_2O$, CH_2Cl_2, −40 °C; then Ac_2O, pyridine; (ii) $N_2H_4{\cdot}AcOH$, DMF; (iii) $CF_3C(NPh)Cl$, Cs_2CO_3, CH_2Cl_2, DCM, 66% over three steps for **4** (for a detailed description of the synthesis of compound **4** see the supporting information of [5]); 62% over three steps for **5**.

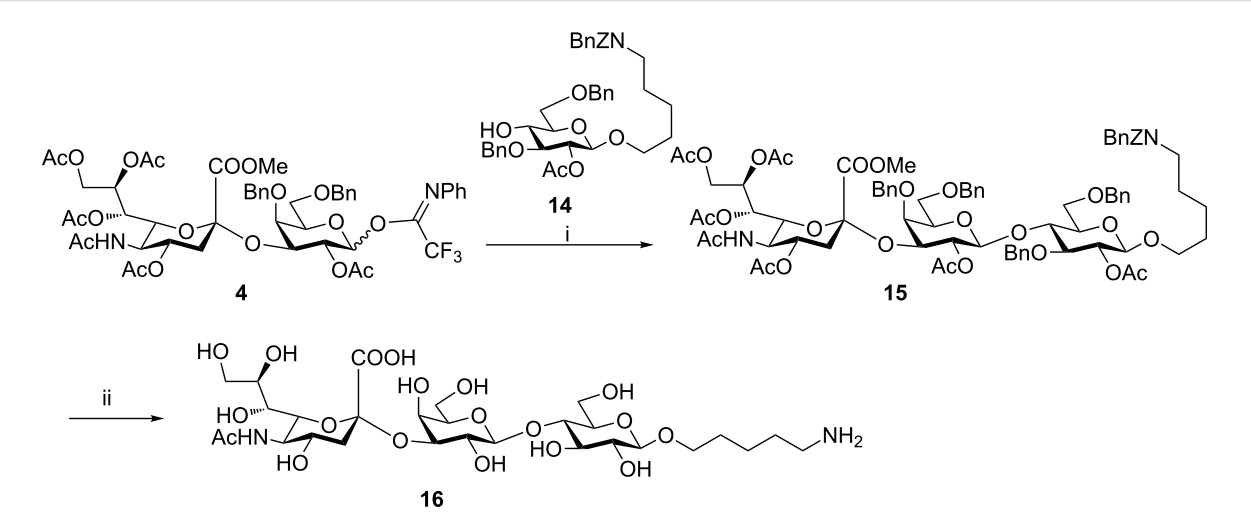

Scheme 2: Reagents and conditions. (i) TMSOTf, DCM, −10 °C, 80%; (ii) NaOMe, MeOH; then KOH, MeOH, 60 °C; then Pd/C, H_2, AcOH, MeOH, THF, H_2O, rt, 76% over three steps.

thetic oligosaccharides. Furthermore, conditions applied to the preparation of **16** can be easily adapted for solid-phase synthesis making **4** a valuable candidate for automation.

Automated synthesis of sialosides

Automated synthesis of linear α-(2→3) sialosides

The new integrated platform for automated synthesis of oligosaccharides [5] offers the possibility to construct a diverse set of glycans rapidly and efficiently. The automated synthesizer proved capable of performing iterative glycosylation–deprotection cycles under conditions commonly employed for solution-phase oligosaccharide synthesis. The synthetic strategy relies on the solid support-bound linker **17** (Scheme 3), which contains a latent amino spacer useful for conjugation. In addition, manual operations are minimized by performing the trichloroacetyl (TCA) reduction, ester removal and cleavage from the solid support by automation. In many cases, only hydrogenolytic cleavage of the remaining benzyl ethers and carbamates has to be performed manually at the end of an automated sequence. These features make the automated platform very attractive for sialoside synthesis. Based on the encouraging results obtained for the solution-phase synthesis of **16**, building blocks **4** and **5** were used for the automated solid-phase synthesis of various sialosides. Some of the results presented herein have been communicated in preliminary form [5]. Sialyl lactosamine **20** (Scheme 3) [25], which serves as a site of attachment for viruses during infections, and sialyl lactose (GM3) **16** (Scheme 4) were chosen to confirm the viability of building block **4** for the automated solid-phase synthesis of linear sialosides.

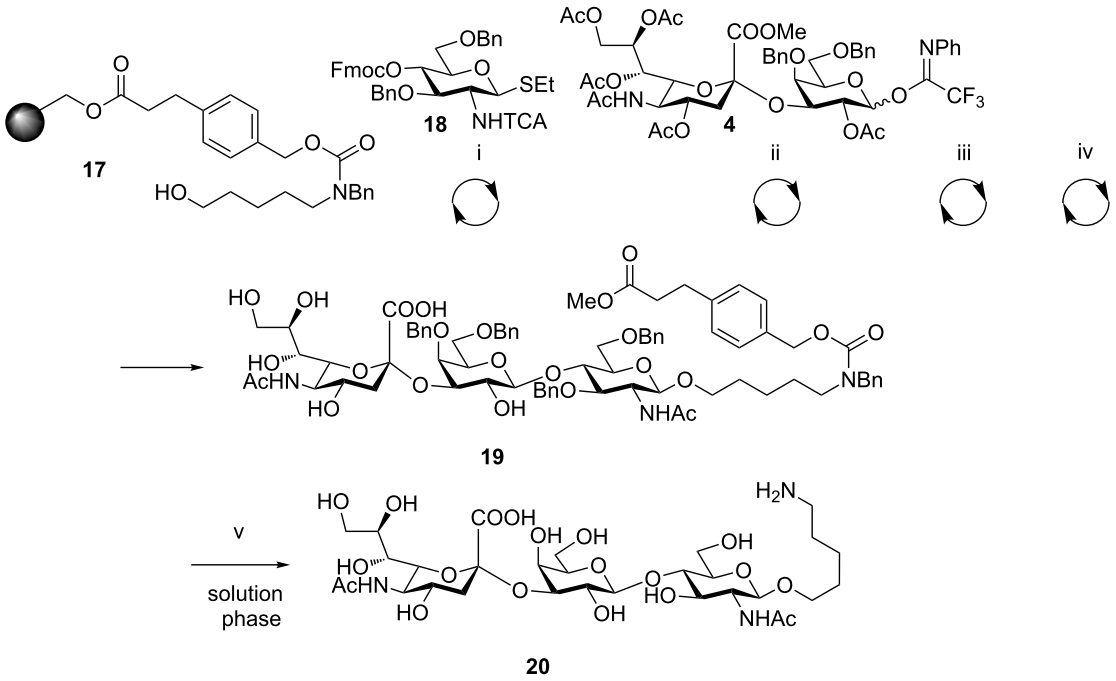

Scheme 3: Automated synthesis of **20**. Reagents and conditions: (i) (a) NIS, TfOH, dioxane, DCM, −40 to −20 °C, 40 min; (b) piperidine, DMF. (ii) (a) TMSOTf, DCM, 0 °C, 2 h; (b) piperidine, DMF. (iii) AIBN (cat.), Bu_3SnH (10 equiv), xylene, 90 °C. (iv) NaOMe, MeOH, DCM, 1.5 h, 33%. (v) Pd/C, H_2, MeOH/H_2O, cat. AcOH, 78% (for experimental details see the supporting information of [5]).

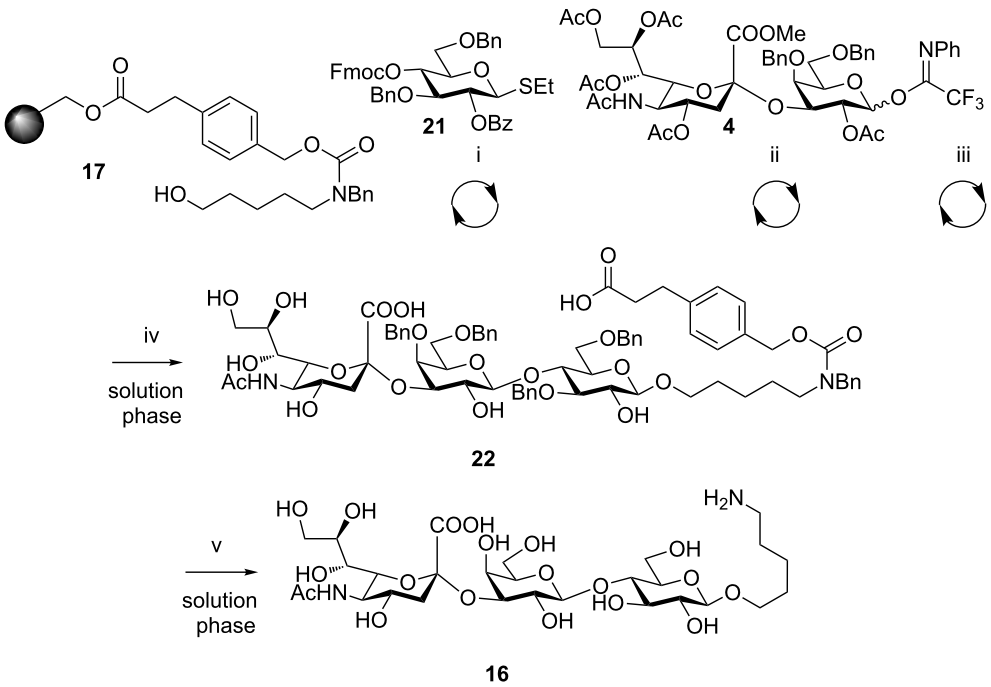

Scheme 4: Automated synthesis of **16**. Reagents and conditions: (i) (a) NIS, TfOH, dioxane, DCM, −40 to −20 °C, 40 min; (b) piperidine, DMF. (ii) (a) TMSOTf, DCM, 0 °C, 2 h; (b) piperidine, DMF. (iii) NaOMe, MeOH, DCM, 1.5 h. (iv) KOH, MeOH, H_2O, THF, 60 °C, 40%. (v) Pd/C, H_2, MeOH/H_2O, cat. AcOH, 91% (for experimental details see the supporting information of [5]).

For all sialosides, a similar synthetic route was followed, consisting of automated glycosylation and deprotection cycles, followed by TCA reduction (when glucosamines are present) and final ester removal/cleavage to afford the semi-protected oligosaccharide. The automated synthesis of **20** (Scheme 3) started with the glycosylation of resin-bound linker **17** with glucosamine building block **18** (2 × 5 equiv) [5] in the presence of *N*-iodosuccinimide and triflic acid. Fluorenylmethoxycarbonyl (Fmoc) removal was followed by glycosylation with building block **4** (2 × 5 equiv) for 1 h at −10 °C with TMSOTf used for activation. Radical reduction using tributyltinhydride and azobisisobutyronitrile (AIBN) was performed to convert the trichloroacetamide into an *N*-acetyl moiety, followed by methoxide-mediated cleavage to provide compound **19**. Analysis of the crude mixture by LC–MS showed incomplete glycosylation of the resin bound glucosamine by building block **4.** The reaction was optimized to identify the best glycosylation conditions for building block **4** under the solid-phase paradigm. Performing the glycosylation at a higher temperature (0 °C) and longer time (2 h) proved sufficient to drive the reaction to higher conversion and trisaccharide **19** was isolated in 33% overall yield with respect to resin loading. Hydrogenolysis under standard conditions afforded the fully deprotected trisaccharide **20** in 78% yield. These conditions were applied to the synthesis of GM3 trisaccharide **16** previously prepared in solution phase (see above*)*. Glucose thioglycoside building block **21** and disaccharide building block **4** served for the assembly of **16** (Scheme 4). Final saponification afforded the partially protected glycan **22** in 40% overall yield before hydrogenolysis gave the final trisaccharide **16** in 91% yield. The efficiency of the solid-phase and the solution-phase syntheses was compared. The solution-phase synthesis of trisaccharide **16** was completed with an overall yield of 42% (taking into account the preparation of compound **14**, 69%) in about one week. The same number of steps was executed in the solid-phase synthesis with little operator interference, to yield the desired compound in a comparable overall yield (36%) in shorter time. An average time of 3 h per glycosylation cycle (coupling and deprotection) or cleavage from the support, allows the assembly of a trisaccharide in roughly 10 h. In general, although an excess of building block is used in the automated solid-phase synthesis, the method provides the final assembled oligosaccharide with much greater efficiency than in the solution-phase synthesis, and avoids the loss of material encountered when performing purifications in between steps.

Automated synthesis of sialyl Lewis^X

Branching is often observed in naturally occurring sialosides. Assembly of branched oligosaccharides is particularly challenging due to the steric hindrance of the branching sites, which can affect glycosylation yields. Working in a solid-phase environment could, in principle, additionally reduce the accessibility of a sterically hindered nucleophile. Thus, the possibility of accessing branched structures was explored on the solid support [5].

Sialyl Lewis^X tetrasaccharide **27** (Scheme 5), has been implicated in inflammation and cancer metastasis [26], and was chosen as a model glycan for the construction of branched compounds. Glucosamine building block **23,** containing C3-levulinoyl (Lev) and C4-Fmoc protecting groups [27], was first reacted with the linker. The glycosylation was followed by Fmoc removal from the C4 hydroxy group and a second glycosylation was performed with building block **4** under the conditions optimized in the context of the synthesis of trisaccharide **20**. Removal of the levulinoyl ester from C3 by treatment with hydrazine hydrate and acetic acid exposed the second hydroxy nucleophile on the central glucosamine. Our first attempt to glycosylate using fucose thioglycoside building block **25** afforded the product in low yield and as a mixture of anomers as confirmed by LC–MS analysis. The use of *N*-phenyl trifluoroacetimidate building block **24** proved more efficient. Nevertheless, when fucosylation with building block **24** was performed in dichloromethane, a mixture of anomers of compounds **26** was detected by NMR analysis. Only running the reaction in ether, which is a strong α-directing solvent [28], ensured stereoselective introduction of the fucose residue. Under these optimized conditions, the branched tetrasaccharide **26** was isolated in 51% overall yield after TCA reduction, cleavage, ester saponification and HPLC purification. Finally, solution-phase hydrogenolysis gave tetrasaccharide **27**.

Automated synthesis of linear α–(2→6) sialosides

α-(2→6) Sialylated oligosaccharides have been identified in humans as a recurring constituent of the upper respiratory epithelial glycocalix [29]. For instance, tetrasaccharide **30** has been reported to bind to haemagglutinins isolated from different H1N1 human viral strains, and was chosen as a target to showcase the solid-phase automated synthesis of α-(2→6) sialosides (Scheme 6).

The synthesis of tetrasaccharide **30** started with the glycosylation of linker **17** by using galactose building block **28** under standard conditions for the activation of thioglycosides, followed by Fmoc removal and a glycosylation with building block **18**. The solid-phase bound disaccharide was further elongated, following removal of the temporary protecting group, by reaction with building block **5**. For this reaction, we applied the reaction conditions optimized for building block **4** without further optimization. Thus, standard TCA reduction, cleavage from the support, saponification and isolation afforded semiprotected tetrasaccharide **29** in 16% overall yield. As

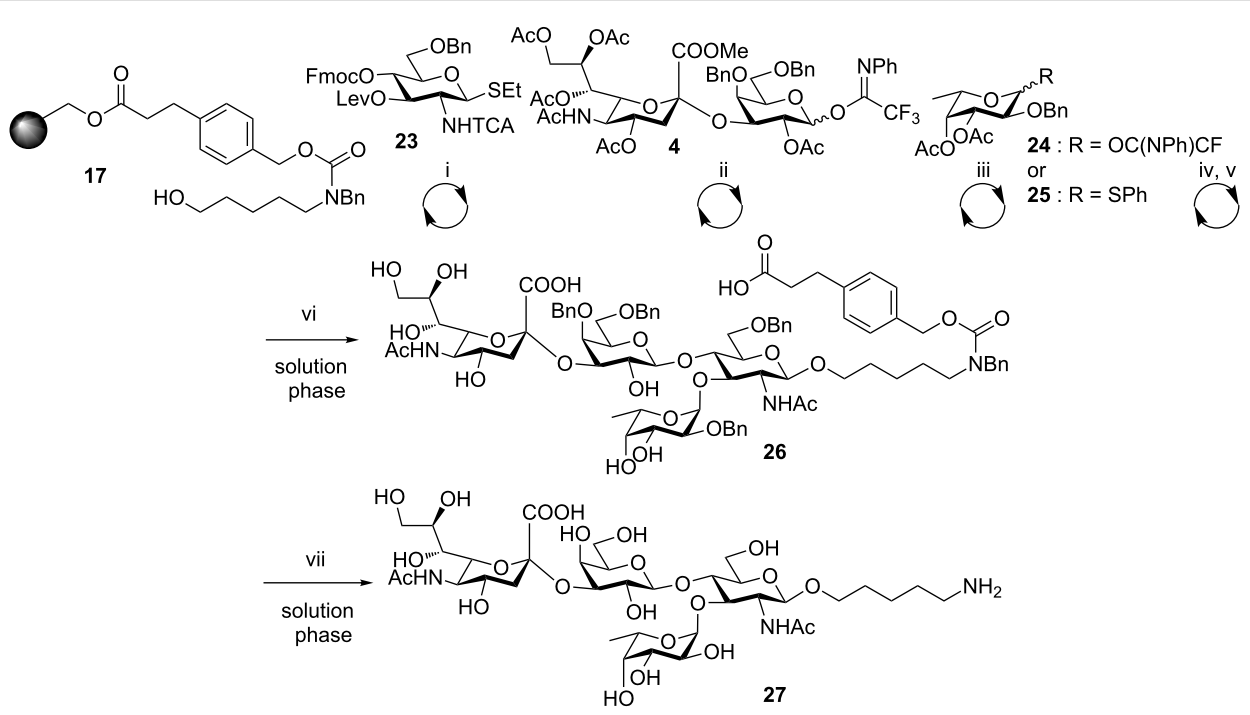

Scheme 5: Automated synthesis of **27**. Reagents and conditions: (i) (a) NIS, TfOH, dioxane, DCM, −40 to −20 °C, 40 min; (b) piperidine, DMF. (ii) (a) TMSOTf, DCM, 0 °C, 2 h; (b) $NH_2NH_2{\cdot}H_2O$, AcOH, pyridine, DCM. (iii with **24**) TMSOTf, Et_2O, −10 °C, 1 h. (iii with **25**) NIS, TfOH, dioxane, DCM, −40 °C to −20 °C, 40 min. (iv) AIBN (cat.), Bu_3SnH (10 equiv), xylene, 90 °C. (v) NaOMe, MeOH, DCM, 1.5 h. (vi) KOH, MeOH, H_2O, THF, 60 °C, 51%. (vii) Pd/C, H_2, MeOH/H_2O, cat. AcOH, 30% (for experimental details see the supporting information of [5]).

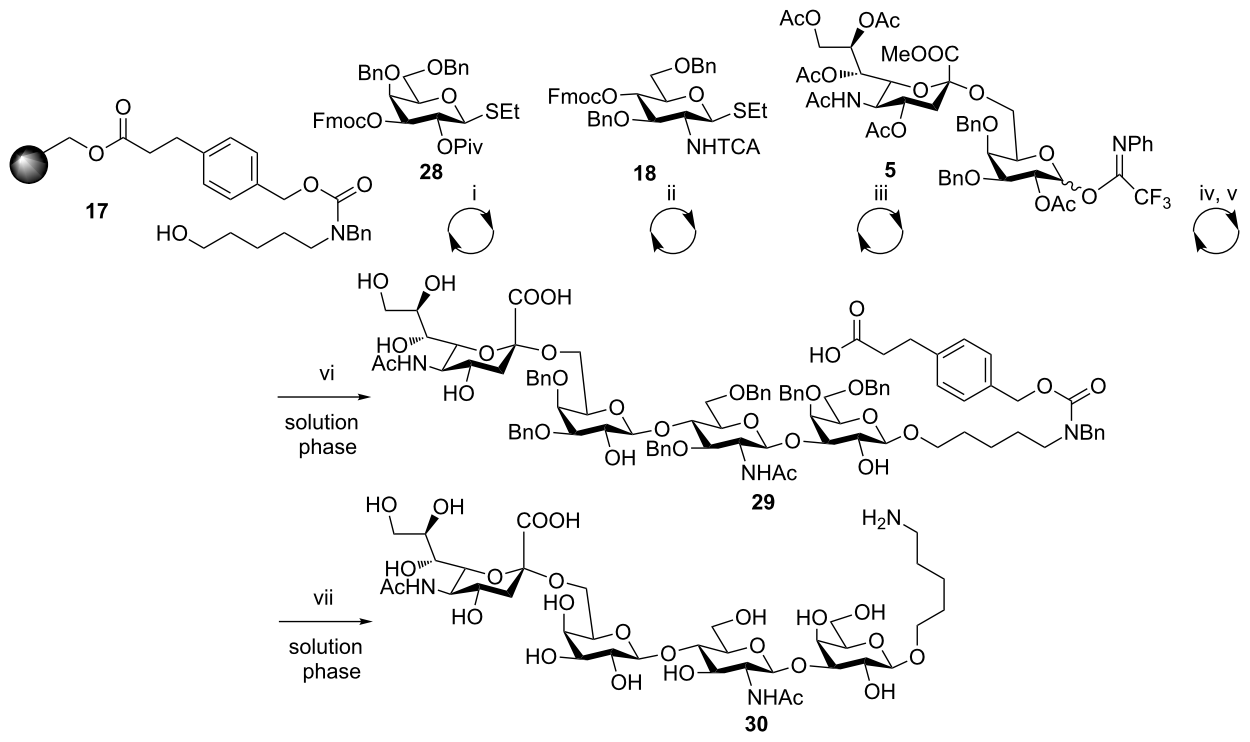

Scheme 6: Automated synthesis of **30**. Reagents and conditions: (i) (a) NIS, TfOH, dioxane, DCM, −40 to −20 °C, 40 min; (b) piperidine, DMF. (ii) NIS, TfOH, dioxane, DCM, −40 to −20 °C, 40 min. (iii) TMSOTf, Et_2O, 0 °C, 2 h. (iv) AIBN (cat.), Bu_3SnH (10 equiv), xylene, 90 °C. (v) NaOMe, MeOH, DCM, 1.5 h. (vi) KOH, MeOH, H_2O, THF, 60 °C, 16%. (vii) Pd/C, MeOH/H_2O/EtOAc, cat. AcOH, 51%.

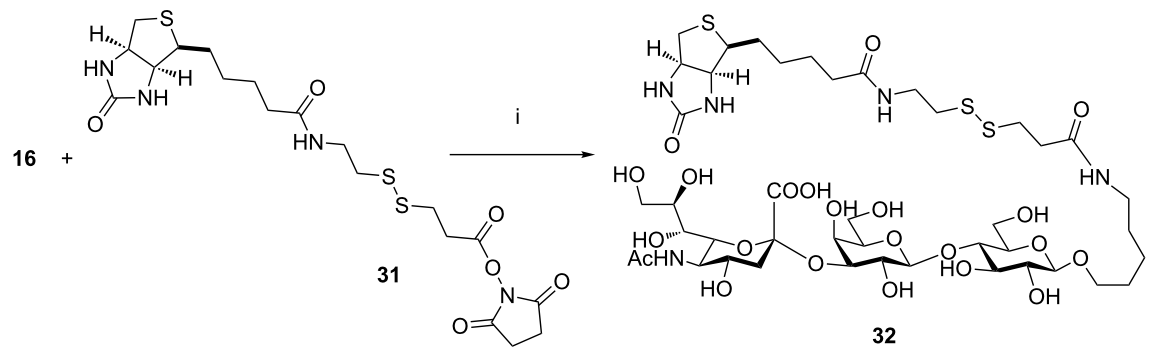

Scheme 7: Reagents and conditions: (i) 10% DMF in PBS buffer pH 7.5, overnight, 80%.

shown by LC–MS analysis (see Supporting Information File 1) the crude mixture contains the desired tetrasaccharide, but also some deletion sequences that can be attributed to the non-optimized conditions used for the synthesis. Moreover, building blocks **18** and **28** have been observed to be a non-ideal donor–acceptor pair (unpublished results). Nevertheless, simple reverse-phase HPLC was sufficient to isolate semiprotected tetrasaccharide **29** in milligram quantities. To complete the synthesis, hydrogenolysis was performed to give final tetrasaccharide **30** in 51% yield. The above example shows that the platform can provide access to target oligosaccharides by using generalized coupling protocols even when conditions are not optimized.

Formation of biotinylated probes

The syntheses of glycans **27** and **30** showed the efficiency of sialyl building blocks **4** and **5** in combination with the automated solid-phase platform for the rapid and reliable access to complex sialosides. Our synthetic strategy makes use of linker **17**, which incorporates an amino spacer for conjugation into the final oligosaccharide. In this way, the synthetic sialosides can be easily conjugated to probes for biological evaluation or labelled for instance with UV-active tags. Biotinylation is a typical example of a commonly employed labelling technique [30] and has been extensively used for instance as a functionalization technique for antigens in antibody selection by phage-display methods [31]. Thus, trisaccharide **16** (Scheme 7) was reacted with biotin derivative **31** in PBS buffer to afford compound **32** in 80% yield after gel filtration.

Conclusion

The synthesis of sialosides is important to create tools for glycobiology. The work presented here demonstrates that several important sialylated oligosaccharides can be accessed by using a standardized automated approach. Two sialic acid containing disaccharide building blocks containing either α-(2→3) or α-(2→6) galactose linkages were obtained in high overall yields from readily accessible starting materials. In combination with a fully automated synthesizer, the disaccharide building blocks have been exploited for the solid-phase synthesis of several oligosaccharides ready for biological evaluation. This work represents the first full account of an automated solid-phase synthesis of sialosides.

Supporting Information

Supporting Information File 1

Experimental procedure and characterization data for new compounds.
[http://www.beilstein-journals.org/bjoc/content/supplementary/1860-5397-8-183-S1.pdf]

Supporting Information File 2

^{1}H and ^{13}C NMR spectra for new compounds.
[http://www.beilstein-journals.org/bjoc/content/supplementary/1860-5397-8-183-S2.pdf]

Acknowledgments

We acknowledge the Max-Planck Society and the Swiss National Science Foundation (200020-117889) for generous financial support. We thank the National Science Council Taiwan for a fellowship to C.-C. Wang and the Minerva Stiftung for a fellowship to M. Hurevich.

References

1. Winter, C.; Schwegmann-Weßels, C.; Cavanagh, D.; Neumann, U.; Herrler, G. *J. Gen. Virol.* **2006,** *87,* 1209–1216. doi:10.1099/vir.0.81651-0
2. Crocker, P. R.; Paulson, J. C.; Varki, A. *Nat. Rev. Immunol.* **2007,** *7,* 255–266. doi:10.1038/nri2056
3. Angata, T.; Varki, A. *Chem. Rev.* **2002,** *102,* 439–470. doi:10.1021/cr000407m
4. Plante, O. J.; Palmacci, E. R.; Seeberger, P. H. *Science* **2001,** *291,* 1523–1527. doi:10.1126/science.1057324

5. Kröck, L.; Esposito, D.; Castagner, B.; Wang, C.-C.; Bindschädler, P.; Seeberger, P. H. *Chem. Sci.* **2012,** *3,* 1617–1622. doi:10.1039/c2sc00940d
6. Schlegel, M. K.; Hütter, J.; Eriksson, M.; Lepenies, B.; Seeberger, P. H. *ChemBioChem* **2011,** *12,* 2791–2800. doi:10.1002/cbic.201100511
7. Walvoort, M. T. C.; van den Elst, H.; Plante, O. J.; Kröck, L.; Seeberger, P. H.; Overkleeft, H. S.; van der Marel, G. A.; Codée, J. D. C. *Angew. Chem., Int. Ed.* **2012,** *51,* 4393–4396. doi:10.1002/anie.201108744
8. Chen, X.; Varki, A. *ACS Chem. Biol.* **2010,** *5,* 163–176. doi:10.1021/cb900266r
9. Ernst, B.; Oehrlein, R. *Glycoconjugate J.* **1999,** *16,* 161–170. doi:10.1023/A:1026496714403
10. Boons, J.-G.; Demchenko, A. V. *Chem. Rev.* **2000,** *100,* 4539–4565. doi:10.1021/cr990313g
11. Hanashima, S.; Castagner, B.; Esposito, D.; Nokami, T.; Seeberger, P. H. *Org. Lett.* **2007,** *9,* 1777–1779. doi:10.1021/ol0704946
12. Gervay, J.; Peterson, J. M.; Oriyama, T.; Danishefsky, S. J. *J. Org. Chem.* **1993,** *58,* 5465–5468. doi:10.1021/jo00072a031
13. Hanashima, S.; Seeberger, P. H. *Chem.–Asian J.* **2007,** *2,* 1447–1459. doi:10.1002/asia.200600424
14. Tanaka, H.; Nishiura, Y.; Takahashi, T. *J. Am. Chem. Soc.* **2006,** *128,* 7124–7125. doi:10.1021/ja0613613
15. Tanaka, K.; Goi, T.; Fukase, K. *Synlett* **2005,** 2958–2962. doi:10.1055/s-2005-921889
16. De Meo, C.; Demchenko, A. V.; Boons, G.-J. *J. Org. Chem.* **2001,** *66,* 5490–5497. doi:10.1021/jo010345f
17. Yu, C.-S.; Niikura, K.; Lin, C.-C.; Wong, C.-H. *Angew. Chem., Int. Ed.* **2001,** *40,* 2900–2903. doi:10.1002/1521-3773(20010803)40:15<2900::AID-ANIE2900>3.0.CO;2-4
18. Marra, A.; Sinay, P. *Carbohydr. Res.* **1989,** *190,* 317–322. doi:10.1016/0008-6215(89)84135-7
19. Cai, S.; Yu, B. *Org. Lett.* **2003,** *5,* 3827–3830. doi:10.1021/ol0353161
20. Martin, T. J.; Schmidt, R. R. *Tetrahedron Lett.* **1992,** *33,* 6123–6126. doi:10.1016/S0040-4039(00)60022-9
21. Sim, M. M.; Kondo, H.; Wong, C.-H. *J. Am. Chem. Soc.* **1993,** *115,* 2260–2267. doi:10.1021/ja00059a023
22. Wang, P.; Zhu, J.; Yuan, Y.; Danishefsky, S. J. *J. Am. Chem. Soc.* **2009,** *131,* 16669–16671. doi:10.1021/ja907136d
23. Shi, L.; Kim, Y.-J.; Gin, D. Y. *J. Am. Chem. Soc.* **2001,** *123,* 6939–6940. doi:10.1021/ja015991a
24. Suzuki, Y.; Matsunaga, M.; Matsumoto, M. *J. Biol. Chem.* **1985,** *260,* 1362–1365.
25. Matsuoka, K.; Kaneko, R.; Koyama, T.; Ma, X. T.; Esumi, Y.; Nakamura, T.; Hatano, K.; Terunuma, D. *Bioorg. Med. Chem.* **2010,** *20,* 4906–4910. doi:10.1016/j.bmcl.2010.06.066
26. Kannagi, R.; Izawa, M.; Koike, T.; Miyazaki, K.; Kimura, N. *Cancer Sci.* **2004,** *95,* 377–384. doi:10.1111/j.1349-7006.2004.tb03219.x
27. Routenberg Love, K.; Seeberger, P. H. *Angew. Chem., Int. Ed.* **2004,** *43,* 602–605. doi:10.1002/anie.200352539
28. Werz, D. B.; Castagner, B.; Seeberger, P. H. *J. Am. Chem. Soc.* **2007,** *129,* 2770–2771. doi:10.1021/ja069218x
29. Chandrasekaran, A.; Srinivasan, A.; Raman, R.; Viswanathan, K.; Raguram, S.; Tumpey, T. M.; Sasisekharan, V.; Sasisekharan, R. *Nat. Biotechnol.* **2008,** *26,* 107–113. doi:10.1038/nbt1375
30. Hermanson, G. T. *Bioconjugate Techniques,* 2nd ed.; Academic Press: San Diego, 2008.
31. Silacci, M.; Brack, S.; Schirru, G.; Mårlind, J.; Ettorre, A.; Merlo, A.; Viti, F.; Neri, D. *Proteomics* **2005,** *9,* 2340–2350. doi:10.1002/pmic.200401273

License and Terms

Beilstein Journal of Organic Chemistry

The Amadori rearrangement as glycoconjugation method: Synthesis of non-natural *C*-glycosyl type glycoconjugates

Katharina Gallas‡, Gerit Pototschnig‡, Florian Adanitsch, Arnold E. Stütz and Tanja M. Wrodnigg*

Full Research Paper

Open Access

Address:
Glycogroup, Institute of Organic Chemistry, Technical University Graz, Stremayrgasse 9, A-8010 Graz, Austria

Email:
Tanja M. Wrodnigg* - t.wrodnigg@tugraz.at

* Corresponding author ‡ Equal contributors

Keywords:
Amadori rearrangement; *C*-glycosyl type glycoconjugates; carbohydrate elongation; non-natural carbohydrate conjugates

Beilstein J. Org. Chem. **2012,** *8,* 1619–1629.
doi:10.3762/bjoc.8.185

Received: 27 April 2012
Accepted: 18 July 2012
Published: 25 September 2012

This article is part of the Thematic Series "Synthesis in the glycosciences II".

Guest Editor: T. K. Lindhorst

Abstract

The Amadori rearrangement was investigated as a potential method for the conjugation of carbohydrate moieties to suitable amino components. Starting from selected aldoheptoses, which are readily available by means of the Kiliani–Fischer C-elongation reaction of the corresponding aldohexoses, glycoconjugates presenting D-*gluco*, D-*manno* and D-*galacto* as well as GlcNAc motifs have been synthesised. Following this strategy, non-natural *C*-glycosyl type glycoconjugates, which can be utilised as building blocks for the composition of larger molecular constructions, are available by a very short synthetic approach.

Introduction

Glycoconjugates such as glycoproteins, glycopeptides, glycolipids and peptidoglycans are ubiquitous in nature [1]. They are found on cell surfaces and are responsible for processes such as cell–cell interaction, recognition and communication. In order to investigate and elucidate their many functions, reliable synthetic methods for the conjugation of carbohydrates to biomolecules are of crucial importance [2]. Several ligation strategies are described in the literature, such as chemical ligation [3], conjugation by means of click chemistry (Huisgen cycloaddition) [4,5], glycosylation protocols [6,7], and Staudinger ligation [8], just to mention the most prominent examples. However, many applications in this respect require a ligation method that is functional in aqueous medium, and, for economic purposes in general, protecting-group manipulations should be kept to a minimum. Considering these aspects, we were interested in probing the Amadori rearrangement as a conjugation method for the synthesis of glycoconjugates. The Amadori rearrangement (AR) allows the formation of 1-aminodeoxyketoses **2** and **3** from the respective aldose **1** and a suitable amine under acid catalysis (Scheme 1).

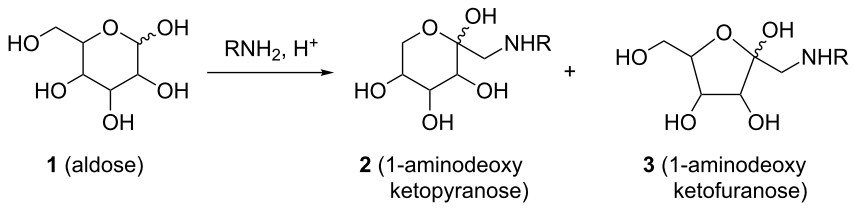

Scheme 1: Amadori rearrangement.

The reaction is known to be very sensitive to the nature of the carbohydrate substrate, the acid catalyst, and the amino component, as well as to the temperature and duration. Additionally, some challenges accompany the reaction limiting its synthetic use, several steps during the introduction of the amine and the subsequent isomerisation to the ketose are reversible, and furthermore, the product itself can enter the Maillard reaction cascade [9,10] pathway. Consequently, a range of side and degradation products can be formed. In general, the rearrangement product can occur as a mixture of different isomers, and in principal the furanoid as well as pyranoid in their α- and β-anomeric forms can be obtained. Thus, isolation of the rearrangement product can be challenging and tedious, and only a few preparatively useful examples of the Amadori rearrangement are known in the literature [11-20]. However, this reaction accomplishes the introduction of various amines onto the position C-1 of aldoses and at the same time the isomerisation to the corresponding 1-aminodeoxyketose without the requirement for protecting-group manipulations, and is thus a very valuable reaction sequence [21-24]. We have succeeded in optimising the reaction conditions for the Amadori rearrangement when introducing D-*glycero*-D-*gulo*-aldoheptose as the starting material. In this special case, all substituents of the resulting 1-aminodeoxy ketose adopt an equatorial position in the $^5C_2$ pyranoid conformation, which is a strong driving force providing excellent preparative yields [25]. In general, this reaction leads to non-natural *C*-glycosyl type glycoconjugates, which are of particular interest for biological investigation because of their chemical stability towards physiological hydrolysis of the glycosidic linkage, compared to the naturally occurring *O*- as well as *N*-glycosides [26].

A broad application of this reaction is not feasible as yet. However, according to its mechanism, the scope of the Amadori rearrangement could well comprise a variety of useful conjugation reactions, including mono- as well as oligo- and polyvalent amines, and the carbohydrate decoration of functionalized surfaces. Fields of application concern the construction of oligovalent glycoconjugates, such as glycoclusters and glycodendrimers, the modification of surfaces (glycosylated surfaces, e.g., "glyco-chips", gold, polystyrene plates, glass, nanoparticles), or labelling and imaging of carbohydrates (fluorescence markers, biotin, photolabelling) [27,28].

Herein we describe the application of the Amadori rearrangement as a key step for the synthesis of non-natural *C*-glycosyl type glycoconjugates in the D-*manno*, D-*galacto* as well as GlcNAc series starting from the respective aldoheptoses and suitable amino components. Aldoheptoses were synthesised by C-elongation of the corresponding hexoses and subsequent reductive hydrolysis following the Kiliani–Fischer cyanohydrin reaction procedure.

Results and Discussion

C-Elongation

In an initial C-elongation attempt, with the aim to avoid HCN as C-synthon, we decided to follow a protocol employing sodium cyanide, as described by Hudson [29] (Scheme 2). By this reaction sequence, starting from aldohexose **1**, the obtained heptonolactones **4** are expected to be formed as a mixture of diastereomers at position C-2. Consequently, the respective aldoheptoses **5**, obtained by reduction of the lactones employing sodium borohydride, will be present as C-2 diastereomers as well. However, during the Amadori rearrangement this centre will be oxidised to a keto group, thus the stereochemical outcome of the chain elongation is not of relevance and therefore a separation is not necessary. As a side product, the fully reduced heptitol **6** is expected to be formed.

To probe this reaction sequence, i.e., C-elongation followed by Amadori rearrangement, D-glucose (**8**) was employed as a model substrate, since in this case NMR data of the obtained D-*glycero*-D-*gulo* aldoheptose **10** can be compared with a commercially available sample (Scheme 3). An aqueous solution of D-glucose (**8**) was treated with sodium cyanide at 100 °C for two days. Hydrolysis of the resulting cyanohydrin to aldonolactone **9** was accomplished by treatment with strong acidic ion-exchange resin IR-120 H^+. In contrast to the described reduction employing sodium amalgam, we preferred sodium borohydride, which has been reported as a suitable agent for the reduction of lactones to the corresponding acetals when the pH value is kept below 6 [30]. In the D-*gluco* series,

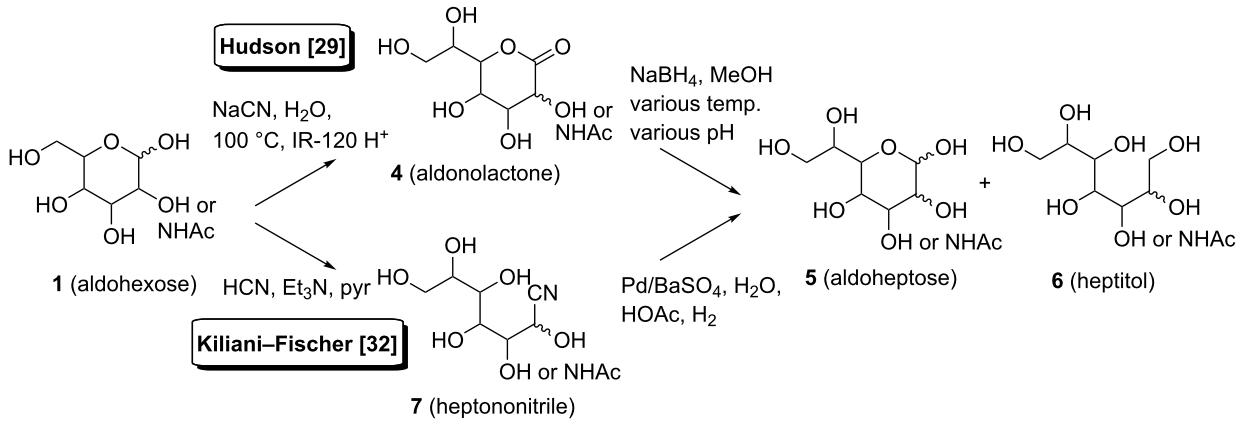

Scheme 2: C-Elongation using the sodium cyanide/sodium borohydride and HCN/Pd($BaSO_4$) method.

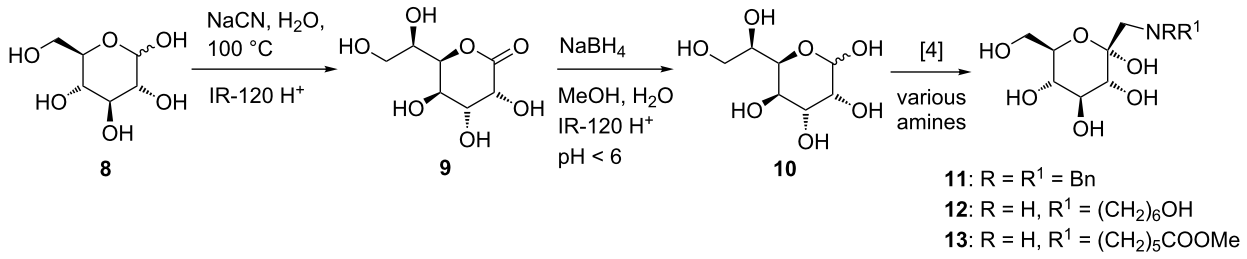

Scheme 3: C-Elongation as well as Amadori rearrangement in the D-*gluco* series.

D-*glycero*-D-*gulo*-aldoheptose **10** was isolated in 81% yield, and no C-2 epimer was detected, as shown by comparison of the NMR data with a commercial sample [31]. Aldoheptose **10** was taken to the Amadori rearrangement without further purification. Three typical amines, dibenzylamine, 6-aminohexanol as well as 6-aminohexanoic acid methyl ester hydrochloride were investigated [25]. In all cases the corresponding Amadori products **11**, **12** as well as **13** were formed, which was confirmed by comparison of the NMR data [25].

Despite thorough investigation of the conditions for the reduction with sodium borohydride by adjusting the pH value, the amount of reagent, and the temperature, it was not possible to obtain the desired aldoheptose in the D-*galacto* as well as the D-*manno* series in satisfactory yields (Scheme 2). In all cases, a mixture of the unreacted lactone **4**, the fully reduced alditol **6** as the main product, and a small amount of the desired aldoheptose **5** was formed. When *N*-acetyl-D-glucosamine was subjected to this reduction method, the corresponding heptitol **6** was isolated as the main product under all conditions tried.

These unsatisfactory results caused us to change the strategy for the C-elongation reaction sequence. Following a slightly modified procedure of the Kiliani–Fischer cyanohydrin reaction reported by Kuhn and Baschang [32], aldoses were exposed to hydrocyanic acid in pyridine and triethylamine, replacing water as solvent, and thereby shortening the reaction time from 15 to 3 days (Scheme 2). A small amount of the reaction mixture was per-*O*-acetylated in order to monitor the reaction by TLC, thus avoiding hydrolysis of the cyanohydrin on the TLC plate, and to track the progress of the reaction. The subsequent reductive hydrolysis of the heptononitrile **7** to the desired aldoheptoses **5** was performed as described by these authors employing Pd/$BaSO_4$ in water and acetic acid. Thus, the corresponding heptose **5**, in some cases as mixtures of C-2 epimers, were isolated in preparatively useful yields. With this method in hand, D-galactose (**14**), D-mannose (**17**) as well as GlcNAc (**20**) were successfully converted to the corresponding aldoheptoses (Scheme 4), namely D-*glycero*-L-*manno*/L-*gluco*-heptopyranose **16a** and **16b**, D-*glycero*-D-*galacto*/D-*talo*-heptopyranose **19a** and **19b**, and 3-acetamido-3-deoxy-D-*gluco*-D-*ido*/D-*gulo*-heptopyranose **22a** and **22b**, via the respective cyanohydrins **15**, **18** and **21**, in preparatively expedient yields.

Amadori rearrangement

With these aldoheptoses in hand we investigated the Amadori rearrangement. The product mixture, containing mainly a C-2 epimeric mixture of α,β-aldoheptoses and minor amounts of

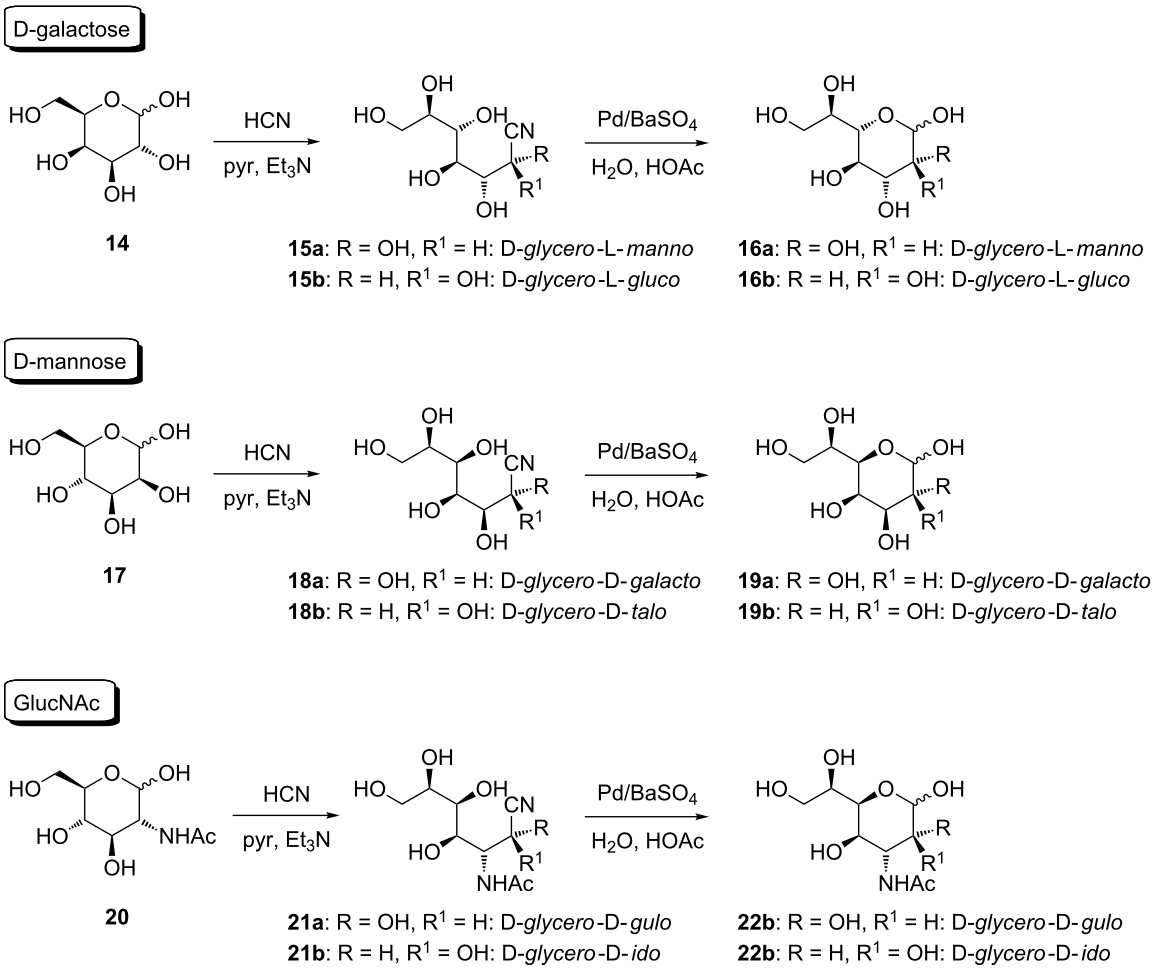

Scheme 4: C-Elongation method by modified Kiliani–Fischer protocol from of D-galactose, D-mannose as well as GlcNAc.

side products from the reductive hydrolysis, was used without further purification. It was expected that the respective aldoheptose would undergo predominantly the Amadori rearrangement, whereas the remaining aldohexose and side products would be rather unreactive under the reaction conditions employed.

In the D-*galacto* series, the mixture containing D-*glycero*-L-*manno*/L-*gluco*-heptopyranose **16a** and **16b** was treated with dibenzylamine in ethanol and 1,4-dioxane as co-solvent, employing one equivalent of acetic acid, to give, after purification by silica-gel chromatography, predominantly the α-anomer of 1-(*N*,*N*-dibenzyl)amino-1-deoxy-α-D-*galacto*-hept-2-ulose in a yield of 71% and as mixture of the pyranoid **23a** and furanoid **23b** forms in a ratio of 3:1 (Scheme 5). 6-Aminohexanol as amino component in aqueous ethanol, containing one equivalent of acetic acid gave, after three days at 50 °C, 1-(6-hydroxyhexylamino)-1-deoxy-α-D-*galacto*-hept-2-ulose in a yield of 74% and with a 4:1 ratio of the pyranoid **24a** and furanoid **24b** forms. In the case of 6-aminohexanoic acid methyl ester hydrochloride, the Amadori rearrangement was performed in ethanol with 1,4-dioxane and water as co-solvent in the presence of triethylamine in order to liberate the free amine from the corresponding ammonium hydrochloride. After purification, 1-(5-(methoxycarbonyl)pentylamino-1-deoxy-α-D-*galacto*-hept-2-ulose was also obtained as a mixture of pyranoid **25a** and furanoid **25b** forms with a 5:1 ratio and a combined yield of 35%. The Amadori products featuring a secondary amine at position C-1, compounds **24** and **25**, were further reacted with triphosgene [25]. In this reaction, the anomeric hydroxy group and the amine at position C-1 formed a cyclic carbamate, thereby stabilising the hemiacetal at the anomeric position. Compounds **24** (**a** and **b**) gave the corresponding 1-*N*,2-*O*-cyclic carbamates in 95% yield with a 3:2 ratio of the pyranoid **26a** and furanoid **26b** forms, and compounds **25** (**a** and **b**) reacted accordingly and gave cyclic carbamates **27a** and **27b** in a 5:3 ratio and a combined yield of 50%.

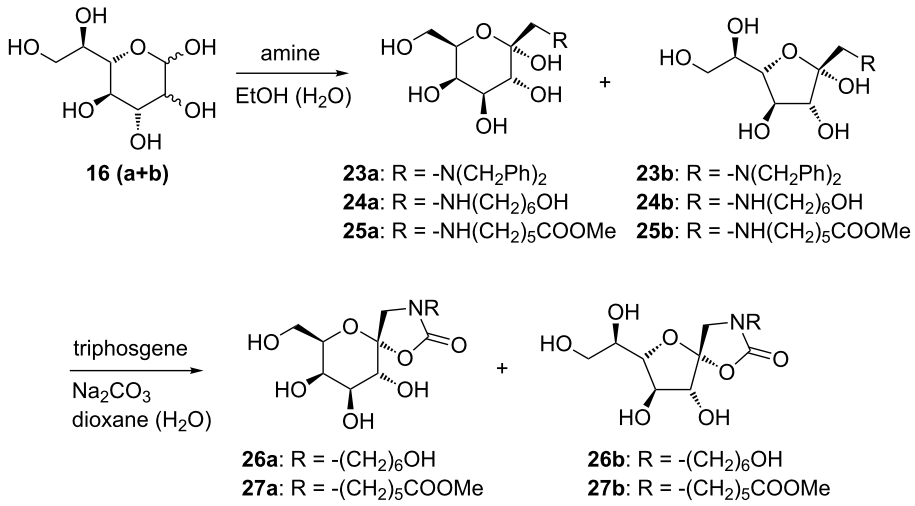

Scheme 5: Amadori rearrangement in the D-*galacto* series.

In the D-*manno* series, the C-elongation employing HCN in pyridine and triethylamine and subsequent reductive hydrolysis of the corresponding nitriles **18** (**a** and **b**) gave very good conversion to D-*glycero*-D-*galacto* heptose **18a**, together with a minor amount of D-*glycero*-D-*talo*-heptopyranose **19b** (Scheme 4). From the NMR analysis of the crude product mixture it was obvious that the predominant product was the β-anomer of D-*glycero*-D-*galacto*-aldoheptose. This was verified by ^{1}H NMR data analysis, the β-anomer presenting a coupling constant of $J_{1,2}$ = 7.8 Hz between protons H-1 and H-2. The Amadori rearrangement with dibenzylamine gave 1-(*N*,*N*-dibenzylamino)-1-deoxy-α-D-*manno*-hept-2-ulopyranose (**28**) in 72% yield, exclusively (Scheme 6). Likewise, with 6-aminohexanol as amino component, the Amadori rearrangement of aldoheptoses **19** (**a** and **b**) gave the corresponding 1-(*N*-6-hydroxyhexyl)amino-1-deoxy-α-D-manno-hept-2-ulose (**29**), exclusively in an isolated yield of 70%. No β-anomer formation could be observed from NMR analysis. Treatment of compound **29** with triphosgene and sodium carbonate in 1,4-dioxane and H_2O gave 1-*N*-(hydroxyhexyl)amino-α-D-*manno*-1-*N*,2-*O*-carbamate **30** in 75% yield. With 6-aminohexanoic acid hydrochloride, the Amadori rearrangement, employing triethylamine for liberation of the free amine from the hydrochloride, gave a 90% yield of the α-anomer **31**. Its treatment with triphosgene provided 1-*N*-2-*O*-cyclic carbamate **32** in 50% yield.

3-Acetamido-3-deoxy-D-*gluco*-D-*ido*/D-*gulo*-heptopyranose **22** (**a** and **b**) gave under Amadori rearrangement conditions with dibenzylamine predominantly 1-(*N*,*N*-dibenzyl)amino-3-acetamido-3-deoxy-α-D-*gluco*-heptulose (**33a**, Scheme 7), and a small amount of the corresponding furanoid form **33b** could be detected by NMR analysis. 6-Aminohexanol as amino component gave exclusively the α-anomer of 1-(*N*-6-hydroxyhexyl)amino-3-acetamido-D-*gluco*-heptulose **34** in the pyranoid form and in 50% yield after purification by column chromatography. Methyl 6-aminohexanoate hydrochloride gave the corresponding α-pyranose **35**, albeit in only 25% yield. With the α-*N*-Boc protected L-lysine derivative Boc-L-Lys(Z)-OMe, the Amadori rearrangement gave the 1-[(5*S*-*tert*-butoxylcarbonylamino)-6-methoxycarbonylpentyl]amino-3-acetamido-1,3-dideoxy-α-D-*gluco*-hept-2-ulopyranose (**36**) in the pyranoid form in 30% yield.

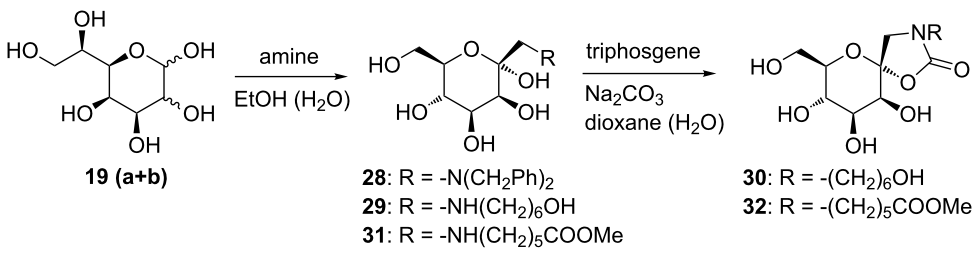

Scheme 6: Amadori rearrangement in the D-*manno* series.

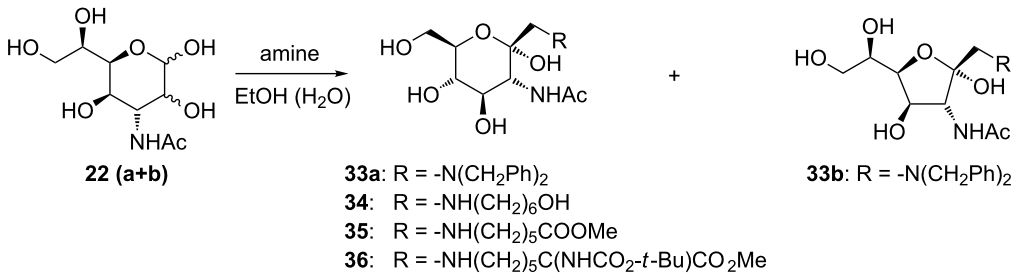

Scheme 7: Amadori rearrangement in the GlcNAc series.

Conclusion

In conclusion, we have successfully developed a protocol for the conjugation of carbohydrate moieties to amine containing molecules through the Amadori rearrangement. By reaction of respective aldoheptoses, non-natural *C*-glycosyl type glycoconjugates presenting the sugar motif in D-*gluco*, D-*manno*, and D-*galacto* as well as GlcNAc configuration are available. This indicates that the Amadori rearrangement is a valuable tool in the repertoire of ligation methods, with the advantage that no protecting-group manipulations are necessary in the carbohydrate moiety and the reaction can be carried out in aqueous environment offering obvious advantages in glycobiology. In preliminary studies, several disaccharidic structures, such as cellobiose, lactose and *N*-DTPM-2-aminodeoxylactose [33], were successfully converted to the respective *C*-glycosyl type glycoconjugates by this method. Optimisation of yields is currently under progress [34].

Experimental

General methods: NMR spectra were recorded on a Bruker Ultrashield spectrometer at 300.36 or 75.53 MHz, in methanol-d_4 or D_2O as indicated. Chemical shifts are listed in parts per million (ppm) employing residual, nondeuterated solvent as the internal standard. Structures of crucial intermediates were unambiguously assigned by 1D-TOCSY and HSQC experiments. Optical rotations were measured on a Perkin Elmer 341 polarimeter at a wavelength of 589 nm and a path length of 10 cm at 20 °C. Analytical TLC was performed on precoated aluminium plates Silica Gel 60 F_{254} (E. Merck 5554), detected with UV light (254 nm), 10% vanillin/sulfuric acid and ceric ammonium molybdate (100 g ammonium molybdate/8 g ceric sulfate in 1 L 10% H_2SO_4), and heated on a hotplate. Preparative TLC was performed on precoated glass plates silica gel 60 F_{254}, 0.5 mm (E. Merck 5744). For column chromatography silica gel 60 (230–400 mesh, E. Merck 9385) was used.

General procedure for generation of HCN [35]**:** Equipment for all reactions in which HCN or cyanides were involved, was placed in a well-ventilated hood. For safety, an electrochemical sensor for HCN detection was used. The required amount of HCN was freshly prepared by adding a saturated NaCN solution dropwise to aqueous sulfuric acid (60%) at 80 °C. HCN was transferred in a nitrogen stream through a drying column ($CaCl_2$) and collected in a cooling trap at −12 °C. Waste solutions containing cyanides were treated with aqueous sodium hypochlorite (10%).

General procedure for preparation of aldoheptoses [32]**:** The respective aldose was dissolved in pyridine, then triethylamine (0.08 equiv) and HCN (8 equiv) were added, and the reaction was kept in a sealed flask at room temperature for several days. For monitoring of the reaction by TLC, a small amount of the reaction mixture was subjected to a per-*O*-acetylation. After complete consumption of the starting material, the remaining HCN and solvents were removed under reduced pressure. The remaining material was azeotroped/co-evaporated with EtOH, and subsequently the products were precipitated by treatment of the residue with ether/ethylacetate 1:1 v/v at 4 °C. The obtained heptononitriles were used for the next step immediately. For the reductive hydrolysis, the respective heptononitrile was dissolved in water, and then acetic acid (1.1 equiv) and $Pd/BaSO_4$ (0.6 g per g heptononitrile) were added, and the reaction mixture was stirred under a hydrogen atmosphere at ambient pressure and temperature until the starting material was consumed. The catalyst was removed by filtration and the pH adjusted with ion-exchange resin (IR-120 H^+) to 2. Filtration of the resin and removal of the solvent under reduced pressure afforded a mixture of products, containing mainly the respective aldoheptoses. This mixture was used for the Amadori rearrangement immediately without further purification.

General method A (Amadori rearrangement with free amines) [25]**:** The respective aldose was dissolved in abs. EtOH, and then 1.2 equiv of the free amine and 1.2 equiv of AcOH were added, and the reaction mixture was stirred at 40 °C until TLC showed satisfactory conversion of the starting material. The reaction mixture was concentrated under reduced pressure, and the obtained products were separated by flash

chromatography with the solvent system indicated in the experimental section.

General method B (Amadori rearrangement with amine hydrochlorides) [25]**:** The respective amine hydrochloride was dissolved in abs. EtOH, 1 equiv of Et_3N was added, and the mixture was stirred for 20 min at rt. To this mixture the aldose was added, and the reaction mixture was stirred at 40 °C until TLC showed satisfactory conversion of the starting material. The reaction mixture was concentrated under reduced pressure and the obtained residue was purified by flash chromatography with the solvent system indicated in the experimental section.

General method C (cyclic carbamate formation with triphosgene) [25]**:** The Amadori rearrangement compound was dissolved in water, and in indicated cases 1,4-dioxane was added to enhance the solubility. A large access of Na_2CO_3, typically >6 equiv, was added at 0 °C. After 15 min triphosgene was added and the reaction mixture stirred for 20 min at 0 °C followed by stirring at room temperature until TLC showed conversion of the starting material. The reaction was concentrated under reduced pressure and the obtained compound mixture separated by flash chromatography with the solvent mixture indicated in the experimental section.

1-(*N*,*N*-Dibenzylamino)-1-deoxy-α-D-*galacto*-hept-2-ulopyranose (23a) and -furanose (23b): The general procedure for the preparation of aldoheptoses was applied to D-galactose (**14**, 3 g, 16.7 mmol) by using pyridine (45 mL), triethylamine (0.18 mL, 1.3 mmol, 0.08 equiv) and HCN (5.6 mL, 0.14 mmol, 8.5 equiv) as described. After five days complete consumption of the aldose was indicated by TLC (per-*O*-acetylation of a sample of the reaction mixture was performed, EE/C (ethyl acetate/cyclohexane) 1:1 v/v) and 5 g of the crude heptononitriles **15a** and **15b** was obtained. This mixture of heptononitriles (2.5 g) was treated in water (50 mL) containing acetic acid (0.75 mL, 1.1 equiv) with $Pd/BaSO_4$ (1.5 g) under a hydrogen atmosphere at ambient pressure. After TLC ($CHCl_3$/MeOH 1:1 v/v containing 0.25% concd NH_4OH) indicated complete consumption of the starting material and workup as described, 3 g of crude aldoheptoses **16a** and **16b** were obtained, which were used for the Amadori rearrangement immediately without any further purification. General procedure A was applied to the mixture of aldoheptose **16a** and **16b** (400 mg) employing EtOH (4 mL) and 1,4-dioxane as co-solvent, dibenzylamine (360 µL, 1.9 mmol) and acetic acid (110 µL, 1.9 mmol). The reaction mixture was stirred at 50 °C for five days. Column chromatography (EE/MeOH 15:1 v/v) gave 480 mg of a mixture of pyranoid **23a** and furanoid **23b** product in a ratio of 3:1 and in an overall yield of 70%. α-Anomer: $[\alpha]_D$ = +20 (*c* 1.4, MeOH); ^{1}H NMR (methanol-d_4) δ 7.37–7.35 (m, 10H, Ph), 4.06 (d, J = 13.4 Hz, 2H, CH_2Ph), 4.06–4.00 (m, 1H, H-6), 3.93 (dd, $J_{4,5}$ = 3.4 Hz, $J_{5,6}$ = 3.5 Hz, 1H, H-5), 3.78–3.71 (m, 2H, H-4, H-7), 3.69–3.65 (m, 1H, H-7), 3.55 (d, 2H, CH_2Ph), 3.52 (d, $J_{3,4}$ = 9.8 Hz, 1H, H-3), 3.05 (d, $J_{1,1}$ = 13.4 Hz, 1H, H-1), 2.72 (d, 1H, H-1); ^{13}C NMR δ 139.6, 130.5, 129.8, 129.6 (Ph), 98.7 (C-2), 72.6, 72.4, 71.5, 70.9 (4C, C-3, C-4, C-5, C-6), 62.6 (C-7), 60.0 (2C, CH_2Ph), 58.8 (C-1); anal. calcd for $C_{21}H_{27}NO_6$: C, 64.77; H, 6.43; found: C, 63.09; H, 6.52.

1-(*N*-(6-Hydroxyhexyl)amino)-1-deoxy-α-D-*galacto*-hept-2-ulopyranose (24a) and -furanose (24b): Following general method A, the aldoheptoses **16a** and **16b** (370 mg) were treated with 6-aminohexanol (200 mg, 1.76 mmol, 1 equiv) in EtOH (5 mL) and 1,4 dioxane as co-solvent in the presence of acetic acid (0.1 mL, 1.76 mmol, 1 equiv) at 50 °C for three days. Silica-gel chromatography ($CHCl_3$/MeOH 4:1 v/v containing 10% of concd NH_4OH) gave the respective Amadori compound in a mixture of α-pyranose **24a** and α-furanose **24b** in a ratio of 4:1 and an overall yield of 74%. Pyranoid α-anomer **24a**: ^{1}H NMR (methanol-d_4) δ 4.00 (m, 1H, H-6), 3.88 (m, 1H, H-5), 3.81–3.69 (m, 3H, H-4, 2 × H-7), 3.63 (d, $J_{3,4}$ = 9.6 Hz, 1H, H-3), 3.57 (t, 2H, H-13), 3.29 (d, $J_{1,1}$ = 12.5 Hz, 1H, H-1), 3.15 (d, 1H, H-1), 3.02 (t, 2H, H-8), 1.82–1.68 (m, 2H, H-9), 1.64–1.53 (m, 2H, H-12), 1.51–1.40 (m, 4H, H-10, H-11); ^{13}C NMR δ 96.7 (C-2), 73.6 (C-6), 71.8, 71.5, 71.1 (3C, C-3, C-4, C-5), 62.9 (C-7), 62.7 (C.13), 54.6 (C-1), 49.7 (C-8), 33.3 (C-12), 27.5, 27.1, 26.5 (3C, C-9, C-10, C-11); anal. calcd for $C_{13}H_{27}NO_7$: C, 50.50; H, 8.82; found: C, 50.46; H, 8.88.

1-(*N*-(5-(Methoxycarbonyl)pentyl)amino)-1-deoxy-α-D-*galacto*-hept-2-ulopyranose (25a) and -furanose (25b): Following general method B, a solution of 6-aminohexanoic acid methyl ester hydrochloride (480 mg, 2.7 mmol, 1.0 equiv) in EtOH (6 mL) with 1,4-dioxane (1 mL) as co-solvent containing Et_3N (370 µL, 2.6 mmol, 1.0 equiv) was applied to the aldoses **16a** and **16b** (560 mg, 2.7 mmol). The reaction mixture was stirred at 60 °C for one day. The solvents were removed under reduced pressure and silica-gel chromatography ($CHCl_3$/MeOH 4:1 v/v containing 10% of concd NH_4OH) gave 300 mg of a mixture of pyranose **25a** and furanose **24b** in 5:1 ratio and 35% yield as a yellow oil. Pyranose **25a** signals: ^{1}H NMR (methanol-d_4) δ 3.91–3.84 (m, 1H, H-6), 3.81–3.73 (m, 1H, H-5), 3.68 (dd, $J_{4,5}$ = 3.2 Hz, $J_{3,4}$ = 9.7 Hz, 1H, H-4), 3.63–3.57 (m, 2H, H-7), 3.56 (s, 3H, OCH_3), 3.53 (d, 1H, H-3), 2.79 (d, $J_{1,1}$ = 12.1 Hz, 1H, H-1), 2.73 (d, 1H, H-1), 2.62–2.48 (m, 2H, H-8), 2.25 (t, 2H, H-12), 1.60–1.48 (m, 2H, H-10), 1.48–1.40 (m, 2H, H-11), 1.33–1.23 (m, 2H, H-9); ^{13}C NMR δ 175.9 (C-13), 98.2 (C-2), 72.8, 72.4, 71.6, 71.3 (3C, C-3, C-4, C-5, C-6), 62.9 (C-7), 56.0 (C-1), 52.1 (OCH_3), 50.8 (C-8), 34.7

(C-12), 30.0 (C-11), 27.7 (C-9), 25.9 (C-10); anal. calcd for $C_{14}H_{27}NO_8$: C, 49.87; H, 8.09; found: C, 49.79; H, 8.11.

1-(*N*-(6-Hydroxyhexyl)amino)-1-*N*,2-*O*-carbonyl-1-deoxy-β-D-galacto-hept-2-ulopyranose 26a and -furanose 26b: General method C was applied to compounds **24a** and **24b** (349 mg) in H_2O (10 mL) and 1,4-dioxane (2 mL), employing Na_2CO_3 (1.3 g, 11.8 mmol, 6 equiv) and triphosgene (0.6 g, 2.0 mmol, 1.8 equiv). Silica-gel chromatography ($CHCl_3$/MeOH 3:1 v/v containing 1% of concd NH_4OH) gave a mixture of pyranose **26a** and furanose **26b** (350 mg, 95%) in a 3:2 ratio. Pyranose **26a** signals: ^{1}H NMR (methanol-d_4) δ 4.07–3.99 (m, 2H, H-5, H-6), 3.87 (d, $J_{1,1}$ = 10.0 Hz, 1H, H-1), 3.84–3.79 (m, 2H, H-3, H-4), 3.79–3.69 (m, 2H, H-7), 3.58 (t, 2H, H-13), 3.47 (d, 1H, H-1), 3.32–3.25 (m, 2H, H-8), 1.67–1.49 (m, 4H, H-9, H-12), 1.49–1.30 (m, 4H, H-10, H-11); ^{13}C NMR δ 158.8 (C=O), 104.6 (C-2), 75.7 (C-5), 71.9, 70.6, 70.8 (3C, C-3, C-4, C-6), 62.9 (C-13), 62.4 (C-7), 53.5 (C-1), 44.5 (C-8), 33.5 (C-12), 28.1, 27.4, 26.5 (3C, C-9, C-10, C-11); anal. calcd for $C_{14}H_{25}NO_8$: C, 50.17; H, 7.53; found: C, 50.10; H, 7.59.

1-(*N*-(5-Methoxycarbonylpentyl)amino)-1-*N*,2-*O*-carbonyl-1-deoxy-β-D-*galacto*-hept-2-ulopyranose (27a) and -furanose (27b): General method C was applied to the mixture of Amadori products **26a** and **26b** (200 mg, 0.6 mmol), Na_2CO_3 (680.0 mg, 6.4 mmol, 6.0 equiv) and triphosgene (320 mg, 1.1 mmol, 1.8 equiv) in H_2O (7 mL) and 1,4-dioxane as co-solvent (1 mL). When TLC indicated complete consumption of the starting material, the solvents were removed under reduced pressure, and silica-gel chromatography ($CHCl_3$/MeOH 6:1 v/v containing 1% of concd NH_4OH) gave a mixture of cyclic carbamates in the pyranoid **27a** and furanoid **27b** form in a ratio of 5:3 (280 mg, 50%) as a yellow oil. Pyranose **27a** signals: ^{1}H NMR (methanol-d_4) δ 4.06–3.94 (m, 2H, H-5, H-6), 3.87–3.79 (m, 2H, H-1, H-4), 3.87–3.70 (m, 3H, H-3, H-7), 3.68 (s, 3H, OCH_3), 3.45 (d, $J_{1,1}$ = 9.8 Hz, 1H, H-1), 2.37 (t, 2H, H-12), 1.72–1.55 (m, 4H, H-9, H-11), 1.42–1.31 (m, 3H, H-10); ^{13}C NMR δ 176.0 (C-13), 158.6 (NCO), 104.5 (C-2), 75.7, 72.0, 70.9, 70.8 (4C, C-3, C-4, C-5, C-6), 62.5 (C-7), 53.4 (C-1), 52.1 (OCH_3), 44.3 (C-8), 34.7 (C-12), 27.8 (C-9), 27.0 (C-10), 25.7 (C-11); anal. calcd for $C_{15}H_{25}NO_9$: C, 49.61; H, 6.95; found: C, 49.58; H, 6.97.

1-(*N*,*N*-Dibenzylamino)-1-deoxy-α-D-*manno*-hept-2-ulopyranose (28): General method for sugar elongation was applied to D-mannose **17** (3 g, 16.7 mmol), pyridine (50 mL), triethylamine (0.18 mL, 1.3 mmol, 0.08 equiv) and HCN (4.5 mL, 0.11 mmol, 6.9 equiv). After five days, complete consumption of the aldose was indicated by TLC, and 8 g of the crude heptononitrile **18** (**a** and **b**) were obtained. For the reductive hydrolysis the heptononitriles **18** (4.5 g) were treated as described employing dist. water (90 mL), acetic acid (1.35 mL, 1.1 equiv) and Pd/$BaSO_4$ (2.7 g). After TLC ($CHCl_3$/MeOH 1:1 v/v containing 0.25% concd NH_4OH) showed complete consumption of the starting material, and workup with ion-exchange resin IR-120 H^+, 3.7 g of crude aldoheptoses **19a** and **19b** were obtained. NMR analysis of the crude product mixture indicated the D-*glycero*-D-*galacto*-β-aldoheptose **19a** as the predominant compound (4.48 ppm, $J_{1,2}$ = 7.8 Hz, 1H, H-1β) next to its α-anomer (5.14 ppm, $J_{1,2}$ = 3.6 Hz, 1H, H-1α) in a ratio of 5:2. This compound mixture was used for the Amadori rearrangement. General procedure A was applied to the mixture of aldoheptoses **19** (400 mg) employing EtOH (5 mL) and 1,4-dioxane (1 mL) as cosovlent, dibenzylamine (360 µL, 1.9 mmol) and acetic acid (110 µL, 1.9 mmol). The reaction mixture was stirred at 50 °C for three days. Column chromatography (EE/MeOH 20:1 v/v) gave product **28** in a yield of 72% (540 mg). α-Anomer **28**: $[\alpha]_D$ = +20 (*c* 1.1, MeOH); ^{1}H NMR (methanol-d_4) δ 7.51–7.24 (m, 10H, Ph), 3.94 (d, *J* = 13.3 Hz, 2H, CH_2Ph), 3.85–3.75 (m, 4H, H-4, H-5, 2 × H-7), 3.73–3.60 (m, 3H, H-6, CH_2Ph), 3.47 (d, $J_{3,4}$ = 3.1 Hz, 1H, H-3), 2.93 (d, $J_{1,1}$ = 13.7 Hz, 1H, H-1), 2.77 (d, 1H, H-1); ^{13}C NMR δ 139.8, 130.6, 130.3, 129.6 (Ph), 97.5 (C-2), 75.8, 74.2, 73.3, 68.7 (4C, C-3, C-4, C-5, C-6), 63.2 (C-7), 60.2 (2C, CH_2Ph), 59.9 (C-1); anal. calcd for $C_{21}H_{27}NO_6$: C, 64.77; H, 6.43; found: C, 63.07; H, 6.50.

1-(*N*-(6-Hydroxyhexyl)amino)-1-deoxy-α-D-*manno*-hept-2-ulose (29): Following general method A, the mixture of aldoheptoses **19** (360 mg) was treated with 6-aminohexanol (200 mg, 1.71 mmol, 1 equiv) in EtOH (5 mL) and 1,4-dioxane as co-solvent in the presence of acetic acid (0.1 mL, 1.71 mmol, 1 equiv) at 50 °C for three days. When TLC indicated complete consumption of the starting material, silica-gel chromatography ($CHCl_3$/MeOH 4:1 v/v containing 10% of concd NH_4OH) gave the respective Amadori compound **29** (360 mg) exclusively in the α-pyranose form in a yield of 70%. $[\alpha]_D$ = +7 (*c* 1.0, MeOH); ^{1}H NMR (methanol-d_4) δ 3.93–3.83 (m, 3H, H-3, H-5, H-7), 3.83–3.71 (m, 2H, H-6, H-7), 3.71–3.62 (m, 1H, H-4), 3.59 (t, 2H, H-13), 3.36 (d, 1H, H-1), 3.12 (d, $J_{1,1}$ = 12.6 Hz, 1H, H-1), 3.04 (q, 2H, H-8), 1.81–1.69 (m, 2H, H-9), 1.64–1.53 (m, 2H, H-12), 1.51–1.40 (m, 4H, H-13, H-14); ^{13}C NMR δ 96.3 (C-2), 75.2, 74.6, 72.6, 67.9 (4C, C-3, C-4, C-5, C-6), 62.8 (C-13), 62.6 (C-7), 55.0 (C-1), 49.4 (C-8), 33.6 (C-12), 27.5, 26.8, 26.5 (3C, C-9, C-10, C-11); anal. calcd for $C_{13}H_{27}NO_7$: C, 50.50; H, 8.82; found: C, 50.45; H, 8.89.

1-(*N*-(6-Hydroxyhexyl)amino)-1-*N*,2-*O*-carbonyl-1-deoxy-β-D-*manno*-pyranose (30): General method C was applied to compound **29** (200 mg, 0.6 mmol) in H_2O (5 mL) and 1,4-dioxane (1 mL), Na_2CO_3 (0.74 g, 6.9 mmol, 6 equiv) and

triphosgene (0.35 g, 1.12 mmol, 1.8 equiv). Silica-gel chromatography ($CHCl_3$/MeOH 6:1 v/v containing 1% of concd NH_4OH) gave the corresponding cyclic carbamate **30** in the pure β-anomeric pyranoid form (160 mg) in a yield of 75%. β-Anomer: $[\alpha]_D$ = +22 (0.9, MeOH); ^{1}H NMR (methanol-d_4) δ 3.92 (d, $J_{3,4}$ = 2.6 Hz, 1H, H-3), 3.83 (d, $J_{1,1}$ = 10.7 Hz, 1H, H-1), 3.81–3.65 (m, 5H, H-4, H-5, H-6, 2 × H-7), 3.56 (t, 2H, H-13), 3.48 (d, 1H, H-1), 3.32–3.22 (m, 2H, H-8), 1.64–1.47 (m, 4H, H-9, H-12), 1.46–1.26 (m, 4H, H-10, H-11); ^{13}C NMR δ 158.2 (C=O), 103.8 (C-2), 77.1, 73.2, 72.6, 67.3 (4C, C-3, C-4, C-5, C-6), 62.9 (C-13), 62.3 (C-7), 54.4 (C-1), 44.7 (C-8), 33.5 (C-12), 28.1, 27.3, 26.5 (3C, C-9, C-10, C-11); anal. calcd for $C_{14}H_{25}NO_8$: C, 50.17; H, 7.53; found: C, 50.13; H, 7.60.

1-(*N*-(5-(Methoxycarbonyl)pentyl)amino)-1-deoxy-α-D-*manno*-hept-2-ulopyranose (31): Following general method B, aldose **19** (350 mg, 1.7 mmol) was treated with a mixture of 6-aminohexanoic acid methyl ester hydrochloride (600 mg, 3.4 mmol, 2.0 equiv) in EtOH (5 mL) and H_2O (1 mL) as co-solvent containing Et_3N (480.0 μL, 3.4 mmol, 2.0 equiv), and the reaction mixture was stirred at 40 °C for four days. The solvents were removed under reduced pressure and silica-gel chromatography ($CHCl_3$/MeOH 3:1 v/v containing 1 % of concd NH_4OH) gave 600 mg of pyranose **31** in a yield of 90% as a yellow oil. $[\alpha]_D$ = +8 (*c* 1.2, MeOH); ^{1}H NMR (methanol-d_4) δ 3.99–3.72 (m, 6H, H-3, H-4, H-5, H-6, 2 × H-7), 3.68 (s, 3H, OCH_3), 3.38 (d, 1H, $J_{1,1}$ = 12.3 Hz, H-1), 3.18 (d, 1H, H-1), 3.06 (bt, 2H, H-8), 2.39 (t, 2H, H-12), 1.84–1.62 (m, 4H, H-9, H-11), 1.51–1.39 (m, 2H, H-10); ^{13}C NMR δ 175.8 (C-13), 96.2 (C-2), 75.2, 74.6, 72.5, 67.8 (4C, C-3, C-4, C-5, C-6), 62.5 (C-7), 55.1 (C-1), 52.1 (OCH_3), 47.7 (C-8), 34.4 (C-12), 27.1, 26.4, 25.5 (3, C-9, C-10, C-11); anal. calcd for $C_{14}H_{27}NO_8$: C, 49.87; H, 8.09; found: C, 49.78; H, 8.12.

1-(*N*-(5-(Methoxycarbonyl)pentyl)amino)-1-*N*,2-*O*-carbonyl-1-deoxy-β-D-*manno*-hept-2-ulopyranose (32): General method C was applied to Amadori product **31** (200 mg, 0.6 mmol), Na_2CO_3 (680.0 mg, 6.4 mmol, 6.0 equiv) and triphosgene (320 mg, 1.1 mmol, 1.8 equiv) in H_2O (7 mL) and 1,4-dioxane as co-solvent (1 mL). After complete consumption of the starting material, the solvent was removed under reduced pressure, and silica-gel chromatography ($CHCl_3$/MeOH 6:1 v/v containing 1% of concd NH_4OH) gave cyclic carbamate **32** (110 mg, 50%) in the β-anomeric pyranoid form exclusively as a slightly yellow oil. $[\alpha]_D$ = +46 (*c* 1.4, MeOH); ^{1}H NMR (methanol-d_4) δ 3.89–3.83 (m, $J_{3,4}$ = 2.7 Hz, 2H, H-3, H-7), 3.81 (d, $J_{1,1}$ = 10.4 Hz, 1H, H-1), 3.79–3.69 (m, 4H, H-4, H-5, H-6, H-7), 3.68 (s, 3H, OCH_3), 3.47 (d, 1H, H-1), 3.36–3.30 (m, 2H, H-8), 2.38 (t, 2H, H-12), 1.74–1.55 (m, 4H, H-9, H-11), 1.44–1.30 (m, 2H, H-10); ^{13}C NMR δ 175.9 (C-13), 158.1 (NCO), 103.8 (C-2), 77.2, 72.7, 72.6, 67.5 (4C, C-3, C-4, C-5, C-6), 62.6 (C-7), 54.3 (C-1), 52.1 (OCH_3), 44.5 (C-8), 34.6 (C-12), 27.9, 27.0, 25.6 (3C, C-9, C-10, C-11); anal. calcd for $C_{15}H_{25}NO_9$: C, 49.61; H, 6.95. found: C, 49.56; H, 6.98.

1-(*N*,*N*-Dibenzylamino)-3-acetamido-1,2-dideoxy-α-D-*gluco*-hept-2-ulopyranose (33a) and -furanose (33b): General method for sugar elongation was applied to GlcNAc **20** (3 g, 13.6 mmol) dissolved in pyridine (45 mL, 0.56 mmol) and triethylamine (0.15 mL, 1.1 mmol, 12.6 equiv) employing HCN (4.5 mL, 0.11 mmol, 8.5 equiv). After four days complete consumption of the starting material was indicated by TLC (per-*O*-acetylation of a small sample, C/EE 1:1 v/v) and 3.5 g of the crude heptononitriles **21a** and **21b** were obtained. Heptononitriles **21a** and **21b** (3.5 g, 14.1 mmol) were treated as described in distd water (40 mL) employing acetic acid (1.23 mL, 1.5 equiv) and Pd/$BaSO_4$ (2.1 g). After TLC ($CHCl_3$/MeOH 1:1 v/v containing 0.25% concd NH_4OH) showed complete consumption of the starting material, the workup was applied as described, and 2.8 g of a mixture of 3-acetamido-3-deoxy-D-*gluco*-D-*ido*/D-*gulo*-heptoses **22a** and **22b** were obtained, which were used for the Amadori rearrangement immediately without any further purification. General procedure A was applied to aldoheptoses **22** (300 mg, 1.2 mmol) in EtOH (6 mL) employing dibenzylamine (460 mL, 2.4 mmol, 2 equiv) and acetic acid (120 mL, 2.1 mmol, 1.8 equiv). The reaction mixture was stirred at 40 °C for three days. When TLC indicated complete consumption of the starting material the solvent was removed under reduced pressure. Column chromatography ($CHCl_3$/MeOH 3:1 v/v containing 1% concd NH_4OH) gave 210 mg of the pyranoid product **33a** and a minor amount of furanoid compound **33b** in an overall yield of 41%. α-Anomer: ^{1}H NMR (methanol-d_4) δ 7.39–7.20 (m, 10H, Ph), 4.02 (d, 1H, $J_{3,4}$ = 9.6 Hz, H-3), 4.06 (d, 2H, *J* = 13.4 Hz, CH_2Ph), 3.71–3.44 (m, 4H, H-6, 2 × H-7, H-5), 3.27 (dd, $J_{4,5}$ = 8.3 Hz, 1H, H-4), 3.26 (d, 2H, CH_2PH), 2.51–2.41 (2 × d, $J_{1,1}$ = 14.2 Hz, 2H, 2 × H-1), 1.46 (s, 3H, CH_3); ^{13}C NMR δ 173.7 (NHCO), 140.1, 130.5, 129.6, 128.5 (Ph), 98.3 (C-2), 74.4, 73.8, 72.2 (3C, C-3, C-4, C-5, C-6), 63.0 (C-7), 60.5 (2C, CH_2Ph), 57.4 (C-1), 56.5 (C-3); anal. calcd for $C_{23}H_{30}N_2O_6$: C, 64.17; H, 7.04; found: C, 64.12; H, 7.09.

1-(*N*-(6-Hydroxyhexyl)amino)-3-acetamido-1,2-dideoxy-α-D-*gluco*-hept-2-ulopyranose (34): Following general method A, the mixture of 3-NHAc-aldoheptoses **22** (**a** and **b**) (300 mg, 1.2 mmol) was treated with 6-aminohexanol (220 mg, 1.9 mmol, 1.6 equiv) in EtOH (6 mL) in the presence of acetic acid (0.26 mL, 4.54 mmol, 3.8 equiv) at 60 °C for two days. When TLC indicated complete consumption of the starting material, the solvent was removed under reduced pressure. Silica-gel chromatography ($CHCl_3$/MeOH 5:1 v/v containing 30% of

concd NH_4OH) gave the respective Amadori compound as α-pyranose **34** (210 mg) in a yield of 50%. α-Anomer: $[\alpha]_D$ = +19 (*c* 3.1, MeOH); ^{1}H NMR (methanol-d_4) δ 3.83–3.75 (m, 5H, H-3, H-4, H-5, 2 × H-7), 3.58 (t, 2H, H-13), 3.47 (ddd, $J_{5,6}$ = 7.8 Hz, $J_{6,7'}$ = 2.4 Hz, $J_{6,7}$ = 8.9 Hz, 1H, H-6), 2.79 (d, $J_{1,1}$ = 12.3 Hz, 1H, H-1), 2.67 (t, 2H, H-8), 2.61 (d, 1H, H-1), 2.05 (s, 3H, CH_3), 1.45–1.36 (m, 4H, H-10, H-11); ^{13}C NMR δ 174.6 (NHCO), 98.1 (C-2), 74.2, 73.4, 71.7 (3C, C-4, C-5, C-6), 62.9 (C-13), 62.5 (C-7), 56.0 (2C, C-1, C-3), 50.9 (C-8), 33.6 (C-12), 29.9, 28.0, 26.8 (3C, C-9, C-10, C-11), 22.7 (CH_3); anal. calcd for $C_{15}H_{30}N_2O_7$: C, 51.41; H, 8.64; found: C, 51.36; H, 8.68.

1-(*N*-(5-(Methoxycarbonyl)pentyl)amino)-2-acetamido-1,2-dideoxy-α-D-*gluco*-hept-2-ulopyranose (35): Following general method B, a mixture of 6-aminohexanoic acid methyl ester hydrochloride (350 mg, 1.9 mmol, 1.6 equiv) in EtOH (6 mL) containing Et_3N (260.0 µL, 1.9 mmol, 1.6 equiv) was applied to the mixture of 3-NHAc-aldoses **22** (**a** and **b**) (300 mg, 1.2 mmol), and the reaction mixture was stirred at 40 °C for four days. The solvents were removed under reduced pressure, and silica-gel chromatography ($CHCl_3$/MeOH 5:1 v/v containing 1% of concd NH_4OH) gave 115 mg of 3-NHAc-pyranose **35** in a yield of 25% (115 mg) as a yellow oil. $[\alpha]_D$ = +6 (*c* 0.9, MeOH); ^{1}H NMR (methanol-d_4) δ 3.92–3.77 (m, 4H, H-3, H-4, 2 × H-7), 3.74 (d, $J_{2,3}$ = 10.3 Hz, 1H, H-3), 3.69 (s, 3H, OCH_3), 3.50 (dd, $J_{5,6\,=\,5,4}$ = 9.0 Hz, 1H, H-5), 3.15–2.93 (m, 4H, 2 × H-1, 2 × H-8), 2.58 (t, 2H, H-12), 2.1 (s, 3H, $COCH_3$), 1.86–1.63 (m, 4H, H-9, H-11), 1.54–1.41 (m, 2H, H-10); ^{13}C NMR δ 175.7, 175.5 (2C, NHCO, C-13), 96.7 (C-2), 74.5, 72.1, 71.4 (3C, C-4, C-5, C-6), 61.7 (C-7), 56.0 (C-3), 54.1 (C-1), 52.1 (OCH_3), 49.5 (C-8), 34.4 (C-13), 26.9, 26.7, 25.4 (3C, C-9, C-10, C-11), 22.5 (CH_3); anal. calcd for $C_{16}H_{30}N_2O_8$: C, 50.78; H, 8.00; found: C, 50.83; H, 8.06.

1-*N*-[(5*S*)-(*tert*-Butoxycarbonylamino)-5-(methoxycarbonyl)pentyl]amino-3-acetamido-1,2-dideoxy-α-D-*gluco*-hept-2-ulopyranose (36): Following general method B, a mixture of Boc-Lys-OMe [36] (360 mg, 1.2 mmol, 1.0 equiv) in EtOH (6 mL) and acetic acid (70.0 µL, 1.2 mmol, 1.0 equiv) was applied to the mixture of 3-NHAc-aldoses **22** (**a** and **b**) (300 mg, 1.2 mmol), and the reaction mixture was stirred at 50 °C for two days. After complete conversion of the starting material, the solvents were removed under reduced pressure, and silica-gel chromatography ($CHCl_3$/MeOH 7:1 v/v containing 10% of concd NH_4OH) gave 3-NHAc-pyranose **36** in a yield of 30% (180 mg) as a yellow oil. $[\alpha]_D$ = +12 (*c* 0.4, MeOH); ^{1}H NMR (methanol-d_4) δ 4.17–4.07 (m, 2H, H-12), 3.58–3.69 (m, 8H, H-3, H-4, H-6, 2 × H-7, OCH_3), 3.48 (dd, $J_{4,5\,=\,5,6}$ = 8.6 Hz, 1H, H-5), 2.75 (d, $J_{1,1}$ = 12.2 Hz, 1H, H-1), 2.61 (t, 2H, H-8), 2.53 (d, 1H, H-1), 2.05 (s, 3H, $COCH_3$), 1.87–1.63 (m, 4H, H-10, H-11), 1.63–1.49 (m, 2H, H-9), 1.46 (s, 9H, 3 × CH_3); ^{13}C NMR δ 175.1, 174.1, 158.2 (3C, 3 × C=O), 98.3 (C-2), 80.6 (C-13), 74.1, 73.7, 71.8 (3C, C-3, C-4, C-5), 62.6 (C-7), 56.3 (C-1), 55.9 (C-9), 55.1 (C-12), 52.7 (OCH_3), 50.7 (C-8), 32.5, 29.9 (2C, C-10, C-11), 28.8 (3C, 2 × CH3), 24.5 (C-9), 22.7 (OCH_3); anal. calcd for $C_{21}H_{39}N_3O_{10}$: C, 51.11; H, 7.99; found: C, 51.16; H, 8.06.

Supporting Information

Supporting Information File 1

NMR data of compounds **16**, **19**, **23**–**36**.
[http://www.beilstein-journals.org/bjoc/content/supplementary/1860-5397-8-185-S1.pdf]

Acknowledgements

This work was supported by the Austrian Science Fund (FWF): Era-Chemistry [I 945-B11].

References

1. Haltiwanger, R. S.; Lowe, J. B. *Annu. Rev. Biochem.* **2004,** *73,* 491–537. doi:10.1146/annurev.biochem.73.011303.074043
2. Boltje, T. J.; Buskas, T.; Boons, G.-J. *Nat. Chem.* **2009,** *1,* 611–622. doi:10.1038/nchem.399
3. Sletten, E. M.; Bertozzi, C. R. *Angew. Chem., Int. Ed.* **2009,** *48,* 6974–6998. doi:10.1002/anie.200900942
4. Payne, R. J.; Wong, C.-H. *Chem. Commun.* **2010,** *46,* 21–43. doi:10.1039/B913845E
5. Dondoni, A.; Marra, A. *Chem. Soc. Rev.* **2012,** *41,* 573–586. doi:10.1039/c1cs15157f
6. Wang, L.-X.; Huang, W. *Curr. Opin. Chem. Biol.* **2009,** *13,* 592–600. doi:10.1016/j.cbpa.2009.08.014
7. Zhu, X.; Schmidt, R. R. *Angew. Chem., Int. Ed.* **2009,** *48,* 1900–1934. doi:10.1002/anie.200802036
8. van Berkel, S. S.; van Eldijk, M. B.; van Hest, J. C. M. *Angew. Chem., Int. Ed.* **2011,** *50,* 8806–8827. doi:10.1002/anie.201008102
9. Davidek, T.; Blank, I. *Chimia* **2005,** *59,* 862.
10. Ames, J. M. The Maillard reaction. In *Biochemistry of Food Proteins;* Hudson, B. J. F., Ed.; Elsevier Applied Science: London, 1992; pp 99–153.
11. Hotchkiss, D. J.; Soengas, R.; Booth, K. V.; Weymouth-Wilson, A. C.; Eastwick-Field, V.; Fleet, G. W. J. *Tetrahedron Lett.* **2007,** *48,* 517–520. doi:10.1016/j.tetlet.2006.11.137
12. Fernández-Bolaños, J. G.; Ulgar, V.; Maya, I.; Fuentes, J.; Diánez, M. J.; Estrada, M. D.; López-Castro, A.; Pérez-Garrido, S. *Tetrahedron: Asymmetry* **2003,** *14,* 1009–1018. doi:10.1016/S0957-4166(03)00160-5
13. Kadokawa, J.; Hino, D.; Karasu, M.; Tagaya, H.; Chiba, K. *Eur. Polym. J.* **2000,** *36,* 225–230. doi:10.1016/S0014-3057(99)00096-8
14. Shu, L.; Shen, Y.-M.; Burke, C.; Goeddel, D.; Shi, Y. *J. Org. Chem.* **2003,** *68,* 4963–4965. doi:10.1021/jo0206770

15. Wrodnigg, T. M.; Stütz, A. E.; Tarling, C. A.; Withers, S. G. *Carbohydr. Res.* **2006,** *341,* 1717–1722. doi:10.1016/j.carres.2006.03.010
16. Wrodnigg, T. M.; Diness, F.; Gruber, C.; Häusler, H.; Lundt, I.; Rupitz, K.; Steiner, A. J.; Stütz, A. E.; Tarling, C. A.; Withers, S. G.; Wölfler, H. *Bioorg. Med. Chem.* **2004,** *12,* 3485–3495. doi:10.1016/j.bmc.2004.04.037
17. Wrodnigg, T. M.; Withers, S. G.; Stütz, A. E. *Bioorg. Med. Chem. Lett.* **2001,** *11,* 1063–1064. doi:10.1016/S0960-894X(01)00126-3
18. Hermetter, A.; Scholze, H.; Stütz, A. E.; Withers, S. G.; Wrodnigg, T. M. *Bioorg. Med. Chem. Lett.* **2001,** *11,* 1339–1342. doi:10.1016/S0960-894X(01)00209-8
19. Wrodnigg, T. M.; Gaderbauer, W.; Greimel, P.; Häusler, H.; Sprenger, F. K.; Stütz, A. E.; Virgona, C.; Withers, S. G. *J. Carbohydr. Chem.* **2000,** *19,* 975–990. doi:10.1080/07328300008544129
20. Wrodnigg, T. M.; Stütz, A. E.; Withers, S. G. *Tetrahedron Lett.* **1997,** *38,* 5463–5466. doi:10.1016/S0040-4039(97)01198-2
21. Amadori, M. *Atti R. Accad. Lincei* **1925,** *2,* 337–342.
22. Hodge, J. E.; Fisher, B. E. *Meth. Carbohydr. Chem.* **1963,** *2,* 99–107.
23. Wrodnigg, T. M.; Eder, B. In *Glycoscience – Epimerization, Isomerization, Rearrangement Reactions of Carbohydrates;* Stütz, A. E., Ed.; Springer, 2001; pp 115–152.
24. Mossine, V. V.; Mawhinney, T. P. *Adv. Carbohydr. Chem. Biochem.* **2010,** *64,* 291–402. doi:10.1016/S0065-2318(10)64006-1
25. Wrodnigg, T. M.; Kartusch, C.; Illaszewicz, C. *Carbohydr. Res.* **2008,** *343,* 2057–2066. doi:10.1016/j.carres.2008.02.022
26. Dondoni, A.; Marra, A. *Chem. Rev.* **2000,** *100,* 4395–4422. doi:10.1021/cr9903003
See for stability of C-glycosides.
27. Nicotra, F.; Cipolla, L.; Peri, F.; La Ferla, B.; Redaelli, C. *Adv. Carbohydr. Chem. Biochem.* **2007,** *61,* 353–398. doi:10.1016/S0065-2318(07)61007-5
28. Kiessling, L. L.; Splain, R. A. *Annu. Rev. Biochem.* **2010,** *79,* 619–653. doi:10.1146/annurev.biochem.77.070606.100917
29. Hudson, C. S. *J. Am. Chem. Soc.* **1951,** *73,* 4498–4499. doi:10.1021/ja01153a548
30. Bock, K.; Lundt, I.; Pedersen, C. *Carbohydr. Res.* **1981,** *90,* 7–16. doi:10.1016/S0008-6215(00)85607-4
31. Gallas, K. Investigation of the Kiliani-Fischer reaction for the preparation of aldoheptoses and their application for the synthesis of C-glycosyl glycoconjugates. Diploma Thesis, TU Graz, Graz, Austria, 2009.
32. Kuhn, R.; Baschang, G. *Justus Liebigs Ann. Chem.* **1960,** *636,* 164–173. doi:10.1002/jlac.19606360117
33. Stütz, A. E.; Dekany, G.; Eder, B.; Illaszewicz, C.; Wrodnigg, T. M. *J. Carbohydr. Chem.* **2003,** *22,* 253–265. doi:10.1081/CAR-120023468
34. Adanitsch, F. Synthesis of Biological Active Carbohydrates and Analogues. Diploma Thesis, TU Graz, Graz, Austria, 2009.
35. Avi, M.; Gaisberger, R.; Feichtenhofer, S.; Griengl, H. *Tetrahedron* **2009,** *65,* 5418–5426. doi:10.1016/j.tet.2009.04.048
36. Steiner, J.; Stütz, A. E.; Tarling, C. A.; Withers, S. G.; Wrodnigg, T. M. *Carbohydr. Res.* **2007,** *342,* 1850–1858. doi:10.1016/j.carres.2007.03.024

License and Terms

Beilstein Journal of Organic Chemistry

A new approach toward the total synthesis of (+)-batzellaside B

Jolanta Wierzejska, Shin-ichi Motogoe, Yuto Makino, Tetsuya Sengoku, Masaki Takahashi and Hidemi Yoda*

Full Research Paper

Open Access

Address:
Department of Materials Science, Faculty of Engineering, Shizuoka University, 3-5-1 Johoku, Naka-ku, Hamamatsu, Shizuoka 432-8561, Japan

Email:
Hidemi Yoda* - tchyoda@ipc.shizuoka.ac.jp

* Corresponding author

Keywords:
asymmetric dihydroxylation; (+)-batzellaside B; iminosugar; L-pyroglutamic acid; total synthesis

Beilstein J. Org. Chem. **2012,** *8,* 1831–1838.
doi:10.3762/bjoc.8.210

Received: 04 August 2012
Accepted: 24 September 2012
Published: 25 October 2012

This article is part of the Thematic Series "Synthesis in the glycosciences II".

Guest Editor: T. K. Lindhorst

Abstract

A new synthetic approach to (+)-batzellaside B from naturally abundant L-pyroglutamic acid is presented in this article. The key synthetic step involves Sharpless asymmetric dihydroxylation of an olefinic substrate functionalized with an acetoxy group to introduce two chiral centres diastereoselectively into the structure. Heterocyclic hemiaminal **4**, which could be converted from the resulting product, was found to provide stereospecific access to enantiomerically enriched allylated intermediate, offering better prospects for the total synthesis of this natural product.

Introduction

Iminosugars, monosaccharide analogues in which the endocyclic oxygen has been replaced by nitrogen, display beneficial therapeutic activity as sugar-mimicking glycosidase inhibitors [1-4]. Since the discovery of nojirimycin (Figure 1), which was isolated from *Streptomyces roseochromogenes* R-468 and *S. lavendulae* SF-425 in the 1960s [5], this class of compounds has attracted a great deal of interest in the medical community due to their promising pharmaceutical potential as antidiabetic [6], antitumor [7] and antiviral [8] agents. Undoubtedly, approval of Glyset [9] and Miglustat [10] (Figure 1) for treatment of type II diabetes and Gaucher disease, respectively, has imparted therapeutic applications of this class of natural products.

In this context, (+)-batzellasides A–C (**1a**–**c**) (Figure 2), *C*-alkylated azasugars isolated in 2004 from a sponge *Batzella* sp. collected off the west coast of Madagascar, represent the first example of iminosugars from a marine organism [11]. These naturally occurring products have been demonstrated to retain a remarkably high degree of potency against *Staphylo-*

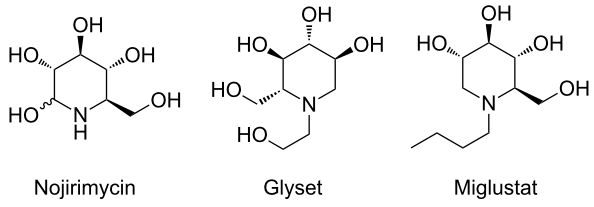

Figure 1: Examples of naturally occurring iminosugars.

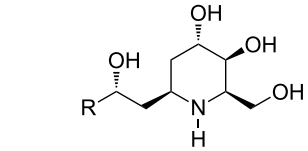

Figure 2: The chemical structures of (+)-batzellasides A–C (**1a**–**c**).

coccus epidermidis with MICs of ≤6.3 μg/mL, thus serving as new potent antibacterial agents [11]. As a part of our research program on the synthesis and investigation of biologically active natural products [12-18], we have pursued the synthetic elaboration of (+)-batzellaside B (**1b**) as a represent member of this new class of iminosugar alkaloids.

In a previous publication, we communicated the first total synthesis of (+)-batzellaside B (**1b**) by the use of L-arabinose, wherein the absolute stereochemistry of this natural product was completely established by the modified Mosher analysis of a synthetic intermediate prepared through a separate route (Scheme 1) [19]. In this approach involving nucleophilic cyclization of acyclic aldehyde in situ generated from olefin **2** for constructing the piperidine ring system, proper synthetic manipulation of the three inherent stereocenters contained in the chiral source was a key strategy for ensuring effective stereocontrol to achieve completion of the target-directed synthesis. The overall yield in 22 steps from 2,3,5-tri-*O*-benzyl-L-arabinose (**3**) was 3.9%. Although **1b** and its related analogues are now accessible through the pathway established above,

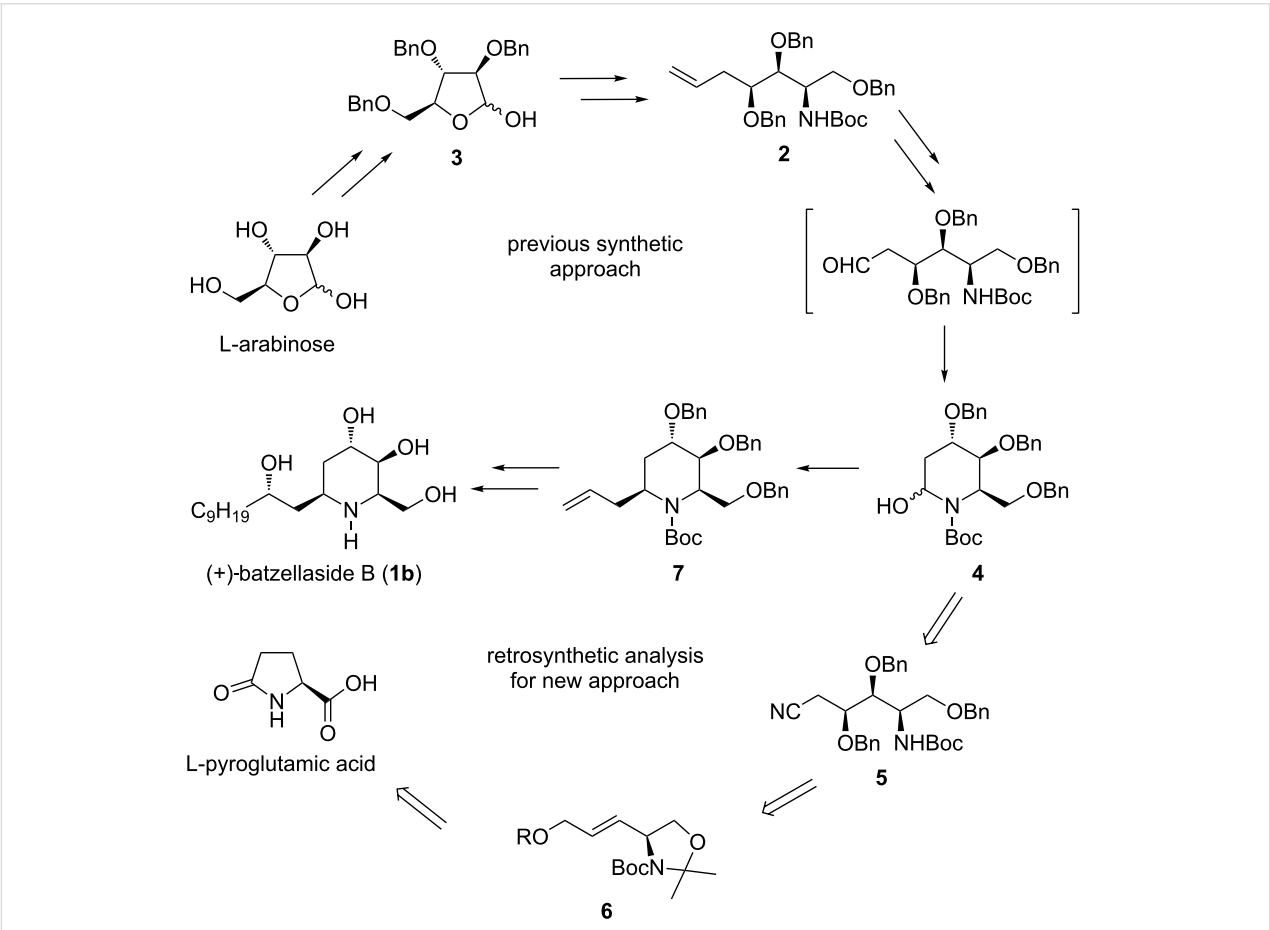

Scheme 1: Our previous approach to (+)-batzellaside B and retrosynthetic analysis for the new synthetic strategy.

pursuing a new synthetic approach strongly appealed to us, because the existing route is still rather unsatisfactory mainly in terms of the insufficient supply and the time-consuming preparation of the tribenzyl ether **3**, which is not commercially available [20]. We thus decided to explore new alternative strategies allowing for a more efficient and convenient access to this natural product and its derivatives. From a retrosynthetic point of view, L-pyroglutamic acid, whose rich natural abundance makes it a commercially and economically viable substrate [21], can be envisaged as a potentially practical starting material for this purpose (Scheme 1). Furthermore, it can be considered that the heterocyclic hemiaminal **4**, a common precursor of the target molecule for both synthetic strategies, would be derived by an analogous cyclization of the acyclic aldehyde generated in situ from cyanide **5**. In this proposed strategy, the key transformation will involve Sharpless asymmetric dihydroxylation to install stereoselectively the hydroxy groups at C3 and C4 positions of the olefinic substrate **6**, and an intramolecular cyclization of aldehyde generated in situ from **5** to construct the piperidine ring system.

The present publication describes the results of our continuing challenges associated with this targeted natural product on the basis of the above synthetic strategy. As a result, and in addition to improvement of the inefficient stereoselectivity observed in allylation process from **4** to **7**, we established the new alternative synthetic route to (+)-batzellaside B from L-pyroglutamic acid, which offers the advantages of convenience and simplicity of total synthesis.

Results and Discussion

The synthesis began with the preparation of *N*-Boc-protected γ-lactam **8** by stepwise functionalization of L-pyroglutamic acid, using literature procedures (Scheme 2) [22]. As indicated previously, this compound underwent efficient ring opening upon treatment with sodium methoxide in methanol to provide acyclic ester **9** in 98% yield [23]. In the next step, the TBS protecting group in **9** was removed by exposure to methanolic *p*-TsOH to give the corresponding alcohol, which was then subjected to reaction with 2,2-dimethoxypropane (2,2-DMP) in the presence of $BF_3{\cdot}Et_2O$ [24] to produce *N*,*O*-acetonide **10** in

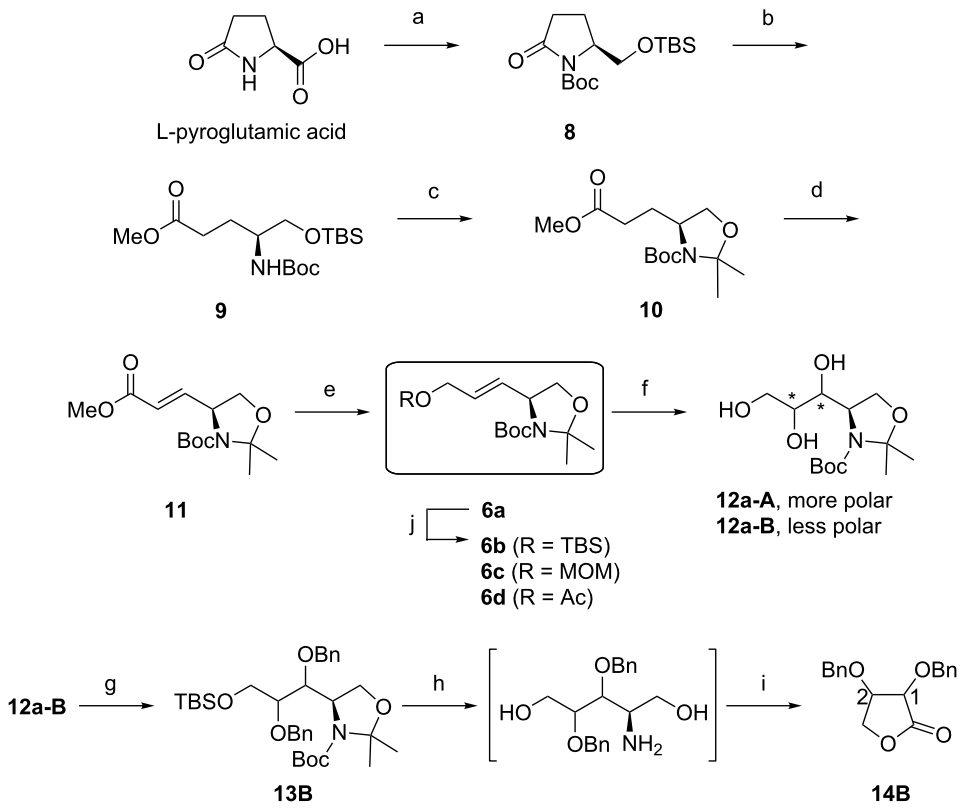

Scheme 2: Reagents and conditions: (a) see [22]; (b) MeONa, MeOH, rt; 98%; (c) (i) *p*-TsOH, MeOH, rt; (ii) $BF_3{\cdot}Et_2O$, 2,2-DMP, acetone, rt; 93% (two steps); (d) (i) LDA, HMPA, PhSeBr, THF, −78 °C; (ii) *m*-CPBA, CH_2Cl_2, −40 °C; 90% (two steps); (e) DIBAL-H, THF, 0 °C; 95%; (f) OsO_4, NMO, *t*-BuOH/H_2O (1/1), rt; 30%, **12a-A**/**12a-B** = 24/76; (g) (i) TBSCl, Et_3N, CH_2Cl_2, rt; (ii) BnBr, NaH, Bu_4NI, THF, rt; (h) (i) *p*-TsOH, MeOH, rt; (ii) TFA, CH_2Cl_2, rt; (i) (i) $NaIO_4$, Et_2O/H_2O (1/1), rt; (ii) PCC, MS 4 Å, CH_2Cl_2, rt; 17% (six steps); (j) TBSCl, imidazole, DMF; 77% (**6b**); or MOMCl, NaH, THF; 68% (**6c**); or Ac_2O, DMAP, Et_3N, CH_2Cl_2; 99% (**6d**).

93% yield over two steps. For the preparation of the *E*-isomer of α,β-unsaturated ester **11**, Wittig–Horner reaction employing Garner's aldehyde has been well known [25,26]; however, we selected stereoselective olefination through deprotonation of **10** with LDA followed by the addition of phenylselenyl bromide [27] and subsequent oxidative elimination of the resulting phenylseleno group with *m*-CPBA according to our previous report [28], which gave *E*-isomer **11** in quantitative geometric purity and 90% yield over two steps. Then, the ester moiety of this compound was reduced with DIBAL-H to the corresponding hydroxymethyl functionality to afford **6a** in 95% yield [29].

With this olefinic compound in hand, we examined the dihydroxylation of **6a**, which was carried out with OsO_4 and NMO in 50% aqueous *t*-BuOH at room temperature [30-33]. Under these conditions, **6a** provided an approximately 1:3 ratio of the more- and less-polar diastereomeric triols **12a-A** and **12a-B**, respectively, in 30% yield. These diastereomers were separated by silica-gel column chromatography and then derivatized to *trans*-1,2-dibenzyloxy-substituted γ-lactone, which allows a precise assignment of the absolute configuration by comparison with the specific optical rotation value [34]. Accordingly, the primary hydroxy group of **12a-B** was chemoselectively protected as the TBS ether [35] and the remaining diol moiety was then etherified with NaH and benzyl bromide, affording **13B** in a crude form. Deprotection of the acetal and TBS groups of this product was carried out by stepwise reactions with *p*-TsOH and TFA to give a dihydroxyamine intermediate, which underwent spontaneous cyclization upon treatment with $NaIO_4$ [36] followed by PCC oxidation to form the corresponding *trans*-1,2-dibenzyloxy-substituted γ-lactone **14B** in 17% yield over six steps. For comparison, optical rotation measurement was performed on a solution of **14B** in $CHCl_3$ at *c* 0.36. Indeed, this compound exhibited optical activity with an $[\alpha]_D^{24}$ value of −51.6, indicative of an opposite sense of absolute configuration in comparison to the literature data given for (1*S*,2*S*)-dibenzyloxy γ-lactone ($[\alpha]_D^{25}$ +60.1, *c* 1.0, $CHCl_3$) [34]. From this, we can conclude, as seen in Scheme 2, that the more polar triol **12a-A** obtained as a minor component of this dihydroxylation process could be identified as the (1*S*,2*S*)-isomer that should be supplied to advance our ongoing synthetic strategy, albeit with low yield for its preparation.

In an effort to improve selectivity of stereogenesis for the dihydroxylation step, we prepared three other olefinic substrates, in which the hydroxy group in **6a** was replaced by *tert*-butyldimethylsilyloxy (TBSO), methoxymethyloxy (MOMO) and acetoxy (AcO) groups, according to standard procedures [37,38], to give moderate to high yields (68–99%) of **6b**–**d**, respectively. Having the four different olefinic compounds **6a**–**d** available, we turned to an asymmetric technique of dihydroxylation to synthesize the (1*S*,2*S*)-constituent in preference to another (Table 1). Indeed, the Sharpless methodology was initially applied to **6a**, by carrying out the reactions at room temperature under a standard set of the asymmetric hy-

Table 1: Asymmetric dihydroxylation of **6a**–**d**.

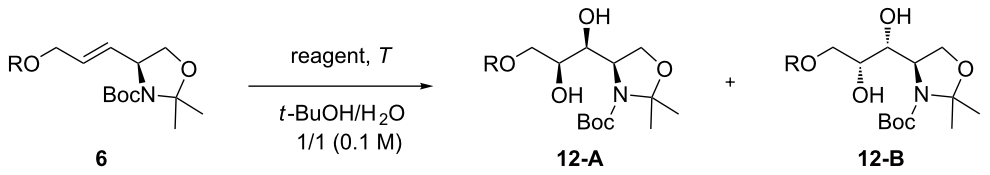

6 **12-A** **12-B**

Entry	**6**	R	Reagent (amount [mol %])	*T*	Yield [%][a] (**12-A**/**12-B**)[b]
1	**a**	H	AD-mix-α (0.5), $MeSO_2NH_2$ (100)	rt	32 (45/55)
2	**a**	H	AD-mix-β (0.5), $MeSO_2NH_2$ (100)	rt	77 (13/87)
3	**b**	TBS	AD-mix-α (0.5), $MeSO_2NH_2$ (100)	rt	33 (14/86)
4	**b**	TBS	AD-mix-β (0.5), $MeSO_2NH_2$ (100)	rt	35 (40/60)
5	**c**	MOM	AD-mix-α (0.5), $MeSO_2NH_2$ (100)	rt	52 (50/50)
6	**c**	MOM	AD-mix-β (0.5), $MeSO_2NH_2$ (100)	rt	88 (0/100)
7	**d**	Ac	AD-mix-α (0.5), $MeSO_2NH_2$ (100)	rt	48 (69/31)
8	**d**	Ac	AD-mix-β (0.5), $MeSO_2NH_2$ (100)	rt	51 (9/91)
9	**d**	Ac	AD-mix-α (0.5), $MeSO_2NH_2$ (100)	0 °C	54 (78/22)
10	**d**	Ac	AD-mix-α (0.5)	0 °C	52 (84/16)
11	**d**	Ac	AD-mix-α (0.5), $(DHQ)_2PHAL$ (10)	0 °C	53 (83/17)

[a]Isolated yield. [b]Diastereomeric ratios were determined by ^1H NMR (300 MHz).

droxylation conditions [39-41]. Using AD-mix-α and -β, we obtained mixtures of **12a-A** and **12a-B** in 45:55 and 13:87 ratios with overall isolated yields of 32 and 77%, respectively (Table 1, entries 1 and 2). Analogously, the asymmetric dihydroxylations of **6b** and **6c** produced predominantly the undesired less-polar diastereomers **12b-B** and **12c-B**, which could be converted by acidic deprotection to **12a-B** (Table 1, entries 3,4 and 6), while the reaction of **6c** with AD-mix-α afforded a 50:50 mixture of diastereomers (Table 1, entry 5).

A remarkable change in the product profile occurred when **6d** was used for this reaction. By employing AD-mix-α under the above reaction conditions, **6d** gave rise to a 69:31 mixture of **12d-A** and **12d-B** in 48% yield, leading to **12a-A** and **12a-B** through hydrolysis under basic conditions, respectively, whereas the use of AD-mix-β resulted in predominant formation of the undesired diastereomer (Table 1, entries 7 and 8). The above observations led us to explore the AD-mix-α-mediated reaction of **6d** at lower temperatures. When the reaction was performed at 0 °C with the same set of the reagents, the product selectivity for **12d-A** was slightly improved (Table 1, entry 9). Remarkably, **6d** underwent slow reaction in the absence of $MeSO_2NH_2$ to give the product mixture in 52% yield, and the diastereomeric ratio could be further enriched to 84:16 (Table 1, entry 10). Additionally, a similar result was obtained by carrying out the reaction using 0.1 equiv of $(DHQ)_2PHAL$ (53%, 83:17 in Table 1, entry 11). The above observations clearly suggested a possibility of improving the product selectivity by lowering the reaction temperature and/or introducing an additional catalytic amount of chiral ligand.

Having established the optimized conditions for the preparation of **12d-A**, our next objective was the construction of the piperidine ring system. As shown in Scheme 3, the acetyl group of the diastereomerically enriched mixture of **12d-A** and **12d-B** was removed by exposure to K_2CO_3 in methanol to give the separable mixture of alcohols **12a-A** and **12a-B**, respectively [42]. After purification by silica-gel column chromatography, **12a-A** was subjected to the TBS protection–benzylation sequence, as illustrated for the preparation of **13B**, to generate **13A** in 50% yield over three steps. In the next step, deprotection of the TBS group with TBAF [37] and subsequent tosylation of the resulting hydroxy group with TsCl in the presence of pyridine was carried out to yield the corresponding tosylate, whose activated ester group could be displaced with NaCN in DMSO to provide cyanide **15** in 80% yield over three steps [43]. Then, the *N*,*O*-acetonide group of **15** was cleaved upon treatment with *p*-TsOH in methanol [44], and the released primary hydroxy group was subsequently protected as the benzyl ether to produce the key intermediate **5** in 67% yield over two steps. As expected, conversion of this compound into the heterocyclic hemiaminal **4** was achieved in one pot with DIBAL-H by the formation of the aldehyde followed by spontaneous intramolecular cyclization with a yield of 67%. The structural identity of this product was precisely confirmed by ^1H NMR spectroscopic data, which proved to be in good agreement with those on record for **4** [19]. Hence, we can conclude that a formal total synthesis of (+)-batzellasides B was accomplished, considering that the synthetic route from **4** to **1b** has been established previously.

At this point, it was thus suggested that the remaining challenge was to improve the stereoselectivity of the allylation of **4**. In the first approach of our previous work [19], we demonstrated that the heterocyclic hemiaminal **4** was allylated by following a protocol using allyltributylstannane ($AllylSnBu_3$) and *tert*-butyldimethylsilyl triflate (TBSOTf) at −78 °C in

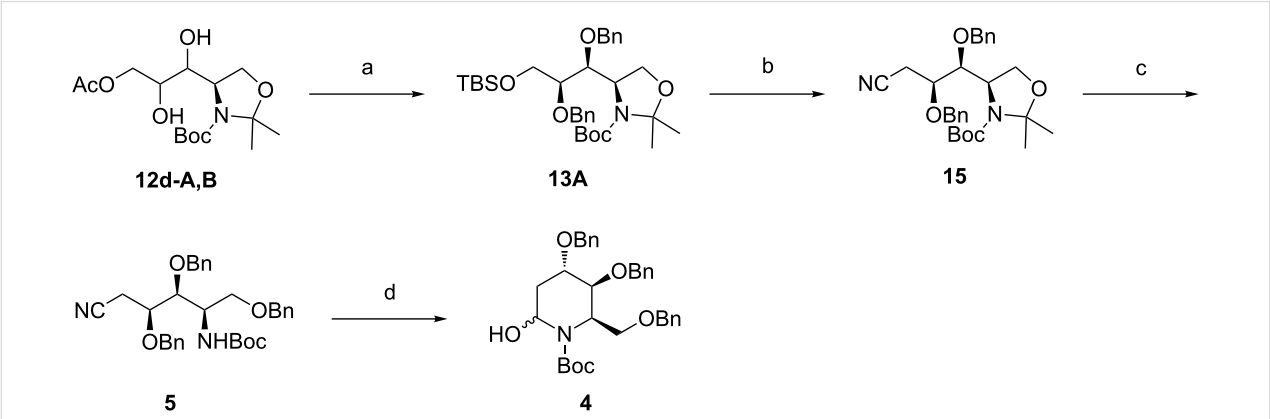

Scheme 3: Reagents and conditions: (a) (i) K_2CO_3, MeOH, rt; (ii) TBSCl, Et_3N, CH_2Cl_2, rt; (iii) BnBr, NaH, Bu_4NI, THF, rt; 50% (three steps); (b) (i) TBAF, THF, rt; (ii) TsCl, pyridine, 0 °C to rt; (iii) NaCN, $NaHCO_3$, DMSO, 60 °C; 80% (three steps); (c) (i) *p*-TsOH, MeOH, rt; (ii) BnBr, Ag_2O, AcOEt, rt; 67% (two steps); (d) DIBAL-H, toluene, −78 °C; 67%.

toluene to furnish the product **7** as a 69:31 mixture of diastereomeric isomers in 96% yield (Table 2, entry 1). Despite the appealing performance observed in the above synthetic process, this reaction protocol has the major disadvantage of low stereoselectivity causing operational inconvenience associated with the laborious chromatographic separation of the two stereoisomers. From the practical considerations, we next explored a more efficient synthetic method for the stereoselective allylation of **4** using an appropriate combination of allylic reagent and Lewis acid to produce the desired diastereomer **7** preferentially. Beginning with a reaction employing indium chloride ($InCl_3$) instead of TBSOTf at 0 °C in dichloromethane, we observed no substantial improvement in the stereoselectivity of the allylation, affording a 44:56 mixture of **7** and **7'** in quantitative yield (Table 2, entry 2). A much greater preference for the formation of **7** was observed in the cases where allyltrimethylsilane (AllylTMS) was used as an allylic reagent (Table 2, entries 3–5). In fact, the reaction carried out with zinc chloride ($ZnCl_2$) at room temperature in toluene led to exclusive stereoselectivity for **7** with 98% de, albeit in low yield (24%, Table 2, entry 3). Furthermore, the use of TBSOTf as a Lewis acid resulted in significant enhancement of the reaction rate to give almost the same stereochemical outcome (98 and 92% de) with slightly and moderately higher yields (29 and 41%) for the periods of 2 and 3 h (Table 2, entries 4 and 5), respectively. In spite of its increased susceptibility, which should be discriminated from those of unsubstituted structural systems [45-50], it became apparent that this multiply functionalized hemiaminal **4** is well tolerated to undergo direct allylation with the silyl reagents. The results of the above investigations provide one particularly successful route that has the potential to allow direct asymmetric access to the advanced-stage intermediate **7** under precise stereochemical control as well as for circumventing the purification problems related to the diastereomeric impurity in this product.

Conclusion

We have described a new synthetic approach to (+)-batzellaside B from L-pyroglutamic acid. Starting from this chiral material, the formal total synthesis of the heterocyclic hemiaminal **4**, a key intermediate elaborated commonly in the first total synthesis, has been achieved in an efficient 21-step protocol in 7.1% overall yield. Furthermore, the stereospecificity in the allylation of **4** has been exemplified by performing the procedures with AllylTMS and two types of Lewis acids, which allows for simpler synthetic operation due to the ease of purification of the products. The present study clearly demonstrates that L-pyroglutamic acid can be used as a versatile chiral source for synthesizing this class of biologically potent piperidine alkaloids and related analogues.

Supporting Information

Supporting Information File 1

Full experimental details and characterization data.
[http://www.beilstein-journals.org/bjoc/content/supplementary/1860-5397-8-210-S1.pdf]

Acknowledgements

We thank Ms. Manami Ohshima for partial support of this research. This research was supported by a Grant-in-Aid for Scientific Research from the Ministry of Education, Culture, Sports, Science and Technology, Japan.

Table 2: Diastereoselective allylation of **4**.

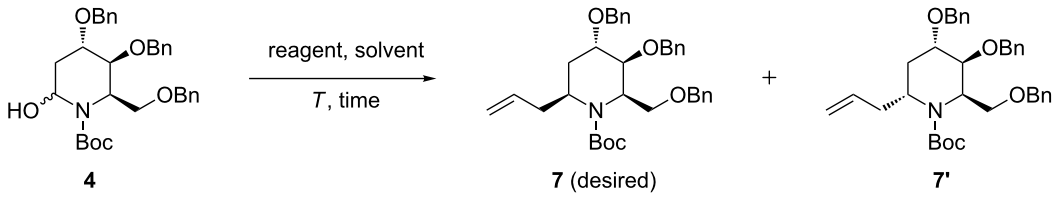

4 **7** (desired) **7'**

Entry	Reagent (amount [equiv])	Solvent	*T*	Time	Yield [%][a] (**7**/**7'**)[b]
1	$AllylSnBu_3$ (3.0), TBSOTf (1.5)	toluene	−78 °C	9 h	96 (69/31)
2	$AllylSnBu_3$ (3.0), $InCl_3$ (1.5)	CH_2Cl_2	0 °C	0.75 h	quant. (44/56)
3	AllylTMS (4.0), $ZnCl_2$ (4.0)	toluene	rt	16 h	24 (99/1)
4	AllylTMS (4.0), TBSOTf (2.0)	CH_2Cl_2	−78 to −45 °C	2 h	29 (99/1)
5	AllylTMS (10.0), TBSOTf (1.5)	toluene	−78 °C	3 h	41 (96/4)

[a]Isolated yield. [b]Diastereomeric ratios were determined by ^1H NMR (300 MHz).

References

1. Ganem, B. *Acc. Chem. Res.* **1996,** *29,* 340–347. doi:10.1021/ar9502184
2. Stutz, A. E. *Iminosugars as Glycosidase Inhibitors: Norjirimycin and Beyond;* Wiley-VCH: New York, 1999.
3. Felpin, F.-X.; Lebreton, J. *Eur. J. Org. Chem.* **2003,** 3693–3712. doi:10.1002/ejoc.200300193
4. Afarinkia, K.; Bahar, A. *Tetrahedron: Asymmetry* **2005,** *16,* 1239–1287. doi:10.1016/j.tetasy.2005.02.020
5. Inoue, S.; Tsuruoka, T.; Niida, T. *J. Antibiot.* **1966,** *19,* 288–292.
6. Somsak, L.; Nagya, V.; Hadady, Z.; Docsa, T.; Gergely, P. *Curr. Pharm. Des.* **2003,** *9,* 1177–1189.
7. Greimel, P.; Spreitz, J.; Stutz, A. E.; Wrodnigg, T. M. *Curr. Top. Med. Chem.* **2003,** *3,* 513–523.
8. Nishimura, Y. *Curr. Top. Med. Chem.* **2003,** *3,* 575–591.
9. Jacob, G. S. *Curr. Opin. Struct. Biol.* **1995,** *5,* 605–611. doi:10.1016/0959-440X(95)80051-4
10. McCormack, P. L.; Goa, K. L. *Drugs* **2003,** *63,* 2427–2434. doi:10.2165/00003495-200363220-00006
11. Segraves, N. L.; Crews, P. *J. Nat. Prod.* **2005,** *68,* 118–121. doi:10.1021/np049763g
12. Sengoku, T.; Murata, Y.; Mitamura, H.; Takahashi, M.; Yoda, H. *Tetrahedron Lett.* **2012,** *53,* 435–437. doi:10.1016/j.tetlet.2011.11.066
13. Sengoku, T.; Wierzejska, J.; Takahashi, M.; Yoda, H. *Synlett* **2010,** 2944–2946. doi:10.1055/s-0030-1259045
14. Takahashi, M.; Suzuki, T.; Wierzejska, J.; Sengoku, T.; Yoda, H. *Tetrahedron Lett.* **2010,** *51,* 6767–6768. doi:10.1016/j.tetlet.2010.10.098
15. Sengoku, T.; Satoh, Y.; Takahashi, M.; Yoda, H. *Tetrahedron Lett.* **2009,** *50,* 4937–4940. doi:10.1016/j.tetlet.2009.06.072
16. Takahashi, M.; Maehara, T.; Sengoku, T.; Fujita, N.; Takabe, K.; Yoda, H. *Tetrahedron* **2008,** *64,* 5254–5261. doi:10.1016/j.tet.2008.03.029
17. Matsuura, D.; Mitsui, T.; Sengoku, T.; Takahashi, M.; Yoda, H. *Tetrahedron* **2008,** *64,* 11686–11696. doi:10.1016/j.tet.2008.10.014
18. Takahashi, M.; Takada, K.; Matsuura, D.; Takabe, K.; Yoda, H. *Heterocycles* **2007,** *71,* 2113–2118. doi:10.3987/COM-07-11119
19. Wierzejska, J.; Ohshima, M.; Inuzuka, T.; Sengoku, T.; Takahashi, M.; Yoda, H. *Tetrahedron Lett.* **2011,** *52,* 1173–1175. doi:10.1016/j.tetlet.2011.01.018
20. Tejima, S.; Fletcher, H. G., Jr. *J. Org. Chem.* **1963,** *28,* 2999–3004. doi:10.1021/jo01046a015
21. Panday, S. K.; Prasad, J.; Dikshit, D. K. *Tetrahedron: Asymmetry* **2009,** *20,* 1581–1632. doi:10.1016/j.tetasy.2009.06.011
22. Sengoku, T.; Satoh, Y.; Oshima, M.; Takahashi, M.; Yoda, H. *Tetrahedron* **2008,** *64,* 8052–8058. doi:10.1016/j.tet.2008.06.078
23. Flynn, D. L.; Zelle, R. E.; Grieco, P. A. *J. Org. Chem.* **1983,** *48,* 2424–2426. doi:10.1021/jo00162a028
24. Xu, Z.; Zhang, F.; Zhang, L.; Jia, Y. *Org. Biomol. Chem.* **2011,** *9,* 2512–2517. doi:10.1039/c0ob01115k
25. Jako, I.; Uiber, P.; Mann, A.; Wermuth, C.-G.; Boulanger, T.; Norberg, B.; Evrard, G.; Durant, F. *J. Org. Chem.* **1991,** *56,* 5729–5733. doi:10.1021/jo00019a055
26. Jako, I.; Uiber, P.; Mann, A.; Taddei, M.; Wermuth, C.-G. *Tetrahedron Lett.* **1990,** *31,* 1011–1014. doi:10.1016/S0040-4039(00)94416-2
27. Silverman, R. B.; Invergo, B. J.; Mathew, J. *J. Med. Chem.* **1986,** *29,* 1840–1846. doi:10.1021/jm00160a007
28. Yoda, H.; Shirai, T.; Katagiri, T.; Takabe, K.; Kimata, K.; Hosoya, K. *Chem. Lett.* **1990,** *19,* 2037–2038. doi:10.1246/cl.1990.2037
29. Spangenberg, T.; Schoenfelder, A.; Breit, B.; Mann, A. *Eur. J. Org. Chem.* **2010,** 6005–6018. doi:10.1002/ejoc.201000865
30. Dondoni, A.; Merino, P.; Perrone, D. *Tetrahedron* **1993,** *49,* 2939–2956. doi:10.1016/S0040-4020(01)80389-6
31. Krishna, P. R.; Reddy, P. S. *Synlett* **2009,** 209–212. doi:10.1055/s-0028-1087669
32. Passiniemi, M.; Koskinen, A. M. P. *Synthesis* **2010,** 2816–2822. doi:10.1055/s-0029-1218843
33. Upadhyay, P. K.; Kumar, P. *Synthesis* **2010,** 3063–3066. doi:10.1055/s-0030-1258185
34. Pabba, J.; Rempel, B. P.; Withers, S. G.; Vasella, A. *Helv. Chim. Acta* **2006,** *89,* 635–666. doi:10.1002/hlca.200690066
35. Reetz, M. T.; Kesseler, K. *J. Org. Chem.* **1985,** *50,* 5434–5436. doi:10.1021/jo00225a103
36. House, H. O.; Berkowitz, W. F. *J. Org. Chem.* **1963,** *28,* 2271–2276. doi:10.1021/jo01044a028
37. Corey, E. J.; Venkateswarlu, A. *J. Am. Chem. Soc.* **1972,** *94,* 6190–6191. doi:10.1021/ja00772a043
38. Kluge, A. F.; Untch, K. G.; Fried, J. H. *J. Am. Chem. Soc.* **1972,** *94,* 7827–7832. doi:10.1021/ja00777a027
39. VanRheenen, V.; Kelly, R. C.; Cha, D. Y. *Tetrahedron Lett.* **1976,** *17,* 1973–1976. doi:10.1016/S0040-4039(00)78093-2
40. Sharpless, K. B.; Akashi, K. *J. Am. Chem. Soc.* **1976,** *98,* 1986–1987. doi:10.1021/ja00423a067
41. Francais, A.; Bedel, O.; Haudrechy, A. *Tetrahedron* **2008,** *64,* 2495–2524. doi:10.1016/j.tet.2007.11.068
42. Plattner, J. J.; Gless, R. D.; Rapoport, H. *J. Am. Chem. Soc.* **1972,** *94,* 8613–8615. doi:10.1021/ja00779a072
43. Mast, C. A.; Eißler, S.; Stončius, A.; Stammler, H.-G.; Neumann, B.; Sewald, N. *Chem.–Eur. J.* **2005,** *11,* 4667–4677. doi:10.1002/chem.200500282
44. Wen, S.-J.; Zhang, H.-W.; Yao, Z.-J. *Tetrahedron Lett.* **2002,** *43,* 5291–5294. doi:10.1016/S0040-4039(02)01043-2
45. Polniaszek, R. P.; Belmont, S. E.; Alvarez, R. *J. Org. Chem.* **1990,** *55,* 215–223. doi:10.1021/jo00288a036
46. Butters, M.; Davies, C. D.; Elliott, M. C.; Hill-Cousins, J.; Kariuki, B. M.; Ooi, L.-l.; Wood, J. L.; Wordingham, S. V. *Org. Biomol. Chem.* **2009,** *7,* 5001–5009. doi:10.1039/b914744f
47. Ukaji, Y.; Tsukamoto, K.; Nasada, Y.; Shimizu, M.; Fujisawa, T. *Chem. Lett.* **1993,** *22,* 221–224. doi:10.1246/cl.1993.221
48. Pilli, R. A.; Robello, L. G. *Synlett* **2005,** 2297–2300. doi:10.1055/s-2005-872659
49. Wang, Y.; Zhu, S.; Ma, D. *Org. Lett.* **2011,** *13,* 1602–1605. doi:10.1021/ol200004s
50. Sakagami, H.; Kamikubo, T.; Ogasawara, K. *Chem. Commun.* **1996,** 1433–1434. doi:10.1039/cc9960001433

Beilstein Journal of Organic Chemistry

Acylsulfonamide safety-catch linker: promise and limitations for solid–phase oligosaccharide synthesis

Jian Yin[1,2,§], Steffen Eller[1,2,§], Mayeul Collot[1,2] and Peter H. Seeberger[*1,2]

Letter

Open Access

Address:
[1]Department of Biomolecular Systems, Max Planck Institute of Colloids and Interfaces, Am Mühlenberg 1, 14776 Potsdam, Germany and [2]Freie Universität Berlin, Institut für Chemie und Biochemie, Arnimallee 22, 14195 Berlin, Germany

Email:
Peter H. Seeberger[*] - peter.seeberger@mpikg.mpg.de

* Corresponding author
§ Equally contributing authors

Keywords:
glycosaminoglycans (GAGs); glycosylation; resins; safety-catch linker; solid-phase synthesis

Beilstein J. Org. Chem. **2012,** *8,* 2067–2071.
doi:10.3762/bjoc.8.232

Received: 01 September 2012
Accepted: 01 November 2012
Published: 26 November 2012

This article is part of the Thematic Series "Synthesis in the glycosciences II".

Guest Editor: T. K. Lindhorst

Abstract

Safety-catch linkers are useful for solid-phase oligosaccharide synthesis as they are orthogonal to many common protective groups. A new acylsulfonamide safety-catch linker was designed, synthesized and employed during glycosylations using an automated carbohydrate synthesizer. The analysis of the cleavage products revealed shortcomings for oligosaccharide synthesis.

Findings

Solid-phase oligosaccharide synthesis [1,2] has been automated [3-5] to rapidly assemble complex oligosaccharides. Key to the success of solid-phase syntheses is the linker that connects the first carbohydrate building block to the solid support [6]. This linker has to remain stable throughout oligosaccharide synthesis but must be cleaved at the end of the reaction sequence to release the oligosaccharide and reveal a functional group for ready conjugation to array surfaces and carrier proteins. Since the first successful automated system for solid-phase oligosaccharide synthesis was introduced [7], alternative linker strategies have been explored [8-12]. Recently, a bifunctional amino–ester linker **1** [13,14] (Figure 1) has been developed, which can be readily cleaved from the resin by basic methanolysis. The released chromophore-containing part, such as aromatic benzyl ether protecting groups, facilitates the purification of the synthetic oligosaccharides by HPLC. Final deprotection of the product provides a terminal amine at the reducing end of the oligosaccharide for the fabrication of carbohydrate microarrays.

An acylsulfonamide safety-catch linker **2** (Figure 1), was developed in combination with TentaGel resin to provide orthogonality to temporary ester protecting groups. This linker was employed in the successful synthesis of a sialyl LewisX

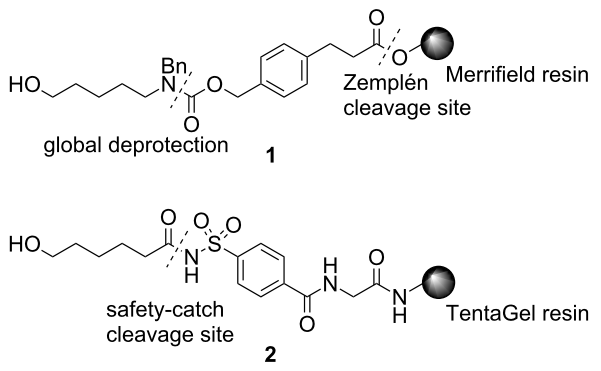

Figure 1: Structures of two novel linkers on different resins.

tetrasaccharide [15] and a sialyl Tn antigen [16]. In the search for a linker suitable for the solid-phase synthesis of complex glycosaminoglycans (GAGs) [17,18], we designed a new acylsulfonamide safety-catch linker that combined the advantageous features of linker **1**, the amino–ester bifunctional linker, and linker **2**, the safety-catch linker, to create a connection to the solid support that remains stable under conditions for cleaving temporary ester protective groups. Furthermore, the safety-catch linker should enable a variety of different reaction conditions on solid support since cleavage only occurs following preactivation. Thus, different modification reactions, such as Staudinger reduction, ester saponification or sulfation, necessary for the synthesis of GAGs, can be performed on solid support in an automated carbohydrate synthesizer. In the process of evaluating the performance of this linker in solid-phase glycosylation reactions, the potential as well as some severe limitations became apparent.

Linker **10** is the newly designed acylsulfonamide safety-catch linker (Scheme 1). The safety-catch linkage to the resin permits methanolysis of temporary ester protecting groups. This linker can only be cleaved after activation with $TMSCH_2N_2$ or ICH_2CN, afterwards, the subsequent aromatic protection of the masked amine enables UV detection during HPLC purification of the resultant oligosaccharide [13]. Finally, the terminal amine group revealed during final deprotection serves in the formation of glycoconjugates and glycan microarrays [19].

Synthesis of **10** relied on key intermediates **4** and **6** (Scheme 1). Monobenzylated amine **4** was prepared by reductive amination [20]. An established three-step synthesis starting with hydrocinnamic acid generated ester **6** with an overall yield of only 28% [21,22]. In contrast, when commercially available 4-formylcinnamic acid (**5**) served as starting material, ester **6** was prepared in just two steps and with an increased overall yield of 88% [23]. Reaction of alcohol **6** and disuccinimidyl carbonate (DSC) in the presence of NEt_3 afforded a crude carbonate, which was

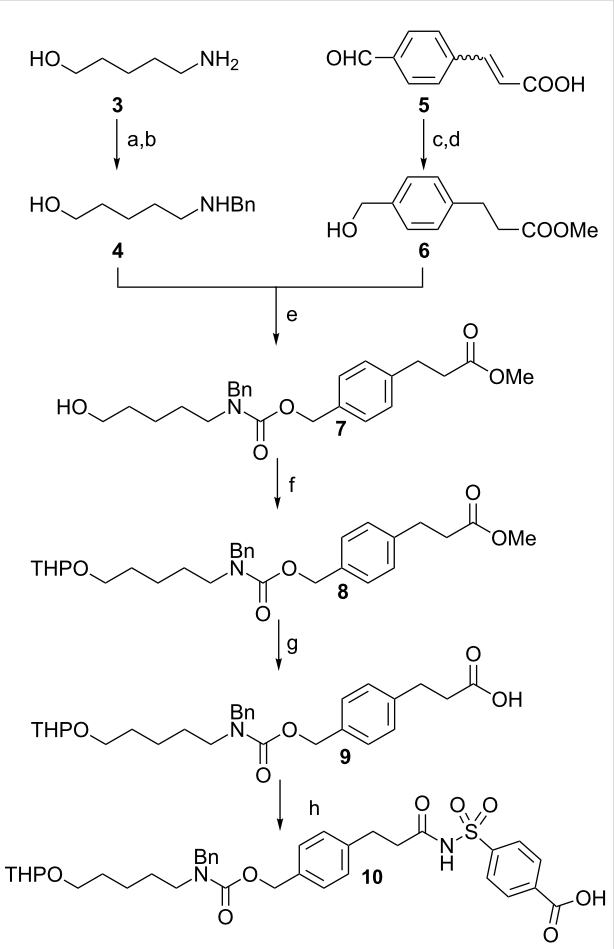

Scheme 1: Synthesis of a new acylsulfonamide safety-catch linker. Reagents and conditions: (a) benzaldehyde, Na_2SO_4, DCM; (b) $NaBH_4$, EtOH; 82% over two steps; (c) H_2, 10% Pd/C, EtOH, DIPEA; (d) cat. H_2SO_4, MeOH, 88% over two steps; (e) DSC, Et_3N, DCM/CH_3CN, 85%; (f) DHP, *p*-TsOH·H_2O, DCM, 86%; (g) LiOH·H_2O, THF/H_2O, reflux, 95%; (h) 4-sulfamoylbenzoic acid, DCC, DMAP, DCM/DMF, 60%.

smoothly reacted with amine **4** to provide carbamate **7** with 85% yield. Carbamate **7** was converted to the free acid **9** by simple protection to form THP ether **8** followed by saponification. Finally, coupling acid **9** with 4-sulfamoylbenzoic acid [15] afforded linker **10**.

To support oligosaccharide synthesis, the safety-catch linker was first coupled to different resins (Scheme 2). In addition, since the activation and cleavage of safety-catch linkers is typically quite slow, a second, base-labile (Zemplén [24]) cleavage site was integrated to facilitate the fast release and analysis of glycosides. Linker-functionalized resin **11** contains both cleavage sites, and was accessed by coupling the cesium salt of linker **10** with Merrifield chloride resin prior to capping and deprotection (Scheme 2). A second resin **12**, containing only the safety-catch cleavage site, was created by installing linker **10** on

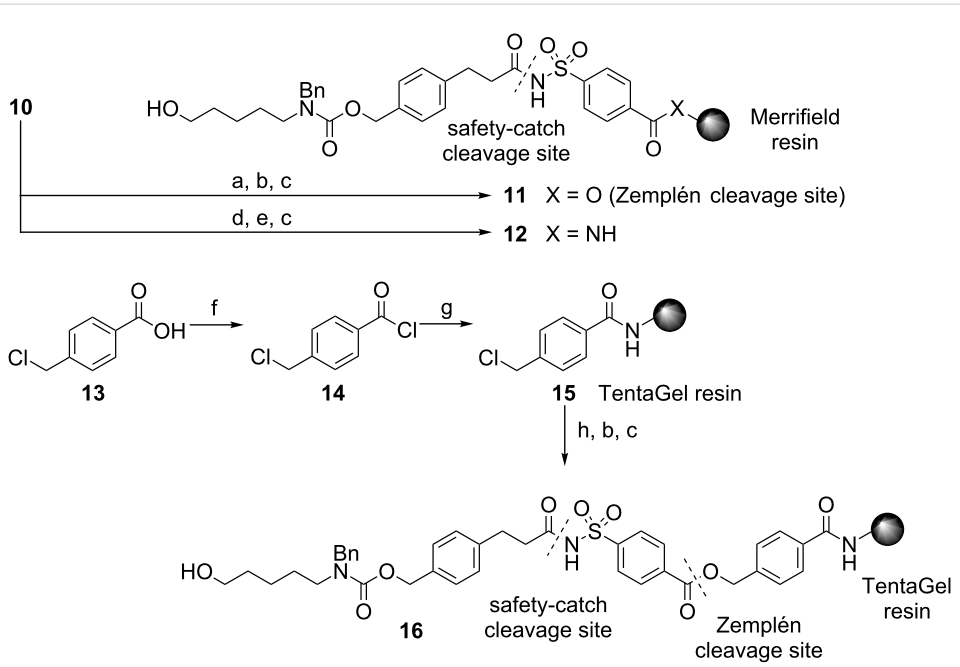

Scheme 2: Functionalization of different resins. Reagents and conditions: (a) Cs_2CO_3, DMF, TBAI, Merrifield chloride resin; (b) CsOAc, DMF, TBAI; (c) *p*-TsOH·H_2O, MeOH; (d) DIC, HOBt, DCM, Merrifield amine resin; (e) Ac_2O, pyridine; (f) $(COCl)_2$, DMF (cat), 99%; (g) TentaGel amine resin, DCM, pyridine, then Ac_2O; (h) **10**, Cs_2CO_3, DMF, TBAI.

Merrifield amine resin by treatment with DIC and HOBt (Scheme 2) [15]. After capping with acetic anhydride and removing the THP protecting group with *p*-TsOH·H_2O, the functionalized resin **12** was ready for use. Finally, a third linker-functionalized resin **16** was created with TentaGel resin [15,16], which swells in water, because encouraging results have been achieved previously with this resin. 4-(Chloromethyl)benzoic acid (**13**) served as an additional spacer [25] between **10** and TentaGel amino resin to incorporate the Zemplén cleavage site. Treatment of acid **13** with oxalyl chloride yielded acyl chloride **14**, which, in turn, was coupled to linker **10** under the conditions established for the construction of resins **11** and **12**, and afforded modified TentaGel resin **16** with both cleavage sites (Scheme 2).

Functionalized resins **11** and **16**, both containing acylsulfonamide safety-catch linker **10** plus the Zemplén cleavage site, were employed in glycosylation reactions on a solid phase using an automated synthesizer [13], subsequently cleaved with NaOMe, and the products were analyzed by HPLC (Scheme 3, see Supporting Information File 1). Glycosylations were performed with either glucosamine thioglycoside **17** and glucosamine trichloroacetimidate **18** or perbenzylated thioglycoside **19**, which are both important building blocks for the synthesis of heparin and heparan sulfate. Three repetitions of a glycosylation using each three equivalents trichloroacetimidate **18** activated by TMSOTf were conducted, and followed by Zemplén cleavage. Similarly, three equivalents of thioglycosides **17** and **19** were added three times (triple coupling) for each glycosylation employing DMTST or NIS/TfOH as an activator. In both instances, surprisingly, only *N*-glycoside **20** (minor product) and glycosylated linker **21** (major product) rather than the desired product **22** were found (Scheme 3). *N*-Glycosidic sulfonamides were previously used during the synthesis of inhibitors of hepatocellular carcinoma cells [26]. This observation illustrates a limitation of the linker system since these undesired reactions result in the preactivation of the safety-catch linker, which can lead to cleavage in presence of nucleophiles. Similar results were observed when the experiments were repeated. The desired product **22** was detected in trace amounts only in the case of the coupling of thioglycoside **17** activated by NIS/TfOH to Merrifield resin **11**, as determined by HPLC (see Supporting Information File 1).

Based on these unexpected findings, we hypothesized that excess glycosylating agent may alkylate the sulfamyl group during glycosylation, such that subsequent cleavage provides products **20** and **21**. To test this, the amount of glycosylating agent was decreased during a reaction, which resulted in the production of glycosylated linkers **21** and **22**. It was evident that two unexpected reactions had occurred. First, the use of excess glycosylating agent, common practice for solid-phase-synthesis protocols, leads to activation of the sulfamyl group of the acylsulfonamide safety-catch linker, permitting cleavage at this

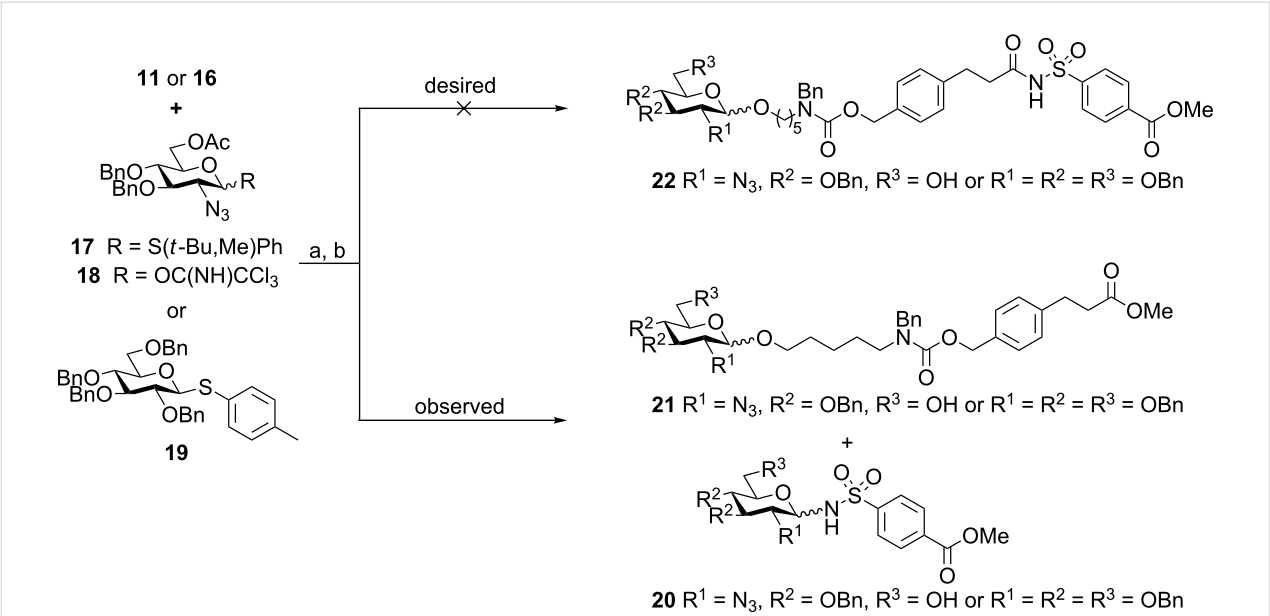

Scheme 3: Glycosylation and cleavage reactions for analysis. Reagents and conditions: (a) automated glycosylations using **17**, **18** or **19**; (b) NaOMe, MeOH.

location. This reaction had not been reported previously [15,16], because the architecture of this safety-catch linker means that the modified sulfamyl group remains on the resin after cleavage and release of the product, and this was not examined. As the new bifunctional resins **11** and **16** contain the additional Zemplén cleavage site, the product of this dominant but undesired reaction was evident. Second, the observation that reducing the concentration of the glycosylation agent caused an increase in the production of glycosylated linker **21**, implied that sodium methoxide may directly cleave safety-catch linkers without prior activation.

To examine linker reactivity in more detail, additional automated glycosylations were performed by using thioglycoside **19** activated with NIS/TfOH, on Merrifield resin **12** containing only the safety-catch cleavage site (Scheme 4). The presence of glycosylated linker **23** as the main product confirmed that premature linker cleavage had occurred. Even nonglycosylated resin **12** was cleaved by treatment with sodium methoxide to afford linker **7** (Scheme 4). A possible explanation is provided by Unverzagt and co-workers [27], who reported, when using another acylsulfonamide safety-catch linker on a solid support, that capping the remaining amino group using acetic anhydride preactivates the sulfamyl group. To test this hypothesis, linker **10** was transformed by benzylation and deprotection to afford **24** prior to treatment with sodium methoxide (Scheme 4). Surprisingly, linker **7** was again isolated as the major product as determined by TLC and NMR, indicating that the nucleophilicity or basicity of NaOMe was responsible for cleavage. Other reagents, such as aqueous NaOH, hydrazine acetate, pyridine and benzylamine failed to cleave the linker. Even the strongly basic and weakly nucleophilic *t*-BuOK was not sufficient to induce premature cleavage. Thus, it is the nucleophilic action of sodium methoxide that is strong enough to induce cleavage of the safety-catch linker (Scheme 4).

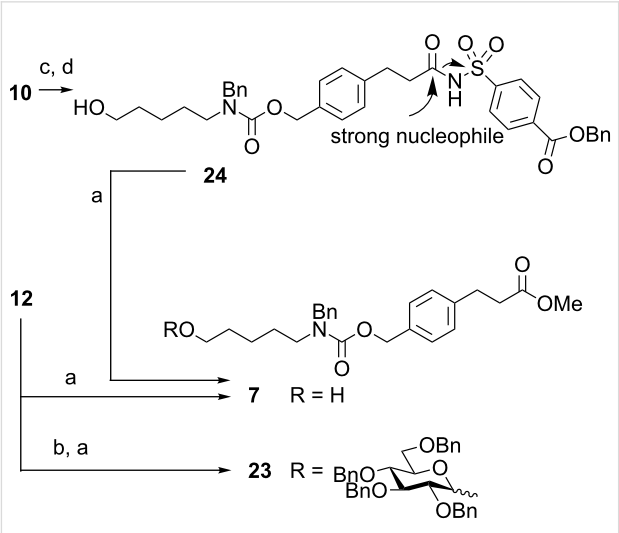

Scheme 4: Further investigations of safety-catch linker. Reagents and conditions: (a) NaOMe, MeOH; (b) **19**, NIS, TfOH, DCM; (c) DCC, BnOH, DCM; (d) *p*-TsOH·H_2O, MeOH; 55% over two steps.

In conclusion, we described a new acylsulfonamide safety-catch linker with an additional Zemplén cleavage site, designed for

automated solid-phase synthesis of glycosaminoglycans. With this novel linker, inherent but previously unknown limitations of the safety-catch concept for solid-phase oligosaccharide synthesis were discovered. The sulfamyl group can be attacked by excess glycosylating agent to give the unexpected resin-bound *N*-glycoside, which may block additional reaction sequences and extension of the oligosaccharide [28]. In addition, sodium methoxide can directly cleave the sulfamyl group, prohibiting its use in conjunction with safety-catch linkers in general. While safety-catch linkers offer many attractive features for the solid-phase synthesis of complex molecules, particularly peptides, they should be used with great caution for oligosaccharide assembly.

Supporting Information

Supporting Information File 1

Experimental section.
[http://www.beilstein-journals.org/bjoc/content/supplementary/1860-5397-8-232-S1.pdf]

Acknowledgements

We thank the Max Planck Society for very generous support, and the European Research Council (ERC Advanced Grant AUTOHEPARIN to PHS) is also gratefully acknowledged. We thank Dr. V. Mountain for critically editing the manuscript.

References

1. Seeberger, P. H.; Haase, W.-C. *Chem. Rev.* **2000,** *100,* 4349. doi:10.1021/cr9903104
2. Seeberger, P. H., Ed. *Solid Support Oligosaccharide Synthesis and Combinatorial Carbohydrate Libraries;* John Wiley & Sons Inc.: New York, 2001. doi:10.1002/0471220442
3. Seeberger, P. H. *Chem. Commun.* **2003,** 1115. doi:10.1039/b210230g
4. Seeberger, P. H.; Werz, D. B. *Nature* **2007,** *446,* 1046. doi:10.1038/nature05819
5. Seeberger, P. H. *Chem. Soc. Rev.* **2008,** *37,* 19. doi:10.1039/b511197h
6. Guillier, F.; Orain, D.; Bradley, M. *Chem. Rev.* **2000,** *100,* 2091. doi:10.1021/cr980040+
7. Plante, O. J.; Palmacci, E. R.; Seeberger, P. H. *Science* **2001,** *291,* 1523. doi:10.1126/science.1057324
8. Love, K. R.; Seeberger, P. H. *Angew. Chem., Int. Ed.* **2004,** *43,* 602. doi:10.1002/anie.200352539
9. Werz, D. B.; Castagner, B.; Seeberger, P. H. *J. Am. Chem. Soc.* **2007,** *129,* 2770. doi:10.1021/ja069218x
10. Codée, J. D. C.; Kröck, L.; Castagner, B.; Seeberger, P. H. *Chem.–Eur. J.* **2008,** *14,* 3987. doi:10.1002/chem.200701864
11. Bindschädler, P. Different aspects of automeated heparin synthesis: *de novo* synthesis of building blocks, a new linker, and synthesis of heparin oligosaccharides. Ph.D. Thesis, Eidgenössische Technische Hochschule Zürich, Switzerland, 2008.
12. Czechura, P.; Guedes, N.; Kopitzki, S.; Vazquez, N.; Martin-Lomas, M.; Reichardt, N.-C. *Chem. Commun.* **2011,** *47,* 2390. doi:10.1039/c0cc04686h
13. Kröck, L.; Esposito, D.; Castagner, B.; Wang, C.-C.; Bindschädler, P.; Seeberger, P. H. *Chem. Sci.* **2012,** *3,* 1617. doi:10.1039/c2sc00940d
14. Christ, W.; Kröck, L.; Plante, O. J.; Castagner, B.; Seeberger, P. H. Automated Oligosaccharide Synthesizer. WO Patent 2010011828, Jan 28, 2010.
15. Kanemitsu, T.; Wong, C.-H.; Kanie, O. *J. Am. Chem. Soc.* **2002,** *124,* 3591. doi:10.1021/ja0167396
16. Kanemitsu, T.; Daikoku, S.; Kanie, O. *J. Carbohydr. Chem.* **2006,** *25,* 361. doi:10.1080/07328300600778785
17. Yeung, B. K. S.; Chong, P. Y. C.; Petillo, P. A. *J. Carbohydr. Chem.* **2002,** *21,* 799. doi:10.1081/CAR-120016490
18. Karst, N. A.; Linhardt, R. J. *Curr. Med. Chem.* **2003,** *10,* 1993. doi:10.2174/0929867033456891
19. Yin, J.; Seeberger, P. H. *Methods Enzymol.* **2010,** *478,* 197. doi:10.1016/S0076-6879(10)78009-5
And references therein.
20. De Michelis, C.; Rocheblave, L.; Priem, G.; Chermann, J. C.; Kraus, J. L. *Bioorg. Med. Chem.* **2000,** *8,* 1253. doi:10.1016/S0968-0896(00)00055-9
21. Arshady, R.; Atherton, E.; Clive, D. L. J.; Sheppard, R. C. *J. Chem. Soc., Perkin Trans. 1* **1981,** 529. doi:10.1039/P19810000529
22. Párkányi, C.; Yeh Huang, L. S.-C.; Chu, S. G.; Jeffries, A. T., III. *Collect. Czech. Chem. Commun.* **1996,** *61,* 342. doi:10.1135/cccc19960342
23. Bolli, M.; Lehmann, D.; Mathys, B.; Mueller, C.; Nayler, O.; Velker, J.; Weller, T. Novel thiophene derivatives. PCT Int. Appl. WO 2006/100635 A2, Sept 28, 2006.
24. Zemplén, G.; Kunz, A. *Ber. Dtsch. Chem. Ges.* **1923,** *56,* 1705. doi:10.1002/cber.19230560736
25. Wu, X.; Schmidt, R. R. *Eur. J. Org. Chem.* **2004,** 2826. doi:10.1002/ejoc.200400111
26. Colinas, P. A.; Bravo, R. D. *Tetrahedron Lett.* **2005,** *46,* 1687. doi:10.1016/j.tetlet.2005.01.065
27. Mezzato, S.; Schaffrath, M.; Unverzagt, C. *Angew. Chem., Int. Ed.* **2005,** *44,* 1650. doi:10.1002/anie.200461125
28. de Paz, J. L.; Kayser, M. M.; Macchione, G.; Nieto, P. M. *Carbohydr. Res.* **2010,** *345,* 565. doi:10.1016/j.carres.2009.12.021

License and Terms

Beilstein Journal of Organic Chemistry

S-Fluorenylmethyl protection of the cysteine side chain upon N^{α}-Fmoc deprotection

Johannes W. Wehner and Thisbe K. Lindhorst*

Letter

Open Access

Address:
Otto Diels Institute of Organic Chemistry, Christiana Albertina University of Kiel, Otto-Hahn-Platz 3/4, 24098 Kiel, Germany

Email:
Thisbe K. Lindhorst* - tklind@oc.uni-kiel.de

* Corresponding author

Keywords:
Fmoc protecting group; glycoamino acids; *N*-Fmoc→*S*-Fm transprotection; protecting groups

Beilstein J. Org. Chem. **2012,** *8,* 2149–2155.
doi:10.3762/bjoc.8.242

Received: 05 September 2012
Accepted: 01 November 2012
Published: 10 December 2012

This article is part of the Thematic Series "Synthesis in the glycosciences II".

Associate Editor: S. Flitsch

Abstract

Deprotection of an N^{α}-Fmoc-protected glycocysteine derivative **7** with an excess of morpholine unexpectedly led to the fluorenylmethyl-protected thioether **8** in high yield. The suggested mechanism for this reaction comprises the addition of the cysteine thiolate on the exocyclic double bond of dibenzofulvene, which is formed during Fmoc deprotection. The influence of base concentration on this transprotection reaction was studied.

Introduction

In the course of our work on the synthesis of glycoamino acids, we have recently used L-cysteine as a scaffold for the synthesis of various glycoclusters [1-3]. This is an attractive concept, because it can be combined with solid-phase peptide synthesis (SPPS) [4,5], as well as with native chemical ligation (NCL) utilizing an *S*→*N* acyl shift [3,6-10]. In addition, glycocysteine derivatives can be easily converted into the corresponding dimers by oxidiation of the cysteine moiety into the respective cystine form.

Indeed, preparation of glycoamino acid derivatives such as **3-dimer**, an oxidized cysteine, or cystine derivative, is facile and can be realized via different synthetic routes. However, as we employed the fluorenylmethoxycarbonyl (Fmoc) protecting group for the synthesis of **3-dimer**, we observed an unexpected but high-yielding *S*-fluorenylmethyl (Fm) protection of the cysteine side chain during *N*-Fmoc deprotection. Hence, this side reaction was further investigated under different reaction conditions and the results of this study are described in this account together with a survey of the synthetic approaches to obtain **3** and **3-dimer**.

Results and Discussion

Synthesis of **3-dimer** was started from the known *N*,*S*-protected glycoamino acid derivative **1** [2], which can be obtained by peptide coupling of 2-aminoethyl α-D-mannopyranoside [11]

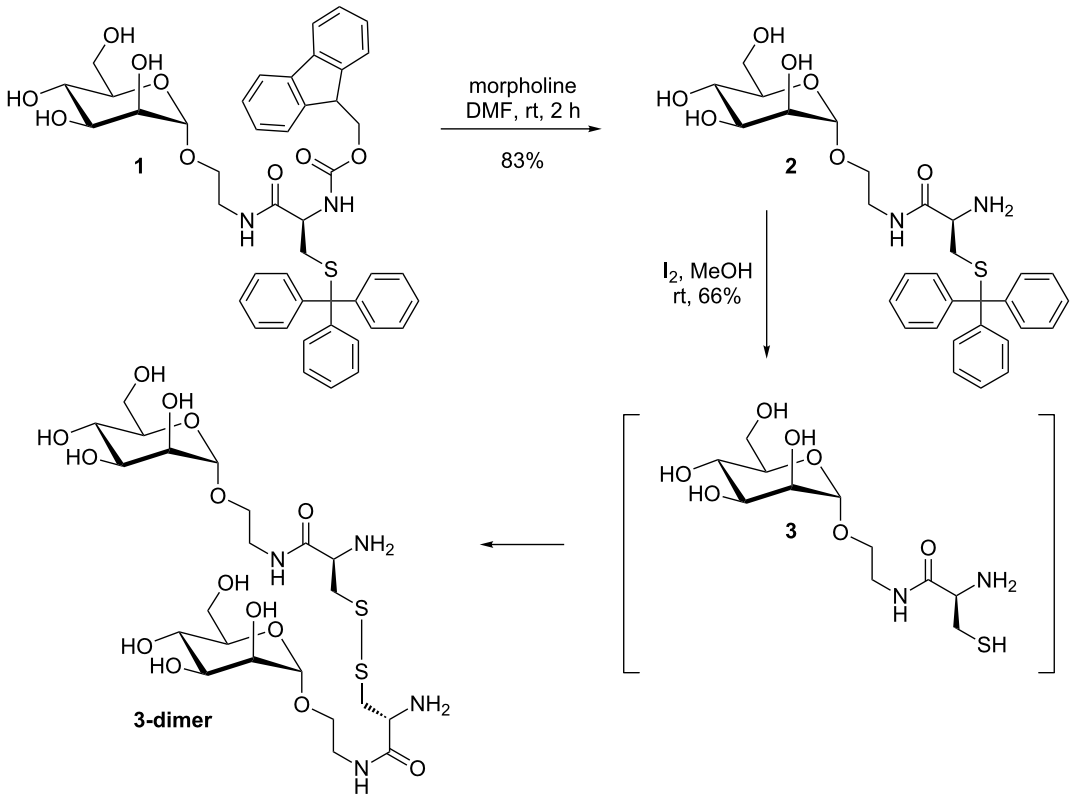

Scheme 1: Synthesis of glycoamino acid derivative **3** and its dimer, from the known mannopyranoside **1**.

and the corresponding protected cysteine derivative, Fmoc-Cys(Trt)-OH (Scheme 1). Fmoc-deprotection by using morpholine as the base gave the free amine **2**, and then removal of the *S*-trityl protecting group under oxidative conditions (iodine in methanol) led to the cystine derivative **3-dimer** after in situ oxidation of the intermediate free thiol in good yield.

As *O*-acetylated building blocks are often advantageous over the OH-free analogues for SPPS [2-4], our next step was to apply the synthesis outlined in Scheme 1 to the *O*-acetylated glycoamino acid derivative **4** (Scheme 2). The *O*-acetylated mannopyranside **4** can be prepared by Staudinger ligation of *O*-acetyl-protected 2-azidoethyl α-D-mannopyranoside [11] and the cysteine derivative Fmoc-Cys(Trt)-OH as described earlier [1]. Then, a sequence of Fmoc-deprotection, leading to **5** and acidic removal of the trityl group by using TFA and triethylsilane (TES) as cation scavenger [12] yields the *O*-acetylated glycoamino acid derivative **6** together with its respective disulfide (not shown in Scheme 2), and de-*O*-acetylation under Zemplén conditions [13] furnishes the unprotected compound **3-dimer** after oxidation in air, as reported previously [3]. However, when the trityl group in **4** was removed first, thiol **7** was obtained as expected, but the following Fmoc deprotection under standard conditions [14], employing 6 equiv of morpholine in DMF, unexpectedly led to the *S*-fluorenylmethyl (Fm)-protected glycoamino acid **8** in 77% yield (Scheme 2). The anticipated glycoamino acid derivative **6** was not obtained. De-*O*-acetylation of **8** gave mannopyranoside **9** with maintained fluorenylmethyl protection at the sulfur atom.

The structure of the *S*-Fm-protected glycoamino acid derivative **8** could be unequivocally confirmed by NMR analysis and MALDI–TOF mass spectrometry. The HMBC NMR spectrum of **8** (Figure 1) clearly indicates that the formerly unprotected thiol group of the cysteine side chain of **7** became protected by a fluorenylmethyl (Fm) moiety. This is indicated by the respective cross peaks between C-β and the Fm-CH_2 protons on one hand and between Fm-*C*H and the H-βa and H-βb protons on the other hand.

N-Fmoc→*S*-Fm transprotection was reported earlier by Katritzky et al. for cysteine peptides [15]. In this case, DBU was employed as the base and the reaction was conducted in dry THF at 0 °C for 15 min to give the rearrangement products in 69–87% yield. The mechanistic rational proposed by the Katrizky group is based on a report by Rich et al., where the influence of the employed base on *N*-Fmoc→*S*-Fm transprotection was studied [16]. According to the proposal provided by

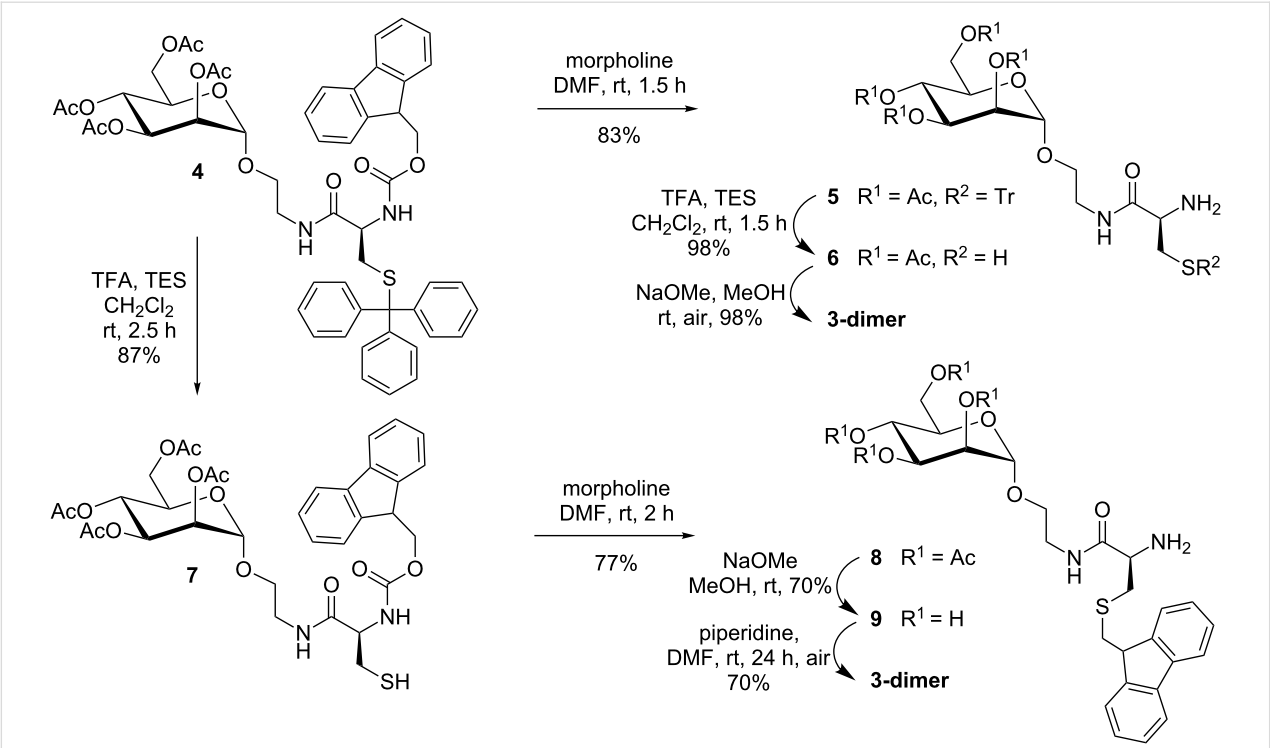

Scheme 2: To obtain the glycocystine derivative **3-dimer** from the protected cysteine mannopyranoside precursor **4**, the sequence of deprotection steps matters. When the thiol function was deprotected first to give **7**, then *N*-Fmoc deprotection resulted in *N*-Fmoc→*S*-Fm transprotection. On the other hand, Fmoc deprotection was no problem starting from **4** with the thiol function protected.

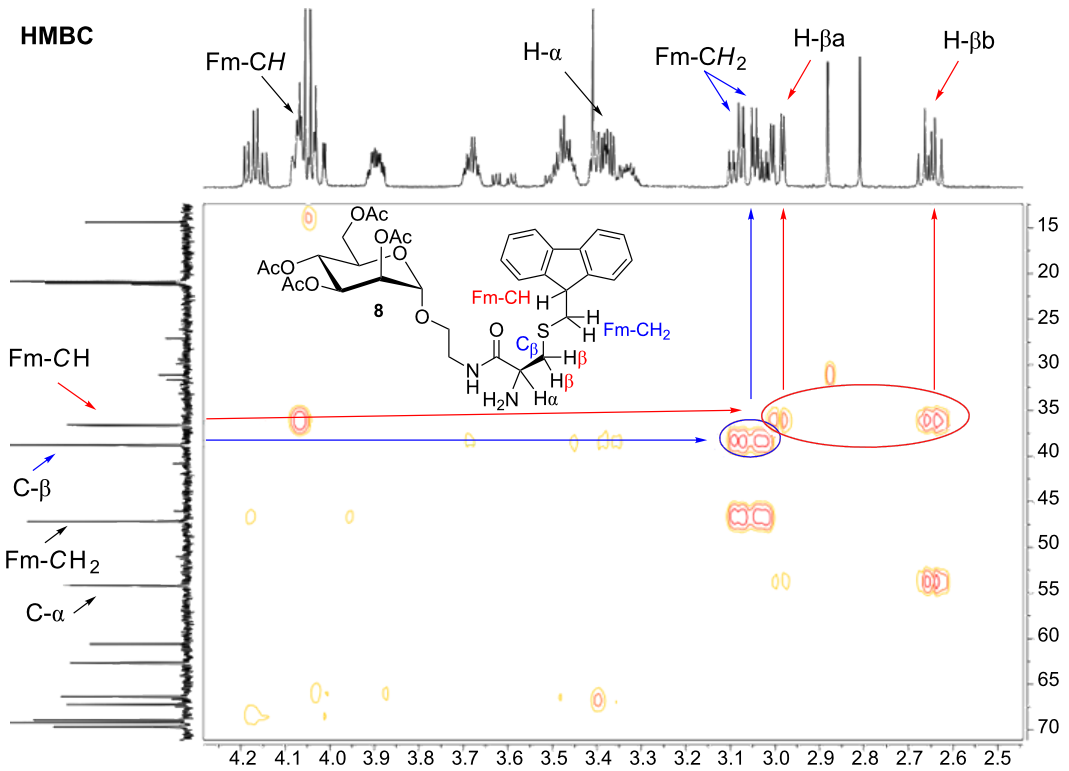

Figure 1: In the $^{1}H/^{13}C$ HMBC NMR spectrum of the *S*-Fm-protected glycoamino acid derivative **8**, protecting-group rearrangement is confirmed by the cross peaks between C-β and the Fm-CH_2 protons (in blue) and between Fm-*C*H and the H-βa,β protons (in red).

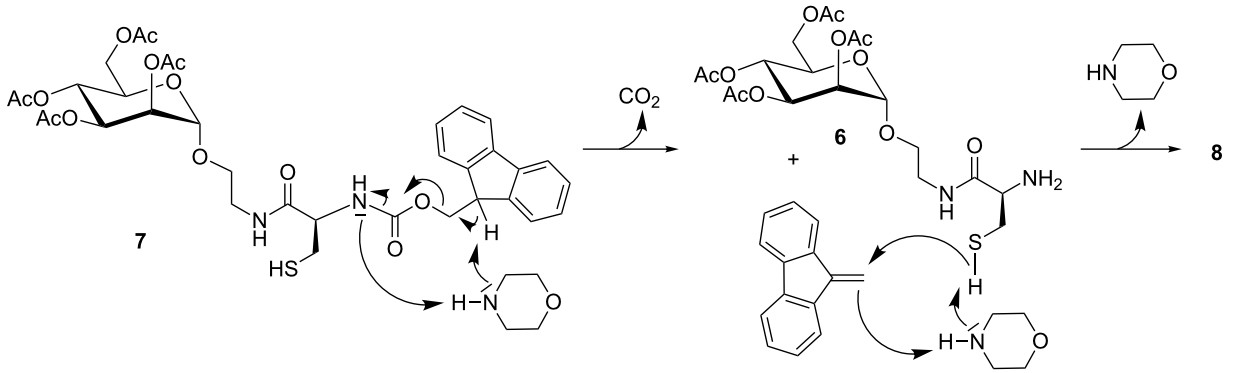

Scheme 3: Proposed mechanism for the formation of *S*-Fm-protected **8** from *N*-Fmoc-protected **7** according to Rich and co-workers [16].

Rich et al., formation of the cysteine derivative **7** can be explained by an elimination reaction of the E1cb type, in which N^{α} is deprotected with the release of carbon dioxide and formation of dibenzofulvene (Scheme 3). Then, presumably, the cysteine thiol is deprotonated by morpholine. Since the nucleophilicity of the so formed thiolate is higher than that of morpholine or the generated primary N^{α} amino group, the in situ generated fulvene is quenched by the cysteine thiolate, leading to *S*-Fm-protected **8**.

Next, we have investigated different reaction conditions for the conversions of **7** and **9** with piperidine, which is the common base used in SPPS. Deprotection of the *S*-Fm-protected glycoamino acid derivative **9** was possible by using 50% piperidine in DMF at room temperature to yield the fully deprotected disulfide **3-dimer** in 70% yield (Table 1). Separately, **7** was treated with different concentrations of piperidine. When 0.1 equiv of piperidine in DMF was employed, only about 20% of the fully deprotected mannopyranoside **6** was obtained, whereas

Table 1: Product analysis of deprotection reactions under different basic reaction conditions.[a]

Starting material/ used base[b]	Products		
9/50% piperidine[c]			70% **3-dimer**
	8	**6** and its disulfide	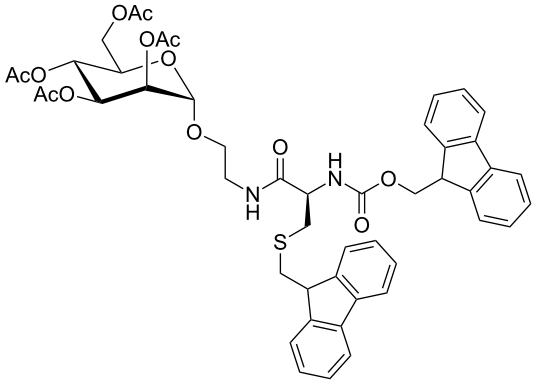 **10**
7/0.1 equiv piperidine	43%	22%	22%[d]
7/1 equiv piperidine[a]	66%	32%	–
7/6 equiv piperidine	47%	46%	–
7/6 equiv morpholine[e]	62%	35%	–
7/20% piperidine	–	93%	–

[a]Only products obtained with yields >5% were isolated and analyzed;
[b]reaction conditions: **7** (50 mg in dry DMF) was reacted at a concentration of 100 mM for 2 h at rt under a nitrogen atmosphere;
[c]this reaction was carried out at a concentration of 57.5 mM;
[d]confirmed by MALDI–TOF mass spectrometry;
[e]6 equiv morpholine at a concentration of 173 mM led to 77% **8** (see above).

over 40% of the *N*→*S*-transprotected product **8** was formed. Concurrently, the doubly *N*,*S*-protected derivative **10** was identified as an additional product (Table 1). When 1 equiv of piperidine was employed, the overall yield of **8** and **6** was increased, while no doubly *N*,*S*-protected compound **10** was detected. However, transprotection occurred with 66%. Further increase of the piperidine concentration to 6 equiv led to 47% transprotection, whereas when the same amount of morpholine was used at 100 mM concentration, 62% transprotection occurred. Standard SPPS Fmoc deprotection conditions with 20% piperidine in DMF, however, led to complete deprotection of **7** and a high combined yield of the desired glycoamino acid derivative **6** and its respective cystine dimer.

These experiments show that the amount of base is crucial to avoid *N*-Fmoc→*S*-Fm transprotection during *N*-Fmoc removal. The problem of transprotection can be solved by choosing the appropriate base at appropriate concentrations.

Conclusion

Glycocysteine/cystine derivatives are versatile building blocks for the synthesis of a wide variety of glycoconjugates, which are thus accessible by, among other methods, NCL or SPPS. In addition, mannosidic glycoamino acids are of interest as ligands for mannose-specific lectins in solution [17] as well as for the fabrication of glycoarrays on solid support [10,18,19]. Moreover, we are interested to advance glycoamino acid deriatives such as **3** into ligands that can be "switched" between two states by oxidation/reduction. A key step, when glycoamino acids are further conjugated, is Fmoc protection and deprotection. Here, we have shown an *N*-Fmoc→*S*-Fm transprotection reaction, which can occur upon *N*-Fmoc deprotection, and how it can be controlled under different basic reaction conditions. Though this type of transprotection reaction has been described before, here the first example with glycoamino acid derivatives is reported. The results of our study can be utilized wherever glycocysteine derivatives are employed in the synthesis of glycoclusters or glycopeptides, for example, in the context of an orthogonal protection/deprotection approach.

Experimental

General methods

Commercially available starting materials and reagents were used without further purification unless otherwise noted. Glycoamino acid derivatives **1** [1], **2** [2], **3** [3], **4** [2], **5** [2] and **6** [3] were prepared according to the literature. Anhydrous DMF was purchased; other solvents were dried for reactions or distilled for chromatography. Air- or moisture-sensitive reactions were carried out under an atmosphere of nitrogen. Thin-layer chromatography was performed on silica-gel plates (GF 254, Merck). Detection was effected by UV irradiation and subsequent charring with 10% sulfuric acid in EtOH followed by heat treatment. Flash chromatography was performed on silica gel 60 (230–400 mesh, particle size 0.040–0.063 mm, Merck). Preparative MPLC was performed on a Büchi apparatus by using a LiChroprep RP-18 column (40–60 µm, Merck) for reversed-phase silica-gel chromatography. ^{1}H and ^{13}C spectra were recorded on Bruker DRX-500 and AV-600 spectrometers at 300 K. 2D NMR experiments ($^{1}H/^{1}H$ COSY, $^{1}H/^{13}C$ HSQC and $^{1}H/^{13}C$ HMBC) were performed for full assignment of the spectra. Chemical shifts are relative to internal TMS (^{1}H: δ 0.00 ppm) or were calibrated relative to solvent peaks of $CHCl_3$ (^{13}C: δ 77.0 ppm), MeOH (^{1}H: δ 3.31 ppm; ^{13}C: δ 49.0 ppm), or H_2O (δ 4.65 ppm). For peak assignment, atoms were numbered according to conventions for carbohydrate and amino-acid nomenclature. The abbreviation "Fmoc" refers to fluorenylmethoxycarbonyl and "Fm" to fluorenylmethyl. ESI mass spectra were recorded on a Mariner ESI-TOF 5280 (Applied Biosystems) instrument and MALDI-MS measurements on a MALDI-TOF-MS-Biflex III (Bruker) instrument by using 2,5-dihydroxybenzoic acid (DHB) or α-cyano-4-hydroxycinnamic acid (CCA) as matrix. IR-spectroscopic measurements were recorded on a FTIR spectrometer Paragon 1000 (Perkin-Elmer) by using a Golden-Gate diamond-ATR unit with a sapphire stamp. Optical rotations were measured on a Perkin-Elmer 241 polarimeter (Na-D-line: 589 nm, length of cell 1 dm).

L-Cystine-bis[2-(α-D-mannopyranosyloxy)ethyl]-amide (**3-dimer**)

The *S*-Fm-protected glycoamino acid derivative **9** (290 mg, 575 µmol) was dissolved in dry DMF (5 mL), and then piperidine (5 mL) was added, and the reaction mixture was stirred for 24 h at ambient temperature under a nitrogen atmosphere. Then the reaction mixture was concentrated in vacuo, and the crude product was purified by two subsequent RP-MPLC purification steps: (i) RP-18, A = water, B = methanol, B: 10% → 50%, 60 min; (ii) RP-18, A = water, B = ethanol, B: 95% → 20%, 60 min). After lyophilization, the title compound **3** (130 mg, 200 µmol, 70% based on monomeric starting material) was obtained. R_f 0.74 (RP-18, MeOH); $[\alpha]_D^{23}$ +15 (*c* 0.6, MeOH); IR (ATR) $\tilde{\nu}$ 3270, 2919, 1648, 1546, 1409, 1200, 1130, 1050, 963, 609, 458 cm^{-1}; ^{1}H NMR (600 MHz, D_2O) δ 4.91 (d, $^{3}J_{1,2}$ = 1.8 Hz, 2H, 2 H-1), 3.99 (dd, $^{3}J_{1,2}$ = 1.8 Hz, $^{3}J_{2,3}$ = 3.4 Hz, 2H, 2 H-2), 3.92 (dd, $^{3}J_{5,6}$ = 4.3 Hz, $^{2}J_{6,6'}$ = 12.0 Hz, 2H, 2 H-6), 3.90–3.88 (m, 2H, 2 H-α), 3.87–3.83 (m, 4H, 2 H-3, 2 man-OC*H*H), 3.78 (dd, $^{3}J_{5,6}$ = 5.9 Hz, $^{2}J_{6,6'}$ = 12.0 Hz, 2H, 2 H-6'), 3.69–3.65 (m, 6H, 2 H-4, 2 H-5, 2 man-OC*H*H), 3.58 (m_c, 2H, 2 man-OCH_2CHH), 3.45 (ddd ~ tdd, ^{3}J = 4.0 Hz, ^{3}J = 6.7 Hz, ^{2}J = 14.6 Hz, 2H, 2 man-OCH_2CHH), 3.15–3.06 (m, 4H, 2 H-β, 2 H-β') ppm; ^{13}C NMR (150 MHz, D_2O) δ 175.5 (2 *C*(O)C-α), 101.5 (2 C-1), 74.6 (2 C-5), 72.3 (2 C-3), 71.8 (2

C-2), 68.5 (2 C-4), 67.5 (2 man-O *C* H_2CH_2), 62.7 (2 C-6), 55.2 (2 *C*-α), 42.7 (2 *C*-β), 40.9 (2 man-OCH_2 *C* H_2) ppm; HRMS–ESI (*m*/*z*): calcd for $C_{22}H_{42}N_4NaO_{14}S_2$, 673.2031; found, 673.2183.

Procedure for the preparation of **3-dimer** by iodine oxidation of **2** (Scheme 1)

Manoside **2** (500 mg, 880 µmol) was dissolved in methanol (2 mL), and then iodine (334 mg, 2.62 mmol) dissolved in methanol (9 mL) was added dropwise. After being stirred for 45 min at ambient temperature, the reaction was quenched with saturated sodium thiosulfate solution (3 mL), and solvents were removed under reduced pressure. The crude product was subjected to size-exclusion chromatography (LH-20, methanol) yielding **3-dimer** (377 mg, 580 µmol, 66%) as a colorless lyophylisate. Analytical data are according to the literature [3].

N-(Fluoren-9-ylmethoxycarbonyl)-L-cysteine-[2-(2,3,4,6-tetra-*O*-acetyl-α-D-mannopyranosyloxy)ethyl]amide (**7**)

The *S*-protected glycoamino acid derivative **4** (1.35 g, 1.41 mmol) was dissolved in dry dichloromethane (8 mL), and then triethylsilane (1.26 mL, 7.91 mmol) and TFA (600 µL, 7.79 mmol) were added, and the reaction mixture was stirred for 2 h at ambient temperature under a nitrogen atmosphere. Then another portion of TFA (600 µL, 7.79 mmol) was added and stirring was continued for 30 min until no further conversion of **1** was observed by TLC (toluene/ethyl acetate, 1:1). The reaction mixture was concentrated under reduced pressure and repeatedly codistilled with toluene (3 × 20 mL). The crude product was purified by flash column chromatography (toluene/ethyl acetate, 2:1) yielding **7** (884 mg, 1.23 mmol, 87%) as a colorless foam. R_f 0.06 (toluene/ethyl acetate, 2:1); $[\alpha]_D^{23}$ +25 (*c* 0.7, $CHCl_3$); IR (ATR) $\tilde{\nu}$ 3311, 2932, 1741, 1661, 1519, 1449, 1367, 1215, 1135, 1079, 1042, 977, 910, 728, 644, 598, 463 cm^{-1}; ^{1}H NMR (600 MHz, $CDCl_3$, TMS) δ 7.70 (d, ^3J = 7.6 Hz, 2H, aryl-H_{Fmoc}), 7.53 (d, ^3J = 7.3 Hz, 2H, aryl-H_{Fmoc}), 7.33 (dd ~ t, ^3J = 7.5 Hz, ^3J = 7.5 Hz, 2H, aryl-H_{Fmoc}), 7.29 (dd ~ t, ^3J = 7.5 Hz, ^3J = 7.3 Hz, 2H, aryl-H_{Fmoc}), 6.62 (br s, 1H, NHα), 5.81 (d, ^3J = 8.0 Hz, 1H, man-OCH_2CH_2-N*H*), 5.26 (dd, $^3J_{2,3}$ = 3.6 Hz, $^3J_{3,4}$ = 9.5 Hz, 1H, H-3), 5.21–5.15 (m, 2H, H-2, H-4), 4.77 (br s, 1H, H-1), 4.42 (m_c, 1H, C*H*H_{Fmoc}), 4.33–4.26 (m, 2H, CH*H*$_{Fmoc}$, H-α), 4.18 (dd, $^2J_{6,6'}$ = 12.2 Hz, $^3J_{5,6}$ = 5.6 Hz, 1H, H-6), 4.16 (t, $^3J_{2,3}$ = 6.9 Hz, 1H, fluorenyl-H), 4.06–4.02 (m, 1H, H-6'), 3.94 (m_c, 1H, H-5), 3.72 (dd, ^3J = 4.4 Hz, ^2J = 9.0 Hz, 1H, man-OC*H*H), 3.56–3.38 (m, 3H, man-OCH*HCH*$_2$), 3.00 (m_c, 1H, H-β), 2.70 (m_c, 1H, H-β'), 2.08, 2.02, 1.95, 1.91 (each s, each 3H, 4 C(O)C*H*$_3$), 1.50 (br s, 1H, S-H) ppm; ^{13}C NMR (150 MHz, $CDCl_3$) δ 170.7 (*C*(O)CH_3), 170.2 (*C*(O)C-α), 170.0, 169.9, 169.8 (3 *C*(O)CH_3), 156.1 (Fmoc-O-*C*O), 143.7, 141.4, 127.8, 127.1, 125.0, 120.0 (12 C-Ar_{Fmoc}), 97.7 (C-1), 69.4 (C-2), 68.9 (C-3), 68.7 (C-5), 67.2 (*C*H_2-Fmoc), 67.0 (man-O*C*H_2CH_2), 66.3 (C-4), 62.6 (C-6), 56.3 ($C_α$), 47.2 (CH_2-*C*H_{Fmoc}), 39.3 (man-OCH_2*C*H_2), 26.8 (*C*-β), 21.0, 20.8, 20.7, 20.7 (4 C(O)*C*H_3) ppm; HRMS–ESI (*m*/*z*): calcd for $C_{34}H_{40}N_2NaO_{13}S$, 739.2143; found, 739.2033.

S-(Fluoren-9-yl)-L-cysteine-[2-(2,3,4,6-tetra-*O*-acetyl-α-D-mannopyranosyloxy)ethyl]amide (**8**)

The *N*-protected L-cysteine derivative **7** (864 mg, 1.21 mmol) was dissolved in dry DMF (7 mL), and then morpholine (640 µL, 7.30 mmol) was added, and the reaction mixture was stirred for 2 h at ambient temperature under a nitrogen atmosphere. Then the solvent was removed under reduced pressure, the residue was dissolved in methanol, and the formed precipitate was filtered off. The filtrate was concentrated under reduced pressure and the crude product was purified by gradient flash column chromatography (cyclohexane/ethyl acetate, 1:12 → ethyl acetate/methanol, 9:1 → ethyl acetate/methanol, 3:1) yielding **8** (630 mg, 936 µmol, 77%) as a colorless foam. R_f 0.45 (ethyl acetate/methanol, 9:1); $[\alpha]_D^{23}$ +14 (*c* 0.7, $CHCl_3$); IR (ATR) $\tilde{\nu}$ 3355, 1930, 1742, 1666, 1518, 1446, 1366, 1216, 1135, 1081, 1043, 977, 911, 729, 599 cm^{-1}; ^{1}H NMR (600 MHz, $CDCl_3$, TMS) δ 7.68 (d, ^3J = 7.5 Hz, 2H, aryl-H_{Fm}), 7.61 (m_c, 2H, aryl-H_{Fm}), 7.32 (dd ~ t, ^3J = 7.5 Hz, 2H, aryl-H_{Fm}), 7.25 (dt, ^3J = 7.5 Hz, ^4J = 1.0 Hz, 2H, aryl-H_{Fm}), 5.27 (dd, $^3J_{3,4}$ = 10.0 Hz, $^3J_{2,3}$ = 3.5 Hz, 1H, H-3), 5.21–5.16 (m, 2H, H-4, H-2), 4.75 (d, $^3J_{1,2}$ =1.2 Hz, 1H, H-1), 4.17 (dd ~ dt, $^3J_{5,6}$ = 5.6 Hz, $^2J_{6,6'}$ = 12.3 Hz, 1H, H-6), 4.09–4.03 (m, 2H, fluorenyl-H, H-6'), 3.90 (ddd, $^3J_{4,5}$ = 10.1 Hz, $^3J_{5,6}$ = 5.2 Hz, $^3J_{5,6'}$ = 2.4 Hz, 1H, H-5), 3.68 (m_c, 1H, man-OC*H*H), 3.52–3.44 (m, 2H, man-OCH*H*, man-OCH_2C*H*H), 3.40–3.31 (m, 2H, H-2, man-OCH_2CH*H*), 3.09 (dd, ^3J = 6.2 Hz, ^2J = 12.9 Hz, 1H, C*H*H_{Fm}), 3.03 (dd, ^3J = 6.4 Hz, ^2J = 12.9 Hz, 1H, CH*H*$_{Fm}$), 2.99 (dd, ^3J = 3.9 Hz, ^2J = 13.7 Hz, 1H, H-β), 2.65 (dd ~ dt, ^3J = 8.9 Hz, ^2J = 13.7 Hz, 1H, H-β'), 2.07, 2.01, 1.97, 1.92 (each s, each 3H, 4 C(O)C*H*$_3$) ppm; ^{13}C NMR (125 MHz, $CDCl_3$) δ 173.6 (*C*(O)C-α), 170.6, 170.1, 170.0, 169.7 (4 *C*(O)CH_3), 145.8, 141.1, 127.6, 127.0, 124.7, 119.9 (12 C-Ar_{Fm}), 97.6 (C-1), 69.5 (C-2), 69.0 (C-3), 68.7 (C-5), 67.0 (man-O*C*H_2CH_2), 66.1 (C-4), 62.4 (C-6), 54.0 (*C*-α), 46.9 (*C*H_2-Fm), 38.7 (*C*-β), 38.6 (man-OCH_2*C*H_2), 36.4 (CH_2-*C*H_{Fm}), 21.0, 20.9, 20.7, 20.7 (4 C(O)*C*H_3) ppm; HRMS–ESI (*m*/*z*): calcd for $C_{33}H_{41}N_2O_{11}S$, 673.24; found, 673.21; MALDI–TOF–MS (CCA) *m*/*z* 673.73.

S-(Fluoren-9-yl)-L-cysteine-[2-(α-D-mannopyranosyloxy)ethyl]amide (**9**)

The *O*-acetylated glycoamino acid derivative **8** (600 mg, 892 µmol) was dissolved in dry methanol (8 mL), and then freshly prepared sodium methanolate solution (200 µL, 1 M in MeOH) was added, and the reaction mixture was stirred

overnight at ambient temperature under a nitrogen atmosphere. Then acidic ion-exchange resin (Amberlite IR 120) was added, and the mixture was stirred for 5 min to allow neutralization of the solution. After filtration of the resin, the solvent was removed under reduced pressure, and the crude product was purified on silica gel (ethyl acetate/ethanol, 7:1) yielding **9** (316 mg, 626 μmol, 70%) as a colorless foam. R_f 0.24 (ethyl acetate/methanol,10:1); IR (ATR) $\tilde{\nu}$ 3286, 2919, 1660, 1409, 1298, 1027, 738, 501 cm^{-1}; ^1H NMR (600 MHz, CD_3OD) δ 7.81 (d, ^3J = 7.5 Hz, 2H, aryl-H_{Fm}), 7.76 (dd, ^3J = 4.4 Hz, ^3J = 7.5 Hz, 2H, aryl-H_{Fm}), 7.34 (t, ^3J = 7.5 Hz, 2H, aryl-H_{Fm}), 7.33 (t, ^3J = 7.5 Hz, 2H, aryl-H_{Fm}), 4.80 (d, $^3J_{1,2}$ = 1.5 Hz, 1H, H-1), 4.17 (t, $^3J_{1(Fm),2(Fm)}$ = 6.3 Hz, 1H, fluorenyl-H), 3.87 (dd, $^3J_{5,6}$ = 2.3 Hz, $^2J_{6,6'}$ = 11.7 Hz, 1H, H-6), 3.85 (dd, $^3J_{2,3}$ = 3.4 Hz, $^2J_{1,2}$ = 1.8 Hz, 1H, H-2), 3.79 (ddd, ^3J = 6.4 Hz, ^3J = 4.5 Hz, ^2J = 10.7 Hz, 1H, man-OC*H*H), 3.75–3.70 (m, 2H, H-3, H-6'), 3.63 (dd, $^3J_{3,4}$ = 9.2 Hz, $^3J_{4,5}$ = 9.6 Hz, 1H, H-4), 3.60–3.54 (m, 2H, H-5, man-OCH*H*), 3.50–3.43 (m, 3H, H-α, man-OCH_2CH_2), 3.17 (ddt, ^4J = 0.7 Hz, ^3J = 6.3 Hz, ^2J = 13.0 Hz, 2H, $CH_{2\ Fm}$), 2.90 (ddd, ^4J = 0.7 Hz, ^3J = 5.6 Hz, ^2J = 13.6 Hz, 1H, H-β), 2.74 (dd, ^3J = 7.2 Hz, ^2J = 13.6 Hz, 1H, H-β') ppm; ^{13}C NMR (150 MHz, CD_3OD) δ 175.9 (*C*(O)C-α), 147.4, 142.5, 128.6, 128.1, 126.0, 120.8 (12 C-Ar_{Fm}), 101.7 (C-1), 74.8 (C-5), 72.6 (C-3), 72.1 (C-2), 68.7 (C-4), 67.2 (man-OCH_2CH_2), 63.0 (C-6), 55.6 (*C*-α), 48.2 (CH_2-CH_{Fm}), 40.3 (man-OCH_2CH_2), 39.3 (C-β), 37.6 (CH_2-CH_{Fm}) ppm.

Supporting Information

Supporting Information File 1

Analytical material: NMR and mass spectra of products **3-dimer**, **6**, **7**, **8**, **9** and **10**.
[http://www.beilstein-journals.org/bjoc/content/supplementary/1860-5397-8-242-S1.pdf]

Acknowledgements

We thank the Evonik Foundation for financial support (stipend for JWW) and Dipl. Chem. Christian Müller for technical assistance.

References

1. Schierholt, A.; Shaikh, H. A.; Schmidt-Lassen, J.; Lindhorst, T. K. *Eur. J. Org. Chem.* **2009,** 3783–3789. doi:10.1002/ejoc.200900437
2. Schierholt, A.; Hartmann, M.; Schwekendiek, K.; Lindhorst, T. K. *Eur. J. Org. Chem.* **2010,** 3120–3128. doi:10.1002/ejoc.201000185
3. Wehner, J. W.; Lindhorst, T. K. *Synthesis* **2010,** 3070–3082. doi:10.1055/s-0030-1258157
4. Shaikh, H. A.; Sönnichsen, F.; Lindhorst, T. K. *Carbohydr. Res.* **2008,** *343,* 1665–1674. doi:10.1016/j.carres.2008.04.015
5. Schierholt, A.; Hartmann, M.; Lindhorst, T. K. *Carbohydr. Res.* **2011,** *346,* 1519–1526. doi:10.1016/j.carres.2011.04.023
6. Hsieh-Wilson, L. C. *Nature* **2007,** *445,* 31–33. doi:10.1038/445031a
7. Hackenberger, C. P. R.; Schwarzer, D. *Angew. Chem.* **2008,** *120,* 10182–10228. doi:10.1002/ange.200801313
Angew. Chem., Int. Ed. **2008,** *47,* 10030–10074. doi:10.1002/anie.200801313
8. Gamblin, D. P.; Scanlan, E. M.; Davis, B. G. *Chem. Rev.* **2009,** *109,* 131–163. doi:10.1021/cr078291i
9. Payne, R. J.; Wong, C.-H. *Chem. Commun.* **2010,** *46,* 21–43. doi:10.1039/b913845e
10. Weissenborn, M. J.; Castangia, R.; Wehner, J. W.; Šardzík, R.; Lindhorst, T. K.; Flitsch, S. *Chem. Commun.* **2012,** 4444–4446. doi:10.1039/c2cc30844d
11. Lindhorst, T. K.; Bruegge, K.; Fuchs, A.; Sperling, O. *Beilstein J. Org. Chem.* **2010,** *6,* 801–809. doi:10.3762/bjoc.6.90
12. Branderhorst, H. M.; Liskamp, R. M. J.; Pieters, R. J. *Tetrahedron* **2007,** *63,* 4290–4296. doi:10.1016/j.tet.2007.03.051
13. Zemplén, G.; Pacsu, E. *Ber. Dtsch. Chem. Ges. B* **1929,** *62,* 1613–1614. doi:10.1002/cber.19290620640
14. Carpino, L. A.; Han, G. Y. *J. Am. Chem. Soc.* **1970,** *92,* 5748–5757. doi:10.1021/ja00722a043
15. Katritzky, A. R.; Abo-Dya, N. E.; Abdelmajeid, A.; Tala, S. R.; Amine, M. S.; El-Feky, S. A. *Org. Biomol. Chem.* **2011,** *9,* 596–599. doi:10.1039/c0ob00663g
16. West, C. W.; Angels Estiarte, M.; Rich, D. H. *Org. Lett.* **2001,** *3,* 1205–1208. doi:10.1021/ol015678d
17. Hartmann, M.; Lindhorst, T. K. *Eur. J. Org. Chem.* **2011,** 3583–3609. doi:10.1002/ejoc.201100407
18. Weissenborn, M. J.; Wehner, J. W.; Gray, C. J.; Šardzík, R.; Eyers, C. E.; Lindhorst, T. K.; Flitsch, S. L. *Beilstein J. Org. Chem.* **2012,** *8,* 753–762. doi:10.3762/bjoc.8.86
19. Wehner, J. W.; Weissenborn, M. J.; Hartmann, M.; Gray, C. J.; Šardzík, R.; Eyers, C. E.; Flitsch, S. L.; Lindhorst, T. K. *Org. Biomol. Chem.* **2012,** *10,* 8919–8926. doi:10.1039/c2ob26118a

License and Terms

Beilstein Journal of Organic Chemistry

Peptoids and polyamines going sweet: Modular synthesis of glycosylated peptoids and polyamines using click chemistry

Daniel Fürniss[1], Timo Mack[2], Frank Hahn[2], Sidonie B. L. Vollrath[1], Katarzyna Koroniak[1], Ute Schepers[*3] and Stefan Bräse[*1,3]

Full Research Paper

Open Access

Address:
[1]Institute of Organic Chemistry, Karlsruhe Institute of Technology (KIT), Fritz-Haber-Weg 6, 76131 Karlsruhe, Germany, [2]Kekulé Institute of Organic Chemistry and Biochemistry, Rheinische Friedrich Wilhelms University of Bonn, Germany and [3]Institute of Toxicology and Genetics, Karlsruhe Institute of Technology (KIT), Hermann-von-Helmholtz-Platz 1, 76344 Eggenstein-Leopoldshafen, Germany

Email:
Ute Schepers* - ute.schepers@kit.edu; Stefan Bräse* - braese@kit.edu

* Corresponding author

Keywords:
click chemistry; glycans; peptoids; polyalkynes; polyamines; solid-phase chemistry

Beilstein J. Org. Chem. **2013,** *9,* 56–63.
doi:10.3762/bjoc.9.7

Received: 21 April 2012
Accepted: 10 December 2012
Published: 10 January 2013

This article is part of the Thematic Series "Synthesis in the glycosciences II".

Guest Editor: T. K. Lindhorst

Abstract

Sugar moieties are present in a wide range of bioactive molecules. Thus, having versatile and fast methods for the decoration of biomimetic molecules with sugars is of fundamental importance. The glycosylation of peptoids and polyamines as examples of such biomimetic molecules is reported here. The method uses Cu-catalyzed azide alkyne cycloaddition to promote the reaction of azido-sugars with either polyamines or peptoids. In addition, functionalized nucleic acids were attached to polyamines via the same route. Based on a modular solid-phase synthesis of peralkynylated peptoids with up to six alkyne groups, the latter were modified with azidosugar building blocks by using copper-catalyzed azide alkyne cycloadditions. In addition, the up-scaling of some particular azide-modified sugars is described.

Introduction

To date, oligosaccharides have gained more and more interest as potential drugs in the treatment of a variety of diseases. However, the rendering of nucleic acids and oligosaccharides as therapeutically active substances often requires a derivatization or a chemical coupling reaction that permits the selective and simple formation of covalent adducts. Some modifications permit the attachment to other molecules through a variety of functional groups, such as amines ($-NH_2$) and carboxylic acids

(–COOH) resulting in peptide bonds, thiols (–SH) resulting in disulfides, thioethers or thioesters, aldehydes (–CHO) and hydroxy (–OH) groups. Nonetheless, coupling to these groups often requires a laborious protection of other reactive functional groups as they can compete in the coupling step. A matched pair of groups, which are selective in reacting with each other while being unreactive with other functional groups in the molecule would, therefore, be highly useful in the preparation of functional structures. Likewise, the coupling reaction should be permitted in hydrophilic solvents such as water or DMSO, since both unprotected nucleic acids and oligosaccharides, as well as many other biomacromolecules, prefer a hydrophilic reaction environment.

With the advent of mild and biocompatible conjugation methods such as the Staudinger ligation [1] or the copper-catalyzed alkyne azide cycloaddition (CuAAC) [2,3], a large number of versatile and functional bioconjugates are accessible for various applications in chemical biology [4].

To date, many therapeutically active molecules are synthetic derivatives of biomacromolecules that have to be soluble in hydrophilic environments to be taken up in vivo or in cell culture. Common solubilizers that enhance the cellular uptake are polyamines and other polycationic moieties such as particular peptoids.

Recently, polycationic polyamines have been shown to be efficacious in the cellular delivery of oligonucleotides such as DNA [5-7] and RNA [8-11]. Conjugates of polyamines with aliphatic lipids or cholesterol yielding, i.e., dioctadecylaminoglycylspermine (DOGS, transfectam) are well established reagents for the transfection of DNA and oligonucleotides [5-7,11-13] displaying only very little toxicity towards mammalian cells [11]. They have also been shown to function in the recognition of biomacromolecules. Likewise, other polycationic species, such as the *N*-alkylated glycine oligomers (peptoids) [14-25], have emerged as powerful tools in the context of drug delivery [26-29], peptidomimetics and other biologically relevant applications [28,30-32] as well as materials science [33,34].

During the last decade the synthesis of polyamines and peptoids has been well established on solid phases [26,27,29,35-39]. However, the on-bead addition of oligosaccharide or monosaccharide modifications are not known so far. The modification of polyamines or peptoids is usually achieved by alternation of the termini [36,40] or by direct use of different side-chain functionalities. For peptoids, CuAAC has already been used successfully to introduce diverse side-chain functionalities directly during solid-phase synthesis of peptoids starting from both, azido- and alkyne-functionalized side chains [41,42]. In addition CuAAC has also been used in order to constrain peptoid secondary structures [43].

CuAAC reactions for the attachment of sugar residues to peptoid backbones have been reported for some cases [44,45]; however, a fully glycosylated structure is unknown (for glycodendrons see [46]). In this study, we describe the first solid-phase synthesis of glycosylated polyamines and a fully glycosylated hexapeptoid.

Results and Discussion

Synthesis of azidosugars

Although the syntheses of the azidosugars **1**–**3** and **5** (Figure 1) were described before [47], we optimized and revised the procedure reported by Laughlin and Bertozzi [48] due to some difficulties in obtaining reproducible results.

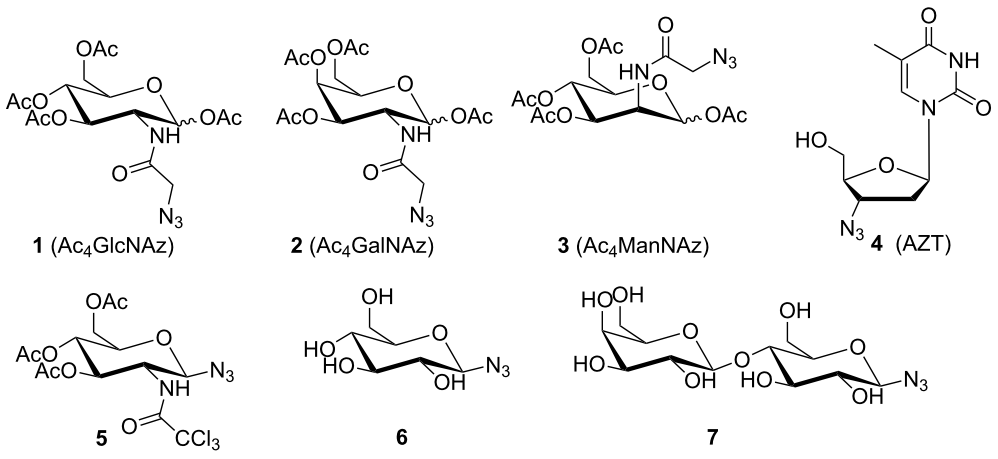

Figure 1: Azidosugars used in this study. The synthesis of the azidosugars **1**–**3** was modified from [47,48], compounds **4**, **6** and **7** were commercially available.

Instead of 5.00 equiv of chloroacetic anhydride only 1.10 equiv were used. A change from LiN_3 to NaN_3, which is more stable and cheaper, in conjunction with lowering the amount of the azide salt from 5.00 equiv to less than 3.60 equiv gave similar results. The solvent was changed from DMF to MeOH. By applying revised conditions 55% yield (on a 4.64 mmol scale) was obtained with a comparable yield on a 1.16 mmol scale (61%). In contrast to the originally reported procedure, the purification and isolation of intermediates could be omitted. We tried to use fewer equivalents of sodium azide during the scale-up of the reaction but this caused a decrease of the overall reaction yields.

In all cases, the test reactions were performed starting from D-glucosamine hydrochloride as a model compound for the synthesis of 1,3,4,6-tetra-*O*-acetyl-*N*-azidoacetyl-D-glucosamine (Ac_4GlcNAz = **1**). Optimal variations from Bertozzi's protocol for this model compound were the use of 1.10 equiv chloroacetic anhydride in the first step and 3.50 equiv sodium azide as well as methanol in the second step (for further details, see Table 1). Eventually, we applied these optimized reaction conditions to synthesize also 1,3,4,6-tetra-*O*-acetyl-*N*-azidoacetyl-D-galactosamine (Ac_4GalNAz = **2**) and 1,3,4,6-tetra-*O*-acetyl-*N*-azidoacetyl-D-mannosamine (Ac_4ManNAz = **3**) with similar yields under these optimized conditions (see Supporting Information File 1).

Click reaction on alkynylated polyamines and peptoids

The covalent coupling of many biomacromolecules to solid-phase-bound polycationic moieties, such as polyamines or peptoids, often requires a hydrophilic reaction environment as well as very mild cleaving conditions of the final product from the solid support. To avoid a degradation of the coupled biomacromolecules at high concentrations of strong acids, a polystyrene resin was chosen that contains a tritylchloride linker. The resin was obtained by treatment of Merrifield resin with *p*-hydroxytriphenylmethyl alcohol and subsequent chlorination [49,50]. This tritylchloride linker allowed a mild cleavage of the acid labile products using less than 0.5% trifluoroacetic acid (TFA) in dichloromethane. The loading of the Merrifield resin occurred in pretty good yields as the ratio of the measured to the calculated loading value was 0.70 mmol/g to 0.78 mmol/g (Scheme 1).

The synthesis started with the assembly of the 2-nitrobenzenesulfonyl-(Nosyl, further abbreviated with Ns)-protected spermine backbone **8** on a solid phase via Fukuyama Ns strategy [51]. The next step was the Ns protection of the residual primary amine with 6.00 equiv of Ns-chloride and 12.0 equiv 2,4,6-collidine in CH_2Cl_2 followed by *N*-alkylation with 5-chloropent-1-yne to insert the terminal alkyne moiety. To accomplish that, we used 10.0 equiv of alkyne and 15.0 equiv of K_2CO_3 in DMF; the reaction led to resin **9** with virtually quantitative yield, as shown in Scheme 1. For the CuAAC with the azides moieties **4**, **6** and **7**, respectively, we used 0.500 equiv of $CuSO_4{\cdot}5H_2O$ and 5.00 equiv sodium ascorbate as the catalytic system, which is a slightly higher catalyst concentration than reported for the reaction in solution [52]. To ensure, that the reaction proceeds completely we chose 2 days of agitation at ambient temperature and obtained resin **10**–**12**.

Finally, the Ns deprotection was achieved in 18 h with 20.0 equiv of 1,8-diazabicyclo[5.4.0]undec-7-ene (DBU) and 20.0 equiv of β-mercaptoethanol. The cleavage from the resin was carried out with 1% TFA in dichloromethane at 10 min

Table 1: Optimization of the synthesis of azide **1**.

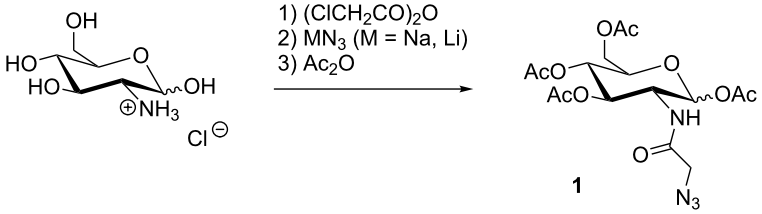

1

Entry	Reaction scale	Solvent (2nd step)	MN_3	Overall reaction yield (over 3 steps)
1	1.16 mmol	DMF	5.00 equiv (M = Li)	61%
2	4.64 mmol	DMF	5.00 equiv (M = Na)	23%
3	4.64 mmol	MeOH	2.10 equiv (M = Na)	35%
4	4.64 mmol	MeOH	3.50 equiv (M = Na)	55%
5	13.4 mmol	MeOH	2.10 equiv (M = Na)	38%
6	23.2 mmol	MeOH	2.00 equiv (M = Na)	42%

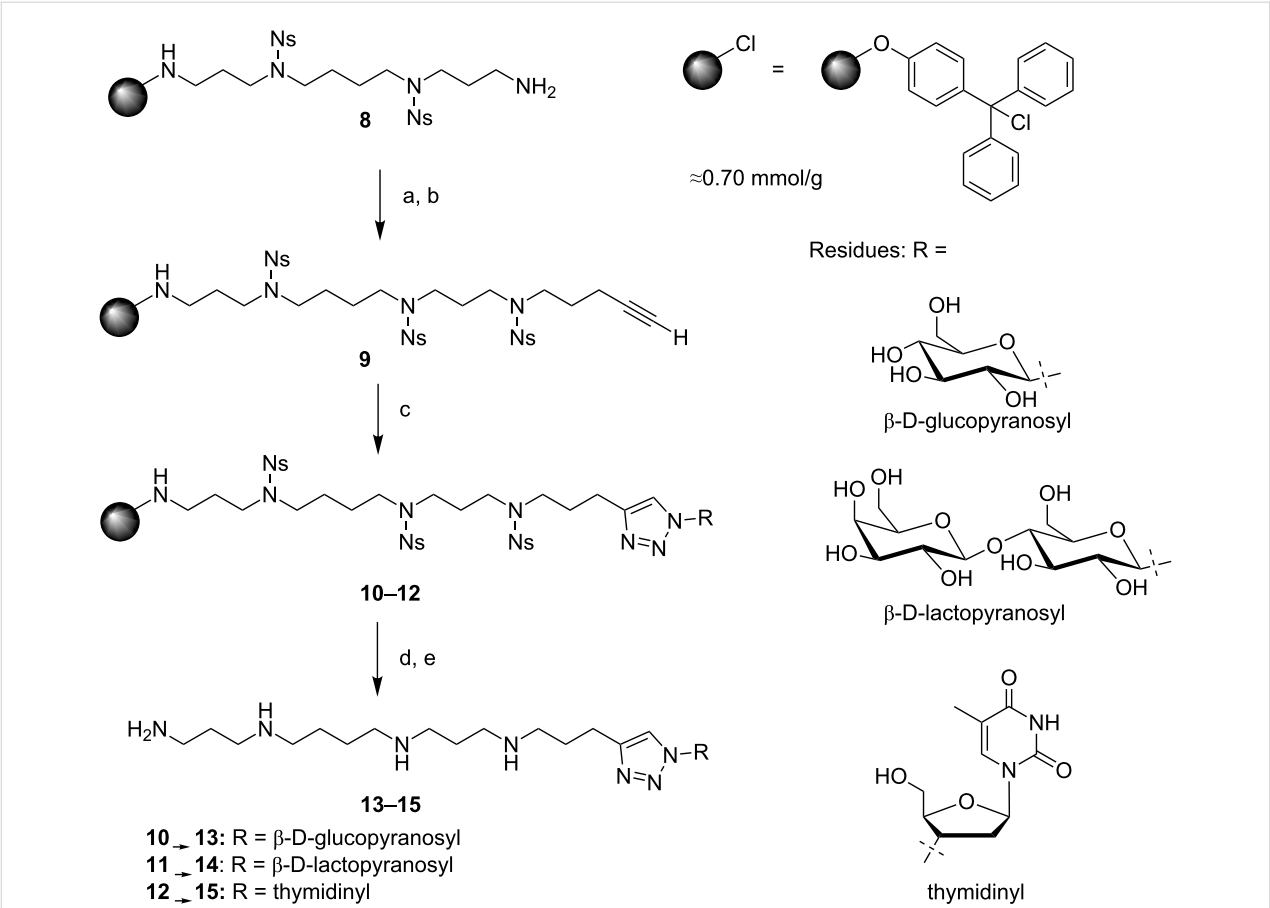

Scheme 1: Reaction conditions and reagents: (a) Ns-chloride (6.00 equiv), 2,4,6-collidine (12.0 equiv), CH_2Cl_2, rt, 16 h; (b) 5-chloropent-1-yne (10.0 equiv), K_2CO_3 (15.0 equiv), DMF, 60 °C, 16 h; (c) azidosugars **6, 7** or AZT (**4**) (2.00 equiv/1.86 equiv), $CuSO_4 \cdot 5H_2O$ (0.500 equiv), sodium ascorbate (5.00 equiv), DMF/H_2O (6:1), rt, 2 d; (d) DBU (20.0 equiv), β-mercaptoethanol (20.0 equiv), DMF, rt, 18 h; (e) 1% TFA in CH_2Cl_2, rt, 10 min.

residence time. The products **13**–**15** were obtained with >90% yield, calculated on the initial loading of the resin (0.70 mmol/g). The ^{1}H NMR data clearly showed the aromatic shift of the triazole proton at 8.02 ppm, 8.03 ppm and 7.94 ppm for **13**–**15**, respectively. The ^{13}C NMR spectra indicated the presence of the anomeric carbon atoms at 89.70 ppm for **13** as well as at 89.41 ppm and 105.47 ppm for **14**.

In a different approach, we synthesized glycosylated spermine derivatives by our optimized procedure on a 2-chlorotrityl chloride resin [35,37-39]. The reaction of the resin **16** and **17** with the Ac_4GlcNAz derivative **1** proceeded smoothly in the presence of copper ions. In some cases, changing the base from DIPEA to DBU was beneficial (Scheme 2).

After these encouraging results, we turned our attention to peptoids. For the glycosylation of peptoids, we envisaged the generation of a fully glycosylated peptoid in order to investigate the compatibility of peptoid synthesis and decoration with sugars.

As a model compound we started with the synthesis of a hexaglycosylated peptoid hexamer. Therefore, we synthesized a hexaalkynated peptoid structure **26**,**27** on resin (Scheme 3).

The synthesis of a hexaalkynated peptoid backbone **26**,**27** was carried out on Rink or Barlos resin containing a 2-chlorotrityl chloride linker by standard methods using the submonomer strategy [14]. By using this method, the peptoid backbone is assembled in two subsequently repeated steps: In the first step (acylation), bromoacetic acid is reacted with the resin, and in the second step (amination) a primary amine is used to substitute the bromine to give the peptoid residue. This approach avoids the use of *N*-terminally protected monomers, which have to be synthesized in advance.

For the incorporation of the alkyne side chains we chose propargylamine as building block. A sixfold repetitive coupling sequence resulted in the peptoids, which were further modified with rhodamine B (Rho-CO_2H) as an easily accessible and versatile fluorescent tag.

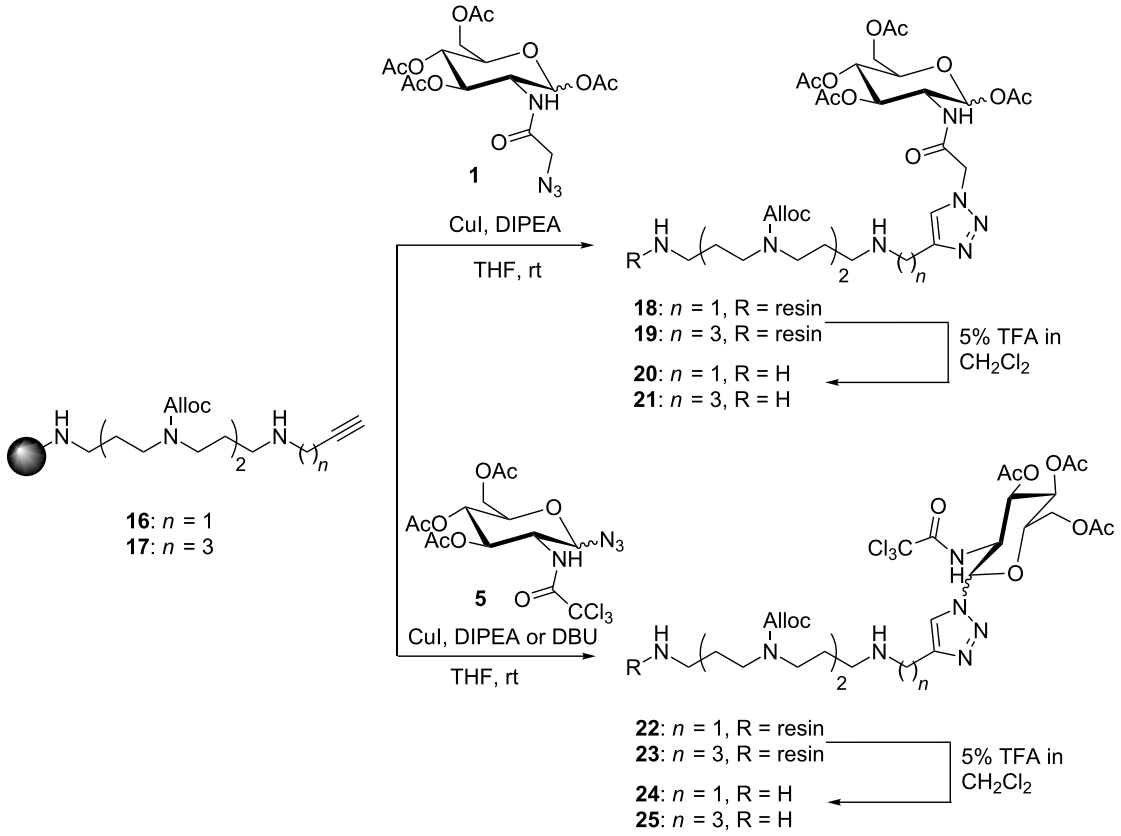

Scheme 2: Synthesis of spermine conjugates **20**,**21** and **24**,**25**. 2-chlorotrityl chloride resin was used as a solid support.

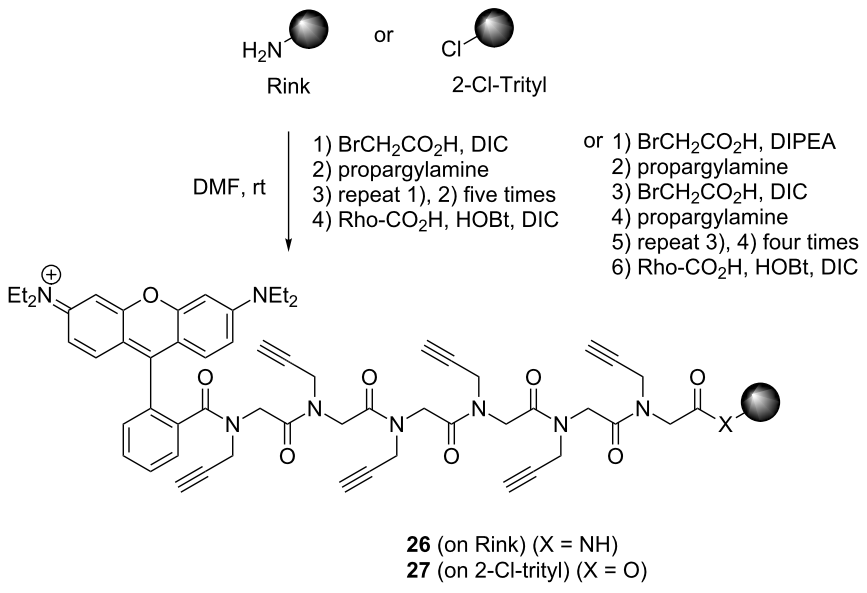

Scheme 3: Synthesis of hexaalkynyl peptoids **26** and **27** on solid supports.

Rhodamine B was coupled to the *N*-terminus in order to provide a label for future biological applications, such as the study of the cellular uptake. For both resins, the peptoid synthesis was successful; the only differences are the functional groups on the *C*-terminus. After cleavage from Rink-amide resin with trifluoroacetic acid, an amide is obtained, whereas cleavage from 2-chlorotrityl chloride resin with hexafluoroisopropanol (HFIP) gives the carboxylic acid. The mild cleavage conditions of the 2-chlorotrityl linker did not harm the sugar moieties of the final glycosylated compound, and this linker was therefore favored over the Rink linker.

For the conjugation of Ac_4GalNAz (**2**), the same conditions were used as described for the spermine conjugation (Scheme 2) with minor modifications. The CuAAC was carried out by using $Cu(CH_3CN)_4PF_6$ in THF with 2,6-lutidine as base. Only 1.60 equiv of the azidosugar were necessary to achieve full conversion after 18 h, and no shorter oligomers were observed in the MALDI–TOF spectrum. Cleavage from the resin by treatment with 33% hexafluoroisopropanol (HFIP) in dichloromethane and subsequent HPLC purification resulted in the fully glycosylated hexameric product **28** (Scheme 4).

Conclusion

In conclusion, we were able to improve protocols for the synthesis of tetra-*O*-acetyl protected sugars. Applying this, better yields as well as upscaling was possible. With these sugar building blocks, functionalization of polyamine derivatives was possible directly on solid supports by using copper-catalyzed alkyne azide cycloaddition conditions. In addition to that, the

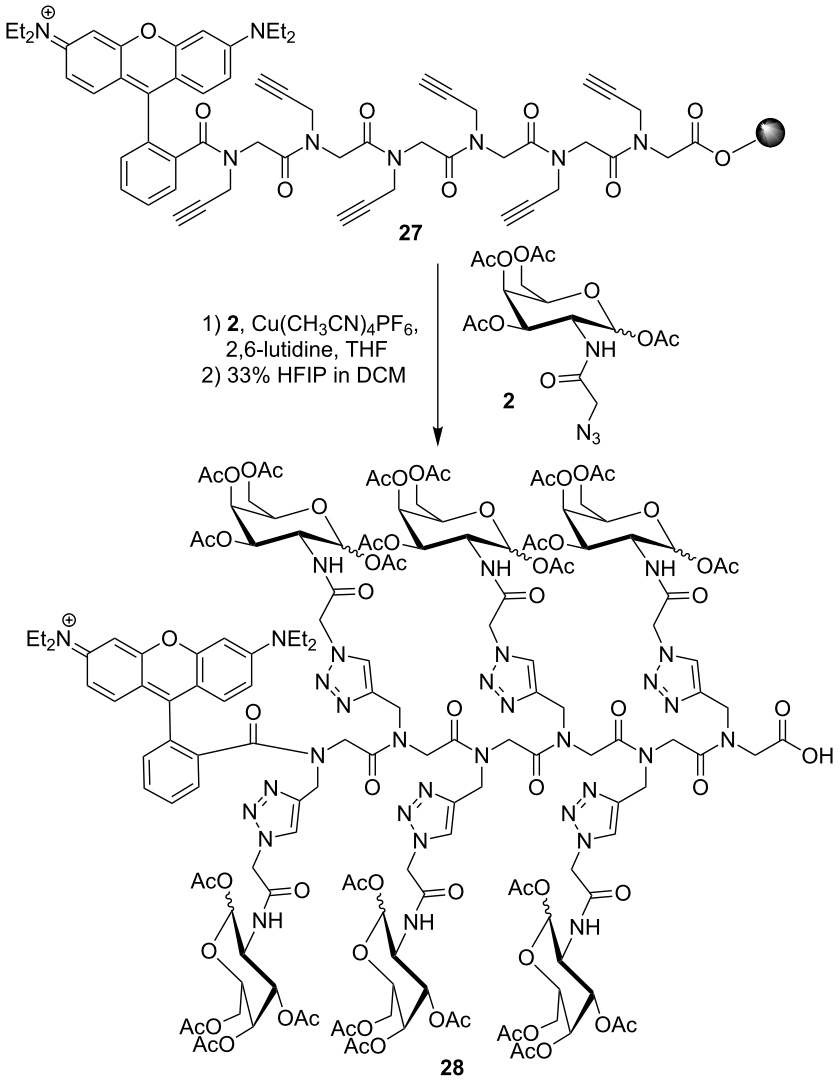

Scheme 4: Synthesis of a hexa-glycosylated peptoid **28**.

functionalization of a peptoid-hexaalkyne was also possible. By using the more labile 2-chlorotrityl chloride resin, the cleavage of peptoid **28** could be achieved without degradation.

Supporting Information

Supporting Information File 1

Methods and NMR spectra.
[http://www.beilstein-journals.org/bjoc/content/supplementary/1860-5397-9-7-S1.pdf]

Acknowledgements

We acknowledge funding from the Landesgraduiertenprogramm Baden-Württemberg (fellowship to S.B.L.V), the Carl-Zeiss foundation (fellowship to D.F.), Theodor Laymann Foundation (fellowships to T.M. and F.H.), the Fonds der Chemischen Industrie, the SFB 645 (Project Z1), the Helmholtz Program "Biointerface" and the Center for Functionalized Nanostructures (CFN), Karlsruhe.

References

1. Schilling, C. I.; Jung, N.; Biskup, M.; Schepers, U.; Bräse, S. *Chem. Soc. Rev.* **2011,** *40,* 4840–4871. doi:10.1039/c0cs00123f
2. Rostovtsev, V. V.; Green, L. G.; Fokin, V. V.; Sharpless, K. B. *Angew. Chem., Int. Ed.* **2002,** *41,* 2596–2599. doi:10.1002/1521-3773(20020715)41:14<2596::AID-ANIE2596>3.0.CO;2-4
3. Tornøe, C. W.; Christensen, C.; Meldal, M. *J. Org. Chem.* **2002,** *67,* 3057–3064. doi:10.1021/jo011148j
4. Holub, J. M.; Kirshenbaum, K. *Chem. Soc. Rev.* **2010,** *39,* 1325–1337. doi:10.1039/b901977b
5. Mack, K. D.; Walzem, R.; Zeldis, J. B. *Am. J. Med. Sci.* **1994,** *307,* 138–143. doi:10.1097/00000441-199402000-00013
6. Boletta, A.; Benigni, A.; Lutz, J.; Remuzzi, G.; Soria, M. R.; Monaco, L. *Hum. Gene Ther.* **1997,** *8,* 1243–1251. doi:10.1089/hum.1997.8.10-1243
7. Kichler, A.; Mechtler, K.; Behr, J.-P.; Wagner, E. *Bioconjugate Chem.* **1997,** *8,* 213–221. doi:10.1021/bc970009z
8. Lu, D.; Benjamin, R.; Kim, M.; Conry, R. M.; Curiel, D. T. *Cancer Gene Ther.* **1994,** *1,* 245–252.
9. Aoki, Y.; Kawa, S.; Karasawa, Y.; Horiuchi, A.; Kiyosawa, K. *Clin. Exp. Pharmacol. Physiol.* **1998,** *25,* 702–705. doi:10.1111/j.1440-1681.1998.tb02279.x
10. Wong, F. M. P.; MacAdam, S. A.; Kim, A.; Oja, C.; Ramsay, E. C.; Bally, M. B. *J. Drug Targeting* **2002,** *10,* 615–623. doi:10.1080/1061186021000066246
11. Guy-Caffey, J. K.; Bodepudi, V.; Bishop, J. S.; Jayaraman, K.; Chaudhary, N. *J. Biol. Chem.* **1995,** *270,* 31391–31396. doi:10.1074/jbc.270.52.31391
12. Lee, E. R.; Marshall, J.; Siegel, C. S.; Jiang, C.; Yew, N. S.; Nichols, M. R.; Nietupski, J. B.; Ziegler, R. J.; Lane, M. B.; Wang, K. X.; Wan, N. C.; Scheule, R. K.; Harris, D. J.; Smith, A. E.; Cheng, S. H. *Hum. Gene Ther.* **1996,** *7,* 1701–1717. doi:10.1089/hum.1996.7.14-1701
13. Lee, J.-H.; Nam, S.-H.; Hwang, S.-B.; Hong, M.-G.; Kwon, J.-Y.; Joeng, K.-S.; Im, S.-H.; Shim, J.-W.; Park, M.-C. *J. Biochem. Mol. Biol.* **2004,** *37,* 107–113. doi:10.5483/BMBRep.2004.37.1.107
14. Zuckermann, R. N.; Kerr, J. M.; Kent, S. B. H.; Moos, W. H. *J. Am. Chem. Soc.* **1992,** *114,* 10646–10647. doi:10.1021/ja00052a076
15. Wu, C. W.; Seurynck, S. L.; Lee, K. Y. C.; Barron, A. E. *Chem. Biol.* **2003,** *10,* 1057–1063. doi:10.1016/j.chembiol.2003.10.008
16. Wender, P. A.; Mitchell, D. J.; Pattabiraman, K.; Pelkey, E. T.; Steinman, L.; Rothbard, J. B. *Proc. Natl. Acad. Sci. U. S. A.* **2000,** *97,* 13003–13008. doi:10.1073/pnas.97.24.13003
17. Sanborn, T. J.; Wu, C. W.; Zuckerman, R. N.; Barron, A. E. *Biopolymers* **2002,** *63,* 12–20. doi:10.1002/bip.1058
18. Burkoth, T. S.; Fafarman, A. T.; Charych, D. H.; Connolly, M. D.; Zuckermann, R. N. *J. Am. Chem. Soc.* **2003,** *125,* 8841–8845. doi:10.1021/ja0352101
19. Fafarman, A. T.; Borbat, P. P.; Freed, J. H.; Kirshenbaum, K. *Chem. Commun.* **2007,** 377–379. doi:10.1039/b612198e
20. Gorske, B. C.; Jewell, S. A.; Guerard, E. J.; Blackwell, H. E. *Org. Lett.* **2005,** *7,* 1521–1524. doi:10.1021/ol0502984
21. Kruijtzer, J. A. W.; Hofmeyer, L. J. F.; Heerma, W.; Versluis, C.; Liskamp, R. M. J. *Chem.–Eur. J.* **1998,** *4,* 1570–1580. doi:10.1002/(SICI)1521-3765(19980807)4:8<1570::AID-CHEM1570>3.0.CO;2-2
22. Li, S.; Bowerman, D.; Marthandan, N.; Klyza, S.; Luebke, K. J.; Garner, H. R.; Kodadek, T. *J. Am. Chem. Soc.* **2004,** *126,* 4088–4089. doi:10.1021/ja039565w
23. Olivos, H. J.; Alluri, P. G.; Reddy, M. M.; Salony, D.; Kodadek, T. *Org. Lett.* **2002,** *4,* 4057–4059. doi:10.1021/ol0267578
24. Saha, U. K.; Roy, R. *J. Chem. Soc., Chem. Commun.* **1995,** 2571–2573. doi:10.1039/C39950002571
25. Saha, U. K.; Roy, R. *Tetrahedron Lett.* **1995,** *36,* 3635–3638. doi:10.1016/0040-4039(95)00620-R
26. Schröder, T.; Schmitz, K.; Niemeier, N.; Balaban, T. S.; Krug, H. F.; Schepers, U.; Bräse, S. *Bioconjugate Chem.* **2007,** *18,* 342–354. doi:10.1021/bc0602073
27. Schröder, T.; Niemeier, N.; Afonin, S.; Ulrich, A. S.; Krug, H. F.; Bräse, S. *J. Med. Chem.* **2008,** *51,* 376–379. doi:10.1021/jm070603m
28. Seo, J.; Ren, G.; Liu, H.; Miao, Z.; Park, M.; Wang, Y.; Miller, T. M.; Barron, A. E.; Cheng, Z. *Bioconjugate Chem.* **2012,** *23,* 1069–1079. doi:10.1021/bc300091d
29. Eggenberger, K.; Birtalan, E.; Schröder, T.; Bräse, S.; Nick, P. *ChemBioChem* **2009,** *10,* 2504–2512. doi:10.1002/cbic.200900331
30. Aditya, A.; Kodadek, T. *ACS Comb. Sci.* **2012,** *14,* 164–169. doi:10.1021/co200195t
31. Chen, X.; Wu, J.; Luo, Y.; Liang, X.; Supnet, C.; Kim, M. W.; Lotz, G. P.; Yang, G.; Muchowski, P. J.; Kodadek, T.; Bezprozvanny, I. *Chem. Biol.* **2011,** *18,* 1113–1125. doi:10.1016/j.chembiol.2011.06.010
32. Levine, P. M.; Imberg, K.; Garabedian, M. J.; Kirshenbaum, K. *J. Am. Chem. Soc.* **2012,** *134,* 6912–6915. doi:10.1021/ja300170n
33. Uejio, J. S.; Schwartz, C. P.; Duffin, A. M.; England, A.; Prendergast, D.; Saykally, R. J. *J. Phys. Chem. B* **2010,** *114,* 4702–4709. doi:10.1021/jp911007k
34. Brown, N. J.; Johansson, J.; Barron, A. E. *Acc. Chem. Res.* **2008,** *41,* 1409–1417. doi:10.1021/ar800058t
35. Hahn, F.; Müllen, K.; Schepers, U. *Synlett* **2008,** 2785–2790. doi:10.1055/s-0028-1083566

36. Hahn, F.; Schepers, U. Solid Phase Chemistry for the Directed Synthesis of Biologically Active Polyamine Analogs, Derivatives, and Conjugates. In *Combinatorial Chemistry on Solid Supports;* Bräse, S., Ed.; Topics in Current Chemistry, Vol. 278; Springer: Berlin, 2007; pp 135–208. doi:10.1007/128_2007_135
37. Hahn, F.; Schepers, U. *J. Comb. Chem.* **2008,** *10,* 267–273. doi:10.1021/cc700119g
38. Hahn, F.; Schepers, U. *Synlett* **2009,** 2755–2760. doi:10.1055/s-0029-1217987
39. Hahn, F.; Schmitz, K.; Balaban, T. S.; Bräse, S.; Schepers, U. *ChemMedChem* **2008,** *3,* 1185–1188. doi:10.1002/cmdc.200800013
40. Brown, N. J.; Dohm, M. T.; de la Serna, J. B.; Barron, A. E. *Biophys. J.* **2011,** *101,* 1076–1085. doi:10.1016/j.bpj.2011.04.055
41. Fritz, D.; Bräse, S. *Synlett* **2010,** 1544–1548. doi:10.1055/s-0029-1219925
42. Roy, O.; Faure, S.; Thery, V.; Didierjean, C.; Taillefumier, C. *Org. Lett.* **2008,** *10,* 921–924. doi:10.1021/ol7030763
43. Holub, J. M.; Jang, H.; Kirshenbaum, K. *Org. Lett.* **2007,** *9,* 3275–3278. doi:10.1021/ol071169l
44. Norgren, A. S.; Budke, C.; Majer, Z.; Heggemann, C.; Koop, T.; Sewald, N. *Synthesis* **2009,** 488–494. doi:10.1055/s-0028-1083302
45. Disney, M. D.; Lee, M. M.; Pushechnikov, A.; Childs-Disney, J. L. *ChemBioChem* **2010,** *11,* 375–382. doi:10.1002/cbic.200900716
46. Papadopoulos, A.; Shiao, T. C.; Roy, R. *Mol. Pharmaceutics* **2012,** *9,* 394–403. doi:10.1021/mp200490b
47. Saxon, E.; Bertozzi, C. R. *Science* **2000,** *287,* 2007–2010. doi:10.1126/science.287.5460.2007
48. Laughlin, S. T.; Bertozzi, C. R. *Nat. Protoc.* **2007,** *2,* 2930–2944. doi:10.1038/nprot.2007.422
49. Hidai, Y.; Kan, T.; Fukuyama, T. *Tetrahedron Lett.* **1999,** *40,* 4711–4714. doi:10.1016/S0040-4039(99)00851-5
50. Hidai, Y.; Kan, T.; Fukuyama, T. *Chem. Pharm. Bull.* **2000,** *48,* 1570–1576. doi:10.1248/cpb.48.1570
51. Kan, T.; Fukuyama, T. *Chem. Commun.* **2004,** *4,* 353–359. doi:10.1039/b311203a
52. Kolb, H. C.; Finn, M. G.; Sharpless, K. B. *Angew. Chem., Int. Ed.* **2001,** *40,* 2004–2021. doi:10.1002/1521-3773(20010601)40:11<2004::AID-ANIE2004>3.3.CO;2-X

License and Terms

Beilstein Journal of Organic Chemistry

Glycosylation efficiencies on different solid supports using a hydrogenolysis-labile linker

Mayeul Collot[1,2], Steffen Eller[1,2], Markus Weishaupt[1,2] and Peter H. Seeberger[*1,2]

Letter

Open Access

Address:
[1]Department of Biomolecular Systems, Max Planck Institute of Colloids and Interfaces, Am Mühlenberg 1, 14776 Potsdam, Germany and [2]Institut für Chemie und Biochemie, Freie Universität Berlin, Arnimallee 22, 14195 Berlin, Germany

Email:
Peter H. Seeberger[*] - peter.seeberger@mpikg.mpg.de

* Corresponding author

Keywords:
glycosylation; hydrogenolysis; linkers; oligosaccharides; resins; solid-phase synthesis

Beilstein J. Org. Chem. **2013,** *9,* 97–105.
doi:10.3762/bjoc.9.13

Received: 27 September 2012
Accepted: 14 December 2012
Published: 16 January 2013

This article is part of the Thematic Series "Synthesis in the glycosciences II".

Guest Editor: T. K. Lindhorst

Abstract

Automated oligosaccharide assembly requires suitable linkers to connect the first monosaccharide to a solid support. A new hydrogenolysis-labile linker that is stable under both acidic and basic conditions was designed, synthesized and coupled to different resins. Glycosylation and cleavage efficiencies on these functionalized solid supports were investigated, and restrictions for the choice of solid support for oligosaccharide synthesis were found.

Findings

Since Bruce Merrifield introduced the concept of solid-phase peptide synthesis in 1963 [1], synthesis on solid supports has evolved as a powerful tool for organic chemists [2]. Over the past fifty years this strategy has been successfully applied to the synthesis of other biopolymers, such as oligonucleotides [3] and oligosaccharides [4]. Solid-phase synthesis is performed on insoluble supports that are functionalized with a linker that connects the growing molecule with the resin (Scheme 1). Once the target molecule has been assembled, it is cleaved from the solid support. The solid-phase paradigm allows for the use of excess reagents to drive reactions to completion, as any leftovers are easily removed by washing of the resin between reaction steps.

Given the repetitive character of solid-supported synthesis, the process was successfully automated for all types of biopolymers [5-7]. As glycobiology is rapidly expanding [8], the need for synthetic tools has prompted synthetic carbohydrate chemists to develop methods for the accelerated synthesis of all types of glycans [9-19]. Automated synthesis of oligosaccharides is beginning to provide molecules for biological evaluation [20-23]. It was early on recognized that the linker plays a pivotal role for oligosaccharide synthesis, as its chemical properties determine the conditions that can be used for glycosylation and deprotection reactions [7,20,23-25]. Equally important is the choice of solid support and many different resins were briefly explored [26]. However, for automated

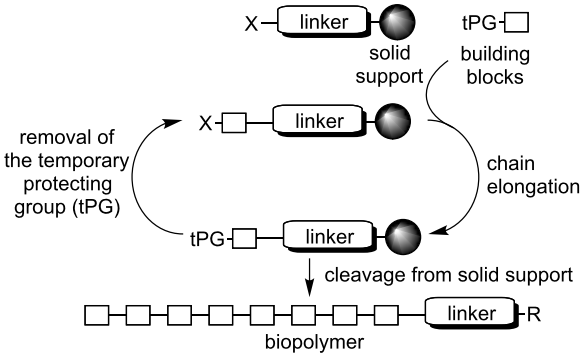

Scheme 1: Solid-phase synthesis of biopolymers. X represents a reactive site such as an amino group for peptide synthesis or a hydroxy group for oligonucleotide and oligosaccharide synthesis.

solid-phase oligosaccharide synthesis, Merrifield polystyrene resin has almost exclusively been used as the solid support.

Here, we describe the development of a new linker system that was tested in the context of different solid supports. In order to be suitable for automated solid-phase synthesis the resins have to be stable, chemically and mechanically, have to be permeable for the reagents, have to allow for reproducible loadings, and must exhibit good swelling behavior in a wide range of solvents. Mindful of these requirements, different solid supports have been developed (Figure 1, [27,28]). The most commonly used solid support for organic synthesis is the Merrifield resin [1]. This polystyrene (PS) resin shows good swelling properties in organic media but is not compatible with the aqueous condi-

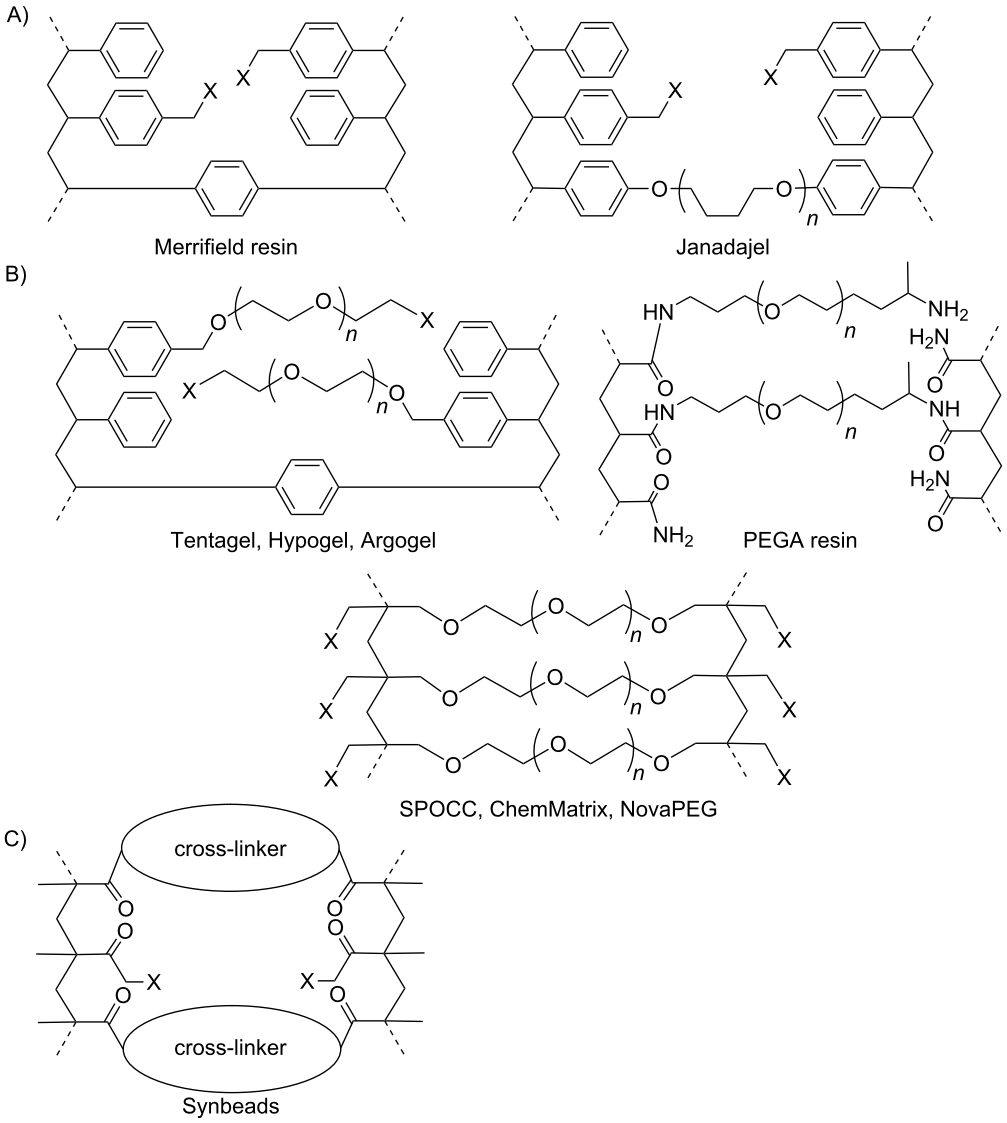

Figure 1: Different resins used for solid-phase synthesis. (A) Hydrophobic PS resins. (B) Water-compatible resins with PEG chains. (C) Nonswelling solid support compatible with aqueous reactions. X represents the functional groups, such as chlorides or amines.

tions that are often required for hydrolysis or enzymatic reactions. There are different variations of pure polystyrene resins. Jandajel resin for example features crosslinking of PS chains by tetrahydrofuran derivatives [29,30]. To improve the swelling behavior of PS resins in polar solvents, the PS core was grafted with polyethylene glycol (PEG) chains [31], resulting in solid supports such as Tentagel, Hypogel or Argogel. These resins were successfully used for the synthesis of peptides [31]. Meldal and co-workers developed PEGA resins [32] with good swelling behavior in water and polar solvents. Since the amide bonds of this solid support mimic peptides, the degree of aggregation of peptide chains during solid-phase synthesis is decreased, which facilitates the synthesis of peptides and glycopeptides [33]. Since amides are incompatible with many organic reactions, pure PEG resins, such as SPOCC [34], ChemMatrix [35] or NovaPEG, were introduced. To perform enzymatic reactions on a solid support, nonswelling resins (Synbeads) with large surfaces and big cavities that can be accessed even by proteins were developed [36].

For the design of linkers for oligosaccharide synthesis on solid support, several key features have to be considered. Not only has the linker to be orthogonal to the reaction conditions necessary for chain elongation, which are in general acidic for glycosylations and basic for the removal of temporary protecting groups; the linker also has to allow for the introduction of many naturally occurring modifications such as sulfation or phosphorylation, as well as non-native features for biological experiments, such as linkers for glycoconjugation. This results in a high requirement concerning the chemical stability of the linker and solid support. Orthogonal linker **1** (Scheme 2) was designed to address these issues. Cleavage of the linker by hydrogenolysis results in a free amine functionality for the immobilization of oligosaccharides on glycan arrays or for the synthesis of glycoconjugates. Hydrogenolysis on a solid support has been used previously in peptide chemistry [37]. In the early 1980s, catalytic-transfer-hydrogenation conditions proved to be very efficient for both deprotection and cleavage of the peptide from the solid support [38]. In this context, in situ generation of palladium black by reduction of palladium(II) acetate with ammonium formate in DMF yielded the best results. Although hydrogenolysis is widely used in carbohydrate chemistry as a means to achieve the final deprotection step, few examples for hydrogenolytic cleavage of an oligosaccharide from a support have been reported [39,40]. To assemble oligosaccharides, linker **1** was equipped with a primary hydroxy group as a glycosylation site, which was obtained by removal of the tetrahydropyran (THP) protecting group after coupling to the solid support. A terephthalic chromophore was incorporated into the linker to facilitate the UV detection during HPLC analysis or purification. The linker was directly attached to chloro-functionalized resins leading to an ester linkage. Cleavage of this

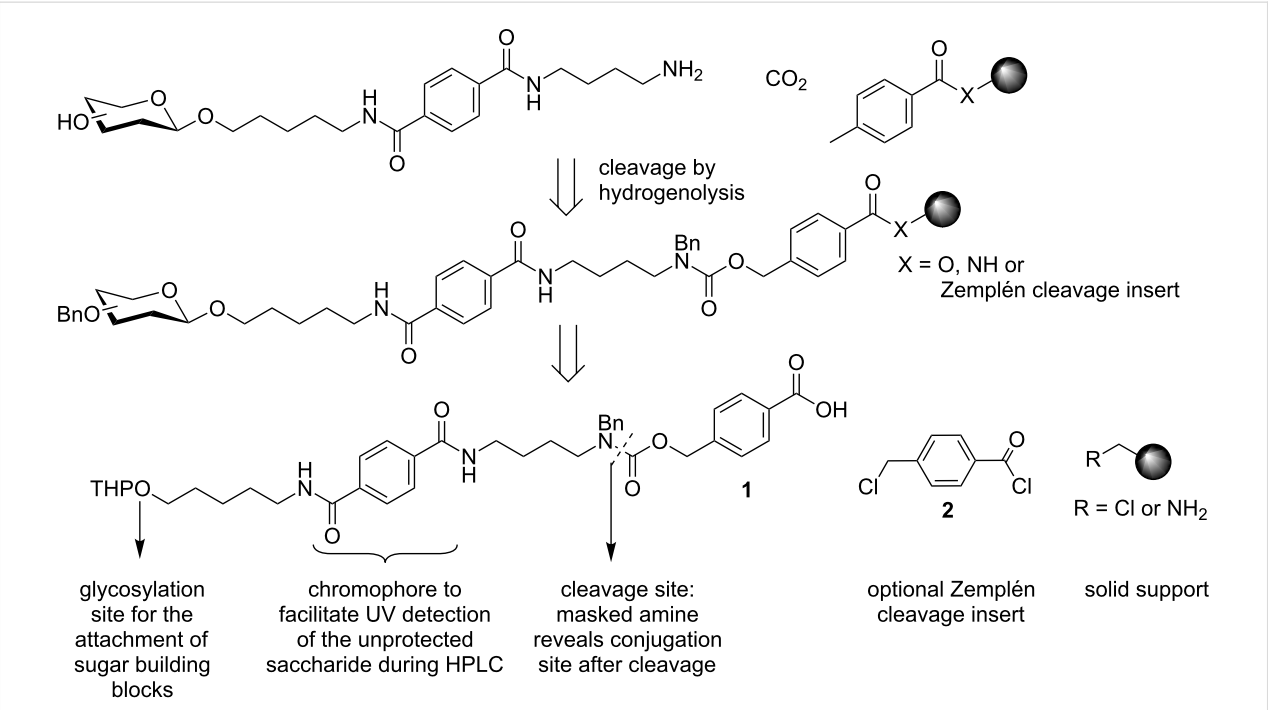

Scheme 2: Design of linker **1**. Cleavage by hydrogenolysis from a solid support reveals a conjugation site for the synthesis of glycoconjugates or glycan arrays and simultaneously removes permanent benzyl protecting groups. The linker can be coupled to amino- and chloro-functionalized resins. By placement of insert **2** on amino resins, an additional Zemplén cleavage site for fast LC–MS analysis is introduced.

ester under Zemplén conditions provides quick access to samples for HPLC analysis that may be used to control the glycosylation efficiency during chain elongation. When amino-functionalized resins were used, insert **2** was placed to obtain the additional Zemplén cleavage site in addition to the stable amide linkage to the solid support. This construct was used for linker evaluation where rapid cleavage for HPLC analysis was of key importance. After the utility of the linker had been established the linker could be directly coupled to amino-functionalized resins, which resulted in an amide bond that is stable under Zemplén conditions.

Linker **1** was prepared starting from chromophore fragment **7** and masked amine **12** (Scheme 3, Supporting Information File 1). Fragment **7** was synthesized starting from aminopentanol **3** and acyl chloride **4**. Following the condensation of **3** and **4**, the primary hydroxy group of the resulting intermediate **5** was protected and the ester was hydrolyzed to afford **7** in 76% yield over three steps. The synthesis of fragment **12** started with the transformation of **8** to carbonate **9**. Subsequent nucleophilic attack of secondary amine **10** [41,42] to afford intermediate **11** and removal of the Boc protecting group furnished amine **12**. Condensation of **7** and **12** provided precursor **13** in 63% yield. Finally, linker **1** was obtained by saponification of methyl ester **13**.

In the next step, solution-phase studies towards cleavage of linker **1** from a solid support were conducted. To this end, compound **14** was prepared and subjected to different conditions for hydrogenolysis (Scheme 3, Supporting Information File 1). Compound **14** was reduced by using palladium(II) acetate and ammonium formate. When the cleavage reaction was carried

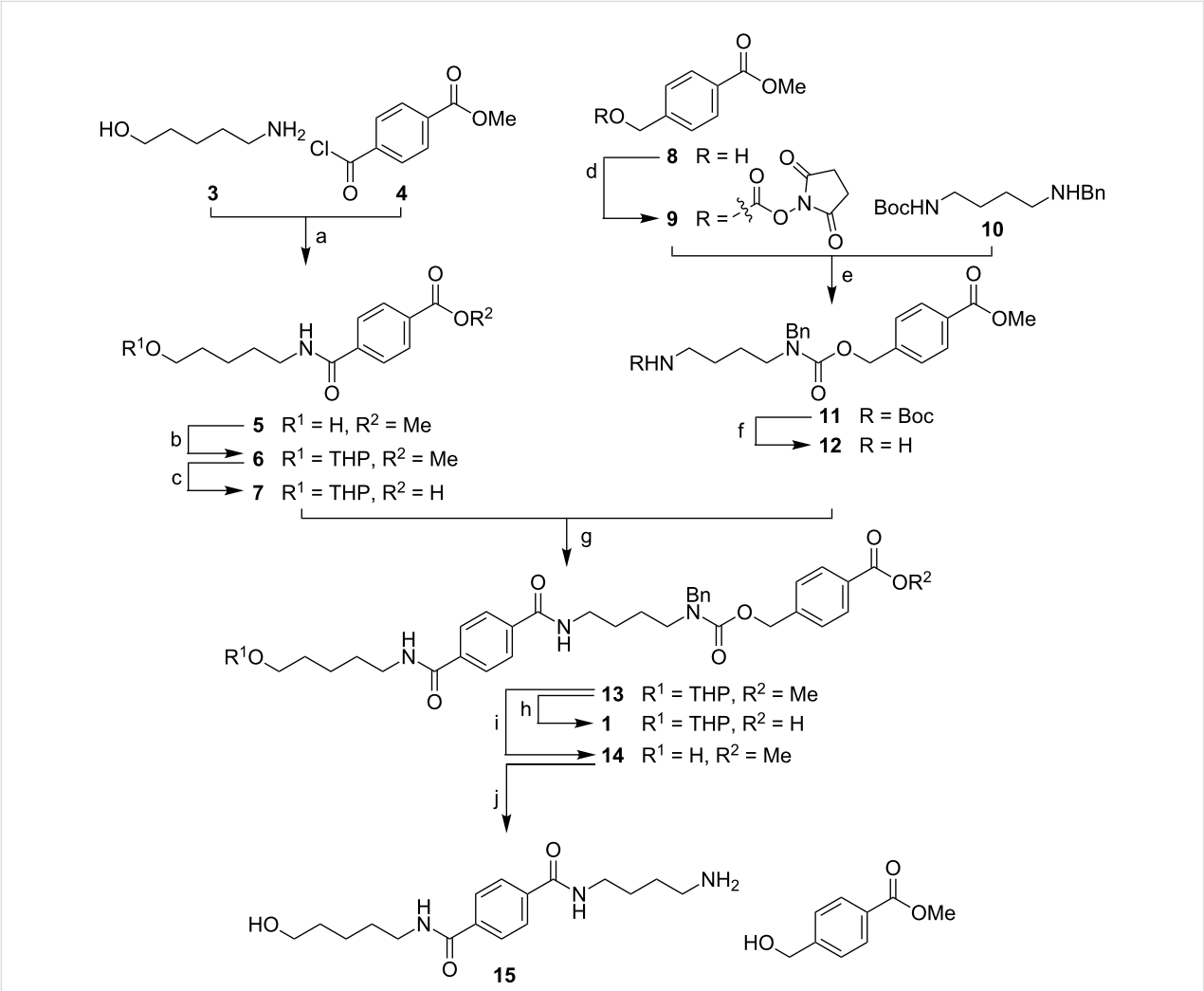

Scheme 3: Synthesis of linker **1**. Reactions and conditions: (a) NEt_3, DCM, rt, 84%; (b) DHP, pyridinium *p*-toluenesulfonate, DCM, rt, quant.; (c) 2 M aq NaOH, THF, rt, 91%; (d) DSC, NEt_3, CH_3CN, 0 °C to rt; (e) NEt_3, DCM, rt, 80% over 2 steps; (f) TFA, DCM, rt, 99%; (g) NHS, DCC, DMAP, CH_3CN, DCM, rt, 63%; (h) 2 M aq NaOH, THF, 55 °C, 92%; (i) *p*-TsOH·H_2O, MeOH, DCM, rt, 94%; (j) $Pd(OAc)_2$, $HCOONH_4$, MeOH, H_2O, 90%.

out in a mixture of methanol/ethyl acetate (3:2), *N*-methylation and *N*-formylation were observed (Supporting Information File 1). Considering prior evidence that methanol can generate formaldehyde in the presence of Pd(0) by an oxidative addition mechanism [43,44] and the observation that apolar solvents cause *N*-formylation during the hydrogenolysis reactions [45], our experimental results could be explained. To avoid any such side reactions, the hydrogenolytic cleavage was performed in MeOH and water resulting in pure **15** in 90% yield. Encouraged by the good cleavage result of model compound **14**, different solid supports were functionalized with linker **1** (Scheme 4). Coupling to both chloro-functionalized Merrifield resin **16** and Jandajel **17** was achieved by a tetrabutylammonium iodide (TBAI) mediated substitution in the presence of Cs_2CO_3. Capping of unreacted chlorides by cesium acetate and subsequent acidic hydrolysis of the THP protecting group led to ester-bound linkers **23** and **24**. Fluorenylmethoxycarbonyl (Fmoc) protection and deprotection of the hydroxy group of an aliquot enabled the determination of the loading by measurement of the UV absorption of the corresponding dibenzofulvene released upon Fmoc deprotection (Table 1, Supporting Information File 1, [46]).

Attachment of linker **1** to the amino-functionalized resins Tentagel (**18**), Hypogel200 (**19**), Hypogel400 (**20**), NovaPEG (**21**) and Synbeads (**22**) was achieved by dehydrative coupling in the presence of diisopropylcarbodiimide (DIC) and hydroxybenzotriazole (HOBt; Scheme 4). To avoid neutralization of the activator during glycosylation reactions, unreacted amino groups were capped by acetylation. Resin loadings with the

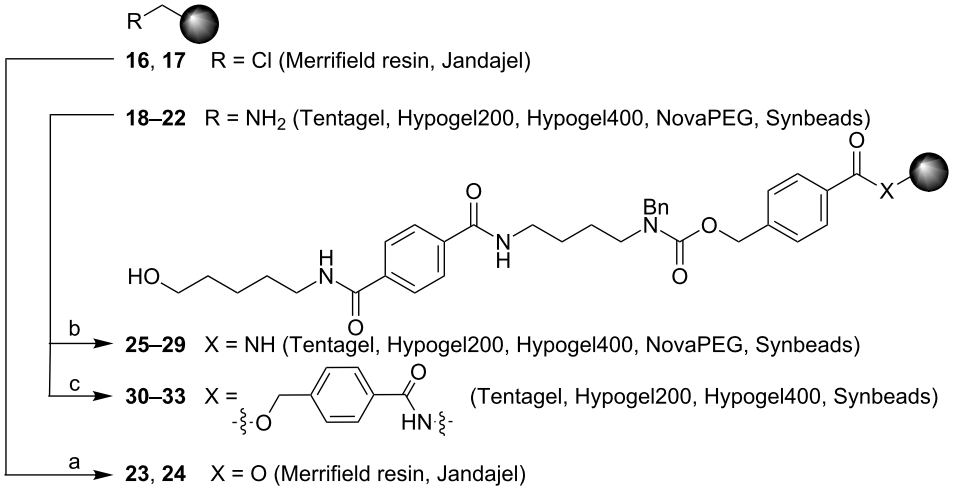

Scheme 4: Coupling of linker **1** to different resins. Reactions and conditions: (a) 1. **1** and **16** or **17**, Cs_2CO_3, DMF, TBAI, 60 °C; 2. CsOAc, TBAI, DMF, 60 °C; 3. *p*-TsOH·H_2O, MeOH, DCM, rt; (b) 1. **1** and **18**, **19**, **20**, **21** or **22**, HOBt, DIC, DMF, rt; 2. Ac_2O, pyridine, DCM, rt; 3. *p*-TsOH·H_2O, MeOH, DCM, rt; (c) 1. **2** and **18**, **19**, **20** or **22**, pyridine, DCM, rt; 2. Ac_2O, pyridine, DCM, rt; 3. **1**, Cs_2CO_3, DMF, TBAI, 60 °C; 4. CsOAc, TBAI, DMF, 60 °C; 5. *p*-TsOH·H_2O, MeOH, DCM, rt.

Table 1: Functionalization of different resins with linker **1** and loading determination.

	chloro-functionalized PS resins		amino-functionalized water-compatible resins				
	Merrifield **16**	Jandajel **17**	Tentagel **18**	Hypogel200 **19**	Hypogel400 **20**	NovaPEG **21**	Synbeads **22**
initial loading [mmol/g]	0.74	1.00	0.30	0.92	0.71	0.66	0.70
	23	**24**	**25**	**26**	**27**	**28**	**29**
linker loading [mmol/g]	0.14	0.61	0.22	0.44	0.40	0.29	0.25
coupling efficiency	19%	61%	73%	48%	56%	44%	36%
			30	**31**	**32**		**33**
linker loading via insert [mmol/g]	–	–	0.13	0.23	0.21	–	0.05
coupling efficiency	–	–	43%	25%	30%	–	7%

amide-bound linkers **25**–**29** were determined by using variants including the ester insert for rapid cleavage (Table 1).

Glycosylation with monosaccharide building blocks **34** or **35** was performed by using an automated oligosaccharide synthesizer (Scheme 5, Supporting Information File 1). This synthesizer is an improved version of a recently disclosed synthesizer prototype [20] whereby a separate unit to accommodate aqueous chemistry was added. To avoid cross contamination of the anhydrous solutions that are used for glycosylation reactions, all aqueous solutions are completely separated from the organic units by an additional syringe pump. Building blocks **34** and **35** can be used for the synthesis of heparin, a major subclass of GAGs. The synthesis of heparin necessitates aqueous solutions to perform Staudinger reductions in the placement of amino groups as well as for ester saponification used to remove temporary protective groups prior to sulfation. A range of different glycosylation conditions were explored, whereby the couplings were performed either twice by using five equivalents of the building block each time or were carried out three times by using three equivalents of the building block each time. Glycosyl trichloroacetimidate **34** was activated by catalytic amounts of trimethylsilyl trifluoromethanesulfonate (TMSOTf) at −15 °C in dichloromethane or toluene. Thioglycoside **35** was activated with *N*-iodosuccinimide (NIS) and triflic acid (TfOH) in dichloromethane and dioxane. In order to establish optimal reaction conditions, temperatures ranging from −40 °C to 25 °C were screened and the reaction time was varied between 15 and 45 minutes.

After completion of the glycosylations, the products were cleaved from the resin by hydrogenolysis before the crude products were analyzed by LC–MS. In order to obtain high cleavage efficiencies and to ensure that all permanent protecting groups are removed during the cleavage process, an excess of Pd catalyst was used. Unfortunately, an efficient cleavage of the products from Merrifield resin was impossible since PS resins fail to swell in water. When dioxane was used to swell the PS resin, some partially deprotected compounds were detected. Other polar solvents that suppress the described side reactions and swell PS solid supports may have to be further investigated. Additionally, the suspension can be filtered and the solution can be resubmitted for a second hydrogenolysis reaction to remove the remaining protecting groups.

On the other hand, when resins that are compatible with aqueous reaction conditions, such as Tentagel, were employed, glycosylation reactions proved to be ineffective and resulted in nonglycosylated linker **36** as the major product (Figure 2, A). A possible explanation for the low conversion to **37** is the long PEG chains contained in the resin structure that can either trap water to hydrolyze the monosaccharide building blocks or may complex the acidic activators due to the presence of many Lewis basic sites on PEG chains [47].

Since the hydrogenolytic linker cleavage did not work equally well for all types of solid support, this cleavage method was ill suited for the comparison of glycosylation efficiencies on different types of resin. Therefore, Zemplén conditions were

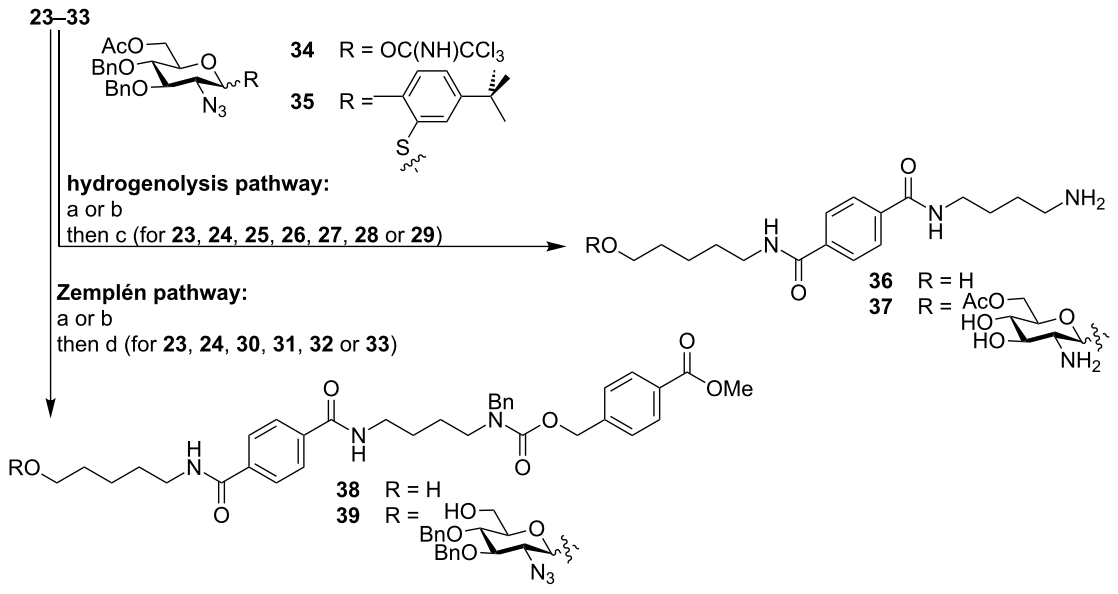

Scheme 5: Model glycosylation by using an automated oligosaccharide synthesizer. Reactions and conditions: (a) **34**, TMSOTf, DCM, −15 °C (30 min); (b) **35**, NIS, TfOH, DCM, dioxane, different temperatures and reaction times; (c) $Pd(OAc)_2$, $HCOONH_4$, H_2O; (d) NaOMe, MeOH, DCM, rt.

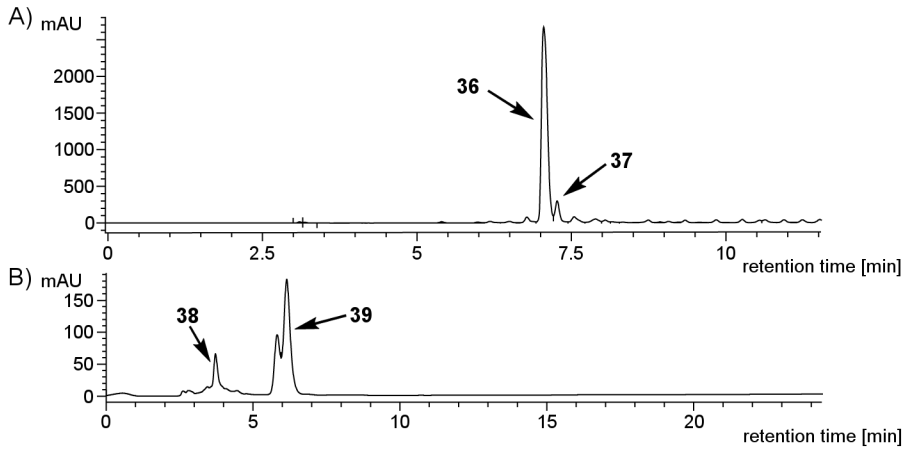

Figure 2: Representative HPLC chromatograms of glycosylation experiments on PS-based and water-compatible resins. (A) Tentagel (Nucleosil C4, 5% → 95% in 20 min, eluents: H_2O and MeCN, detection at 254 nm). (B) Merrifield resin (Nucleosil C4, 50% → 80% in 30 min, eluents: H_2O and MeCN, detection at 254 nm; the double peak for **39** is caused by an anomeric mixture).

employed as an alternative cleavage method. Sodium methoxide-mediated cleavage of the ester bond between linker **1** and the solid support in the case of polystyrene resins, as well as the ester bond between linker **1** and insert **2** in the case of all water-compatible resins, reliably afforded the crude products of the automated syntheses for analysis. For automated solid-phase syntheses on Merrifield resin, LC–MS analysis of the crude products indicated good glycosylation efficiencies. Only small quantities of nonglycosylated linker **38** were detected when compared to the desired product **39** (Figure 2B). It is well known that glycosylations on PS resins can be optimized to achieve full conversion [7,20-22]. However, due to the problems encountered regarding the hydrogenolytic linker cleavage on Merrifield resin, a further optimization of this system was not pursued.

To enable rapid LC–MS analysis and to exclude solubility issues caused by aqueous conditions during hydrogenolysis, the amino-functionalized resins **18**–**22** were equipped with an additional Zemplén cleavage site. To this end, insert **2** was coupled to these resins by amide-bond formation (Scheme 4, Supporting Information File 1). In the next step, the alkyl chlorides were displaced by the cesium carboxylate of **1**. Resin loadings were determined by Fmoc quantification (Table 1). Glycosylations on functionalized solid supports **30**–**33** were performed on the automated oligosaccharide synthesizer, and subsequent linker cleavage with sodium methoxide afforded the crude products, which were analyzed by LC–MS. These analyses clearly showed lower glycosylation efficiencies for all water-compatible resins when compared to PS resins **23** and **24**. To prevent the basic residues on the water-compatible resins from interfering with the acidic activators used during the glycosylations, solid supports **25**–**33** were washed before glycosylations with the acidic solutions. By using such prewashes, the ratio between the desired product **39** and the unglycosylated linker **38** improved, but complete conversions in glycosylations that are possible by using PS resins could not be achieved with water-compatible solid supports (data not shown).

To investigate the orthogonality of the linker for the introduction of naturally occurring modifications in oligosaccharides, the azide protecting group of the glucosamine was reduced under Staudinger conditions (Scheme 6, Supporting Information File 1). Therefore, imidate **34** was glycosylated to function-

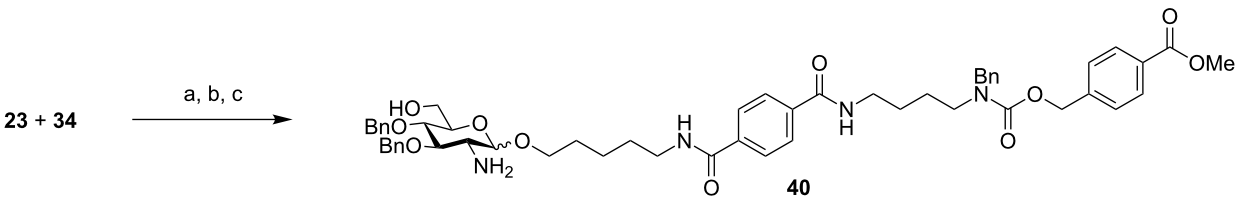

Scheme 6: Glycosylation of **34** to linker **23** and subsequent Staudinger reduction of the azide. Reactions and conditions: (a) TMSOTf, DCM, −15 °C, 30 min; (b) PMe_3, NEt_3, H_2O, THF, 25 °C, 30 min; (c) NaOMe, MeOH, DCM, rt.

alized resin **23**. In the next step the azide was reduced by using PMe_3 under basic and aqueous conditions. The use of THF swelled the PS resin, granting access to the reactive sites on the solid support. The azide reduction can be used as a key step to facilitate *N*-sulfation, which is necessary in the synthesis of heparin [48], or for the introduction of prevalent *N*-acetates.

In summary, we demonstrate that PS-based resins perform best in the automated solid-phase oligosaccharide synthesis. A linker that can be cleaved by hydrogenolysis and incorporates a chromophore to facilitate LC–MS analysis and purification was developed and served as example for glycosylation studies involving different solid supports. Cleavage of this linker is more efficient in aqueous media and necessitates the use of PEG-containing resins for the best results.

Supporting Information

Supporting Information File 1

Experimental details, characterization data and spectra.
[http://www.beilstein-journals.org/bjoc/content/supplementary/1860-5397-9-13-S1.pdf]

Acknowledgements

The Max-Planck Society and the European Research Council (ERC Advanced Grant AUTOHEPARIN to PHS) are also gratefully acknowledged for very generous support. We thank Ms. O. Calin for critically editing the manuscript.

References

1. Merrifield, R. B. *J. Am. Chem. Soc.* **1963,** *85,* 2149. doi:10.1021/ja00897a025
2. Dörwald, F. Z. *Organic Synthesis on Solid Phase: Supports, Linkers, Reaction;* Wiley VCH: Weinheim, Germany, 2002.
3. Letsinger, R. L.; Mahadevan, V. *J. Am. Chem. Soc.* **1966,** *88,* 5319. doi:10.1021/ja00974a053
4. Frechet, J. M.; Schuerch, C. *J. Am. Chem. Soc.* **1971,** *93,* 492. doi:10.1021/ja00731a031
5. Merrifield, R. B.; Stewart, J. M. *Nature* **1965,** *207,* 522. doi:10.1038/207522a0
6. Caruthers, M. H. *Science* **1985,** *230,* 281. doi:10.1126/science.3863253
7. Plante, O. J.; Palmacci, E. R.; Seeberger, P. H. *Science* **2001,** *291,* 1523. doi:10.1126/science.1057324
8. Varki, A.; Cummings, R.; Esko, J.; Freeze, H.; Hart, G.; Marth, J., Eds. *Essentials of glycobiology,* 2nd ed.; Cold Spring Harbor Laboratory Press: Cold Spring Harbor, New York, 2009.
9. Mootoo, D. R.; Konradsson, P.; Udodong, U.; Fraser-Reid, B. *J. Am. Chem. Soc.* **1988,** *110,* 5583. doi:10.1021/ja00224a060
10. Kanie, O.; Ito, Y.; Otawa, T. *J. Am. Chem. Soc.* **1994,** *116,* 12073. doi:10.1021/ja00105a066
11. Crich, D.; Sun, S. *J. Am. Chem. Soc.* **1998,** *120,* 435. doi:10.1021/ja9734814
12. Zhang, Z.; Ollmann, I. R.; Ye, X.-S.; Wischnat, R.; Baasov, T.; Wong, C.-H. *J. Am. Chem. Soc.* **1999,** *121,* 734. doi:10.1021/ja982232s
13. Tanaka, H.; Adachi, M.; Tsukamoto, H.; Ikeda, T.; Yamada, H.; Takahashi, T. *Org. Lett.* **2002,** *4,* 4213. doi:10.1021/ol020150+
14. Ko, K.-S.; Jaipuri, F. A.; Pohl, N. L. *J. Am. Chem. Soc.* **2005,** *127,* 13162. doi:10.1021/ja054811k
15. Wang, Y.; Ye, X.-S.; Zhang, L.-H. *Org. Biomol. Chem.* **2007,** *5,* 2189. doi:10.1039/b704586g
16. Geiger, J.; Reddy, B. G.; Winterfeld, G. A.; Weber, R.; Przybylski, M.; Schmidt, R. R. *J. Org. Chem.* **2007,** *72,* 4367. doi:10.1021/jo061670b
17. Eller, S.; Schuberth, R.; Gundel, G.; Seifert, J.; Unverzagt, C. *Angew. Chem., Int. Ed.* **2007,** *46,* 4173. doi:10.1002/anie.200604788
18. Wang, P.; Zhu, J.; Yuan, Y.; Danishefsky, S. J. *J. Am. Chem. Soc.* **2009,** *131,* 16669. doi:10.1021/ja907136d
19. Cai, H.; Huang, Z.-H.; Shi, L.; Zou, P.; Zhao, Y.-F.; Kunz, H.; Li, Y.-M. *Eur. J. Org. Chem.* **2011,** 3685. doi:10.1002/ejoc.201100304
20. Kröck, L.; Esposito, D.; Castagner, B.; Wang, C.-C.; Bindschädler, P.; Seeberger, P. H. *Chem. Sci.* **2012,** *3,* 1617. doi:10.1039/c2sc00940d
21. Walvoort, M. T. C.; van den Elst, H.; Plante, O. J.; Kröck, L.; Seeberger, P. H.; Overkleeft, H. S.; van der Marel, G. A.; Codée, J. D. C. *Angew. Chem., Int. Ed.* **2012,** *51,* 4393. doi:10.1002/anie.201108744
22. Walvoort, M. T. C.; Volbeda, A. G.; Reintjens, N. R. M.; van den Elst, H.; Plante, O. J.; Overkleeft, H. S.; van der Marel, G. A.; Codée, J. D. C. *Org. Lett.* **2012,** *14,* 3776. doi:10.1021/ol301666n
23. Yin, J.; Eller, S.; Collot, M.; Seeberger, P. H. *Beilstein J. Org. Chem.* **2012,** *8,* 2067–2071. doi:10.3762/bjoc.8.232
24. Guillier, F.; Orain, D.; Bradley, M. *Chem. Rev.* **2000,** *100,* 2091. doi:10.1021/cr980040+
25. Yin, J.; Eller, S.; Collot, M.; Seeberger, P. H. *Beilstein J. Org. Chem.* **2012,** *8,* 2067. doi:10.3762/bjoc.8.232
26. Seeberger, P. H., Ed. *Solid Support Oligosaccharide Synthesis and Combinatorial Carbohydrate Libraries;* John Wiley & Sons, Inc.: New York, 2001. doi:10.1002/0471220442
27. Gerritz, S. W. *Curr. Opin. Chem. Biol.* **2001,** *5,* 264. doi:10.1016/S1367-5931(00)00201-5
28. Basso, A.; Braiuca, P.; Ebert, C.; Gardossi, L.; Linda, P. *J. Chem. Technol. Biotechnol.* **2006,** *81,* 1626. doi:10.1002/jctb.1593
29. Toy, P. H.; Janda, K. D. *Tetrahedron Lett.* **1999,** *40,* 6329. doi:10.1016/S0040-4039(99)01251-4
30. Toy, P. H.; Reger, T. S.; Garibay, P.; Garno, J. C.; Malikayil, J. A.; Liu, G.-y.; Janda, K. D. *J. Comb. Chem.* **2001,** *3,* 117. doi:10.1021/cc000083f
31. Kates, S. A.; McGuinness, B. F.; Blackburn, C.; Griffin, G. W.; Solé, N. A.; Barany, G.; Albericio, F. *Biopolymers* **1998,** *47,* 365. doi:10.1002/(SICI)1097-0282(1998)47:5<365::AID-BIP4>3.0.CO;2-8
32. Auzanneau, F.-I.; Meldal, M.; Bock, K. *J. Pept. Sci.* **1995,** *1,* 31. doi:10.1002/psc.310010106
33. Meldal, M.; Auzanneau, F.-I.; Hindsgaul, O.; Palcic, M. M. *J. Chem. Soc., Chem. Commun.* **1994,** 1849. doi:10.1039/C39940001849
34. Rademann, J.; Grøtli, M.; Meldal, M.; Bock, K. *J. Am. Chem. Soc.* **1999,** *121,* 5459. doi:10.1021/ja984355i
35. García-Martín, F.; Quintanar-Audelo, M.; García-Ramos, Y.; Cruz, L. J.; Gravel, C.; Furic, R.; Côté, S.; Tulla-Puche, J.; Albericio, F. *J. Comb. Chem.* **2006,** *8,* 213. doi:10.1021/cc0600019
36. Basso, A.; Braiuca, P.; De Martin, L.; Ebert, C.; Gardossi, L.; Linda, P.; Verdelli, S.; Tam, A. *Chem.–Eur. J.* **2004,** *10,* 1007. doi:10.1002/chem.200305243

37. Schlatter, J. M.; Mazur, R. H. *Tetrahedron Lett.* **1977,** *18,* 2851. doi:10.1016/S0040-4039(01)83091-4
38. Gowda, D. C.; Abiraj, K. *Lett. Pept. Sci.* **2002,** *9,* 153. doi:10.1007/BF02538377
39. Douglas, S. P.; Whitfield, D. M.; Krepinsky, J. J. *J. Am. Chem. Soc.* **1995,** *117,* 2116. doi:10.1021/ja00112a035
40. Manabe, S.; Ito, Y.; Ogawa, T. *Synlett* **1998,** 628. doi:10.1055/s-1998-1750
41. Muller, D.; Zeltser, I.; Bitan, G.; Gilon, C. *J. Org. Chem.* **1997,** *62,* 411. doi:10.1021/jo961580e
42. Tzouros, M.; Bigler, L.; Bienz, S.; Hesse, M.; Inada, A.; Murata, H.; Inatomi, Y.; Nakanishi, T.; Darnaedi, D. *Helv. Chim. Acta* **2004,** *87,* 1411. doi:10.1002/hlca.200490129
43. Bailey, P. D.; Beard, M. A.; Dang, H. P. T.; Phillips, T. R.; Price, R. A.; Whittaker, J. H. *Tetrahedron Lett.* **2008,** *49,* 2150. doi:10.1016/j.tetlet.2008.01.104
44. Fu, X.; Cook, J. M. *J. Org. Chem.* **1993,** *58,* 661. doi:10.1021/jo00055a019
45. Reddy, P. G.; Baskaran, S. *Tetrahedron Lett.* **2002,** *43,* 1919. doi:10.1016/S0040-4039(02)00143-0
46. Gude, M.; Ryf, J.; White, P. D. *Lett. Pept. Sci.* **2002,** *9,* 203. doi:10.1007/BF02538384
47. Delgado, M.; Janda, K. D. *Curr. Org. Chem.* **2002,** *6,* 1031. doi:10.2174/1385272023373671
48. Noti, C.; de Paz, J. L.; Polito, L.; Seeberger, P. H. *Chem.–Eur. J.* **2006,** *12,* 8664. doi:10.1002/chem.200601103

License and Terms

Beilstein Journal of Organic Chemistry

De novo synthesis of D- and L-fucosamine containing disaccharides

Daniele Leonori[1,§] and Peter H. Seeberger[*1,2]

Full Research Paper

Open Access

Address:
[1]Department of Biomolecular Systems, Max Planck Institute of Colloids and Interfaces, Am Mühlenberg 1, 14476 Potsdam, Germany and [2]Institute for Chemistry and Biochemistry, Freie Universität Berlin, Arnimallee 22, 14195 Berlin, Germany

Email:
Peter H. Seeberger[*] - peter.seeberger@mpikg.mpg.de

* Corresponding author
§ Current Address: School of Chemistry, University of Bristol, Cantock's Close, Bristol, BS8 1TS, UK

Keywords:
de novo synthesis; fucosamine; glycan; *pseudomonas aeruginosa*; vaccine

Beilstein J. Org. Chem. **2013,** *9,* 332–341.
doi:10.3762/bjoc.9.38

Received: 14 October 2012
Accepted: 16 January 2013
Published: 14 February 2013

This article is part of the Thematic Series "Synthesis in the glycosciences II".

Guest Editor: T. K. Lindhorst

Abstract

The availability of rare monosaccharides that cannot be isolated from natural sources is currently limiting the access to the synthesis and the biological evaluation of complex bacterial cell-surface glycans. Here, we report the synthesis of D- and L-fucosamine building blocks by a *de novo* approach from L- and D-Garner aldehydes. These differentially protected monosaccharide building blocks were utilized to prepare disaccharides present on the surface of *Pseudomonas aeruginosa* bacteria.

Introduction

Protein functions are directly influenced by their glycosylation patterns [1,2]. Therefore, an understanding of protein glycosylation is of utmost importance in order to develop new therapeutics [3-6]. The ability of bacteria to colonize human hosts and cause diseases is directly influenced by their capacity to synthesize glycoproteins and express them on cell surfaces. This evidence makes it particularly relevant especially for the identification of novel antibacterial agents as well as vaccines [7-9]. Those bacterial glycans often contain unusual monosaccharides that are not present in the human body. An immune response against these cell-surface glycans is the basis for the development of new vaccine candidates against bacterial infections [10-13].

Our efforts were directed to the development of new vaccine candidates [14-16] to prevent bacterial infections, including glycans of the highly pathogenic bacteria *Pseudomonas aeruginosa*. *P. aeruginosa* is a nosocomial pathogen that is involved in ventilator-associated pneumonia and has become resistant to many antimicrobials. The somatic pili of *P. aeruginosa* are a

major virulence factor playing a pivotal role in the adherence and invasiveness of the bacterium. In 2001, the *P. aeruginosa* pilin *O*-linked glycans were found to be linear trisaccharides that are covalently attached to serine (Figure 1). The *O*-glycans contain a D-fucosamine residue at the protein-binding site. This unusual monosaccharide is not present in eukaryotes, and therefore may be used to stimulate an antibacterial response in the host organism [17-23]. Access to differentially protected D- and L-fucosamine building blocks, which can be used in preparing the corresponding glycans, is instrumental for the evaluation of oligosaccharide-based vaccine candidates against this bacterium [24-28].

The synthesis of fucosamine building blocks has been reported in the literature, but it is highly affected by long synthetic sequences, extensive protecting group manipulations and expensive starting materials [29-33]. The *de novo* synthesis of rare sugars [34-43] provides an attractive alternative for rapid access to the required building blocks, but this approach has not been reported for D- or L-fucosamine [29-33,44-46].

Here, a full account of the *de novo* synthesis of differentially protected D- and L-fucosamine building blocks is described following a recent preliminary communication [47]. The building blocks prepared by *de novo* synthesis were used in the assembly of two disaccharides that are found on *P. aeruginosa*.

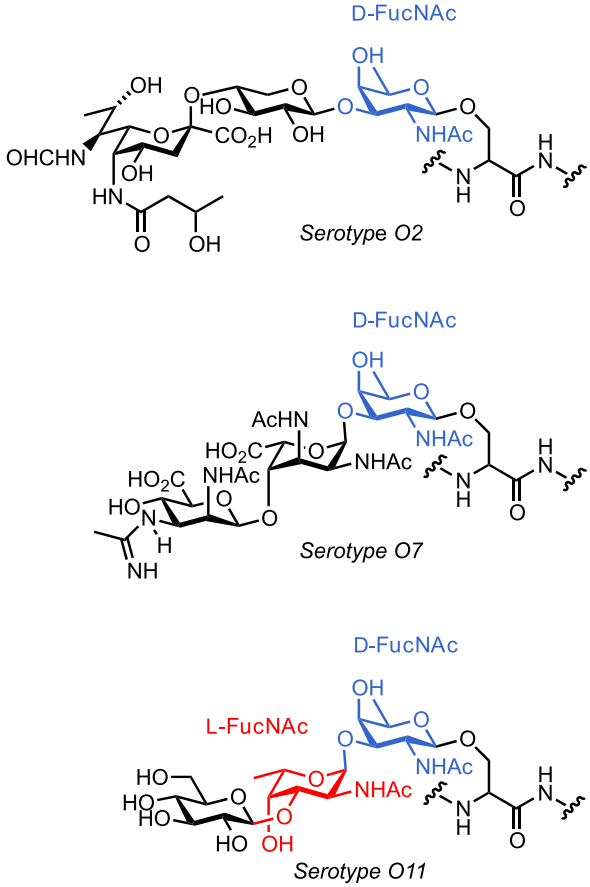

Figure 1: Structure of some *O*-linked glycans found on the cell surface of *P. aeruginosa*.

Results and Discussion

De novo synthesis of D- and L-fucosamine building blocks

Our retrosynthetic analysis of D-fucosamine envisioned the installation of the *syn*-1,2-diol unit by osmium-catalysed dihydroxylation of allylic ether **A**. It was anticipated that the conformation adopted by the molecule would allow for the formation of the required *anti* relationship between *C*3 and *C*4 hydroxy groups. **A** in turn would be accessed by the addition of a carbon nucleophile to L-Garner aldehyde L-**1** (Scheme 1) [48]. The fact that D- and L-Garner aldehydes are commercially available greatly facilitates the synthesis of both D- and L-fucosamine building blocks. The fucosamine residues are usually further elongated at the *C*3 position in *P. aeruginosa* requiring two orthogonal protecting groups (PGs) at *C*3 and *C*4

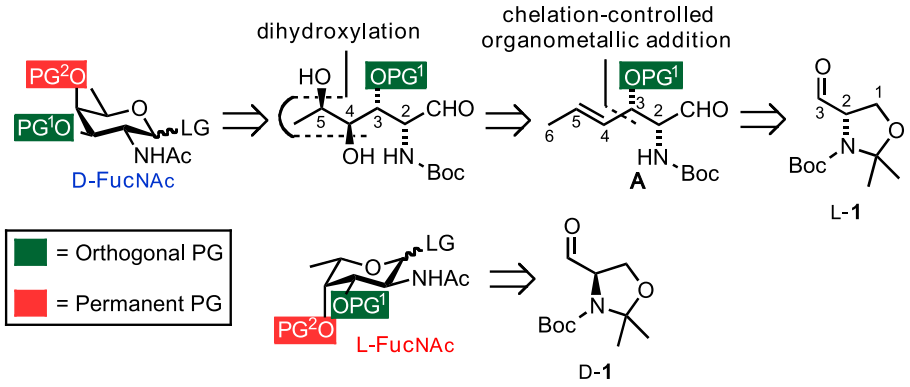

Scheme 1: Retrosynthetic analysis of D- and L-fucosamine building blocks.

of the building block in order to differentiate the two hydroxy groups at a later stage.

The three carbon *C*4–*C*6 fragment of D-fucosamine was introduced by chelation-controlled addition [49,50] of commercially available propynylmagnesium bromide to L-**1** (Scheme 2A) [51,52] The following *E*-selective alkyne reduction was accomplished by using diluted RedAl in Et_2O [53]. This reaction proved to be highly dependent on the quality of the aluminium reagent obtained from commercial sources. Inspired by the work from the Trost group [54,55], an alternative reduction protocol based on a Ru-catalyzed hydrosilylation–protodesilylation sequence was pursued (Scheme 2B). Thus, exposure of alkyne **2** to $Cp^*Ru(CH_3CN)_3PF_6$ catalyst in the presence of the appropriate trialkylsilane gave the desired silylated products **7a**–**c** (Table 1). The alkene geometry was confirmed as *Z* by nuclear Overauser effect (nOe). Treatment of **7a**–**c** with TBAF and CuI delivered **3** in high yields. Generally, $BnMe_2SiH$ has been found to be optimal for these transformations [54,55]. In our hands however, the best results were achieved using the cheaper Et_3SiH (Table 1). With a gram amount of **3** in hand, the *C*3 hydroxy group was protected and the acetonide removed by treatment with *p*-TSA. Oxidation of primary aminoalcohols **5a**–**b** with the Dess–Martin reagent [56] yielded the desired aldehydes **6a**–**b**, in five steps from commercially available starting materials. The two different *O*-protecting groups, namely naphthyl ether (Nap) [57-59] and benzoate ester (Bz), were introduced to gain access to two sets of electronically different and orthogonally protected derivatives (Scheme 2A).

Table 1: Hydrosilylation yields.

entry		R	yield (%)
1	**7a**:	Et_3	81
2	**7b**:	Et_2Me	71
3	**7c**:	Me_2Bn	traces

Dihydroxylation of aldehyde **6a** under standard Upjohn conditions gave, after peracetylation with Ac_2O, D-fucosamine building block D-**8a** in 81% yield and 5:1 dr (*anti*/*syn*, diastereomers separable by column chromatography) (Scheme 3) [60-62]. The formation of the desired *C*3–*C*4–*C*5 *syn*,*syn* cyclic product was confirmed based on observation of a $^3J_{H3-H4}$ coupling of 3.5 Hz. When the same sequence of dihydroxylation–peracetylation was performed on Bz-substituted aldehyde **6b**, compound D-**8b** was formed in 71% as a single diastereomer (Scheme 3). This product was crystallized from *n*-hexane/EtOAc solvent mixture, and the stereochemical assignment was confirmed by X-ray analysis (data shown in Supporting Information File 1).

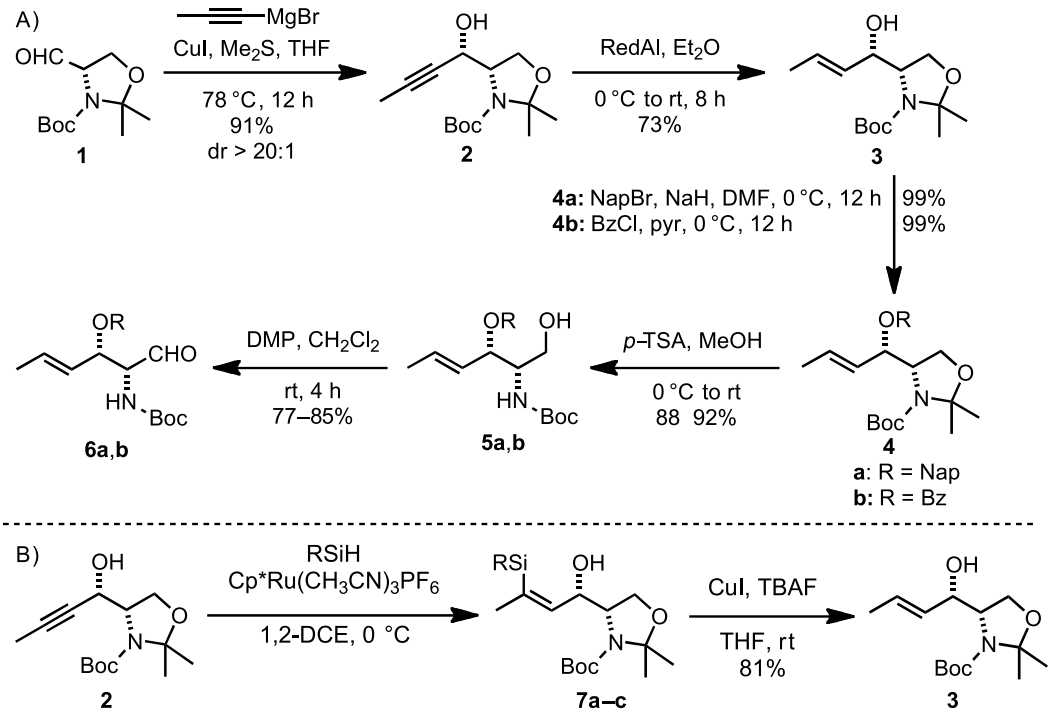

Scheme 2: (A) Synthesis of aldehydes **6a** and **6b**. (B) Alkyne reduction by hydrosilylation–protodesilylation sequence (see Table 1).

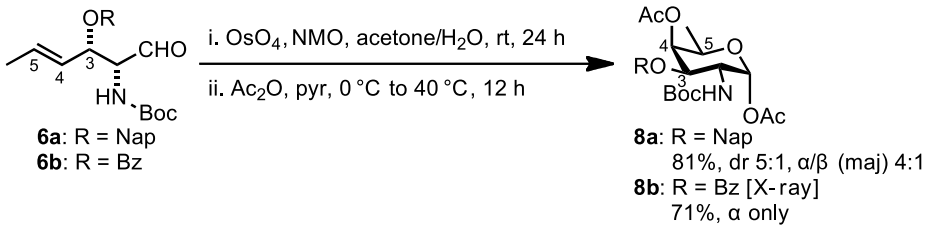

Scheme 3: Synthesis of D-fucosamine building blocks **8a** and **8b**.

During the optimization of the synthetic sequence we explored potentially more economic oxidation protocols to convert the primary alcohol **5a** to the D-fucosamine building block. Since α-amino protected aldehydes easily undergo α-epimerization, oxidation had to proceed under mild conditions in order to avoid the formation of the undesired D-talosamine building block D-**9** (Scheme 4).

Several oxidation methods were tested (Table 2). All the reactions were performed sequentially without column-chromatographic purification of the aldehyde. Classic Swern oxidation [63] (Table 2, entry 2) gave a 2:1 mixture of *C*2 epimers demonstrating the acid lability of aldehyde **6a**. This ratio in favour of the desired product was improved to 8:1 by switching the base from Et_3N to iPr_2EtN as reported by Dondoni and co-workers (Table 2, entry 3) [64]. Parrikh–Doering oxidation [65] and TCCA–TEMPO mediated oxidation [66] (Table 2, entries 4 and 6, respectively) were not suitable as considerable amounts of D-talosamine building block were formed. DMP emerged as the reagent of choice for the oxidation of **5a**. Interestingly, the dihydroxylation of aldehyde *epi*-**6a** resulted in the formation of talosamine D-**9** as a single diastereomer while the dihydroxylation of **6a** gave D-**8a** in 5:1 dr (Scheme 3).

Carrying out the synthetic sequence optimized for the synthesis of D-**8a**, on D-Garner aldehyde (D-**1**, commercially available)

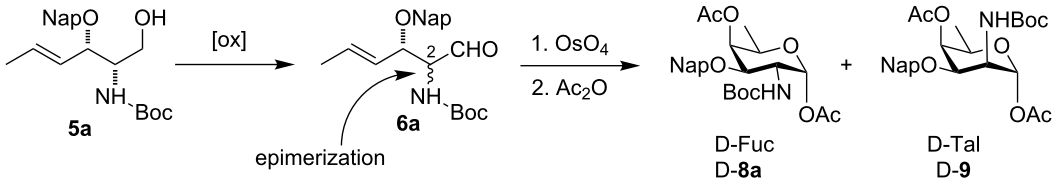

Scheme 4: Epimerization of aldehyde **6a**.

Table 2: Oxidation of **5a** to D-fucosamine D-**8a**.

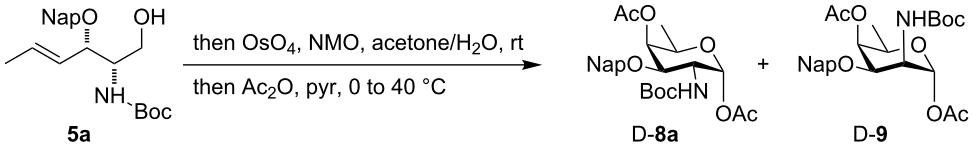

entry	reaction conditions	D-Fuc/D-Tal[a]
1[b]	DMP, CH_2Cl_2, rt then 1 M $Na_2S_2O_3$ in $NaHCO_3$, sat.	>20:1
2	DMSO, $(COCl)_2$, Et_3N, CH_2Cl_2, −78 °C	2:1
3	DMSO, $(COCl)_2$, iPr_2NEt, CH_2Cl_2, −78 °C	8:1
4	SO_3·pyr, DMSO, CH_2Cl_2, 0 °C	2:1
5	TCCA, TEMPO, CH_2Cl_2, 0 °C	3:1

[a]Determined by ^1H NMR analysis of the crude product after dihydroxylation and peracetylation. [b]Reaction run on 1 g scale.

gave alcohol *ent*-**5a** (four steps, two chromatographic purifications) that after the direct oxidation–dihydroxylation–peracetylation protocol yielded the desired L-fucosamine building block L-**8a** (Scheme 5).

Synthesis of fucosamine-containing disaccharides

To facilitate the use of the bacterial monosaccharides in the glycan microarray platform and their conjugation to carrier proteins, an appropriate linker was required at the anomeric position [67]. Placement of a *C*3 naphthyl ether anticipated the site for further glycosylation at this position, which typically serves as the connection to the next sugar. Therefore, building block **8a** is ideal in terms of orthogonality and chemical synthesis. Hence, we tested the ability of D-**8a** to undergo anomeric functionalization and to effect glycosylation at the *C*3 hydroxy group. Due to the presence of *N*-acetylated D- and L-fucosamine residues in *P. aeruginosa O*-linked glycans, the strategic *N*-protecting group was evaluated. Direct glycosylation by using the building block D-**8a** was not possible. Hence, a direct *N*-Boc deprotection/*N*-acetylation sequence afforded D-**10** in 84% yield (Scheme 6A). Direct glycosylation of D-**10** by using glycosylating agent **11** [67] and $BF_3{\cdot}Et_2O$ as the activating agent, yielded the linker-functionalized monosaccharide D-**12** as the β-anomer ($^3J_{H1-H2}$ = 8.3 Hz, Scheme 6A). At this point, the *C*3 naphthyl ether was cleaved under oxidative conditions and the corresponding alcohol was revealed by using a two-step deprotection protocol consisting of ester hydrolysis and hydrogenation. Monosaccharide D-**13** was obtained in 85% yield (the β-linkage further confirmed by $^1J_{C1-H1}$ 164.1 Hz, Scheme 6A). Direct glycosylation after DDQ-deprotection was possible and the use of differentially protected glucose building block **15** [68] yielded the desired β-disaccharide **16** in 61% yield over two steps (β anomer, $^3J_{H1-H2}$ of 7.8 Hz, Scheme 6A). Global deprotection employed saponification, and hydrogenation gave the fully deprotected D-fucosamine containing disaccharide **17** (Scheme 6A).

When the same synthetic sequence was performed on L-FucNAc building block L-**10** the fully deprotected monomer L-**13** and disaccharide **19** were obtained in similar yields and selectivities (Scheme 6B). Diagnostic $^1J_{C-H}$ analysis also corroborated the formation of the β-glycosydic linkages (Scheme 6B). Linker-terminated disaccharide **19** represents the terminal unit of the *P. aeruginosa* serotype *O*11 *O*-linked glycan (Figure 1).

Conclusion

The *de novo* synthesis of differentially protected D- and L-fucosamine building blocks from D- and L-Garner aldehyde is reported. Placement of a naphthyl ether protecting group at the *C*3 position allows for further elongation by glycosylation. The key oxidation step was optimized to minimize the formation of the unwanted D-talosamine building block D-**9**. The fucosamine building blocks prepared by *de novo* synthesis enabled the preparation of monosaccharides and disaccharides for attachment to microarray surfaces. The terminal disaccharide of *P. aeruginosa O*11 *O*-linked glycan has been prepared and will be the basis for biological studies involving this pathogen.

Experimental

General experimental details

All reagents were obtained from commercial suppliers and were used without further purification unless otherwise specified. All reactions were conducted under an Ar atmosphere by using standard Schlenk techniques. THF and Et_2O were distilled from purple Na/benzophenone diketyl; CH_2Cl_2, pyridine and $BF_3{\cdot}Et_2O$ were distilled from CaH_2. Deionized water was obtained from an in-house purification system. The compounds purified by flash chromatography were further concentrated by the removal of residual solvent under high vacuum (<0.2 mbar). ^{1}H NMR and ^{13}C NMR spectra were measured with a Varian 400-MR or Varian 600 spectrometer. The proton signal of residual, nondeuterated solvent (δ 7.26 ppm for $CHCl_3$ or δ 4.79 ppm for HDO) was used as an internal reference for ^{1}H spectra. For ^{13}C spectra, the chemical shifts are reported relative to the δ 77.36 ppm resonance of $CDCl_3$. Coupling constants (*J* values) are quoted to one decimal place with values in hertz (Hz) and were corrected. Infrared (IR) spectra were recorded as thin films on a Perkin Elmer Spectrum 100 FTIR spectrophotometer. Optical rotations (OR) were measured with a Schmidt & Haensch UniPol L 1000 spectrometer at a concentration (*c*) expressed in grams per hundred millilitres (g/100 mL). High-

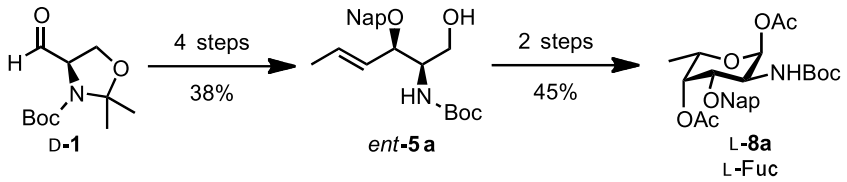

Scheme 5: Synthesis of L-fucosamine building block L-**8a** from D-Garner aldehyde.

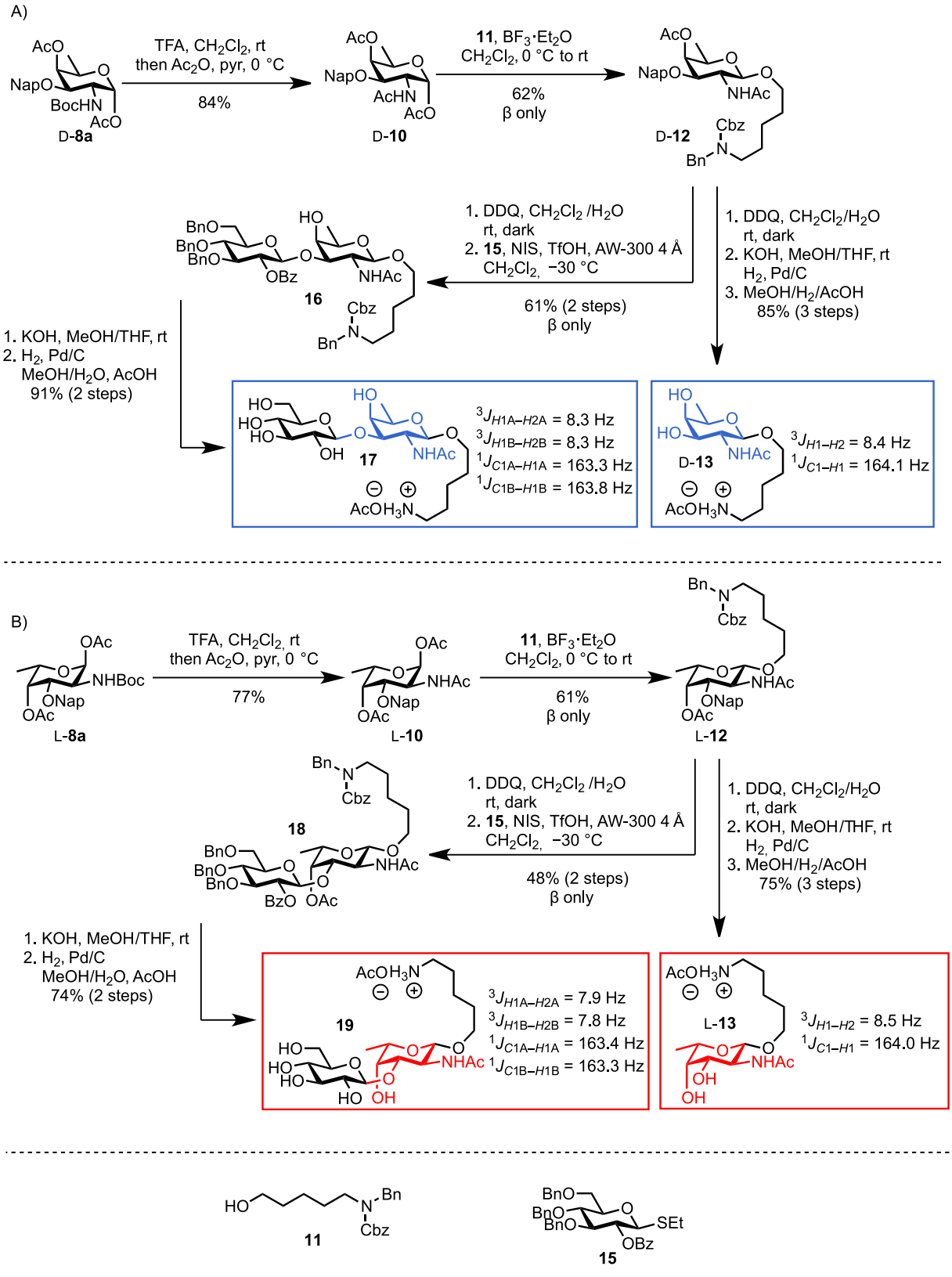

Scheme 6: Synthesis of D- and L-fucosamine-containing mono- and disaccharides carrying the pentanolamine linker.

resolution mass spectra (HRMS) were recorded with an Agilent 6210 ESI–TOF mass spectrometer at the Freie Universität Berlin, Mass Spectrometry Core Facility. Analytical thin-layer chromatography (TLC) was performed on Kieselgel 60 F_{254} glass plates precoated with a 0.25 mm thickness of silica gel. The TLC plates were visualized with UV light and by staining with Hanessian solution (ceric sulfate and ammonium molybdate in aqueous sulfuric acid) or potassium permanganate solution (potassium permanganate in basic aqueous solution). Column chromatography was performed by using Kieselgel 60 (230–400 mesh) silica gel with a typical 50–100:1 weight ratio of silica gel to crude product. For the preparation and characterization of compounds **2**–**10**, D-**12** and D-**16** see [14].

L-Fucosamine monosaccharide L-**12**

Under the same reaction conditions reported in [14], L-**10** (75 mg, 0.17 mmol, 1.0 equiv), **11** (86 mg, 0.26 mmol, 1.5 equiv) and $BF_3{\cdot}Et_2O$ (33 mL, 0.26 mmol, 1.5 equiv) gave L-**12** (74 mg, 61%) as an oil; $[\alpha]_D^{20}$ −63.2 (*c* 2.0, $CHCl_3$), other data as above.

D-Fucosamine monosaccharide D-**13**

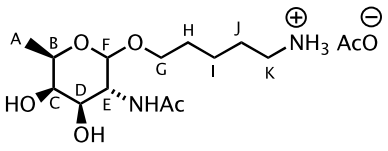

A solution of D-**12** (56 mg, 80.0 mmol, 1.0 equiv) in CH_2Cl_2 (0.9 mL) and H_2O (90 mL) was treated with DDQ (21 mg, 94.0 mmol, 1.2 equiv) and stirred in the dark at rt for 2 h. Saturated $NaHCO_3$ (2 mL) and CH_2Cl_2 (5 mL) were added and the layers were separated. The aqueous layer was extracted with CH_2Cl_2 (2 × 3 mL). The combined organic layers were dried ($MgSO_4$), filtered and concentrated. The crude was purified by filtration over a short plug of silica gel eluting with CH_2Cl_2/MeOH 9:1 (34 mg, 76%) and immediately used for the next step. The monodeprotected compound (18 mg, 32.0 mmol, 1.0 equiv) in MeOH (0.4 mL) and THF (0.4 mL) was treated with KOH (1.8 mg, 32.0 mmol, 1.0 equiv) and stirred at rt for 30 min. H_2O (2 mL) was added and the solvents were removed under vacuum. CH_2Cl_2 (5 mL) was added and the layers were separated. The aqueous layer was extracted with CH_2Cl_2 (2 × 5 mL). The combined organic layers were dried ($MgSO_4$), filtered and concentrated. The crude product was solubilised in MeOH/H_2O/AcOH (2.0:1.0:0.05 mL) and Pd/C (10 mg) was added. The heterogeneous mixture was stirred under an atmosphere of H_2 for 24 h. The mixture was filtered over celite to give D-**13** (8 mg, 85%) as an amorphous solid; $[\alpha]_D^{20}$ +112.9 (*c* 1.1, H_2O); ^{1}H NMR (400 MHz, D_2O) δ 4.38 (d, *J* = 8.4 Hz, 1H, CH^F), 3.83 (dt, *J* = 10.1, 6.3 Hz, 1H, CH^G), 3.79 (dd, *J* = 10.7, 8.4 Hz, 1H, CH^E), 3.75–3.69 (m, 2H, CH^C and NH), 3.68 (dd, *J* = 10.7, 3.4 Hz, 1H, CH^D), 3.66 (dt, *J* = 10.1, 6.3 Hz, 1H, CH^G), 3.41 (q, *J* = 6.4 Hz, 1H, CH^B), 2.95 (t, *J* = 7.6 Hz, 2H, CH_2^K), 1.99 (s, 3H, CH_3), 1.87 (AcOH), 1.71–1.62 (m, 2H, CH_2^J), 1.59–1.51 (m, 2H, CH_2^H), 1.39–1.29 (m, 2H, CH_2^I), 1.23 (d, *J* = 6.4 Hz, 3H, CH_3^A); ^{13}C NMR (100 MHz, D_2O) δ 101.4 (CH^F), 71.0 (CH^D), 70.4 (CH^C), 70.3 (CH^B), 69.8 (CH_2^G), 52.0 (CH^E), 39.2 (CH_2^K), 28.0 (CH_2^J), 26.3 (CH_2^H), 23.1 (CH_3), 22.1 (CH_3), 21.9 (CH_2^I), 15.3 (CH_3^A); LRMS–ESI (*m*/*z*): 291.2 [M + H^+]; HRMS–ESI (*m*/*z*): [M + H^+] calcd for $C_{13}H_{27}N_2O_5$, 291.1914; found, 291.1919.

L-Fucosamine monosaccharide L-**13**

Using the same reaction conditions reported for D-**13**, D-**12** (24 mg, 34.0 mmol, 1.0 equiv), DDQ (21 mg, 41.0 mmol, 1.2 equiv), KOH (1.8 mg, 34.0 mmol, 1.0 equiv) and Pd/C (10 mg), gave L-**13** (9 mg, 75%) as an amorphous solid; $[\alpha]_D^{20}$ −111.1 (*c* 1.0, H_2O), other data as above.

D-Fucosamine disaccharide **17**

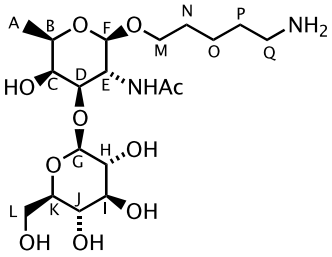

A solution of **16** (21 mg, 19.0 mmol, 1.0 equiv) in MeOH (0.4 mL) and THF (0.4 mL) was treated with KOH (1.0 mg, 19.0 mmol, 1.0 equiv) and stirred at rt for 30 min. H_2O (2 mL) was added and the solvents were removed under vacuum. CH_2Cl_2 (5 mL) was added and the layers were separated. The aqueous layer was extracted with CH_2Cl_2 (2 × 5 mL). The combined organic layers were dried ($MgSO_4$), filtered and concentrated. The crude product was solubilised in MeOH/H_2O/AcOH (2.0:1.0:0.05 mL) and Pd/C (20 mg) was added. The heterogeneous mixture was stirred under an atmosphere of H_2 for 24 h. The mixture was filtered over celite to give **17** (9 mg, 91%) as an amorphous solid; $[\alpha]_D^{20}$ +13.5 (*c* 0.9, H_2O); ^{1}H NMR (400 MHz, D_2O) δ 4.47 (d, *J* = 7.9 Hz, 1H, CH^G), 4.41 (d, *J* = 7.9 Hz, 1H, CH^F), 3.94 (d, *J* = 2.7 Hz, 1H, CH^C), 3.90 (dd, *J* = 10.3, 7.9 Hz, 1H, CH^E), 3.87–3.77 (m, 3H, CH^L & CH^M & CH^D), 3.70 (q, *J* = 6.5 Hz, 1H, CH^B), 3.68 (dd, *J* = 12.1, 3.4 Hz, 1H, CH^L), 3.54 (dt, *J* = 10.0, 6.2 Hz, 1H, CH^M), 3.44–3.32 (m, 3H, CH^I, CH^J and CH^K), 3.25 (t, *J* = 7.9 Hz, 1H, CH^H), 2.94 (t, *J* = 7.6 Hz, 2H, CH_2^Q), 1.97 (s, 3H, CH_3), 1.90 (s, 3H, AcOH), 1.68–1.59 (m, 2H, CH_2^P), 1.58–1.50 (m, 2H, CH_2^N), 1.41–1.32 (m, 2H, CH_2^O), 1.22 (d, *J* = 6.5 Hz, 3H, CH_3^A); ^{13}C NMR (100 MHz, D_2O) δ 104.2 (CH^G), 101.1

(CH^{F}), 80.2 (CH^{D}), 75.5 (CH), 75.4 (CH), 72.7 (CH^{H}), 70.4 (2 × CH$^{B\&C}$), 69.8 (CH$_2^{L}$), 69.2 (CH), 60.3 (CH$_2^{M}$), 50.8 (CH^{E}), 39.1 (CH$_2^{Q}$), 28.0 (CH$_2^{N}$), 26.2 (CH$_2^{P}$), 23.1 (CH$_3$), 22.1 (CH$_3$), 22.0 (CH$_2^{O}$), 15.3 (CH$_3^{A}$); LRMS–ESI (*m*/*z*): 453.2 [M + Na$^+$]; HRMS–ESI (*m*/*z*): [M + H$^+$] calcd for $C_{19}H_{37}N_2O_{10}$, 453.2443; found, 453.2468.

L-Fucosamine disaccharide **18**

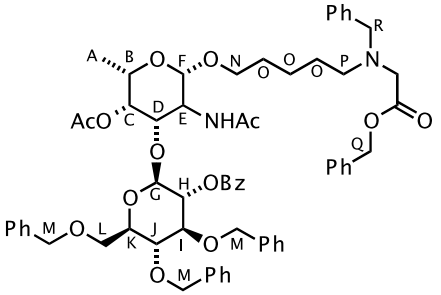

A solution of L-**12** (60 mg, 86 mmol, 1.0 equiv) in CH_2Cl_2 (1 mL) and H_2O (0.1 mL) was treated with DDQ (21 mg, 95 mmol, 1.2 equiv) and stirred in the dark at rt for 2 h. Saturated $NaHCO_3$ (2 mL) and CH_2Cl_2 (5 mL) were added and the layers were separated. The aqueous layer was extracted with CH_2Cl_2 (2 × 3 mL). The combined organic layers were dried ($MgSO_4$), filtered and concentrated. The crude was purified by filtration over a short plug of silica gel eluting with CH_2Cl_2/MeOH (9:1) and immediately used for the next step. An oven-dried flask was immediately charged with the product and **15** (77 mg, 0.12 mmol, 1.5 equiv) was added. The flask was left under high vacuum for 4 h. After refilling the flask with argon, freshly distilled CH_2Cl_2 (1.5 mL) was added, and the mixture was cooled to −30 °C. NIS (29 mg, 0.13 mmol, 1.5 equiv) and TfOH (4 mL, 43 mmol, 0.5 equiv) were added. The mixture was stirred at −30 °C for 4 h and then it was allowed to warm to rt overnight. Saturated Na_2SO_3 (3 mL) and CH_2Cl_2 (3 mL) were added and the layers were separated. The aqueous layer was extracted with CH_2Cl_2 (2 × 5 mL). The combined organic layers were dried ($MgSO_4$), filtered and evaporated. Purification by column chromatography on silica gel, eluting with *n*-hexane/EtOAc (6:4), gave **18** (45 mg, 48%) as an oil; R_f 0.22 [*n*-hexane/EtOAc (4:1)]; $[\alpha]_D^{20}$ −5.5 (*c* 0.3, $CHCl_3$); FTIR (film) ν_{max} (cm^{-1}): 3321, 2925, 2857, 1743, 1716, 1705, 1662, 1368, 1271, 1240, 1071; ^{1}H NMR (400 MHz, $CDCl_3$, rotamers) δ 8.04 (d, 2H, *J* = 7.3 Hz, 2 × CH), 7.57 (tt, *J* = 7.4, 1H, 1.2 CH), 7.44 (t, *J* = 7.7 Hz, 2H, 2 × CH), 7.35–7.22 (m, 17H, 17 × CH), 7.17–7.04 (m, 8H, 8 × CH), 5.88 (br d, *J* = 6.5 Hz, 0.5H, NH), 5.73 (br d, *J* = 6.0 Hz, 0.5H, NH), 5.21 (dd, *J* = 9.1, 8.0 Hz, 1H, CH^{H}), 5.17 (br s, 1H, CH^{Q}), 5.14 (br s, 1H, CH^{Q}), 5.13 (d, *J* = 3.5 Hz, 1H, CH^{C}), 5.07 (d, *J* = 8.0 Hz, 1H, CH^{F}), 4.79 (d, *J* = 10.8 Hz, 1H, CH^{M}), 4.70 (d, *J* = 11.0 Hz, 1H, CH^{M}), 4.65–4.53 (m, 6H, CH^{D} & CH^{G} & 4 × CH^{M}), 4.52–4.46 (m, 2H, CH$_2^{R}$), 3.86 (t, *J* = 9.3 Hz, 1H, CH^{I}), 3.82–3.74 (m, 4H, CH^{J}, CH$_2^{L}$, CH^{N}), 3.67 (q, *J* = 6.4 Hz, 1H, CH^{B}), 3.50 (br dt, *J* = 9.6, 2.3 Hz, 1H, CH^{K}), 3.44–3.40 (m, 1H, CH^{N}), 3.23–3.17 (m, 3H, CH^{E} and CH$_2^{P}$), 1.85 and 1.81 (s, 3H, CH$_3$), 1.53–1.50 (m, 3H, 3 × CH^{O}), 1.45 (s, 3H, CH$_3$), 1.29–1.21 (m, 3H, 3 × CH^{O}), 1.08 (d, *J* = 6.4 Hz, 3H, CH$_3^{A}$); ^{13}C NMR (100 MHz, $CDCl_3$, rotamers) δ 171.2 (C=O), 170.5 (C=O), 165.1 (C=O), 137.9 (2 × C), 137.7 (2 × C), 137.6 (C), 133.2 (2 × CH), 130.1 (2 × CH), 129.5 (C), 128.5 (2 × CH), 128.4 (4 × CH), 128.3 (4 × CH), 128.2 (4 × CH), 127.9 (2 × CH), 127.8 (4 × CH), 127.7 (CH), 127.6 (CH), 127.3 (CH), 127.2 (CH), 127.1 (CH), 99.6 (CH), 98.4 (CH), 82.9 (CH), 77.7 (CH), 75.2 (CH$_2$), 75.0 (CH$_2$), 74.7 (CH), 73.5 (CH), 73.4 (CH$_2$), 72.5 (CH), 69.7 and 69.5 (CH$_2$), 69.1 (CH), 68.9 (CH), 68.7 (CH$_2$), 67.1 (CH$_2$), 54.4 (CH), 50.4 and 50.1 (CH$_2$), 47.1 and 46.1 (CH$_2$), 29.7 and 29.1 (CH$_2$), 27.8 and 27.4 (CH$_2$), 23.5 (CH$_3$), 23.1 (CH$_2$), 19.9 (CH$_3$), 16.4 (CH$_3$); LRMS–ESI (*m*/*z*): 1115.4 [M + Na$^+$].

L-Fucosamine disaccharide **19**

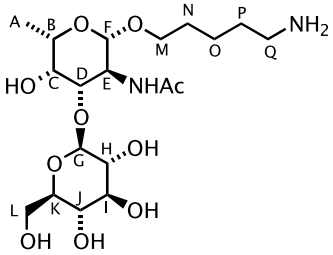

A solution of **18** (29 mg, 27.0 mmol, 1.0 equiv) in MeOH (0.6 mL) and THF (0.6 mL) was treated with KOH (0.8 mg, 13.5 mmol, 0.5 equiv) and stirred at rt for 30 min. H_2O (2 mL) was added and the solvents were removed under vacuum. CH_2Cl_2 (5 mL) was added and the layers were separated. The aqueous layer was extracted with CH_2Cl_2 (2 × 5 mL). The combined organic layers were dried ($MgSO_4$), filtered and concentrated. The crude product was solubilised in MeOH/H_2O/AcOH (3.0:1.5:0.06 mL) and Pd/C (30 mg) was added. The heterogeneous mixture was stirred under an atmosphere of H_2 for 24 h. The mixture was filtered over celite to give **19** (10 mg, 74%) as an amorphous solid; $[\alpha]_D^{20}$ +59.2 (*c* 0.9, H_2O); ^{1}H NMR (400 MHz, D_2O) δ 4.48 (d, *J* = 7.9 Hz, 1H, CH^{G}), 4.43 (d, *J* = 7.9 Hz, 1H, CH^{F}), 3.96–3.89 (m, 3H, CH^{C}, CH^{D} and CH^{L}), 3.88–3.80 (m, 2H, CH^{E} and CH^{M}), 3.72 (q, *J* = 6.5 Hz, 1H, CH^{B}), 3.67 (dd, *J* = 12.1, 6.5 Hz, 1H, CH^{L}), 3.56 (dt, *J* = 10.2, 6.2 Hz, 1H, CH^{M}), 3.45 (t, *J* = 9.5 Hz, 1H, CH^{I}), 3.42–3.46 (m, 1H, CH^{J}), 3.36–3.31 (m, 1H, CH^{K}), 3.27 (dd, *J* = 9.5, 7.9 Hz, 1H, CH^{H}), 2.95 (t, *J* = 7.6 Hz, 2H, CH$_2^{Q}$), 1.99 (s, 3H, CH$_3$), 1.97 (s, 3H, AcOH), 1.69–1.60 (m, 2H, CH$_2^{P}$), 1.59–1.50 (m, 2H, CH$_2^{N}$), 1.42–1.32 (m, 2H, CH$_2^{O}$), 1.26 (d, *J* = 6.5 Hz, 3H, CH$_3^{A}$); ^{13}C NMR (100 MHz, D_2O) δ 177.0 (C=O), 103.9 (CH^{F}), 102.7 (CH^{G}), 80.1 (CH^{D}), 79.5 (CH^{I}),

77.9 (CH^J), 75.3 (CH^B), 73.0 (CH^H), 72.4 (CH_2^L), 72.2 (CH^K), 70.4 (CH^C), 63.5 (CH_2^M), 52.8 (CH^E), 41.7 (CH_2^Q), 30.5 (CH_2^N), 28.8 (CH_2^P), 24.8 (CH_3), 24.5 (CH_2^O), 24.4 (CH_3), 17.8 (CH_3); LRMS–ESI (*m*/*z*): 453.2 [M + H^+]; HRMS–ESI (*m*/*z*): [M + H^+] calcd for $C_{19}H_{37}N_2O_{10}$, 453.244; found, 453.2468.

Supporting Information

Supporting Information File 1

^{1}H NMR, COSY, ^{13}C NMR and HSQC spectra and the crystallographic data file for D-**8b**.
[http://www.beilstein-journals.org/bjoc/content/supplementary/1860-5397-9-38-S1.pdf]

Acknowledgements

The authors gratefully thank the Max Planck Society for generous funding, Dr. A. Hagelbach (FU) and Dr. A. Barandov (MPI) for X-ray crystallographic analyses, and Dr. I. Vilotjevic for helpful comments during the preparation of the manuscript.

References

1. Mariño, K.; Bones, J.; Kattla, J. J.; Rudd, P. M. *Nat. Chem. Biol.* **2010,** *6,* 713. doi:10.1038/nchembio.437
2. Arnold, J. N.; Wormald, M. R.; Sim, R. B.; Rudd, P. M.; Dwek, R. A. *Annu. Rev. Immunol.* **2007,** *25,* 21. doi:10.1146/annurev.immunol.25.022106.141702
3. Dube, D. H.; Bertozzi, C. R. *Nat. Rev. Drug Discovery* **2005,** *4,* 477. doi:10.1038/nrd1751
4. Stallforth, P.; Lepenies, B.; Adibekian, A.; Seeberger, P. H. *J. Med. Chem.* **2009,** *52,* 5561. doi:10.1021/jm900819p
5. Dube, D. H.; Champasa, K.; Wang, B. *Chem. Commun.* **2011,** *47,* 87. doi:10.1039/c0cc01557a
6. Boltje, T. J.; Buskas, T.; Boons, G.-J. *Nat. Chem.* **2009,** *1,* 611. doi:10.1038/nchem.399
7. Bieber, D.; Ramer, S. W.; Wu, C.-Y.; Murray, W. J.; Tobe, T.; Fernandez, R.; Schoolnik, G. K. *Science* **1998,** *280,* 2114. doi:10.1126/science.280.5372.2114
8. Banerjee, A.; Wang, R.; Supernavage, S. L.; Ghosh, S. K.; Parker, J.; Ganesh, N. F.; Wang, P. G.; Gulati, S.; Rice, P. A. *J. Exp. Med.* **2002,** *196,* 147. doi:10.1084/jem.20012022
9. Power, P. M.; Ku, S. C.; Rutter, K.; Warren, M. J.; Limnios, E. A.; Tapsall, J. W.; Jennings, M. P. *Infect. Immun.* **2007,** *75,* 3202. doi:10.1128/IAI.01501-06
10. Takeuchi, K.; Taguchi, F.; Inagaki, Y.; Toyoda, K.; Shiraishi, T.; Ichinose, Y. *J. Bacteriol.* **2003,** *185,* 6658. doi:10.1128/JB.185.22.6658-6665.2003
11. Horzempa, J.; Carlson, P. E., Jr.; O'Dee, D. M.; Shanks, R. M. Q.; Nau, G. J. *BMC Microbiol.* **2008,** *8,* No. 172. doi:10.1186/1471-2180-8-172
12. van Sorge, N. M.; Bleumink, N. M. C.; van Vliet, S. J.; Saeland, E.; van der Pol, W.-L.; van Kooyk, Y.; van Putten, J. P. M. *Cell. Microbiol.* **2009,** *11,* 1768. doi:10.1111/j.1462-5822.2009.01370.x
13. Verma, A.; Arora, S. K.; Kuravi, S. K.; Ramphal, R. *Infect. Immun.* **2005,** *73,* 8237. doi:10.1128/IAI.73.12.8237-8246.2005
14. Yang, Y.; Martin, C. E.; Seeberger, P. H. *Chem. Sci.* **2012,** *3,* 896. doi:10.1039/c1sc00804h
15. Martin, C. E.; Weishaupt, M. W.; Seeberger, P. H. *Chem. Commun.* **2011,** *47,* 10260. doi:10.1039/c1cc13614c
16. Ohara, T.; Adibekian, A.; Esposito, D.; Stallforth, P.; Seeberger, P. H. *Chem. Commun.* **2010,** *46,* 4106. doi:10.1039/c000784f
17. Smedley, J. G., III; Jewell, E.; Roguskie, J.; Horzempa, J.; Syboldt, A.; Stolz, D. B.; Castric, P. *Infect. Immun.* **2005,** *73,* 7922. doi:10.1128/IAI.73.12.7922-7931.2005
18. Castric, P.; Cassels, F. J.; Carlson, R. W. *J. Biol. Chem.* **2001,** *276,* 26479. doi:10.1074/jbc.M102685200
19. Chamot-Rooke, J.; Rousseau, B.; Lanternier, F.; Mikaty, G.; Mairey, E.; Malosse, C.; Bouchoux, G.; Pelicic, V.; Camoin, L.; Nassif, X.; Duménil, G. *Proc. Natl. Acad. Sci. U. S. A.* **2007,** *104,* 14783. doi:10.1073/pnas.0705335104
20. Kus, J. V.; Kelly, J.; Tessier, L.; Harvey, H.; Cvitkovitch, D. G.; Burrows, L. L. *J. Bacteriol.* **2008,** *190,* 7464. doi:10.1128/JB.01075-08
21. Castric, P. *Microbiology (Reading, U. K.)* **1995,** *141,* 1247. doi:10.1099/13500872-141-5-1247
22. Sugawara, K.; Tsunakawa, M.; Konishi, M.; Kawaguchi, J.; Krishnan, B.; He, C. H.; Clardy, J. *J. Org. Chem.* **1987,** *52,* 996. doi:10.1021/jo00382a005
23. Myers, A. G.; Liang, J.; Hammond, M.; Harrington, P. M.; Wu, Y.; Kuo, E. Y. *J. Am. Chem. Soc.* **1998,** *120,* 5319. doi:10.1021/ja980588y
24. Zhu, X.; Schmidt, R. R. *Angew. Chem., Int. Ed.* **2009,** *48,* 1900. doi:10.1002/anie.200802036
25. Bongat, A. F. G.; Demchenko, A. V. *Carbohydr. Res.* **2007,** *342,* 374. doi:10.1016/j.carres.2006.10.021
26. Buskas, T.; Ingale, S.; Boons, G.-J. *Glycobiology* **2006,** *16,* 113R. doi:10.1093/glycob/cwj125
27. Codée, J. D. C.; Litjens, R. E. J. N.; van den Bos, L. J.; Overkleeft, H. S.; van der Marel, G. A. *Chem. Soc. Rev.* **2005,** *34,* 769. doi:10.1039/b417138c
28. Boons, G.-J.; Demchenko, A. V. *Chem. Rev.* **2000,** *100,* 4539. doi:10.1021/cr990313g
29. Liav, A.; Hildesheim, J.; Zehavi, U.; Sharon, N. *Carbohydr. Res.* **1974,** *33,* 217. doi:10.1016/S0008-6215(00)82799-8
30. Busca, P.; Martin, O. R. *Tetrahedron Lett.* **2004,** *45,* 4433. doi:10.1016/j.tetlet.2004.04.074
31. Jones, G. B.; Lin, Y.; Xiao, Z.; Kappen, L.; Goldberg, I. H. *Bioorg. Med. Chem.* **2007,** *15,* 784. doi:10.1016/j.bmc.2006.10.052
32. Weerapana, E.; Glover, K. J.; Chen, M. M.; Imperiali, B. *J. Am. Chem. Soc.* **2005,** *127,* 13766. doi:10.1021/ja054265v
33. Amin, M. N.; Ishiwata, A.; Ito, Y. *Carbohydr. Res.* **2006,** *341,* 1922. doi:10.1016/j.carres.2006.04.031
34. Schmidt, R. R. *Pure Appl. Chem.* **1987,** *59,* 415. doi:10.1351/pac198759030415
35. Kirschning, A.; Jesberger, M.; Schöning, K.-U. *Synthesis* **2001,** 507. doi:10.1055/s-2001-12342
36. Hemeon, I.; Bennet, A. J. *Synthesis* **2007,** 1899. doi:10.1055/s-2007-983723
37. Vogel, P. In *The Organic Chemistry of Sugars;* Levy, D. E.; Fugedi, P., Eds.; Taylor and Francis Group/CRC Press: Boca Raton, FL, 2006; pp 629 ff.
38. Voigt, B.; Scheffler, U.; Mahrwald, R. *Chem. Commun.* **2012,** *48,* 5304. doi:10.1039/c2cc31541f
39. Crich, D.; Navuluri, C. *Org. Lett.* **2011,** *13,* 6288. doi:10.1021/ol202773t
40. Lorpitthaya, R.; Suryawanshi, S. B.; Wang, S.; Pasunooti, K. K.; Cai, S.; Ma, J.; Liu, X.-W. *Angew. Chem., Int. Ed.* **2011,** *50,* 12054. doi:10.1002/anie.201104516

41. Northrup, A. B.; MacMillan, D. W. C. *Science* **2004,** *305,* 1752. doi:10.1126/science.1101710
42. Babu, R. S.; Zhou, M.; O'Doherty, G. A. *J. Am. Chem. Soc.* **2004,** *126,* 3428. doi:10.1021/ja039400n
43. Enders, D.; Grondal, C. *Angew. Chem., Int. Ed.* **2005,** *44,* 1210. doi:10.1002/anie.200462428
44. Calin, O.; Pragani, R.; Seeberger, P. H. *J. Org. Chem.* **2012,** *77,* 870. doi:10.1021/jo201883k
45. Pragani, R.; Seeberger, P. H. *J. Am. Chem. Soc.* **2011,** *133,* 102. doi:10.1021/ja1087375
46. Pragani, R.; Stallforth, P.; Seeberger, P. H. *Org. Lett.* **2010,** *12,* 1624. doi:10.1021/ol1003912
47. Leonori, D.; Seeberger, P. H. *Org. Lett.* **2012,** *14,* 4954. doi:10.1021/ol3023227
48. Garner, P. *Tetrahedron Lett.* **1984,** *25,* 5855. doi:10.1016/S0040-4039(01)81703-2
49. Cram, D. J.; Kopecky, K. R. *J. Am. Chem. Soc.* **1959,** *81,* 2748. doi:10.1021/ja01520a036
50. O'Brien, A. G. *Tetrahedron* **2011,** *67,* 9639. doi:10.1016/j.tet.2011.10.002
51. Zhang, X.; van der Donk, W. A. *J. Am. Chem. Soc.* **2007,** *129,* 2212. doi:10.1021/ja067672v
52. Garner, P.; Park, J. M.; Malecki, E. *J. Org. Chem.* **1988,** *53,* 4395. doi:10.1021/jo00253a039
53. Blot, V.; Jacquemard, U.; Reissig, H.-U.; Kleuser, B. *Synthesis* **2009,** 759. doi:10.1055/s-0028-1083373
54. Trost, B. M.; Ball, Z. T.; Jöge, T. *J. Am. Chem. Soc.* **2002,** *124,* 7922. doi:10.1021/ja026457l
55. Trost, B. M.; Ball, Z. T. *J. Am. Chem. Soc.* **2005,** *127,* 17644. doi:10.1021/ja0528580
56. Dess, D. B.; Martin, J. C. *J. Org. Chem.* **1983,** *48,* 4155. doi:10.1021/jo00170a070
57. Gaunt, M. J.; Yu, J.; Spencer, J. B. *J. Org. Chem.* **1998,** *63,* 4172. doi:10.1021/jo980823v
58. Liao, W.; Locke, R. D.; Matta, K. L. *Chem. Commun.* **2000,** 369. doi:10.1039/a908511d
59. Lipták, A.; Borbás, A.; Jánossy, L.; Szilágyi, L. *Tetrahedron Lett.* **2000,** *41,* 4949. doi:10.1016/S0040-4039(00)00735-8
60. Cha, J. K.; Kim, N.-S. *Chem. Rev.* **1995,** *95,* 1761. doi:10.1021/cr00038a003
61. Cha, J. K.; Christ, W. J.; Kishi, Y. *Tetrahedron Lett.* **1983,** *24,* 3943. doi:10.1016/S0040-4039(00)88231-3
62. Karjalainen, O. K.; Koskinen, A. M. P. *Org. Biomol. Chem.* **2011,** *9,* 1231. doi:10.1039/c0ob00747a
63. Mancuso, A. J.; Swern, D. *Synthesis* **1981,** 165. doi:10.1055/s-1981-29377
64. Dondoni, A.; Perrone, D. *Org. Synth.* **2004,** *Coll. Vol. 10,* 320.
65. Parikh, J. R.; Doering, W. v. E. *J. Am. Chem. Soc.* **1967,** *89,* 5505. doi:10.1021/ja00997a067
66. De Luca, L.; Giacomelli, G.; Masala, S.; Porcheddu, A. *J. Org. Chem.* **2003,** *68,* 4999. doi:10.1021/jo034276b
67. Snapper, C. M.; Mond, J. J. *J. Immunol.* **1996,** *157,* 2229.
68. Plé, K.; Chwalek, M.; Voutquenne-Nazabadioko, L. *Tetrahedron* **2005,** *61,* 4347. doi:10.1016/j.tet.2005.03.003

License and Terms